U.S. Department of Transportation
Federal Highway Administration

Publication No. FHWA-NHI-16-009
FHWA GEC 012 – Volume I
September 2016

NHI Courses No. 132021 and 132022

Design and Construction of Driven Pile Foundations – Volume I

Developed following:

AASHTO LRFD Bridge Design Specifications, 7th Edition, 2014, with 2015 Interim.

and

AASHTO LRFD Bridge Construction Specifications, 3rd Edition, 2010, with '11, '12, '13, '14, and '15 Interims.





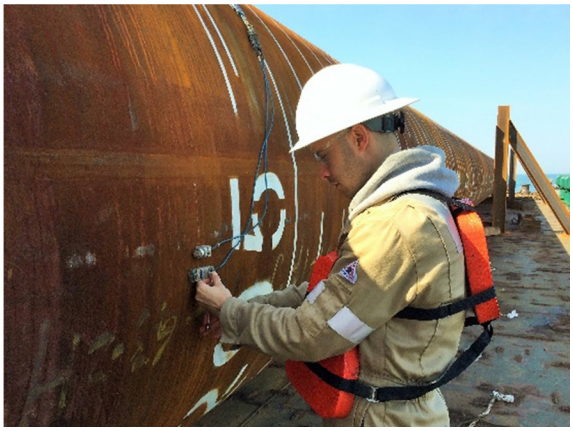

NATIONAL HIGHWAY INSTITUTE
Training Solutions for Transportation Excellence

NOTICE

The contents of this report reflect the views of the authors, who are responsible for the facts and accuracy of the data presented herein. The contents do not necessarily reflect policy of the Department of Transportation. This report does not constitute a standard, specification, or regulation. The United States Government does not endorse products or manufacturers. Trade or manufacturers′ names appear herein only to illustrate methods and procedures, and are considered essential to the objective of this document.

Technical Report Documentation Page

1. REPORT NO.	2. GOVERNMENT ACCESSION NO.	3. RECIPIENT'S CATALOG NO.
FHWA-NHI-16-009		

4. TITLE AND SUBTITLE	5. REPORT DATE
Geotechnical Engineering Circular No. 12 – Volume I Design and Construction of Driven Pile Foundations	September 2016
	6. PERFORMING ORGANIZATION CODE

7. AUTHOR(S)	8. PERFORMING ORGANIZATION REPORT NO.
Patrick J. Hannigan, PE, Frank Rausche, PhD, PE, Garland E. Likins, PE, Brent R. Robinson, PE, and Matthew L. Becker, EI.	

9. PERFORMING ORGANIZATION NAME AND ADDRESS	10. WORK UNIT NO.
Ryan R. Berg & Associates, Inc. 2190 Leyland Alcove Woodbury, MN 55125	11. CONTRACT OR GRANT NO. DTFH61-11-D-00049

12. SPONSORING AGENCY NAME AND ADDRESS	13. TYPE OF REPORT & PERIOD COVERED
National Highway Institute U.S. Department of Transportation Federal Highway Administration, Washington, DC 20590	Final Report
	14. SPONSORING AGENCY CODE

15. SUPPLEMENTARY NOTES

FHWA COTR: Heather Shelsta

FHWA Technical Working Group: Naser Abu-Hejleh, PhD, PE; Scott Anderson, PhD, PE; and Silas Nichols, PE

16. ABSTRACT

This document presents information on the analysis, design, and construction of driven pile foundations for highway structures. This document updates and replaces FHWA NHI-05-042 and FHWA NHI-05-043 as the primary FHWA guidance and reference document on driven pile foundations. The manual addresses design aspects including subsurface exploration, laboratory testing, pile selection, aspects of geotechnical and structural limit states, as well as technical specifications. Construction aspects including static load tests, dynamic tests, rapid load tests, wave equation analyses, dynamic formulas and development of driving criteria, as well as pile driving equipment, pile driving accessories, and monitoring of pile installation inspection are also covered. Step by step procedures are included for most analysis procedures and design examples.

17. KEY WORDS	18. DISTRIBUTION STATEMENT
Driven pile foundations, foundation economics, site characterization, geomaterial properties, axial compression resistance, axial tension resistance, lateral resistance, pile groups, specifications, nominal resistance determination tests, construction monitoring and quality assurance.	No restrictions.

19. SECURITY CLASSIF.	20. SECURITY CLASSIF.	21. NO. OF PAGES	22. PRICE
Unclassified	Unclassified	517	

CONVERSION FACTORS

Approximate Conversions to SI Units			Approximate Conversions from SI Units		
When You Know	**Multiply By**	**To Find**	**When You Know**	**Multiply By**	**To Find**
(a) Length					
inch (in.)	25.4	millimeter (mm)	millimeter (mm)	0.039	inch (in.)
foot (ft)	0.305	meter (m)	meter (m)	3.28	foot (ft)
yard (yd)	0.914	meter (m)	meter (m)	1.09	yard (yd)
mile (mi)	1.61	kilometer (km)	kilometer (km)	0.621	mile (mi)
(b) Area					
square inches (in^2)	645.2	square millimeters (mm^2)	square millimeters (mm^2)	0.0016	square inches (in^2)
square feet (ft^2)	0.093	square meters (m^2)	square meters (m^2)	10.764	square feet (ft^2)
Acres (ac)	0.405	hectares (ha)	hectares (ha)	2.47	Acres (ac)
square miles (mi^2)	2.59	square kilometers (km^2)	square kilometers (km^2)	0.386	square miles (mi^2)
square inches (in^2)	645.2	square millimeters (mm^2)	square millimeters (mm^2)	0.0016	square inches (in^2)
(c) Volume					
fluid ounces (oz)	29.57	milliliters (mL)	milliliters (mL)	0.034	fluid ounces (oz)
Gallons (gal)	3.785	liters (L)	liters (L)	0.264	Gallons (gal)
cubic feet (ft^3)	0.028	cubic meters (m^3)	cubic meters (m^3)	35.32	cubic feet (ft^3)
cubic yards (yd^3)	0.765	cubic meters (m^3)	cubic meters (m^3)	1.308	cubic yards (yd^3)
(d) Mass					
ounces (oz)	28.35	grams (g)	grams (g)	0.035	ounces
pounds (lb)	0.454	kilograms (kg)	kilograms (kg)	2.205	pounds
short tons (2000 lb) (T)	0.907	megagrams (tonne) (Mg)	megagrams (tonne) (Mg)	1.102	short tons (2000 lb)
(e) Force					
pound (lb)	4.448	Newton (N)	Newton (N)	0.2248	pound (lb)
(f) Pressure, Stress, Modulus of Elasticity					
pounds per square foot (psf)	47.88	Pascals (Pa)	Pascals (Pa)	0.021	pounds per square foot (psf)
pounds per square inch (psi)	6.895	kiloPascals (kPa)	kiloPascals (kPa)	0.145	pounds per square inch (psi)
(g) Density					
pounds per cubic foot (pcf)	16.019	kilograms per cubic meter (kgm^3)	kilograms per cubic meter (kgm^3)	0.0624	pounds per cubic feet (pcf)
(h) Temperature					
Fahrenheit temperature (^oF)	5/9(^oF- 32)	Celsius temperature (^oC)	Celsius temperature (^oC)	9/5(^oC)+ 32	Fahrenheit temperature (^oF)

Notes:

1) The primary metric (SI) units used in civil engineering are meter (m), kilogram (kg), second (s), Newton (N), and Pascal ($Pa=N/m^2$).

2) In a "soft" conversion, an English measurement is mathematically converted to its exact metric equivalent.

3) In a "hard" conversion, a new rounded metric number is created that is convenient to work with and remember.

PREFACE

The purpose of this manual is to provide updated, state-of-the-practice information for the design and construction of driven pile foundations in accordance with the Load and Resistance Factor Design (LRFD) platform. Engineers and contractors have been designing and installing pile foundations for many years. During the past three decades, the industry has experienced several major improvements including newer and more accurate methods of predicting and measuring geotechnical resistance, vast improvements in design software, highly specialized and sophisticated equipment for pile driving, and improved methods of construction control. Previous editions of the FHWA Design and Construction of Driven Pile Foundations manual were published 1985, 1996, and 2006 and chronical the many changes in design and construction practice over the past 30 years. This two volume edition, GEC-12, serves as the FHWA reference document for highway projects involving driven pile foundations.

Volume I, FHWA-NHI-16-009, covers the foundation selection process, site characterization, geotechnical design parameters and reporting, selection of pile type, geotechnical aspects of limit state design, and structural aspects of limits state design. Volume II, FHWA-NHI-16-010, addresses static load tests, dynamic testing and signal matching, rapid load testing, wave equation analysis, dynamic formulas, contract documents, pile driving equipment, pile accessories, driving criteria, and construction monitoring. Comprehensive design examples are presented in publication FHWA-NHI-16-064.

Throughout this manual, numerous references will be made to the names of software or technology that are proprietary to a specific manufacturer or vendor. Please note that the FHWA does not endorse or approve commercially available products, and is very sensitive to the perceptions of endorsement or preferred approval of commercially available products used in transportation applications. Our goal with this development is to provide recommended technical guidance for the safe design and construction of driven pile foundations that reflects the current state of practice and provides information on advances and innovations in the industry. To accomplish this, it is necessary to illustrate methods and procedures for design and construction of driven pile foundations. Where proprietary products are described in text or figures, it is only for this purpose.

The primary audience for this document is: agency and consulting engineers specialized in geotechnical and structural design of highway structures; engineering geologists and consulting engineers providing technical reviews, or who are engaged in the design, procurement, and construction of driven pile foundations This document is also intended for management, specification and contracting specialists, as well as for construction engineers interested in design and contracting aspects of driven pile systems.

This document draws material from the three earlier FHWA publications in this field; FHWA-DP-66-1 by Vanikar (1985), FHWA HI 97-013 and FHWA HI 97-014 by Hannigan et al. (1998), and FHWA NHI-05-042 and FHWA NHI-05-043 by Hannigan et al. (2006). Photographs without specific acknowledgement in this two volume document are from these previous editions, their associated training courses, or from the consulting practice of GRL Engineers, Inc.

The following individuals were part of the Ryan R. Berg & Associates internal peer review team and are acknowledged for their technical advice and contributions to this version of the document:

Mr. Jerry DiMaggio – Applied Research Associates, Inc.
Mr. Van E. Komurka – Wagner Komurka Geotechnical Group, Inc.
Mr. Billy Camp – S&ME, Inc.
Dr. Brian Anderson – Auburn University

TABLE OF CONTENTS

LIST OF TABLES

LIST OF FIGURES

LIST OF SYMBOLS

A - Pile cross sectional area (7.3).

A_b - Brown's regression analysis factor based on soil type (7.2).

A_d - Angular distortion (7.3).

A_{dm} - Modified angular distortion (7.3).

A_p - Pile toe area (7.1);
Cross sectional area of pile material at pile toe (7.2) (7.10).

A_{pp} - Cross sectional area of soil plug in open end pipe or H-piles at pile toe (7.2); Cross sectional area of pile and soil plug at pile toe (7.10).

A_{ps} - Cross sectional area of prestressing steel (8.6).

A_s - Pile shaft surface area (7.1) (7.2) (7.10);
Peak seismic ground acceleration coefficient modified by short-period site factor (7.4).

A_{si} - Pile shaft interior surface area (7.10).

A_{so} - Pile shaft exterior surface area (7.10).

A_{st} - Cross sectional area of steel (8.5). (8.7) (9.5).

A_{stc} - Cross sectional area of compression reinforcing steel (8.9).

A_{str} - Cross sectional area of longitudinal reinforcing steel (8.6) (8.7).

A_{stt} - Cross sectional area of tension reinforcing steel (8.9).

A_{stv} - Area of transverse reinforcement within distance, s (8.9).

A_1 - Constant based on soil type and subsurface condition (7.2).

A_2 - Constant based on pile type (7.2).

$\mathrm{a(t)}$ - Acceleration measured at the gage location (10.4).

B - Width of pile group (7.2) (7.3);

B_b - Database calibrated regression factor (7.2).

b - Pile width or diameter (3.5) (7.1) (8.4);
Width/ Height of square (8.2);
Depth of beam or width of dimension lumber (8.4);
Width of the compression face (8.9).

b_c - Column side for square columns (8.9).

b_f - Flange width of pile section (8.2) (8.5).

b_o - Critical punching shear perimeter (8.9).

b_v - Width of interface (8.9).

C - Perimeter of pier excluding half circles at ends of oblong pier (7.4).

C' - Dimensionless bearing capacity index, determined from average corrected SPT N value, for layer with consideration of SPT hammer type (7.3).

C_a - Pile adhesion (7.2) (7.10).

C_c - Compression index (5.2) (7.3).

C_d - Pile perimeter at depth d (7.2);
Deck factor for timber pile structural resistance (8.4).

C_F - Correction factor for K_δ when $\delta \neq \phi$ (7.2).

C_F - Size factor for timber pile structural resistance (8.4).

C_f - Conversion factor for cone tip resistance to sleeve friction (7.2).

C_{fu} - Flat-use factor for timber pile structural resistance (8.4).

C_h - Pore water pressure dissipation factor (7.2).

C_i - Incising factor for timber pile structural resistance (8.4).

C_M - Wet service factor for timber pile structural resistance (8.4).

C_n - Correction factor for SPT N value (5.1).

C_p - Toe correction coefficient for Eslami and Fellenius CPT Method (7.2).

C_r - Recompression index (5.2) (7.3).

C_s - Swell index (5.2);
Shaft correlation coefficient for Eslami and Fellenius CPT Method (7.2).

C_{sm} - Elastic seismic response coefficient (7.4).

C_v - Coefficient of consolidation (5.2) (7.3);
Volume factor for timber pile structural resistance (8.4).

C_α - Secondary compression index (5.2).

C_λ - Time effect factor for timber pile structural resistance (8.4).

C_1 - Composite column constant 1 (8.7).

C_2 - Composite column constant 2 (8.7).

C_3 - Composite column constant 3 (8.7).

C_4 - Damping constant for Statnamic test (11.4).

c - Cohesion (5.2) (7.1);
Distance from centroid to outer edge (8.2);
Distance between the neural axis and the compressive face (8.9).

c' - Effective cohesion (5.2).

c_o - Column diameter (8.9).

c_1 - Small column side for rectangular columns (8.9).

c_2 - Large column side for rectangular columns (8.9).

D - Pile embedded length (3.5) (7.2) (7.3) (7.10);
Pile penetration below the rock surface (7.2).
Outside pile diameter (8.2);

DA - Design angular distortion (7.3).

DWT - Deadweight tonnage (7.4).

D_B - Pile embedded length into bearing stratum (7.3).

D_{il} - Depth from reference to top of incompressible layer (7.3).

D_{np} - Depth from reference to neutral plane (7.3).

D_r - Relative density (5.1) (5.2).

Dδ - Design differential settlement (7.3).

D' - Effective depth, 2/3 pile embedded length (7.1).

D_1 - Inside pile diameter (8.2).

d - Equilibrium depth (7.10).

d_c - Clear space (8.9).

d_f - Depth to fixity below the ground (8.3); Pile embedment into cap (8.9).

d_s - Distance to center of steel (8.9).

d_{sc} - Distance from extreme compression fiber to the centroid of the compression reinforcement (8.9).

d_{st} - Distance from extreme compression fiber to the centroid of the tensile reinforcement (8.9).

d_v - Vane diameter (for Vane Shear Test) (5.2);
Effective depth to reinforcement (8.9).

d_w - Web depth of pile section (8.5).

E - Elastic modulus of material (Youngs modulus) (5.2) (7.3);
Elastic modulus of pile material (7.3) (8.3).

E_c - Elastic modulus of concrete (8.2).

E_e - Modified elastic modulus of steel for composite column (8.7).

E_m - Rock Mass Modulus (5.1).

E_n - Rated hammer energy (5.1).

E_o - Timber reference value for elastic modulus (8.2).

ER - SPT Hammer efficiency as determined by energy measurements in accordance with ASTM D4633 (5.1).

E_r - Manufacturers rated hammer energy (3.5);
Modulus of Intact Rock (5.1).

E_s - Elastic modulus of soil (5.1) (5.2) (7.3) (8.3) .

E_{sm} - Secant modulus (7.3).

E_{st} - Elastic modulus of steel (8.5);
Elastic modulus of prestressing steel (8.6).

E_{50} - 50% secant modulus (5.4).

e - Void ratio (7.3).

e_o - Initial soil layer void ratio (5.2.4) (7.3).

F - Vertical force (7.4).

F_a - Short period site factor (7.4);

F_b - Adjusted timber pile structural flexural resistance (8.4).
F_{bo} - Timber reference value for strength in flexure (8.4).
F_c - Adjusted timber pile structural axial resistance (8.4).
F_{co} - Timber reference value for compressive stress parallel to grain (8.2) (8.4).
F_e - Nominal compressive resistance of composite section (8.7).
F_p - Plug mobilization factor (7.2).
F_{PGA} - Zero period site factor (7.4).
F_v - Long period site factor (7.4).
F_{vo} - Timber reference value for strength in shear (8.4).
F_{vs} - Factor for pile driving method (1.0 for impact or 0.68 for vibratory) (7.2).
F_y - Yield stress of steel (8.2) (8.5) (8.7) (8.8).
F_{yf} - Minimum yield strength of lower strength flange (8.5).
F_{yr} - Yield stress of reinforcing steel (8.6) (8.7).
F_{yw} - Yield stress of web (8.5).
f_c - Consolidation factor (non-dimensional regression factor) (7.2).
f'_c - Ultimate compression strength for concrete,
Concrete compressive strength at 28 days (8.2) (8.6) (8.7).
f_{cr} - Elastic local buckling stress (8.5).
f_n - Unit negative shaft resistance (7.3).
f_{pe} - Effective prestress in concrete (8.6).
f_r - Remolding recovery rate (non-dimensional regression factor) (7.2).
f_s - Unit sleeve friction; Average unit sleeve friction (5.1) (7.2).
f_s - Unit shaft resistance over the pile surface area (7.1) (7.2);
Unit positive shaft resistance (7.3).
f_{sc} - Stress in the mild steel compression reinforcement at nominal flexural resistance (8.9).
f_{si} - Interior unit shaft resistance (7.10).
f_{so} - Exterior unit shaft resistance (7.10).
f_{st} - Stress in the mild steel tension reinforcement at nominal flexural resistance (8.9).
f_1 - Correction factor for undrained shear strength determination (5.2).
G - Shear modulus (5.2) (8.5).
G_s - Specific Gravity (5.2).
H_o - Initial soil layer thickness (5.2) (7.3).
H_v - Maximum vertical drainage path in cohesive layer (7.3).
h - Total Thickness of sublayers (7.3);
Distance between flange and centroid for warping torsional constant (8.5); Structural depth, thickness of cap less pile embedment (8.9).

h_f - Height of embankment fill (7.3).

h_i - Thickness of soil strata (5.2).

h_v - Vane height (for Vane Shear Test) (5.2).

h_w - Height of water (pressure head) for calculation of pore water pressure (5.2).

I - Moment of inertia (8.2);
Weak axis moment of inertia (8.3).

I_f - Influence factor for group embedment (7.3).

I_x - Moment of inertia about the major principal axes of cross section (8.5).

I_y - Moment of inertia about the minor principal axes of cross section (8.5).

j - Stress exponent (7.3).

K - Effective length factor for buckling (7.2) (8.2) (8.5) (8.7).

K_o - At rest earth pressure coefficient (5.2) (7.2).

K_s - Ratio of unit pile shaft resistance to cone unit sleeve friction for cohesionless soils (7.2).

K_δ - Coefficient of lateral earth pressure (7.2).

k_c - Modulus of subgrade reaction for cyclic lateral loading (7.3).

k_s - Modulus of subgrade reaction for static lateral loading (7.3).

k_1 - Regression factor (0.17 for PSC, 0.12 for CEP and 0.15 for OEP) (7.2).

k_2 - Regression factor (0.00044 for PSC piles, 0.00078 for CEP, and 0.00060 for OEP) (7.2).

L - Total pile length (7.3).

L% - Pile length subject to heave (7.10).

L_e - Effective pile length considering unbraced length (8.4).

L_o - Embedded pile length at the time of initial driving (7.2).

L_s - Span length (7.3).

L_t - embedded pile length at time “t” after initial driving (7.2).

l - Unbraced length, or laterally unsupported length plus d_f (8.3) (8.5) (8.7).

M_b - Bending moment (7.3).

M_n - Nominal flexural resistance (structural) (8.4) (8.5) (8.6).

M_p - Plastic moment about the weak axis (8.5).

M_r - Factored flexural resistance (structural) (8.3) (8.5) (8.6).

M_{rx} - Factored flexural resistance about x-axis (8.5) (8.6).

M_{ry} - Factored flexural resistance about y-axis (8.5) (8.6).

M_u - Factored moment load (structural) (2.3) (8.3).

M_{ux} - Factored moment about x-axis (8.5) (8.6) (8.8).

M_{uy} - Factored moment about y-axis (8.5) (8.6) (8.8).

m_n - Dimensionless modulus number (7.3).

m_{nr} - Dimensionless recompression modulus number (7.3).

m_s - Semilog-linear slope of R_s vs t from multiple restrike tests (7.2).

N - Uncorrected field SPT resistance value (5.1) (5.2) (5.4) (5.5) (7.2) (7.3) (7.4).

N_a - Average SPT N-Value over pile length (7.2).

N_c - Dimensionless bearing capacity factor (7.2).

N_k - Bearing capacity factor, typically from 15 to 20 (5.2).

N_q - Dimensionless bearing capacity factor (API Method) (7.2).

N'_q - Dimensionless bearing capacity factor (7.2).

N_t - Toe resistance coefficient (7.2).

N_{60} - SPT N value corrected for 60% energy transfer (5.1.1) (7.2) (7.3).

$(N_1)_{60}$ - SPT N value corrected for energy and overburden stress (5.1) (5.2) (7.2) (7.4) (7.10);
Average corrected SPT N value within a depth B below pile toe (7.3).

$(N_1)_{60e}$ - Equivalent clean sand blow count (7.4).

N_{corr} - SPT N value corrected for percent fines (7.4.).

N_γ - Bearing capacity factor (7.2).

n - Exponent typically equal to 1 in clays (e.g., Olsen 1997) and 0.5 in sandy soils (e.g. Lio and Whitman 1986) (5.1);
Number of piles in pile group (7.2) (7.3) (8.8).

n_h - Rate of increase of soil modulus with depth (8.3).

n_i - Number of piles whose centers lie inside the two-way shear critical section (8.9).

n_o - Number of piles whose centers lie outside the two-way shear critical section (8.9).

P_e - Elastic critical buckling resistance (8.5).

$P_e(x)$ - Equivalent static horizontal seismic force acting on superstructure (7.4).

PGA - Peak ground acceleration coefficient (7.4).

P_m - P-multiplier for p-y curve (7.3).

P_n - Nominal axial resistance (structural) (8.4.2) (8.5) (8.6) (8.7).

P_o - Equivalent nominal axial yield resistance (structural) (8.5) (8.6).

P_r - Factored axial resistance (structural) (3.4.1) (8.3) (8.5) (8.6) (8.7).

P_{rx} - Factored axial resistance determined on the basis that only eccentricity, e_y, is present (8.6).

P_{rxy} - Factored axial resistance in biaxial flexure (8.6).

P_{ry} - Factored axial resistance determined on the basis that only eccentricity, e_x, is present (8.6).

P_s - Pile shape factor (7.2);

P_s - Equivalent static vessel impact force (7.4).

P_t - Pile base factor (7.2).

P_u - Factored axial load (structural) (8.3.3) (8.6) (8.8) (8.9).

P_{ui} - Maximum single pile axial load (8.8).

P_{uz} - Factored axial load from superstructure/substructure acting upon pile cap (8.8).

p - Soil resistance per unit pile length (7.3).

p_a - Atmospheric pressure (5.1) (5.2).

p_f - Design foundation pressure (7.3.4).

Q - Total factored load (2.3); Factored axial load (7.3) (7.6); Slender element reduction factor (8.5).

Q_c - Scour Design Check Flood Frequency (7.2).

Q_d - Hydraulic design flood frequency (7.2); Unfactored permanent load (7.3).

Q_{max} - Maximum axial compressive force in the pile (7.3).

Q_l - Live load on a pile (7.3).

Q_i - Force effect (2.3) (7.3) (7.4).

Q_L - Lateral pile load (7.3).

Q_s - Scour Design Flood Frequency (7.2).

q - Surcharge (7.3).

q_c - Cone tip resistance (5.1) (5.2) (7.2).

q_{ca} - Average cone tip resistance within a depth of B below the pile toe (7.3).

q_{c1} - Average q_c over a distance of x_b below the pile toe (7.2).

q_{c2} - Average q_c over a distance of 8b above the pile toe (7.2).

q_{DMT} - Dilatometer test tip resistance (5.5).

q_E - Eslami cone stress (7.2).

q_{Eg} - Geometric average of the corrected cone tip resistance over the influence zone (7.2).

q_L - Limiting unit toe resistance (7.2).

q_p - Unit toe resistance (7.1) (7.2) (7.1).

q_t - Corrected cone tip resistance (5.1) (7.2).

q_u - Unconfined compressive strength (5.1) (5.2) (5.3) (5.5) (7.2).

R - Radius of pier (7.4).

R_f - Friction ratio or f_s/q_t (5.1).

R_n - Nominal resistance (2.4) (3.4) (7.1) (7.2) (7.3) (7.6) (7.10). Nominal resistance of each individual pile in the group (7.2).

R_{ndr} - Nominal driving resistance (3.4) (7.6).

R_{ng} - Nominal resistance of pile group (7.2).

R_{no} - Initial nominal resistance at time "t_o" of driving (7.2).

R_p - Nominal toe resistance (7.1) (7.2) (7.3).

R_r - Factored resistance (2.4) (7.2) (8.8) (8.9).

R_{relax} - Resistance loss from relaxation (7.6).
R_{rg} - Factored resistance of the pile group (7.3).
R_s - Nominal shaft resistance (3.4) (7.1) (7.2) (7.3) (12.7).
R_{scour} - Resistance loss from scour (7.6).
R_{so} - Initial shaft resistance at "t_o" of driving (7.2).
R_s^+ - Positive Shaft Resistance (7.3).
R_s^- - Negative Shaft Resistance (7.3).
R_{ug} - Nominal uplift resistance of the pile group (7.2).
r_p - Equivalent pile radius (7.2).
r_s - Minimum radius of gyration (8.3);
Radius of gyration about axis normal to plane of buckling (8.5) (8.7).
S - Settlement (7.1); Estimated total settlement (7.3);
Elastic section modulus (8.2) (8.4).
S_{avg} - Average settlement (3.5).
S_d - Differential settlement of the foundation (7.3).
S_{dd} - downdrag movement (7.3).
S_c - Settlement from primary consolidation (5.2) (7.3).
S_{DS} - C_{sm} value with a period of 0.2 seconds = F_aS_s (7.4).
S_{D1} - C_{sm} value with a period of 0.2 seconds = F_vS_1 (7.4).
S_h - Horizontal abutment movement (7.3).
S_{max} - Maximum settlement (3.5).
S_p - Pile slope (7.3).
S_s - Short period spectral acceleration (7.4).
S_t - Sensitivity of a cohesive soil (5.2).
S_{ta} - Total foundation settlement (7.3).
S_{tp} - Total foundation settlement before construction (7.3).
S_{tr} - Relevant total settlement (7.3).
S_v - Vertical fill settlement (7.3).
S_y - Elastic section modulus about weak axis (8.5).
S_1 - Long period coefficient (7.4).
s - Spacing of the transverse reinforcement (8.9).
s_r - Residual shear strength (7.4).
s_u - Undrained shear strength (3.4) (5.1) (5.2) (5.5) (7.2) (7.4) (8.3);
Vane Shear Test undrained shear strength (5.5);
Average undrained shear strength (7.3);
Undrained shear strength of soft cohesive soil (7.3) (7.10).
T - Theoretical time factor for percentage of primary consolidation (7.3).
T_m - Period of vibration of m^{th} mode(s) (7.4).
T_o - Reference period to define spectral shape = $0.2T_s$ (7.4).

T_s - Corner period when spectrum changes from independent to inversely proportional = S_{D1} /$S_{DS.}$ (7.4).

T_v - Input torque during shear (for Vane Shear Test) (5.2).

t - Time after driving (7.2);
Time for settlement to occur (7.3);

t - Pipe pile wall thickness (8.2) (8.5).

t_{cap} - Thickness of pile cap (8.9).

t_f - Flange thickness of pile section (8.2) (8.5).

t_i - Ice thickness (7.4).

t_o - Time after driving from which the increase in resistance is linear in logarithmic time (days) (typically 0.5 for sand, 1.0 for clay) (7.2).

t_{soil} - Thickness of compressible soil beneath neutral plane (7.3).

t_w - Web thickness of pile section (8.2) (8.5).

U - Displacement (7.3).

u - Pore water pressure (5.1) (5.2) (7.1).

u_e - Excess pore water pressure (7.2).

u_h - Hydrostatic pore water pressure (7.2).

V - Volume of soil displaced per unit length of pile (7.2);
Vessel impact velocity (7.4).

V_c - Nominal shear resistance provided by concrete tensile strength (8.9).

V_n - Nominal shear resistance (8.9).

V_r - Factored shear resistance (structural) (8.3).

V_s - Shear wave velocity (7.4);
Nominal shear resistance provided by steel reinforcement (8.9).

V_u - Factored shear load (structural) (2.3) (8.3) (8.9).

W - Pier or Abutment Width (4.2);
Equivalent weight of the superstructure (7.4).

W_c - Estimated weight of pile cap (8.8).

W_g - Effective weight of the pile/soil block including pile cap weight (7.2).

W_p - Weight of soil plug (7.10).

W_s - Estimated weight of soil above pile cap (8.8).

w - Moisture Content (5.1) (5.2) (7.2) (7.4).

x - Distance along x-axis from the center of the column to each pile center (8.8).

Y_o - Pile head deflection (7.3).

y - Lateral soil (or pile) deflection (7.3);
Distance along y-axis from the center of the column to each pile center (8.8).

Z - Length of pile group (7.2) (7.3).

Z_y - Plastic section modulus about weak axis (8.5).

α - Compression factor for settlement (3.4) (3.5);
Dimensionless adhesion factor (7.2).

α' - Ratio of pile unit shaft resistance to cone unit sleeve friction for cohesive soils (7.2).

α_t - Dimensionless factor in Nordlund method (7.2).

β - Bjerrum-Burland beta coefficient (7.2).

β_c - Ratio of the long side to the short side of the load (8.9).

β_m - Mobilized angle for strain wedge analysis (7.3).

β_1 - Stress block factor (8.9).

Δ - Elastic compression (7.3).

Δd - Length of pile segment (7.2).

ΔH - Total settlement at Pier or Abutment (7.3).

ΔH_{100} - Differential settlement over 100 Feet within a pier or abutment, or the differential settlement between piers (7.3).

Δ_{um} - Maximum excess pore pressure (7.2).

$\Delta\sigma$ - Additional stress at mid-point of soil layer from loading (5.2);
Additional pressure from structural loading (7.3).

$\Delta\sigma_h$ - Changes in deviator stress in the direction of loading (7.3).

$\Delta\varepsilon$ - Strain from the increase in effective stress (7.3);

δ - Friction angle between pile and soil (7.2) (7.3);

ε - Strain (5.2) (7.3).

ε_{cu} - Failure strain of concrete in compression (8.6).

ε_v - Vertical strain (5.2).

ε_{50} - Strain at one half the maximum principal stress (7.3) (7.4).

η_g - Pile group efficiency (7.2).

η_i - Load modifier based on ductility, redundancy, or operation classification (2.3) (2.4).

γ - Total unit weight of soil (5.1) (5.2) (5.5).

γ' - Buoyant unit weight of soil (5.5).

γ_d - Dead Load Factor (7.3).

γ_f - Unit weight of embankment fill (7.3).

γ_i - Load factor, statistically based multiplier applied to force effect (2.3) (2.4) (7.4) (7.3);
Unit weight of soil strata for calculation of in-situ stress (5.2).

γ_l - Load factor for force effect due to live loads (7.3).

γ_p - Load factor for force effect due to permanent loads (2.3) (7.3) (7.4).

γ_{SE} - Load factor for force effect due to vertical settlement (7.3).

γ_{TG} - Load factor for force effect due to temperature gradient (2.3).

γ_w - Unit weight of water (5.2).

λ - Normalized column slenderness factor (8.7).

λ_f - Slenderness ratio for flange (8.5).

λ_{pf} - Limiting slenderness ratio for a compact flange (8.5).

λ_{rf} - Limiting slenderness ratio for a non-compact flange (8.5).

v - Poisson ratio (5.2) (5.4).

σ - Normal stress (pressure) on plane of failure, stress (5.2).

σ' - Effective normal stress (pressure) on plane of failure (σ - u) (5.2).

σ'_d - Vertical effective stress at the center of depth increment d (7.2).

σ_{dr} - Driving stress (8.4) (8.5) (8.6).

σ'_{ho} - Horizontal effective stress at the sample depth (5.2).

σ'_o - Effective stress prior to stress increase (7.3).

σ_p - Preconsolidation pressure or stress (5.1) (5.2) (7.3).

σ'_p - Vertical effective stress at the pile toe (7.2).

σ_r - Reference stress for settlement with Janbu Tangent Modulus (7.3).

σ_v - Total stress (7.1).

σ'_v - Vertical effective stress (7.1).

σ'_{vi} - Initial vertical effective stress prior to pile driving (7.2).

σ'_{vo} - Vertical effective stress at the sample depth (5.1.1) (5.2) (7.2); Vertical effective stress at midpoint of each layer (prior to stress increase) (7.3).

σ'_1 - Effective stress after stress increase (7.3).

τ - Shear stress at failure (shear strength) (5.2); Shear strength of soil (7.1).

ϕ - Resistance factor, statistically based multiplier on nominal resistance (2.4); Angle of internal friction (2.4) (5.1) (5.2) (5.5) (7.1) (7.2) (7.3).

ϕ' - Effective Stress Friction Angle (5.1) (5.5) (7.2.) (7.10).

ϕ_c - Resistance factor (pile structural resistance in compression) (8.3) (8.5) (8.6).

ϕ_{b1} - Block Failure (7.1).

ϕ_{da} - Resistance factor (pile structural resistance during driving) (8.3) (8.4) (8.5) (8.6).

ϕ_{dyn} - Resistance factor (based on the construction control method) (2.10) (3.4) (7.1) (7.2) (7.6).

ϕ_f - Resistance factor (pile structural resistance in flexure) (8.3) (8.5) (8.6).

ϕ_m - Mobilized angle of internal friction (7.3).

ϕ_{stat} - Resistance factor (based on the static analysis method) (7.1) (7.2).

ϕ_{ug} - Resistance factor for group uplift (based on the uplift analysis method) (7.1) (7.2).

ϕ_{up} - Resistance factor (based on the uplift analysis method) (3.4) (7.1) (7.2).

ϕ_v - Resistance factor (pile structural resistance in shear) (8.3).

ψ - Ratio of undrained shear strength divided by effective overburden pressure,s_u/σ'_{vo} (7.2).

ω - Angle of pile taper from vertical (7.2).

μ - Correction factor (5.2).

LIST OF ACRONYMNS

AASHTO	-	American Association of State Highway and Transportation Officials
ASTM	-	American Society for Testing and Materials
BL	-	Blast load
BOR	-	Beginning of Restrike
BR	-	Vehicular braking force
CD	-	Consolidated Drained triaxial test
CE	-	Vehicular centrifugal force
CED	-	Closed End Diesel hammer
CEP	-	Closed End Pipe
CFA	-	Continuous Flight Auger
COR	-	Coefficient of Restitution
CPT	-	Cone Penetration Test
CPTu	-	Piezo Cone Penetration Test
CR	-	Force effects due to creep
CT	-	Vehicular collision force
CU	-	Consolidated Undrained triaxial test
CV	-	Vessel collision force
DA	-	Design Angular Distortion
DC	-	Dead load components and attachments
DD	-	Downdrag
DF	-	Drag force
DLT	-	Dynamic Load Test
DMT	-	Dilatometer test
DW	-	Wearing surface and utilities
DWT	-	Deadweight tonnage
EH	-	Horizontal earth pressure
EL	-	Locked-in stress
EOD	-	End of Drive
EQ	-	Earthquake load
ER	-	SPT hammer efficiency as determined by energy measurements
ES	-	Earth surcharge
EV	-	Vertical earth pressure
FHWA	-	Federal Highway Administration
FR	-	Friction load
I.D.	-	Inner diameter

IC	-	Ice load
IM	-	Vehicular dynamic load allowance
KE	-	Kinetic Energy
LL	-	Liquid Limit; Vehicular live load
LS	-	Live Load Surcharge
LVDT	-	Linear Variable Differential Transformer
MUP	-	Modified Unloading Point Method
NHI	-	National Highway Institute
O.D.	-	Outer Diameter
OED	-	Open Ended Diesel hammer
OEP	-	Open Ended Pipe
PE	-	Potential Energy
PGA	-	Peak Ground Acceleration coefficient
PI	-	Plasticity Index
PL	-	Plastic Limit; Pedestrian live load
PS	-	Secondary forces from post-tensioning
RSA	-	Residual Stress Analysis
SA	-	Static Analysis
SE	-	Force effect due to settlement
SH	-	Force effects due to shrinkage
SLT	-	Static Load Test
SPT	-	Standard Penetration Test
SRD	-	Soil Resistance to Driving
SUP	-	Segmental Unloading Point Method
TG	-	Force effect due to temperature gradient
TU	-	Force effect due to uniform temperature
UPM	-	Unloading Point Method
UU	-	Unconsolidated Undrained triaxial test
VST	-	Vane shear test
WA	-	Water load and steam pressure
WD	-	Downward traveling wave, Wave Down
WE	-	Wave Equation
WEAP	-	Wave Equation Analysis Program
WL	-	Wind on live load
WS	-	Wind load on structure
WU	-	Upward traveling wave, Wave Up

CHAPTER 1

DRIVEN PILE FOUNDATION MANUAL

1.1 INTRODUCTION

In 1985 the Federal Highway Administration (FHWA) published the first edition of this manual. Subsequent editions were published in 1997 and 2006. Since the last published update, significant changes in pile design, construction, and performance requirements have occurred which make it necessary to once again update the manual. This 2015 update is primarily dictated by the need to revise and update manual content in accordance with the Load and Resistance Factor Design (LRFD) methodology which replaced the Allowable Strength Design (ASD) method for the design of transportation substructures in 2007. Other significant changes in practice addressed by this edition of the manual include:

- emphasis on a rational economic evaluation of the foundation design,
- use of higher strength pile materials and/or larger driven pile sections to support greater foundation loads,
- updates in computer programs for pile foundation analysis and design,
- use and quantification of soil setup in pile design and construction,
- improvements in pile installation equipment and equipment performance monitoring,
- increased use of instrumented static load test programs, and
- improvements in QA/QC methods for nominal resistance and pile integrity verifications.

1.2 PURPOSE OF THE MANUAL

The purposes of the previous driven pile foundation manual editions remain largely unchanged. It is worthwhile to restate the purpose and objectives of the manual.

1. There exists a vast quantity of information on driven pile foundations which presently is not compiled in a form which is useful to most practicing engineers. There are proven rational design procedures, information on construction materials, equipment and techniques, and useful case histories.

Unfortunately, much of this information is fragmented and scattered. Standard textbooks and other publications on the subject tend to be theoretically oriented and practicing design and construction engineers often find them lacking in practical aspects. One of the primary goals of this manual is to meet that need for the practicing engineer.

2. Many historical design methods lead to unnecessarily conservative designs because they were based solely on experience and tradition with little theoretical background. Well established rational design procedures and techniques are summarized herein that provide more economical driven pile foundation systems that can safely support the applied structural loads.

3. There are opportunities for substantial cost savings on driven pile foundation projects through the use of improved methods of design and construction technology. A minimum of fifteen percent of the substructure cost can be easily saved by utilizing such methods and, in most cases, the savings are more significant.

4. Since the adoption of LRFD methodology for all transportation projects, a comprehensive driven pile foundation manual has been needed. This manual is intended to fulfill that need as well as to establish minimum design standards and recommendations.

5. Design criteria for bridges and other structures are becoming more complex and sophisticated. Extreme design events such as scour, debris loading, vessel impact, and seismic events require that foundation performance be evaluated under lateral and uplift loading, group behavior, and substructure - superstructure interaction. In addition, deformation performance requirements (lateral and vertical deflections) are routinely included in project requirements. This new series of performance criteria frequently results in foundations which are more costly, more complex to design, and more difficult to construct.

6. The loading conditions noted above have can have a substantial impact on the structural design of the piles. In the past, driven piles were often designed structurally for axial loads only using an allowable stress approach. The allowable stresses had been established primarily to assure pile drivability. However, the requirement that piles be analyzed for combined horizontal and axial loads requires a change in the evaluation procedure. The pile top is subjected to both horizontal and axial loads and in a pile group the

pile resistance to lateral loads varies with each pile row. Of course this complicates the geotechnical analysis. It also complicates the pile structural analysis. A combined bending and axial load analysis of the structural behavior of the pile must be performed. Particularly for concrete piles this analysis must be based on an ultimate strength analysis and it is not always obvious which pile within a group is the critical one. Comprehensive software is now available to perform the necessary analyses and is discussed herein.

7. Alternative contracting methods (ACM), design-build (D-B) and CM/GC (construction manager/general contractor), are increasingly replacing the conventional design-bid-build (DBB) method as the preferred methods of project development and delivery. Among the changes which these ACM's affect is an intentional, but yet aggressive challenge to existing design specifications.

8. Final pile design selection should involve a cost evaluation. In the past, such evaluations have been implied but they were not a routine part of the design process. Methods have been developed to perform cost evaluations of pile foundations that include the effects of soil setup. These concepts will be presented in this edition of the manual.

9. A larger selection of pile hammer types and sizes, improvements in hammer performance, advancements in equipment controllability and installation aids allow efficient pile installation in most subsurface conditions.

1.3 SCOPE OF MANUAL

The manual is limited to driven piles and consists of eighteen chapters and four appendices. The first half of the manual covers the design aspects of pile foundations including cost evaluations, geotechnical data collection and analysis, selection of pile type, as well as geotechnical and structural aspects of limit state design. The second half of the manual covers methods of nominal resistance verification as well as chapters on pile driving equipment, accessories and inspection procedures. Theoretical discussions have been included only where necessary. Specific recommendations are made where appropriate. Example problems are included to provide hands-on knowledge to manual users.

The manual is a standalone document that provides guidance for engineers on the design and construction of driven pile foundations. A separate training course will

be used to transfer knowledge in this area and will continue with the original goal of updating transportation department practice. Also, new engineers continue to join transportation agencies and require expanding their knowledge in the practical aspects of pile design and installation.

1.4 HISTORY OF DRIVEN PILE FOUNDATIONS

The detailed history of driven pile foundations has been lost to time. It has been postulated that some of the earliest use of driven timber piles dates back to 800 BC where the piles were installed with mauls or drop hammers. Reinforced concrete piles debuted in Europe in 1897 and in Chicago in 1901. Structural steel piles including, pipe, I-beams, and H-piles followed not too long thereafter. Octagonal and square, precast, prestressed concrete piles as well as 36 inch and 54 inch diameter post-tensioned concrete cylinder piles developed in the 1950's.

As noted above, the first pile hammers were simple drop hammers. The first modern pile driving hammer was a Scottish steam hammer patented by Naysmith in 1839. In the U.S., steam pile driving hammers were reported between the mid- to late 1800's. In the mid 1920's, the diesel pile hammer was invented in Germany. Vibratory hammers were invented in the Soviet Union in the 1940's and made their way into the U.S. market in the 1960's. The first hydraulic pile hammers were developed in Scandinavia in the 1960's. In the 1960's, Bodine developed a resonant pile hammer but the hammer had limited use in the market due to mechanical reliability issues. The resonant pile driver re-emerged in the 2000's. Many improvements in hammer features and operation have occurred over the years for all hammer types. Rausche (2000) summarized the development of pile driving equipment along with equipment capabilities and properties.

1.5 INFORMATION SOURCES

The information presented in this manual has been collected from several sources. The primary references are the 7th Edition of the AASHTO LRFD Bridge Design Specifications (2014) with 2015 Interim Revisions and the 3rd Edition of the AASHTO LRFD Bridge Construction Specifications with 2010, 2011, 2012, and 2014 Interim Revisions. Additional sources of information include: "Evaluation of Soil and Rock Properties," GEC-5 by Sabatini et al. (2002), "Implementation of AASHTO LRFD Design Specifications for Driven Piles" by Abu-Hejleh et al. (2013), "Drilled Shafts: Construction Procedures and LRFD Design Methods" GEC-10 by Brown et

al. (2010), “LRFD Seismic Analysis and Design of Transportation Geotechnical Features and Structural Foundations” GEC-3 by Kavazanjian et al. (2011) as well as “Evaluating Scour at Bridges, Fifth Edition” HEC-18 by Arneson et al. (2012).

The information within has been condensed, modified and updated as needed. The sources also include state-of-the-art technical publications, manufacturers' literature, existing Federal Highway Administration (FHWA), National Highway Institute (NHI) and Transportation Research Board (TRB) publications, standard textbooks, and information provided by State and Federal transportation engineers. Reference lists are provided at the end of each chapter.

Many of the documents used in the development or updating of this manual, as well as useful industry links are available at www.fhwa.dot.gov/engineering/geotech/.

REFERENCES

Abu-Hejleh, N., Kramer, W.M., Mohamed, K., Long, J.H., and Zaheer, M.A. (2013). Implementation of AASHTO LRFD Design Specifications for Driven Piles, FHWA-RC-13-001. U.S. Dept. of Transportation, Federal Highway Administration, 71 p.

American Association of State Highway and Transportation Officials (AASHTO). (2014). AASHTO LRFD Bridge Design Specifications, US Customary Units, Seventh Edition, with 2015 Interim Revisions. American Association of State Highway and Transportation Officials, Washington, D.C., 1960 p.

Arneson, L.A., Zevenbergen, L.W., Lagasse, P.F., and Clopper, P.E. (2012). Evaluating Scour at Bridges, Fifth Edition, FHWA-HIF-12-003, Hydraulic Engineering Circular (HEC) No. 18. U.S. Dept. of Transportation, Federal Highway Administration, 340 p.

Brown, D. A., Turner, J.P. and Castelli R.J. (2010). Drilled Shafts: Construction Procedures and LRFD Design Methods, FHWA-NHI-10-016, Geotechnical Engineering Circular (GEC) No. 10. U.S. Dept. of Transportation, Federal Highway Administration, 970 p.

Kavazanjian, E., Wan, J-N. J., Martin, G.R., Shamsabadi, A., Lam, I., Dickenson, S.E., and Hung, C.J. (2011). LRFD Seismic Analysis and Design of Transportation Geotechnical Features and Structural Foundations, FHWA-NHI-11-032, Geotechnical Engineering Circular (GEC) No. 3. U.S. Dept. of Transportation, Federal Highway Administration, 592 p.

Rausche, F. (2000). Keynote Lecture: Pile Driving Equipment: Capabilities and Properties, Proceedings of the Sixth International Conference on the Application of Stress Wave Theory to Piles, A.A. Balkema, pp. 75-90.

Sabatini, P.J., Bachus, R.C., Mayne, P.W., Schneider, J.A., and Zettler, T.E. (2002). Evaluation of Soil and Rock Properties, FHWA-IF-02-034, Geotechnical Engineering Circular (GEC) No. 5. U.S. Dept. of Transportation, Federal Highway Administration, 385 p.

CHAPTER 2

OVERVIEW OF PILE FOUNDATION DESIGN & CONSTRUCTION

2.1 INTRODUCTION

As stated by Professor R. B. Peck, “driving piles for a foundation is a crude and brutal process.” The interactions among the piles and the surrounding soil are complex. Insertion of piles alters the character of the soil and intense strains are set up locally near the piles. The non-homogeneity of soils, along with the effects of the pile group and pile shape, adds further difficulties to the understanding of soil-pile interaction. For piles driven to hard rock or into soft rock, the strength and structure of the rock mass including joints, bedding planes, and the degree of weathering complicate our understanding of rock-pile interaction.

Broad generalizations about pile behavior are unrealistic. An understanding of the significance of several factors involved is required to be successful in the design of pile foundations. Because of the inherent complexities of pile behavior, it is necessary to use practical semi-empirical methods of design, and to focus attention on significant factors rather than minor or peripheral details.

To arrive at the optimum driven pile foundation solution, the foundation engineer must have a thorough understanding of the subsurface conditions including soil/rock parameters and behavior, the applicable limit states, the factored loads and load combinations, project performance requirements, foundation costs, and the current foundation design and construction practices where the foundation is located.

2.2 LIMIT STATES

Four limit states are identified in the AASHTO LRFD Bridge Design Specifications (AASHTO 2014): strength, service, extreme event, and fatigue. In addition, these limit states have several load combination cases such that up to thirteen limit states may require evaluation in a bridge design. There are five strength limit cases, two extreme event limit cases, four service limit cases, and two fatigue limit cases as described in Table 2-1.

Limit states that commonly govern driven pile foundation designs include: Strength I, Strength IV, Extreme Event I (earthquake), Extreme Event II (ice, vessel, blast, and vehicle collision), and Service I. All applicable limit states have equal importance in a driven pile foundation design. Service Limit States II, III, and IV and Fatigue Limit States I and II are relevant to the behavior of superstructure elements and are not generally applicable to foundation design.

Table 2-1 Limit State, Load Case, and Load Combination (after AASHTO 2014)

Limit State and Load Case	Load Combination
Strength I	Basic load combination related to normal vehicular use of the bridge without wind.
Strength II	Load combination relating to use of the bridge by owner-specified special vehicles, evaluation permit vehicles, or both, without wind.
Strength III	Load combination for bridge exposed to wind velocity exceeding 55 mph without live loads.
Strength IV	Load combination for very high dead load to live load force effect ratios. (Typical for bridge spans greater than 250 feet).
Strength V	Load combination for normal vehicular use of the bridge with wind velocity of 55 mph.
Extreme Event I	Load combinations including earthquake.
Extreme Event II	Load combinations relating to ice load, collision by vessels and vehicles, and certain hydraulic events with a reduced live load other than that which is part of the vehicular collision load.
Service I	Load combinations relating to normal operational use of the bridge with a 55 mph wind and all loads taken at their nominal values.
Service II	Load combinations intended to control yielding of steel structures and slip of slip-critical connections due to vehicular live load.
Service III	Load combinations relating to tension in prestressed concrete superstructures with the objective of crack control and to principal tension in the webs of segmental concrete girders.
Service IV	Load combinations intended to control tension in prestressed concrete columns with the objective of crack control.
Fatigue I	Fatigue and fracture load combination related to infinite load-induced fatigue life.
Fatigue II	Fatigue and fracture load combination related to finite load-induced fatigue life.

2.3 LOADS, LOAD COMBINATIONS, AND LOAD FACTORS

The total factored load, *Q*, associated with a given limit state is calculated based on the applicable force effect, load modifiers, and load factors.

$$Q = \sum \eta_i \gamma_i Q_i \qquad \text{Eq. 2-1}$$

Where:

- η_i = load modifier based on ductility, redundancy, or operation classification.
- γ_i = load factor, a statistically based multiplier applied to force effect.
- Q_i = force effect.

A specific load combination applies for each limit state case. A general description of the applicable load, load combinations and load factors associated with each limit state is presented in Table 2-2. The two letter codes in the second column in Table 2-2 correspond to permanent loads and the remaining two letter code descriptions correspond to transient loads.

For example, the total factored load, *Q*, for Strength Limit State I is defined as follows:

$$Q = \gamma_p DC + \gamma_p DD + \gamma_p DW + \gamma_p EH + \gamma_p EV + \gamma_p ES + \gamma_p EL + \gamma_p PS + \gamma_p CR + \gamma_p SH + 1.75LL + 1.75IM + 1.75CE + 1.75BR + 1.75PL + 1.75LS + WA + FR + 1.20TU + \gamma_{TG} TG + \gamma_{SE} SE$$

The load factor for permanent loads, γ_p, has maximum and minimum values as prescribed in Table 2-3. For permanent force effects, the load factor that produces the more critical load combination is selected from Table 2-3.

Table 2-2 Load Combinations and Load Factors (after AASHTO 2014)

Load Combination Limit State	DC DD DW EH EV ES EL PS CR SH	LL IM CE BR PL LS	WA	WS	WL	FR	TU	TG	SE	EQ*	BL*	IC*	CT*	CV*
Strength I	γ_p	1.75	1.00	- - -	- - -	1.00	0.50/1.20	γ_{TG}	γ_{SE}	- - -	- - -	- - -	- - -	- - -
Strength II	γ_p	1.35	1.00	- - -	- - -	1.00	0.50/1.20	γ_{TG}	γ_{SE}	- - -	- - -	- - -	- - -	- - -
Strength III	γ_p	- - -	1.00	1.40	- - -	1.00	0.50/1.20	γ_{TG}	γ_{SE}	- - -	- - -	- - -	- - -	- - -
Strength IV	γ_p	- - -	1.00	- - -	1.00	1.00	0.50/1.20	- - -	- - -	- - -	- - -	- - -	- - -	- - -
Strength V	γ_p	1.35	1.00	0.40	- - -	1.00	0.50/1.20	γ_{TG}	γ_{SE}	- - -	- - -	- - -	- - -	- - -
Extreme Event I	γ_p	γ_{EQ}	1.00	- - -	- - -	1.00	- - -	- - -	- - -	1.00	- - -	- - -	- - -	- - -
Extreme Event II	γ_p	0.50	1.00	- - -	- - -	1.00	- - -	- - -	- - -	- - -	1.00	1.00	1.00	1.00
Service I	1.00	1.00	1.00	0.30	1.00	1.00	1.00/1.20	γ_{TG}	γ_{SE}	- - -	- - -	- - -	- - -	- - -
Service II	1.00	1.30	1.00	- - -	- - -	1.00	1.00/1.20	- - -	- - -	- - -	- - -	- - -	- - -	- - -
Service III	1.00	0.80	1.00	- - -	- - -	1.00	1.00/1.20	γ_{TG}	γ_{SE}	- - -	- - -	- - -	- - -	- - -
Service IV	1.00	- - -	1.00	0.70	- - -	1.00	1.00/1.20	- - -	1.00	- - -	- - -	- - -	- - -	- - -
Fatigue I -** LL, IM & CE	- - -	1.50	- - -	- - -	- - -	- - -	- - -	- - -	- - -	- - -	- - -	- - -	- - -	- - -
Fatigue II -** LL, IM & CE	- - -	0.75	- - -	- - -	- - -	- - -	- - -	- - -	- - -	- - -	- - -	- - -	- - -	- - -

* - Use one of these at a time ** - Load factors only applied to LL, IM and CE

The two letter load descriptions correspond to permanent and transient loads as follows:

DC – dead load components and attachments
DD – downdrag
DW – wearing surface and utilities
EH – horizontal earth pressure
EV – vertical earth pressure
ES – earth surcharge
EL – locked-in stress
PS – secondary forces from post-tensioning
CR – force effects due to creep
SH – force effects due to shrinkage
LL – vehicular live load
IM – vehicular dynamic load allowance
CE – vehicular centrifugal force
BR –vehicular braking force
PL – pedestrian live load
LS – live load surcharge
WA – water load and steam pressure
WS – wind load on structure
WL – wind on live load
FR – friction load
TU – force effect due to uniform temp.
TG – force effect due to temp. gradient
SE – force effect due to settlement
EQ – earthquake load
BL – blast load
IC – ice load
CT – vehicular collision force
CV – vessel collision force

Table 2-3 Load Factors for Permanent Loads (after AASHTO 2014)

Type of Load	Max. Load Factor, γ_p	Min. Load Factor, γ_p
DC: Components and Attachments	1.25	0.90
DC: Strength IV only	1.50	0.90
DD: Downdrag (Tomlinson α-Method)	1.40	0.25
DD: Downdrag: (λ Method)	1.05	0.30
DW: Wearing Surface and Utilities	1.50	0.90
EH: Horizontal Earth Pressure (Active)	1.50	0.90
EH: Horizontal Earth Pressure (At-rest)	1.35	0.90
EH: Horizontal Earth Pressure (AEP for anchored walls)	1.35	N/A
EL: Locked-in Construction Stresses	1.00	1.00
EV: Vertical Earth Pressure (overall stability)	1.00	N/A
EV: Vertical Earth Pressure (retaining walls and abutments)	1.35	1.00
EV: Vertical Earth Pressure (rigid buried structures)	1.30	0.90
EV: Vertical Earth Pressure (rigid frames)	1.35	0.90
EV: Vertical Earth Pressure (flexible buried str. - metal box, plate, fiberglass)	1.50	0.90
EV: Vertical Earth Pressure (flexible buried str. - thermoplastic)	1.30	0.90
EV: Vertical Earth Pressure (flexible buried str. – all others)	1.95	0.90
ES: Earth Surcharge	1.50	0.75

Brown et al. (2010) summarized the basic limit state design process for a bridge or other structure. For each limit state, the structural engineer determines the foundation force effects using a preliminary structural model of the proposed structure. This structural model is developed and analyzed under the limit state load combinations described in Table 2-2. Factored loads are used in the analyses.

Figure 2-1 illustrates the reactions at a column-cap joint computed by the structural analysis. These are the force effects transmitted to the deep foundation supported cap. For driven pile designs, these reactions are resolved into vertical, horizontal, and moment components, and are taken as the factored values of axial, lateral, and moment force effects, respectively at the top of the pile cap. Multiple iterations are typically performed to obtain agreement between deformations and forces calculated by the structural analysis and those based on geotechnical analysis at the structure/foundation (column-cap) interface. The resulting factored force effects must be less than the factored resistance. This is an oversimplified description of

the process but it describes the general procedure by which factored foundation force effects are determined for each applicable limit state.

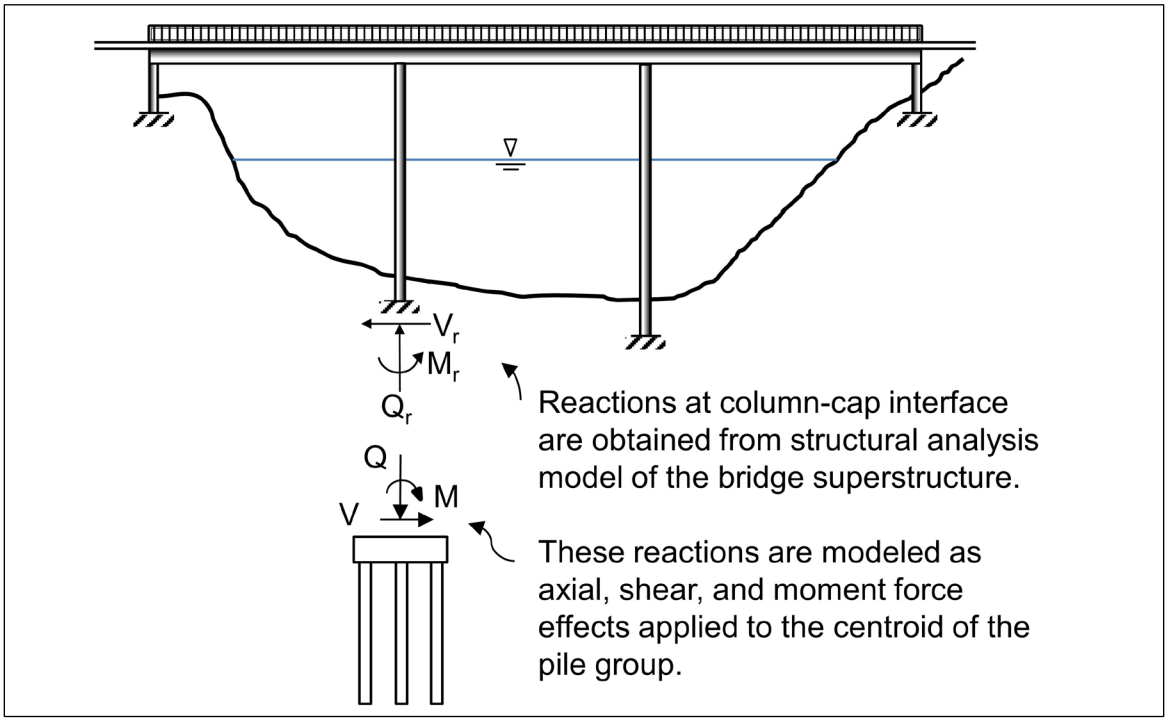

Figure 2-1 Structural analysis of bridge used to establish foundation force effects (modified from Brown et al. 2010).

In the structure model, the load factors in Tables 2-2 and 2-3 are varied over the specified ranges to determine the load combinations resulting in maximum force effects on the foundation. These maximum force effects are then used in the limit state checks.

An example of the final structure loads determined for a 45 foot wide, three span structure having a total length of 350 feet and a main span length of 100 feet is presented in Figure 2-2. The structure will be subjected to both scour and seismic events. At Abutment 1, the highest factored axial loads are 2749 kips for the Strength I limit state and 1982 kips for the Service II limit state. The abutment also has a lateral shear load of 1980 kips transverse to the bridge for the Extreme Event I limit state. At Pier 2, the highest factored axial loads are 5542 kips for the Strength I limit state and 4307 kips for the Service II limit state. The pier is also subjected to a lateral shear load of 1267 kips longitudinal to the bridge, and a moment of 40,800 ft-kips at the Extreme Event I limit state. Each limit state load combination is then checked independently based on all appropriate factored loads and moments and compared to the corresponding factored resistance and performance criteria (tolerable deforations) for each case.

Load Combination Limit State	DC DD DW EH EV ES EL PS CR SH	LL IM CE BR PL LS	WA	WS	WL	FR	TU	TG	SE	EQ*	BL*	IC*	CT*	CV*
Strength I	γ_p	1.75	1	---	---	1	0.50/1.20	γ_{TG}	γ_{SE}	---	---	---	---	---
Strength II	γ_p	1.35	1	---	---	1	0.50/1.20	γ_{TG}	γ_{SE}	---	---	---	---	---
Strength III	γ_p	---	1	1.4	---	1	0.50/1.20	γ_{TG}	γ_{SE}	---	---	---	---	---
Strength IV	γ_p	---	1	---	1	1	0.50/1.20	---	---	---	---	---	---	---
Strength V	γ_p	1.35	1	0.4	---	1	0.50/1.20	γ_{TG}	γ_{SE}	---	---	---	---	---
Extreme I	γ_p	γ_{EQ}	1	---	---	1	---	---	---	1	---	---	---	---
Extreme II	γ_p	0.5	1	---	---	1	---	---	---	---	1	1	1	1
Service I	1	1	1	0.3	1	1	1.00/1.20	γ_{TG}	γ_{SE}	---	---	---	---	---
Service II	1	1.3	1	---	---	1	1.00/1.20	---	---	---	---	---	---	---
Service III	1	0.8	1	---	---	1	1.00/1.20	γ_{TG}	γ_{SE}	---	---	---	---	---
Service IV	1	---	1	0.7	---	1	1.00/1.20	---	1	---	---	---	---	---
Fatigue I	---	1.5	---	---	---	---	---	---	---	---	---	---	---	---
Fatigue II	---	0.75	---	---	---	---	---	---	---	---	---	---	---	---

Abutment 1	Axial loads at base of abutment									Perpendicular (or transverse) to Bridge					
Load (kips)	1252	562	0	0	0	0	0	0	0	1980	0	0	0	0	Total
Strength I	1565	1184	0	0	0	0	0	0	0	0	0	0	0	0	2749
Strength II	1565	758	0	0	0	0	0	0	0	0	0	0	0	0	2323
Strength III	1565	0	0	0	0	0	0	0	0	0	0	0	0	0	1565
Strength IV	1878	0	0	0	0	0	0	0	0	0	0	0	0	0	1878
Strength V	1565	758	0	0	0	0	0	0	0	0	0	0	0	0	2323
Extreme I	0	0	0	0	0	0	0	0	0	1980	0	0	0	0	1980
Extreme II	0	0	0	0	0	0	0	0	0	0	0	0	0	0	0
Service I	1252	562	0	0	0	0	0	0	0	0	0	0	0	0	1814
Service II	1252	730	0	0	0	0	0	0	0	0	0	0	0	0	1982
Service III	1252	450	0	0	0	0	0	0	0	0	0	0	0	0	1702
Service IV	1252	0	0	0	0	0	0	0	0	0	0	0	0	0	1252
Fatigue I	0	422	0	0	0	0	0	0	0	0	0	0	0	0	422
Fatigue II	0	211	0	0	0	0	0	0	0	0	0	0	0	0	211

Extreme I - Lateral shear load: 1980 kips (transverse to bridge)

Pier 2	Axial loads at base of pier									Longitudinal (or transverse) to Bridge					
Load (kips)	2660	1267	0	0	0	0	0	0	0	3840	0	0	0	0	Total
Strength I	3325	2217	0	0	0	0	0	0	0	0	0	0	0	0	5542
Strength II	3325	1710	0	0	0	0	0	0	0	0	0	0	0	0	5035
Strength III	3325	0	0	0	0	0	0	0	0	0	0	0	0	0	3325
Strength IV	3990	0	0	0	0	0	0	0	0	0	0	0	0	0	3990
Strength V	3325	1710	0	0	0	0	0	0	0	0	0	0	0	0	5035
Extreme I	0	0	0	0	0	0	0	0	0	1267	0	0	0	0	1267
Extreme II	0	0	0	0	0	0	0	0	0	0	0	0	0	0	0
Service I	2660	1267	0	0	0	0	0	0	0	0	0	0	0	0	3927
Service II	2660	1647	0	0	0	0	0	0	0	0	0	0	0	0	4307
Service III	2660	1014	0	0	0	0	0	0	0	0	0	0	0	0	3674
Service IV	2660	0	0	0	0	0	0	0	0	0	0	0	0	0	2660
Fatigue I	0	950	0	0	0	0	0	0	0	0	0	0	0	0	950
Fatigue II	0	475	0	0	0	0	0	0	0	0	0	0	0	0	475

Extreme I - Moment at base: 40,800 k-ft

Extreme I - Lateral shear load: 1267 kips (longitudinal to bridge)

Figure 2-2 Example of factored load calculation.

2.4 NOMINAL AND FACTORED RESISTANCE

The nominal resistance, R_n, is calculated and then multiplied by the applicable resistance factor to determine the factored resistance, R_r. Nominal geotechnical resistances and associated resistance factors are discussed in Chapter 7. Nominal structural resistances and applicable resistance factors are presented in Chapter 8. The factored resistance must be greater than or equal to the sum of all factored force effects in all applicable limit states. The basic LRFD methodology equation is given as:

$$\sum \eta_i \gamma_i Q_i \leq \phi R_n = R_r \qquad \text{Eq. 2-2}$$

Where:

- η_i = load modifier based on ductility, redundancy, or operation classification, applied to the force effect.
- γ_i = load factor, statistically based multiplier applied to force effect.
- Q_i = force effect.
- ϕ = resistance factor, statistically based multiplier applied to nominal resistance.
- R_n = nominal resistance.
- R_r = factored resistance.

The load modifiers for redundancy, η_r, described in AASHTO Article 1.3.4 were developed for superstructures. Paikowsky (2004) in NCHRP Report 507 defined redundancy in driven pile foundation designs based on the number of piles in a pile cap with redundant piles defined as 5 or more piles per pile cap and non-redundant piles defined as 4 piles or less per pile cap. For non-redundant driven pile foundation designs, AASHTO Article C10.5.5.2.3 recommends the resistance factor be reduced by 20%.

2.5 STRENGTH LIMIT STATES

The strength limit states ensure local and global strength and stability against statistically significant load combinations occurring during the structure design life. Strength limit state design of driven pile foundations includes an evaluation of the nominal geotechnical and structural resistances as well as the loss of lateral and vertical support in the design flood event (100 year) due to scour. For driven pile designs, strength limit state considerations include:

- axial compression resistance of single piles and pile groups,
- uplift resistance of single piles and pile groups,
- lateral resistance of single piles and pile groups,
- bearing stratum punching failure,
- structural resistance in axial compression, combined axial and flexural loading, and shear, and
- drivability including and driving stresses.

Geotechnical and structural strength limit state considerations are described in detail in Chapters 7 and 8, respectively of this manual.

2.6 SERVICE LIMIT STATES

The service limit states provide limits on stress, deformation, and cracking under regular service conditions. Service limit state considerations in driven pile foundation designs include:

- vertical deformation – settlement,
- horizontal movements,
- rotation,
- overall stability, and
- deformations due to scour at the design flood (100 year event).

Service limit state considerations are further discussed in AASHTO (2014) Articles 10.5.2.1 through 10.5.2.4 and associated commentary. All applicable service limit state load combinations must be evaluated.

2.7 EXTREME EVENT LIMIT STATES

Extreme event limit states ensure structural survival of a bridge under unique major occurrences such as earthquakes, floods, and vehicle, vessel collisions, or blasts with return periods significantly greater than the bridge design life. Extreme event limit states for driven pile foundation design include:

- the check flood (500 year event) for scour,
- vessel collision,
- vehicle collision,
- blast loading,
- seismic loading, and
- other site-specific situations determined by the design engineer.

A liquefaction assessment is required as part of the design for multi-span bridges if the site is classified as Seismic Zone 2, 3, or 4. Extreme event limit states are discussed further in Section 7.4 of this manual.

2.8 CONSTRUCTION OF PILE FOUNDATIONS

Construction of a successful driven pile foundation that meets the design objectives depends on relating the load requirements to the resistance requirements of the field installation and resistance determination method. The means for obtaining such a foundation must be explicitly incorporated into the plans and specifications as well as adhered to in the construction administration.

A pile foundation must be installed to meet the limit state requirements for compressive, lateral and uplift resistance. This may dictate driving piles for a required nominal resistance or to a predetermined penetration depth established by the designer to satisfy strength, service and extreme event limit state performance requirements. It is equally important to avoid pile damage or foundation cost overruns by excessive driving. These objectives can all be satisfactorily achieved by use of wave equation analysis, dynamic monitoring of pile driving, and/or static load testing. Some agencies have calibrated and/or developed new dynamic formulas for nominal resistance verification to replace more unreliable dynamic formulas such as the Engineering News formula.

Knowledgeable construction supervision and inspection are the keys to proper installation of piles. State-of-the-art designs and detailed plans and specifications

must be coupled with good construction supervision to achieve desired results. Post construction review of pile driving results versus predictions regarding pile penetration resistances, pile lengths, field problems, and static and/or dynamic load test nominal resistances is essential.

These reviews add to the experience of all engineers involved on the project and will enhance their skills. In addition, the implementation of LRFD in pile foundation design with rationally determined resistance factors makes it possible to use data from the post construction review to improve the resistance factors for future projects.

2.9 FOUNDATION SPECIALIST INVOLVEMENT

The input of an experienced foundation specialist is essential to produce a successful driven pile foundation. A foundation specialist has both a structural and geotechnical background in design and construction. The foundation specialist is the most knowledgeable person for selecting the pile type, estimating pile length, and choosing the most appropriate and cost effective method to determine the nominal resistance. In some agencies, the role of the foundation specialist may be divided amongst individuals and disciplines. Regardless of how the foundation specialist role is fulfilled, geotechnical and structural expertise in both design and construction knowledge is essential as design input.

The foundation specialist should be involved from the planning stage through the design and construction process. In some project phases (i.e. preliminary explorations, preliminary design, and final design), the foundation specialist will have significant involvement. In other project phases, such as construction, and post construction review, the foundation specialist's involvement may be more of a technical support role. The foundation specialist's involvement provides the needed continuity of design personnel in dealing with design related issues that develop throughout the construction stage. The importance of this continuity of knowledge, experience, and communication applies to all types of contracting methods.

2.10 THE DRIVEN PILE DESIGN AND CONSTRUCTION PROCESS

The driven pile design and construction process includes aspects that are unique in all of structural design. Because pile driving characteristics are related to the nominal geotechnical resistance for most soils, they can be used to improve the accuracy of the estimated nominal geotechnical resistance. In general, the various methods of determining nominal geotechnical resistance from dynamic data such as penetration resistance with wave equation analysis or with dynamic measurements are more accurate than the static analysis methods based on subsurface exploration information. It should be clearly understood that the static analysis based on the subsurface exploration information has the primary function of providing an estimate of the pile length for contractor bidding purposes.

Pile drivability is a critical aspect of the design process and must be considered during the design phase. If the design is completed, a contractor is selected, and then the piles cannot be driven, large additional costs can often result. Therefore, it is absolutely necessary that driven pile foundation design and construction be linked to a greater degree than in the design and construction of other foundation types.

During construction, the pile driving criterion is usually a blow count criterion that is established at the early stage of field installation, and individual pile penetration depths may vary depending on the subsurface variability. In some instances, piles may need to meet a minimum penetration depth and a blow count criterion. Minimum pile penetration depths are sometimes established to satisfy uplift or lateral loads, or for serviceability consideration. In other cases, satisfying a required pile penetration depth established from static analysis may be the sole pile installation criterion.

The driven pile design-construction process is outlined in the flow chart of Figure 2-3. The design and construction process will be discussed block by block using the numbers in the blocks as a reference and will serve to guide the designer through all of the tasks that must be completed. The block border depicts whether the structural engineer, geotechnical engineer, or construction engineer has the lead role for a given step in the design or construction process. This highlights the importance of interdisciplinary communication. The foundation specialist may perform some or a portion of the outlined structural and geotechnical steps based on their background and the organizational structure of the transportation agency.

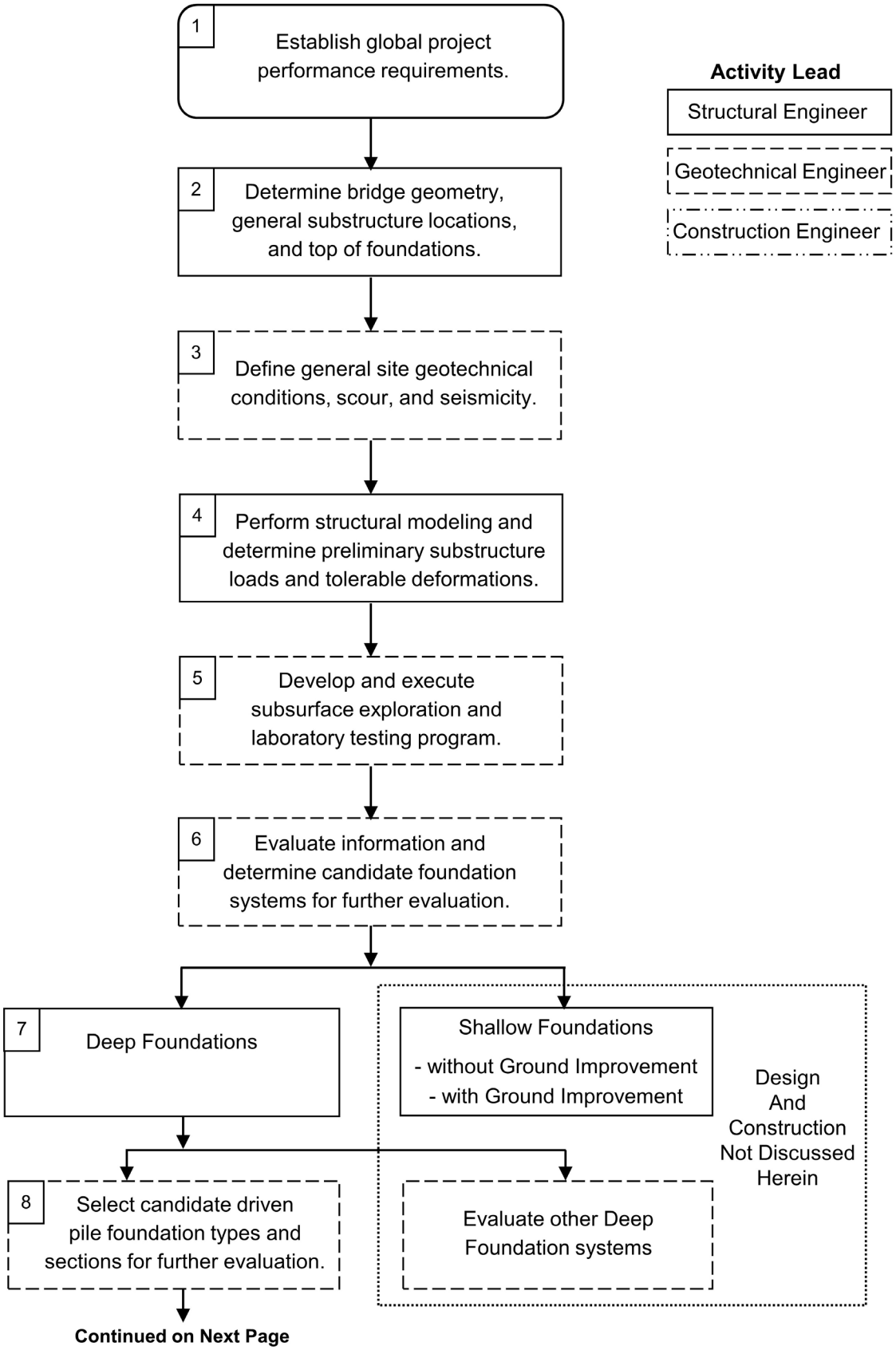

Figure 2-3 Driven pile design and construction process.

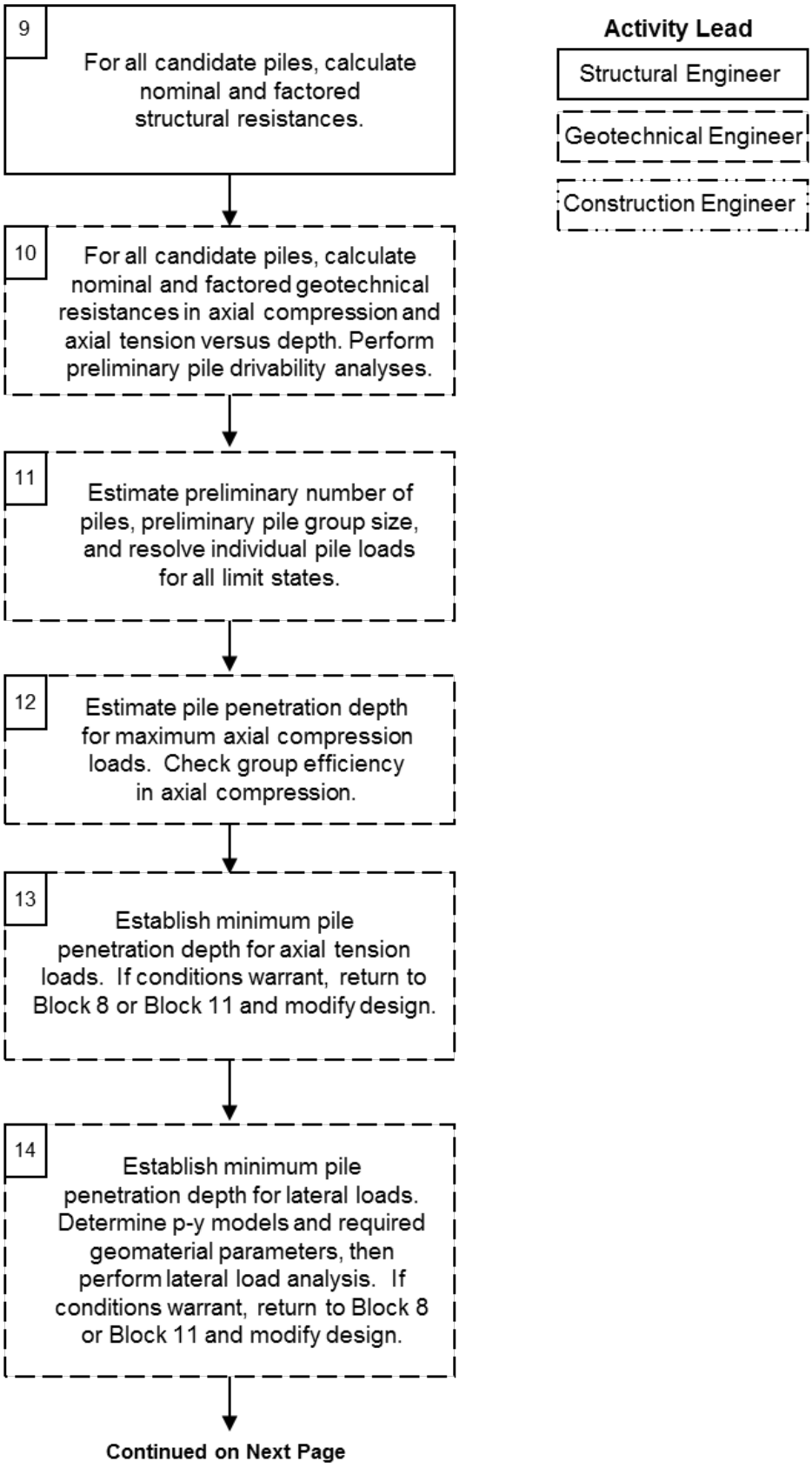

Figure 2-3 Driven pile design and construction process (continued).

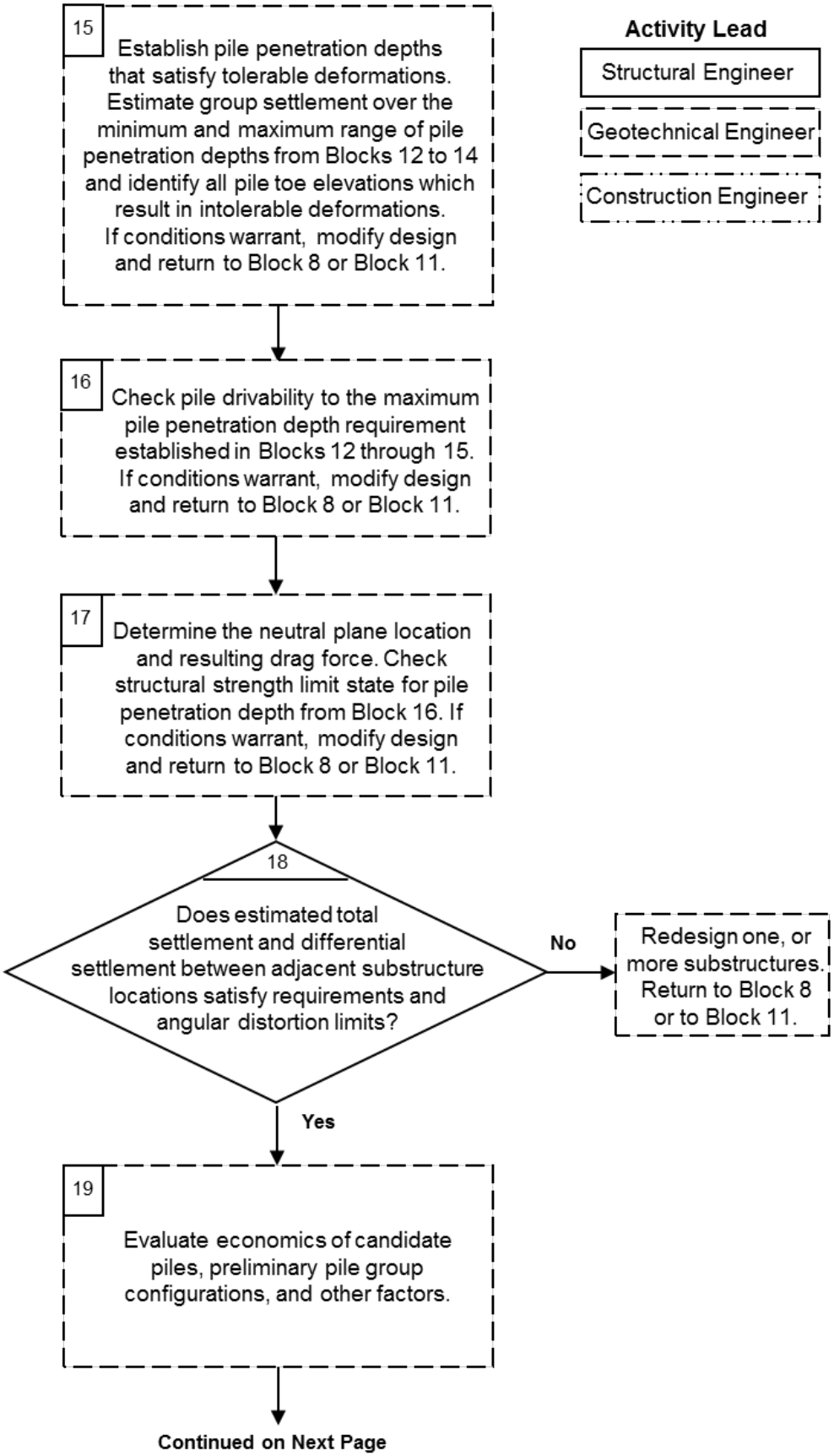

Figure 2-3 Driven pile design and construction process (continued).

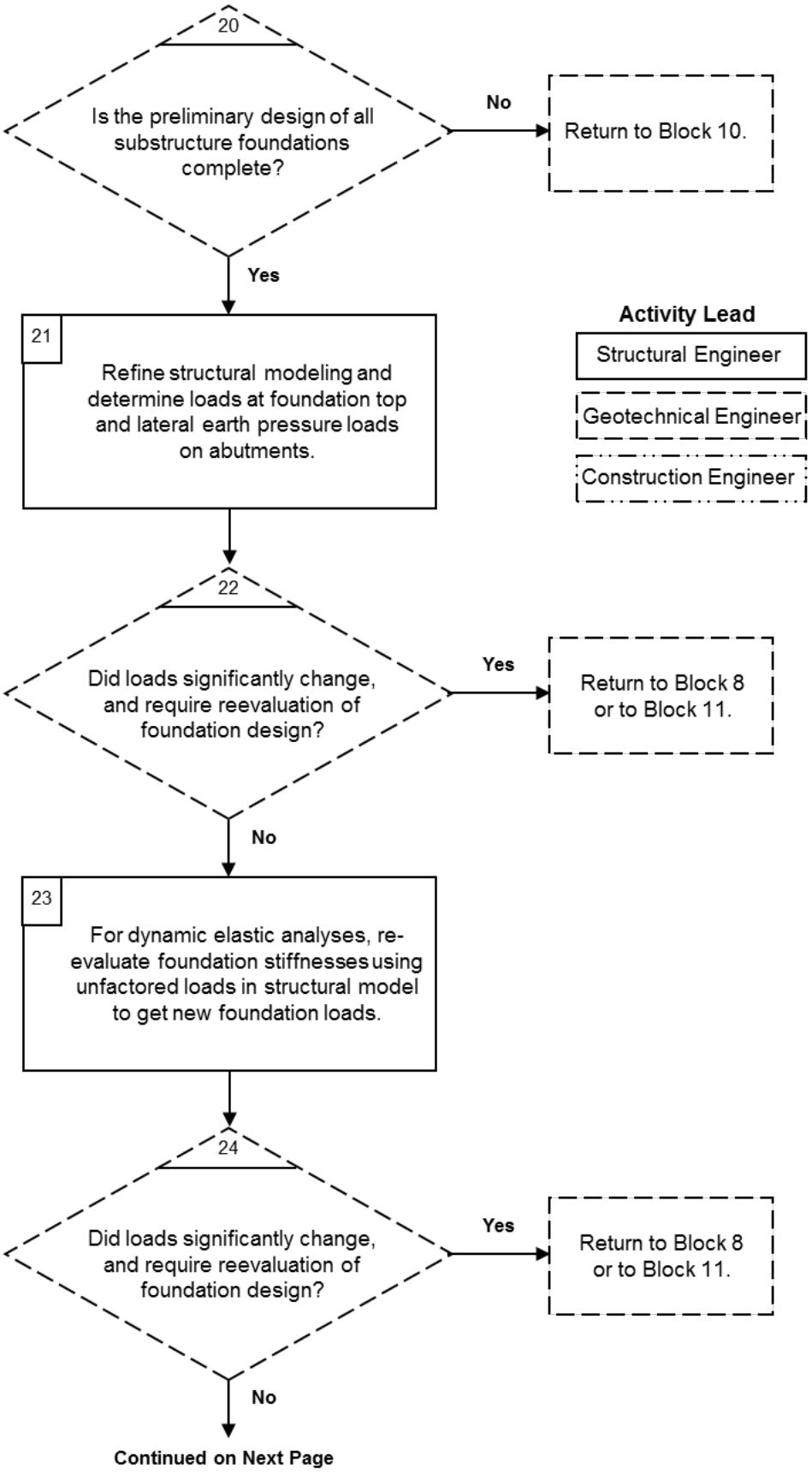

Figure 2-3 Driven pile design and construction process (continued).

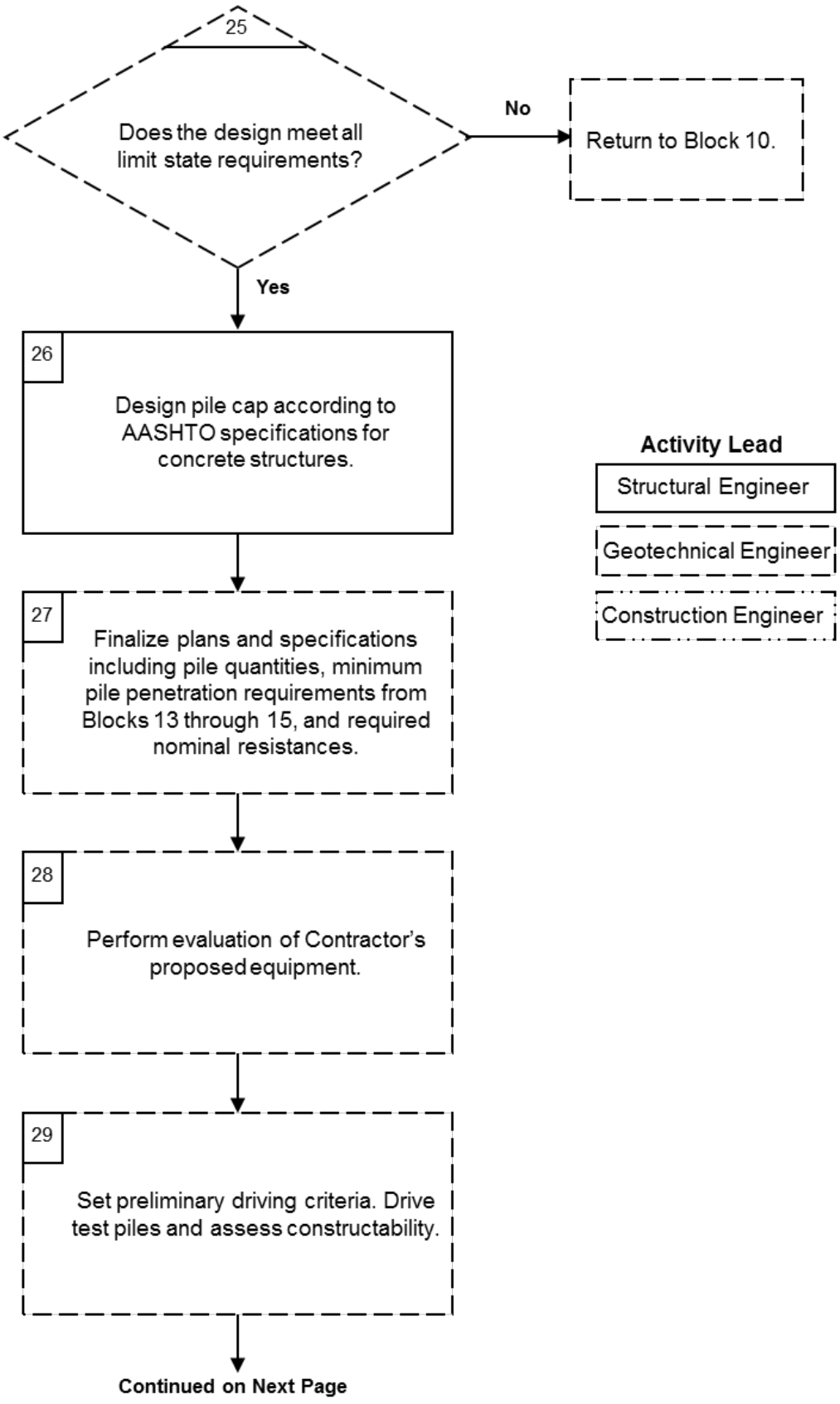

Figure 2-3 Driven pile design and construction process (continued).

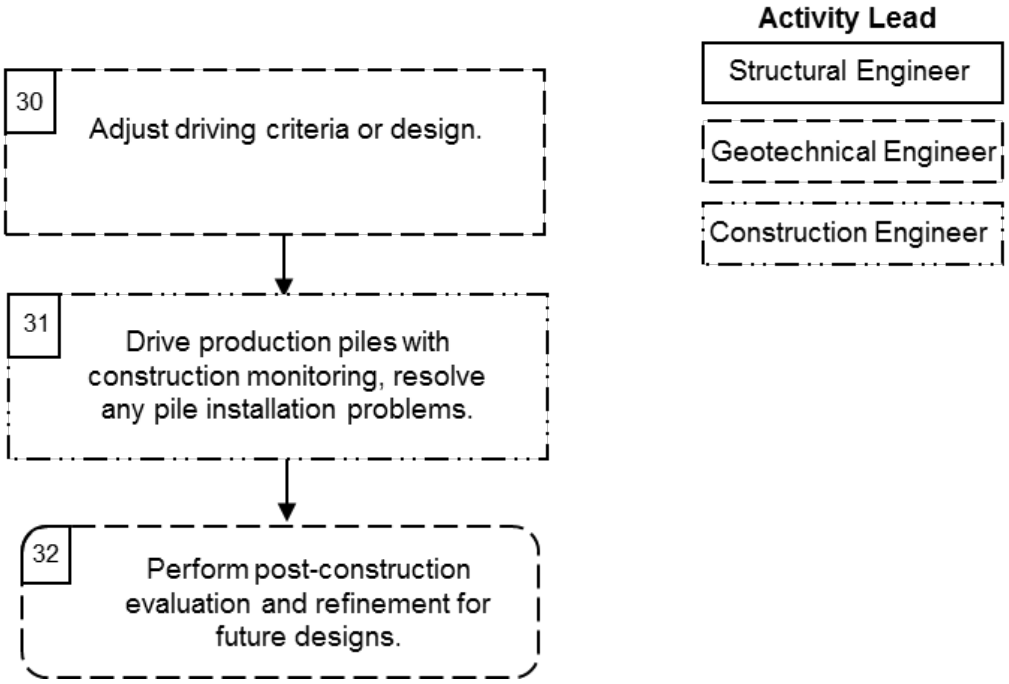

Figure 2-3 Driven pile design and construction process (continued).

Figure 2-3 is representative of the key steps in a typical design-bid-build project. The contractor in a design-bid-build project would be retained between Blocks 27 and 28, however the design and construction tasks for projects delivered using design-build or construction manager/general contractor contracts will vary. In a design-build contract, the contractor would be retained early on in the process once the project's general requirements and preliminary supporting information has been established. Hence, the early steps of the flow chart in a design-build contract will vary. While the responsibility for the individual tasks will differ in alternative contracting methods, the identified key design or construction activities are still performed.

Block 1: Establish Global Project Performance Requirements.

The first step in the design process is to determine the structure requirements.

1. Is the project a new bridge, a replacement bridge, a bridge renovation, a bridge widening, a retaining wall, a noise wall, or sign or light standard?

2. Will the project be constructed in phases or all at one time?

3. What are the general structure layout and approach grades?

4. What are the surficial site characteristics?

5. What are the approximate foundation loads? What are the deformation or deflection limits (total settlement, differential settlement, and lateral deformations) for the service and extreme event limit states?

6. Will the structure be subjected to any extreme event limit states such as seismic, scour, debris loading, vessel or vehicle impact, etc.?

7. Are there any special considerations to be evaluated such as lateral squeeze?

8. Are there modifications in the design that may be desirable for the site under consideration such as changes in substructure locations or span length?

9. Are there site or surrounding environmental considerations that must be considered in the design (low headroom, utility conflicts, aggressive soil environments, environmentally impacted soil and/or groundwater, limitations on noise, vibrations, etc.)? These factors may influence the selection of suitable deep foundation types, the deep foundation installation equipment, as well as the need for installation aids such as predrilling for driven pile options.

10 Are there other factors influencing bridge span lengths including river navigation channel width, road or railroad crossings; or avoidance of previous foundations?

Block 2: Determine Structure (bridge) Geometry, Substructure Locations and Elevations.

The general bridge geometry, probable substructure locations, and the top of foundation elevations should be established at this time.

Block 3: Define General Site Geotechnical Conditions, Scour, and Seismicity.

A great deal can be learned about the foundation requirements with even a very general understanding of both the site geology and area geotechnical conditions. Frequently there is information available on foundations that have been constructed in the area. This information can be of assistance in avoiding problems. Both subsurface exploration information and foundation construction experience should be collected prior to beginning the foundation design. This step is sometimes overlooked in practice.

If scour will be a design consideration, the hydraulic engineer should be consulted to determine probable scour depths that may impact the foundation selection.

Block 4: Perform Preliminary Structure Modeling. Determine Preliminary Substructure Loads and Tolerable Deformations.

Preliminary structural analysis and modeling of the proposed bridge or structure is performed at this time. The strength, service and extreme event limit states load demands and performance requirements at the foundation top have been established. For major bridge structures such as cable-stayed and balanced cantilever bridges, construction stage loads may govern the foundation design.

Many agencies also have total and differential settlement criteria for typical bridges which must be satisfied by the design. Lateral deformation limits for the proposed structure should also now be known and conveyed to the foundation specialist.

It is imperative that the foundation specialist obtain a completely defined and unambiguous set of foundation loads and deformation limits in order to proceed through the foundation design process. Accurate load information and deformation criteria are essential in the development and implementation of an adequate subsurface exploration program for the planned structure. It is important for the foundation specialist to address the level of uncertainty in their deformation

predictions and distinguish between total final loads and incremental loading such that post-construction deformation can be distinguished from total deformations. Of course, post-construction deformations are those of most interest.

Block 5: Develop and Execute Subsurface Exploration and Laboratory Testing Program for Feasible Foundation Systems.

Based on the information obtained in Blocks 1-4, it is possible to make decisions regarding the necessary information that must be obtained for the technically feasible foundation systems at the site. The subsurface exploration program including the associated laboratory testing must meet the project needs for design and construction at a cost consistent with the size and complexity of the project. Depending upon the project size and complexity, it may be advantageous to perform the subsurface exploration program in phases, one for preliminary planning and general site evaluation and a second phase for final design.

The results of the subsurface exploration soil boring and in-situ testing program along with laboratory test results are used to prepare a subsurface profile; define soil and rock parameters including strength, compressibility, parameter variation, liquefaction susceptibility, and seismic earth pressure parameters; subsurface water conditions, as well as identify critical cross sections for design. The design profile for each substructure location will be developed from the information gathered in this block and used in later blocks. Site characterization and design parameter selection are covered in detail in Chapters 4 and 5.

Block 6: Evaluate Information and Determine Candidate Foundation Systems.

The information collected in Blocks 1-5 must be evaluated and candidate foundation systems selected. The question to be answered is what candidate foundation systems are appropriate for consideration based on the site conditions. This question will be answered based primarily on the strength and compressibility of the geomaterials, the proposed loading conditions, the project deformation limits, the project schedule, and the foundation cost. Shallow foundations may be determined to be technically feasible and the most economical solution provided all project performance requirements can be addressed. Ground improvement techniques in conjunction with shallow foundations should also be evaluated. Shallow and deep foundation interaction with approach embankments and approach slabs must also be considered.

If the performance of a shallow foundation exceeds the established deformation limit, or if excessive scour is a concern, a deep foundation must be used. The design of shallow foundations and ground improvement techniques are not covered in this manual. Information on design consideration for shallow foundations can be found in Munfakh et al. (2001), Kimmerling (2002), Samtani et al. (2010), and in Abu-Hejleh et al. (2014). The effects of settlement can be more comprehensively examined by using a construction point concept and estimating the differential settlement between supports as discussed by Modjeski and Masters, Inc, et al. (2015) in SHRP 2 Report S2-R19B-RW-1. Information on ground improvement techniques can be found in Elias et al. (2006) and at www.geotechtools.org. The selection of the appropriate foundation system including cost considerations is discussed in greater detail in Chapter 3, while Chapter 6 presents pile type selection along with advantages and disadvantages.

Block 7: Determine if a Deep Foundation is Required.

Once candidate foundation systems have been identified in Block 6, it has been determined that a deep foundation system is required. Therefore, driven piles and other deep foundation systems must be further evaluated. These other deep foundation systems are primarily drilled shafts, but also include micropiles, continuous flight auger (CFA) piles, and other drilled-in deep foundation systems. The questions that must be answered in deciding between driven piles and other deep foundation systems will center on both the technical feasibility and the relative costs of available systems. Foundation support cost can be conveniently calculated based on the cost per unit of load carried. The foundation cost analysis should address all temporary and permanent requirements (e.g., pile caps, effects of pile cap elevation, cofferdams, use of vertical and/or batter piles, load tests, construction control tests) for that specific foundation type. In addition, constructability and productivity (i.e., schedule) must be considered. This manual is concerned with driven piles; therefore other types of deep foundations will not be further discussed. Design guidance on drilled shafts can be found in Brown et al. (2010). For micropile design guidance refer to Sabatini et al. (2005), and for CFA piles refer to in Brown et al. (2007). Economic considerations in the foundation selection process are discussed in Chapter 3.

Block 8: Select 2 to 5 Candidate Driven Pile Types and Sections for Further Evaluation.

At this point on the flow chart, the primary concern is for the design of a driven pile foundation. The pile type must be selected consistent with the factored loads (compression, tension, and lateral) to be resisted per pile. Consider this problem. The general magnitude of the pier load is known from the information obtained in Blocks 1 and 4. However, a large number of combinations of pile types and nominal geotechnical resistances can satisfy the nominal resistance requirements for the factored loads. In the case of axial compression resistance, should twenty piles with a nominal resistance of 225 kips be used to support a 4,500 kip factored load, or would it be better to use ten piles with a nominal resistance of 450 kips, or five piles with a nominal resistance of 900 kips? This decision should consider the nominal structural resistance of the piles, the realistic geotechnical nominal resistances and deformations for the soil conditions at the site, the cost of the different pile types, and the capability of construction contractors to install the piles. Changes in the foundation selection from twenty 225 kip piles to five 900 kip piles will also affect structure and foundation response and therefore adjust the lateral and axial loads as well as pile cap requirements and costs. At this point in the design process, 2 to 5 candidate pile types and/or sections that meet the general project requirements should be selected for further evaluation. Pile type and selection considerations are covered in greater detail in Chapter 6.

Approximate loads determined in Block 1 were refined in Block 4. At those stages of the design process, the other aspects of the total structural design were probably insufficiently advanced to establish the final factored loads. By the time that Block 7 has been reached, the foundation loads and deformation limits should be closer to being finalized.

If there are extreme event limit states applicable to the structure, the design must satisfy those load and deformation requirements. Vessel impact will be evaluated primarily by the structural engineer and the results of that analysis will give factored loads for that case. There may be stiffness considerations in dealing with vessel impact since the design requirement is basically that some vessel impact energy be absorbed.

Scour presents a different requirement. AASHTO (2014) Article 3.7.5 requires changes in foundation conditions resulting from the design flood (100 year event) be evaluated at the strength and service limit states. Foundation condition changes from the check flood (500 year event) must be considered and evaluated at the

extreme event limit state. Scour is not a force effect. However, scour can change the substructure conditions and alter the consequences of force effects acting on the structure. It must be assured that after scour, the pile will still satisfy geotechnical and structural resistance demands.

In many locations, seismic design will be an important factor. Since the 1971 San Fernando Earthquake, significant emphasis has been placed on the design of highway bridges in seismic events. AASHTO (2014), Section 10, Appendix A10 discusses seismic analysis and design requirements. Additional seismic design guidance is available in GEC-3, LRFD Seismic Analysis and Design of Transportation Geotechnical Features and Structural Foundations, by Kavazanjian et al. (2011), as well as in the AASHTO (2011) Guide Specifications for LRFD Seismic Bridge Design, 2nd Edition, with 2012, 2014, and 2015 Interims.

Block 9: Calculate Nominal and Factored Structural Resistance.

The maximum nominal and factored structural resistances of all candidate pile types in axial compression, bending, and combined axial compression and flexure resistance are calculated at this time. Pile structural resistance is covered in Chapter 8.

The maximum factored resistance for a given pile type is the lesser of the factored structural resistance or the factored geotechnical resistance for that pile.

Block 10 Calculate the Nominal and Factored Geotechnical Resistance, as well as Perform a Preliminary Drivability Assessment of Candidate Pile Types.

The maximum nominal and factored geotechnical resistance in axial compression and uplift are calculated as a function of pile penetration depth for all candidate pile types. A static analysis method(s) appropriate for the pile type(s), the soil conditions, and the loading condition should be selected. These methods are presented in detail in Chapter 7. Factored geotechnical resistances are most often calculated based on the resistance determination method used in the field but can also be calculated solely on the basis of an appropriate static analysis method. Review of the nominal and factored geotechnical resistances versus depth for candidate pile sections and various resistance determination methods assists the designer in selecting the foundation type and associated resistance determination method.

Deposits within the subsurface strata which are unsuitable as load carrying geomaterial must be identified. The geotechnical resistance from these layers must be determined by static analysis. Unsuitable layers may include urban fills, organic deposits, soft and very soft cohesive soils, as well as potentially scourable or liquefiable materials.

Preliminary wave equation drivability assessments of candidate pile sections should be performed at this time. These analyses must consider the geotechnical resistance from suitable as well as unsuitable layers. A commonly available pile hammer having a ram weight of 1 to 2% of the required nominal resistance is a good initial trial hammer size for preliminary drivability assessments.

Block 11: Estimate the Preliminary Number of Piles, Preliminary Group Size, and Resolve Individual Pile Loads at All Limit States.

The preliminary number of piles at a substructure location can be estimated by dividing the largest factored axial load by an individual pile's factored geotechnical resistance. Axial compression and axial tension requirements should both be considered. In some cases, lateral load requirements may control the design. Therefore, similar past experience may also be used to estimate the preliminary number of piles, trial group configurations, and pile spacing. Using the factored loads with the trial group configurations, determine the limit state reactions on the substructure unit and the resulting maximum factored load per pile at the strength, service, and extreme limit states for each candidate pile type.

Block 12: Estimate Pile Penetration Depth for Axial Compression Loads and Check Group Efficiency in Axial Compression.

For each candidate pile section and each group configuration, determine the estimated pile penetration depth where the factored geotechnical resistance exceeds the factored load. Note that the factored geotechnical resistance will vary based on the resistance verification method. Block 12 establishes an estimated pile penetration depth for compression loading for each of the candidate pile types. Note this estimated depth is a function of the resistance determination method. Check that group axial compression resistance meets design requirements. If the group resistance group does not satisfy requirements, modify the design.

Block 13: Establish Minimum Pile Penetration Depth for Axial Tension Loads.

Determine the maximum factored axial tension load to be resisted in any limit state. From the nominal axial tension resistance versus depth results calculated in Block 10, determine the minimum pile penetration depth necessary to obtain a factored geotechnical resistance greater than the maximum factored axial tension load. Block 13 establishes a minimum pile penetration depth for tension loading for each of the candidate pile types. Note that this minimum depth is a function of the resistance determination method. Check that group axial tension resistance meets design requirements. If axial tension requirements cannot be achieved, modify the design. Return to Block 8 and select a new pile type or new pile section, or return to Block 11 and evaluate new group configurations.

Block 14: Establish Minimum Pile Penetration Depth for Lateral Loads.

Determine p-y models and required geomaterial properties for each layer in the subsurface profile. The p-y model and parameters chosen depend on the soil or rock response being modelled in the service or extreme event limit case. Results of this analysis will be compared to the tolerable lateral deformation requirements. Check that the deformation and lateral resistance of the trial group configuration meets design requirements. Determine the minimum pile penetration depth necessary to resist the maximum applied lateral loads within the permissible deformation limit. This depth establishes the minimum pile penetration depth for lateral loading for the candidate pile type and group. This topic is covered in greater detail in Section 7.3.4.2. If lateral deformation requirements cannot be achieved, modify the design. Return to Block 8 and select a new pile type or pile section, or return to Block 11 and evaluate new group configurations.

Block 15: Establish Pile Penetration Depths that Satisfy Tolerable Deformations Based on Group Settlement Computations.

Preliminary group configurations should now be evaluated for settlement. One of the primary objectives at this stage is to determine if a minimum pile penetration depth is required and, if so, to determine the required minimum pile toe elevation. In some subsurface profiles, piles could attain the requisite nominal resistance near the bottom of a dense layer overlying a compressible layer. In order to satisfy tolerable deformation limits, it may be necessary to drive through, or otherwise penetrate, the higher, suitable layer to preclude large future settlements. Hence, in some

stratigraphy cases, it is necessary to calculate group settlements over a range of pile termination depths to determine the minimum (highest pile toe elevation) and, in unique stratigraphy cases, the maximum (lowest pile toe elevation) acceptable for tolerable group settlements. Any penetration depths that will result in intolerable deformations should be identified. Where appropriate, Block 15 establishes a minimum pile penetration depth, maximum pile penetration depth, or both. If tolerable deformation requirements cannot be achieved, modify the design. Return to Block 8 and select a new pile type, or return to Block 11 and evaluate new group configurations.

Block 16: Check Pile Drivability.

Identify the maximum pile penetration depth required by each block in Block 12 through Block 15. Perform a wave equation drivability analysis for each candidate section to the maximum pile penetration depth determined in any of these blocks. Candidate pile types that cannot be driven to the required nominal resistance and/or the minimum pile penetration depth without exceeding material stress limits and within a reasonable blow count of 30 to 120 blows per foot with appropriately sized driving systems are eliminated at this time. It should be noted that 120 blows per foot or 10 blows per inch is considered refusal driving conditions by many hammer manufacturers. Therefore, depending on the expected driving conditions (e.g., an extended duration of hard driving compared to a quick transition onto hard rock), it may more reasonable to assess candidate pile drivability based on an upper limit of 96 blows per foot or 8 blows per inch. In some cases pile installation aids such as jetting or predrilling may be evaluated subject to other design limitations.

The drivability analyses should also consider what influence the group configuration (pile spacing) and construction procedures and constraints (i.e., predrilling, cofferdams, etc.) may have on pile installation conditions. If the selected pile type does not meet drivability requirements, a different pile section, pile type, or group configuration is required. Return to Block 8 and select a new pile type, or return to Block 11 and evaluate new group configurations.

Block 17: Determine Location of Neutral Plane and Magnitude of Drag Force.

The neutral plane location for drag force evaluation is performed in this step. Note that the neutral plane location may have already been determined in Block 15 depending upon the settlement analysis approach selected by the designer. The

neutral plane is defined as the location where the sum of the permanent structure load and drag force is balanced by the sum of the shaft and toe resistances occurring below the neutral plane. The maximum drag force, caused by differential movement between the pile and the geomaterials, occurs at the neutral plane. The drag force magnitude is related to the pile properties, loading conditions, soil stress state, and deformation. The sum of the permanent structure load plus the maximum drag force should be less than the pile's factored structural resistance. If it is not, a different pile section or pile type is required, and the design process returns to Block 8, or a new group configuration is required and the design process returns to Block 11. Determination of the neutral plane location and drag force is discussed further in Section 7.2.10.

It should be noted that the AASHTO (2014) design specifications do not specifically address drag force considerations relative to the pile structural resistance. For example, the factored structural resistance of an H-pile is the nominal structural resistance multiplied by the resistance factor for axial compression, ϕ_c. This resistance factor is 0.70 for combined axial and flexural resistance of undamaged piles, 0.60 for the axial resistance of piles in compression under good driving conditions, and 0.50 for the axial resistance of piles in compression subject to damage due to severe driving conditions. While not equivocally stated, it follows that if the neutral plane is located below the point of fixity and above the depth where H-piles are subject to potential damage during driving, then the sum of the permanent load plus drag force at the neutral plane is limited to 0.70 of the nominal structural resistance.

Block 18: Does the Computed Total Settlement, Differential Settlement, and Angular Distortion Satisfy Design Requirements?

In this block, the total settlement should be computed and compared to project deformation limits. At the same time, the computed differential settlement between the current substructure location and adjacent substructure units should be compared to differential settlement and angular distortion limits. The construction point concept described in Section 7.3.3 and the recommended procedure for vertical deformation analysis in Section 7.3.4 should be followed.

If the total settlement, differential settlement, or angular distortion limits are exceeded, the design process returns to an earlier block. If a new pile type or section needs to be considered, the design process returns to Block 8. If existing

candidate pile types or sections are considered for the redesign of one or more of the substructure units, then the design process returns to Block 11.

Block 19: Evaluate Economics of Candidate Pile Types and/or Sections.

The next step is to determine the pile support cost versus pile penetration depth for each candidate pile type and/or section. The support cost, which is the cost per ton supported, is the pile cost at a given penetration depth divided by the nominal resistance at that penetration depth. The pile cost can be calculated from the unit cost per foot multiplied by the pile length between the pile cutoff elevation and the pile penetration depth. These plots should be evaluated to identify possible pile termination depths to obtain the lowest pile support cost. In some instances, uplift load rather than axial compression load may control the design in which case the same concept could be used for nominal tension resistance. The pile cost should include all costs associated with a given candidate section including material, transportation, and installation. In addition, the cost of the pile cap, cofferdams, dewatering or other related construction items should be included. This economic assessment should be modified appropriately in cases where lateral load demand and deformation control the design. The cost of the resistance determination method should be considered when evaluating the economics of candidate piles. Economic evaluation is presented in detail in Chapter 3.

Block 20: Is the Preliminary Design Complete at All Substructure Locations?

The preliminary design process in Blocks 9 through 19 is completed for each substructure location until the preliminary design is complete at all foundation units.

Block 21: Refine Structural Modeling and Loads.

At this point, the structure and foundation response to the loading cases can be further refined based on the structural and geotechnical analyses completed in Block 9 through Block 17. The structural model is now reanalyzed using the results from these preliminary substructure analyses to better determine the structure loads at the foundation top, and lateral earth pressure loads on the abutments.

Block 22: Did the Loads Significantly Change Requiring Reevaluation of the Foundation Design?

Based on the refined structural modeling, review the preliminary design based on the refined loads. If necessitated by the refined modelling, return to Block 8 and modify the design.

Block 23: Re-evaluate Foundation Stiffness and Loads.

For dynamic elastic analyses in seismic or other dynamic extreme events, the structural engineer now re-evaluates foundation stiffness. The structural model will be rerun to get new foundation loads.

Block 24: Did the Loads Significantly Change Requiring Reevaluation of the Foundation Design?

Review the preliminary design based on the refined loads from the dynamic elastic analyses. If loads from lateral pile analysis do not match the new foundation top loads within 5%, re-iterate the process until convergence is achieved. See Section 7.4.2.1 and GEC 3, (Kavazanjian et al. 2011). If necessary, return to Block 8 and modify the design.

Block 25: Does the Design Meet All Limit State Requirements?

The foundation specialist checks the estimated and/or minimum pile toe elevation for nominal geotechnical resistance in axial compression and tension, deformation under lateral load, serviceability, and drivability. If any limit state checks are not satisfied, the design process returns to Block 8.

Block 26: Design Pile Caps and Abutments.

The final design of the pile cap (and abutment walls) is completed according to AASHTO specifications for concrete structures. The size and thickness of the pile cap in evaluating trial group configurations should have been previously evaluated and the cost of the resulting pile cap estimated. Pile cap cost is a key component in selecting the most cost effective foundation and should not be overlooked in the

design process. A procedure for preliminary sizing of pile caps is provided in Chapter 8.

Block 27: Prepare Plans and Specifications, Set Nominal Resistance Field Verification Procedure.

When the design has been finalized, the structural engineer prepares the project plans and the geotechnical engineer the project specifications. It is important that all of the quality assurance procedures are clearly defined for the bidders to avoid claims after construction is underway. The factored pile load should be shown on the plans along with nominal resistance, the resistance determination method and the method's resistance factor, ϕ_{dyn}. If changes in the resistance determination method are later appropriate, the required nominal resistance with the new method can readily be evaluated. Any minimum or maximum pile penetration depth requirements should also be clearly identified. This information should also be readily apparent in the project specifications so that the contractor has no question regarding the installation requirements. Quality assurance procedures should be in place that address commonly occurring pile installation issues such as obstructions, drivability and construction records. Contract documents and specifications are discussed in Chapter 14, and the foundation report is covered in Chapter 5.

Block 28: Perform Evaluation of Contractor's Equipment Submission.

At this point the engineering effort shifts to the field. The contractor will be required to submit a description of the pile driving equipment that is intended to be used on the project for the engineer's evaluation. On most projects, a wave equation analysis is performed to estimate the blow count that must be achieved in the field to meet the required nominal driving resistance as well as to check if the pile can be driven to the required pile penetration depth, if specified. Driving stresses are also determined and evaluated. If all conditions are satisfactory, the equipment is approved for driving. Some design specifications make this information advisory to the contractor rather than mandatory. Chapters 12 and 14 provide additional information in this area.

Block 29: Set Preliminary Driving Criteria, Drive Test Pile(s), Perform Resistance Evaluation Tests, and Evaluate the Nominal Resistance Achieved.

Depending on the specified resistance determination method, the blow count needed to achieve the required nominal resistance can be established and used as the preliminary driving criteria. With some methods, the preliminary criteria can be determined before driving a pile and with other methods a pile must be driven, tested, and results evaluated. Preliminary driving criteria are generally established using wave equation analysis or a dynamic formula since these can be performed before driving a pile. Additional details on wave equation analysis and dynamic formulas are presented in Chapters 12 and 13, respectively.

The test pile(s), if required, are driven to the preliminary criteria. Driving requirements may be defined by blow count, minimum penetration depth, dynamic monitoring results, or a combination of these conditions. The nominal resistance can be evaluated using the observed blow count and hammer performance (e.g., stroke, energy readout) in a wave equation analysis or dynamic formula. Alternatively, the nominal resistance achieved by the test pile can be evaluated by more reliable methods such as a static load test, dynamic load test, or rapid load test. Details on static load testing are presented in Chapter 9, dynamic load testing in Chapter 10, rapid load testing in Chapter 11.

Each field resistance determination method has its own resistance factor, ϕ_{dyn}. Therefore, it is important to determine the resistance determination method during the design process. The selected resistance determination method determines the required nominal resistance. Post-design modification to the resistance determination method changes the resistance factor and the required nominal resistance. Changing to a more reliable resistance determination method reduces the required nominal resistance, which generally shortens the piles. Conversely, changing to a less reliable resistance determination method increases the required nominal resistance. This may result in the original design no longer meeting design or constructability requirements.

On smaller projects, a dynamic formula might be used to evaluate the nominal resistance. The modified Gates Formula is frequently used for this purpose but some transportation agencies have also developed or adopted other dynamic formulas. If a dynamic formula is used, then drivability and hammer selection will be based on the blow count given by the formula only, since stresses and drivability to a penetration depth are not determined. Dynamic formula usage is covered in Chapter 13.

Block 30: Adjust Driving Criteria or Design.

At this stage the final installation criteria can be set or, if test results from Block 29 indicate the nominal resistance is inadequate, the driving criteria may have to be changed. Occasionally, it may be necessary to make changes in the design as far back as Block 8. It may also be possible to change to a more reliable resistance determination method with a higher resistance factor and thereby reduce the required nominal resistance to a nominal resistance that can be achieved without a major design change.

In some cases, it is desirable to perform preliminary field testing before final design. When the project is very large and the subsurface conditions are difficult, it may be possible to achieve substantial cost savings by having results from a design stage test pile program, including actual driving records at the site. Such results can be used to optimize the design, and reduce contractor contingencies when included as part of the bid package.

Block 31: Drive Production Piles with Construction Monitoring.

After the driving criteria is established, the production pile driving begins. Quality control and quality assurance procedures have been established and are applied. Construction inspection items are discussed in greater detail in Chapter 18. Problems may arise and must be handled as they occur in a timely fashion.

Block 32: Post-Construction Evaluation and Refinement of Design.

After completion of the foundation construction, the design should be reviewed and evaluated for its effectiveness in satisfying the design requirements and also its cost effectiveness. This review benefits future similar projects constructed in similar conditions.

2.11 COMMUNICATION

Good communication between all organizations and disciplines involved in the design and construction of a pile foundation is essential to reach a successful completion of the project. In the design stage, communication and interaction is needed between the structural, geotechnical, geologic, hydraulic, and construction

disciplines, as well as with consultants, drill crews and laboratory personnel. In the construction stage, structural, geotechnical and construction disciplines need to communicate for a timely resolution of construction issues as they arise. Tables 2-4 and 2-5 highlight some of the key issues to be communicated in the design and construction stages.

Table 2-4 Design Stage Communication

Subject	Structural	Geotechnical	Hydraulic	Construction	Field Crews	Laboratory
Preliminary Structure Loads and Performance Criteria.	X	X	X			
Determination of Scour Potential.	X	X	X			
Determination of Applicable Extreme Events.	X	X	X			
Review of Past Construction Problems in Project Area.	X	X	X	X		
Implement Subsurface Exploration and Testing Programs.	X	X	X	X	X	X
Determination of Pile Type, Length and Nominal Resistance.	X	X		X		
Select Construction Control and Quality Assurance Methods.	X	X		X		
Effects of Approach Fills on Design.	X	X				
Prepare Plans and Specifications.	X	X	X	X		

Table 2-5 Construction Stage Communication

Subject	Structural	Geotechnical	Construction
Perform Required Methods of Construction Control and Quality Assurance.	X	X	X
Perform Wave Equation Analysis of Contractors Driving System to Establish Driving Criteria.	X	X	X
Perform Static Load Test(s) and/or Dynamic Monitoring and Adjust Driving Criteria.	X	X	X
Resolve Pile Installation Problems / Construction Issues.	X	X	X

REFERENCES

Abu-Hejleh, N., Kramer, W.M., Mohamed, K., Long, J.H., and Zaheer, M.A. (2013). Implementation of AASHTO LRFD Design Specifications for Driven Piles, FHWA-RC-13-001. U.S. Dept. of Transportation, Federal Highway Administration, 71 p.

American Association of State Highway and Transportation Officials (AASHTO). (2011). Guide Specifications for LRFD Seismic Bridge Design, 2nd Edition, with 2012, 2014, and 2015 Interim Revisions. American Association of State Highway and Transportation Officials, Washington, D.C., 331 p.

American Association of State Highway and Transportation Officials (AASHTO). (2014). AASHTO LRFD Bridge Design Specifications, US Customary Units, Seventh Edition, with 2015 Interim Revisions. American Association of State Highway and Transportation Officials, Washington, D.C., 1960 p.

Brown, D.A., Dapp, S.D., Thompson, W.R., and Lazarte, C.A. (2007). Design and Construction of Continuous Flight Auger (CFA) Piles. FHWA-HIF-07-03, Geotechnical Engineering Circular (GEC) No.08. U.S. Dept. of Transportation, Federal Highway Administration, 289 p.

Brown, D. A., Turner, J.P. and Castelli R.J. (2010). Drilled Shafts: Construction Procedures and LRFD Design Methods, FHWA-NHI-10-016, Geotechnical Engineering Circular (GEC) No. 10. U.S. Dept. of Transportation, Federal Highway Administration, 970 p.

Elias, V., Welsh, J.P., Warren, J., Lukas, R.G., Collin J.G., and Berg, R.R. (2006). Ground Improvement Methods Volumes I and II, FHWA-NHI-06-019 and FHWA NHI-06-020. National Highway Institute, Federal Highway Administration, U.S. Department of Transportation, Washington D.C.

Kavazanjian, E., Wan, J-N. J., Martin, G.R., Shamsabadi, A., Lam, I., Dickenson, S.E., and Hung, C.J. (2011). LRFD Seismic Analysis and Design of Transportation Geotechnical Features and Structural Foundations, FHWA-NHI-11-032, Geotechnical Engineering Circular (GEC) No. 3. U.S. Dept. of Transportation, Federal Highway Administration, Washington, D.C., 592 p.

Kimmerling, R.E. (2002). Shallow Foundations, FHWA-IF-02-054, Geotechnical Engineering Circular (GEC) No. 6. U.S. Dept. of Transportation, Federal Highway Administration, Washington, D.C., 310 p.

Modjeski and Masters, Inc. (2015). Bridges for Service Life Beyond 100 Years: Service Limit State Design. SHRP2 Report S2-R19B-RW-1. Transportation Research Board, Washington D.C., 268 p.

Munfakh, G., Arman, A., Collin, J.G., Hung, J.C.-J., and Brouillette, R.P. (2001). Shallow Foundations Reference Manual, FHWA-NHI-01-023. National Highway Institute, Federal Highway Administration, Washington, D.C., 222 p.

Paikowsky, S.G. (2004), with contributions from Birgisson, B., McVay, M., Nguyen, T., Kuo, C., Baecher, G., Ayyub, B., Stenersen, K., O.Malley, K., Chernauskas, L., and O'Neill, M., Load and Resistance Factor Design (LRFD) for Deep Foundations, NCHRP Report 507. Transportation Research Board, Washington, D.C., 76 p.

Sabatini, P.J., Tanyu, B., Armour., P., Groneck, P., and Keeley, J. (2005). Micropile Design and Construction, FHWA-NHI-05-039. National Highway Institute, U.S. Dept. of Transportation, Federal Highway Administration, Washington, D.C., 436 p.

Samtani, N.C., Nowatzki, E.A., and Mertz, D.R. (2010). Selection of Spread Footings on Soils to Support Highway Bridge Structures, FHWA-RC TD-10-001. U.S. Department of Transportation, Federal Highway Administration, Washington, D.C., 98 p.

CHAPTER 3

CONSIDERATIONS IN FOUNDATION SELECTION

A foundation is the interfacing element between the superstructure, substructure, and the underlying geomaterial (i.e., soil or rock). The loads transmitted by the foundation to the underlying geomaterial must not cause shear failure or damaging deformations of the superstructure. It is essential to systematically consider various foundation types and to select the most appropriate alternative based on the superstructure requirements, the subsurface conditions, and foundation cost. Foundation types include shallow foundations consisting of spread footing or mat foundations with or without ground improvement; or deep foundations consisting of driven piles, micropiles, drilled shafts, or continuous flight auger (CFA) piles.

Subsequent chapters of this manual provide guidance on driven pile foundation design and construction. FHWA guidance for other foundation solutions is shown in Table 3-1 below.

Table 3-1 Foundation Information Sources Provided by the Federal Highway Administration

Foundation Solution	FHWA Reference	Author(s)
Spread Footings	GEC-6, FHWA-SA-02-054	Kimmerling (2002)
Ground Improvement	FHWA-NHI-06-019/020	Elias et al. (2006)
Micropiles	FHWA-NHI-05-039	Sabatini et al. (2005)
Drilled Shafts	GEC-10, FHWA NHI-10-016	Brown et al. (2010)
CFA Piles	GEC-8, FHWA-HIF-07-03	Brown et al. (2007)

Complete references for the above design manuals are provided at the end of this chapter. Information on the availability of these documents is provided at www.fhwa.dot.gov/bridge/geopub.htm.

3.1 FOUNDATION DESIGN APPROACH

The following design approach is recommended to determine the most appropriate foundation alternative.

1. Determine the foundation loads to be supported, structure layout, limits on total and differential settlements, lateral deformations, lateral loads, scour, seismic and other extreme event loading conditions, and special requirements such as construction phasing and time constraints on construction. A complete knowledge of these issues is of paramount importance.

2. Evaluate the subsurface exploration and laboratory testing data. Ideally, the subsurface exploration and laboratory testing programs were performed with knowledge of the foundation loads and the needed geomaterial resistances. If the subsurface information is insufficient, perform a second subsurface exploration program, laboratory testing program, or in-situ testing program.

3. Prepare a final subsurface profile and critical cross sections. Determine subsurface layers suitable or unsuitable for spread footings, pile foundations, or drilled shaft load transfer. Also consider if ground improvement techniques could modify unsuitable layers into suitable bearing layers.

4. Determine the most feasible foundation alternatives. Both shallow foundations and deep foundations should be considered. Deep foundation alternatives include driven piles, drilled shafts, micropiles, and CFA piles. Proprietary deep foundations systems should not be excluded as they may be the most economical alternative in a given condition. Consideration should be given to the following foundation options.

Shallow Foundations:
a. Spread footings (without ground improvement).
b. Mat foundations.

Shallow Foundations:
a. Spread footings (with ground improvement).
b. Mat foundations.

Deep Foundations:

a. Driven pile foundations.
    i. Candidate pile types.
    ii. Viable pile sections.
b. Drilled shafts.
c. Micropile.
d. Continuous Flight Auger (CFA) piles.

5. Prepare cost estimates for technically feasible alternative foundation designs including all associated substructure and construction control method costs. The cost estimates should consider the concept of foundation support cost introduced in Section 3.4.1. The foundation support cost should include all associated temporary and permanent substructure costs required for foundation construction (e.g. sheeting or cofferdam requirements, concrete tremie seal, pile cap requirement and size), the effect of environmental or construction limitations (noise, vibration, low overhead, access restrictions), as well as any required mitigation procedures (noise shrouds, predrilling, bubble nets, etc.).

6. Select the most appropriate foundation alternative. Generally the most economical alternative (lowest foundation support cost) should be selected and recommended. The ability of the local construction force as well as the availability of materials and equipment should also be considered.

For major projects, if the estimated costs of technically feasible foundation alternatives (during the design stage) are within 15 percent of each other, then alternate foundation designs should be considered for inclusion in the contract documents. The most economical foundation design will then be determined by construction demand and material pricing rather than subtleties in the design estimate.

3.2 FOUNDATION ALTERNATIVES

To determine the most preferred foundation alternatives, both shallow foundations and deep foundations should be considered. Table 3-2 summarizes shallow and deep foundation types and uses, as well as applicable and non-applicable subsurface conditions.

Table 3-2 Foundation Types and Typical Uses (Modified from Bowles 1977)

Foundation Type	Use	Applicable Soil Conditions	Non-suitable or Difficult Soil Conditions
Spread footing, wall footings.	Individual columns, walls, bridge piers.	Any conditions where bearing capacity is adequate for applied load. May use on single stratum; firm layer over soft layer, or weaker layer over firm layer. Check immediate, differential and consolidation settlements.	Any conditions where foundations are supported on soils subject to excessive scour or liquefaction.
Mat foundation.	Same as spread and wall footings. Very heavy column loads. Usually reduces differential settlements and total settlements.	Generally soil bearing value is less than for spread footings. Over one-half area of structure covered by individual footings. Check settlements.	Same as footings.
Driven pile foundations.	In groups to transfer heavy column and bridge loads to suitable soil and rock layers. Also to resist uplift and/or lateral loads.	Poor surface and near surface soils. Geomaterials suitable for load support 15 to 300 feet below ground surface. Check settlement and lateral deformation of pile groups.	Shallow depth to hard stratum. Sites where pile driving vibrations or heave would adversely impact adjacent facilities. Boulder fields.
Drilled shafts.	In groups to transfer heavy column loads. Monoshafts and small groups sometimes used. Cap sometimes eliminated by using drilled shafts as column extensions.	Poor surface and near surface soils. Geomaterial suitable for load support located 25 to 300 feet below ground surface.	Caving formations difficult to stabilize. Artesian conditions. Boulder fields. Contaminated soil. Areas with concrete delivery or concrete placement logistic problems.
Micropiles.	Often used for seismic retrofitting, underpinning, very difficult drilling through overburden materials, in low head room situations, and for projects with noise or vibration restrictions.	Any soil, rock, or fill conditions including areas with rubble fill, boulders, and karstic conditions.	High slenderness ratio may present buckling problems from loss of lateral support in liquefaction susceptible soils. Low lateral resistance. Offshore applications.
CFA Piles.	In groups to transfer heavy loads to suitable geomaterials. Projects with noise and vibration restrictions.	Medium to very stiff clays, cemented sands or weak limestone, residual soils, medium dense to dense sands, rock overlain by stiff or cemented deposits.	Very soft soils, loose saturated sands, hard bearing stratum overlain by soft or loose soils, karst conditions, areas with flowing water. Highly variable subsurface conditions. Conditions requiring long piles due to deep scour, liquefiable layers, or penetrating very hard strata or rock, offshore conditions.

3.2.1 Shallow Foundations

The feasibility of using spread footings for shallow foundation support should be considered in any foundation selection process. Spread footings are generally more economical than deep foundations in situations where geomaterial and loading conditions are conducive for their use. Favorable conditions include: competent soils within shallow depth; foundation width is expected to be relatively small; spread footing can be placed at an economical depth (e.g., 10-feet); quality granular fills are available (Abu-Hejleh et al. 2014). Spread footings on engineered compacted granular fills and mechanically stabilized earth (MSE) granular fills to support bridge abutments provide a satisfactory alternative to deep foundations with good performance and significant cost savings (Abu-Hejleh et al. 2014). Bridge foundations that are subject to scour, liquefaction, or large settlement, as well as those with large uplift or lateral load demand are typically not suitable for shallow foundations. Additional details on spread footings for highway bridges may be found in FHWA GEC-6, Shallow Foundations by Kimmerling (2002).

3.2.2 Shallow Foundations with Ground Improvement

In some situations, ground improvement methods can be used to improve subsurface conditions thereby allowing the use of shallow spread footing foundations. Ground improvement in conjunction with spread footings should be economically evaluated provided they meet strength and service limit state requirements as this combination may be more cost effective than deep foundation solutions. Additional information on ground improvement may be found in FHWA-NHI-06-019/020 Ground Improvement Methods (Elias et al. (2006), and at www.GeoTechTools.org.

3.2.3 Deep Foundations

Deep foundations are generally needed where the axial compression, axial tension, lateral load demand or a combination of the above cannot be satisfied by the near surface soil conditions. However, deep foundations should not be used indiscriminately for all subsurface conditions and for all structures. There are subsurface conditions where a driven pile, drilled shaft, micropile, or CFA pile may be very difficult or costly to install. Ground improvement techniques can also be used with deep foundations as an economical means to improve lateral resistance in weak surficial soils (Rollins and Brown 2011).

3.2.3.1 Driven Piles

Driven piles are the most commonly used deep foundation system for transportation projects. Piles are typically installed in groups using an impact pile driving hammer. Multiple pile types with various section properties are available to resist almost any load demand. Pile lengths for some pile types can be easily adjusted and spliced in the field to accommodate variations in subsurface conditions. Further guidance on pile selection, pile type advantages and disadvantages, as well as the best pile type for a given subsurface condition may be found in Chapter 6.

3.2.3.2 Drilled Shafts

Drilled shafts are frequently used for transportation projects with large axial compression or lateral load demand. They are installed by mechanically or percussion drilling a hole to the required depth and filling the hole with concrete. Sometimes an enlarged base or bell is formed mechanically to increase the toe bearing area. Drilling slurry and/or temporary casings can be used when the sides of the hole are unstable. Reinforcing steel is installed as a cage inserted prior to concrete placement. For complete details on drilled shafts, reference should be made to FHWA GEC-10, Drilled Shafts: Construction Procedures and LRFD Design Methods by Brown et al. (2010) and AASHTO (2014) design specifications Section 10.8.

3.2.3.3 Micropiles

Micropiles are often used for transportation projects in karst areas as well as for underpinning, seismic retrofitting, and projects with difficult drilling conditions. Micropiles are a small diameter (< 12 inches), reinforced, drilled, and grouted deep foundation element. Many different tools and installation methods are available to construct micropiles. They are often installed by rotating a casing with a cutting edge into the geomaterial or by percussion methods. Cuttings are removed with circulating drilling fluid. Reinforcing steel is then inserted and a sand-cement grout is pumped through a tremie. Pressurized two-stage grouting techniques are also used. The casing can be partially or fully withdrawn. Due to the wide variety of micropile types and construction techniques, reference should be made to FHWA-05-039, Micropile Design and Construction, Sabatini et al. (2005), and AASHTO (2014) design specifications Section 10.9 for complete details.

3.2.3.4 Continuous Flight Auger (CFA) Piles

Continuous Flight Auger (CFA) or alternatively Auger Cast-in-Place (ACIP) piles are usually installed by turning a continuous-flight hollow-stem auger into the ground to the required depth. As the auger is withdrawn, grout or concrete is pumped under pressure through the hollow stem, filling the hole from the bottom up. Vertical reinforcing steel is pushed down into the grout or concrete column before it hardens. Uplift tension reinforcing can be installed by placing a single high strength steel bar through the hollow stem of the auger before grouting. After reinforcing steel is placed, the pile head is cleaned of any lumps of soil which may have fallen from the auger. For complete details on CFA piles, reference should be made to FHWA GEC-8, Design and Construction of Continuous Flight Auger Piles by Brown et al. (2007).

3.3 ESTABLISHMENT OF A NEED FOR A DEEP FOUNDATION

The first difficult problem facing the foundation designer is to establish whether or not the site conditions dictate that a deep foundation must be used. Vesic (1977) summarized typical situations in which piles may be needed. These typical situations as well as additional uses of deep foundations are shown in Figure 3-1.

Figure 3-1(a) shows the most common case in which the upper soil strata are too compressible or too weak to support heavy vertical loads. In this case, deep foundations transfer loads to a deeper competent stratum and act as predominantly toe bearing foundations. In the absence of a competent stratum within a reasonable depth, the loads must be gradually transferred, mainly through soil resistance along the shaft, Figure 3-1(b). An important point to remember is that deep foundations transfer load through unsuitable layers to suitable layers. The foundation designer must define at what depth suitable soil layers begin in the soil profile.

Deep foundations are frequently needed because of the relative inability of shallow footings to resist inclined, lateral, or uplift loads and overturning moments or excessive deformations. Deep foundations resist uplift loads by shaft resistance, Figure 3-1(c). Lateral loads are resisted either by vertical deep foundations in bending, Figure 3-1(d), or by groups of vertical and battered piles, which combine the axial and lateral resistances of all piles in the group, Figure 3-1(e). Lateral loads from overhead highway signs and noise walls may also be resisted by groups of deep foundations, Figure 3-1(f).

Deep foundations are often required when scour around footings could cause loss of bearing capacity at shallow depths, Figure 3-1(g). In this case the deep foundations must extend below the depth of scour and develop their full nominal resistance in the support zone below the level of expected scour. FHWA scour guidelines using the Hydraulics Engineering Circular No. 18 (Arneson et al. 2012) require the geotechnical analysis of bridge foundations to be performed on the basis that all stream bed materials in the scour prism have been removed and are not available for bearing or lateral support. Costly damage and the need for future underpinning can be avoided by properly designing for scour conditions.

Liquefaction and other seismic effects on deep foundation performance must be considered for deep foundations in seismic areas. Soils subject to liquefaction in a seismic event may dictate that a deep foundation be used, Figure 3-1(h). Seismic events can also induce significant lateral loads to deep foundations. During a seismic event, liquefaction susceptible soils offer less lateral resistance, reduced shaft resistance, and can add drag load to a deep foundation.

Deep foundations are often used as fender systems to protect bridge piers from vessel impact, Figure 3-1(i). Fender system sizes and group configurations vary depending upon the magnitude of vessel impact forces to be resisted. In some cases, vessel impact loads must be resisted by the bridge pier foundation elements. Single deep foundations may also be used to support navigation aids.

In urban areas, deep foundations may occasionally be needed to support structures adjacent to locations where future excavations are planned or could occur, as in Figure 3-1(j). Use of shallow foundations in these situations could require future underpinning in conjunction with adjacent construction.

Deep foundations are also used in areas of expansive or collapsible soils to resist undesirable seasonal movements of the foundations. Under such conditions, deep foundations are designed to transfer foundation loads, including uplift or downdrag, to a level unaffected by seasonal moisture movements, Figure 3-1(k).

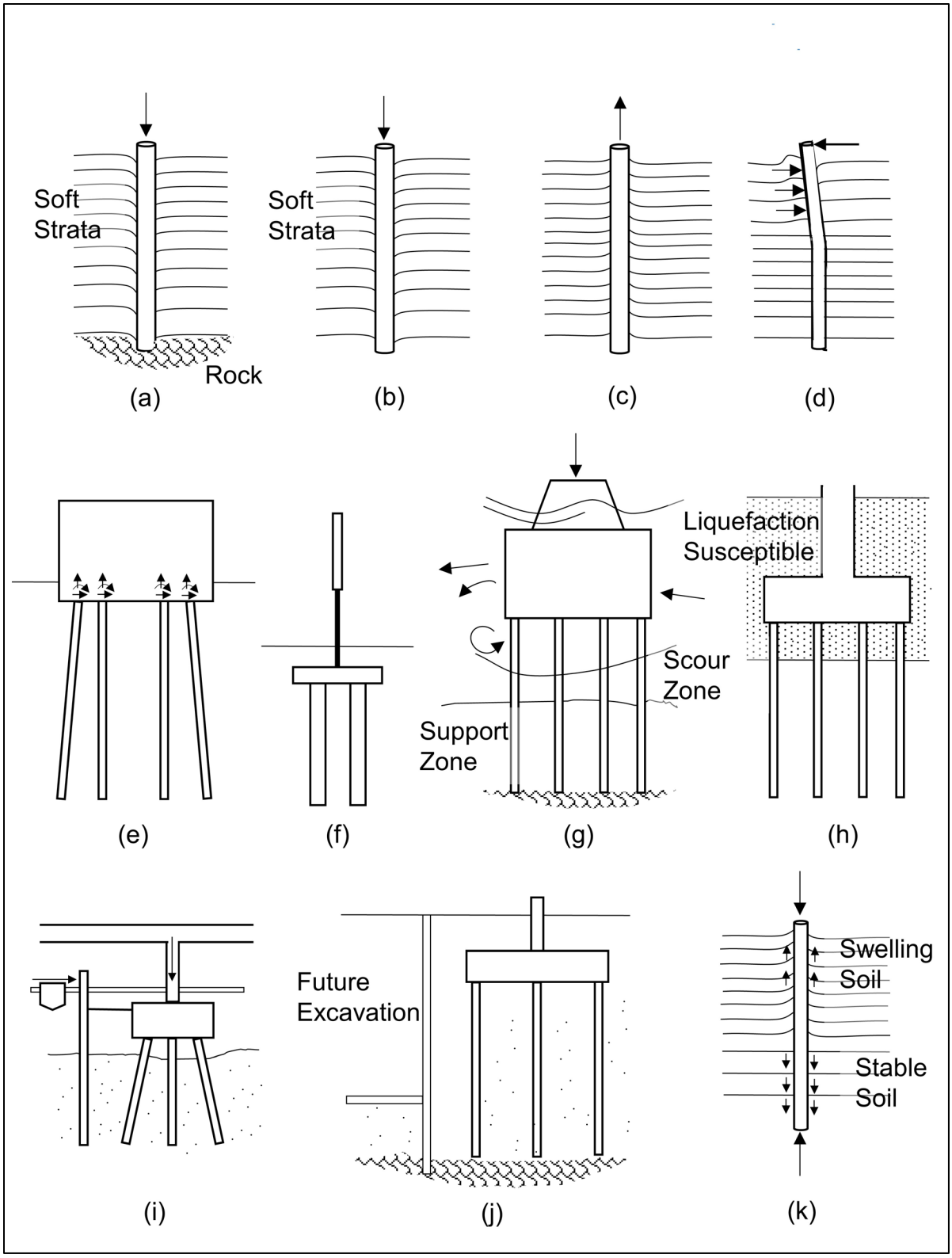

Figure 3-1 Situations in which deep foundations may be needed (modified from Vesic 1977).

3.4 ECONOMIC ASPECTS OF FOUNDATION SELECTION

In many instances, either a shallow or deep foundation alternative is technically feasible. Feasible conditions for the use of a shallow spread footing foundation are summarized in Abu-Hejleh et al. (2014). Under these circumstances, an evaluation of the shallow foundation should include; 1) the dimensions and depth of shallow footings based on bearing resistance, 2) the magnitude and time rate of settlement under anticipated loads, and 3) detailed cost analysis including such factors as need for cofferdams, overall substructure cost, dewatering and foundation seals, construction time, construction risk, claims potential, and other project constraints. A comparative analysis of feasible deep foundation alternatives should also be performed. The cost analysis of feasible alternatives generally has a significant role in final selection of the foundation type.

Because this manual deals only with driven pile foundations, other types of foundations will not be discussed further.

3.4.1 Foundation Support Cost

A rational comparison of technically viable foundation systems can be made based on the foundation support cost of each candidate foundation type. The foundation support cost is defined as the total cost of the foundation divided by the factored load the foundation supports in tons or kips. Factored loads are used since resistance factors vary by foundation type. For driven pile foundation projects, the total foundation support cost where axial loading governs can be separated into three major components; the pile support cost, the pile cap support cost, and the construction control method support cost. The total foundation cost should also include all costs associated with a given foundation system including the need for excavation or retention systems, dewatering, pile caps and cap size, environmental restrictions on construction activities, etc. A detailed discussion on foundation support cost applications to driven pile design is presented in Komurka (2015).

It should be noted that the above discussion assumes that the axial compression load controls the foundation design. On projects where the axial tension load, lateral load, or combined axial and lateral loads govern the foundation design, the support cost concept can still be applied. In those situations, the cost per ton of factored uplift load or factored lateral load should be used in the selection process.

3.4.1.1 Cost Optimization Example

Figure 3-2 presents a layered soil profile that will be used to illustrate the cost optimization process. The first step in the cost optimization of a candidate pile section is to perform a static analysis to determine its nominal geotechnical resistance versus the pile penetration depth. Static analysis methods are described in greater detail in Chapter 7. A static analysis was performed for a HP 14x117 H-pile using the FHWA method in the APILE computer program. The results of that static analysis are presented in Figure 3-2, and include the nominal geotechnical resistance which is comprised of the nominal shaft resistance and the nominal toe resistance at a given pile penetration depth.

Several possible pile penetration termination depths and associated nominal resistances are apparent in Figure 3-2. Piles could be driven into the medium dense sand layer at a depth of 60 feet for a nominal resistance of 150 kips; seated into the medium dense sand layer near a depth of 70 feet for 300 kips; driven through the medium dense sand layer and underlying stiff clay layer and into the extremely dense sand layer at 110 feet for 1000 kips; or driven to bedrock near 118 feet for 1700 kips. A rational economic assessment of these potential pile termination depths and nominal resistances is needed for cost effective design. For most pile types, the pile cost can usually be assumed as linear with depth based on unit price as illustrated in Figure 3-3. However, this may not be true for very long concrete piles or long, large section steel piles. These exceptions may require the cost analysis to reflect special transportation, handling, or splicing costs for the concrete piles or extra splice time and cost for steel piles.

Figure 3-4 presents a plot of nominal resistance pile support cost versus pile penetration depth. This figure is obtained by dividing the pile cost at a given depth from Figure 3-3 by the nominal resistance at that same depth from Figure 3-2. Note that Figure 3-4 includes the nominal resistance versus depth in addition to the pile support cost. For the H-pile section evaluated, a general conclusion can quickly be reached; piles penetrating to more than 60 feet will be more cost effective than shorter piles. At the top of the sand layer near 60 feet, the pile has a nominal resistance of 150 kips and a nominal resistance support cost of $39 per kip. Near the middle of this sand layer at a penetration depth of 70 feet, the pile has a nominal resistance of 300 kips and a much lower nominal resistance support cost of $19 per kip. The nominal resistance pile support cost drops further to $9 per kip at a depth of 110 feet and a nominal resistance of 1000 kips. Finally, the nominal resistance pile support cost continues to decrease to $5.50 per kip at a depth of 118 feet and a nominal resistance of 1722 kips.

A HP 14x117 H-pile section with a yield strength of 50 ksi has a nominal structural resistance of 1720 kips when fully embedded. An example detailing the calculation of the nominal structural resistance of an H-pile is provided in Section 8.5.3. The maximum factored load that can be placed on the pile is the lesser of the factored structural resistance or the factored geotechnical resistance. For the H-pile section used, the maximum factored structural resistance is 1032 kips when good driving conditions are anticipated based on the subsurface conditions, pile damage is unlikely, and a driving shoe is therefore not required. The maximum factored structural resistance decreases to 860 kips when severe driving conditions are anticipated based on the subsurface conditions, damage is possible, and a driving shoe is required. Figure 3-5 includes the nominal and factored structural resistances in the strength limit state under axial compression loading. The structural resistance for all pile types is discussed in Chapter 8.

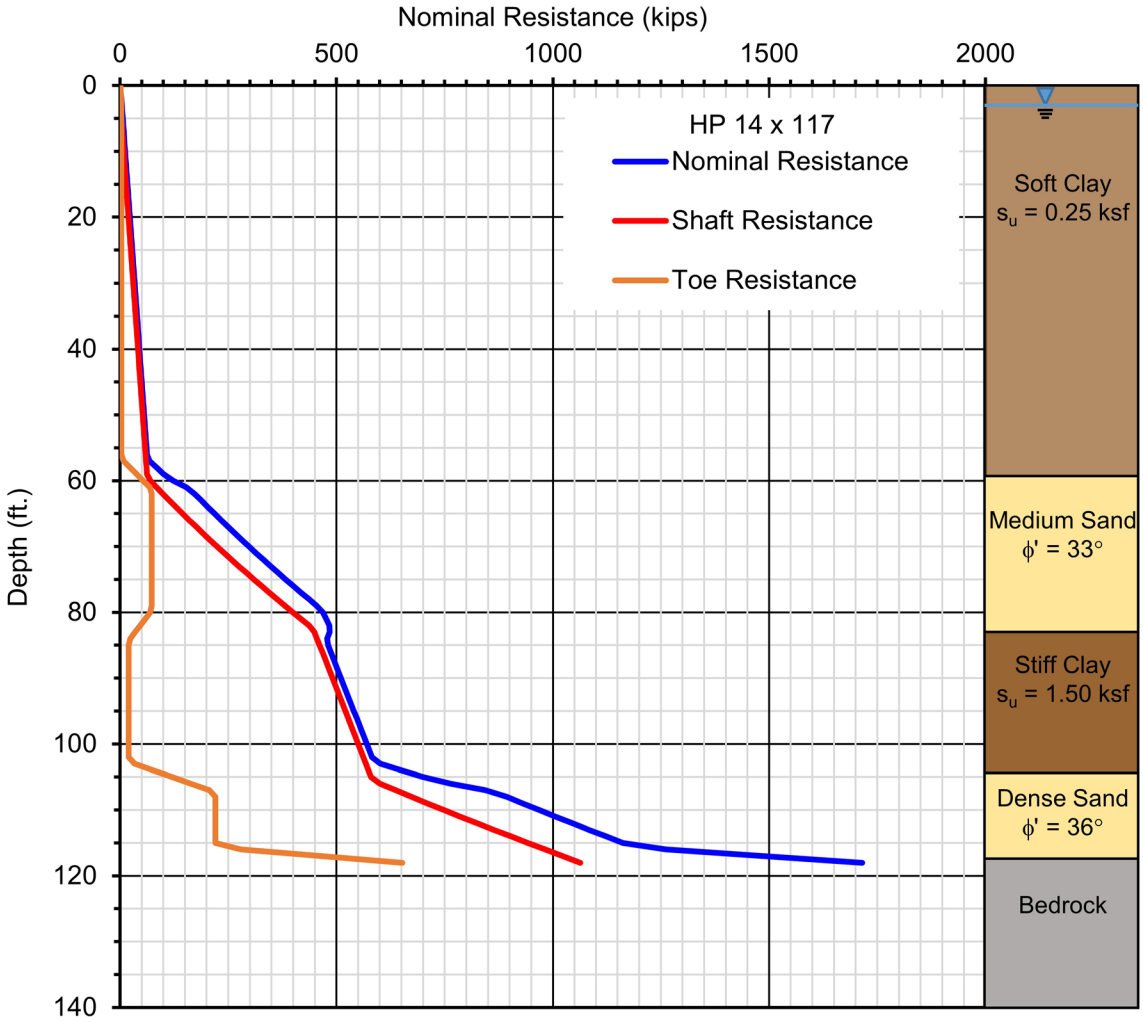

Figure 3-2 Soil profile and nominal geotechnical resistances versus depth.

Figure 3-3 Pile cost versus pile penetration depth.

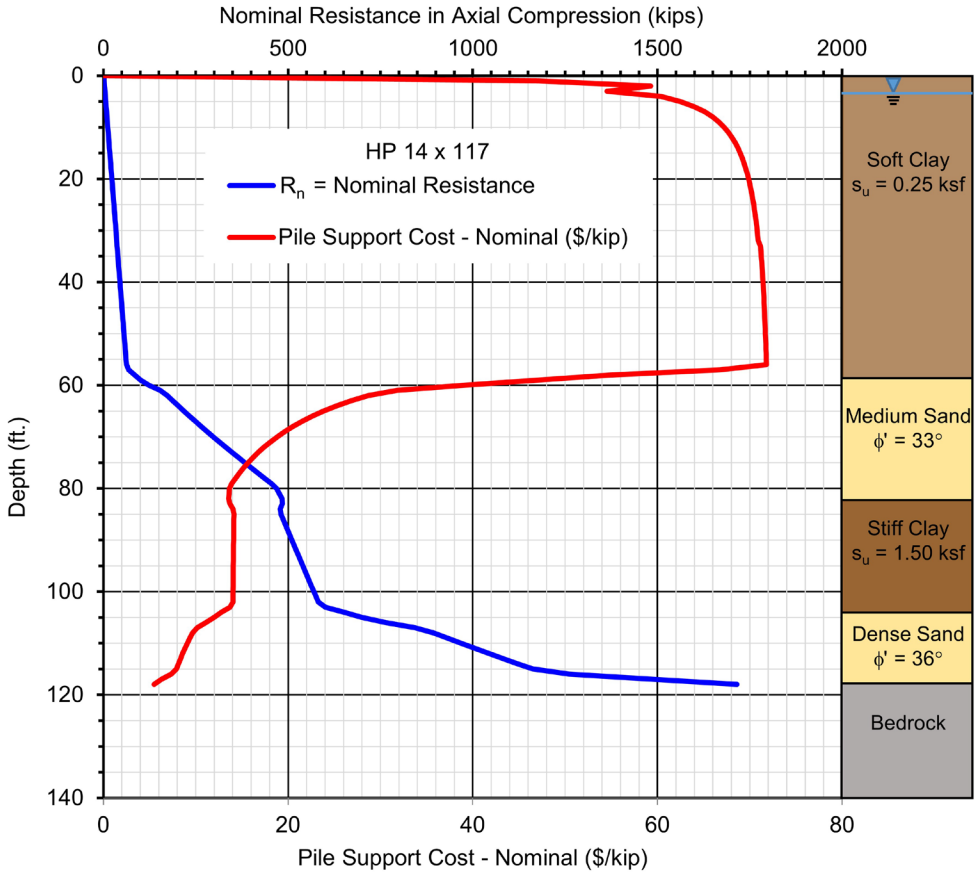

Figure 3-4 Nominal resistance of pile support cost versus penetration depth.

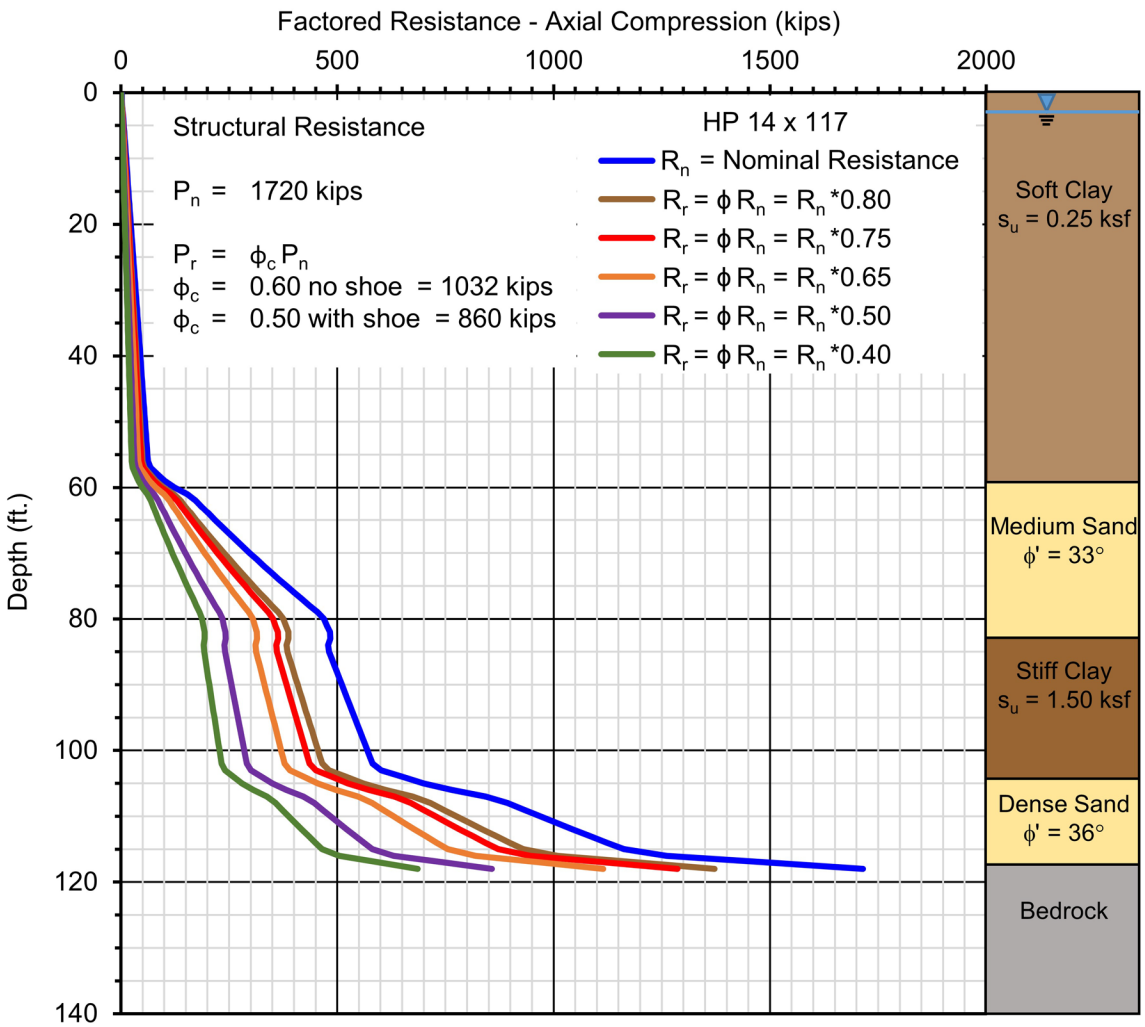

Figure 3-5 Nominal and factored resistances for axial compression loads.

Figure 3-5 also includes the nominal and factored geotechnical resistances in the strength limit state under axial compression loading. Geotechnical aspects of limit state design are covered in Chapter 7. The factored geotechnical resistances versus pile penetration depth shown in Figure 3-5 are based on construction control with the following field verification methods:

ϕ_{dyn} = 0.80 Driving criteria established by successful static load test of at least one pile per site condition and dynamic testing with signal matching of at least two piles per site condition, but no less than 2% of production piles.

ϕ_{dyn} = 0.75 Driving criteria established by successful static load test of at least one pile per site condition without dynamic testing or by dynamic testing with signal matching on 100% of the production piles.

ϕ_{dyn} = 0.65 Driving criteria established by dynamic testing with signal matching of at least two piles per site condition, but no less than 2% of production piles.

ϕ_{dyn} = 0.50 Driving criteria established by wave equation analysis based on end of drive conditions only.

ϕ_{dyn} = 0.40 Driving criteria established by FHWA modified Gates dynamic formula based on end of drive conditions only.

The required nominal driving resistance, R_{ndr}, needed to utilize the full factored structural resistance, P_r, of either 1032 or 860 kips with a given resistance verification field method is provided in Table 3-3. The required nominal driving resistance for full utilization of the factored structural resistance can be calculated by dividing the factored structural resistance by the resistance factor of the field verification method, ϕ_{dyn}.

The estimated pile length for the nominal driving resistance, R_{ndr}, can then be determined from Figure 3-5 by the depth where the nominal geotechnical resistance, R_n equals the nominal driving resistance value for the field method. The abbreviations used in the table for the field verification methods are as described above with SLT for static load test, DLT for dynamic load test, WEA for wave equation analysis and DF for dynamic formula. Note that a drivability strength limit check will preclude use of the maximum factored structural resistance, P_r in some cases due to the nominal driving resistance, R_{ndr}, required by that field method.

Table 3-3 Pile Length Estimates Based on Field Methods and Factored Resistances

Field Method	ϕ_{dyn}	R_{ndr} P_r = 1032 kips	Estimated Length	R_{ndr} P_r = 860 kips	Estimated Length
SLT & 2% DLT	0.80	1290 kips	116 ft	1075 kips	113 ft
SLT or 100% DLT	0.75	1376 kips	117 ft	1147 kips	115 ft
2% DLT	0.65	1588 kips	118 ft	1323 kips	117 ft
WEA	0.50	2064 kips	118 ft+ Rock	1720 kips	118 ft
FHWA Gates DF	0.40	2580 kips	118 ft+ Rock	2150 kips	118 ft+ Rock

Figure 3-5 also illustrates the benefit of using a more reliable field verification method for piles terminated in the geomaterials above bedrock. If an HP 14x73 section is chosen for this subsurface condition instead of the HP 14x117 section, the maximum factored structural resistance for a fully embedded HP 14x73 section in severe driving conditions is 520 kips. For illustrative purposes, the static analysis

results are assumed unchanged for a HP 14x73 section compared to the HP 14x117 section based on roughly the same pile perimeter and the same plugged pile toe area. The estimated pile length from Figure 3-5 to geotechnically utilize the maximum factored structured resistance is 104 feet for field verification with a static load test and dynamic testing (ϕ_{dyn} = 0.80) compared to an estimated length of 116 feet for field verification with the modified Gates dynamic formula (ϕ_{dyn} = 0.40).

The results of the static analysis on the HP 14x117 H-pile section can be also used to evaluate the pile penetration requirements for the axial tension load demand. The shaft resistance from Figure 3-2 is presented once again in Figure 3-6 and labeled R_s for the nominal shaft resistance. The pile cost at a given depth from Figure 3-3 can be divided by the nominal shaft resistance at that same depth to obtain a plot of the pile support cost in dollars per kip of nominal uplift resistance versus pile penetration depth. Figure 3-6 presents plots of both the nominal uplift resistance pile support cost versus depth and the nominal uplift resistance versus depth. Two distinct plateaus in the pile support cost for tension loading are apparent, $90 to $100 per kip of nominal uplift resistance above 60 feet and $15 to $25 per kip of nominal uplift resistance below 70 feet.

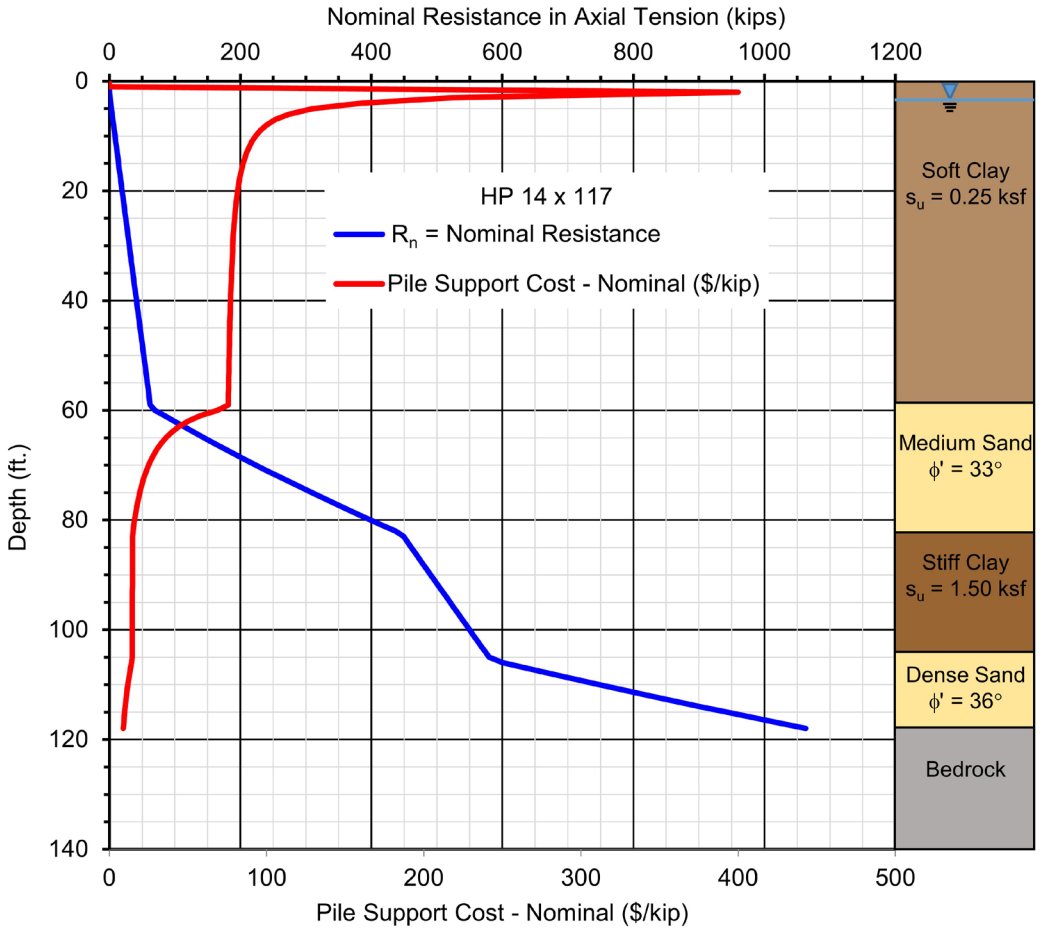

Figure 3-6 Nominal resistance and pile support cost.

Figure 3-7 presents the nominal shaft resistance, R_s, and the factored axial tension resistance versus depth, R_r. In Figure 3-7, the nominal shaft resistance, R_s, is multiplied by the uplift resistance factors, ϕ_{up}, of 0.60 if the uplift resistance is determined with a static load test, 0.50 if obtained from a dynamic load test with signal matching, and 0.25 in clay layers and 0.35 in sand layers for uplift resistance determined by the α-method and Nordlund static analysis methods.

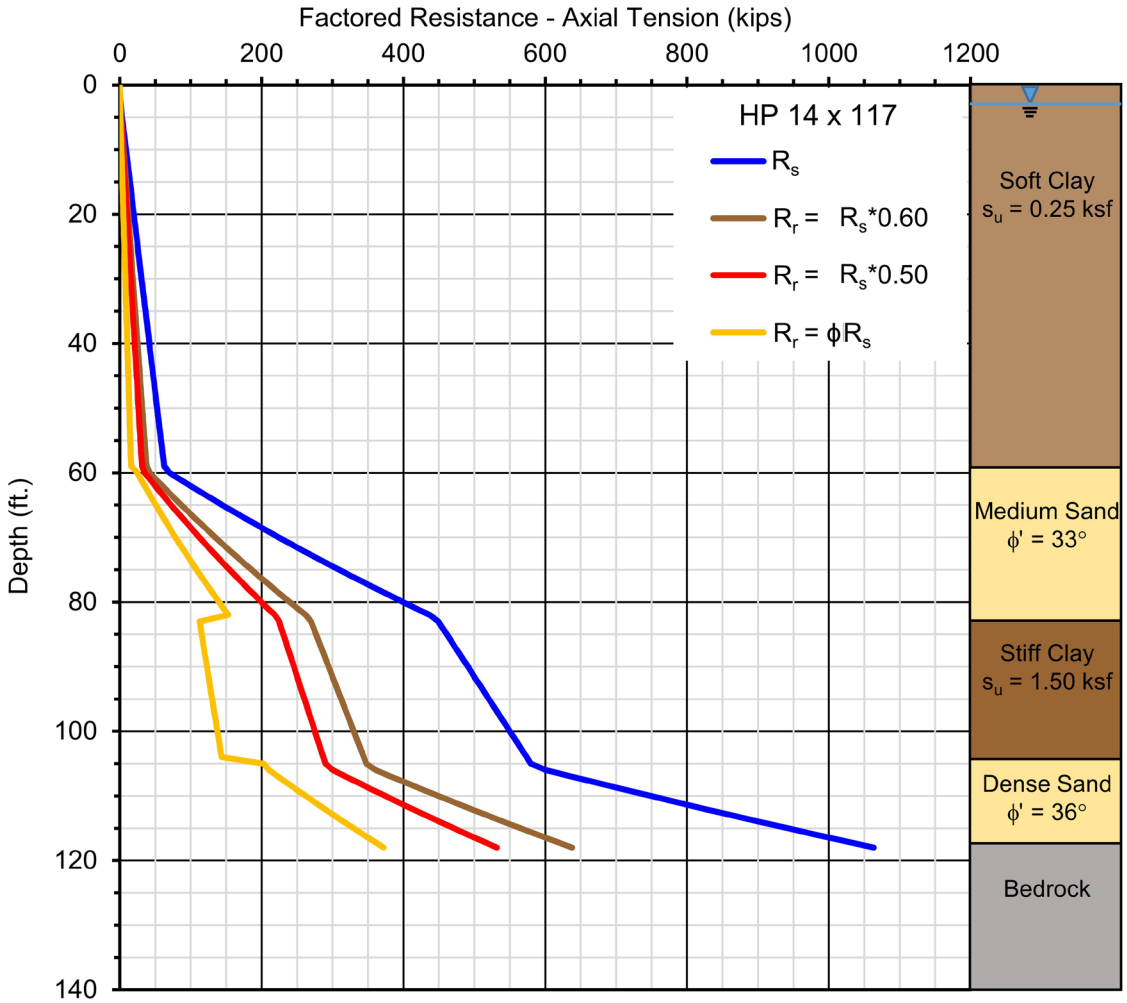

Figure 3-7 Nominal and factored resistances for axial tension loads.

3.5 OTHER CONSIDERATIONS

In many instances, several driven pile alternatives may be technically feasible for satisfying the project load and deformation requirements. Other considerations such as constructability, noise, vibrations, effects on nearby structures and utilities, durability, long term maintenance, and other considerations should also be evaluated to determine the most appropriate driven pile selection.

3.5.1 Constructability

Constructability should also be assessed during the design stage with any construction considerations factored into the pile selection and final design. Drivability is a key component of constructability and must be evaluated. The chosen pile section must be capable of being installed to the specified minimum penetration depth dictated by scour, extreme event or deformation considerations. The design and drivability assessment should consider the presence of any hard layers that must be penetrated to meet design requirements that could necessitate use of pile penetration aids such as predrilling or jetting. Constructability considerations and drivability analysis should also consider potential densification effects of soils constrained within cofferdams or soils that may densify from driving large pile groups. Similarly, the influence of soil heave on adjacent structures, utilities, or other piles from driving displacement piles in a cohesive deposit should be considered along with the need for pile penetration aids to mitigate the heave potential, if present. The cost of a driven pile foundation will increase on projects with limitations or restrictions on head room, work space, and construction access. Similarly, environmental restrictions on vibrations, noise, work hours, marine mammals, and fish will likely increase foundation costs.

3.5.2 Consideration of Pile Driving Noise

Driven piles are installed by impact hammers. Noise levels associated with typical impact pile driving activities depend upon the hammer and pile type used. Noise from impact pile driving operations typically ranges from around 80 to 135 dBa. If local ordinances dictate allowable noise levels at or below this level, some driving equipment may not meet these requirements. Manufacturers of a few diesel and hydraulic hammers can provide optional noise suppression devices that may reduce the pile driving generated noise by about 10 dBa. Independently manufactured devices are also available. Additional information on noise suppression equipment is presented in Chapter 15.

In noise sensitive areas, the foundation designer should review any noise ordinances to determine if pile driving noise suppression devices would be necessary and if so, the impact this may have on the contractor’s equipment selection and productivity. If limits on work hours, pile equipment type, or noise suppression equipment are required, costs associated with these limitations should be considered in the foundation selection process.

3.5.3 Pile Driving Induced Vibrations

Since piles are driven by impact or vibratory hammers, ground vibrations of some magnitude are always induced into the surrounding soils during pile installation. In many situations these vibrations do not pose a significant threat or risk to structures. The vibrations created by pile driving depend on the soil type, pile type and section, pile hammer, installation techniques, penetration resistance, pile toe penetration depth, and distance from the pile. Therefore, the distance from a pile driving operation where these variables combine to cause vibration levels that are a threat to structures, facility operations, or utilities varies.

The ground vibration level where vibration induced soil densification and settlement or structural damage from direct vibrations may occur depends upon the vibration magnitude, frequency, and number of cycles as well as the type and condition of the existing structure or facility. In addition, nearby structures may house sensitive equipment whose operation may be adversely affected by pile driving vibrations. Establishing appropriate vibration limits for sensitive equipment can be difficult, which makes identifying and addressing such installations all the more important.

For pile driving projects with structures, facilities, or utilities within a zone potentially affected by pile driving vibrations, careful evaluation of the pile driving procedures and/or monitoring of ground vibrations during pile installations should be performed by personnel with vibration monitoring and mitigation experience. Even if a designer is satisfied the pile driving vibrations pose no threat to structures or equipment, advance notification to neighbors of pile driving activities, pre-construction condition surveys, and vibration monitoring plans promotes a “good neighbor” policy which can reduce the risk of claims.

Potential damage to nearby structures can result from two mechanisms:

1. Vibrations induced soil densification and settlement.

2. The effects of vibrations on the structure itself.

Lacy and Gould (1985) found that vibratory induced soil densification settlements and resulting structural damage can occur at ground surface peak particle velocities much less than 2 inches per second and that soil gradation is an important factor in this phenomenon. They reported that significant vibration induced settlements occurred at some sites with peak particle velocities measured on the ground surface as low as 0.1 to 0.2 inches per second. Sands particularly susceptible to vibratory

densification were late Pleistocene deposits with uniformity coefficients of up to 4 or 5 and relative densities of up to 50 or 55%.

Wiss (1981) reported typically recommended "safe" ground vibration levels for structures between 0.5 and 4 inches per second. In codes, such as NFPA 495 (2013), the maximum allowable particle velocity to prevent the onset or propagation of hairline cracks in plaster or drywall is a function of the vibration frequency. For example, a particle velocity of 1 inch per second at 30 Hz would be below NFPA 495 code limits but would be above code limits if the vibration frequency were 10 Hz.

Bay (2003) summarized relationships between peak particle velocity and the distance from the pile as a function of rated hammer energy. These results were plotted against typical damage thresholds for various types of structures. Charts for Class II and Class III soils were provided and are reproduced in Figure 3-8. Class II soils were defined as competent soils with SPT-N values of 5 to 15 blows per foot. Class III soils are hard soils with SPT N values of 15 to 50 blows per foot. Bay noted that stiff soil crusts near the ground surface can significantly increase the vibration levels from those noted in the charts and that other factors that can influence the vibration levels include nearby deep excavations, rock outcrops, and shallow bedrock. Soil-structure interaction should also be considered in assessing vibration levels and damage potential. Therefore, while informative, these charts should not be used to eliminate vibration monitoring.

If the potential for damaging ground vibrations is high, pile installation techniques should be specified to reduce vibration levels. Specifications could require predrilling or jetting, cutoff trenches, as well as use of a different pile type or use of a specific type of pile hammer. Since predrilling and jetting influence compression, uplift, and lateral pile capacities, a determination of probable vibration levels and remediation measures should be evaluated in the design stage. A case history illustrating how changing pile installation procedures reduced vibratory induced soil densification and off-site settlement damage was reported by Lukas and Gill (1992).

NCHRP Project 20-5, Dynamic Effects of Pile Installations on Adjacent Structures, by Woods (1997), provides a synthesis of pile driving induced vibrations and typical mitigation practices. This synthesis noted that vibration problem management is the key to minimizing vibration damage, delays and claims. Two important elements in vibration management are a vibration specification with limits on the frequency dependent maximum peak particle velocity and a predriving survey of surrounding structures. An example vibration specification that details the requirements of a preconstruction survey as well as particle velocity controls is included in the NCHRP

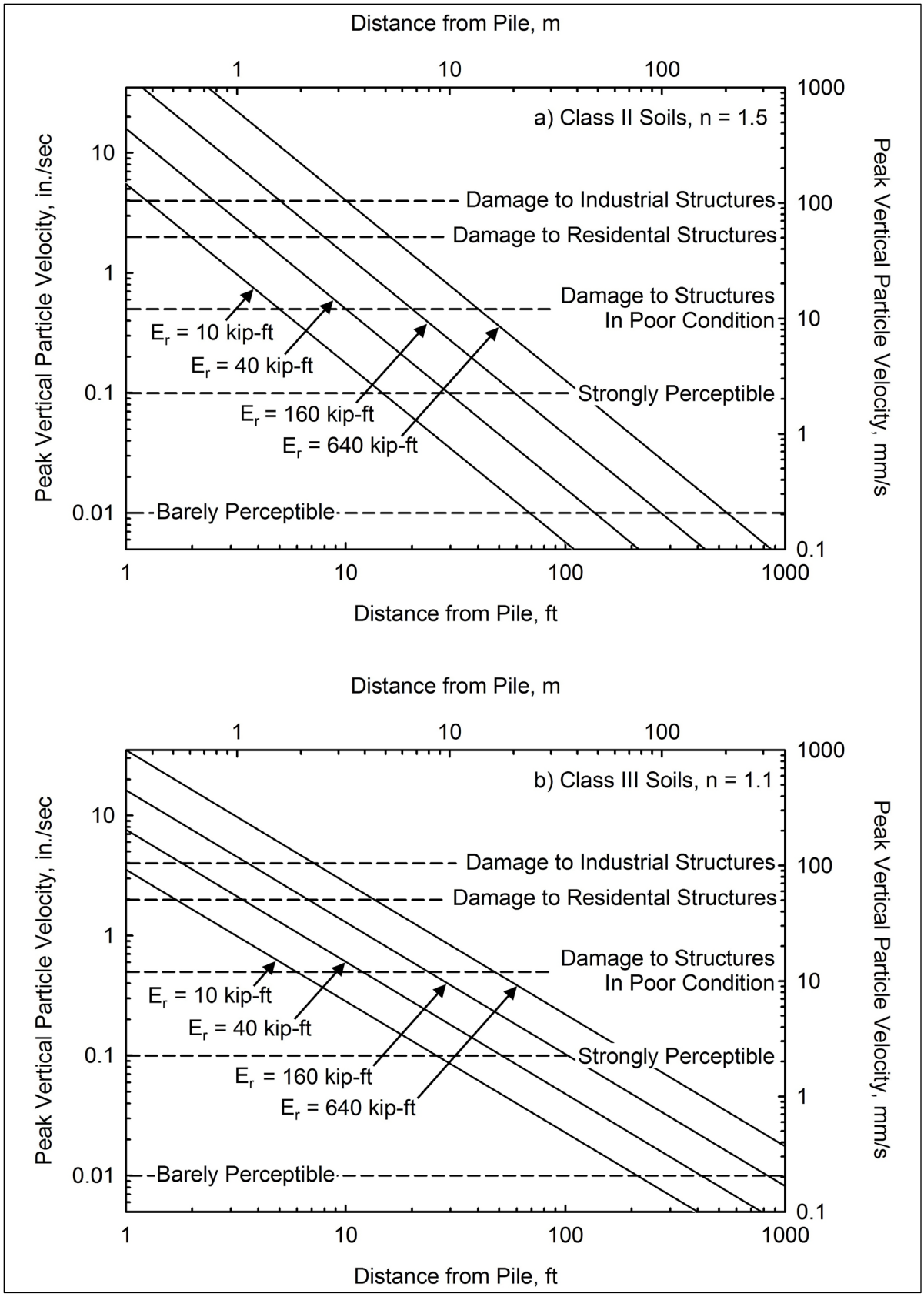

Figure 3-8 Predicted vibration levels for class II and class III soils (after Bay 2003).

synthesis. The predriving survey needs to document conditions within the potential effected area. Woods reported that vibration damage is not likely to occur at a distance from a driven pile of 50 feet for piles 50 feet long or less, or at a distance greater than one pile length away from driving for piles longer than 50 feet.

Piles with low impedances, EA/C, tend to transmit the hammer energy to the soils along the pile shaft and thus increase ground vibrations, whereas piles with higher impedances tend to more effectively transmit the hammer energy to the pile toe resulting in lower ground vibration levels (Woods 1997; Massarsch and Fellenius 2008). Hence, selection of a stiffer pile section at sites where vibrations are a concern may help reduce vibration problems.

Massarsch and Fellenius (2014) describe ground vibration effects on soil settlement. In loose sands and silts, vibratory densification beneath adjacent structures can occur, therefore causing deformation of the adjacent foundation. As discussed, pile dimensions influence the area affected by ground vibrations. Furthermore they propose that settlement occurs in an inverted 2(V):1(H) triangular region around the pile as depicted in Figure 3-9. Maximum settlement adjacent to the pile and average settlement within a distance of 3*b* + *D*/2 from the pile are estimated using Equations 3-1 and 3-2. A compression factor is applied based on in-situ soil density and vibration magnitude, as shown in Table 3-4 for sands.

Maximum settlement $$S_{max} = \alpha\,(D + 6b)$$ Eq. 3-1

Average settlement $$S_{avg} = \frac{\alpha\,(D+3b)}{3}$$ Eq. 3-2

Where:

- α = compression factor.
- D = pile embedded length (feet).
- b = pile diameter or width (feet).

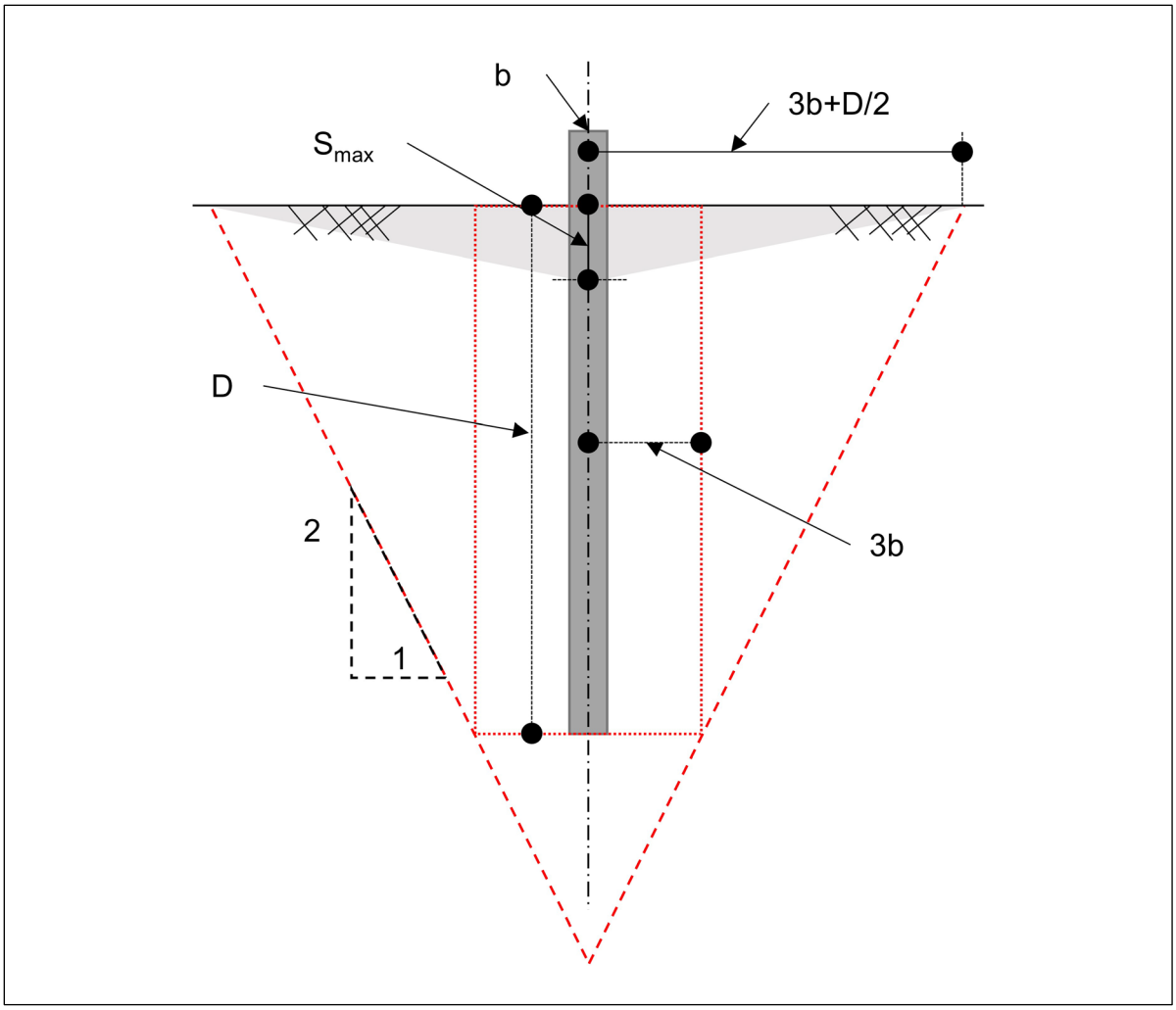

Figure 3-9 Settlement area and magnitude around a pile in homogeneous sand deposit (after Massarsch and Fellenius 2014).

Table 3-4 Compression Factor, *α*, for Sand Based on Soil Density and Level of Driving Energy (after Massarsch and Fellenius 2014)

Soil Density	Low Ground Vibration	Medium Ground Vibration	High Ground Vibration
Very Loose	0.02	0.03	0.04
Loose	0.01	0.02	0.03
Medium	0.005	0.01	0.02
Dense	0.00	0.005	0.01
Very Dense	0.00	0.00	0.005

The Pile Driving Contractors Association (2015) while working with The Citadel and WPC has a pile driving vibration database with 23 case histories and over 1800 individual pile-ground vibration measurements. Data has been submitted from a number of design and testing firms, with the goal of allowing contractors and designers to make reasonable assessments of the potential vibration effects from driven pile installations. This database should only be used for general guidance as differing site conditions, construction equipment and installation techniques may not be applicable in each unique situation.

3.5.4 Condition Surveys and Vibration Monitoring of Adjacent Facilities

Many projects are built in populated urban areas where existing condition surveys and vibration monitoring programs are warranted. Prior to starting construction, the internal and external condition of structures potentially affected by the construction activity should be documented using photos and videos. The condition of any existing cracks should be documented and crack monitors installed as needed. This documentation provides a preconstruction baseline of the existing conditions that can later be compared to any damage claims should they occur. Following construction, a similar survey should be performed with photos to document the change, if any, in the existing structures. Condition surveys should be performed using film rather than digital photography should damage claims be made.

The distance that should be surveyed on pile driving projects depends on the soil conditions, the pile type, the pile driving equipment, and the pile driving procedures. Many states have adopted a survey distance based on the rated pile hammer energy. Others agencies have policies based solely on the distance away from the pile driving operation. For most routine cases, a preconstruction and post construction survey along with a vibration monitoring program that documents conditions within 200 feet of the pile driving operation should be sufficient. However, this distance may need to be extended to as much as 500 feet for older structures, structures or utilities in poor condition, or highly vibration sensitive equipment.

3.5.5 Durability Considerations

The durability of a pile foundation can be defined by how long it performs satisfactorily, without unforeseen high maintenance costs relative to the foundations expected service life. AASHTO has mandated a design life of 75 years for new ordinary bridges. Complex major bridge structures may have a design life of 100 years. Hence, structure foundation durability over the design life is an important consideration. In general, driven piles have proved very durable in most

environments. However, environments exist for driven piles as well as any other deep foundation type where durability is an important design consideration to satisfy design life requirements.

In 2013, a pier supported on H-piles at the Leo Frigo bridge carrying I-43 over the Fox River in Green Bay, WI settled 2 feet during the night. The sudden settlement of the 32 year old structure resulted from severe corrosion and the resultant buckling and shearing of the foundation H-piles. Figure 3-10 illustrates the corrosion of the foundation piles uncovered at the pier location during the post event investigation. In the final investigation report on the event by Michael Baker, Jr. Inc., (2015) the corrosion and deterioration was attributed to a highly unusual set of occurrences at the pier location. Fill materials included the presence of porous, industrial fly ash in contact with the H-piles. The porous material permitted oxygen access to the piles. Also the fill material contained high amounts of sulfates and the water and soil surrounding the pile section contained high concentrations of chlorides. This unusual set of conditions created a highly aggressive environment for steel piles.

Figure 3-10 Corrosion and resulting buckling of foundation pile (courtesy Wisconsin Department of Transportation).

Gu at al. (2015) reported on the results of a corrosion study performed to evaluate the reuse of 34 year old H-pile foundations. The original project was for the Girard Avenue Bridge in Philadelphia, PA and piles were installed through a cinder ash fill located at the water table in close proximity to a tidal river. This study found that the piles had a 12% loss in section over their 34 year old life. This site specific corrosion rate was then used to assess future section loss over the rehabilitated structure life for both existing piles that were reused as well as new piles. The section loss rate was also used to evaluate the nominal pile resistance under axial and lateral loading. It was also noted that site specific corrosion rate of 0.0015 inches/year was less than published rates. Section 6.13 provides details on steel pile protection measures and design considerations for durability in aggressive environments.

Figure 3-11 Concrete pile damage from corrosion effects on concrete pile reinforcement (courtesy of Moser 2011).

Figure 3-12 Concrete surface abrasion and deterioration in tidal zone (courtesy of Moser 2011).

The durability of concrete piles should also be evaluated during design so that the foundation satisfies the target design life. Concrete piles can deteriorate due to chloride intrusion and resulting reinforcement and prestressing strand corrosion. Moser et al. (2011) noted the three main factors contributing to concrete deterioration in coastal structures include the high chloride content in seawater, the potential for high temperature and relative humidity, and the cyclic wetting due to tidal and splash action. Figure 3-11 shows two concrete piles with severe damage and cracking due to corrosion of the reinforcement steel. Abrasion of concrete piles in intertidal zone, as depicted in Figure 3-12, can also accelerate deterioration. Concrete abrasion can also occur at the mudline due to littoral drift of bottom sediments. Moser (2011) reported that some prestressed concrete piles in coastal Georgia have severe corrosion damage in the splash zone after less than 25 years of service which is well under the target design life.

Holland et al (2014) summarized multiple deterioration mechanisms affecting the concrete piles on a 38 year old I-95 bridge over Tuttle Creek. Their forensic investigation determined damage occurred from chloride-induced corrosion, severe deterioration of concrete from sulfate attack, and coarse aggregate attack from Cliona boring sponges.

To increase concrete pile durability in aggressive environments, high performance concrete mixes are being design and studied. The dense, impermeable, concrete that results with high performance concrete mixes should better protect reinforcement against the ingress of chlorides, sulfates, and seawater, as well as resist freeze/thaw and chemical attacks.

Timber piles also have durability considerations. Bigelow et al. (2007) evaluated several timber pile supported bridges in Iowa as part of a structure life assessment. Figure 3-13 illustrates the durability issues they documented as a result of a break down in the preservative barrier including a) mechanical damage, b) abrasion or debris damage, c) fire damage, and d) weathering. One of the most common durability issues occurred on piles in the stream channel as abrasion or debris damage from floating debris and/or ice. The study found that creosote treated timber piles up and away from the stream channel lased 60 to 70 or more years and those in the stream channel have a life expectancy of 40 to 50 years.

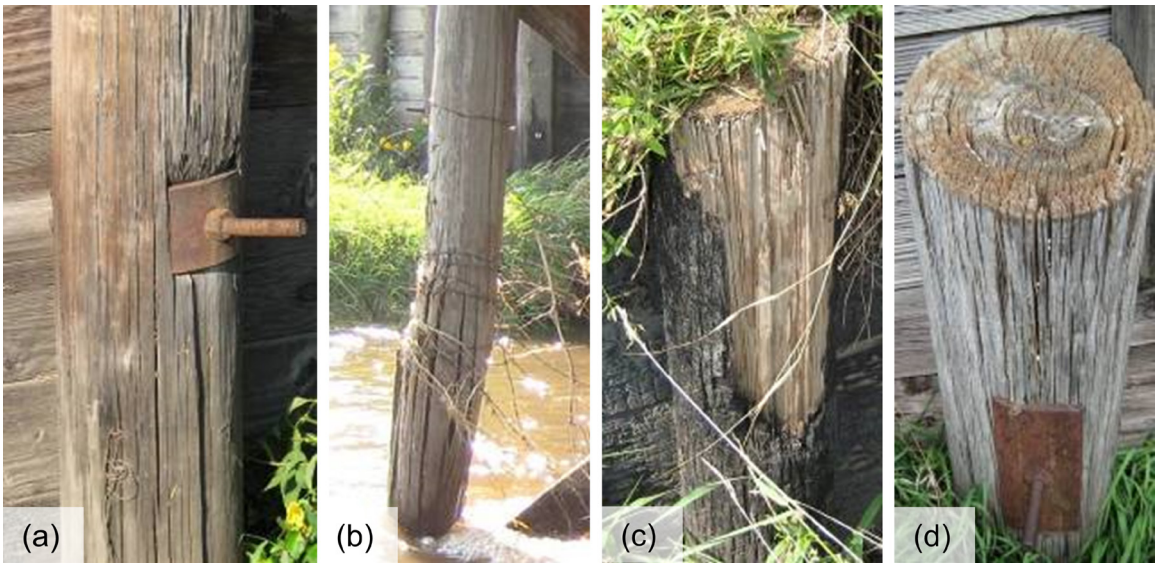

Figure 3-13 Examples of timber pile deterioration
(courtesy Bridge Engineering Center at Iowa State University).

3.6 UNANTICIPATED OCCURRENCES

The long term performance of a foundation is generally assessed by its total and differential settlement within and between substructure locations. Unanticipated occurrences can result from outside influences, such as a fill stockpile can affect a foundation's long term performance as shown in Figure 3-14 and Figure 3-15. Construction of a new pile foundation can also result in unanticipated outside influences as described in Section 3.6.2.

3.6.1 Fill Stockpile

During the summer of 2104, a portion of the 40 year old elevated section of I-495 near Wilmington, Delaware was noticed to have substantially tilted over a relatively short time period. The tops of some of the 50 feet tall columns supporting the elevated roadway were noted to be almost 2 feet out of alignment from their base as shown in Figure 3-14. Engineers determined a roughly 50,000 ton stockpile of fill material had been placed near the four affected piers. The weight of this fill had caused lateral movement of soil beneath the bridge, deformed the H-piles supporting the piers, and cracked the pile caps as illustrated in Figure 3-15. This caused four of the piers supporting the elevated roadway to tilt. In the above case, the structure was performing as expected based on its previous inspection report until being affected by the stockpile of fill material.

Figure 3-14 Tilting columns adjacent to stockpile (courtesy DelDOT).

Figure 3-15 Cracked pile cap from lateral soil movements (courtesy DelDOT).

3.6.2 Adjacent Construction

In 2015, the five span bridge carrying I-65 over Wildcat Creek was being widened from two to three travel lanes. Due to scour considerations, the new construction was supported on a driven H-pile foundation rather than spread footings. Shortly after production pile installation, the pier supported by the adjacent spread footing foundation settled as much as 10 inches and rotated 7 inches, ENR (2015). This resulted in closing the I-65 bridge to stabilize the pier. The movements were attributed to the release of artesian pressures and sand beneath the spread footing supported pier foundation.

REFERENCES

Abu-Hejleh, N., Kramer, W.M., Mohamed, K., Long, J.H., and Zaheer, M.A. (2013). Implementation of AASHTO LRFD Design Specifications for Driven Piles, FHWA-RC-13-001. U.S. Dept. of Transportation, Federal Highway Administration, 71 p.

Arneson, L.A., Zevenbergen, L.W., Lagasse, P.F., and Clopper, P.E. (2012). Evaluating Scour at Bridges, Fifth Edition, FHWA-HIF-12-003, Hydraulic Engineering Circular (HEC) No. 18. U.S. Dept. of Transportation, Federal Highway Administration, 340 p.

Bay, J.A. (2003). A Summary of the Research on Pile Driving Vibrations. Proceedings of the Pile Driving Contractor's Association 7th Annual Winter Roundtable, Atlanta, 13 p.

Bigelow, J., Clausen, C., Lebow, S., Greimann, L. (2007). Field Evaluation of Timber Preservation Treatments for Highway Applications, CRTE 06-252. Iowa Highway Research Board, Iowa Dept. of Transportation, Ames, IA, 104 p.

Bowles, J.E. (1977). Foundation Analysis and Design. Second Edition, McGraw-Hill Book Company, Blacklick, OH, 750 p.

Brown, D.A., Dapp, S.D., Thompson, W.R., and Lazarte, C.A. (2007). Design and Construction of Continuous Flight Auger (CFA) Piles. FHWA-HIF-07-03, Geotechnical Engineering Circular (GEC) No.08. U.S. Dept. of Transportation, Federal Highway Administration, 289 p.

Brown, D. A., Turner, J.P. and Castelli R.J. (2010). Drilled Shafts: Construction Procedures and LRFD Design Methods, FHWA-NHI-10-016, Geotechnical Engineering Circular (GEC) No. 10. U.S. Dept. of Transportation, Federal Highway Administration, 970 p.

Elias, V., Welsh, J.P., Warren, J., Lukas, R.G., Collin J.G., and Berg, R.R. (2006). Ground Improvement Methods Volumes I and II, FHWA-NHI-06-019 and FHWA NHI-06-020. National Highway Institute, Federal Highway Administration, U.S. Department of Transportation, Washington D.C.

Engineering News Record (2015). Pile Driving and Poor Soils Prompt Indiana I-65 Shutdown.

Gu, L., McInnes, S.E., Fenton, J.H., Welsh, S.J., and Mouradian, A.G. (2015). Corrosion Study of Existing Steel H-pile Installed Through Cinder-Ash Fill. Proceeding of the 2015 International Foundations Congress and Equipment Expo, San Antonio, TX, pp. 961-972.

Holland, R.B., Kurtis, K.E., Moser, R.D. Kahn, L.F., Aguayo, F. and Singh, P.M. (2014). Multiple Deterioration Mechanisms in Coastal Concrete Piles, A Forensic Case Study, Concrete International, Vol. 36, No. 7, pp. 45-52.

Kimmerling, R.E. (2002). Shallow Foundations, FHWA-IF-02-054, Geotechnical Engineering Circular (GEC) No. 6. U.S. Dept. of Transportation, Federal Highway Administration, Washington, D.C., 310 p.

Komerka, V. (2015). Foundation Support Cost – Applications to Driven-Pile Design. Proceedings of the 2015 International Foundations Conference and Equipment Exposition, San Antonio, TX, pp. 990-1005.

Lacy H.S. and Gould, J.P. (1985). Settlement from Pile Driving in Sands, Vibration Problems in Geotechnical Engineering. American Society of Civil Engineers (ASCE), Special Technical Publication, New York, NY, pp. 152-173.

Lukas, R.G. and Gill, S.A. (1992). Ground Movement from Piling Vibrations. Piling-European Practice and Worldwide Trends, Proceeding of the Conference ICE Telford House, London, pp. 163-169.

Massarsch, K.M, and Fellenius, G.H. (2008). Ground Vibrations Induced by Impact Pile Driving. The Sixth International Conference on Case Histories in Geotechnical Engineering, Arlington, VA, 38 p.

Massarsch, K.R., and Fellenius, B.H. (2014). Ground Vibrations from Pile and Sheet Pile Driving. Part 1 Building Damage. Proceedings of the DFI-EFFC International Conference on Piling and Deep Foundations, Stockholm, Sweden, pp. 131-139.

Michael Baker, Jr., Inc. (2015). Investigation Report, I-43 Leo Frigo Memorial Bridge, Volume I, 181 p.

Moser, R., Holland, B. Kahn, L., Singh, P., and Kurtis, K. (2011). Durability of Precast Prestressed Concrete Piles in Marine Environment: Reinforcement Corrosion and Mitigation Part 1. GDOT Research Project No. 07-30. Office of Materials and Research Georgia Department of Transportation, 243 p.

Munfakh, G., Arman, A., Collin, J.G., Hung, J.C.-J., and Brouillette, R.P. (2001). Shallow Foundations Reference Manual, FHWA-NHI-01-023. National Highway Institute, Federal Highway Administration, Washington, D.C., 222 p.

National Fire Protection Association, (NFPA). (2013). Explosive Materials Code (495) - Chapter 11, Ground Vibration, Air Overpressure, Flyrock, and Gases, National Fire Protection Association, Quincy, MA, 58 p.

Pile Driving Contractors Association (PDCA). (2015). National Pile Driving Noise and Vibration Database, www.piledrivers.org.

Rollins, K.M., and Brown, D.A., (2011). Design Guidelines for Increasing the Lateral Resistance of Highway-Bridge Pile Foundations by Improving Weak Soils. NCHRP Report No. 697. Washington, D.C., 98 p.

Sabatini, P.J., Tanyu, B., Armour., P., Groneck, P., and Keeley, J. (2005). Micropile Design and Construction, FHWA-NHI-05-039. National Highway Institute, U.S. Dept. of Transportation, Federal Highway Administration, Washington, D.C, 436 p.

Vesic, A.S. (1977). Design of Pile Foundation, Synthesis of Highway Practice No. 42. National Cooperative Highway Research Program, Transportation Research Board, National Research Council, Washington, D.C., 68 p.

Wiss, J.F. (1981). Construction Vibrations: State-of-the-Art. American Society of Civil Engineers (ASCE), Journal of the Geotechnical Engineering Division, , Vol. 107, No. 2, pp. 167-181.

Woods, R.D. (1997). Dynamic Effects of Pile Installations on Adjacent Structures. NCHRP Synthesis 253, National Cooperative Highway Research Program, Transportation Research Board, Washington, D.C., 96 p.

CHAPTER 4

SITE CHARACTERIZATION

4.1 INTRODUCTION

The design of a structure's foundation requires adequate knowledge of the subsurface conditions at the construction site. The absence of a thorough foundation study or adequate geotechnical data often leads to (1) a foundation system with a large safety margin which is generally a more expensive foundation and in some cases one that may be difficult to construct, or to (2) an unsafe foundation, or to (3) construction disputes and claims.

Site characterization consists of a subsurface exploration program and subsequent testing to determine geomaterial parameters for foundation design. This information is also used in construction feasibility and planning decisions. For reliability based design, reducing uncertainty with respect to geomaterial properties may lead to more economical foundations, therefore a carefully implemented soil exploration and testing program is beneficial. This chapter will focus on site characterization based on the assumption that a driven pile deep foundation has been selected for design.

An experienced geotechnical engineer is of great value to the design team and assists with planning the subsurface exploration, ordering field and laboratory tests of geomaterials, determining the design subsurface profile, and recommending technically feasible and appropriate foundation systems. Subsurface exploration and/or laboratory testing results are often relayed in technical documents from specialty firms directly to the geotechnical engineer who then compiles this information into a geotechnical design report. This document is used by multiple engineering disciplines during the foundation design and construction phases. In some agencies, design memoranda and transmittals are used instead of geotechnical reports. In these situations, regular communication between engineering disciplines is essential for effective foundation design and construction.

Guidance on site characterization and the evaluation of geomaterial properties for geotechnical design is provided in several FHWA reference documents including FHWA-NHI-01-031, Mayne et al. (2002); GEC-5, Sabatini et al. (2002); and FHWA-NHI-06-088, Samtani and Nowarzki (2006). Laboratory and in-situ testing are also

integral to a site characterization program. These topics will be discussed further in Chapter 5 of this manual.

4.2 SITE CHARACTERIZATION PROGRAM

Site characterization encompasses the gathering and reporting of site conditions required to safely and economically design foundations and other earth structures, as well as to address constructability considerations. The information necessary to adequately characterize the site will vary depending upon the site geologic conditions, foundation types being considered for the structure, the structure performance requirements, the acceptable risk level for the structure, constructability, as well as owner preferences.

The site exploration should be carefully organized, and consists of three main phases. These are (1) planning the exploration program and data collection (office work), (2) completing a field reconnaissance survey, and (3) performing a detailed subsurface exploration program (boring, sampling, and in-situ testing). Each phase should be planned so that a maximum amount of information can be obtained at a minimum cost. Each phase also adds to, or supplements, the information from the previous phase. Table 4-1 lists the purpose of each exploration phase.

Depending upon the project size and contract delivery method, a single phase or staged subsurface exploration program may be appropriate. A single phase program is common for small project and staged subsurface exploration programs are often used for large projects. Staged programs are common for design-build projects where the owner performs a preliminary subsurface exploration program and the design-build team performs the final subsurface exploration program.

4.2.1 Data Collection

The purpose of this phase is to obtain information about the proposed structure and general information on subsurface conditions. The structural information can be obtained from studying the preliminary structure plan prepared by the bridge design office and by meeting with the structural designer. Approach embankment preliminary design and performance requirements can be obtained from the roadway office. General information about the subsurface conditions can be obtained from a variety of sources, some of which are listed in Table 4-2. Additional sources of historical data are listed in GEC-5, Sabatini et al. (2002). The data collection phase

Table 4-1 Subsurface Exploration Phases

Phase	Activity	Purpose	Remarks
1.	Planning the Exploration (Office Work).	A. Obtain structure information. Determine: 1. Type of structure. 2. Preliminary location of piers and abutments. 3. Loading and special design events. 4. Allowable differential settlement, lateral deformations, and other performance criteria. 5. Any special features and requirements. B. Obtain drilling records for nearby structures and from local well drillers. C. Perform literature reviews including maintenance records, pile driving records, scour history, etc. Obtain overall picture of subsurface conditions in the area.	See Table 4-2 for sources of information.
2.	Field Reconnaissance Survey.	Verify information gained from the office phase and plan the detailed subsurface exploration. A. Observe, confirm and collect information regarding: 1. Topographic, geologic, and hydrologic features. 2. New and old construction in the area including utilities. Performance of existing structures. 3. Drilling equipment required, cost, and access for the equipment. B. If appropriate, conduct geophysical testing to obtain preliminary subsurface information.	Field reconnaissance is often conducted by a multi-disciplined team.
3.	Detailed Subsurface Exploration.	Develop a preliminary boring plan based on phases 1 and 2. Conduct a preliminary evaluation for viable foundation systems including ground improvement. Determine subsurface requirements for all of the viable foundation systems. The boring plan should be modified if needed as the borings are performed and detailed subsurface information is obtained. The subsurface exploration should provide the following: 1. Depth and thickness of strata (subsurface profile). 2. In-situ field tests to determine soil design parameters. 3. Samples to determine soil and rock design parameters. 4. Groundwater levels including perched, regional, and any artesian conditions.	For major structures, the pilot boring program is often supplemented with control and verification boring programs.

Table 4-2 Sources of Subsurface Information and Use

Source	Use
Preliminary structure plans prepared by the bridge design office.	Determine: 1. Type of structure. 2. Preliminary locations of piers and abutments. 3. Footing loads and special design events. 4. Allowable differential settlement, lateral deformations, and performance criteria. 5. Any special features and requirements.
Geotechnical databases.	Nearby soil boring logs, laboratory test results, and in-situ test results.
Construction plans and records for nearby structures.	Foundation type, old boring data, construction information including construction problems.
Topographic maps prepared by the United States Coast and Geodetic Survey (USC and GS), United States Geological Survey (USGS) and State Geology survey.	Existing physical features shown; find landform boundaries and determine access for exploration equipment. Maps from different dates can be used to determine topographic changes over time.
County agricultural soil survey maps and reports prepared by the United States Department of Agriculture (USDA).	Boundaries of landforms shown; appraisal of general shallow subsurface conditions.
Aerial photos prepared by the United States Geological Survey (USGS) or satellite imagery such as Google Earth.	Detailed physical relief shown; gives indication of major problems such as old landslide scars, fault scarps, buried meander channels, sinkholes, or scour; provides basis for field reconnaissance.
Well drilling record or water supply bulletins from state geology or water resources department.	Old well records or borings with general soils data shown; estimate required depth of explorations and preliminary cost of foundations.
Geologic maps and Geology bulletins.	Type, depth and orientation of rock formations.

prepares the engineer for the field reconnaissance survey, and identifies possible problems and areas to scrutinize.

4.2.2 Field Reconnaissance Survey

Site visits by the geotechnical engineer and other members of the design team are necessary to properly characterize the site. Field reconnaissance presents an opportunity to locate and record many constructability issues such as site access, headroom restrictions, and other working conditions that may be otherwise overlooked from reviewing site or aerial photos and satellite images. This phase enables the engineer to substantiate the information gained from the office phase and to plan the detailed site exploration program.

The field reconnaissance for a structure foundation exploration includes, but is not limited to:

a. Inspection of nearby structures to determine their performance with the particular foundation type used.

b. Inspection of existing structure footings and stream banks for evidence of scour (for stream crossings) and movement. Large boulders in a stream are often an indication of obstructions which may be encountered in pile installations.

c. Recording of the location, type and depth of existing structures which may be affected by the new structure construction.

d. Visual examination of terrain for evidence of landslides.

e. Location of trees and other vegetation, as well as surface water.

f. Relating site conditions to proposed boring operations. This includes recording the locations of both overhead and below ground utilities, site access, private property restrictions, water depth and access points for marine borings, and other access restrictions or obstructions.

g. Recording of any feature or constraint which may impact the constructability of potential foundation systems.

Figure 4-1 contains an example of a field reconnaissance form modified from the AASHTO Foundation Investigation Manual (1978) for recording data pertinent to a site. At conclusion of the data collection and field reconnaissance phases, the

Bridge Foundation Investigation
Field Reconnaissance Report
_____ Department of Transportation

Project No: _____ County _____ Sta. No. _____

Reported By: _____ Date _____

1. Staking of Line
   - Well Staked
   - Poorly Staked (We can work)
   - Request Division to Restake

2. Bench Marks
In Place: Yes _____ No _____
Distance from bridge - (ft) _____

3. Property Owners
Granted Permission: Yes _____ No _____
Remarks on Back

4. Utilities
Will Drillers Encounter Underground or
Overhead Utilities? Yes _____ No _____
Maybe _____ At Which Holes? _____
What Type? _____
Who to See for Definite Location _____
_____

5. Geologic Formation

6. Surface Soils
Sand _____ Clay _____ Sandy Clay _____
Muck _____ Silt _____ Other _____

7. General Site Description
Topography
Level _____ Rolling _____ Hillside_____
Valley _____ Swamp _____ Gullied_____
Groundcover
Cleared _____ Farmed _____ Buildings _____
Heavy Woods _____ Light Woods_____
Other _____
Remarks on Back _____

8. Bridge Site
   - Replacing _____
   - Widening _____
   - Relocation _____

Check Appropriate Equipment

Truck Mounted Drill Rig	Failing 1500
Track Mounted Drill Rig	Skid Rig
Truck Mounted Skid Rig	
Rock Coring Rig	
Wash Boring Equipment	
Water Wagon	
Pump	Hose _____ (ft)

8. Bridge Site – Continued
   - Cut Section - (ft) _____
   - Fill Section - (ft) _____
   - If Stream Crossing:

Will Pontoons Be Necessary? _____
Can Pontoons Be Placed in Water Easily?
_____
Can Cable Be Stretched Across Stream?
How Long?_____
Is Outboard Motorboat Necessary? _____
Current:
Swift _____ Moderate _____ Slow_____
Describe Streambanks scour.
If Present Bridge Nearby:
Type of Foundation _____
Any Problems Evident in Old Bridge Including
Scour _____
(describe on back)
Is Water Nearby for Wet Drilling - (ft) _____
Are Abandoned Foundations in Proposed
Alignment? _____

9. Ground Water Table
   - Close to Surface - (ft) _____
   - Nearby Wells - Depth - (ft) _____
   - Intermediate Depth - (ft)_____
   - Artesian head - (ft) _____

10. Rock
   - Boulders Over Area? Yes _____ No _____
   - Definite Outcrop? Yes _____ No _____
   - (show sketch on back)
   - What kind? _____

11. Special Equipment Necessary

12. Remarks on Access
(Describe any Problems on Access)

13. Debris and Sanitary Dumps
   - Stations _____
   - Remarks_____

_____
_____

Reference: Modified from 1978 AASHTO Foundation Investigation Manual

Figure 4-1 Typical field reconnaissance form.

engineer should have in mind geotechnical loading requirements, which would therefore dictate the planning of the field exploration program.

4.2.3 Detailed Field Exploration

The purpose of any field exploration program is to obtain representative information on subsurface conditions, to recover disturbed and undisturbed soil samples, to perform in-situ testing, and to determine groundwater levels. This information provides factual basis upon which all subsequent steps in the pile design and construction process are founded. Its quality and completeness are of paramount importance. Each step in the process directly or indirectly relies on this data. It is assumed that a preference to a driven pile foundation is given. Therefore, the field exploration plan will focus on items related to the design of driven pile foundations.

The first step in this phase is to prepare a preliminary boring, sampling, and in-situ testing plan. For major structures, pilot borings are usually performed at a few select locations during the preliminary planning stage. These pilot borings establish a preliminary subsurface profile and thus identify key soil strata for testing and analysis in subsequent design stage borings. Then, during the design stage of major structures, geophysical surveys and a two phase boring program are recommended. First, control borings are performed at key locations identified in the preliminary subsurface profile to determine what, if any, adjustments are appropriate in the design stage exploration program. Following analysis of the control boring data, verification borings are then performed to fill in the gaps in the design stage exploration program.

A preliminary structural design plan should also be established at this point such that borings are properly located with respect to structural or earthen elements. Geophysical surveys and in-situ testing are included in this category. Information on developing a site exploration program may be found in Sabatini et al. (2002).

4.2.3.1 Geophysical Surveys

Geophysical surveys aide in subsurface characterization over a wide area, and supplement borings and other invasive tests. Primarily, seismic and electrical methods are used to measure depth to groundwater and bedrock and to resolve intermediate soil strata thickness. These methods may identify and locate subsurface anomalies requiring further evaluation by soil borings or in-situ tests. Geophysical surveys may also locate voids, debris or buried objects as well as measure divisions in soil stiffness.

Seismic surface wave methods involve using an applied impact or simply ambient earthborn noise (traffic, wind, microtremors, etc.) to produce surface waves or vibrations that travel through the ground and reflect off changes in subsurface materials. These reflected waves are generally measured with geophones located on the surface. The collected data can be analyzed to compute soil stiffness, allowing the bedrock depth, groundwater depth, and other soil strata to be located. Additional details on seismic surface wave methods can be found in Wightman et al. (2003), Sirles (2006), Rosenblad and Li (2009), and Sirles et al. (2009).

Ground penetrating radar is a common geophysical option and is useful to detect near surface voids in the 20 to 30 feet depth range, buried objects, and to locate the water table. However, this technique decreases in effectiveness with depth, and is not effective in saturated clayey soils.

Electrical test methods employ electrical currents to measure resistively which may be correlated to locate soil strata changes, as well as to detect voids or buried objects. DC resistivity testing does produce soil resistivity results below the groundwater table, as this medium conducts electrical current, Lucius et al. (2007). Results from this test can be modeled to show coarse versus fine grained material, as well as the groundwater table location, and bedrock.

It should be noted that geophysical surveys are often performed in the preliminary site exploration phase to provide a larger sense of site geology, and should further model soil stratigraphy. They should and always be performed in combination with direct exploration methods such as soil borings or in-situ testing.

4.2.3.2 Depth, Spacing, and Frequency of Boring & In-Situ Tests

The cost of a subsurface exploration program is comparatively small in relation to the foundation cost. For example, the cost of one 2.4 inch diameter boring is less than the cost of one 12 inch diameter pile. However, in the absence of adequate boring data, the design engineer must rely on extremely conservative designs with high safety margins. At the same time, the designer assumes enormous risk and uncertainty during the project's construction.

The number of borings required, their spacing, and sampling intervals depend on the uniformity of soil strata and loading conditions. Erratic subsurface conditions require closely spaced borings while more uniform soil profiles may require less frequent exploration. Structures sensitive to settlements or subjected to heavy loads require more detailed subsurface knowledge, and in this case, borings should be closely

spaced. Minimum guidelines for depth and quantity of borings for given structures are provided by Sabatini et al. (2002) and AASHTO (2014). For deep foundations, Table 4-3 provides minimum quantity guidelines.

Table 4-3 Minimum Number of Exploration Points per Substructure (modified from Sabatini et al. 2002)

Pier or Abutment Width, *W*	Exploration Points per Substructure[1]
W ≤ 100-ft	1
W > 100-ft	2

[1]Additional exploration points should be provided if erratic subsurface conditions are encountered.

Minimum exploration depths should be met as well. Exploration points should extend a minimum of 20 feet below the expected pile toe elevation, or at least two times the pile group width. If piles will bear on rock, at least 10 feet of rock coring should be performed. Although these minimum values are provided by AASHTO (2014), additional boring and in-situ testing depths may be required due to site specific geology. Adjustments to the exploration program may be required as information becomes available, and likewise, additional rock coring length may be required if highly variable bedrock is present. Where unsuitable soil strata such as peat, highly organic materials, uncontrolled fills, soft fine grained soils, and loose coarse-grained soils are encountered, structure borings should extend through these deposits to reach and characterize suitable foundation support materials.

In-situ test spacing and frequency should be used to determine geomaterial design parameters based on project requirements. These tests generally supplement other aspects of the site exploration and will be performed after preliminary borings have been performed. In-situ tests are often done where undisturbed sampling is not easily performed. This includes both vane shear and pressuremeter testing among others. For in-situ testing and soil borings, many times a standard sampling interval is used. However, a customized soil boring and in-situ testing program may be formulated if general site geology or loading conditions warrant alternative intervals. This could aid with locating the contact between two soil strata, as well as discovering a thin layer of unsuitable material. Liquefaction and aggressive environment studies may also dictate appropriate sampling intervals.

4.2.3.3 Soil Boring Methods

Soil borings are the most frequently used soil exploration technique for projects in the public and private sector. Soil borings offer the ability to collect disturbed and undisturbed samples from various depths, as well as to perform in-situ tests. Common boring methods include augered borings, wash borings, and rotary drilling in soil. These methods, as well as sonic drilling, are presented in Table 4-4.

Continuous flight augers are either solid stem or hollow stem and are both used to bore into the subsurface and allow for sampling and/or in-situ testing. A solid stem auger is essentially a solid rod with flights, and must be removed in order to test native soil. They are therefore not useful in soft soils, sands or areas of high groundwater due to the probability of borehole collapse and are best used when soil sampling only at relatively shallow depths is required. Hollow stem augers act as a casing that stays in place during drilling, whereby subsequent sampling and testing is performed through the bottom of the hollow stem. This auger type is therefore practical for a variety of subsurface conditions and utilizes a plug when advancing the auger. Hollow stem auger diameters range from 2.25 inch I.D. up to 12.25 inch I.D with larger sizes reserved for more complex sampling and testing techniques.

Rotary drilling may be performed in soil or rock and involves inserting a drill bit to cut and grind the material. Water or drilling mud flushes out the cuttings, and provides borehole stability. Air has also been used to force out cuttings in lieu of drilling mud, however borehole stability issues remain. To sample soil or perform an in situ test, the drill bit is removed and a sampling device is then inserted to collect material.

Wash borings are advanced by the chopping action of a light bit in combination with the jetting action of water or drill fluid coming through the bit. Casing may be used to maintain an open bore hole, although typically a bentonite or drilling mud of similar properties is adequate. Drilling mud can contaminate recovered soil samples as well as add difficulty when trying to classify soil stratigraphy from wash cuttings. In addition, heavier particles such as gravel or cobbles may be left at the bottom of the hole if the wash system is undersized. Wash borings are infrequently used in the United States.

4.2.3.4 Soil Sampling Methods

Soil samples may be collected via disturbed or undisturbed methods. Disturbed soil samples contain representative material that may be used for visual classification and more routine laboratory testing which is further described in Chapter 5. These

Table 4-4 Soil Boring Methods

Method	Depth	Advantages	Disadvantages	Remarks
Auger Borings.	Most equipment can drill to depths of 100 to 200 feet.	Boring advanced without water or drilling mud. Hollow stem auger acts as a casing.	Difficult to detect change in material. Heavy equipment required. Water level must be maintained in boring equal to or greater than existing water table to prevent sample disturbance.	Boring advanced by rotating and simultaneously pressing an auger into the ground either mechanically or hydraulically.
Rotary Drilling.	Most equipment can drill to depths of 200 feet or more.	Suited for borings 4 to 6 inches in diameter. Most rapid method in most soils and rock. Relatively uniform hole with little disturbance to the soil below the bottom of hole. Experienced driller can detect changes based on rate of progress.	Drilling mud if used does not provide an indication of material change as the wash water does. Use of drilling mud hampers the performance of permeability tests.	Borehole advanced by rapid rotation of drilling bit and removal of material by water or drilling mud. Rock coring is performed by rotary drilling. Liquefaction evaluation methods require mud rotary drilling methods.
Wash Boring.	Most equipment can drill to depths of 100 feet or more.	Borings of small and large diameter. Equipment is relatively inexpensive. Equipment is light. Wash water provides an indication of change in materials.	Slow rate of progress. Not suitable for materials containing stones and boulders.	Boring advanced by a combination of the chopping action of a light bit and jetting action of the water coming through the bit.
Sonic Coring.	Up to 1000 feet.	Generally a 100% recovery rate. Can collect samples in soils and bedrock.	Expensive for large amounts of dense rock sampling.	Borehole advanced in 10 feet cased sections. Can collect any soil type with minimal to no fluids.

soil samples are not suitable for strength or compressibility testing as the sampling disturbance alters their condition. When in-situ particle arrangements, water content and other properties must be preserved for laboratory testing, undisturbed samples are taken. These samples are collected in devices designed to minimize sample disturbance. However, even while using utmost care for removal and transport, no sample will be completely undisturbed.

Disturbed soil samples may be collected with a split barrel sampler, sonic cores, or through test pits. Split barrel samplers typically range from 1.5 to 2.5 inches in diameter and are 18 or 24 inches long. Although multiple sizes exist, the standard split spoon sampler used for the Standard Penetration Test (SPT) has an inner diameter of 1.375 inches and outer diameter of 2 inches (ASTM D1586). A photograph of a standard SPT sampler is presented in Figure 4-2. This test is further discussed in Section 5.1.1.

Relatively undisturbed soil samples may be collected with thin walled tubes (Shelby tubes), a piston sampler or other specialized means. Thin walled tubes are produced in various sizes, and are typically used to collect fine grained soils as illustrated in Figure 4-3. These tubes are pushed into the soil and removed after a brief swelling of the soil occurs. ASTM D1587 provides detailed guidance on this sampling technique.

Piston samplers were developed to prevent soil from entering the sampling tube before the sample depth and to reduce sample loss during tube extraction. They are basically a thin wall tube sampler with a piston, rod, and a modified sampler head. There are numerous types of piston samplers; free or semi-fixed piston samplers, fixed-piston samplers, and retractable piston samplers.

The Pitcher sampler is a core barrel sampler that may be used for sampling a broad range of materials including undisturbed samples of stiff to hard clays, soft rocks and cemented sands. This sampler consists of a rotating outer core barrel with an inner thin walled sampling tube. The sampling tube leads the core barrel when sampling soft soils and the core barrel leads the sampling tube when sampling hard materials. This makes the Pitcher sampler particularly attractive for sampling materials with alternating hard and soft layers.

Figure 4-2 Standard split spoon sampler.

Figure 4-3 Shelby tubes (after Mayne et al. 2002).

4.2.3.5 Rock Exploration Methods (Coring / Drilling)

Rock drilling and coring is typically performed at the end of a soil boring once bedrock is encountered. Special drilling bits are used to cut and grind through rock, so that sampling can be performed. Fluid or air is circulated to flush out cuttings,

and an inner core barrel collects rock samples. The recovered rock core is classified by rock type, and the core recovery length and recovery percentage noted as a percentage of the core run. Table 4-5 summarizes several rock coring methods.

Conventional rotary coring is primarily used to collect rock samples. For this, a circular diamond or tungsten drill bit grinds rock so that a core is cut from the surrounding rock. To collect intact rock samples, the drill barrel typically has an inner and outer tube, of which the inner tube remains stationary during drilling. The inner tube is removable such that intact samples may be brought to the surface, while the outer tube acts as casing, and remains in place. However, several barrel types exist, which are discussed further in Sabatini et al. (2002).

Wire line rotary coring is similar to conventional rotary coring however; the inner barrel is connected to a wire retrieval line as opposed to a rod or tube. This retrieval method significantly speeds up sampling at deeper depths.

Table 4-5 Summary of Rock Coring Methods

Method	Depth	Type of Samples Taken	Advantages	Disadvantages	Remarks
Conventional Rotary Coring in Rock.	Most equipment can drill to depths of 200 feet or more.	Continuous Rock Cores.	Helps differentiate between boulders and bedrock.	Can be slow and fairly expensive.	Several types of core barrels are used.
Wire Line Rotary Coring in Rock.	Most equipment can drill to depths of 200 feet or more.	Continuous Rock Cores.	Improved recovery rate of fractured rock. Typically faster drilling rate when coring rock at deep depths.	Fairly expensive.	Inner tube retrieved by cable suspended lifting device. Preferred method for depths greater than 80 feet.
Rotary Coring of Swelling Clay or Soft Rock.	Most equipment can drill to depths of 200 feet or more.	Plastic tube encased sample.	Inner plastic tube protects soil and soft rock.	More complex equipment.	Smaller sample due to coring equipment.

A specialized barrel may be used when sampling swelling soil and soft rock. This barrel contains a third inner liner which contains the swelling soil or soft rock and is

more easily removed due to the 5% to 10% difference in liner and drill bit size (Acker 1974). A smaller diameter sample results from this barrel design, as opposed to samples collected via rotary coring. However, this collection method may exhibit less soil disturbance than thin walled sampling for some soil types.

Rock cores should be stored in a structurally sound box designed for the size of core collected as illustrated in Figure 4-4. Cores should be set carefully to retain natural bedding and fractures, and handled such that accidental breaks do not occur after retrieval. Features should be noted including bedding, fractures, and weathered zones, and photographs should be taken, always using a visible reference scale such as a tape measure. Sometimes wetting the rock surface can increase color contrast for photos. Labels identifying the project, borehole, depth interval and number of core runs should be written on the core box, in addition to standard field notes.

Rock cores are also given a rock quality designation (RQD). The RQD index test allows for a description of rock mass quality and should be performed in the field upon core recovery. The RQD index test, described in ASTM D6032, is used to provide estimates of overall rock quality. Deere and Deer (1989) proposed the RQD to be equal to the sum of the length of sound core pieces, 4 inches or greater in length, divided by the total length of core run. Core lengths should be measured from the axis centerline, while the RQD is expressed as a percentage. RQD designations are shown in Table 4-6, with a further discussion of rock quality index parameters provided in Section 5.4.

Figure 4-4 Rock core samples.

RQD values may be indicative of the pile penetration into the rock needed to satisfy resistance requirements when reviewed in combination with additional test results. However, the RQD value alone should not be used to correlate rock strength. In

addition to the coring methods presented here, various drill bits exist as well as core barrel types, which influence ease of drilling, core size and recovery rate. These should be selected accordingly based on experience and recovery requirements. Further descriptions of these may be found in Acker (1974), ASCE (2001), and ASTM D2113. Core samples should be retained for the duration of the project and beyond if needed due to any construction claims.

Table 4-6 Rock Quality Designation

Rock Mass Description	RQD
Excellent	90 – 100
Good	75 – 90
Fair	50 – 75
Poor	25 – 50
Very Poor	< 25

4.2.3.6 Groundwater

Accurate ground water level information is needed for the estimation of soil densities, determination of effective soil pressures and for the preparation of effective stress diagrams. Water levels will also indicate the construction difficulties which may be encountered in excavations and the dewatering effort required.

In most structure foundation explorations, water levels should be monitored during drilling of the boring, upon completion of the boring, and 24 hours after the completion of boring. More than one week may be required to obtain representative water level readings in low permeability cohesive soils or in bore holes stabilized with some drilling muds. In these cases, an observation well or piezometer should be installed in a boring to allow long term ground water monitoring. An observation well is typically used to monitor changes in the water level in a select aquifer whereas a piezometer is used to monitor changes in the hydrostatic pressure in a confined aquifer or specific stratum.

An observation well is usually a slotted section of small diameter PVC pipe installed in a bore hole. The bottom section of the slotted PVC pipe is capped and solid PVC sections are used to extend the observation well from the top of the slotted PVC section to a height above grade. The annulus between the slotted section and the sides of the bore hole is backfilled with sand. Once the sand is above the slotted

PVC section, a bentonite seal is placed in the annulus sealing off the soil stratum in which the water table fluctuations will be monitored. Grout or auger cuttings are used to backfill the remaining void, while a locking removable cover may be placed over the annulus top. The water level reading in the observation well will be the highest of the water table in any soil layer that the slotted section penetrates.

Piezometers are generally used to monitor hydrostatic pressure changes in a specific soil stratum. Piezometers may be either pneumatic or vibrating wire diaphragm devices and are installed in a sand pocket with a bentonite seal similar to an observation well. Single and multiple piezometers can be installed in a single bore hole using a cement-bentonite grout. Additional piezometer information is available in FHWA-NHI-01-031, Subsurface Investigations – Geotechnical Site Characterization (Mayne et al. 2002).

4.2.4 Information Required for Construction

The subsurface exploration and subsequent soil and rock testing program provides essential information for driven pile design and construction. Engineers and contractors use this information to select the most appropriate pile type for the loading requirements, size pile driving hammer equipment, determine if pile installation aids are needed to meet design objectives, prepare cost estimates and bid documents, establish construction control methods and generate construction schedules. To reduce the risk of unplanned cost and claims, a well-defined and executed site characterization program is vital.

As described in Chapter 6, a variety of driven pile types and sections exist and may derive their nominal resistance from end bearing, shaft resistance or both. The pile type is generally selected based on local practice, structural requirements and subsurface conditions, while size and length are contingent upon soil properties and bearing layers. Pile drivability and other construction considerations are affected by the overall site characterization including permeability, relative density, layering and soil response to pile driving.

REFERENCES

Acker, W.L. III, (1974). Basic Procedures for Soil Sampling and Core Drilling, Acker Drill Company, Inc., Scranton, PA, 246 p.

American Association of State Highway and Transportation Officials (AASHTO). (1978). Manual on Foundation Investigations Second Edition. AASHTO Highway Subcommittee on Bridges and Structures, Washington, D.C., 196 p.

American Association of State Highway and Transportation Officials (AASHTO). (2014). AASHTO LRFD Bridge Design Specifications, US Customary Units, Seventh Edition, with 2015 Interim Revisions. American Association of State Highway and Transportation Officials, Washington, D.C., 1960 p.

ASTM D1586-11. (2014). Standard Test Method for Standard Penetration Test (SPT) and Split-Barrel Sampling of Soils. Annual Book of ASTM Standards, Vol. 4.08, ASTM International, West Conshohocken, PA, 9 p.

ASTM D1587-12. (2014). Standard Practice for Thin-Walled Tube Sampling of Soils for Geotechnical Purposes. Annual Book of ASTM Standards, Vol. 4.08, ASTM International, West Conshohocken, PA, 4 p.

ASTM D2113-14. (2014). Standard Practice for Rock Core Drilling and Sampling of Rock for Site Investigation. Annual Book of ASTM Standards, Vol. 4.08, ASTM International, West Conshohocken, PA, 20 p.

ASTM D6032-08. (2014). Standard Test Method for Determining Rock Quality Designation (RQD) of Rock Core. Annual Book of ASTM Standards, Vol. 4.09, ASTM International, West Conshohocken, PA, 5 p.

ASTM Vol 4.08. (2014). Soil and Rock I, Vol. 4.08, ASTM International, West Conshohocken, PA, 1826 p.

ASTM Vol 4.09. (2014). Soil and Rock II, Vol. 4.09, ASTM International, West Conshohocken, PA, 1754 p.

Brown, D. A., Turner, J.P. and Castelli R.J. (2010). Drilled Shafts: Construction Procedures and LRFD Design Methods, FHWA-NHI-10-016, Geotechnical Engineering Circular (GEC) No. 10. U.S. Dept. of Transportation, Federal Highway Administration, 970 p.

Cheney, R.S. and Chassie, R.G. (2000). Soils and Foundations Workshop Reference Manual. FHWA HI-00-045, U.S. Department of Transportation, National Highway Institute, Federal Highway Administration, Washington, D.C., 358 p.

Federal Highway Administration (FHWA). (1996). Geotechnical Engineering Notebook DT-15. Differing Site Conditions. U.S. Dept. of Transportation, Federal Highway Administration, Washington, D.C., 36 p.

Louie, J, N. (2001). Faster, Better: Shear-wave Velocity to 100 Meters Depth from Refraction Microtremor Arrays: Bulletin of the Seismological Society of America, V. 91.02, Alexandria, VA, pp. 347-364.

Lucius, J.E., Langer W.H. and Ellefsen, K. (2007). An Introduction to Using Surface Geophysics to Characterize Sand and Gravel Deposits. U.S. Geological Survey Circular, Reston, VA, 1310, 33 p.

Mayne, P.W., Christopher, B., Berg, R., and DeJong, J. (2002). Subsurface Investigations (Geotechnical Site Characterization), FHWA NHI-01-031, U.S. Dept. of Transportation, National Highway Institute, Federal Highway Administration, Washington, D.C., 300 p.

Sabatini, P.J., Bachus, R.C., Mayne, P.W., Schneider, J.A., and Zettler, T.E. (2002). Evaluation of Soil and Rock Properties, FHWA-IF-02-034, Geotechnical Engineering Circular (GEC) No. 5, U.S. Dept. of Transportation, Federal Highway Administration, 385 p.

Samtani, N.C. and Nowatzki, E.A. (2006). Soils and Foundations: Reference Manual, Vol. 1, FHWA-NHI-06-088, U.S. Dept. of Transportation, National Highway Institute, Federal Highway Administration, Washington, D.C., 462 p.

Sirles, P.C. (2006). Use of Geophysics for Transportation Projects, NCHRP Synthesis 357, Transportation Research Board of the National Academies, Washington, D.C., 109 p.

Sirles, P., Shawver, J.B., Pullammanappallil, S., and Batchko, Z. (2009). Mapping Top-of-Bedrock and Soft-Soil Zones Beneath High-Traffic Areas Using 2D REMI, Symposium on the Application of Geophysics to Engineering and Environmental Problems (SAGEEP 2009), Environmental and Engineering Geophysical Society, Denver, CO, (available on CD; online @:www.eegs.org).

Rosenblad B.L., and Li J. (2009). Comparative study of Refraction Microtremor (ReMi) and Active Source Methods for Developing Low-Frequency Surface Wave Dispersion Curves. Journal of Environmental and Engineering Geophysics. 14 (3), pp. 101-113.

Wightman, W., Jalinoos, F., Sirles., and Hanna, K. (2003). Applications of Geophysical Methods to Related Highway Problems. U.S. Dept. of Transportation, Federal Highway Administration, 716 p.

CHAPTER 5

GEOMATERIAL DESIGN PARAMETERS AND GEOTECHNICAL REPORTS

Properties of cohesive soil, cohesionless soil, soft rock, and hard rock affect the design and construction of driven piles. Depending on subsurface conditions, additional consideration may be given to aggressive soils or areas effecting pile integrity. As discussed in chapter 4, in-situ tests are performed during subsurface exploration while samples may be collected for further evaluation in a soils engineering laboratory. Results of in-situ and laboratory tests define material properties that are often correlated to design parameters, if not directly measured. Primary design parameters include shear strength and deformation values. This chapter will focus on the determination of soil and rock parameters that influence the design and construction of driven piles. Table 5-1 provides a summary of field and laboratory tests used for geomaterial characterization and determination of design parameters.

A discussion of in-situ and laboratory testing to acquire design parameters is provided in subsequent sections. For a more in depth discussion on the collection of design parameters, please refer to AASHTO (2014), Bowles (1992), Mayne et al. (2002), Duncan and Wright (2005) among other sources. In addition, the latest version of GEC-5, Evaluation of Soil and Rock Properties, should be consulted for updates in practice. The version at the time of this manual revision is Sabatini et al. (2002).

5.1 IN-SITU SOIL TESTING

In-situ testing provides soil parameters for the design of structure foundations especially in conditions where standard drilling and sampling methods cannot be used to obtain high quality undisturbed samples. Therefore, representative strength test data is difficult to obtain on these soils in the laboratory. To overcome these difficulties, test methods have been developed to evaluate soil properties, particularly strength and compressibility, in-situ.

Table 5-1 Field and Laboratory Tests for Geomaterial Parameter Determination

Design Parameter or Information Needed	Cohesionless Soil	Cohesive Soil	Rock
Subsurface Conditions			
Subsurface Stratigraphy	Drilling and Sampling; SPT, CPTu, CPT; Geophysical methods	Drilling and Sampling; SPT, USS, CPTu, CPT, DMT; Geophysical methods	Drilling and Sampling; Rock Core Logging
Groundwater Conditions	Well / Piezometer	Well / Piezometer	Well / Piezometer
Index Properties			
Classification	USCS Group	USCS Group	Rock Type
Gradation	Sieve Analysis	Sieve Analysis Hydrometer Analysis	N/A
Atterberg Limits	N/A	Liquid Limit Plastic Limit	N/A
Moisture Content, *w*	Wet and Oven-Dried Weights	Wet and Oven-Dried Weights	Lab
Unit Weight, γ	SPT, DMT	USS-Lab	USS-Lab
Sensitivity	N/A	VST, USS-Lab	N/A
RQD and GSI	N/A	N/A	Rock Core Recovery and Logging
Engineering Properties			
Effective Stress Friction Angle, ϕ'	SPT, CPTu, CPT, DMT	CD or CIU triaxial on USS	Correlate to GSI
Undrained Shear Strength, s_u	N/A	UU, CIU and UC on USS, VST, CPT	N/A
Preconsolidation Stress, σ_p	SPT, CPT	Consolidation test, DMT, CPTu, CPT	N/A
Elastic Modulus of Soil, E_s	SPT, CPT, PMT, DMT; correlate with Index Properties	DMT, PMT, Triaxial Tests; correlate with Index Properties	N/A
Unconfined Compressive Strength, q_u	N/A	N/A	UC on Rock Core
Modulus of Intact Rock, E_r	N/A	N/A	Compression Test on Rock Core
Rock Mass Modulus, E_m	N/A	N/A	Correlate to GSI and q_u or E_r; PMT

Table Key:

CD – Consolidated Drained Triaxial Test (Section 5.2)
CIU – Consolidated Undrained Triaxial test with pore pressure measurements (Section 5.2)
CPT – Cone Penetration Test (Section 5.1.2)
CPTu – Cone Penetration Test with pore water pressure measurements (Section 5.1.2)
CU – Consolidated Undrained Triaxial Test (Section 5.2)
DMT – Dilatometer Test (Section 5.1)
GSI – Geological Strength Index
PMT – Pressuremeter Test (Section 5.1)
RQD – Rock Quality Designation Test (Section 4.2)
SPT – Standard Penetration Test (Section 5.1.1)
UU – Unconsolidated, Undrained Triaxial Test (Section 5.2)
UC – Unconfined Compression Test (Section 5.2)
USS – Undisturbed soil sample (Section 4.2)
USCS – Unified Soil Classification System
VST – Vane Shear Test (Section 5.1.3)

In-situ test methods can be effective when used to supplement conventional exploration programs. In addition, these methods help identify key strata for further conventional sampling and laboratory tests. In the absence of an adequate program to determine subsurface design parameters, the engineer must use a more conservative approach based on less certain data. This situation also results in additional uncertainty and risk and is not recommended.

Primary in-situ tests that provide data for foundation design are the Standard Penetration Test (SPT), cone penetration test (CPT), the cone penetration test with pore pressure measurements (CPTu), the seismic cone penetration test with pore pressure measurements (SCPTu), and the vane shear (VST). Other lesser used in-situ testing devices include the pressuremeter test (PMT) and flat dilatometer test (DMT). Each of these test methods apply different loading conditions (orientation and rate of strain) to gain information on strength and or/stiffness such as torsion for VST or axial loading for SPT. The net result is that all in-situ tests are index tests that require local correlations and where possible should be benchmarked to laboratory tests. In-situ test method schematics are depicted in Figure 5-1.

The applicability, advantages and disadvantages of all the in-situ testing methods are briefly summarized in Table 5-2. For a detailed discussion of a particular in-situ testing method, the reader is referred to the publications listed at the end of this chapter. NHI course 132031, Subsurface Investigations – Geotechnical Site Characterization and the accompanying course manual by Mayne et al. (2002) provides a thorough coverage of in-situ testing methods.

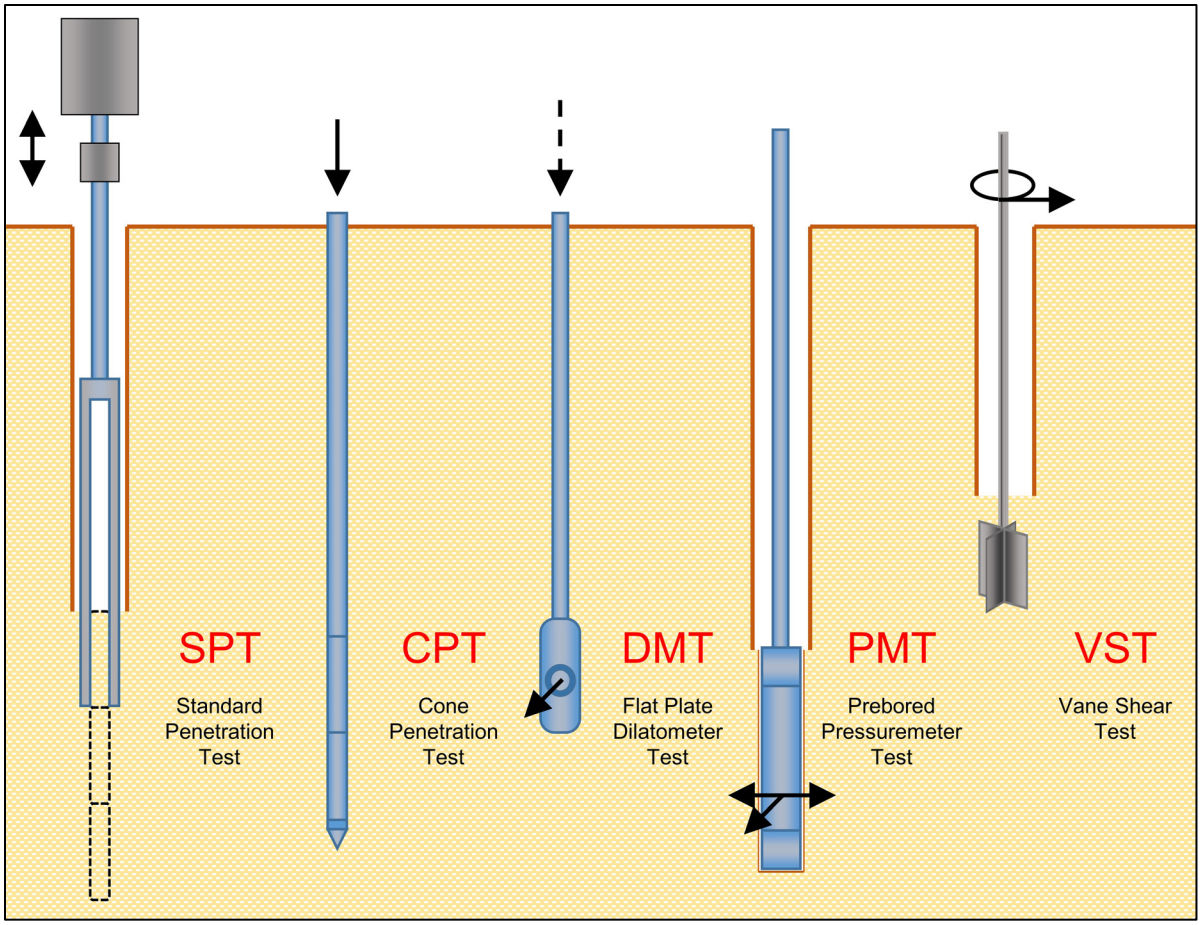

Figure 5-1 Schematic of common of in-situ tests (after Mayne et al. 2001).

5.1.1 Standard Penetration Test

The most common in-situ test in current use is the Standard Penetration Test (SPT) (ASTM D1586). During borehole advancement, the standard split spoon is driven using a 140 lb hammer from a 30 inch drop height. The sampler tip starts at the current borehole bottom and is driven 18 or 24 inches depending on sampler length. The number of blows for each 6 inch drive interval is counted, with the second and third interval summed to establish an N value. If the sampler penetrates over the increment under the weight of the drill rods or after the SPT hammer is set atop the rods, a WOR (weight of rods) or WOH (weight of hammer) designation is recorded on the boring log. Furthermore, if very dense or hard material is encountered and blow counts exceed 50 blows before finishing a 6 inch sampling interval, the SPT event is ended and the N value is designated as 50/x where x is the actual sampler penetration in inches measured for the 50 blows. This blow count and partial penetration increment should be recorded in lieu of an N value on the respective boring logs.

Table 5-2 Summary of In-Situ Methods

In-Situ Test	Information Obtained for Pile Foundation Design in Appropriates Soil Types	Advantages	Disadvantages
Standard Penetration Test (SPT) ASTM D1586	Collection of soil samples to confirm subsurface soil type. Correlations for determination of in-situ density, liquefaction susceptibility, and friction angle of sands, undrained shear strength of clays. Best suited for sand, silt, and clay materials. Not suitable in large gravel, rubble, and rock.	1. Simple test. 2. Can retrieve samples to confirm soil type. 3. Equipment is widely available. 4. Correlations available for estimating soil parameters.	1. Operator and equipment dependent. 2. Samples are disturbed. 3. Cannot evaluate in-situ pore pressure. 4. Accuracy of estimated soil parameters.
Cone Penetration Test with Pore Pressure Measurements (CPTu) ASTM D5778	Continuous evaluation of subsurface stratigraphy. Correlations for determination of in-situ density and friction angle of sands, undrained shear strength of clays, and liquefaction susceptibility. Best suited for sand, silt, and clay materials. Not suitable in gravel, rubble, and rock.	1. Cone can be considered as a model pile. 2. Quick and simple test. 3. Can reduce number of borings. 4. Relatively operator independent. 5. Pore pressure measurements can be used to assess soil setup effects. 6. Can help determine if penetration is drained or undrained.	1. Does not provide soil samples. 2. Should be used in conjunction with soil borings in an exploration program. 3. Local correlations can be important in data interpretation. 4. Location and saturation of porous filter can influence pore pressure measurements.
Pressuremeter Test (PMT) ASTM D4719	Bearing capacity from limit pressure and compressibility from pressure meter deformation modulus. Best suited in sand, silt, clay and soft rock. Not suitable in organic soils and hard rock.	1. Tests can be performed in and below hard strata that may stop other in-situ testing devices. 2. Tests can be made on non-homogenous soil deposits.	1. Bore hole preparation very important. 2. Limited number of tests per day. 3. Limited application for axially loaded pile design.
Dilatometer Test (DMT) ASTM D6635	Correlations for soil type, earth pressure at rest, over consolidation ratio, undrained shear strength, and dilatometer modulus. Best suited for low to medium strengths sand and clay. Not suitable in dense deposits, gravel, and rock.	1. Quick, inexpensive test. 2. Relatively operator independent.	1. Less familiar test method. 2. Intended for soils with particle sizes smaller than fine gravel. 3. Limited application for axially loaded pile design.
Vane Shear Test ASTM D2573	Undrained shear strength. Best suited in soft to medium clays. Not suitable in silt, sand or gravel.	1. Quick and economical. 2. Compares well with unconfined compression test results at shallow depths.	1. Can be used to depths of only 13 to 20 feet without casing bore hole.
Dynamic Cone Test	Qualitative evaluation of soil density. Qualitative comparison of stratigraphy. Best suited in sand and gravel. Not suitable in clay.	1. Can be useful in soil conditions where static cone (CPT) reaches refusal.	1. An unknown fraction of resistance is due to side friction. 2. Overall use is limited.

In addition to the penetration resistance that is recorded during driving, soil enters the hollow sampler, thus providing a disturbed soil sample. A schematic of the Standard Penetration Test is presented in Figure 5-2. A description of the SPT sampler was previously presented in Chapter 4 along with a photograph of the sampler in Figure 4-2.

The SPT hammer type and operational characteristics have a significant influence on the resulting SPT N values. There are two main hammer types currently in use in the U.S., the safety hammer and the automatic hammer. A third hammer type, the donut hammer, was used almost exclusively prior to about 1970 but not any longer due to safety considerations. Figure 5-3 provides illustrations of these SPT hammer types.

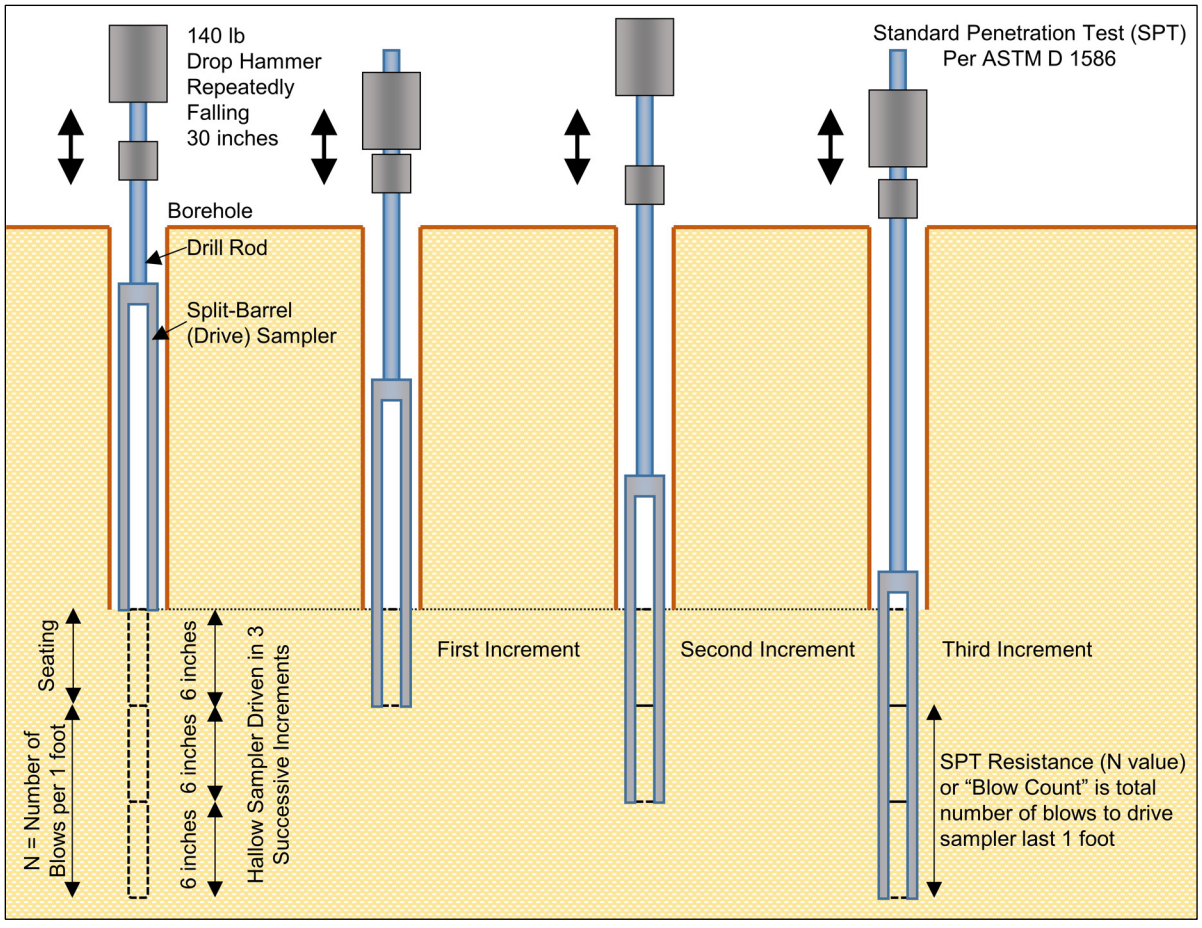

Figure 5-2 Standard Penetration Test schematic (after Mayne et al. 2001).

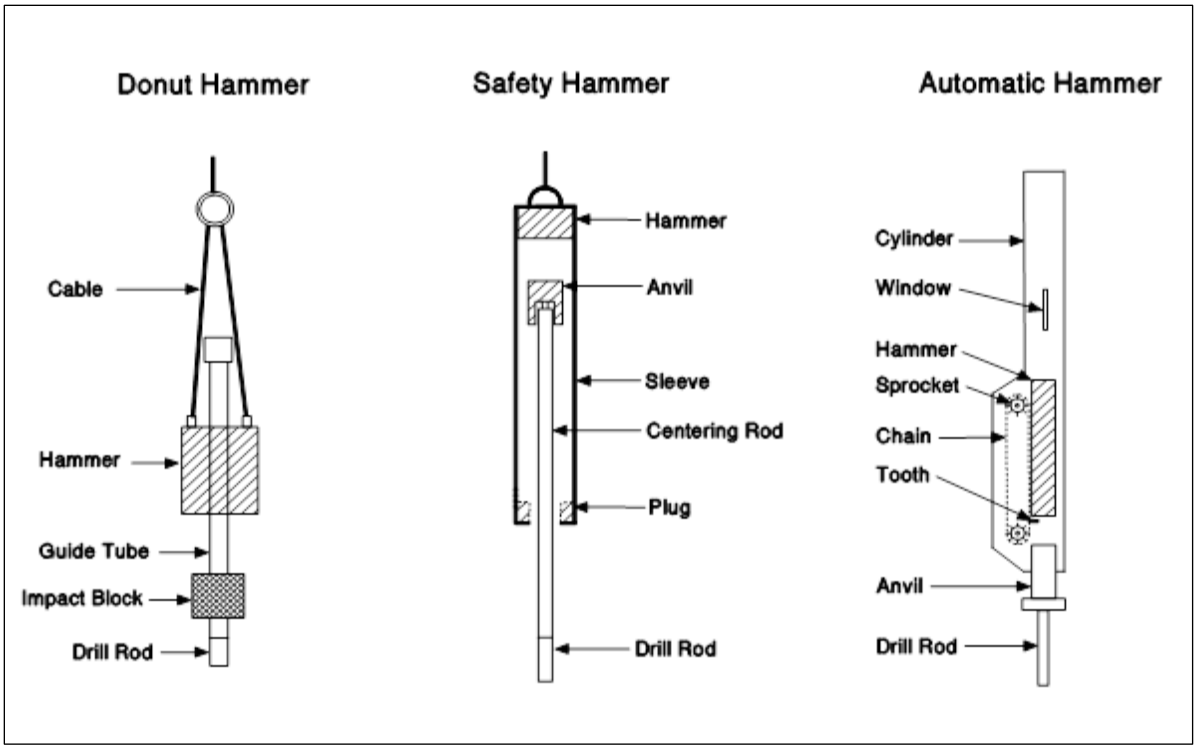

Figure 5-3 Standard Penetration Test hammer types.

Measurement studies on SPT energy transfer have been performed (e.g. Kovacs et al. 1983; Honeycutt et al. 2014). In general, these studies have indicated that the typical energy transfer from donut, safety, and automatic hammers are on the order of 45%, 60%, and 80% of the SPT test potential energy, respectively. It should not be assumed that all SPT hammers of a given type will have the energy transfer values noted above. Energy transfer for a given hammer type can and does vary according to hammer maintenance, hammer manufacturer, driller, and operating procedures. Because of these variations, it is recommended that SPT hammers undergo a yearly calibration in accordance with ASTM D4633 to document hammer performance. It may be particularly advantageous to conduct these calibrations prior to undertaking major projects. A photograph of energy transfer measurements being taken during a SPT sampling event is provided in Figure 5-4.

The use of reliable qualified drillers and adherence to recommended sampling practice cannot be overemphasized. Procurement practices should consider the drilling quality, sampling, and testing requirements needed for economical driven pile foundation design and construction.

Figure 5-4 Instrumented 2 foot long AW rod atop drill string for SPT hammer energy measurements.

The significance of the SPT hammer type and energy transfer on N values is very apparent in a pile capacity prediction symposium reported by Finno (1989). For this event, two soil borings were drilled less than 33 feet apart in a uniform sand soil profile. Figure 5-5 presents the results of the two borings, one with SPT N values obtained using a safety hammer and the other with an automatic hammer. The SPT N values from the safety hammer range from 1.9 to 2.7 times the comparable N value from the automatic hammer. This significant variation in N values clearly indicates that the type of SPT hammer used should be recorded on all drilling logs. It is recommended that SPT N values be corrected and reported as N_{60} values whenever possible. Cheney and Chassie (2000) identified ten common errors that influence SPT test results which should also be reviewed by designers and boring crews.

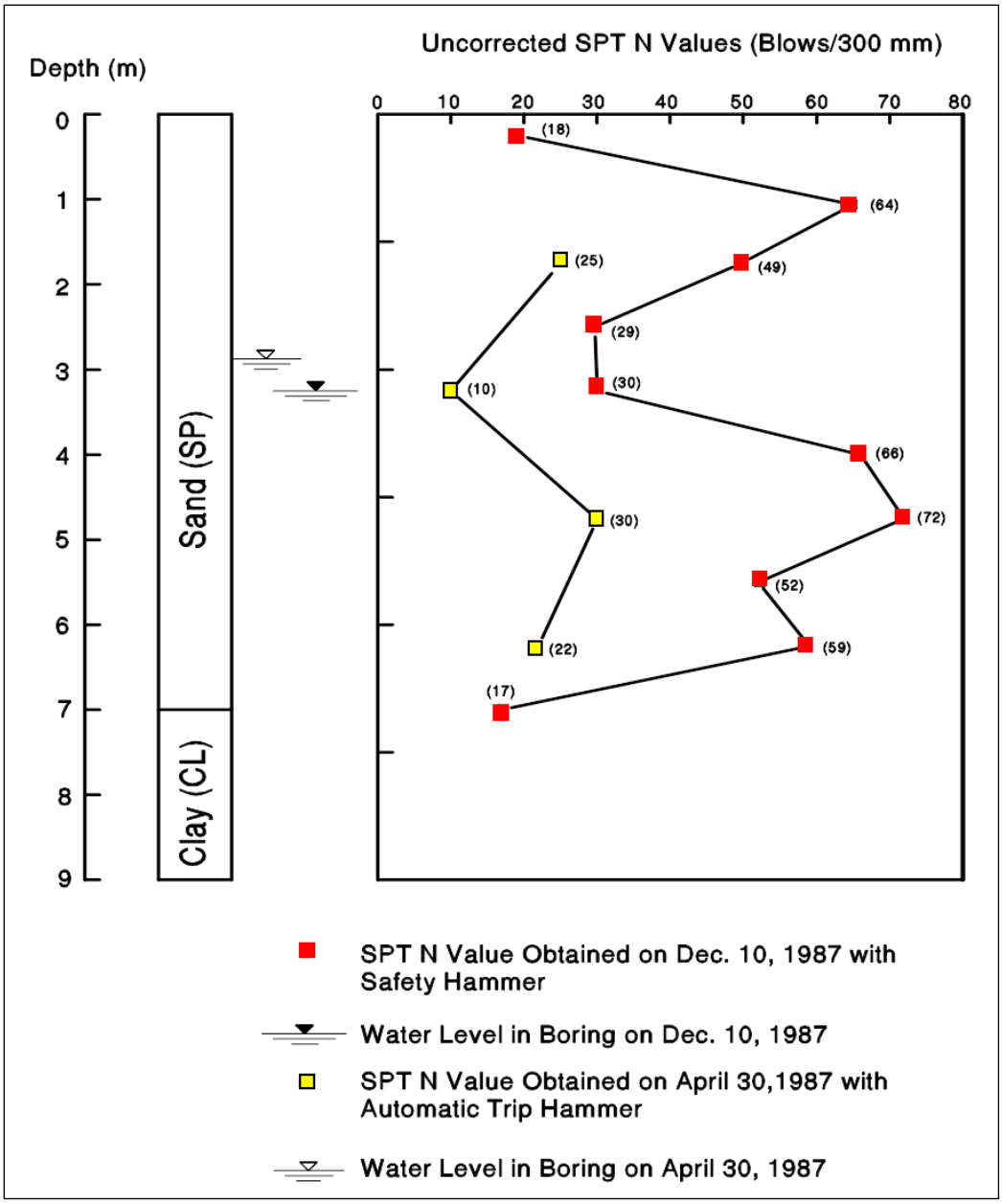

Figure 5-5 Adjacent borings with different SPT hammer types (after Finno 1989).

Although sources of error exist in the SPT test, correction and/or normalization factors have been developed to aid designers. The pile design charts and methods provided in this manual are the current standard of practice in the United States and use SPT N values based on safety hammer correlations, i.e., 60% energy transfer. Therefore SPT N values established on the basis of 60% energy transfer are referred to as N_{60}. Conversion of field SPT N values to N_{60} values based on energy transfer measurements are as follows:

$$N_{60} = N\left(\frac{\mathrm{ER}}{60}\right) \qquad \text{Eq. 5-1}$$

Where:

N_{60} = SPT N value corrected for 60% energy transfer.
N = uncorrected field SPT resistance value.
ER = hammer efficiency as determined by energy measurements in accordance with ASTM D4633.

Typical SPT hammer efficiencies may also be found in geotechnical literature such as FHWA GEC-5, Sabatini et al. (2002) as well as Das (2007). The energy-corrected N_{60} value may be normalized for the effects of overburden stress, designated $(N_1)_{60}$, before being used in correlations between N values and soil properties. The general conversion is shown in Equation 5-2.

$$(N_1)_{60} = C_n N_{60} \qquad \text{Eq. 5-2}$$

Where:

$(N_1)_{60}$ = SPT N value corrected for energy and overburden stress.
N_{60} = SPT N value corrected for 60% energy transfer.
C_n = correction factor for SPT N value.

AASHTO specifications recommend SPT N values be corrected for overburden pressure using Equation 5-3 unless otherwise specified by the design method. Relationships for this factor have been published in the literature whereas Equation 5-3 is the recommended correction in AASHTO specifications from Peck et al. (1974). An alternate correction approach from Lio and Whitman (1986) is presented in Equation 5-4.

$$C_n = 0.77 \log\left[\frac{40}{(\sigma'_{vo})}\right] \leq 2.0 \qquad \text{Eq. 5-3}$$

$$C_n = \left(\frac{p_a}{\sigma'_{vo}}\right)^n \qquad \text{Eq. 5-4}$$

Where:

p_a = atmospheric pressure (ksf).
σ'_{vo} = vertical effective stress at the sample depth (ksf).
n = exponent typically equal to 1 in clays (Olsen 1997) and 0.5 in sandy soils (Lio and Whitman 1986).

Corrected N values are used for soil strength parameter correlations presented in Section 5.2. Note that correlations between cohesive soil and physical properties with N values are crude and, therefore, correction of N values in cohesive soils is generally not necessary.

5.1.2 Cone Penetration Test

The cone penetration test (CPT) was first introduced in the U.S. in 1965. By the mid 1970's, the electronic cone began to replace the mechanical cone, and in the early 1980's, the piezocone or cone penetration test with pore pressure measurements (CPTu) became readily available. A NCHRP synthesis by Mayne (2007) provides a good summary of cone penetration testing practices and use by transportation agencies in the US and Canada. The CPT/CPTu has developed into one of the most popular in-situ testing devices. Part of this popularity is due to the CPT's ability to provide large quantities of useful data quickly and at an economical cost. Depending upon equipment capability as well as soil conditions, 300 to 1200 feet of penetration testing may be completed in one day.

Current cone penetration testing relies on the use of electronic cone penetrometers with pore pressure measurements. In the cone penetration test, a cone penetrometer with a cross sectional area of 1.55 or 2.33 inch^2 and a 60° conical tip is attached to a series of rods and is continuously pushed into the ground. The cone also contains a friction sleeve located behind the conical tip. Pore pressure measurements are obtained with all modern cones from a pore pressure transducer located behind the conical tip and just before the friction sleeve. Pore pressure measurements at this location are referred to as the u_2 position.

Typically, a hydraulic ram with 10 to 40 kips of thrust is used to continuously advance the cone into the ground at a rate of 0.8 in/sec. Built in load cells are used to continuously measure the cone tip resistance, q_c, the unit sleeve friction resistance, f_s, and the pore pressure, u, during penetration. The pore pressure measurement is used to correct the measured cone tip resistance, q_c, for geometrical effects that reduce the measured value in proportion to the amount of pore pressure that is generated. The resulting corrected tip resistance is referred to as q_t. The friction ratio, R_f, is the defined as f_s/q_t and is commonly used in the interpretation of test results. Careful porous element and cavity saturation is essential to obtain pore pressure measurements. Test procedures may be found in ASTM D5778. Both size cones are displayed in Figure 5-6 with a CPT rig shown in Figure 5-7.

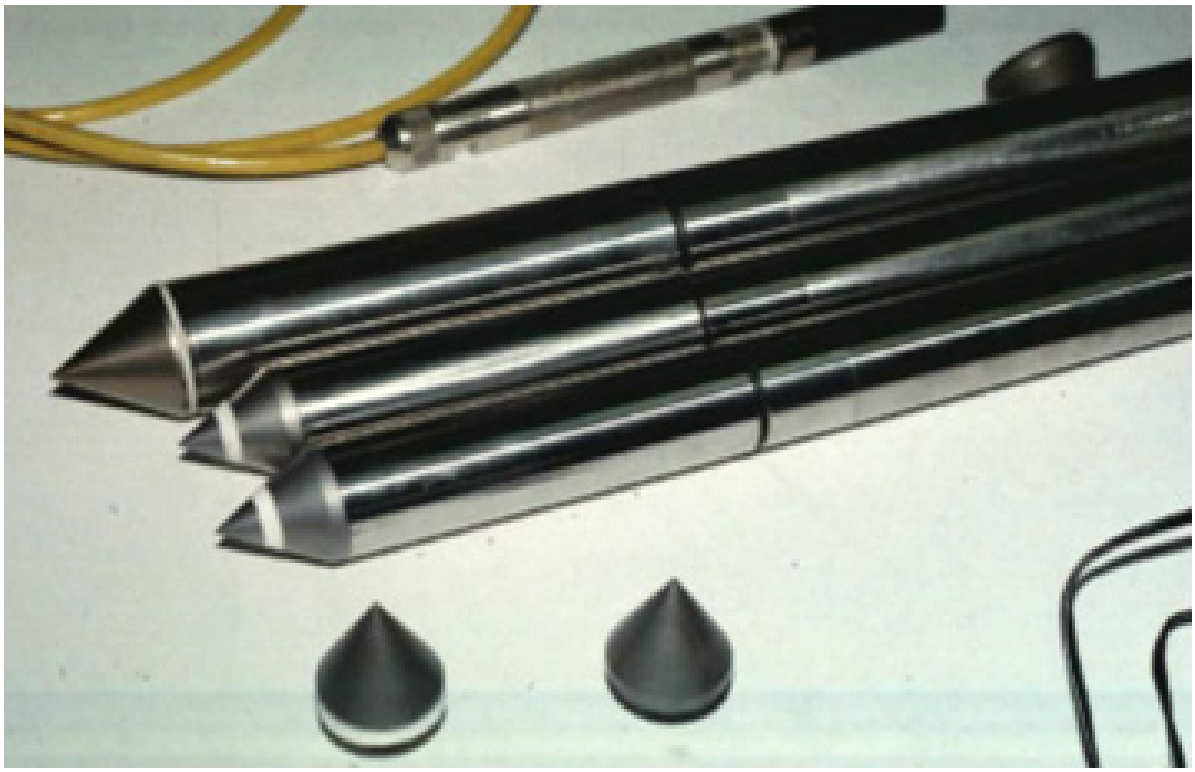

Figure 5-6 Cone penetrometers (after Mayne et al. 2001).

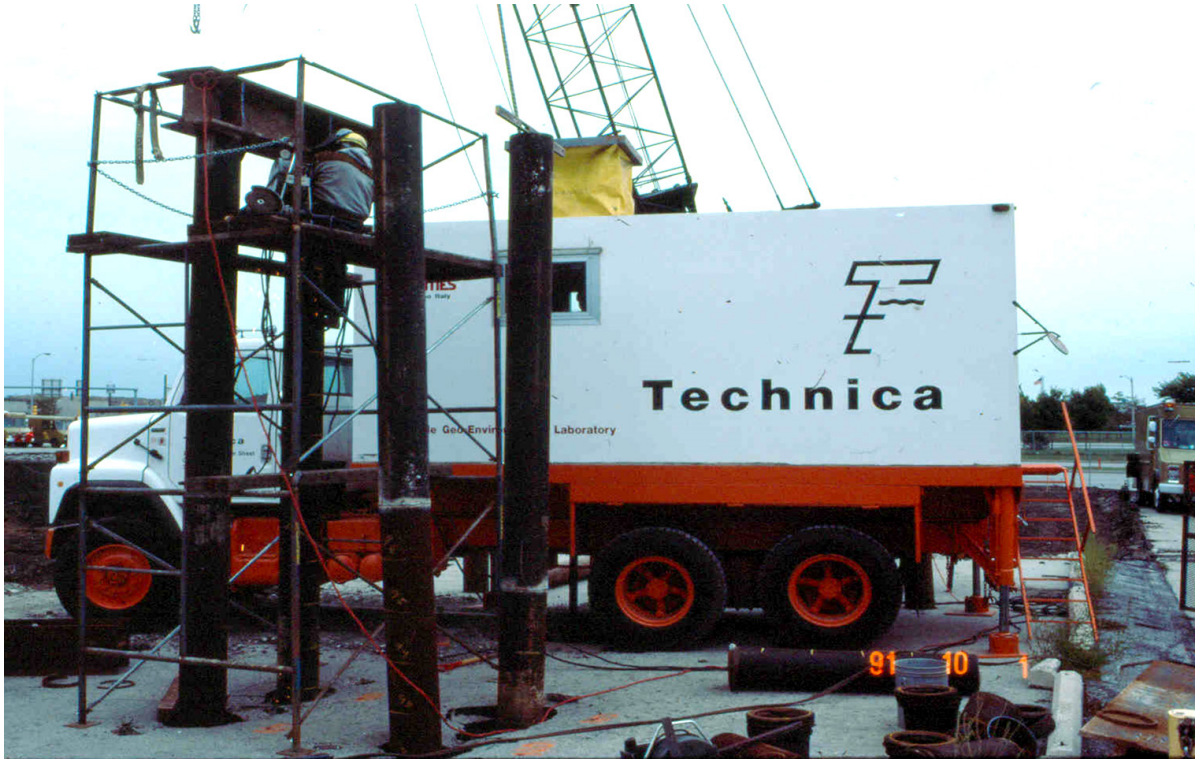

Figure 5-7 CPT rig.

Modern cones may be further divided into three main types, the piezocone (CPTu), the seismic piezocone (SCPTu), and the resistivity piezocone (RCPTu). The CPTu can also be used to monitor pore pressure dissipation. The seismic cone includes a horizontal geophone above the friction sleeve which allows calculation of shear wave velocity at selected depths. The resistivity cone uses electrical conductivity or resistivity which allows detection of the freshwater – salt water interface or profiling of contaminated groundwater plumes. Since pore pressure measurements are made with all modern electronic cone penetrometers, the abbreviation CPT will be used hereafter and assume that pore pressure measurements are included.

Data collected with CPT can provide a continuous profile of the subsurface stratigraphy. A soil behavior chart developed by Robertson (1990) for CPT data is presented in Figure 5-8. From correlations with CPT data, evaluations of in-situ relative density, D_r, and effective friction angle, ϕ', of cohesionless soils as well as the undrained shear strength, s_u, of cohesive soils can be made. Correlations for determination of other soil properties, liquefaction susceptibility, and estimates of SPT N_{60} values may also be determined. The accuracy of these correlations may vary depending upon geologic conditions. Correlation confirmation with local conditions is therefore important.

The primary advantage of CPT testing is the ability to rapidly develop a continuous profile of subsurface conditions more economically than other subsurface exploration or in-situ testing tools. Because the CPT collects continuous data, it can delineate fine changes in stratigraphy and characterize site variability better than other methods. Engineering properties can be assessed through empirical correlations. For cohesionless soils, these empirical engineering property correlations are accurate and commonly used. For cohesive soils, engineering property correlations are less accurate. CPT results are relatively operator independent and highly repeatable. Because of these advantages, the CPT is increasingly being used as an equal or superior subsurface exploration method in some stratigraphic conditions such as alluvial sites and liquefiable soils. In other subsurface conditions, CPT may be used to reduce the number of conventional borings needed on a project, or to focus attention on discrete zones for detailed soil sampling and testing.

Limitations of CPT testing include the inability to push the cone in dense or coarse soil deposits. In general, soils with SPT N values greater than about 30 to 40 are difficult to test with CPT equipment. To penetrate dense layers, cones are sometimes pushed in bore holes advanced through the dense strata. While CPT can be used in marine environments, the soundings must be performed from a fixed

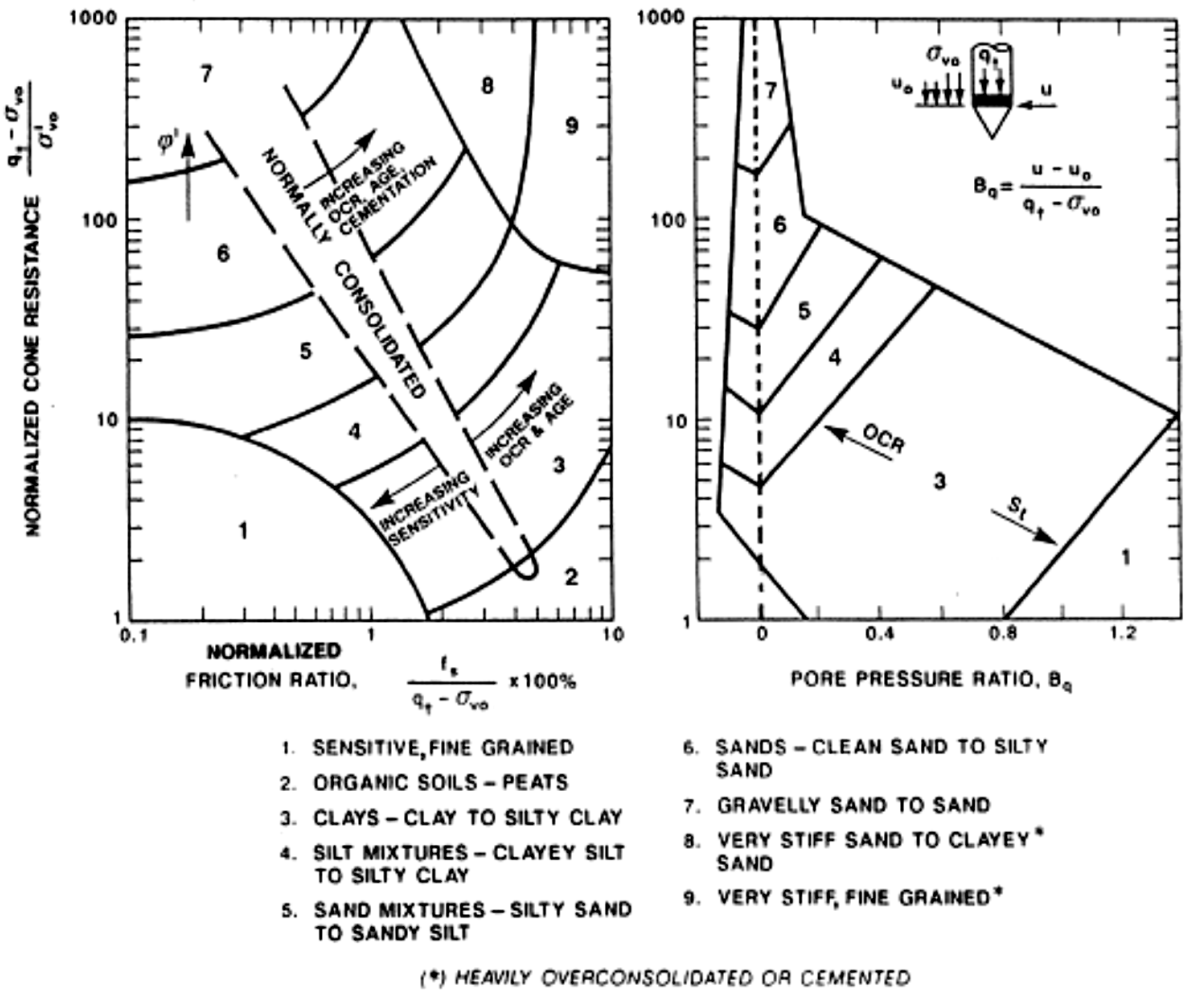

Figure 5-8 Soil behavior type classification chart based on normalized CPT data (after Robertson 1990).

platform (e.g., a jack-up barge) with sufficient casing to provide lateral support for the rods or specialized submersible equipment is will be required. Another limitation is that soil samples are generally not obtained during routine CPT programs for confirmation of stratigraphy. Local correlations are also important in data interpretation.

5.1.3 Vane Shear Test

The vane shear test is an in-situ test for determining the undrained shear strength of soft to medium clays. Figure 5-9 is a schematic drawing of the essential components and test procedure. The test consists of forcing a four bladed vane into undisturbed soil and rotating it until the soil shears. Two shear strengths are usually

recorded, the peak shearing strength and the remolded shearing strength. These measurements are used to determine the sensitivity of clay and allows for analysis of the soil resistance to be overcome during pile driving. It is necessary to measure skin friction along the steel connector rods which must be subtracted to determine the actual shear strength. The vane shear test generally provides the most accurate undrained shear strength values for clays when undrained shear strengths are less than 1 ksf. A detailed test procedure may be found ASTM D2573.

It should be noted that the sensitivity of clay determined from a vane shear test provides insight into the setup potential of the clay deposit. Soil setup may then be used for pile drivability and resistance evaluations. However, the sensitivity value is a qualitative and not a quantitative indicator of soil setup.

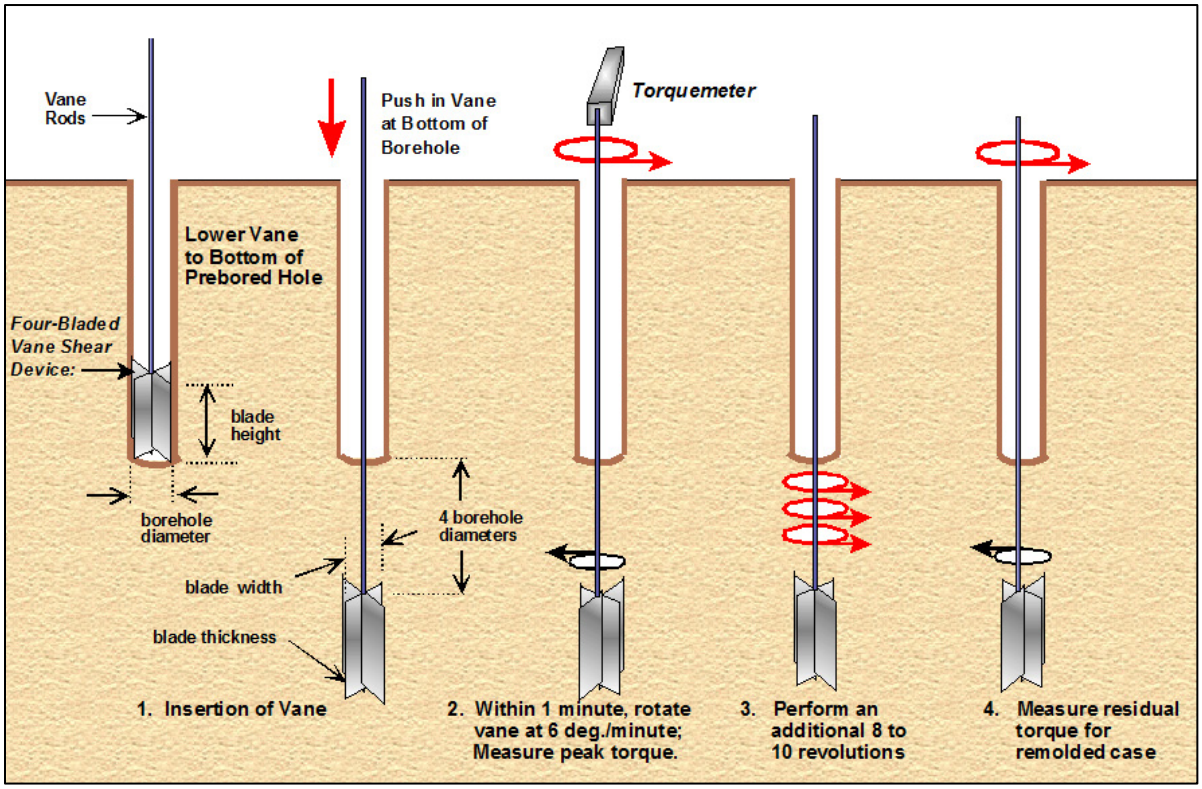

Figure 5-9 Vane shear test schematic (after Mayne et al. 2001).

5.1.4 Other In-Situ Tests

Other in-situ tests with limited application to pile foundation design include the dilatometer, the pressuremeter, and the dynamic cone. These are briefly discussed in the following sections.

5.1.4.1 Dilatometer Test

The dilatometer test (DMT) is an in-situ testing device that was developed in Italy in the early 1970's and first introduced in the U.S. in 1979. Like the CPT, the DMT is generally hydraulically pushed into the ground although it may also be driven. When the DMT can be pushed into the ground with tests conducted at 8 inch increments, 100 to 300 feet of DMT sounding may be completed in a day. The primary utilization of the DMT in pile foundation design is the delineation of subsurface stratigraphy and interpreted soil properties. However, it would appear that the CPT/CPTu is generally better suited to this task than the DMT. The DMT may be a potentially useful test for design of piles subjected to lateral loads. For axially loaded piles, the dilatometer test has limited direct value. The test procedures for DMT are presented in ASTM D6635.

5.1.4.2 Pressuremeter Tests

The pressuremeter test (PMT) is an in-situ device used to evaluate soil and rock properties, and imparts lateral pressures to the soil, allowing for soil shear strength and compressibility to be determined by interpretation of a pressure-volume relationship. Deposits such as soft clays, fissured clays, sands, gravels and soft rock can be tested with a pressuremeter. A pressuremeter test produces information on the elastic modulus of the soil as well as the at rest horizontal earth pressure, the creep pressure, and the soil limit pressure. For piles subjected to lateral loads, the pressuremeter test is a useful design tool and can be used for determination of p-y curves. However for design of vertically loaded piles, the pressuremeter test has limited value. Pile design procedures using pressuremeter data have been developed and may be found in FHWA-IP-89-008, The Pressuremeter Test for Highway Applications, Briaud (1989). Details on test procedures may be found in ASTM D4719, Standard Test Method for Pressuremeter Testing in Soils.

5.1.4.3 Dynamic Cone

There are two types of dynamic penetrometers with conical points. The dynamic cone type that is most often used has a shaft diameter that is smaller than the cone diameter. Theoretically, due to the cone being larger than the shaft, the penetrometer measures only point resistance. A lesser used cone type has a shaft and cone of the same diameter. This type of dynamic cone penetrometer records both skin friction and point resistance, but the two components cannot be analyzed independently. Equations have been developed for determining the geotechnical

resistance of pile foundations by using the dynamic cone test data. However, these are not used extensively and the dynamic cone penetrometer is not recommended for final foundation design unless specific local correlations with load tests to geotechnical failure have been taken.

5.2 SOIL PARAMETERS

Index properties and engineering properties for geomaterials are derived from field and laboratory testing. Differing soil and rock types may be segregated through index tests which aid in the division of subsurface strata for design. These properties are typically obtainable through routine sampling and testing methods, and assist with constructability limitations or preliminary pile selection based on soil type and loading conditions. Engineering properties for soil and rock include shear strength, compressibility and permeability. Shear strength values can be used to determine driven pile geotechnical resistances while compressibility information can be used to check service limit states. Permeability is not generally quantified for pile design purposes, however certain slow draining soils can influence pile drivability, and therefore knowledge of these areas may assist in constructability concerns. Further information on laboratory testing of soils may be found in Bowles (1992), as well is in GEC-5 by Sabatini et al. (2002) and Samtani and Nowatzki (2006) among other sources.

5.2.1 Soil Classification and Index Properties

Two soil classification systems are in common use for transportation projects. The AASHTO soil classification system is used by many transportation agencies for pavement features while the Unified Soil Classification System (USCS) is utilized for nearly all other geotechnical work. The USCS is better suited to deep foundation design and will therefore be solely used in this manual.

Routine index tests for classification include a particle size distribution, Atterberg limits and moisture content. Additional index tests include specific gravity and soil unit weight. A summary of these index tests is shown in Table 5-3.

Laboratory tests to determine the fine content and gradation of cohesionless soils and the remolded shear strength of cohesive soils are important in assessing pile drivability and potential soil setup effects (changes in nominal resistance with time).

Table 5-3 Soil Index Tests used for Driven Pile Design
(modified from Brown et al. 2010)

Test	Index Property Determined	Soil Type	Application	Standard Test Procedure
Particle Size Distribution (Mechanical and Hydrometer)	Grain Size Distribution	Sieve on all Soils; Hydrometer on Minus #200	USCS classification Aids in evaluation of densification and liquefaction potential for cohesionless soils	ASTM D422 AASHTO T88
Atterberg Limits	Liquid Limit (LL) Plastic Limit (PL) Plasticity index (PI) PI = LL - PL Liquidity Index (LI) LI = (w_n - PL) / PI	Minus #40	USCS classification Soil consistency Engineering property correlations	ASTM D4318 AASHTO T89 AASHTO T90
Moisture Content	Moisture Content, w_n	Undisturbed Samples; Split-Spoon Samples with Moisture Change	Soil Consistency May aid in determination of water table elevation	ASTM D2216 AASHTO T265
Unit Weight (Undisturbed)	Total Unit Weight, γ or Density, ρ	Fine-grained (Cohesive)	Aids evaluation of underground soil stresses	ASTM D7263 AASHTO T38
Specific Gravity	Specific Gravity, G_s	Minus #4	Aids evaluation of soil density and compressibility	ASTM D854 AASHTO T100
Soil Classification	USCS Group Name and Group Symbol;	All Soils	Physical characteristics define soil types	ASTM D2487

The relative density, gradation, and fine content of cohesionless soils provide useful information in assessing pile drivability. Soils with a high fine content generally have lower angles of internal friction than lower fine content soils of similar density. A high fine content can also affect soil drainage and pore pressures during shear, and thus, the effective stresses acting on a pile during driving. Depending upon soil density, cohesionless soils with high fine contents are also more likely to

demonstrate soil setup than cohesionless soils with little or no fines. The gradation and angularity of the soil grains also influences the angle of internal friction. Gradation information is also useful in assessing the densification and liquefaction potential of cohesionless soils.

Routine laboratory grain size analyses (mechanical and hydrometer) can quantify gradation and fine content. With this information, improved assessments of pile drivability and soil setup potential in cohesionless soils can be made. Cohesive soils may lose a significant portion of their shear strength when disturbed or remolded, as during the pile driving process. The ability to estimate the soil strength at the time of driving and the resulting strength gain with time or soil setup is a key component of economical pile design in cohesive soils. Soil setup is discussed further in Chapter 7. The sensitivity of a cohesive soil can provide a qualitative but not quantitative indication of potential soil setup. Sensitivity determined in-situ with a vane shear device provides the best assessment of cohesive soil sensitivity. However, the sensitivity of a cohesive soil can also be determined from laboratory tests on undisturbed and remolded samples to determine respective shear strength values.

The sensitivity of a cohesive soil, S_t, is defined as:

$$S_t = \frac{q_u\ undisturbed}{q_u\ remolded} \qquad \text{Eq. 5-5}$$

Table 5-4 contains typical values of sensitivity as reported by Sowers (1979) which may be useful for preliminary estimates of remolded shear strength. Terzaghi and Peck (1967) noted that clays with sensitivities less than 16 generally regain a portion to all of their original shear strength with elapsed time. Based upon typical sensitivity values reported by Terzaghi et al. (1996) as well as by Sowers (1979), the remolded shear strength of many cohesive soils during pile driving would be expected to range from about 1/3 to 1/2 the undisturbed shear strength.

Table 5-4 Typical Values of Sensitivity (after Sowers 1979)

Soil Type	Sensitivity
Clay of medium plasticity, normally consolidated	2 – 8
Highly flocculent, marine clays	10 – 80
Clays of low to medium plasticity, overconsolidated	1 – 4
Fissured clays, clays with sand seams	0.5 – 2

Additional information on index testing of soil may be found in GEC-5 by Sabatini et al. (2002) as well as in Samtani and Nowatzki (2006). Section 5.4 provides additional insight and discussion on drivability considerations.

5.2.2 In-Situ Stress

For the design of driven piles, the in-situ state of stress at a given depth is needed to calculate geotechnical resistance. A basic assessment of stress calculation in soil is provided in this section. Further detail is provided in the literature including Sabatini et al. (2002), Samtani and Nowatzki (2006), and Das (2007) among other sources. The reader is directed to these resources for in depth coverage of this topic.

For geotechnical analyses, the effective soil stress is utilized for design. The effective stress, σ', is the difference of total stress, σ, and pore water pressure, u, and may be expressed as Equation 5-6.

$$\sigma' = \sigma - u \qquad \text{Eq. 5-6}$$

The total stress at a given depth is generally the product of total soil unit weight for each soil strata, γ_i, and strata thickness, h_i. Often multiple soils with ranges in unit weight exist at a given location. Therefore a summation of these layers accounts for the total stress calculation with depth as illustrated in Equation 5-7. Pore water pressure is a function of the unit weight of water, γ_w, and the pressure head, h_w, as shown in Equation 5-8.

$$\sigma = \sum_i^n (\gamma_i h_i) \qquad \text{Eq. 5-7}$$

$$u = \gamma_w h_w \qquad \text{Eq. 5-8}$$

The vertical effective stress at a given depth may be calculated as follows:

$$\sigma'_{vo} = \sum_i^n (\gamma_i h_i) - \gamma_w h_w \qquad \text{Eq. 5-9}$$

Above the water table, free draining, coarse grained soils may be assumed dry. More likely however, this soil is partially saturated, particularly in the vadose zone where negative pore water pressure results from capillary effects. Accurate soil unit weights should be therefore be reflected in this effective stress calculation. The lateral resistance for deep foundations is affected by the horizontal effective stress. Determination of the effective horizontal stress at a given depth, σ'_{ho}, condition may

be evaluated by relating the vertical effective stress and the at rest lateral earth pressure coefficient, K_o, using Equation 5-10.

$$K_o = \frac{\sigma'_{ho}}{\sigma'_{vo}} \qquad \text{Eq. 5-10}$$

Selection of effective stress or total stress usage for design is contingent upon the structural loading conditions and soil properties. For piles driven in free draining clean sands, an analysis would generally include the use of effective stress parameters since it may be assumed pore water pressure dissipates almost immediately after loading the soil. Conversely for clays or other slow draining soils, an increase in pore water pressure will be apparent immediately after loading. A total stress analysis may therefore be practical for this condition. The responsible engineer should exercise clear judgment involving loading conditions and the selection of design parameters.

5.2.3 Shear Strength

Shear strength is an internal resistance per unit area that the geomaterial can provide to resist failure along a plane. Compositional, environmental and in-situ factors combine to define the overall shear strength of a soil, which contributes to the geotechnical strength limit state for design. Geomaterial shear strength is also influenced by the manner (static, dynamic, cyclic) and rate of loading.

GEC-5 by Sabatini et al. (2002) notes several issues relevant to shear strength evaluations for driven pile designs. These include variation of the soil shear strength between the time the pile is driven and when load application occurs. Time dependent strength increases, referred to as soil setup, are often observed in saturated, normally consolidated to moderately over consolidated clays and fine-grained material. Conversely, a decrease in strength with time, referred to as relaxation, is often observed for heavily over consolidated clays, dense silts, dense fine sands, and weak laminated rock. Therefore, shear strength evaluations should consider both of these long and short term conditions.

Shear strength may also vary due to changes in site conditions that affect the in-situ effective stress state. Site conditions that may increase or decrease soil shear strength values include site dewatering, surface loading, and excavations. Granular soil strengths may also change over time due to densification from driving. This potential shear strength increase should be evaluated relative to pile drivability and constructability considerations.

The Mohr-Coulomb failure criterion will be the only model discussed herein and is shown in Equation 5-11.

$$\tau = c + \sigma \, tan \, \phi \qquad \text{Eq. 5-11}$$

Where:

- τ = shear stress at failure (shear strength).
- c = cohesion.
- σ = total normal stress (pressure) on plane of failure.
- ϕ = angle of internal friction.

Equation 5-11 is used for total stress analysis and uses an undrained friction angle and cohesion. For cases where effective stress or drained parameters are necessary, this equation is modified to Equation 5-12.

$$\tau = c' + \sigma' \, tan \, \phi' \qquad \text{Eq. 5-12}$$

Where:

- τ = shear stress at failure (shear strength).
- c' = effective cohesion.
- σ' = effective normal stress (pressure) on plane of failure.
- ϕ' = effective stress angle of internal friction.

In this drained situation, typically cohesionless soils exist, therefore *c'* is assumed equal to zero. However upon careful evaluation, *c'* may be included to account for certain conditions including cemented soils, partially saturated soils and heavily over consolidated clays. Determination of *c'* should be carefully selected on interpretation of the test data due to its strong influence on pile design results.

For short-term, undrained loading of cohesive soils, Equation 5-11 can be simplified to a total stress approach. Typically, cohesive soils exhibit a friction angle, ϕ, equal to zero, therefore Equation 5-13 reflects this behavior.

$$\tau = c = s_u \qquad \text{Eq. 5-13}$$

Where:

- τ = shear stress at failure (shear strength).
- c = cohesion.
- s_u = undrained shear strength.

In addition to the above mentioned case, rapid loading of slow draining (low permeability) soil generates excess pore water pressure that is not easily quantified. Moreover, to simplify the shear stress calculation, the cohesion determined via testing may be assumed equal to the design shear strength while in-situ states of stress, water content, loading rate, and other variables are unknown.

5.2.3.1 Laboratory Tests for Soil Shear Strength

Three test methods are commonly used to measure shear strength in the laboratory. A brief description of each test method is provided in the subsequent sections. Further details on the test procedure and analysis may be found in GEC-5 by Sabatini et al. (2002), as well as the respective ASTM designations. The three test methods are as follows:

1. Direct shear test (AASHTO T236 / ASTM D3080).

2. Unconfined compression test (AASHTO T208 / ASTM D2166).

3. Triaxial compression test (AASHTO T234 / ASTM D2850).

5.2.3.1.1 Direct Shear

The direct shear test is performed by placing a sample of soil into a shear box which is split into two parts at mid height. A normal load is then applied to the top of the sample and one half of the shear box is pulled or pushed horizontally past the other half. The shear stress is calculated from the horizontal force divided by the sample area and is plotted versus horizontal deformation. A plot of at least three normal stresses and their corresponding maximum shear stresses provides the shear strength parameters c and ϕ. Bowles (1977) notes that the ϕ values determined from plane strain direct shear tests are approximately 1.1 times the ϕ values determined from triaxial tests. Direct shear tests are primarily performed on recompacted granular soils, which may not represent their in-situ conditions, and are generally not recommended for cohesive soils due to limitations on drainage control during shear.

5.2.3.1.2 Unconfined Compression

The unconfined compression test is a widely used laboratory test to evaluate the shear strength of cohesive soil and rock. In the unconfined compression test, an axial load is applied on a cylindrical sample while maintaining a zero lateral or confining pressure. Axial loading is increased to failure and the shear strength is

then considered to be one half the axial stress at failure. Unconfined compression tests are performed only on cohesive soil and rock samples.

Unconfined compression tests on cohesive soil samples recovered from deeper depths or samples with a secondary structure, such as sand seams, fissures, or slickensides, can give misleadingly low shear strengths. This is due to the removal of the in-situ confining stress normally present. Triaxial compression tests provide improved information on soil shear strength in these cases.

5.2.3.1.3 Triaxial Compression Test

The most versatile shear strength test is the triaxial compression test. Triaxial tests allow a soil sample to be subjected to three principal stresses under controlled conditions. A cylindrical test specimen is encased in a rubber membrane and is then subjected to a confining pressure. Drainage from the sample is controlled through its two ends as the shearing force is applied axially and increased to failure. A plot of normal stress versus shear stress is developed and parameters c and ϕ are determined. In triaxial tests where full drainage is allowed during shear, or in undrained tests with pore pressure measurements during shear, the effective stress parameters c' and ϕ' can be determined.

In triaxial compression tests, the drainage, consolidation, and loading conditions are selected to simulate the applicable field conditions for the shear strength evaluation. Triaxial compression tests are classified according to the consolidation and drainage conditions allowed during testing. The three test types normally conducted are unconsolidated undrained (UU) (ASTM D 2850), consolidated undrained (CU) (ASTM D 4767), and consolidated drained (CD) (ASTM D 7181). Unconsolidated undrained tests provide more reliable shear strength values than those obtained from unconfined compression tests. Consolidated undrained tests with pore pressure measurements provide both effective stress and total stress parameters.

5.2.3.2 Effective Stress Friction Angle Correlations, Cohesionless Soils

For pile design in cohesionless soil, the effective internal friction angle is typically correlated from in-situ test results. Usually, the SPT N value or CPT cone resistance provides this relationship. Care should be exercised when using any SPT N value to soil parameter correlation. Depending upon the date and method, the correlation may be based on an uncorrected N value from a certain SPT hammer type or a corrected $(N_1)_{60}$. AASHTO (2014) design specifications note that the designer should ascertain the basis of the correlation and use $(N_1)_{60}$ or N, as appropriate. The

SPT $(N_1)_{60}$ correlation to ϕ' in AASHTO is presented in Table 5-5 and is the basis of the AASHTO resistance factors associated with the AASHTO calibrations.

Table 5-5 AASHTO (2014) Correlation Between SPT $(N_1)_{60}$ values to Drained Friction Angle of Granular Soils (modified after Bowles 1997)

SPT Blow Count, $(N_1)_{60}$ (blows/ft)	Angle of Internal Friction Φ' (degree)
< 4	25 - 30
4	27 - 32
10	30 - 35
30	35 - 40
50	38 - 43

FHWA GEC-5 (2002) provides a different correlation for effective friction angle based upon the SPT N value. This correlation, presented in Table 5-6, was originally tabulated in Meyerhof (1956) for relatively clean sands. Sabatini et al. (2002) in GEC-5 recommended ϕ' be reduced by 5° for clayey sand and increased by 5° for gravelly sand.

Table 5-6 Correlation Between Relative Density, SPT N value, and Internal Friction Angle for Cohesionless Soils in GEC-5 (2002) (after Meyerhof 1956)

State of Packing	Relative Density, D_r (%)	SPT Blow Count, N (blows/ft)	Angle of Internal Friction Φ' (degree)
Very Loose	< 20	< 4	< 30
Loose	20-40	4-10	30-35
Compact	40-60	10-30	35-40
Dense	60-80	30-50	40-45
Very Dense	> 80	> 50	> 45

Note: In saturated fine sand or silty sand, N = 15 + (N'-15) / 2 for N' > 15 where N is the blow count corrected for dynamic pore pressure effects during the SPT, and N' is the measured blow count.

Other correlation methods between corrected N values and laboratory test results have been published to provide drained friction angle equations for sands and gravels. Each method provides a correlation based upon the respective soil type, sampling method, and testing technique used.

Schmertmann (1975) assessed test data from clean sands and provides a correlation between friction angle, SPT N values and overburden stress. The data is interpreted for depths greater than 7-ft, for which Kulhawy and Mayne (1990) approximated a relationship as Equation 5-14.

$$\phi' = \tan^{-1}\left[\frac{N_{60}}{12.2+20.3\left(\frac{\sigma'_{vo}}{p_a}\right)}\right]^{0.34} \quad \text{Eq. 5-14}$$

Hatanaka and Uchida (1996) utilized ground freezing to extract undisturbed samples of fine and medium sands. After subjecting samples to drained triaxial compression tests, an effective friction angle correlation to $(N_1)_{60}$ was established as shown in Equation 5-15.

$$\phi' = \sqrt{20\ (N_1)_{60}} + 20 \quad \text{Eq. 5-15}$$

Kulhawy and Chen (2007) performed strength tests on samples of sand and gravel. Although this study was performed to assess the uplift capacity of drilled shafts, a variable spread of sands and gravels were analyzed, and compared well with the Meyerhof (1956) correlations. For the combined 57 samples, a regression analysis (r^2=0.356, n =57) provided the relationship in Equation 5-16.

$$\phi' = 27.5 + 9.2\log[(N_1)_{60}] \quad \text{Eq. 5-16}$$

Similar to correlations developed for the SPT, the effective friction angle may be compared to the CPT/CPTu generally via cone tip resistance, q_c. Meyerhof (1976) correlations are shown in Table 5-7 for relatively clean sands.

Table 5-7 Correlation Between Relative Density, CPT Cone Resistance, and Angle of Internal Friction for Clean Sands (after Meyerhof 1976)

State of Packing	Relative Density D_r (%)	Cone Tip Resistance q_c (tons/ft^2)	Angle of Internal Friction Φ' (degree)
Very Loose	< 20	< 4	< 30
Loose	20-40	4-10	30-35
Compact	40-60	10-30	35-40
Dense	60-80	30-50	40-45
Very Dense	> 80	> 50	> 45

Robertson and Campanella (1983) compared cone resistance to drained triaxial compression tests results on clean, quartz sands. Using the cone tip resistance, a relationship to effective friction angle was presented by Kulhawy and Mayne (1990). This is shown in Equation 5-17.

$$\phi' = \tan^{-1}\left[0.1 + 0.38\log\left(\frac{q_c}{\sigma'_{vo}}\right)\right] \qquad \text{Eq. 5-17}$$

Where:

ϕ' = effective stress angle of internal friction.
q_c = cone tip resistance.
σ'_{vo} = vertical effective stress at the sample depth.

For layers with cobbles and boulders, SPT N value correlations for the material friction angle can be problematic particularly when the material contains particles larger than the size of the split spoon sampler. The resultant inflated N values can result in overestimation of the friction angle of the rockfill materials. Therefore, the drained friction angle of rockfills, gravels, and sands can be estimated from Figure 5-10 using the appropriate rockfill grade from Table 5-8 in conjunction with the effective normal stress. The rockfill grades of A through E identified in Table 5-8 are based on the unconfined compressive strength of the rockfill particles. Once the rockfill grade is determined, a representative drained friction angle can obtained from Figure 5-10 using the average effective normal stress in the layer. The secant friction angle is based on a straight line constructed from the origin of the Mohr circle diagram to the intersection with the strength envelope at the effective normal stress as detailed in Terzaghi et al (1996).

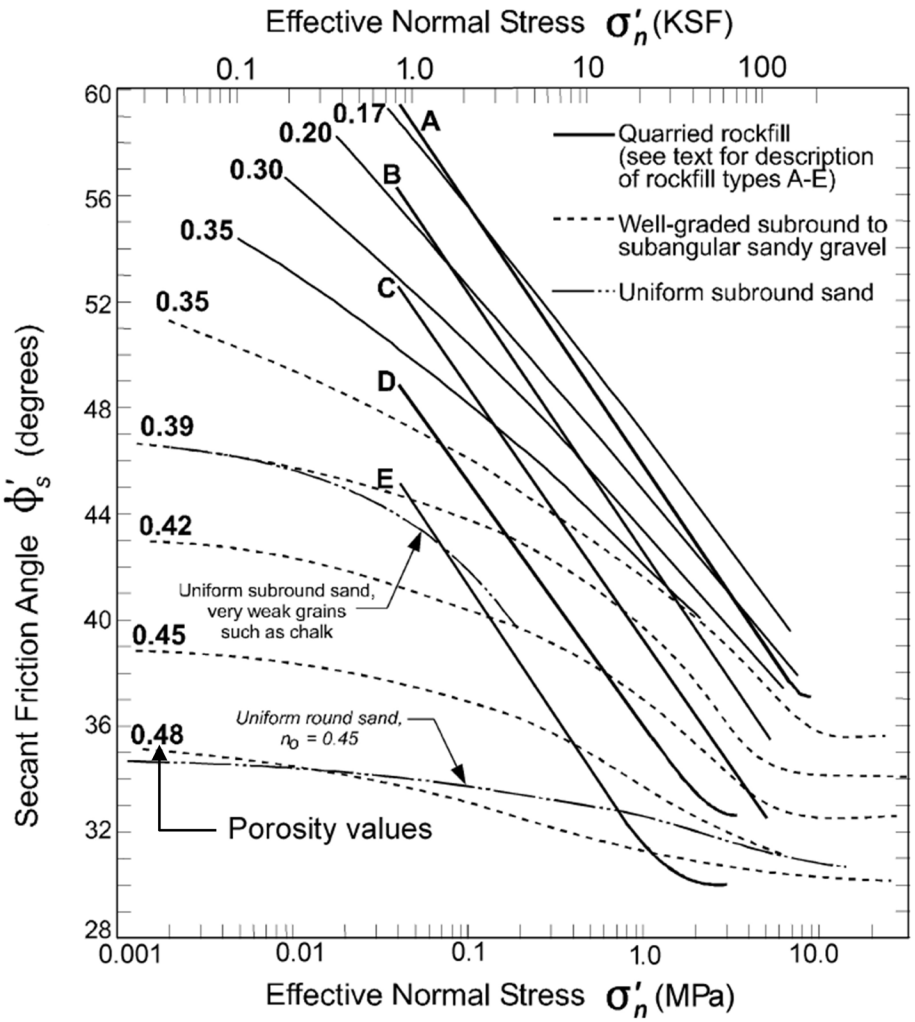

Figure 5-10 Typical ranges of friction angle for rockfills, gravels and sands (Note: 1 kPA = 0.145 psi) (after Terzaghi et al. 1996).

Table 5-8 Unconfined Compressive Strength of Particles for Rockfill Grades in Figure 5-12

Rockfill Grade	Particle Unconfined Compressive Strength (ksf)
A	≥ 4610
B	3460 – 4610
C	2590 – 3460
D	1730 – 2590
E	≤ 1730

5.2.3.3 Fully Drained Shear Strength of Fine-Grained Cohesive Soils

Effective stress analysis methods may be used for fine grained soils under fully drained loading. This approach is useful to assess driven pile resistances a significant time after pile installation when pore water pressure has stabilized. For these cases, laboratory testing is recommended by AASHTO (2014) to produce effective stress design parameters ϕ' and c'. Consolidated drained direct shear tests, consolidated drained (CD) triaxial tests or consolidated undrained (CU) triaxial tests with pore pressure measurements may be used to determine these shear strength parameters. Consideration for shear rate should be provided during these laboratory tests. Furthermore, complete dissipation of excess pore pressure for drained tests or equalization of pore pressure throughout the sample in undrained tests should be confirmed.

Preliminary estimates for effective friction angle may be interpreted from plasticity index (PI) tests. Terzaghi et al. (1996) assessed a range of clayey soils and shale to provide correlations between PI and effective friction angle. These results are presented in Figure 5-11. For these estimates FHWA GEC-5, Sabatini et al. (2002), recommends utilizing a cohesion value equal to zero (c' =0).

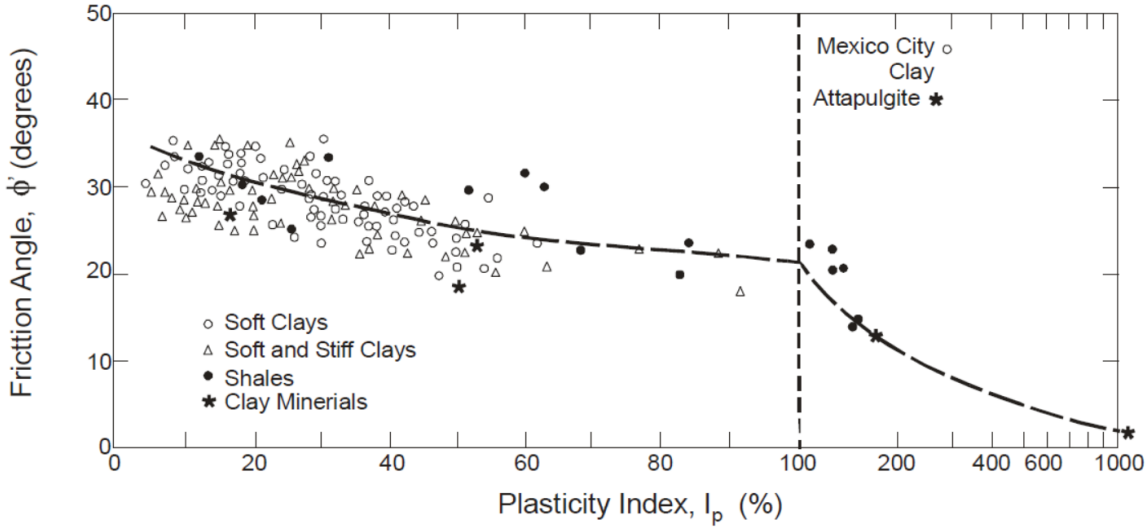

Figure 5-11 Relationship between ϕ' and PI (after Terzaghi et al. 1996).

5.2.3.4 Undrained Shear Strength of Fine-Grained Cohesive Soils

The undrained shear strength, s_u, of cohesive soils may be measured via laboratory testing or through correlations with in-situ tests. However, laboratory testing of undisturbed samples is recommended. This may be accomplished through simple

unconfined compression (UC) tests or by triaxial unconsolidated undrained (UU), or consolidated undrained (CU) testing. Sampler disturbance, strain rate variations and uncertain drainage conditions can affect shear strength results, although more conservative values are produced from these effects (Brown et al. 2010). CU triaxial tests offer the advantage of reconsolidating the sample to in-situ stress states before shearing, thus providing more representative shear strength values. AASHTO (2014) specifically recommends the use of CU and UU testing where possible.

For cases where undisturbed sampling is difficult or does not yield well preserved samples, in-situ testing may implemented as an alternative. A discussion of in-situ test methods is provided in Section 5.1. Common correlations between the CPT, SPT, and VST are provided below. Additional correlations may be found in GEC-5 by Sabatini et al. (2002) among other sources.

A CPT to s_u correlation is provided in Equation 5-18. Local calibration of N_k is recommended.

$$s_u = \frac{q_c - \sigma'_{vo}}{N_k} \qquad \text{Eq. 5-18}$$

Where:

q_c = cone tip resistance.
σ'_{vo} = vertical effective stress at the sample depth.
N_k = cone factor, typically 14 to 16, may vary from approximately 10 to 18.

A preliminary estimate of undrained shear strength can be made from a corrected SPT N value in combination with atmospheric pressure, and a correction factor, f_1, based on the plasticity index. Stroud (1974; 1989) utilized the f_1 empirical correction as follows:

$$s_u = \frac{f_1 N_{60} p_a}{100} \qquad \text{Eq. 5-19}$$

Where:

f_1 = 4.5 for PI = 50.
f_1 = 5.5 for PI =15.
p_a = atmospheric pressure.
N_{60} = SPT N value corrected for 60% energy transfer.

A preliminary estimate of s_u can also be made from uncorrected SPT N values (blows / ft). Table 5-9 contains an empirical relationship between the uncorrected SPT N value, unconfined compressive strength, and saturated unit weight for

cohesive soils. The undrained shear strength is one half of the unconfined compressive strength ($s_u = q_u / 2$). Correlation of N values to the undrained shear strength of clays is crude and unreliable for final design and as stated, should only be used for preliminary estimating purposes.

Table 5-9 Empirical Values for Unconfined Compressive Strength, q_u, and Consistency of Cohesive Soils Based on Uncorrected N- Value (after Bowles 1977)

Consistency	Very Soft	Soft	Medium	Stiff	Very Stiff	Hard
q_u, ksf	0 – 0.5	0.5 – 1.0	1.0 – 2.0	2.0 – 4.0	4.0 – 8.0	8.0+
Standard Penetration N value	0 - 2	2 - 4	4 – 8	8 - 16	16 - 32	32+
γ (saturated), lb/ft^3	100 – 120	100 – 120	110 – 130	120 – 140	120 – 140	120 – 140

The Vane Shear Test (VST) can be used for soft to medium clays and produces a correlation for s_u from the input torque, T_v, and vane diameter, d_v. During the VST both peak and residual shear strengths are measured, thus the sensitivity can be calculated (Equation 5-5). When the vane height to diameter ratio is equal to two, $h_v/d_v = 2$, a widely used relationship found in GEC-5 by Sabatini et al. (2002) is shown in Equation 5-20. Furthermore, Bjerrum (1972) developed a correction based on static equilibrium theory as shown in Equation 5-21.

$$s_u = \frac{6T_v}{7\pi(d_v)^3} \qquad \text{For } \frac{h_v}{d_v} = 2 \qquad \text{Eq. 5-20}$$

Where:

s_u = undrained shear strength.
T_v = input torque during shear.
d_v = vane diameter.
h_v = vane height.

$$\mu = 2.5(PI)^{-0.3} \leq 1.1 \qquad \text{Eq. 5-21}$$

Where:

μ = correction factor.
PI = plasticity Index.

5.2.4 Deformation

Deformation is a measure of the soil response to an applied load. For the design of driven piles, tolerable deformations relate to a structure's serviceability limit state. These values are obtained through tests that quantify strain to provide modulus and consolidation parameters.

5.2.4.1 Elastic Deformation

Modulus, *E*, is determined through direct measurement of a strain from an applied load via Hooke's Law (Equation 5-22) or through correlations with other laboratory and in-situ tests.

$$\sigma = E\varepsilon \qquad \text{Eq. 5-22}$$

Where:

σ = stress.
E = elastic modulus of material.
ε = strain.

A stress- strain curve developed for modulus determination is shown in Figure 5-12. In this figure, the origin and half the peak stress are designated as points to develop the 50% secant modulus, E_{50}.

Shear modulus, *G*, is sometimes used in load- deformation calculations and is related to the elastic modulus, *E*, and Poisson ratio, *v*, using Equation 5-23 below. Elastic deformation of soil will be further discussed in Chapter 7.

$$G = \frac{E}{2(1+\nu)} \qquad \text{Eq. 5-23}$$

A compilation of soil elastic modulus and poison ratio values have been made by Bowles (1988) and Department of the Navy (1982). These values were tabulated by AASHTO (2014) so that preliminary estimates of elastic soil deformation could be established. Correlations to corrected SPT N values and CPT cone resistance are also included. Testing should be performed to confirm or supersede these tabulated values. Table 5-10 to Table 5-12 are modified from AASHTO (2014).

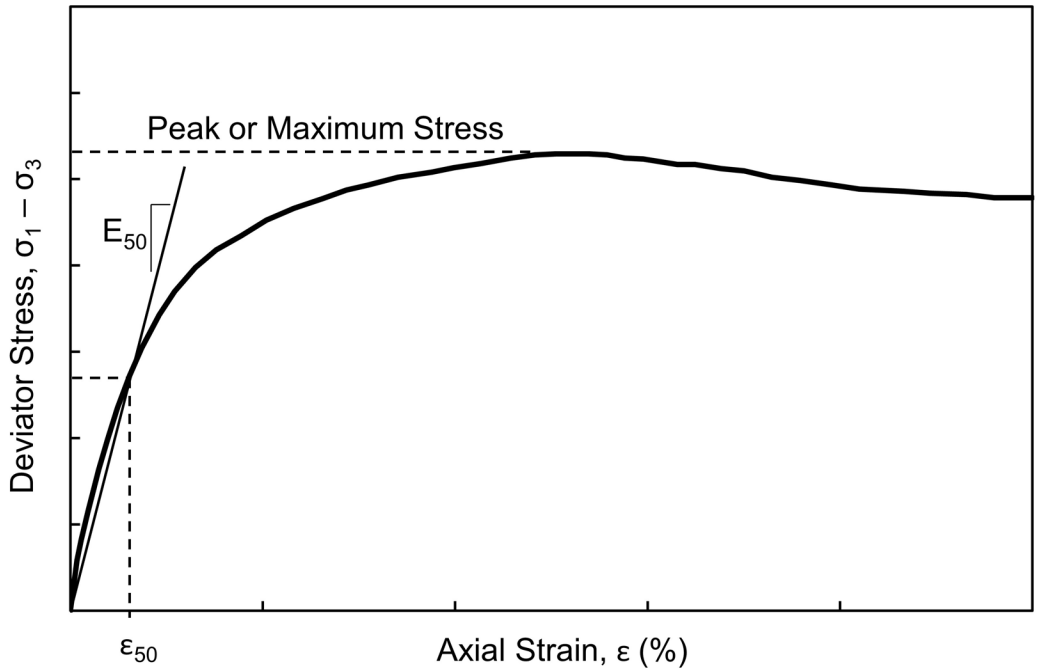

Figure 5-12 Soil stress strain curve and 50% secant modulus (after Brown et al. 2010).

Table 5-10 Estimating Soil Modulus, E_s, Based on Soil Type (after AASHTO 2014)

Soil Type	Typical Range of Young's Modulus, E_s (ksf)	Poisson Ratio, v
Clay:		
Soft Sensitive	50 – 300	0.40 – 0.50 (undrained)
Medium Stiff to Stiff	300 – 1,000	
Very Stiff	1,000 – 2,000	
Loess	300 – 1,200	0.10 – 0.30
Silt	40 – 400	0.30 – 0.35
Sand:		
Loose	200 – 600	0.20 – 0.36
Medium Dense	600 – 1,000	
Dense	1,000 – 1,6000	0.30 – 0.40
Gravel:		
Loose	600 – 1,600	0.20 – 0.35
Medium Dense	1,600 – 2,000	
Dense	2,000 – 4,000	0.30 – 0.40

Table 5-11 Estimating Soil Modulus, E_s, from SPT N value (after AASHTO 2014)

Soil Type	E_s (ksf)
Silts, Sandy Silts, Slightly Cohesive Mixtures	8 $(N_1)_{60}$
Clean Fine to Medium Sands, Slightly Silty Sands	14 $(N_1)_{60}$
Coarse Sands and Sands with Little Gravel	20 $(N_1)_{60}$
Sandy Gravels and Gravels	24 $(N_1)_{60}$

Table 5-12 Estimating Soil Modulus, E_s, from Cone Resistance, q_c (after AASHTO 2014)

Soil Type	E_s (ksf)
Sandy Soils	2 q_c

5.2.4.2 Primary Consolidation Settlement

A one dimensional consolidation test (AASHTO T216 / ASTM D2435) is often performed to estimate the amount and rate at which a cohesive soil deposit will consolidate under an applied load. This test provides consolidation parameters including the coefficient of consolidation, C_v, compression index, C_c, recompression or swell index, C_r (alternatively C_s), and secondary compression index, C_α.

For this test, a saturated soil sample is constrained laterally while being compressed vertically. The vertical compression is measured and related to the change in the soil void ratio. Loading the cohesive sample increases pore water pressure within the soil voids. Over a period of time, as the water is squeezed from the soil, this excess water pressure will dissipate resulting in the soil grains (or skeleton) supporting the load. The amount of water squeezed from the sample is a function of load magnitude and compressibility of soil deposit while the rate of pressure dissipation is a function of the permeability of the soil. Test background and analysis information may be found in numerous sources such as Bowles (1977), GEC-5, Sabatini et al. (2002), and Samtani and Nowatzki (2006).

The results from the test are used to plot void ratio, e, versus vertical effective stress, σ'_{vo}, on a semi log scale to determine the preconsolidation pressure, σ_p, and other quantities. An illustration of a typical e-log σ'_v curve is presented in Figure 5-13. A plot of log time versus sample compression is used to determine coefficient of consolidation. Consolidation test results can be used to estimate magnitude and

settlement rate of pile foundations in cohesive soils. Consolidation tests can also be plotted as the vertical strain, ε versus vertical effective stress, σ'_v, on a semi log scale.

Equations 5-24 to 5-26 utilize the results of consolidation testing to determine primary consolidation settlement of cohesive soil.

For normally consolidated ($\sigma'_{vo} = \sigma_p$) cohesive soil layers:

$$S_c = \sum_i^n \frac{C_c}{1+e_o} H_o \log\left(\frac{\sigma'_{vo}+\Delta\sigma}{\sigma'_{vo}}\right) \qquad \text{Eq. 5-24}$$

For overconsolidated soil with ($\sigma'_{vo} + \Delta\sigma \leq \sigma_p$):

$$S_c = \sum_i^n \frac{C_r}{1+e_o} H_o \log\left(\frac{\sigma'_{vo}+\Delta\sigma}{\sigma'_{vo}}\right) \qquad \text{Eq. 5-25}$$

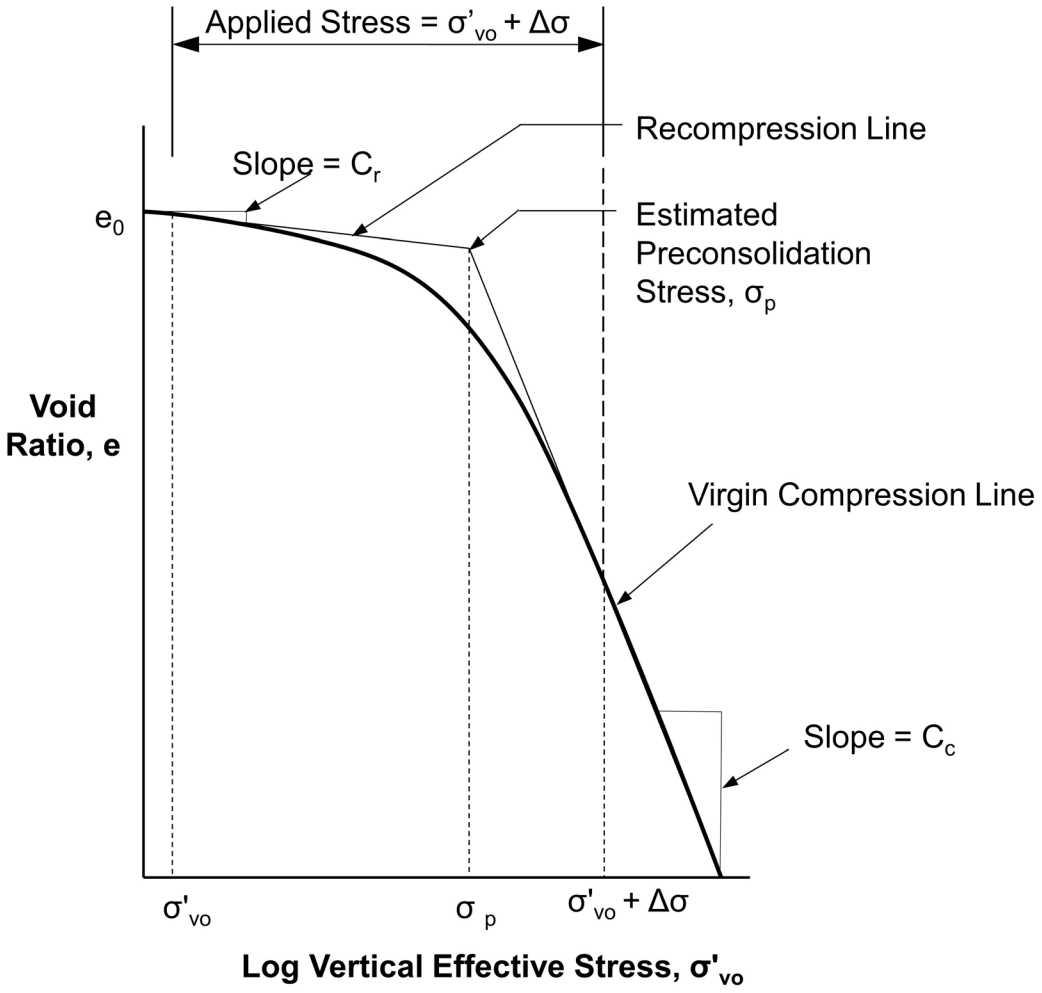

Figure 5-13 Plot of Void Ratio vs Vertical Effective Stress from consolidation test.

For overconsolidated soil with ($\sigma'_{vo} + \Delta\sigma > \sigma_p$):

$$S_c = \sum_i^n \frac{C_r}{1+e_o} H_o \log\left(\frac{\sigma_p}{\sigma'_{vo}}\right) + \frac{C_c}{1+e_o} H_o \log\left(\frac{\sigma'_{vo}+\Delta\sigma}{\sigma_p}\right) \quad \text{Eq. 5-26}$$

Where:

S_c = settlement from primary consolidation.
e_o = initial soil layer void ratio.
H_o = initial soil layer thickness.
σ_p = preconsolidation stress.
σ'_{vo} = average vertical effective stress at the mid-point of the soil layer before loading.
$\Delta\sigma$ = additional stress at mid-point of soil layer from loading.

5.2.5 Electro Chemical Properties

The soil and groundwater can contain constituents detrimental to pile materials. Electro chemical classification tests can be used to determine the aggressiveness of the subsurface conditions and the potential for pile deterioration. For pile design, corrosion rates for steel piles or disintegration rates for concrete may be required to evaluate long term structural resistance. These electro chemical tests include:

a. pH (AASHTO T289 / ASTM D4972).

b. Resistivity (AASHTO T288 / ASTM D1125).

c. Sulfate ion content (AASHTO T290 / ASTM D4230).

d. Chloride ion content (AASHTO T291 / ASTM D512).

Additional discussions on the influence of environmental conditions on pile section selection are presented in Section 6.14 of Chapter 6.

5.3 ROCK PARAMETERS

For the design of driven piles, rock property determination is necessary to assess end bearing resistance as well as long term deformation. Shallow rock profiles may necessitate predrilling pile locations into these materials to satisfy minimum penetration requirements. A designer's understanding of rock classification and associated rock characteristics is therefore essential. To properly classify and rate a given quantity of rock, a distinction between intact rock and rock mass should be

noted (Brown et al. 2010). Intact rock is a collection of consolidated and cemented particles forming rock material, where rock core samples are used to determine index and strength properties. Joints, faults, and other bedding features serve to break up intact rock, therefore this inclusive system combines to form a rock mass.

5.3.1 Rock Index Properties and Classification

When designing foundations that bear on rock, proper rock classification is essential. Physical and chemical properties of the rock should be noted during the subsurface exploration as the rock mass quality may affect design and construction. Rock classification should include color, texture, lithology (e.g. igneous, metamorphic, or sedimentary), field hardness, weathering, and geologic discontinuities.

The slake durability test (ASTM D4644) is useful to assess if rock will weather and deteriorate. The slake durability test is useful for weak rocks including shale, mudstone, and siltstone. These deposits are particularly susceptible to weathering or fracturing during the pile driving process. Low slake durability index results may help identify deposits in which driven piles are subject to relaxation.

The slake durability test requires representative rock fragments be dried to a constant weight in a wire mesh drum. After submerging and rotating the drum with containing rock fragments for 10-minutes in water, the sample is again dried to constant weight. This process is repeated a second time, and the ratio of final to initial dry weights results in the slake durability index, I_D. An I_D of less than 60% correlates to a rock prone to rapid degradation.

5.3.2 Rock Mass Shear Strength

Rock shear strength is typically measured in the laboratory through uniaxial compression testing where recovered core samples are prepared and subjected to loading in accordance with ASTM D7012. As load is applied during this test, axial strain is measured and plotted to determine the elastic modulus. The peak load is divided by the specimen's cross sectional area to provide an unconfined compressive strength, q_u. AASHTO and other methods for determining the nominal resistance of end bearing piles on rock utilizes the rock unconfined compressive strength.

5.3.3 Rock Mass Deformation

Rock deformation is typically elastic. Laboratory uniaxial compression test results can provide information on modulus values if rock deformation calculations are required. Rock deformation for most rock formations is generally not a design consideration as piles typically penetrate into weak rock or terminate on hard rock. If heavily loaded piles are terminated just into or above soil-like weak rock formations such as marl, rock mass deformation properties may be needed for design. To estimate the modulus values for rock, the designer should consider the RQD, GSI, and core recovery and use correlations of these parameters with rock mass modulus.

As noted in the previous section, the material modulus, E, is measured by plotting load versus strain during the uniaxial compression test. Careful axial and diametrical measurements also yield the material's Poisson ratio, v. The modulus is the slope of the stress-strain curve. Figure 5-12 utilizes a 50% secant modulus, E_{50}, where a stress value equal to one-half of the maximum deviator stress was selected. Test result tables complied by Kulhawy (1978) for numerous rock types have been in use to estimate elastic modulus and Poisson ratio. These tables are reproduced in a number of manuals including Samtani and Nowatzki (2006) and Table C10.4.6.5-1 of AASHTO (2014).

5.4 CONSIDERATIONS FOR PILE DRIVABILITY

AASHTO Article 10.7.8 stipulates that an evaluation of pile drivability should be performed during the design stage. Pile drivability is defined as the ability to drive the pile to the estimated nominal axial resistance anticipated during driving at or above the required penetration depth and to achieve penetration requirements within the driving stress limits of the pile material. To satisfy this objective, a detailed identification of the subsurface conditions and a thorough understanding of the soil behavior and its response to pile installation are needed.

Some subsurface issues that influence drivability are fairly obvious such as the presence of boulders above the bearing strata that increase the risk of pile damage or the identification of artesian conditions that can result in reduced geotechnical resistances. Other factors such as fine content, angularity, density, as well as high soil plasticity can all have a significant influence on drivability.

Cases of large soil quakes or high elastic behavior have been reported in dense silty sand, hard silty clay, glacial tills and other fine grained saturated soils (e.g., Likins 1983; Hannigan 1985; Hussein et al. 2006). Furthermore, Cosentino et al. (2010) researched cases of high rebound soils for the Florida DOT. High rebound is an effect of increased pore water pressure due to driving generally occurring near the pile toe. As driving continues, pore water pressure increases and causes a larger elastic response and rebound, leading to refusal driving conditions. If pile driving is paused, the pore water pressure dissipates and subsequently smaller rebound occurs. The research performed on the Hawthorn Group formation, a Florida soil formation, determined that high silt content and N value changes within the strata appeared to have strong correlations with soil zones of high elastic rebound.

Some sand deposits have also exhibited high dynamic resistances during pile driving. Thompson and Goble (1988) summarized details from nine projects that had this behavior. Unfortunately no clear relationship was identified between soil deposition, geologic, or mineralogical characteristics. This suggests drivability assessments should consider a range in dynamic soil properties rather than a specific value. Similarly, a range of dynamic soil properties should be evaluated in drivability analyses in highly plastic CH and MH soils where conventional values may underestimate the dynamic soil resistances encountered in these materials.

For certain weathered rock such as shale and siltstone, competent material is typically encountered during initial drive. However, a reduction in pile end bearing resistance can occur with time due to the release of locked in horizontal stresses in the laminated rock. Driving of adjacent piles to the same depth or below previously installed piles can also shatter the weak rock causing a reduction in end bearing resistance. Because rock types vary by region, local experience and analysis methods are advantageous in this regard.

5.5 SELECTION OF PARAMETERS FOR DESIGN AND CONSTRUCTION

Soil and rock parameters should be carefully selected based on site specific in-situ and laboratory testing results and relevant design methods for driven pile foundations. In some cases, resistance factors were developed for a specific design methodology based on a specific correlation approach between N and ϕ, between N and s_u, or a design method limit on the maximum friction angle.

5.5.1 Soil Parameters

Preliminary estimates of the soil shear strength and density parameters are often made from published correlations with SPT N values. Many of these correlations were provided in Section 5.2.3.3 and 5.2.3.4. While these correlations are very useful for preliminary design assessments, soil parameter confirmation and refinement should be obtained through additional in-situ and laboratory tests. Parameter variability for each layer must be considered for final soil parameter selection and final design. The shear strength, compressibility and index properties of each layer should be adequately quantified for design.

In coarse granular deposits, the selection of the design friction angle should be done conservatively. A comparison of nominal resistances from static load test results with static analysis predictions indicates that static analyses often overpredict the shaft resistance in these deposits. This is particularly true for coarse granular deposits comprised of uniform sized or rounded particles. Cheney and Chassie (1993) recommended limiting the shearing resistance by neglecting particle interlock forces. For shaft resistance calculations in gravel deposits, this results in a maximum ϕ' angle of 32° for gravels comprised of soft rounded particles, and in a maximum ϕ' angle of 36° for hard angular gravel deposits. The ϕ' angle used to calculate the toe resistance is determined using normal procedures.

Final design methods are often selected based on a given foundation type or from prior satisfactory design experience with the design method in similar subsurface conditions. The soil parameters required for method use must be acquired during the subsurface exploration program. Necessary parameters may include USCS classification, moisture content, density, grain size distribution, and Atterberg limits in addition to shear strength and compressibility information. In AASHTO Article 10.4, resistance factors have been developed for specific design method equations using specific procedural guidance. Hence, the soil parameters necessary to perform the analyses should be obtained in the prescribed manner. Design methods are discussed further in Chapter 7.

5.5.2 Rock Parameters

Design parameters for rock must be determined for piles driven either into soft rock or to hard rock. Rock cores should be collected for both soft and hard rock layers and the extent of rock weathering and fracturing should also be determined. The value of local experience with a given rock mass behavior cannot be overstated, as regional rock formations pose their own unique features.

A clear definition of soft and hard rock is not available in technical literature, in AASHTO, or in other building codes. In many intact rock classification systems, the transition between hard soil and soft rock occurs at an unconfined compression strength, q_u, of around 20 ksf. Similarly, the transition between soft rock and hard rock occurs between unconfined compression strength of 200 and 1000 ksf. In driven pile design and construction, soft rock is defined as rock that can be penetrated by pile driving and hard rock is defined as rock that cannot be penetrated. Hence, piles are driven into soft rock and driven to hard rock.

Soft and weak rocks are difficult materials to sample, test, and quantify. They have shear strengths greater than that of conventional soils and less than hard rock. Soft rock strengths can be too strong to be tested in soil laboratory equipment and too weak to be tested in rock mechanics equipment. Soft rocks often exhibit additional problematic characteristics such as crumbling, laminations, disaggregation, high plasticity, slaking, and variable strengths depending on weathering. All of these considerations complicate determination of representative parameter selection for pile design in soft rocks. Usual types of soft rock were identified by Kanji (2014) and are listed in Table 5-13.

Table 5-13 Usual Types of Soft Rocks (after Kanji 2014).

Rock Classification	Subclasses
Sedimentary Rocks	Mudstones, shales, siltstones, sandstones, conglomerates, breccias, marl, limestone, dolomites, gypsum, coal, salt rock, carnallite,
Igneous Rocks	Volcanic breccias and lahars, basaltic breccias, pyroclastic deposits, volcanic ash, tuff, igimbrite, and weathering products of crystalline rocks (granite, gneiss)
Metamorphic Rocks	Slate, phyllite, schists, quartzite little cemented, and metavolcanic deposits.

As noted above, piles can be driven into soft and weak rocks. In these materials, rock classification, core recovery, RQD, unconfined compression strength, density, and slake durability index parameters should be quantified. Piles cannot be driven into hard rock as pile toe damage or yielding occurs before hard rock failure. As with soft and weak rocks, rock classification, core recovery, RQD, unconfined compression strength, and density parameters should be quantified for pile designs on hard rock.

5.5.3 Site Variability

After a thorough site investigation and characterization of material properties, a subsurface profile is then generated for design and constructability purposes. Often times, throughout a relatively uniform soil model, results of laboratory tests and in situ tests present conflicting information. Soil cohesion, relative density and permeability among other properties may vary within a given strata along a horizontal plane or with depth. Final selection of material parameters then becomes reliant upon the use of engineering judgment.

Chapter 8 of GEC-5, Sabatini et al. (2002), provides a detailed overview of incorporating engineering judgment into the selection of design parameters when site variability is encountered. When facing situations of this nature, the Engineer can reevaluate subsurface parameters by either (1) locating inconsistencies with reported test results or (2) using historical information (i.e. experience, published data) to assess the inherent site variability.

Site variability relates to the variability within similar site conditions of the same site, not between sites. Furthermore, determination of site variability should be performed for each substructure location. When pile designs are prepared (Chapter 7 and 8), they are done so with respect to the encountered subsurface conditions which directly correlate to performance criteria for construction and the resulting structure. Generally, the nearest boring(s) or in-situ test(s) are utilized for this purpose. Judgment may be applied when establishing a subsurface profile. However, the following three steps provided in Paikowsky et al. (2004) serve to aide this process.

1. Relate each significant bearing layer and determine average parameters used for strength analysis at each boring location.

2. Check the Coefficient of Variation (COV) between the average values for each identifiable significant layer obtained at each boring location.

3. Categorize site variability based on COV as low, medium, or high.

    a. COV < 25% - Low
    b. 25% ≤ COV < 40% - Medium
    c. 40% ≤ COV – High

When analysis results yield a high COV, additional tests, different tests, engineering judgement, or further division of the project site into smaller less variable sub-sites may be required.

A larger statistical analysis of design parameters can also serve as a means to identify variability. For this, a database of similar geomaterials is constructed with the goal of assessing variation within a particular property and the effect on the project at large. Duncan and Wright (2005) compiled Table 5-14 based on the variability of geotechnical properties from in situ tests. They present the COV for a select number of soil parameters, which have been compiled from a number of sources. It should be noted that these values are obtained from projects covering a wide range of material, and this should not be applied to specific cases.

Sabatini et al. (2002) suggests the use of statistics and sensitivity analyses as a minimum practice for design parameter selection. Based on reported test results, determination of the sample mean and standard deviation is a relatively straightforward process. The COV is a statistical measure of the extent of variability and is calculated by dividing the sample standard deviation by the sample mean. By applying these statistics to a sensitivity study for design methods, the influence of a given design parameter can be assessed. Several designs can then be completed efficiently with the use of computer software or spreadsheets.

Table 5-14 Coefficients of Variation for Geotechnical Properties and In-Situ Tests (after Duncan and Wright 2005)

Property or In-Situ Test	COV (%)
Unit Weight (γ)	3 - 7
Buoyant Unit Weight (γ')	0 - 10
Effective Stress Friction Angle (ϕ')	2 - 13
Undrained Shear Strength (s_u)	13 - 40
Undrained Strength Ratio (s_u/σ'_{vo})	5 - 15
Standard Penetration Test N value (N)	15 - 45
Electric Cone Penetration Test (q_c)	5 - 15
Mechanical Cone Penetration Test (q_c)	15 - 37
Dilatometer Test Tip Resistance (q_{DMT})	5 - 15
Vane Shear Test Undrained Strength (s_u)	10 - 20

5.6 GEOTECHNICAL REPORTING

Upon conclusion of the site characterization program, the geotechnical engineer summarizes the factual data and prepares a geotechnical report. Three types of geotechnical reports are appropriate for driven piles: 1) geotechnical data reports; 2) geotechnical foundation design reports; and 3) geotechnical baseline reports. The type of geotechnical report prepared depends on project type and owner requirements.

Geotechnical data reports simply document and transmit a record of the exploration performed and the collected data. These data reports may be used on conventional Design-Bid-Build or Design-Build projects. Other agencies prefer foundation design reports that include the results of the subsurface exploration program as well as an assessment of the subsurface conditions with supporting design recommendations. The third type of report, a geotechnical baseline report, provides a contractual understanding of the subsurface conditions to be expected during construction. Geotechnical baseline reports are relatively uncommon on driven pile projects but are increasing in use particularly on Design-Build projects with highly variable site conditions. Dwyre et al. (2010) provides suggested guidelines for the application of geotechnical baseline reports to foundation projects. The various methods of geotechnical reporting are discussed in greater detail in the subsequent sections. Table 5-15 summarizes the decisions in driven pile design and construction that are influenced by the subsurface conditions.

5.6.1 Geotechnical Data Reports

A Geotechnical Data Report (GDR) contains only factual information from the performed site exploration. This includes a description of the geologic setting, site exploration program, and field and laboratory testing program. Also included are completed boring logs as well as field and laboratory test results. The GDR does not offer subsurface interpretations, or design recommendations, and is typically used when a subcontracted consultant performs the field exploration and associated soil or rock testing for the foundation designer. Information included in Geotechnical Data Reports is summarized in Table 5-16. The Owner's design team is responsible for interpreting the GDR. For design-build projects, the GDR may be used for construction bidding and must be included as a Contract Document.

Table 5-15 Pile Foundation Decisions Influenced by Subsurface Information

Decisions	Subsurface Information
Project Constraints and Auxiliary Equipment	Old foundations, boulders, obstructions. Site accessibility and terrain. Site constraints, overhead and underground utilities, adjacent buildings.
Pile Type and Accessory Selection	Subsurface strata and installation conditions. Structural resistance needs. Geotechnical resistance available. Pile lengths. Need for pile splices. Bedrock type and depth. Water table. Coatings due to aggressive or abrasive environment. Pile driving shoes.
Pile Driving Equipment Selection	Hammer type requirements. Hammer size and energy requirements. Crane, leads, template, and other equipment. Drilling equipment, augers, spuds, jets.
Construction Control	Hammer energy control. Resistance determination method. Time dependent soil strength changes.

Table 5-16 Information Included in Geotechnical Data Reports
(after Brown et al. 2010)

Background Information	Overview of project (bridge, structure, retaining wall, or other facility. General site conditions (geology, topography, drainage, accessibility). Specific methods used for site exploration.
Scope of Site Exploration	Plans showing location of all borings, test pits, and in-situ test locations. Number, locations, and depths of all borings and in-situ tests. Types and frequency of samples obtained; standards used. Types and numbers of laboratory tests; standards used. Subcontractors performing the work and dates of work.
Data Presentation	Final logs of borings and test pits. Water level readings and other groundwater data. Data tabulations and plots from each in-situ test hole. Summary tables and data sheets for lab tests performed. Photographs of rock core. Results of geophysical tests. Geological mapping data sheets and summary plots. Existing information from previous site explorations (boring logs, data).

5.6.2 Geotechnical Foundation Design Reports

A foundation design report is prepared to present the results of the subsurface explorations, laboratory test data, analysis, and specific design and construction recommendations for the foundation system of a structure. A foundation design report includes all the information noted in Table 5-16. In addition, the foundation design report includes an assessment of the subsurface conditions, identifies the soil and rock stratigraphy, provides design parameters for each soil and rock layer, presents analyses performed and their results, and provides recommendations for foundation design and construction. The report should make a clear distinction between factual and interpretive information. Foundation design reports are referred to frequently during the design and construction period as well as in resolving post construction issues such as claims. It is therefore important that the foundation design report be clear, concise and accurate. The foundation report is a very important document and should be prepared and reviewed accordingly.

Preliminary design recommendations based on, and/or transmitted with initial subsurface data does not constitute a foundation design report. A foundation design report must address each design issue such as axial compression resistance, uplift resistance, settlement, lateral resistance and response to lateral loading, seismic, scour, etc., in accordance with applicable limit state design methodologies. Only with this information can a foundation design report be prepared with appropriate content and quality.

The parts of a foundation design report are described below, and are modified from Cheney and Chassie (2000).

I. Table of Contents.

II. Introduction.
    1. Summary of proposed construction, including factored foundation loads.
    2. Summary of applicable extreme event limit states and loads.
    3. Foundation performance criteria (total and differential settlements, lateral deformation).
    4. Hydraulic information (if applicable).
    5. Summary of site constraints including accessibility, environmental restrictions (noise, vibrations, contaminated soil or groundwater, marine mammals, fish, wildlife), utility conflicts, as well as any limitations on headroom or equipment.

III. Scope of Explorations.
    1. Field explorations (summary of dates and methods, appended results).
    2. Laboratory testing (summary of types of tests, appended results).

IV. Interpretation of Subsurface Conditions.
    1. Description of formations.
    2. Soil types.
    3. Rock types.
    4. Dip and strike of rock.
        a. Regional.
        b. Local.
    5. Water table data.
        a. Perched.
        b. Regional.
        c. Artesian.

V. Geomaterial Design Parameters. (Narrative to describe procedure for evaluating factual data to establish design values for all soil and rock layers).
   1. Shear strength.
   2. Compressibility.
   3. Design analysis.

VI. Description of Design Procedures.
   1. Summary of results.
   2. Explanation of interpretation.

VII. Geotechnical Conclusions and Recommendations.

Pile foundations.
   1. Type of pile geotechnical resistance: shaft resistance, toe resistance, or both.
   2. Delineation of unsuitable layers due to compressibility, scour, or liquefaction.
   3. Suitable pile types: reasons for choice and/or exclusion of types and optimization of the recommended section.
   4. Estimated pile toe elevation, (average estimated values with probable variation potential).
   5. Estimated pile lengths.
   6. Minimum pile penetration (AASHTO Article 10.7.7 summarizes reasons why a minimum penetration depth could be specified to satisfy all applicable limit states).
   7. Nominal axial compression and axial tension resistances. Lateral load resistance and deformation.
   8. Location of the neutral plane and drag force.
   9. Estimated pile group settlement. Very important for pile groups in cohesive soils and large groups in a cohesionless soil deposit underlain by compressible soils.
   10. Number of test piles and specific test pile locations for maximum utility.
   11. Static pile load tests. If used, specify test locations for maximum utility.
      a. Axial compression.
      b. Axial tension.
      c. Lateral.
   12. Dynamic pile load tests. If used, specify test locations and restrike time and frequency.
   13. Rapid load tests. If used, specify test locations.

14. Resistance determination method (driving criteria). Nominal driving resistance depends on the resistance determination method per AASHTO Table 10.5.5.2.3-1.
15. Nominal driving resistance.
16. Pre-boring, pile toe reinforcement, or other requirements to reach pile penetration requirements or handle potential obstructions.
17. Pile driving requirements: hammer size, alignment and location tolerances, sequence of driving, etc.
18. Cofferdams and seals; seal design should consider potential conflicts between batter piles driven at alignment tolerance limits and depth of sheeting. Group densification inside sheeting for displacement piles in sands, or heave for displacement piles in clays should be considered.
19. Corrosion effects or chemical attack; particular concern in marine environments, old dumps, areas with soil or groundwater contaminants.
20. Effects of pile driving on adjacent construction; settlements from vibrations and development of excess pore water pressures in soil.
21. Other pile foundation construction issues.
    a. Conflicts with existing foundations, foundation remnants, or other obstructions.
    b. Cobbles and boulders.
    c. Groundwater control and/or pile cap excavation stability.

VIII. Appendix: Graphic Presentations.

1. Map showing project location.
2. Detailed plan of the site showing proposed structure(s) borehole locations and existing structures.
3. Laboratory test data.
4. Finished boring logs and interpreted soil profile.

IX. Report Distribution.

Copies of the completed Foundation Report should be transmitted in accordance with agency protocol.

The foundation report should be widely distributed to design, construction and maintenance engineers involved in the project. The foundation report should also furnish information regarding anticipated construction problems and solutions. This will provide a basis for the contractor's cost estimates.

On conventional design-bid-build contracts, the foundation design report should be completed and available to the designer prior to final design. The foundation drawings, special provisions, and foundation design report should all be cross-checked for compliance upon completion of final design documents. Conflicts between any of these documents greatly increase the potential for construction problems. For design-build contracts, factual data is provided by the owner to the design-build team that then performs the final geotechnical exploration and foundation design report.

5.6.3 Geotechnical Baseline Reports

Uncertainties in subsurface construction and resulting claims resulted in the concept of a Geotechnical Baseline Report (GBR). This concept originated in the tunneling industry where due to the linear nature of construction activities an unexpected condition disrupting construction quickly had significant cost and schedule implications. Geotechnical Baseline Reports establish a single source document where the geotechnical conditions to be expected (or assumed) are established on a contractual basis. This allows the Owner and Contractor to allocate geotechnical construction risk according to the established baseline of expected subsurface conditions. Risks associated with subsurface conditions equivalent to or better than the baseline conditions are borne by the contractor and risk associated with more severe subsurface conditions are allocated to the owner.

A GBR represents what is assumed that will be encountered for contract purposes. Baselines stated in the GBR should be well defined, reasonable and realistic. These should be derived from the site exploration performed, and/or local experience, and provide rational for specific requirements, designs or methods to be used. A GBR is not a warranty. It does provide a legal foundation for differing site condition claims. An example of a GBR statement relative to pile driving would be “Obstructions will be encountered between EL 610 and EL 605. For baseline purposes, these obstructions are reinforced concrete footing rubble, up to 3 feet thick, covering 15% of the substructure footprint at Pier 4.”

A GDR also provides a summary of the site characterization and expected subsurface conditions. For projects where both a GDR and GBR exist, a GBR should take precedence over a GDR in the hierarchy of contract documents. More information on the GBR concept may be found in Essex (2007).

REFERENCES

Acker, W.L. III, (1974). Basic Procedures for Soil Sampling and Core Drilling, Acker Drill Company, Inc., Scranton, PA, 246 p.

American Association of State Highway and Transportation Officials (AASHTO). (2014). AASHTO LRFD Bridge Design Specifications, US Customary Units, Seventh Edition, with 2015 Interim Revisions. American Association of State Highway and Transportation Officials, Washington, D.C., 1960 p.

ASTM D1452-09. (2014). Standard Practice for Soil Exploration and Sampling by Auger Borings. Annual Book of ASTM Standards, Vol. 4.08, ASTM International, West Conshohocken, PA, 6 p.

ASTM D1586-11. (2014). Standard Test Method for Standard Penetration Test (SPT) and Split-Barrel Sampling of Soils. Annual Book of ASTM Standards, Vol. 4.08, ASTM International, West Conshohocken, PA, 9 p.

ASTM D1587-12. (2014). Standard Practice for Thin-Walled Tube Sampling of Soils for Geotechnical Purposes. Annual Book of ASTM Standards, Vol. 4.08, ASTM International, West Conshohocken, PA, 4 p.

ASTM D2113-14. (2014). Standard Practice for Rock Core Drilling and Sampling of Rock for Site Investigation. Annual Book of ASTM Standards, Vol. 4.08, ASTM International, West Conshohocken, PA, 20 p.

ASTM D2573-08. (2012). Standard Test Method for Field Vane Shear Test in Cohesive Soil. Annual Book of ASTM Standards, Vol. 4.08, ASTM International, West Conshohocken, PA, 8 p.

ASTM D4633-10. (2014). Standard Test Method for Energy Measurement for Dynamic Penetrometer. Annual Book of ASTM Standards, Vol. 4.08, ASTM International, West Conshohocken, PA, 7 p.

ASTM D4719-07. (2014). Standard Test Methods for Prebored Pressuremeter Testing in Soils Annual. Annual Book of ASTM Standards, Vol. 4.08, ASTM International, West Conshohocken, PA,10 p.

ASTM D4971-02. (2014). Standard Test Method for Determining the In Situ Modulus of Deformation of Rock Using the Diametrically Loaded 76-mm (3-in.) Borehole Jack. Annual Book of ASTM Standards, Vol. 4.08, ASTM International, West Conshohocken, PA, 7 p.

ASTM D5778-12. (2014). Standard Test Method for Electronic Friction Cone and Piezocone Penetration Testing of Soils. Annual Book of ASTM Standards, Vol. 4.08, ASTM International, West Conshohocken, PA, 20 p.

ASTM D6635-07. (2014). Standard Test Method for Performing the Flat Dilatometer. Annual Book of ASTM Standards, Vol. 4.09, ASTM International, West Conshohocken, PA, 16 p.

ASTM D7012-14. (2014). Standard Tests Method for Compressive Strength and Elastic Moduli of Intact Rock Core Specimens under Varying States of Stress and Temperatures. Annual Book of ASTM Standards, Vol. 4.09, ASTM International, West Conshohocken, PA, 9 p.

ASTM Vol 4.08. (2014). Soil and Rock I, Vol. 4.08, ASTM International, West Conshohocken, PA, 1826 p.

ASTM Vol 4.09. (2014). Soil and Rock II, Vol. 4.09, ASTM International, West Conshohocken, PA, 1754 p.

Bowles, J.E. (1977). Foundation Analysis and Design. Second Edition, McGraw-Hill Book Company, Blacklick, OH, 750 p.

Bowles, J E. (1992). Engineering Properties of Soils and Their Measurement. Fourth Edition. New York: McGraw-Hill, 480 p.

Brown, D. A., Turner, J.P. and Castelli R.J. (2010). Drilled Shafts: Construction Procedures and LRFD Design Methods, FHWA-NHI-10-016, Geotechnical Engineering Circular (GEC) No. 10. U.S. Dept. of Transportation, Federal Highway Administration, 970 p.

Cheney, R.S. and Chassie, R.G. (2000). Soils and Foundations Workshop Reference Manual. FHWA HI-00-045, U.S. Department of Transportation, National Highway Institute, Federal Highway Administration, Washington, D.C., 358 p.

Cosentino, P.J., Kalajian, E., Misilo III, T.J., Fong, Y.C.,Davis, K., Jarushi, F., Bleakley, A. (2010). Design Phase Identification of High Pile Rebound Soils. FL/DOT/BDK81 977-01. Florida Department of Transportation, Tallahassee, FL, 128 p.

Das, B. M. (2007). Principles of Foundation Engineering. Sixth Edition. Toronto, Ontario, Canada: Thomson, 750 p.

Department of the Navy, (1982). Foundations and Earth Structures Design Manual. DM 7.2. Naval Facilities Engineering Command, (NAVFAC), Alexandria, VA, 279 p.

Duncan, J. M., and S. G. Wright. (2005). Soil Strength and Slope Stability, Hoboken, N.J.: John Wiley, 297 p.

Dwyre, E.M., Batchko, Z., and Castelli, R.J. (2010). Geotechnical Baseline Reports for Foundation Projects, Proceedings, GeoFlorida 2010: Advances in Analysis, Modeling & Design, (GSP 199), Orlando, FL, pp. 1-10.

Essex, R.J. (2007). Geotechnical Baseline Reports for Construction: Suggested Guidelines. The Technical Committee on Geotechnical Reports of the Underground Technology Research Council, Sponsored by the Construction Institute of ASCE and American Institute of Mining, Metallurgical, and Petroleum Engineers, ASCE. Reston, VA, 62 p.

Hannigan, P.J. (1985). Large Quakes Developed During Driving of Low Displacement Piles. Proceedings of the Second International Conference on the Application of Stress-Wave Theory on Piles, Stockholm, 27-30, May, 1984 Rotterdam, The Netherlands: Balkema, pp. 118-125.

Hatanaka, M., and Uchida, A. (1996). Empirical Correlation Between Penetration Resistance and Internal Friction Angle of Sandy Soils, Japanese Geotechnical Society, Soils and Foundations, Vol. 36, No. 4, pp. 1-9.

Honeycutt, J., Kiser, S., and Anderson, J. (2014). Database Evaluation of Energy Transfer for Central Mine Equipment Automatic Hammer Standard Penetration Tests. Journal of. Geotechnical and Geoenvironmental. Engineering, 140(1), pp. 194–200.

Hussein, M., Woerner, II, W., Sharp, M., and Hwang, C. (2006). Pile Driveability and Bearing Capacity in High-Rebound Soils. Proceeding of Geocongress 2006: Geotechnical Engineering in the Information Technology Age. Atlanta, GA, February 26-March 1, 2006, ASCE, Reston, VA, pp. 1-4.

Kanji, M.A. (2014). Critical Issues in Soft Rocks. Journal of Rock Mechanics and Geotechnical Engineering 6, pp. 186-195.

Kovacs, W. D. Salomone, L. A., and Yokal, F. Y. (1983). Comparison of Energy Measurements in the Standard Penetration Test Using the Cathead and Rope Method, US Nuclear Regulatory Commission, (NUREG) CR-3545, Washington, D.C.

Kulhawy, F. H. (1978). Geomechanical Model for Rock Foundation Settlement. Journal of Geotechnical Engineering, Vol. 104, No. 2, pp. 211–227.

Kulhawy, F.H. and Chen, J.-R. (2007). Discussion of 'Drilled Shaft Side Resistance in Gravelly Soils' by Kyle M. Rollins, Robert J. Clayton, Rodney C. Mikesell, and Bradford C. Blaise. Journal of Geotechnical and Geoenvironmental Engineering, ASCE, Vol. 133, No. 10, pp. 1325-1328.

Kulhawy F. H. and Mayne, P. W. (1990). Manual on Estimating Soil Properties for Foundation Design, EL-6800, Electrical Power Research Institute (EPRI), Palo Alto, CA, 306 p.

Liao, S.S.C. and Whitman, R.V.(1986). Overburden Correction Factors for SPT in Sand. Journal of Geotechnical Engineering, American Society of Civil Engineers (ASCE), Vol. 112, No. 3, pp. 373-377.

Likins, G. E. (1983). Pile Installation Difficulties in Soils with Large Quakes. Dynamic Measurement of Piles and Piers, American Society of Civil Engineers, Geotechnical Engineering Division: Philadelphia, PA, 13 p.

Mayne, P.W., Christopher, B., Berg, R., and DeJong, J. (2002). Subsurface Investigations (Geotechnical Site Characterization), FHWA NHI-01-031, U.S. Dept. of Transportation, National Highway Institute, Federal Highway Administration, Washington, D.C., 300 p.

Mayne, P.W. (2007). Cone Penetration Testing. National Cooperative Highway Research Program (NCHRP) Synthesis 368, Washington D.C., 117 p.

Meyerhof, G. G. (1956). Penetration Tests and Bearing Capacity of Piles, American Society of Civil Engineers (ASCE), Journal of the Soil Mechanics and Foundation Division, Vol. 82, No. 1, paper 886, pp. 1-29 .

Meyerhof, G.G. (1976). Bearing Capacity and Settlement of Pile Foundations, American Society of Civil Engineers (ASCE), Journal of Geotechnical Engineering, Vol. 102, No. 3, pp. 195-228.

Mokwa, R. L. and Brooks, H. (2008). Axial Capacity of Piles supported on Intermediate Geomaterials. FHWA/ MT Report No. 08-008/8117-32. Montana DOT, Helena, MT, 79 p.

Peck, R.B., Hanson, W.E., and Thornburn, T.H. (1974). Foundation Engineering, Second Edition., Wiley, New York, NY, 544 p.

Robertson, P.K. (1990). Soil Classification Using the Cone Penetration Test. Canadian Geotechnical Journal, Vol. 27, No. 1, pp. 151-158.

Robertson, P.K. and Campanella, R. G. (1983). Interpretation of Cone Penetration Tests. Part I: Sand. Canadian Geotechnical Journal, Vol. 20, No. 4, pp. 718-733.

Robertson P.K., Campanella, R.G., Gillespie, D. and Grieg, J. (1986). Use of Piezometer Cone Data. Proceedings of Use of In-Situ Tests in Geotechnical Engineering 1986, ASCE Special Publication No. 6, Blacksburg, pp 1263-1280.

Sabatini, P.J., Bachus, R.C., Mayne, P.W., Schneider, J.A., and Zettler, T.E. (2002). Evaluation of Soil and Rock Properties, FHWA-IF-02-034, Geotechnical Engineering Circular (GEC) No. 5, U.S. Dept. of Transportation, Federal Highway Administration, 385 p.

Samtani, N.C. and Nowatzki, E.A. (2006). Soils and Foundations: Reference Manual, Vol. 1, FHWA-NHI-06-088. U.S. Dept. of Transportation, National Highway Institute, Federal Highway Administration, Washington, D.C., 462 p.

Schmertmann, J.H. (1975). Measurement of In Situ Shear Strength, Proceedings of the Conference on In Situ Measurement of Soil Properties, Vol. 2, ASCE, New York, NY, pp. 57-138.

Sowers, G.F. (1979). Introductory Soil Mechanics and Foundations. Geotechnical Engineering, Fourth Edition, MacMillan Publishing Co. Inc., New York, NY, 592 p.

Stroud, M.A. (1974). The Standard Penetration Test in Insensitive Clays and Soft Rocks, Proceedings of the European Symposium on Penetration Testing, Vol. 2 No. 2, Stockholm, Sweden, pp. 367-375.

Stroud, M.A. (1989). Standard Penetration Test: Introduction Part 2, Penetration Testing in the U.K., Thomas Telford, London, pp. 29-50.

Terzaghi, K., and Peck, R.B. (1967). Soil Mechanics in Engineering Practice, Second Edition, Wiley and Sons, Inc., New York, NY, 729 p.

Terzaghi, K., Peck, R.B., and Mesri, G. (1996). Soil Mechanics in Engineering Practice, Third Edition, Wiley and Sons, Inc., New York, NY, 592 p.

Thompson, C.D., and Goble, G.G. (1988). High Case Damping Constants in Sand. Proceedings of the Third International Conference on the Application of Stress-wave Theory to Piles 1988, Ottawa, Canada, BiTech Publishers, Vancouver, B.C., pp. 555-566.

CHAPTER 6

PILE TYPES FOR FURTHER EVALUATION

The economic selection of a pile foundation type and section for a structure should be based on the specific subsurface conditions as well as the foundation loading requirements, performance criteria, construction limitations and schedule, as well as the foundation support cost. Piles can be broadly categorized in two main types: foundation piles for support of structural loads and piles for earth retention systems. The use of piles for earth retention systems is outside the scope of this manual. This chapter focuses on the characteristics of driven pile types typically used for highway structure foundations. Additional details on pile splices and toe protection devices are presented in Chapter 16.

6.1 OVERVIEW OF TYPICAL PILE TYPES

There are numerous types of piles used for foundation support. Figure 6-1 shows a pile classification system based on type of material, configuration, installation technique and equipment used for installation. Foundation piles can also be classified on the basis of their method of load transfer from the pile to the surrounding geomaterial. Load transfer can be by shaft resistance, toe resistance or a combination of both.

Tables 6-1 to 6-7, modified from NAVFAC (1982), summarize characteristics and uses of common driven pile types. The tables are for preliminary guidance only, and should be confirmed by local practice. The typical factored resistance may be controlled by the structural or available geotechnical resistance which may in turn be limited by installation conditions or performance requirements. Although drilled and bored piles are included in the pile classification chart shown in Figure 6-1, these foundation types are outside the scope of the FHWA driven pile foundation manual. Reference should be made to the FHWA reference manuals for drilled shafts (Brown et al. 2010), continuous flight auger (CFA) piles (Brown et al. 2007) and micropiles (Sabatini et al. 2005) for detailed information on these deep foundation types.

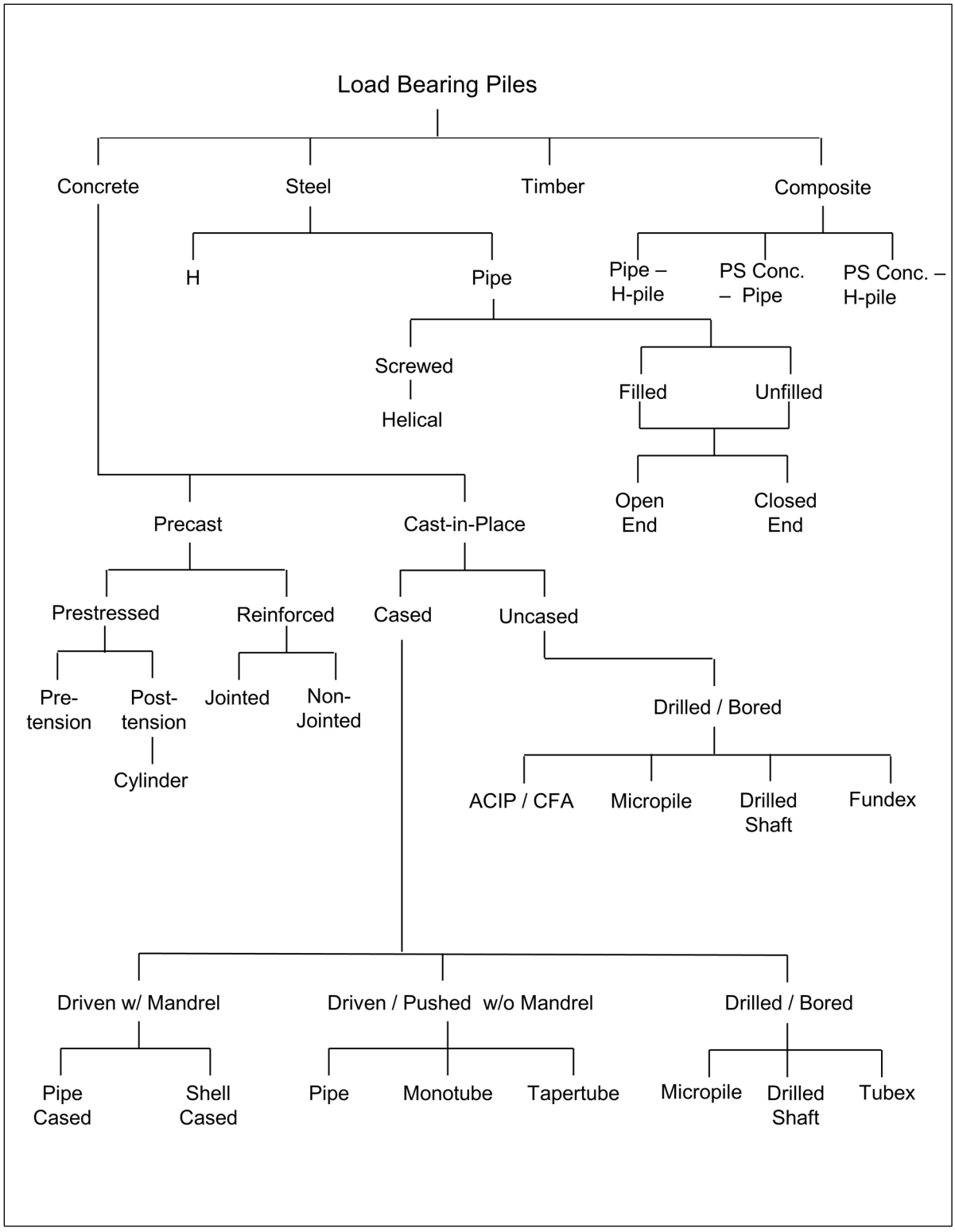

Figure 6-1 Pile classification chart.

Table 6-1 Timber Piles Technical Summary

PILE TYPE	TIMBER PILES
TYPICAL LENGTHS	15 to 75 feet for Southern Pine. 15 to 120 feet for Douglas Fir.
MATERIAL SPECIFICATIONS	ASTM D25. AWPA UC4A, UC4B, UC4C, UC5A, UC5B and UC5C.
TYPICAL FACTORED RESISTANCE	50 to 120 kips.
MAXIMUM DRIVING STRESS	$\sigma_{dr} = \phi_{da} (F_{co})$. $\phi_{da} = 1.15$. F_{co} = 1.25 ksi for Douglas Fir, 1.20 ksi for Southern Pine.
ADVANTAGES	• Comparatively low in initial cost. • Permanently submerged piles are resistant to decay. • Easy to handle.
DISADVANTAGES	• Difficult to splice. • Vulnerable to damage in hard driving; both pile head and pile toe may need protection. • Intermittently submerged piles are vulnerable to decay unless treated.
REMARKS	• Best suited for friction piles in granular material. • Suitable for friction piles with lower factored resistances in cohesive soils.

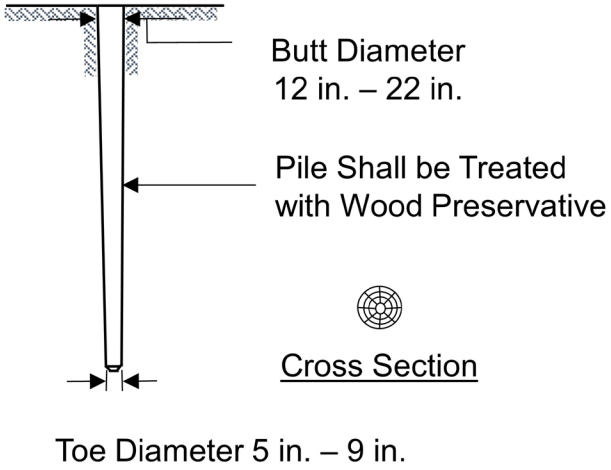

Figure 6-2 Timber pile typical illustration.

Table 6-2 Steel H-Piles Technical Summary

PILE TYPE	STEEL – H-PILES
TYPICAL LENGTHS	15 to 200 feet.
MATERIAL SPECIFICATIONS	ASTM - A572, A588, or A690 Grade 50, 60. (A572 Grade 50 is standard).
TYPICAL FACTORED RESISTANCE	260 to 1,600 kips.
MAXIMUM DRIVING STRESS	$\sigma_{dr} = 0.9\ \phi_{da}\ F_y$. $\phi_{da} = 1.00$. F_y = Yield strength of steel (ksi).
ADVANTAGES	• Available in various lengths and sizes. • High factored resistance. • Small soil displacement. • Easy to splice. • Pile toe protection will assist penetration through harder layers and some small obstructions.
DISADVANTAGES	• Vulnerable to corrosion where exposed and in corrosive soil conditions. • HP section may be damaged or deflected by major obstructions.
REMARKS	• Best suited for toe bearing on rock. • Factored resistance reduced in corrosive environments. • Length and cost overruns often occur when used as a friction pile in granular materials.

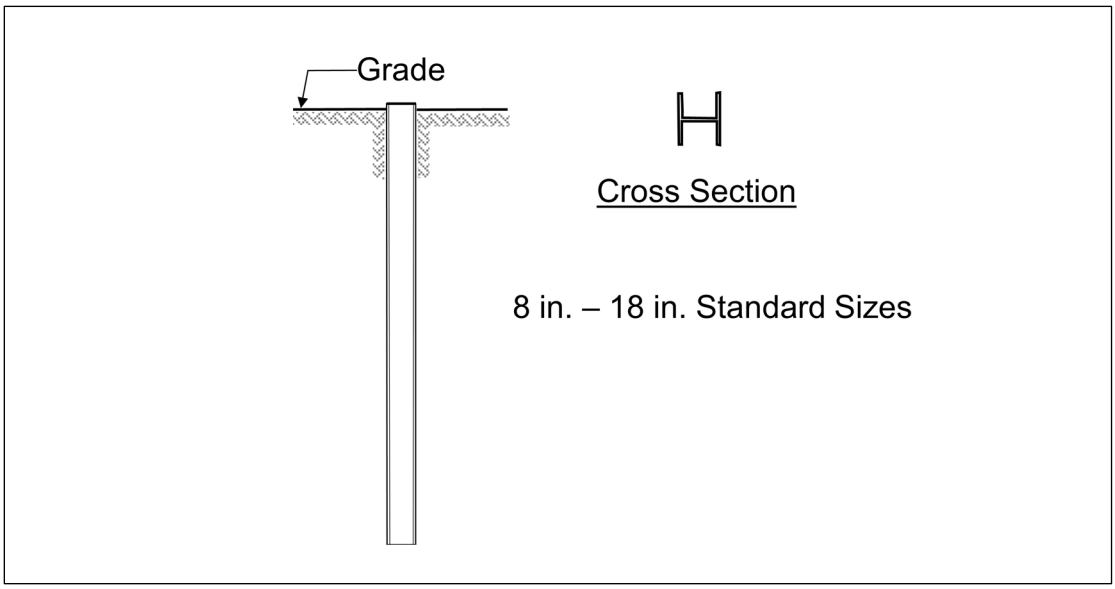

Figure 6-3 Steel H-pile typical illustration.

Table 6-3 Steel Pipe Piles Technical Summary

PILE TYPE	STEEL – PIPE PILES
TYPICAL LENGTHS	15 to 200 feet.
MATERIAL SPECIFICATIONS	ASTM A252 Grade 2 or 3, API 5L, or API 2B - for pipe. ACI 318 - for concrete (if filled). ASTM A572 - for core (if used).
TYPICAL FACTORED RESISTANCE	100 to 1,250 kips (closed end, D ≤ 30 in.) with concrete fill. 660 to 6,500 kips (open end, 16 in. ≤ D ≤ 72 in.) no concrete.
MAXIMUM DRIVING STRESS	$\sigma_{dr} = 0.9\ \phi_{da}\ F_y$. ϕ_{da} = 1.00 for non-composite during driving. F_y = Yield strength of steel (ksi).
ADVANTAGES	• Closed end pipe can be internally inspected after driving. • Low soil displacement for open end installation. • High factored resistances depending on section. • Open end pipe with shoe can be used for obstructions. • Open end pipe can be cleaned out and driven further. • Easy to splice.
DISADVANTAGES	• Vulnerable to corrosion where exposed and in corrosive soil conditions. • Potential soil displacement from larger closed end pipe.
REMARKS	• Provides high bending resistance where unsupported length is loaded laterally. • Open end not recommended as a friction pile in granular material due to tendency for length and cost overruns.

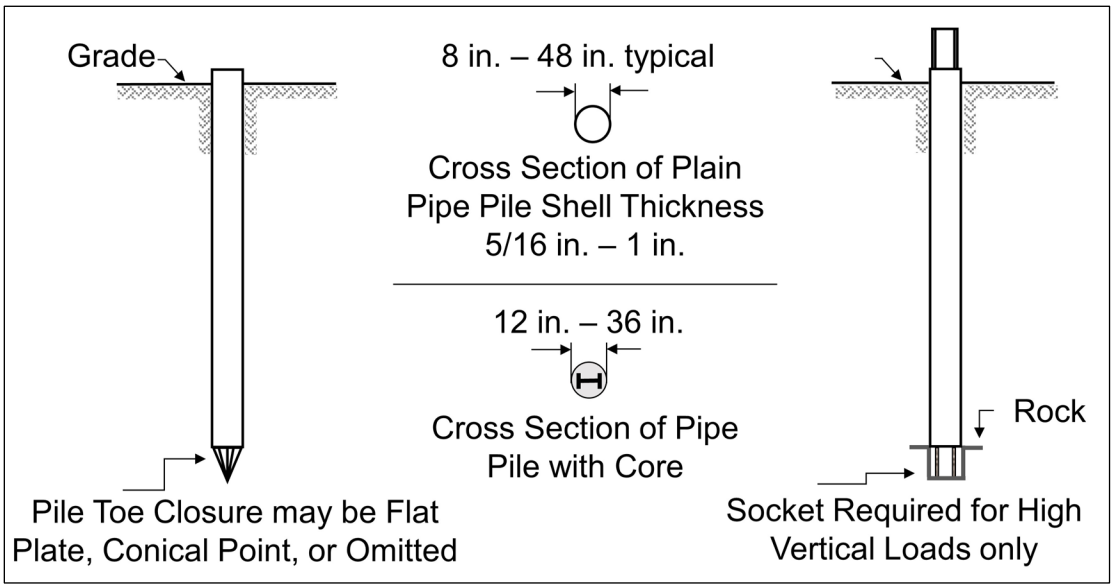

Figure 6-4 Steel pipe piles typical illustration.

Table 6-4 Precast, Prestressed Concrete Technical Summary

PILE TYPE	PRECAST PRESTRESSED CONCRETE PILES
TYPICAL LENGTHS	30 to 150 feet.
MATERIAL SPECIFICATIONS	ACI 318 - for concrete. ASTM - A82, A615, A722, and A884 - for reinforcing steel. ASTM - A416, A421, and A882 - for prestressing.
TYPICAL FACTORED RESISTANCE	350 to 2,200 kips on solid square piles. 1,500 to 3,000 kips on spun cast cylinder piles.
MAXIMUM DRIVING STRESS	$\sigma_{dr} = \phi_{da}$ (0.85 f'_c- f_{pe}) In compression. $\sigma_{dr} = \phi_{da}$ (0.095$\sqrt{f'_c}$ +f_{pe}) In tension (normal conditions). $\sigma_{dr} = \phi_{da}$ (f_{pe}) In tension (severe conditions). ϕ_{da} = 1.00. f'_c = Concrete compressive strength (ksi). f_{pe} = Effective prestress (ksi).
ADVANTAGES	• High factored resistances. • Corrosion resistance obtainable. • Hard driving possible.
DISADVANTAGES	• Vulnerable to handling damage. • Can have relatively high breakage rate. • Potential soil displacement effects from large sections. • Difficult to splice when insufficient length ordered.
REMARKS	• Cylinder piles are well suited for bending resistance.

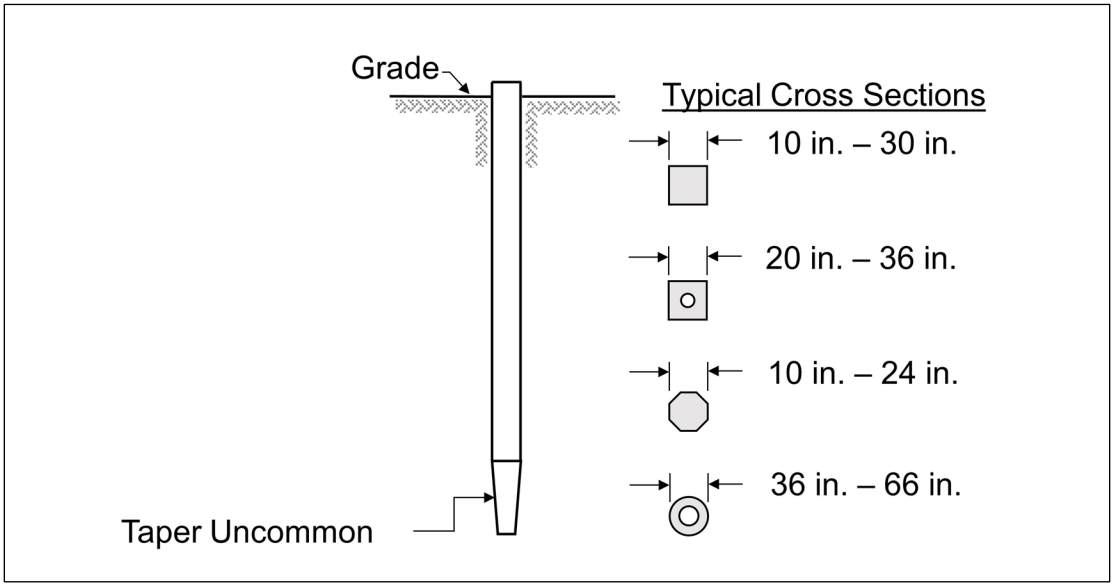

Figure 6-5 Precast, prestressed concrete typical illustration.

Table 6-5 Monotube Pile Technical Summary

PILE TYPE	MONOTUBE PILES
TYPICAL LENGTHS	15 to 100 feet.
MATERIAL SPECIFICATIONS	ACI 318 - for concrete. ASTM A252 - for steel pipe.
TYPICAL FACTORED RESISTANCE	100 to 450 kips.
MAXIMUM DRIVING STRESS	$\sigma_{dr} = 0.9\ \phi_{da}\ F_y$. ϕ_{da} = 1.00 for non-composite during driving. F_y = Yield strength of steel (ksi).
ADVANTAGES	• High factored resistance for relatively shorter lengths. • Increased shaft resistance from tapered section. • Fluted shell not easily damaged.
DISADVANTAGES	• Potential soil displacement effects. • Vulnerable to corrosion where exposed and in corrosive soil conditions.
REMARKS	• Best suited as a friction pile in granular soils.

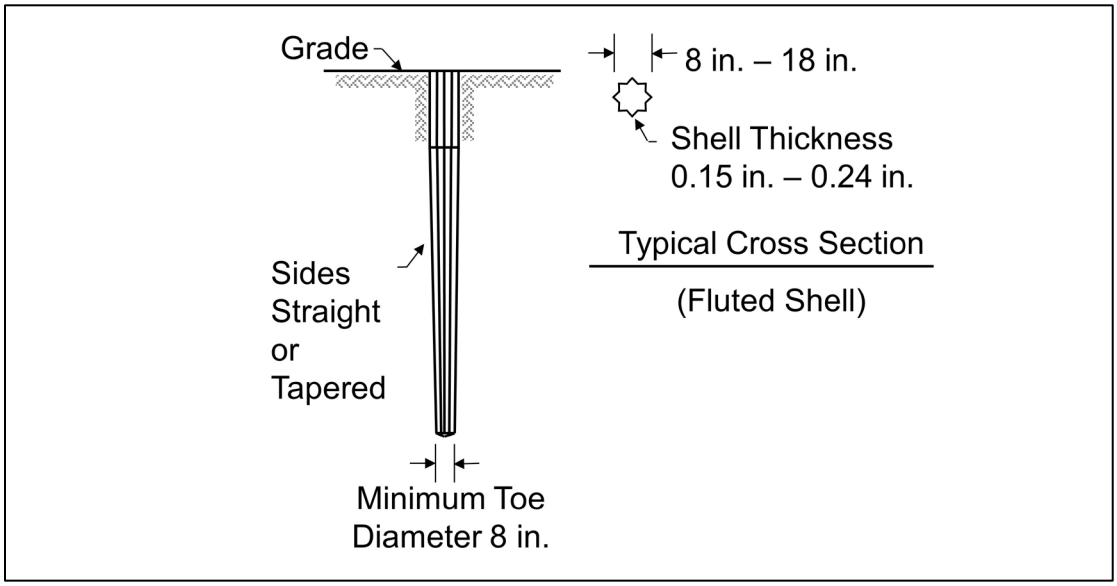

Figure 6-6 Monotube pile typical illustration.

Table 6-6 Tapertube Piles Technical Summary

PILE TYPE	TAPERTUBE PILES
TYPICAL LENGTHS	50 to 150 feet.
MATERIAL SPECIFICATIONS	ACI 318 - for concrete. ASTM A252 - for steel pipe.
TYPICAL FACTORED RESISTANCE	200 to 850 kips.
MAXIMUM DRIVING STRESS	$\sigma_{dr} = 0.9\ \phi_{da}\ F_y$. ϕ_{da} = 1.00 for non-composite during driving. F_y = Yield strength of steel (ksi).
ADVANTAGES	• High factored resistance for relatively shorter lengths. • Standard pipe piles may be spliced to tapered sections. • Increased shaft resistance from tapered section. • Reduced concrete fill volume in tapered section.
DISADVANTAGES	• Potential soil displacement effects. • Vulnerable to corrosion where exposed and in corrosive soil conditions.
REMARKS	• Best suited as a friction pile in granular soils.

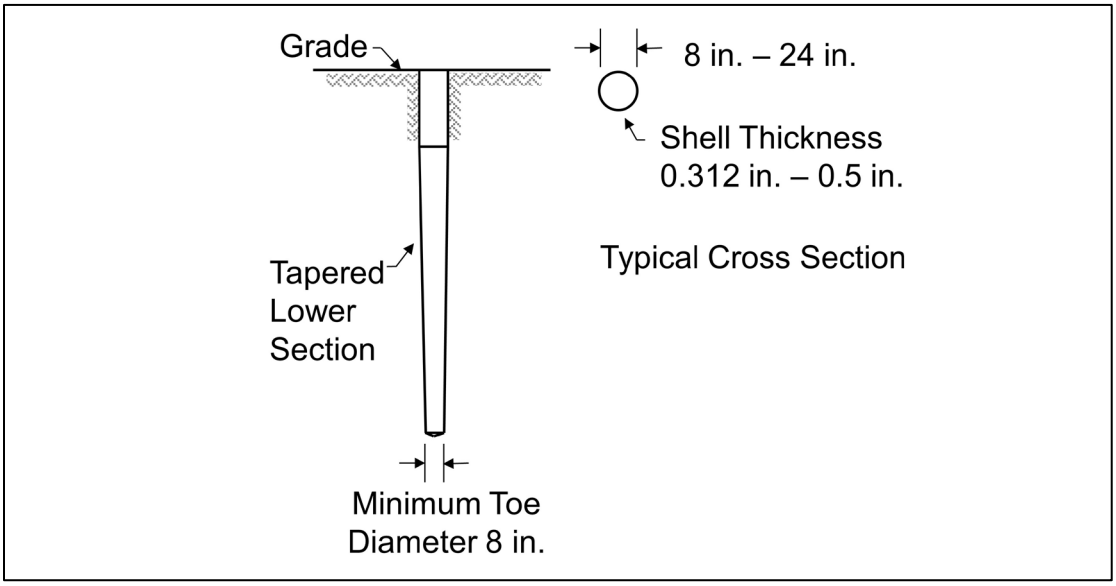

Figure 6-7 Tapertube pile typical illustration.

Table 6-7 Composite Piles Technical Summary

PILE TYPE	COMPOSITE PILES
TYPICAL LENGTHS	50 to 200 feet.
MATERIAL SPECIFICATIONS	ASTM A572 - for HP section. ASTM A252 - for steel pipe. ASTM D25 - for timber. ACI 318 - for concrete.
TYPICAL FACTORED RESISTANCE	100 to 1,250 kips.
MAXIMUM DRIVING STRESS	Varies depending on pile materials.
ADVANTAGES	• Composite section can be designed to address loading conditions and/or specific site requirements. • Considerable length can be provided at comparatively low cost for wood composite piles. • High factored resistance for some composite piles. • Internal inspection for pipe composite piles.
DISADVANTAGES	• More complex pile fabrication. • Difficult to attain good joints between two materials except for concrete and H or pipe composite piles.
REMARKS	• The weakest of any material used will govern the structural design and factored resistance.

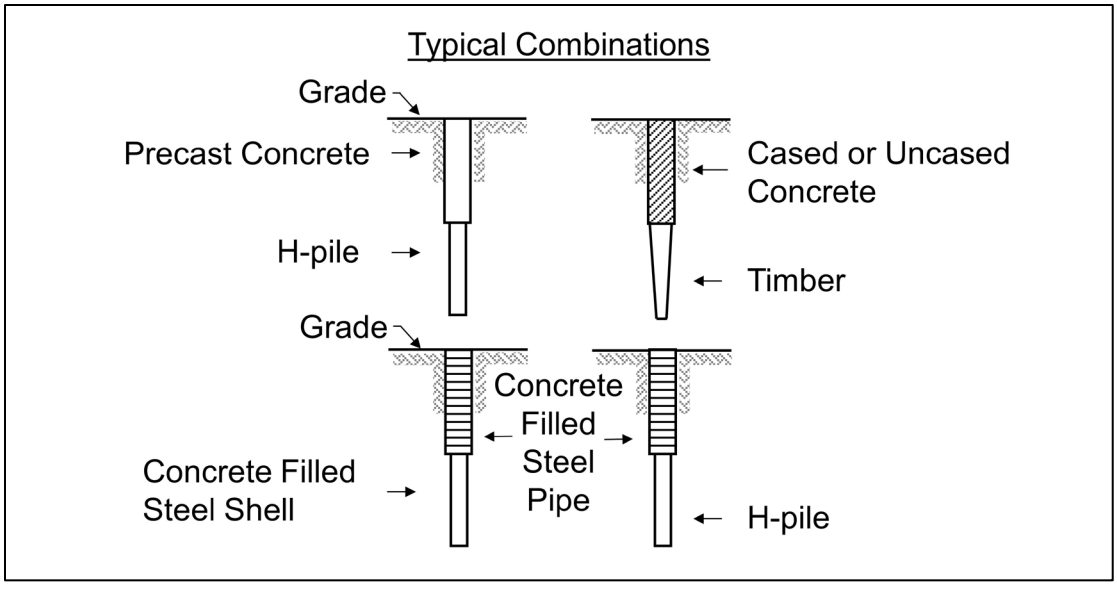

Figure 6-8 Composite piles typical illustration.

6.2 TIMBER PILES

Timber piles are usually of round, tapered cross section made from tree trunks of Southern Pine or Douglas Fir driven with the smaller end used as the pile toe. Southern Pine timber piles can be found to lengths up to 75 feet, and some west coast Douglas fir may be up to 120 feet in length. Oak and other timber types have also been used for piles, but their use is infrequent today. ASTM D25, Standard Specification for Round Timber Piles, presents guidelines on minimum timber pile dimensions, straightness, knot sizes, etc. AWPA C3, Piles - Preservative Treatment by Pressure Process, contains penetration and retention values for the various preservatives. Figure 6-9 presents a photograph of timber piles.

Figure 6-9 Timber piles.

Timber piles are best suited to support modest loads as friction piles in sands, silts and clays. The taper of timber piles is effective in increasing the shaft resistance, particularly in loose sands. They are not recommended as piles to be driven through dense gravel, boulders, or till, or for toe bearing piles on rock since they are vulnerable to damage at the pile head and toe in hard driving. Overdriving of timber piles can result in the crushing of fibers or brooming at the pile head. This can be controlled by using a helmet with cushion material and/or metal strapping around the head of the pile. In hard driving situations, a metal shoe should be attached to the pile toe. Timber piles are favored for the construction of bridge fender systems and small jetties due to the good energy absorption properties of wood.

Timber pile splices are difficult and undesirable. AASHTO (2010) LRFD Bridge Construction Specifications state that timber piles should not be spliced unless specified in the contract documents and approved by the engineer.

Durability is generally not a design consideration if a timber pile is below the permanent water table. However, when a timber pile is subjected to alternate wetting and drying cycles or located above the water table, damage and decay by insects may result. Bacteria and fungi attack can also result in pile damage and decay. Such damage reduces the service life of timber piles significantly unless the pile is treated with a wood preservative. The most common treatments for timber piling are Chromated Copper Arsenate (CCA) for Southern Pine, and Ammoniacal Copper Zinc Arsenate (ACZA) for Douglas Fir. Creosote remains a common treatment option in some areas of the United States but prohibited in others. Creosote cannot be used alone in southern waters due to attack by limnoria tripunctata, but should be used as part of a dual treatment with CCA or ACZA. If cracking of the pile shaft or head occurs and extends below the prescribed pile cut-off level, the initial preservative treatment will not be effective, and the trimmed end of the pile should be treated a second time.

According to Graham (1995), the durability of round timber piling is a function of site-specific conditions:

1. Foundation piles permanently submerged in ground water will typically last indefinitely.

2. Fully embedded, treated foundation piles partially above the ground water with a concrete cap will typically last on the order of 100 years or longer.

3. Treated trestle piles over land will generally last as long as utility poles in the area, i.e., about 75 years in northern areas and about 40 years in southern areas of the United States.

4. Treated piles in fresh water will typically last about five to ten years less than land trestle piles in the same area.

5. For treated piles in brackish water, the longevity should be determined by the experience in the area.

6. Treated marine piles will typically last about 50 years in northern climates and 25 years in southern climates of the United States.

6.3 STEEL H-PILES

Steel H-piles consist of rolled wide flange sections that have flange widths approximately equal to the section depth. In most H-piles sections, the flange and web thicknesses are the same. They are manufactured in standard sizes ranging from 8 to 18 inches. In some cases, W-sections have also been used for piles. However, this is generally customized on a project to project basis. Figure 6-10 contains a photograph of H-piles with driving shoes.

Figure 6-10 H-piles with driving shoes.

H-piles produced today meet the requirements of ASTM A572, Grade 50 steel, as ASTM A36 steel H-piles are no longer readily available. Steel sections meeting the requirements of ASTM A588 and ASTM A690 are also available. These are high strength, low alloy steels developed for improved corrosion resistance in atmospheric (ASTM A588) and marine (ASTM A690) environments. However, ASTM A588 and A690 steels are typically hard to obtain, and long lead times may be necessary if they are specified. ASTM A572, A588 and A690 are all Grade 50 steels. Some H-piles can also be obtained in A572 Grade 60 steel. Therefore, it is possible to use the higher strength of Grade 50 or 60 steel if the pile can be installed to maximize the geotechnical resistance in the project soil conditions. Steel H-piles

are very effective when driven into soft rock. They can be driven very hard with modern high impact velocity hammers with little likelihood of pile toe damage.

H-piles can develop their nominal resistance through shaft resistance, toe resistance or a combination of both. Since H-piles generally displace a minimum amount of soil, they can be driven more easily through dense granular layers and very stiff clays than displacement piles. In addition, problems associated with soil heave during foundation installation are often reduced by using H-piles. However, sometimes H-piles will "plug". That is, the soil being penetrated will adhere to the web and the inside flange surfaces creating a closed end, solid section. The pile will then drive as if it were a displacement pile below the depth of plug formation. Plugging can have a substantial effect on both the soil resistance during driving and the nominal geotechnical resistance. H-piles can be problematic when used as friction piles in some granular deposits. In these conditions they often don't plug during driving, have low dynamic resistances during installation, and result in excessive pile lengths.

Experience indicates that corrosion is not a practical problem for steel piles driven in natural soil, due primarily to the absence of oxygen in the soil. However, in fill materials at or above the water table, moderate corrosion may occur and protection may be needed. In 2013, an H-pile supported pier at the I-43 Leo Frigo Bridge suddenly settled due severe corrosion. While the concurrent factors that lead to the corrosion were considered highly unusual, this occurrence emphasizes the need for identifying corrosive environments during the design stage. As noted previously, high strength, low allow steels are available for improved corrosion resistance. Another common protection method requires the application of pile coatings before and after driving. Coal-tar epoxies, fusion bonded epoxies, metallized zinc, metallized aluminum and phenolic mastics are some of the pile coatings available. Encasement by cast-in-place concrete, precast concrete jackets, or cathodic protection can also provide protection for piles extending above the water table. Another design option for piles subject to corrosion is to select a heavier section than that required by the design loads, anticipating the loss of material caused by corrosion. Corrosion losses can be estimated using the information provided in Section 6.14.1. However, even with the corrosion protection options or allowances mentioned above, certain aggressive soil conditions will preclude the use of steel piles altogether.

One of the key advantages of H-piles is the ease of extension or reduction in pile length. This makes them suitable for nonhomogeneous soils with layers of hard strata or natural obstructions. Splices are commonly made by full penetration

groove welds so that the splice is as strong as the pile in both compression and bending. The welding should always be done by qualified welders in accordance with approved procedures. Proprietary splices are also commonly used for splicing H-piles and Chapter 16 presents additional information on typical splices. A steel load transfer cap is not required by AASHTO if the pile head is embedded 12 inches into the concrete pile cap. Pile toe reinforcement using commercially manufactured pile shoes is recommended for H-piles driven through or into very dense soil or soil containing boulders or other obstructions. Pile shoes are also used for H-piles driven to rock, particularly for penetration into sloping rock surfaces. Chapter 16 provides details on available driving shoes.

The disadvantages of H-piles include a tendency to deviate when natural obstructions are encountered. Nominal resistance verification of H-piles used as friction piles in granular soils based on the observed blow count can also be problematic, and can result in significant length overruns. An H-pile in a granular profile will often not plug during the dynamic loading of pile installation but may plug under the slower static loading condition. Length for length, steel piles tend to be more expensive than concrete piles. On the other hand, steel's high factored resistance for a given weight can reduce pile driving costs.

6.4 STEEL PIPE PILES

6.4.1 Closed End Steel Pipe

Closed end steel pipe piles consist of seamless, welded or spiral welded steel pipes in diameters typically ranging from 8 to 30 inches. Larger pipe pile sizes are available, but larger diameters are more commonly driven open ended. Typical wall thicknesses for closed end pipe piles range from 0.188 to 1 inch. Pipe piles should be specified by grade with reference to ASTM A252, API-5L, or API-2B. In some situations, a contractor may propose to supply used pipe not produced under ASTM standards. Used pipe piles not meeting ASTM standards must be evaluated by an engineer for general condition, drivability, and weldability prior to approval.

A closed end pipe pile is generally formed by welding a 0.75 to 2 inch thick flat steel plate to the pile toe. The toe plate thickness generally increases with pile diameter and/or with anticipated harder driving conditions. When pipe piles are driven to weathered rock or through boulders, a cruciform-reinforced end plate or a conical point with rounded nose is often used to minimize pile toe distortion. Figure 6-11 presents a picture of a typical closed end pipe pile with a flat closure plate.

Figure 6-11 Typical 16 inch closed end pipe pile.

Closed end steel pipe piles can be used as friction piles, toe bearing piles, a combination of both, or as rock socketed piles. They are commonly used where variable pile lengths are required since splicing is relatively easy. With the increased ductility requirements for earthquake resistant design, pipe piles are being used extensively in seismic areas.

Pipe piles may be left open or filled with concrete. If concrete filled, the piles can also have a reinforcing steel cage or structural shape such as an H-section inserted into the concrete. Reinforcing steel is required only when the concrete in the pile may be under tension from such conditions as uplift, high lateral loads, or for unsupported pile lengths.

Most often, pipe piles are driven from the pile head. However, thin wall, closed end pipe piles can also be bottom driven using a mandrel. A mandrel is usually a heavy tubular steel section inserted into the pile that greatly improves pile drivability. After driving, the mandrel is removed and the pile is inspected internally before concrete is placed. Typically, pipe piles are spliced using full penetration groove welds. Proprietary splicing sleeves are available and should be used only if the splice can provide full strength in bending and tension (unless the splice will be located at a distance below ground where bending moments and tension loads are small). Typical pile splices are described in Chapter 16. The corrosion discussion on H-piles is also applicable to steel pipe piles.

6.4.2 Open End Steel Pipe

Open end pipe piles are frequently installed when hard driving conditions, significant penetration depths, or debris is expected. Open end pipe piles are available in diameters that range from 8 to 160 inches. When pipe piles are driven open ended, wall thicknesses of 0.5 inches or greater are commonly used. Similar to closed end pipe piles, the open end piles can be seamless, rolled and welded, or spiral welded steel pipes. Open end pipe piles should be specified by grade with reference to ASTM A252, API-5L, or API-2B. In some situations, a contractor may propose to supply used pipe not produced under ASTM standards. Used pipe piles not meeting ASTM standards must be evaluated by an engineer for general condition, drivability, and weldability prior to approval.

Large diameter open end pipe piles are defined as greater than 36 inches in diameter (Brown and Thompson 2015). These are often selected due to their ability to resist significant vessel impacts and overturning moments, and/or due to scour, ice, or seismic design considerations. Other common applications of large diameter open end pipe include fender systems, mooring dolphins, and offshore facilities. Large diameter open end pipe piles are frequently used to support main piers on major river bridges or other structures with large lateral resistance demands. Large diameter open end pipes are typically driven to bear in dense sand or soft rock, or are installed as long friction piles. Figure 6-12 shows a group of 42 inch diameter, spiral weld, open end pipe piles for a main bridge pier support. A photo of a 12 foot diameter open end pipe is presented in Figure 6-13.

Open end pipe piles can be socketed into bedrock (rock socketed piles), or when driving through dense materials, may form a soil plug. The plug makes the pile act like a closed end pile and can significantly increase the pile toe resistance. Plugging is discussed in greater detail in Section 7.10.7 and is a complex phenomenon. The soil plug should not be removed unless the pile is to be internally cleaned out and filled with concrete or unless the soil plug is preventing the pile from achieving the required penetration depth.

Large diameter open end pipe typically core through the soil during driving due to mass soil inertia effects. However, under static loading conditions, these piles generally plug providing significant toe bearing resistance. Some recent large diameter open end pipe pile projects have incorporated a constrictor plate inside the pile to force plugged behavior during driving. A diagram of a constrictor plate design and a companion photograph are presented in Figures 6-14 and 6-15, respectively. Constrictor plates are also discussed in Section 16.3.3.

Figure 6-12 42 inch diameter, spiral weld, open end, pipe for main river pier.

Figure 6-13 Large diameter open end pipe piles.

Open end pipe piles are seldom cleaned out full length unless a rock socket is planned or short pile lengths are used. Before concrete placement, steel reinforcement and uplift resisting dowels can be added, as necessary.

Open ended piles can also be equipped with internal or external steel cutting shoes to reduce the potential for toe damage. When hard driving conditions are expected such as sloping rock, cobbles and boulders, etc., large diameter open end pipes are frequently designed with a thicker wall pipe section over the bottom two diameters to lessen the risk of toe damage from high localized stresses.

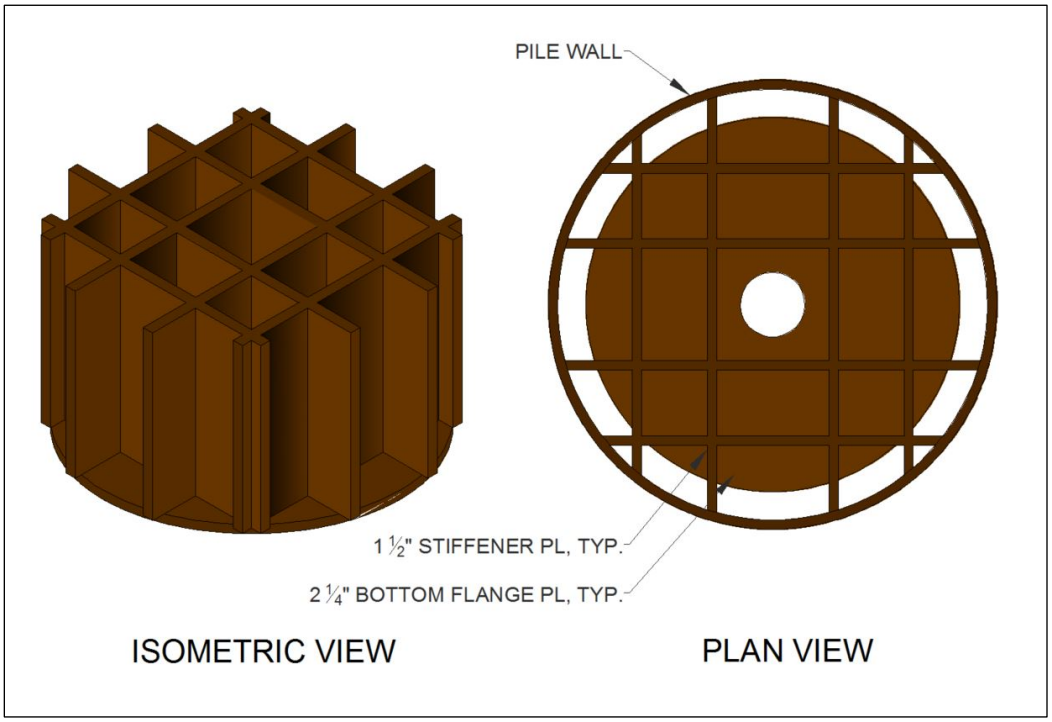

Figure 6-14 Constrictor plate.

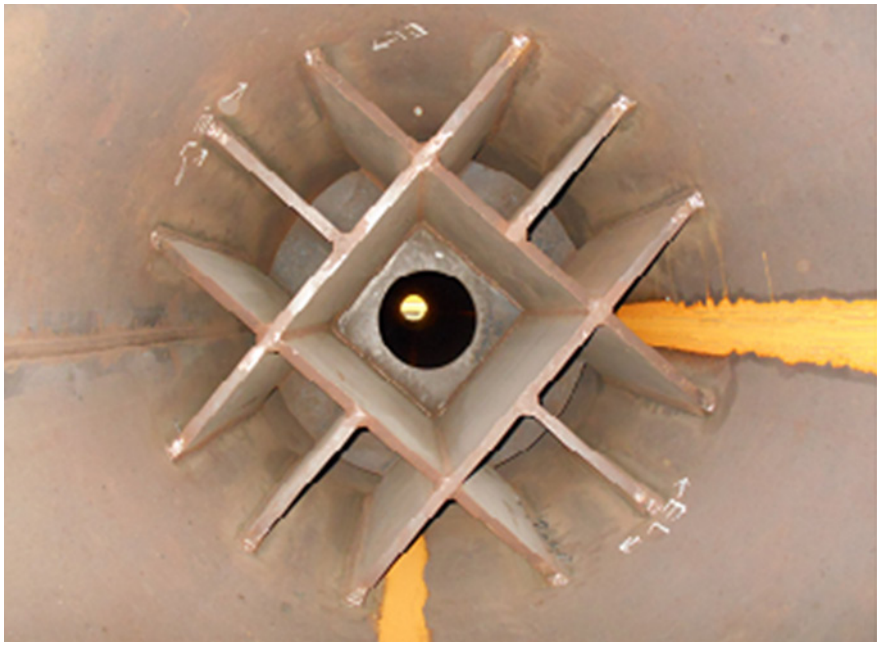

Figure 6-15 Constrictor plate installed inside pipe pile.

6.5 MONOTUBE PILES

The Monotube pile, shown in Figure 6-16, is a proprietary pile driven without a mandrel. Monotubes are longitudinally fluted and are tapered over the lower pile section. Depending upon the pile section selected nominal pile toe diameters of 8 or 8.5 inches taper to a butt diameter of 12, 14, 16, or 18 inches over tapered section lengths of 10 to 75 feet. Non-tapered extensions are available in 20 and 40 feet for splicing to the lower tapered section. Monotube piles are available in 9 to 3 gage shell thicknesses or roughly 0.15 to 0.24 inches. Monotube sections are spliced by inserting the slightly smaller bottom section of the extension into the top of the previously driven section. A fillet weld is then used along the interface between the extension and the lower pile section into which it is inserted. Four V shaped notches cut into the lower pile section at 90 degree locations are often added to increase weld length and splice strength. After driving, Monotube piles are filled with concrete.

The fluted and tapered design of Monotube piles has several functional advantages. The flutes add stiffness necessary for handling and driving lightweight piles. These also increase the surface area while the tapered section improves the soil resistance per unit length in compression loading. The flutes are formed by cold working when the pile is manufactured as this increases the yield point of the steel to more than 50 ksi, further improving the pile drivability.

Figure 6-16 Tapered Monotube section (right) with add-on sections (left).

6.6 TAPERTUBE PILES

This pile consists of a tapered, 12 sided polygon over the lower section with conventional steel pipe pile material as the upper add-on sections. The 15 to 30 feet long tapered section steel is available with pile toe diameters ranging from 8 to 14 inches and pile head diameters of 12 to 24 inches. Wall thickness of the tapered sections ranged from 0.1875 to 0.625 inches. The tapered tube bottom section has a yield strength of 50 ksi, and the upper pipe pile sections conform to ASTM A252 Grade 3 steel with a yield strength of 45 ksi. The tapered and pipe sections are connected using a full penetration weld.

Tapertube piles are driven from the top and filled with concrete after driving. Specialty sleeve splices may be used as an alternative to welding sections together. Please see Chapter 16 for more information. A photo of Tapertube piles is presented in Figure 6-17.

Figure 6-17 Tapertube piles (courtesy DFP Foundation Products, LLC).

6.7 SPIN FIN PILES

The Spin Fin pile is a variation of a pipe pile introduced on the west coast in 1983. It is a pipe pile with an outside “thread” made of fins that gradually wind around a bottom portion of the pile. These fins cause the pile to rotate into the ground during driving. Following driving, the pile is incorporated into a pile cap. Pile rotation is

then restrained by the cap preventing the pile from twisting. This results in a plugging effect that increases the pile's resistance to tension loads as depicted in Figure 6-18. The Spin Fin pile is particularly attractive on projects needing increased uplift resistance such as for seismic events or in soils with limited overburden materials overlying a hard bearing layer such as a glacial till over bedrock. The fins also increase the compression resistance by increasing the bearing area in the pile section having fins. A photograph of a 30 inch diameter spin fin pile is presented in Figure 6-19.

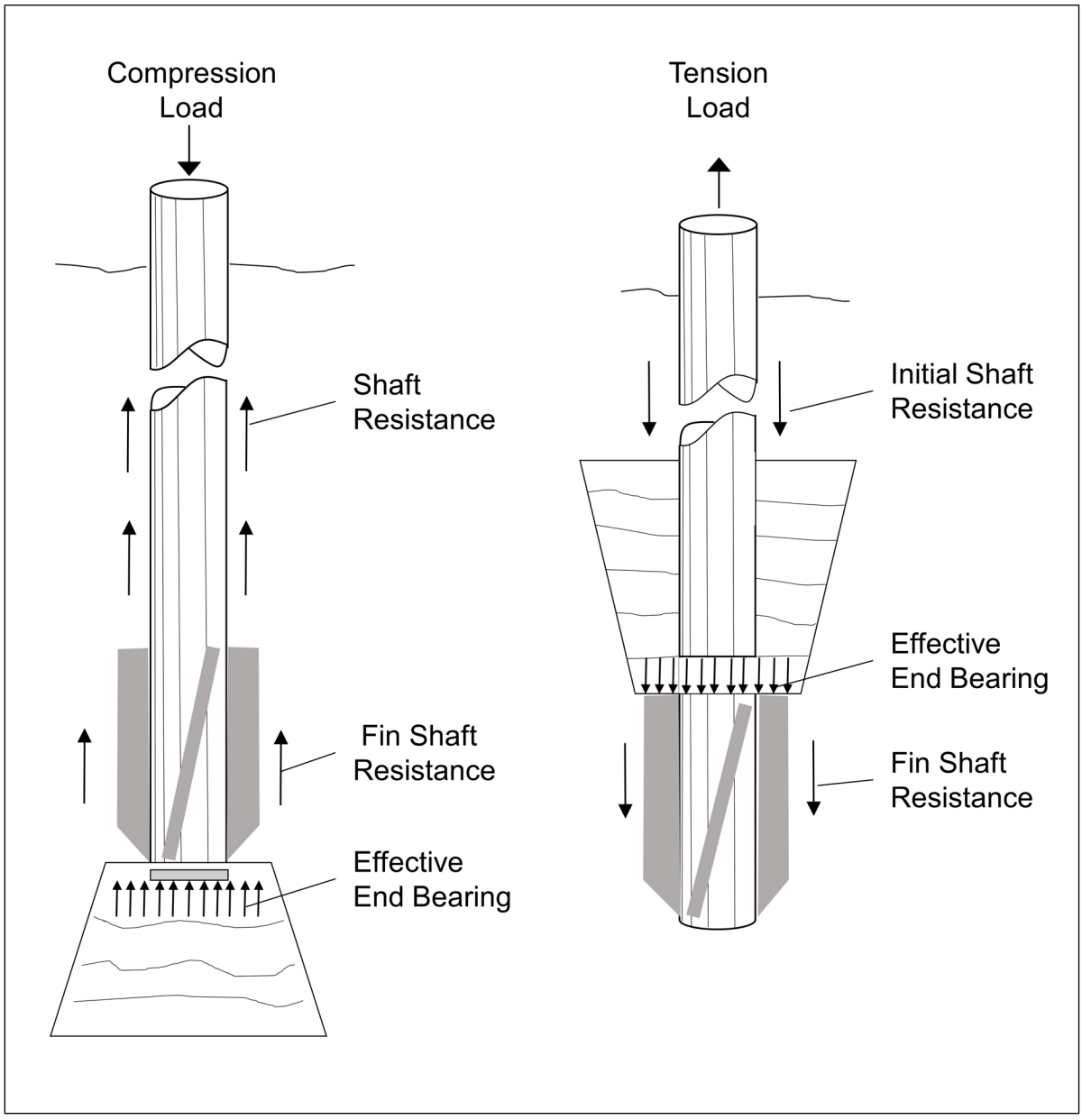

Figure 6-18 Spin Fin pile load transfer illustration.

Figure 6-19 30 inch diameter Spin Fin pile.

6.8 PRESTRESSED CONCRETE PILES

Prestressed concrete piles vary from the most common solid square section to a solid octagonal section. As sections increase in size, they are often cast with an internal void to reduce handling weight. Prestressed piles can either be pre-tensioned or post-tensioned. Pre-tensioned piles are usually cast to their full length in permanent casting beds. Post-tensioned piles are usually manufactured in sections, most commonly cylindrical, and assembled and prestressed to the required pile lengths at the manufacturing plant or on the job site. Figure 6-20 depicts common prestressed concrete pile sections and Figure 6-21 presents a photograph of prestressed piles stored on a barge prior to driving.

The prestressing steel may be in the form of strands or wires which are enclosed in a conventional steel spiral and placed in tension. Prestressing steel must conform to ASTM A416, A421, and A882. Due to the effects of prestressing, these piles can usually be made lighter and longer than reinforced concrete piles of the same size. In cases of extreme environmental conditions, an epoxy coating has been used on prestressing strands. If this coating is used, it should be dusted with sand before the epoxy sets. Then the strand will have sufficient bond strength to carry the prestress

development bond stresses. If an epoxy coating has been used on the strand, it should also be used on the tie or spiral reinforcement. However, epoxy coating is generally not necessary for prestressed piles since the prestressing force will keep the concrete in compression making deterioration less likely.

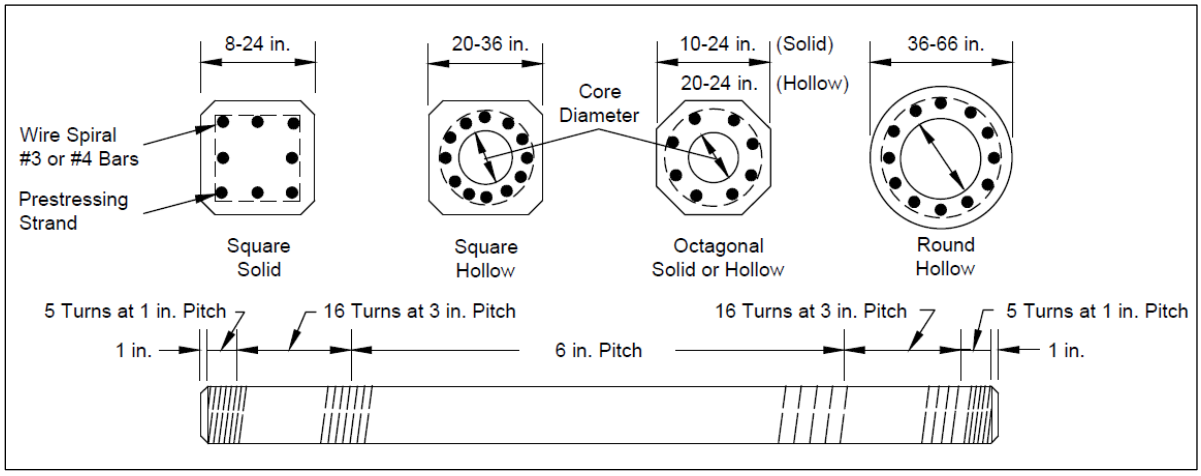

Figure 6-20 Typical prestressed concrete piles.

Figure 6-21 Square prestressed concrete piles.

The primary advantage of prestressed concrete piles compared to conventional reinforced concrete piles is durability. Since the concrete is under continuous compression, hairline cracks are kept tightly closed and thus prestressed piles are usually more resistant to weathering and corrosion than conventionally reinforced piles. This characteristic of prestressed concrete removes the need for special steel coatings since corrosion is not as serious a problem as for reinforced concrete.

Another advantage of prestressing is that the tensile stresses which can develop in the concrete under certain driving and handling conditions are less critical.

Prestressed concrete piles are more vulnerable to damage from striking hard layers of soil or obstructions during driving than reinforced concrete piles. This is due to the decrease in axial compression strength due to the application of the prestressing force. When driven in soft soils, care must also be used since large tension stresses can be generated in easy driving.

Prestressed concrete piles cutoff and splicing problems are considered much more serious by contractors that drive them infrequently than by those that drive only this pile type. Special reinforcement required at the pile head in seismic areas can pose problems if actual lengths vary significantly from the planned length. In these cases, a splice detail must be included so that the seismic reinforcement is extended into the pile cap.

Concrete used for most prestressed concrete piles typically has a 28 day compressive strength between 5 and 6 ksi. Recent developments in prestressed concrete piles include studies on the use of high performance concrete (e.g., Moser 2011) to improve pile durability, or ultra-high performance concrete (e.g., Vande Voort et al. 2008) for improved durability and load support relative to steel H-piles. Belk (2013) studied the use of lightweight aggregate on prestressed concrete piles relative to drivability, load support and weight. At the present time, these developments have not progressed into mainstream practice.

6.9 CONCRETE CYLINDER PILES

Concrete cylinder piles include spun cast, non-spun cast, and Industrial Concrete Products pile types. Each of these cylinder piles types is discussed further below. Cylinder piles are sometimes difficult to drive. However, they usually extend directly to the superstructure support level avoiding the need for a pile cap, which can result in substantial cost savings. Jetting is often used to install cylinder piles to the near the desired depth followed by impact driving to attain the required nominal resistance. When jetting is used, it must be controlled to minimize degradation of the lateral soil resistance and disturbance and removal of soils below the specified jetting elevation. The design of the pile wall often includes periodic vent holes that are used to reduce the build-up of internal water pressure during driving as well as to later avoid build-up of internal gas pressure from organic soil decomposition during service life.

6.9.1 Spun-Cast Cylinder Piles

Spun-cast concrete cylinder piles are hollow concrete piles which are cast in 8, 12, or 16 foot sections. Depending on the manufacturer, cylinder piles are generally available in diameters of 36, 42, 54 and 66 inches. Wall thicknesses of 5, 6, or 6.5 inches are available depending on the pile diameter. Cylinder pile sections are spun centrifugally during the casting process to obtain a high density, durable concrete that is virtually impervious to moisture. The concrete quality from the spun-casting process is unique to spun-cast cylinder piles and concrete compressive strengths of 8 ksi can routinely be achieved. Once cured, sections are assembled to form a pile with the desired pile length. An adhesive joint compound is used between sections. The assembled pile is post tensioned and then the post tensioning ducts grouted.

Results of chloride ion penetration and permeability tests on prestressed cylinder piles indicate that the spun-cast cylinder piles have excellent resistance to chloride intrusion. The post-tensioning process results in a typical prestress level of 1.5 ksi. Figure 6-22 shows the typical configuration of this cylinder pile type. A photograph of concrete cylinder piles is presented in Figure 6-23.

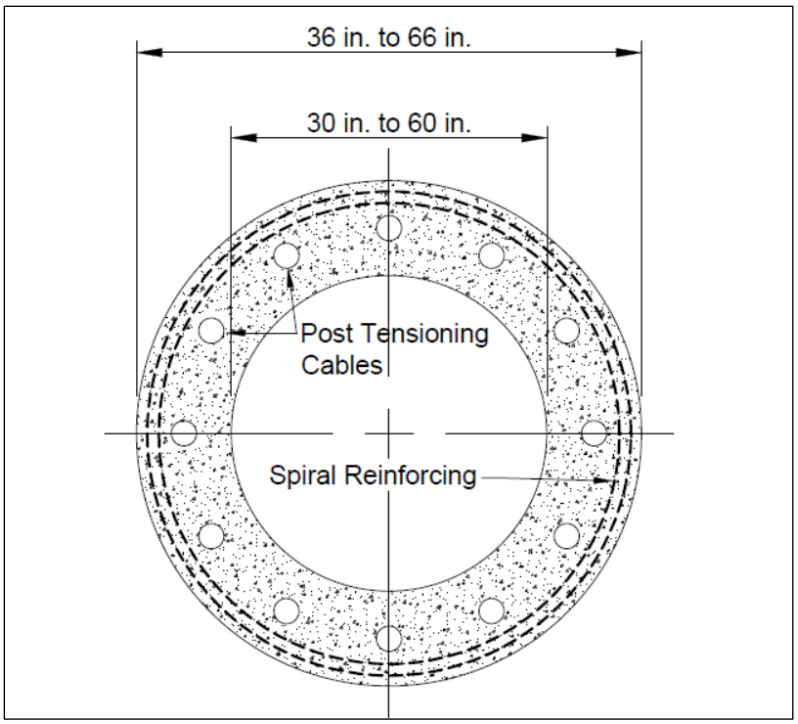

Figure 6-22 Typical spun-cast concrete cylinder pile section.

Generally spun-cast cylinder piles are used for marine structures or land trestles and have high resistance to corrosion and high lateral resistance. To prevent freeze-thaw degradation, air entrainment and adequate spiral reinforcement are important

considerations. The piles typically extend above ground and are designed to resist a combination of axial loads and bending moments. Additional design and installation considerations associated with concrete cylinder piles are summarized in Hartman et al. (2007).

Figure 6-23 Concrete cylinder pile.

6.9.2 Bed-Cast Cylinder Piles

Cylinder piles can also be cast in a bed with forms rather than centrifugally spun cast. These piles are produced to the required length in a single piece and are pretensioned instead of being post tensioned like the spun-cast piles. Due to the differences in the casting process, these piles do not have the high density, low porosity concrete that is characteristic of spun-cast cylinder piles and will therefore not have the same resistance to chloride intrusion. Bed-cast cylinder piles have typical specified concrete compressive strengths of 5.5 ksi, a diameter of 60 inches, and a wall thickness of 7.5 inches.

6.9.3 Industrial Concrete Products (ICP) Piles

These cylindrical piles are pretensioned and spun to compact concrete while curing. The spinning process creates a high density mix by forcibly removing water during the hydration process while pretension adds tensile strength. Typically, ICP piles are cast in sections with steel end plates. Field splices are made by welding the section end plates. Sizes range from 10 inch diameter with a 2.25 inch thick wall to a 48 inch diameter with a 5.9 inch wall. ICP section lengths vary with the pile diameter from 20 to 39 feet on the smallest diameter section up to 33 to 138 feet on the largest diameter section. Piles are supplied open end with a flat shoe or with an X-pointed shoe.

6.10 COMPOSITE PILES

In general, a composite pile is made up of two or more sections of different materials or different pile types. Depending upon the soil conditions, various composite sections may be used. The upper pile section is often precast concrete, steel pipe, or corrugated shell. The lower pile section may consist of steel H, steel pipe, or timber pile. Composite piles have limited application and are generally used only under special conditions. Some of the more common composite piles are discussed below.

6.10.1 Precast Concrete - Steel H-pile Composite Piles

One of the more commonly used composite piles consists of a lower section of steel H-pile or pipe pile embedded in an upper pile section of precast concrete. These concrete-steel composite piles are often used when scour or uplift requirements dictate pile penetration depths that a displacement pile cannot achieve, in subsurface conditions where surficial soil layers have high corrosion potential, or in other conditions that dictate their use. A photograph of composite square concrete piles each with H-pile stinger is presented in Figure 6-24.

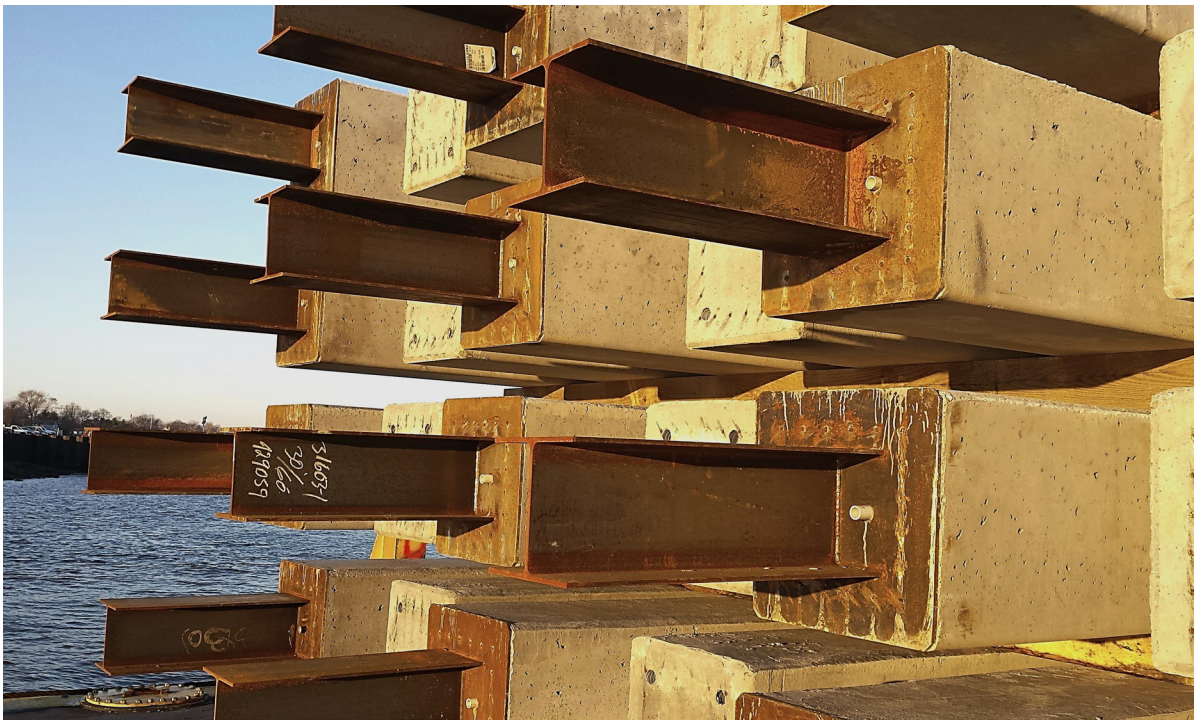

Figure 6-24 Precast concrete piles each with H-pile stinger.

6.10.2 Steel Pipe - H-pile Composite Piles

Steel pipe - H-pile composite piles are comprised of a steel pipe upper section with a transition to an H-pile lower section. This composite selection may be applicable where lateral load demands require the bending resistance of a pipe pile in the upper pile length and dense soil conditions necessitate a low displacement pile over the lower pile length to satisfy minimum pile penetration depth or bearing layer requirements. A steel pipe - H-pile composite piles are shown in Figure 6-25.

Figure 6-25 Steel pipe - H-pile composite piles.

6.10.3 Corrugated Shell - Timber Composite Piles

Corrugated shell - timber composite piles are sometimes used as foundation piles. For this composite pile the timber pile section is permanently located below the groundwater level. A concrete filled shell pile is used above the treated or untreated timber pile. In the case of the composite corrugated shell - timber pile, the timber pile is driven below the water table. A corrugated steel shell is connected to the pile

head of the timber section with a wedge ring driven into the wood. The shell is filled with concrete to the cutoff elevation and the pile is complete.

6.10.4 Corrugated Shell - Pipe Composite Piles

This composite pile consists of a pipe pile for the lower section and a corrugated shell for the upper portion of the pile. A variety of pipe and shell diameters can be used to accommodate a range of loading conditions. The corrugated shell - pile composite pile is mandrel driven. The mandrel provides a guide for alignment of the two pile sections provided it extends to the pipe pile head or partially into the pipe pile. Possible pile joints include: a sleeve joint, a welded joint, and a drive-sleeve joint. Once the pipe and shell are driven and connected, they are filled with concrete to cutoff grade and any excess shell is removed.

6.11 PILE TYPES INFREQUENTLY USED ON TRANSPORTATION PROJECTS

Additional pile types exist that are sometimes used in specialty applications. Others were used more frequently in the past and could be encountered if existing foundations are re-used on reconstruction projects. These include Fundex piles, Tubex piles, mandrel driven piles, reinforced concrete piles, and pressure injected footings. Experience and field testing (load and integrity tests) should be used in new designs using these systems or in re-use of existing foundations.

6.11.1 Fundex Piles

The Fundex pile is a unique form of a pipe-cased, cast-in-place concrete displacement pile. Instead of the pile being driven into the ground with a hammer, it is screwed into the ground with a special 18 inch diameter boring tip. The boring tip is fitted to a 14 inch diameter drilling mandrel with a chuck assembly. A drill table forces the drilling mandrel into the ground utilizing a constant vertical load and torque. When the bearing layer or required penetration depth is reached, a reinforcing cage is suspended within the mandrel and concrete is placed. The drilling mandrel is then oscillated out of the ground leaving the drill point behind. This process results in a cast-in place pile typically installed for unfactored design loads in the 40 to 125 ton range.

Some of the advantages of the Fundex piles include minimal vibrations and very low noise during installation, drilling equipment that can be used in confined places, and a removable mast that allows installation with only 20 feet of overhead clearance.

6.11.2 Tubex Piles

Tubex piles are installed similarly to Fundex piles. A pipe-cased hole is created for the Tubex pile as the drill point is advanced into the soil. Pipe sections may be spliced if additional length is required or if required by headroom limitations. Since the steel casing is in place after drilling to the final installation depth, an internal inspection can also be performed prior to concrete and reinforcement placement. However, unlike the Fundex pile, this casing is then left in place along with the drill point. A grout injected version of the Tubex pile is also available. Typically Tubex pile diameters are 14 inches or greater. If grouted, this pile is typically installed for unfactored design loads of up to 230 tons.

Some of the advantages of the Tubex piles include minimal vibrations and very low noise during installation, drilling equipment that can be used in confined places, and a removable mast that allows installation with only 20 feet of overhead clearance. In addition, the grout injected Tubex pile can be used to insulate the steel casing from corrosive environments.

6.11.3 Pressure Injected Footings (PIF)

This type of driven, cast-in-place pile is often referred to as a Franki pile or pressure injected footing. The best site conditions for these piles are loose to medium dense granular soils.

This pile type is installed by bottom driving a temporary steel casing into the ground using a drop weight driving on a zero slump concrete plug at the bottom of the casing. When the required depth has been reached, the steel casing is restrained from above and the concrete plug is driven out the bottom of the tube. An enlarged base is formed by adding and driving out small batches of zero slump concrete.

Steel reinforcing is then installed prior to adding more concrete to the shaft. It is suggested that widely spaced bars be used to allow the low workability mix to penetrate to the exterior of the piles. After the base is formed and reinforcement is placed, concrete continues to be added and the uncased shaft is formed by compacting the concrete with a drop weight in short lifts as the casing is being withdrawn. Alternatively, if a high workability mix is used to complete the pile, a vibrator can be clamped to the top of the tube and used to compact the concrete into place as the casing is withdrawn.

6.11.4 Mandrel Driven Piles

In the past, mandrel driven piles were used in many soil conditions except where obstacles such as cobbles and boulders were present that could damage the thin shells during driving. The thin shells were susceptible to collapse under hydrostatic pressure prior to concrete placement. They were best suited for friction piles in granular material. Thin shell mandrel driven piles are rarely used today for new construction. They may however be encountered when widening or rehabilitating existing structures so a general overview of their characteristics remains useful.

The pile shells for mandrel driven piles were generally produced from sections of corrugated steel and were either of constant diameter, steadily decreasing in diameter from the pile head to the pile toe, or diameter decreasing in discrete steps over the pile length. Typical tapers were on the order of 1 inch per 8 foot length. It was also possible to have different lengths for each section. Separate shell sections were usually screw-connected and waterproofed with an O-ring gasket. The Raymond Step Taper, Armco Hel-Cor, Republic Corwel, and Guild pile were among the pile types previously driven with mandrels. However most of these corrugated shell type piles are no longer manufactured. Thin wall pipe piles have also been mandrel driven with the mandrel driving on a reinforced section at the pile toe.

The properties of the reusable mandrels dictated the drivability of these shell or thin wall pipe pile sections. This resulted in a significant cost advantage for a mandrel driven pile since the mandrels result in improved pile drivability and soil resistance at low material costs. Construction control of mandrel driven piles should include a wave equation analysis that accounts for the improved pile drivability from the mandrel. A dynamic formula should not be used for construction control of mandrel driven piles. Mandrel driven piles may be costly if it is necessary to drive piles to an unanticipated depth that exceeds the mandrel length available at the job site.

6.11.5 Reinforced Concrete Piles

Prestressed concrete piles have replaced reinforced concrete piles in the U.S. market. Reinforced concrete piles were manufactured from concrete and had reinforcement consisting of a steel cage made up of several longitudinal bars and lateral or tie steel in the form of individual hoops or a spiral. While they are no longer used in the U.S., a limited discussion on them is presented in case they are encountered on a rehabilitation or widening project. Steel reinforcing for reinforced concrete piles was governed by ASTM A82, A615, and A884. High yield strength steel reinforcement to resist uplift loads had to conform to ASTM A722.

Reinforced concrete piles were more susceptible to damage during handling and driving because of tensile stresses compared to prestressed piles. Advantages of reinforced concrete piles included their lower net compressive stress during driving and under foundation loads, and a reduced danger of pile head cracking. In addition, these piles were easier to splice than prestressed piles. To reduce corrosion of the reinforced concrete joints, splices were located below the ground surface, or if under water, the mudline. Segmental pile sections were used to produce piles with varied lengths to accommodate variable soil conditions, and were easily transported to job sites.

The most common type of jointed pile was a square cross section made of high density concrete with each successive unit of shorter length. Typical pile cross sections ranged from 10 to 16 inches, but sizes above and below this range were produced. Joints between these pile sections were of the mechanical type, including bayonet fittings or wedges. The joints had to be well aligned or energy was lost during driving and bending stresses would be introduced due to an eccentric connection. These piles were best suited for friction piles in sand, gravel and clay.

Another jointed reinforced concrete pile type utilized a hexagonal section. The advantages of this cross sectional shape were an improved stress distribution over the pile section and an improved resistance to torsional loading.

Special precautions had to be taken when placing piles during cold weather. If piles were driven through ice and water before reaching soil, the air and concrete may have been at low temperatures relative to the soil and water. Such temperature gradients could cause concrete to crack due to non-uniform shrinkage and expansion. Although most reinforced concrete piles were jointed, there were occasions when non-jointed piles were more economical due to the cost of pile segments. Often for a very large project when thousands of piles were used, the piles were economically cast on site. Most non-jointed piles had a square cross section and were difficult to change in length. Only a few splicing procedures existed if a situation arose where a reinforced concrete pile needed to be lengthened. The first method of pile lengthening involved the breakdown of the projecting pile head to provide a suitable lap for reinforcing steel. Concrete was cast to form a joint. A second option was to butt the two piles together within a steel sleeve, and use an epoxy cement to join the two piles. The last lengthening method involved the use of dowel bars to be inserted into drilled holes with epoxy cement to form the joint. If piles were lengthened, the connecting pile sections had to be carefully aligned, since excessive bending stresses would result if any eccentricity

existed. Splicing problems tended to become less severe or even non-existent when contractors developed experience and techniques. Special reinforcement required at the pile head in seismic areas posed problems if actual lengths varied significantly from the planned length. In these cases, a splice detail had to be included so that the seismic reinforcement was extended into the pile cap.

Reinforced concrete piles are no longer used in the United States. However, they are routinely used in Europe, Australia, and many Asian countries for economic reasons.

6.12 DESIGN CONSIDERATIONS IN AGGRESSIVE SUBSURFACE ENVIRONMENTS

For every design, consideration should be given to the possible deterioration of the pile over its design life due to the surrounding environment. This section will address design considerations in aggressive subsurface environments where corrosion, chemical attack, abrasion, and other factors can adversely affect pile durability after installation. An assessment of the in-situ soil conditions, fill materials, and groundwater properties is necessary to completely categorize an aggressive subsurface condition.

An aggressive environment can generally be identified by soil resistivity and pH tests. If either the pH or soil resistivity tests indicate the subsurface conditions are aggressive, then the pile selection and foundation design should be based on an aggressive subsurface environment. The design of pile foundations in an aggressive environment is a developing field. Therefore, a corrosion/degradation specialist experienced in underground corrosion should be retained for major projects with pile foundations in aggressive environments.

Whenever the pH value of the soil or water is less than 4.5, the foundation design should be based on an aggressive subsurface environment. Alternatively, if the resistivity is less than 2000 ohms-cm the site should also be treated as aggressive. When the soil resistivity test results are between 2000 and 5000 ohms-cm then chloride ion content and sulfate ion content tests should be performed. If these test results indicate a chloride ion content greater than 100 parts per million (ppm) or a sulfate ion content greater than 200 ppm, then the foundation design should be based on an aggressive subsurface environment. Resistivity values greater than 5000 ohms-cm are considered non-aggressive environments. Electro chemical classification tests for aggressive environments are described in Chapter 5.

Contaminated soil and groundwater can cause significant damage to foundation piles in direct contact with the aggressive chemicals. Acidic groundwater is common at sites with organic soils, industrial contamination, or mine runoff. The subsurface exploration program should indicate if the soil or groundwater is contaminated. If industrial contamination is found, the maximum likely concentrations should be determined as well as an estimate of the lateral and vertical extent of the contamination.

6.12.1 Corrosion of Steel Piles

Steel piles driven through contaminated soil and groundwater conditions may be subject to high corrosion rates and should be designed appropriately. Corrosion of steel or steel reinforced piles may also occur if piles are driven into disturbed ground, landfills or cinder fills, or low pH soils. Corrosion should also be evaluated for piles located in a marine environment, or if piles are subject to alternate wetting and drying from tidal action. Corrosion rates are a function of the ambient temperature, pH, access to oxygen, and chemistry of the aqueous environment surrounding the steel member.

6.12.1.1 Corrosion in Non-Marine Environments

AASHTO Standard R 27-01 (2010) provides a recommended assessment procedure for evaluating corrosion of steel piling in non-marine applications. This recommended procedure consists of a Phase I and Phase II assessment. In the Phase I assessment, information on the location of the pile cap relative to the groundwater table, the soil characteristics, and soil contaminants is obtained. This information is used to determine if a Phase II assessment is required.

If the pile cap is at or above the water table, a Phase II assessment is performed to evaluate the corrosivity of the site. The Phase II assessment consists of collecting continuous soil samples to a depth of 3 feet below the water table and conducting laboratory tests on the recovered samples. The site sampling and testing protocol is outlined in Figure 6-26. After collecting the necessary information, the possibility of uniform or macro cell corrosion is evaluated using the flow chart presented in Figure 6-27. The final step in the evaluation process includes determining the necessity for electrochemical testing, corrosion monitoring, and mitigation techniques. A flow chart of this process is presented in Figure 6-28.

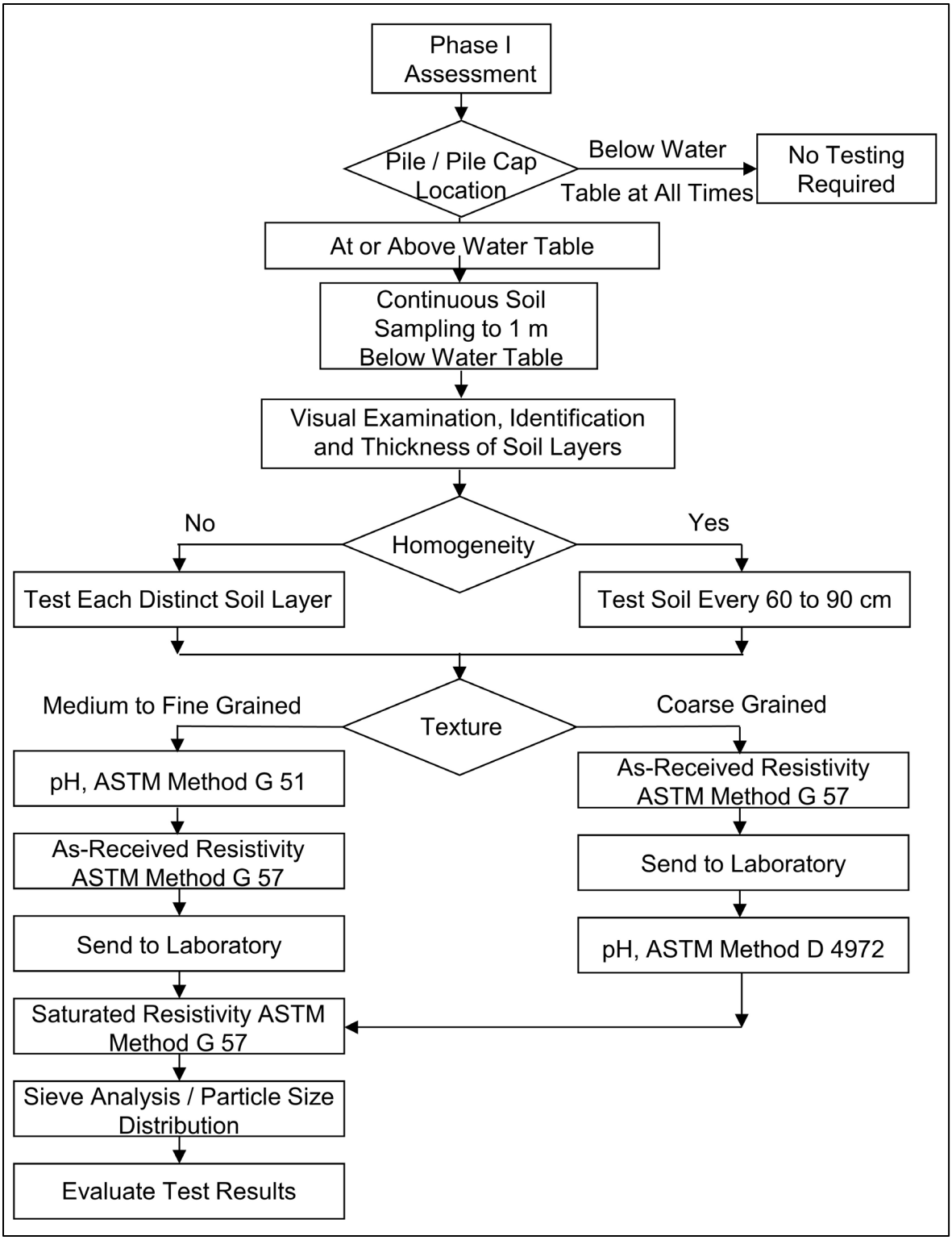

Figure 6-26 Soil sampling and testing protocol for corrosion assessment of steel piles in non-marine applications.

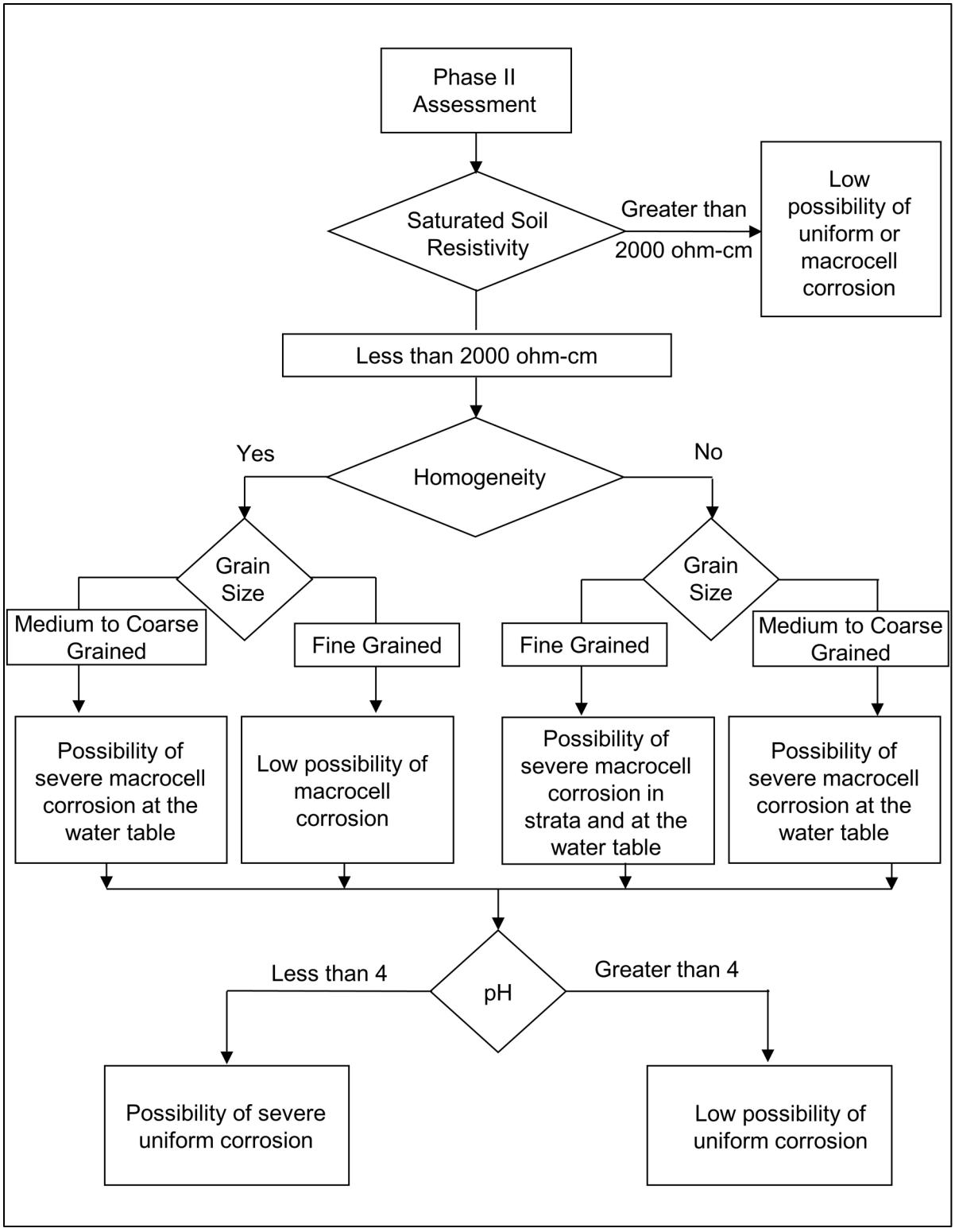

Figure 6-27 Procedure for uniform or macrocell corrosion assessment of steel piles in non-marine applications.

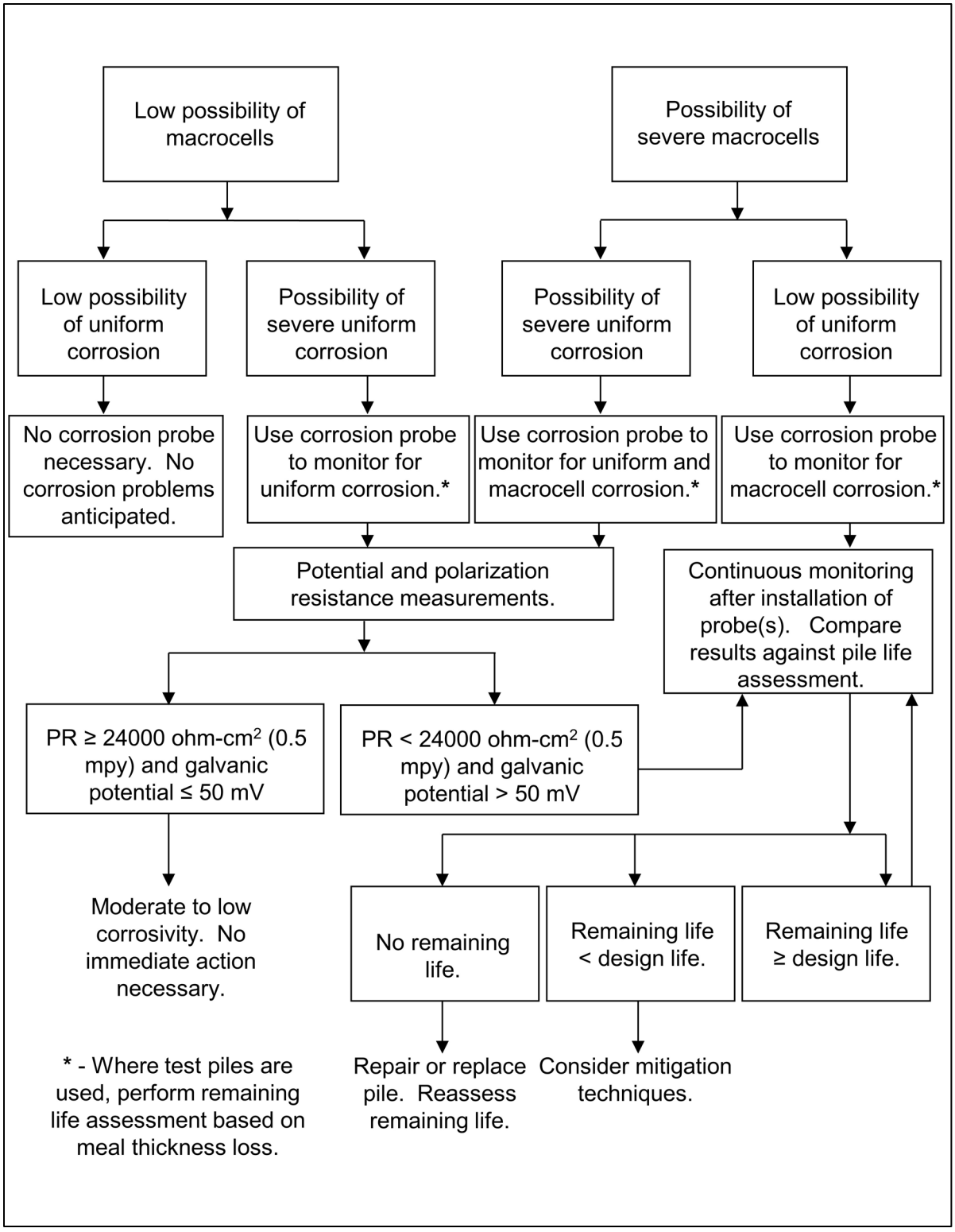

Figure 6-28 Procedure for determination of electrochemical testing, corrosion monitoring and corrosion mitigation techniques.

It should be noted that the flow charts do not cover all possibilities for corrosion of steel piling at a site. Factors not addressed include chemical contamination, stray DC currents, and the presence of high concentrations of microbes. When these conditions are present on a project, an underground corrosion specialist should be consulted.

For steel piles buried in fill or disturbed natural soils, a conservative estimate of the corrosion rate is 0.003 inches per year. Morley (1979) reported corrosion rates of 0.002 inches per year for steel piles immersed in fresh water, except at the waterline in canals where the rate was as high as 0.013 inches per year. The high rate of corrosion at the water line was attributed to debris abrasion and/or cell action between other parts of the structure.

AASHTO Standard R 27-01 (2010) should be consulted for a detailed step by step procedure of corrosion evaluation process and estimation of remaining service life. Additional insight into the corrosion of steel piles in non-marine environments is also presented in NCHRP Report 408 by Beavers and Dunn (1998).

6.12.1.2 Corrosion in Marine Environments

For steel piles in marine environments (salt water), separate zones, each with a different corrosion rate, are present along the length of the pile. Tomlinson (1994) identifies these zones as follows:

1. Atmospheric zone: exposed to the damp atmospheric conditions above the highest water level or subject to airborne spray.

2. Splash zone: above the mean high tide, but exposed to waves, spray, and wash from passing ships.

3. Intertidal zone: between mean high and low tides.

4. Continuous immersion zone: below lowest low tide.

5. Underground zone: below the mudline.

Figure 6-29, after Morley and Bruce (1983), summarizes average and maximum probable marine corrosion rates in these zones as well as in the low water zone. In corrosive environments, the designer should apply one of the design options for piles in corrosive environments discussed in Section 6.12.4.

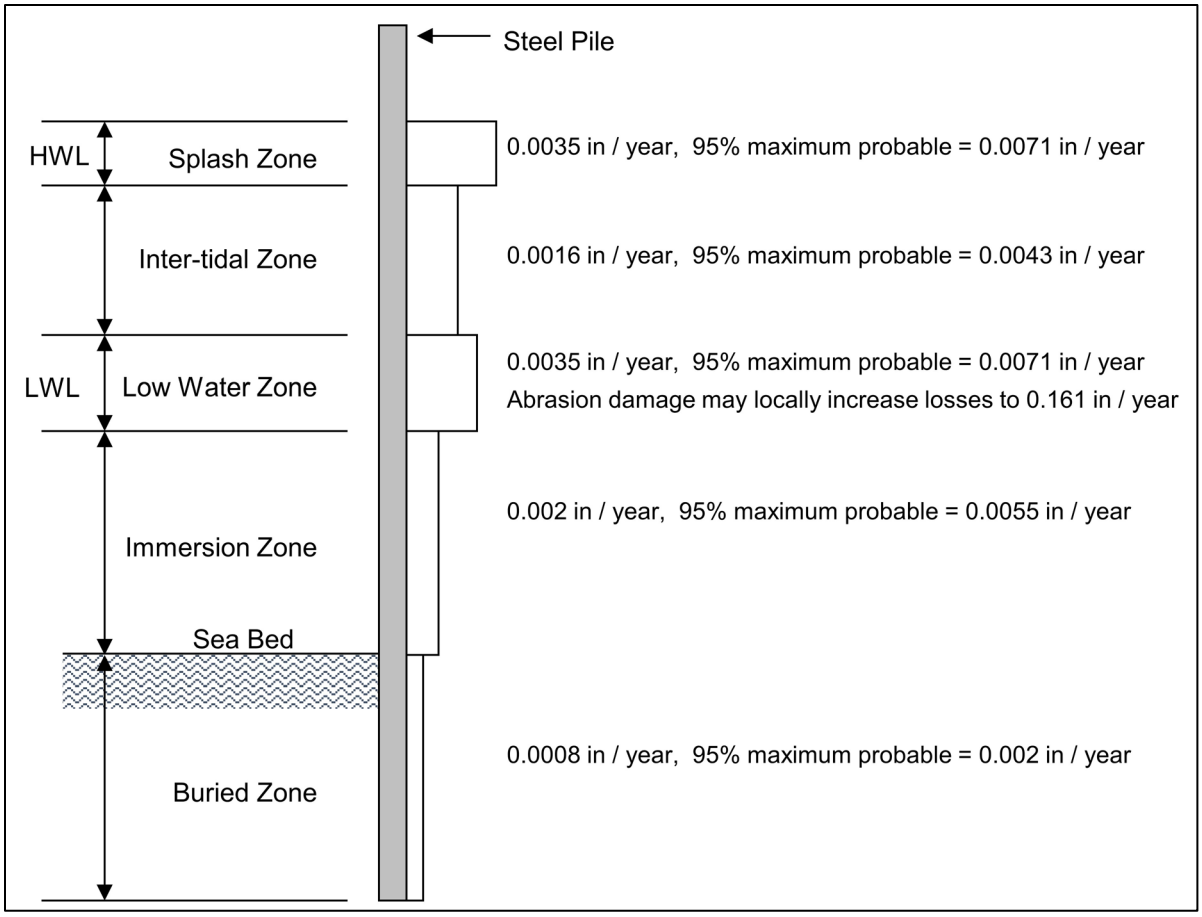

Figure 6-29 Loss of thickness by corrosion for steel piles in seawater (after Morley and Bruce 1983).

6.12.2 Sulfate and Chloride Attack on Concrete Piles

Attack on precast and cast-in-place concrete occurs in soils with high sulfate or chloride concentrations. Factors influencing the rate of deterioration on concrete piles include the pH of the soil, the solubility of the sulfate or chloride, the movement of the groundwater relative to the piles, and the density of the pile concrete.

The reaction between concrete and sulfate begins with sulfate ions in solution. Once the sulfate ions in the groundwater come in contact with Portland cement, an expansive chemical reaction takes place. Expansion of concrete often leads to cracking and spalling which can significantly reduce the available structural resistance of a pile foundation.

One method of reducing sulfate attack is to use a dense concrete which is less permeable to sulfate ions. Other possible deterrents include using sulfate-resisting

cement, using cement with 25% pozzolanic material, or creating a physical barrier between the concrete and the groundwater with some form of pile sleeve.

Chlorides are commonly found in soils, groundwater, or industrial wastes. Instead of attacking concrete, chlorides cause corrosion of reinforcement steel with consequential expansion and bursting of concrete as the products of steel corrosion are formed. Once corrosion begins, it continues at an accelerated rate. This can lead to a loss of bond between steel and concrete and extreme reduction of pile structural resistance. Protective measures which can reduce corrosion include increased concrete cover around the reinforcing steel, and the use of galvanized, or epoxy coated reinforcement.

6.12.3 Bacteria, Fungi, Insect, and Marine Borer Attacks on Timber Piles

Timber piles are subject to attack on land by bacteria, fungi, termites, and beetles, or in water by bacteria, fungi, and marine borers. Incidences of marine borer attack on timber piles have re-emerged in some areas as previously polluted water has improved. As mentioned in Section 6.2, arsenate and creosote pressure treatments are the most effective means of protecting timber piles from premature deterioration. In southern waters, creosote must be combined with other preservative treatments because of attack by limnoria tripuncata. Table 6-8 provides a summary of AWPI recommended preservative treatments depending upon foundation use, preservative, and wood species. Any environmental restrictions or regulations on a preservative treatment in a given situation must be considered.

When designing with timber piles, the wood species is usually not specified unless a specific species of wood is more suitable for design loads and/or environmental conditions. Certain species are not suitable for preservative treatment, while others may provide increased durability. As expected, ASTM standards for timber piles vary with geologic region, as land and fresh water piles have less stringent preservative treatment requirements than piles used in marine environments.

If timber piles are installed in other aggressive environments such as environments containing chemical wastes, a timber pile specialist should be consulted in determining the appropriate preservative treatment.

Table 6-8 Preservative Retention Requirements (after Collin 2002)

Pile Use Category	Southern Pine Creosote (pcf)	Douglas Fir Creosote (pcf)	Southern Pine CCA (pcf)	Douglas Fir ACZA (pcf)
Foundation	12	17	0.8	1.0
Land & Fresh Water	12	17	0.8	1.0
Marine (Saltwater) N. of Delaware[1] or San Francisco[1]	16	16	1.5	1.5
Marine (Saltwater) S. of New Jersey[2] or San Francisco[2]	20	20	2.5	2.5
Marine (Saltwater) Dual Treatment[3]	20	20	1.0	1.0

[1] Where Teredo is expected and Limnoria tripunctata is not expected, creosote or creosote solutions provide adequate protection.

[2] Where Teredo and Limnoria tripunctata are expected and where pholad attack is not expected, either dual treatment, or high retentions of CCA for Southern Pine or ACZA for Douglas Fir provide maximum protection.

[3] In those areas where Limnoria tripunctata and pholad attack is expected or known, dual treatment provides the maximum protection.

6.12.4 Design Options for Piles Subject to Degradation or Abrasion

When a pile must be installed in an aggressive or abrasive environment, several design options can be considered. These design options include:

1. A heavier steel section than required can be used to provide extra thickness (H and pipe sections). This method is not effective in running water with active bedload to scour the corroded surface.

2. Cathodic protection of steel piles in soil below the water table or in marine environments. Note that this method of protection tends to be a costly solution and requires periodic anode replacement.

3. Concrete encasement of steel piles above the mud line. This method may alter the impact absorbing properties of the pile.

4. Use of copper-bearing steel is effective against atmospheric corrosion but the cost is greater than conventional steel.

5. Sleeving or encapsulating of reinforced, cast-in-place piles by using metal casings, polymer or fiberglass jackets isolates contaminants from concrete.

6. Use of a low water/cement ratio, resistant aggregate, and minimum air content consistent with the environment to improve abrasion resistance of precast concrete piles.

7. Use of a protective metallic or epoxy paint (isocyanate-cured) or fusion bonded epoxy coating on exposed sections of the pile. These options may not as effective in running water with active bedload.

8. Use of coal-tar epoxies for corrosion protection in marine environments. This method can also lose effectiveness in running water with active bedload.

Protective coatings cannot be replaced after a pile is driven. Therefore, if a protective coating is used, the coating should be designed to be durable enough to remain undamaged during pile transportation, handling, and placement in the leads for driving as well as resistant to the abrasion resulting from pile driving. The designer should also note that the shaft resistance on a coated pile may be significantly different than on an uncoated pile, depending on the coating.

6.13 SELECTION OF PILE TYPE AND SIZE FOR FURTHER EVALUATION

The selection of appropriate pile types for any project involves the consideration of several design and installation factors including pile characteristics, subsurface conditions and performance criteria. This selection or elimination process should consider the factors listed in Tables 6-1 to 6-7, 6-9, and 6-10. Tables 6-1 to 6-7 summarize typical pile characteristics and uses. Table 6-9 provides pile type

recommendations for various subsurface conditions. Table 6-10 presents the placement effects of pile shape characteristics.

In addition to the considerations provided in the tables, the problems posed by the specific project location and topography must be considered in any pile selection process. Following are some of the usually encountered issues:

1. Vibrations from driven pile installation may affect pile type selection, dictate installation equipment selection and/or use of special installation techniques such as predrilling, and/or necessitate vibration monitoring of adjacent structures.

2. Urban areas, remote areas, or other locations with limited access may restrict driving equipment size and, therefore, pile type and size.

3. Local availability of certain materials and capability of contractors may have decisive effects on pile selection.

4. Waterborne operations may dictate use of shorter pile sections due to pile handling limitations.

5. Steep terrain may make the use of certain pile equipment costly or impossible.

Often several different pile types meet all the requirements for a particular structure. In such cases, the final choice should be made on the basis of a cost analysis that assesses the over-all cost of the foundation alternatives. This requires that candidate pile types be carried forward in the design process for determination of the pile section requirements for design loads and constructability. The cost analysis should also include time and space limitations, time delays, cost of load testing programs, as well as the differences in the cost of pile caps and other elements of the structure that may differ among alternatives. For major projects, alternate foundation designs should be considered for inclusion in the contract documents if there is a potential for cost savings.

Table 6-9 Pile Type Selection Based on Subsurface and Hydraulic Conditions.

TYPICAL PROBLEM	RECOMMENDATIONS
Boulders overlying bearing stratum	Use heavy non-displacement pile with a cast steel driving shoe and include contingent predrilling item in contract.
Loose cohesionless soil	Use a tapered pile to develop the maximum unit shaft resistance.
Downdrag and Drag Force	Avoid use of battered piles due to ground settlement. A pile-soil bond breaker such as a bitumen coating or plastic wrap (if feasible) can be used to reduce large drag forces.
Deep soft clay	Use rough concrete piles to increase adhesion and rate of pore water dissipation.
Artesian pressure	Use solid prestressed concrete pile, tapered piles with sufficient collapse strength, or thick wall closed end pipe with flush boot plate depending upon local practice. H-piles without driving shoes may also be viable selection. Do not use mandrel driven thin-wall shells, as generated hydrostatic pressure may cause shell collapse. Pile heave also common to closed end pile.
Scour	Use uniform section pile with sufficient structural resistance to act as a column through scour zone. Do not use tapered piles unless a large part of the taper extends well below scour depth.
Coarse gravel deposits	Use prestressed concrete piles where hard driving is expected. In coarse soils, use of H-piles and open end pipe piles often results in excessive pile lengths and cost overruns due to pile running during installation.

***** Table modified and reproduced (Cheney and Chassie 1993).

Table 6-10 Pile Type Selection Based on Pile Shape Effects.

SHAPE CHARACTERISTICS	PILE TYPE	PLACEMENT EFFECT
Displacement	Closed end pipe Precast concrete	Increases lateral ground stress. Densifies cohesionless soils, remolds and weakens cohesive soils temporarily. May cause heave and lateral displacement of previously driven piles. Setup time for large pile groups in sensitive clays may be up to six months.
Non-displacement	Steel H Open end pipe	Minimal disturbance to soil. Not suited for friction piles in coarse granular soils. Piles often have low dynamic resistances in these deposits making resistance verification in the field difficult thereby often resulting in excessive pile lengths.
Tapered	Timber Monotube Tapertube	Increased densification of soil, high soil resistance for short penetration lengths in granular soils.

* Table modified and reproduced (Cheney and Chassie 1993).

6.14 HISTORICAL PRICE INFORMATION

Many state transportation agencies post project bid and award information. This media may be downloaded for use by designers, contractors, and project managers to aid in cost estimating. The corresponding agency standard specifications are also typically available to download and should be reviewed to determine the description of the work as well as the method of measurement and payment. Tables 6-11 to 6-17 present recent historical statewide price information for several state agencies.

The description of the work requirements vary from state to state. Prices for furnishing piles and driving piles are listed separately for some state agencies, while a combined bid price is used by others. Items such as pile shoes, splices, sleeves, load tests and mobilization may or may not be incidental, and vary by agency.

6.14.1 California

According to the CALTRANS specification, furnished cost includes any length of pile installed in the ground, including splices and materials to splice. Driving costs included installing and cutting off piles, providing pile tips or shoes and any predrilling involved. Table 6-11 presents costs tabulated from 2014 for various pile types, including the quantity, weighted unit price per linear foot and number of projects for each. Both steel and concrete piles are driven in California and are presented in this table. Pile class 90, 140, or 200 identifies the axial compression resistance in kips for the prestressed concrete piles in the service limit state.

Table 6-11 CALTRANS, 2014 Contract Cost Data

Description	Quantity[1,2]	Weighted Unit Price	No. of Projects
FURNISH STEEL PILING (HP 10 X 57)	12,882	$30.53	3
FURNISH STEEL PILING (HP 14 X 89)	12,100	$45.55	1
FURNISH STEEL PILING (HP 14 X 117)	22,593	$63.69	2
FURNISH 24” CIS SHELL PIPE PILING	8,497	$135.31	3
FURNISH 30” CIS SHELL PIPE PILING	1,262	$145.00	1
FURNISH 48” CIS SHELL PIPE PILING	1,242	$448.19	2
FURNISH PILING (CLASS 90)	3,729	$50.00	1
FURNISH PILING (CLASS 140)	25,583	$25.00	1
FURNISH PILING (CLASS 200)	19,256	$62.87	2
DRIVE STEEL PILE (HP 10 X 57)	280	$2,034.57	3
DRIVE STEEL PILE (HP 14 X 89)	310	$1,050.00	1
DRIVE STEEL PILE (HP 14 X 117)	424	$1,283.02	2
DRIVE 24" STEEL PIPE PILE	132	$5,863.63	3
DRIVE 30" STEEL PIPE PILE	18	$20,200.00	1
DRIVE 48" STEEL PIPE PILE	23	$23,130.43	2
DRIVE PILE (CLASS 90)	94	$1,550.00	1
DRIVE PILE (CLASS 140)	336	$3,100.00	1
DRIVE PILE (CLASS 200)	261	$2513.22	2

[1]Furnished Units in Linear Feet.

[2]Driven Units in Individually Driven Sections.

www.dot.ca.gov/hq/esc/oe/awards/2014CCDB/2014ccdb.pdf

6.14.2 Florida

Although prestressed concrete piles are primarily driven in Florida, steel piles are also included by the Florida Department of Transportation in their 2015 Historical Cost Summary. Costs are summarized on a statewide basis on a moving 12 month average. The data presented below is for the 12 month period ending January 31, 2016. Prices include furnishing and driving piles, per linear foot, with splices included in the per foot price. Pile points or driving shoes are paid per each. Table 6-12 presents the piling related costs.

Table 6-12 FDOT 2015 Historical Cost Information

Description	Quantity[1,2]	Weighted Average Price	No. of Projects
PRESTRESSED CONCRETE PILING, 14" SQ	460	$230.00	1
PRESTRESSED CONCRETE PILING, 18" SQ	21,755	$93.73	7
PRESTRESSED CONCRETE PILING, 24" SQ	105,468	$90.12	10
STEEL PILING, HP 12 X 53	28,113	$49.11	1
STEEL PILING, HP 14 X 89	5,185	$90.57	2
STEEL PILING, 24" DIA. PIPE	560	$224.28	1
POINT PROTECTION , HP 12 X 53	297	$240.24	1
POINT PROTECTION , HP 14 X 89	61	$262.55	1
POINT PROTECTION , 24” PIPE	20	$340.69	1
STEEL PILING, 24" DIA. PIPE	7,936	$121.27	5
TEST PILES - PREST CONCRETE,18" SQ	4,335	$198.65	6
TEST PILES - PREST CONCRETE,24" SQ	9,650	$181.58	9
TEST PILES - STEEL, HP 12 X 53	1,783	$85.63	1
TEST PILES - STEEL, HP 14 x 89	535	$128.69	1
TEST PILES - STEEL, 24" DIA. PIPE	140	$521.59	1

[1]Units in Linear Feet for Piles.
[2]Units in Per Each for Point Protection.
www.dot.state.fl.us/specificationsoffice/Estimates/HistoricalCostInformation/HistoricalCost.shtm

6.14.3 Indiana

Steel piles are used almost exclusively across the Midwest. Table 6-13 presents the weighted average unit bid price for Indiana Department of Transportation pile driving items in 2015. This information is tabulated annually and is available on their website. Pile costs are per linear foot and include furnishing and driving the piles including splices. For closed end steel pipe piles, the price includes the flat end plate and concrete fill. Conical tip protection or inside cutting shoes for pipe piles, driving shoes for H-piles, and mobilization of the driving system are separate pay items. Piles are priced per linear foot installed.

Table 6-13 INDOT 2015 Unit Price Summaries

Description	Quantity[1,2]	Weighted Average Price
PILE, STEEL PIPE, 14 IN O.D. X 0.250 IN WALL	5,370	$48.45
PILE, STEEL PIPE, 14 IN O.D. X 0.312 IN WALL	13,352	$42.10
PILE, STEEL PIPE, 14 IN O.D. X 0.375 IN WALL	3,318	$55.39
PILE, STEEL PIPE, 14 IN O.D. X 0.50 IN WALL	2,861	$58.51
PILE, STEEL PIPE, 18 IN O.D. X 0.50 IN WALL	1,254	$95.00
PILE, STEEL PIPE, 24 IN O.D. X 0.50 IN WALL	838	$65.00
PILE, STEEL PIPE, 24 IN O.D. X 0.75 IN WALL	7,700	$75.00
PILE, STEEL H, HP 12 X 53	17,314	$44.21
PILE, STEEL H, HP 12 X 74	8,362	$67.82
PILE, STEEL H, HP 12 X 84	3,548	$64.39
PILE, STEEL H, HP 14 X 73	59	$325.00
PILE, STEEL H, HP 14 X 89	669	$109.50
CONICAL PILE TIP, 14 IN	327	$277.81
CONICAL PILE TIP, 16 IN	15	$1000.00
PILE SHOE, 24 IN INSIDE CUTTING SHOE	102	$400.00
PILE SHOE, HP 12 X 53	286	$123.43
PILE SHOE, HP 12 X 74	152	$113.85
PILE SHOE, HP 12 X 84	22	$118.17
PILE SHOE, HP 14 X 73	4	$125.00
PILE SHOE, HP 14 X 89	12	$140.00

[1] Units in Linear Feet.

[2] Tip Reinforcement Unit Price for Each.

www.in.gov/dot/div/contracts/pay/

6.14.4 Maryland

The Maryland State Highway administration maintains a price index that is updated twice per year. The piling items, quantities and associated unit costs summarized in the July 2015 price index are presented in Table 6-14. In Maryland, furnishing and driving pile are included in the same pay item and are priced per linear foot. Mobilization of the pile driving system and pile splices are incidental items included in the per foot price. However H-pile shoes (pile points) are a separate bid item, unless specified and are priced per item. Projects for the Maryland State Highway Administration primarily utilize steel piles.

Table 6-14 MDSHA Price Index Published July 2015

Description	Quantity[1,2]	Weighted Average Price	Projects
UNTREATED TIMBER PILE	25,855	$21.19	6
STEEL HP 8 X 36 BEARING PILE	188	$65.00	1
STEEL HP 12 X 53 BEARING PILE	17,703	$47.74	4
STEEL HP 12 X 63 BEARING PILE	2,460	$85.00	1
STEEL HP 12 X 74 BEARING PILE	7,472	$55.00	1
STEEL HP 14 X 73 BEARING PILE	4,328	$55.32	1
STEEL HP 14 X 89 BEARING PILE	66,092	$60.25	9
STEEL HP 14 X 102 BEARING PILE	1,020	$106.51	1
STEEL HP 8 X 36 BEARING TEST PILE	13	$180.00	1
STEEL HP 12 X 53 BEARING TEST PILE	568	$110.30	4
STEEL HP 12 X 63 BEARING TEST PILE	260	$85.00	1
STEEL HP 12 X 74 BEARING TEST PILE	285	$85.00	1
STEEL HP 14 X 73 BEARING TEST PILE	183	$100.00	1
STEEL HP 14 X 89 BEARING TEST PILE	2,250	$87.13	9
STEEL HP 14 X 102 BEARING TEST PILE	255	$196.19	1
PILE POINT FOR 12 INCH HP BEARING PILE	144	$119.63	2
PILE POINT FOR 14 INCH HP BEARING PILE	48	$126.00	1

[1] Pile Units in Linear Feet.
[2] Pile Point Unit Price for Each.

www.roads.maryland.gov/ohd2/MDSHA_PriceIndex_Jul2015.pdf

6.14.5 North Carolina

Multiple geologic conditions dictate that both concrete and steel piles are driven in North Carolina. Table 6-15 presents the 2015 average bid prices compiled by the North Carolina Department of Transportation. Piles are priced per linear foot, while pile points and pile plates are separate items. More detailed information on the scope of measurement and payment may be found in the most recent agency standard specification.

Table 6-15 2015 NCDOT Bid Quantities and Averages

Description	Quantity[1,2]	Weighted Average Price
12" PRESTRESSED CONCRETE PILE	18,220	$58.94
16" PRESTRESSED CONCRETE PILE	28,315	$73.39
24" PRESTRESSED CONCRETE PILE	6,076	$144.80
HP12X53 PILES	43,983	$49.45
HP14X53 GALVANIZED PILES	680	$85.00
HP14X73 PILES	10,016	$62.42
HP14X73 GALVANIZED PILES	1,660	$71.52
HP14X89 PILES	1,195	$75.00
14 IN O.D. X 0.50 STEEL PIPE	3,000	$67.37
36 IN O.D. X 0.625 STEEL PIPE	95	$230.00
14 IN O.D. X 0.50 GALVANIZED STEEL PIPE	480	$145.87
16 IN O.D. X 0.50 GALVANIZED STEEL PIPE	400	$124.53
18 IN O.D. X 0.50 GALVANIZED STEEL PIPE	3,570	$101.47
24 IN O.D. X 0.50 GALVANIZED STEEL PIPE	7,680	$152.39
30 IN O.D. X 0.50 GALVANIZED STEEL PIPE	8,560	$193.34
30 IN O.D. X 0.625 GALVANIZED STEEL PIPE	4,850	$212.30
36 IN O.D. X 0.625 GALVANIZED STEEL PIPE	770	$215.00
PREDRILLING FOR PILES	13,169	$20.38
STEEL PILE POINTS	673	$386.19
PIPE PILE PLATES	262	$168.74

[1] Pile Units in Linear Feet.
[2]Pile Point & Plate Unit Price for Each.

https://connect.ncdot.gov/letting/pages/central-letting-resources.aspx

6.14.6 Pennsylvania

Price history for the Pennsylvania Department of Transportation is presented in Table 6-16 . The latest PennDOT price history covers projects let between April 2013 and April 2015. The majority of PennDot projects involve steel piles, many of which are H-piles driven to rock due to local geology. For bearing piles, the unit price per linear foot includes furnished and driven pile including splices and cutoff. Driving shoes (tips) are a separate pay item. Shoes for timber piles are included in the unit price.

Table 6-16 2015 PennDOT Bid Quantities and Averages

Description	Quantity[1,2]	Weighted Average Price	No. of Projects
TREATED TIMBER BEARING PILES	14,800	$40.00	1
CAST-IN-PLACE CONCRETE PILES	4,907	$74.37	7
CAST-IN-PLACE CONCRETE PILE TIP	22	$804.23	3
STEEL BEAM BEARING PILES, HP10X42	150	$144.50	1
STEEL BEAM BEARING PILES, HP10X57	10,376	$63.01	8
STEEL BEAM BEARING PILES, HP12X53	673	$60.49	3
STEEL BEAM BEARING PILES, HP12X63	3,350	$54.79	3
STEEL BEAM BEARING PILES, HP12X74	63,600	$70.31	47
STEEL BEAM BEARING PILES, HP 12X84	5,278	$96.46	5
STEEL BEAM BEARING PILES, HP14X73	4,497	$71.95	3
STEEL BEAM BEARING PILES, HP14X89	134,174	$85.00	19
STEEL BEAM BEARING PILES, HP14X102	126,960	$68.90	15
STEEL BEAM BEARING PILES, HP14X117	26,458	$91.33	3
NORMAL DUTY PILE TIP - HP 10X57	56	$118.58	2
NORMAL DUTY PILE TIP - HP 12X63	44	$151.59	2
NORMAL DUTY PILE TIP - HP 12X74	410	$151.17	13
NORMAL DUTY PILE TIP - HP 14X73	50	$149.04	2
NORMAL DUTY PILE TIP - HP 14X89	26	$129.00	1
HEAVY DUTY PILE TIP - HP 12X74	405	$141.92	11
HEAVY DUTY PILE TIP - HP 12X84	49	$104.08	2
HEAVY DUTY PILE TIP - HP 14X89	1,388	$134.28	18
HEAVY DUTY PILE TIP - HP 14X117	254	$135.00	1

[1] Pile Units in Linear Feet.

[2]Tip Reinforcement Unit Price for Each.

ftp.dot.state.pa.us/public/Bureaus/design/Pub287/Pub%20287.pdf

6.14.7 Texas

A 12-month statewide moving average of bid prices and quantities from the Texas Department of Transportation is presented below in Table 6-17. The weighted average prices cover the period from March 1, 2015 to February 28, 2016. The unit bid price for piling is per linear foot in place. However, splices and pile tips, when necessary, are a separate bid item. The majority of driven piles in Texas are concrete piles. Please consult the most recent Texas Department of Transportation Standard Specification for further information on measurement and payment items, as well as the average project bid awards as these values are updated monthly.

Table 6-17 TxDOT 12-Month Project Bid Averages

Description	12 Month Quantity[1]	12 Month AVG BID	No. of Projects
STEEL H-PILING (HP 12 X 53)	640	$150.00	1
STEEL H-PILING (HP 14 X 117)	201	$20.00	1
PRESTR CONCRETE PILING (16 IN SQ)	48,679	$113.38	17
PRESTR CONCRETE PILING (18 IN SQ)	7,133	$100.20	8
PRESTR CONCRETE PILING (20 IN SQ)	8,151	$118.80	3
PRESTR CONCRETE PILING (24 IN SQ)	3,304	$135.00	1

[1] Units in Linear feet.

www.txdot.gov/business/letting-bids/average-low-bid-unit-prices.html

A brief summary of pay items was presented for selected state agencies covering a range of pile types and installation conditions. The designer should consult the most current price information from the appropriate agency as price histories and specifications change over time.

REFERENCES

American Concrete Institute (ACI), (2012). Guide to Design, Manufacture and Installation of Concrete Piles. ACI-543R-12, 64 p.

American Association of State Highway and Transportation Officials (AASHTO). (2001). Standard Recommended Practice for Assessment of Corrosion of Steel Piling for Non-Marine Applications. AASHTO Standard Specifications for Transportation Materials and Methods of Sampling and Testing, Part 1B: Specifications, 24th Edition, 13 p.

American Association of State Highway and Transportation Officials (AASHTO). (2014). AASHTO LRFD Bridge Design Specifications, US Customary Units, Seventh Edition, with 2015 Interim Revisions. American Association of State Highway and Transportation Officials, Washington, D.C., 1960 p.

Beavers, J.A. and Durr, C.L. (1998). Corrosion of Steel Piling in Non-Marine Applications. NCHRP Report 408, National Cooperative Highway Research Program, Transportation Research Board, Washington, D.C., 35 p.

Belk, N.A. (2013). Evaluation of Lightweight Aggregate Concrete for Precast, Prestressed Driven Piles. PhD Dissertation, Auburn University, 215 p.

Brown, D.A., Dapp, S.D., Thompson, W.R., and Lazarte, C.A. (2007). Design and Construction of Continuous Flight Auger (CFA) Piles. FHWA-HIF-07-03, Geotechnical Engineering Circular (GEC) No. 8. U.S. Dept. of Transportation, Federal Highway Administration, 289 p.

Brown, D. A., Turner, J.P. and Castelli R.J. (2010). Drilled Shafts: Construction Procedures and LRFD Design Methods, FHWA-NHI-10-016, Geotechnical Engineering Circular (GEC) No. 10. U.S. Dept. of Transportation, Federal Highway Administration, 970 p.

Brown, D.A., and Thompson III, W.R. (2015). Current Practices for Design and Load Testing of Large Diameter Open-End Driven Pipe Piles. Final Report. NCHRP Report 20-05, Topic 45-05, National Cooperative Highway Research Program, Washington, D.C., 175 p.

Chellis, R.D. (1961). Pile Foundations. Second Edition, McGraw-Hill Book Company, New York, NY, 704 p.

Cheney, R.S. and Chassie, R.G. (2000). Soils and Foundations Workshop Reference Manual. FHWA HI-00-045, U.S. Department of Transportation, National Highway Institute, Federal Highway Administration, Washington, D.C., 358 p.

Collin, J.G. (2002). Timber Pile Design and Construction Manual. American Wood Preservers Institute (AWPI), 122 p.

Department of the Navy, (1982). Foundations and Earth Structures Design Manual. DM 7.2. Naval Facilities Engineering Command, (NAVFAC), Alexandria, VA, 279 p.

Fleming, W.G.K., Weltman, A.J., Randolph, M.F. Elson, W.K. (2008). Piling Engineering, Third Edition, Taylor and Francis, New York, New York, NY, 398 p.

Fuller, F.M. (1983). Engineering of Pile Installations. McGraw-Hill, New York, NY, 286 p.

Graham, J. (1995). Personal Communication.

Hartman, J.J., Castelli, R.J., and Malhotra, S. (2007). Design and Installation of Concrete Cylinder Piles. Proceeding of GeoDenver 2007, GSP 158 Contemporary Issues in Deep Foundations, ASCE, pp. 1-14.

Moser, R., Holland, B. Kahn, L., Singh, P., and Kurtis, K. (2011). Durability of Precast Prestressed Concrete Piles in Marine Environment: Reinforcement Corrosion and Mitigation Part 1. GDOT Research Project No. 07-30. Office of Materials and Research Georgia Department of Transportation, 243 p.

Morley, J. (1979). The Corrosion and Protection of Steel Piling, British Steel Corporation, Teesside Laboratories, Report No. T/CS/906/4/78/C.

Morley, J. and Bruce, D.W. (1983). Survey of Steel Piling Performance in Marine Environments, Final Report, Commission of the European Communities, Document EUR 8492 EN, 25 p.

Portland Cement Association (PCA). (1951). Concrete Piles: Design, Manufacture and Driving, 80 p.

Prakash, S. and Sharma, H. (1990). Pile Foundations in Engineering Practice. John Wiley and Sons, Inc., New York, NY, 768 p.

Rausche, F. (1994). Design, Installation and Testing of Nearshore Piles. Proceedings of the 8th Annual Symposium on Deep Foundations, Vancouver.

Sabatini, P.J., Tanyu, B., Armour., P., Groneck, P., and Keeley, J. (2005). Micropile Design and Construction, FHWA-NHI-05-039. National Highway Institute, U.S. Dept. of Transportation, Federal Highway Administration, Washington, D.C., 436 p.

Tomlinson, M.J. (1994). Pile Design and Construction Practice, Fourth Edition, E & FN Spon, London, 432 p.

Transportation Research Board. (1977). Design of Pile Foundations. NCHRP Synthesis of Highway Practice No. 42, 68 p.

Vande Voort, T., Suleiman, M. T., and Sritharan, S. (2008). Design and Performance Verification of Ultra-High Performance Concrete Piles for Deep Foundations. Final Report, Iowa DOT, IHRB Project TR-558, CTRE Project 06-264, Iowa Dept. of Transportation, Ames, IA, 206 p.

CHAPTER 7

GEOTECHNICAL ASPECTS AND LIMIT STATE DESIGN

7.1 INTRODUCTION

Static analysis methods can be categorized as analytical methods that use geomaterial strength and compressibility properties to determine nominal geotechnical resistance and deformation. This chapter will focus on analysis methods for determining the nominal geotechnical resistance of single piles and pile groups in axial compression, uplift, and lateral loading as well as the resulting vertical and lateral deformations. Important considerations are as follows:

1. Static analysis methods are an integral part of the design process. Static analysis methods are necessary to determine the most cost effective pile type and to estimate the number of piles and the required pile lengths for the design of substructure elements. The foundation designer must have knowledge of the design loads and the project performance criteria in order to perform the appropriate static analyses.

2. Many static analysis methods are available. The methods presented in this chapter are relatively simple methods that have proven to provide reasonable agreement with full scale field results. Many of these methods are also included in the AASHTO (2014) design specifications. Other more sophisticated analysis methods may be used and in some cases may provide better results. Regardless of the method used, it is important to continually apply experience gained from past field performance of the analysis method.

3. Designers should fully understand the basis for, the limitations of, and the applicability of a chosen method. This is particularly true of computer solutions where some underlying assumptions may not be readily apparent. A selected method should also have a proven agreement with full scale field results.

4. Evaluation and confirmation of pile drivability is an integral part of limit state design. Foundation designs with fewer, larger, pile sections having greater nominal resistances are more frequently being used. The ability of these

piles to achieve the required pile penetration depths necessary to satisfy all nominal resistance and deformation requirements is a critical design check. A pile drivability analysis requires combining the geotechnical aspects detailed in this chapter with the wave equation analysis procedures described in Chapter 12. A drivability analysis should be performed by the engineer during the design stage to assess the constructability of the pile design.

Construction procedures can have a significant influence on the behavior of pile foundations. The analysis methods described in this chapter lead to successful designs of deep foundations only if appropriate construction techniques and construction monitoring methods are used. Construction monitoring should be an integral part of the design and construction of any foundation. Static load tests, wave equation analysis or dynamic monitoring for construction control should, whenever possible, be used to confirm the results of a static design method. These topics are discussed in detail in subsequent chapters.

The first few sections of this chapter will briefly cover background information. Static analysis procedures for piles subject to compression, uplift, and lateral loads will be covered, as well as pile group settlement. The influence of special design events on driven pile designs will also be discussed. Limited guidance on design in liquefaction susceptible soils is provided. Detailed seismic design is beyond the scope of this manual and is covered in GEC-3 by Kavazanjian et.al (2011). Finally, this chapter will address construction issues pertinent to static analysis methods and foundation design. In all cases, existing character notation for soil resistances as well as load and resistance factors utilized by AASHTO (2014) will be presented.

7.1.1 Static Analysis Methods in Limit State Design

There are four general types of static analyses addressed in this chapter. Static analyses are performed to determine:

1. Nominal resistance in axial compression of a pile or pile group. These calculations are performed to determine the long term resistance of a foundation as well as to determine the soil resistance provided from soil layers subject to scour, liquefaction, downdrag, or that are otherwise unsuitable for long term load support. Static analyses are used to establish minimum pile penetration requirements, pile lengths for bid quantities, as well as to estimate the soil resistance at the time of driving (SRD) and the required nominal driving resistance, R_{ndr}.

2. Nominal resistance in axial tension of a pile or pile group. These calculations are performed to determine the soil resistance to uplift or tension loading which, in some cases, may also determine the minimum pile penetration requirements.

3. Nominal lateral resistance and lateral deformation of a pile or pile group. These soil-structure interaction analysis methods consider the soil strength and deformation behavior as well as the pile structural properties and are used in pile section selection.

4. Settlement of a pile group. These calculations are performed to estimate the vertical foundation deformation under the structure's service loads.

The factored geotechnical resistance of a pile can be defined as the sum of geomaterial resistances along the pile shaft and at the pile toe available to support the factored loads on the pile. As noted above, static analyses are performed to determine the factored resistance of an individual pile and of a pile group as well as the deformation response of a pile group to the factored loads. The factored resistance of an individual pile and of a pile group is the smaller of: (1) the factored geotechnical resistance of surrounding soil/rock medium to support the loads transferred from the pile(s) or, (2) the factored structural resistance of the pile(s). Soil-structure interaction analysis methods are used to determine the deformation response of a pile and pile groups to lateral loads. The results from these analyses in conjunction with pile group settlement analysis are compared to the performance criteria established for the structure. Both vertical (settlement) and lateral deformation analyses of pile groups are computed using factored loads at the service limit state.

The static pile resistance from the sum of the soil/rock resistances along the pile shaft and at the pile toe can be estimated from geotechnical engineering analysis using:

1. Laboratory determined shear strength parameters of the soil and rock surrounding the pile.

2. In-situ test data (i.e., SPT, CPT).

3. Back analysis of geomaterial design parameters based on performance data.

Prior to discussing static design methods for estimating pile resistance in detail, it is desirable to review events that occur in the pile soil system during and after pile driving as well as basic load transfer mechanisms.

7.1.2 Events During and After Pile Driving

The soil and some weaker rocks in which a pile foundation is installed are almost always disturbed. Several factors influence the degree of disturbance. These include the soil and rock type and density, the pile type (displacement, low-displacement), and the method of pile installation (driven, vibrated, drilled, jetted). For driven piles, substantial disturbance and remolding is unavoidable in soils and weaker rocks where the in-situ stresses and rock structure are changed during pile installation.

Over the long term, scour, settlement, pore pressure fluctuations, seismic and other extreme events may occur. These situations should be addressed in the applicable strength, extreme, and service limit states such that sufficient embedment and foundation stiffness is achieved. These topics, among others, will be discussed throughout this chapter.

7.1.2.1 Cohesionless Soils

The resistance of piles driven into cohesionless soil depends primarily on the relative density of the soil. During driving, the relative density of loose to medium dense cohesionless soil is increased close to the pile due to vibrations and lateral displacement of soil. This effect is most pronounced in the immediate vicinity of displacement piles. Broms (1966) and more recent studies found the zone of densification extends as far as 3 to 5.5 diameters away from the pile shaft and 3 to 5 diameters below the pile toe as depicted in Figure 7-1.

The increase in relative density increases the resistance of single piles and pile groups. The pile type selection also affects the amount of change in relative density. Piles with large displacement characteristics such as closed end pipe and precast concrete piles increase the relative density of cohesionless material more than low-displacement open end pipe or steel H-piles. Similarly, vibratory installation may increase the relative density of loose to medium dense cohesionless material more than driving with an impact hammer.

In dense cohesionless soil, the relative density may actually decrease since dense soils will dilate during shear and displacement. As a result, negative pore pressures

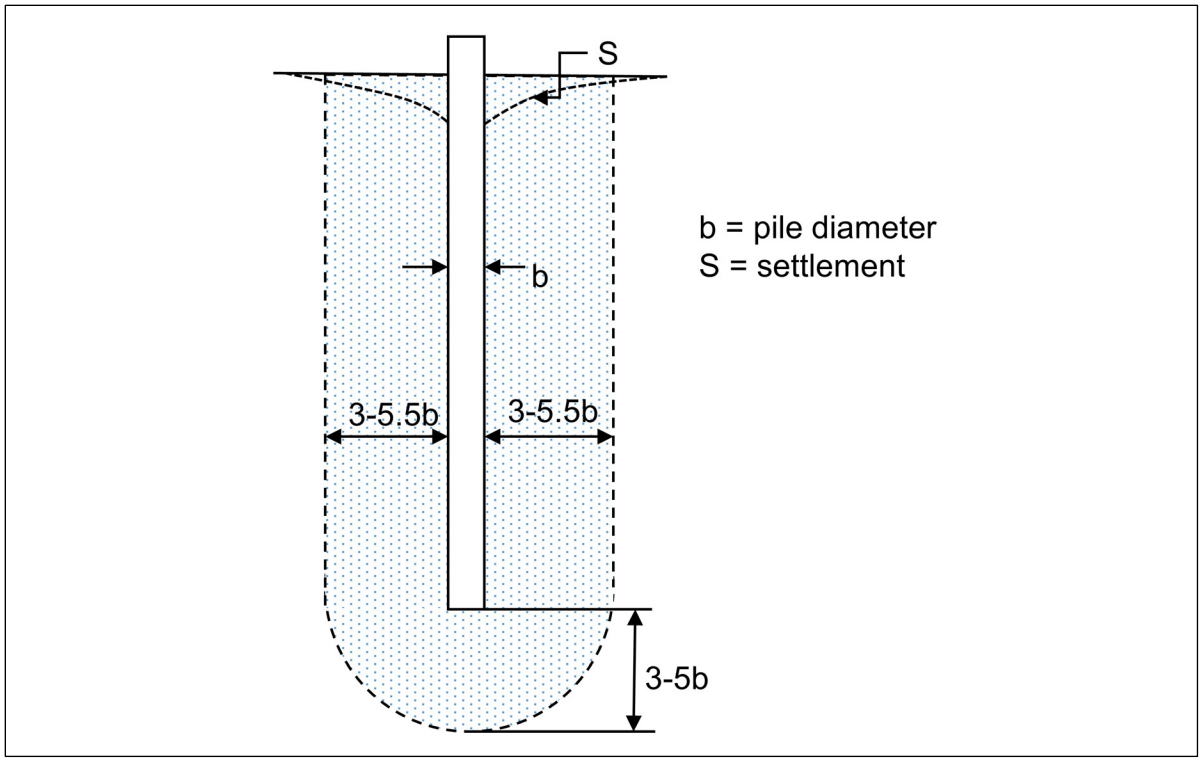

Figure 7-1 Compaction of cohesionless soils during pile driving (after Broms 1966).

may temporarily be generated during driving which could lead to a temporarily increased resistance. The increase in stress, which can occur adjacent to the pile shaft and/or below the pile toe during the driving process, can be lost by relaxation in dense sand and gravels as the negative pore pressures generated during driving are dissipated. The phenomena can be explained by the shear strength equation presented in Equation 7-1.

$$\tau = c + (\sigma - u)\ tan\ \phi \qquad \text{Eq. 7-1}$$

Where:

- τ = shear strength of soil.
- c = cohesion.
- σ = total normal stress (pressure) on plane of failure.
- u = pore water pressure.
- ϕ = angle of internal friction.

Negative pore pressures temporarily increase the soil shear strength, and therefore pile resistance, by changing the $(\sigma - u)$ tan ϕ component of shear strength to $(\sigma + u)$ tan ϕ. As negative pore pressures dissipate, the shear strength and pile resistance decrease.

The pile driving process can also generate high positive pore water pressures in saturated cohesionless silts and loose to medium dense fine sands. Positive pore pressures temporarily reduce the soil shear strength and the pile resistance. This phenomena is identical to the one described below for cohesive soils. The gain in resistance with time or soil setup is generally quicker for sands and silts than for clays because the pore pressures dissipate more rapidly in cohesionless soils than in cohesive soils.

7.1.2.2 Cohesive Soils

When piles are driven into saturated cohesive materials, the soil near the piles is disturbed and radially compressed. For soft or normally consolidated clays, the zone of disturbance is generally within one pile diameter around the pile. For piles driven into saturated stiff clays, there are also significant changes in secondary soil structure (closing of fissures) with remolding and loss of previous stress history effects in the immediate vicinity of pile. Figure 7-2 illustrates the disturbance zone for piles driven in cohesive soils as observed by Broms (1966). This figure also notes the heave that can occur when driving displacement piles in cohesive soils.

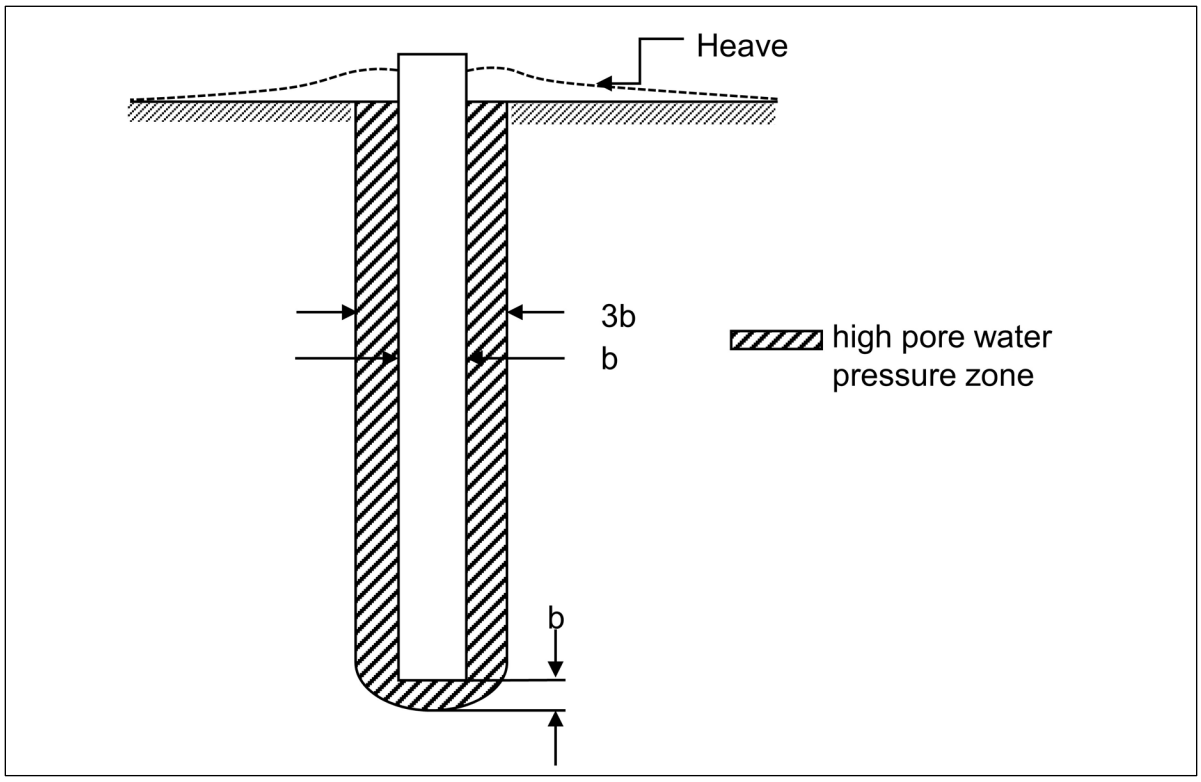

Figure 7-2 Disturbance of cohesive soils during pile driving (after Broms 1966).

The disturbance and radial compression generate high pore pressures (excess positive pore pressures) which temporarily reduce soil shear strength, the nominal geotechnical resistance, and therefore the pile penetration resistance or blow count. As reconsolidation of cohesive soils around the pile occurs, the high pore pressures are diminished, which leads to an increase in shear strength and pile resistance (setup). This phenomenon is opposite to "relaxation" described for cohesionless soils. The zone and magnitude of soil disturbance are dependent on the soil properties of soil sensitivity, driving method, and the pile foundation geometry. Limited data available for partially saturated cohesive soils indicates that pile driving does not generate high pore pressures and hence significant soil setup does not occur.

7.1.2.3 Additional Soil Resistance Considerations

On many driven pile projects, multiple static analyses are required for a design. First, a static analysis is necessary to determine the number and length of piles necessary to support the structure loads. A second static analysis may also be required to determine the nominal resistance the pile will encounter during installation. This second analysis enables the design engineer to determine the necessary capability of the driving equipment and the minimum pile section requirements based on drivability. Figures 7-3 and 7-4 illustrate situations that require two static analyses.

Figure 7-3 shows a situation where piles are to be driven for a bridge pier. In this case, the first static analysis performed should neglect the soil resistance in the soil zone subject to scour, since this resistance may not be available for long term support. The number of piles and pile lengths determined from this analysis will then be representative of the long term conditions in the event of scour. At the time of pile driving however, the scour zone soil will provide resistance to pile penetration. Therefore, a second static analysis is required to estimate the nominal resistance encountered by the pile during driving to the embedment depth determined in the first analysis. The second static analysis includes the soil resistance in the materials above the scour depth as well as the underlying strata.

Figure 7-4 shows another frequently encountered situation in which piles are driven through loose uncompacted fill material into the natural ground. The loose fill material offers unreliable resistance and is usually neglected in determining the number of piles and the pile lengths required. A second static analysis is then performed to determine nominal resistance encountered by the pile during driving, which includes the resistance in the fill material.

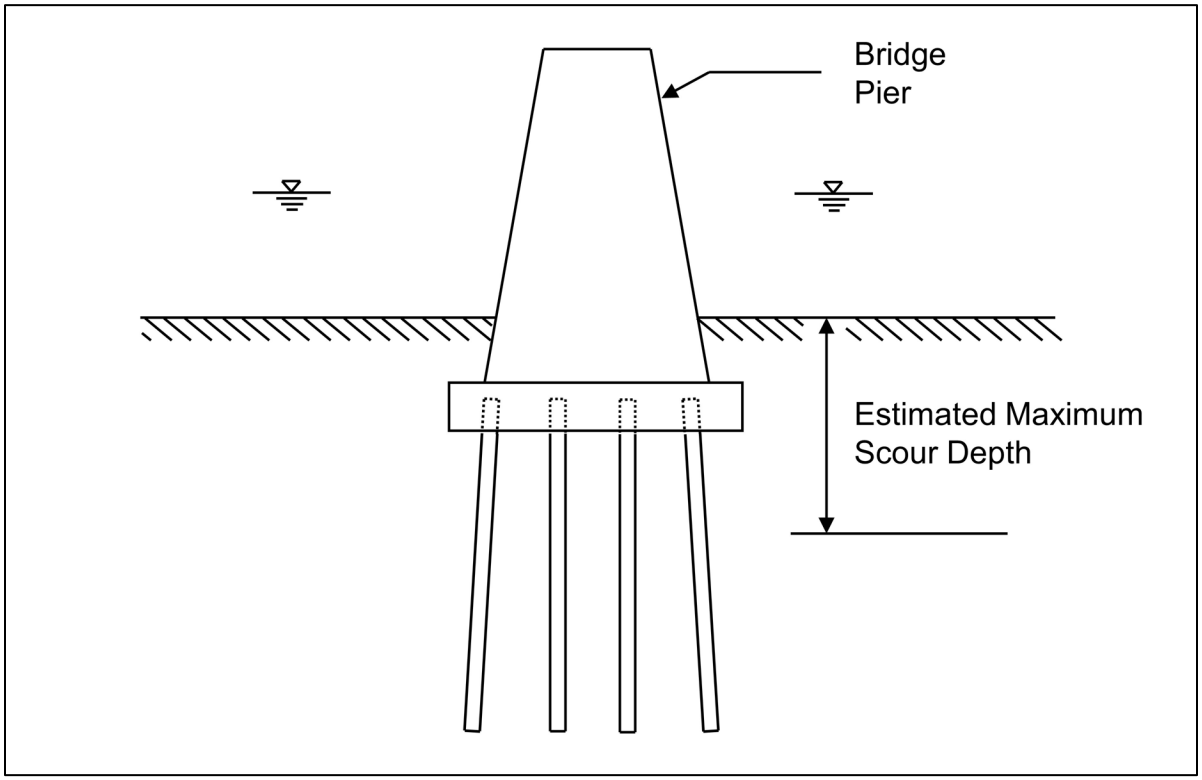

Figure 7-3 Situation where two static analyses are necessary due to scour.

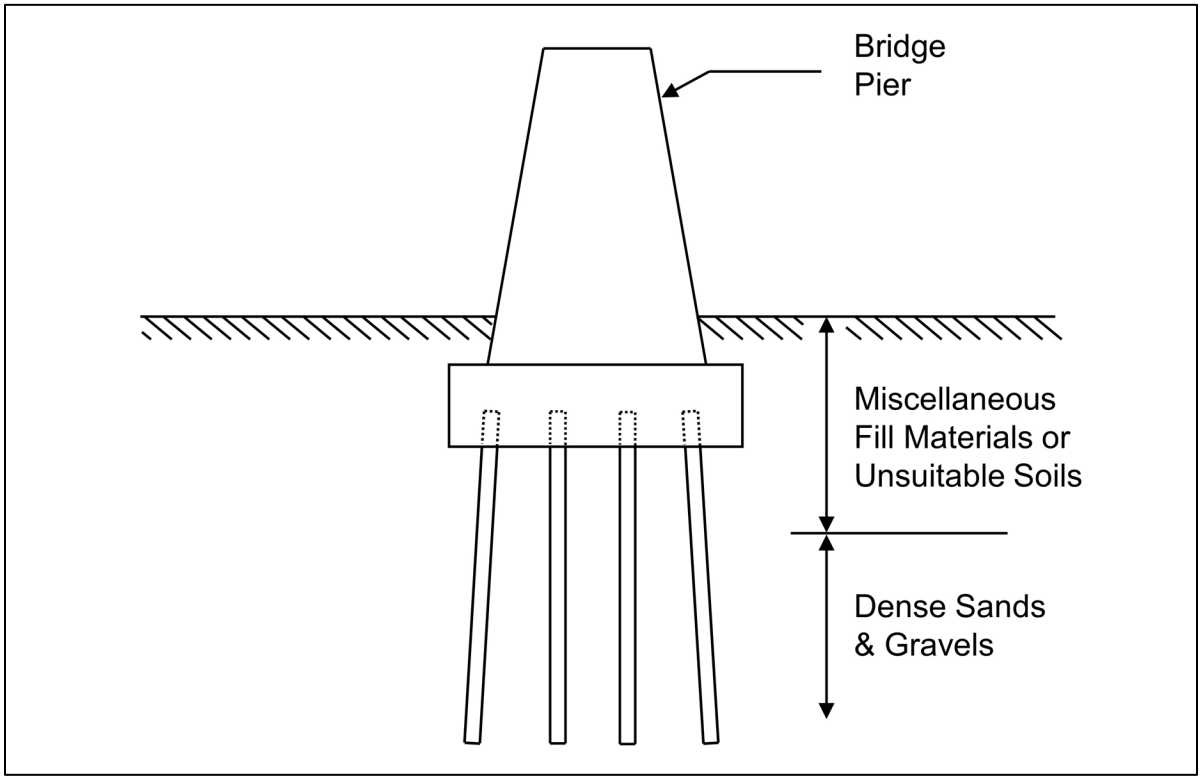

Figure 7-4 Situation where two static analyses are necessary due to fill materials.

In both examples, the soil resistance to be overcome during driving will be substantially greater than the required nominal resistance, R_n. The geotechnical resistance computed in the scourable or unsuitable layer, determined from static analysis, is then added to the required nominal resistance when determining the required nominal driving resistance, R_{ndr}.

The results of multiple static analyses should be considered in the development of project plans and specifications. For example, consider a case where scour, uplift loading, or some other design consideration (e.g., seismic event) dictates that a greater pile penetration depth be achieved than that required for support of the axial compressive loads. The static analyses indicate that a soil resistance of 420 kips must be overcome to obtain the minimum penetration depth needed for a 300 kip nominal resistance in axial compression. This information is germane to the drivability assessment for pile section selection. It should also be conveyed in the construction documents so that the driving equipment can be properly sized and so that the intent of the design is clearly and correctly interpreted by the contractor and construction personnel. Specifying only the 300 kip nominal resistance or providing only the factored load on the plans could easily be misinterpreted and can lead to construction claims. In the above example, the controlling factored load, the nominal resistance, the required nominal driving resistance, and the minimum penetration depth should all be provided. A more in depth discussion on driving criteria is presented in Chapter 17.

7.1.3 Load Transfer

The nominal resistance, R_n, of a pile in homogeneous soil may be expressed by the sum of the shaft resistance R_s and toe resistance R_p, or

$$R_n = R_s + R_p \qquad \text{Eq. 7-2}$$

The above equation for nominal resistance assumes that both the pile toe and the pile shaft have moved sufficiently with respect to the adjacent soil to simultaneously develop the nominal shaft and toe resistances. Generally, the displacement needed to mobilize the shaft resistance is smaller than that required to mobilize the toe resistance. This simple rational approach has been commonly used for all piles except very large piles greater than 36 inches in diameter or width.

Figure 7-5 illustrates typical load transfer profiles for a single pile. The load transfer distribution can be obtained from a static load test where strain gages or telltale rods

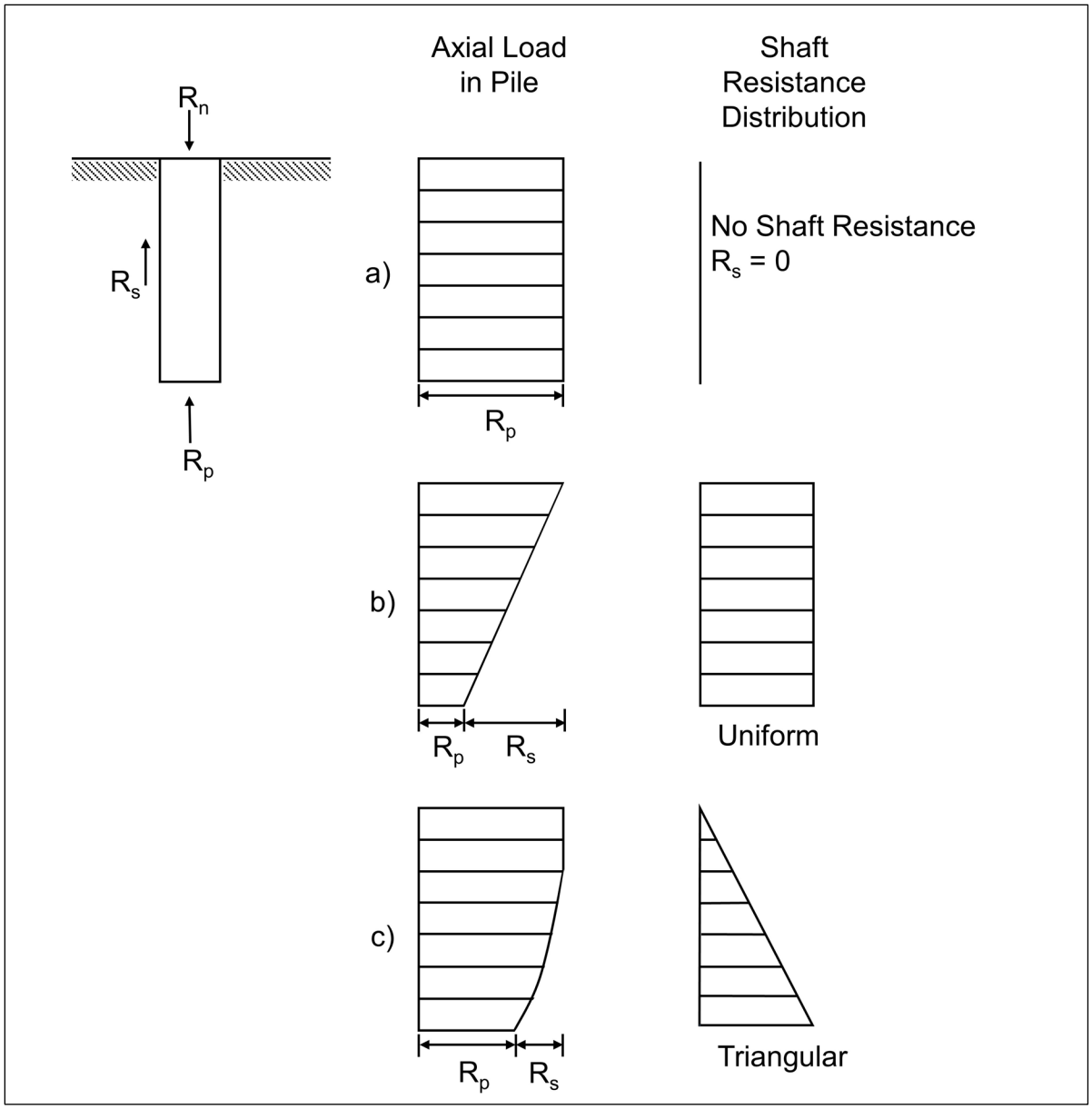

Figure 7-5 Typical load transfer profiles.

are attached to a pile at different depths along the pile shaft. Figure 7-5 shows the nominal resistance, R_n, in the pile plotted against depth. The shaft resistance transferred to the soil is represented by R_s, while R_p represents the resistance at the pile toe. In Figure 7-5(a), the load transfer distribution for a pile with no shaft resistance is illustrated. In this case the full axial load at the pile head is transferred to the pile toe. In Figure 7-5(b), the axial load versus depth for a uniform shaft resistance distribution typical of a cohesive soil is illustrated. Figure 7-5(c) presents the axial load in the pile versus depth for a triangular shaft resistance distribution and is typical of cohesionless soils.

7.1.4 Effective Stress

The vertical effective stress at a given depth below ground surface is the vertical stress at that depth due to the weight of the overlying soils. An Effective Stress Diagram plots the vertical effective stress versus depth, and is used in many static resistance and settlement calculations. An understanding of how to construct and use an Effective Stress Diagram is therefore important.

Information needed to construct an Effective Stress Diagram includes the total unit weight and thickness of each soil layer as well as the depth of the water table. The soil layer thickness and depth of the water table should be available from the project boring logs. The total unit weight of each soil layer may be obtained from density tests on undisturbed cohesive samples or estimated from Standard Penetration Test (SPT) N values in conjunction with the soil visual classification.

The first step in constructing an Effective Stress Diagram is to calculate the total vertical stress, σ_{vo}, versus depth. This is done by summing the product of the total unit weight times the layer thickness versus depth which was demonstrated in Section 5.2.2. Similarly, the pore water pressure, u, is summed versus depth by multiplying the unit weight of water, γ_w = 62.4 lb/ft^3, times the water height. The vertical effective stress, σ'_{vo}, at any depth is then the total vertical stress minus the pore water pressure at that depth.

The vertical effective stress at any depth is determined by summing the weights of all layers above that depth as follows:

1. For soil deposits above the static water table:
   σ'_{vo}= (total soil unit weight, γ)(thickness of soil layer above the desired depth).

2. For soil deposits below the static water table:
   σ'_{vo} = (total soil unit weight, γ)(depth) - (unit weight of water, γ_w)(height of water, h_w).

The design water table elevation should be carefully selected. It should compared to the water level determined in the subsurface exploration and consider seasonal variations.

Figures 7-6 and 7-7 present examples of Effective Stress Diagrams for cases where the water table is above and below the ground surface level.

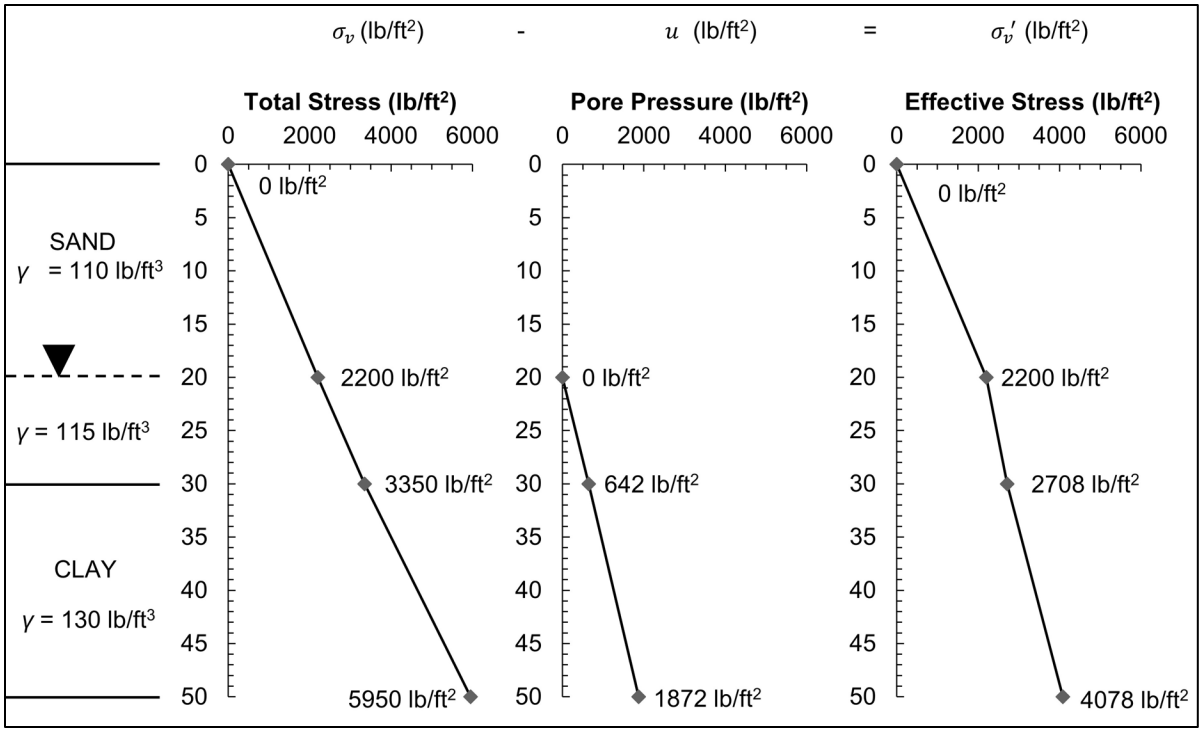

Figure 7-6 Effective stress diagram – water table below ground surface.

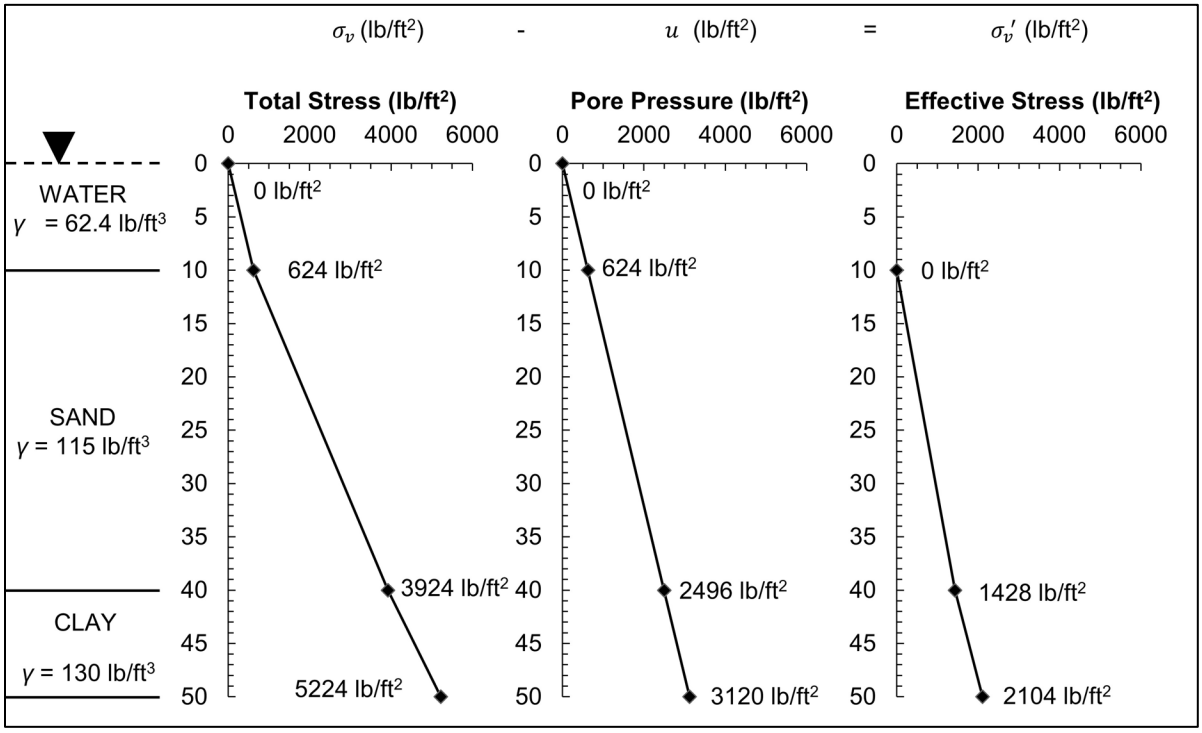

Figure 7-7 Effective stress diagram – water table above ground surface.

7.1.5 Resistance Factors

As discussed in Chapter 2, limit state design for highway structures in the U.S. has been mandated since 2007, and is specified to achieve objectives of safety, serviceability, constructability, and economy. Resistance factors applicable to driven pile design are contained in AASHTO (2014) Table 10.6.5.2.3-1. Section 7.2 of this chapter reviews nominal resistance methods for the strength limit state, while Section 7.3 describes lateral deflection and group settlement for the service limit state. Section 7.4 discusses extreme limit state design which must address strength and serviceability requirements for the respective factored loads and performance requirements.

Resistance factors should not be viewed as a direct replacement for the factor of safety previously used in the allowable stress design (ASD) platform. As discussed in Chapter 2, a resistance factor is a statistically based multiplier applied to the nominal resistance determined from a specific analysis method or analysis procedure. It may be a value determined by national practice (i.e. AASHTO) or it may be a locally calibrated value determined from past practice, databases, and correlation studies. Similarly, load factors are applied to address the uncertainty on the load side, with the load factor also acting as a statistically based multiplier on the force effect. Both the load and resistance factors are tied to a target reliability index, β, which quantifies the probability of non-performance or failure.

Resistance factors to determine the factored resistance via static analysis calculations are summarized in Table 7-1. Several static analysis methods are documented in the literature. However, only those most commonly used in the US transportation industry will be presented in this chapter. Table 7-1 includes several static analysis methods that are presented in this manual that do not have calibrated resistance factors in AASHTO. The presented resistance factors are the best guidance available at the present time. Further research and calibration studies are needed in this area. Brown and Thompson (2015) noted that the AASHTO resistance factor calibration study considered few large diameter pipe piles. Therefore the designer should consider this factor if performing analyses for piles larger than 24 inches in diameter regardless of pile type.

Where a static analysis method is used to determine nominal resistance, the factored resistance, R_r, shall be less than or equal to the sum of the shaft resistance multiplied by the resistance factor associated with the shaft resistance computation method plus the toe resistance multiplied by the resistance factor for the toe resistance computation method as presented in Equation 7-3.

$$R_r \leq \phi R_n = \phi_{stat} R_s + \phi_{stat} R_p \quad \text{Eq. 7-3}$$

Where:

R_r = factored resistance (kips).
ϕ_{stat} = resistance factor (based on the static analysis method).
R_n = nominal resistance (kips).

Table 7-1 Resistance Factors for Static Analysis Methods Presented in this Manual (modified from AASHTO 2014)

Condition	Resistance Determination Method	Resistance Factor
Nominal Geotechnical Resistance of Single Piles in Compression - Static Analysis Methods, ϕ_{stat}	Shaft Resistance and Toe Resistance: Clay and Mixed Soils	
	α-method	0.35
	β-method (1991)	Differs in Manual[1]
	Brown (2001)	not in AASHTO
	API RP2A (1993)	not in AASHTO
	Elsami and Fellenius	not in AASHTO
	Schmertmann (1975)	0.50
	Shaft Resistance and Toe Resistance: Sand	
	Nordlund Method	0.45
Block Failure, ϕ_{b1}	Cohesive	0.60
Nominal Geotechnical Resistance of Single Piles in Tension, ϕ_{up}	Nordlund Method	0.35
	α-method	0.25
	β-method (1991)	0.20
	λ-method	0.30
	SPT-method	0.25
	CPT-method	0.40
Group Uplift Resistance, ϕ_{ug}	Sand and Clay	0.50
Lateral Geotechnical Resistance of Single Pile or Pile Group	All Soils and Rock	1.0

Note: 1 – AASHTO based on Skempton (1951), manual based on Fellenius (1991).

The pile shaft resistance, R_s, and pile toe resistance, R_p, can further be expressed in terms of unit resistance values as shown in Equations 7-4 and 7-5.

$$R_s = f_s A_s \quad \text{Eq. 7-4}$$

$$R_p = q_p A_p \quad \text{Eq. 7-5}$$

Where:

f_s = unit shaft resistance over the pile surface area (ksf).
A_s = pile shaft surface area (ft^2).
q_p = unit toe resistance over the pile toe area (ksf).
A_p = pile toe area (ft^2).

The range in the resistance factors has primarily depended upon the reliability of the particular analysis method with consideration of the following items.

1. The level of confidence in the input parameters. This is a function of the type and extent of the subsurface exploration and laboratory testing program. It is assumed that AASHTO Section 10.4 on soil and rock properties is followed.

2. Variability of the soil and rock deposits.

3. Method of static analysis. Resistance factors for some static analysis methods are tied to specific correlation procedures for soil properties.

4. Effects of and consistency of the proposed pile installation method.

AASHTO (2014) Article C10.5.5.2.3 notes that where the nominal resistance is determined by static load test, dynamic testing, wave equation analysis or dynamic formulas, the uncertainty in the nominal resistance is solely due to the reliability of the field resistance determination method. Therefore, the resistance factor for the field method, $\phi_{dyn,}$ should be used to determine the number of piles of a given factored resistance needed to resist the factored loads in the strength limit state. Table 7-2 summarizes resistance factors for field resistance determination methods. Individual chapters provide expanded details on the field test methods as well as associated performance, analysis, and interpretation information. Chapter 9 covers static load tests, Chapter 10 dynamic pile testing, Chapter 11 rapid load tests, Chapter 12 wave equation analysis, and Chapter 13 dynamic formulas.

If the pile foundation design consists of a small group (i.e. less than 3 piles per substructure unit in this manual) AASHTO (2014) recommends the resistance factors in Tables 7-1 and 7-2 be reduced by 20% to reflect the limited ability of the small group to accommodate the overstressing of one pile. The definition of a small group ranges from 2 or 3 according to Isenhower and Long (1997) to 5 according to Paikowsky et al. (2004).

Table 7-2 Resistance Factors for Field Determination Methods (after AASHTO 2014)

Condition	Resistance Determination Method	Resistance Factor
Nominal Geotechnical Resistance of Single Pile in Compression Dynamic Analysis and Static Load Test Methods, ϕ_{dyn}	Driving criteria established by successful static load test of at least one pile per site condition and dynamic testing* of at least two piles per site condition, but no less than 2% of the production piles.	0.80
	Driving criteria established by successful static load test of at least one pile per site condition without dynamic testing.	0.75
	Driving criteria established by dynamic testing* conducted on 100% of production piles.	0.75
	Driving criteria established by dynamic testing,*quality control by dynamic testing* of at least two piles per site condition, but no less than 2% of the production piles.	0.65
	Wave equation analysis, without pile dynamic measurements or load test, at End of Drive conditions only.	0.50
	FHWA Modified Gates dynamic pile formula (End of Drive condition only).	0.40
	Engineering News (as defined in AASHTO) dynamic pile formula (End of Drive condition only).	0.10
Nominal Geotechnical Resistance of Single Pile in Tension, ϕ_{dyn}	Static load test. Dynamic testing* with signal matching.	0.60 0.50

* - Dynamic testing requires signal matching, and best estimates of nominal resistance are made from a restrike test. Dynamic tests are calibrated to the static load test, when available.

7.1.6 Interdiscipline Communication and Coordination

The design and construction process requires clear and concise communication among the project professionals practicing in the structural, geotechnical, geologic, hydraulic, and construction fields. Figure 2-3 in Chapter 2 presented a flow chart of the driven pile design and construction process that highlighted the major corroboration areas required in LRFD design and construction of surface transportation projects. The content of the interdiscipline communication was further detailed in Tables 2-4 and 2-5. Effective communication is essential to achieve a cost effective foundation meeting all of the strength, extreme, and service limit state design requirements.

7.2 STRENGTH LIMIT STATES

The strength limit state ensures local and global strength and stability against statistically significant load combinations occurring during the structure design life. Strength limit state design includes an evaluation of the nominal geotechnical and structural resistances as well as the loss of lateral and vertical support in the design flood event due to scour. Geotechnical aspects of strength limit state design includes:

- axial compression resistance of single piles,
- axial compression resistance of pile groups,
- uplift resistance of single piles,
- uplift resistance of pile groups,
- bearing stratum punching failure, and
- constructability including drivability.

7.2.1 Determination of Nominal Resistance for Single Piles

7.2.1.1 General

Numerous static analysis methods are available for calculating the nominal geotechnical resistance of a single pile. Section 7.2.1.3 of this chapter will detail analysis methods for piles in cohesionless, cohesive, and layered soil profiles using readily available SPT or laboratory test information. Additional methods based on cone penetration test results are also presented. As noted earlier, designers should fully understand the basis for, the limitations of, and the applicability of a chosen method. The selected method should also have a proven agreement with full scale

field results in soil conditions similar to the project being designed, with the pile type being evaluated, and the pile installation conditions (impact driving, vibratory driving, etc.) to be used. The AASHTO resistance factors for some static analysis methods require specific procedures for determining soil strength properties.

To perform a static analysis, a pile depth is iteratively assumed based on geomaterial design parameters and selected design methods. This manual presents several design methods with AASHTO (2014) specified resistance factors. However, regional geologic settings or construction control techniques may offer unique conditions not accounted for in these provided methods, therefore reliability calibrations for design methods and resistance factors are encouraged, and may supersede the presented guidelines herein if justified. Table 7-3 compares the static analysis methods presented in AASHTO (2014) design specifications with those contained in this manual. Methods shaded in gray are presented in both documents and have a static analysis resistance factor, ϕ_{stat}. Methods without a static analysis resistance factor require local calibration or must rely on the resistance factor for the field verification method.

Table 7-3 Summary of Static Analysis Methods in GEC-12 and AASHTO (2014) for Determination of Nominal Resistance

Analysis Method	Soil Type	Soil Information Required	Presented in GEC-12	Presented in 2014 AASHTO Code	AASHTO ϕ_{stat}
Meyerhof (1976)	Cohesionless	SPT N	No	Yes	0.30
Nordlund (1963)	Cohesionless	ϕ'	Yes	Yes	0.45
α-method (1980)	Cohesive	s_u	Yes	Yes	0.35
β-method (1951)(1979)*	Cohesive	s_u	No	Yes	0.25
λ-method (1972)	Cohesive	s_u	No	Yes	0.40
API RP2A (1993)	Mixed	s_u, ϕ'	Yes	No	- - -
β-method (1991)**	Mixed	ϕ'	Yes	No	Differs[1]
Brown (2001)	Mixed	SPT N	Yes	No	- - -
Elsami & Fellenius (1997)	Mixed	CPTu	Yes	No	- - -
Schmertmann (1975)	Mixed	CPT	Yes	Yes	0.50

Notes: ϕ' = effective stress friction angle
s_u = undrained shear strength
SPT = standard penetration test
CPT = cone penetration test
[1] = β-method in AASHTO uses Skempton (1951), Ersig and Kirby (1979)*; β-method in GEC-12 based on Fellenius (1991)**

7.2.1.2 Static Analysis Overview

Agencies often specify the use of select design methodologies based on experience. The design methods presented in this chapter should be used based on applicability to soil conditions, pile type and laboratory testing or subsurface exploration in-situ data. Tables 7-4 and 7-5 present an overview of design methods commonly used for calculating the nominal resistance of piles in cohesionless and cohesive soils, respectively. In layered profiles, the nominal resistance can be calculated by using the applicable cohesionless and cohesive static analysis methods in appropriate soil layers. Table 7-3 identified additional methods that may be used to estimate the nominal resistance in mixed profiles as well as commonly used CPT methods.

Static analysis methods are typically used to estimate the required pile length for a given nominal resistance to establish pile length quantities in the contract documents. The estimated pile lengths and nominal resistance are then confirmed during construction using a field resistance determination method. A driving criterion as discussed in Chapter 17 is established from these results and used to install the remaining production piles. In some cases, static analyses alone are used as the resistance determination method and piles are driven to a predetermined toe elevation. In this latter case, site variability must be addressed in the design pile lengths. Regardless of the static analysis method used, the designer should clearly understand the applications and limitations of the selected method, the soil strength parameters needed to properly use the method, and the procedures and/or correlations used to determine those soil parameters for the method.

The FHWA recommended static analysis methods are the Nordlund method in cohesionless soils (Section 7.2.1.3.1), the α-method in cohesive soils (Section 7.2.1.3.2), and the API method for large diameter pipe piles (Section 7.2.1.3.3). The Nordlund and α-method are recommended methods based on FHWA experience with their reliability in estimating pile length and the associated nominal resistance for conventional pile types in most subsurface conditions. The API method was specifically developed for large diameter pipe piles, and thus is the recommended static analysis method for evaluating highway structure foundations of this pile type.

Table 7-4 Methods of Static Analysis for Piles in Cohesionless Soils

Method	Approach	Method of Obtaining Design Parameters	Advantages	Disadvantages	Remarks
Nordlund Method.	Semi-Empirical.	Charts provided by Nordlund. Estimate of soil friction angle is needed.	Allows for increased shaft resistance of tapered piles and includes effects of pile-soil friction coefficient for different pile materials.	No limiting value on unit shaft resistance is recommended. Soil friction angle often estimated from SPT data. Limit on pile sizes.	Good approach to design that is widely used. Method is based on field observations. Details provided in Section 7.2.1.3.1.
API RP2A.	Empirical, effective stress analysis.	N_q selected from Table 7-8 based on soil type.	Developed specifically for large diameter open end pipe.	Application to non-LDOEPs is limited.	Used almost exclusively for offshore pile design.
Effective Stress Method.	Semi-empirical.	β and N_t selected based on soil classification and estimated friction angle.	β value considers pile-soil friction coefficient for different pile materials. Soil resistance related to effective vertical stress.	Results affected by range in β values and in particular by range in N_t chosen.	Good approach for design. Details provided in Section 7.2.1.3.3.
Brown Method.	Empirical.	Results of SPT tests based of N_{60} values.	Widespread use of SPT test and input data availability. Simple method to use.	Relies solely on N_{60} values, which may not always be available.	Simple method based on correlations with 71 static load test results. Details provided in Section 7.2.1.3.5.
Methods based on Cone Penetration Test (CPT) data.	Empirical.	Results of CPT tests.	Testing analogy between CPT and pile. Reliable correlations and reproducible test data.	Limitations on pushing cone into dense strata.	Good approach for design. Details provided in Sections 7.2.1.3.6 and 7.2.1.3.7.

Table 7-5 Methods of Static Analysis for Piles in Cohesive Soils

Method	Approach	Method of Obtaining Design Parameters	Advantages	Disadvantages	Remarks
α-Method (Tomlinson Method).	Empirical, total stress analysis.	Undrained shear strength estimate of soil is needed. Adhesion calculated from Figures 7-17 and 7-18.	Simple calculation from laboratory undrained shear strength values to adhesion.	Wide scatter in adhesion versus undrained shear strengths in literature. Limits on s_u strengths in soft and medium cohesive soils.	Widely used method described in Section 7.2.1.3.2.
API RP2A.	Empirical, effective stress analysis.	Undrained shear strength estimate of soil is needed.	Developed specifically for large diameter open end pipe piles.	Application to non-LDOEPs is limited.	Used almost exclusively for offshore pile design.
Effective Stress Method.	Semi-Empirical, based on effective stress at failure.	β and N_t values are selected from Table 7-9 based on drained soil strength estimates.	Ranges in β and N_t values for most cohesive soils are relatively small.	Range in N_t values for hard cohesive soils such as glacial tills can be large.	Good design approach theoretically better than undrained analysis. Details in Section 7.2.1.3.3.
Methods based on Cone Penetration Test data.	Empirical.	Results of CPT tests.	Testing analogy between CPT and pile. Reproducible test data.	Cone can be difficult to advance in very hard cohesive soils such as glacial tills.	Good approach for design. Details in Section 7.2.1.3.6 and Section 7.2.1.3.7.

7.2.1.3 Nominal Resistance of Single Piles in Soils

The nominal resistance of a single pile is taken as the sum of shaft and toe resistances ($R_n = R_s + R_p$). The calculation assumes that the shaft resistance and toe resistance can be determined separately and that these two factors do not affect each other. Many analytical and empirical methods have been developed for estimating the nominal resistance of piles using this approach. For typical pile sizes 18 inches and smaller in diameter or width, the nominal resistance is often calculated using the Nordlund Method in cohesionless soils and the α-method in cohesive materials. The Nordlund Method is described in Section 7.2.1.3.1 and the α-method is detailed in Section 7.2.1.3.2. It should be noted that piles larger than 18 inches were not in the correlation database for either the Nordlund Method or the α-method. In layered soil profiles, the nominal resistance can be calculated by combining these methods in cohesionless and cohesive layers as applicable. Table 7-3 identified additional methods that may be used to estimate the nominal resistance in mixed profiles as well as commonly used CPTu and CPT methods.

7.2.1.3.1 Nordlund Method – Cohesionless Soils

The Nordlund Method (1963) is based on field observations and considers the shape of pile taper and its soil displacement in calculating the shaft resistance. This method also accounts for the differences in soil-pile coefficient of friction for different pile materials, and is based on the results of load test programs in cohesionless soils. Several pile types were used in these test programs including timber, H, closed end pipe, Monotube, and Raymond step taper piles. These piles, which were used to develop the method's design curves, had pile widths generally in the range of 10 to 20 inches. The larger pile types used today including large diameter open end pipe piles, concrete cylinder piles, 24 inch and greater square prestressed concrete piles as well as16 and 18 inch H-pile sections are not in the calibration database. The Nordlund Method tends to over predict the nominal resistance for piles widths larger than 24 inches. Alternative static analysis methods should be evaluated for these other pile types and larger pile sizes.

According to the Nordlund Method, the shaft resistance is a function of the following variables:

1. The friction angle of the soil.
2. The friction angle on the sliding surface.
3. The taper of the pile.
4. The effective unit weight of the soil.

5. The pile length.
6. The minimum pile perimeter.
7. The volume of soil displaced.

These factors are considered in the Nordlund equation as illustrated in Figure 7-8. The Nordlund Method equation for computing the nominal resistance of a pile is as follows:

$$R_n = \sum_{d=0}^{d=D} K_\delta \; C_F \; \sigma'_d \; \frac{\sin(\delta+\omega)}{\cos(\omega)} \; C_d \; \Delta d + \alpha_t \; N'_q \; A_p \; \sigma'_p \qquad \text{Eq. 7-6}$$

Where:

d = depth (feet).
D = embedded pile length (feet).
K_δ = coefficient of lateral earth pressure at depth d.
C_F = correction factor for K_d when $\delta \neq \phi$.
σ'_d = vertical effective stress at the center of depth increment d.
δ = friction angle between pile and soil.
ω = angle of pile taper from vertical.
C_d = pile perimeter at depth d (feet).
Δd = length of pile segment.
α_t = dimensionless factor (dependent on pile depth width relationship).
N'_q = bearing capacity factor.
A_p = pile toe area (feet).
σ'_p = vertical effective stress at the pile toe (ksf).

For a pile of uniform cross section (ω=0) and embedded length *D*, driven in soil layers of the same effective unit weight and friction angle, the Nordlund equation becomes:

$$R_n = K_\delta \; C_F \; \sigma'_d \; \sin(\delta) \; C_d \; \Delta d + \alpha_t \; N'_q \; A_p \; \sigma'_p \qquad \text{Eq. 7-7}$$

The soil angle of internal friction, ϕ, influences most of the calculations in the Nordlund method. In the absence of laboratory test data, ϕ can be estimated from corrected SPT N values. Section 5.2.3 provides several means of estimating soil friction angle based on these corrected SPT N values. Figures 7-8 to 7-14 should be used to include associate parameters for design. In addition, Table 7-6 and 7-7 provide factors to evaluate the coefficient of lateral earth pressure with depth.

Nordlund developed this method in 1963 with updates in 1979 and did not place a limiting value on the shaft resistance. However, Nordlund recommended that the vertical effective stress at the pile toe, σ'_p, used for computing the pile toe resistance be limited to 3 ksf.

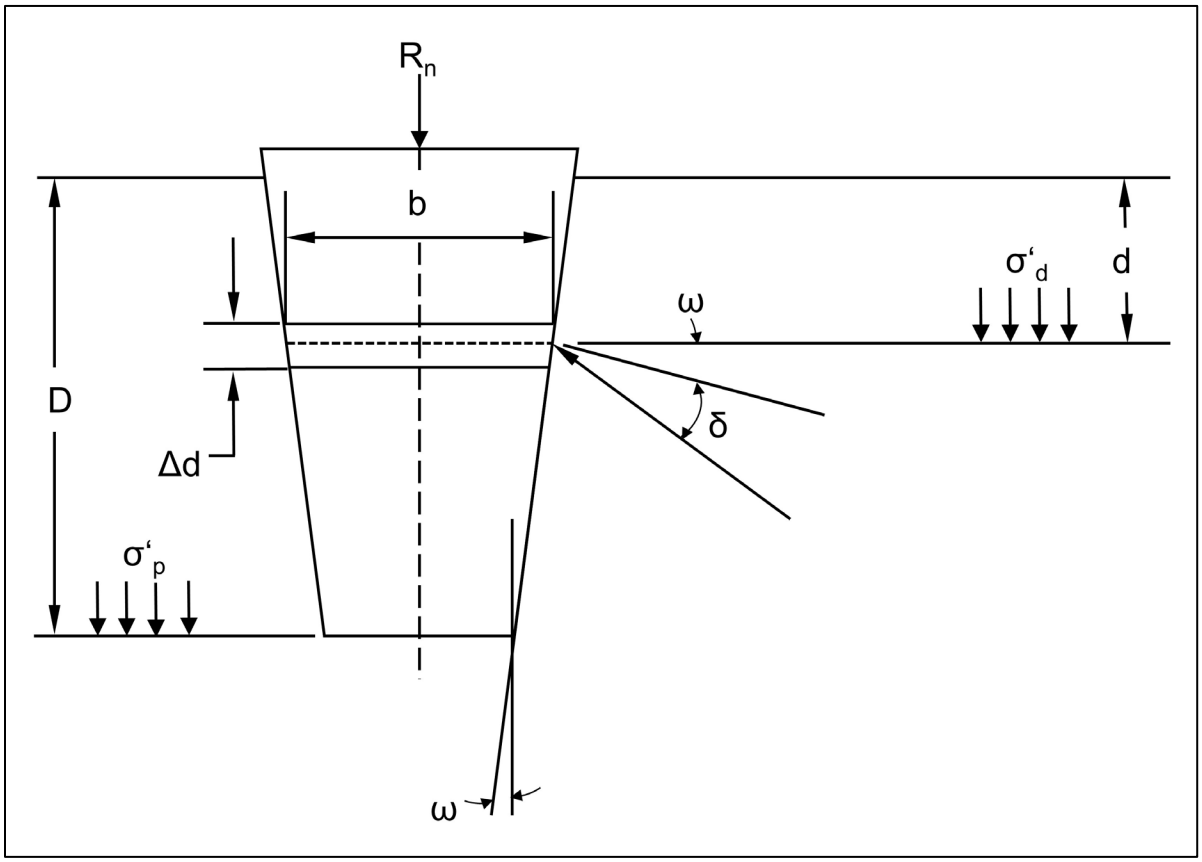

Figure 7-8 Nordlund's general equation diagram for nominal resistance.

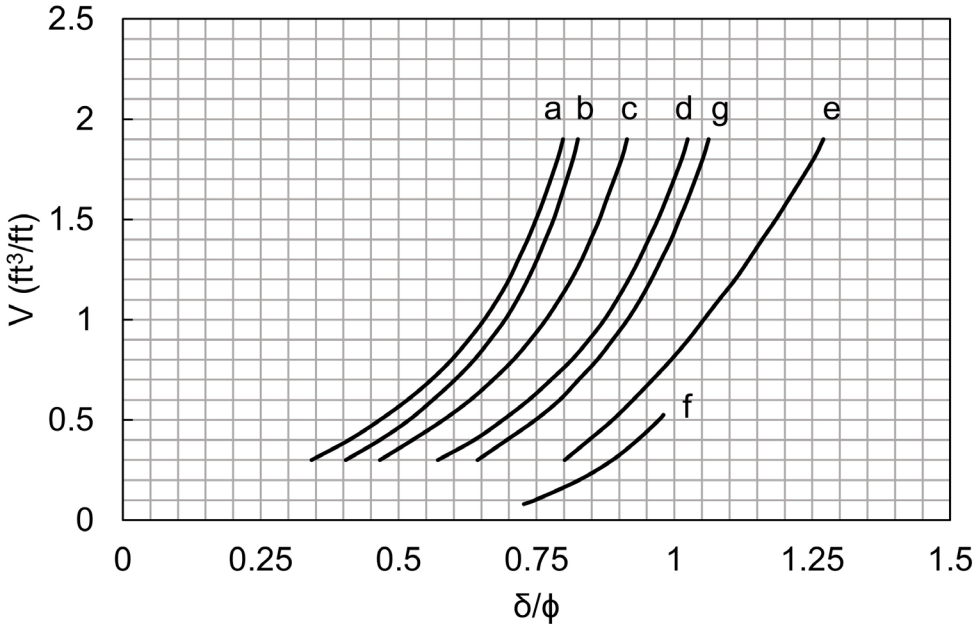

a. Pipe piles and non-tapered portion of monotube piles
b. Timber piles
c. Precast concrete piles
d. Raymond step-taper piles
e. Raymond uniform taper piles
f. H-piles and augercast piles
g. Tapered portion of monotube piles

Figure 7-9 Relationship of δ/ϕ and pile soil displacement, *V*, for various pile types (after Nordlund 1979).

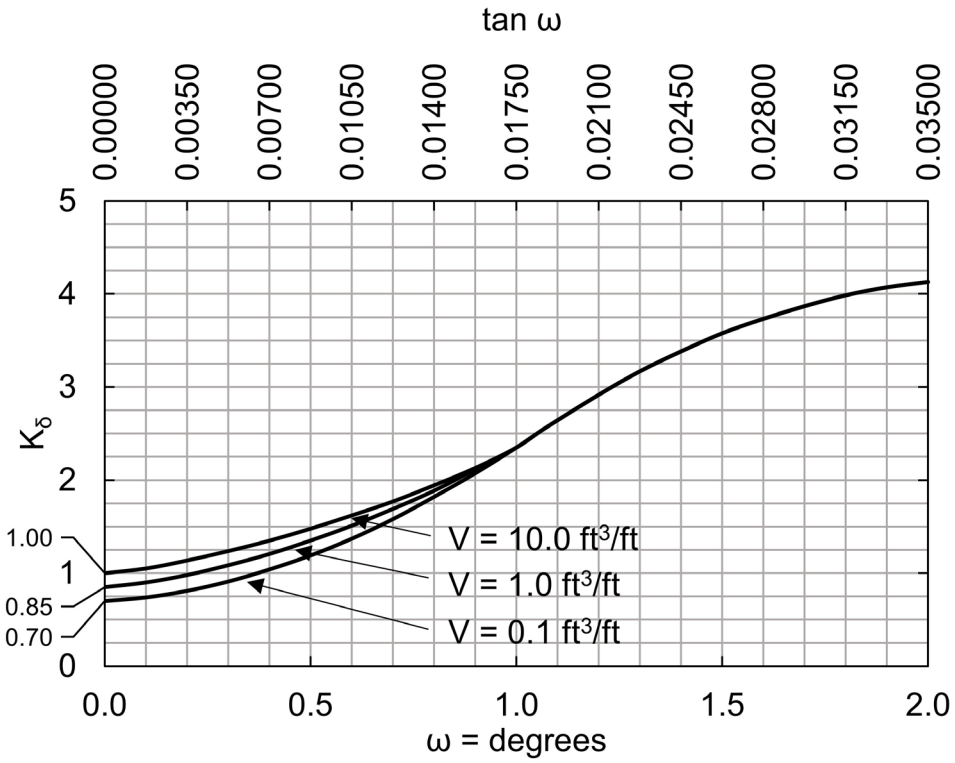

Figure 7-10 Design curve for evaluating K_δ for piles when $\phi = 25^\circ$ (after Nordlund 1979).

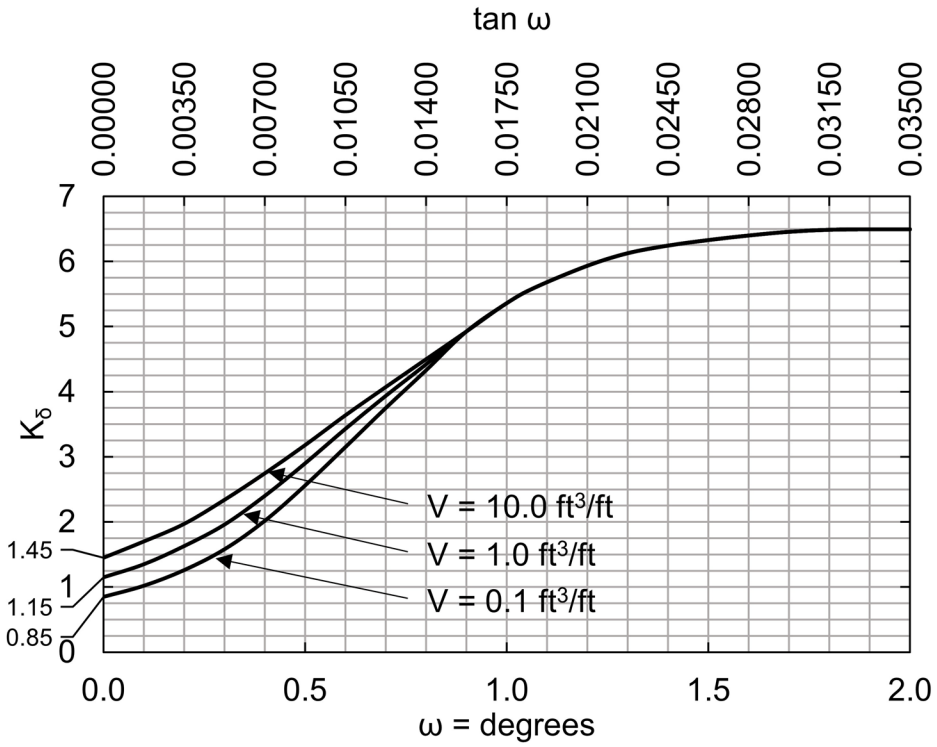

Figure 7-11 Design curve for evaluating K_δ for piles when $\phi = 30^\circ$ (after Nordlund 1979).

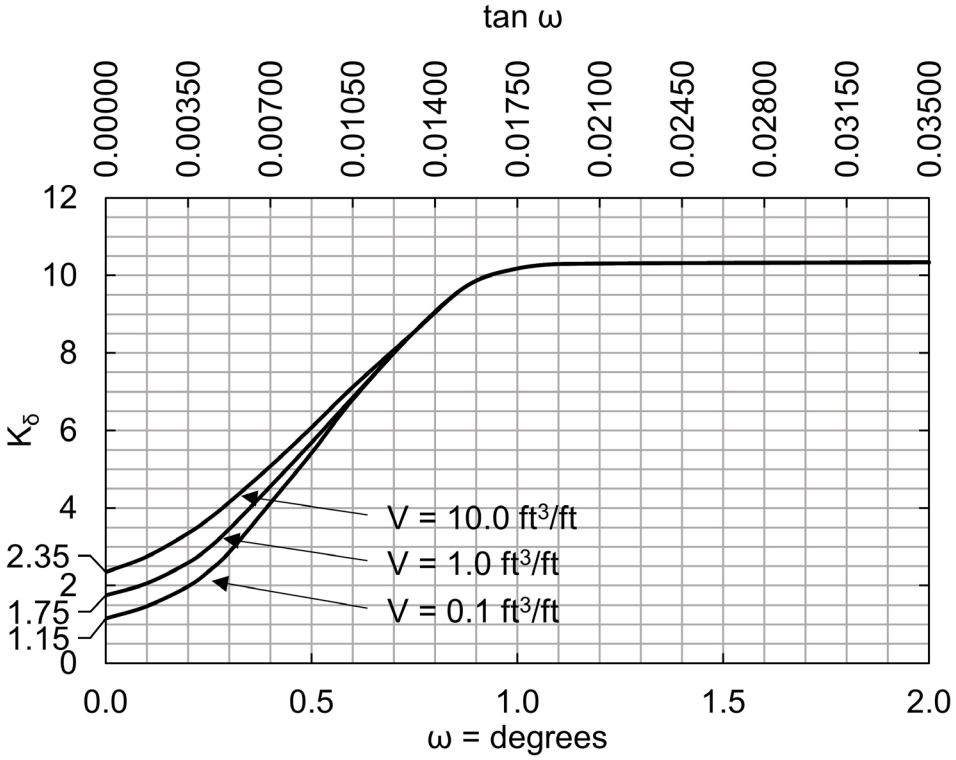

Figure 7-12 Design curve for evaluating K_δ for piles when $\phi = 35^\circ$ (after Nordlund 1979).

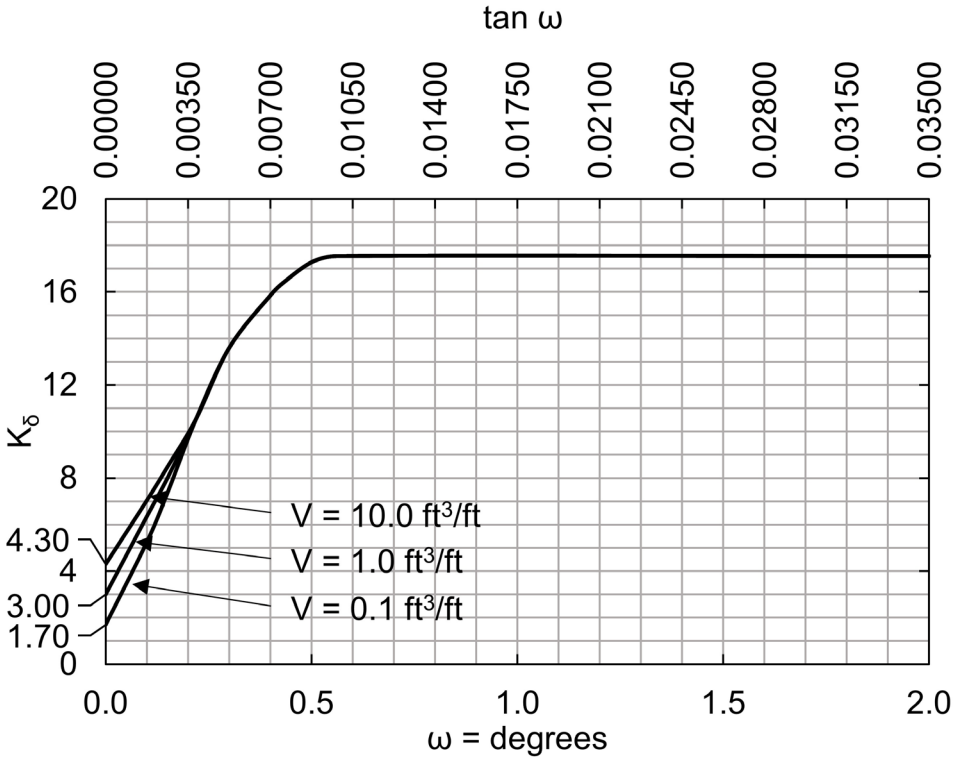

Figure 7-13 Design curve for evaluating K_δ for piles when $\phi = 40^\circ$ (after Nordlund 1979).

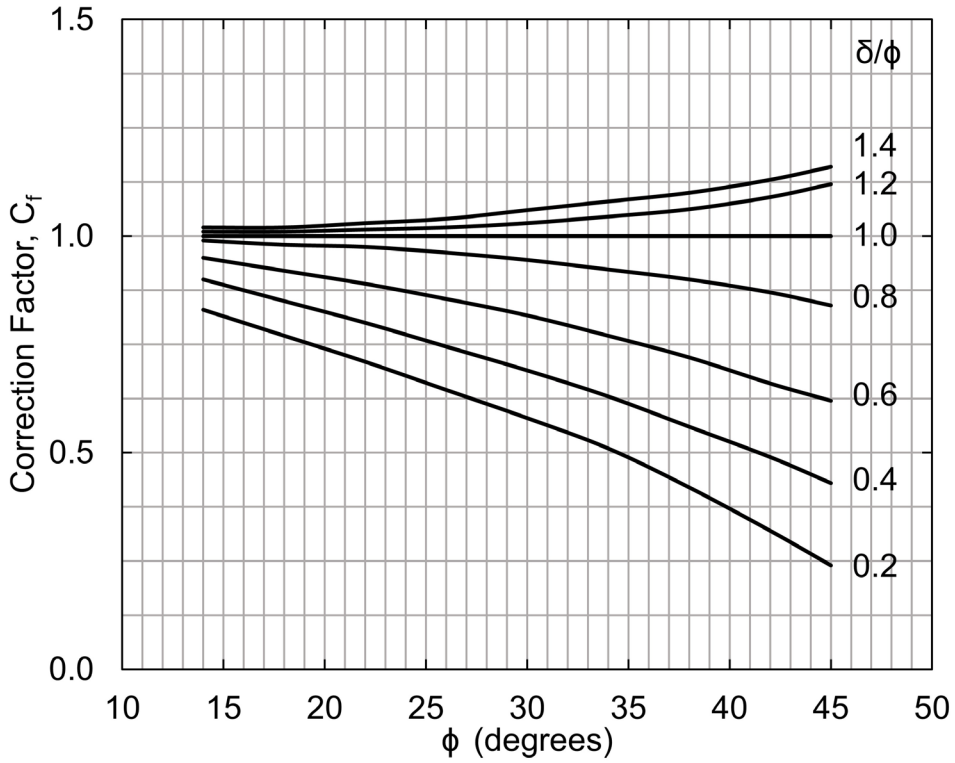

Figure 7-14 Correction factor for K_δ when $\delta \neq \phi$ (after Nordlund 1979).

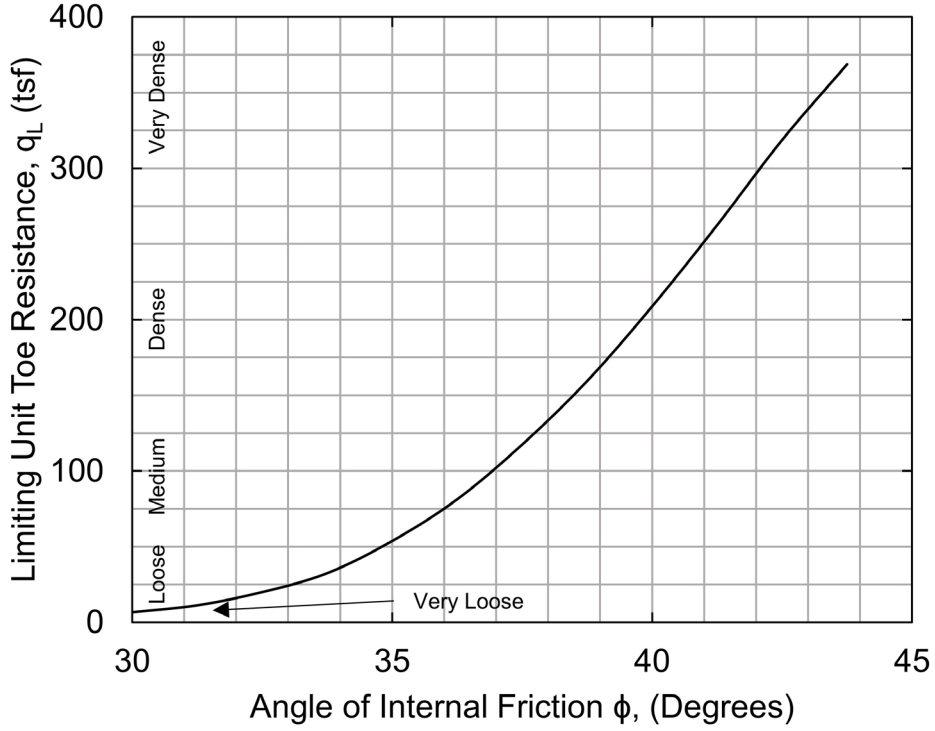

Figure 7-15 Relationship between maximum unit toe resistance and friction angle for cohesionless soils (after Meyerhof 1976).

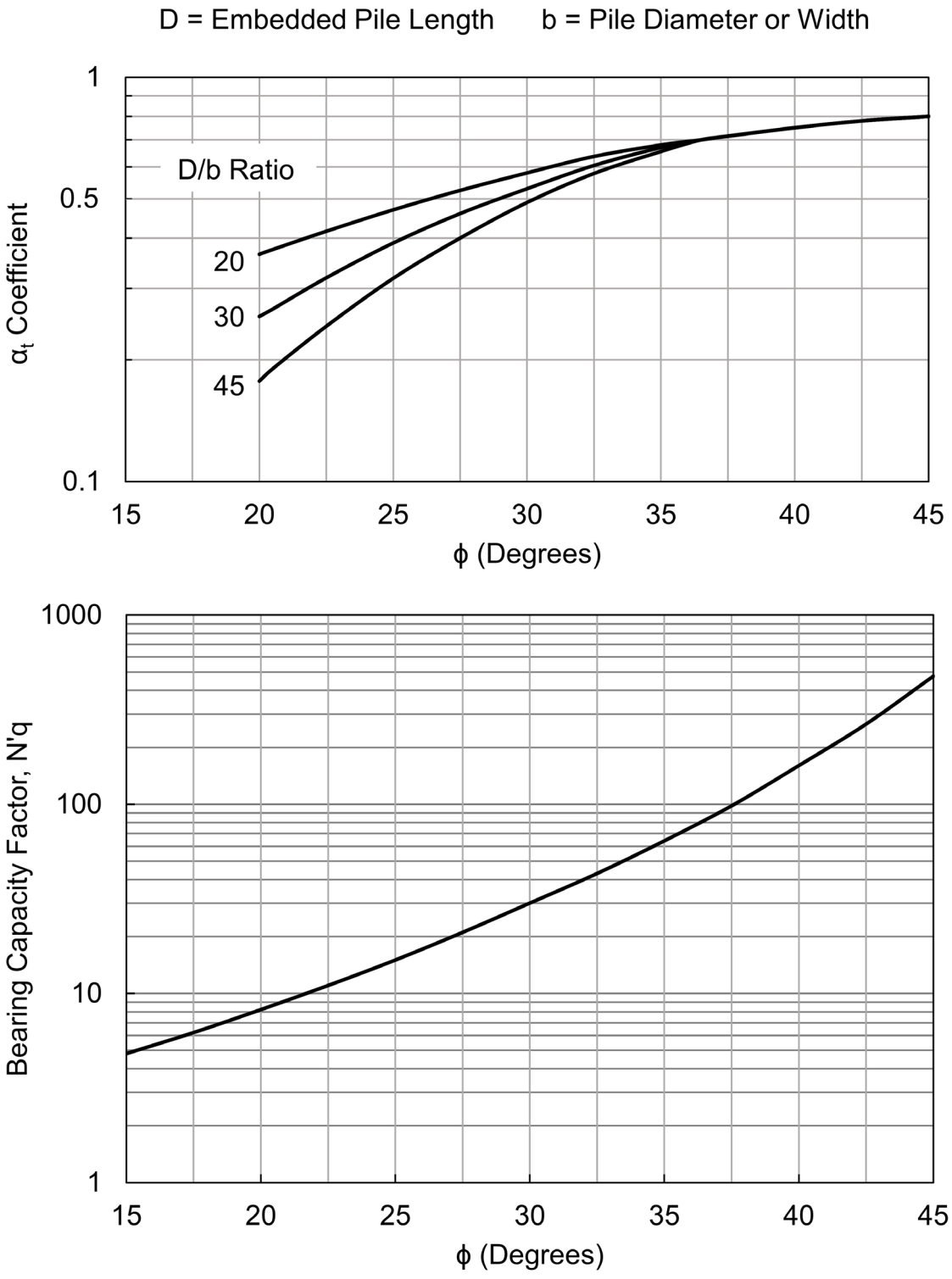

Figure 7-16 Chart for estimating α_t coefficient and bearing capacity factor N'_q (after Bowles 1977).

Table 7-6 Design Table for Evaluating K_δ for Piles when $\omega = 0°$ and $V = 0.10$ to 1.00 ft^3/ft

	Displaced Volume -V, ft^3/ft									
ϕ	0.10	0.20	0.30	0.40	0.50	0.60	0.70	0.80	0.90	1.00
25	0.70	0.75	0.77	0.79	0.80	0.82	0.83	0.84	0.84	0.85
26	0.73	0.78	0.82	0.84	0.86	0.87	0.88	0.89	0.90	0.91
27	0.76	0.82	0.86	0.89	0.91	0.92	0.94	0.95	0.96	0.97
28	0.79	0.86	0.90	0.93	0.96	0.98	0.99	1.01	1.02	1.03
29	0.82	0.90	0.95	0.98	1.01	1.03	1.05	1.06	1.08	1.09
30	0.85	0.94	0.99	1.03	1.06	1.08	1.10	1.12	1.14	1.15
31	0.91	1.02	1.08	1.13	1.16	1.19	1.21	1.24	1.25	1.27
32	0.97	1.10	1.17	1.22	1.26	1.30	1.32	1.35	1.37	1.39
33	1.03	1.17	1.26	1.32	1.37	1.40	1.44	1.46	1.49	1.51
34	1.09	1.25	1.35	1.42	1.47	1.51	1.55	1.58	1.61	1.63
35	1.15	1.33	1.44	1.51	1.57	1.62	1.66	1.69	1.72	1.75
36	1.26	1.48	1.61	1.71	1.78	1.84	1.89	1.93	1.97	2.00
37	1.37	1.63	1.79	1.90	1.99	2.05	2.11	2.16	2.21	2.25
38	1.48	1.79	1.97	2.09	2.19	2.27	2.34	2.40	2.45	2.50
39	1.59	1.94	2.14	2.29	2.40	2.49	2.57	2.64	2.70	2.75
40	1.70	2.09	2.32	2.48	2.61	2.71	2.80	2.87	2.94	3.0

Table 7-7 Design Table for Evaluating K_δ for Piles when $\omega = 0°$ and V = 1.0 to 10 ft^3/ft

	Displaced Volume -V, ft^3/ft									
ϕ	1.0	2.0	3.0	4.0	5.0	6.0	7.0	8.0	9.0	10.0
25	0.85	0.90	0.92	0.94	0.95	0.97	0.98	0.99	0.99	1.00
26	0.91	0.96	1.00	1.02	1.04	1.05	1.06	1.07	1.08	1.09
27	0.97	1.03	1.07	1.10	1.12	1.13	1.15	1.16	1.17	1.18
28	1.03	1.10	1.14	1.17	1.20	1.22	1.23	1.25	1.26	1.27
29	1.09	1.17	1.22	1.25	1.28	1.30	1.32	1.33	1.35	1.36
30	1.15	1.24	1.29	1.33	1.36	1.38	1.40	1.42	1.44	1.45
31	1.27	1.38	1.44	1.49	1.52	1.55	1.57	1.60	1.61	1.63
32	1.39	1.52	1.59	1.64	1.68	1.72	1.74	1.77	1.79	1.81
33	1.51	1.65	1.74	1.80	1.85	1.88	1.92	1.94	1.97	1.99
34	1.63	1.79	1.89	1.96	2.01	2.05	2.09	2.12	2.15	2.17
35	1.75	1.93	2.04	2.11	2.17	2.22	2.26	2.29	2.32	2.35
36	2.00	2.22	2.35	2.45	2.52	2.58	2.63	2.67	2.71	2.74
37	2.25	2.51	2.67	2.78	2.87	2.93	2.99	3.04	3.09	3.13
38	2.50	2.81	2.99	3.11	3.21	3.29	3.36	3.42	3.47	3.52
39	2.75	3.10	3.30	3.45	3.56	3.65	3.73	3.80	3.86	3.91
40	3.00	3.39	3.62	3.78	3.91	4.01	4.10	4.17	4.24	4.30

STEP BY STEP PROCEDURE FOR: “NORDLUND METHOD”

Steps 1 through 6 are for computing the shaft resistance and Steps 7 through 9 are for computing the pile toe resistance.

STEP 1 Delineate the soil profile into layers and determine the ϕ angle for each layer.

a. Construct Effective Stress Diagram using procedure described in Section 7.1.4.

b. Correct SPT field N values for vertical stress using methods from Section 5.1.1 to obtain corrected SPT N values, $(N_1)_{60}$. Delineate soil profile into layers based on corrected SPT N values.

c. Determine ϕ angle for each layer from laboratory tests or in-situ data.

d. In the absence of laboratory or in-situ test data, determine the average corrected SPT N value, $(N_1)_{60}$, for each soil layer and estimate ϕ angle from Table 5-5 in Chapter 5.

STEP 2 Determine δ, the friction angle between pile and soil based on displaced soil volume, V, and the soil friction angle, ϕ.

a. Compute volume of soil displaced per unit length of pile, V.

b. Use Figure 7-9 with V and determine δ/ϕ ratio for pile type.

c. Calculate δ from δ/ϕ ratio.

STEP 3 Determine the coefficient of lateral earth pressure, K_δ, for each ϕ angle.

a. Determine K_δ for ϕ angle based on displaced volume, V, and pile taper angle, ω, using either Figure 7-10, 7-11, 7-12, or 7-13 and the appropriate procedure described in Step 3b, 3c, 3d, or 3e.

b. If the displaced volume is 0.1, 1.0 or 10.0 ft^3/ft, which correspond to one of the curves provided in Figures 7-10 through 7-13 and the ϕ

angle is one of those provided, K_δ can be determined directly from the appropriate figure.

c. If the displaced volume is 0.1, 1.0 or 10.0 ft^3/ft which correspond to one of the curves provided Figures 7-10 through 7-13 but the ϕ angle is different from those provided, use linear interpolation to determine K_δ for the required ϕ angle. Tables 7-6 and 7-7 also provide interpolated K_δ values at selected displaced volumes versus ϕ angle for uniform piles ($\omega = 0$).

d. If the displaced volume is other than 0.1, 1.0 or 10.0 ft^3/ft which corresponds to one of the curves provided in Figures 7-10 through 7-13 but the ϕ angle corresponds to one of those provided, use log linear interpolation to determine K_δ for the required displaced volume. Tables 7-6 and 7-7 also provide interpolated K_δ values at selected displaced volumes versus ϕ angle for uniform piles ($\omega = 0$).

e. If the displaced volume is other than 0.1, 1.0 or 10.0 ft^3/ft which correspond to one of the curves provided in Figures 7-10 through 7-13 and the ϕ angle does not correspond to one of those provided, first use linear interpolation to determine K_δ for the required ϕ angle at the displaced volume curves provided for 0.1, 1.0 or 10.0 ft^3/ft. Then use log linear interpolation to determine K_δ for the required displaced volume. Tables 7-6 and 7-7 also provide interpolated K_δ values at selected displaced volumes versus friction angle for uniform piles ($\omega = 0$).

STEP 4 Determine the correction factor, C_F, to be applied to K_δ if $\delta \neq \phi$.

Use Figure 7-14 to determine the correction factor for each K_δ. Enter figure with ϕ angle and δ/ϕ value to determine C_F.

STEP 5 Compute the average vertical effective stress at the midpoint of each soil layer, σ'_d (psf).

Note: A limiting value is not applied to σ'_d.

STEP 6 Compute the shaft resistance in each soil layer. Sum the shaft resistance from each soil layer to obtain the nominal shaft resistance, R_s (kips).

$$R_s = K_\delta \, \mathrm{C}_F \, \sigma'_d \, \sin(\delta) \, \mathrm{C}_d \, \mathrm{D} \qquad \text{Eq. 7-8}$$

(for uniform pile cross section)

For H-piles in cohesionless soils, the "box" area should generally be used for shaft resistance calculations. An additional discussion on the behavior of open pile sections is presented in Section 7.10.7.

STEP 7 Determine the α_t coefficient and the bearing capacity factor, N'_q, from the ϕ angle near the pile toe.

a. Enter Figure 7-16(a) with ϕ angle near the pile toe to determine α_t coefficient based on pile length to diameter ratio.

b. Enter Figure 7-16(b) with ϕ angle near the pile toe to determine N_q.

c. If ϕ angle is estimated from SPT data, compute the average corrected SPT N value, $(N_1)_{60}$, over the zone from the pile toe to 3 diameters below the pile toe. Use this average corrected SPT N value to estimate ϕ angle near pile toe.

STEP 8 Compute the vertical effective stress at the pile toe, σ'_p (ksf).

Note: The limiting value of σ'_p is 3 ksf.

STEP 9 Compute the nominal toe resistance, R_p (kips).

$$R_p = \alpha_t \, \mathrm{N}'_q \, \mathrm{A}_p \, \sigma'_p \qquad \text{Eq. 7-9}$$

a. While limiting $R_p = q_L A_p$ where q_L value is obtained from:

1. Entering Figure 7-15 with ϕ angle near pile toe determined from laboratory or in-situ test data.

2. Entering Figure 7-15 with ϕ angle near the pile toe estimated and the average corrected SPT N value, $(N_1)_{60}$, near toe as described in Step 7.

b. Use lesser of the two R_p values obtained in steps a and b.

For steel H and open end pipe piles, the selection of the pile toe area (steel area only or full cross sectional area of steel and enclosed soil) for toe resistance calculations should be based on past experience and local correlations with static load test results.

STEP 10 Compute the nominal resistance, R_n, from the sum of the shaft and toe resistances, $R_n = R_s + R_p$.

STEP 11 Compute the factored resistance, R_r (kips), using select resistance factors provided in Section 7.1.5 and Equation 7-3.

AASHTO (2014) provides a recommended resistance factor for this method in Table 7-1 for the nominal resistance determined by static analysis. The nominal resistance at the strength limit state could also be determined using the resistance factor associated with the field verification method, ϕ_{dyn}, as recommended in Table 7-2.

7.2.1.3.2 α-Method - Cohesive Soils

For piles in clay, a total stress analysis is often used where nominal resistance is calculated from the undrained shear strength of the soil. This approach assumes that the shaft resistance is independent of the vertical effective stress and that the unit shaft resistance can be expressed in terms of an empirical adhesion factor times the undrained shear strength.

The unit shaft resistance, f_s, is equal to the adhesion which is the shear stress between the pile surface and the soil at failure. This may be expressed in equation form as:

$$f_s = \mathrm{C}_a = \alpha\, \mathrm{s}_u \qquad \text{Eq. 7-10}$$

Where:

C_a = adhesion (ksf).
s_u = undrained shear strength (ksf).
α = adhesion factor.

The adhesion factor α depends on the nature and strength of the clay, pile dimension, method of pile installation, and time effects. The values of α vary within wide limits and decreases rapidly with increasing shear strength.

It is recommended that Figure 7-17 generally be used for adhesion calculations, unless one of the special soil stratigraphy cases identified in Figure 7-18 is present at a site. In cases where either Figures 7-17 or 7-18 could be used, the inexperienced user should select and use the smaller value obtained from either figure. The undrained shear strengths addressed in the design charts ranges from approximately 0.5 ksf on the low end to 3.5 to 5.0 ksf on the high end, depending on the design chart. All users should confirm the applicability of a selected design chart in a given soil condition with local correlations between static resistance calculations and static load tests results. This is particularly for cases where the shear strength approaches either the upper or lower limit of the design chart.

In Figure 7-17, the pile adhesion, C_a, is expressed as a function of the undrained shear strength, s_u, with consideration of both the pile type and the embedded pile length, D, to pile diameter, b, ratio. The embedded pile length used in Figure 7-17 should be the minimum value of the length from the ground surface to the bottom of the clay layer, or the length from the ground surface to the pile toe.

Figure 7-18 presents the adhesion factor, α, versus the undrained shear strength of the soil as a function of unique soil stratigraphy and pile embedment. The adhesion factor from these soil stratigraphy cases should be used only for determining the adhesion in a stiff clay layer in that specific condition. For a soil profile consisting of clay layers of significantly different consistencies such as soft clays over stiff clays, adhesion factors should be determined for each individual clay layer.

The top graph in Figure 7-18 may be used to select the adhesion factor when piles are driven through a sand or sandy gravel layer and into an underlying stiff clay stratum. This case results in the highest adhesion factors as granular material is dragged into the underlying clays. The greater the pile penetration into the clay stratum, the less influence the overlying granular stratum has on the adhesion factor. Therefore, for the same undrained shear strength, the adhesion factor decreases with increased pile penetration into the clay stratum.

The middle graph in Figure 7-18 should be used to select the adhesion factor when piles are driven through a soft clay layer overlying a stiff clay layer. In this case, the soft clay is dragged into the underlying stiff clay stratum thereby reducing the adhesion factor of the underlying stiff clay soils. The greater the pile penetration into

the underlying stiff clay soils, the less the influence the overlying soft clays have on the stiff clay adhesion factor. Therefore, the stiff clay adhesion factor increases with increasing pile penetration into the stiff clay soils.

Last, the bottom graph in Figure 7-18 may be used to select the adhesion factor for piles driven in stiff clays without any different overlying strata. In stiff clays, a gap often forms between the pile and the soil along the upper portion of the pile shaft. In this case, the shallower the pile penetration into a stiff clay stratum the greater the effect the gap has on the shaft resistance that develops. Hence, the adhesion factor for a given shear strength is reduced at shallow pile penetration depths and increased at deeper pile penetration depths.

In highly overconsolidated clays, undrained shear strengths may exceed the upper limits of Figures 7-17 and 7-18. In these cases, it is recommended that adhesion factor, α, be calculated according to API Recommended Practice 2A (1993). Further information for this is provided in Section 7.2.1.3.3 of this chapter.

In the case of H-piles in cohesive soils, the shaft resistance should not be calculated from the surface area of the pile, but rather from the "box" area of the four sides. The shaft resistance for H-piles in cohesive soils consists of the sum of the adhesion, C_a, times the flange surface area along the exterior of the two flanges, plus the undrained shear strength of the soil, s_u, times the area of the two remaining sides of the "box", due to soil-to-soil shear along these faces. This computation can be approximated by determining the adhesion using the appropriate corrugated pile curve in Figure 7-17 and multiplying the adhesion by the H-pile "box" area. Additional information on the behavior of open pile sections is presented in Section 7.10.7.

In clays with large shrink-swell potential, static resistance calculations should ignore the shaft resistance from the adhesion in the shrink-swell zone. During dry times, shrinkage will create a gap between the clay and the pile in this zone and therefore the shaft resistance should not be relied upon for long term support.

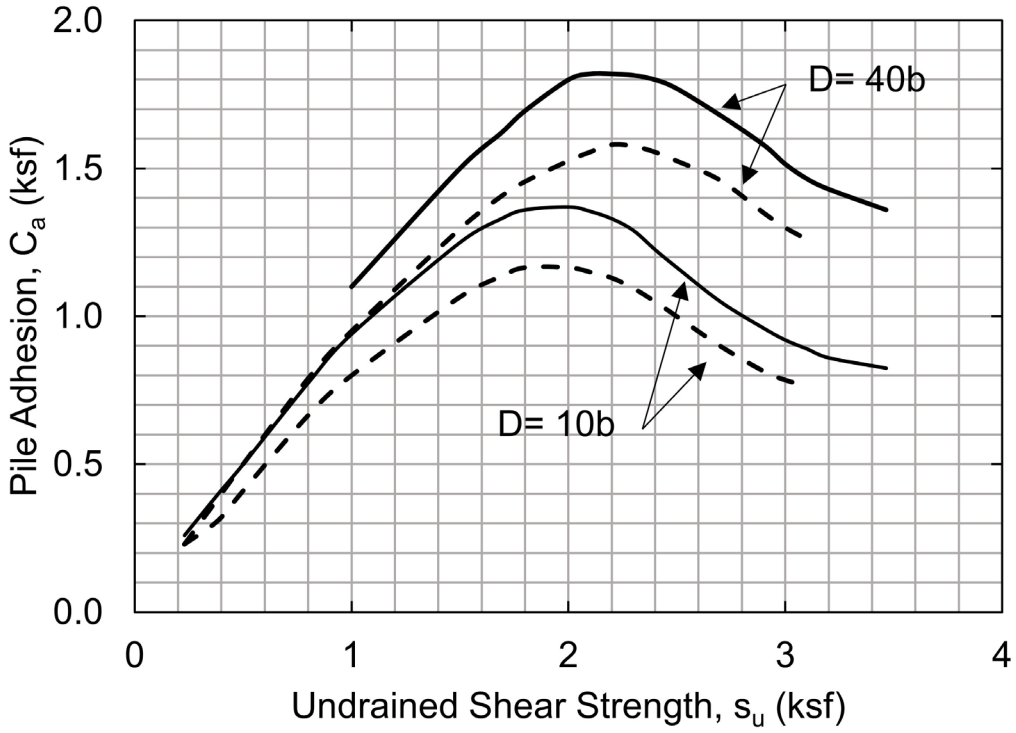

Legend
D = Distance from Ground Surface to Bottom of Clay Layer
b = Pile Diameter
——— Concrete, Timber, Corrugated Steel Piles
– – – – – – – – Smooth Steel Piles

Figure 7-17 Adhesion values for piles in cohesive soils (after Tomlinson 1979).

The unit toe resistance, q_p, in a total stress analysis for homogeneous cohesive soil can be expressed as:

$$q_p = \mathrm{N}_c \, s_u \qquad \text{Eq. 7-11}$$

Where:

N_c = bearing capacity factor.
s_u = undrained shear strength (ksf).

The term N_c is a dimensionless bearing capacity factor which depends on the pile diameter and the depth of embedment. The bearing capacity factor, N_c, is usually taken as 9 for deep foundations.

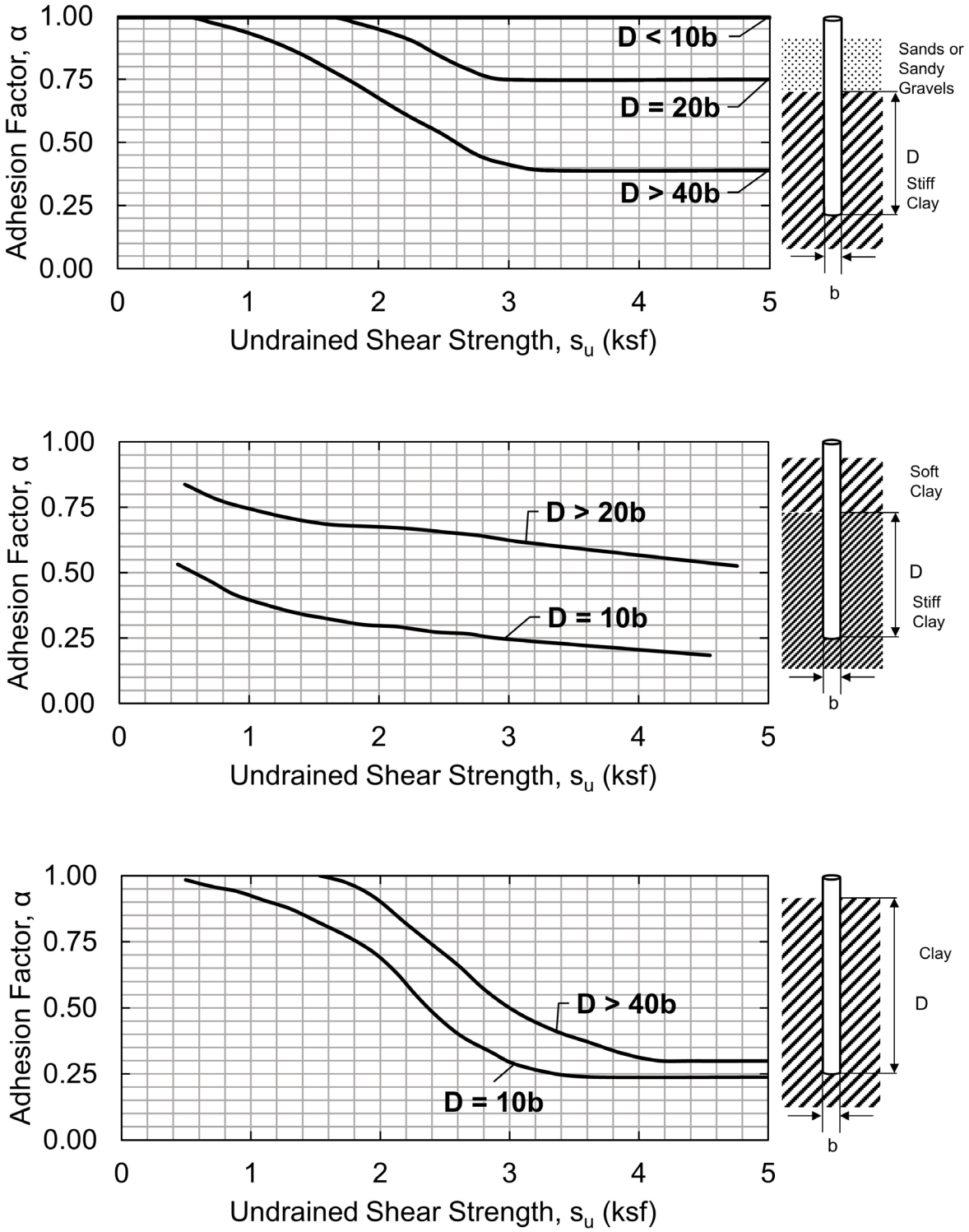

Figure 7-18 Adhesion factors for driven piles in clay (Tomlinson 1980).

On smaller piles in cohesive soils, the toe resistance contribution to the nominal resistance is a low percentage of the overall resistance and is therefore sometimes ignored. On larger piles, the movement required to mobilize the toe resistance is

several times greater than that required to mobilize the shaft resistance. At the movement required to fully mobilize the toe resistance, the shaft resistance may have decreased to a residual value. These factors should be considered when performing nominal resistance assessments of various pile sections.

STEP BY STEP PROCEDURE FOR: "α-METHOD"

STEP 1 Delineate the soil profile into layers and determine the pile adhesion, C_a, from Figure 7-17 or adhesion factor, α, from Figure 7-18 for each layer.

Enter appropriate figure with the undrained shear strength of the soil, s_u, and determine pile adhesion or adhesion factor based on the embedded pile length in clay, D, and pile diameter, b. Use the curve for the appropriate soil and embedment condition. For highly overconsolidated clays where s_u exceeds the chart values, see Section 7.2.1.3.3 for guidance on α.

STEP 2 For each soil layer, compute the unit shaft resistance, f_s (ksf), using Equation 7-10.

STEP 3 Compute the shaft resistance in each soil layer and the nominal shaft resistance, R_s (kips), from the sum of the layer shaft resistances.

STEP 4 Compute the unit toe resistance, q_p (ksf) using Equation 7-11.

STEP 5 Compute the nominal toe resistance, R_p (kips).

For open pile sections, refer to the discussion of pile plugging presented in Section 7.10.7.

STEP 6 Compute the nominal pile resistance, R_n, from the sum of the shaft and toe resistances, $R_n = R_s + R_p$.

STEP 7 Compute the factored resistance, R_r (kips), using the resistance factors provided in Section 7.1.5 and Equation 7-3.

AASHTO (2014) provides a recommended resistance factor for this method in Table 7-1 for the nominal resistance determined by static analysis. The nominal resistance in the strength limit state could also be determined using the resistance factor associated with the field verification method, ϕ_{dyn}, as recommended in Table 7-2.

7.2.1.3.3 P2A Method – Mixed Soil Profiles

The American Petroleum Institute (API) provides a static analysis procedure design developed for offshore construction. These projects almost exclusively use large diameter, open-end, steel pipe piles which are driven by impact hammer to final penetration (API 1993). In NCHRP Report 20-05 on large diameter pipe piles by Brown and Thompson (2015), large diameter open end pipe piles are defined as having a diameter of 36 inches or greater. Large diameter open end pipe piles can be either steel pipe piles or concrete cylinder piles. Recently, large diameter open end pipe pile usage has increased significantly on transportation projects. This has heightened the need for more accurate nominal resistance estimates on these larger piles.

Similar to other design methodologies, the API approach gives consideration to soil type. For cohesive soil, shaft resistance, f_s, can be determined from Equation 7-12.

$$f_s = \alpha\, s_u \qquad \text{Eq. 7-12}$$

Where:

α = dimensionless adhesion factor.

s_u = undrained shear strength at the location in question (ksf).

The factor α_f varies based on effective stress and may be calculated using Equations 7-13 through 7-15 below.

$$\alpha = 0.5\,\psi^{-.5} \text{ when } \psi \leq 1.0 \qquad \text{Eq. 7-13}$$

$$\alpha = 0.5\,\psi^{-.25} \text{ when } \psi > 1.0 \qquad \text{Eq. 7-14}$$

$$\psi = \frac{s_u}{\sigma'_{vo}} \qquad \text{Eq. 7-15}$$

Where:

α = dimensionless factor.
s_u = undrained shear strength at the sample depth (ksf).
σ'_{vo} = vertical effective stress at the sample depth (ksf).

An α value of 1.0 is recommended for unconsolidated clays. Reductions in resistance may be practical for very long piles where residual soil strength values are approached due to extended driving and subsequent soil displacement. For these cases, API (1993) recommends the use of engineering judgment.

The unit toe resistance, q_p, for piles in cohesive soil can be determined using Equation 7-16.

$$q_p = 9\, s_u \qquad \text{Eq. 7-16}$$

Because of the dynamic events during driving, the pile may be installed in an unplugged condition, however when static loads are applied, a plugged condition may exist. Consideration should be given to these cases when performing a static analysis and drivability study.

When installing piles in cohesionless soils, the unit shaft resistance may be determined with Equation 7-17.

$$f_s = K_\delta\, \sigma'_{vo} \tan\delta \qquad \text{Eq. 7-17}$$

Where:

K_δ = coefficient of lateral earth pressure.
σ'_{vo} = vertical effective stress (ksf).
δ = friction angle between the soil and pile wall.

API (1993) notes that assuming K_δ=0.8 for both tension and compression loading of unplugged, open ended pipe pile is appropriate. In addition, for the plugged or closed end case the assumption of K_δ=1.0 is recommended.

The unit toe resistance, q_p for piles in cohesionless soils may be determined using the following relationship:

$$q_p = \sigma'_{vo}\, N_q \qquad \text{Eq. 7-18}$$

Where:

σ'_{vo} = vertical effective stress (ksf).

N_q = dimensionless bearing capacity factor.

Table 7-8 is modified from API (1993) and presents guidelines for design parameters using steel pipe piles installed in cohesionless soils. Subsurface exploration and testing data for sites in question should be considered where necessary, in lieu of these guidelines.

Table 7-8 Design Parameter Guidelines for Cohesionless Siliceous Soil (after API 1993)

Density	Soil	Soil-Pile Friction Angle, δ	Limiting Unit Shaft Resistance, (ksf)	N_q	Limiting Unit Toe Resistance, (ksf)
Very loose Loose Medium	Sand Sand-Silt* Silt	15	1.0	8	40
Loose Medium Dense	Sand Sand-Silt* Silt	20	1.4	12	60
Medium Dense	Sand Sand-Silt*	25	1.7	20	100
Dense Very Dense	Sand Sand-Silt*	30	2.0	40	200
Dense Very Dense	Gravel Sand	35	2.4	50	250

* - In sand-silt soils (soils with significant fractions of both sand and silt), the strength values generally increase with increasing sand fractions and decrease with increasing silt fractions.

STEP BY STEP PROCEDURE FOR: “API METHOD”

STEP 1 Delineate the soil profile into cohesive and cohesionless layers.

For cohesive layers, determine the average undrained shear strength, s_u, for the layer and the vertical effective stress σ'_{vo}, at the mid-point of the layer. Determine the adhesion factor, α, based on the s_u/σ'_{vo} ratio and Equation 7-13 or 7-14.

For cohesionless layers, determine the soil-pile friction angle, δ, for the layer and the vertical effective stress σ'_{vo}, at the mid-point of the layer. Determine the coefficient of lateral earth pressure, K_δ, based on the pile type and loading direction.

STEP 2 For each soil layer, compute the unit shaft resistance, f_s (ksf) using Equation 7-12 in cohesive soil layers and Equation 7-17 in cohesionless soil layers.

Note: A limiting unit shaft resistance is applied in cohesionless soils.

STEP 3 Using Equation 7-4, compute the shaft resistance in each soil layer and the nominal shaft resistance, R_s, from the sum of the shaft resistance from each layer.

STEP 4 Compute the unit toe resistance, q_p (ksf).

For piles terminated in a cohesive layer, use the average undrained shear strength, s_u, in Equation 7-16.

For piles terminated in a cohesionless layer, determine bearing capacity factor, N_q, from Table 7-8 and Equation 7-18.

Note: A limiting unit toe resistance is applied in cohesionless soils.

STEP 5 Compute the nominal toe resistance, R_p (kips) using Equation 7-5.

For open pile sections, refer to the discussion of pile plugging presented in Section 7.10.7.

STEP 6 Compute the nominal pile resistance, R_n from the sum of the shaft and toe resistances, $R_n = R_s + R_p$.

STEP 7 Compute the factored resistance, R_r (kips), using the applicable resistance factor for the field verification method.

In NCHRP Report 507, Paikowsky (2004) evaluated the reliability of the API method in cohesive soils but not in sands or mixed profiles. AASHTO (2014) also does not provide a recommended resistance factor for the nominal resistance determined by the API method. Therefore, the nominal resistance at the strength limit state should be determined using the resistance factor associated with the field verification method, ϕ_{dyn}, as recommended in Table 7-2.

7.2.1.3.4 Effective Stress β-Method – Mixed Soil Profiles

Static resistance calculations in cohesionless, cohesive, and layered soils can also be performed using an effective stress method. Effective stress methods were developed to model the long term drained shear strength conditions. Therefore, the effective stress friction angle, ϕ', should be used in parameter selection.
In an effective stress analysis, the unit shaft resistance is calculated from the following expression:

$$f_s = \beta \ \sigma'_{vo} \qquad \text{Eq. 7-19}$$

Where:

β = Bjerrum-Burland beta coefficient = $K_\delta \tan \delta$.
σ'_{vo} = average vertical effective stress along the pile shaft (ksf).
K_δ = coefficient of lateral earth pressure.
δ = friction angle between pile and soil.

The unit toe resistance is calculated from:

$$q_p = N_t \ \sigma'_p \qquad \text{Eq. 7-20}$$

Where:

N_t = toe resistance coefficient.

σ'_p = vertical effective stress at the pile toe (ksf).

Recommended ranges of β and N_t coefficients as a function of soil type and ϕ' angle from Fellenius (2014) are presented in Table 7-9. Fellenius notes that factors affecting the β and N_t coefficients consist of the soil composition including the grain size distribution, angularity and mineralogical origin of the soil grains, the original soil density and density due to the pile installation technique, the soil strength, as well as other factors. While Table 7-9 provides the approximate range of β coefficients for various soil types, Fellenius noted that values can deviate significantly from those in the table. β coefficients seldom exceed 1.0.

For sedimentary cohesionless deposits, Fellenius states N_t ranges from about 30 to a high of 120. In very dense deposits such as glacial tills, N_t can be much higher, but can also approach the lower bound value of 30. In clays, Fellenius notes that the toe resistance calculated using an N_t of 3 is similar to the toe resistance calculated from a traditional analysis using undrained shear strength. Therefore, the use of a relatively low N_t coefficient in clays is recommended unless local correlations suggest higher values are appropriate.

As with any design method, the user should also confirm the appropriateness of selected coefficients in a given soil condition with local correlations between static resistance calculations and load tests results.

It should be noted that the effective stress method places no limiting values on either the shaft or toe resistance.

Table 7-9 Approximate Range of β and N_t Coefficients
(after Fellenius 2014)

Soil Type	ϕ'	β	N_t
Clay	25 - 30	0.15 - 0.35	3 - 30
Silt	28 - 34	0.25 - 0.50	20 - 40
Sand	32 - 40	0.30 - 0.90	30 - 150
Gravel	35 - 45	0.35 - 0.80	60 - 300

STEP BY STEP PROCEDURE FOR: “EFFECTIVE STRESS β-METHOD”

STEP 1 Delineate the soil profile into layers and determine ϕ' angle for each layer.

a. Construct Effective Stress Diagram using previously described procedure in Section 7.1.4.

b. Divide soil profile throughout the pile penetration depth into layers and determine the vertical effective stress, σ'_{vo}, (ksf) at the midpoint of each layer.

c. Determine the ϕ' angle for each soil layer from laboratory or in-situ test data.

d. In the absence of laboratory or in-situ data for cohesionless layers, determine the average corrected SPT *N* value, $(N_1)_{60}$, for each layer and estimate ϕ' angle from a select method in Section 5.2.3 of Chapter 5.

STEP 2 Select the β coefficient for each soil layer.

a. Use local experience to select β coefficient for each layer.

b. In the absence of local experience, use Table 7-9 to estimate β coefficient from ϕ' angle for each layer.

STEP 3 For each soil layer compute the unit shaft resistance, f_s (ksf) using Equation 7-19.

STEP 4 Compute the shaft resistance in each soil layer and the nominal shaft resistance, R_s (kips), from the sum of the shaft resistance from each soil layer.

Refer to Section 7.10.7 for additional information on the behavior of open pile sections.

STEP 5 Compute the unit toe resistance, q_p (ksf) using Equation 7-20.

a. Use local experience to select N_t coefficient.

b. In the absence of local experience, estimate N_t from Table 7-9 based on ϕ' angle.

c. Calculate the vertical effective stress at the pile toe, σ'_p (ksf).

STEP 6 Compute the nominal toe resistance, R_p (kips) using Equation 7-5.

For open pile sections, refer to the discussion of pile plugging presented in Section 7.10.7.

STEP 7 Compute the nominal pile resistance, R_n from the sum of the shaft and toe resistances, $R_n = R_s + R_p$.

STEP 8 Compute the factored resistance, R_r (kips), using resistance factors provided in Section 7.1.5 and Equation 7-3.

AASHTO (2014) does not provide a recommended resistance factor for the nominal resistance determined by the β-Method by Fellenius. Therefore, the nominal resistance at the strength limit state should be determined using the resistance factor associated with the field verification method, ϕ_{dyn}, as recommended in Table 7-2.

7.2.1.3.5 Brown Method – Mixed Soil Profiles – SPT Data

The Brown Method (2001) is a simple empirical method that uses SPT N_{60} values for calculating unit shaft resistance and unit toe resistance values. The Brown Method was based on resistance correlations with 71 static load tests from Caltrans projects in a wide variety of soil types. The pile types included closed end pipe, open end pipe, H-piles, and precast concrete piles. The method considers compression and uplift loading as well as pile installation method (impact driving and partial vibratory installation).

Brown reported that the average unit shaft resistance, f_s, (ksf) is:

$$f_s = \mathrm{F}_{vs}\,(\,\mathrm{A}_b + \mathrm{B}_b\ \mathrm{N}_{60}\,) \qquad \text{Eq. 7-21}$$

Where:

F_{vs} = factor for pile driving method (1.0 for impact or 0.68 for vibratory).
A_b = Brown's regression analysis factor based on soil type in (ksf).
B_b = Brown's regression analysis factor based on soil type in (ksf/bpf).
N_{60} = SPT N-Value corrected for 60% energy transfer.

Limits on the value of N_{60} were also recommended. If N_{60} is greater than 50, a value of 50 should be used and if N_{60} is less than 3, use 3. Brown recommended that the shaft resistance, R_s, be calculated by multiplying the unit shaft resistance times the pile perimeter with the "box" perimeter used for H-piles rather than the actual pile/soil contact area and for open end pipe piles only the external surface area. Regression factors A_b and B_b, as well as the pile installation factor, F_{vs}, are given in Table 7-10.

Brown (2001) recommended that for impact driven piles, the unit toe resistance, q_p (ksf) is calculated:

$$q_p = 3.55\ N_{60} \qquad \text{Eq. 7-22}$$

For vibratory installed piles this unit toe resistance should then be multiplied by 0.56. The pile toe resistance, R_p, in kips is then calculated as follows:

$$R_p = q_p\ (A_p + A_{pp}\ F_p) \qquad \text{Eq. 7-23}$$

Where:

A_p = cross sectional area of the pile material at pile toe (ft^2).
A_{pp} = cross sectional area of soil plug (ft^2) for open end pipe piles or H-piles at pile toe.
F_p = plug mobilization factor, 0.42 for pipe piles or 0.67 for H-piles.

Brown recommended the actual steel area at the pile toe be used for A_p on H-piles and open end pipe piles.

While the simplicity of Brown's method is attractive, it is recommended that the method be used only for preliminary length estimates until a greater experience base is obtained with the method results. Caltrans continues to study and expand on Brown's work as reported by Olson and Shantz (2004). AASHTO (2014) does not provide a recommended resistance factor for the nominal resistance determined by this method. Therefore, the resistance factor for the applicable field verification method, ϕ_{dyn}, should be used if this method is used.

Table 7-10 Input Factors for Brown's Method

Loading Condition	Installation Method	Soil Type	F_{vs}	A_b (ksf)	B_b (ksf/bpf)
Compression	Impact	Clay to Sand	1.0	0.555	0.040
"	"	Gravelly Sand to Boulders	1.0	0.888	0.888
"	"	Rock	1.0	2.89	2.89
Tension	Impact	Clay to Sand	1.0	0.522	0.0376
"	"	Gravelly Sand to Boulders	1.0	0.835	0.0
"	"	Rock	1.0	2.71	0.0
"	Vibratory	Clay to Sand	0.68	0.522	0.0376
"	"	Gravelly Sand to Boulders	0.68	0.835	0.0
"	"	Rock	0.68	2.71	0.0

7.2.1.3.6 Eslami and Fellenius Method – CPT Data

In the Eslami and Fellenius method, the unit shaft resistance is correlated to the average effective cone tip resistance with a shaft correlation coefficient applied based on the soil profile. The unit shaft resistance, f_s, (ksf) is calculated from:

$$f_s = \mathrm{C}_s \, \mathrm{q}_E \qquad \text{Eq. 7-24}$$

In Which:

$$\mathrm{q}_E = \mathrm{q}_t - U2 \qquad \text{Eq. 7-25}$$

$$\mathrm{q}_t = \mathrm{q}_c + U2(1 - a) \qquad \text{Eq. 7-26}$$

Where:

- C_s = shaft correlation coefficient from Table 7-11.
- q_E = Eslami cone stress.
- $U2$ = pore water pressure measured at cone shoulder.
- q_c = measured cone tip stress.
- a = ratio between shoulder area (cone base) unaffected by the pore water pressure to total area.

Table 7-11 C_s Values for Eslami and Fellenius Method (after Fellenius 2014)

Soil Type	C_s (%)
Soft sensitive soil	8.0
Clay	5.0
Silty clay, stiff clay and silt	2.5
Sandy silt and silt	1.5
Fine sand or silty sand	1.0
Sand	0.4

The unit toe resistance is computed using geometric averaging of the cone tip resistance over the influence zone at the pile toe, after the cone tip resistances have been corrected for pore pressure on the cone shoulder and effective stress. The zone of influence at the pile toe is based on the pile diameter, b, and ranges from 4b below the pile toe to 8b above the pile toe when the pile is installed through a weak zone overlying a dense zone. When a pile is driven through a dense soil into a weak soil, the zone of influence is from 4b below the pile toe to 2b above the pile toe. The unit toe resistance is calculated from:

$$q_p = \mathrm{C}_p \, \mathrm{q}_{Eg} \qquad \text{Eq. 7-27}$$

Where:

C_p = toe correction coefficient equal to 1.0 in most cases.

q_{Eg} = geometric average of the cone tip resistance in ksf over the influence zone after correction for pore pressure on shoulder and adjustment to effective stress.

The toe correction coefficient is a function of the pile size since larger piles require greater movement to mobilize the pile toe resistance. For pile diameters greater than 16 inches, the toe correction coefficient should be calculated as follows:

$$C_p = \frac{12}{b} \qquad \text{Eq. 7-28}$$

Where:

b = pile width or diameter (inches).

STEP BY STEP PROCEDURE FOR: “ESLAMI AND FELLENIUS METHOD”

STEP 1 Obtain CPT test results with outputs of cone stress and pore pressure measurements.

STEP 2 For each depth increment, compute the unit shaft resistance, f_s (ksf) using Equation 7-24 and coefficients provided in Table 7-11.

STEP 3 Compute the shaft resistance in each soil layer and the nominal shaft resistance, R_s (kips), from the sum of the shaft resistance from each layer using Equation 7-4.

STEP 4 Compute the unit toe resistance, q_p (ksf), using Equation 7-27.

STEP 5 Compute the nominal toe resistance, R_p (kips) using Equation 7-5.

STEP 6 Compute the nominal pile resistance, R_n from the sum of the shaft and toe resistances, $R_n = R_s + R_p$.

STEP 7 Compute the factored resistance, R_r (kips), using select resistance factors provided in Section 7.1.5 and Equation 7-3.

AASHTO (2014) does not provide a recommended resistance factor for this method. Therefore, the nominal resistance in the strength limit state should be determined using the resistance factor associated with the field verification method, ϕ_{dyn}, as recommended in Table 7-2.

7.2.1.3.7 Nottingham and Schmertmann Method – CPT Data

One empirical procedure used in U.S. practice was derived from work originally published by Nottingham and Schmertmann (1975), and summarized in publication FHWA-TS-78-209, "Guidelines for Cone Penetration Test, Performance and Design" by Schmertmann (1978).

The nominal shaft resistance, R_s, in cohesionless soils may be derived from unit sleeve friction of the CPT using the following expression:

$$R_s = K_s \left[\frac{1}{2}(\mathrm{f}_s A_s)_{0\ to\ 8b} + (\mathrm{f}_s A_s)_{8b\ to\ D}\right] \qquad \text{Eq. 7-29}$$

Where:

- K_s = ratio of unit pile shaft resistance to unit cone sleeve friction from Figure 7-20 as a function of the full penetration depth, D.
- f_s = average unit sleeve friction over the depth interval indicated by subscript.
- A_s = pile shaft surface area over fs depth interval.
- b = pile width or diameter.
- D = embedded pile length.
- 0 to 8b = range of depths for segment from ground surface to a depth of 8b.
- 8b to D = range of depths for segment from a depth equal to 8b to the pile toe.

The transfer function K_s, relating pile shaft resistance to CPT sleeve friction, varies as a function of total pile penetration (depth of embedment/pile diameter), pile material type, and type of cone penetrometer used. No limit was imposed on sleeve friction values in the procedure originally proposed by Nottingham and Schmertmann (1975).

If cone sleeve friction data is not available, R_s can be determined from the cone tip resistance as follows:

$$R_s = \mathrm{C}_f \sum q_c A_s \qquad \text{Eq. 7-30}$$

Where:

- C_f = correction obtained from Table 7-12.
- q_c = average cone tip resistance along the pile length.
- A_s = pile shaft surface area (length).

For shaft resistance in cohesive soils, the nominal shaft resistance, R_s, is obtained from the sleeve friction values using the following expression:

$$R_s = \alpha' \mathrm{f}_s A_s \qquad \text{Eq. 7-31}$$

Where:

α' = ratio of pile shaft resistance to cone sleeve friction, patterned after Tomlinson's α-method.

f_s = unit sleeve friction.

A_s = pile shaft surface area (length).

The value of α' varies as a function of sleeve friction, f_s, as shown in Figure 7-20. It is expected that this method of calculating pile shaft resistance is less appropriate in sensitive soils as the friction sleeve of the cone encounters severely disturbed soils behind the cone tip.

The estimation of pile toe resistance is described in Figure 7-21. In essence, an elaborate averaging scheme is used to weigh the cone tip resistance values, from 8 pile diameters above the pile toe, to as much as 3.75 pile diameters below the pile toe, favoring the lower cone tip resistance, q_c, values within the depth range. The authors make reference to a "limit" value of q_c between 105 to 315 ksf, that should be applied to the nominal unit pile toe resistance, q_p, unless local experience warrants use of higher values. In the case of mechanical cone soundings in cohesive soils, the q_p value is reduced by 40 percent to account for toe resistance effects on the base of the friction sleeve. As discussed in Section 7.10.7, careful consideration of soil plugging phenomena is needed in choosing the cross-sectional area over which q_p is applied for low displacement open ended pipe and H-piles.

Table 7-12 CPT C_f VALUES

Type of Piles	C_f
Precast Concrete	0.012
Timber	0.018
Steel Displacement	0.012
Open End Steel Pipe	0.008

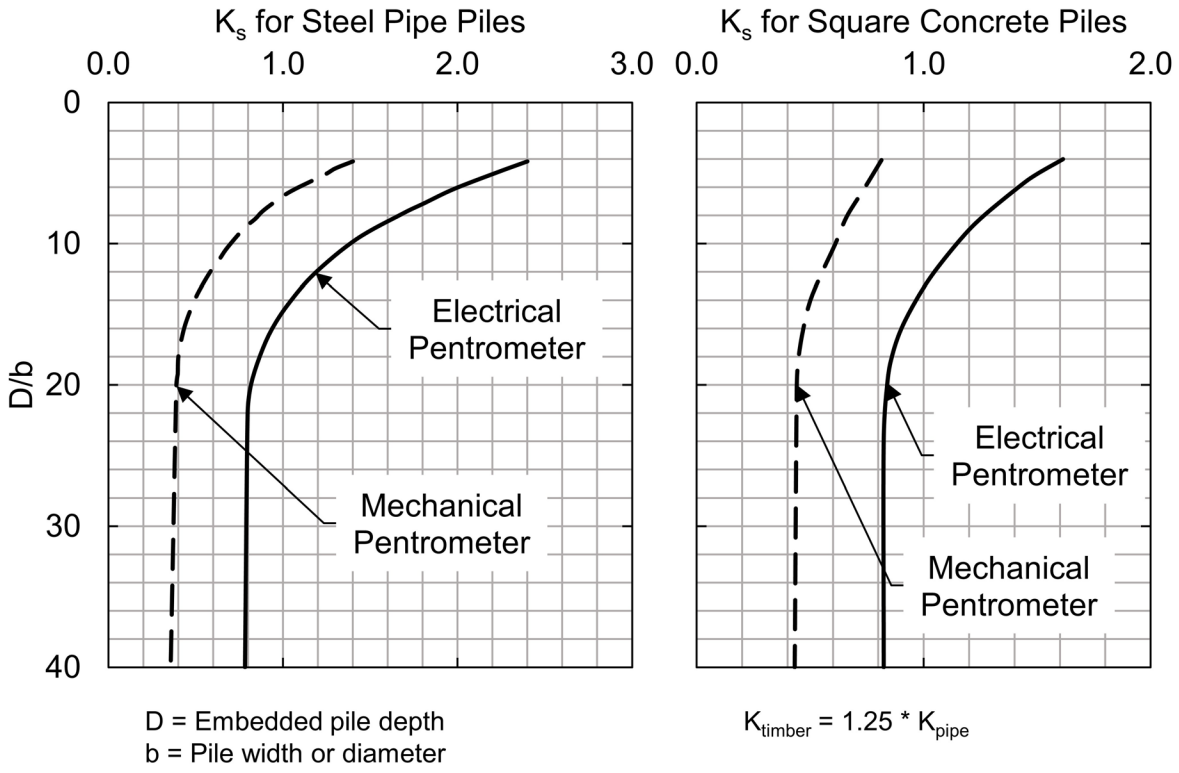

Figure 7-19 Penetrometer design curves for pile shaft friction in sand (after FHWA Implementation Package, FHWA-TS-78-209).

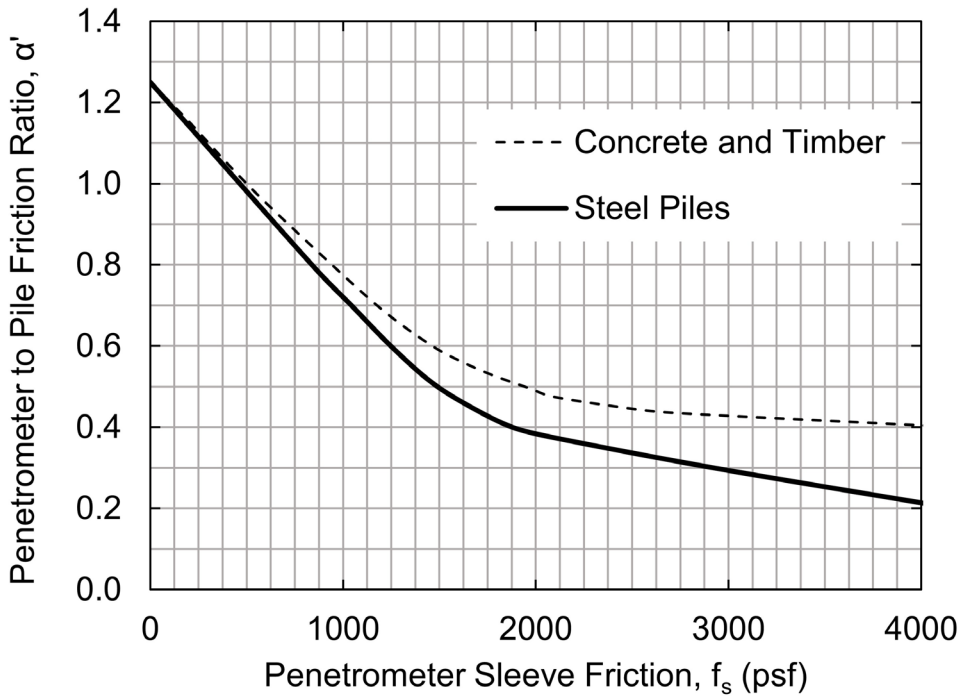

Figure 7-20 Design curve for pile shaft friction in clay (after Schmertmann 1978).

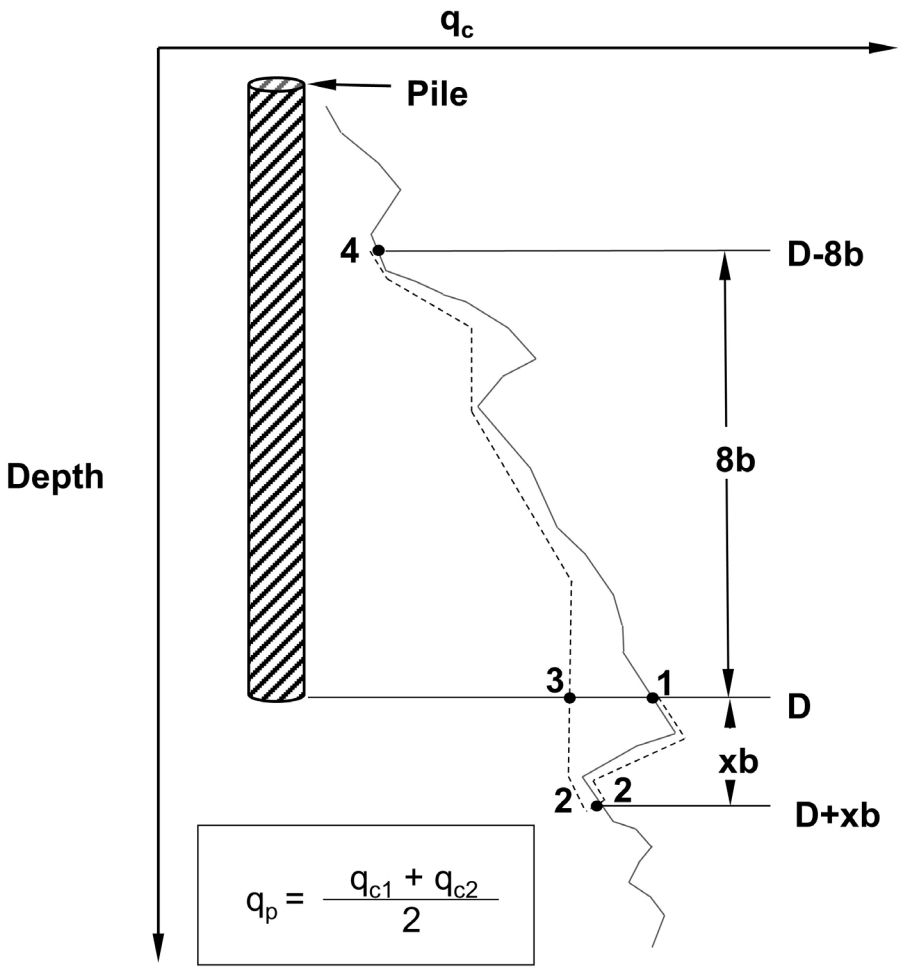

q_{c1} = Average q_c over a distance of xb below the pile toe (path 1-2-3). Sum q_c values in both the downward (path 1-2) and upward (path 2-3) direction. Use actual q_c values along path 1-2 and the minimum path rule along path 2-3. Compute q_{c1} for x-values from 0.7 to 3.75 below the pile toe and use the minimum qc1 value obtained.

q_{c2} = Average q_c over a distance of 8b above the pile toe (path 3-4). Use the minimum path rule as for path 2-3 in the q_{c1} computations.

b = Pile width or diameter.

D = Embedded pile length.

Figure 7-21 Illustration of Nottingham and Schmertmann Procedure for estimating pile toe resistance (FHWA-TS-78-209).

STEP BY STEP PROCEDURE FOR: “NOTTINGHAM AND SCHMERTMANN METHOD”

STEP 1 Delineate the soil profile into layers using the cone tip resistance, q_c, and sleeve friction, f_s, values.

STEP 2 Compute the shaft resistance for each soil layer, R_s (kips).

a. For piles in cohesionless soils, compute shaft resistance, R_s, using the average sleeve friction value for the layer, f_s, and the K value. Note that K should be determined using the full pile penetration depth to diameter ratio from Figure 7-19, and not the penetration depth for the layer. Conversely, the depth d corresponds to the pile toe depth, or the depth to the bottom of the layer, whichever is less. For H-piles in cohesionless soils, the pile-soil surface area A_s, should be the "box" area.

For cohesionless layers below a depth of 8b, Equation 7-29 for shaft resistance in a layer reduces to:

$$R_s = K_s \mathrm{f}_s A_s \qquad \text{Eq. 7-32}$$

Where:

K_s = ratio of unit pile shaft resistance to unit cone sleeve friction from Figure 7-19 as a function of the full penetration depth, D.

f_s = average unit sleeve friction over the depth interval indicated by subscript.

A_s = pile shaft surface area over f_s depth interval.

For piles in cohesionless soils without sleeve friction data, compute the shaft resistance from Equation 7-30.

b. For piles in cohesive soils, compute the shaft resistance using the average sleeve friction value for the layer and Equation 7-31.

STEP 3 Compute the shaft resistance in each soil layer and the nominal shaft resistance, R_s (kips), from the sum of the shaft resistance from each layer.

STEP 4 Compute the unit pile toe resistance, q_p (ksf) using Equation 7-33.

$$q_p = \frac{q_{c1}+q_{c2}}{2} \quad \text{Eq. 7-33}$$

Where:

q_{c1} = average q_c over a distance of *xb* below the pile toe (path 1-2-3 from Figure 7-21). Sum q_c values in both the downward (path 1-2) and upward (path 2-3 direction. Use actual q_c values along path 1-2 and the minimum path rule along path 2-3. Compute q_{c1} for x-values from 0.7 to 3.75 below the pile toe and use the minimum qc_1 value obtained.

q_{c2} = average q_c over a distance of 8b above the pile toe (path 3-4 from Figure 7-21). Use the minimum path rule as for path 2-3 in the q_{c1} computations.

b = pile width or diameter.

D = embedded pile length.

STEP 5 Compute the nominal toe resistance, R_p (kips).

For steel H and unfilled open ended pipe piles, use only the steel cross section area at the pile toe unless there is reasonable assurance and previous experience that a soil plug would form. For a plugged condition use the "box" area of the H-pile and the full cross section area for pipe pile. Additional information on the plugging of open pile sections is presented in Section 7.10.7.

STEP 6 Compute the nominal resistance, R_n from the sum of the shaft and toe resistances, $R_n = R_s + R_p$.

STEP 7 Compute the factored resistance, R_r (kips), using select resistance factors provided in Section 7.1.5 and Equation 7-3.

AASHTO (2014) provides a recommended resistance factor for this method in Table 7-1 for the nominal resistance determined by static analysis. The nominal resistance in the strength limit state could also be determined using the resistance factor associated with the field verification method, ϕ_{dyn}, as recommended in Table 7-2.

7.2.1.4 Nominal Resistance of Single Piles to Rock

Pile foundations on rock are normally designed to carry large loads. For pile foundations driven to rock, which include steel H-piles, pipe piles or precast concrete piles, the exact area in contact with the rock, the depth of penetration into rock, as well as the quality of rock in the immediate pile contact area are largely unknown. Pile installation can also alter the characteristics of the rock formation, further complicating design procedures.

The distinction between soft rock and hard rock is not well defined. The AASHTO definition of soft and hard rock for driven pile foundation design is limited. In general, soft rock is defined as rock that can be penetrated by pile driving and hard rock is defined as rock that cannot be penetrated. Hence, piles are driven into soft rock and driven to hard rock. In many intact rock classification systems, the transition between soft rock and hard rock occurs between an unconfined compression strength of 200 and 1000 ksf. Kulhawy (1991) proposed 400 ksf as the an unconfined compression strength denoting the transition between weak and moderate rock. AASHTO notes that a definition of hard rock based on measureable rock characteristics has not been widely accepted.

Likins and Goble (1978) reported on the results of an Ohio DOT and FHWA sponsored research study on HP 10x42 H-piles driven to shallow bedrock with multiple, similarly sized pile hammers. Static and dynamic load tests were conducted at the two sites, one with hard rock and one with soft rock. The H-piles were driven to a penetration resistance of 20 blows per inch on rock at both sites. At the hard rock site, hard limestone with an unconfined compression strength of up to 1094 ksf was encountered around 22 feet. At the soft rock site, weathered shale with unconfined compressive strength of 172 to 316 ksf was encountered around 15 feet. The A-36 steel H-piles at the hard limestone site were statically load tested to as high as $0.93F_y$ without reaching the Davisson load test failure criteria which is described in Chapter 9. At the weathered shale site, significantly lower nominal resistances were achieved with failure occurring between 0.28 to $0.71F_y$. Relaxation occurred on the H-piles driven at the weathered shale site and higher nominal resistances were observed on piles that penetrated deeper into the shale. This study, even though it was performed with smaller hammers and piles then commonly used today, demonstrates that geotechnical aspects control soft rock design and structural aspects control hard rock design.

Tomlinson and Woodward (2015) state that piles driven to rock can create very high concentrated loads on the rock beneath the pile toe. The ability of the rock to

support the concentrated load depends in part on the compressive strength of the rock, the frequency of fissures and joints in the rock mass, and whether the fissures and joints are tightly closed or are open and filled with weathered material. They further note that very high loads can be supported if the rock is strong and has closed joints or joints on a shallow angle to horizontal. Conversely, steeply inclined and open joints may provide little resistance as the rock beneath the pile toe slides until the joints are closed or the rock mass becomes locked together. The driving of piles through weak or broken rock to hard rock can shatter weak rock such that shaft resistance is significantly reduced or eliminated. The resulting concentrated load may be acceptable for strong intact rock but it may be excessive for a strong but closely jointed rock mass.

Published results as well as empirical values for nominal shaft resistances are presented in Table 7-13. These results may be used for preliminary estimating purposes or as a check of values obtained from field tests. However, they are not intended to be used as final design values without the user determining the applicability of the underlying method or the suitability of a reported nominal resistance value to a given site or geologic formation.

Table 7-13 Published Nominal Shaft Resistance Values in Weak Rock Materials

Rock Description	Pile Type	Nominal Unit Shaft Resistance (ksf)	Source
Moderately strong, slightly weathered, Slaty Mudstone	H-pile	0.6	1.
Moderately strong, slightly weathered, Slaty Mudstone	H-pile	3.3	1.
Faintly to moderately weathered , moderately strong to strong, Mudstone	Pipe Pile	2.6	2.
Very weak, closely fissured argillaceous Siltstone (Mercia Mudstone)	Precast Concrete	2.7	3.
Very weak, coral detrital Limestone (carbonate sandstone/siltstone)	Pipe pile	0.9	2.
Limestone	H-pile	24.0	4.
Weak calcareous Sandstone	Pipe Pile	0.9	2.
Sandstone	H-pile	20.0	4.
Shale	H-pile	12.0	4.

Information sources:
1) George et al. (1976)
2) Tomlinson and Woodward (2015)
3) Leach and Mallard (1980)
4) Illinois DOT Geotechnical Pile Design Guide, AGMU 10.2 (2011)

Published results and recommended empirical values for nominal toe resistances are presented in Table 7-14. Once again these values may be used for preliminary estimating purposes or as a check of values obtained from field tests. However, they are not intended to be used as final design values without the user determining the applicability of the underlying method or the suitability of a reported nominal resistance value to a given site or geologic formation.

Table 7-14 Published Nominal Toe Resistance Values in Weak Rock Materials

Rock Description	Pile Type	Nominal Unit Toe Resistance (ksf)	Source
Weak carbonate Siltstone/Sandstone (coral detrital limestone)	N.A.	106.7	1.
Limestone	H-pile	240.0	2.
Weak calcareous Sandstone	Pipe Pile	62.6	1.
Sandstone	H-pile	200.0	2.
Shale	H-pile	120.0	2.

Information sources: 1) Tomlinson and Woodward (2015)
2) Illinois DOT Geotechnical Pile Design Guide, AGMU 10.2 (2011)

Based on the above discussion and information, the determination of nominal shaft and toe resistances of piles driven into or on rock is best made on the basis of static or dynamic load tests in conjunction with pile driving observations and local experience. In general, the design of small diameter piles supported on fair to excellent quality rock will be controlled by their nominal structural resistance as described in Chapter 8. A pile on hard intact rock will fail structurally before hard intact rock failure. Piles supported in soft, weakly laminated or weathered rock should be designed based on the results of static or dynamic load tests.

7.2.1.4.1 Piles Driven into Soft and Weak Rock

Tomlinson and Woodward (2015) note that the shaft resistance on piles driven into weak weathered rocks cannot always be calculated from the results of laboratory tests on rock cores. Factors such as degradation of the weak rock, reduction in shaft resistance due to shattering of the rock structure from driving adjacent piles, and formation of an enlarged hole around the pile hamper analytical methods.

The design of axial loaded piles in soft rock should be performed using the same procedures and methods used for piles in soil as presented in Section 7.2.2. Static and dynamic tests are recommended for design verification until local correlations

and design methods are available. The empirical values provided above for H-piles in shale, sandstone, and limestone were developed by Illinois DOT for their practice and have been found to yield reasonable estimates of pile length and nominal resistance in the regional geology.

The nominal toe resistance of piles in soft and hard rocks can also be computed according to Equation 7-34 in Section 7.2.1.4.2 below. For this calculation, the rock friction angle, undrained shear resistance, and effective density are needed from laboratory tests.

It is recommended that unit resistance values calculated from this equation be compared to values obtained from static or dynamic tests and that these comparisons be compiled in a local or regional database. This will assist and improve foundation design procedures in soft and weak rocks. Piles driven into soft rock may not require pile toe protection (i.e. driving shoe).

7.2.1.4.2 Piles Driven to Hard Rock

For piles driven to hard rock, the nominal resistance is generally controlled by the structural limit state. In hard rock designs, the nominal structural resistance will generally be less than the nominal geotechnical resistance of hard rock.

Where laboratory tests can be made on undisturbed samples of weak or hard rock and the undrained shear strength, s_u, and the rock friction angle, ϕ, can be obtained, the nominal unit toe resistance, q_p, in ksf can be calculated using Equation 7-34.

$$q_p = P_s\, s_u\, N_c + \gamma D\, N_q + P_t\, \gamma \left(\frac{b\, N_\gamma}{2}\right) \qquad \text{Eq. 7-34}$$

Where:

- s_u = undrained shear resistance of the rock (ksf).
- γ = effective density of the rock mass (kcf).
- D = pile penetration below the rock surface (ft).
- b = pile width or diameter (ft).
- P_s = pile toe shape factor of 1.25 for square pile or 1.2 for a circular pile.
- P_t = pile base factor of 0.8 for a square pile or 0.7 for a circular pile.

  N_c, N_q, and N_γ are bearing capacity factors from Figure 7-22.

Equation 7-34 represents wedge failure below a foundation modified with shape factors and it should not be confused with Terzaghi's equation for a spread footing

foundation. Tomlinson and Woodward (2015) added the recommended correction factors P_s and P_t for driven pile shapes.

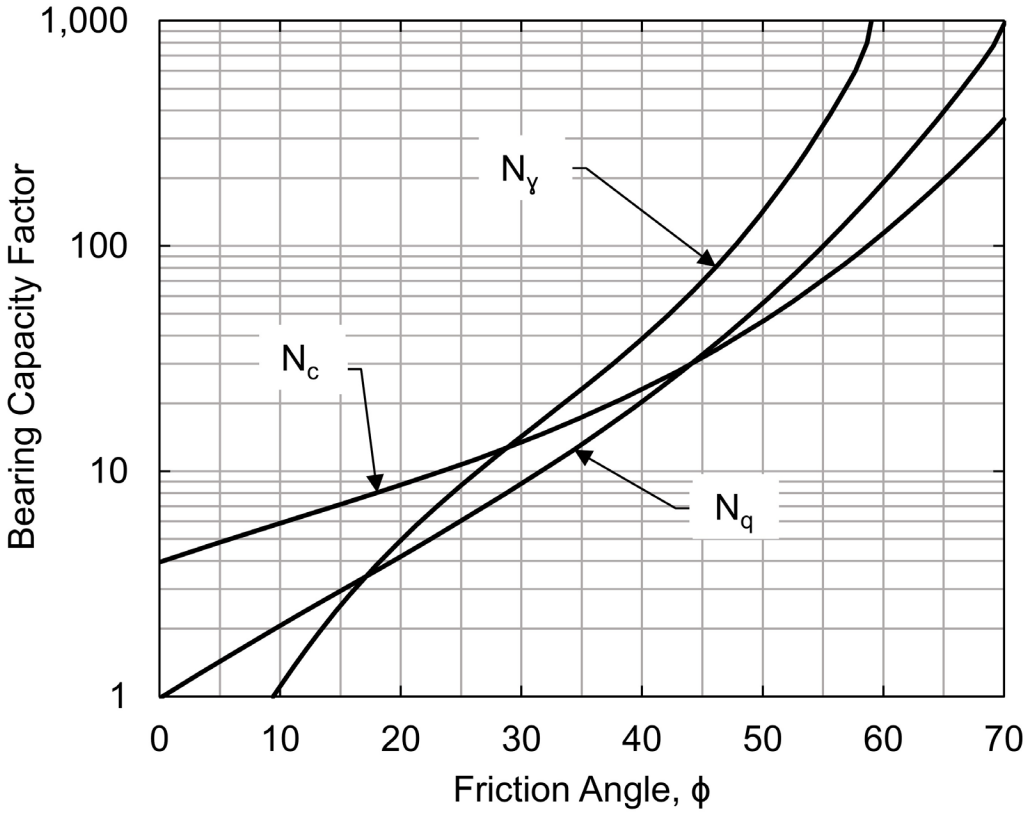

Figure 7-22 Bearing capacity factors for foundations on rock (modified from Pells and Turner 1980).

Data from Kulhawy and Goodman (1980; 1987) showed that the unit toe resistance, q_p, can also be estimated from the Rock Quality Designation (RQD) value of the intact rock mass and the unconfined compression strength of the rock, q_u. RQD was described previously in Chapter 4. For RQD values of 0 to 70%, the nominal unit toe resistance can be estimated as $0.33q_u$. For RQD values of 70 to 100%, the nominal unit toe resistance can be linearly interpolated from $0.33q_u$ at an RQD value of 70% to $0.80q_u$ at an RQD value of 100%. In hard rock cases, pile toe protection should be considered in the design.

A static analysis resistance factor, ϕ_{stat}, for any of the above nominal resistance calculation methods for rock is not available. Therefore, the calculated nominal resistance should be verified during construction using a nominal resistance field verification method and its associated resistance factor, ϕ_{dyn}.

7.2.1.5 Software for Single Pile Nominal Resistance Computations

The FHWA previously sponsored the development and use of the DRIVEN computer program for static analysis computations. This program used the FHWA recommended Nordlund Method and α-method as presented in this manual for calculation of the nominal resistance. The public domain version of the DRIVEN program is no longer available from the FHWA. However, a commercial version of the program, DrivenPiles, was released in 2015. Numerous other static analysis programs are also commercially available. Table 7-15 summarizes the static analysis methods incorporated in commercially available programs. It should be emphasized that the FHWA does not endorse any particular analysis program and the programs are listed alphabetically in Table 7-15.

Table 7-15 Summary of Computer Analysis Software for Axial Single Pile Analysis

Computer Program	Static Analysis Methods in Program	Method Presented in GEC-12 (2016)	Method Presented in AASHTO 7th Edition (2014)
AllPile	Navfac DM-7	No	No
A-Pile	API-RP2A	Yes	No
	US Army COE	No	No
	FHWA (alpha / Nordlund)	Yes	Yes
	Lambda Method	No	Yes
	NGI (CPT)	No	No
	ICP (CPT)	No	No
DrivenPiles	Alpha Method	Yes	Yes
	Nordlund Method	Yes	Yes
FB-Deep	FDOT SPT Method	No	No
	Schmertmann (CPT)	Yes	Yes
	UF (CPT)	No	No
	LCPC (CPT)	No	No
Unipile	Alpha Method	Yes	Yes
	Beta Method	Yes	Yes, but differs
	Elsami and Fellenius (CPT)	Yes	No
	Schmertmann (CPT)	Yes	Yes
	LCPC (CPT)	No	No

An example soil profile is presented in Figure 7-23 along with the necessary soil input parameters for the selected static analysis software programs. Figure 7-24 presents DRIVEN results of nominal resistance, shaft resistance, and toe resistance versus depth. For comparison purposes, results for the same soil profile are presented in Figures 7-25 and 7-26 for the APILE using the Nordlund and alpha Methods and UNIPILE using the Beta Method, respectively.

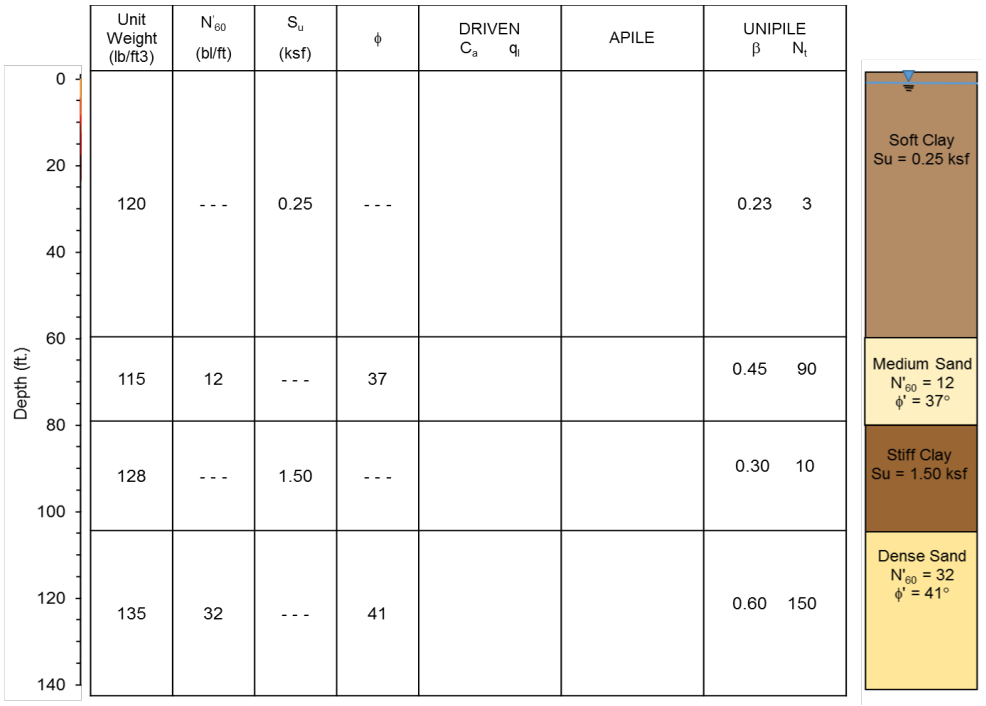

Figure 7-23 Soil profile for computer software comparison.

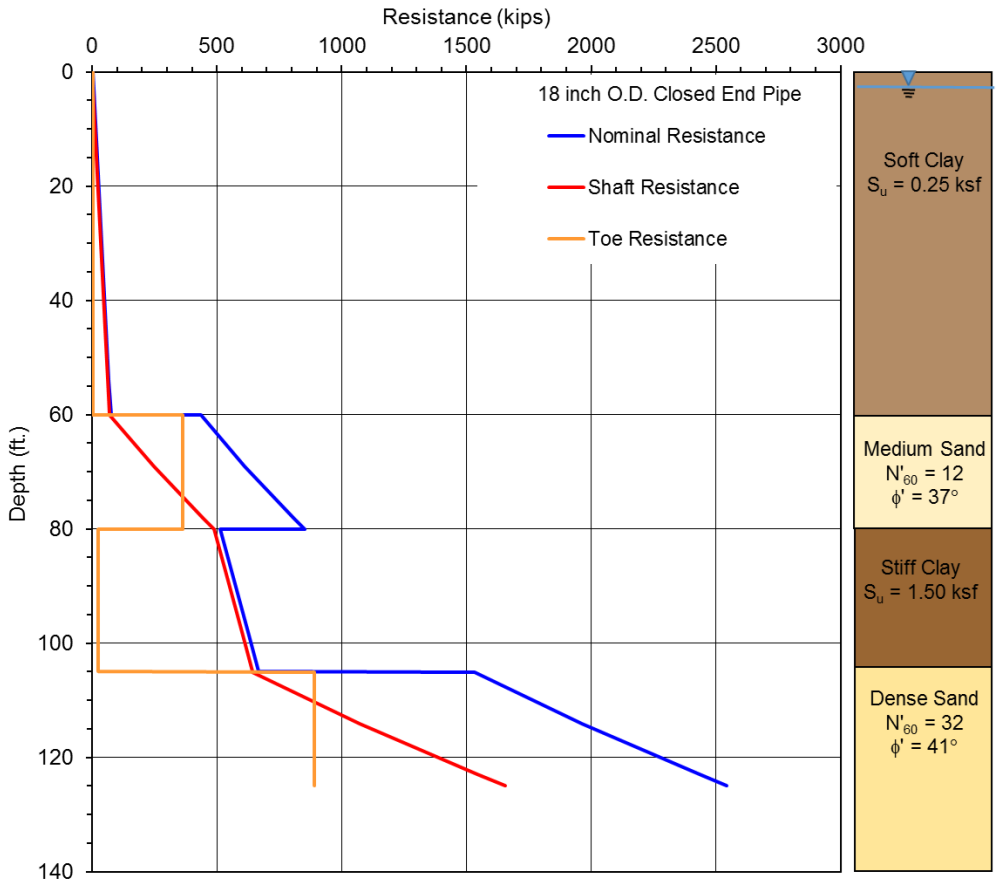

Figure 7-24 Nominal resistance from DRIVEN program using FHWA method.

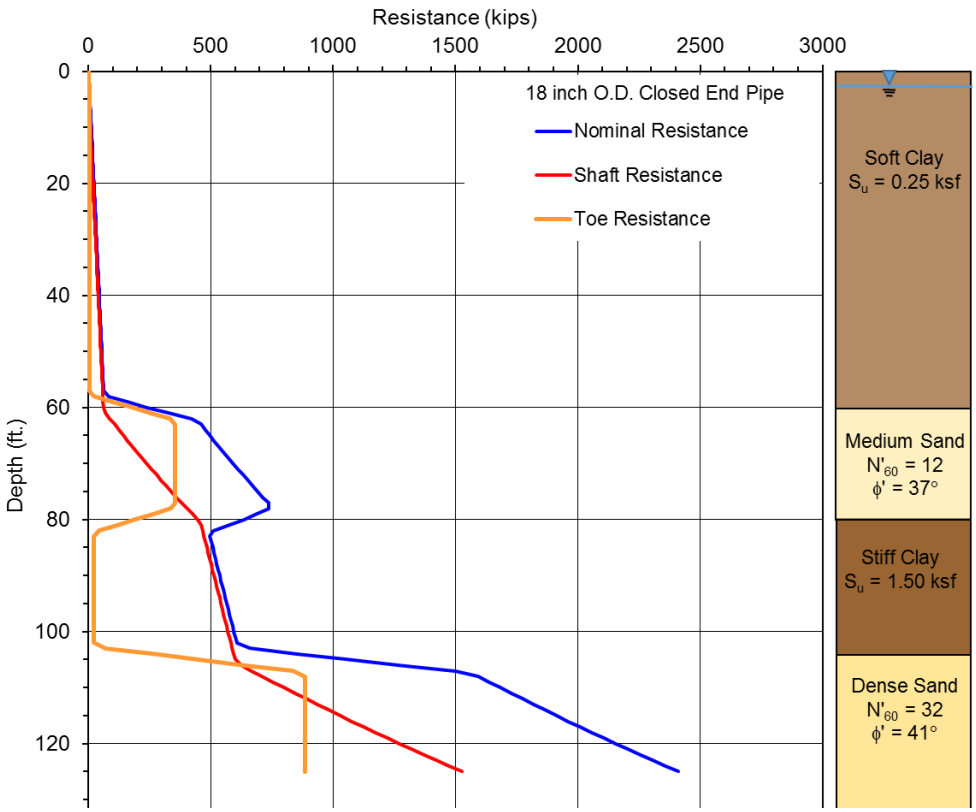

Figure 7-25 Nominal resistance from APILE program using FHWA Method.

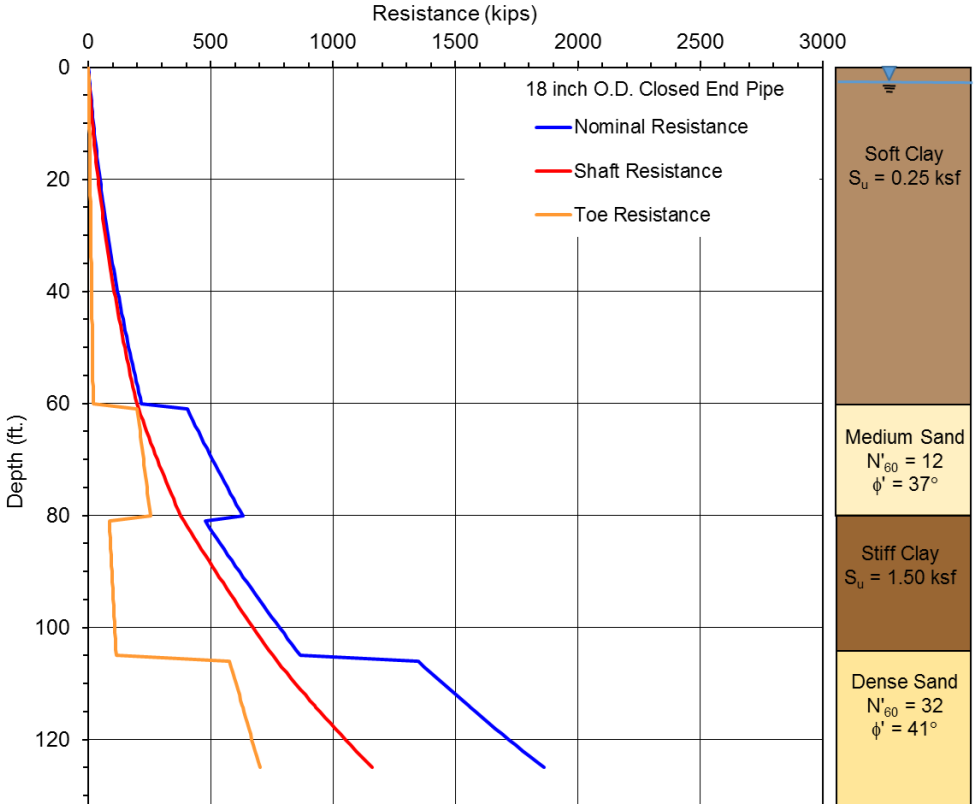

Figure 7-26 Nominal resistance from UNIPILE program using Beta Method.

Of particular note is the difference between the DRIVEN results and the APILE FHWA method results. One could reasonably expect both programs to yield the same results. However, subtle differences in software coding results in about a 10% variation in the toe resistance and nominal resistance at the final 125 foot penetration depth. The programs also have differences in the toe resistance and nominal resistance at the transition depths between soil layers. The APILE program uses an averaging of the toe resistance around layer transitions whereas the DRIVEN program does not. The results from the UNIPILE program which calculates the resistance using effective stresses in all layers yields a lower resistance solution.

Figure 7-27 presents nominal resistance results generated by the APILE - FHWA method for three different pile types in the same soil profile. The pile types include an HP 18 x 204 H-pile, a 18 inch O.D. closed end pipe pile, an a 24 inch square prestressed concrete pile. Note the displaced volume of a 24 inch concrete pile exceeds the 2.0 pcf volume limit in Figure 7-9.

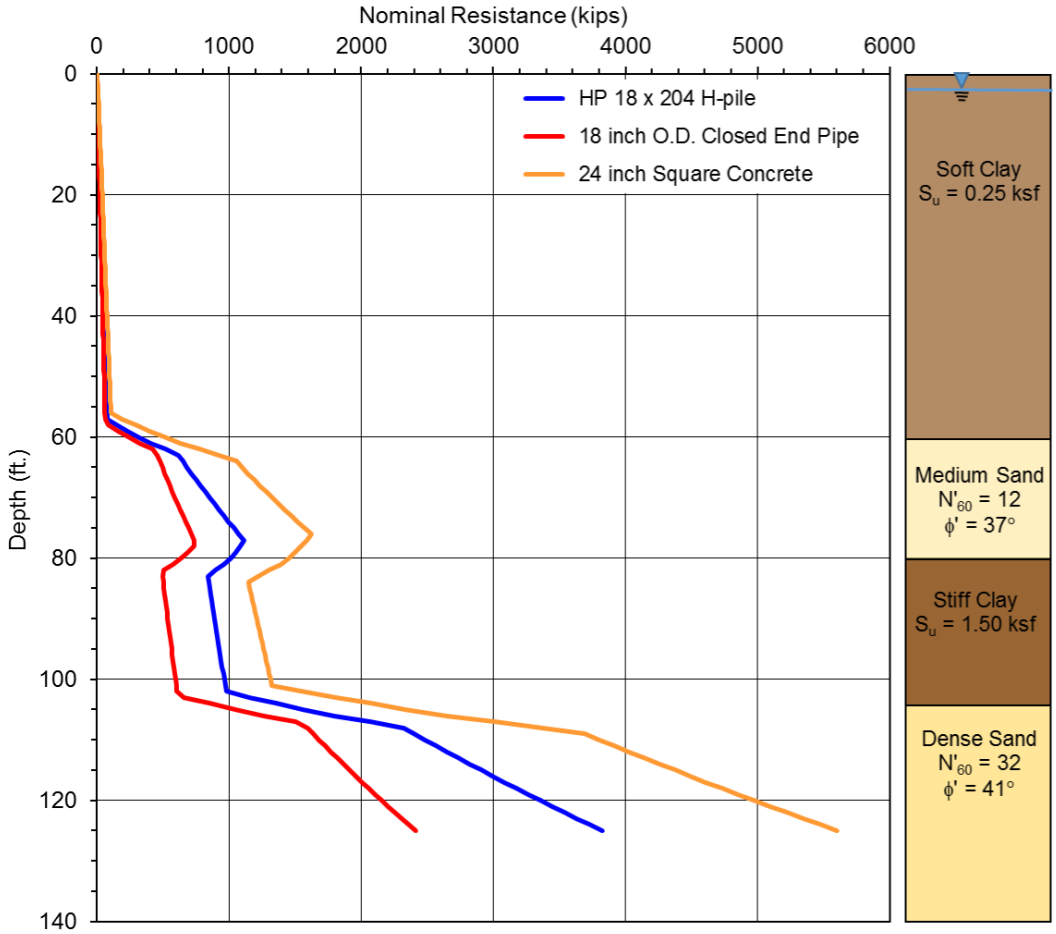

Figure 7-27 Nominal resistance versus depth for three pile types calculated by the APILE program with the FHWA Method.

Both of these examples emphasize the importance of the program user to fully understand the methodology behind a given program, its accuracy, and its limitations in a given application.

In Figure 7-28, a design chart for an 18 inch diameter closed-end pipe pile is presented. The nominal resistance results versus depth were calculated using the APILE - FHWA method. In the same figure, the factored resistance versus depth is presented for different field verification methods. For a factored resistance of 1000 kips in the soil conditions depicted, a relatively small difference exists between the estimated pile penetration depth of 106 feet based on a resistance factor of 0.80 (static load test and dynamic tests on 2% of the production piles) and the estimated pile penetration depth of 108 feet based on a resistance factor of 0.65 (dynamic tests on 2% of the production piles). Hence, a static load test may not be justifiable based on cost in this situation. Conversely, a significant difference exists between the estimated pile penetration depth of 108 feet based on a resistance factor of 0.65 (dynamic tests on 2% of the production piles) and the estimated pile penetration depth of 117 feet based on a resistance factor of 0.50 (wave equation analysis) or 127 feet based on a resistance factor of 0.40 (Modified Gates formula). An evaluation of the nominal and factored resistances versus depth considering the cost of the pile length as well as the field verification method allows the designer to determine the most appropriate method of field verification for the design.

The design chart in Figure 7-28 allows an evaluation of the nominal and factored resistances versus depth considering the cost of the pile length as well as the field verification method. This type of analysis allows the designer to determine the most appropriate method of field verification for the design.

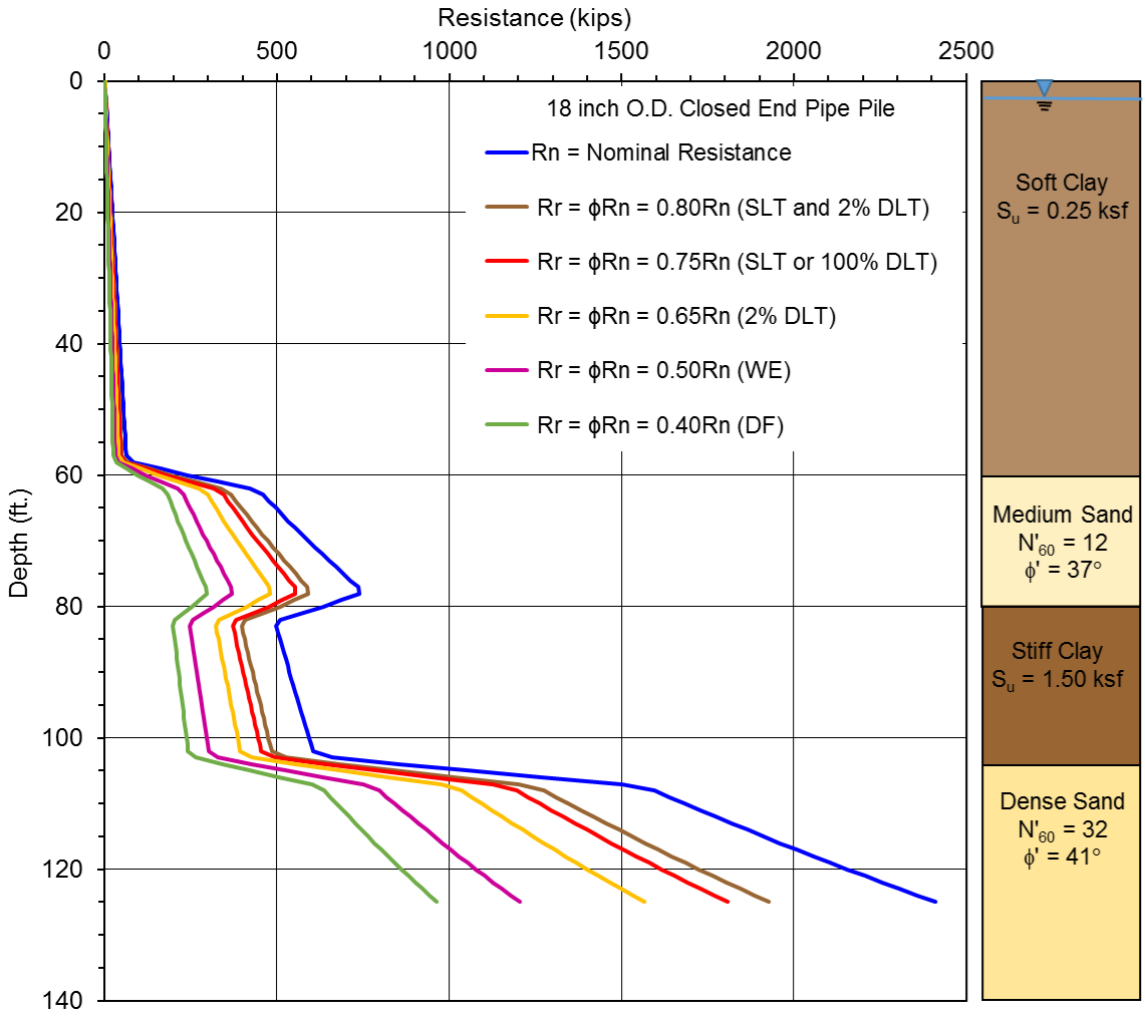

Figure 7-28 Design chart of nominal resistance, R_n, and factored resistance, R_r, versus depth for one pile type with different field control methods.

7.2.2 Resistance of Pile Groups in Axial Compression

The previous sections dealt with design procedures for single piles. However piles for almost all highway structures are installed in groups, due to the heavy foundation loads. The following sections of this chapter will address foundation design procedures for evaluating the nominal resistance in axial compression of pile groups. The nominal resistance in axial compression and settlement of pile groups are interrelated; settlement will be further discussed in Section 7.3.2 of this chapter. Pile group design computations are primarily performed using computer programs designed for this purpose such as FB-Pier or Group 6.0 rather than the simple hand calculations presented in this manual.

The efficiency of a pile group in supporting the foundation load is defined as the ratio of the nominal resistance of the group to the sum of the nominal resistance of the individual piles comprising the group. This may be expressed in equation form as:

$$\eta_g = \frac{R_{ng}}{n\,R_n} \qquad \text{Eq. 7-35}$$

Where:

η_g = pile group efficiency.
R_{ng} = nominal resistance of pile group.
n = number of piles in pile group.
R_n = nominal resistance of each individual pile in pile group.

If piles are driven into relatively weak cohesive soil or in dense cohesionless material underlain by weaker soil, then the nominal resistance in axial compression of a pile group may be less than that of the sum of the nominal resistance in axial compression of the individual piles. In this case, the pile group has a group efficiency of less than 1. In cohesionless soils, the nominal resistance in axial compression of a pile group is generally greater than the sum of the nominal resistance in axial compression of the individual piles comprising the group. In this case, the pile group has group efficiency greater than 1.

Guidance on the group efficiency for piles driven to or into rock is not contained in AASHTO. Provided the pile group is driven to or into rock with equally strong material beneath, the pile group efficiency should be 1 or greater. Group efficiency of groups driven into highly weathered, karst, or other variable conditions should be further evaluated by the designer based on local conditions.

The soil medium supporting a pile group is also subject to overlapping stress zones from individual piles in the group. The overlapping effect of stress zones for a pile group supported by shaft resistance is illustrated in Figure 7-29.

Piles are typically driven into mixed soil and rock profiles. For pile group analysis, the stratum that provides the majority of the nominal geotechnical resistance may be considered the controlling stratum.

7.2.2.1 Pile Groups in Cohesionless Soils

In cohesionless soils, the nominal group resistance of driven piles with a center to center spacing of less than 3 pile diameters is greater than the sum of the nominal resistance of the individual piles. The greater group resistance is due to the overlap of individual soil compaction zones around each pile which increases the shaft resistance due to soil densification. Piles in groups at center to center spacings greater than three times the average pile diameter generally act as individual piles.

Design recommendations for estimating group resistance for driven piles in cohesionless soil are as follows:

1. The nominal group resistance for driven piles in cohesionless soils not underlain by a weak deposit may be taken as the sum of the individual nominal pile resistances, provided jetting or predrilling was not used in the pile installation process. Jetting or predrilling can result in group efficiencies less than 1. Therefore, jetting or predrilling should be avoided whenever possible and controlled by detailed specifications when necessary.

2. If a pile group founded in a firm bearing stratum of limited thickness is underlain by a weak deposit, then the nominal group resistance is the smaller value of either the sum of the nominal resistances of the individual piles, or the group resistance against block failure of an equivalent pier, consisting of the pile group and enclosed soil mass punching through the firm stratum into the underlying weak soil. From a practical standpoint, block failure in cohesionless soils can only occur when the center to center pile spacing is less than 2 pile diameters, which is less than the minimum center to center spacing of 2.5 diameters allowed by AASHTO (2014). The method shown for cohesive soils in the Section 7.2.2.3 may be used to evaluate the possibility of a block failure.

3. Piles in groups should not be installed at center to center spacing less than 3 times the average pile diameter unless dictated otherwise by pile size, site constraints, pile cap requirements, and construction costs. The minimum center to center spacing of 3 diameters is recommended to optimize nominal group resistance and to minimize pile installation problems associated with a center to center pile spacing of 2.5 diameters.

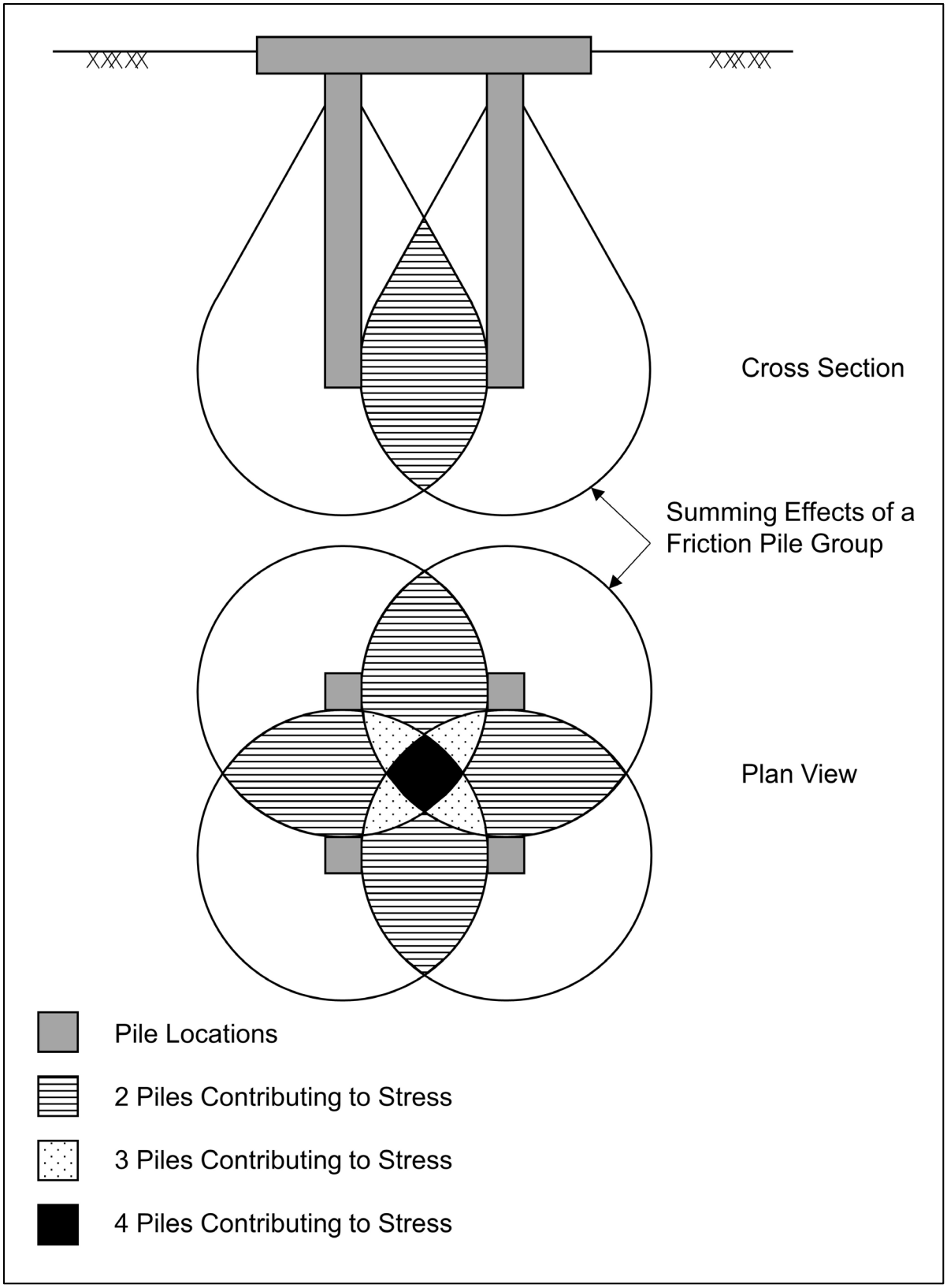

Figure 7-29 Overlap of stress zones for friction pile group (after Bowles 1988).

7.2.2.2 Pile Groups in Cohesive Soils

The nominal group resistance in cohesive soil is usually governed by the sum of the nominal resistance of the individual piles, with some reduction due to overlapping zones of shear deformation in the surrounding soil. AASHTO (2014) design specifications states that the group resistance is influenced by whether the pile cap is in firm contact with the ground. If the pile cap is in firm contact with the ground, the soil between the piles and the pile group act as a unit.

The following design recommendations are for estimating nominal group resistance in cohesive soils. The lesser value of the nominal group resistance, calculated from Steps 1 to 4, should be used.

1. For pile groups driven in clays with undrained shear strengths of less than 2 ksf and the pile cap not in firm contact with the ground, a group efficiency of 0.65 should be used for center to center pile spacing of 2.5 times the average pile diameter. If the center to center pile spacing is greater than 6 times the average pile diameter, then a group efficiency of 1.0 may be used. Linear interpolation should be used for intermediate center to center pile spacing.

2. For piles in clays with undrained shear strengths less than 2 ksf, and the pile cap in firm contact with the ground, a group efficiency of 1.0 may be used.

3. For pile groups in clays with undrained shear strength in excess of 2 ksf, a group efficiency of 1.0 may be used regardless of the pile cap - ground contact.

4. Calculate the nominal pile group resistance against block failure using the procedure described in Section 7.2.2.3.

5. Piles in cohesive soils should not be installed at center to center pile spacing less than 3 times the average pile diameter unless dictated otherwise by pile size, site constraints, pile cap requirements, and construction costs. The center to center pile spacing should also not be less than 3 feet.

It is important to note that the driving of pile groups in cohesive soils can generate large excess pore water pressures. This can result in short term (1 to 2 months after

installation) group efficiencies on the order of 0.4 to 0.8. As these excess pore pressures dissipate, the pile group efficiency will increase. Figure 7-30 presents observations on the dissipation of excess pore water pressure versus time for pile groups driven in cohesive soils. Depending upon the group size, the excess pressures typically dissipate within 1 to 2 months after driving. However, in very large groups, full pore pressure dissipation may take up to a year.

If a pile group will experience the full group load shortly after construction, the foundation designer must evaluate the reduced group resistance that may be available for load support. In these cases, piezometers should be installed to monitor pore pressure dissipation with time. Effective stress resistance calculations can then be used to determine if the increase in pile group resistance versus time during construction meets the load support requirements.

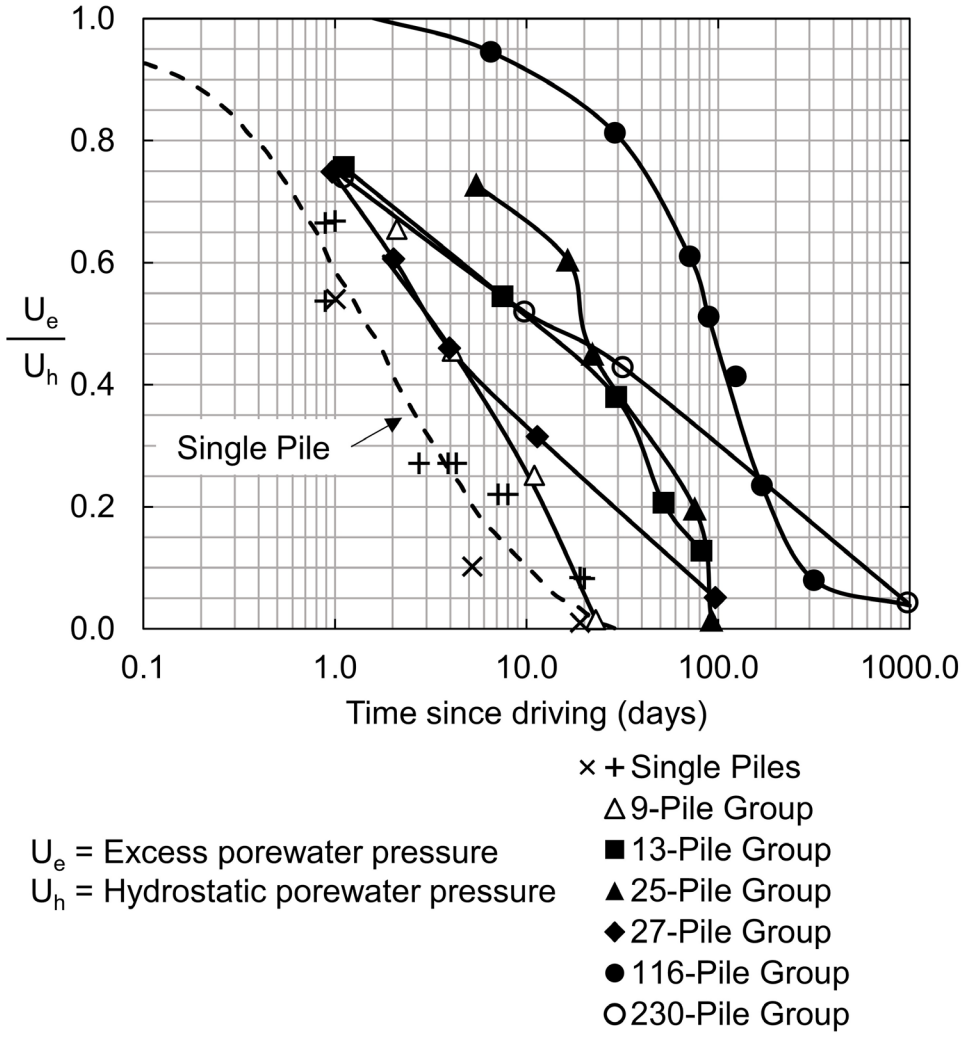

Figure 7-30 Measured dissipation of excess pore water pressure in soil surrounding full scale pile groups (after O'Neill 1983).

7.2.2.3 Block Failure of Pile Groups

Block failure of pile groups is generally only a design consideration for pile groups in soft cohesive soils or in cohesionless soils underlain by a weak cohesive layer. For a pile group in cohesive soil as shown in Figure 7-31 the nominal resistance of the pile group against a block failure is provided by the following expression:

$$R_{ng} = 2\mathrm{D}\ (\mathrm{B} + \mathrm{Z})s_{u1} + \mathrm{BZ}\ s_{u2}\ N_c \qquad \text{Eq. 7-36}$$

Where:

- R_{ng} = nominal resistance of the pile group.
- D = pile embedded length.
- B = width of pile group.
- Z = length of pile group.
- s_{u1} = weighted average of the undrained shear strength over the depth of pile embedment for the cohesive soils along the pile group perimeter.
- s_{u2} = average undrained shear strength of the cohesive soils at the base of the pile group to a depth of 2B below pile toe level.
- N_c = dimensionless bearing capacity factor.

If a pile group will experience the full group load shortly after construction, the nominal group resistance against block failure should be calculated using the remolded or reduced shear strength rather than the average undrained shear strength for s_{u1}.

The bearing capacity factor, N_c, for a rectangular pile group is generally 9. However, for pile groups with small pile embedment depths and/or large widths, N_c should be calculated from the following equation:

$$N_c = 5\left[1 + \frac{D}{5B}\right]\left[1 + \frac{B}{5Z}\right] \leq 9 \qquad \text{Eq. 7-37}$$

Where:

- N_c = dimensionless bearing capacity factor.
- D = pile embedded length.
- B = width of pile group.
- Z = length of pile group.

When evaluating possible block failure of pile groups in cohesionless soils underlain by a weak cohesive deposit, the weighted average unit shaft resistance for the cohesionless soils should be substituted for s_{u1} in calculating the nominal group resistance. The pile group base strength determined from the second part of the nominal group resistance equation should be calculated using the strength of the underlying weaker layer.

Additional guidance can be found in AASHTO (2014) Article 10.6.3.1.2d on the punching failure of a footing situated in a strong layer overlying a weak layer. The equivalent footing concept for the pile group can be used in conjunction with the spread footing guidance.

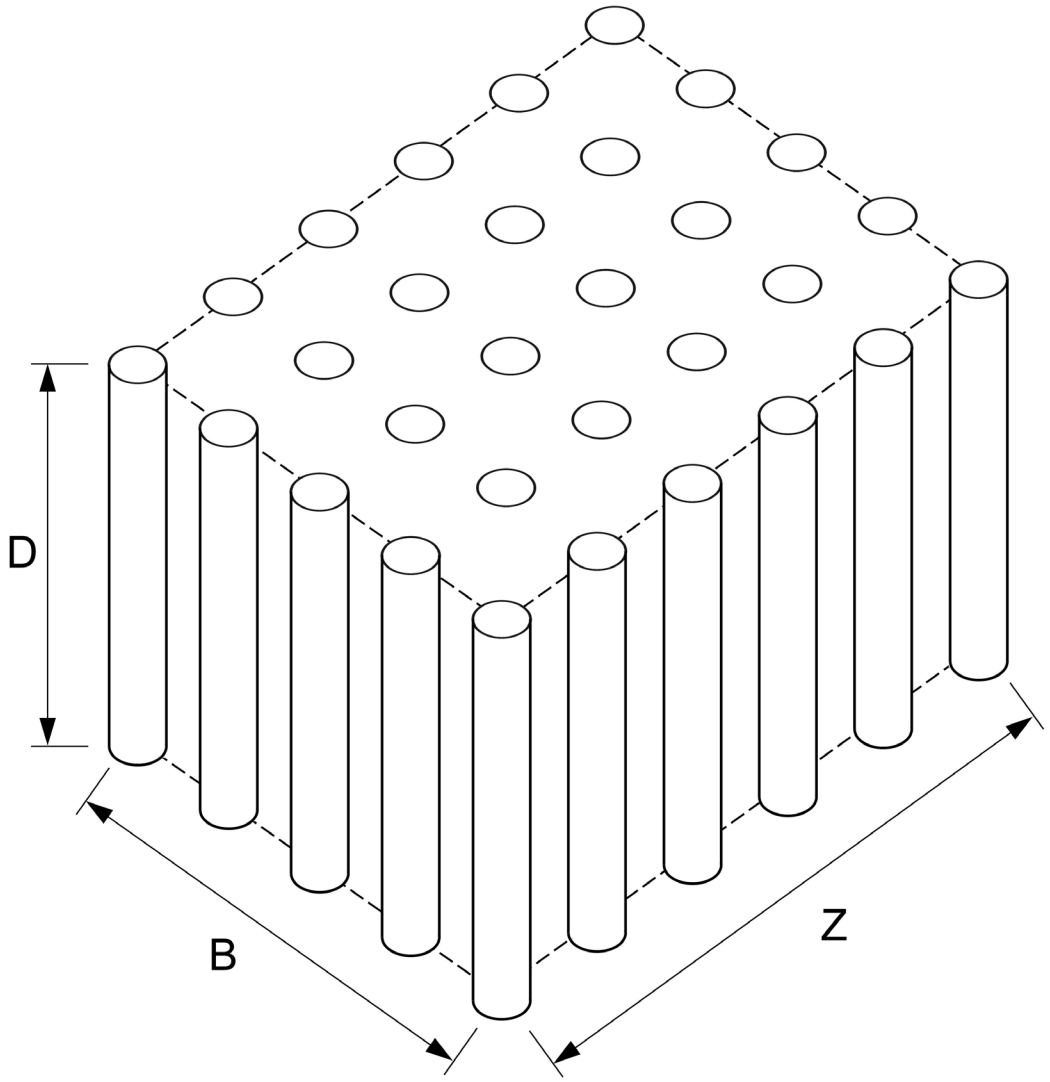

Figure 7-31 Three dimensional pile group configuration (after Tomlinson 1994).

7.2.3 Design for Axial Tension Resistance

The design of piles for axial tension or uplift loading conditions has become increasingly important for structures subject to seismic loading. In some cases, the uplift resistance determines the minimum pile penetration requirements. In those situations, axial tension load tests may be very cost effective as the higher resistance factor as a result of testing may reduce minimum pile penetration requirements and overall pile lengths. Tension load test procedures are described by Kyfor et al. (1992) in FHWA-SA-91-042 as well as in Chapter 9.

7.2.3.1 Axial Tension Resistance of Single Piles

De Nicola and Randolph (1993) note that in fine grained cohesive soils, where loading is assumed to occur under undrained conditions, the shaft resistance is generally considered equal in compression and in uplift.

In non-cohesive or free draining soils, the uplift resistance of a pile has been more controversial. De Nicola and Randolph (1993) state that it has been customary to assume that the shaft resistance in uplift is approximately 70% of the shaft resistance in compression. Based upon a finite difference parametric study, they concluded that a reduction in shaft resistance for uplift in free draining soils should be used, and that piles have lower uplift resistance than their compression shaft resistance. Conversely, the American Petroleum Institute's (1993) recommended design practice considers the pile shaft resistance to be equal in uplift and compression loading. Likewise, Altaee et al. (1992) presented a case of an instrumented pile in sand where the shaft resistance was approximately equal in compression and uplift when residual stresses were considered.

Tomlinson (1994) notes that the shaft resistance under cyclic loading is influenced by the rate of application of load as well as the degree of degradation of soil particles at the soil-pile interface. Under cyclic or sustained uplift loading in clays, the uplift resistance can decrease from the peak value to a residual value. In sands, particle degradation or reorientation can also result in decrease in uplift resistance under cyclic or sustained uplift loading. Therefore, the designer should consider what effect, if any, sustained or cyclic uplift loading will have on soil strength degradation.

Based on the above issues, the factored uplift resistance of a single pile should be taken as that of the nominal shaft resistance calculated from any of the AASHTO static analysis methods with a resistance factor for uplift, ϕ_{up}, from Table 7-1. From AASHTO (2014) Article C10.7.3.10, the uplift resistance factor from static analysis

methods is reduced to 80 percent of the resistance factor for static shaft resistance in compression. Therefore, the shaft resistance does not need to be further reduced for the uplift case.

Equation 7-38 is modified from the general static analysis equation to account for uplift. Selection of the factored uplift resistance should also consider the potential for soil strength degradation due to the duration or frequency of uplift loading, which may not be apparent in the short term static or dynamic test results.

$$R_r = \phi R_n = \phi_{up} R_s \qquad \text{Eq. 7-38}$$

Where:

R_r = factored resistance (Equation 7-3).
R_s = nominal shaft resistance (Equation 7-4).
ϕ_{up} = resistance factor for uplift analysis method per Table 7-1.

If a tension static load test is performed for design confirmation, a design uplift resistance factor of up to 0.60 may be used. Dynamic tests with signal matching can also be used to determine uplift resistance per AASHTO (2014) Article 10.7.3.10. Based on a dynamic test, an uplift resistance factor of up to 0.50 is recommended.

Figure 7-32 illustrates a design chart for uplift loading. The nominal resistance and nominal shaft resistance in the figure were calculated using the FHWA method (Nordlund / α-method) in APILE. The nominal shaft resistance has also been factored by 0.60 to yield the factored resistance in axial tension expected based on a static load test, 0.50 for a dynamic test with signal matching, and by 0.25 in the clay layers (α-method) and 0.35 (Nordlund Method) in the sand layers to yield the factored resistance in axial tension based solely on static analysis.

For a factored resistance in axial tension of 100 kips, the uplift design chart indicates estimated pile lengths of 72, 74, and 78 feet for a tension load test, dynamic test with signal matching, and static analysis. Hence, a static analysis may be the most cost effective approach for this factored load for a project with a limited number of piles. On the other hand, the uplift design chart indicates estimated pile lengths of 81, 84, and 112 feet for a factored uplift resistance of 200 kips based on a tension load test, dynamic test with signal matching, and static analysis. In this case, the pile length savings from either static load testing or dynamic testing may be economically justified.

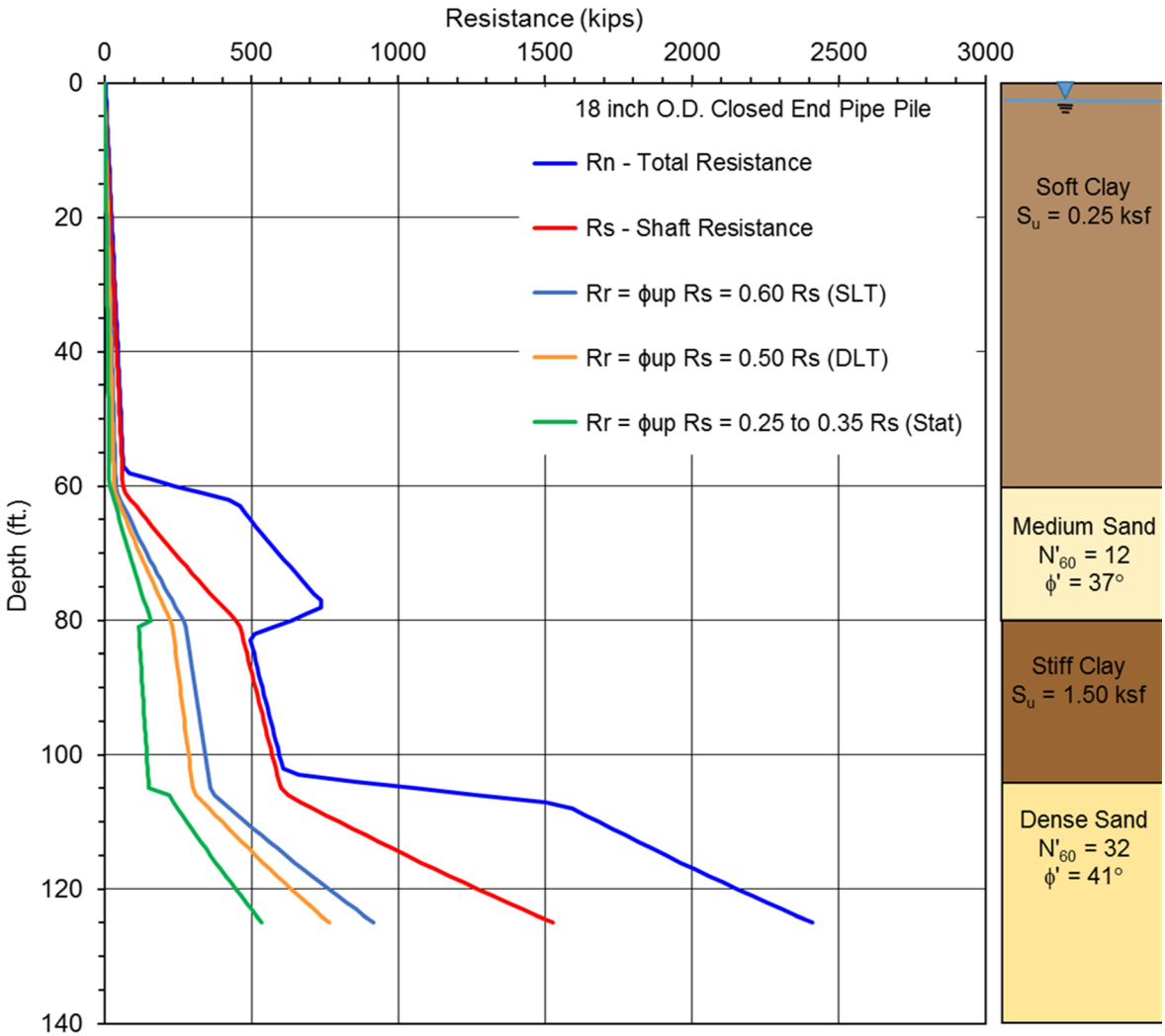

Figure 7-32 Design chart for nominal and factored resistance in axial tension.

7.2.3.2 Axial Tension Resistance of Pile Groups

Axial tension or uplift resistance of a pile group is often a significant factor in determining the minimum pile penetration requirements and in some cases can control the foundation design. A few common conditions where group uplift resistance may significantly influence the foundation design include cofferdam seals that create large buoyancy forces, cantilever segmental bridge construction, and seismic, vessel impact, or debris loading. When piles with uplift loads are driven to a relatively shallow bearing stratum, uplift resistance may control the foundation design. AASHTO (2014) specifications for group uplift resistance are considered relatively conservative, particularly in cohesionless soils.

AASHTO specifications (2014) limit uplift resistance of a pile group to the lesser of:

1. The sum of individual pile resistance in axial tension.

2. The resistance in axial tension of the pile group considered as a block.

Equation 7-39 is modified for factored uplift which considers the total resistance of a pile group. Meanwhile, the group uplift resistance is determined differently for cohesive and cohesionless soils, which is described in the following two sections.

$$R_r = \phi R_n = \phi_{ug} R_{ug} \qquad \text{Eq. 7-39}$$

Where:

R_r = factored resistance in axial tension (Eq. 7-4).
R_{ug} = nominal resistance in axial tension of the pile group.
ϕ_{ug} = resistance factor for axial tension, 0.50 per Table 7-1.

7.2.3.2.1 Axial Tension Resistance of Groups in Cohesionless Soils

In cohesionless soils, AASHTO (2014) Article 10.7.3.11 limits the nominal group resistance in axial tension to the lesser of two resistances. The first resistance is the sum of the individual pile nominal shaft resistance times the analysis method resistance factor for uplift, times the number of piles in the group. This is expressed in Equation 7-40.

$$R_r = \phi R_{ug} = \emptyset_{up} R_s n \qquad \text{Eq. 7-40}$$

Where:

R_{ug} = nominal resistance in axial tension of pile group.
R_s = nominal shaft resistance.
$\emptyset_{\mathrm{up}}$ = resistance factor for uplift analysis method per Table 7-1.
n = number of piles in group.

The second resistance is defined by the weight of soil contained with the pile group block depicted by Figure 7-33. This approach outlined by Tomlinson (1994), uses the effective weight of the block of soil extending upward from the pile toe level at a slope of 1H:4V. For simplicity in performing the calculation, the weights of the piles within the soil block are considered equal to the weight of the soil. The group uplift resistance is the lesser resistance determined from Equation 7-40 or Figure 7-33.

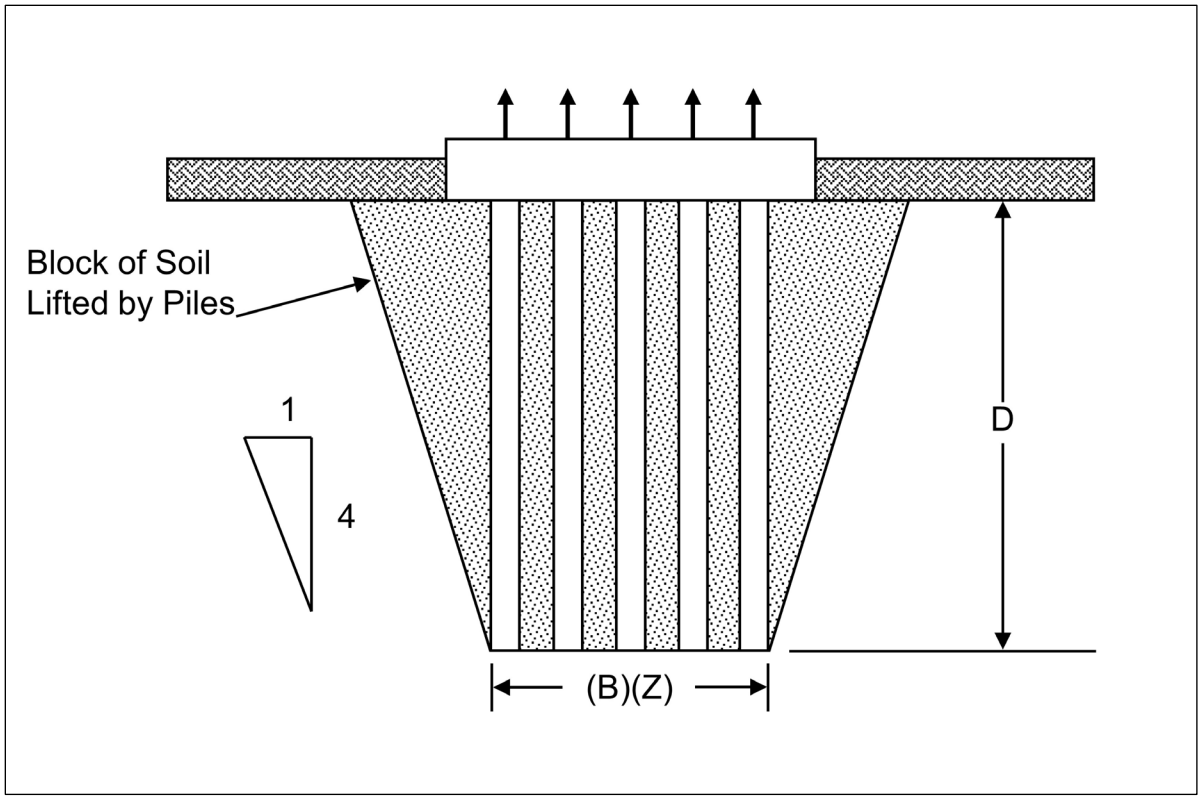

Figure 7-33 Uplift of pile group in cohesionless soil (after Tomlinson 1994).

7.2.3.2.2 Axial Tension Resistance of Groups in Cohesive Soils

Similarly in cohesive soils, AASHTO (2014) Article 10.7.3.11 limits the nominal group uplift resistance to the lesser of the resistance computed by Equation 7-40 or Equation 7-41. Figure 7-34 depicts the nominal group resistance provided by the soil weight contained within the pile group block and the soil shear resistance along the group perimeter, as should be used for Equation 7-41.

$$R_n = R_{ug} = 2\,\mathrm{D}\,(\mathrm{B}+\mathrm{Z})s_u + W_g \qquad \text{Eq. 7-41}$$

Where:

R_n = nominal resistance (kips).
R_{ug} = nominal resistance in axial tension of the pile group (kips).
D = pile embedded length (feet).
B = width of pile group (feet).
Z = length of pile group (feet).
s_u = weighted average of the undrained shear strength over the depth of pile embedment along the pile group perimeter (ksf).
W_g = effective weight of the pile/soil block including pile cap weight (kips).

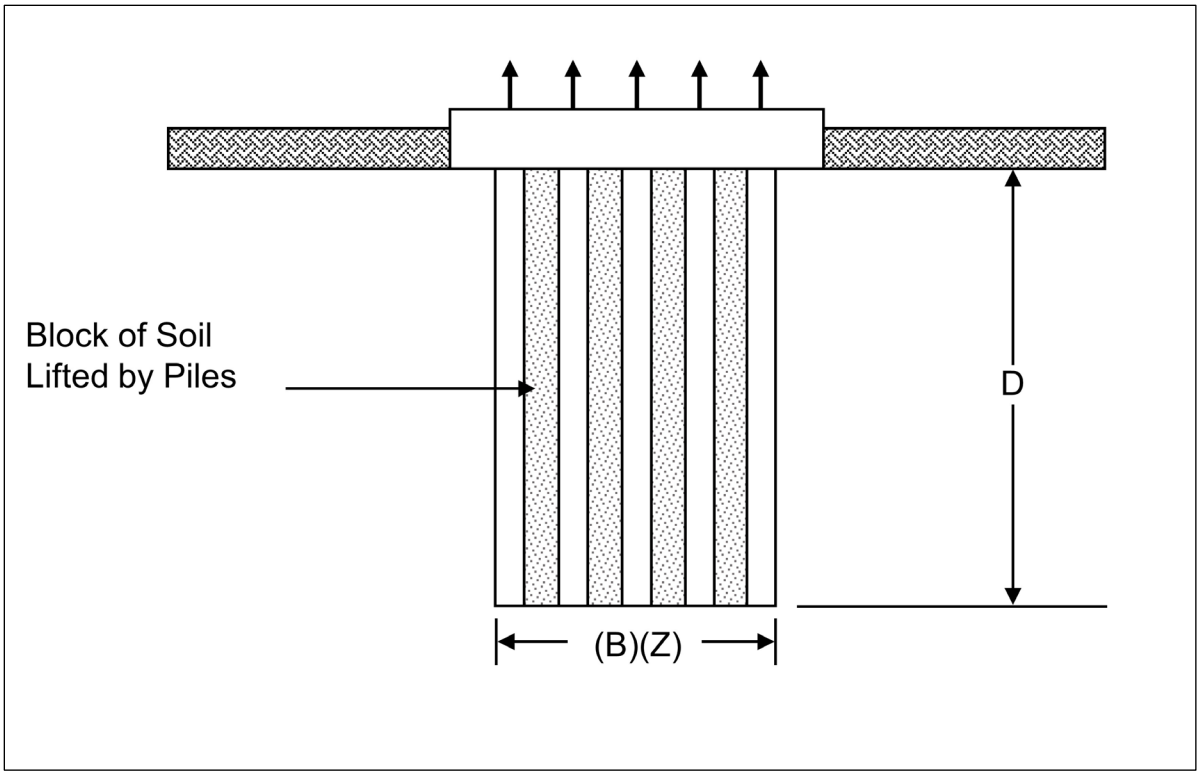

Figure 7-34 Uplift of pile group in cohesive soils (after Tomlinson 1994).

7.2.4 Nominal Axial Resistance Changes after Pile Driving

The surrounding soil is greatly disturbed when a pile is driven into it. As the soil surrounding the pile regains strength following the installation disturbance, a time dependent change in geotechnical resistance occurs. Frequently piles driven in saturated clays, and loose to medium dense silts or fine sands gain significant resistance after driving has been completed. This phenomenon is called soil setup. Occasionally piles driven into dense saturated fine sands, dense silts, or weak laminated rocks such as shale, will exhibit a decrease in resistance after the driving has been completed. This phenomenon is called relaxation. Case history discussions on soil setup and relaxation may be found in Fellenius et al. (1989), and Thompson and Thompson (1985), respectively.

7.2.4.1 Relaxation

The nominal resistance of driven piles can decrease with time following driving. This decrease in nominal resistance is known as relaxation. Relaxation has been observed in dense, saturated, fine grained soils such as non-cohesive silts and fine sands. In these cases, the driving process is believed to cause the dense soil near the pile toe to dilate (tendency for volume increase), thereby generating negative

pore pressures (suction). The negative pore pressures temporarily increase the effective stresses acting on the pile, resulting in a temporarily higher soil strength and driving resistance. When these pore pressures dissipate, the effective stresses acting on the pile decrease, as does the nominal resistance. Several cases of relaxation in silts and fine sands have been reported in the literature including Yang (1970), York et al. (1994), Morgano and White (2004), and Richardson (2011).

Relaxation in weak laminated rocks has also been reported. Thompson and Thompson (1985) attributed this to a release of locked in horizontal stresses. Rock formations reported in the literature to exhibit relaxation include shales; Thompson and Thompson (1985), Hussein et al. (1993), Morgano and White (2004); and phyllite, Seidel et al. (1992). However, relaxation is possible in other weak laminated rock formations such as mudstone, claystone, and siltstone among others.

Because the nominal resistance may decrease (relaxation) after the end of driving, nominal resistance assessments from static load testing or dynamic test restrikes should be made after equilibrium conditions in the soil have been re-established. In the absence of site specific pore pressure data from piezometers, it is suggested that static load testing or restriking of piles in dense silts and fine sands be delayed for a few days to a week after driving, or longer if possible. In relaxation prone shales, it is suggested that static load testing or restrike testing be delayed a minimum of ten days to two weeks after driving.

Published cases of the relaxation magnitude of various soil types are quite limited. However, data from Thompson and Thompson (1985) as well as Hussein et al. (1993) suggest relaxation factors for piles founded in some shales can range from 0.5 to 0.9. The relaxation factor is defined as the static load test failure load divided by the nominal resistance at the end of initial driving. Relaxation factors of 0.5 and 0.8 have also been observed in two cases where piles were founded in dense sands and extremely dense silts, respectively. The importance of evaluating time dependent decreases in nominal resistance for piles founded in these materials cannot be over emphasized. AASHTO (2014) Article 10.7.3.4.2 states that a restrike test should be done after a sufficient time for relaxation to develop if relaxation is possible in the soils at the site.

7.2.4.2 Soil Setup

When saturated cohesive soils are compressed and disturbed due to pile driving, large excess pore pressures develop. These excess pore pressures are generated partly from the shearing and remolding of the soil and partly from radial compression

as the pile displaces the soil. The excess pore pressures cause a reduction in the effective stresses acting on the pile, and a reduction in the soil shear strength. This results in a reduced nominal resistance during, and for a period of time after, driving.

After driving, the excess pore pressures will dissipate primarily through radial flow of the pore water away from the pile (Randolph et al. 1979). With the dissipation of pore pressures, the soil reconsolidates and increases in shear strength. This increase in soil shear strength results in an increase in the nominal resistance and is called soil setup. A similar decrease in resistance to pile penetration with subsequent soil setup may occur in loose to medium dense, saturated, fine grained sands or silts. The magnitude of the gain in nominal resistance depends on soil characteristics, pile material and pile dimensions.

Because the nominal resistance may increase after the end of driving, nominal resistance assessments should be made from static load tests, dynamic testing, or hammer restrike events performed after equilibrium conditions in the soil have been re-established. The time for the return of equilibrium conditions is highly variable and depends on soil type and degree of soil disturbance.

In research studies, piezometers installed within three diameters of the pile can be used to monitor pore pressure dissipation with time. Effective stress static nominal resistance calculations can be used to evaluate the increase in resistance with time once pore pressures are quantified.

To quantify the largest magnitude of soil setup, static load testing or restrike dynamic testing of piles in fine grained soils should be delayed until pore pressures dissipate and return to equilibrium. In the absence of site specific pore pressure data or local experience, it is preferable that static load testing or dynamic restrike tests of piles in clays and other predominantly fine grained soils be delayed for two weeks after driving or longer if possible. Unfortunately, delays of this magnitude to quantify or confirm the soil setup magnitude are not frequently feasible on most routine projects. Therefore, it is best to quantify the soil setup magnitude and time rate of setup in a design stage test program in high setup locales. The design stage program should include multiple restrike events on dynamic test piles and static load test(s) so that both the time rate of setup as well as the setup magnitude can be determined and later used for production driving where only shortened restrike intervals can be accommodated due to the construction schedule. In sandy silts and fine sands, pore pressures generally dissipate more rapidly. In these more granular deposits, three to seven days is often a sufficient time delay.

Hannigan et al. (2012) presented a case history multiple dynamic monitoring events on test piles were used to quantify the time dependent soil setup magnitude and its spatial variation for a four-level interchange project. Static load tests were also used to confirm the nearly five-fold increase in shaft resistance over time.

Several methods have been proposed to predict soil setup effects. A study by Skov and Denver (1988) looked at predicting the nominal resistance in cohesive and cohesionless soils sometime after initial driving based on initial driving measurements using Equation 7-42.

$$R_n = R_{no}\left(1 + A_1 \log\frac{t}{t_o}\right) \qquad \text{Eq. 7-42}$$

Where:

R_n = nominal resistance after time "t" of driving (kips).
R_{no} = initial nominal resistance at "t_o" of driving (kips).
A_1 = constant based on soil type and subsurface condition. (0.2 for sand and 0.6 for clay).
t = time after driving (days).
t_o = time after driving from which the increase in resistance is linear in logarithmic time (days) (typically 0.5 for sand, 1.0 for clay).

Komurka et al. (2003) summarized the state of the practice in estimating and measuring soil setup in a report to the Wisconsin Highway Research Program. This report summarizes the mechanisms associated with soil setup development and reviews several empirical relationships for estimating setup.

A study by Bullock et al. (2005) assessed five square prestressed concrete piles driven in various soils throughout Florida. Resistance was measured through initial drive and restrike dynamic testing followed by subsequent O-cell tests. For this, they expanded upon the Skov and Denver approach.

$$R_s = R_{so}\left[\left(\frac{m_s}{R_{so}}\right)\log\left(\frac{t}{t_0}\right) + 1\right] \qquad \text{Eq. 7-43}$$

Where:

R_s = shaft resistance after time "t" of driving (kips).
R_{so} = initial shaft resistance at "t_o" of driving (kips).
m_s = semilog-linear slope of R_s vs t from multiple restrike tests.
t = time after driving (days).
t_o = time of driving (days) (1 day for all tests).

Ng (2011) investigated soil setup on steel HP 10x42 piles driven into cohesive soils throughout Iowa. Initial drive and restrike dynamic testing was performed to assess time dependent resistance changes. This dissertation was presented in SI units, therefore the pore water dissipation factor, C_h, should be determined first using Equation 7-44, and then converted to English units for inclusion in Equation 7-45.

$$C_h = \frac{3.179}{N^{2.08}} \quad (\text{cm}^2/\text{min}) \qquad \text{Eq. 7-44}$$

In which:

$$\frac{R_s}{R_{so}} = \left[\left(\frac{f_c\, C_h}{N_a r_p{}^2} + f_r\right) \log\frac{t}{t_o} + 1\right] \frac{L_t}{L_o} \qquad \text{Eq. 7-45}$$

Where:

- R_s = shaft resistance after time "t" of driving (kips).
- R_{so} = initial shaft resistance at "t_o" of driving (kips).
- f_c = consolidation factor (non-dimensional regression factor).
- C_h = pore water pressure dissipation factor (in^2/min for Equation 7-45).
- N_a = average SPT N-Value over pile length.
- N = SPT N-Value.
- r_p = equivalent pile radius (inches).
- f_r = remolding recovery rate (non-dimensional regression factor).
- L_t = embedded pile length at time "t" after initial driving (feet).
- L_o = embedded pile length at the time of initial driving (feet).
- t = time after initial driving (days).
- t_o = time of driving (days) (0.00694 days for all tests).

Another recent study comparing the nominal resistance from initial drive and restrike dynamic testing was performed by Reddy and Stuedlein (2014). They reviewed data from 76 piles in the Puget Sound Lowlands of Oregon, with restrikes varying from 5 to 310 hours. Both closed (CEP) and open end (OEP) steel pipe piles, as well as prestressed concrete piles (PSC) were utilized. The setup prediction model developed followed a hyperbolic curve and is presented as Equation 7-46.

$$R_s = \frac{R_{so}\, A_2\, \log\left(\frac{t}{t_o}\right)}{k_1 + k_2\, R_{so}\, A_2\, \log\left(\frac{t}{t_o}\right)} + R_{so} \qquad \text{Eq. 7-46}$$

Where:

R_s = shaft resistance after time "t" of driving (kips).
R_{so} = initial shaft resistance at "t_o" of driving (kips).
A_2 = constant based on pile type (1.72 for PSC piles, 0.70 for CEP, and 0.77 for OEP).
t = time after driving (hours).
t_o = time of driving (hours) (1 hour for all tests).
k_1 = regression factor (0.17 for PSC, 0.12 for CEP and 0.15 for OEP).
k_2 = regression factor (0.00044 for PSC piles, 0.00078 for CEP, and 0.00060 for OEP).

For the studies presented above, specific contributing factors were explored (i.e. regional soil, pile type, etc.). Therefore, these predictive methods may not translate to other areas with different conditions unless modified by local correlation experience. However, many of these studies provide a suggested approach for agencies to generate a database of tested piles with initial driving, restrike testing and static load tests are available to better assess the time dependent changes.

Limited information is available regarding soil setup in unsaturated soils. However, it is anticipated that setup would occur in these deposits.

Rausche et al. (1996) calculated general soil setup factors based on the predominant soil type along the pile shaft. The soil setup factor was defined as the static load test failure load divided by the end-of-drive wave equation resistance. These results are presented in Table 7-16. The database for this study was comprised of 99 test piles from 46 sites. The number of sites and the percentage of the database in a given soil condition is included in the table. While these soil setup factors may be useful for preliminary estimates, soil setup is better estimated based on site specific data gathered from pile restriking, dynamic measurements, static load testing, and local experience.

Table 7-16 Soil Setup Factors (after Rausche et al. 1996)

Predominant Soil Type Along Pile Shaft	Range in Soil Setup Factor	Recommended Soil Setup Factors*	Number of Sites and (Percentage of Database)
Clay	1.2 - 5.5	2.0	7 (15%)
Silt - Clay	1.0 - 2.0	1.0	10 (22%)
Silt	1.5 - 5.0	1.5	2 (4%)
Sand - Clay	1.0 - 6.0	1.5	13 (28%)
Sand - Silt	1.2 - 2.0	1.2	8 (18%)
Fine Sand	1.2 - 2.0	1.2	2 (4%)
Sand	0.8 - 2.0	1.0	3 (7%)
Sand - Gravel	1.2 - 2.0	1.0	1 (2%)

* Confirmation with Local Experience Recommended.

7.2.4.2.1 Estimation of Pore Pressures During Driving

According to Lo and Stermac (1965), the maximum pore pressure induced from pile driving may be estimated from the following equation.

$$\Delta_{\mathrm{um}} = \left[(1 - K_o) + \left(\frac{\Delta \mathrm{u}}{\sigma'_{\mathrm{v}}}\right)_m\right]\sigma'_{vi} \qquad \text{Eq. 7-47}$$

Where:

Δ_{um} = maximum excess pore pressure (ksf).
K_o = at rest earth pressure coefficient.
σ'_{vi} = initial vertical effective stress prior to pile driving (ksf).
$(\Delta \mathrm{u}/\ \sigma'_{\mathrm{vo}})_{\mathrm{m}}$ = maximum value of the pore pressure ratio, $\Delta u/\sigma'_{vo}$, measured in a CU triaxial test with pore pressure measurements.

Ismael and Klym (1979) presented a case history where the above procedure was used. They reported good agreement between measured excess pore pressures with estimates from the Lo and Stermac procedure.

Poulus and Davis (1980) summarized measurements of excess pore pressures due to pile driving from several case histories. In this compilation, the reported excess pore pressure measurements divided by the vertical effective stress were plotted versus the radial distance from the pile surface divided by the pile radius. These

results are presented in Figure 7-35 and indicate that the excess pore pressure at the pile-soil interface can approach 1.4 to 1.9 times the vertical effective stress, depending upon the clay sensitivity.

The foundation designer should evaluate the potential change in nominal resistance with time. Once pore pressures are measured or estimated, effective stress static resistance calculation methods can be used to quantify the probable change in nominal resistance with time.

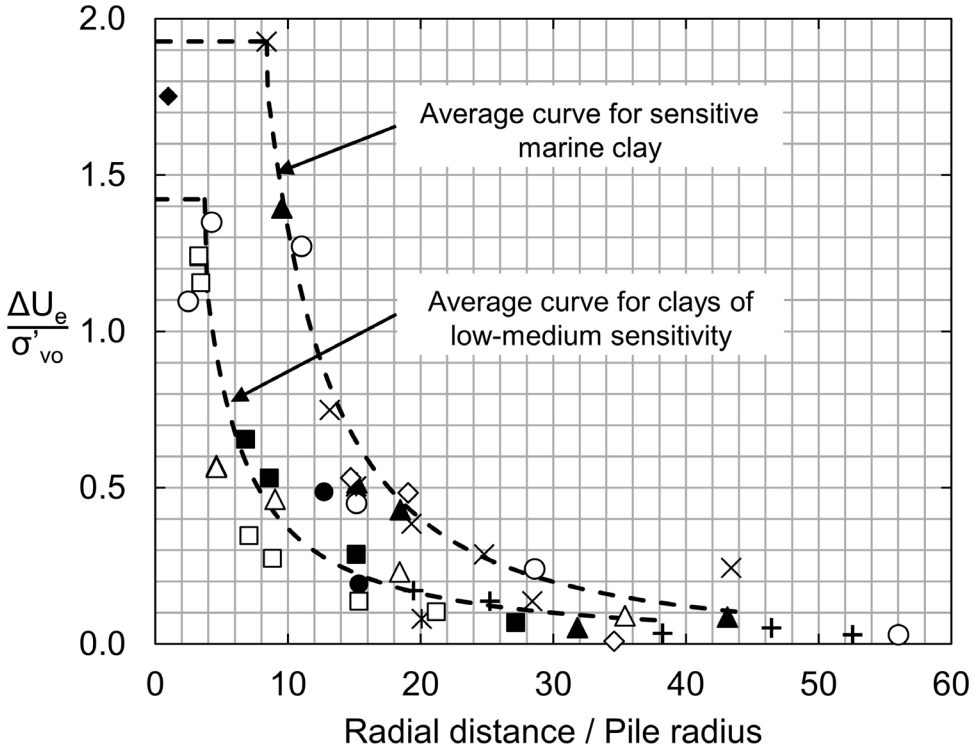

Figure 7-35 Excess pore water pressure due to pile driving (after Poulos and Davis 1980).

7.2.4.3 Implementation of Time Effects During Construction

As discussed above in the relaxation and soil setup sections, changes in nominal resistance occur after driving. These are permanent physical changes to the nominal resistance. Significant cost savings can be achieved when soil setup is effectively used. Many state transportation agencies are aware of soil setup effects, and as mentioned in Komurka et al. (2003), if setup effects could be predicted in the design phase, it may be possible to reduce pile lengths, reduce pile sections (use smaller-diameter or thinner-wall pipe piles, or smaller-section H-piles), or reduce the size of driving equipment (use smaller hammers and/or cranes).

Conversely, relaxation effects have been studied to a lesser degree, and in areas with known weathered shale or weak laminated bedrock, initial drive and restrike dynamic testing can prove useful to evaluate the extent of resistance loss (Long and Anderson 2014). Potentially problematic pile installations can be avoided when relaxation is identified early on and modified construction procedures adopted.

7.2.5 Nominal Lateral Resistance

In addition to axial compression and uplift loads, piles are routinely subjected to lateral loads. Potential sources of lateral loads on bridge structures include vehicle acceleration and braking forces, wind loads, wave and current forces, debris loading, ice forces, vessel impact loads, construction procedures, thermal expansion and contraction, earth pressures on the back of abutment walls, slope movements, and seismic events. These lateral loads can be of the same magnitude as axial compression loads and therefore warrant careful consideration during design.

AASHTO (2014) Article 10.7.3.12 addresses the nominal resistance of piles subjected to lateral loads. For a long pile, the nominal lateral resistance is controlled by the strength of the pile material since the pile will fail structurally before soil failure occurs along the entire pile length. The nominal lateral resistance of a short pile, defined as a pile with insufficient embedment to prevent toe rotation, is controlled by the soil. While short and rigid piles with very large lateral loads are relatively uncommon in practice, when encountered, they should be further evaluated in a p-y analysis considering both the properties of the geomaterials and the pile's structural resistance. The p-y method is described in detail in Section 7.3.7.3.

AASHTO (2014) notes that the strength limit state for nominal lateral resistance is, in most cases, only structural for the reasons described above. Chapter 8 provides guidance on structural limit states. The foundation deformation under lateral loading must also be within the established performance criterion for the structure. Section 7.3.7 discusses horizontal pile deflection under the service limit state.

7.2.6 Pile Length Estimates for Contract Documents

Pile length estimates and contract pile quantities should be carefully established using a combination of the site subsurface information, static analysis methods, and preconstruction test pile programs. Sometimes, pile length estimates can be determined from an obvious bearing layer. In other cases, construction control or static analysis methods may be relied upon, but the potential bias in either method

should be considered. Local pile driving experience should also be reviewed when determining the pile length estimates.

Minimum pile penetration requirements for effects of uplift, settlement, scour, lateral deflection, or downdrag should also factor into the contract pile length estimates. In cases where the depth of penetration required to achieve the nominal resistance in axial compression is less than the depth to satisfy these strength, service or extreme limit state requirements, the minimum pile penetration required to satisfy all limit state requirements should be used for contract pile quantities. The contract documents should also explicitly note the minimum pile penetration depth and the required nominal resistance below that depth during driving, R_{ndr}, to avoid construction control problems if the required nominal resistance is achieved above the minimum pile penetration depth. It is important to note that a minimum pile penetration depth is not always required and that the estimated length may be all that is necessary for contract documents.

7.2.7 Groundwater Effects and Buoyancy

The nominal resistance in axial compression and tension as well as the lateral resistance can be influenced by groundwater elevation changes and the resulting change in vertical effective stress. Groundwater elevation changes can be influenced by droughts, regional construction events such as construction of tunnels, or by local site events such as excavation dewatering. Events which cause temporary lowering of the groundwater elevation increases vertical effective stresses and thus the effective stress acting on the pile. Hence, a pile driven for the required nominal resistance in a temporarily lowered groundwater condition will have a nominal resistance less than required when the groundwater returns to its normal elevation.

Buoyant forces should also be considered in driven pile foundation design. A closed-end pipe pile driven through soft soils to rock or a hard bearing layer may need a thicker wall section or other measures to counter-act buoyancy effects. In this situation, buoyancy effects can raise a sealed closed-end pile from the bearing layer if the shaft resistance alone is insufficient to resist buoyancy forces.

7.2.8 Site Dewatering

When a site is dewatered during construction, a temporary increase in effective stresses will occur. This causes a corresponding temporary increase in soil shear strength that will result in piles driven in a dewatered site to develop a greater

resistance at a shallower pile penetration depth as compared to the non-dewatered condition. The soil resistance to be overcome to reach a specified penetration depth will also be greater than in the non-dewatered condition. If not considered in the design stage, the selected pile type may not be drivable to the required penetration depth in the dewatered construction condition. When dewatering is terminated, the effective stresses acting on the pile will decrease as the water table rises. This will result in a decrease in the soil shear strength and a decrease in long term nominal resistance. Hence piles driven to the nominal resistance in the dewatered condition would have less than the required nominal resistance once dewatering is terminated.

For projects where significant dewatering is required, the effects of the dewatering on nominal resistance and pile drivability should be evaluated. In these cases, multiple static analyses should be performed to determine the nominal resistance and drivability requirements under the short term dewatered condition, as well as the long term nominal resistance after dewatering has been terminated.

Dewatering can also have negative impacts on nearby structures supported on deep and shallow foundations. The increase in effective stress can cause or increase drag force on deep foundations or cause consolidation settlements that affect the performance of deep and shallow foundations systems. The potential dewatering effects on adjacent structures should be evaluated during the design phase.

7.2.8.1 Artesian Conditions

Artesian conditions develop where a permeable soil layer or aquifer is confined by two impermeable layers and the permeable soil layer outcrops at an elevation higher than where it is encountered in-situ. In this situation the effective stresses acting on the pile are directly related to the head of water. Artesian conditions can result in lower than expected nominal resistance in the soil layer as well as potential vertical groundwater migration issues along the pile-soil interface. Harris et al. (2003) describe a driven pile case history where the back calculated effective stress design parameters from a static load test program where significantly lower than expected due to artesian conditions. A detailed subsurface exploration program can aid in identifying artesian conditions. Nominal resistances that require pile lengths that punch through confining layers should be avoided in design. Artesian conditions should be noted on foundation plans to reduce the risk of construction problems.

7.2.9 Scour

Scour is defined as the erosion of soil and rock materials from the streambed and/or stream banks due to flowing water. Foundations subject to scour require input from all disciplines; hydraulics, structures, geotechnical, and construction. Multidiscipline input and communications are required to achieve the most cost effective design.

Though often considered as being localized, scour may consist of multiple components including long term aggradation and degradation, local scour, and contraction scour. Aggradation and degradation involve the long term streambed elevation changes due to an abundance or deficit, respectively, in upstream sediment supply. Local scour involves the removal of material from the immediate vicinity of a substructure unit and can be either clear-water (free of disturbed upstream sediment), or live-bed scour, complicated by the transport of upstream sediment into the scour hole following the storm event. In contrast, contraction scour occurs due to a constriction of the flow and involves erosion across all or most of the channel width and relates directly with the stream stratigraphy at the scour location. Contraction scour may be cyclic and or relate to the passing of a flood.

Different materials, subject to any of the above mentioned types of scour, erode at different rates. In a flood event, loose granular soils can be eroded away in a few hours. Cohesive or cemented soils typically erode more gradually and over several cycles of flooding but can experience the same nominal scour depths as those of cohesionless deposits. As noted earlier in this chapter, the nominal resistance of a driven pile is due to soil resistance along the pile shaft and at the pile toe. Therefore, the erosion of the soil materials providing pile support can have significant detrimental effects on nominal resistance and must clearly be evaluated during the design stage.

Depending on the type of scour and the scour susceptibility of the streambed soils, multiple static resistance calculations may be required to evaluate the nominal resistance of a pile and to establish minimum pile penetration requirements. In the case of local scour, the soil in the scour zone provides resistance at the time of driving that cannot be counted on for long term support. Hence, shaft resistance in the scour zone, although included for drivability considerations, is ignored for design purposes. However, because the erosion is localized, nominal resistance calculations should assume that the vertical effective stress is unchanged. The effects of non-localized scour on long term pile resistance are more severe. In all of degradation, contraction scour, and general scour, a reduction in both the scour zone soil resistance and the vertical effective stress is applied to long term

resistance calculations, due to the widespread removal of the streambed materials. This added reduction in effective stresses can have a significant effect on the calculated shaft and toe resistances. Figure 7-36 provides an illustration of localized and non-localized scour. Table 7-17 presents HEC-18 recommended minimum scour design flood frequencies and scour design check flood frequencies as a function of the hydraulic design flood frequencies.

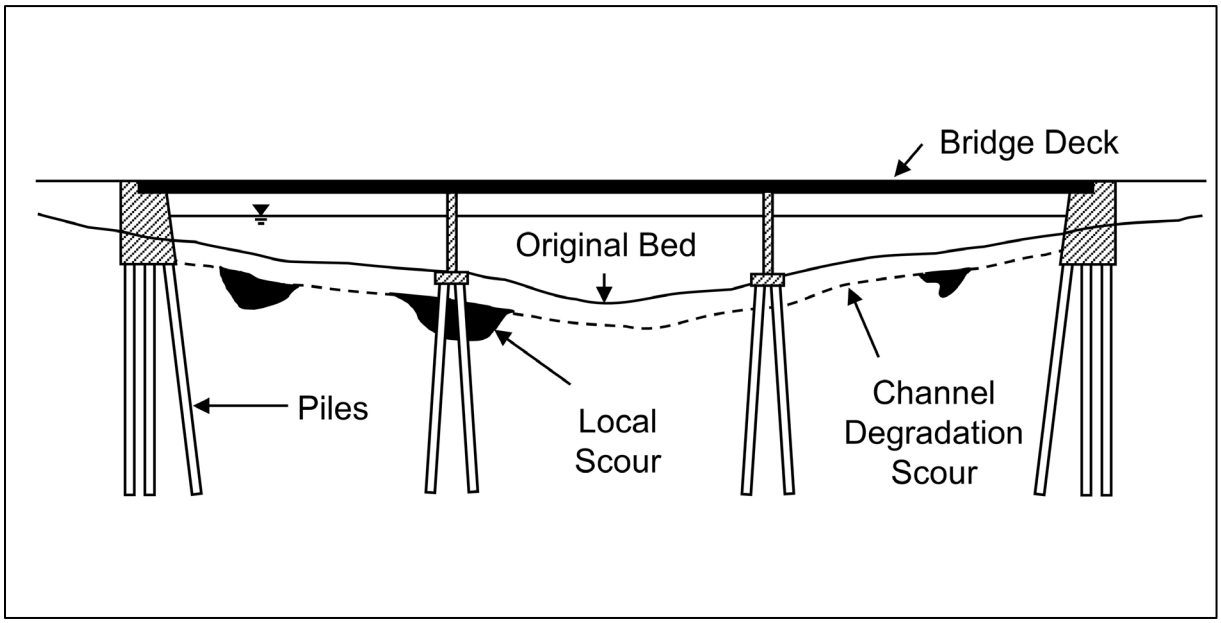

Figure 7-36 Local and channel degradation scour.

Table 7-17 Hydraulic Design, Scour Design, and Scour Design Check Flood Frequencies per HEC-18 (after Arneson et al. 2012)

Hydraulic Design Flood Frequency, Q_D	Scour Design Flood Frequency, Q_S	Scour Design Check Flood Frequency, Q_C
Q_{10}	Q_{25}	Q_{50}
Q_{25}	Q_{50}	Q_{100}
Q_{50}	Q_{100}	Q_{200}
Q_{100}	Q_{200}	Q_{500}

The FHWA publication FHWA HIF-12-003, “Evaluating Scour at Bridges” by Arneson et al. (2012) more commonly known as HEC-18, recommends that the following pile design issues also be considered at bridge sites subject to scour.

1. For pile supported substructures subjected to scour, a reevaluation of the foundation design may require a change in the pile length, number, cross-sectional dimension and type based on the loading and performance requirements and site-specific conditions.

2. Piling should be designed for additional lateral restraint and column action because of the increase in unsupported pile length after scour. The unsupported pile length is discussed in Chapter 8.

3. Local scour holes at piers and abutments may overlap one another in some instances. If local scour holes do overlap, the scour is indeterminate and may be deeper. The top width of a local scour hole on each side of the pier ranges from 1.0 to 2.8 times the depth of local scour. A top width value of 2.0 times the depth of local scour on each side of a pier is recommended.

4. Perform the bridge foundation analysis on the basis that all streambed material in the scour prism above the total scour line has been removed and is not available for nominal resistance or lateral support. In areas where the local scour is confined to the proximity of the footing, the lateral ground stresses on the pile length which remains embedded may not be significantly reduced from the pre-local scour conditions.

5. Placing the top of the footing or pile cap below the streambed a depth equal to the estimated long term degradation and contraction scour depth will minimize obstruction to flood flows and resulting local scour. Even lower footing elevations may be desirable for pile supported footings when the piles could be damaged by erosion and corrosion from exposure to river or tidal currents. However, in deep water situations, it may be more cost effective to situate the pile cap above the mudline and design the foundation accordingly.

6. Stub abutments positioned in the embankment should be founded on piling driven below the elevation of the thalweg including long term degradation and contraction scour in the bridge waterway to assure structural integrity in the event the thalweg shifts and the bed material around the piling scours to the thalweg elevation.

AASHTO (2014) Article 10.7.3.6 notes that scour effects must be considered in determining the minimum pile embedment depth and the required nominal driving resistance, R_{ndr}. The pile penetration depth after the design scour event must satisfy the required nominal resistance for axial and lateral loading. Therefore, the piles need to be driven to the required nominal resistance plus the shaft resistance lost due to scour. The shaft resistance in the scour zone should be calculated using the same static analysis procedure used for design except the scour zone resistance should not be included in the long term nominal resistance. The bias of the static analysis method should also be considered.

If restrike dynamic measurements with signal matching are performed during construction, the shaft resistance in the scour zone materials can be determined and that resistance subtracted from the nominal resistance. The material below the scour elevation must provide the required nominal resistance after the scour event.

7.2.10 Downdrag

Downdrag is ground settlement, or downward soil movement, relative to a pile. Current AASHTO (2014) guidance treats downdrag and the resulting drag force as an additional load that must be supported by the pile foundation. Therefore, downdrag is addressed in AASHTO under the geotechnical strength limit state. The AASHTO approach has generally been conservative in practice as there have been relatively few transportation structures where drag forces have been problematic and corrective action required. However, a design procedure that addresses the effects of downdrag in the geotechnical service limit state and in the pile structural strength limit state is preferred to the current AASHTO geotechnical strength limit state approach. The recommended design approach for downdrag is presented under the service limit state in Section 7.3.6.1.

7.3 SERVICE LIMIT STATES

Service limit states for foundations include settlement, lateral movement, overall stability and scour at the design flood. Foundation movement should be limited to structural tolerances for both the total and differential deformations. As mentioned in AASHTO (2014), the economics of limiting settlement, rotation and horizontal movements should be compared with the cost of designing the respective superstructure to tolerate such movement. This includes maintenance of either structural or roadway elements. Deformations should be computed assuming scour will occur at the design flood.

The service limit state provides limits on stress, deformation, and cracking under regular service conditions. Service limit state geotechnical considerations in driven pile foundation designs include:

- vertical deformation – settlement,
- horizontal movements,
- rotation,
- overall stability, and
- deformations due to scour at the design flood (100 year event).

Settlements should be determined using the Service I Load combination which includes normal operational factors only. If the pile foundation is supported in or on cohesive deposits subject to time dependent consolidation settlement, transient loads may be excluded from the settlement analysis. Settlement methods are covered in Section 7.3.5.

Load combinations for all applicable service limit states should be evaluated for horizontal movement and foundation rotation. Horizontal movement is measured at the foundation top, and should be within structural limits based on column length and stiffness. Sufficient geotechnical resistance and structural stiffness to resist shear and overturning loads should be checked during design. Lateral loading from the structure or earthen elements is covered in Section 7.3.7. Rotational movement is likewise measured at the foundation top and should be restricted.

Service limit state considerations are further discussed in AASHTO (2014) Articles 10.5.2.1 through 10.5.2.4 and associated commentary. All applicable service limit state load combinations must be evaluated.

7.3.1 Tolerable Vertical Deformations and Angular Distortion

Tolerable deformations are limited by the structure type and function, design service life, and anticipated performance at respective displacement levels. Vertical, horizontal, and rotational displacements should be considered during design, where tolerable movement criteria shall be established by empirical procedures, structural analysis, or both (AASHTO 2014).

Agencies often limit tolerable vertical deformations to restrictive values such as 1 inch or less without a rational basis. While there are no technical reasons to set arbitrary deformation limits, there are practical reasons for limits such as the deformation tolerances of attached structures and utilities. Drainage, ride quality, and safety are additional considerations in evaluating the deformation magnitude that can be tolerated by the design.

Moulton (1985) performed a detailed study of 314 bridges to develop a tolerable movement criterion for highway bridges. He recommended limiting values of angular distortion for multi-span and simple span structures. Angular distortion is illustrated in Figure 7-37, and is defined by the differential settlement of the foundation, S_d, relative to the span length, L_s. Both the differential settlement and span length should be expressed in the same units. The tolerable movement criteria recommend by Moulton and illustrated in SHRP 2 Project R19B is presented in Table 7-18. Moulton also recommended that lateral deformations be limited to 1.5 inches for all structures.

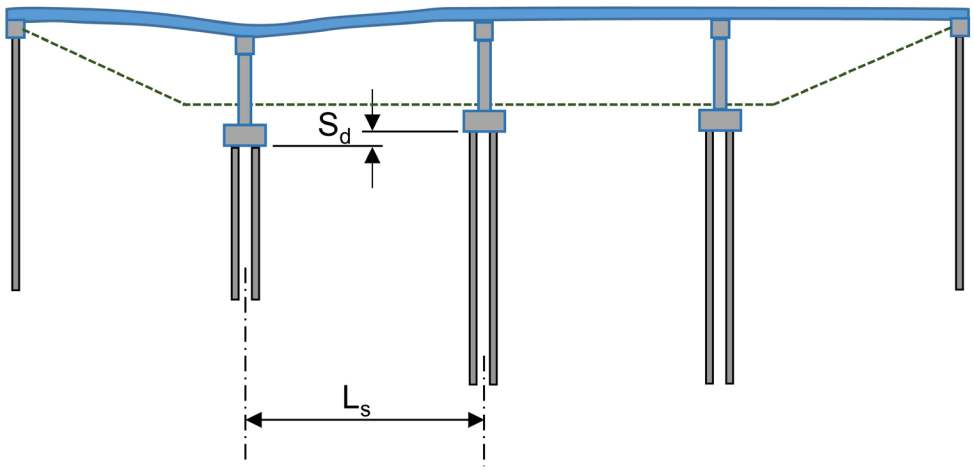

Angular Distortion, $A_d = S_d / L_s$

Figure 7-37 Angular distortion due to non-uniform bridge settlement.

Table 7-18 Tolerable Movement Criteria for Bridges

Type of Bridge	Limiting Angular Distortion, S_d/L_s (radians)
Multi-span bridges	0.004
Simple-span bridges	0.005

Note the limiting angular distortion criterion was developed for tolerable bridge movements in the longitudinal direction and should not be used for tolerable bridge movements in the transverse direction.

7.3.1.1 Load Factor for Vertical Deformations

AASHTO (2014) specifications include a load factor for vertical deformations or settlement, γ_{SE}, which is to be considered on a project-specific basis. AASHTO specifications currently recommend a value of 1.0 for this load factor in lieu of project-specific information to the contrary. This load factor is used to assess force effects from settlement on the structural design such as the generation of secondary moments within a given span due to settlement of a substructure support. For example, a settlement load factor of 1.25 does not indicate the computed settlements from a given method should be multiplied by 25% to limit the probability of exceeding tolerable settlements. Rather, the settlement load factor is applied to the limit state load combinations to determine the settlement effects on service and strength limit states. A research effort is in progress to develop additional guidance on application and use of the γ_{SE} load factor.

7.3.2 S-0 Concept for Vertical Deformations

Due to the variability of subsurface conditions, the vertical deformation that occurs at each substructure location will generally vary. In addition, the predicted deformation and actual deformation will differ. Therefore, a bridge structure should be designed to accommodate a realistic value of differential settlement and angular distortion in the longitudinal direction using the S-0 concept proposed by Duncan and Tan (1991). The key points of this method are as follows:

1. The actual settlement of a substructure unit can be as large as the value calculated by a given method.

2. The actual settlement of an adjacent substructure unit can be zero instead of the value calculated using the same method.

The maximum differential settlement between two adjacent foundations using this approach is therefore the maximum total settlement calculated for either foundation unit supporting the span. The maximum angular distortion is then the maximum total settlement divided by the span length. These values represent the design differential settlement, DS_d, and the design angular distortion, *DA*, respectively.

Figure 7-38 illustrates the computed settlement and associated computed angular distortion for a four span bridge supported by two abutments and three piers. The design differential settlement and design angular distortion using the S-0 concept are illustrated in Figure 7-39.

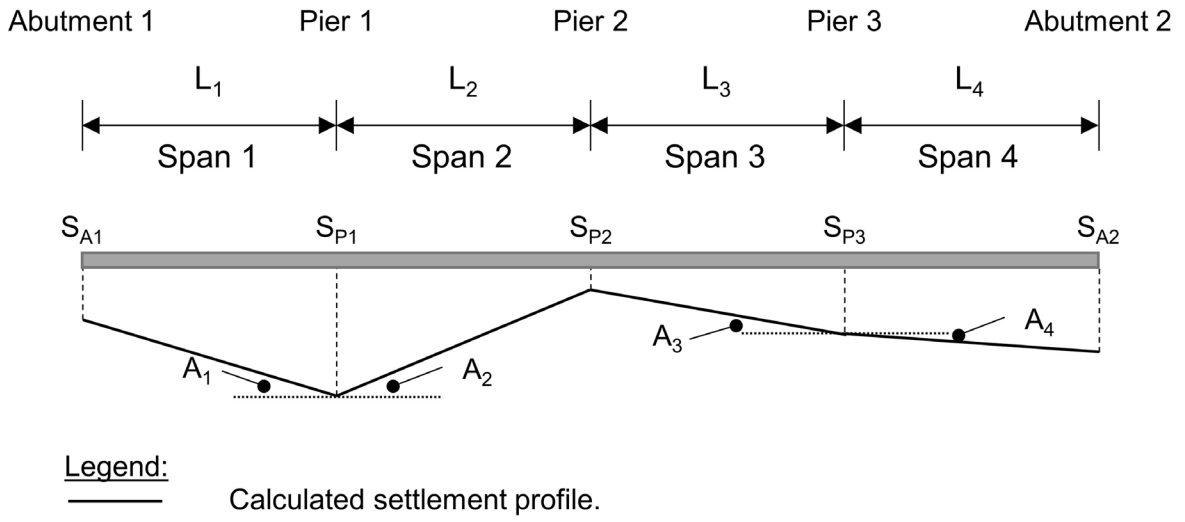

Support Element	Settlement, S
Abutment 1	S_{A1}
Pier 1	S_{P1}
Pier 2	S_{P2}
Pier 3	S_{P3}
Abutment 2	S_{A2}

Span	Differential Settlement	Angular Distortion, A
1	$\lvert S_{A1} - S_{P1} \rvert$	$A = \lvert S_{A1} - S_{P1} \rvert / L_1$
2	$\lvert S_{P1} - S_{P2} \rvert$	$A = \lvert S_{P1} - S_{P2} \rvert / L_2$
3	$\lvert S_{P2} - S_{P3} \rvert$	$A = \lvert S_{P2} - S_{P3} \rvert / L_3$
4	$\lvert S_{P3} - S_{A2} \rvert$	$A = \lvert S_{P3} - S_{A2} \rvert / L_4$

Figure 7-38 Example settlement and angular distortion profile (after Modjeski and Masters 2015).

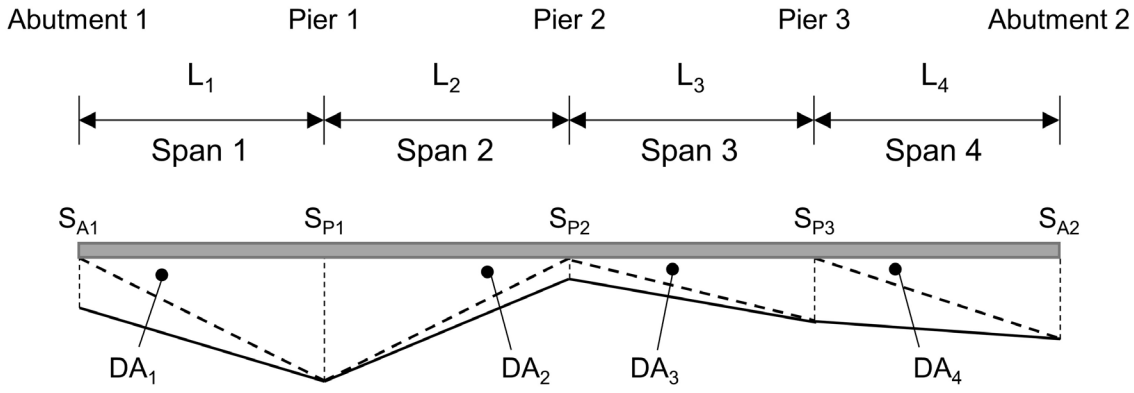

Legend:

——— Calculated settlement profile (refer to Figure 7-38).

- - - - - Hypothetical settlement profile assumed for computation of maximum angular distortion, based on S = 0 concept.

Span	Design Differential Settlement, Dδ	Design Angular Distortion, DA
1	$DS_{P1} = S_{P1}$ (assume $S_{A1} = 0$)	$DA_1 = S_{P1}/L_1$
2	$DS_{P1} = S_{P1}$ (assume $S_{P2} = 0$)	$DA_2 = S_{P1}/L_2$
3	$DS_{P3} = S_{P3}$ (assume $S_{P2} = 0$)	$DA_3 = S_{P3}/L_3$
4	$DS_{A2} = S_{A2}$ (assume $S_{P3} = 0$)	$DA_4 = S_{A2}/L_4$

Figure 7-39 Settlement profile with design differential settlement and design angular distortion from S-0 concept (after Modjeski and Masters 2015).

7.3.3 Construction Point Concept

In the example presented in Figure 7-39, the computed settlements and resultant angular distortion are based on the foundation loads applied instantaneously at the same time. In reality, the loads on the foundation are gradually applied. Similarly, settlements from those incrementally applied loads occur as construction progresses. Therefore, settlement and angular distortion relative to several critical points during construction process should be evaluated separately by the designer.

Figure 7-40(a) illustrates the typical sequences in the construction of a bridge pier, while Figure 7-40(b) shows the associated applied load from each sequence and resulting vertical deformation. Plotting the load and deformation results as shown in this figure allow settlement and resulting distortion to be assessed relative to a given

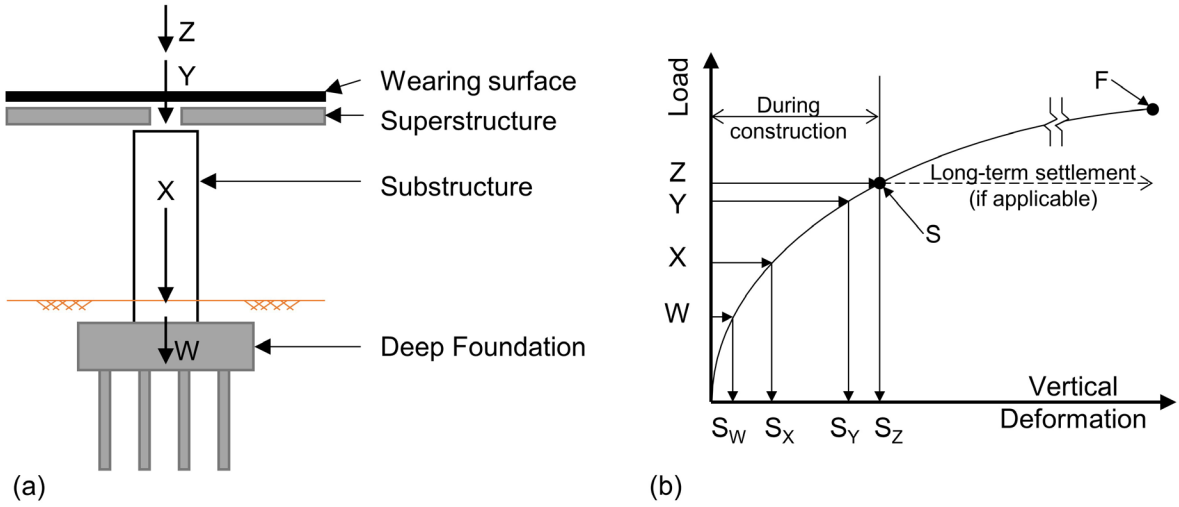

Legend:

W	Load after foundation construction
X	Load after pier column and wall placement
Y	Load after superstructure construction
Z	Load after wearing surface construction
S	Service load (service limit state)
F	Factored load (strength limit state)

S_W	Settlement under load W
S_X	Settlement under load X
S_Y	Settlement under load Y
S_Z	Settlement under load Z

Figure 7-40 Construction point concept: (a) identification of key construction points, (b) estimated load-deformation behavior (after Modjeski and Masters 2015).

point in the construction process. In a typical bridge structure project, settlement that occurs after pier column and superstructure construction but prior to wearing surface construction is often the most relevant. For example, settlement occurring prior to superstructure construction may not be significant to the superstructure design.

Vertical deformation and angular distortion should be determined and evaluated using the construction point concept in limit state designs. The four span bridge example from Figure 7-38 is revisited to illustrate the construction point concept. In Figure 7-41, the calculated settlements (solid line), and hypothetical maximum angular distortion (dashed line) from the S-0 concept are once again plotted. Using construction point load and deformation data similar to Figure 7-40, the range in anticipated settlement and the resulting range in angular distortion are then computed. The results are then depicted by the hatched zone pattern in Figure 7-41.

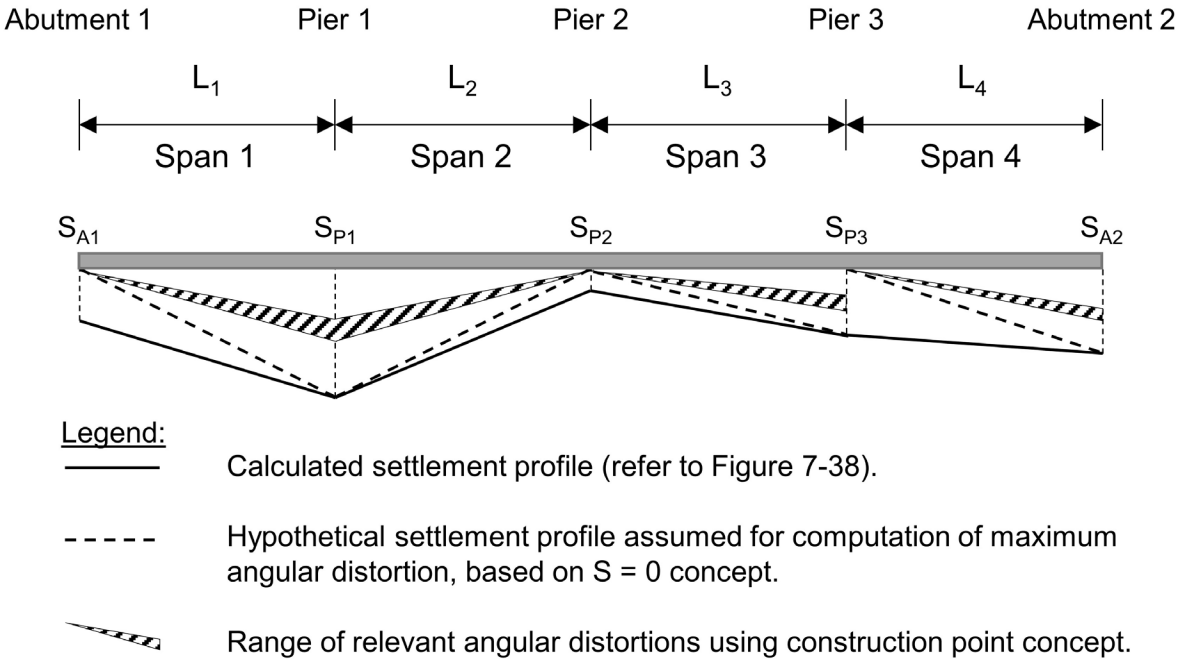

Figure 7-41 Settlement profile with angular distortion from construction point concept (after Modjeski and Masters 2015).

7.3.4 Recommended Procedure for Vertical Deformation Analysis

Modjeski and Masters, Inc., et al. (2015) in SHRP2 Report S2-R19B-RW-1 presented a recommended design procedure for determining vertical deformations or settlement. Their recommended procedure can be summarized as follows:

1. The total foundation settlement should be computed at each substructure location using an appropriate analysis method. Several appropriate analysis methods are described in detail in Section 7.3.5.

    a. Calculate the total foundation settlement, S_{ta}, using all applicable loads in the Service I load combination.

    b. Calculate the total foundation settlement, S_{tp}, before construction of the bridge superstructure using all applicable substructure loads in the Service I load combination.

    c. Calculate, S_{tr}, the relevant total settlement: $S_{tr} = S_{ta} - S_{tp}$.

2. a. Assume that the relevant settlement at each substructure support location can be as large as the magnitude calculated from an appropriate analysis method and that the settlement at the adjacent substructure support is zero. Hence, the differential settlement, S_d, for a bridge span is the maximum relevant settlement value of either support location.

   b. As illustrated in Figure 7-37, calculate the angular distortion, A, in radians from the ratio of the differential settlement, S_d, divided by the span length, L_s, or: $A_d = S_d / L_s$.

3. Compute the modified angular distortion, A_m, by multiplying A from step 2b by the load factor for settlement, γ_{SE}.

4. Check the modified angular distortion with the owner-specified criteria. Alternatively, angular distortion should be limited to 0.004 radians for multi-span bridges and 0.005 radians for single span bridges if no owner-specified criteria are provided. Other angular distortion limits may be applicable or appropriate due to:

   - vertical clearance,
   - cost of mitigation via larger foundations, realignment, ground improvement, or surcharge,
   - rideability,
   - tolerable deformation limits of other associated structures,
   - roadway drainage,
   - aesthetics, and
   - safety.

5. Evaluate the ramifications of the computed angular distortions on the structure. Modify the foundation design if necessary based on the structural ramifications.

6. The above procedure is also recommended for structures where foundations have been designed for equal total settlement due to the uncertainty in the settlement prediction from any given method.

7.3.5 Pile Group Settlement

Pile groups supported in and underlain by cohesionless soils will produce only immediate settlements. This means the settlements will occur immediately as the pile group is loaded. Pile groups supported in and underlain by cohesive soils may produce both immediate settlements and primary consolidation and secondary compression settlements that occur over a period of time. In highly over-consolidated clays, the majority of the foundation settlement will occur immediately. Primary consolidation settlements will generally be the major source of foundation settlement in normally consolidated clays.

The settlement of a pile group is likely to be many times greater than the settlement of an individual pile carrying the same load per pile as each pile in the pile group. Figure 7-42 illustrates that for a single pile, only a small zone of soil around and below the pile toe is subjected to vertical stress. This also illustrates that for a pile group, a considerable depth of soil around and below the pile group is stressed. The settlement of the pile group may be large, depending on the compressibility of the soils within the stressed zone.

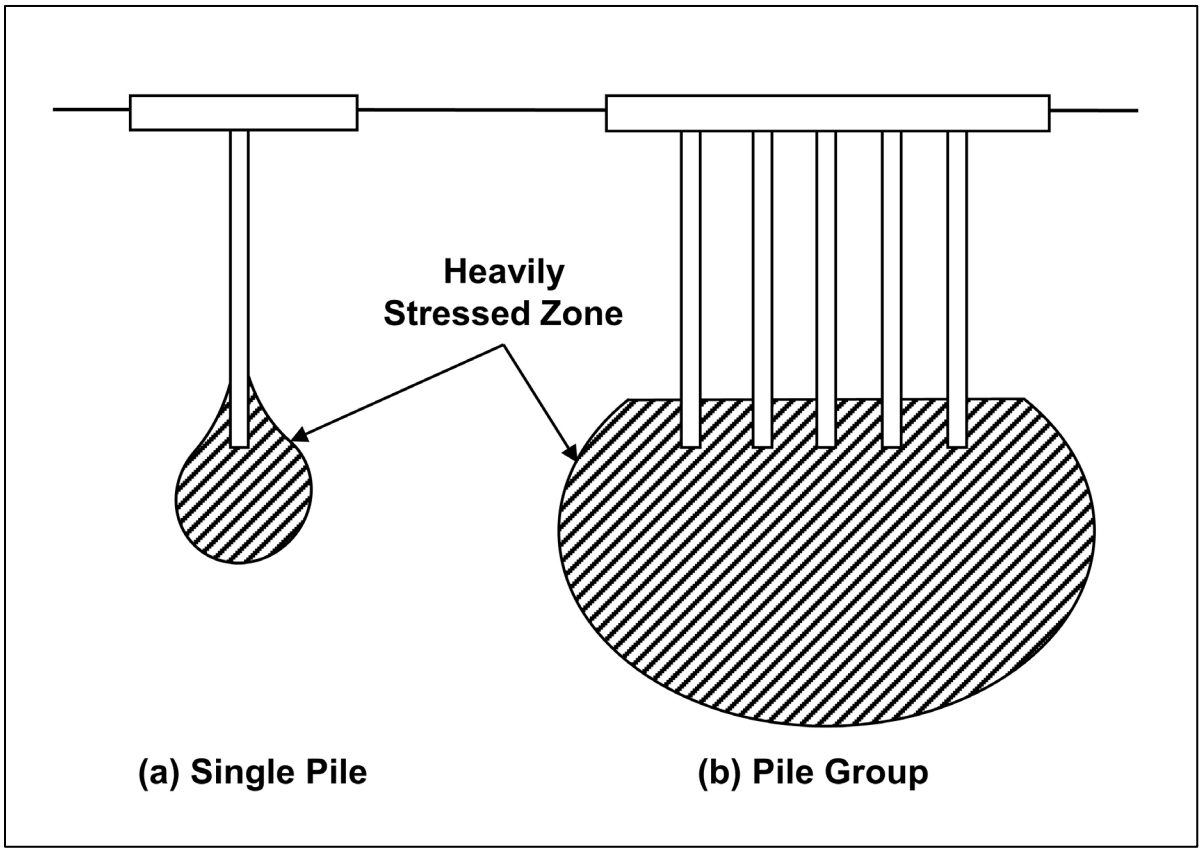

Figure 7-42 Stress zone from single pile and pile group (after Tomlinson 1994).

Methods for estimating settlement of pile groups are provided in the following sections. Methods for estimating single pile settlements are not provided because piles are usually installed in groups.

7.3.5.1 Elastic Compression of Piles

The pile group settlement methods discussed in the following sections only consider soil settlements and do not include the settlement caused by elastic compression of pile material due to the imposed axial load. Therefore, the elastic compression should also be computed and this settlement added to the group settlement estimates of soil settlement. The elastic compression, Δ, can be computed by the following expression:

$$\Delta = \frac{QL}{AE} \qquad \text{Eq. 7-48}$$

Where:

Q = unfactored axial load (kips).
L = total pile length (inches).
A = pile cross sectional area (in^2).
E = elastic modulus of pile material (ksi).

The modulus of elasticity for steel piles is 29,000 ksi. For concrete piles, the modulus of elasticity varies with concrete compression strength and is generally on the order of 4,000 ksi. The elastic compression of short piles is usually quite small and can often be neglected in design. For pile with significant shaft resistance, much of the load will be transferred to the soil over the length of the pile. In those cases, the elastic compression will be overestimated by Equation 7-48.

7.3.5.2 Group Settlement in Cohesionless Soils

Settlement in cohesionless soils is generally considered elastic for deformation calculations. Meyerhof (1976) provided elastic settlement correlations based on SPT and CPT test data as described in 7.3.5.2.1 and 7.3.5.2.2, respectively. Elastic settlement may also be estimated by the Hough (1959) method shown in Equation 7-49. The stress increase in a soil layer due to the foundation loads should be determined using the equivalent footing method with consideration of the soil stratigraphy.

$$S = H_o \left[\frac{1}{C'} \log \frac{\sigma'_{vo} + \Delta\sigma}{\sigma'_{vo}}\right] \qquad \text{Eq. 7-49}$$

Where:

S = total layer settlement (feet).

H_o = initial soil layer thickness (feet).

C' = dimensionless bearing capacity index from Figure 7-43, determined from the average corrected SPT N value for the layer with consideration of the SPT hammer type.

σ'_{vo} = vertical effective stress at midpoint of layer prior to stress increase (ksf).

$\Delta\sigma$ = average change in vertical stress in the layer in (ksf).

Cheney and Chassie (2002) report that FHWA experience with this method indicates the method is usually conservative and can overestimate settlements by a factor of 2. This conservatism is attributed to the use of the original bearing capacity index chart from Hough (1959) which was based upon SPT donut hammer data. Based upon average energy variations between SPT donut, safety, and automatic hammers reported in technical literature, Figure 7-43 now includes a correlation between SPT N values from safety and automatic hammers and bearing capacity index. The safety hammer values are considered N_{60} values. This modification should improve the accuracy of settlement estimates with this method.

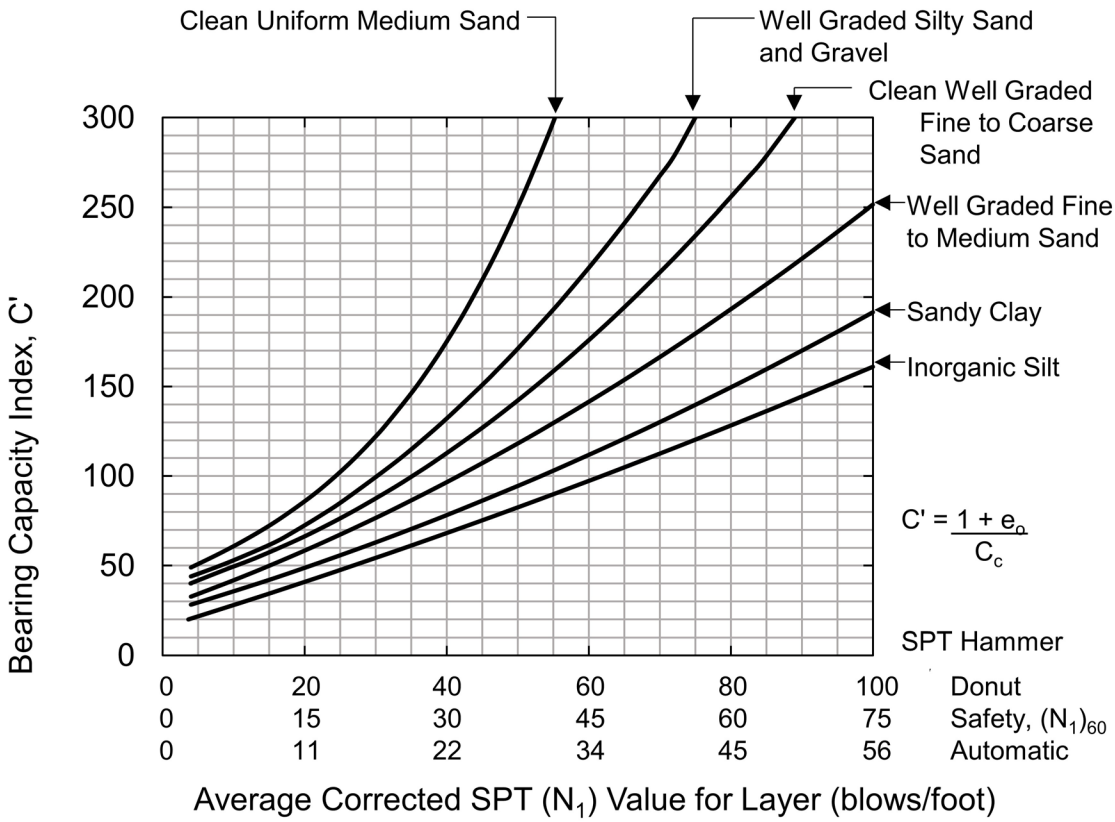

Figure 7-43 Values of the bearing capacity index, C', for granular soil (data from Hough 1959).

7.3.5.2.1 Method Based on SPT Test Data

Meyerhof (1976) recommended that the settlement of a pile group in a homogeneous sand deposit not underlain by a more compressible soil at a greater depth may be conservatively estimated by the following expression:

$$S = \frac{4\, p_f\, I_f \sqrt{B}}{N_{1(60)}} \qquad \text{Eq. 7-50}$$

For silty sand, use:

$$S = \frac{8\, p_f\, I_f \sqrt{B}}{N_{1(60)}} \qquad \text{Eq. 7-51}$$

In which

$$I_f = 1 - \frac{D\prime}{8B} \geq 0.5 \qquad \text{Eq. 7-52}$$

Where:

S	=	estimated total settlement (inches).
p_f	=	design foundation pressure (ksf).
B	=	width of pile group (feet).
$N_{1(60)}$	=	average corrected SPT N value within a depth B below pile toe.
D'	=	2/3 pile embedded length (feet).
I_f	=	influence factor for group embedment.

For piles in cohesionless soils underlain by cohesive deposits, the method presented in Sections 7.3.5.3 should be used.

7.3.5.2.2 Method Based on CPT Test Data

Meyerhof (1976) recommended the following relationship to estimate maximum settlements using cone penetration test results for saturated cohesionless soils.

$$S = \frac{p_f\, B\, I_f}{2\, q_{ca}} \qquad \text{Eq. 7-53}$$

In which

$$I_f = 1 - \frac{D\prime}{8B} \geq 0.5 \qquad \text{Eq. 7-54}$$

Where:

S	=	estimated total settlement (inches).
p_f	=	design foundation pressure (ksf).
B	=	width of pile group (feet).

I_f = influence factor for group embedment.

q_{ca} = average cone tip resistance within depth of B below the pile toe (ksf).

D' = 2/3 pile embedded length (feet).

7.3.5.3 Group Settlement in Cohesive Soils

Terzaghi and Peck (1967) proposed that pile group settlements could be evaluated using an equivalent footing situated at a depth of 1/3 *D* above the pile toe. This concept is illustrated in Figure 7-44. For a pile group consisting of only vertical piles, the equivalent footing has a plan area (*B*)(*Z*) that corresponds to the perimeter dimensions of the pile group as depicted previously in Figure 7-31. The pile group load over this plan area is then the stress transferred to the soil through the equivalent footing. The load is assumed to spread within the frustum of a pyramid with side slopes at 30˚ and to cause uniform additional vertical stress at lower levels.

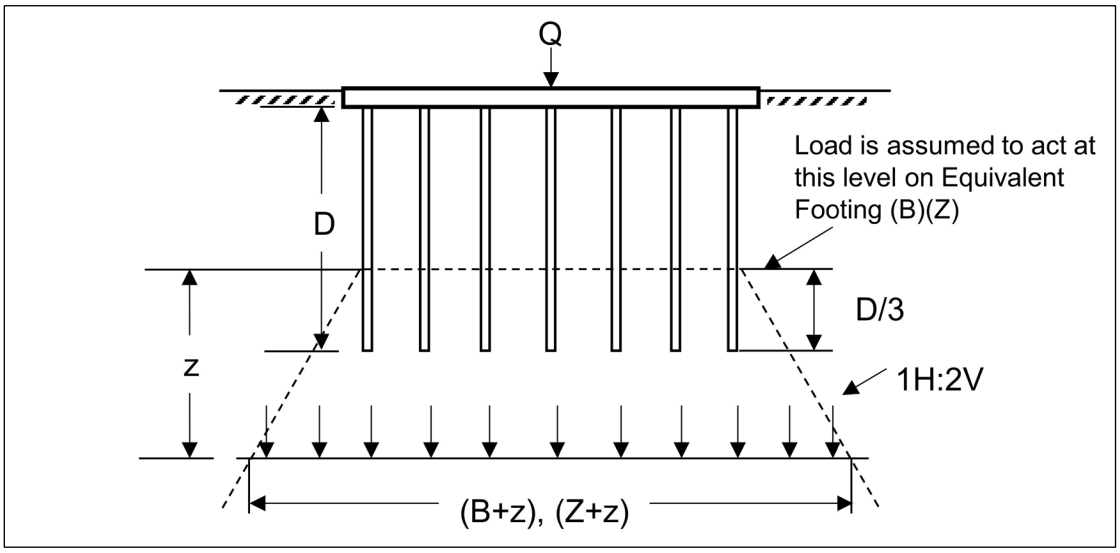

Figure 7-44 Equivalent footing concept.

The stress at any level is equal to the load carried by the group divided by the plan area of the base of the frustum at that level. AASHTO (2014) Article 10.7.2.3.1 states that the load used in calculating group settlement is the permanently applied load. Equation 7-55 should be used to calculate the change in stress for a given depth, z, below the equivalent footing.

$$\Delta\sigma'_d = \frac{Q}{(B+z)*(Z+z)} \qquad \text{Eq. 7-55}$$

Where:

$\Delta\sigma'_d$ = change in stress below equivalent footing (inches).

Q = unfactored permanent load (kips).
B = width of pile group (feet).
Z = length of pile group (feet).
z = depth below equivalent footing.

Rather than fixing the equivalent footing at a depth of a *D* above the pile toe for all soil conditions, the depth of the equivalent footing should be adjusted based upon soil stratigraphy and load transfer mechanism to the soil. Figure 7-45 presents the recommended equivalent footing location and stress distribution proposed by Duncan and Buchignani, (1976) for a pile group driven through a soft clay layer and into a medium or firm layer.

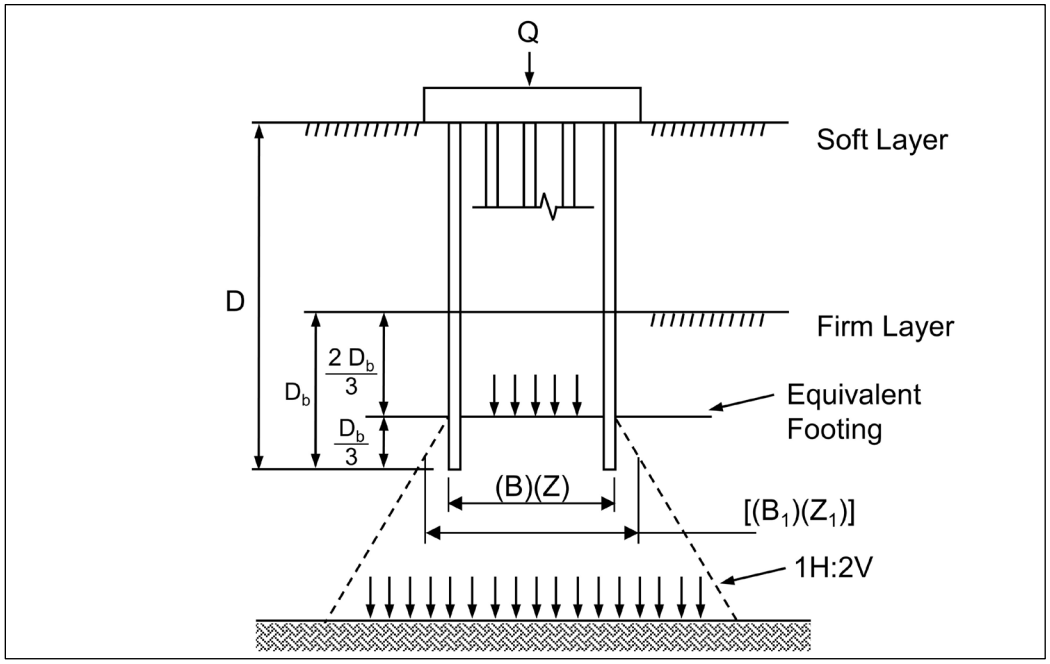

Figure 7-45 Stress distribution below equivalent footing for a pile group in firm clay (after Duncan and Buchignani, 1976).

Figure 7-46 presents other recommended locations of the equivalent footing for the following load transfer and soil resistance conditions:

a. toe resistance piles in hard clay or sand underlain by soft clay,

b. piles supported by shaft resistance in clay,

c. piles supported by shaft resistance in sand underlain by clay, and

d. piles supported by shaft and toe resistance in layered soil profile.

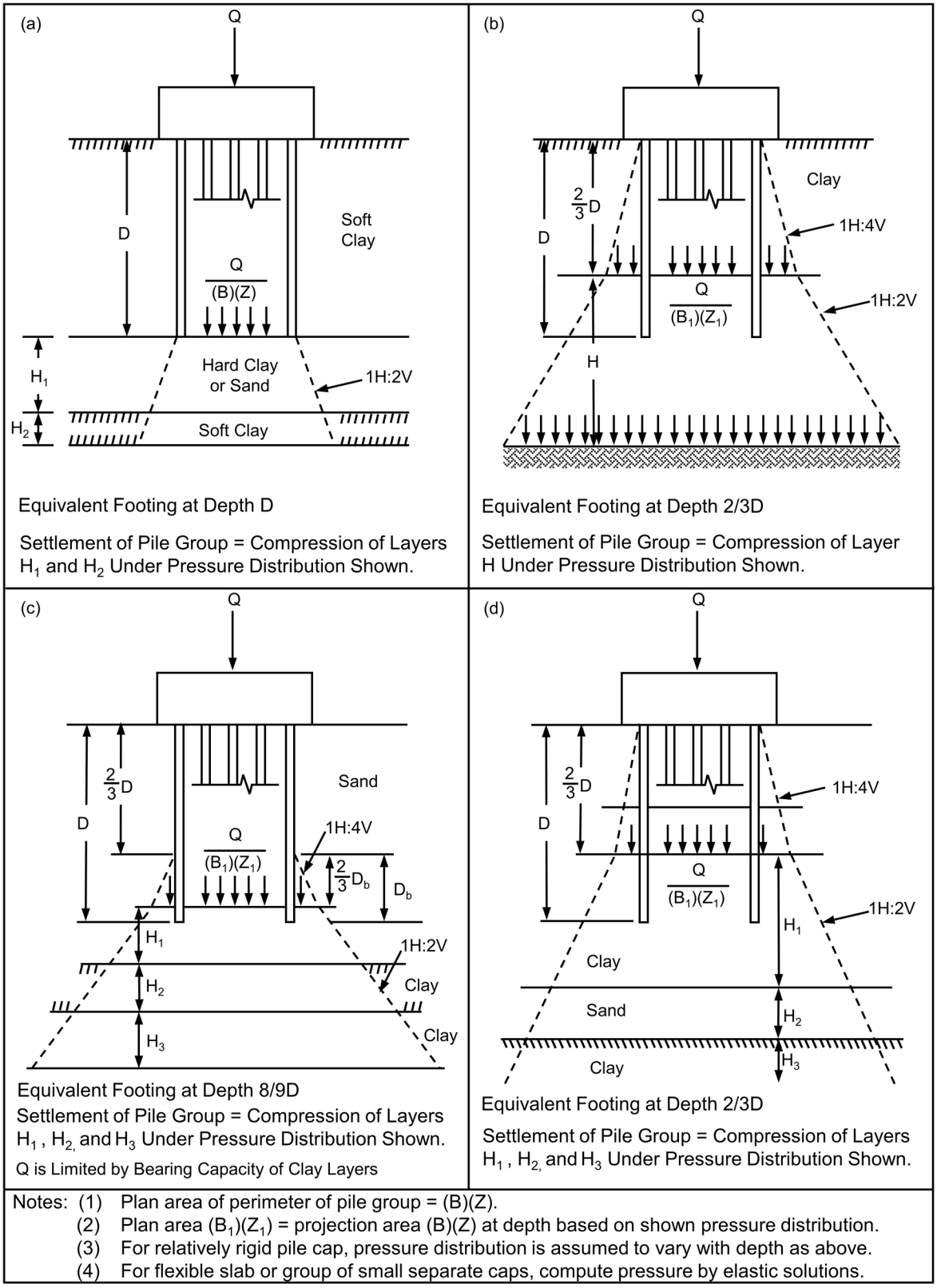

Notes: (1) Plan area of perimeter of pile group = (B)(Z).
(2) Plan area $(B_1)(Z_1)$ = projection area (B)(Z) at depth based on shown pressure distribution.
(3) For relatively rigid pile cap, pressure distribution is assumed to vary with depth as above.
(4) For flexible slab or group of small separate caps, compute pressure by elastic solutions.

Figure 7-46 Stress distribution below equivalent footing for a pile group (modified from Cheney and Chassie 2000).

Consolidation settlements are calculated based on the stress increase in the underlying layers. Equations 7-56 through 7-58 provide primary consolidation settlement estimations for cohesive soil. Parameters determined from a consolidation test are shown in the plot of void ratio versus vertical effective stress in Figure 7-47.

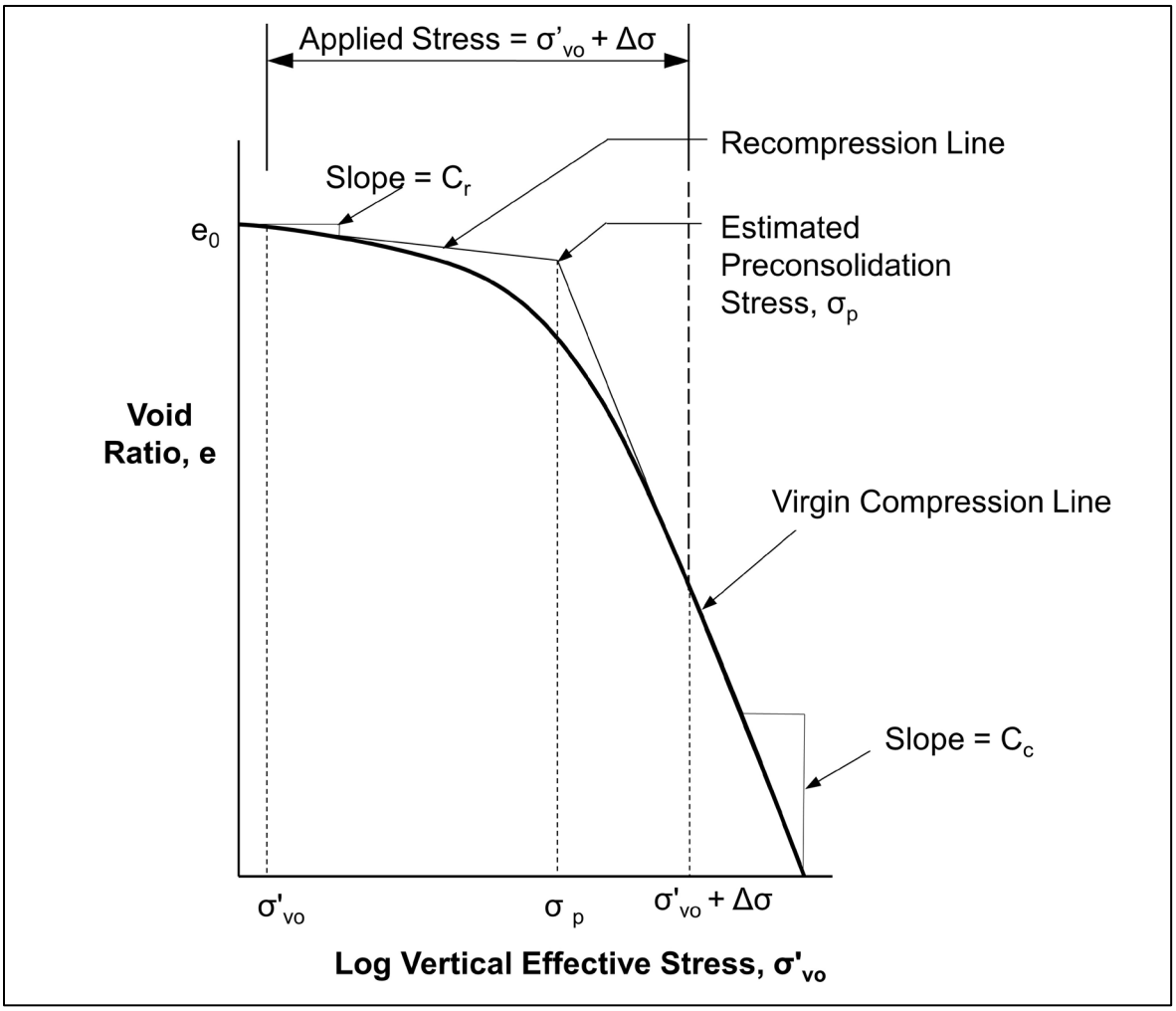

Figure 7-47 Plot of void ratio vs. vertical effective stress from consolidation test.

For normally consolidated ($\sigma'_{vo} = \sigma_p$) cohesive soil layers:

$$S_c = \sum_i^n \frac{C_c}{1+e_o} H_o \log\left(\frac{\sigma'_{vo}+\Delta\sigma}{\sigma'_{vo}}\right) \qquad \text{Eq. 7-56}$$

For overconsolidated soil with ($\sigma'_{vo} + \Delta\sigma \leq \sigma_p$):

$$S_c = \sum_i^n \frac{C_r}{1+e_o} H_o \log\left(\frac{\sigma'_{vo}+\Delta\sigma}{\sigma'_{vo}}\right) \qquad \text{Eq. 7-57}$$

For overconsolidated soil with ($\sigma'_{vo} + \Delta\sigma > \sigma_p$):

$$S_c = \sum_i^n \frac{C_r}{1+e_o} H_o \log\left(\frac{\sigma_p}{\sigma'_{vo}}\right) + \frac{C_c}{1+e_o} H_o \log\left(\frac{\sigma'_{vo}+\Delta\sigma}{\sigma_p}\right) \quad \text{Eq. 7-58}$$

Where:

S_c = settlement estimate from primary consolidation (feet).
e_o = initial soil layer void ratio.
H_o = initial soil layer height (feet).
σ_p = preconsolidation stress (psf).
σ'_{vo} = vertical effective stress at midpoint of each layer prior to loading (psf).
$\Delta\sigma$ = additional pressure from structural loading (psf).
C_r = recompression index from consolidation test.
C_c = compression index from consolidation test.

STEP BY STEP PROCEDURE FOR GROUP SETTLEMENT IN COHESIVE SOILS

STEP 1 Determine the new load imposed on soil by the pile group.

a. Determine the location of the equivalent footing. For pile groups supported primarily by toe resistance, the equivalent footing is placed at the pile toe as illustrated in Figure 7-46 (a). For pile groups supported primarily by shaft resistance, the equivalent footing is placed at a depth of ⅔ *D* as shown in Figure 7-46 (b, c, and d).

b. Determine the dimensions of the equivalent footing. For pile groups consisting only of vertical piles, the equivalent footing (unless modified for load transfer as in Figure 7-46) has the same dimensions as the length and width of the pile group from Figure 7-31. For pile groups supported primarily by shaft resistance that include batter piles, the plan area of the footing should be calculated from the dimensions of the pile group at depth ⅔ *D*, including the plan area increase due to the pile batter. For toe resistance groups with batter piles, the equivalent footing area should be the dimensions of the pile group at depth *D*, including the area increase due to pile batter.

c. Determine the stress distribution to soil layers below the equivalent footing up to the depth at which the stress increase from the equivalent footing is less than 10% of existing vertical effective stress at that depth. Remember that the equivalent footing size may be increased and the

footing stress correspondingly reduced as a result of load transfer above the footing location or in groups with batter piles. The depth at which the stress increase is less than 10% will provide the total thickness of cohesive soil layer or layers to be used in performing settlement computations. AASHTO (2014) Article 10.7.2.3.1 states that the load used in calculating settlement is the permanently applied load.

d. Divide the cohesive soil layers in the affected stress increase zone into several thinner layers with thickness of 5 to 10 feet. The thickness of each layer is the thickness *H* for the settlement computation for that layer.

e. Determine the existing vertical effective stress, σ'_{vo}, at the midpoint of each layer.

f. Determine the imposed stress increase, $\Delta\sigma$, at the midpoint of each affected soil layer based on the appropriate stress distribution.

STEP 2 Determine consolidation test parameters.

Plot the results of consolidation test(s) as shown in Figure 7-47 followed by determination of settlement parameters.

STEP 3 Compute settlements.

Using the appropriate settlement equation, Equation 7-56, 7-57 or 7-58, compute the settlement of each affected soil layer. Sum the settlements of all layers to obtain the total estimated soil settlement from the pile group. Add the elastic compression of the pile under the design load to obtain the total estimated pile group settlement.

7.3.5.4 Time Rate of Settlement in Cohesive Soils

Settlement analyses in cohesive soils should also evaluate the time required for the anticipated settlement to occur. In time rate computations, the time for 90% consolidation to occur is typically used to determine the total time required for primary settlement. The time rate of settlement of a cohesive soil deposit can be calculated from:

$$t = \frac{T{H_v}^2}{C_v} \qquad \text{Eq. 7-59}$$

Where:

t = time for settlement to occur (days).

T = theoretical time factor for percentage of primary consolidation to occur (Table 7-19).

H_v = maximum vertical drainage path in the cohesive layer (feet).

C_v = coefficient of consolidation (ft^2/day).

The term H_v should not be confused with the term H_o used in the settlement equations for cohesive soils. H_v is the maximum distance water must travel from the compressible cohesive deposit to reach a more permeable layer. In the case of a cohesive layer overlain and underlain by a permeable granular layer, H_v would be ½ the cohesive layer thickness. However, if the cohesive layer were overlain by a permeable granular layer and underlain by a non-permeable rock layer, H_v would be the full thickness of the cohesive deposit. Additional discussion on time rate of consolidation can be found in Samtani and Nowatzki (2006).

Table 7-19 Time Factors for Settlement

Primary Settlement (%)	Time Factor (T)
10	0.008
20	0.031
30	0.071
40	0.126
50	0.197
60	0.287
70	0.403
80	0.567
90	0.848

7.3.5.5 Group Settlement in Layered Soils

Piles are often installed in a layered soil profile consisting of cohesionless and cohesive soils or in soil profiles where an underlying soil stratum of different consistency is affected by the pile group loading. In these cases, group settlement will be influenced by the stress increase in and compressibility of the affected layers.

Figures 7-46(a), 7-46(c) and 7-46(d) may be used to determine the location of the equivalent footing and to evaluate the resulting stress increase in a soil layer. The settlement of each layer is then calculated using the appropriate settlement equation presented in Section 7.3.5.2 or Section 7.3.5.3.

STEP BY STEP PROCEDURE FOR GROUP SETTLEMENT IN LAYERED SOIL PROFILES

STEP 1 Determine the new load imposed on soil by the pile group.

a. Determine the location of the equivalent footing. For pile groups supported primarily by toe resistance, the equivalent footing is placed at the pile toe as illustrated in Figure 7-46 (a). For pile groups supported primarily by shaft resistance in sands underlain by cohesive soils, the equivalent footing is placed at a depth of 8/9 *D* as shown in Figure 7-46 (c). For pile groups in layered soils supported by a combination of shaft and toe resistance, the equivalent footing is placed at ⅔ *D* as shown in Figure 7-46 (d).

b. Determine the dimensions of the equivalent footing. For pile groups consisting only of vertical piles, the equivalent footing (unless modified for load transfer as in Figures 7-46 (c) and 7-46 (d)) has the same dimensions as the length and width of the pile group from Figure 7-31. For pile groups supported primarily by shaft resistance that include batter piles, the plan area of the footing should be calculated from the dimensions of the pile group at the equivalent footing depth that includes the plan area increase due to the pile batter. For toe resistance groups with batter piles, the equivalent footing area should be calculated from the dimensions of the pile group at depth *D*, including the plan area increase due to the pile batter.

c. Determine the stress distribution to soil layers below the equivalent footing up to the depth at which the stress increase from the equivalent footing is less than 10% of existing vertical effective stress at that depth. Remember that the equivalent footing size may be increased and the footing stress correspondingly reduced as a result of load transfer above the footing location or in groups with batter piles. The depth at which the stress increase is less than 10% will provide the total thickness of soil to be evaluated in the settlement

computations. AASHTO (2014) Article 10.7.2.3.1 states that the load used in calculating settlement is the permanently applied load.

d. Divide the soil layers in the affected stress increase zone into several thinner layers of 5 to 10 feet in thickness. The thickness of each layer is the thickness *H* for the settlement computation for that layer.

e. Determine the existing vertical effective stress, σ'_{vo}, at the midpoint of each soil layer.

f. Determine the imposed stress increase, $\Delta\sigma$, at the midpoint of each affected soil layer based on the appropriate stress distribution.

STEP 2 Determine consolidation test parameters for each cohesive layer.

Plot results of consolidation test(s) as shown in Figure 7-47. Determine σ_p, e_o, C_r and C_c values from the consolidation test data.

STEP 3 Determine bearing capacity index for each cohesionless layer.

Determine the average corrected SPT N value, for each cohesionless layer. Use N_{60} or the appropriate SPT hammer type in Figure 7-43 to obtain the bearing capacity index for each layer. The safety hammer N values in Figure 7-43 are considered representative N_{60} values.

STEP 4 Compute settlements.

Using the appropriate settlement equation, compute the settlement of each affected soil layer. Sum the settlements of all layers to obtain the total estimated soil settlement from the pile group. Add the elastic compression of the pile under the design load to obtain the total estimated pile group settlement.

7.3.5.6 Group Settlement Using the Janbu Tangent Modulus Approach

The previous methods of group settlement analyses assume a linear relationship between induced stress and soil strain. However except at very small strains, a non-linear relationship exists between stress and strain. Figure 7-48 illustrates that a stress increase at a small original stress will result in a larger strain than the same stress increase applied at a greater original stress.

Janbu (1963, 1965) proposed a tangent modulus approach that is referenced in the Canadian Foundation Engineering Manual (1985). In this method, the stress strain relationship of soils is expressed in terms of a dimensionless modulus number, *m*, and a stress exponent, *j*. Values of the modulus number can be determined from conventional laboratory triaxial or oedometer tests. The stress exponent, *j*, can generally be taken as 0.5 for cohesionless soils and 0 for cohesive soils.

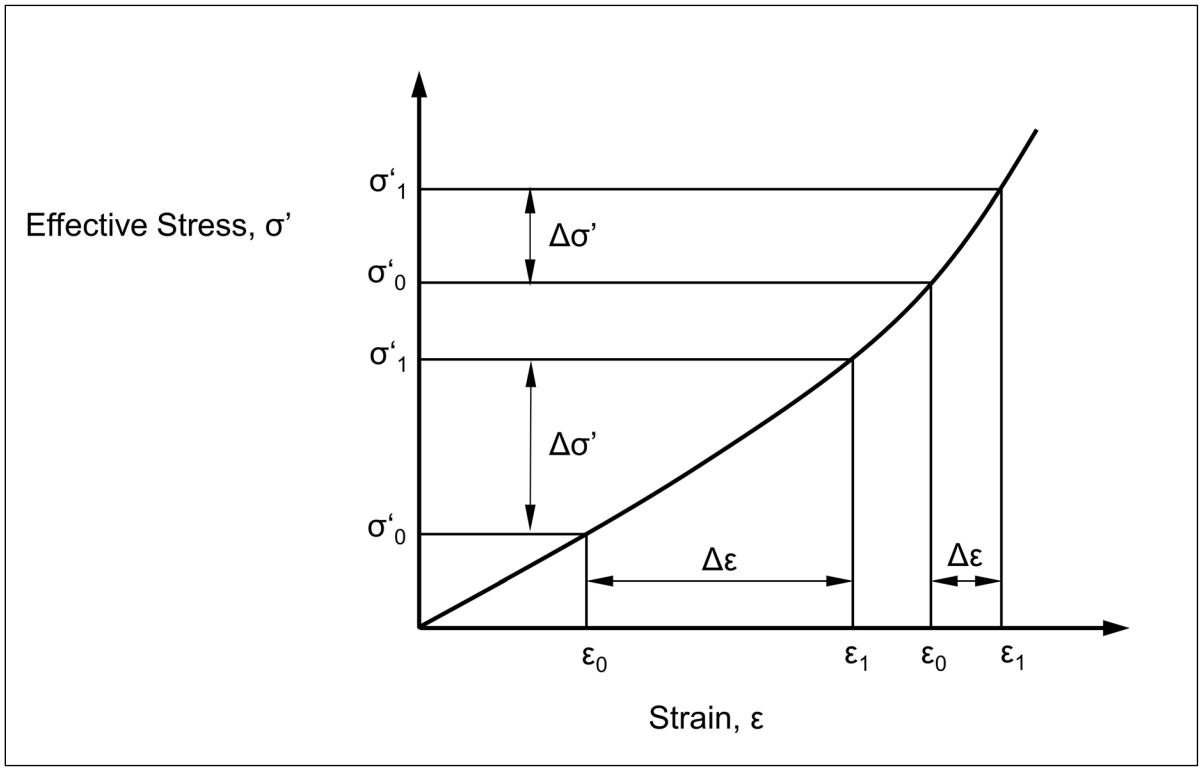

Figure 7-48 Non-linear relation between stress and strain in soil (after Fellenius 1990).

The following seven equations are used to calculate the strain for normally and over consolidated, cohesionless and cohesive soils. The terms used in these four equations are as follows:

ε = strain from the increase in effective stress.
E_s = elastic modulus of soil (ksf).
m_n = dimensionless modulus number.
m_{nr} = dimensionless recompression modulus number.
j = stress exponent in Table 7-20.
σ'_1 = new effective stress after stress increase (ksf).
σ'_o = effective stress prior to stress increase (ksf).
σ'_p = preconsolidation stress (ksf).
σ_r = constant reference stress = 2 ksf.

For cohesionless soils ($j > 0$), the strain induced by an increase in effective stress may be expressed as shown in Equation 7-60:

$$\varepsilon = \frac{1}{m_n j}\left[\left(\frac{\sigma'_1}{\sigma_r}\right)^j - \left(\frac{\sigma'_0}{\sigma_r}\right)^j\right] \quad \text{Eq. 7-60}$$

For dense coarse grained soils ($j = 1$), the following equation should be used to calculate the strain induced by an increase in effective stress:

$$\varepsilon = \frac{1}{E_s}[\sigma'_1 - \sigma'_o] \quad \text{Eq. 7-61}$$

For sandy or silty soil ($j = 0.5$), the Equation 7-62 should be used to calculate the strain induced by an increase in effective stress:

$$\varepsilon = \frac{\sqrt{2}}{m_n}\left[\sqrt{\sigma'_p} - \sqrt{\sigma'_o}\right] \quad \text{Eq. 7-62}$$

For overconsolidated sandy or silty soil, where the final stress will exceed the preconsolidation stress, Equation 7-63 should be used to calculate the induced strain:

$$\varepsilon = \frac{\sqrt{2}}{m_{nr}}\left[\sqrt{\sigma'_1} - \sqrt{\sigma'_o}\right] + \frac{\sqrt{2}}{m_n}\left[\sqrt{\sigma'_1} - \sqrt{\sigma'_p}\right] \quad \text{Eq. 7-63}$$

For cohesive soils, the stress exponent is zero, ($j = 0$). The strain induced by an increase in effective stress in a normally consolidated cohesive soil is then as follows:

$$\varepsilon = \frac{1}{m_n}\ln\left[\left(\frac{\sigma'_1}{\sigma'_o}\right)\right] \quad \text{Eq. 7-64}$$

For overconsolidated cohesive soils, if the applied foundation stress exceeds the preconsolidation stress, the following equation should be used to calculate the strain:

$$\varepsilon = \frac{1}{m_{nr}}\ln\left[\left(\frac{\sigma'_p}{\sigma'_0}\right)\right] + \frac{1}{m_n}\ln\left[\left(\frac{\sigma'_1}{\sigma'_p}\right)\right] \quad \text{Eq. 7-65}$$

For overconsolidated cohesive soils, if the applied foundation stress does not exceed the preconsolidation stress, the following equation should be used to calculate strain:

$$\varepsilon = \frac{1}{m_{nr}} \ln\left[\left(\frac{\sigma'_1}{\sigma'_{vo}}\right)\right] \quad \text{Eq. 7-66}$$

In cohesionless soils, the modulus number can be calculated from the soil modulus of elasticity, E_s (ksf), and the previously described terms using Equation 7-67:

$$m_n = \frac{\sqrt{2}E_s}{(\sqrt{\sigma'_1} + \sqrt{\sigma'_0})} \quad \text{Eq. 7-67}$$

In cohesive soils, the modulus number, m_n, or recompression modulus number, m_{nr}, can be calculated from the initial void ratio, e_o, and the compression index, C_c, or recompression index, C_r. The modulus number is calculated from:

$$m_n = 2.30\left[\frac{1+e_0}{C_c}\right] \quad \text{Eq. 7-68}$$

The recompression modulus number, m_{nr}, is calculated by substituting the recompression index, C_r, for the compression index, C_c, as follows:

$$m_{nr} = 2.30\left[\frac{1+e_0}{C_r}\right] \quad \text{Eq. 7-69}$$

The Janbu tangent modulus approach is quite adaptable to calculating pile group settlements in any soil profile. For reference purposes, typical and normally conservative modulus number and stress exponent values from the Canadian Foundation Engineering Manual (1985) are presented in Table 7-20. These values may be useful for preliminary settlement estimates. A step by step procedure for this method follows.

STEP BY STEP PROCEDURE FOR PILE GROUP SETTLEMENT BY JANBU METHOD

STEP 1 Determine the new load imposed on soil by the pile group.

a. Determine the location of the equivalent footing. For pile groups supported primarily by toe resistance, the equivalent footing is placed at the pile toe as illustrated in Figure 7-46 (a). For pile groups supported primarily by shaft resistance in sands underlain by cohesive soils, the equivalent footing is placed at a depth of 8/9 *D* as shown in Figure 7-46(c). For pile groups in layered soils supported by a combination of shaft and toe resistance, the equivalent footing is placed at ⅔ *D* as shown in Figure 7-46 (d).

b. Determine the dimensions of the equivalent footing. For pile groups consisting only of vertical piles, the equivalent footing (unless modified for load transfer as in Figures 7-46 (c) and 7-46 (d) has the same dimensions as the length and width of the pile group from Figure 7-31. For pile groups supported primarily by shaft resistance that include batter piles, the plan area of the footing should be calculated from the dimensions of the pile group at the equivalent footing depth that includes the plan area increase due to the pile batter. For toe resistance groups with batter piles, the equivalent footing area should be calculated from the dimensions of the pile group at depth *D*, including the plan area increase due to the pile batter.

c. Determine the stress distribution to soil layers below the equivalent footing up to the depth at which the stress increase from the equivalent footing is less than 10% of existing vertical effective stress at that depth. Remember that the equivalent footing size may be increased, and the footing stress correspondingly reduced, as a result of load transfer above the footing location, or in groups with batter piles. The depth at which the stress increase is less than 10% will provide the total thickness of the soil to be analyzed and the number of soil layers for settlement calculations. AASHTO (2014) Article 10.7.2.3.1 states that the load used in calculating settlement is the permanently applied load.

d. Divide the soil layers in the affected stress increase zone into several thinner layers of 5 to 10 feet in thickness. The thickness of each layer is the thickness *H* for the settlement computation for that layer.

e. Determine the existing effective stress, σ'_{vo}, at the midpoint of each soil layer.

f. Determine the preconsolidation stress, σ_p, at the midpoint of each soil layer and whether the soil layer is overconsolidated or normally consolidated.

g. Determine the new effective stress, σ'_1, at the midpoint of each affected soil layer based on the equivalent footing stress distribution.

Table 7-20 Typical Modulus and Stress Exponent Values
(after Canadian Geotechnical Society 1985)

Soil Type	Consistency	Range in Modulus Number, m_n	Stress Exponent, *j*
Glacial Till	Very Dense to Dense	1000 - 300	1.0
Gravel	---	400 - 40	0.5
Sand	Dense	400 - 250	0.5
Sand	Medium Dense	250 - 150	0.5
Sand	Loose	150 - 100	0.5
Silt	Dense	200 -80	0.5
Silt	Medium Dense	80 - 60	0.5
Silt	Loose	60 - 40	0.5
Silty Clay & Clayey Silt	Hard - Stiff	60 - 20	0
Silty Clay & Clayey Silt	Stiff - Firm	20 - 10	0
Silty Clay & Clayey Silt	Soft	10 – 5	0
Marine Clay	Soft	20 – 5	0
Organic Clay	Soft	20 – 5	0
Peat	---	5 – 1	0

STEP 2 Determine modulus number and stress exponent for each soil layer.

Use laboratory test data to compute modulus number for each layer. Preliminary settlement estimates can be made by using assumed modulus numbers based on soil type as indicated in Table 7-20.

STEP 3 Select the appropriate strain computation equation for each layer.

Select the strain equation applicable to each layer depending upon whether the soil layer is cohesive or cohesionless, and overconsolidated or normally consolidated.

STEP 4 Compute settlements.

Using the appropriate strain computation equation, compute the settlement, *S*, of each affected soil layer of thickness, H_o. Sum the settlements of all layers until the stress increase is less than 10% of the

existing vertical effective stress at that depth obtain the total estimated soil settlement from the pile group. Add the elastic compression of the pile under the design load to obtain the total estimated pile group settlement.

7.3.5.7 Group Settlement Using the Neutral Plane Method

As the previous sections demonstrate, most of the group settlement methods select the depth of the equivalent footing based upon the assumed load transfer behavior. A preferred solution is to determine the depth of the neutral plane, and place the equivalent footing at or below the neutral plane location. The neutral plane occurs at the depth where the unfactored permanent load plus the load from negative shaft resistance is equal to the positive shaft resistance plus the toe resistance. The design should aim to locate the neutral plane in competent soils. When this is done, group settlements are usually well within acceptable limits.

The position of the neutral plane and the resulting negative shaft resistance can be determined from a static calculation. As previously stated, the neutral plane is the depth at which the sum of the unfactored permanent load plus the negative shaft resistance is equal to the positive shaft resistance plus the toe resistance. Above the neutral plane, the settlement of the soil is greater than the settlement of the pile. Any shaft resistance above the neutral plane is negative shaft resistance, since by definition the soil settlement is greater than the pile settlement. Therefore, the soil settlement transfers load to the pile. Below the neutral plane, the settlement of the soil is less than the settlement of the pile and load is transferred from the pile to the soil. Accordingly, pile settlement equals soil settlement at the neutral plane. Therefore, pile settlement is controlled by the soil compressibility below the neutral plane.

The following step by step procedure adapted from Goudreault and Fellenius (1994) is recommended for determination of the neutral plane.

STEP BY STEP PROCEDURE FOR DETERMINING THE NEUTRAL PLANE DEPTH

STEP 1 Perform a static resistance calculation.

a. Determine the nominal resistance, R_n, from a static resistance calculation.

b. Plot the load transfer versus depth by subtracting the shaft resistance at a given depth from the nominal resistance. This computation is identified as Curve A in Figure 7-49.

STEP 2 Determine the load transfer to the pile above the neutral plane.

a. Determine the unfactored permanent load, Q_d.

b. Plot the load transfer to the pile versus depth by adding the shaft resistance at a given depth to the sustained load. This computation is labeled as Curve B in Figure 7-49.

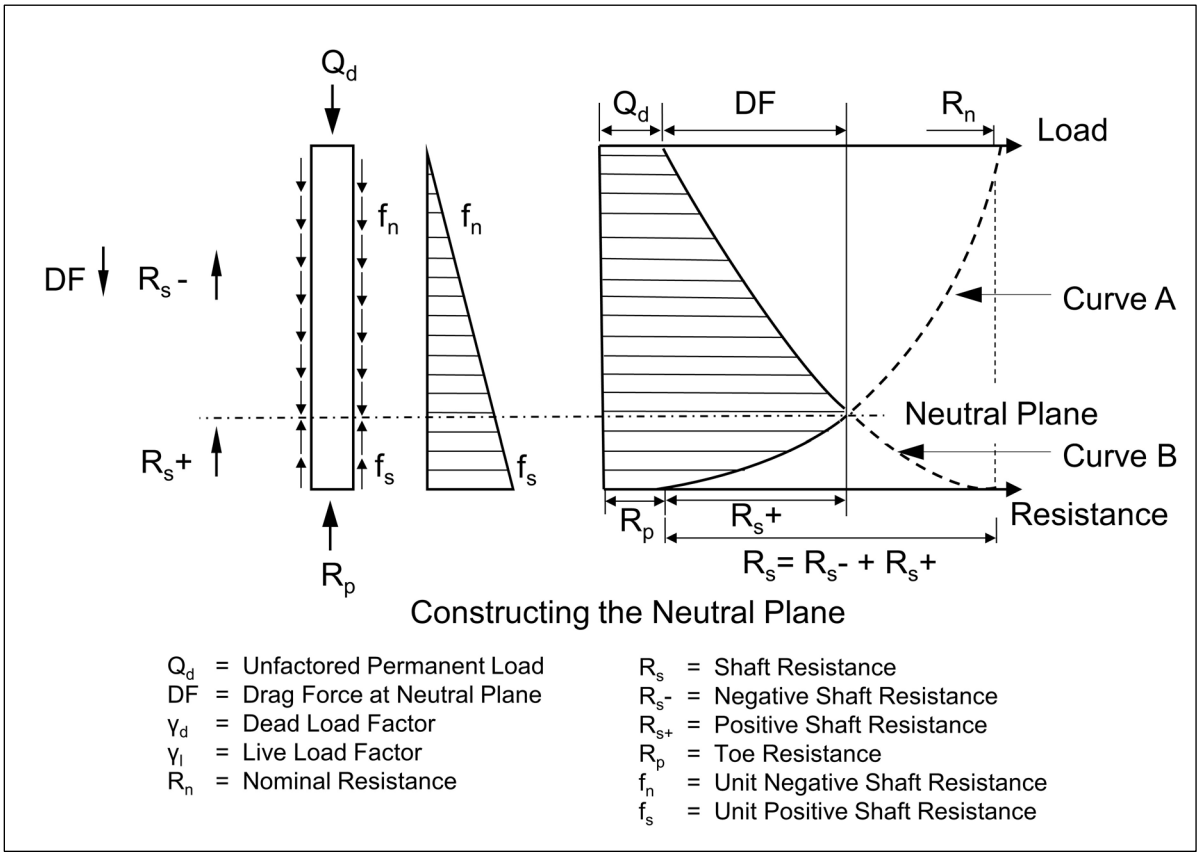

Figure 7-49 Neutral plane (after Goudrealt and Fellenius 1994).

STEP 3 Determine the depth of the neutral plane.

a. The neutral plane is at the depth of where Curves A and B intersect.

b. The location of the neutral plane will move if the permanent load is changed or the soil resistance versus depth is altered. Hence, design or construction decisions altering the permanent load, or soil

resistance versus depth, will require reevaluation of the neutral plane location under the changed conditions. Preaugering, jetting, use of bitumen coatings, etc. are but a few of the factors that can change the soil resistance versus depth and thus the neutral plane location.

Goudreault and Fellenius (1994), note that the magnitude of group settlement between the neutral plane and the pile toe level is generally small. This is because the piles below the neutral plane act as reinforcing elements and the compression of the pile-reinforced soil is small. Therefore, for most cases they recommend calculating the pile group settlements based on locating the neutral plane at the pile toe.

The group load is distributed below the neutral plane at a slope of 1H:2V. As in the previous methods, the soil materials below the neutral plane should be evaluated for settlement until the stress increase is less than 10%. Group settlements are generally calculated based upon the stress increase and the resulting strain as presented for the Janbu method in Section 7.3.5.6. However, the methods presented for layered soils in Section 7.3.5.5 could also be used.

7.3.6 Settlement Due to Downdrag

When soil moves downward relative to the pile, it creates a drag force on, and therefore within, the pile. The downward soil movement creates the potential for downward pile movement. This downward pile movement is referred to as downdrag. The subsurface conditions, pile installation methods, pile loading sequences, as well as the pile and ground surface configuration determine the magnitude of the drag force and the downdrag movement.

The design approach for downdrag specified by AASHTO treats drag force as an additional load to be resisted in a geotechnical strength limit state analysis. However, drag force does not affect geotechnical strength. As the pile head axial compression load approaches the nominal geotechnical resistance, all shaft resistance is positive or acting upward, hence no drag force exists. This section provides further explanation of these concepts and a recommended approach for calculating drag force and downdrag movement is presented in Section 7.3.6.1. The recommended approach is based on the neutral plane method developed by Fellenius (1989), and modified by Siegel et al. (2013). The recommended method should be used in evaluating the structural strength and geotechnical service limit states, respectively.

The drag force and/or the downdrag movement may be large or small, but for practical consideration they always exist primarily due to the contrasting-stiffness between the pile and the surrounding geomaterials as well as due to soil disturbance and soil stress changes caused by pile installation. This is an important realization. It means that drag force and downdrag are not design considerations in only special circumstances. Rather, drag force and downdrag should be evaluated in all driven pile designs. The determination of drag force and its effect on the structural resistance should be considered in the structural strength limit state analysis. Determination of the downdrag movement, since it contributes to pile head settlement, should be part of a geotechnical service limit state analysis.

Negative shaft resistance occurs as the soil moves downward relative to the pile. The accumulation of negative shaft resistance with depth produces the drag force on the pile. When piles are installed through a soil deposit undergoing consolidation, a large drag force can develop. Battered piles should be avoided in soil conditions where large soil settlements are expected because of the additional bending forces imposed on the piles which can cause pile deformation and damage.

There exists a depth along the pile where the sum of the permanent load on the pile plus the negative shaft resistance is equal to the positive shaft resistance on the pile plus the toe resistance. This depth is the location of the neutral plane. The maximum drag force and the maximum axial compression stress in the pile occur at the neutral plane.

Figure 7-50 presents plots of the calculated load in a pile versus depth as a function of time. This data set was collected by the Minnesota Department of Transportation (MnDOT) using sister bar mounted vibrating wire strain gages embedded in a 12.75 inch O.D. concrete filled pipe pile. A large abutment footing and wall were constructed atop the pile concurrent with abutment backfilling. As the sustained pile head load increased, the development and location of the neutral plane 30 feet above the pile toe is readily apparent. The maximum compression force in the pile and the drag force at the neutral plane are also easily identified. The effects of any residual driving stresses are not included in the load versus depth profiles due to installation of the embedded instrumentation following pile driving.

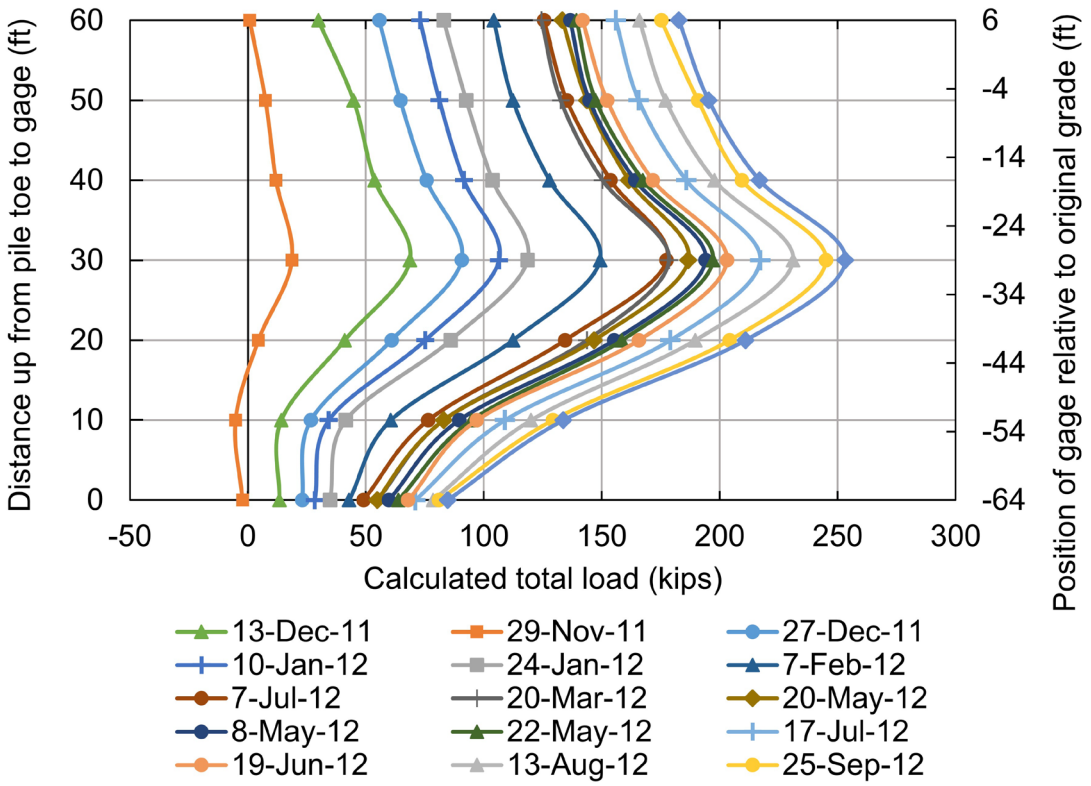

Figure 7-50 Calculated load versus depth in 12.75 inch O.D. concrete filled pipe pile as a function of time (after MnDOT Geotechnical Manual).

Figure 7-51 illustrates the changes that occur as the pile approaches the geotechnical strength limit state. Note that the location of the neutral plane moves up the pile toward the ground surface. This results in a reduction in the magnitude of the negative shaft resistance as well as the drag force in the pile. At the geotechnical strength limit state, geotechnical failure, all shaft resistance is positive as the entire pile is moving downward relative to the soil during plunging failure. Hence, drag force does not alter the geotechnical strength limit state.

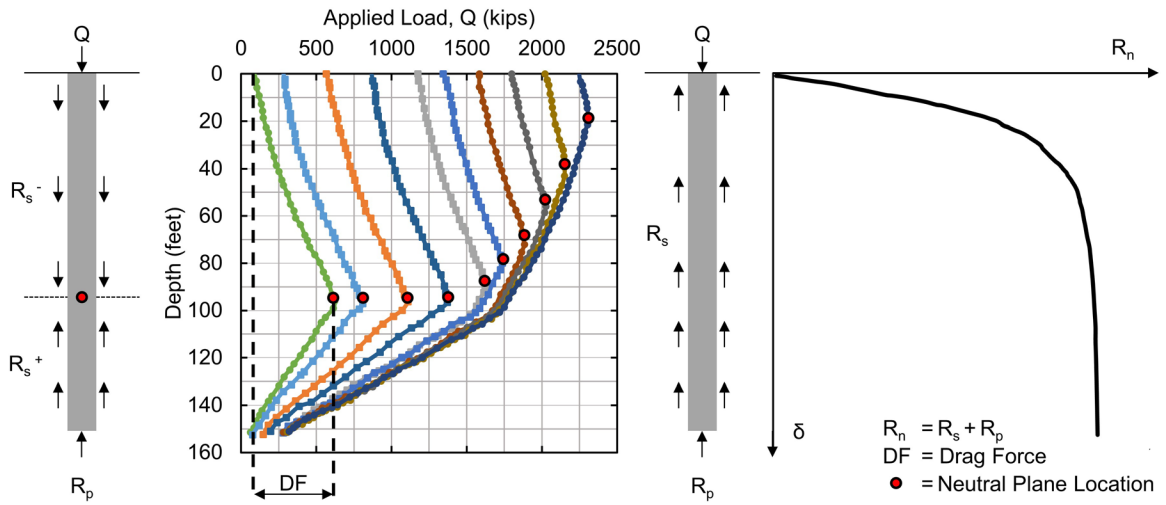

Figure 7-51 Change in neutral plane, negative shaft resistance, and drag force during transition to geotechnical strength limit (after MnDOT Geotechnical Manual).

The recommended design procedure for downdrag is presented in Section 7.3.6.1. The recommended approach addresses settlement considerations due to downdrag in the geotechnical service limit state and pile structural considerations in the structural limit state. Figure 7-52 presents a conceptual illustration of soil and pile movement and resulting pile forces.

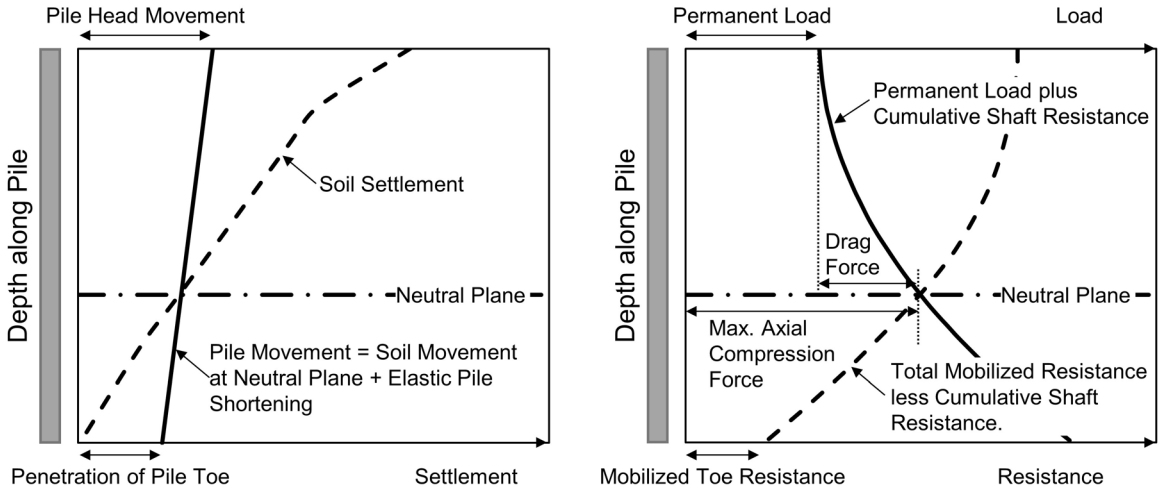

Figure 7-52 Conceptual illustration of soil and pile movement (left) and resulting neutral plane and pile forces (right) (adapted from Siegel et al. 2013).

Figure 7-53 illustrates the most common situation where large negative shaft resistance develops when fill is placed over a compressible layer immediately prior to, or after, piles are driven. Effective stress changes due to dewatering can also cause negative shaft resistance to develop such as shown in Figure 7-54.

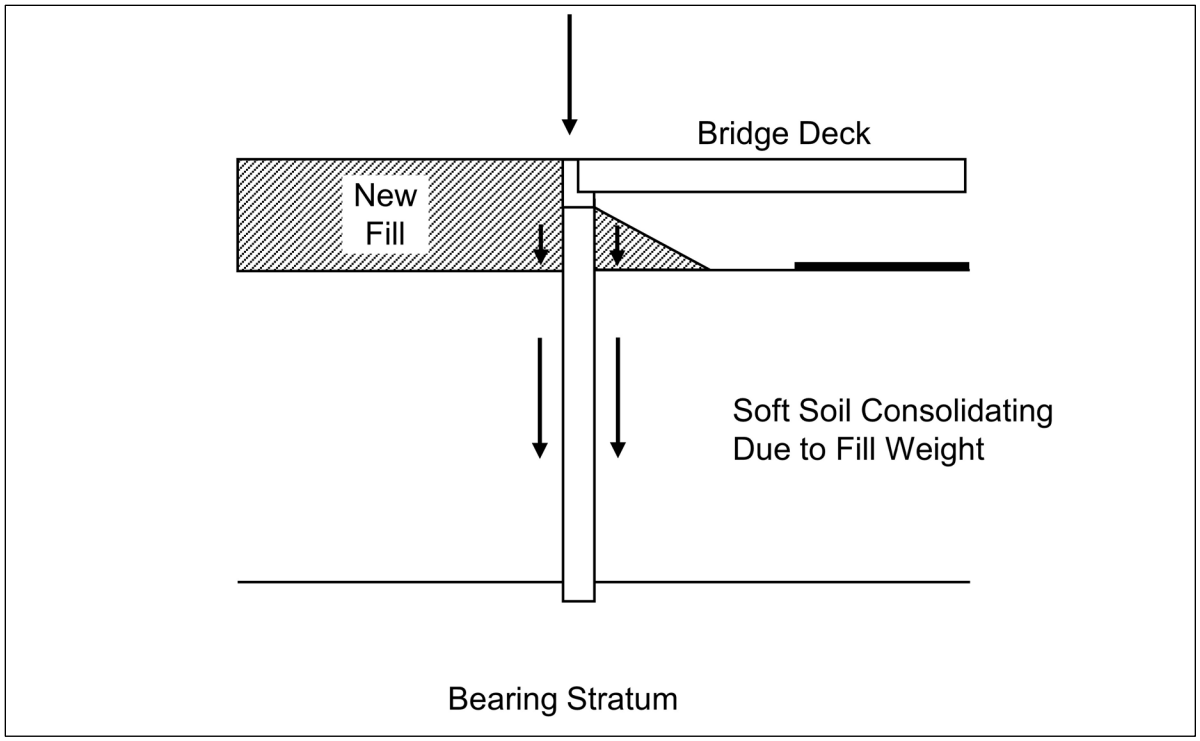

Figure 7-53 Common downdrag situation due to fill weight.

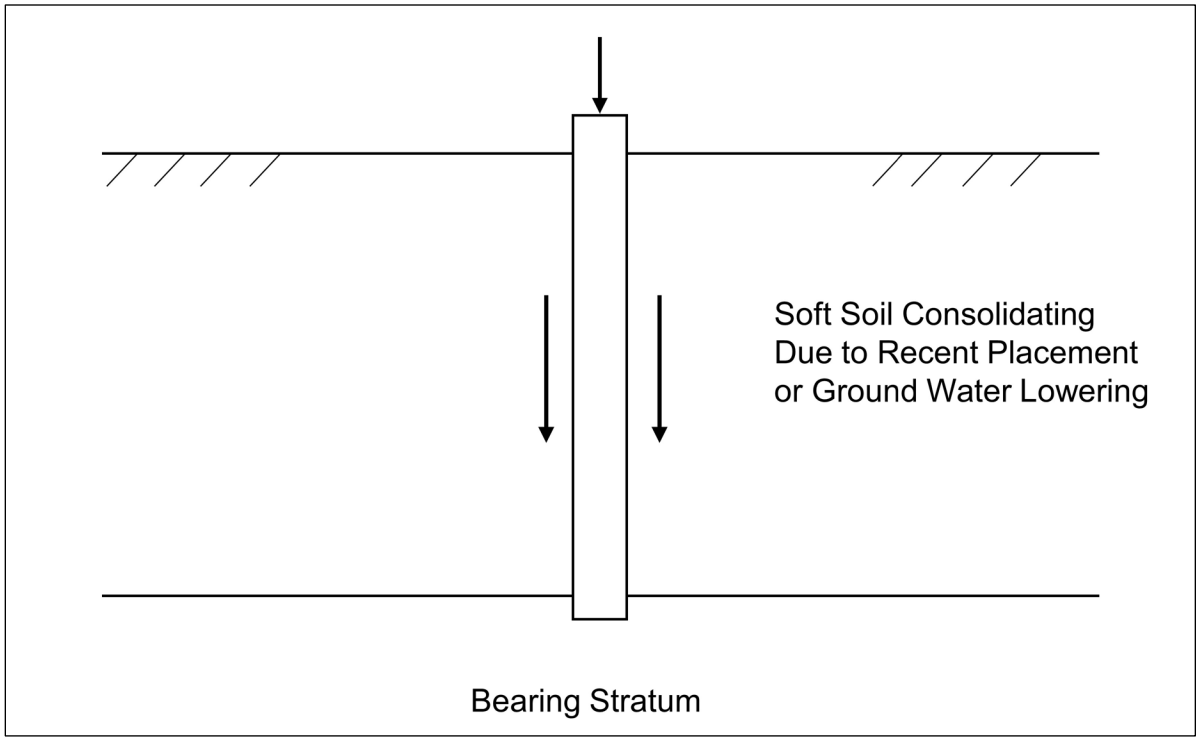

Figure 7-54 Common downdrag situation due to ground water lowering.

Briaud and Tucker (1993) presented the following criteria to assist in identifying situations where drag force and downdrag may be significant and should be carefully

evaluated in the design. This list is not meant to be all inclusive and other situations can also cause significant drag force and downdrag. Ultimately the designer must determine when the magnitude of the drag force and/or downdrag movement must be addressed in the design. Briaud and Tucker listed the following events for where significant drag force and downdrag merits careful consideration in the design:

1. The total settlement of the ground surface will be larger than 4 inches.

2. The settlement of the ground surface after the piles are driven will be larger than 0.4 inches.

3. The height of the embankment placed on the ground surface exceeds 5 feet.

4. The thickness of the soft compressible layer is larger than 30 feet.

5. The water table will be lowered by more than 10 feet.

6. The piles will be longer than 80 feet.

7.3.6.1 Recommended Approach for Downdrag

Siegel et al. (2013) proposed a downdrag design approach using the neutral plane method within the LRFD framework. This approach is the FHWA recommended design method for downdrag. It does not treat the drag force as an additional load that must be supported. Rather, drag force is a settlement consideration in the geotechnical service limit state and is a structural consideration in the pile structural limit state. The approach recognizes that drag force develops on all piles, regardless of soil and loading conditions.

The information necessary to implement the downdrag analysis procedure includes:

- Unfactored structural loads to determine the permanent load.
- Defined subsurface stratigraphy with appropriate parameters for all layers.
- Soil behavior models to characterize load-deformation response, (instrumented load tests, or t-z and q-z models).
- Information on fill placement including amount, lateral extent, and timeline.

In the recommended approach, all loads and resistances should be unfactored. The use of factored loads or factored resistances will distort load-transfer relationships and lead to erroneous predictions of settlement and drag force.

STEP BY STEP PROCEDURE FOR DOWNDRAG ANALYSIS

STEP 1 Assume soil consolidation and ground settlement will occur.

STEP 2 Using an appropriate static analysis method for the pile type and subsurface conditions, determine the nominal shaft, mobilized toe, and total mobilized resistance as a function of pile penetration depth.

Shaft resistance is typically fully mobilized at relatively small pile movements of 0.10 inches or less. The full toe resistance however may require a toe movement as much as 4 to 5% of the pile diameter depending on the geomaterial at the pile toe. An assessment of the mobilized toe resistance magnitude can be made using engineering judgment along with t-z and q-z behavior in static analysis software, or from t-z and q-z values derived from instrumented static load tests.

Example output of the required static analysis results versus pile penetration depth is included in Figure 7-55. An illustration of the percentage toe resistance mobilized relative to the toe movement normalized by the pile diameter is presented in Figure 7-56.

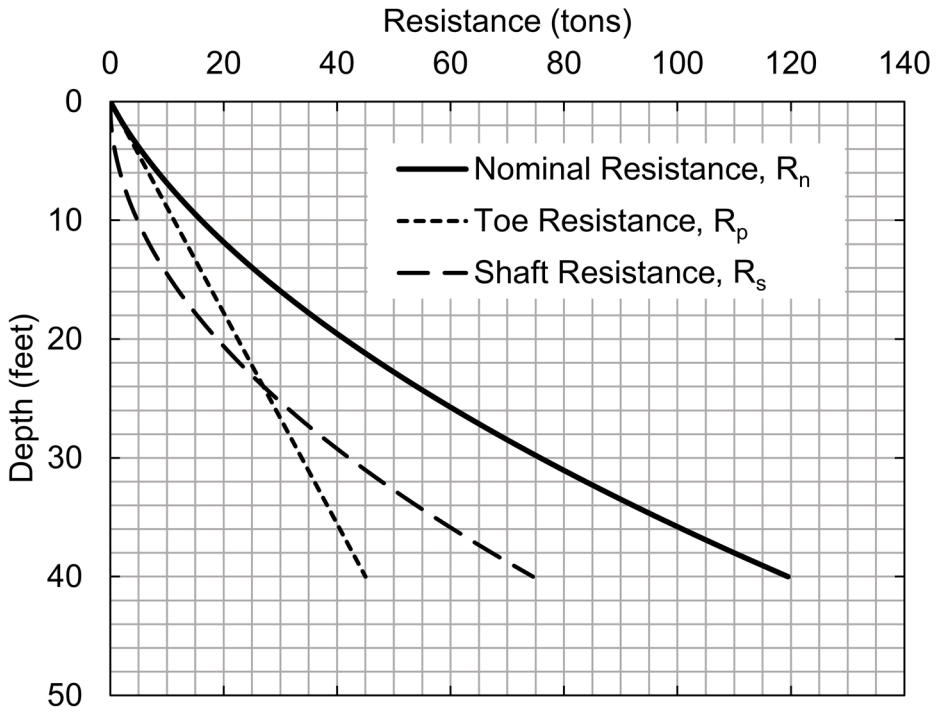

Figure 7-55 Plot of static analysis results (after Siegel et al. 2013).

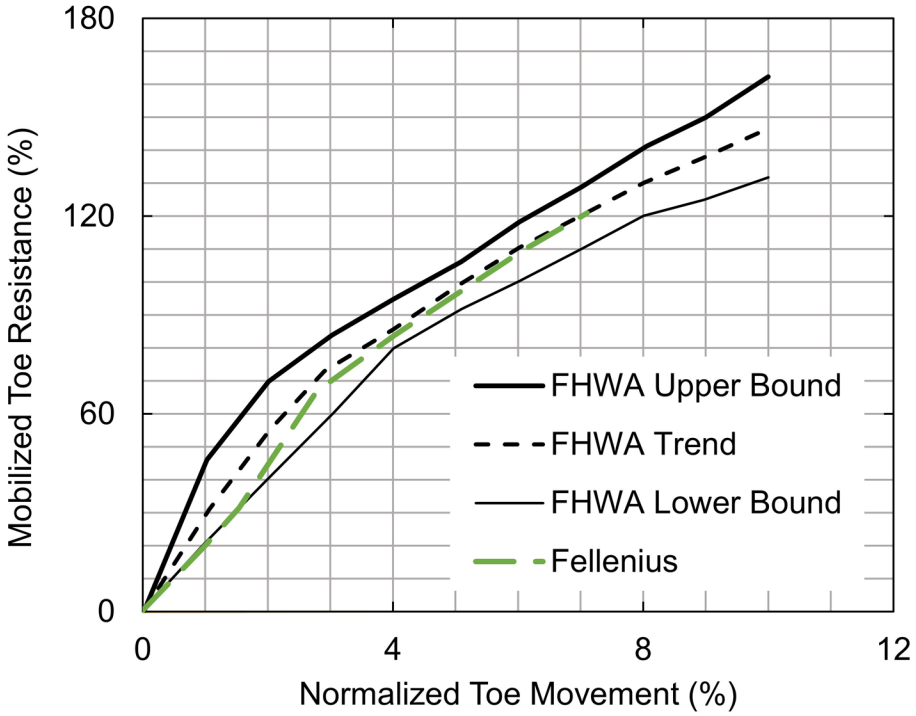

Figure 7-56 Plot of normalized toe resistance versus toe movement (after Siegel et al. 2013).

STEP 3 Select the pile toe elevation for analysis.

STEP 4 Develop the axial load and resistance versus depth diagram at the selected pile toe elevation.

Plot the accumulated shaft resistance versus depth ($\sum R_s$) from Step 2 on the load and resistance diagram. This is depicted by the solid line in Figure 7-57.

Determine the unfactored permanent load on the pile. Add the unfactored permanent load to the accumulated shaft resistance versus depth. This is indicated by the solid line in Figure 7-58.

Subtract the sum of the accumulated shaft resistance at a given depth from the nominal resistance at the selected the pile toe elevation ($R_n - \sum R_s$). Plot this resistance on the load and resistance diagram. This is denoted by dashed lines in Figure 7-59. Graphs a, b, and c, represent the total mobilized resistance based on the shaft resistance plus a

mobilized toe resistance of 100%, 50%, and 0% of the nominal toe resistance, respectively.

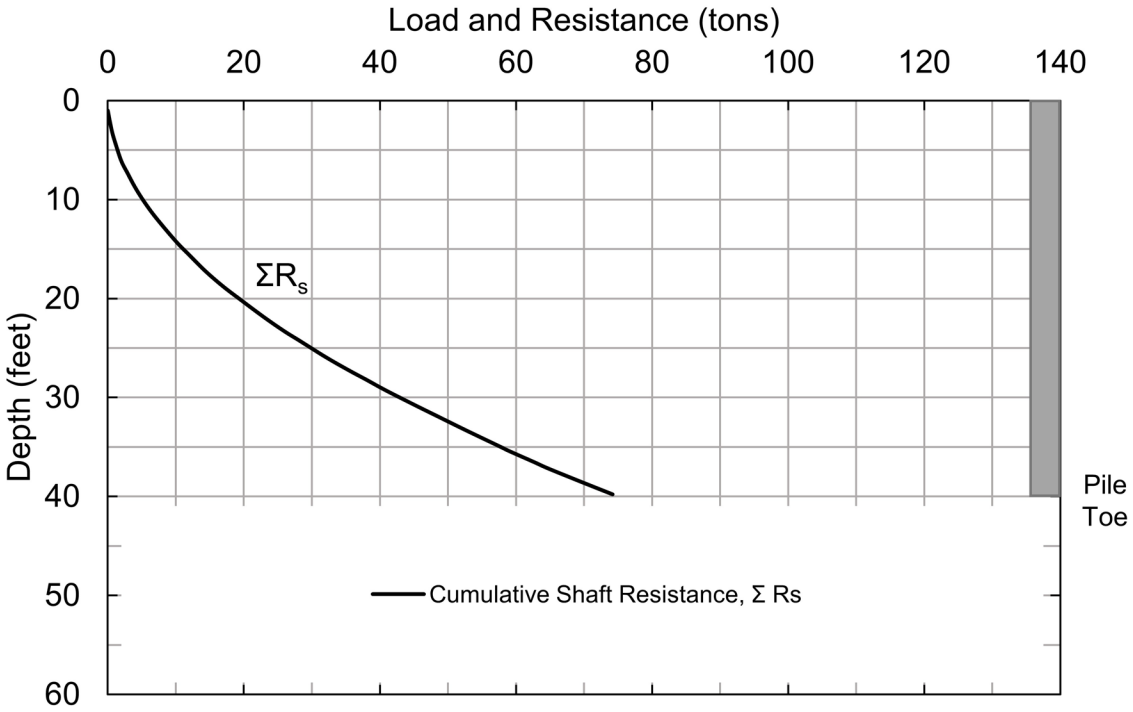

Figure 7-57 Axial load and resistance plot of cumulative shaft resistance vs. depth (after Siegel et al. 2013).

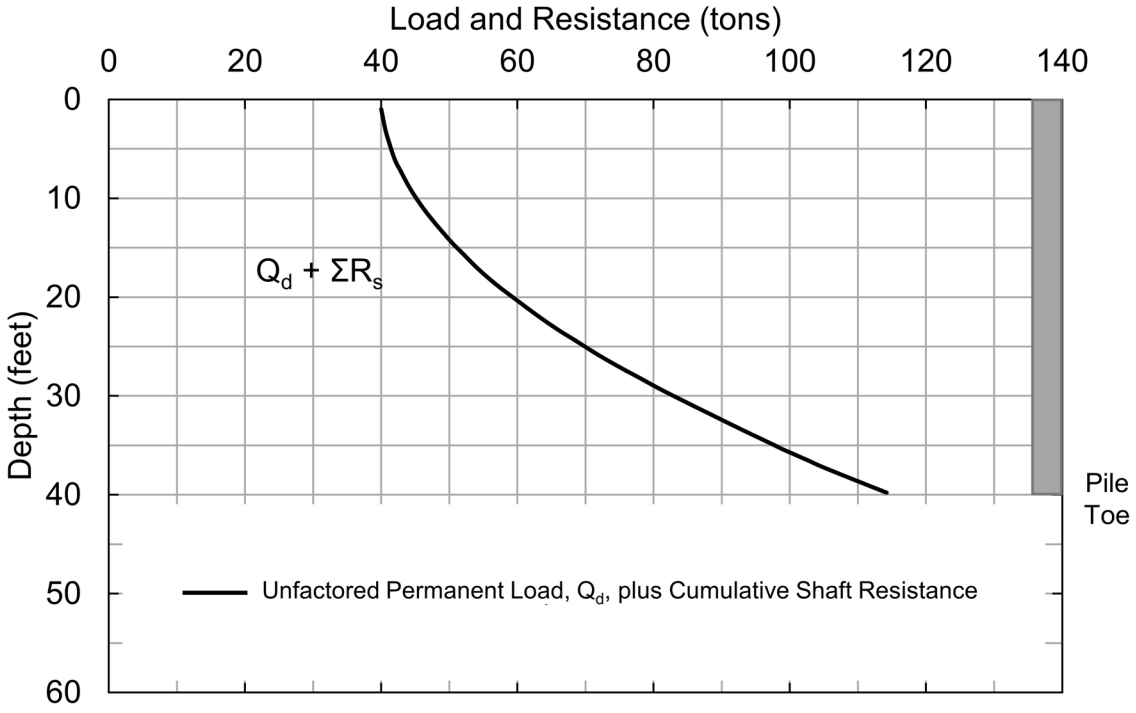

Figure 7-58 Axial load and resistance plot of unfactored permanent load plus cumulative shaft resistance vs depth (after Siegel et al. 2013).

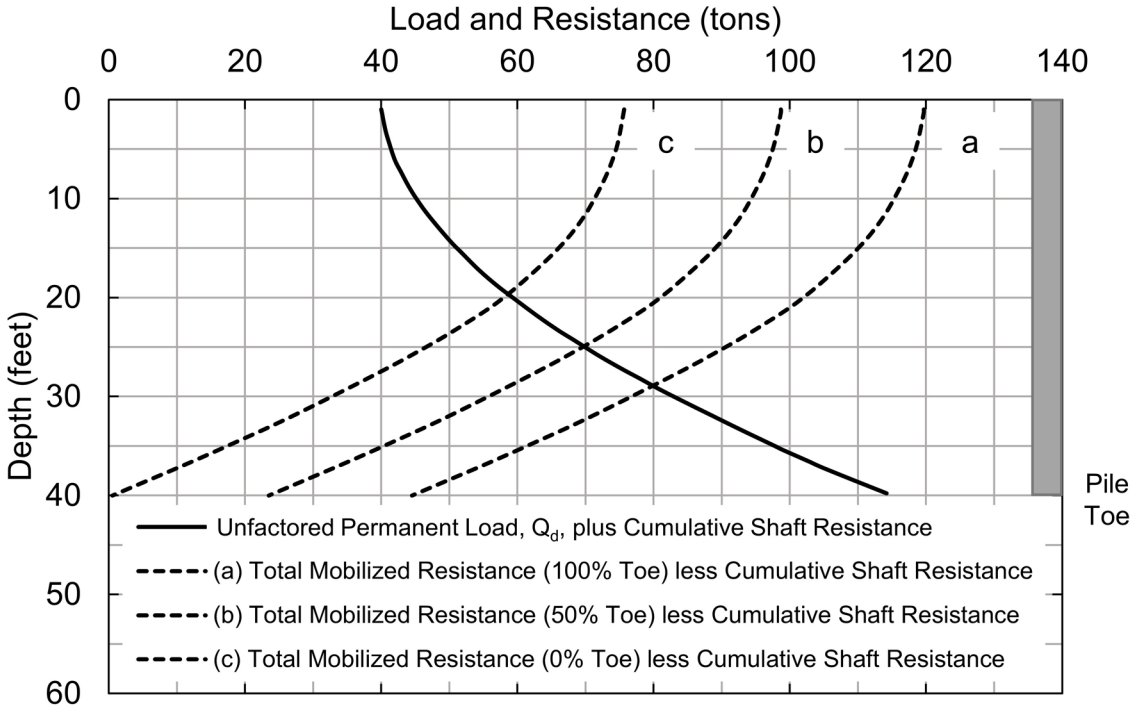

Figure 7-59 Axial load and resistance plot including mobilized resistances (after Siegel et al. 2013).

STEP 5 Determined the location of the neutral plane, the magnitude of the maximum axial compression load in the pile, and the magnitude of the drag force.

For the example given in Figure 7-60, the neutral plane occurs at depth A, B, or C, depending on the magnitude of the mobilized toe resistance. If 100% of the toe resistance is mobilized, the neutral plane occurs at a depth of 30 feet (point A), the maximum axial load in the pile is 80 tons, and the drag force is 40 tons (80 tons – 40 ton permanent pile head load). Conversely, if no toe resistance is mobilized, the neutral plane occurs at a depth of 20 feet (point C), the maximum axial load in the pile is 60 tons, and the drag force is 20 tons (60 tons – 40 ton permanent pile head load).

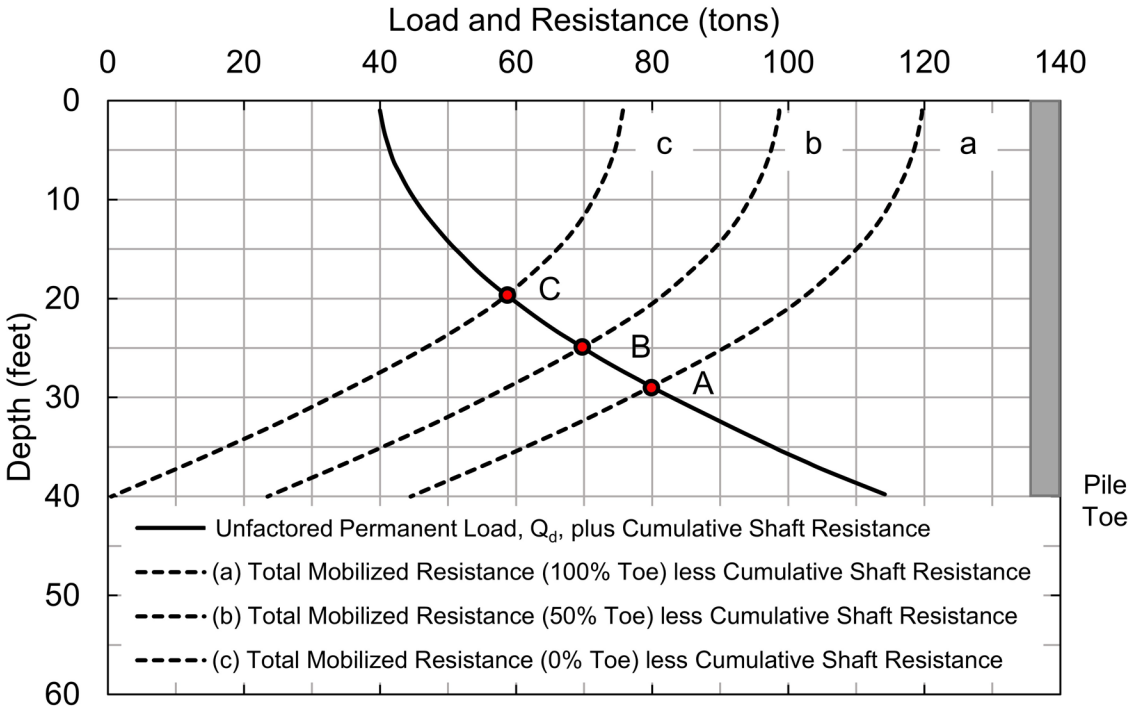

Figure 7-60 Axial Load and resistance plot including neutral plane location based on mobilized toe resistance (after Siegel et al. 2013).

STEP 6 Check the structural strength limit state due to loading conditions including drag force. The factored structural resistance of the pile in the strength limit state in axial compression, P_r, must exceed the factored permanent load and factored drag force per Equation 7-70.

$$1.25\ (Q_d) + \gamma_p(DF) < P_r \qquad \text{Eq. 7-70}$$

Where:

Q_d = permanent load on pile (kips).
DF = drag force on pile (kips).
γ_p = load factor for drag force in neutral plane analysis.
P_r = factored axial compression resistance of pile (kips).

An AASHTO load factor for drag force, γ_p, determined by static analysis methods using the neutral plane procedure is not yet available. Therefore, local calibration is required for implementation of this approach. The Minnesota DOT has adopted a load factor of 1.1 for drag force with the neutral plane downdrag procedure while a local calibration effort is in progress. This load factor was based on an equivalent minimum factor of safety 1.5 for material strength evaluation.

STEP 7 Calculate the settlement due to downdrag with respect to the neutral plane.

a. Calculate the thickness of compressible soil, t_{soil}, beneath the neutral plane.

$$t_{soil} = D_{il} - D_{np} \quad \text{Eq. 7-71}$$

Where:

t_{soil} = thickness of compressible soil beneath neutral plane (feet).
D_{il} = depth from reference to top of incompressible layer (feet).
D_{np} = depth from reference to neutral plane (feet).

b. Determine settlement due to downdrag from stress increase.

$$S_{dd} = t_{soil}\left(\frac{\gamma_p \Delta\sigma}{E_s}\right) \quad \text{Eq. 7-72}$$

Where:

S_{dd} = settlement due to downdrag (feet).
t_{soil} = thickness of compressible soil beneath neutral plane (feet).
γ_p = load factor for downdrag.
$\Delta\sigma$ = increase in vertical stress (ksf).
E_s = elastic modulus of in-situ soil (ksf).

It should be noted that effective stress changes such as approach fill placement after pile driving will alter the plot of the permanent load plus cumulative shaft resistance. This will in turn alter the location of the neutral plane, the maximum compression force in the pile, the magnitude of the drag force, and calculated settlement due to downdrag. Similarly, changes in the permanent load to be applied to the pile or changes in the pile toe elevation will also alter the analysis results.

7.3.6.2 Methods for Reducing Downdrag and Drag Force

In situations where the permanent load and drag force exceed the structural strength limit state, or where pile settlement exceeds the geotechnical service limit state, methods for mitigating the drag force should be evaluated. The following techniques have been used in cases with large drag forces:

a. Increase the structural resistance

In cases where the factored structural resistance is insufficient, the pile structural resistance may be increased by using a pile section with greater structural resistance. The use of a thicker wall section in a steel pipe pile, a heavier H-pile section of the same size, or use of higher strength pile materials are possible solutions. A larger pile size can also be evaluated although this will also increase the pile surface area and therefore drag force.

b. Increase the number of piles

An increase in the number of piles will result in a decrease in the permanent load carried per pile. This will reduce the maximum axial compression force carried by the pile section.

c. Reduce soil settlement by preloading

Preconsolidation of compressible soils can be achieved by preloading and consolidating the soils prior to pile installation. This approach is often used for bridge foundations in fill sections. Prefabricated vertical drains are often used in conjunction with preloading to shorten the time required for consolidation. Additional information on prefabricated vertical drains is available in “Prefabricated Vertical Drains,” FHWA RD 86/168 by Rixner et al. (1986) and in "Ground Improvement Methods" manual by Elias et al. (2004).

d. Use lightweight fill material

Construct structural fills using lightweight fill material to reduce the drag forces. Lightweight fill materials often used, depending upon regional availability, include geofoam, foamed concrete, wood chips, blast furnace slag, and expanded shales. Additional information on lightweight fills is available in Elias et al. (2004). Geofoam blocks being placed for embankment construction are shown in Figure 7-61.

e. Use a friction reducer

Bitumen coating and plastic wrap are two methods commonly used to reduce the friction at the pile-soil interface. Bitumen coatings should only be applied to the portion of the pile which will be embedded in the negative shaft resistance zone. Case histories on bitumen coatings have reported reductions in negative shaft resistance from as little as 47% to as much as 90%. Goudreault and Fellenius (1994) suggest that the reduction effect of bitumen may be analyzed by using an upper limit of 200 psf as the pile-soil shear resistance or adhesion in the bitumen coated zone.

Figure 7-61 Geofoam block approach embankment (courtesy MnDOT).

One of the major problems with bitumen coatings is protecting the coating during pile installation, especially when driving through coarse soils. An inexpensive solution to this problem is to weld an oversized collar around the pile where the bitumen ends. The collar opens an adequate size hole to permit passage of the bitumen for moderate pile lengths in fine grained soils. Figure 7-62 presents a photograph on an over-sized collar between the uncoated lower pile section and white washed bitumen coating on the upper pile section.

Bitumen coatings can also present additional construction problems associated with field coating and handling. The bitumen coating used must have relatively low viscosity to permit slippage during soil consolidation, yet high enough viscosity and adherence to insure the coating will stick to the pile surface during storage and driving. The bitumen must also have sufficient ductility to prevent cracking and spalling of the bitumen during handling and driving. Therefore, the climate at the time of pile installation should be considered in selection of the proper bitumen coating. The use of bitumen coatings can be quite successful provided proper construction control methods are followed. However, bitumen coatings should not be casually specified as the solution to drag forces.

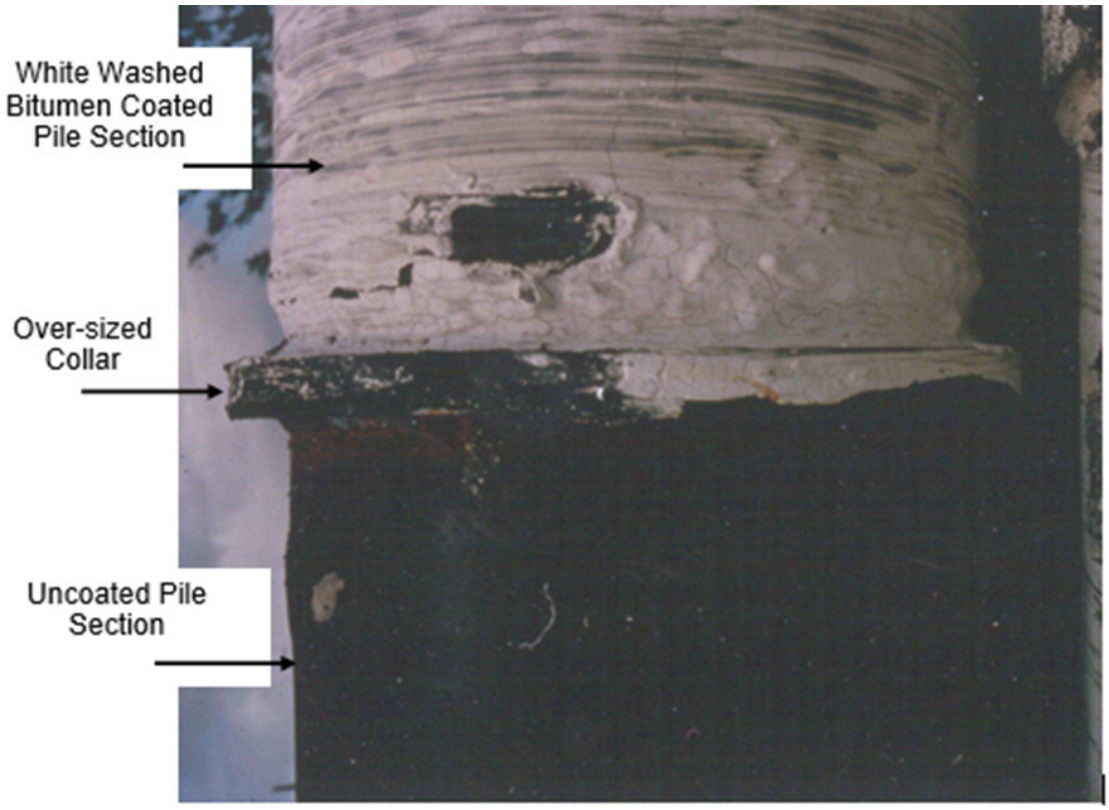

Figure 7-62 Over-sized collar for bitumen coating protection.

Plastic wrap has proven to be an economically attractive friction reducer, particularly for abutment piles driven behind and before construction of MSE walls. Tawfig (1994) performed laboratory tests on 0.006 inch thick polyethylene sheets used as a friction reducer. The laboratory test results indicated plastic wraps reduced the pile-soil shear resistance from between 78% for a one wrap layer to 98% for a two layer wrap with mineral oil lubricant. The laboratory test data indicated the pile-soil shear resistance of a one wrap layer was about 200 psf and only 20 psf for the lubricated two wrap system.

f. Prevent direct contact between soil and pile

Pile sleeves are sometimes used to eliminate direct contact between pile and soil. Bentonite slurry has been used in the past to achieve the same purpose. However these methods are generally more expensive and less effective than other solutions.

7.3.7 Horizontal Pile Foundation Deflection

Historically, designers often used prescriptive values for the lateral load resistance of vertical piles, or have added batter piles to increase a pile group's lateral resistance when it was believed that vertical piles could not provide the needed lateral resistance. However, vertical piles can be designed to withstand significant lateral loads. Modern analysis methods should be employed in the selection of the pile type and pile section.

Coduto (1994) notes that a foundation system consisting of only vertical piles designed to resist both axial and lateral loads is more flexible, and thus more effective at resisting dynamic loads, as well as less expensive to build. Bollman (1993) reported that the Florida Department of Transportation often uses only vertical piles to resist lateral loads, including ship impact loads because vertical piles are often less expensive than batter piles. In areas where seismic lateral loading is a serious concern, batter piles can deliver excessively large horizontal forces to the structure during the earthquake event. This phenomenon was observed during the Loma Prieta earthquake of 1989 in California and discussed in greater detail by Hadjian et al. (1992). In earthquake areas, lateral loads should be resisted by ductile vertical piles, and batter piles should be avoided whenever possible.

Sophisticated analysis methods are now readily available that allow the lateral load-deflection behavior of piles to be rationally evaluated. Lateral loads and moments on a vertical pile are resisted by the flexural stiffness of the pile and mobilization of resistance in the surrounding soil as the pile deflects. The flexural stiffness of a pile

is defined by the pile's modulus of elasticity, *E*, and moment of inertia, *I*. The geomaterial resistance to an applied lateral load is a combination of geomaterial compression and shear resistance, as shown in Figure 7-63.

The design of laterally loaded piles must evaluate both the pile structural response and geomaterial deformation to lateral loads. The nominal structural resistance must be determined. In addition, the pile deformation under the service loading conditions must be calculated and compared to foundation performance criteria.

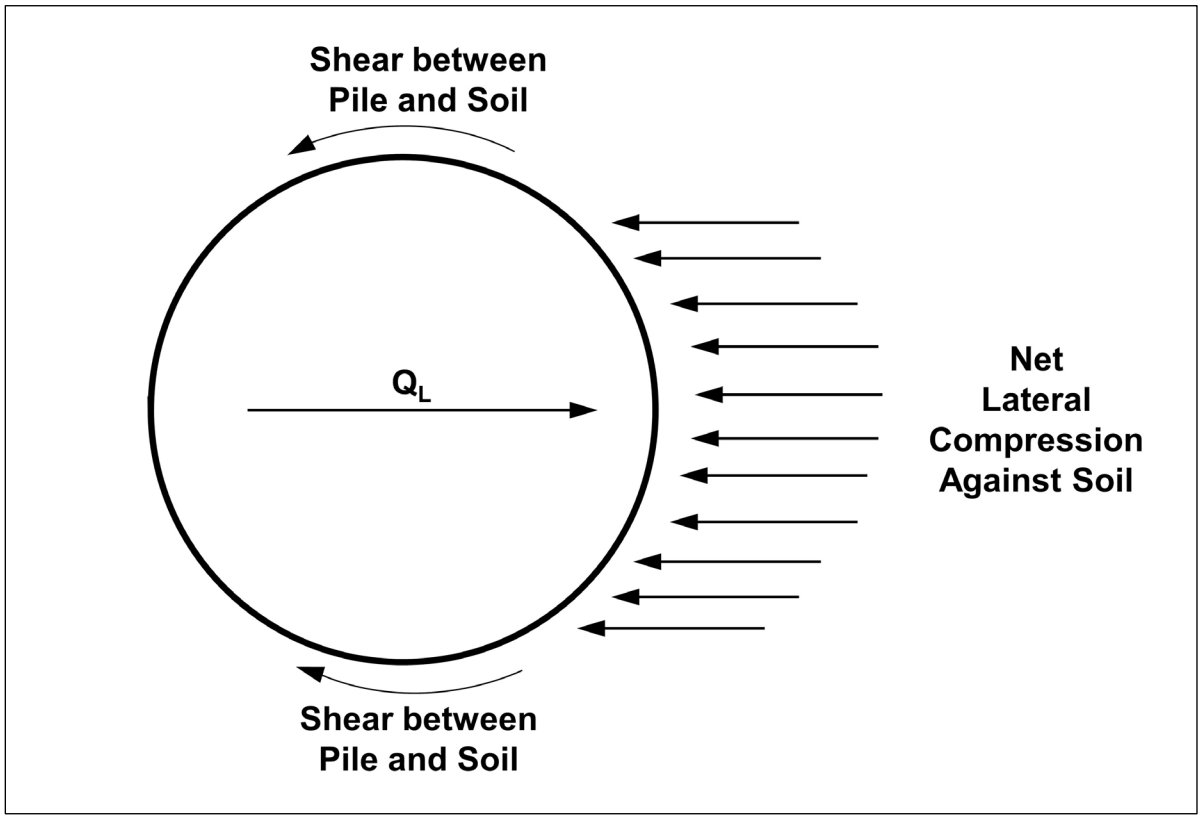

Figure 7-63 Soil resistance to a lateral pile load (after Smith 1989).

The design of laterally loaded piles requires the combined skills of the geotechnical and structural engineer. It is inappropriate for the geotechnical engineer to analyze a laterally loaded pile without a full understanding of pile-structure interaction. Likewise it is inappropriate for the structural engineer to complete a laterally loaded pile design without a full understanding of how pile section or spacing changes may alter the geotechnical response. Because of the interaction of pile structural and geotechnical considerations, the economical solution of lateral pile loading problems requires interdisciplinary coordination between the structural and geotechnical engineer.

Soil, pile, and load parameters have significant effects on the lateral resistance of piles. The factors influencing these parameters are as follows:

1. Geomaterial Parameters

    a. Soil or rock type and physical properties such as shear strength, friction, density, groundwater level, and moisture content.

    b. Coefficient of horizontal subgrade reaction in (pcf). This coefficient is defined as the ratio between a horizontal stress per unit area of vertical surface (psf) and the corresponding horizontal displacement (inches). For a given deformation, the greater the coefficient, the greater the lateral load resistance.

2. Pile Parameters

    a. Physical properties such as shape, material, and dimensions.

    b. Pile head conditions (rotational constraint, if any).

    c. Method of pile placement such as driving, jetting, etc.

    d. Group action.

3. Lateral Load Parameters

    a. Static (monotonic or cyclic) or dynamic.

    b. Eccentricity (moment coupled with shear force).

7.3.7.1 Pile Head Fixity

The pile to pile cap connection can behave as a pinned connection, fixed connection, or somewhere in between depending on the design detail. Wilson et al. (2006) summarized the design effect of pile to pile cap connection. If the pile extends only a nominal distance into the pile cap, it will behave as a pinned connection. A pinned connection provides restraint against translational movements but does not restrain rotation of the pile head relative to the cap. Conversely, a fixed connection requires the pile to be embedded two to three diameters into pile cap or

to be fitted with a specially designed connection. A fixed connection provides restraint against rotation and all directions of movement of the pile head relative to the pile cap.

At the service limit state, a pinned connection will typically have more horizontal movement than a fixed connection as illustrated in Figure 7-64. At the strength limit state, Figure 7-65 illustrates that a fixed head condition will generally result in a larger bending moment at the pile head compared to a pinned connection, but may or may not have larger bending moments below the pile head.

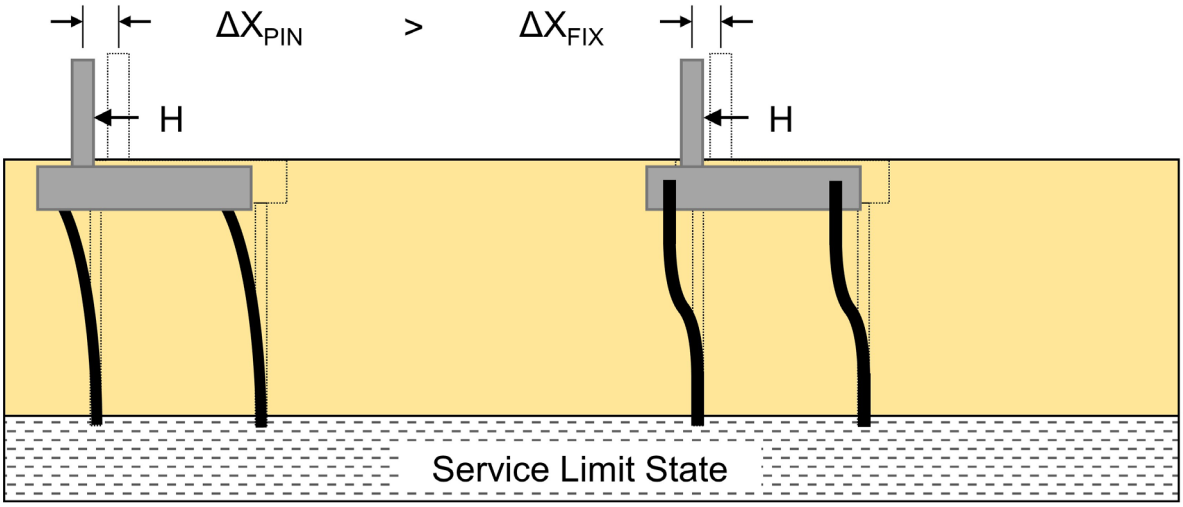

Figure 7-64 Effect of pile head fixity on translation at service limit state (after Wilson et al. 2006).

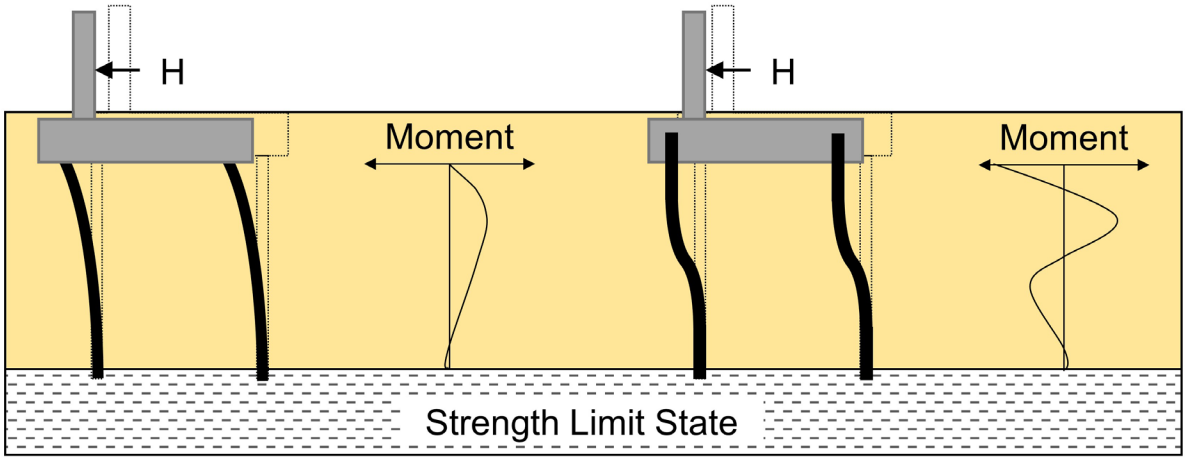

Figure 7-65 Effect of pile head fixity on moment in piles at strength limit state (after Wilson et al. 2006).

7.3.7.2 Lateral Design Methods

The basic design approaches for lateral soil resistance analysis of vertical piles consist of lateral load tests or analytical methods. Both of these approaches are described in greater detail in the following sections.

1. Lateral Load Tests

Full scale lateral load tests can be conducted at a site during either the design or construction stage. The load-deformation data obtained is used to finalize or confirm the design for the particular site. Factors such as loading rate, cyclic (single or multi-directional) versus monotonic application of design forces, and magnitude of axial load should be considered in developing appropriate field testing procedures. Lateral load tests may not be economically justifiable on many projects but are essential on projects controlled by lateral load demand. Chapter 9 provides additional details on lateral load test procedures and interpretation.

2. Analytical Methods

The analytical methods are based on theory and empirical data and permit the rational consideration of various site parameters. Two common approaches are Broms' (1964a, 1964b) hand calculation method, and Reese's (1984) computer solution. Both approaches consider the pile to be analogous to a beam on an elastic foundation. FHWA IP-84-11 by Reese (1984) presents details of both methods. Broms' method provides a relatively easy hand calculation procedure to determine lateral loads and pile deflections at the ground surface. Broms' method also ignores the axial load on the pile. As lateral load demand has increased along with the need for improved deformation estimates more detailed load-deformation computer analyses have become the norm.

Reese's p-y method is a more rigorous computer analysis that was originally available in the 1993 DOS based COM624 computer program which was developed under an FHWA research grant. That method is now incorporated in that program’s proprietary successor, the LPILE program (Isenhower and Wang 2014). The p-y method permits the inclusion of more complete modeling parameters of a specific problem. The program output provides distributions versus depth of moment, shear, soil and pile moduli, and soil resistance for the entire length of pile, including moments and shears in above ground sections.

For the design of all major pile foundation projects, the p-y method should be used. Some of the more common software programs that perform lateral loading analysis using the p-y method include LPILE, FBPIER, and ALLPILE. It should be emphasized that the FHWA does not endorse the use of any particular software program. However the p-y method, described further in the following section, is the FHWA recommended analysis method for lateral load design.

7.3.7.3 p-y Method

The interaction of a pile-soil system subjected to lateral load has long been recognized as a complex function of nonlinear response characteristics of both pile and soil. The most widely used nonlinear analysis method is the p-y method, where p is the soil resistance per unit pile length and y is the lateral soil or pile deflection. This method, illustrated in Figure 7-66, models the soil resistance to lateral load as a series of nonlinear springs. As noted previously, some of the more common software programs that perform lateral loading analysis using the p-y method include LPILE, FBPIER, and ALLPILE.

Reese (1984, 1986) has presented procedures for describing the soil response surrounding a laterally loaded pile for various soil conditions by using a family of p-y curves. The procedures for constructing these curves are based on experiments using full sized, instrumented piles and theories for the behavior of soil and rock under stress.

The geomaterial modulus subgrade reaction is defined as follows:

$$k = -\frac{p}{y} \qquad \text{Eq. 7-73}$$

Where:

k = modulus of subgrade reaction (psi).
p = soil resistance per unit pile length (lbs/inch).
y = lateral deflection (inch).

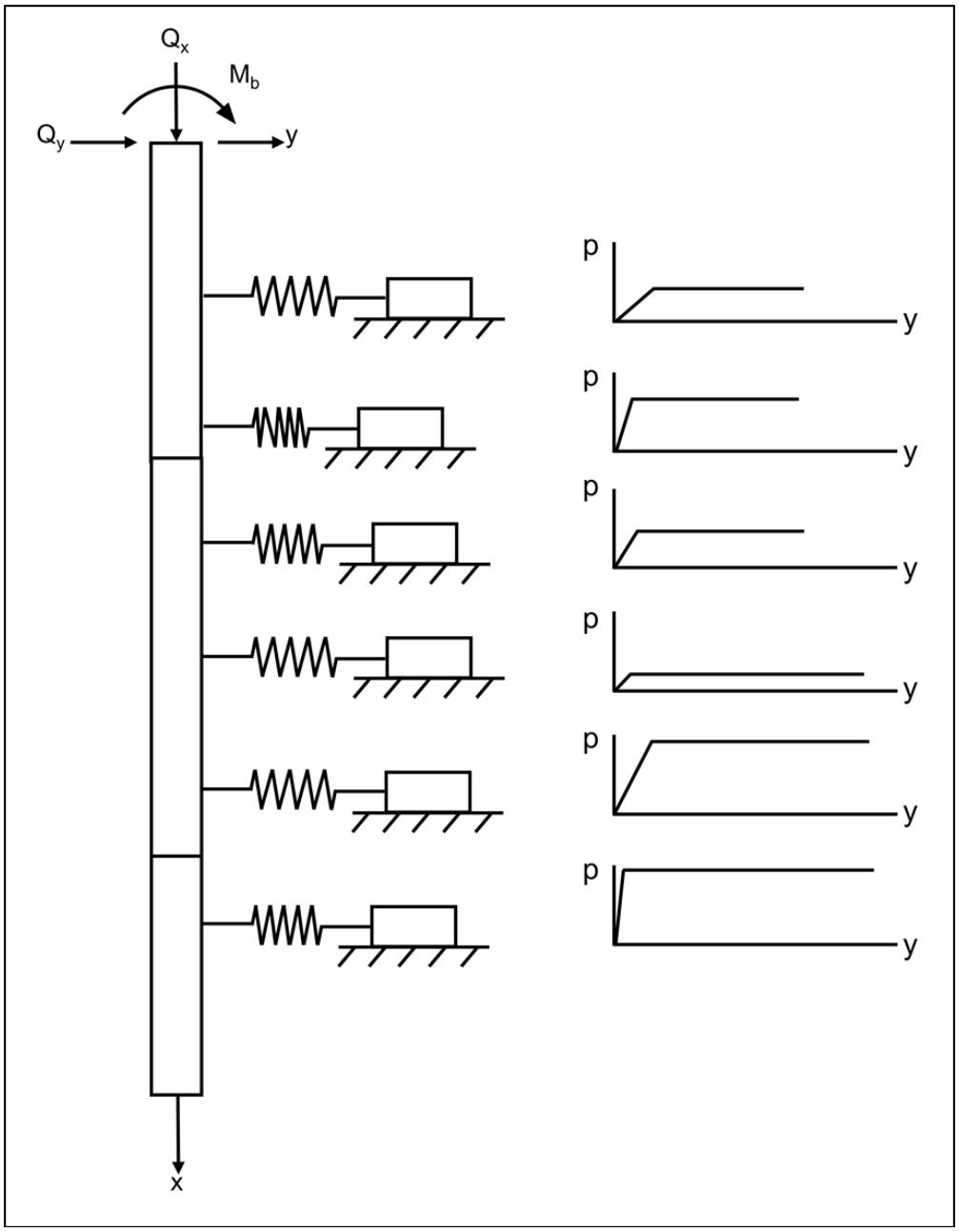

Figure 7-66 Typical lateral analysis pile-soil model.

The negative sign indicates that the ground resistance opposes pile deflection. The ground's modulus is the secant modulus of the p-y curve and is not constant except over a small range of deflections. Typical p-y curves are shown in Figure 7-67. Ductile p-y curves, such as curve A, are typical of the response of soft clays under static loading and sands. Brittle p-y curves, such as curve B, can be found in some stiff clays under dynamic loading conditions.

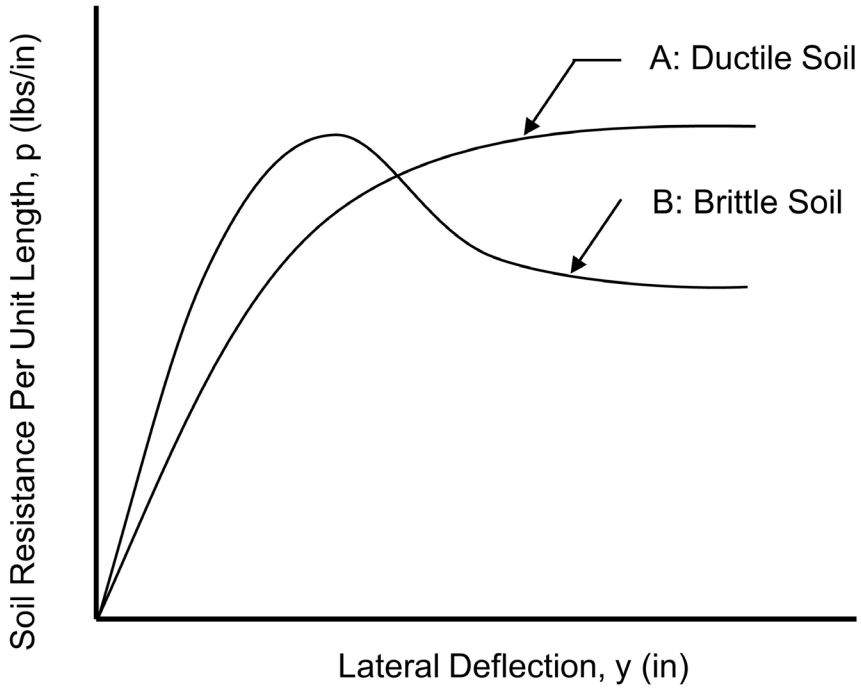

Figure 7-67 Typical p-y curves for ductile and brittle soil (after Coduto 1994).

The factor most influencing the shape of the p-y curve is the soil properties. However, the p-y curves also depend upon depth, soil stress strain relationships, pile width, water table location, and loading conditions (static or cyclic). Representative values for the clay ε_{50} strain parameter are provided in Table 7-21 while modulus of subgrade reaction values for clays and sand are shown in Table 7-22. Procedures for constructing p-y curves for various soil and water table conditions as well as static or cyclic loading conditions are typically provided in the p-y program documentation.

Table 7-21 Representative Values of ε_{50} for Clays

Clay Consistency	Average Undrained Shear Strength, s_u, (ksf)	ε_{50}
Soft Clay	0.25 – 0.50	0.02
Medium Clay	0.50 - 1.0	0.01
Stiff Clay	1.0 – 2.0	0.007
Very Stiff Clay	2.0 – 4.0	0.005
Hard Clay	4.0 – 8.0	0.004

Table 7-22 Representative Modulus of Subgrade Reaction Values, k_s *and* k_c, for Clays and Sands

Soil Type	Avg. Undrained Shear Strength, s_u, (ksf)	Soil Condition Relative to Water Table	k_s - Static Loading (pci)	k_c – Cyclic Loading (pci)
Soft Clay	0.25 - 0.50	---	30	---
Medium Clay	0.50 - 1.0	---	100	---
Stiff Clay	1.0 – 2.0	---	500	200
Very Stiff Clay	2.0 – 4.0	---	1000	400
Hard Clay	4.0 – 8.0	---	2000	1000
Loose Sand	---	Submerged	20	20
Loose Sand	---	Above	25	25
Med Dense Sand	---	Submerged	60	60
Med Dense Sand	---	Above	90	90
Dense Sand	---	Submerged	125	125
Dense Sand	---	Above	225	225

The p-y programs solve the nonlinear differential equations representing the behavior of the pile-soil system to lateral (shear and moment) loading conditions in a finite difference formulation using Reese's p-y method of analysis. The strongly nonlinear reaction of the surrounding soil to pile-soil deflection is represented by the p-y curve prescribed to act on each discrete element of the embedded pile. For each set of applied boundary (static) loads the program performs an iterative solution which satisfies static equilibrium and achieves an acceptable compatibility between force and deflection (p and y) in every element.

The shape and discrete parameters defining each individual p-y curve may be input by the user or generated by the program. Layered soil systems are characterized by conventional geotechnical data including soil type, shear strength, density, depth, and stiffness parameters, and whether the loading conditions are monotonic or cyclic in nature.

For batter piles, Awoshika and Reese (1971) proposed a modifying constant ranging from 0 to 2 be applied to the p_{ult} value based on the direction of the applied lateral load relative to the orientation of the pile batter. This modifying constant proportionally modifies the p-values. If the pile head is inclined away from the

direction of the horizontal load, the modifying constant ranges from 1 to 2. If the pile head is inclined toward the applied horizontal load the modifying constant ranges from 1 to 0. With this approach, predicted behavior has been reported to reasonable agree with lateral test results on outwardly battered piles but less successful for inwardly battered piles. Hence, full scale load tests to better evaluate batter pile response should be considered on important projects.

The influence of applied loads (axial, lateral and moment) at each element can be modeled with flexural rigidity varying as a function of applied moment. In this manner, progressive flexural damage such as cracking in a reinforced concrete pile can be treated more rigorously. Programs typically include a subroutine which calculates the value of flexural rigidity at each element under the boundary conditions and resultant pile-soil interaction conditions.

Typical p-y analysis output summarizes the input information and the analysis results. The input data summarized includes the pile geometry and properties, and soil strength data. Output includes the generated p-y curves at various depths below the pile head and the computed pile deflections, bending moments, stresses and soil moduli as functions of depth below the pile head. This information allows an analysis of the pile's structural resistance. Internally generated (or input) values of flexural rigidity for cracked or damaged pile sections are also output. Graphical output presentations versus depth include the computed deflection, slope, moment, and shear in the pile, and soil reaction forces similar to those illustrated in Figure 7-68.

The p-y analyses characterize the behavior of a single pile under lateral loading conditions. A detailed view is obtained of the load transfer and structural response mechanisms to design conditions. Considerable care is required in extrapolating the results to the behavior of pile groups (pile-soil-pile interaction, etc.), and accounting for the effects of different construction processes such as predrilling or jetting.

In any lateral analysis case, the analyst should verify that the intent of the modeling assumptions, all elastic behavior for example, is borne out in the analysis results. When a lateral load test is performed, the measured load-deflection results versus depth should be plotted and compared with the analysis predicted behavior so that an evaluation of the validity of the p-y curves used for design can be made. Figure 7-69 illustrates a comparison between the measured load–deflection curve and one predicted by COM624P.

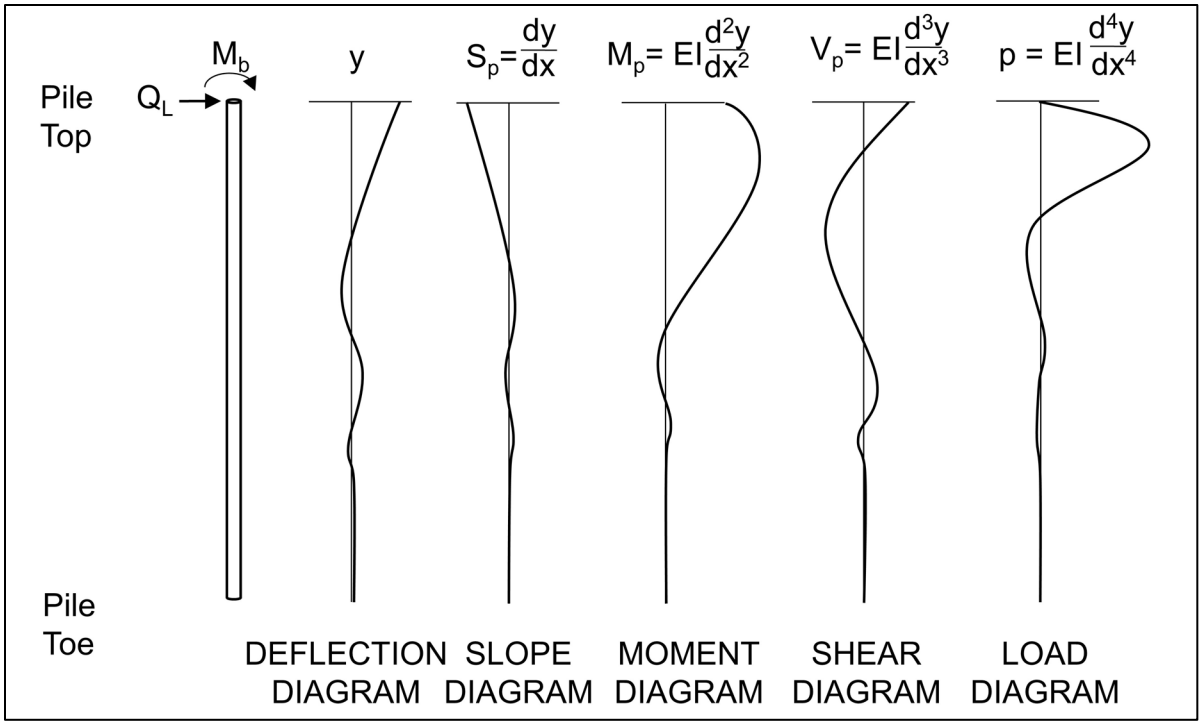

Figure 7-68 Graphical presentation of p-y analysis results (after Reese 1986).

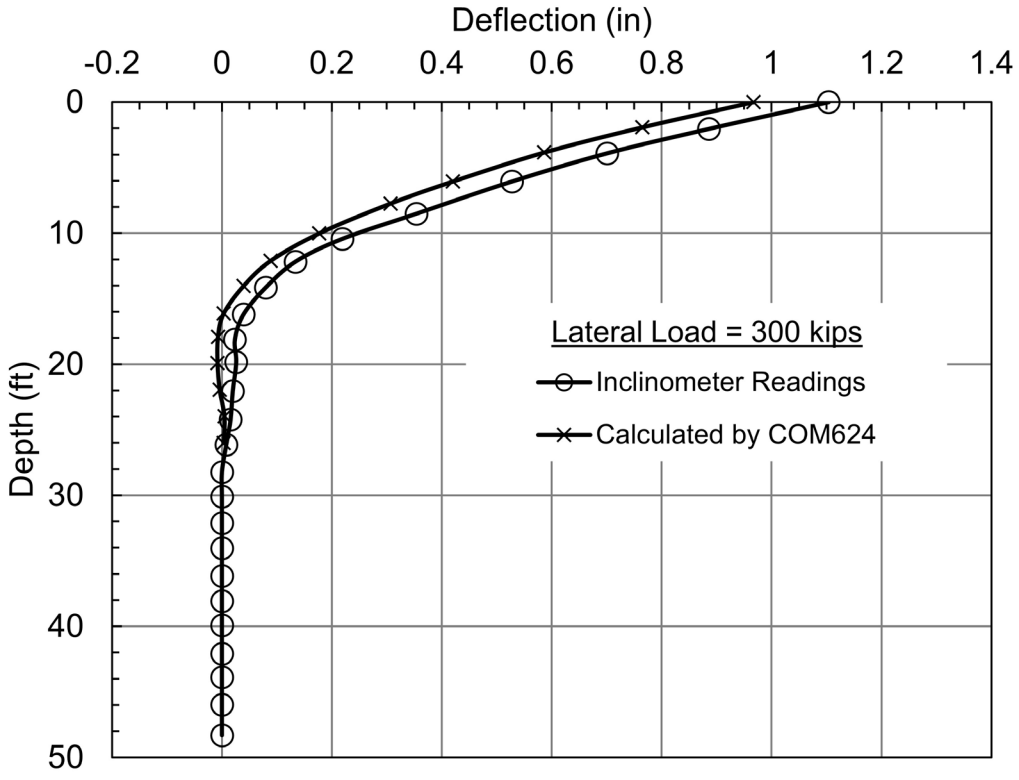

Figure 7-69 Comparison of measured and COM624P predicted load-deflection behavior versus depth (after Kyfor et al. 1992).

7.3.7.4 Strain Wedge Method

The p-y methods are generally applicable to piles that have the ability to bend and deflect. For short, stiff, piles, the strain wedge (SW) method may be a more realistic modeling approach as a short stiff pile tends to rotate rather than bend. Background details on the strain wedge method are provided in Norris (1986) and Ashour et al. (1998a).

In the strain wedge method, a passive soil wedge is modelled to resist lateral pile loads. A three dimensional wedge is incorporated into the beam on elastic foundation problem and can accommodate variations in shape, depth, loading and pile deflection due to changes in strain. Additional research with this model has added the use of multiple soil layers and the effect of pile head conditions (Ashour et al. 2002). Within the wedge, the mobilized strains form the relationship between passive resistance and horizontal displacement as shown in Figure 7-70.

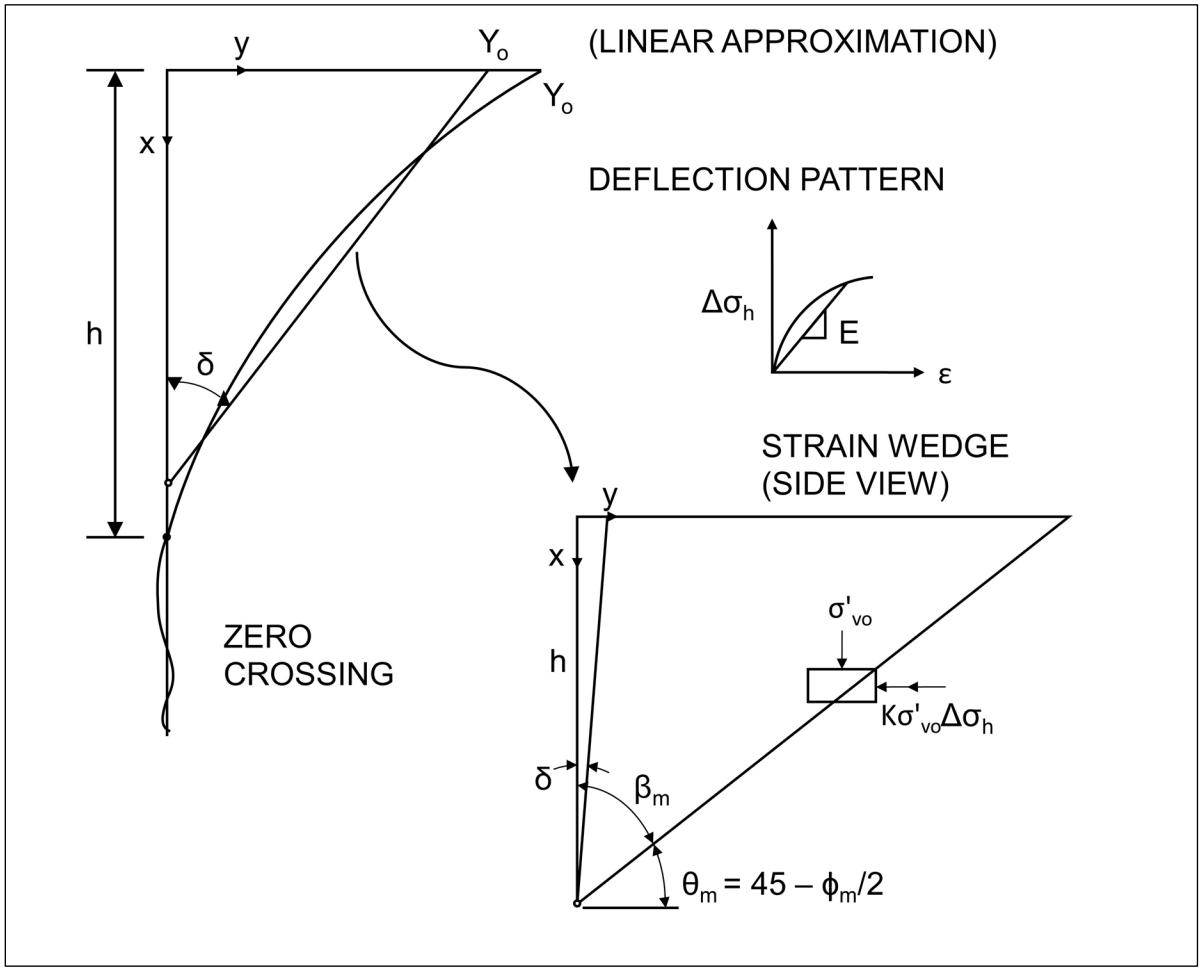

Figure 7-70 Strain wedge developed in soil (after Ashour et al. 1998a).

The soil stress-strain behavior can be estimated or directly incorporated from laboratory tests and included in the wedge profile. For the so called multi-sublayer technique, individual soil parameters are assigned for each respective soil layer in the wedge. The wedge shape changes with variations in soil properties as depicted in Figure 7-71. This analysis method therefore offers a potential benefit over traditional p-y modeling; the elastic springs are not independently modeled along the continuous pile length as shown in Figure 7-72. In addition, pile group effects are addressed from the overlapping wedges of each pile in the group.

Implementation of the SW method may be performed with software such as the Deep Foundation System Analysis Program (DFSAP), and has shown positive correlation with measured pile response from field tests (Ashour et al. 1998a). However widespread use of DFSAP has yet to occur, and many transportation agencies continue to use p-y based lateral pile analyses.

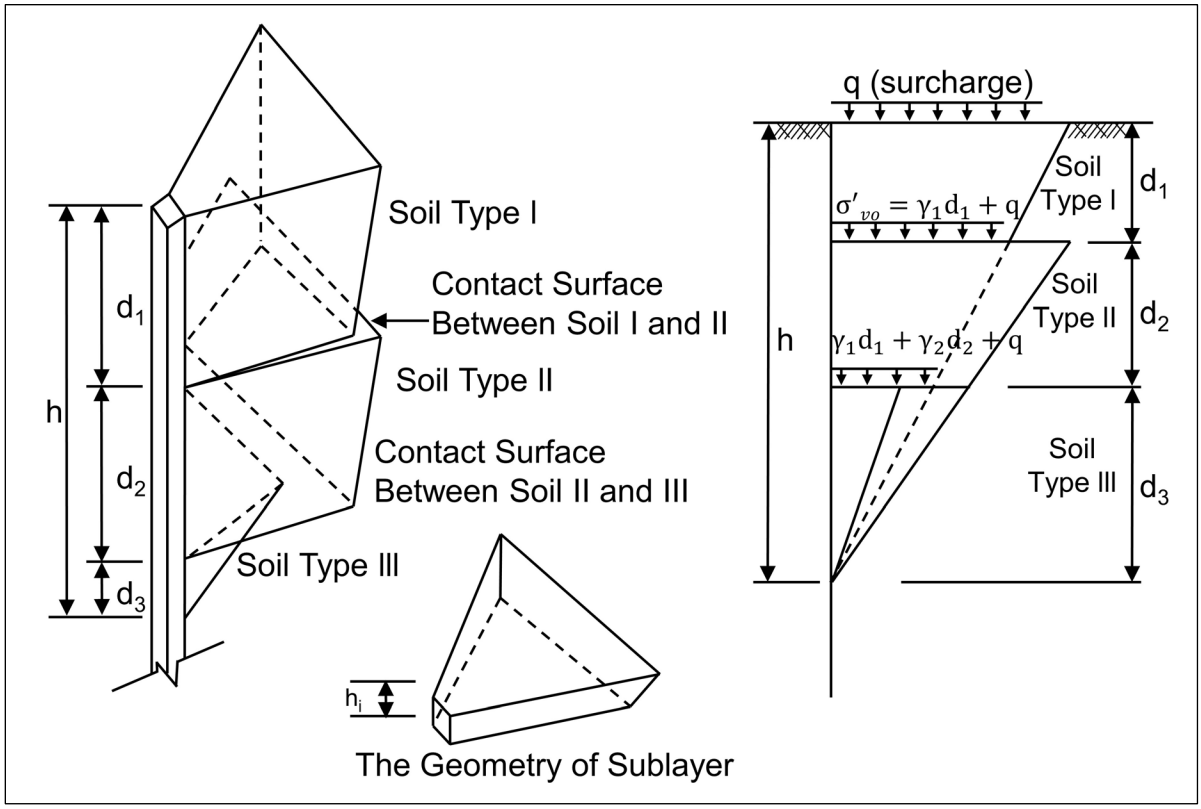

Figure 7-71 Proposed geometry of compound passive wedge (after Ashour et al. 1998a).

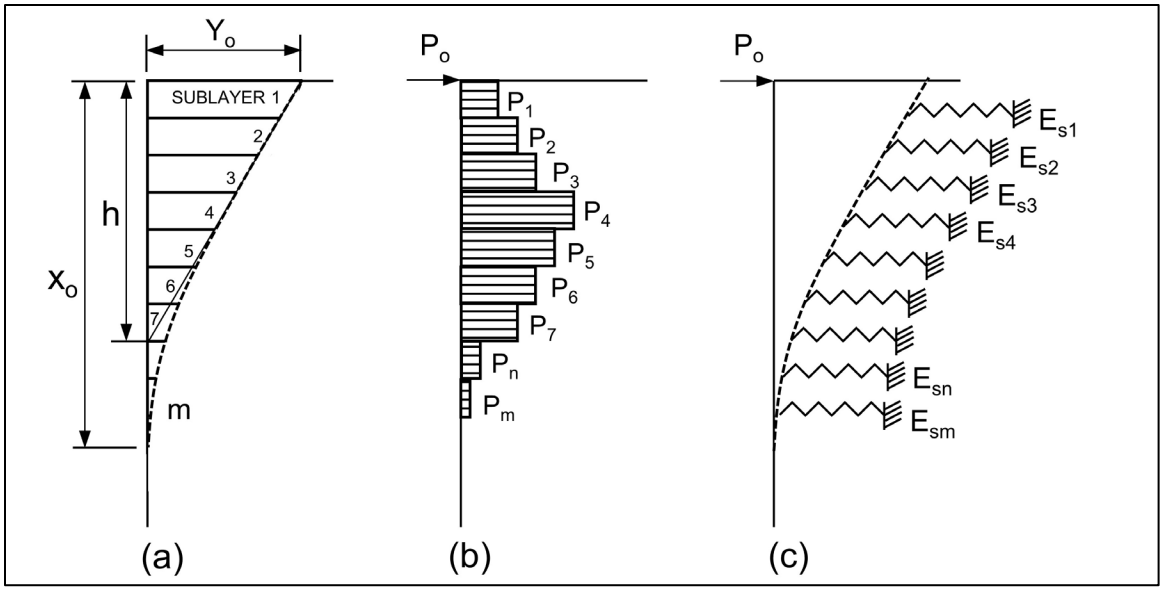

Figure 7-72 Soil-pile interaction with multiple soil layers (after Ashour et al. 1998a).

7.3.7.5 Single Piles

Lateral analysis software readily performs lateral analysis for a single pile. The applied loads to be analyzed should be factored loads (at the respective strength, service, and extreme event limit states) while the geotechnical resistance has a resistance factor of 1.0 per AASHTO (2014). Pile bents frequently consist of a single row of piles. Therefore, these are modeled as a single pile along the alignment of a bridge, and as a pile group in the perpendicular axis. More frequently, piles are installed in groups with two or more rows of piles. The following section addresses lateral pile analysis in greater detail with content applicable to both a single pile (lead row) and pile groups.

7.3.7.6 Pile Groups

The ability of a pile group to resist lateral loads from vessel impact, debris, wind, or wave loading, seismic events, and other sources is a significant design issue. The deflection of a pile group under a lateral load is typically 2 to 3 times larger than the deflection of a single pile loaded to the same intensity. Holloway et al. (1981) and Brown et al. (1988) reported that piles in trailing rows of pile groups (nearest the point of load application) have significantly less resistance to a lateral load than piles in the lead row, and therefore exhibit greater deflections. This is due to the pile-soil-pile interaction that takes place in a pile group. The pile-soil-pile interaction results in the lateral resistance of a pile group being less than the sum of the lateral resistance of the individual piles comprising the group. Hence, laterally loaded pile groups have a group efficiency of less than 1.

The lateral resistance of an individual pile in a pile group is a function of its position in the group and the center to center pile spacing. Brown et al. (1988) proposed a p-multiplier, P_m, be used to modify the p-y curve of an individual pile based upon the piles row position. An illustration of the p-multiplier concept is presented in Figure 7-73. For piles in a given row, the same P_m value is applied to all p-y curves along the length of the pile. In a lateral load test of a 3 by 3 pile group in very dense sand with a center to center pile spacing of 3b, Brown found the leading row of piles had a P_m of 0.8 times that of an individual pile. The P_m values for the middle and back row of the group were 0.4 and 0.3, respectively.

McVay et al. (1995) performed centrifuge model tests on a 3 by 3 pile group having center to center pile spacings of 3b and 5b. A dense and loose sand condition was simulated in the centrifuge model tests. For the dense sand case at a center to center spacing of 3b, the centrifuge model test results were similar to Brown's field results. However, McVay also found that the P_m values were influenced by soil density and the center to center spacing. The P_m results from McVay's centrifuge tests as well as other recent results for vertical piles in 3 x 3 pile groups are summarized in Table 7-23. McVay's centrifuge tests indicated lateral load group efficiencies in sands on the order of 0.74 for a center to center pile of 3b and 0.93 for a center to center spacing of 5b. Field studies in cohesive soils have also shown that pile-soil-pile interaction occurs. Brown et al. (1987) reported P_m values of 0.7, 0.5, and 0.4 for the lead, second, and third row of a laterally loaded pile group in stiff clays.

Additional work on this topic has included full scale lateral load testing of a 16 pile group in loose sand by Ruesta and Townsend (1997), and a 9 pile group in clayey silt by Rollins et al. (1998). A scaled model study of a cyclically laterally loaded pile group in medium clay has also been reported by Moss (1997). The center to center pile spacing, P_m results, and pile head deflections reported in these studies are included in Table 7-23. NCHRP Project 24-09 entitled “Static and Dynamic Lateral Loading of Pile Groups” was also completed by Brown et al. (2001). The objective of this study was to develop and validate an improved design method for pile groups subjected to static and dynamic lateral loads. The information summarized in Table 7-23 has been averaged and incorporated into AASHTO (2014). However, the distinction between soil type and test type is not made. The designer should consider if other p-multiplier, P_m, values may be more applicable in situations similar to those described in Table 7-22 which have comparatively lower P_m values than AASHTO.

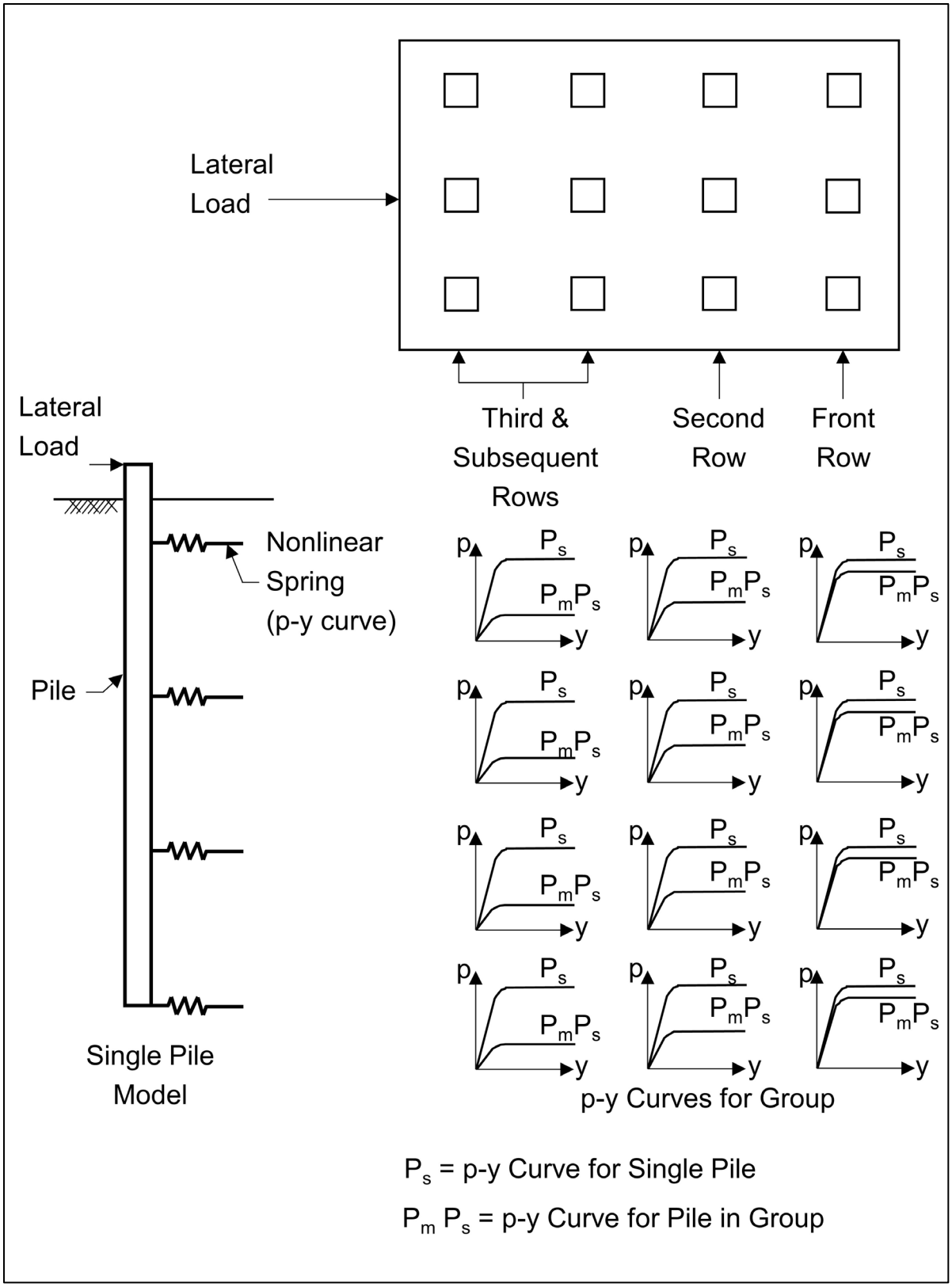

Figure 7-73 Illustration of p-multiplier concept for lateral group analysis.

Table 7-23 Laterally Loaded Pile Group Studies

Soil Type	Test Type	Center to Center Pile Spacing	Calculated p-Multipliers, P_m For Rows 1, 2, & 3+	Deflection, inches	Reference
Stiff Clay	Field Study	3b	0.70, 0.50, 0.40	2	Brown *et al*. (1987)
Stiff Clay	Field Study	3b	0.70, 0.60, 0.50	1.2	Brown *et al*. (1987)
Stiff Clay	Field Study	3.3b	0.82, 0.61, 0.45	3.5	Rollins *et al.* (2006)
Stiff Clay	Field Study	4.4b	0.90, 0.80, 0.69	1.6	Rollins *et al*. (2006)
Stiff Clay	Field Study	5.65b	0.95, 0.88, 0.77	2.6	Rollins *et al*. (2006)
Medium Clay	Scale Model-Cyclic Load	3b	0.60, 0.45, 0.40	2.4 at 50 cycles	Moss (1997)
Clayey Silt	Field Study	3b	0.60, 0.40, 0.40	1.0 - 2.4	Rollins *et al*. (1998)
V. Dense Sand	Field Study	3b	0.80, 0.40, 0.30	1	Brown *et al*. (1988)
M. Dense Sand	Centrifuge Model	3b	0.80, 0.40, 0.30	3	McVay *et al*. (1995)
M. Dense Sand	Centrifuge Model	5b	1.0, 0.85, 0.70	3	McVay *et al*. (1995)
Loose M. Sand	Centrifuge Model	3b	0.65, 0.45, 0.35	3	McVay *et al*. (1995)
Loose M. Sand	Centrifuge Model	5b	1.0, 0.85, 0.70	3	McVay *et al*. (1995)
Loose F. Sand	Field Study	3b	0.80, 0.70, 0.30	1-3	Ruesta *et al*. (1997)

Brown and Bollman (1993) proposed a p-multiplier procedure for the design of laterally loaded pile groups. It is recommended that this approach, outlined in the step by step procedure that follows, be used for the design of laterally loaded pile groups. For a center to center pile spacing of 3b, AASHTO (2014) design specifications recommend p-multiplier, $P_{m,}$ values of 0.8 for the lead row, 0.4 for the second row, and 0.3 for the third and subsequent rows. For a center to center pile spacing of 5b, the AASHTO specified P_m values are 1.0 for the lead row, 0.85 for the second row, and 0.7 for the third and subsequent rows. For center to center pile spacing between 3B and 5B, interpolation is recommended to determine the

appropriate P_m value. Figure 7-74 shows typical load and moment versus deflection plots from this procedure which can be performed using multiple individual analyses with a p-y software program. The analyses can also be performed with less effort using pile group software such as the FB-Pier, FB-MultiPier or GROUP computer programs.

The computer program FB-Pier was developed with FHWA support as the primary design tool for analysis of pile groups under axial and lateral loads. This program, which is a successor of the LPGSTAN program by Hoit and McVay (1994) is a non-linear, finite element analysis, soil structure interaction program. FB-Pier uses a p-multiplier approach in evaluation of laterally loaded pile groups under axial, lateral, and combined axial and lateral loads. The program is capable of analyzing driven pile and drilled shaft foundation supported sound walls, retaining walls, signs and high mast lighting. FB-MultiPier replaced FB-Pier and functions similarly. FB-Multipier contains additional features and can apply loading variations from multiple piers connected by bridge spans.

Fayyazi et al. (2012) studies the effects of the center to center pile spacing between rows as well as the spacing between piles within the same row in two model pile groups in sand. They observed that the spacing within a row can have a significant effect of the lateral pile group resistance due to the edge effects from overlapping zones of influence between two piles in the same row. They found that edge effects can result in overestimating the lateral load resistance by as much as 30%. Their research is ongoing with the goal of providing a procedure of p-multiplier selection that considers both row and inter row pile spacing within a group.

STEP BY STEP DESIGN PROCEDURE FOR LATERALLY LOADED PILE GROUPS USING LATERAL SINGLE PILE ANALYSIS

STEP 1 Obtain factored lateral loads.

STEP 2 Develop p-y curves for single pile.

a. Obtain site specific single pile p-y curves from instrumented lateral pile load test at site.

b. Use p-y curves based on published correlations with soil properties.

c. Develop site specific p-y curves based on in-situ test data.

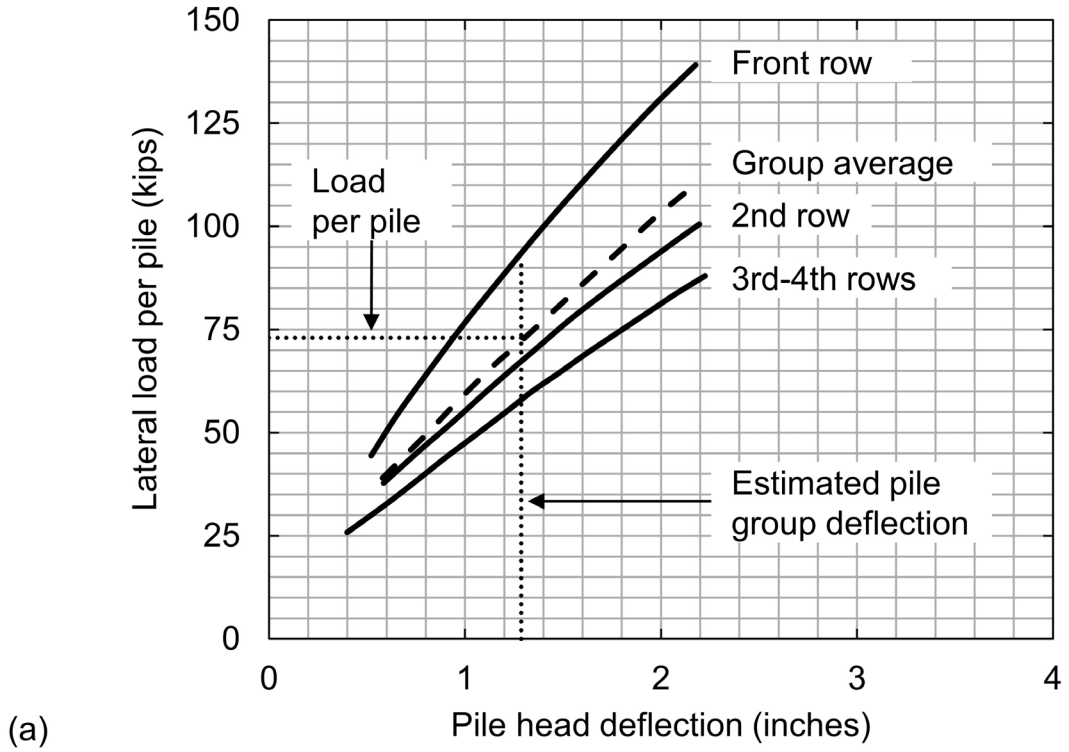

(a)

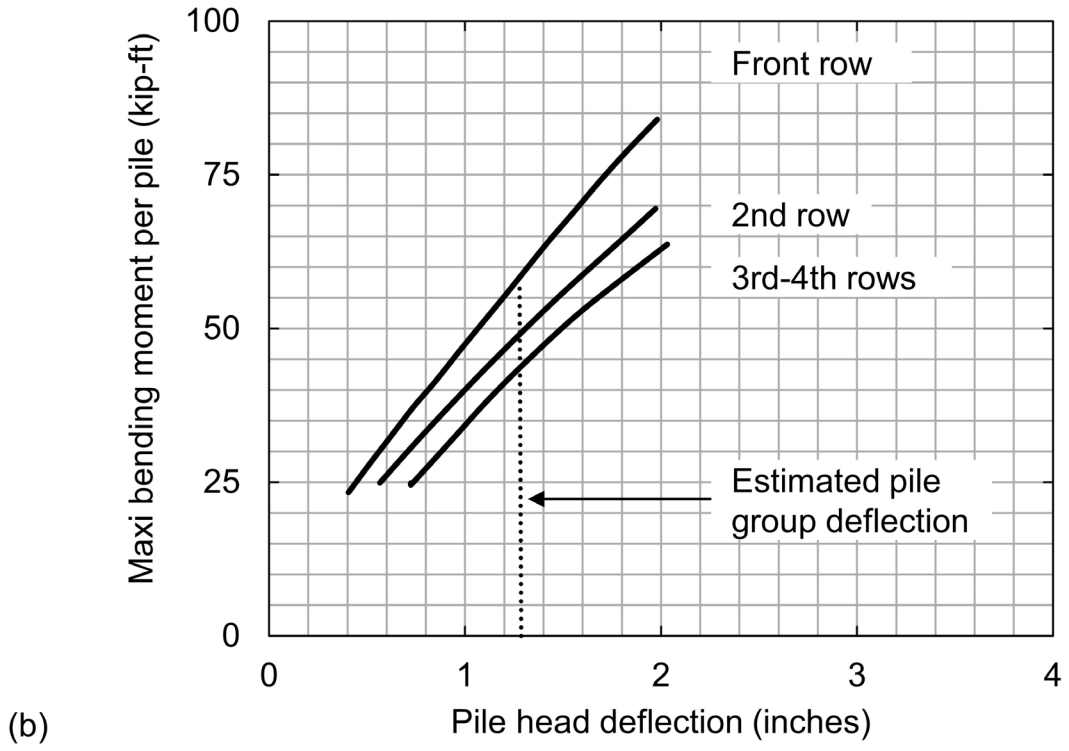

(b)

Figure 7-74 Typical plots of (a) Load versus deflection and (b) Bending moment versus deflection for pile group analysis (adapted from Brown and Bollman 1993).

STEP 3 Run software analyses.

a. Perform p-y analyses using the P_m value for each row position to develop load-deflection and load-moment data.

b. Use AASHTO (2014) design specification recommendations for P_m values. For a center to center pile spacing of 3b, recommended P_m values are 0.8 for the lead row, 0.4 for the second row, and 0.3 for the third and subsequent rows. For a center to center pile spacing of 5b, recommended P_m values are 1.0 for the lead row, 0.85 for the second row, and 0.7 for the third and subsequent rows. Interpolate for center to center pile spacing between 3b and 5b to determine for the appropriate P_m value.

c. Determine shear load versus deflection behavior for piles in each row. Plot load versus pile head deflection results similar to as shown in Figure 7-74(a).

STEP 4 Estimate group deflection under lateral load.

Average the load for a given deflection from all piles in the group (i.e. each of the four rows) to determine the average group response to a lateral load as shown in Figure 7-74(a).

Divide the lateral load to be resisted by the pile group by the number of piles in the group to determine the average lateral load resisted per pile.

Enter load-deflection graph similar to Figure 7-74(a) with the average load per pile to estimate group deflection using the group average load deflection curve.

STEP 5 Evaluate pile structural acceptability.

a. Plot the maximum bending moment determined from p-y software analyses versus deflection for each row of piles as illustrated in Figure 7-74(b).

b. Check the pile structural adequacy for each p. Use the estimated group deflection under the lateral load per pile to determine the maximum bending moment for an individual pile in each row.

c. Determine maximum pile stress from p-y software output associated with the maximum bending moment.

d. Compare maximum pile stress with pile yield stress.

STEP 6 Perform refined pile group evaluation that considers superstructure-substructure interaction.

7.3.7.6.1 Lateral Resistance Increases Through Ground Improvement

Methods to improve the lateral resistance of pile groups in weak near surface soils were evaluated by Rollins and Brown (2011) in NCHRP Report 698, Design Guidelines for Increasing the Lateral Resistance of Highway-Bridge Pile Foundations by Improving Weak Soils. This study concluded that significant increases in lateral resistance in soft clays and loose sands can be achieved through soil replacement or ground improvement techniques. Figure 7-75 illustrates the appropriate treatment areas to improve lateral resistance around new foundations in weak soils as well as the treatment areas around existing foundations to improve their lateral resistance.

Tables 7-24 and 7-25 summarize the treatment options studied, the improvement in lateral resistance achieved, the treatment costs, and the cost savings. The standard alternative to ground improvement is to add more piles in order to resist the same lateral load. This option would also require a larger pile cap. The approximate cost of the additional piles and larger cap necessary to resist the same lateral load was estimated for each ground improvement technique and is reported in the third column of Table 7-25. The difference between this cost and the ground improvement cost in column 2 is the reported cost savings in column 4. For more detailed information, please refer to the NCHRP study.

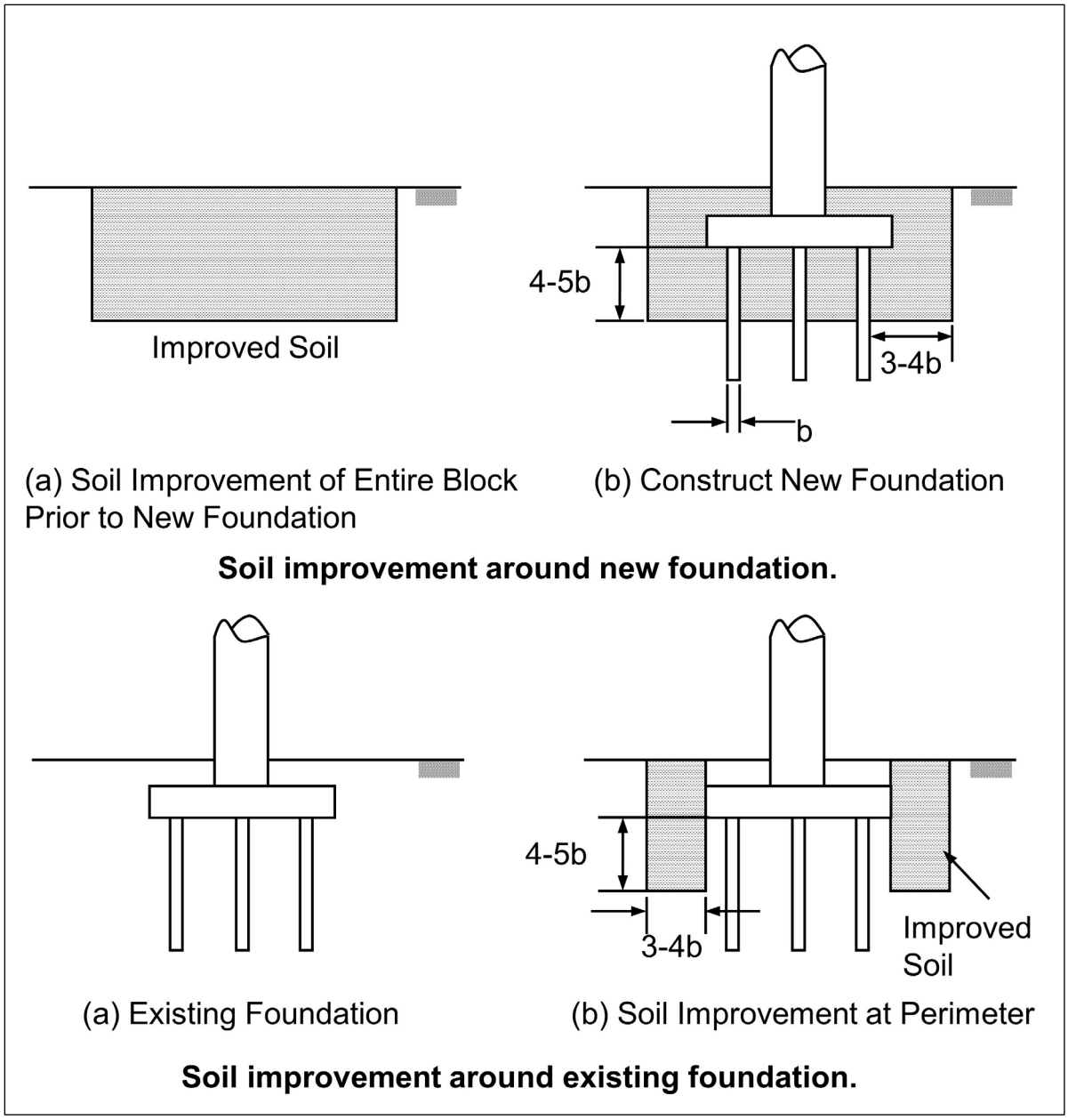

Figure 7-75 Ground improvement treatment areas for increased lateral resistance of pile groups in weak soils (Rollins and Brown 2011).

Table 7-24 Summary of Ground Improvement Method and Increase in Lateral Resistance (after Rollins and Brown 2011)

Treatment Method	Treatment Dimensions (LxWxD)	Treatment Volume (yd^3)	Untreated Lateral Resistance (kips)	Increase in Lateral Resistance (kips)	Percent Increase in Resistance
Jet grouting below cap.	15' x 10.5' x 10'	58.3	282	500	160
Jet grouting adjacent to cap.	6,6' x 13' x 12'	38.1	214	398	185
Soil mixing adjacent to cap.	4' x 11' x 10'	16.3	282	170	60
Weal flowable fill below cap.	13.5' x 8.8' x 6'	26.4	232	24	10
Flowable fill adjacent to cap.	6' x 12' x 6'	16.0	265	145	55
Compacted fill to edge of cap.	9.6' x 8.75' x 3.5'	10.9	232	23	10
Compacted fill 5 feet beyond edge of cap.	14.6' x 8.75' x 3.5'	16.6	232	40	18
Rammed aggregate piers adjacent to cap top.	13, 2.5 dia x 13' deep	29.5	285	40	14
Rammed aggregate piers adjacent to cap top.	13, 2.5' dia. X 10.5 deep	23.6	50	35	70

Table 7-25 Summary of Ground Improvement Method and Associated Costs for Increase in Lateral Resistance after (Rollins and Brown 2011)

Treatment Method	Ground Improvement Cost	Pile and Pile Cap Cost for Same Lateral Load Increase	Savings Relative to Adding Additional Piles	Ground Improvement Lateral Support Cost ($ / kip)
Jet grouting below cap.	$28,500	$84,200	$55,700	57
Jet grouting adjacent to cap.	$38,000	$69,360	$31,360	95
Soil mixing adjacent to cap.	$10,000	$30,345	$20,345	59
Weak flowable fill below cap.	$3,180	$4,335	$1,155	133
Flowable fill adjacent to cap.	$3,600	$26,010	$22,410	25
Compacted fill to edge of cap.	$544	$4,335	$3,791	24
Compacted fill 5 feet beyond edge of cap.	$828	$8,670	$7,842	21
Rammed aggregate piers adjacent to cap top.	$4,225	$8,670	$4,445	106
Rammed aggregate piers adjacent to cap top.	$4,225	$8,670	$4,445	121

7.3.8 Lateral Squeeze of Foundation Soil and Solutions

Bridge abutments supported on piles driven through soft compressible cohesive soils may tilt forward or backward depending on the geometry of the backfill and the abutment. This problem is illustrated in Figure 7-76. Large horizontal movements may cause damage to the structure. The unbalanced fill loads displace the soil laterally. This lateral displacement may bend the piles, causing the abutment to tilt toward or away from the fill. Lateral squeeze can similarly adversely affect pier locations if stockpiles are placed adjacent to a pier location.

The following rules of thumb are recommended for determining whether tilting will occur, as well as estimating the magnitude of horizontal movement.

1. Lateral squeeze and abutment tilting can occur if:

$$\gamma_f \, h_f > 3 \, s_u \qquad \text{Eq. 7-74}$$

Where:

γ_f = unit weight of fill (pcf).
h_f = height of fill (feet).
s_u = undrained sear strength of soft cohesive soil (psf).

2. If abutment tilting can occur, the magnitude of the horizontal movement can be estimated by the following formula:

$$S_h = 0.25 \, S_v \qquad \text{Eq. 7-75}$$

Where:

S_h = horizontal abutment movement (inches).
S_v = vertical fill settlement (inches).

Mitigation of lateral squeeze may be provided by several means. The four solutions below represent primary methods to prevent lateral squeeze.

a. Delay installation of abutment piling until after fill settlement has stabilized (best solution).

b. Provide expansion shoes large enough to accommodate the movement.

c. Use steel H-piles to provide high tensile strength in flexure.

d. Use lightweight fill materials to reduce driving forces.

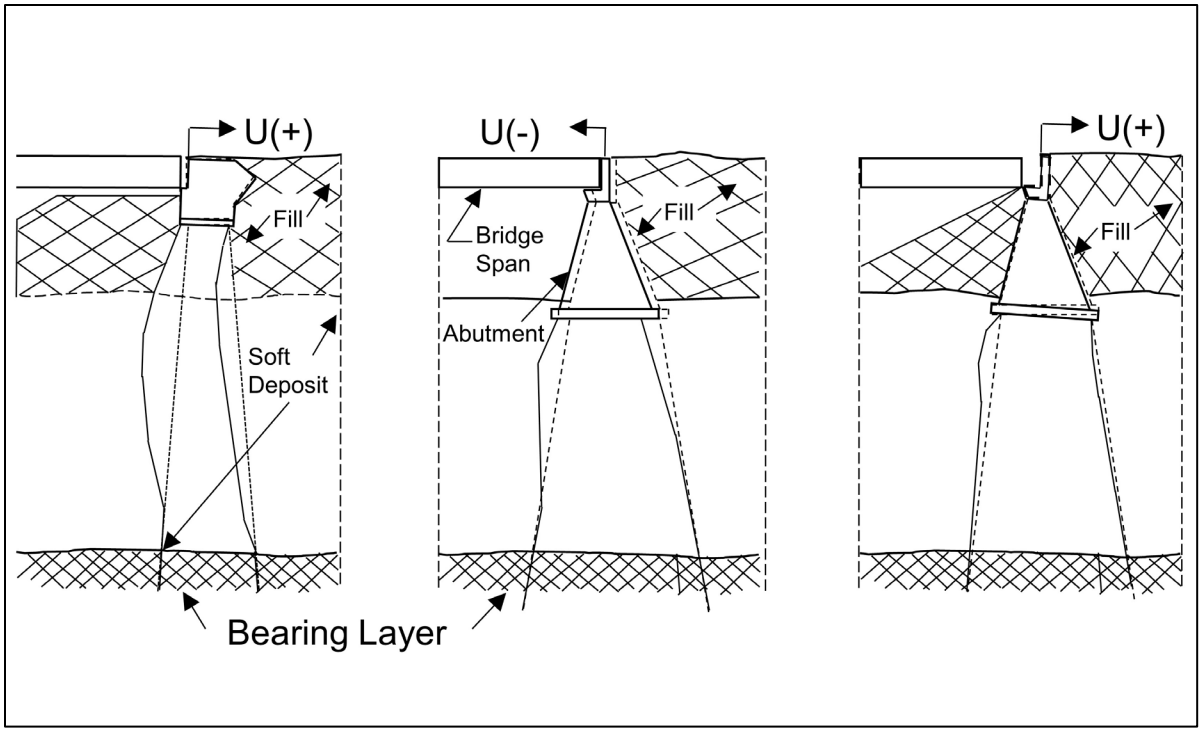

Figure 7-76 Examples of abutment tilting due to lateral squeeze.

7.3.9 Overall Stability

Abutments are often supported by a deep foundation system and are also subject to the potential for overall stability failure. Although the stiffness of deep foundations may provide resistance against this shear loading, if the slip surface is below the pile tip elevation, or if large earthen loads are generated, global stability failure should be evaluated. To a lesser extent, this situation may apply to walls or other cut slopes which are also founded on structural elements. Per AASHTO (2014), the Service I Load Combination and load factor should be used to assess global stability. When the stabilizing system includes a structural element (deep foundation), a resistance factor of 0.65 for sliding is recommended for use in stability calculations. As provided in the AASHTO (2014) commentary, the 0.65 resistance factor is taken as the inverse of the typical 1.5 safety factor used in the ASD approach. A detailed discussion on the mechanisms of shear failure and slope stability is beyond the scope of this manual. References can be made to Sabatini et al. (1997), Duncan and Wright (2005) and Tanyu et al. (2008).

7.4 EXTREME EVENT LIMIT STATES

Extreme event limit states involve events with a low occurrence probability. However, these events can have a detrimental impact on the foundation and structure if not considered in design. As noted in AASHTO (2014), the extreme event limit state exists to protect against structural collapse and preserve life. Furthermore, AASHTO (2014) provides guidance on extreme event loading cases, including ice loading and vehicle and vessel impacts. Arneson et al. (2012) details scour development near bridge piers and abutments, while Kavazanjian et al. (2011) provides an in depth discussion on seismic events. Background information on ice loads can be found in in Montgomery et al. (1984). In depth coverage for vessel impact design is available in AASHTO (2009) Guide Specifications and Commentary for Vessel Collision Design of Highway Bridges. The following sections provide a discussion on these event types, while the documents referenced above address these topics in greater detail.

Extreme event limit state evaluations ensure structural survival of a bridge under unique major occurrences such as earthquakes, floods, and vehicle or vessel collisions having return periods significantly greater than the bridge design life. Extreme event limit states for driven pile foundation design include:

- the check flood for scour,
- vessel collision,
- vehicle collision,
- seismic loading,
- ice and debris loading, and
- other site-specific situations determined by the design engineer.

7.4.1 Extreme Event Scour During Check Flood

Many bridges are constructed over rivers, bodies of water, and tidal areas where scour is a consideration in the foundation design. These structures encounter repeated aggradation or degradation of material in the scour zone which affects the foundation resistance. The check flood is an extreme event that is unlikely to happen during the design life of the structure. Arneson et al. (2012) details design requirements for the check flood where soil materials within the scour zone are assumed to be removed and provide no geotechnical resistance for lateral, axial compression, or tension loads.

For the applicable factored loads, the pile foundation must have adequate factored axial and lateral resistance. In the extreme event limit state, the check flood for scour differs from the design flood as follows:

1. The 500-year check flood has a different and typically deeper scour prism.

2. The loads used for structural modeling in the extreme event limit state are unfactored.

3. Resistance factors of 1.0 are used for the geotechnical resistances on lateral and axial compression loads, and 0.8 or less for uplift loads.

Overall stability of the bridge should be evaluated during the check flood, where storm surges, tides or other floods can detrimentally impact the foundation and overall structure. Debris loads during the check flood should likewise be included in this analysis. Piles should be driven to penetration depths to overcome the loss of shaft resistance within the scour prism.

Loading combinations with the check flood are further explained in Section 7.4.4, as well as in HEC-18 (Arneson et al. 2012). Section 7.2.9 also provides additional background on scour design considerations.

7.4.2 Seismic and Seismic Induced Downdrag

The design issues associated with pile foundation design for seismic events are significant and include liquefaction effects on soil resistance, ground movements, seismic induced foundation loads, and seismic induced drag forces. As noted in AASHTO (2014) design specifications, bridges shall be designed for a low probability of collapse but may suffer significant damage or disruption of service as a result of earthquake loading. A pseudo-static analysis approach is commonly utilized for many bridges and will be covered in this section. In addition, subsequent sections of this manual will discuss seismic action effects with respect to the extreme event limit states. However, more detailed references should be consulted on the seismic design procedure including Geotechnical Engineering Circular No. 3 by Kavazanjian et al. (2011) and FHWA-NHI-15-004 LRFD Seismic Analysis and Design of Bridges by Marsh et al. (2014).

7.4.2.1 AASHTO Recommendations for the Equivalent Static Seismic Force

For earthquake loads, the horizontal ground displacements are transmitted from the foundation to superstructure where accelerations occur. As a result, inertial forces are generated and applied back to the foundation which must then resist these loads. The superstructure must be designed to resist brittle failure as a result of seismic loading (Marsh et al. 2014) while the foundation must resist effects of liquefaction, ground movement, drag forces and the increased superstructure loads. Before defining the required nominal geotechnical resistance, the increased loads resulting from seismic action must first be determined.

STEP BY STEP PROCEDURE FOR: “EVALUATION OF EARTHQUAKE LOAD”

The seismic hazard of a site contributes to expected loads that can develop for a 1000 year design earthquake (AASHTO 2014). AASHTO Article 3.10 outlines steps to determine the elastic seismic coefficient, C_{sm}. However the end goal is to define the equivalent static horizontal seismic force, $P_e(x)$. This relationship is shown in Equation 7-76, with the following steps providing a discussion of this process.

$$P_e(x) = C_{sm}W \qquad \text{Eq. 7-76}$$

Where:

$P_e(x)$= equivalent static horizontal seismic force acting on superstructure.
C_{sm} = elastic seismic response coefficient (dimensionless).
W = equivalent weight of the superstructure.

STEP 1 Define the Site Ground Coefficient and Spectral Coefficients.

The site peak ground acceleration coefficient, PGA, short period spectral coefficient, S_s and long period spectral coefficient, S_1, are determined by inspecting contour seismic maps developed for such a purpose. These maps were developed by the U.S. Geological Survey for AASHTO and may be found in the Chapter 3 of AASHTO (2014) design specifications. In addition, the U.S. Geological Survey website includes an application (http://earthquake.usgs.gov/designmaps/us/application.php) which performs a search and presents these output values, after the user enters the site location and site classification.

STEP 2 Determine the Site Classification.

Using results of the subsurface investigation, the site is classified as A to F. The upper 100 feet of the subsurface profile is to be averaged to define the shear wave velocity, SPT N-Value, and undrained shear strength. Table 7-26 should be used for this determination.

Table 7-26 Site Class Definition

Site Class	Soil Type and Profile
A	Hard rock with measured shear wave velocity, $\bar{v}_s$ > 5,000 ft/s.
B	Rock with 2,500 ft/sec < $\bar{v}_s$ < 5,000 ft/s.
C	Very dense soil and soil rock with 1,200 ft/sec < $\bar{v}_s$ < 2,500 ft/s, or with either $\bar{N}$ > 50 blows/ft, or $\bar{s}_u$ > 2.0 ksf.
D	Stiff soil with 600 ft/s < $\bar{v}_s$ < 1,200 ft/s, or with either 15 < $\bar{N}$ < 50 blows/ft, or 1.0 < $\bar{s}_u$ < 2.0 ksf.
E	Soil profile with $\bar{v}_s$ < 600 ft/s or with either $\bar{N}$ < 15 blows/ft or $\bar{s}_u$ < 1.0 ksf, or any profile with more than 10 ft of soft clay defined as soil with PI > 20, *w* > 40 percent and $\bar{s}_u$ < 0.5 ksf.
F	Soils requiring site-specific evaluations, such as: • Peats or highly organic clays (H > 10 ft of peat or highly organic clay where H = thickness of soil). • Very high plasticity clays (H > 25 ft with PI > 75). • Very thick soft/medium stiff clays (H >120 ft).

$\bar{v}_s$ = average shear wave velocity
$\bar{N}$ = average SPT N-value
$\bar{s}_u$ = averageundrained shear strength
w = moisture content
PI = Plasticity Index

STEP 3 Determine the Site Factors.

Site factors corresponding to the zero, short and long periods of acceleration should be determined using Table 7-27 to Table 7-29. Straight line interpolation should be used for intermediate values in any of the three tables. If the site is classified as Class F, a site-specific geotechnical investigation with dynamic response analysis should be performed to determine these acceleration period parameters.

Table 7-27 Site Factor Values, F_{pga}, at Zero Period Acceleration

Site Class	PGA < 0.1	PGA = 0.2	PGA = 0.3	PGA = 0.4	PGA > 0.5
A	0.8	0.8	0.8	0.8	0.8
B	1.0	1.0	1.0	1.0	1.0
C	1.2	1.2	1.1	1.0	1.0
D	1.6	1.4	1.2	1.1	1.0
E	2.5	1.7	1.2	0.9	0.9
F	*	*	*	*	*

Table 7-28 Site Factor Values, F_a, for Short Period Coefficient S_s

Site Class	S_s < 0.25	S_s = 0.5	S_s = 0.75	S_s = 1.0	S_s > 1.25
A	0.8	0.8	0.8	0.8	0.8
B	1.0	1.0	1.0	1.0	1.0
C	1.2	1.2	1.1	1.0	1.0
D	1.6	1.4	1.2	1.1	1.0
E	2.5	1.7	1.2	0.9	0.9
F	*	*	*	*	*

Table 7-29 Site Factor Values, F_v, for Long Period Coefficient, S_1

Site Class	S_1 < 0.1	S_1 = 0.2	S_1 = 0.3	S_1 = 0.4	S_1 > 0.5
A	0.8	0.8	0.8	0.8	0.8
B	1.0	1.0	1.0	1.0	1.0
C	1.7	1.6	1.5	1.4	1.3
D	2.4	2.0	1.8	1.6	1.5
E	3.5	3.2	2.8	2.4	2.4
F	*	*	*	*	*

STEP 4 Characterize the Design Response Spectrum and Determine the Elastic Seismic Response Coefficient, C_{sm}.

The Design Response Spectrum as shown in Figure 7-77 is created using the zero, short, and long period acceleration values as well as the site factor values determined from the steps above.

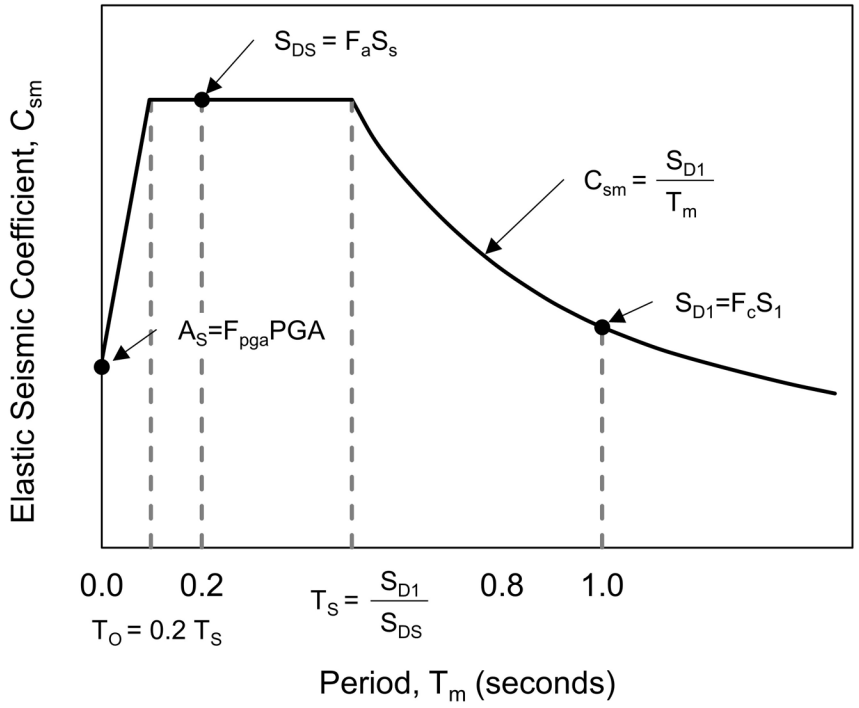

Figure 7-77 Design response spectrum (after AASHTO 2014).

The elastic seismic response coefficient is a function of the Design Response Spectrum and a hand calculation may be used to determine this exact value. Equation 7-77 to Equation 7-79 should be employed for this purpose.

$$C_{sm} = A_S + (S_{DS} - A_S)\left(\frac{T_m}{T_o}\right) \quad \text{Eq. 7-77}$$

In which

$$A_S = F_{PGA}\, PGA \quad \text{Eq. 7-78}$$

$$S_{DS} = F_a\, S_S \quad \text{Eq. 7-79}$$

Where:

C_{sm} = elastic seismic response coefficient (dimensionless).

A_S = peak seismic ground acceleration coefficient modified by short-period site factor (dimensionless).

S_{DS} = C_{sm} value with a period of 0.2 second = $F_a S_S$.

T_m = period of vibration of *m*th mode(s).

T_o = reference period to define spectral shape = $0.2T_s$.

T_s = corner period when spectrum changes from independent to inversely proportional = S_{D1} /S_{DS}.

F_{PGA} = zero period site factor.

PGA = peak ground acceleration coefficient.
F_a = short period site factor.
S_S = short period spectral coefficient.
S_{D1} = C_{sm} value with a period of 1.0 seconds = $F_v S_1$.

The elastic seismic response coefficient, C_{sm}, is then substituted into Equation 7-76 as noted to determine the equivalent static force. The structural engineer applies this force to the superstructure using a method outlined in Article 4.7.4.3 of the AASHTO (2014) design specifications. The minimum analysis requirement depends on the seismic zone in which the bridge exists, as well as the bridge regularity and operational classification. Table 7-30 classifies the site as Seismic Zone 1 through 4 depending on the acceleration coefficient, S_{D1}. If the site is classified as Seismic Zone 2 through 4, a liquefaction assessment is required for multispan bridges.

Table 7-30 Seismic Zones

Acceleration Coefficient, S_{D1}	Seismic Zone
$S_{D1} \leq 0.15$	1
$0.15 < S_{D1} \leq 0.30$	2
$0.30 < S_{D1} \leq 0.50$	3
$0.50 < S_{D1}$	4

For the Extreme Event I check, the factored loads resulting from seismic action are then applied to the foundation for an axial, lateral and overturning analysis. A resistance factor of 1.0 is used on the resistances for axial compression loads and 0.8 or less for lateral and uplift loads as recommended by AASHTO (2014).

7.4.2.2 Liquefaction

Liquefaction is defined as a loss of shear strength and stiffness which results from built-up pore water pressure during cyclic loading. Soil types most susceptible to liquefaction are saturated, very loose to medium dense, fine to medium grained sands and non-plastic silts. However, liquefaction has also occurred in saturated, very loose to medium dense gravels.

In seismically active areas where peak earthquake acceleration will be greater than 0.1g, the soil susceptibility to liquefaction should be evaluated. A commonly used procedure for identification of liquefaction susceptible soils was proposed by Seed et al. (1983). This liquefaction evaluation approach is detailed in Lam and Martin

(1986), the Commentary for Article 10.5.4 of AASHTO (2014), and Chapter 6 of GEC-3 by Kavazanjian et al. (2011). If the soils are found to be subject to liquefaction during the design event, the pile foundation must be designed to accommodate the following resulting behavior: the loss of resistance in the liquefied zone, the seismic induced loads, as well as the anticipated vertical and horizontal displacements, and the resulting drag force. Alternatively, the liquefaction potential may be mitigated through ground improvement techniques.

Pile foundations in liquefiable soils must penetrate through the zone of liquefaction and develop adequate resistance in the underlying deposits. Evaluation of compression and uplift resistances during the seismic event can be made by assigning residual strength properties to the liquefiable layers. Appropriate residual strengths should be used to analyze axial and lateral loading. Residual strengths of sands and silty sands can be approximated from SPT resistance values using a correlation proposed by Seed (1987) and updated by Seed and Harder (1990). Additional correlations on the residual strengths of sands and silty sands have been reported by Olson and Stark (2002), as well as Idriss and Boulanger (2007). Figure 7-78 presents the correlation developed by Idriss and Boulanger between the equivalent clean sand SPT corrected blow count and the ratio of the residual shear strength, s_r, divided by the vertical effective stress, σ'_{vo}.

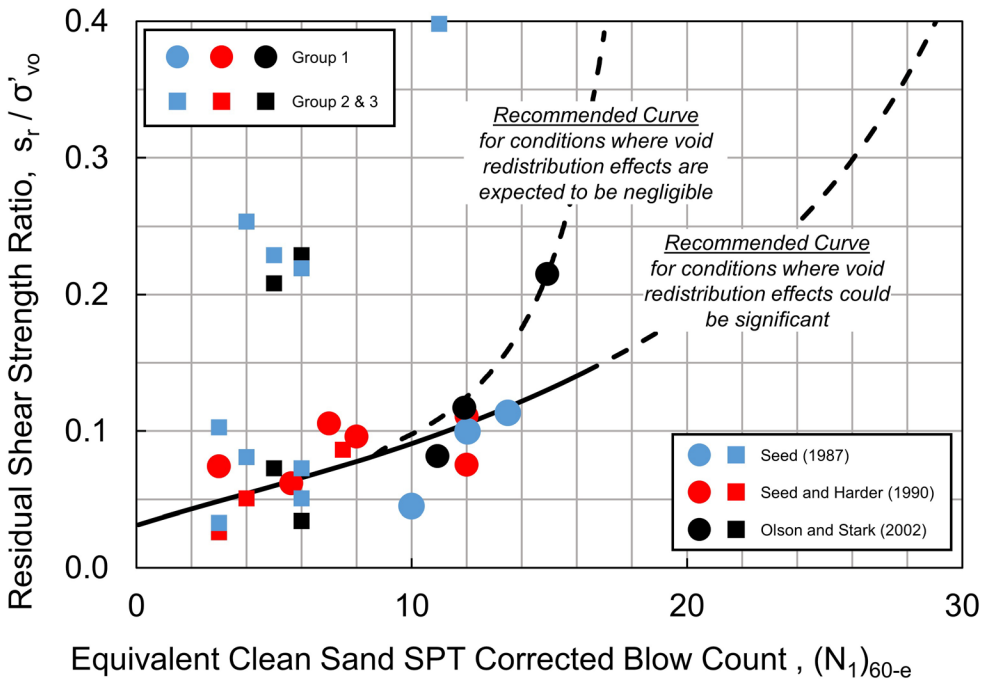

Figure 7-78 Correlation between the Residual Undrained Strength Ratio, s_r / σ'_{vo} and equivalent clean sand SPT blow count, $(N_1)_{60\text{-}e}$ (Idriss and Boulanger 2007).

The SPT N-value used for the equivalent clean sand in Figure 7-78 should be corrected for both energy and vertical effective stress as well as for the percent fines, as described by Seed and Harder (1990). The correction for the percent fines is provided in Table 7-31.

Table 7-31 Blow Count Correction, N_{corr}, for the Equivalent Clean Sand Blow Count, $(N_1)_{60\text{-}e}$

Percent Passing #200 Sieve	N_{corr}
0 – 9	0
10 – 24	1
25 – 49	2
50 – 74	4
> 75	5

The equivalent clean sand blow count is then determined using Equation 7-80 below.

$$(N_1)_{60-e} = (N_1)_{60} + N_{corr} \qquad \text{Eq. 7-80}$$

Where:

$(N_1)_{60-e}$ = equivalent clean sand blow count.
$(N_1)_{60}$ = SPT N value corrected for energy and overburden stress.
N_{corr} = correction for percent fines from Table 7-31.

In a Washington State research report, Kramer (2008) proposed an alternate approach for estimating the residual strength of liquefied soil. This approach estimated the residual strength based on a weighted value determined by four methods. This residual strength was based on 20% of the value determined following Idriss (1998), 20% of the value determined in accordance with from Olson and Stark (2002), 20% of the value determined following Idriss and Boulanger (2007), and 40% of the value determined using the Kramer-Wang hybrid model, Kramer and Wang (2007).

Following a seismic event that induces soil liquefaction, the liquefied layer will generally consolidate as pore water pressure dissipates. Settlement magnitude can be estimated using procedures in Kavazanjian et al. (2011). Fellenius and Siegel (2008) noted that the location of the zone of liquefaction relative to the neutral plane is very important. If liquefaction occurs in soil layers above the location of the neutral plane before liquefaction, the liquefaction event will have limited effect on the

pile. If liquefaction occurs in soil layers located below the pre-liquefaction location of the neutral plane, it will increase the axial compression load in the pile as well as result in additional pile settlement. The structural design of the pile section and the settlement resulting from liquefaction occurring below the neutral plane should be evaluated in the design. The pile foundation must be structurally capable of supporting the increased drag force and foundation settlement occurring after liquefaction must be within the structure's performance criteria.

Liquefaction induced lateral spread can impose significant bending moments in piles driven through liquefiable soils. Therefore, piles in liquefiable soils should be flexible and ductile in order to accommodate lateral loads. The maximum bending moment of piles in liquefiable soils is often evaluated in a p-y analysis by assigning Reese's soft clay p-y curve with low residual shear strengths and high ε_{50} values to the liquefiable layer. Brandenberg et al. (2007) performed centrifuge model tests and found p-multiplier values of 0.05 in loose sand and 0.30 in dense sand could be used to model pile p-y response in fully liquefied granular layers.

7.4.3 Ice and Collisions

Vehicle and vessel collision as well as ice loads are included in the Extreme Event II load combination provided in AASHTO (2014). Each is treated as an independent extreme event. However they often occur in tandem with other loading cases such as large wind loads and vessel impact. Since these loads are typically applied to the superstructure, they are analyzed for structural loading cases, and therefore do not directly alter the geotechnical resistance as with scour and earthquakes. The Extreme Event II limit state equation can be expressed as Equation 7-81 below.

$$\sum \gamma_i Q_i = \gamma_p DL + 0.5LL + 1.0WA + 1.0FR + 1.0\ (IC\ or\ CT\ or\ CV) \qquad \text{Eq. 7-81}$$

Where:

γ_i = load factor.
Q_i = force effect.
γ_p = load factor for permanent loads (from Table 2-3 of Chapter 2).
DL = dead loads.
LL = live loads.
WA = water load.
FR = friction load.
IC = ice load.
CT = vehicular collision force.
CV = vessel collision force.

From the equation above, ice loads as well as vehicle and vessel collisions are treated as separate events. Therefore they will be independently discussed.

7.4.3.1 Ice Loads

AASHTO (2014) provides consideration for ice loading that occurs in freshwater bodies such as lakes and rivers. Specific mention of saltwater ice loading is left to specialists in that area, and are thus beyond the scope of this manual. The expected ice forces are assumed to act directly on piers. Four loading conditions may occur including; 1) dynamic impact from ice sheet collision with the bridge pier, 2) static load resulting from thermal expansion of ice sheets around piers, 3) load from hanging dams or ice jams and 4) static uplift or vertical loads that result from ice adhesion when water levels fluctuate.

Section 3.9 of AASHTO (2014) provides in depth detail on the magnitude and application of ice loads resulting from the above mentioned factors. A discussion of dynamic forces resulting from ice collisions is mainly provided by Montgomery et al. (1984), where forces depend on the flow size, the ice strength and thickness, and pier geometry. Meanwhile, presumed values are noted in AASHTO (2014) as to ice crushing strength.

Static loads applied from thermal expansion and hanging dams or ice jams are accounted for in the structural design of superstructure members. Increased forces are therefore applied during a static structural analysis, where they generate alternative loading conditions for the foundations. To account for vertical forces from ice adhesion in rapid water level fluctuations, AASHTO (2014) recommends Equation 7-82 to determine the vertical force surrounding circular piers. Equation 7-83 should be used for oblong piers.

$$F = 80{t_i}^2 \left(0.35 + \frac{0.03R}{{t_i}^{0.75}}\right) \quad \text{Eq. 7-82}$$

$$F = 0.2{t_i}^{1.25}C + 80.0{t_i}^2 \left(0.35 + \frac{0.03R}{{t_i}^{0.75}}\right) \quad \text{Eq. 7-83}$$

Where:

- F = vertical force.
- t_i = ice thickness (feet).
- C = perimeter of pier excluding half circles at ends of oblong pier (feet).
- R = radius of pier (feet).

7.4.3.2 Vehicle Collison

When bridge piers are within 30 feet of the roadway edge or within 50 feet of the railway centerline, vehicular collision should be evaluated. In the absence of crash protection, an equivalent 600 kip static force is to be applied 5 feet above grade and at an angle of 0 to 15 feet from the edge of pavement. This loading condition is based on full scale tractor trailer collision tests. A distributed load of no more than 5 feet wide by 2 feet high may be alternatively applied for wall piers, if considered a suitable replacement for an anticipated vehicle.

The designer may also utilize a barrier to redirect or absorb the vehicular collision. For this, an embankment, guardrail or other crash protection system may be used. AASHTO (2014) requires this barrier to be structurally independent of the pier and ground mounted. If within 10 feet of the pier, the barrier must be 54 inches high, while a height of 42 inches must be reached if outside of this distance.

7.4.3.3 Vessel Collision

Bridges that span navigable bodies of water should be designed for vessel impact. Bow, deck house, or mast impacts are typically applied to superstructure elements. A head on collision with piers may occur and should consider the full vessel mass. Based on an assessment of vessels passing the bridge, a design vessel is selected and given a deadweight tonnage (DWT) value of representative size and weight. The head on collision force to the pier may be calculated as follows.

$$P_s = 8.15\, V \sqrt{DWT} \qquad \text{Eq. 7-84}$$

Where:

P_s = equivalent static vessel impact force (kips).
DWT = deadweight tonnage (tonne).
V = vessel impact velocity (ft/s).

After determination of the equivalent static impact force, the load is to be applied as either 100 percent in the direction parallel to the channel centerline or 50 percent in the direction normal to the channel centerline. Both loading cases should be evaluated. Overall stability is determined by applying a point load at the mean high water level as shown in Figure 7-79. AASHTO (2014) notes that all substructure components exposed to direct impacts shall be designed to resist the applied loads.

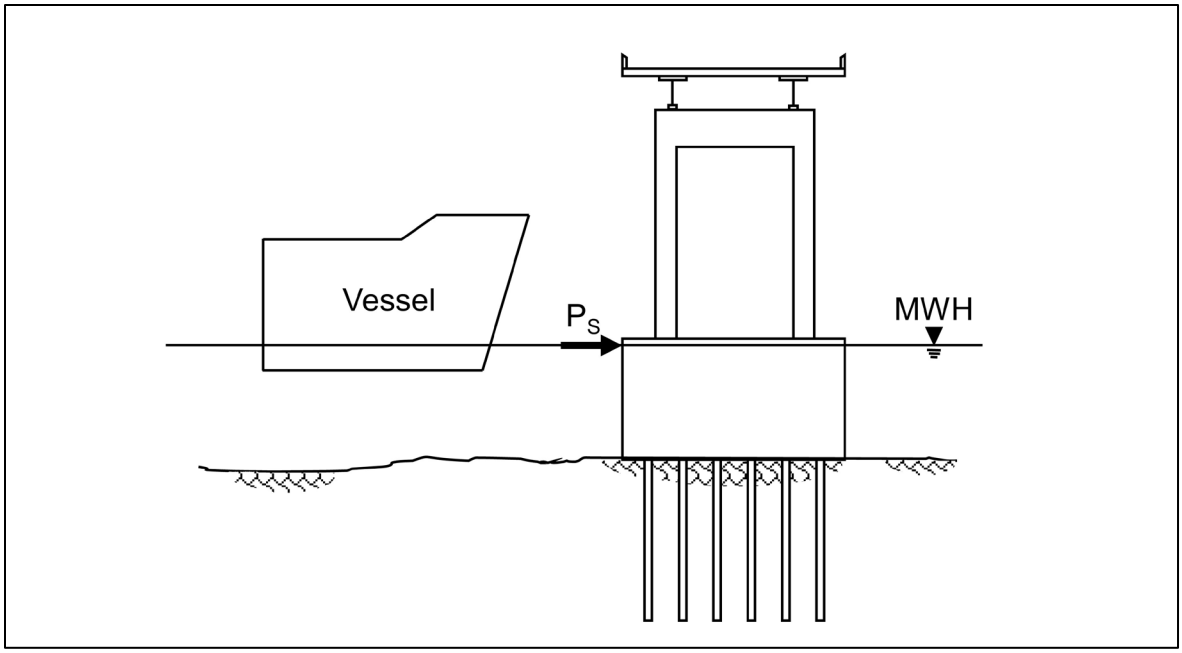

Figure 7-79 Application of equivalent impact force (after AASHTO 2014).

7.4.4 Combined Extreme Events

Two extreme event combinations with scour are given in AASHTO (2014). Extreme Event I is in combination with earthquake loading, while the Extreme Event II combination includes ice, vessel and vehicle collisions and hydraulic loads. As noted in Arneson et al. (2012), the Extreme Event I combination has a low occurrence probability for both the check flood and earthquake loading. Therefore scour for the mean discharge or normal non-flood flow may be applied to this event combination. For the Extreme Event II combination, research is ongoing to assess the probability of joint loading conditions during the check flood, and judgement should be used based on site-specific factors. If ice or debris jams near the structure dictates the use of a more extreme flood event than the check flood, this may be used to assess the extreme event limit state.

7.5 DETERMINATION OF MINIMUM PILE PENETRATION

Foundation settlement and resultant structure deformation should be kept within tolerable limits as described in Section 7.3.1. Once all limit state analyses have been performed, minimum pile penetration depths should be specified, if necessary. Minimum pile penetration depths may be required to limit structure vertical or lateral deformations under applied loads.

A minimum pile penetration depth should be specified only if needed. In many cases, the inclusion of only an estimated length is satisfactory with recognition that once piles achieve their required nominal driving resistance, driving may be terminated shorter than the estimated length. The ability of an appropriately sized pile hammer to drive piles to the specified minimum penetration depth should be evaluated during the design phase in a wave equation drivability analysis. The drivability analysis is used to check constructability and viability of achieving the minimum pile penetration depth. An alternative pile type or use of pile installation aids may need to be specified if the drivability analysis indicates the minimum pile penetration depth is not obtainable using conventional driving procedures.

AASHTO (2014) design specifications state that the minimum pile penetration depth shall be the pile toe elevation needed to satisfy the following requirements, as applicable, to the site and loading conditions. Additional guidance on each topic affecting the minimum pile penetration requirement is provided in the noted sections.

a. Single pile and pile group settlement (service limit state – Section 7.3.5).

b. Lateral deflection (service limit state – Section 7.3.7).

c. Uplift (strength limit state – Section 7.2.3).

d. Penetration depth into soils to accommodate drag forces from static settlement stresses (service limit state – Section 7.3.6).

e. Penetration depth into soils due to liquefaction (strength and extreme event limit states – Section 7.4.2).

f. Penetration depth into soils needed to provide adequate pile axial (compression and uplift) and lateral resistance after scour (strength limit state – Section 7.2.9, and extreme event limit states – Section 7.4.1).

g. Penetration depth into soils necessary to achieve fixity for resisting the applied lateral loads (strength limit state – Section 7.2.5, and service limit state – Section 7.3.7). It should be noted that AASHTO is silent on the definition of fixity, which can vary if defined by the deflection profile, the bending moment profile, or the pile head deflection.

h. Axial uplift and lateral resistance to resist extreme event limit states loads (extreme event limit state – Section 7.4).

7.6 DETERMINATION OF R_{ndr} TO ESTABLISH CONTRACT DRIVING CRITERIA

The required nominal driving resistance, R_{ndr}, is used to establish the driving criteria. This resistance along with the field method for resistance verification should be specified in contract documents. The nominal driving resistance includes many factors such as the axial compression loads, resistance from scourable or liquefiable layers, as well as time dependent soil strength changes. Some of these conditions result in an increased soil resistance at the time of installation. In these cases, the pile should be driven to a higher nominal resistance to accommodate these future resistance losses. Inclusion of the R_{ndr} in conjunction with the factored load and the field verification method can reduce the risk of contractor claims. A minimum penetration depth may also be required in addition to the R_{ndr} to also satisfy uplift or lateral loading requirements and/or serviceability.

An example calculation for determining R_{ndr} is illustrated in Equation 7-85 based on the project information provided in Table 7-32. The factored axial load, *Q*, is 200 kips in compression. Given the site conditions, some resistance will be lost in a soil layer subject to scour. The resistance lost in the scour zone should be determined by an appropriate static analysis method and should not be factored per AASHTO (2014) Article 10.7.3.6. For this example, it is estimated that 50 kips of resistance will be lost in the scour zone. The pile will also be driven into a weathered shale formation that historically has exhibited a loss in toe resistance following initial driving. The resistance lost to relaxation should be factored based the resistance verification method. For this example, it is estimated that 100 kips of toe resistance will be lost. Based on field verification by dynamic testing with signal matching, the resistance loss from relaxation is then 154 kips.

Equations 7-85 and 7-86 are simplified from AASHTO (2014) to provide the necessary calculation steps.

Table 7-32 Summary of Load and Resistance Information

Q (kips)	200
ϕ_{dyn}	0.65
R_n (kips)	308
R_{scour} (kips)	50
R_{relax} (kips)	154
R_{ndr} (kips)	512

Example computation of R_n

$$R_n = \frac{\mathrm{Q}}{\Phi_{dyn}} \qquad \text{Eq. 7-85}$$

$$R_n = \frac{200}{0.65} = 308\ kips$$

Example computation of R_{ndr}

$$R_{ndr} = R_n + R_{scour} + R_{relax} \qquad \text{Eq. 7-86}$$

$$R_{ndr} = 308 + 50 + (\frac{100}{0.65}) = 512\ kips$$

As shown in the above example, $R_{ndr}$is considerably higher than the nominal resistance due to the site specific considerations of scour and relaxation. The load and resistance factors used in this determination may be found respectively in Table 2-3 in Chapter 2 and Table 7-2 of this chapter.

7.7 DRIVABILITY ANALYSIS

Greater pile penetration depths are increasingly being required to satisfy minimum penetration depth requirements due to extreme events such as scour, vessel impact, ice and debris loading, as well as seismic events. Therefore, the ability of a pile to be driven to the required penetration depth has become increasingly more important. AASHTO (2014) Article 10.7.8 states that a drivability analysis should be performed by the engineer and that it be conducted during the design stage. Pile drivability refers to the ability of a pile to be driven to the required pile penetration depth and/or to the required resistance, and within specified material strength limits. All of the previously described static analysis methods are meaningless if the pile cannot be driven to the required depth and nominal resistance without sustaining damage. The limit of pile drivability is the maximum soil resistance a pile can overcome at a reasonable blow count without being damaged while being driven by an appropriately sized and properly operating driving system.

Primary factors controlling the nominal geotechnical resistance of a pile are the pile type and length, the soil conditions, and the method of installation. Since the pile type, length and method of installation can be specified, it is often erroneously assumed that the pile can be installed as designed to the estimated penetration depth. However, the pile must have sufficient drivability to overcome the soil

resistance encountered during driving to reach the estimated or specified pile penetration depth. If a pile section does not have a drivability limit in excess of the soil resistance to be overcome during driving, it will not be drivable to the desired pile penetration depth. The failure to adequately evaluate pile drivability is one of the most common deficiencies in driven pile design practice.

In evaluating the drivability of a pile, the soil disturbance during installation and the time dependent soil strength changes should be considered. Both soil setup and relaxation have been described earlier in this chapter. For economical pile design, the foundation designer must match the soil resistance to be overcome at the time of driving with the pile impedance (discussed below), the pile material strength, and the pile driving equipment.

7.7.1 Factors Affecting Drivability

A pile must satisfy two aspects of drivability. First, the pile must have sufficient stiffness to transmit driving forces large enough to overcome soil resistance. Second, the pile must have sufficient structural strength to withstand the driving forces without damage.

The primary controlling factor on pile drivability is the pile impedance, EA/C. Once the pile material is selected, and thus the pile modulus of elasticity, E, and the pile wave speed, C, only increasing the pile cross sectional area, A, will improve the pile drivability. For steel H-piles, the designer can improve pile drivability by increasing the H-pile section without increasing the H-pile size. This will increase the area and impedance without significantly changing the soil resistance on the section. The drivability of steel pipe piles can be improved by increasing the pipe wall thickness. This again increases the pile impedance without increasing the soil resistance. For open ended pipe piles, an inside-fitting cutting shoe can improve drivability by delaying the formation of a soil plug and thereby reducing the soil resistance to be overcome. Most concrete piles are solid cross sections. Therefore, increasing the pile area to improve drivability is usually accompanied by an increase in the soil resistance to driving.

A lesser factor influencing pile drivability is the pile material strength. The influence of pile material strength on drivability is limited, since strength does not alter the pile impedance. However, a pile with a higher pile material strength can tolerate higher driving stresses that may allow a larger pile hammer to be used. This may allow a slightly higher nominal resistance to be obtained before refusal driving conditions or pile damage occurs.

Other factors that may affect pile drivability include the driving system characteristics such as ram weight, stroke, and speed, as well as the actual system performance in the field. The dynamic soil response can also affect pile drivability. Soils may have higher damping characteristics or elasticity than assumed, both of which can reduce pile drivability. Dynamic soil response is discussed in greater detail in Chapters 10, 11, and 12. Pile installation aids such as predrilling, jetting and spudding, can assist in meeting project pile penetration requirements. However, these installation aids do not change the drivability of the pile section.

Even if the geotechnical and structural resistance both indicate a large geotechnical resistance could be used, this large geotechnical resistance may still not be obtainable because driving stresses may exceed material driving stress limits. A pile cannot be driven to a static nominal resistance that is as high as the structural resistance of the pile because of the additional dynamic resistance or damping forces generated during pile driving. Pile structural resistance and driving stresses are presented in Chapter 8.

7.7.2 Methods for Determining Pile Drivability

There are three available methods for predicting and/or checking pile drivability. As design tools, all of the methods have advantages and disadvantages and are therefore presented in order of increasing cost and reliability.

1. Wave Equation Analysis

   This computer program accounts for pile impedance and calculates estimated driving stresses as well as the relationship of pile penetration resistance (blow count) versus nominal resistance (Goble and Rausche 1986). Wave equation analyses performed in the design stage require assumptions on the hammer type and performance level, the drive system components, as well as the soil response during driving. These shortcomings are reflected in variations between predicted and actual field behavior. Even with these shortcomings, the wave equation is a powerful design tool that can and should be used to check drivability in the design stage, to design an appropriate pile section, or to specify driving equipment characteristics. As noted previously, AASHTO (2014) design specification state that a wave equation drivability analysis should be performed during design in the strength limit state. Additional information on the wave equation, including its use as a construction control tool, is presented in Chapter 12.

2. Dynamic Testing and Analysis

Dynamic measurements can be made during pile installation to calculate driving stresses and to estimate nominal resistance at the time of driving. Time dependent changes in nominal resistance can be evaluated during restrike tests. Signal matching analysis of the dynamic test data can provide soil parameters for a refined wave equation analysis. A shortcoming of this method as a design tool is that it must be performed during pile driving. Therefore, in order to use dynamic testing information to confirm drivability or to refine a design, a test program is required during the design stage. Additional details on dynamic testing and analysis, including its use as a construction control tool, is presented in Chapter 10.

3. Static Load Tests

Static load tests are useful for confirming pile drivability and the nominal resistance prior to production pile driving (Kyfor et al. 1992). Test piles are normally driven to estimated lengths and load tested. The confirmation of pile drivability through static load test programs is the most accurate method of confirming drivability and nominal resistance since a pile is actually driven and statically load tested. However, this advantage also illustrates one of its shortcomings as a design tool, in that a test program is required during the design stage. Other shortcomings associated with static load tests for determining drivability include:

a. cost and time delay that limit their suitability to certain projects.

b. assessment of driving stresses and the extent of pile damage, if any, is not provided by the test.

c. can be misleading on projects where soil and/or rock conditions are highly variable.

Additional details on static load tests, including its use as a construction control tool, are presented in Chapter 9. Rapid load tests can also be used to evaluate nominal resistance and are discussed in Chapter 11.

As design and construction control tools, methods 1 and 2 offer additional information and complement static load tests. Used properly, methods 1 and 2 can yield significant savings in material costs or reduction of construction delays and

risks of claims. These methods can be used to reduce the number of static load tests and increase the usefulness and applicability of the static load test performed. A determination of the increase (soil setup) or decrease (relaxation) in geotechnical resistance with time can also be made if piles are tested under restrike conditions after initial driving.

7.7.3 Drivability versus Pile Type

Drivability should be checked during the design stage of all driven piles. It is particularly important for closed end steel pipe piles where the impedance of the steel casing may limit pile drivability. Although the designer may attempt to specify a thin wall pipe in order to save material cost, a thin wall pile may lack the drivability to develop the required nominal resistance or to achieve the necessary pile penetration depth. This concept is illustrated in the wave equation example problem presented in Section 12.5.8 of Chapter 12. Wave equation drivability analyses should be performed in the design stage to select the pile section and wall thickness per AASHTO (2014) design specifications. An example of a wave equation drivability assessment is presented in Section 12.5.3.

Steel H-piles and open pipe piles, prestressed concrete piles, and timber piles are also subject to drivability limitations. This is particularly true as extreme events and the trend to use larger nominal resistances require increased pile penetration depths. The drivability of long prestressed concrete piles can be limited by the pile's tensile strength.

7.8 CONSIDERATIONS FOR BATTER PILE DESIGN AND CONSTRUCTION

Battered or inclined piles are piles that are driven on an inclination from vertical and are often considered when large static lateral loads are expected or where structural rigidity is required. A battered pile can typically resist larger horizontal loads and experience less deflection than their vertical counterparts at the same loading levels. When static loads are applied, battered piles generally perform well. However under dynamic horizontal loads or for seismic events, the increased structural stiffness benefit decreases. In seismic design particularly, earthquake induced displacements generate load, and as force is a function of stiffness, the increased stiffness from battered piles results in larger applied horizontal forces to the structure. Where significant drag forces are expected, battered piles should be avoided due to the increased bending moment loads along the pile length.

The response of a pile group to applied loads will differ if the pile group consists solely of vertical piles, or if the pile group consists of a combination of vertical and batter piles. Figure 7-80 illustrates the response of a foundation unit subjected to a horizontal load and an overturning moment. In Case A, the foundation unit is supported by a single pile that rotates about a point below the ground surface in response to the applied load and moment. In Case B, the foundation unit is supported by two vertical piles and it translates horizontally and displaces vertically downward in response to the applied load and overturning moment. In Case C, the foundation unit is supported by an outwardly battered lead pile and a trailing vertical pile. This foundation unit translates horizontally and displaces vertically upward in response to the applied load and overturning moment. Hence, the influence of batter piles on the foundation response must be considered in the foundation design.

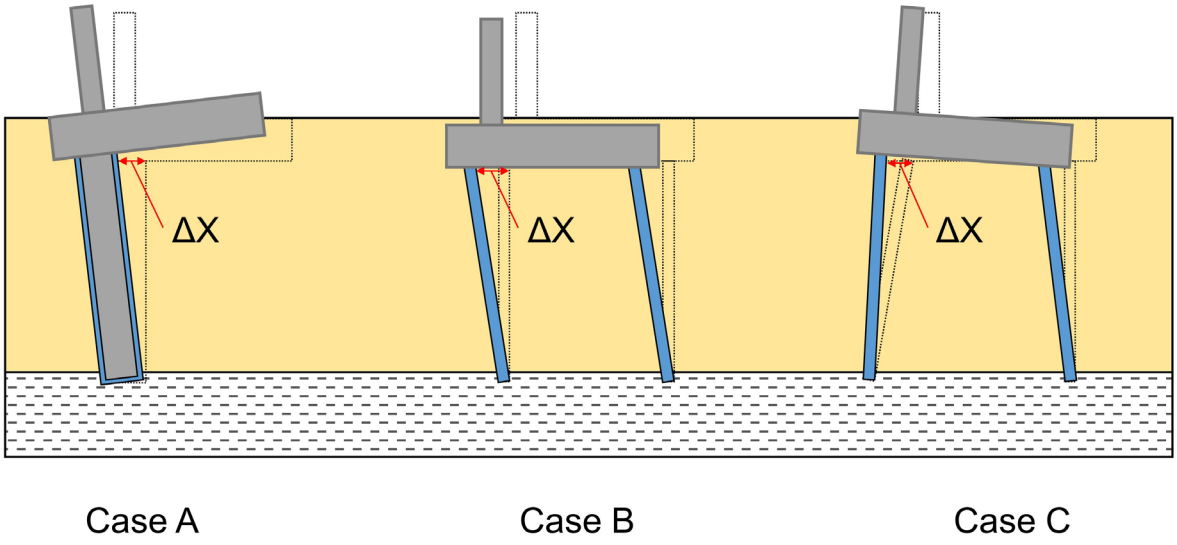

Figure 7-80 Variation of foundation response depending on group configuration and batter (after Wilson et al. 2006).

For batter piles, the horizontal component of the axial load contributes to, or subtracts from the horizontal resistance of the group depending on the batter pile direction relative to the applied load. Wilson et al. (2006) noted that the analysis for a pile group containing batter piles is similar to the procedures described earlier in Section 7.3.7.5 with the following exceptions:

1. Using a rigid cap assumption, the vertical load at the head of each pile is resolved into the axial pile load based on the batter angle. The horizontal component of the axial pile load is then computed.

2. The sum of all horizontal components is computed, and the total compared to the applied horizontal load. If the sum of the horizontal components is less than the applied horizontal load, the remainder of the horizontal load must be resisted through pile bending computed in a p-y analysis. If the sum of the horizontal components are greater and opposite of the applied horizontal load, the piles will bend in the opposite direction of the applied load.

3. If no vertical load is applied to a batter pile by the pile cap, the batter pile will have no axial load. Without an axial load, it will have no horizontal component to resist an applied horizontal load. A battered pile in this scenario behaves as a vertical pile and the horizontal resistance is provided by pile bending.

Careful assessment of the direction of the applied horizontal loads and corresponding need, location, and orientation of batter piles is required when batter piles are incorporated into a foundation design. As noted above, adding batter piles to resist horizontal loads is inefficient and could be more economically handled by vertical piles if the batter pile receives no vertical load from the pile cap.

Batter pile interference with the surrounding environment should be carefully reviewed during the design. The selected batter angle as well as pile deviation from the selected batter angle should be evaluated for potential conflicts with adjacent in-use foundations, cofferdams and excavation support systems, utilities, abandoned deep foundations from previous construction, tunnels, and other constraint posed by the surrounding environment. In situations where an offshore lead and template system are used with batter piles, additional bending stresses from the weight of the pile hammer and the unsupported portion of the pile above the template can cause additional stresses that must be considered in addition to the axially oriented driving stresses. From a constructability standpoint, batter angles greater than 1H:3V should be avoided.

7.9 CORROSION AND DETERIORATON

Corrosion and deterioration of all pile types must be considered for the respective environmental conditions. Section 6.12 of Chapter 6 provides extensive detail on

design considerations for aggressive subsurface environments. AASHTO (2014) recommends at minimum, an evaluation for steel corrosion particularly in fill soils, low pH soils, and marine environments. For concrete piles, sulfate, chloride and acid attack should be evaluated. Timber piles are subject to decay from wetting and drying cycles as well as attack from marine bores and insects. Additional details can be found in AASHTO (2014) Article 10.7.5 and associated commentary.

7.10 ADDITIONAL DESIGN AND CONSTRUCTION CONSIDERATIONS

The previous sections of this chapter addressed typical geotechnical design and analysis procedures for pile foundation design. However, the designer should be aware of additional design and construction considerations that can influence the reliability of static analysis procedures in estimating nominal resistance. These issues include the influence of time, predrilling or jetting, driving piles though embankments, soil densification, and the plugging of open pile sections on soil resistance. Pile driving induced vibrations can also influence the final design and resistance calculation results if potential vibration levels dictate changes in pile type or installation procedures. These final sections serve to fill the gaps between design and construction events that may influence long term resistance and/or construction procedures.

7.10.1 Minimum Pile Spacing, Clearance, and Cap Embedment

AASHTO (2014) design specifications recommend a minimum center-to-center pile spacing of no less than 30 inches or 2.5 pile diameters. In addition, the pile cap edge should be greater than 9 inches from the side of the nearest pile. As discussed previously in this chapter, center-to-center spacing less than 3.0 diameters can create construction difficulties and lower pile group axial and lateral resistances. Therefore, the benefit of a smaller cap size should be weighed against the reduced resistances and constructability issues that can arise with the smaller spacing.

The pile head should extend a minimum of 12 inches into the pile cap. Any damaged portions of the pile head should be trimmed and the damaged portion removed down to undamaged material before pouring the cap. If piles are attached to the cap by embedded bars or strands, the piles should extend a minimum of 6 inches into the pile cap.

When a reinforced concrete bent cap is cast in place atop piles, the concrete cover should be a minimum of 6 inches on all sides of the piles. Pile misalignment may occur. Therefore an additional allowance should be given for cover in conjunction with specified maximum permissible pile misalignment and its remedy. Where pile reinforcement is anchored into the cap satisfying AASHTO (2014) Article 5.13.4.1 requirements, the projection may be less than 6.0 inches.

7.10.1.1 Special Considerations for Large Pile Sizes

AASHTO design specifications do not address minimum pile spacing requirements or pile cap embedment for large diameter open end pipe piles. The synthesis study on large diameter pipe piles by Brown and Thompson (2015) presents limited details on this subject and most state agencies do not currently have standard plan details for these large pile sizes.

One detail used to connect large diameter pipe piles into the pile cap consists of internally cleaning out the pipe pile to the desired depth, if necessary, and then inserting a reinforcing cage into the pile that also extends up into the pile cap. The pile is then filled with a concrete plug. In some cases, design details require the internal cleanout extended to the scour depth or mudline, and in other instances, the concrete plug extends only for the length needed for load transfer.

Another design approach is use an internal reinforcing cage in conjunction with welded shear studs on the exterior surface of the pile that extends into the pile cap. At least two rows of shear studs are frequently used to develop sufficient load transfer from the pile to cap. In addition to the use of rebar cages or cages and shear studs, large diameter piles heads typically extend on the order of 3 feet into the pile cap to develop the required structural connection.

Little information was provided with respect to center to center pile spacing. However because of the large diameter, comparison with drilled shaft minimum spacing guidelines may be appropriate. The presented pile layout in Brown and Thompson (2015) shows the minimum spacing to be on the order of 3 pile diameters center-to- center. Since large diameter open end piles are often selected for a foundation design due to their high lateral load resistance, greater center-to-center pile spacing may be applicable for the lateral load demand.

7.10.2 Identification of High Rebound Soils

During pile driving, the hammer impact causes temporary compression of the soil and pile system. For certain soil types, the deformed soil system can spring back close to its original position. When this occurs, it proves difficult to continue pile driving operations and to achieve the nominal resistance (Hussein et al. 2006). This effect is known as high rebound, or elastic rebound, and is generally due to increased pore water pressure from driving occurring near the pile toe. As driving continues, pore water pressure increases and causes a larger rebound, leading to refusal like driving conditions. If pile driving is paused, the pore water pressure dissipates and subsequently smaller rebound occurs.

Studies have shown that for dense silty sand, hard silty clay, glacial tills, silt and other fine grained saturated soils, high elastic rebound can occur when using displacement piles (Likins 1983; Hussein et al. 2006; Cosentini et al. 2010). Research is ongoing to determine what specific soil properties or in-situ tests may be used to locate and quantify high rebound soils beyond a basic assessment of soil types and saturation. Local experience may be of great value in areas where these soil conditions exist, as recommendations on pile drivability may provide a significant cost savings in design and construction. Pile driving equipment with heavy rams operating at short hammer strokes is helpful in these installation conditions.

7.10.3 Soil and Pile Heave

As noted by Hagerty and Peck (1971), whenever piles are driven, soil is displaced. This can result in both upward movement (pile heave) and lateral movements of previously driven piles. These soil movements can be detrimental to the resistance of previously driven piles as well as to adjacent facilities. Obviously, the greater the volume of soil displaced by pile driving, the greater the potential for undesirable movements of previously driven piles, or damage to adjacent structures. Heave of piles primarily supported by toe resistance is particularly troublesome since the pile may be lifted from the bearing stratum, thereby greatly reducing the soil resistance and increasing the foundation settlement when loaded. Haggerty and Peck noted that saturated, insensitive clays display incompressible behavior during pile driving and have the greatest heave potential.

When piles are to be installed in cohesive soils, it is recommended that the potential magnitude of vertical and lateral soil movements be considered in the design stage. If calculations indicate that movements may be significant, use of an alternate low displacement pile, or specifying a modified installation procedure (such as predrilling

to reduce the volume of displaced soil) should be evaluated. A step by step procedure adapted from Haggerty and Peck for estimating soil and pile heave in saturated insensitive clay follows. The procedure assumes a regular pile driving sequence and a level foundation surface. The paper by Haggerty and Peck should be consulted for modifications to the recommended procedure for conditions other than those stated.

STEP BY STEP PROCEDURE FOR ESTIMATING SOIL AND PILE HEAVE

STEP 1 Calculate the estimated soil heave at the ground surface.

a. Divide the volume of inserted piles by the volume of soil enclosed by the pile foundation to obtain the volumetric displacement ratio.

b. Estimate the normalized soil heave (soil heave / pile length) from ½ the volumetric displacement ratio calculated in Step 1a.

c. Calculate the soil heave at the ground surface by multiplying the normalized soil heave in Step 1b by the average length of piles.

STEP 2 Determine the depth of no pile-soil movement.

a. Figure 7-81 illustrates that an equilibrium depth, d, exists where the potential upward pushing and downward resisting forces on the pile shaft are equal.

b. Calculate the pile-soil adhesion along the entire pile shaft using the α-method described in Section 7.2.1.3.2.

c. Through multiple iterations determine the equilibrium depth, d, where the adhesion from the upward pushing force equals the adhesion from the downward resisting force. Note that only shaft resistance is considered in calculating the downward resisting force.

STEP 3 Calculate the estimated pile heave.

a. Calculate the percentage of pile length resisting heaving soil.

$$L\% = \frac{D-d}{D} \qquad \text{Eq. 7-87}$$

Where:

$L\%$ = percentage of pile length resisting heaving soil (%).
D = pile embedded length (feet).
d = equilibrium depth (feet).

b. Calculate the estimated pile heave by multiplying the estimated soil heave from Step 1c by the percentage of pile length resisting heave from Step 3a.

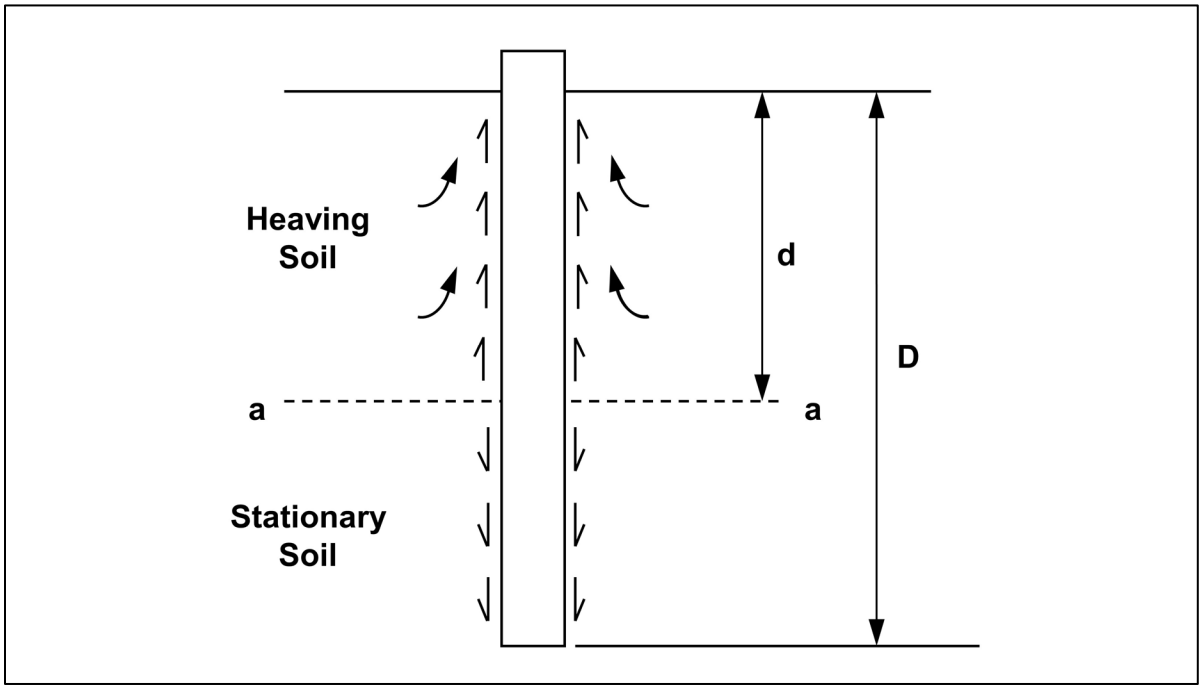

Figure 7-81 Balance of forces on pile subject to heave (after Haggerty and Peck 1971).

More recent work on this topic was present in Sagaseta and Whittle (2001) where the shallow strain path method (SSPM) was used to predict ground movements due to pile driving in clay. Results from this method typically yield a reasonable first estimate of pile heave.

7.10.4 Piles Driven Through Embankment Fills

Approach embankments are frequently constructed before the commencement of pile driving operations. Piles driven through embankment fills should penetrate a minimum of 10 feet below original grade unless refusal driving conditions are

encountered on bedrock or a competent bearing layer. An alternative foundation type may be more effective in cases where refusal driving conditions occur at a pile penetration depth less than 10 feet below the embankment base. Ideally, bedrock or a bearing layer that may cause refusal driving conditions is identified by the subsurface exploration program performed before foundation construction begins. To minimize drag forces, piles should not be driven through embankments or constructed over compressible materials until after 90% primary settlement is complete.

7.10.5 Effect of Predrilling, Jetting and Vibratory Installation on Nominal Resistance

Piles are sometimes predrilled or jetted to a prescribed depth in order to attain the pile penetration depths required, as well as to reduce other foundation installation concerns, such as ground vibrations. Jetting is usually performed in cohesionless soils that can be freely eroded by water jets. Jetting, which can be very effective in sands, is usually ineffective in cohesive soils. For clays, and other drillable materials, such as thin layers of rock, predrilling the pile locations is more effective. The predrilled hole can be slightly smaller, equal to, or slightly larger than the pile diameter.

The use of predrilling or jetting will result in greater soil disturbance than considered in standard static pile resistance calculations. Therefore, when predrilling or jetting is contemplated, the effect of either of these construction procedures on calculated compression, uplift, and lateral soil resistance should be considered. Poulos and Davis (1980) reported that the shaft resistance should be reduced by 50% of the originally calculated resistance in the jetted zone, if the pile is jetted and then driven to the final penetration. McClelland et al. (1969) reported that a decrease in shaft resistance over a predrilled depth can range from 50 to 85% of that calculated without predrilling, depending upon the size of the predrilled hole. Hence, the probable reduction in compression, uplift, and lateral resistance from jetting or predrilling should be evaluated whenever predrilling or jetting is being considered.

Agencies are often requested to allow pile installation with a vibratory pile hammer instead of an impact hammer. Mosher (1987) summarized the results from five sites where piles were installed by both impact and vibratory hammers. This study concluded that for a majority of the cases, piles installed in sand with a vibratory hammer had a lower nominal resistance than impact driven piles at the same site. Mosher also concluded that time dependent soil strength changes occurred equally for both installation methods. Hence, even with soil setup, the resistance of the

vibratory installed piles did achieve the resistance of the impact driven piles. However, it was also observed that impact driving a vibratory installed pile would increase the resistance of the vibratory installed pile to that of an impact driven pile.

O'Neill and Vipulanandan (1989) performed a laboratory evaluation of piles installed with vibratory hammers. This laboratory study found impact driven piles had a 25% greater unit shaft resistance and a 15 to 20% higher unit toe resistance than vibratory installed piles in medium dense to dense, uniform, fine sand. However, in very dense, uniform, fine sand, the impact driven pile had a 20 to 30% lower unit shaft resistance and approximately a 30% lower unit toe resistance than the vibratory installed pile.

Ghose-Hajra et al. (2015) compared the effects of pile installation using an impact and a vibratory hammer on the long term soil setup on two H-piles and two open-end pipe piles driven in a soft clay formation in southeast Louisiana. This study found that the impact driven piles always had a greater soil resistance than the companion vibratory installed pile at comparable time intervals.

The above studies indicate use of vibratory pile installation rather than impact driving will affect the nominal pile resistance that can be achieved at a given pile penetration depth. Therefore, communication between design and construction personnel should occur, and the influence of vibratory pile installation be evaluated when it is proposed. Impact driving a specific final depth of vibratory installed piles may provide a foundation that meets the engineer's performance requirements at reduced installation cost.

7.10.6 Densification Effects on Nominal Resistance and Installation Conditions

As illustrated in the previously presented Figure 7-1, driving a pile in cohesionless soil influences the surrounding soils to a distance of about 3 to 5 pile diameters away from the pile. The soil displacement and vibrations resulting from driving pile groups in cohesionless soils can further densify cohesionless materials. The use of displacement piles also intensifies group densification effects in cohesionless soils.

Densification can result in the soil resistance as well as the resistance during pile driving being significantly higher than that calculated for a single pile in static analysis calculations. The added confinement provided by cofferdams or the sequence of pile installation can further aggravate a group densification issue. Piles should be installed from the center of the group outward in order to reduce group densification effects due to installation sequence. Densification can cause

significant construction problems if scour, seismic, or other considerations require achieving pile penetration depths that cannot be achieved.

Potential densification effects should be considered in the design stage. Studies by Meyerhof (1959) and Kishida (1967) indicate that an increase in the soil friction angle of up to 4 degrees would not be uncommon for piles in loose to medium dense sands. It is expected that the increase in soil friction angle would be less for dense sands or cohesionless soils with a significant fine content. Densification affects the nominal resistance to be overcome during driving. As a constructability check, static analyses should be performed using higher soil strength parameters than used for design to assess nominal resistance due to densification. Results from these static analyses may indicate that a low displacement pile should be used, the pile spacing should be increased, or that a pile installation aid should be specified in order to obtain the required pile penetration depth.

7.10.7 Plugging of Open Pile Sections

Open pile sections include open end pipe piles and H-piles. The use of open pile sections has increased, particularly where special design events dictate large pile penetration depths. When open pile sections are driven, they may behave as low displacement piles and "core" through the soil, or act as displacement piles if a soil plug forms near the pile toe. It is generally desired that open sections remain unplugged during driving and plugged under static loading conditions.

Stevens (1988) reported that plugging of pipe piles in clays does not occur during driving if pile accelerations (along the plug zone) are greater than 22g's. Holloway and Beddard (1995) reported that hammer blow size (impact force and energy) influenced the dynamic response of the soil plug. With a large hammer blow, the plug "slipped" under the dynamic event, whereas under a lesser hammer blow the pile encountered toe resistance typically of a plugged condition. From a design perspective, these cases indicate that pile penetration of open sections can be facilitated if the pile section is designed to accommodate a large pile hammer. Wave equation analyses can provide calculated accelerations at selected pile segments.

Static soil resistance calculations must determine whether an open pile section will exhibit plugged or unplugged behavior. Studies by O'Neill and Raines (1991), Raines et al. (1992), as well as Paikowsky and Whitman (1990) suggest that plugging of open pipe piles in medium dense to dense sands generally begins at a pile penetration to pile diameter ratio of 20, but can be as high as 35. For pipe piles

in soft to stiff clays, Paikowsky and Whitman (1990) reported plugging can occur at penetration-to-pile diameter ratios of 10 to 20.

The above studies suggest that plugging in any soil material may occur under static loading conditions once the penetration to pile diameter ratio exceeds 20 in dense sands and clays, or 20 to 30 in medium sands. However, plugging is difficult to predict with certainty in all cases. For large diameter open ended pipe piles, plugging during driving is significantly less likely to occur particularly for piles larger than 36 inches in diameter. Plugging of large diameter pipe piles under static loading conditions is more likely than in the dynamic conditions. However, it is still subject to uncertainty. Forced plugging of large diameter pipe piles using an internal constrictor plate as illustrated in Figures 6-14 and 6-15 is sometimes used to reduce this uncertainty.

NCHRP Report 20-05 by Brown and Thompson (2015) provides a summary of the current industry practices with large diameter open end piles and provides an in depth discussion on plugging. This report postulates that large inertial effects prevent plug development during driving. Under static loading conditions, plug or unplugged behavior for these large diameter piles is uncertain. Further research is ongoing regarding design methods on large diameter pipe piles.

An illustration of the difference in the soil resistance mechanism that develops on a pipe pile with an open and plugged toe condition is presented in Figure 7-83. Paikowsky and Whitman (1990) recommend that the static resistance of an open end pipe pile be calculated from the lesser of the following equations:

Plugged Condition:

$$R_n = f_{so}A_{so} + q_pA_{pp} \qquad \text{Eq. 7-88}$$

Unplugged Condition:

$$R_n = f_{so}A_{so} + f_{si}A_{si} + q_pA_p - W_p \qquad \text{Eq. 7-89}$$

Where:

R_n = nominal resistance (kips).
f_{so} = exterior unit shaft resistance (ksf).
A_{so} = pile exterior surface area (ft^2).
f_{si} = interior unit shaft resistance (ksf).
A_{si} = pile interior surface area (ft^2).

q_p = unit toe resistance (ksf).
A_{pp} = cross sectional area of pile and soil plug at pile toe (ft^2).
A_p = cross sectional area of pile material at pile toe (ft^2).
W_p = weight of soil plug (kips).

The soil stresses and displacements induced by driving an open pile section and a displacement pile section are not the same. Hence, a lower unit toe resistance, q_p, should be used for calculating the toe resistance of open end pipe piles compared to a typical closed end condition. The value of the interior unit shaft resistance in an open end pipe pile is typically on the order of 1/3 to 1/2 the exterior unit shaft resistance, and is influenced by soil type, pile diameter, and pile shoe configuration. These factors will also influence the length of soil plug that may develop.

For open end pipe piles in cohesionless soils, Tomlinson (1994) recommends that the static soil resistance be calculated using a limiting value of 105 ksf for the unit toe resistance, regardless of the pile size or soil density. Tomlinson states that higher unit toe resistances do not develop, because yielding of the soil plug rather than geotechnical failure of the soil below the plug governs the resistance.

For open end pipe piles driven in stiff clays, Tomlinson (1994) recommends that the static soil resistance be calculated as follows when field measurements confirm a plug is formed and carried down with the pile:

$$R_n = 0.8C_aA_s + 4.5s_uA_p \qquad \text{Eq. 7-90}$$

Where:
R_n = nominal resistance (kips).
C_a = pile adhesion from Figure 7-17 (ksf).
A_s = pile shaft surface area (ft^2).
s_u = average undrained shear strength at the pile toe (ksf).
A_p = toe area of a plugged pile (ft^2).

Static soil resistance calculations for open end pipe piles in cohesionless soils should be performed using the Paikowsky and Whitman equations. Toe resistance should be calculated using the Tomlinson limiting unit toe resistance of 105 ksf, once Meyerhof's limiting unit toe resistance, determined from Figure 7-15, exceeds 105 ksf. For open end pipe piles less than 24 inches in diameter, and in predominantly cohesive soils, the Tomlinson equation should be used. Conversely, for moderate (24 to 36 inch O.D.) and large (36+ inch) diameter open ended pipe piles, plugging is less certain under static conditions and should be carefully analyzed.

The API method incorporated into the APILE program calculates the plugged and unplugged resistance of a open end pipe pile. The program also contains an automated routine that calculates whether a plugged or unplugged condition will develop. The results for a 30 inch open end pipe along with the analyzed soil profile are presented in Figure 7-82.

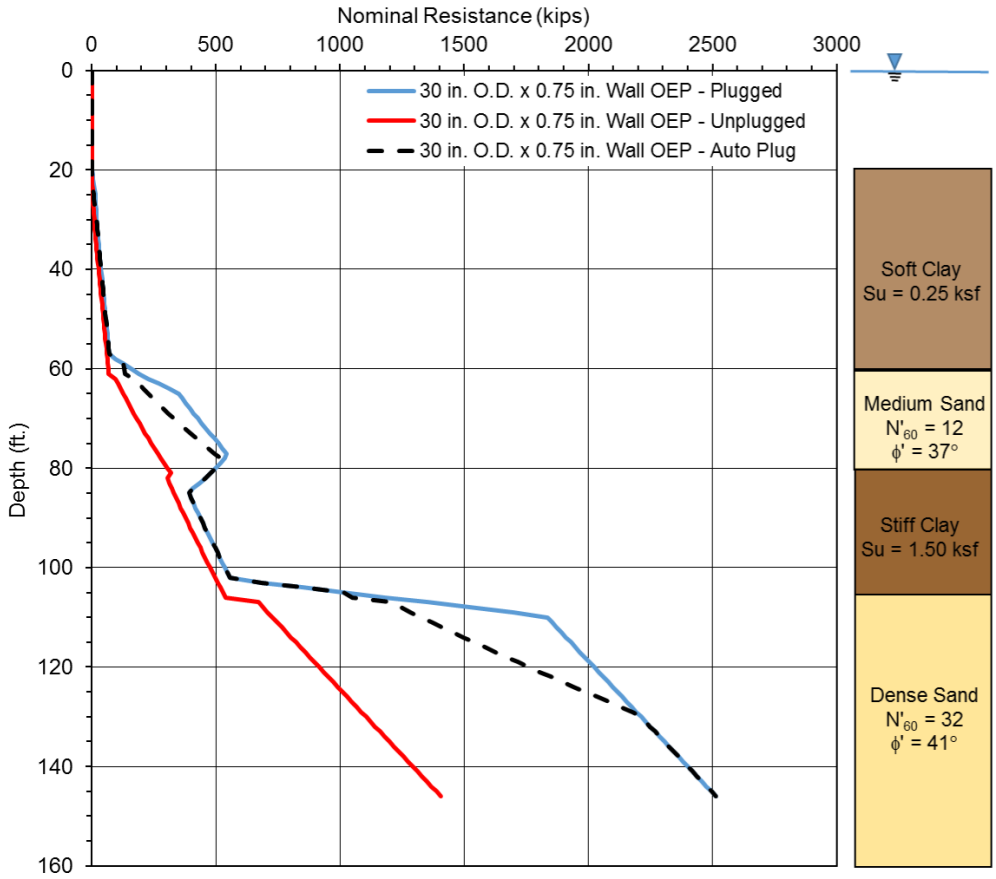

Figure 7-82 Variation in expected static resistance from APILE API method based on plugged, unplugged, and automatic calculated plugging.

The plugging phenomenon in H-piles can be equally difficult to analyze. However, the distance between flanges of an H-pile is smaller than the inside diameter of most open end pipe piles. Therefore, an H-pile is more likely to be plugged under static loading conditions where the “box” area of the pile toe is be used for static calculation of the toe resistance in cohesionless and cohesive soils. The toe resistance for H-piles driven to rock is usually governed by the pile structural strength, calculated based on the steel cross sectional area, and should not include the area of a soil plug, if any.

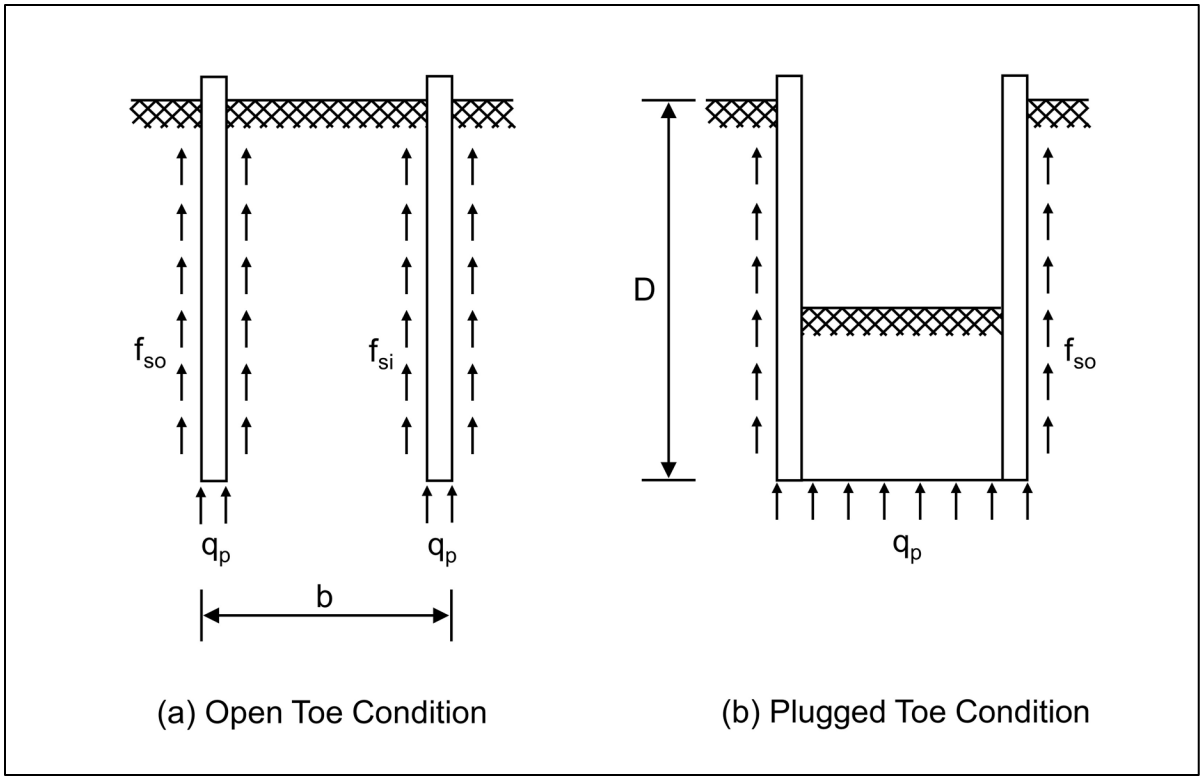

Figure 7-83 Plugging of open end pipe piles
(after Paikowsky and Whitman 1990).

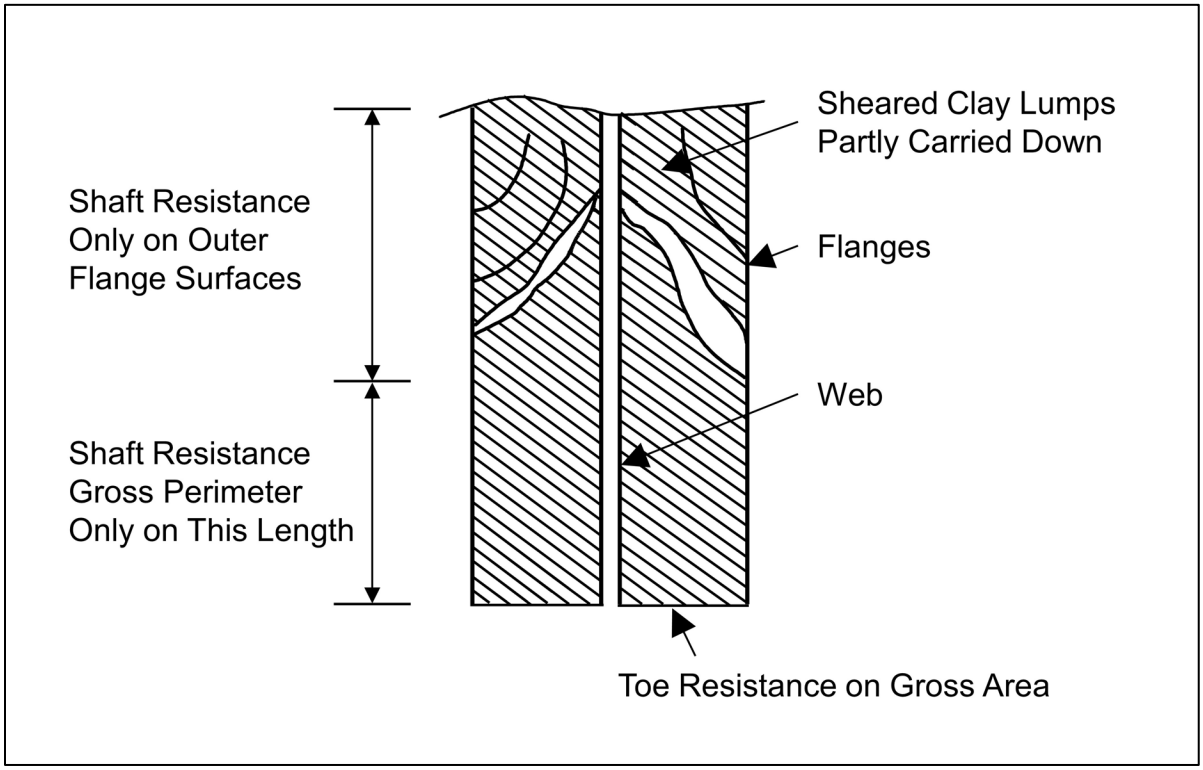

Figure 7-84 Plugging of H-piles (after Tomlinson 1994).

For H-piles in cohesionless soils, arching between the flanges may occur, and the "box" perimeter can be used for shaft resistance calculations. In most cohesive soils, the shaft resistance is calculated from the sum of the adhesion, C_a, along the exterior of the two flanges plus the undrained shear strength of the soil, s_u, times the surface area of the two remaining sides of the "box" due to soil-to-soil shear along these two faces. Figure 7-84 illustrates that the calculation of shaft resistance in H-piles in stiff clays can still be problematic. Sheared clay lumps can develop above the plug zone, in which case the shaft resistance may only develop along the exterior surfaces of the flanges in the sheared lump zone.

The above discussions highlight the point that a higher degree of uncertainty often exists for static soil resistance calculations of open pile sections than for displacement piles. Soil plug formation and plug response is often different under static and dynamic loading. This can complicate nominal resistance evaluations of open pile sections with all dynamic methods (wave equation, dynamic testing, and dynamic formulas). Therefore, for large diameter open end pipe piles, greater than 18 inches, or for H-piles designed to carry their load primarily in shaft resistance, a static load test is recommended for resistance verification.

REFERENCES

Altaee, A., Evgin, E. and Fellenius, B.H. (1992). Axial Load Transfer for Piles in Sand, I:Tests on an Instrumented Precast Pile. Canadian Geotechnical Journal, Vol. 29, No. 1, pp. 11-20.

American Association of State Highway and Transportation Officials (AASHTO). (2010). LRFD Guide Specifications and Commentary for Vessel Collision Design of Highway Bridges, Second Edition, with 2010 Interim, CVCB-2-M. American Association of State Highway and Transportation Officials, Washington, D.C., 244 p.

American Association of State Highway and Transportation Officials (AASHTO). (2014). AASHTO LRFD Bridge Design Specifications, US Customary Units, Seventh Edition, with 2015 Interim Revisions. American Association of State Highway and Transportation Officials, Washington, D.C., 1960 p.

American Petroleum Institute (API). (1993). Recommended Practice for Planning, Designing and Constructing Fixed Offshore Platforms – Load and Resistance Factor Design. API Recommended Practice 2A-LRFD (RP 2A-LRFD), First Edition, Reaffirmed 2003, 242 p.

Arneson, L.A., Zevenbergen, L.W., Lagasse, P.F., and Clopper, P.E. (2012). Evaluating Scour at Bridges, Fifth Edition, FHWA-HIF-12-003, Hydraulic Engineering Circular (HEC) No. 18. U.S. Dept. of Transportation, Federal Highway Administration, 340 p.

Ashour, M., Norris, G., and Pilling, P., (1998a). Lateral Loading of a pile in Layered Soil Using the Strain Wedge Model. American Society of Civil Engineers, (ASCE) Journal of Geotechnical and Geoenvironmental Engineering, Vol. 124, No.4, pp. 303–315.

Ashour, M., Norris, G., and Pilling P., (2002). Strain Wedge Model Capability of Analyzing Behavior of Laterally Loaded Isolated Piles, Drilled Shafts, and Pile Groups. American Society of Civil Engineers, (ASCE) Journal of Bridge Engineering, Vol. 7, No. 4, pp. 245-254.

Awoshika, K., and Reese, L. C., (1971). Analysis of Foundation with Widely-Spaced Batter Piles, Research Report 11 7-3F, Center for Highway Research, The University of Texas at Austin, 321 p.

Bollman, H.T. (1993). Notes on Designing Deep Foundations for Lateral Loads. Proceedings of Design of Highway Bridges for Extreme Events, Crystal City, VA, pp. 175-199.

Bowles, J.E. (1977). Foundation Analysis and Design. Second Edition, McGraw-Hill Book Company, Blacklick, OH, 750 p.

Bowles, J.E. (1988). Foundation Analysis and Design. Fourth Edition, McGraw Hill, New York, NY, 1023 p.

Brandenberg, S.J., Boulanger, R.W., Kutter, B.L., and Chang, D. (2007). Static Pushover Analyses of Pile Groups in Liquefied and Laterally Spreading Ground in Centrifuge Tests. American Society of Civil Engineers (ASCE), Journal of Geotechnical and Geoenvironmental Engineering, Vol. 133, No. 9, pp. 1055-1066.

Briaud J-L. and Miran, J. (1992). The Cone Penetration Test, FHWA-SA-91-043. U.S. Department of Transportation, Federal Highway Administration, Office of Technology Applications, Washington, D.C., 161 p.

Briaud, J. L. and Tucker, L.M. (1993). Downdrag on Bitumen-Coated Piles, NCHRP 24-5. National Cooperative Highway Research Program, (NCHRP), Washington, D.C., 245 p.

Broms, B.B. (1964a). Lateral Resistance of Piles in Cohesive Soils. American Society of Civil Engineers, (ASCE), Journal for Soil Mechanics and Foundation Engineering, Vol. 90, SM2, pp. 27-63.

Broms, B.B. (1964b). Lateral Resistance of Piles in Cohesionless Soils. American Society of Civil Engineers, (ASCE), Journal for Soil Mechanics and Foundation Engineering., Vol. 90, SM3, pp. 123-156.

Broms, B.B. (1966). Methods of Calculating the Ultimate Bearing Capacity of Piles – A Summary. Soils-Soils, No. 18-19, pp. 21-32.

Brown, D.A., Reese, L.C. and O'Neill, M.W. (1987). Cyclic Lateral Loading of a Large-Scale Pile Group in Sand. American Society of Civil Engineers (ASCE), Journal of Geotechnical Engineering., Vol. 113, No. 11, Reston, VA, pp. 1326-1343.

Brown, D.A., Morrison, C. and Reese, L.C. (1988). Lateral Load Behavior of Pile Group in Sand. American Society of Civil Engineers (ASCE), Journal of Geotechnical Engineering , Vol. 114, No. 11, Reston, VA, pp. 1261-1276.

Brown, D.A. and Bollman, H.T. (1993). Pile-Supported Bridge Foundations Designed for Impact Loading. Appended Document to the Proceedings of Design of Highway Bridges for Extreme Events, Crystal City, VA, pp. 265-281.

Brown, D.A., O'Neill, M.W., Hoit, M., McVay, M., El Naggar, M.H., and Chakraborty, S. (2001). Static and Dynamic Lateral Loading of Pile Groups. NCHRP Report 461, Transportation Research Board – National Research Council, Washington, D.C., 50 p.

Brown, D. A., Turner, J.P. and Castelli R.J. (2010). Drilled Shafts: Construction Procedures and LRFD Design Methods, FHWA-NHI-10-016, Geotechnical Engineering Circular (GEC) No. 10. U.S. Dept. of Transportation, Federal Highway Administration, 970 p.

Brown, D.A., and Thompson III, W.R. (2015). Current Practices for Design and Load Testing of Large Diameter Open –End Driven Pipe Piles. Final Report. NCHRP Report 20-05, Topic 45-05 National Cooperative Highway Research Program, Washington, D.C., 175 p.

Brown, R. P. (2001). Predicting the Ultimate Axial Resistance of Single Driven Piles. PhD Dissertation (supervisor: Prof. Roy E. Olson), Department of Civil Engineering, The University of Texas at Austin, 168 p.

Bullock, P.J., Schmertmann, J. H., McVay, M. C., Townsend, F., March (2005). Side Shear Setup. II: Results From Florida Test Piles. American Society of Civil Engineers (ASCE), Journal of Geotechnical Engineering, Vol. 131, No. 3, Reston, VA, pp. 301-310.

Canadian Geotechnical Society. (1985). Canadian Foundation Engineering Manual, Second Edition. Technical Committee on Foundations, BiTech Publishers, Vancouver, B.C., 456 p.

Cheney, R.S. and Chassie, R.G. (2000). Soils and Foundations Workshop Reference Manual. FHWA HI-00-045, U.S. Department of Transportation, National Highway Institute, Federal Highway Administration, Washington, D.C., 358 p.

Cheney, R.S. and Chassie, R.G. (2002). Soils and Foundation Workshop Manual. Second Edition, Report No. HI-88-009. U.S. Department of Transportation, Federal Highway Administration, Office of Engineering, Washington, D.C., 395 p.

Coduto, D.P. (1994). Foundation Design: Principles and Practice. Prentice-Hall, Inc., Englewood Cliffs, NJ, 796 p.

De Nicola, A. and Randolph, M. (1993). Tensile and Compressive Shaft Capacity of Piles in Sand. Journal of Geotechnical Engineering., Vol. 19, No. 12, pp. 1952-1973.

Duncan, J.M., and Buchignani, A.L (1976). An Engineering Manual for Settlement Studies, Department of Civil Engineering, University of California, Berkeley, CA, 94 p.

Duncan, J. M., and S. G. Wright. (2005). Soil Strength and Slope Stability, John Wiley, Hoboken, N.J, 297 p.

Elias, V., Welsh, J.P., Warren, J., Lukas, R.G., Collin J.G., and Berg, R.R. (2006). Ground Improvement Methods Volumes I and II, FHWA-NHI-06-019 and FHWA NHI-06-020. National Highway Institute, Federal Highway Administration, U.S. Department of Transportation, Washington D.C.

Eslami, A., and Fellenius, B. H. (1997). Pile Capacity by Direct CPT and CPTu Methods Applied to 102 Case Histories. Canadian Geotechnical Journal, Vol. 34, No. 6, pp. 880-898.

Fayyazi, M.S., Taiebat, M., Finn, W.D.L., and Ventura, C.E. (2012). Evaluation of P-Multiplier Method for Performance Based Design of Pile Groups. Second International Conference on Perfromance Based Design in Earthquake Geotechnical Engineering, Taormina, Italy. , Vol. 34, No. 6, pp. 880-898.

Fellenius, B.H., Riker, R.E., O'Brien, A.J. and Tracy, G.R. (1989). Dynamic and Static Testing in a Soil Exhibiting Set Up. American Society of Civil Engineers (ASCE), Journal of Geotechnical Engineering, Vol. 115, No. 7, pp. 984-1001.

Fellenius, B.H. (1991). Foundation Engineering Handbook, Chapter 13 - Pile Foundations. Second Edition. Van Nostrand Reinhold Publisher, New York, NY, pp. 511-536.

Fellenius, B.H. and Siegel, T.C., (2008). Pile Design Considerations in a Liquefaction Event. American Society of Civil Engineers (ASCE), Journal of Geotechnical and Geoenvironmental Engineering, Vol. 132, No. 9, pp. 1412-1416.

Fellenius, B.H. (2014). Basics of foundation Design. Electronic Edition. www.Fellenius.net, 410 p.

Goble, G.G. and Rausche, F. (1986). Wave Equation Analysis of Pile Driving - WEAP86 Program. U.S. Department of Transportation, Federal Highway Administration, Implementation Division, McLean, Volumes I-IV.

Ghose-Hajra, M., Jensen, R., and Hulliger, L. (2015). Pile Setup and Axial Capacity Gain for Driven Piles Installed Using Impact Hammer versus Vibratory System. Proceedings of the International Foundations Conference and Equipment Exposition 2015, San Antonio, TX, pp. 1064-1074.

Gouderault, P. and Fellenius, B.H. (1994). UNIPILE Program Background and Manual. Unisoft, Ltd., Ottawa, Canada, 120 p.

Hadjian, A.H., Fallgren, R.B. and Tufenkjian, M.R. (1992). Dynamic Soil-Pile-Structure Interaction, The State-of-Practice. American Society of Civil Engineers (ASCE), Geotechnical Special Publication No. 34, Piles Under Dynamic Loads, pp. 1-26.

Hagerty, D.J. and Peck, R.B. (1971). Heave and Lateral Movements Due to Pile Driving. American Society of Civil Engineers (ASCE), Journal of the Soil Mechanics and Foundations Division, Vol. 97, No.11, pp. 1513-1532.

Harris, D.E., Anderson, D.G., Butler, J.J., Fellenius, B.H., Fisher, G.S., and Hinman. J. (2003). Design of Pile Foundations for the Sand Creek Byway, Sandpoint, Idaho. Proceedings of the Deep Foundation Institute Annual Meeting, Miami, FL, 11 p.

Haque, M., Chen, Q., Abu-Farsakh, M., and Tsai, C. (2014). Effects of Pile Size on Setup Behavior of Cohesive Soils. Proceedings of Geo-Congress 2014: Geo-Characterization and Modeling for Sustainability, Atlanta, GA, pp. 1743-1749.

Hoit, M.I. and McVay, M. (1994). LPGSTAN User's Manual. University of Florida, Gainsville, FL, 27 p.

Holloway, D.M. and Beddard, D.L. (1995). Dynamic Testing Results Indicator Pile Test Program - I-880. Proceedings of the 20th Annual Members Conference of the Deep Foundations Institute. Charleston, SC, pp. 105–126.

Holloway, D.M., Moriwaki, Y., Stevens, J.B. and Perez, J-Y. (1981). Response of a Pile Group to Combined Axial and Lateral Loading. Proceedings of the 10th International Conference on Soil Mechanics and Foundation Engineering, Boulimia Publishers, Stockholm, Sweden, pp. 731-734.

Hough, B.K. (1959). Compressibility as the Basis for Soil Bearing Value. American Society of Civil Engineers (ASCE), Journal for Soil Mechanics and Foundation Division, Vol. 85, No. 4, pp. 11-40.

Hussein, M.H., Likins, G.E. and Hannigan, P.J. (1993). Pile Evaluation by Dynamic Testing During Restrike. Eleventh Southeast Asian Geotechnical Conference, Singapore, pp. 535-539.

Hussein, M., Woerner, II, W., Sharp, M., and Hwang, C. (2006). Pile Driveability and Bearing Capacity in High-Rebound Soils. Proceeding of Geocongress 2006: Geotechnical Engineering in the Information Technology Age. Atlanta, GA, February 26-March 1, 2006, ASCE, Reston, VA, pp. 1-4.

Idriss, I.M. and Boulanger, R.W. (2007). SPT and CPT-based Relationships for the Residual Shear Strength of Liquefied Soils. Proceedings of the 4th International Conference on Earthquake Geotechnical Engineering. The Netherlands, pp. 1-22.

Isenhower, W.M. and Wang, S.T. (2014). User's Manual for LPILE 2013: A Program to Analyze Deep Foundations Under Lateral Loading, ENSOFT. Austin, TX, 177 p.

Ismael, N.F. and Klym, T.W. (1979). Pore-Water Pressures Induced by Pile Driving. American Society of Civil Engineers, Journal of Geotechnical Engineering, Vol. 105, No.11, pp.1349-1354.

Kramer. S.L. and Wang, C.-H. (2007). Estimation of the residual strength of liquefied soil, in preparation.

Kramer, S.L. (2008). Evaluation of Liquefaction Hazards in Washington State. Washington State Research Report WA-RD 668.1, Washington State Department of Transportation, Olympia, WA, 329 p.

Janbu, N. (1963). Soil Compressibility as Determined by Oedometer and Triaxial Tests. European Conference on Soil Mechanics and Foundation Engineering, Wiesbaden, Germany, Vol. 1, pp. 19-25.

Janbu, N. (1965). Consolidation of Clay Layers Based on Non-linear Stress-Strain. Proceedings of the Sixth International Conference on Soil Mechanics and Foundation Engineering, Montreal, Canada, Vol. 2, pp. 83-87.

Kavazanjian, E., Wan, J-N. J., Martin, G.R., Shamsabadi, A., Lam, I., Dickenson, S.E., and Hung, C.J. (2011). LRFD Seismic Analysis and Design of Transportation Geotechnical Features and Structural Foundations, FHWA-NHI-11-032, Geotechnical Engineering Circular (GEC) No. 3. U.S. Dept. of Transportation, Federal Highway Administration, Washington, D.C., 592 p.

Kishida, H. (1967). Ultimate Bearing Capacity of Piles Driven in Loose Sands. Japanese Society of Soil Mechanics and Foundation Engineering, Soils and Foundations. Vol. 7, No. 3, pp. 20-29.

Komurka, V.E., Wagner, A.B., and Edil, T.B. (2003). Estimating Soil/Pile Setup, Final Report. Wisconsin Highway Research Program, Report No. 0305, Wisconsin Department of Transportation, Madison, WI, 42 p.

Kulhawy, F.H. and Goodman, R.E. (1980). Design of Foundations on Discontinuous Rock, Proceedings of the International Conference on Structural Foundation on Rock, Sydney, Australia, Vol. 1, pp. 209-220.

Kulhawy, F.H. and Goodman, R.E. (1987). Foundations in Rock, Ground Engineering, Chapter 15, London, UK.

Kyfor, Z.G., Schnore, A.R., Carlo, T.A. and Bailey, P.F. (1992). Static Testing of Deep Foundations, FHWA-SA-91-042. U.S. Department of Transportation, Federal Highway Administration, Office of Technology Applications, Washington, D.C., 174 p.

Likins, G.E. and Goble, G.G. (1978). Tests on H-piles Driven to Rock. Proceedings of the Thirty Second Annual Ohio Transportation Engineering Conference, pp. 57-67.

Lo, K.Y. and Stermac, A.G. (1965). Induced Pore Pressures During Pile Driving Operations. Proceedings of the Sixth International Conference on Soil Mechanics and Foundation Engineering, Vol. 2, Montreal, Canada, pp. 285-289.

Long, J., and Anderson, A. (2014). Improved of Driven Pile Installation and Design in Illinois: Phase 2, FHWA-ICT-14-019. Illinois Department of Transportation, Bureau of Material and Physical Research, Springfield, IL, 84 p.

Marsh, M.L., Buckle, I.G., and Kavazanjian Jr, E. (2014). LRFD Seismic Analysis and Design of Bridges, FHWA-NHI-15-004. National Highway Institute, U.S. Dept. of Transportation, Federal Highway Administration, Washington, D.C., 608 p.

Modjeski and Masters, Inc. (2015). Bridges for Service Life Beyond 100 Years: Service Limit State Design. SHRP2 Report S2-R19B-RW-1. Transportation Research Board, Washington D.C., 268 p.

McClelland, B., Focht, J.A. and Emrich, W.J. (1969). Problems in Design and Installation of Offshore Piles. American Society of Civil Engineers (ASCE), Journal of the Soil Mechanics and Foundations Division, Vol. 94, No.6, pp. 1491-1514.

McVay, M., Casper, R. and Shang, T-I. (1995). Lateral Response of Three-Row Groups in Loose to Dense Sands at 3D and 5D Pile Spacing. American Society of Civil Engineers (ASCE), Journal of Geotechnical Engineering, Vol. 121, No. 5, pp. 436-441.

Meyerhof, G. G. (1956). Penetration Tests and Bearing Capacity of Piles, American Society of Civil Engineers (ASCE), Journal of the Soil Mechanics and Foundation Division, Vol. 82, No. 1, Paper 886, pp. 1-29 .

Meyerhof, G.G. (1976). Bearing Capacity and Settlement of Pile Foundations, American Society of Civil Engineers (ASCE), Journal of Geotechnical Engineering, Vol. 102, No. 3, pp. 195-228.

Montgomery, C.T., Gerard R., Huiskamp, W.J., and Kornelson,R.W. (1984) Application of Ice Engineering to Bridge Design Standards. Proceedings of the Cold Regions Engineering Specialty Conference, Canadian Society for Civil Engineering, Montrel, QC, Canada, pp. 795-810.

Morgano, C.M., White, B. (2004). Identifying Soil Relaxation from Dynamic Testing. Proceedings of the Seventh International Conference on the Application of Stresswave Theory to Piles 2004, Petaling Jaya, Selangor, Malaysia, pp. 415-421.

Mosher, R.L. (1987). Comparison of Axial Capacity of Vibratory Driven Piles to Impact Driven Piles, ITL-87-7. Department of the Army, Waterways Experiment Station, Vicksburg, MS, 36 p.

Moss, R.E.S. (1997). Cyclic Lateral Loading of Model Pile Groups in Clay Soil, Phase 2B. Department Civil and Environmental Engineering, Geotechnical Division, Utah State University, Logan, UT, 700 p.

Kuthy, R.A., Ungerer, R.P, Renfrew, W.W., Hiss, J.G.F., and Rizzuto, I.F. (1977). Lateral Load Capacity of Vertical Pile Groups. ERD 77 RR47. New York State Department of Transportation, Engineering Research and Development Bureau. Albany, NY, 49 p.

Ng, K. W. (2011). Pile Setup, Dynamic Construction Control, and Load and Resistance Factor Design of Vertically-Loaded Steel H Piles. Theses and Dissertations. Paper 11924. Iowa State University, Ames, IA, 299 p.

Ng, K., Roling, M., AbdelSalam, S., Suleiman, M., and Sritharan, S. (2013). Pile Setup in Cohesive Soil. I: Experimental Investigation. American Society of Civil Engineers (ASCE), Journal of Geotechnical and Geoenvironmental Engineering, Vol. 139, No. 2, pp. 199–209.

Nordlund, R.L. (1963). Bearing Capacity of Piles in Cohesionless Soils. American Society of Civil Engineers, ASCE, Journal of the Soil Mechanics and Foundations Division, Vol. 98, No. 12, pp. 1291-1310.

Nordlund, R.L. (1979). Point Bearing and Shaft Friction of Piles in Sand. Missouri-Rolla 5th Annual Short Course on the Fundamentals of Deep Foundation Design, Rolla, MO.

Norris, G. M. (1986). Theoretically based BEF laterally loaded pile analysis. Proceedings of the Third International Conference on Numerical Methods in Offshore Piling, Nates, France, pp. 361-386.

Nottingham, L.C. (1975). Use of Quasi-Static Friction Cone Penetrometer to Predict Load Capacity of Displacement Piles. Ph.D. dissertation to the Department of Civil Engineering, University of Florida, Gainesville, FL, 552 p.

Olson, R.E., and Shantz T.J., (2004). Axial Load Capacity of Piles in California in Cohesionless Soils. Geotechnical Special Publication No. 125, Current Practices and Future Trends in Deep Foundations, American Society of Civil Engineers (ASCE), Reston, VA, pp. 1-15.

Olson, S.M. and Stark, T.D. (2002). Liquefied Strength ratio from Liquefaction Flow Failure Case Histories. Canadian Geotechnical Journal, Vol 39, No.5, pp. 629-647.

O'Neill, M.W. (1983). Group Action in Offshore Piles. Proceedings of the Conference on Geotechnical Practice in Offshore Engineering, Houston, TX, pp. 25-64.

O'Neill, M.W. and Vipulanandan, C. (1989). Laboratory Evaluation of Piles Installed with Vibratory Drivers. NCHRP Report 316, National Cooperative Highway Research Program, Transportation Research Board, Washington, D.C., 51 p.

O'Neill, M.W. and Raines, R.D. (1991). Load Transfer for Pipe Piles in Highly Pressured Dense Sand. American Society of Civil Engineers, (ASCE), Journal of Geotechnical Engineering, Vol. 117, No. 8, pp. 1208-1226.

Paikowsky, S.G. (2004), with contributions from Birgisson, B., McVay, M., Nguyen, T., Kuo, C., Baecher, G., Ayyub, B., Stenersen, K., O.Malley, K., Chernauskas, L., and O'Neill, M., Load and Resistance Factor Design (LRFD) for Deep Foundations. NCHRP Report 507,Transportation Research Board, Washington, D.C., 76 p.

Paikowsky, S.G. and Whitman, R.V. (1990). The Effects of Plugging on Pile Performance and Design. Canadian Geotechnical Journal, Vol. 27, No. 4, pp. 429-440.

Poulos, H.G. and Davis, E.H. (1980). Pile Foundation Analysis and Design. John Wiley and Sons, New York, NY, pp. 18-51.

Preim, M.J., March, R., and Hussein, M.H. (1989). Bearing Capacity of Piles in Soils with Time Dependent Characteristics. Proceedings of the International Conference on Piling and Deep Foundations, London, England, pp. 363-370.

Raines, R.D., Ugaz, O.G. and O'Neill, M.W. (1992). Driving Characteristics of Open-Toe Piles in Dense Sand. American Society of Civil Engineers (ASCE), Journal of Geotechnical Engineering, Vol. 118, No. 1, pp 72-88.

Randolph, M. F., Carter, J. P., and Wroth, C. P. (1979). Driven Piles in Clay—The Effects of Installation and Subsequent Consolidation. Geotechnique, Vol. 29, No. 4, pp. 361–393.

Rausche, F., Thendean, G., Abou-matar, H., Likins, G. and Goble, G. (1996). Determination of Pile Drivability and Capacity from Penetration Tests, DTFH61-91-C-00047, Final Report. U.S. Department of Transportation, Federal Highway Administration, McLean, VA, 432 p.

Reddy, S. and Stuedlein, A. (2014) Time-Dependent Capacity Increase of Piles Driven in the Puget Sound Lowlands. Geotechnical Special Publication No. 233, From Soil Behavior Fundamentals to Innovations in Geotechnical Engineering, pp. 464-474.

Reese, L.C. (1984). Handbook on Design of Piles and Drilled Shafts Under Lateral Load, FHWA-IP-84-11. U.S. Department of Transportation, Federal Highway Administration, Office of Implementation, Washington, D.C., 392 p.

Reese, L.C. (1986). Behavior of Piles and Pile Groups Under Lateral Load, FHWA-RD-85-106. U.S. Department of Transportation, Federal Highway Administration, Office of Engineering and Highway Operations Research and Development, Washington, D.C., 311 p.

Reese, L.C., Wang, T.C., Arrellaga, J.A., and Vasquez, L.G. (2014). APILE 2014 User's Manual: A Program for the Study of Driven Piles under Axial Load. ENSOFT. Austin, TX, 223 p.

Rixner, J.J., Kraemer, S.R. and Smith, A.D. (1986). Prefabricated Vertical Drains Volume I, Engineering Guidelines, FHWA-RD-86-168. U.S. Department of Transportation, Federal Highway Administration, Office of Engineering and Highway Operations Research and Development, McLean, VA, 117 p.

Rollins, K.M., Peterson, K.T., and Weaver, T.J. (1998) Lateral Load Behavior of a Full-Scale Pile Group in Clay. American Society of Civil Engineers (ASCE), Journal of Geotechnical and Geoenvironmental Engineering, Vol. 124, No. 6, pp. 468-478.

Rollins, K. M., Olsen, R. J., Egbert, J. J., Jensen, D. H., Olsen, K. G., and Garrett, B. H. (2006a). Pile Spacing Effects on Lateral Pile Group Behavior: Load Tests American Society of Civil Engineers (ASCE), Load tests. Journal of Geotechnical and Geoenvironmental Engineering, Vol. 132, No. 10, pp. 1262-1271.

Rollins, K.M., and Brown, D.A., (2011). Design Guidelines for Increasing the Lateral Resistance of Highway-Bridge Pile Foundations by Improving Weak Soils. NCHRP Report No. 697, Washington, D.C., 98 p.

Ruesta, P.F. and Townsend, F.C. (1997). Evaluation of Laterally Loaded Pile Group at Roosevelt Bridge. American Society of Civil Engineers (ASCE), Journal of Geotechnical and Geoenvironmental Engineering, Vol. 123, No. 12, pp. 1153-1161.

Sabatini, P. J., Elias, V., Schmertmann, G. R., and Bonaparte, R. (1997). Earth Retaining Systems, FHWA-SA-96-038. Geotechnical Engineering Circular (GEC) No. 2. U.S. Department of Transportation, Federal Highway Administration, Washington, D.C.

Sagaseta, C., and Whittle, A. J. (2001). Prediction of Ground Movements Due to Pile Driving in Clay. American Society of Civil Engineers (ASCE), Journal of Geotechnical and Geoenvironmental Engineering, Vol. 127, No. 11, pp. 939-949.

Schmertmann, J.H. (1975). Measurement of In Situ Shear Strength. Proceedings of the Conference on In Situ Measurement of Soil Properties, Vol. 2, ASCE, New York, NY, pp. 57-138.

Schmertman, J.H. (1978). Guidelines For Cone Penetration Test, Performance, and Design, FHWA-TS-78-209. U.S. Department of Transportation, Federal Highway Administration, Washington, D.C., 145 p.

Seed, H.B., Idriss, I.M. and Arango, I. (1983). Evaluation of Liquefaction Potential Using Field Performance Data. American Society of Civil Engineers (ASCE), Journal of Geotechnical Engineering, Vol. 109, No. 3, pp. 458-482.

Seed, H.B. (1987). Design Problems in Soil Liquefaction. American Society of Civil Engineers (ASCE), Journal of Geotechnical Engineering, Vol. 113, No. 8, pp. 827-845.

Seed, R.B. and Harder, L.F., Jr. (1990). SPT-Based Analysis of Cyclic Pore Pressure Generation and Undrained Residual Strength. Proceedings of the H.B. Bolton Seed Memorial Symposium, BiTech Publishers, Vol. 2, pp. 351-376.

Seidel, J.P., Anderson, G.D., and Morison, N.J. (1992). The Effects of Pile Relaxation on Toe Capacity and Stiffness. Proceedings of the Fourth International Conference on the Application of Stress-Wave Theory to Piles. The Hague, Netherlands, pp 153-158.

Siegel, T.C., Lamb, R., Dasenbrock, D., and Axtell, P.J. (2013). Alternative Design Approach for Drag Load and Downdrag with the LRFD Framework. Proceedings of the 38th Annual Conference on Deep Foundations 2013, Phoenix, AZ, pp. 23-39.

Smith, T.D. (1989). Fact or Friction: A Review of Soil Response to a Laterally Moving Pile. Proceeding of the Foundation Engineering Congress, Evanston, IL, pp. 588-598.

Stevens, R.F. (1988). The Effect of a Soil Plug on Pile Drivability in Clay. Proceedings of the Third International Conference on the Application of Stress Wave Theory to Piles, BiTech Publishers, Vancouver, Canada, pp. 861-868.

Tanyu B.F., Sabatini, P. J., and Berg, R.R. (2008). Earth Retaining Structures, FHWA-NHI-07-07. U.S. Department of Transportation, Federal Highway Administration, Washington, D.C., 792 p.

Tawfig, K.S. (1994). Polyethylene Coating for Downdrag Mitigation on Abutment Piles. Proceedings of the International Conference on Design and Construction of Deep Foundations, Vol. 2, pp. 685-698.

Terzaghi, K., and Peck, R.B. (1967). Soil Mechanics in Engineering Practice, Second Edition, Wiley and Sons, Inc., New York, NY, 729 p.

Terzaghi, K., Peck, R.B., and Mesri, G. (1996). Soil Mechanics in Engineering Practice, Third Edition, Wiley and Sons, Inc., New York, NY, 592 p.

Thompson, C.D. and Thompson, D.E. (1985). Real and Apparent Relaxation of Driven Piles. American Society of Civil Engineers (ASCE), Journal of Geotechnical Engineering, Vol. 111, No. 2, pp. 225-237.

Tomlinson, M.J. (1980). Foundation Design and Construction, Fourth Edition. Pitman Advanced Publishing Program, Boston, MA, 793 p.

Tomlinson, M.J. (1994). Pile Design and Construction Practice, Fourth Edition, E & FN Spon, London, 432 p.

Wilson, K.E., Kimmerling, R.E., Goble, G.G., Sabatini, P.J., Zang, S.D., Zhou, J.Y., Amrhein, W.A., Bouscher, J.W., and Danovich, L.J. (2006). LRFD for Highway Bridge Substructures and Earth Retaining Structures, FHWA-NHI-05-094. U.S. Dept. of Transportation, Federal Highway Administration, 1730 p.

Yang, Nai C. (1970). Relaxation of Piles in Sand and Inorganic Silt. American Society of Civil Engineers (ASCE), Journal of the Soil Mechanics and Foundations Division, March, Vol. 96, No. 2, pp. 395-409.

York, D., Brusey, W., Clémente, F., and Law, S. (1994). Setup and Relaxation in Glacial Sand. American Society of Civil Engineers (ASCE), Journal of Geotechnical Engineering, Vol 120, No. 9, pp. 1498–1513.

CHAPTER 8

STRUCTURAL ASPECTS AND LIMIT STATES

Driven piles resist a variety of vertical loads, moments and lateral loads. The previous chapter discussed a pile's and pile group's geotechnical resistance to these loads. This chapter considers the pile's structural limit states which can govern the design in situations where both lateral and axial loads are applied. The analysis of the effects of vessel impact, wind, scour, and earthquake events in structure design often generates factored loads that can tax the pile's structural resistance.

8.1 INTRODUCTION

This chapter addresses structural limit states, but is not meant to cover structural design in a comprehensive way. Please review AASHTO (2014) for specific structural design equations and requirements. A driven pile must satisfy stress and buckling checks under static loading conditions during its design life as well as under dynamic, driving induced loads. Therefore, the material strength limits are compared to:

1. The factored driving stresses.
2. The factored design loads during the pile's design life.

In almost all cases, the highest stress levels occur in a pile during driving. High driving stresses are necessary to cause pile penetration. The pile must be stressed to overcome the nominal geotechnical resistance, plus any dynamic resistance forces, in order to be driven to support the pile design load. The high strain rate and temporary nature of the loading during pile driving allow a substantially higher driving stress limitation than for the static design case. Wave equation analyses can be used to predict driving stresses prior to installation. During installation, dynamic testing can be used to monitor driving stresses.

Factored loads are briefly considered in Chapter 2. The factored structural resistance is summarized in this chapter, in conformance with the AASHTO (2014) LRFD Bridge Design Specification. AASHTO (2014) provides a discussion on

concrete piles in Article 5, steel piles in Article 6, and timber piles in Article 8. Composite concrete filled steel pipe piles are also discussed.

The factored structural resistances for piles given in AASHTO (2014) are a function of the following variables:

1. Average section yield strength, such as:

    a. F_y, the yield strength for steel piles or steel reinforcement.

    b. $f'_{c,}$ the ultimate compression strength for concrete, typically at 28 days.

    c. Wood crushing strengths.

2. Factors for incision, loading rate, submersion, cross sectional shape and analysis method for timber piles.

3. Resistance factor,ϕ_i, which allows for variations in loading condition, materials, construction dimensions, and method reliability.

4. Load factor, γ_i, to account for uncertainty in the factored service loads.

Driving stress limits, group layout, preliminary cap design, in-service stress limits, and buckling of piles are addressed in this chapter.

8.2 BASIC STRUCTURAL PROPERTIES OF DRIVEN PILES

8.2.1 Material Properties

Primary pile materials include steel, concrete and timber. The properties of these materials can significantly affect static nominal structural resistance and nominal driving resistance. Steel piles are generally produced to meet a minimum design yield stress which is used during load evaluations. Common steel Pipe pile and H-pile designations are given in Table 8-1 and Table 8-2 respectively, along with the minimum required yield stress. H-pile sections were traditionally available as Grade A-36 steel; however ASTM A572 requires new sections to be produced with a minimum yield stress of 50 ksi. H-piles of grade A-36 are therefore no longer manufactured. For all steel piles, the elastic modulus for static calculations, E_s, is assumed to be 29,000 ksi, per AASHTO (2014) specifications.

Table 8-1 Common Steel Pipe Pile Grades and Yield Stress

Designation/Grade	Yield Stress, F_y, ksi
ASTM A-252 Grade 2	35
ASTM A-252 Grade 3	45
ASTM A-252 Grade 3 (Mod)	50-80

Table 8-2 Common Steel H-pile Grades and Yield Stress

Designation/Grade	Yield Stress, F_y, ksi
A-36	36
ASTM A-572-50	50
ASTM A-572-60	60

For concrete piles, the elastic modulus/concrete strength is likewise a limiting variable. However, reinforcing steel can be added to increase tensile strength. The elastic modulus of concrete is typically estimated based on the compression strength. Without confirming test data, the AASHTO (2014) recommended method to determine the elastic modulus of concrete is presented in Equation 8-1. This approach assumes normal weight concrete with a unit weight of 145 pcf.

$$\mathrm{E}_c = 1820\sqrt{f'_c} \qquad \text{Eq. 8-1}$$

Where:

E_c = elastic modulus of concrete (ksi).

f'_c = concrete compression strength at 28 days, unless otherwise specified (ksi).

Timber pile properties vary by tree species. Douglass-Fir and Southern Pine are the predominant timber pile species used across the United States. However, Red Oak and Red Pine are also used. Reference values for compression stress parallel to grain, F_{co}, and elastic modulus, E_o, are provided in AASHTO (2014) Article 8.4.1.4 and are shown in Table 8-3. These values are typically modified by shape and size factors which are further discussed in Section 8.4.

Table 8-3 Timber Pile Compression Stress and Elastic Modulus Reference Values (after AASHTO 2014)

Species	F_{co} ksi	E_o ksi
Pacific Coast Douglas-Fir	1.25	1500
Red Oak	1.10	1250
Red Pine	0.90	1280
Southern Pine	1.20	1500

8.2.2 Pile Section Definitions

Beyond material properties, the general shape and element dimensions affect modes of structural resistance. The relative thickness of steel generally limits the magnitude of force that can be reasonably transferred to the pile either during driving, or for structural considerations. Axial compression and flexural resistance is also derived from the pile shape, and as relatively large loads are transferred to steel and concrete piles, the element dimensions should be accounted for. Figure 8-1 and Figure 8-3 provide general shape dimensions for H-piles and pipe piles, respectively.

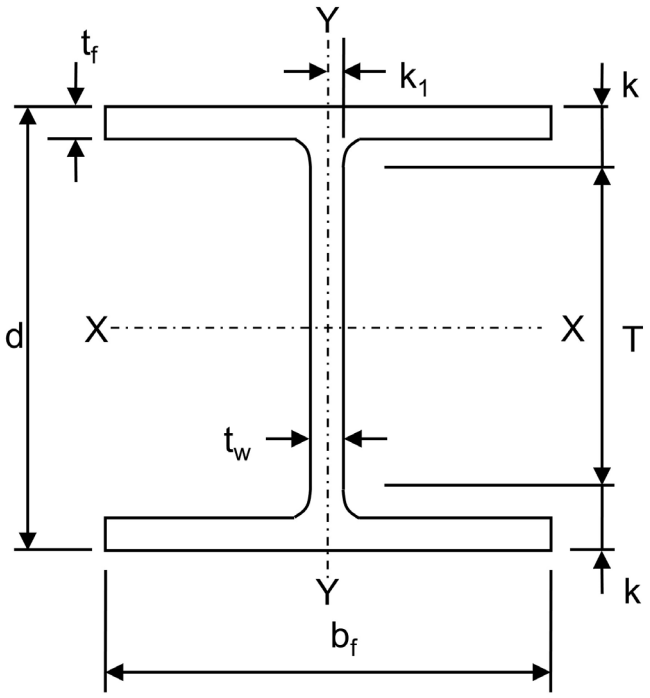

Figure 8-1 H-pile section dimensions.

Section	Weight	Area	Depth	Flange Width	Thickness		Properties							
							X- Axis				Y-Axis			
			d	b_f	Web t_w	Flange t_f	I	Z	S	r	I	Z	S	r
	lb/ft	in^2	in	in	in	in	in^4	in^3	in^3	in	in^4	in^3	in^3	in
HP8X36	36	10.6	8.02	8.16	0.445	0.445	119	33.6	29.8	3.36	40.3	15.2	9.9	1.95
HP10X42	42	12.4	9.70	10.10	0.420	0.415	210	48.3	43.4	4.13	71.7	21.8	14.2	2.41
HP10X57	57	16.7	9.99	10.20	0.565	0.565	294	66.5	58.8	4.18	101	30.3	19.7	2.45
HP12X53	53	15.5	11.80	12.00	0.435	0.435	393	74.0	66.7	5.03	127	32.2	21.1	2.86
HP12X63	63	18.4	11.90	12.10	0.515	0.515	472	88.3	79.1	5.06	153	38.7	25.3	2.88
HP12X74	74	21.8	12.10	12.20	0.610	0.605	569	105.0	93.8	5.11	186	46.6	30.4	2.92
HP12X84	84	24.6	12.30	12.30	0.685	0.685	650	120.0	106.0	5.14	213	53.2	34.6	2.94
HP12x89	89	25.9	12.36	12.32	0.720	0.720	689	126.3	111.6	5.16	225	56.2	36.5	2.94
HP12X102	102	29.9	12.56	12.64	0.819	0.819	811	147.6	129.3	5.20	276	67.1	43.7	3.04
HP12X117	117	34.4	12.76	12.87	0.929	0.929	946	170.8	148.2	5.24	331	79.3	51.4	3.11
HP14X73	73	21.4	13.60	14.60	0.505	0.505	729	118	107	5.84	261	54.6	35.8	3.49
HP14X89	89	26.1	13.80	14.70	0.615	0.615	904	146	131	5.88	326	67.7	44.3	3.53
HP14X102	102	30.1	14.00	14.80	0.705	0.705	1050	169	150	5.92	380	78.8	51.4	3.56
HP14X117	117	34.4	14.20	14.90	0.805	0.805	1220	194	172	5.96	443	91.4	59.5	3.59
HP16X88	88	25.8	15.30	15.70	0.540	0.540	1110	161	145	6.56	349	68.2	44.5	3.68
HP16X101	101	29.9	15.50	15.80	0.625	0.625	1300	187	168	6.59	412	80.1	52.2	3.71
HP16X121	121	35.8	15.80	15.90	0.750	0.750	1590	226	201	6.66	504	97.6	63.4	3.75
HP16X141	141	41.7	16.00	16.00	0.875	0.875	1870	264	234	6.70	599	116.0	74.9	3.79
HP16X162	162	47.7	16.30	16.10	1.000	1.000	2190	306	269	6.78	697	134.0	86.6	3.82
HP16X183	183	54.1	16.50	16.30	1.130	1.130	2510	349	304	6.81	818	156.0	100.0	3.89
HP18X135	135	39.9	17.50	17.80	0.750	0.750	2200	281	251	7.43	706	122.0	79.3	4.21
HP18X157	157	46.2	17.70	17.90	0.870	0.870	2570	327	290	7.46	833	143.0	93.1	4.25
HP18X181	181	53.2	18.00	18.00	1.000	1.000	3020	379	336	7.53	974	167.0	108.0	4.28
HP18X204	204	60.2	18.30	18.10	1.130	1.130	3480	433	380	7.60	1120	191.0	124.0	4.31

Figure 8-2 Table of H-pile section properties (modified from Skyline Steel 2015).

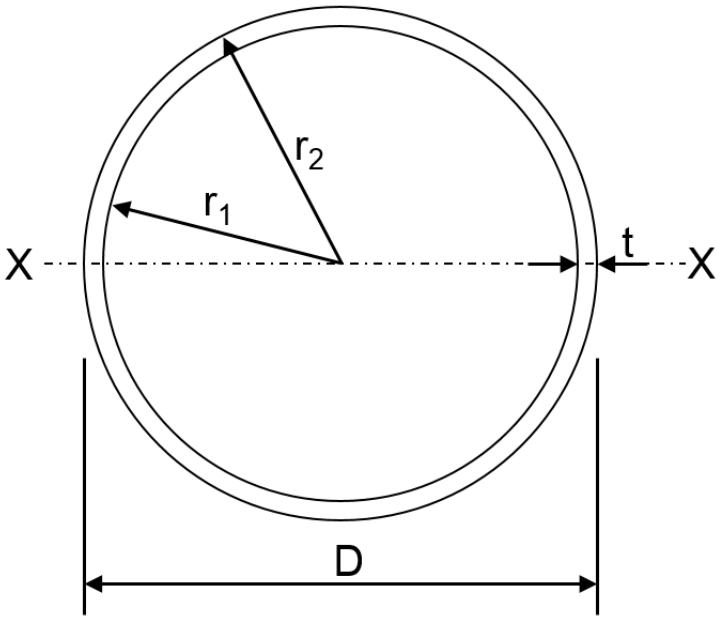

Figure 8-3 Pipe pile section dimensions.

The largest stresses in piles occur at the greatest distance from the neutral axis. This is at the outer edge(s) of a single pile and at the outer edge of the outermost piles of a group. Under combined axial and flexural loading, the pile area, the stiffness or moment of inertia, and distance from neutral axis to the edge of the section, must be defined to check maximum stress.

The moment of inertia, I (in^4), for various common shapes may be computed with Equation 8-2 to 8-4. A reference should be made to the AISC (2011) shape tables or Figure 8-2 for H-piles, where tabulated structural property values about the strong and weak axis are provided. Sections should be selected from those commonly available from local suppliers. Otherwise, scheduling delays may result as manufacturers do not continuously hold all pile sizes in stock.

For solid, circular sections:

$$I = \frac{\pi\,(D)^4}{64} \qquad \text{Eq. 8-2}$$

For voided circular sections:

$$I = \frac{\pi\left[(D)^4 - (D_1)^4\right]}{64} \qquad \text{Eq. 8-3}$$

For solid, square sections:

$$I = \frac{b^4}{12} \qquad \text{Eq. 8-4}$$

Where:

D = outside diameter (inches).
D_1 = inner diameter, 2 r_1 = D-2 t, (inches).
t = pipe pile wall thickness (inches).
b = width/height of square (inches).

To compute moment induced stresses, it is also convenient to compute the elastic section modulus, S, as in Equation 8-5.

$$S = \frac{I}{c} \qquad \text{Eq. 8-5}$$

Where:

S = elastic section modulus (in^3).

I = moment of inertia (in^4).

c = distance from centroid to outer edge (inches).

8.2.3 Effective Length and Buckling

From a structural view, piles act as columns and therefore under axial or moment loads, an effective length could be considered for simplified frame analyses. Pile end conditions are used to approximate an effective length factor, *K*, as shown in Figure 8-4, where the pile toe is generally assumed fixed for both translation and rotation. In the absence of sufficient bracing, (e.g. very soft soils, piles extended though water, large scour) the pile head may be affected by sidesway, and therefore a fixed rotation and translation condition may not apply. For these conditions, the design value of *K* should be applied. For example, if a pile extends into a pier cap, which is subject to severe scour, rotation is generally prevented by the pier cap mass and stiffness, while lateral movement may result from reduced soil confining pressure (reduced lateral bracing) in combination with existing loads. In this case, a fixed rotation and free translation condition may exist. In pile bents, depending on the foundation's connection to the superstructure, the bent cap could allow rotation and translation perpendicular to the long axis of the bent cap, but free translation with fixed rotation along the long axis of the bent cap. To have a rotationally fixed pile top condition, Rollins and Stenlund (2010) observed that rather than defining a rule-of-thumb for minimum pile embedment length into the pile cap, the moment capacity of the pile cap to pile connection should be designed with pile embedment and cap reinforcement details such that the moment capacity of the connection exceeds the moment capacity of the pile.

Buckling is generally of concern when piles extend through water or air, or for liquefaction, where an absence of confining stress is clearly recognizable. Concern for buckling has also been expressed for piles extending through very soft soils or peat. However, pile buckling is a function of the confining stress (bracing) and applied load (Davisson 1963).

To characterize buckling in soft soils, a load test program was performed by the Bethlehem Steel Corporation which suggested that even soft soils provide adequate support (Bethlehem Steel Corporation 1970). One such H-pile in this study extended though 31 feet of water and 29 feet of organic silt where the pile sank under its own weight. A load of 200 tons produced a gross settlement of 0.63 inches while net settlement, after unloading, was measured at 0.02 inches. No pile buckling

occurred. In addition, Coduto et al. (2016) suggests that, “even the softest soils provide enough lateral support to prevent underground buckling in piles subject only to axial loads, especially when a cap is present and provides rotational fixity to the pile top.”

Buckled shape of column is shown by dashed line	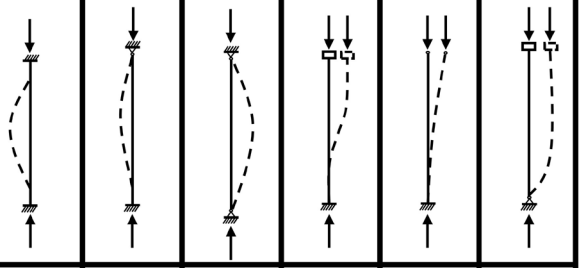					
Theoretical K value	0.5	0.7	1.0	1.0	2.0	2.0
Design value of K when ideal conditions are approximated	0.65	0.80	1.0	1.2	2.1	2.0
End condition code		Rotation fixed	Translation fixed			
		Rotation free	Translation fixed			
		Rotation fixed	Translation free			
		Rotation free	Translation free			

Figure 8-4 Effective length factors, *K* (after AASHTO 2014).

A more conservative approach to this issue is presented in Chance (2003) where the critical buckling load is determined through the use of computer software such as LPILE. For this method, a pile-soil model is generated and incremental loads are applied to evaluate the resulting deflection. This method may provide the design engineer with a deflected pile shape to assess buckling for a given factored load in lieu of using prescriptive minimum soil strength values to characterize an unbraced length.

8.3 STRUCTURAL CONSIDERATIONS AND RESISTANCE FACTORS

The limitations on nominal static design stresses for driven piles in various codes generally represent the static resistance which can be consistently developed with traditional driving equipment and methods.

The factored resistance must be greater than factored loads applied to the pile. The recommended AASHTO limits for factored pile design stresses will generally keep the driving stresses within recommended limits. Factored loads are covered in Article 3 of the AASHTO Specification (2014) while driving stress limits are presented in the respective pile material sections for concrete (Article 5), steel (Article 6), and timber (Article 8).

8.3.1 Depth to Fixity

The unbraced length, l, or laterally unsupported length is defined by AASHTO (2014) as the distance between two braced points that resist buckling or distortion modes. For embedded piles, the unbraced length is considered for scour and pile stickup through air and/or water. For preliminary analysis, when lateral loads are applied, the effective length, *K*, for flexural or torsional resistance calculations is taken as the total unsupported length, plus an embedded depth to "fixity." If a lateral pile analysis with p-y curves for soil-structure interaction has been performed as discussed in Chapter 7, the depth to fixity concept is unnecessary. Most software with lateral analysis also includes additional features to determine a pile's buckling capacity given the soil model and a pile model with the expected stick-up above the ground level.

For preliminary calculations, however, the depth to fixity below the ground may be evaluated based on soil type and soil strength parameters as shown in Equation 8-6 for clays and Equation 8-8 for sands. Table 8-4 contains the rate of increase in soil modulus for sands, n_h, and should be used as applicable in the following depth to fixity estimates.

For clays:

$$d_f = 1.4\left(\frac{E\,I_w}{E_s}\right)^{0.25} \qquad \text{Eq. 8-6}$$

$$E_s = 0.465\,s_u \qquad \text{Eq. 8-7}$$

For sands:

$$d_f = 1.8\left(\frac{E\,I_w}{n_h}\right)^{0.2} \qquad \text{Eq. 8-8}$$

Where:

d_f = depth to fixity below the ground (ft).

E = elastic modulus of pile material (ksi).

E_s = elastic modulus of clay soil (ksi).
s_u = undrained shear strength of clay (ksf).
I_w = weak axis moment of inertia of pile (ft^4).
n_h = rate of increase of soil modulus with depth (Table 8-4) (ksi/ft).

Table 8-4 Rate of Increase of Soil Modulus with Depth for Sands (ksi/ft) (after AASHTO 2014)

Consistency	Dry or Moist	Submerged
Loose	0.417	0.208
Medium	1.110	0.556
Dense	2.780	1.390

8.3.2 Limiting Slenderness Ratio

Piles extending through air or water are unbraced over some length and therefore, for axial compression, the slenderness ratio should be checked during design. For non-composite steel piles, which are not fully embedded, slenderness ratio limits should be satisfied as follows:

$$\frac{Kl}{r_s} \leq 120 \qquad \text{Eq. 8-9}$$

Where:
K = effective length factor (Figure 8-4) (dimensionless).
l = unbraced length, or laterally unsupported length plus d_f (inches).
r_s = minimum radius of gyration, $\sqrt{\frac{I}{A}}$ (inches).

8.3.3 Resistance Factors

A discussion and step by step determination of the nominal structural resistance for timber, steel, and concrete piles is provided in the following sections. The AASHTO (2014) specifications form the basis of these respective sections. Following the Load and Resistance Factor Design (LRFD) approach, a resistance factor is applied to the calculated nominal structural resistance.

In practical terms, the imposed factored load must be less than or equal to the factored resistance. Chapter 2 provides a discussion on load combinations in which load factors are applied to respective load effects. The critical load combination is

applied as axial, shear and moment loads on the structural member and will be described herein as follows:

Factored axial load:

$$\sum(n_i\gamma_i)Q_i = Q \rightarrow \mathrm{P}_u \qquad \text{Eq. 8-10}$$

Factored moment load:

$$\sum(n_i\gamma_i)Q_i = Q \rightarrow \mathrm{M}_u \qquad \text{Eq. 8-11}$$

Factored shear load:

$$\sum(n_i\gamma_i)Q_i = Q \rightarrow \mathrm{V}_u \qquad \text{Eq. 8-12}$$

The nominal structural resistance is specific to pile properties such as material, size, and shape. A separate discussion based on pile material is provided in Section 8.4 through Section 8.7. On the resistance side, the factored structural resistance will be described as shown below.

Factored resistance in axial compression:

$$\sum \phi_i R_i = \varphi_c P_n = \mathrm{P}_r \qquad \text{Eq. 8-13}$$

Factored resistance in flexure:

$$\sum \phi_i R_i = \varphi_f M_n = \mathrm{M}_r \qquad \text{Eq. 8-14}$$

Factored resistance in shear:

$$\sum \phi_i R_i = \varphi_v V_n = \mathrm{V}_r \qquad \text{Eq. 8-15}$$

AASHTO (2014) recommended resistance factors for driving and structural resistance are provided in Table 8-5 and Table 8-6, respectively. As an example, for a steel H-pile with good driving conditions and with the use of a pile tip (e.g. pile point or shoe), ϕ_{da} = 1.0 would be used in Equation 8-33 (Section 8.5.1) along with the material yield stress to determine the nominal driving stress limits. For nominal structural resistance, ϕ_c = 0.60, would be entered into Equation 8-34 (Section 8.5.2). A similar procedure is therefore used for alternative pile types, driving conditions, and loading cases.

Table 8-5 Resistance Factors During Pile Driving

Condition	Resistance Determination Method	Resistance Factor
Pile Drivability, ϕ_{da}	Steel Piles (AASHTO 6.5.4.2)	ϕ_{da} = 1.0
	Concrete Piles (AASHTO 5.5.4.2)	ϕ_{da} = 1.0
	Timber Piles (AASHTO 8.5.4.2)	ϕ_{da} = 1.15

Table 8-6 Structural Limit Resistance Factors for Piles in Compression

Pile Material	Design Resistance	Resistance Factor
Steel (AASHTO 6.5.4.2)	Axial - Good driving conditions where pile tip is not necessary	
	H-piles	ϕ_c = 0.60
	Pipe Piles	ϕ_c = 0.70
	Axial -Pile is subject to damage due to severe driving conditions where pile tip is necessary	
	H-piles	ϕ_c = 0.50
	Pipe Piles	ϕ_c = 0.60
	Combined Axial and Flexural for Undamaged Piles	
	Axial – H-piles	ϕ_c = 0.70
	Axial – Pipe Piles	ϕ_c = 0.80
	Flexure – Both Pile Types	ϕ_f = 1.00
	Shear	ϕ_v = 1.00
Concrete (AASHTO 5.5.4.2)	Tension Controlled	
	Reinforced Concrete	ϕ_c = 0.90
	Prestressed Concrete	ϕ_c = 1.00
	Compression Controlled	
	Prestressed Concrete	ϕ_c = 0.75
Timber (AASHTO 8.5.4.2)	Compression Parallel to Grain	ϕ_c = 0.90
	Flexure	ϕ_f = 0.85
	Shear	ϕ_v = 0.75

8.4 TIMBER PILES

Timber piles are typically round, tapered, and used for modest loading levels. Several species of timber are suitable for use as piles, however Douglas Fir and Southern Pine are by far the most common types used in the United States. Equations to assess maximum driving stresses (Section 8.4.1) or axial and flexural stresses (Section 8.4.2) will be subsequently described, while reference design values shown in Table 8-7 are factored into these calculations. For the load cases described herein, the reference value is modified with an adjustment factor specific to the loading case and pile properties.

Table 8-7 Reference Design Values for Timber Piles, ksi (after AASHTO 2014)

Species	F_{co}	F_{bo}	F_{vo}	E_o
Pacific Coast Douglas-Fir[1]	1.25	2.45	0.115	1500
Red Oak[2]	1.10	2.45	0.135	1250
Red Pine[3]	0.90	1.90	0.085	1280
Southern Pine[4]	1.20	2.40	0.110	1500

[1] Use Douglas Fir-Latch reference values for connection design.
[2] Northern and Southern Red Oak.
[3] United States grown Red Pine. Use Northern Pine reference values for connection design.
[4] Reference strengths apply to Lobololly, Longleaf, Shortleaf and Slash Pine.

Where:

F_{co} = reference value for compression stress parallel to grain (ksi).
F_{bo} = reference value for strength in flexure (ksi).
F_{vo} = reference value for strength in shear (ksi).
E_o = reference value elastic modulus (ksi).

The time effect factor, C_λ, shown in Table 8-8 is utilized in consideration of specific limit states. AASHTO (2014) commentary provides that the Strength I condition be used when the cumulative duration of a bridge live load is two months, while the Strength II condition is used for cumulative live loading less than two months. Furthermore for permanent loads, the Strength IV limit state should be used.

Table 8-8 Time Effect Factors (after AASHTO 2014)

Limit State	C_λ
Strength I	0.8
Strength II	1.0
Strength III	1.0
Strength IV	0.6
Extreme Event I	1.0

A size reduction factor, C_F, is applied to timber piles in flexure; however this factor is only applied if the critical section in bending has a diameter greater than 12 inches (i.e. area of 144 in^2). This would be the sawn lumber beam equivalent of a depth of 12 inches (i.e. area of 144 in^2). If the critical section area is less than 144 in^2, the shape reduction factor is set equal to 1.0. Conversely, if the critical section area is greater than 144 in^2, Equation 8-16 should be used to determine the size reduction factor. Considering the AASHTO (2014) criteria, "the equation should be entered with a *b* equal to the depth of a square beam having the same cross-sectional area as that of a round member" (Showalter 2012).

$$C_F = \left(\frac{12}{b}\right)^{\frac{1}{9}} \qquad \text{Eq. 8-16}$$

Where:

C_F = size factor.
b = depth of beam or width of dimension lumber.

The wet service factor, C_M, provides adjustment based upon moisture content and although not all timber piles are submerged, and assumption of wet use conditions may be made. A wet service factor equal to 1.0 is therefore recommended.

Several adjustment factors provided in the AASHTO (2014) specifications do not apply to timber piles such as the volume factor C_v, incising factor C_i, deck factor C_d, flat-use factor C_{fu}. Since AASHTO (2014) design specifications do not provide specific guidance on these values for timber piles, the values are assumed as 1.0 in this manual to prevent unwarranted increases or reductions in the structural resistance limits.

8.4.1 Driving Stresses

Timber piles should be installed to limit excessive pile stress development that may result in shearing or brooming near the pile top. Additional stresses may develop along the pile as well, especially as the tapered section decreases near the pile toe. AASHTO (2014) specifications limit maximum compression and tension driving stresses as Equation 8-17.

$$\sigma_{dr} = \varphi_{da}\,(F_{co}) \qquad \text{Eq. 8-17}$$

Where:

σ_{dr} = driving stress (ksi).
φ_{da} = resistance factor during driving (1.15 for timber piles, Table 8-5).
F_{co} = reference value for compression stress parallel to grain (Table 8-7).

8.4.2 Structural Resistance

AASHTO (2014) summarizes axial and flexural loading resistance limits in Article 8.6, 8.8 and 8.10. The following sections provide design checks to determine structural strength limits, where Table 8-7 -provides reference values, Table 8-8 contains time effect factors, and Equation 8-16 may be used to determine a size factor. The equations below apply to all timber elements, and therefore several adjustment factors introduced in the AASHTO (2014) specification do not specifically pertain to piles and are assumed to equal 1.0.

8.4.2.1 Axial Compression Parallel to Grain

For axial compression loading, the factored structural limit state is taken as follows:

$$P_r = \varphi P_n \quad \text{Eq. 8-18}$$

Where:

P_r = factored resistance in axial compression (kips).
φ = resistance factor (0.9 for timber pile compression parallel to grain).
P_n = nominal resistance in axial compression (kips).

STEP BY STEP PROCEDURE FOR: “NOMINAL COMPRESSION RESISTANCE”

STEP 1 Determine the adjusted resistance in compression, F_c.

The nominal resistance for axial compression should be evaluated using Equation 8--19 and 8-20 which are provided in AASHTO (2014) Article 8.4.

$$F_c = F_{co} C_{KF} C_M C_F C_i C_\lambda \quad \text{Eq. 8-19}$$

In which:

$$C_{KF} = \frac{2.5}{\varphi} \quad \text{Eq. 8-20}$$

Where:

F_c = adjusted resistance in compression (ksi).
F_{co} = reference resistance in compression (Table 8-7) (ksi).
C_{KF} = format conversion factor where φ_c = 0.9.
C_M = wet service factor (1.0 for piles).
C_F = size factor (1.0 for or Equation 8-16 for piles).
C_i = incising factor (Not Applicable for piles-1.0).
C_λ = time effect factor (Table 8-8).

STEP 2 Determine the nominal resistance in axial compression, P_n.

Following adjustment of the reference resistance in compression, the nominal resistance in axial compression is calculated from Equation 8-21. If the piles are sufficiently braced, the column stability factor, C_p, may be taken as 1.0. However, Equation 8-22 should be used to determine the column stability factor, C_p, if sufficient bracing does not exist.

$$\mathrm{P}_n = F_c A_g C_p \qquad \text{Eq. 8-21}$$

In which:

$$\mathrm{C}_p = \frac{1+B}{2c} - \sqrt{\left(\frac{1+B}{2c}\right)^2 - \frac{B}{c}} \leq 1.0 \qquad \text{Eq. 8-22}$$

$$B = \frac{F_{cE}}{F_c} \leq 1.0 \qquad \text{Eq. 8-23}$$

$$\mathrm{F}_{cE} = \frac{K_{cE} E b^2}{{L_e}^2} \qquad \text{Eq. 8-24}$$

$$E = E_o C_t \qquad \text{Eq. 8-25}$$

Where:

F_c = adjusted resistance in compression parallel to grain (ksi).
P_n = nominal resistance in axial compression (kips).
A_g = gross cross-sectional area (in^2).
C_p = column stability factor.
C_M = wet service factor (1.0 for piles).
C_i = incising factor (Not Applicable for piles-1.0).
c = round timber pile factor (0.85).

K_{cE} = round timber pile factor (0.76).
b = depth or width (inches).
L_e = effective length taken as KL (Figure 8-4, inches).
E_o = reference modulus of elasticity (ksi) (Table 8-7).

8.4.2.2 Flexure

For flexure, the factored structural limit state is taken as:

$$M_r = \varphi M_n \quad \text{Eq. 8-26}$$

Where:
M_r = factored flexural resistance (kip-in).
φ = resistance factor (0.85 for timber pile flexure).
M_n = nominal flexural resistance (kip-in).

STEP BY STEP PROCEDURE FOR: “NOMINAL FLEXURAL RESISTANCE”

STEP 1 Determine the adjusted resistance in flexure, F_b.

A round timber pile is assumed in this manual for flexure. If alternative pile cross sections are used, consideration should be given to the new shape. To determine the adjusted resistance in flexure, the following equations should be applied.

$$\mathrm{F}_b = F_{bo} C_{KF} C_M C_F C_{fu} C_i C_d C_\lambda \quad \text{Eq. 8-27}$$

In which:

$$C_{KF} = \frac{2.5}{\varphi} \quad \text{Eq. 8-28}$$

Where:
F_{bo} = reference resistance in flexure (Table 8-7) (kips).
C_{KF} = format conversion factor where ϕ_f = 0.85.
C_M = wet service factor (1.0 for piles).
C_F = size factor (1.0 or Equation 8-16 for piles).
C_{fu} = flat use factor (Not Applicable for piles-1.0).
C_i = incising factor (Not Applicable for piles-1.0).
C_d = deck factor (Not Applicable for piles-1.0).
C_λ = time effect factor (Table 8-8).

STEP 2 Determine the nominal flexural resistance, M_n.

Following adjustment of the reference resistance in flexure, the nominal flexural resistance is calculated as follows.

$$M_n = F_b S \qquad \text{Eq. 8-29}$$

Where:

M_n = nominal flexural resistance (kip-in).
S = elastic section modulus (in^3).
F_b = adjusted resistance in flexure (Table 8-7) (ksi).

8.4.2.3 Combined Flexure and Axial Compression

For combined flexure and compression, the factored structural limit state must satisfy checks for beam rupture and lateral buckling as shown in Equation 8-30. If the applied loads are not sufficiently resisted by the pile section, an alternative pile design is required.

$$\left(\frac{\mathrm{P}_u}{\mathrm{P}_r}\right)^2 + \frac{M_u}{M_r\left(1-\frac{P_u}{F_{cE}A_g}\right)} \leq 1.0 \qquad \text{Eq. 8-30}$$

In which:

$$\mathrm{F}_{cE} = \frac{K_{cE}Eb^2}{{L_e}^2} \qquad \text{Eq. 8-31}$$

$$E = E_o C_M C_i \qquad \text{Eq. 8-32}$$

Where:

P_r = factored resistance in axial compression (kips) (Equation 8-18).
P_u = factored axial load (kips) (Equation 8-10).
M_r = factored resistance in flexure (kip-in) (Equation 8-26).
M_u = factored moment load (kip-in) (Equation 8-11).
A_g = gross cross-sectional area (in^2).
C_M = wet service factor (N/A -1.0 for piles).
C_i = incising factor (N/A -1.0 for piles).
K_{cE} = round timber pile factor (0.76).
b = pile width or diameter (inches).
L_e = effective length taken as *KL* (Figure 8-4, inches).
E_o = reference modulus of elasticity (ksi) (Table 8-7).

8.5 STEEL PILES

8.5.1 Driving Stresses

Steel piles can handle higher stresses than concrete or timber during driving, and the limit is governed the steel yield strength. Several grades of steel are routinely produced and higher grades may be specified if warranted. Table 8-1 provides an overview of typical steel grades and their respective yield strength. Pile driving does not typically generate sufficiently high tensile stresses to yield steel piles, therefore a stress limit is only required in compression. For steel piles, AASHTO (2014) specifications limit nominal compression driving stresses as follows:

$$\sigma_{dr} = \varphi_{da}\left(0.9\,F_y\right) \qquad \text{Eq. 8-33}$$

Where:

σ_{dr} = driving stress limit (ksi).
φ_{da} = resistance factor during driving (1.0 for steel piles, Table 8-5).
F_y = yield stress of steel (ksi) (Table 8-1).

8.5.2 Structural Resistance

8.5.2.1 Axial Compression

For axial compression loads, the factored structural limit state is taken as:

$$P_r = \varphi_c P_n \qquad \text{Eq. 8-34}$$

Where:

P_r = factored resistance in axial compression (kips).
φ_c = resistance factor (Table 8-6).
P_n = nominal resistance in axial compression (kips).

To determine the nominal resistance in axial compression, pile strength and buckling failure should be considered. The following step by step procedure should be used to calculate the nominal resistance.

STEP BY STEP PROCEDURE FOR: “NOMINAL COMPRESSION RESISTANCE”

STEP 1 Determine the equivalent nominal yield resistance, P_o.

The equivalent nominal yield resistance, P_o, is a function of the material yield stress, cross sectional area and slenderness reduction factor, if applicable. For non-slender piles in compression, the slenderness reduction factor, Q, is taken as 1.0. However for slender piles, the full nominal yield strength under uniform axial compression is limited by local buckling. This reduction factor is governed by section buildup, pile dimensions and material properties, therefore, a further discussion of slender members and direction for calculating Q may be found in AASHTO (2014) Article 6.9.4.2.2.

$$P_o = QF_yA_g \qquad \text{Eq. 8-35}$$

Where:

A_g = gross cross-sectional area (in^2).
P_o = equivalent nominal axial yield resistance (kips).
F_y = yield stress of steel (Table 8-1) (ksi).
Q = slender element reduction factor (dimensionless).

To satisfy the slender element requirement for local buckling, Equation 8-36 is used for H-piles and Equation 8-38 is used for unfilled pipe piles.

$$\frac{b_f}{2t_f} \leq 0.64\sqrt{\frac{k_c\,E_{st}}{F_y}} \qquad \text{Eq. 8-36}$$

And:

$$0.35 \leq k_c \leq 0.76$$

In which:

$$k_c = \frac{4}{\sqrt{\frac{d_w}{t_w}}} \qquad \text{Eq. 8-37}$$

Where:

b_f = flange width (inches).
t_f = flange thickness (inches).
F_y = yield stress of steel (Table 8-1) (ksi).
E_{st} = elastic modulus of steel (ksi).
d_w = web depth (inches).
t_w = web thickness (inches).

$$\frac{D}{t} \leq 0.11 \frac{E_{st}}{F_y}$$ Eq. 8-38

Where:

D = diameter of pipe (inches).
t = wall thickness (inches).
F_y = yield stress of steel (Table 8-1) (ksi).
E_{st} = elastic modulus of steel (ksi).

STEP 2 Determine the elastic critical buckling resistance, P_e.

In determination of the nominal resistance in axial compression, buckling may occur with a lack of sufficient bracing. This topic is discussed further in Section 8.2.3. AASHTO (2014) requires both flexural and torsional modes of buckling be checked if applicable. For fully embedded piles, the flexural buckling mode will be used. However, when the pile extends through water or air, doubly symmetric open section members (e.g., H-piles) must be evaluated for torsional buckling as well. The critical failure mode is the lesser buckling resistance, and is employed to define the nominal resistance in axial compression.

Flexural buckling:

$$P_e = \frac{\pi^2 E_{st} A_g}{\left(\frac{Kl}{r_s}\right)^2}$$ Eq. 8-39

Where:

P_e = elastic critical buckling resistance (kips).
E_{st} = elastic modulus of steel (ksi).
A_g = gross cross-sectional area (in^2).
K = effective length in the plane of buckling (Figure 8-4) (dimensionless).
l = unbraced length in the plane of buckling (Section 8.3) (inches).
r_s = radius of gyration about axis normal to plane of buckling (inches).

Torsional buckling:

$$\mathrm{P}_e = \left[\frac{\pi^2 E_{st} C_w}{(K_z l_z)^2} + GJ\right] \frac{A_g}{\mathrm{I}_x + \mathrm{I}_y}$$ Eq. 8-40

In which:

$$C_w = \frac{I_y h^2}{4} \quad \text{Eq. 8-41}$$

$$G = 0.385 E_{st} \quad \text{Eq. 8-42}$$

Where:

- P_e = elastic critical buckling resistance (kips).
- E_{st} = elastic modulus of steel (ksi).
- C_w = warping torsional constant (doubly symmetric open sections) (in^6).
- K_z = effective length for torsional buckling (Figure 8-4) (dimensionless).
- l_z = unbraced length for torsional buckling (inches).
- G = shear modulus (ksi).
- J = St. Venant torsional constant (in^4).
- A_g = gross cross-sectional area (in^2).
- I_x, I_y = moments of inertia about the major and minor principal axes of cross section, respectively (in^4).
- h = distance between flange and centroids (inches).

STEP 3 Determine the nominal resistance in axial compression, P_n.

With the above resistances defined, the nominal resistance for axial compression may be evaluated using the following equations, which are provided in AASHTO (2014) Article 6.9.4.1.

If $\frac{P_e}{P_o} \geq 0.44$:

$$P_n = P_o \, 0.658^{\frac{P_o}{P_e}} \quad \text{Eq. 8-43}$$

If $\frac{P_e}{P_o} < 0.44$:

$$P_n = 0.877 P_e \quad \text{Eq. 8-44}$$

Where:

- P_n = nominal resistance in axial compression (kips).
- P_o = equivalent nominal yield resistance (Equation 8-35) (kips).
- P_e = elastic critical buckling resistance (Equation 8-39 or 8-40) (kips).

8.5.2.2 Flexure

The factored resistance in flexure is computed as follows:

$$M_r = \varphi_f M_n \qquad \text{Eq. 8-45}$$

Where:

M_r = factored resistance in flexure (kip-in).
φ_f = resistance factor (Table 8-6).
M_n = nominal resistance in flexure (kip-in).

The nominal flexural resistance is a function of pile shape as well as general pile properties. Steel piles are primarily H-piles or pipe piles. Therefore the step by step procedure that follows will consider only these two steel pile types. If alternative sections are used, the engineer is referred to Article 6.12.2.2 of the AASHTO (2014) specifications. Steel H-piles and I-sections are treated equally for flexural resistance. Hence, part A of this procedure applies to both steel H-piles and miscellaneous I sections.

STEP BY STEP PROCEDURE FOR: “NOMINAL FLEXURAL RESISTANCE”

A. Steel H-Sections.

STEP 1 Check flange slenderness ratio and limiting slenderness.

$$\lambda_f = \frac{b_f}{2t_f} \qquad \text{Eq. 8-46}$$

$$\lambda_{pf} = 0.38\sqrt{\frac{E_{st}}{F_{yf}}} \qquad \text{Eq. 8-47}$$

$$\lambda_{rf} = 0.83\sqrt{\frac{E_{st}}{F_{yf}}} \qquad \text{Eq. 8-48}$$

Where:

λ_f = slenderness ratio for flange.
λ_{pf} = limiting slenderness ratio for a compact flange.
λ_{rf} = limiting slenderness ratio for a non-compact flange.

b_f = flange width (inch).
t_f = flange thickness (inch).
E_{st} = elastic modulus of steel (ksi).
F_{yf} = minimum yield strength of lower strength flange (ksi).

STEP 2 Determine the nominal flexural resistance.

To determine the nominal flexural resistance, the above slenderness definitions should first be resolved. These functions serve to define the limiting flexural resistance. In the case where the limiting slenderness ratio of a compact flange is greater than the slenderness ratio, the plastic moment about the weak axis will limit resistance. For H-piles, Eq. 8-49 can be used. Conversely, Eq. 8-51 should be used when the slenderness ratio is greater than the limiting slenderness ratio of a compact flange.

If $\lambda_f \leq \lambda_{pf}$:

$$M_n = M_p \qquad \text{Eq. 8-49}$$

In which, for HP-sections about weak axis:

$$M_p = 1.5\, F_y\, S_y \qquad \text{Eq. 8-50}$$

If $\lambda_{pf} < \lambda_f \leq \lambda_{rf}$ the nominal flexural resistance about the weak axis is:

$$M_n = \left[1 - \left(1 - \frac{S_y}{Z_y}\right)\left(\frac{\lambda_f - \lambda_{pf}}{0.45\sqrt{\frac{E_{st}}{F_{yf}}}}\right)\right] f_{yf} Z_y \qquad \text{Eq. 8-51}$$

Where:

M_n = nominal resistance in flexure (kip-in).
M_p = plastic moment about the weak axis (kip-in).
S_y = elastic section modulus about weak axis (in^3).
Z_y = plastic section modulus about weak axis (in^3).
λ_f = slenderness ratio for flange (Equation 8-46, dimensionless).
λ_{pf} = limiting slenderness ratio for a compact flange (Equation 8-47, dimensionless).

E_{st} = elastic modulus of steel (ksi).
F_y = yield stress of steel (ksi).
F_{yf} = minimum yield strength of lower strength flange (ksi).

B. Steel Pipe Piles.

STEP 1 Check diameter to thickness ratio.

If the diameter to thickness ratio is sufficiently large, local buckling limits flexural resistance. To determine whether the plastic moment or local buckling will govern flexural resistance, Equation 8-52 should be applied. If Equation 8-52 is satisfied, the plastic moment will yield the steel pile and Step 2a should follow. Conversely, local buckling will limit flexural resistance if Equation 8-2 is not satisfied, and therefore Step 2b should follow.

$$\frac{D}{t} \leq 0.07 \frac{E_{st}}{F_y} \qquad \text{Eq. 8-52}$$

Where:
D = outside diameter of pipe (inch).
t = pipe thickness (inch).
E_{st} = elastic modulus of steel (ksi).
F_y = yield strength of steel (Table 8-1) (ksi).

STEP 2a Determine nominal flexural resistance by plastic moment.

The nominal flexural resistance can be taken as follows:

$$M_n = M_p = F_y Z_y \qquad \text{Eq. 8-53}$$

Where:
M_n = nominal resistance in flexure (kip-in).
M_p = plastic moment (kip-in).
Z_y = plastic section modulus about weak axis (in^3).
F_y = yield strength of steel (Table 8-1) (ksi).

STEP 2b Determine nominal flexural resistance by local buckling.

Where local buckling will limit the nominal resistance in flexure, the following checks apply.

If $\frac{D}{t} \leq 0.31\frac{E_{st}}{F_y}$:

$$M_n = \left(\frac{0.021\,E_{st}}{\frac{D}{t}} + F_y\right) S_y \qquad \text{Eq. 8-54}$$

If $\frac{D}{t} > 0.31\frac{E_{st}}{F_y}$:

$$M_n = f_{cr}\,S_y \qquad \text{Eq. 8-55}$$

In which:

$$f_{cr} = \frac{0.33\,E_{st}}{\frac{D}{t}} \qquad \text{Eq. 8-56}$$

Where:

D = outside diameter of pipe (inch).
t = pipe thickness (inch).
E_s = elastic modulus of steel (ksi).
F_y = yield strength of steel (Table 8-1) (ksi).
M_n = nominal flexural resistance (kip-in).
S_y = elastic section modulus about weak axis (in^3).
f_{cr} = elastic local buckling stress (ksi).

8.5.2.3 Combined Axial Compression and Flexure

Combined axial compression and flexure checks are only applied to pile groups with vertical piles. At this time, AASHTO (2014) does not have a recommendation to include battered piles. For combined compression and flexure of vertical piles, AASHTO (2014) requires the factored structural limit state to satisfy the following limit state checks.

If $\frac{P_u}{P_r} < 0.2$:

$$\frac{\mathrm{P}_u}{2.0\ \mathrm{P}_r} + \left(\frac{\mathrm{M}_{ux}}{\mathrm{M}_{rx}} + \frac{\mathrm{M}_{uy}}{\mathrm{M}_{ry}}\right) \leq 1.0 \qquad \text{Eq. 8-57}$$

If $\frac{P_u}{P_r} \geq 0.2$:

$$\frac{\mathrm{P}_u}{\mathrm{P}_r} + \frac{8.0}{9.0}\left(\frac{\mathrm{M}_{ux}}{\mathrm{M}_{rx}} + \frac{\mathrm{M}_{uy}}{\mathrm{M}_{ry}}\right) \leq 1.0 \qquad \text{Eq. 8-58}$$

Where:

P_u = factored load in axial compression (kips).
P_r = factored resistance in axial compression (kips) (Section 8.5.2.1).
M_{ux} = factored moment about x-axis (kip-ft).
M_{rx} = factored resistance in flexure about x-axis (kip-ft) (Section 8.5.2.2).
M_{uy} = factored moment about y-axis (kip-ft).
M_{ry} = factored resistance in flexure about y-axis (kip-ft) (Section 8.5.2.2).

8.5.2.4 Shear

Piles used for bridge foundations are generally not also used to resist high shear loads as significant lateral pile deflections may negatively impact bridge serviceability. For shear loads, the factored structural limit state is taken as:

$$V_r = \varphi_v V_n \qquad \text{Eq. 8-59}$$

Where:

V_r = factored resistance in shear (kips).
φ_v = resistance factor (Table 8-6).
V_n = nominal resistance in shear (kips).

A straightforward calculation of the nominal structural resistance in shear is shown in Equation 8-60 and Equation 8-61 for an H-pile section. Reference should be made to the AASHTO (2014) specifications for additional design requirements concerning piles subject to significant shear loads or for alternative non-composite pile sections.

$$V_n = C\ V_p \qquad \text{Eq. 8-60}$$

$$V_p = 0.58\ F_{yw}\ d_w\ t_w \qquad \text{Eq. 8-61}$$

Where:

V_n = nominal resistance in shear (kips).
C = ratio of shear-buckling resistance to shear yield strength, typically 1.0 for H-piles.
V_p = plastic shear force (kips).
F_{yw} = yield strength of web (Table 8-1) (ksi).
d_w = web depth of pile section (inch).
t_w = web thickness of pile section (inch).

8.5.3 Example Calculations for H Pile Structural Resistance.

The following example provides calculations for an HP 14x117 which will support an integral abutment. This H-pile section is produced with a yield stress, F_y, of 50 ksi, an elastic modulus, E_{st}, of 29,000 ksi while the radius of gyration in the weak direction, r_s, is 3.59 inches (Figure 8-2). Based upon project specific conditions, an unbraced length, l, of 120 inches is assumed for scour. In addition, rotation is fixed while translation is free at the pile head, whereas both rotation and translation are fixed for at the pile toe, thus an effective length factor of 1.2 results (Figure 8-4).

Under the given conditions, the pile section easily satisfies main member slenderness limits (kl/r<120). However a further inspection of local buckling under compression loads is required. First the buckling coefficient is determined.

$$k_c = \frac{4}{\sqrt{\frac{d_w}{t_w}}} = \frac{4}{\sqrt{\frac{14.2\ (\text{inches})}{0.805\ (\text{inches})}}} = 0.952 \qquad \text{[Eq. 8-37]}$$

But, k_c must satisfy:

$$0.35 \leq k_c \leq 0.76$$

Therefore:

$$k_c = 0.76$$

After calculating the buckling coefficient, the following condition is checked.

$$\frac{b_f}{2t_f} \leq 0.64\sqrt{\frac{k_c\, E_{st}}{F_y}} \qquad \text{[Eq. 8-36]}$$

$$\frac{14.9\ (inches)}{2{*}0.805\ (inches)} \leq 0.64\sqrt{\frac{0.76 * 29{,}000\ (ksi)}{50(ksi)}}$$

$$9.25 \leq 13.44 \quad => \quad \mathrm{Q} = 1.0$$

Based upon Equation 8-36, the pile section is a non-slender element, and therefore the slenderness reduction factor *Q* is set equal to 1.0. The equivalent nominal yield resistance is determined using Equation 8-35.

$$P_o = QF_yA_g \qquad \text{[Eq. 8-35]}$$

$$P_o = 1.0 * 50\ (ksi) * 34.4\ (in^2)$$

$$P_o = 1720\ kips$$

Next, elastic critical buckling resistance in the section is determined.

$$P_e = \frac{\pi^2 E_s A_g}{\left(\frac{Kl}{r_s}\right)^2} \qquad \text{[Eq. 8-39]}$$

$$P_e = \frac{\pi^2 * (29{,}000\ \text{ksi}) * (34.4 in^2)}{\left(\frac{(1.2) * (120\ inches)}{(3.59\ inches)}\right)^2}$$

$$P_e = 6120\ kips$$

From Step 3 of Section 8.5.2.1, the nominal resistance in axial compression, P_n, is determined by applying either Equation 8-43 or 8-44. For this example, the ratio of elastic critical buckling resistance, P_e, to yield resistance, P_o, satisfies criteria for Equation 8-43 and is therefore shown in the following calculations.

If $\frac{P_e}{P_o} \geq 0.44$:

$$\frac{P_e}{P_o} = \frac{6120\ kips}{1{,}720\ kips} = 3.56 \geq 0.44$$

Therefore:

$$P_n = P_o\ 0.658^{\frac{P_o}{P_e}} \qquad \text{[Eq. 8-43]}$$

$$P_n = 1{,}720\ kips * 0.658^{\frac{1{,}720\ kips}{6120\ kips}}$$

$$P_n = 1{,}529\ \ kips$$

After calculation of the nominal resistance in axial compression, a resistance factor can be applied to determine the factored structural resistance in axial compression. Because good driving conditions were encountered and pile toe protection was not necessary, a resistance factor, ϕ_c = 0.60, is used (Table 8-6). This factor is applied when only axial compression is considered. When using the combined axial and flexure interaction equations as shown in Section 8.5.2.3, ϕ_c = 0.70 is used.

$$P_r = \varphi_c P_n \quad \text{[Eq. 8-34]}$$

$$P_r = 0.60 * 1{,}529 \ kips$$

$$P_r = 917 \ kips$$

Continuing with the example, the factored resistance in flexure is determined. To begin, the flange slenderness is inspected for the HP 14x117 pile section. In addition, compact and non-compact flange slenderness ratios are calculated.

Flange slenderness ratio:

$$\lambda_f = \frac{b_f}{2t_f} \quad \text{[Eq. 8-46]}$$

$$\lambda_f = \frac{14.9 \ (inches)}{2*0.805 \ (inches)}$$

$$\lambda_f = 9.25$$

Limiting slenderness ratio for a compact flange:

$$\lambda_{pf} = 0.38\sqrt{\frac{E_{st}}{F_{yf}}} \quad \text{[Eq. 8-47]}$$

$$\lambda_{pf} = 0.38\sqrt{\frac{29{,}000 \ (ksi)}{50 \ (ksi)}}$$

$$\lambda_{pf} = 9.15$$

Limiting slenderness ratio for a non-compact flange:

$$\lambda_{rf} = 0.83\sqrt{\frac{E_{st}}{F_{yf}}} \quad \text{[Eq. 8-48]}$$

$$\lambda_{rf} = 0.83\sqrt{\frac{29{,}000\ (ksi)}{50\ (ksi)}}$$

$$\lambda_{rf} = 19.98$$

After determining the slenderness ratio functions, a comparison is then made. For this particular pile, Equation 8-48 will be used to define the nominal flexural resistance. Reference should be made to Figure 8-2 for H-pile section properties such as the elastic and plastic section moduli.

If $\lambda_{pf} < \lambda_f \leq \lambda_{rf}$:

$$9.15 < 9.25 \leq 19.98$$

Therefore:

$$M_n = \left[1 - \left(1 - \frac{S_y}{Z_y}\right)\left(\frac{\lambda_f - \lambda_{pf}}{0.45\sqrt{\frac{E_{st}}{F_{yf}}}}\right)\right] F_{yf} Z_y \qquad \text{[Eq. 8-55]}$$

$$M_n = \left[1 - \left(1 - \frac{59.5\ (\text{in}^3)}{91.4\ (\text{in}^3)}\right)\left(\frac{9.25 - 9.15}{0.45\sqrt{\frac{29{,}000\ (ksi)}{50\ (ksi)}}}\right)\right] 50\ (ksi) * 91.4(\text{in}^3)$$

$$M_n = 4555\ kip - in$$

Following the calculation of nominal resistance in flexure, a resistance factor can be applied to determine the factored structural resistance in flexure. The AASHTO recommended resistance factor for flexure is, ϕ_f = 1.0, is used (Table 8-6).

$$M_r = \varphi_f M_n \qquad \text{[Eq. 8-41]}$$

$$M_r = 1.0 * 4555\ kip - in$$

$$M_r = 4555\ kip - in$$

Finally, the nominal resistance in shear of the pile section is determined using Equations 8-60 and 8-61. For the HP 14x117 pile section, the web depth is 14.2 inches and the web thickness is 0.805 inches (Figure 8-2). The plastic shear force is calculated using Equation 8-61.

$$V_p = 0.58\, F_{yw}\, d_w\, t_w \qquad \text{[Eq. 8-61]}$$

$$V_p = 0.58 * (50\ ksi) * (14.2\ inches) * (0.805\ inches)$$

$$V_p = 332\ kips$$

The nominal structural resistance in shear is calculated using Equation 8-60.

$$V_n = C\, V_p \qquad \text{[Eq. 8-60]}$$

$$V_n = (1.0) * (332\ kips)$$

$$V_n = 332\ kips$$

By multiplying the nominal structural resistance in shear by the AASHTO (2014) recommended resistance factor, the factored structural resistance in shear is determined.

$$V_r = \varphi_v V_n \qquad \text{[Eq. 8-59]}$$

$$V_r = (1.0) * (332\ kips)$$

$$V_r = 332\ kips$$

8.6 CONCRETE PILES

8.6.1 Driving Stresses

Concrete by nature is strong in compression while tensile strength is mainly derived from reinforcing steel and prestressed longitudinal rebar. The additional tensile strength from prestressing allows for somewhat larger tensile stresses to develop and is therefore featured in nearly all concrete piles manufactured in the United States today. Unlike timber and steel piles, concrete piles are susceptible to damage in both compression and tension under normal driving conditions. The use of a pile cushion (Chapter 15) slows the impact velocity and thus, reduces dynamic forces during driving. Pile cushions are therefore employed when driving piles to lessen the probability of damage.

Driving stress limits are applied to the gross concrete area. In severe corrosive environments, the nominal tension stress is limited to the effective prestress after losses. AASHTO (2014) specifications limit the nominal driving stresses in compression and tension for concrete piles as follows.

For compression:

$$\sigma_{dr} = \varphi_{da}\left(0.85\, f'_c - f_{pe}\right) \qquad \text{Eq. 8-62}$$

For tension:

$$\sigma_{dr} = \varphi_{da}\left(0.095\sqrt{f'_c} + f_{pe}\right) \qquad \text{Eq. 8-63}$$

Where:

σ_{dr} = driving stress (ksi).
φ_{da} = resistance factor during driving (1.0 for concrete piles, Table 8-5).
f'_c = concrete compression strength at 28 days, unless otherwise specified (ksi).
f_{pe} = effective prestressing stress in concrete (ksi).

In Chapter 10 of the AASHTO (2014) specifications, the effective prestressing stress in the concrete is designated as f_{pe}, as shown in Equation 8-62 and 8-63. This value should typically be on the order of 0.5 to 1.0 ksi for most piles on highway projects, and should certainly be less than f'_c.

8.6.2 Structural Resistance

8.6.2.1 Axial Compression

For axial compression loading, the factored structural limit state is taken as:

$$\mathrm{P}_r = \varphi_c P_n \qquad \text{Eq. 8-64}$$

Where:

P_r = factored resistance in axial compression (kips).
φ_c = resistance factor (Table 8-6).
P_n = nominal resistance in axial compression (kips).

To determine the nominal resistance in axial compression, a straightforward calculation is performed considering either spiral or tie reinforcement. As mentioned in the ASSHTO (2014) commentary, reduction factors are placed on the respective equations to account for unintended eccentricity. Further details on axial resistance of concrete piles can be found in Article 5.7.4.4 of AASHTO (2014).

For members with spiral reinforcement:

$$P_n = 0.85[0.85f'_c(A_g - A_{str} - A_{ps}) + F_{yr}A_{str} - A_{ps}(f_{pe} - E_{st}\varepsilon_{cu})] \qquad \text{Eq. 8-65}$$

For members with tie reinforcement:

$$P_n = 0.80[0.85f'_c(A_g - A_{str} - A_{ps}) + F_{yr}A_{str} - A_{ps}(f_{pe} - E_{st}\varepsilon_{cu})] \qquad \text{Eq. 8-66}$$

Where:

P_n = nominal resistance in axial compression (kips).
f'_c = concrete compression strength at 28 days, unless otherwise specified (ksi).
f_{pe} = effective stress in the prestressing steel after losses (ksi).
F_{yr} = yield stress of reinforcing steel (ksi).
A_g = gross cross-sectional area (in^2).
A_{str} = cross sectional area of longitudinal reinforcement (in^2).
A_{ps} = cross sectional area of prestressing steel (in^2).
E_{st} = elastic modulus of prestressing steel (in^2).
ε_{cu} = failure strain of concrete in compression (in/in).

8.6.2.2 Biaxial Flexure

For biaxial flexure, the factored structural limit state is taken as:

$$M_r = \varphi_f M_n \qquad \text{Eq. 8-67}$$

Where:

M_r = factored resistance in flexure (kip-ft).
φ_f = resistance factor (Table 8-6).
M_n = nominal resistance in flexure (kip-ft).

Biaxial flexural resistance must satisfy the following checks. Additional information may be found in Article 5.7.4.5 of the AASHTO (2014) specifications.

If $P_u \geq 0.10\varphi f'_c A_g$:

$$\frac{1}{\mathrm{P}_{rxy}} = \frac{1}{\mathrm{P}_{rx}} + \frac{1}{\mathrm{P}_{ry}} - \frac{1}{\varphi P_o} \leq 1.0 \qquad \text{Eq. 8-68}$$

In which:

$$P_o = 0.85 f'_c (A_g - A_{str} - A_{ps}) + F_{yr} A_{str} - A_{ps}(f_{pe} - E_p \varepsilon_{cu}) \qquad \text{Eq. 8-69}$$

If $P_u < 0.10\varphi f'_c A_g$:

$$\left(\frac{\mathrm{M}_{ux}}{\mathrm{M}_{rx}} + \frac{\mathrm{M}_{uy}}{\mathrm{M}_{ry}}\right) \leq 1.0 \qquad \text{Eq. 8-70}$$

Where:

P_u = factored axial load.
P_{rx} = factored resistance in axial compression determined on the basis that only eccentricity, e_y, is present (kips).
P_{ry} = factored resistance in axial compression determined on the basis that only eccentricity, e_x, is present (kips).
P_{rxy} = factored resistance axial compression with biaxial flexure (kips).
M_{ux} = factored moment about x-axis (kip-in).
M_{rx} = factored resistance in flexure about x-axis (kip-in) (Section 8.5.2.3).
M_{uy} = factored moment about y-axis (kip-in).
M_{ry} = factored resistance in flexure about y-axis (kip-in) (Section 8.5.2.3).
φ_c = resistance factor for axial compression (Table 8-6).

f'_c = concrete compression strength at 28 days, unless otherwise specified (ksi).

f_{pe} = effective stress in the prestressing steel after losses (ksi).

F_{yr} = yield stress of reinforcing steel (ksi).

A_g = gross cross-sectional area (in^2).

A_{str} = cross sectional area of longitudinal reinforcing steel (in^2).

A_{ps} = cross sectional area of prestressing steel (in^2).

E_p = elastic modulus of prestressing steel (in^2).

ε_{cu} = failure strain of concrete in compression (in^2).

The analysis of the prestressed concrete section response to a combination of an axial load and two orthogonal moments is complex. A successful and practical approach to the analysis of the pile cross section is offered by the FB-Pier Program. The concrete and the prestressing steel stress strain relationships are assumed. For concrete, the FB-Pier program assumes a maximum concrete strength of $0.85f'_c$ to include loading time effects on the concrete strength and all points on the stress strain curve are reduced to 85 percent of the short time values.

Bi-axial interaction diagrams are determined for each of an increasing set of axial loads up to the maximum axial strength condition. An illustration of one of these interaction diagrams for a particular axial load is shown in Figure 8-5. These diagrams are determined for the entire range of axial loads up to the axial failure case. With increasing axial load the maximum moment strength becomes smaller. A three dimensional interaction diagram can then be constructed with the axial load on the vertical axis and a particular interaction diagram at each level of axial load. Imagine a stack of these interaction diagrams. Thus, a three dimensional failure surface is defined. The equation of the failure surface can be generated by fitting a surface through the interaction diagrams at each level.

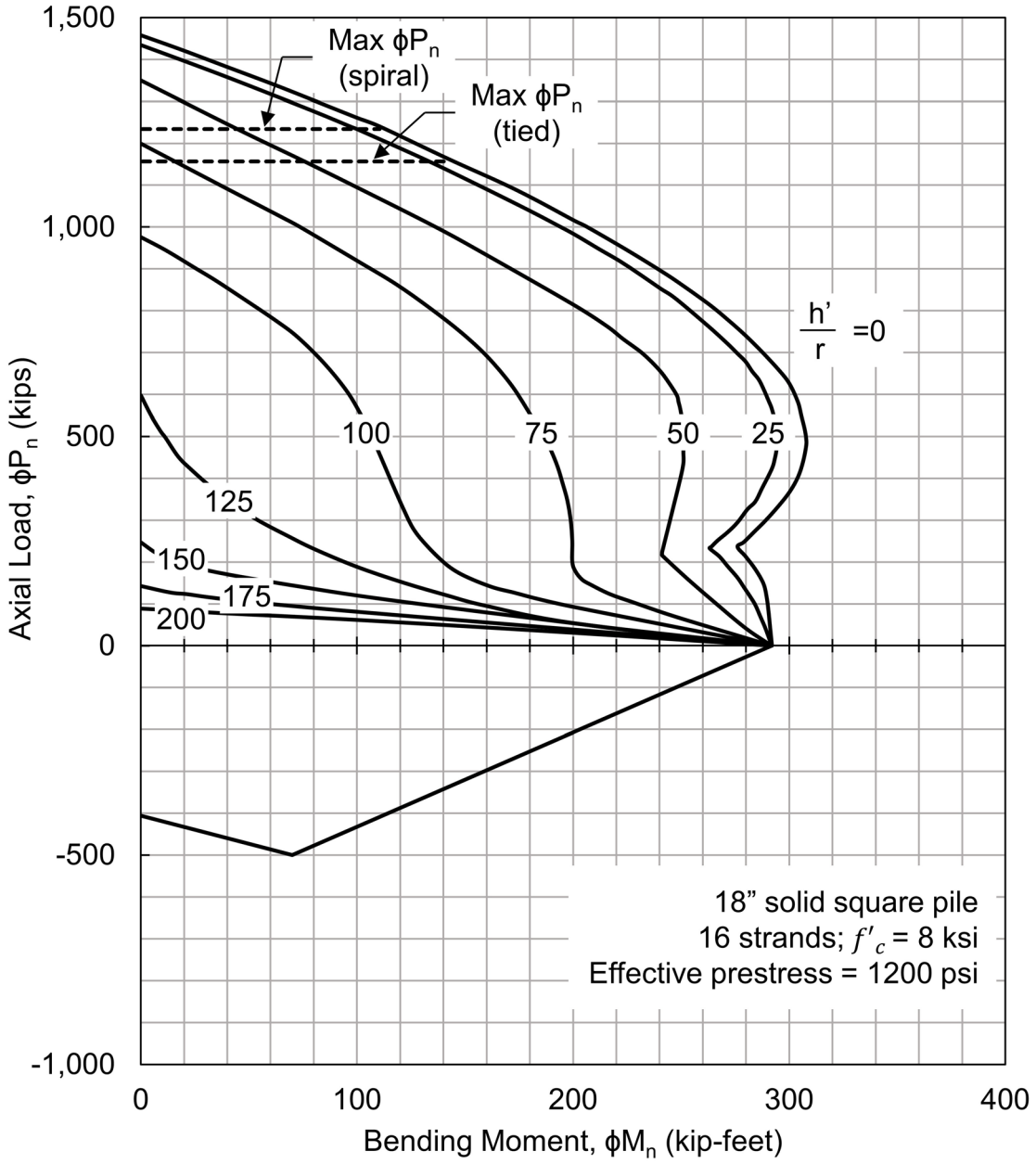

Figure 8-5 Moment interaction diagram.

When the necessary failure surfaces are available, the analysis at a particular load level can be checked by examining whether the vector of the forces on the section (axial, M_x and M_y) falls within or outside the failure envelope. The deformations associated with the three applied forces make it possible to determine the displacements associated with the various load levels. This elegant and powerful

analysis algorithm produces excellent results. Well-designed graphics make it possible for the foundation specialist to easily evaluate the results.

The analysis has been discussed for prestressed concrete piles and they are probably the most challenging to deal with. FB-Pier can also analyze steel piles and concrete filled pipes using the same concepts described above.

8.7 COMPOSITE PILES

Composite piles for structural applications shall be defined as concrete filled steel pipe piles. Guidance for other composite pile types such as a concrete pile with an H-pile stinger is not provided for in AASHTO (2014) specifications. Therefore structural resistances over the length of respective pile materials should be evaluated considering the primary section material.

8.7.1 Driving Stress

Concrete filled steel pipe piles are driven unfilled. Therefore, driving stresses for the non-composite steel section should be used and reference should be made to Section 8.5.1, Driving Stresses: Steel Piles.

8.7.2 Structural Resistance

8.7.2.1 Axial Compression

The behavior of composite sections is somewhat different than non-composite members and is therefore evaluated by alternate means. AASHTO (2014) provides evaluation methods to assess the strength limit state of composite sections, provided the following criteria are met.

1. The cross-sectional area of steel is at least 4 percent of the total cross-sectional area. If the cross sectional area of steel is less than this limit, the pile is considered non-composite and should be evaluated following procedures in Section 8.6 Concrete Piles.

2. The concrete compression strength is between 3.0 ksi and 8.0 ksi. Commentary provided in AASHTO (2014) notes the lower limit is imposed to encourage use of good quality concrete.

3. The yield strength of longitudinal reinforcement to determine the compression resistance cannot exceed 60.0 ksi.

For axial compression loading of concrete filled steel pipes, the factored structural limit state is taken as:

$$P_r = \varphi P_n \qquad \text{Eq. 8-71}$$

Where:

P_r = factored resistance in axial compression (kips).
φ = resistance factor (Table 8-6).
P_n = nominal resistance in axial compression (kips).

STEP BY STEP PROCEDURE FOR: “NOMINAL COMPRESSION RESISTANCE”

STEP 1 Determine the normalized column slenderness factor, λ.

The normalized column slenderness factor is be evaluated using the following equation. However, if the pile is fully embedded, λ may be taken as 0 (AASHTO 2014).

$$\lambda = \left(\frac{Kl}{\pi r_s}\right)^2 \left(\frac{F_e}{E_e}\right) \qquad \text{Eq. 8-72}$$

In which:

$$F_e = F_y + C_1 F_{yr} \left(\frac{A_{str}}{A_{st}}\right) + C_2 f'_c \left(\frac{A_c}{A_{st}}\right) \qquad \text{Eq. 8-73}$$

$$E_e = E_{st} \left[1 + \left(\frac{C_3}{n}\right)\left(\frac{A_c}{A_{st}}\right)\right] \qquad \text{Eq. 8-74}$$

$$n = \frac{E_{st}}{E_c} \qquad \text{Eq. 8-75}$$

Where:

λ = normalized column slenderness factor.
A_{st} = cross sectional area of steel (in^2).
A_c = cross sectional area of concrete (in^2).
A_{str} = cross sectional area of longitudinal reinforcing steel (in^2).
K = effective length factor (Figure 8-4).
l = unbraced length in the plane of buckling (inches).
r_s = radius of gyration about axis normal to plane of buckling (inches).

F_e = nominal compression resistance of composite section (ksi).
F_y = yield stress of steel (Table 8-1) (ksi).
F_{yr} = yield stress of reinforcing steel (ksi).
f'_c = concrete compression strength at 28 days, unless otherwise specified (ksi).
E_e = modified elastic modulus of steel for composite column (ksi).
E_{st} = elastic modulus of steel (ksi).
E_c = elastic modulus of concrete (Equation 8-1) (ksi).
C_1 = composite column constant 1 (1.00 for concrete filled pipes).
C_2 = composite column constant 2 (0.85 for concrete filled pipes).
C_3 = composite column constant 3 (0.40 for concrete filled pipes).

STEP 2 Determine the nominal resistance in axial compression, P_n.

After determining the normalized column slenderness ratio, a relatively straightforward calculation of the nominal resistance in axial compression is made using either Equation 8-73 or Equation 8-74.

If $\lambda \leq 2.25$:

$$P_n = 0.66^{\lambda} F_e A_{st} \quad \text{Eq. 8-76}$$

If $\lambda > 2.25$:

$$P_n = \frac{0.88 F_e A_{st}}{\lambda} \quad \text{Eq. 8-77}$$

Where:

λ = normalized column slenderness factor.
P_n = nominal resistance in axial compression (kips).
A_{st} = cross sectional area of steel (in^2).
F_e = nominal resistance in axial compression of composite section (ksi).

8.8 LAYOUT OF PILE GROUPS

A group of piles is typically required to support large structural loads. An initial group layout must be determined to perform in-service stress checks. The possible loads are illustrated in Figure 8-6. The various load combinations, as given in Article 3.4 of the 2014 AASHTO Standard Specification, should be investigated to determine the pile stress conditions. Pile group layouts can be determined through the use of computer software such as GROUP or FB-Pier, which utilize soil structure interaction (t-z and p-y curves) to distribute loads and deflections throughout the pile group. Alternatively, a hand calculation for the Rigid Cap Method may be performed as follows.

STEP BY STEP PROCEDURE FOR: "LAYOUT OF PILE GROUPS"

STEP 1 Estimate the number of piles required to resist structural loads.

An initial, or trial, group layout may be computed by dividing the factored axial load acting on the pile cap/group by the factored geotechnical resistance of a single pile, and then rounding the number up (say, by 15% or more, depending upon magnitude of the moments and lateral loads) to a constructible pile layout. Therefore, the number of piles is estimated as:

$$\frac{\mathrm{P}_u}{R_r} \cong \ Number\ of\ Piles\ \ (round\ up) \rightarrow n \qquad \text{Eq. 8-78}$$

Where:

P_u = largest factored, axial load of the superstructure (kips).
R_r = factored resistance of a single pile (geotechnical) (kips).
n = number of piles in pile group.

Please note however that for many highway structures, lateral or tension loading may govern the design. Although the Equation 8-78 provides a preliminary guide to estimate the number of piles for axial compression loads, additional piles may be required to resist other loads and limit deflection.

STEP 2 Generate trial pile group configuration.

A trial configuration for the group of piles should be developed with *n*-piles. Minimum center-to-center pile spacing requirements by AASHTO (2014) specifications is the lesser of 2.5 feet or 2.5 pile diameters. However, as

recommended in the previous edition of this manual, experience with pile group loading and efficiency has shown that 3.0 pile diameters is a more practical pile spacing minimum. Example pile group layouts can be found in CRSI Design Handbook (2002) and other sources.

STEP 3 Determine the maximum single pile axial load.

The trial group configuration consisting of *n*-piles should be checked for adequate single pile axial resistance under the combined superstructure/substructure axial loads and moments. The various factored load combinations, and not just the combination with the largest axial load, should be checked to determine the critical loading case. If the stiffness of all piles in the group are equal, then the maximum single pile factored axial load, P_{ui}, may be computed with the rigid cap method as:

$$P_{ui} = \frac{P_{uz}+W_c+W_s}{n} + \frac{M_{ux}y}{\sum y^2} + \frac{M_{uy}x}{\sum x^2} \qquad \text{Eq. 8-79}$$

Where:

P_{ui} = maximum single pile factored axial load (kips).
P_{uz} = factored axial load from superstructure/substructure acting upon pile cap (kips).
W_c = estimated weight of pile cap (kips).
W_s = estimated weight of soil above pile cap, if applicable (kips).
n = number of piles in pile group.
M_{ux} = factored moment about the x axis acting on the pile cap (kip-ft).
M_{uy} = factored moment about the y axis acting on the pile cap (kip-ft).
x = distance along x-axis from the center of the column to each pile center (feet).
y = distance along y-axis from the center of the column to each pile center (feet).

If the maximum single pile factored axial load exceeds the pile factored structural resistance, add one, or more, piles to the group or increase the pile spacing if $P_{ui} > P_{uz}$ and recompute the maximum single pile factored axial load (P_{ui}). If the moments in one direction are substantially larger than the other, it may be desirable to make the cap unsymmetrical.

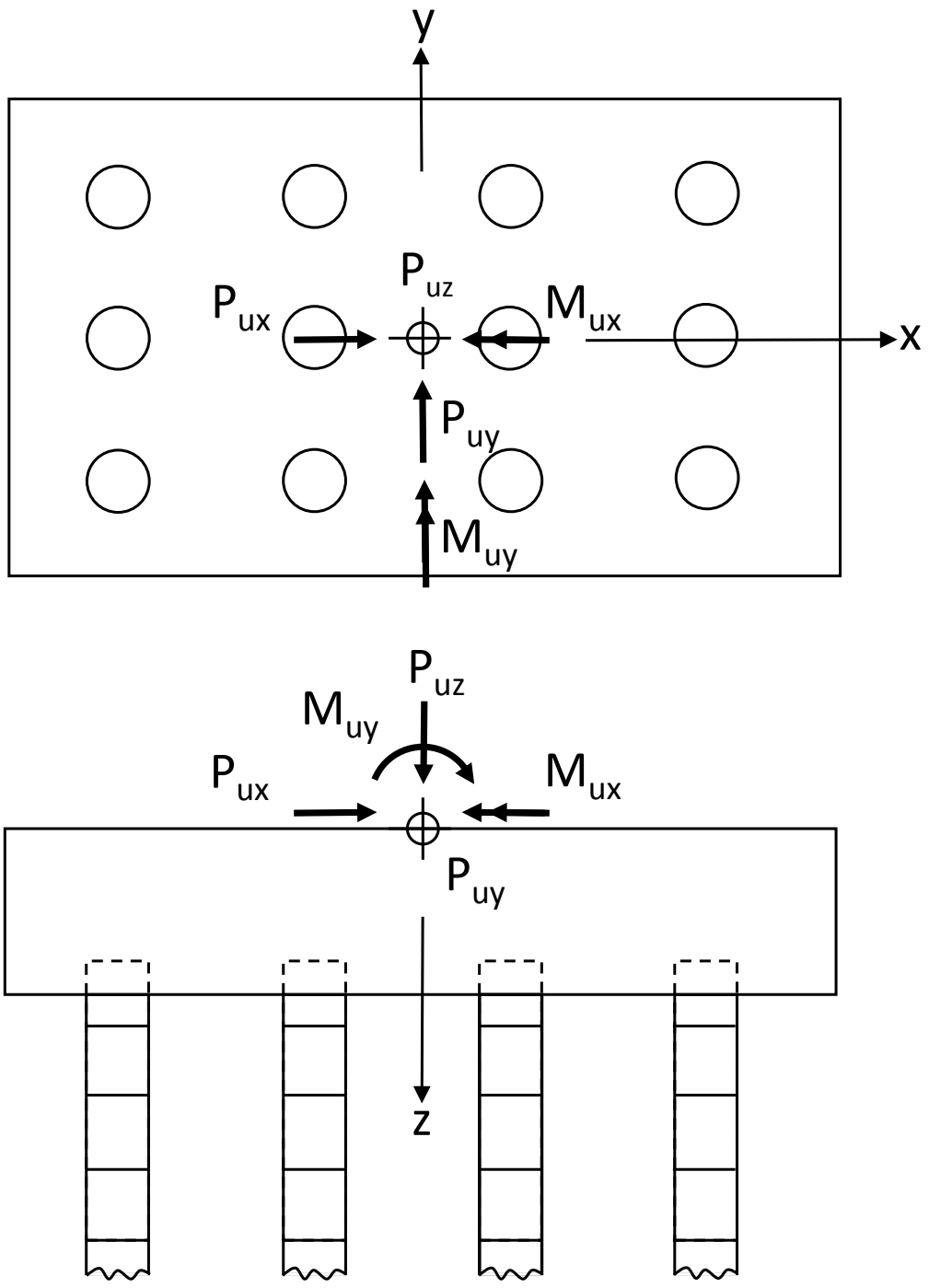

Figure 8-6 Pile group layout.
(Note: Column supported on pile cap not shown for clarity)

8.9 PRELIMINARY DESIGN OF PILE BENT AND GROUP CAPS

The purpose of this section is to provide guidelines to develop a preliminary size of a pile cap for the purposes of cost estimating. Information for complete, comprehensive structural design, including design for seismic and other extreme events, is beyond the scope of this manual, and not presented herein.

A state-of-the-practice manual on pile cap design was recently published by the Concrete Reinforcing Steel Institute (CRSI). This manual, "Design Guide for Pile Caps" (Mays 2015), was developed to provide the practicing engineer with a detailed overview of pile cap design, analysis methods, and detailing. It follows the American Concrete Institute ACI-14: Building Code Requirements for Structural Concrete and Commentary (ACI 2014) and covers piles with nominal loads up to 400 tons. Design procedure for vertical, lateral/overturning, and seismic loading is presented. Spreadsheets for pile cap design, following ACI-14, are available for download at www.crsi.org/pilecaps.cfm. This guide and spreadsheets are useful tools to develop a preliminary cap design for detailed analysis following AASHTO (2014).

In bridge design, the LRFD structural design of a concrete pile bent cap is similar to that of structural design for a concrete pier cap (Wilson et al. 2006). However, several design considerations are unique to cap design including: pile embedment into the cap, structural design depth, pile concrete cover requirements, pile misalignment tolerance, concrete pile anchorage, and minimum pile spacing requirements.

The design and size of the pile cap is dependent on the pile group layout, pile loads, and superstructure loads. Thus, an iterative design is required to optimize overall economics. The horizontal dimensions of the pile cap for the trial pile group configuration may be estimated, per AASHTO (2014) Article 10.7.1.2, by using: (i) the minimum center-to-center pile spacing of not less than 30.0 inches or 2.5 pile diameters; and (ii) a minimum edge of cap to side of pile distance of 9 inches. Maximum width and/or length of pile cap may be dictated by project constraints.

The thickness of the pile cap is a sum of the pile embedment into the cap, clear space between the cap reinforcing steel and the top of (embedded) piles, and thickness required for structural support. Per AASHTO (2014) Article 10.7.1.2, the piles shall project at least 12.0 inches into the cap after damaged pile material has been removed. If the piles and cap are attached by embedded bars or strands, this thickness may be reduced to 6.0 inches. The reinforced concrete must be designed with consideration of flexure and shear, for the factored loads. Potential shear

failures include punching about a single pile, punching about a pair of piles, a single pile across the corner of the cap, and punching of the (superstructure) column across the width(s) of the cap.

STEP BY STEP PROCEDURE FOR: “LAYOUT OF PILE GROUPS”

STEP 1 Estimate the total thickness of cap.

An initial, trial total (including pile embedment and 3 inches clear space between top of piles and reinforcing steel) thickness of the pile cap may be estimated from experience, agency guidelines or standards, or with the following equation:

$$\mathrm{t}_{cap} = \frac{P_{ui}}{12} + 30 \qquad \text{Eq. 8-80}$$

Where:

t_{cap} = thickness of cap (inches).

P_{ui} = maximum single pile factored axial load (kips).

This initial, trial thickness should be refined by examining punching shear in the reinforced concrete pile cap. Equations for these preliminary calculation steps are shown below.

STEP 2 Determine dimensions for computations.

1. Determine effective shear depth to concrete reinforcement, d_v. The effective shear depth, d_v, is taken as the distance between the resultants of the tensile and compression forces due to flexure, as illustrated in Figure 8-7, where:

$$d_v = \mathrm{t}_{cap} - d_c - d_s - d_f \qquad \text{Eq. 8-81}$$

Where:

d_v = effective depth to reinforcement (inches).
t_{cap} = thickness of cap (inches).
d_c = clear space (inches).
d_s = distance to center of steel (inches).
d_f = pile embedment into cap (inches).
h = structural depth, thickness of cap less pile embedment (inches).

The effective shear depth for a regularly reinforced section, per AASHTO (2014) Article 5.8.2.9, need not be taken to be less than the greater of 0.9d_s or 0.72h (inches). Thus, an assumed value of the effective shear depth, d_v, for preliminary sizing may be taken as the maximum of 0.9d_s or 0.72h (inches).

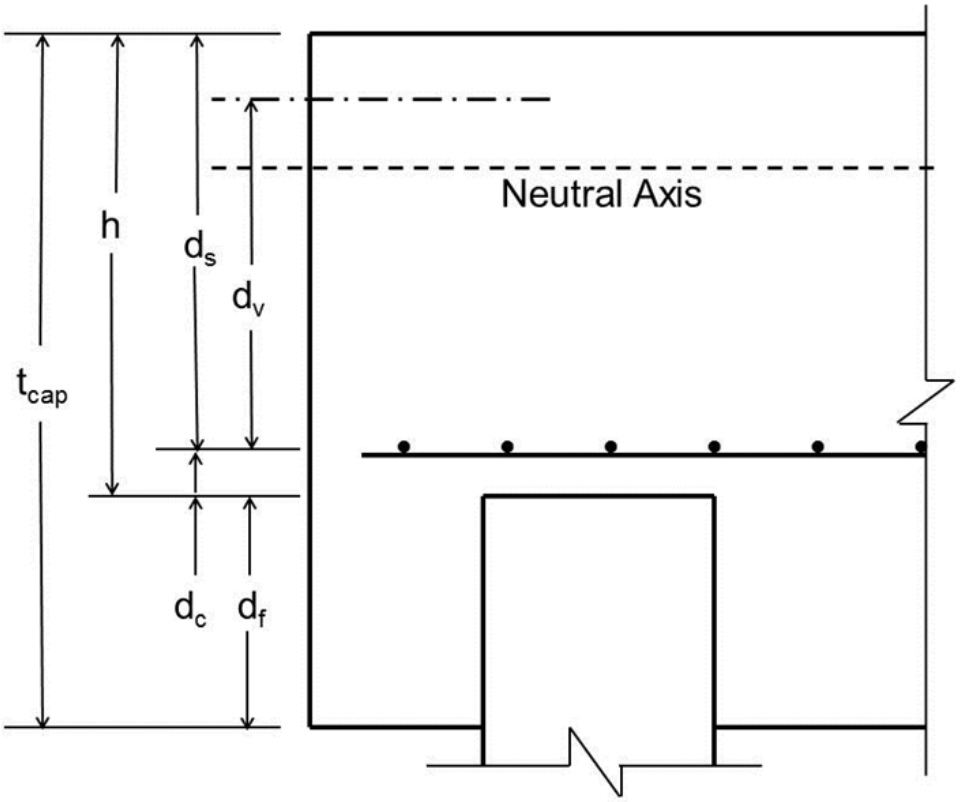

Figure 8-7 Cap section and notation.

2. Determine critical punching shear perimeter, b_o, around the column supported on the pile cap. The shear force applied the shear perimeter is the load acting outside that perimeter.

For square columns:

$$b_o = 4\,(b_c + d_v) \qquad \text{Eq. 8-82}$$

For rectangular columns:

$$b_o = 2\,(c_1 + c_2 + 2d_v) \qquad \text{Eq. 8-83}$$

For circular columns:

$$b_o = c_o + d_v \qquad \text{Eq. 8-84}$$

Where:

b_o = critical punching shear perimeter (inches).
d_v = effective shear depth (inches).
b_c = column side for square columns (inches).
c_1 = small column side for rectangular columns (inches).
c_2 = large column side for rectangular columns (inches).
c_o = column diameter (inches).

STEP 3 Check punching (two-way) shear at: (i) at a distance $d_v/2$ from face of column and at the face of the column, as illustrated in Figure 8-8; and (ii) around individual and pair of piles as illustrated in Figures 8-9 and 8-10.

1. Compute total applied two-way, punching shear stress, V_u, at critical section.

For shear around column:

$$V_u = P_u \qquad \text{Eq. 8-85}$$

Where:

V_u = factored shear force (kips).
P_u = factored axial load of the superstructure (kips).

For shear around individual or pair of piles:

$$V_u = \gamma_i Q_i = n_i R_r \qquad \text{Eq. 8-86}$$

Where:

V_u = factored shear force (kips).

R_r = factored (geotechnical) axial resistance of a single pile (kips).

n_i = number of piles whose centers lie inside the two-way shear critical section.

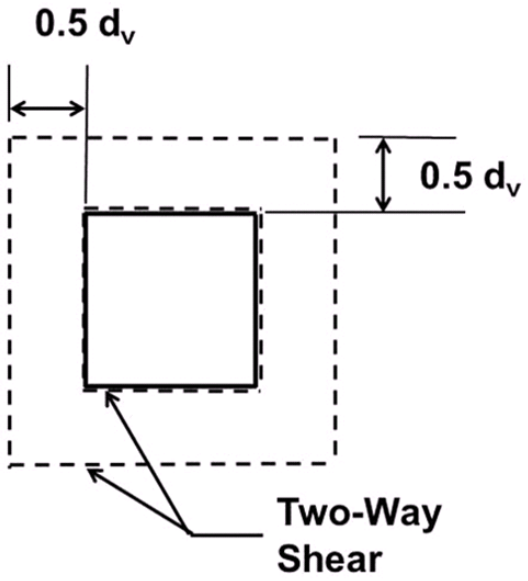

Figure 8-8 Critical punching (two-way) shear sections around column.

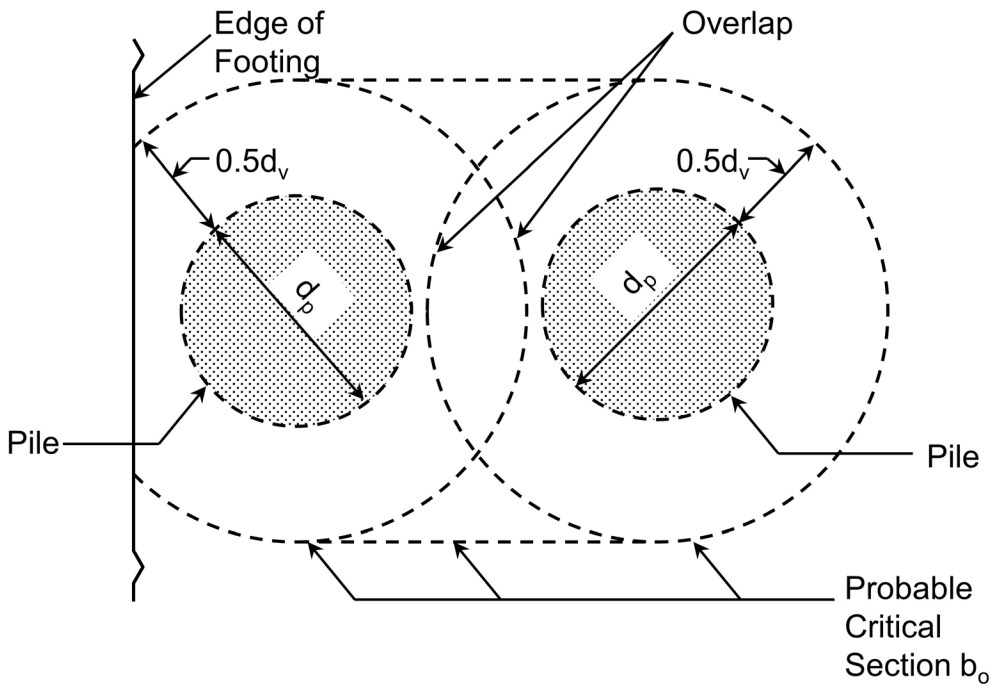

Figure 8-9 Critical section from overlapping critical perimeters (after AASHTO 2014).

2. Determine the nominal shear strength of concrete, per AASHTO Article 5.13.3.6.3, for two way action. Without transverse reinforcement, the nominal resistance is calculated using Equation 8-84. Sections with transverse reinforcement resist shear by means presented in Equation 8-85.

Without Transverse Reinforcement (AASHTO 5.13.3.6.3-1):

$$V_n = \left(0.063 + \frac{0.126}{\beta_c}\right)\sqrt{f'_c}\,b_o d_v \le 0.126\sqrt{f'_c}\,b_o d_v \qquad \text{Eq. 8-87}$$

With Transverse Reinforcement (AASHTO 5.13.3.6.3-2):

$$V_n = V_c + V_s \le 0.192\sqrt{f'_c}\,b_o d_v \qquad \text{Eq. 8-88}$$

In which (AASHTO 5.13.3.6.3-3,-4):

$$V_c = 0.0632\sqrt{f'_c}\,b_o d_v \qquad \text{Eq. 8-89}$$

$$V_s = \frac{A_{stv} F_y d_v}{s} \qquad \text{Eq. 8-90}$$

Where:

V_n = nominal shear resistance (kips).
V_s = nominal shear resistance provided by steel reinforcement (kips).
V_c = nominal shear resistance provided by concrete tensile strength (kips).
β_c = ratio of the long side to the short side of the load.
f'_c = concrete compression strength at 28 days, unless otherwise specified (ksi).
F_y = specified yield stress of reinforcement (ksi).
b_o = critical punching (two-way) shear perimeter (inches).
d_v = effective shear depth (inches).
A_{stv} = area of transverse reinforcement within distance, *s* (in^2).
s = spacing of the transverse reinforcement (inches).

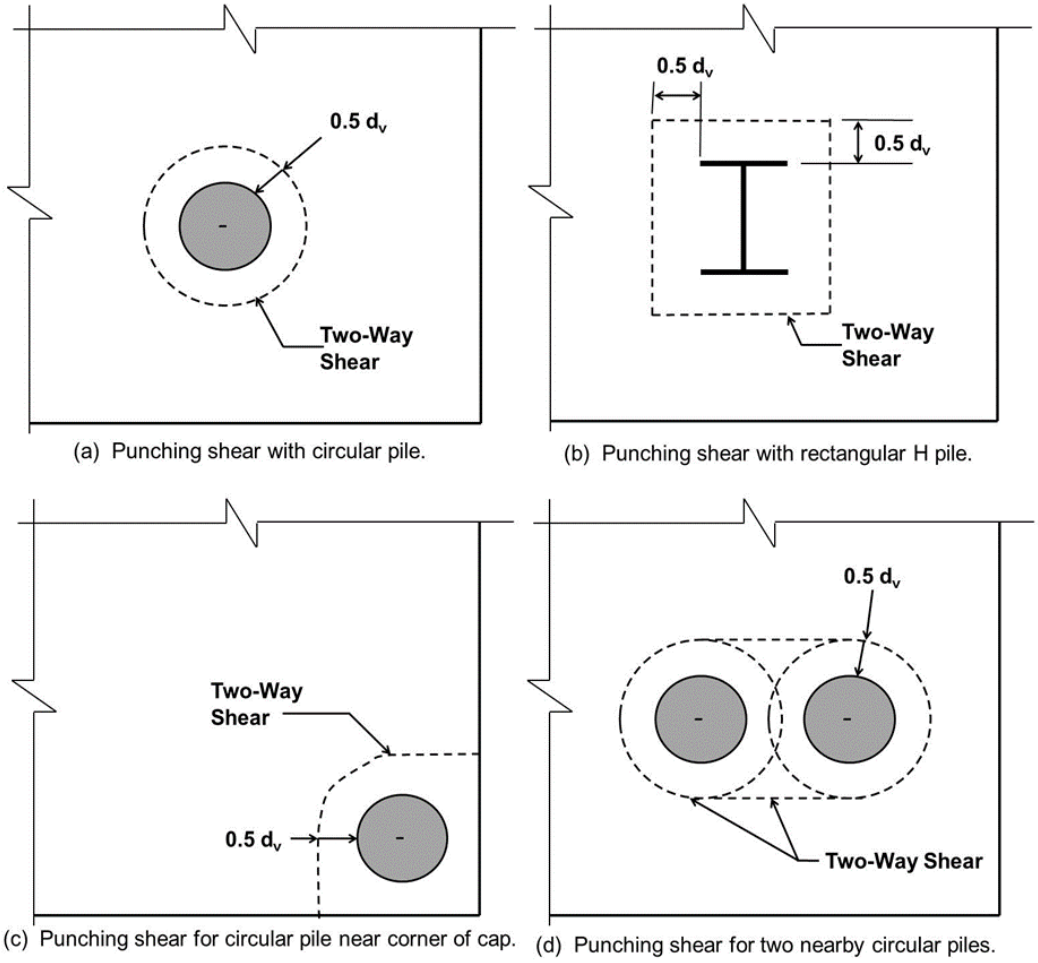

Figure 8-10 Pile punching shear for: (a) circular pile; (b) rectangular H pile; (c) circular pile near corner of cap; and (d) two nearby circular piles.

3. Compute the factored shear resistance from:

$$V_r = \varphi_v V_n \quad \text{Eq. 8-91}$$

Where:

V_r = factored shear resistance (kips).
φ_v = resistance factor (0.9 for normal weight concrete shear).
V_n = nominal shear resistance (kips).

4. Check that the factored shear resistance is greater than the factored shear load.

$$V_u < V_r \quad \text{Eq. 8-92}$$

Where:

V_u = factored shear load (kips).
V_r = factored shear resistance (kips).

If the above condition is not satisfied, increasing shear reinforcement or the effective shear depth should be considered.

STEP 4 Check One-Way Beam Shear, per AASHTO Article 5.13.3.6.2.

1. Compute total applied beam (one-way) shear stress, V_u, at critical sections, per AASHTO (2014) Article 5.8.3.2. Determine the beam shear distance from column to critical section as illustrated in Figure 8-11. Determine beam shear distance from the pile to the critical section(s), as illustrated in Figure 8-12.

2. For each direction of pile cap, check number of piles that lie outside of the critical section. Compute total applied one-way, beam shear stress, V_u, at critical section.

$$V_u = \gamma_i Q_i = n_o R_r \quad \text{Eq. 8-93}$$

Where:

V_u = factored shear stress (kips).
R_r = factored nominal resistance of a single pile (geotechnical) (kips).
n_o = number of piles which lie outside of the one-way critical shear section.

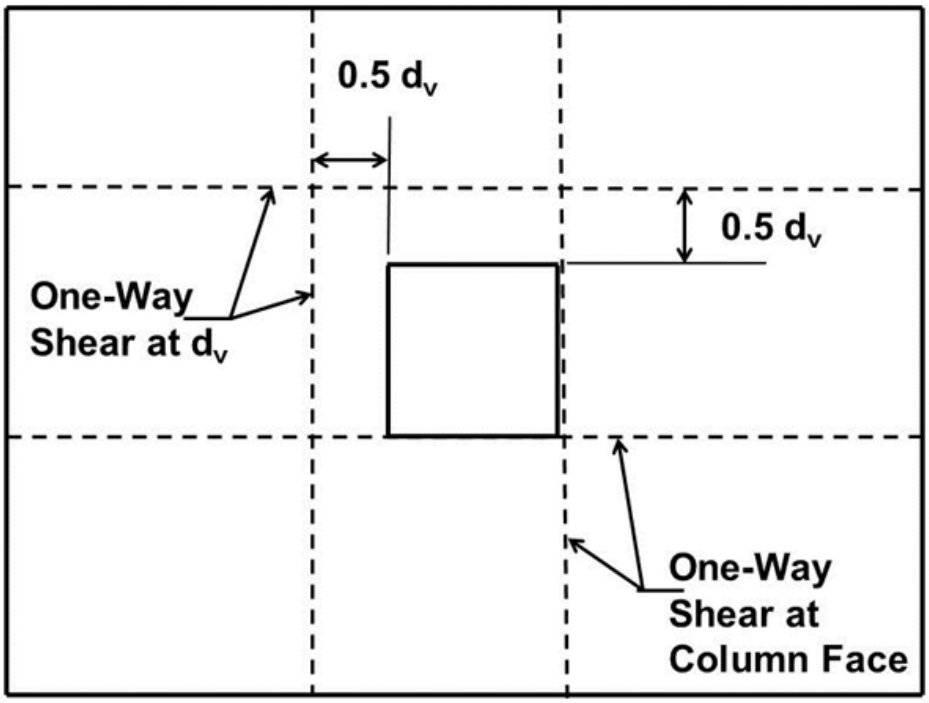

Figure 8-11 One-way beam shear critical sections from column.

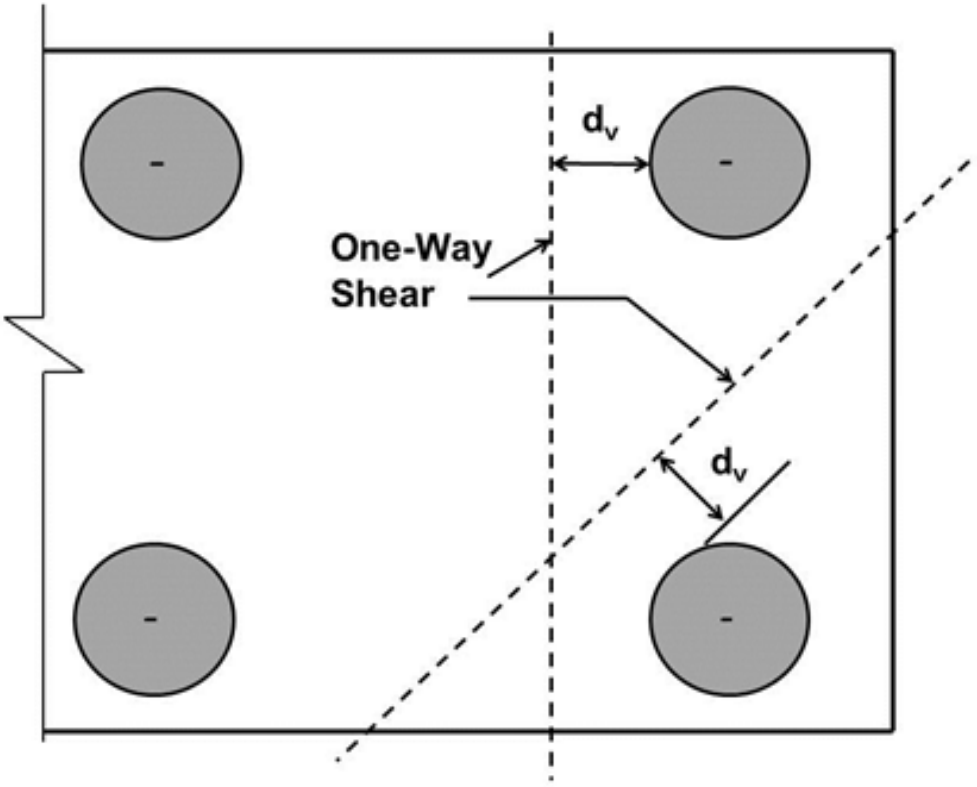

Figure 8-12 One-way beam shear critical sections from pile(s).

3. Determine the nominal shear strength of concrete, per AASHTO Article 5.8.3.3. The nominal shear resistance, V_n, without prestressed reinforcement, is the lesser of Equation 8-91 or 8-92 per AASHTO Article 5.8.3.3-2:

$$V_n = V_c + V_s \quad \text{Eq. 8-94}$$

$$V_n = 0.25\, f_c'\, b_v d_v \quad \text{Eq. 8-95}$$

Where:

V_n = nominal shear resistance (kips).
V_s = nominal shear resistance provided by steel reinforcement (kips).
V_c = nominal shear resistance provided by concrete tensile strength (kips).
f'_c = concrete compression strength at 28 days, unless otherwise specified (ksi).
b_v = width of interface (inches).
d_v = effective depth to reinforcement (inches).

4. Compute the factored shear resistance from:

$$V_r = \varphi_v V_n$$

Where:

V_r = factored shear resistance (kips).
φ_v = resistance factor (0.9 for normal weight concrete shear per AASHTO Article 5.5.4.2.1).
V_n = nominal shear resistance (kips).

5. Check that the factored shear resistance is greater than the factored shear load.

$$V_u < V_r \quad \text{Eq. 8-96}$$

Where:

V_u = factored shear force (kips).
V_r = factored shear resistance (kips).

STEP 5 Check Bending in Cap.

1. Compute factored bending moment, for each direction of pile cap, from piles to edge of column.

$$M_u = \sum R_r\,(x, y) \leq \varphi M_n \qquad \text{Eq. 8-97}$$

Where:

M_u = factored moment load (kip-in).
R_r = factored (geotechnical) axial resistance of a single pile (kip).
x, y = distance from edge of column to each pile (in both x and y directions) (inches).
M_n = nominal flexural resistance (kip-in).
φ = resistance factor (0.9 for normal weight concrete in shear or torsion).

The moment resistance of a reinforced concrete beam is determined based on the assumption of a rectangular distribution of the compression stress in the concrete at failure. The design must fail by yielding the tension steel to assure ductility. The nominal flexural resistance, M_n, for a non-prestressed rectangular section can be computed with the following equation (after AASHTO 5.7.3.2.2-1):

$$M_n = A_{stt} f_{st} \left(d_{st} - \frac{a}{2}\right) - A_{stc} f_{sc} \left(d_{sc} - \frac{a}{2}\right) \qquad \text{Eq. 8-98}$$

In which:

$$a = c\beta_1 = \frac{\beta_1}{\beta_1}\frac{A_s f_s - A'_s f'_s}{0.85 f'_c b} = \frac{A_s f_s - A'_s f'_s}{0.85 f'_c b} \qquad \text{Eq. 8-99}$$

Where:

M_n = nominal flexural resistance (kip-in).
A_{stt} = area of tension reinforcement (in^2).
f_{st} = stress in the mild steel tension reinforcement at nominal flexural resistance (ksi), as specified in AASHTO Article 5.7.2.1.
d_{st} = distance from extreme compression fiber to the centroid of the tensile reinforcement (in).
a = $c\,\beta_1$, depth of the equivalent stress block (in).
b = width of the compression face.
c = distance between the neutral axis and the compression face (in).
β_1 = stress block factor, which cancels in Equation 8-96.
A_{stc} = area of compression reinforcement (in^2).

f_{sc} = stress in the mild steel compression reinforcement at nominal flexural resistance (ksi), as specified in AASHTO Article 5.7.2.1.

d_{sc} = distance from extreme compression fiber to the centroid of the compression reinforcement (in).

The equation for moment strength, M_n, can be solved for the area of steel, A_{st}. However, $a/2$ is small compared with d so an approximate value can be assumed for $a/2$, A_{st} can be calculated and the steel area adjusted to arrive at a satisfactory A_{st}. If $d-a/2$ is assumed to be $0.9d$, A_{st} will be quite close and it will be satisfactory for preliminary design. If an improved A_{st} is desired it can be obtained made by determining an improved a with knowledge of the preliminary A_{st} and with the new a the next cycle of A_{st} can be determined and it will probably be final.

Per AASHTO Article 5.7.3.3.2, the tensile reinforcement should be adequate to develop a factored flexural resistance, M_r of at least 1.33 times the factored moment. See Article 5.7.3.3.2 for more details.

The final, structural design of pile caps is beyond the scope of this manual. See AASHTO (2014), ACI (2014), etc. for guidance on detailed structural design.

8.9.1 Cap Considerations for Large Pile Sizes

For Large Diameter Open-Ended Piles (LDOEPs), general analysis steps in the above section should be followed. No strict guidance can be offered at this time regarding minimum spacing and embedment into the pier cap, specifically for large pile sizes. Case studies presented in Brown and Thompson (2014) present few details on this subject as most state agencies do not currently have standard plans for these pile sizes. Pile tops were however embedded further into the cap, than with smaller pile sections. This was on the order of 3 feet into the pier cap for LDOEPs.

Pile spacing considerations should reflect guidelines proposed for drilled shafts due to the comparable element diameter. The presented pile plan layout in Brown and Thompson (2014) shows a minimum pile spacing on the order of 3 pile diameters (center to center), which is consistent with typical drilled shaft group layouts (Brown et al. 2010).

REFERENCES

American Association of State Highway and Transportation Officials (AASHTO). (2014). AASHTO LRFD Bridge Design Specifications, US Customary Units, Seventh Edition, with 2015 Interim Revisions. American Association of State Highway and Transportation Officials, Washington, D.C., 1960 p.

American Institute of Steel Construction (AISC). (2011). Steel Construction Manual, Fourteen Edition, (Third Printing). American Institute of Steel Construction Chicago, IL, 2192 p.

American Concrete Institute (ACI) (2014). Building Code Requirements for Structural Concrete and Commentary, ACI 318-14. Farmington Hills, MI, 520 p.

Bethlehem Steel Corporation. (1970). Steel H Piles, Handbook 2196-B. Bethlehem Steel Corporation, Bethlehem, PA, 64 p.

Brown, D. A., Turner, J.P. and Castelli R.J. (2010). Drilled Shafts: Construction Procedures and LRFD Design Methods, FHWA-NHI-10-016. Geotechnical Engineering Circular (GEC) No. 10, U.S. Dept. of Transportation, Federal Highway Administration (FHWA), Washington D.C., 970 p.

Brown, D.A., and Thompson III, W.R. (2015). Current Practices for Design and Load Testing of Large Diameter Open-End Driven Pipe Piles. Final Report. NCHRP Report 20-05, Topic 45-05, National Cooperative Highway Research Program, (NCHRP) Washington, D.C., 175 p.

Coduto, D P., and Kitch, W.A., and Yeung, M.R. (2016). Foundation Design: Principles and Practices, Third Edition. Pearson Education, Upper Saddle River, NJ:, 686 p.

Davisson, M.T. (1963). Estimating Buckling Loads for Piles. Proceedings of the Second Pan-American Conference on Soil Mechanics and Foundation Engineering, Brazil, Vol. 1, pp. 351-371.

Davisson, M.T. and K.E. Robinson. (1965). Bending and Buckling of Partially Embedded Piles. Proceedings Sixth International Conference on Soil Mechanics and Foundation Engineering, University of Toronto Press. Montreal, Canada, pp. 243-246.

Mays, T. (2015). Design Guide for Pile Caps, First Edition. Concrete Reinforcing Steel Institute (CSRI), Schaumburg, IL, 152 p.

Reese, L.C. (1984). Handbook on Design of Piles and Drilled Shafts Under Lateral Load, FHWA-IP-84-11. U.S. Department of Transportation, Federal Highway Administration, Office of Implementation, Washington, D.C., 392 p.

Rollins, K. and Stenlund, T. (2010). Laterally Loaded Pile Cap Connections. Utah Department of Transportation, Research Division, Report UT-10.16, 133 p.

Showalter, J. (2012). Round Timber Poles and Piles. Wood Design Focus, Forest Products Society, Vol. 22, No. 4, pp. 14-18.

Skyline Steel. (2015). Steel H-pile Technical Datasheets. Skyline Steel, http://www.skylinesteel.com.

White, C.D., and Castrodale, R.W. (2004). Precast/Prestresed Concrete Institute Bridge Design Manual – Chapter 20 Precast Prestressed Concrete Piles, MNL 133. Precast/Prestressed Concrete Institute, Chicago, IL, 171 p.

Wilson, K.E., Kimmerling, R.E., Goble, G.G., Sabatini, P.J., Zang, S.D., Zhou, J.Y. Amrhein, W.A., Bouscher, J.W. and Danaovich, L.J. (2006). LRFD for Highway Bridge Substructures and Earth Retaining Structures Reference Manual, FHWA NHI-05-094. U.S. Dept. of Transportation, Federal Highway Administration (FHWA), Washington, D.C., 1730 p.

APPENDIX A

LIST OF FHWA/ NHI RESOURCES RELEVANT TO DEEP FOUNDATIONS

Abu-Hejleh, N., DiMaggio, J.A., Kramer, W.M., Anderson, S., and Nichols, S. (2010). Implementation of LRFD Geotechnical Design for Bridge Foundations: Reference Manual. FHWA-NHI-10-039. National Highway Institute, Federal Highway Administration, Washington, D.C.

Abu-Hejleh, N., Kramer, W.M., Mohamed, K., Long, J.H., and Zaheer, M.A. (2013). Implementation of AASHTO LRFD Design Specifications for Driven Piles, FHWA-RC-13-001. U.S. Dept. of Transportation, Federal Highway Administration, 71 p.

Arneson, L.A., Zevenbergen, L.W., Lagasse, P.F., and Clopper, P.E. (2012). Evaluating Scour at Bridges, Fifth Edition, FHWA-HIF-12-003, Hydraulic Engineering Circular (HEC) No. 18. U.S. Dept. of Transportation, Federal Highway Administration, 340 p.

Azizinamini, A., Power, E.H., Myers, G.F., and Ozyildirim, H.C. (2014). Bridges for Service Life Beyond 100 Years, Innovative Systems Subsystems, and Components, S2-R19A-RW-1 Strategic Highway Research Program 2 (SHRP), Transportation Research Board, Washington, D.C., 248 p.

Briaud J-L. and Miran, J. (1992). The Cone Penetration Test, FHWA-SA-91-043. U.S. Department of Transportation, Federal Highway Administration, Office of Technology Applications, Washington, D.C., 161 p.

Brown, D.A., and Thompson, W.R. (2011). Developing Production Pile Criteria from Test Pile Data. National Cooperative Highway Research Program (NCHRP) Synthesis 418, Washington, D.C,. 54 p.

Brown, D. A., Turner, J.P. and Castelli R.J. (2010). Drilled Shafts: Construction Procedures and LRFD Design Methods, FHWA-NHI-10-016, Geotechnical Engineering Circular (GEC) No. 10. U.S. Dept. of Transportation, Federal Highway Administration, 970 p.

Brown, D.A., Dapp, S.D., Thompson, W.R., and Lazarte, C.A. (2007). Design and Construction of Continuous Flight Auger (CFA) Piles. FHWA-HIF-07-03, Geotechnical Engineering Circular (GEC) No.08. U.S. Dept. of Transportation, Federal Highway Administration, 289 p.

Cheney, R.S. and Chassie, R.G. (2000). Soils and Foundations Workshop Reference Manual. FHWA HI-00-045, U.S. Department of Transportation, National Highway Institute, Federal Highway Administration, Washington, D.C., 358 p.

Elias, V., Welsh, J.P., Warren, J., Lukas, R.G., Collin J.G., and Berg, R.R. (2006). Ground Improvement Methods Volumes I and II, FHWA-NHI-06-019 and FHWA NHI-06-020. National Highway Institute, Federal Highway Administration, U.S. Department of Transportation, Washington D.C.

Federal Highway Administration (FHWA). (1996). Geotechnical Engineering Notebook DT-15. Differing Site Conditions. U.S. Dept. of Transportation, Federal Highway Administration, Washington, D.C. 36 p.

Federal Highway Administration (FHWA). (2002a). Life-Cycle Cost Analysis Primer, IF-02-047. Federal Highway Administration, U.S. Department of Transportation. Washington, D.C., 24 p.

Geotechnical Guideline 13 (1985). Geotechnical Engineering Notebook, U.S. Department of Transportation. Federal Highway Administration, Washington, D.C., 37 p.

Ghosn, M., Moses, F., and Wang, J. (2003). Design of Highway Bridges for Extreme Events, NCHRP Report 489. National Cooperative Highway Research Program. Transportation Research Board, Washington, D.C., 174 p.

Goble, G.G. and Rausche, F. (1976). Wave Equation Analysis of Pile Driving – WEAP Program, FHWA IP-76-14.3., U.S. Department of Transportation, Federal Highway Administration, Office of Research and Development, Washington, D.C., Volumes I-IV.

Goble, G.G. and Rausche, F. (1986). Wave Equation Analysis of Pile Driving - WEAP86 Program. U.S. Department of Transportation, Federal Highway Administration, Implementation Division, McLean, Volumes I-IV.

Hawk, H. (2003). Bridge Life-Cycle Cost Analysis, NCHRP483. Transportation Research Board of the National Academies, Washington, D.C. 96 p.

Kavazanjian, E., Wan, J-N. J., Martin, G.R., Shamsabadi, A., Lam, I., Dickenson, S.E., and Hung, C.J. (2011). LRFD Seismic Analysis and Design of Transportation Geotechnical Features and Structural Foundations, FHWA-NHI-11-032, Geotechnical Engineering Circular (GEC) No. 3. U.S. Dept. of Transportation, Federal Highway Administration, Washington, D.C., 592 p.

Kimmerling, R.E. (2002). Shallow Foundations, FHWA-IF-02-054, Geotechnical Engineering Circular (GEC) No. 6. U.S. Dept. of Transportation, Federal Highway Administration, Washington, D.C., 310 p.

Kyfor, Z.G., Schnore, A.R., Carlo, T.A., and Bailey, P.F. (1992). Static Testing of Deep Foundations, FHWA-SA-91-042. U.S. Department of Transportation, Federal Highway Administration, Office of Technology Applications, Washington, D.C., 174 p.

Lam, I.P. and Martin, G.R. (1986). Seismic Design of Highway Bridge Foundations. Volume II - Design Procedures and Guidelines, FHWA-RD-86-102. U.S. Department of Transportation, Federal Highway Administration, Office of Engineering and Highway Operations, McLean, VA, 167p.

Long, J., and Anderson, A. (2014). Improved of Driven Pile Installation and Design in Illinois: Phase 2, FHWA-ICT-14-019. Illinois Department of Transportation, Bureau of Material and Physical Research, Springfield, IL, 84 p.

Marsh, M.L., Buckle, I.G., and Kavazanjian Jr, E. (2014). LRFD Seismic Analysis and Design of Bridges, FHWA-NHI-15-004. National Highway Institute, U.S. Dept. of Transportation, Federal Highway Administration, Washington, D.C., 608 p.

Mayne, P.W., Christopher, B., Berg, R., and DeJong, J. (2001). Manual on Subsurface Investigations, FHWA NHI-01-031, U.S. Dept. of Transportation, National Highway Institute, Federal Highway Administration, Washington, D.C., 301 p.

Munfakh, G., Arman, A., Collin, J.G., Hung, J.C.-J., and Brouillette, R.P. (2001). Shallow Foundations Reference Manual, FHWA-NHI-01-023. National Highway Institute, Federal Highway Administration, Washington, D.C., 222 p.

Rausche, F., Likins, G.E., Goble, G.G., Hussien, M. (1986). The Performance of Pile Driving Systems; Inspector's Manual. U.S. Department of Transportation, Federal Highway Administration, Washington, D.C., 92 p.

Rausche, F., Thendean, G., Abou-matar, H., Likins, G.E. and Goble, G.G. (1996). Determination of Pile Drivability and Capacity from Penetration Tests, DTFH61-91-C-00047, Final Report. U.S. Department of Transportation, Federal Highway Administration, McLean, VA, 432 p.

Reese, L.C. (1984). Handbook on Design of Piles and Drilled Shafts Under Lateral Load. Report No. FHWA-IP-84-11, U.S. Department of Transportation, Federal Highway Administration, Office of Implementation, McLean, VA, 386 p.

Reese, L.C. (1986). Behavior of Piles and Pile Groups Under Lateral Load, FHWA-RD-85-106. U.S. Department of Transportation, Federal Highway Administration, Office of Engineering and Highway Operations Research and Development, Washington, D.C., 311 p.

Rixner, J.J., Kraemer, S.R. and Smith, A.D. (1986). Prefabricated Vertical Drains Volume I, Engineering Guidelines, FHWA-RD-86-168. U.S. Department of Transportation, Federal Highway Administration, Office of Engineering and Highway Operations Research and Development, McLean, VA, 117 p.

Sabatini, P. J., Elias, V., Schmertmann, G. R., and Bonaparte, R. (1997). Earth Retaining Systems FHWA-SA-96-038, Geotechnical Engineering Circular (GEC) No. 2. U.S. Department of Transportation, Federal Highway Administration, Washington, D.C., 161 p.

Sabatini, P.J., Tanyu, B., Armour., P., Groneck, P., and Keeley, J. (2005). Micropile Design and Construction, FHWA-NHI-05-039. National Highway Institute, U.S. Dept. of Transportation, Federal Highway Administration, Washington, D.C., 436 p.

Samtani, N.C. and Nowatzki, E.A. (2006). Soils and Foundations: Reference Manual, Vol. 1, FHWA-NHI-06-088, U.S. Dept. of Transportation, National Highway Institute, Federal Highway Administration, Washington, D.C., 462 p.

Samtani, N.C., Nowatzki, E.A., and Mertz, D.R. (2010). Selection of Spread Footings on Soils to Support Highway Bridge Structures, FHWA-RC TD-10-001. U.S. Department of Transportation, Federal Highway Administration, Washington, D.C., 98 p.

Schmertmann, J.H. (1978). Guidelines For Cone Penetration Test, Performance, and Design, FHWA-TS-78-209. U.S. Department of Transportation, Federal Highway Administration, Washington, D.C., 145 p.

Tanyu B.F., Sabatini, P. J., and Berg, R.R. (2008). Earth Retaining Structures, FHWA-NHI-07-07. U.S. Department of Transportation, Federal Highway Administration, Washington, D.C., 792 p.

Wightman, W., Jalinoos, F., Sirles., and Hanna, K. (2003), Applications of Geophysical Methods to Related Highway Problems. U.S. Dept. of Transportation, Federal Highway Administration (FHWA), Washington D.C., 716 p.

Wilson, K.E., Kimmerling, R.E., Goble, G.C., Sabatini, P.J., Zang, S.D., Zhou, J.Y. Amrhein, W.A., Bouscher, J.W. and Danaovich, L.J. (2006). LRFD for Highway Bridge Substructures and Earth Retaining Structures Reference Manual, FHWA NHI-05-094. U.S. Dept. of Transportation, Federal Highway Administration, Washington, D.C., 1730 p.

Appendix B

LIST OF ASTM AND AASHTO PILE DESIGN AND TESTING SPECIFICATIONS

American Association of State Highway and Transportation Offices (AASHTO). Standard Method of Test for High Strain Dynamic Testing of Piles, AASHTO Designation T-298-33.

American Association of State Highway and Transportation Officials (AASHTO). (1978). Manual on Foundation Investigations Second Edition.. AASHTO Highway Subcommittee on Bridges and Structures, Washington, D.C., 196 p.

American Association of State Highway and Transportation Officials (AASHTO). (2001). Standard Recommended Practice for Assessment of Corrosion of Steel Piling for Non-Marine Applications. AASHTO Standard Specifications for Transportation Materials and Methods of Sampling and Testing, Part 1B: Specifications, 24th Edition, 13 p.

American Association of State Highway and Transportation Officials (AASHTO). (2011) Guide Specifications for LRFD Seismic Bridge Design, 2nd Edition, with 2012, 2014, and 2015 Interim Revisions. American Association of State Highway and Transportation Officials, Washington, D.C., 331 p.

American Association of State Highway and Transportation Officials (AASHTO). (2014). AASHTO LRFD Bridge Design Specifications, US Customary Units, Seventh Edition, with 2015 Interim Revisions. American Association of State Highway and Transportation Officials, Washington, D.C., 1960 p.

ASTM A27-13. (2014). Standard Specification for Steel Castings, Carbon, for General Application. Book of ASTM Standards, Vol. 1.02, ASTM International, West Conshohocken, PA, 4 p.

ASTM A572-15. (2015). Standard Specification for High-Strength Low-Alloy Columbium-Vanadium Structural Steel. Book of ASTM Standards, Vol. 1.04, ASTM International, West Conshohocken, PA, 4 p.

ASTM D1143-07. (2014). Standard Test Methods for Deep Foundations Under Static Axial Compressive Load. Book of ASTM Standards, Vol. 4.08, ASTM International, West Conshohocken, PA, 15 p.

ASTM D1452-09. (2014). Standard Practice for Soil Exploration and Sampling by Auger Borings. Annual Book of ASTM Standards, Vol. 4.08, ASTM International, West Conshohocken, PA, 6 p.

ASTM D1586-11. (2014). Standard Test Method for Standard Penetration Test (SPT) and Split-Barrel Sampling of Soils. Annual Book of ASTM Standards, Vol. 4.08, ASTM International, West Conshohocken, PA, 9 p.

ASTM D1587-12. (2014). Standard Practice for Thin-Walled Tube Sampling of Soils for Geotechnical Purposes. Annual Book of ASTM Standards, Vol. 4.08, ASTM International, West Conshohocken, PA, 4 p.

ASTM D2113-14. (2014). Standard Practice for Rock Core Drilling and Sampling of Rock for Site Investigation. Annual Book of ASTM Standards, Vol. 4.08, ASTM International, West Conshohocken, PA, 20 p.

ASTM D2573-08. (2012). Standard Test Method for Field Vane Shear Test in Cohesive Soil. Annual Book of ASTM Standards, Vol. 4.08, ASTM International, West Conshohocken, PA, 8 p.

ASTM D3689-07. (2014). Standard Test Methods for Deep Foundations Under Static Axial Tensile Load. Book of ASTM Standards, Vol. 4.08, ASTM International, West Conshohocken, PA,13 p.

ASTM D4633-10. (2014). Standard Test Method for Energy Measurement for Dynamic Penetrometer. Book of ASTM Standards, Vol. 4.08, ASTM International, West Conshohocken, PA, 7 p.

ASTM D4719-07. (2014). Standard Test Methods for Prebored Pressuremeter Testing in Soils Annual. Book of ASTM Standards, Vol. 4.08, ASTM International, West Conshohocken, PA, 10 p.

ASTM D4945-12. (2014). Standard Test Method for High-Strain Dynamic Testing of Piles. Book of ASTM Standards, Vol. 4.08, ASTM International, West Conshohocken, PA, 9 p.

ASTM D4971-02. (2014). Standard Test Method for Determining the In Situ Modulus of Deformation of Rock Using the Diametrically Loaded 76-mm (3-in.) Borehole Jack. Book of ASTM Standards, Vol. 4.08, ASTM International, West Conshohocken, PA, 7 p.

ASTM D5778-12. (2014). Standard Test Method for Electronic Friction Cone and Piezocone Penetration Testing of Soils. Book of ASTM Standards, Vol. 4.08, ASTM International, West Conshohocken, PA, 20 p.

ASTM D5882-07. (2013). Standard Test Method for Low-Strain Dynamic Testing of Piles Annual Book of ASTM Standards, Vol. 4.09, ASTM International, West Conshohocken, PA, 6 p.

ASTM D6032-08. (2014). Standard Test Method for Determining Rock Quality Designation (RQD) of Rock Core. Annual Book of ASTM Standards, Vol. 4.09, ASTM International, West Conshohocken, PA, 5 p.

ASTM D6635-07. (2014). Standard Test Method for Performing the Flat Dilatometer. Book of ASTM Standards, Vol. 4.09, ASTM International, West Conshohocken, PA, 16 p.

ASTM D7012-14. (2014). Standard Tests Method for Compressive Strength and Elastic Moduli of Intact Rock Core Specimens under Varying States of Stress and Temperatures. Annual Book of ASTM Standards, Vol. 4.09, ASTM International, West Conshohocken, PA, 9 p.

ASTM D7383-10 (2010). Standard Test Methods for Axial Compressive Force Pulse (Rapid) Testing of Deep Foundations. Annual Book of ASTM Standards, Vol. 4.08, ASTM International, West Conshohocken, PA, 9 p. ASTM

ASTM Vol 4.08. (2014). Soil and Rock I, Vol. 4.08, ASTM International, West Conshohocken, PA, 1826 p.

ASTM Vol 4.09. (2014). Soil and Rock II, Vol. 4.09, ASTM International, West Conshohocken, PA, 1754 p.

Appendix C

PILE HAMMER INFORMATION

Type	Hammer Make	Hammer Model	Hammer Type	Rated Energy kip-feet	Ram Weight kips	Stroke feet
1	DELMAG	D 5	OED	10.51	1.10	9.55
2	DELMAG	D 8-22	OED	20.10	1.76	11.42
3	DELMAG	D 12	OED	22.61	2.75	8.22
4	DELMAG	D 15	OED	27.09	3.30	8.21
5	DELMAG	D 16-32	OED	40.20	3.52	11.42
6	DELMAG	D 22	OED	40.61	4.91	8.27
7	DELMAG	D 22-02	OED	48.50	4.85	10.00
8	DELMAG	D 22-13	OED	48.50	4.85	10.00
9	DELMAG	D 22-23	OED	51.22	4.85	10.56
10	DELMAG	D 25-32	OED	66.34	5.51	12.04
11	DELMAG	D 30	OED	59.73	6.60	9.05
12	DELMAG	D 30-02	OED	66.20	6.60	10.03
13	DELMAG	D 30-13	OED	66.20	6.60	10.03
14	DELMAG	D 30-23	OED	73.79	6.60	11.18
15	DELMAG	D 30-32	OED	75.44	6.60	11.43
16	DELMAG	D 36	OED	83.82	7.93	10.57
17	DELMAG	D 36-02	OED	83.82	7.93	10.57
18	DELMAG	D 36-13	OED	83.82	7.93	10.57
19	DELMAG	D 36-23	OED	88.50	7.93	11.16
20	DELMAG	D 36-32	OED	90.56	7.93	11.42
21	DELMAG	D 44	OED	90.16	9.50	9.49
22	DELMAG	D 46	OED	107.08	10.14	10.56
23	DELMAG	D 46-02	OED	107.08	10.14	10.56
24	DELMAG	D 46-13	OED	96.53	10.14	9.52
25	DELMAG	D 46-23	OED	107.08	10.14	10.56
26	DELMAG	D 46-32	OED	122.19	10.14	12.05
27	DELMAG	D 55	OED	125.00	11.86	10.54
28	DELMAG	D 62-02	OED	152.45	13.66	11.16
29	DELMAG	D 62-12	OED	152.45	13.66	11.16
30	DELMAG	D 62-22	OED	164.60	13.66	12.05
31	DELMAG	D 80-12	OED	186.24	17.62	10.57
32	DELMAG	D 80-23	OED	212.50	17.62	12.06
33	DELMAG	D100-13	OED	265.68	22.07	12.04
35	DELMAG	D 19-52	OED	43.20	4.00	10.80
36	DELMAG	D 6-32	OED	13.52	1.32	10.23

Type	Hammer Make	Hammer Model	Hammer Type	Rated Energy kip-feet	Ram Weight kips	Stroke feet
37	DELMAG	D 12-32	OED	31.33	2.82	11.11
38	DELMAG	D 12-42	OED	33.30	2.82	11.81
39	DELMAG	D 14-42	OED	34.50	3.09	11.18
40	DELMAG	D 19-32	OED	42.44	4.00	10.61
41	DELMAG	D 19-42	OED	43.24	4.00	10.81
42	DELMAG	D200-42	OED	492.04	44.09	11.16
43	DELMAG	D120-42	OED	301.79	26.45	11.41
44	DELMAG	D150-42	OED	377.33	33.07	11.41
45	DELMAG	D125-42	OED	313.63	27.56	11.38
46	DELMAG	D 21-42	OED	55.75	4.63	12.04
47	DELMAG	D 5-42	OED	10.56	1.10	9.60
48	DELMAG	D160-32	OED	393.45	35.27	11.16
49	DELMAG	D260-32	OED	639.36	57.32	11.16
50	FEC	1200	OED	22.50	2.75	8.18
51	FEC	1500	OED	27.09	3.30	8.21
52	FEC	2500	OED	50.00	5.50	9.09
53	FEC	2800	OED	55.99	6.16	9.09
54	FEC	3000	OED	63.03	6.60	9.55
55	FEC	3400	OED	73.01	7.48	9.76
56	FEC	D-18	OED	39.70	3.97	10.00
61	MITSUBIS	M 14	OED	25.25	2.97	8.50
62	MITSUBIS	MH 15	OED	28.14	3.31	8.50
63	MITSUBIS	M 23	OED	43.01	5.06	8.50
64	MITSUBIS	MH 25	OED	46.84	5.51	8.50
65	MITSUBIS	M 33	OED	61.71	7.26	8.50
66	MITSUBIS	MH 35	OED	65.62	7.72	8.50
67	MITSUBIS	M 43	OED	80.41	9.46	8.50
68	MITSUBIS	MH 45	OED	85.43	10.05	8.50
70	MITSUBIS	MH 72B	OED	135.15	15.90	8.50
71	MITSUBIS	MH 80B	OED	149.60	17.60	8.50
81	LINKBELT	LB 180	CED	8.10	1.73	4.68
82	LINKBELT	LB 312	CED	15.02	3.86	3.89
83	LINKBELT	LB 440	CED	18.20	4.00	4.55
84	LINKBELT	LB 520	CED	26.31	5.07	5.19
85	LINKBELT	LB 660	CED	51.63	7.57	6.82
90	HITACHI	HNC65	ECH	56.42	14.33	3.94
91	HITACHI	HNC80	ECH	69.43	17.64	3.94
92	HITACHI	HNC100	ECH	86.79	22.05	3.94
93	HITACHI	HNC125	ECH	108.49	27.56	3.94
101	KOBE	K 13	OED	25.43	2.87	8.86
103	KOBE	K22-Est	OED	45.35	4.85	9.35
104	KOBE	K 25	OED	51.52	5.51	9.35
107	KOBE	K 35	OED	72.18	7.72	9.35

Type	Hammer Make	Hammer Model	Hammer Type	Rated Energy kip-feet	Ram Weight kips	Stroke feet
110	KOBE	K 45	OED	92.75	9.92	9.35
112	KOBE	KB 60	OED	130.18	13.23	9.84
113	KOBE	KB 80	OED	173.58	17.64	9.84
120	ICE	180	CED	8.13	1.73	4.70
121	ICE	422	CED	23.12	4.00	5.78
122	ICE	440	CED	18.56	4.00	4.64
123	ICE	520	CED	30.37	5.07	5.99
124	ICE	640	CED	40.62	6.00	6.77
125	ICE	660	CED	51.63	7.57	6.82
126	ICE	1070	CED	72.60	10.00	7.26
127	ICE	30-S	OED	22.50	3.00	7.50
128	ICE	40-S	OED	40.00	4.00	10.00
129	ICE	42-S	OED	42.00	4.09	10.27
130	ICE	60-S	OED	59.99	7.00	8.57
131	ICE	70-S	OED	70.00	7.00	10.00
132	ICE	80-S	OED	80.00	8.00	10.00
133	ICE	90-S	OED	90.00	9.00	10.00
134	ICE	100-S	OED	100.00	10.00	10.00
135	ICE	120-S	OED	120.00	12.00	10.00
136	ICE	200-S	OED	100.00	20.00	5.00
137	ICE	205-S	OED	170.00	20.00	8.50
139	ICE	32-S	OED	26.01	3.00	8.67
140	ICE	120S-15	OED	132.45	15.00	8.83
142	MKT	DE-20C	OED	20.00	2.00	10.00
143	MKT	DE-30C	OED	28.00	2.80	10.00
144	MKT	DE-33C	OED	33.00	3.30	10.00
145	MKT	DE333020	OED	40.00	4.00	10.00
146	MKT	DE 10	OED	8.80	1.10	8.00
147	MKT	DE 20	OED	16.00	2.00	8.00
148	MKT	DE 30	OED	22.40	2.80	8.00
149	MKT	DA35B SA	OED	23.80	2.80	8.50
150	MKT	DE 30B	OED	23.80	2.80	8.50
151	MKT	DA 35B	CED	21.00	2.80	7.50
152	MKT	DA 45	CED	30.72	4.00	7.68
153	MKT	DE 40	OED	32.00	4.00	8.00
154	MKT	DE 35	OED	35.00	3.50	10.00
155	MKT	DE 42	OED	42.00	4.20	10.00
157	MKT	DE 50C	OED	50.00	5.00	10.00
158	MKT	DE 70C	OED	70.00	7.00	10.00
159	MKT	DE 50B	OED	42.50	5.00	8.50
160	MKT	DA55B SA	OED	40.00	5.00	8.00
161	MKT	DA 55B	CED	38.20	5.00	7.64
162	MKT	DE 70B	OED	59.50	7.00	8.50

Type	Hammer Make	Hammer Model	Hammer Type	Rated Energy kip-feet	Ram Weight kips	Stroke feet
163	MKT	DE-50B	OED	50.00	5.00	10.00
164	MKT	DE-70B	OED	70.00	7.00	10.00
165	MKT	DE-110C	OED	110.00	11.00	10.00
166	MKT	DE-150C	OED	150.00	15.00	10.00
167	MKT	DA 35C	CED	21.00	2.80	7.50
168	MKT	DA 55C	CED	38.20	5.00	7.64
171	CONMACO	C 50	ECH	15.00	5.00	3.00
172	CONMACO	C 65	ECH	19.50	6.50	3.00
173	CONMACO	C 550	ECH	25.00	5.00	5.00
174	CONMACO	C 565	ECH	32.50	6.50	5.00
175	CONMACO	C 80	ECH	26.00	8.00	3.25
176	CONMACO	C 100	ECH	32.50	10.00	3.25
177	CONMACO	C 115	ECH	37.38	11.50	3.25
178	CONMACO	C 80E5	ECH	40.00	8.00	5.00
179	CONMACO	C 100E5	ECH	50.00	10.00	5.00
180	CONMACO	C 115E5	ECH	57.50	11.50	5.00
181	CONMACO	C 125E5	ECH	62.50	12.50	5.00
182	CONMACO	C 140	ECH	42.00	14.00	3.00
183	CONMACO	C 160	ECH	48.75	16.25	3.00
184	CONMACO	C 200	ECH	60.00	20.00	3.00
185	CONMACO	C 300	ECH	90.00	30.00	3.00
186	CONMACO	C 5200	ECH	100.00	20.00	5.00
187	CONMACO	C 5300	ECH	150.00	30.00	5.00
188	CONMACO	C 5450	ECH	225.00	45.00	5.00
189	CONMACO	C 5700	ECH	350.00	70.00	5.00
190	CONMACO	C 6850	ECH	510.00	85.00	6.00
191	CONMACO	C 160 **	ECH	51.78	17.26	3.00
192	CONMACO	C 50E5	ECH	25.00	5.00	5.00
193	CONMACO	C 65E5	ECH	32.50	6.50	5.00
194	CONMACO	C 200E5	ECH	100.00	20.00	5.00
195	CONMACO	C 300E5	ECH	150.00	30.00	5.00
196	CONMACO	C 1750	ECH	1050.00	175.00	6.00
204	VULCAN	VUL 01	ECH	15.00	5.00	3.00
205	VULCAN	VUL 02	ECH	7.26	3.00	2.42
206	VULCAN	VUL 06	ECH	19.50	6.50	3.00
207	VULCAN	VUL 08	ECH	26.00	8.00	3.25
208	VULCAN	VUL 010	ECH	32.50	10.00	3.25
209	VULCAN	VUL 012	ECH	39.00	12.00	3.25
210	VULCAN	VUL 014	ECH	42.00	14.00	3.00
211	VULCAN	VUL 016	ECH	48.75	16.25	3.00
212	VULCAN	VUL 020	ECH	60.00	20.00	3.00
213	VULCAN	VUL 030	ECH	90.00	30.00	3.00
214	VULCAN	VUL 040	ECH	120.00	40.00	3.00

Type	Hammer Make	Hammer Model	Hammer Type	Rated Energy kip-feet	Ram Weight kips	Stroke feet
215	VULCAN	VUL 060	ECH	180.00	60.00	3.00
220	VULCAN	VUL 30C	ECH	7.26	3.00	2.42
221	VULCAN	VUL 50C	ECH	15.10	5.00	3.02
222	VULCAN	VUL 65C	ECH	19.18	6.50	2.95
223	VULCAN	VUL 65CA	ECH	19.57	6.50	3.01
224	VULCAN	VUL 80C	ECH	24.48	8.00	3.06
225	VULCAN	VUL 85C	ECH	25.99	8.52	3.05
226	VULCAN	VUL 100C	ECH	32.90	10.00	3.29
227	VULCAN	VUL 140C	ECH	35.98	14.00	2.57
228	VULCAN	VUL 200C	ECH	50.20	20.00	2.51
229	VULCAN	VUL 400C	ECH	113.60	40.00	2.84
230	VULCAN	VUL 600C	ECH	179.16	60.00	2.99
231	VULCAN	VUL 320	ECH	60.00	20.00	3.00
232	VULCAN	VUL 330	ECH	90.00	30.00	3.00
233	VULCAN	VUL 340	ECH	120.00	40.00	3.00
234	VULCAN	VUL 360	ECH	180.00	60.00	3.00
235	VULCAN	VUL 505	ECH	25.00	5.00	5.00
236	VULCAN	VUL 506	ECH	32.50	6.50	5.00
237	VULCAN	VUL 508	ECH	40.00	8.00	5.00
238	VULCAN	VUL 510	ECH	50.00	10.00	5.00
239	VULCAN	VUL 512	ECH	60.00	12.00	5.00
240	VULCAN	VUL 520	ECH	100.00	20.00	5.00
241	VULCAN	VUL 530	ECH	150.00	30.00	5.00
242	VULCAN	VUL 540	ECH	200.00	40.90	4.89
243	VULCAN	VUL 560	ECH	300.00	62.50	4.80
245	VULCAN	VUL 3100	ECH	300.00	100.00	3.00
246	VULCAN	VUL 5100	ECH	500.00	100.00	5.00
247	VULCAN	VUL 5150	ECH	750.00	150.00	5.00
248	VULCAN	VUL 6300	ECH	1800.00	300.00	6.00
251	RAYMOND	R 1	ECH	15.00	5.00	3.00
252	RAYMOND	R 1S	ECH	19.50	6.50	3.00
253	RAYMOND	R 65C	ECH	19.50	6.50	3.00
254	RAYMOND	R 65CH	ECH	19.50	6.50	3.00
255	RAYMOND	R 0	ECH	24.38	7.50	3.25
256	RAYMOND	R 80C	ECH	24.48	8.00	3.06
257	RAYMOND	R 80CH	ECH	24.48	8.00	3.06
258	RAYMOND	R 2/0	ECH	32.50	10.00	3.25
259	RAYMOND	R 3/0	ECH	40.63	12.50	3.25
260	RAYMOND	R 150C	ECH	48.75	15.00	3.25
261	RAYMOND	R 4/0	ECH	48.75	15.00	3.25
262	RAYMOND	R 5/0	ECH	56.88	17.50	3.25
263	RAYMOND	R 30X	ECH	75.00	30.00	2.50
264	RAYMOND	R 8/0	ECH	81.25	25.00	3.25

Type	Hammer Make	Hammer Model	Hammer Type	Rated Energy kip-feet	Ram Weight kips	Stroke feet
265	RAYMOND	R 40X	ECH	100.00	40.00	2.50
266	RAYMOND	R 60X	ECH	150.00	60.00	2.50
270	MENCK	MHU 100C	ECH	73.71	11.10	6.64
271	MENCK	MH 68	ECH	49.18	7.72	6.37
272	MENCK	MH 96	ECH	69.43	11.02	6.30
273	MENCK	MH 145	ECH	104.80	16.53	6.34
274	MENCK	MHU 195	ECH	143.74	21.36	6.73
275	MENCK	MHU 220	ECH	162.17	24.84	6.53
276	MENCK	MHU 400	ECH	294.82	51.09	5.77
277	MENCK	MHU 600	ECH	442.28	75.52	5.86
278	MENCK	MHU 1000	ECH	737.38	126.98	5.81
279	MENCK	MHU 1700	ECH	1253.24	207.15	6.05
280	MENCK	MHU 2100	ECH	1548.29	257.18	6.02
281	MENCK	MHU 3000	ECH	2211.90	370.23	5.97
282	MENCK	MRBS 500	ECH	45.07	11.02	4.09
283	MENCK	MRBS 750	ECH	67.77	16.53	4.10
285	MENCK	MRBS 850	ECH	93.28	18.96	4.92
286	MENCK	MRBS1100	ECH	123.43	24.25	5.09
287	MENCK	MRBS1502	ECH	135.59	33.07	4.10
288	MENCK	MRBS1800	ECH	189.81	38.58	4.92
289	MENCK	MRBS2500	ECH	262.11	63.93	4.10
290	MENCK	MRBS2502	ECH	225.95	55.11	4.10
291	MENCK	MRBS2504	ECH	225.95	55.11	4.10
292	MENCK	MRBS3000	ECH	325.36	66.13	4.92
293	MENCK	MRBS3900	ECH	513.34	86.86	5.91
294	MENCK	MRBS4600	ECH	498.94	101.41	4.92
295	MENCK	MRBS5000	ECH	542.33	110.23	4.92
296	MENCK	MRBS6000	ECH	759.23	132.27	5.74
297	MENCK	MRBS7000	ECH	631.40	154.00	4.10
298	MENCK	MRBS8000	ECH	867.74	176.37	4.92
299	MENCK	MRBS8800	ECH	954.53	194.01	4.92
300	MENCK	MBS12500	ECH	1581.83	275.58	5.74
301	MKT	No. 5	ECH	1.00	0.20	5.00
302	MKT	No. 6	ECH	2.50	0.40	6.25
303	MKT	No. 7	ECH	4.15	0.80	5.19
304	MKT	9B3	ECH	8.75	1.60	5.47
305	MKT	10B3	ECH	13.11	3.00	4.37
306	MKT	C5-Air	ECH	14.20	5.00	2.84
307	MKT	C5-Steam	ECH	16.20	5.00	3.24
308	MKT	S-5	ECH	16.25	5.00	3.25
309	MKT	11B3	ECH	19.15	5.00	3.83
310	MKT	C826 Stm	ECH	24.40	8.00	3.05
311	MKT	C826 Air	ECH	21.20	8.00	2.65

Type	Hammer Make	Hammer Model	Hammer Type	Rated Energy kip-feet	Ram Weight kips	Stroke feet
312	MKT	S-8	ECH	26.00	8.00	3.25
313	MKT	MS-350	ECH	30.80	7.72	3.99
314	MKT	S 10	ECH	32.50	10.00	3.25
315	MKT	S 14	ECH	37.52	14.00	2.68
316	MKT	MS 500	ECH	44.00	11.00	4.00
317	MKT	S 20	ECH	60.00	20.00	3.00
318	IHC	S-30	ECH	21.70	3.53	6.15
319	IHC	S-40	ECH	28.93	4.85	5.97
320	IHC	S-35	ECH	25.53	6.63	3.85
321	IHC	S-70	ECH	51.25	7.73	6.63
322	IHC	S-90	ECH	65.90	9.94	6.63
323	IHC	S-120	ECH	89.37	13.48	6.63
324	IHC	S-150	ECH	110.06	16.60	6.63
325	IHC	S-200	ECH	145.64	22.00	6.62
326	IHC	S-280	ECH	205.31	30.06	6.83
327	IHC	S-400	ECH	292.60	44.20	6.62
328	IHC	S-500	ECH	366.09	55.30	6.62
329	IHC	S-600	ECH	443.54	67.00	6.62
330	IHC	S-900	ECH	658.36	99.45	6.62
331	IHC	S-1200	ECH	891.05	134.60	6.62
332	IHC	S-1800-L	ECH	1170.39	166.00	7.05
333	IHC	S-2300	ECH	1681.48	254.00	6.62
334	IHC	S-2000	ECH	1473.97	222.65	6.62
335	IHC	SC-30	ECH	21.81	3.76	5.80
336	IHC	SC-40	ECH	29.86	5.51	5.42
337	IHC	SC-50	ECH	36.82	7.29	5.05
338	IHC	SC-60	ECH	44.95	13.30	3.38
339	IHC	SC-75	ECH	54.80	12.15	4.51
340	IHC	SC-110	ECH	81.89	17.46	4.69
341	IHC	SC-150	ECH	109.35	24.30	4.50
342	IHC	SC-200	ECH	152.51	30.20	5.05
343	IHC	SC-250	ECH	179.80	37.26	4.83
344	IHC	S-750	ECH	550.79	83.11	6.63
345	IHC	S-800	ECH	589.97	88.15	6.69
346	IHC	S-1400	ECH	1033.84	147.94	6.99
347	IHC	S-1800	ECH	1340.21	195.64	6.85
348	IHC	S-2500	ECH	1843.16	275.80	6.68
349	HERA	1900	OED	44.41	4.19	10.60
350	HERA	1250	OED	24.85	2.76	9.02
351	HERA	1500	OED	29.81	3.31	9.02
352	HERA	2500	OED	49.70	5.51	9.02
353	HERA	2800	OED	55.70	6.18	9.02
354	HERA	3500	OED	69.59	7.72	9.02

Type	Hammer Make	Hammer Model	Hammer Type	Rated Energy kip-feet	Ram Weight kips	Stroke feet
355	HERA	5000	OED	99.45	11.03	9.02
356	HERA	5700	OED	113.38	12.57	9.02
357	HERA	6200	OED	123.30	13.67	9.02
358	HERA	7500	OED	149.19	16.54	9.02
359	HERA	8800	OED	174.99	19.40	9.02
360	ICE	I-12obs	OED	30.21	2.82	10.71
361	ICE	I-19obs	OED	43.24	4.02	10.77
362	ICE	I-30obs	OED	71.45	6.62	10.80
363	ICE	I-36obs	OED	90.68	7.94	11.42
364	ICE	I-46obs	OED	107.74	10.15	10.62
365	ICE	I-62obs	OED	164.98	14.60	11.30
366	ICE	I-80obs	OED	212.40	17.70	12.00
367	ICE	I-8v2obs	OED	17.60	1.76	10.00
368	ICE	I-100obs	OED	264.45	23.61	11.20
369	BSP	SL20	ECH	14.11	3.31	4.27
370	BSP	SL30	ECH	21.69	5.51	3.94
371	FAIRCHLD	F-45	ECH	45.00	15.00	3.00
372	FAIRCHLD	F-32	ECH	32.55	10.85	3.00
374	BSP	CX40	ECH	28.21	6.61	4.27
375	BSP	CX50	ECH	37.61	8.82	4.27
376	BSP	CX60	ECH	47.01	11.02	4.27
377	BSP	CX75	ECH	52.08	13.23	3.94
378	BSP	CX85	ECH	60.75	15.43	3.94
379	BSP	CX110	ECH	78.11	19.84	3.94
381	BSP	HH3	ECH	26.02	6.61	3.94
382	BSP	HH5	ECH	43.38	11.02	3.94
383	BSP	HH7	ECH	60.78	15.43	3.94
384	BSP	HH8	ECH	69.50	17.64	3.94
385	BSP	HH9	ECH	78.17	19.84	3.94
386	BSP	HH11-1.2	ECH	95.55	24.25	3.94
387	BSP	HH14-1.2	ECH	121.59	30.86	3.94
388	BSP	HH16-1.2	ECH	138.87	35.27	3.94
391	BSP	HA30	ECH	260.37	66.14	3.94
392	BSP	HA40	ECH	347.16	88.18	3.94
393	BSP	HH11-1.5	ECH	119.31	24.25	4.92
394	BSP	HH14-1.5	ECH	151.83	30.86	4.92
395	BSP	HH16-1.5	ECH	173.54	35.27	4.92
396	BSP	CG180	ECH	131.92	26.45	4.99
397	BSP	CG210	ECH	153.91	30.86	4.99
398	BSP	CG240	ECH	175.90	35.27	4.99
399	BSP	CG270	ECH	197.88	39.68	4.99
400	BSP	CG300	ECH	219.87	44.09	4.99
401	BERMINGH	B23	CED	22.99	2.80	8.21

Type	Hammer Make	Hammer Model	Hammer Type	Rated Energy kip-feet	Ram Weight kips	Stroke feet
402	BERMINGH	B200	OED	18.00	2.00	9.00
403	BERMINGH	B225	OED	29.25	3.00	9.75
404	BERMINGH	B300	OED	40.31	3.75	10.75
405	BERMINGH	B400	OED	53.75	5.00	10.75
406	BERMINGH	B-21	OED	53.25	4.63	11.50
410	BERMINGH	B300 M	OED	40.31	3.75	10.75
411	BERMINGH	B400 M	OED	53.75	5.00	10.75
412	BERMINGH	B400 4.8	OED	43.20	4.80	9.00
413	BERMINGH	B400 5.0	OED	45.00	5.00	9.00
414	BERMINGH	B23 5	CED	22.99	2.80	8.21
415	BERMINGH	B250 5	OED	26.25	2.50	10.50
416	BERMINGH	B3505	OED	47.20	4.00	11.80
417	BERMINGH	B4005	OED	59.00	5.00	11.80
418	BERMINGH	B4505	OED	77.88	6.60	11.80
419	BERMINGH	B5005	OED	92.04	7.80	11.80
420	BERMINGH	B5505	OED	108.56	9.20	11.80
421	BERMINGH	B550 C	OED	88.00	11.00	8.00
422	BERMINGH	B2005	OED	18.00	2.00	9.00
424	BERMINGH	B2505	OED	35.40	3.00	11.80
425	BERMINGH	B3005	OED	35.40	3.00	11.80
431	BERMINGH	B6005	OED	160.95	13.64	11.80
432	BERMINGH	B6505 C	OED	253.00	22.00	11.50
433	BERMINGH	B6505	OED	202.86	17.64	11.50
434	BERMINGH	B-9	OED	21.00	2.00	10.50
435	BERMINGH	B-32	OED	81.08	7.05	11.50
436	BERMINGH	B-64	OED	166.50	14.11	11.80
437	BERMINGH	B-6505HD	OED	220.50	22.05	10.00
441	MENCK	MHF5-5	ECH	38.69	11.02	3.51
442	MENCK	MHF5-6	ECH	46.43	13.23	3.51
443	MENCK	MHF5-7	ECH	54.17	15.43	3.51
444	MENCK	MHF5-8	ECH	61.91	17.64	3.51
445	MENCK	MHF5-9	ECH	69.65	19.84	3.51
446	MENCK	MHF5-10	ECH	77.39	22.05	3.51
447	MENCK	MHF5-11	ECH	85.13	24.25	3.51
448	MENCK	MHF5-12	ECH	92.87	26.45	3.51
449	MENCK	MHF3-3	ECH	24.76	7.05	3.51
450	MENCK	MHF3-4	ECH	30.96	8.82	3.51
451	MENCK	MHF3-5	ECH	38.69	11.02	3.51
452	MENCK	MHF3-6	ECH	46.43	13.23	3.51
453	MENCK	MHF3-7	ECH	54.17	15.43	3.51
454	MENCK	MHF10-15	ECH	124.73	33.06	3.77
455	MENCK	MHF10-20	ECH	166.28	44.07	3.77
456	MENCK	MHF 5-14	ECH	108.34	30.86	3.51

Type	Hammer Make	Hammer Model	Hammer Type	Rated Energy kip-feet	Ram Weight kips	Stroke feet
457	MENCK	MHU135T*	ECH	110.59	17.99	6.15
458	MENCK	MHU500T*	ECH	368.74	65.96	5.59
459	MENCK	MHU 300S	ECH	221.20	35.73	6.19
460	MENCK	MHU 270T	ECH	221.20	35.73	6.19
461	MENCK	MHU 200T	ECH	162.24	26.75	6.07
462	MENCK	MHU 400T	ECH	324.37	52.45	6.18
463	MENCK	MHU 500T	ECH	405.53	65.96	6.15
464	MENCK	MHU 700T	ECH	567.72	92.88	6.11
465	MENCK	MHU 840S	ECH	619.22	92.88	6.67
466	MENCK	MHU 600B	ECH	457.03	65.96	6.93
467	MENCK	MHU 600T	ECH	486.63	80.39	6.05
468	MENCK	MHU 800S	ECH	604.57	99.93	6.05
469	MENCK	MHU1200S	ECH	884.84	145.71	6.07
470	MENCK	MHU1500S	ECH	1106.07	178.94	6.18
471	MENCK	MHU1700T	ECH	1400.86	227.36	6.16
472	MENCK	MHU1900S	ECH	1400.86	227.36	6.16
473	MENCK	MHU 150S	ECH	110.59	17.99	6.15
474	MENCK	MHU2700S	ECH	1990.19	318.77	6.24
475	MENCK	MHU 135T	ECH	110.59	17.99	6.15
476	MENCK	MHU 750T	ECH	604.57	99.93	6.05
477	MENCK	MHU1100T	ECH	899.66	145.71	6.18
478	MENCK	MHU150S*	ECH	110.59	17.99	6.15
479	MENCK	MHU600B*	ECH	457.03	65.96	6.93
481	JUNTTAN	HHK3A	ECH	26.05	6.62	3.94
482	JUNTTAN	HHK4A	ECH	34.73	8.82	3.94
483	JUNTTAN	HHK5A	ECH	43.41	11.03	3.94
484	JUNTTAN	HHK6A	ECH	52.10	13.23	3.94
485	JUNTTAN	HHK7A	ECH	60.75	15.43	3.94
486	JUNTTAN	HHK10A	ECH	86.83	22.05	3.94
487	JUNTTAN	HHK12A	ECH	104.19	26.47	3.94
488	JUNTTAN	HHK14A	ECH	121.56	30.88	3.94
491	JUNTTAN	HHK9A	ECH	78.14	19.85	3.94
494	JUNTTAN	HHK16A	ECH	138.92	35.29	3.94
495	JUNTTAN	HHK18A	ECH	156.29	39.70	3.94
496	JUNTTAN	HHK20A	ECH	173.65	44.11	3.94
497	JUNTTAN	HHK4SL	ECH	43.40	8.82	4.92
498	JUNTTAN	HHK3AL	ECH	17.37	6.62	2.63
499	JUNTTAN	HHK4AL	ECH	23.15	8.82	2.63
500	JUNTTAN	HHK5AL	ECH	28.94	11.03	2.63
501	HPSI	110	ECH	44.00	11.00	4.00
502	HPSI	150	ECH	60.00	15.00	4.00
503	HPSI	154	ECH	61.60	15.40	4.00
504	HPSI	200	ECH	80.00	20.00	4.00

Type	Hammer Make	Hammer Model	Hammer Type	Rated Energy kip-feet	Ram Weight kips	Stroke feet
505	HPSI	225	ECH	90.00	22.50	4.00
506	HPSI	650	ECH	32.50	6.50	5.00
507	HPSI	1000	ECH	50.00	10.00	5.00
508	HPSI	1605	ECH	83.00	16.60	5.00
509	HPSI	2005	ECH	95.10	19.02	5.00
510	HPSI	3005	ECH	154.33	30.87	5.00
511	HPSI	3505	ECH	176.33	35.27	5.00
512	HPSI	2000	ECH	80.00	20.00	4.00
514	UDDCOMB	H2H	ECH	16.62	4.40	3.77
515	UDDCOMB	H3H	ECH	24.88	6.60	3.77
516	UDDCOMB	H4H	ECH	33.18	8.80	3.77
517	UDDCOMB	H5H	ECH	41.47	11.00	3.77
518	UDDCOMB	H6H	ECH	49.76	13.20	3.77
519	UDDCOMB	H8H	ECH	82.19	17.60	4.67
520	UDDCOMB	H10H	ECH	86.88	22.05	3.94
521	DAWSON	HPH1200	ECH	8.72	2.30	3.79
522	DAWSON	HPH1800	ECH	13.72	3.30	4.16
523	DAWSON	HPH2400	ECH	17.32	4.19	4.13
524	DAWSON	HPH6500	ECH	46.98	10.25	4.58
525	DAWSON	HPH4500	ECH	32.56	7.72	4.22
526	DAWSON	HPH9000	ECH	66.30	10.47	6.33
530	BRUCE	SGH-0312	ECH	26.00	6.60	3.94
531	BRUCE	SGH-0512	ECH	43.34	11.00	3.94
532	BRUCE	SGH-0712	ECH	60.68	15.40	3.94
533	BRUCE	SGH-1012	ECH	86.77	22.05	3.94
534	BRUCE	SGH-0412	ECH	34.67	8.80	3.94
535	BANUT	S3000	ECH	26.04	6.62	3.94
536	BANUT	S4000	ECH	34.72	8.82	3.94
537	BANUT	S5000	ECH	43.41	11.03	3.94
538	BANUT	S6000	ECH	52.09	13.23	3.94
539	BANUT	S8000	ECH	69.45	17.64	3.94
540	BANUT	S10000	ECH	86.81	22.05	3.94
541	BANUT	3 Tonnes	ECH	17.35	6.61	2.62
542	BANUT	4 Tonnes	ECH	23.14	8.82	2.62
543	BANUT	5 Tonnes	ECH	28.92	11.02	2.62
544	BANUT	6 Tonnes	ECH	34.72	13.23	2.62
545	BANUT	7 Tonnes	ECH	40.49	15.43	2.62
550	ICE	70	ECH	21.00	7.00	3.00
551	ICE	75	ECH	30.00	7.50	4.00
552	ICE	110-SH	ECH	37.72	11.50	3.28
553	ICE	115-SH	ECH	37.95	11.50	3.30
554	ICE	115	ECH	46.00	11.50	4.00
555	ICE	160-SH	ECH	64.00	16.00	4.00

Type	Hammer Make	Hammer Model	Hammer Type	Rated Energy kip-feet	Ram Weight kips	Stroke feet
556	ICE	160	ECH	64.00	16.00	4.00
557	ICE	220	ECH	88.00	22.00	4.00
558	ICE	275	ECH	110.00	27.50	4.00
559	ICE	DKH-3U	ECH	26.00	6.60	3.94
560	HMC	28A	ECH	28.00	7.00	4.00
561	HMC	28B	ECH	21.00	7.00	3.00
562	HMC	62	ECH	46.00	11.50	4.00
563	HMC	86	ECH	64.00	16.00	4.00
564	HMC	119	ECH	88.00	22.00	4.00
565	HMC	149	ECH	110.00	27.50	4.00
566	HMC	187	ECH	138.00	34.50	4.00
567	HMC	19D	ECH	14.00	3.50	4.00
568	HMC	38D	ECH	28.00	7.00	4.00
569	APE	D 8-42	OED	19.80	1.76	11.25
570	APE	D 1-42	OED	1.32	0.21	6.33
571	APE	D 19-42	OED	47.13	4.19	11.25
572	APE	D 30-42	OED	74.42	6.62	11.25
573	APE	D 36-42	OED	89.30	7.94	11.25
574	APE	D 46-42	OED	114.11	10.14	11.25
575	APE	D 62-42	OED	153.80	13.67	11.25
576	APE	D 80-42	OED	198.45	17.64	11.25
577	APE	D 100-42	OED	248.06	22.05	11.25
579	APE	D 16-42	OED	39.69	3.53	11.25
580	APE	D 16-52	OED	39.69	3.53	11.25
581	APE	D 25-42	OED	62.01	5.51	11.25
582	APE	D 125-42	OED	310.08	27.56	11.25
583	APE	D 50-42	OED	124.03	11.03	11.25
584	APE	D 12-42	OED	29.77	2.65	11.25
585	APE	D 36-26	OED	89.30	7.94	11.25
586	APE	D 128-42	OED	317.25	28.20	11.25
587	APE	D 138-42	OED	342.00	30.40	11.25
588	APE	D 160-42	OED	396.90	35.28	11.25
589	APE	D 180-42	OED	446.51	39.69	11.25
590	APE	D 225-42	OED	558.00	49.60	11.25
591	APE	5.4mT	ECH	26.00	12.00	2.17
592	APE	7.2mT	ECH	51.30	16.20	3.17
593	APE	D 220-42	OED	540.81	48.46	11.16
594	APE	15-60	ECH	150.00	30.00	5.00
595	APE	10-60	ECH	100.00	20.00	5.00
596	APE	400U	ECH	400.00	80.00	5.00
598	APE	750U	ECH	750.00	120.00	6.25
599	APE	D 100-13	OED	300.04	23.70	12.66
600	BSP	DX20	ECH	14.11	3.31	4.27

Type	Hammer Make	Hammer Model	Hammer Type	Rated Energy kip-feet	Ram Weight kips	Stroke feet
601	BSP	DX25	ECH	18.09	4.41	4.10
602	BSP	DX30	ECH	21.71	5.51	3.94
603	BSP	LX2.5-SA	ECH	14.47	5.51	2.63
604	BSP	LX4-SA	ECH	23.15	8.82	2.63
605	BSP	LX5-SA	ECH	28.94	11.03	2.63
606	BSP	CGL370	ECH	271.22	55.11	4.92
607	BSP	CGL440	ECH	325.47	66.14	4.92
608	BSP	CGL520	ECH	379.71	77.16	4.92
609	BSP	CGL590	ECH	433.96	88.18	4.92
610	BSP	LX7-SA	ECH	40.52	15.44	2.63
625	BRUCE	SGH-1212	ECH	104.13	26.46	3.94
626	BRUCE	SGH-1312	ECH	112.81	28.66	3.94
627	BRUCE	SGH-1315	ECH	141.01	28.66	4.92
628	BRUCE	SGH-1412	ECH	121.48	30.87	3.94
629	BRUCE	SGH-1415	ECH	151.85	30.87	4.92
630	BRUCE	SGH-1612	ECH	138.84	35.27	3.94
631	BRUCE	SGH-1615	ECH	173.55	35.27	4.92
632	BRUCE	SGH-1618	ECH	208.26	35.27	5.90
633	BRUCE	SGH-1619	ECH	219.83	35.27	6.23
634	BRUCE	SGH-1812	ECH	156.19	39.68	3.94
635	BRUCE	SGH-1815	ECH	195.24	39.68	4.92
636	BRUCE	SGH-2012	ECH	173.55	44.09	3.94
637	BRUCE	SGH-2015	ECH	216.94	44.09	4.92
638	BRUCE	SGH-2312	ECH	199.58	50.71	3.94
639	BRUCE	SGH-2315	ECH	249.48	50.71	4.92
640	BRUCE	SGH-3012	ECH	260.32	66.14	3.94
641	BRUCE	SGH-3013	ECH	282.02	66.14	4.26
642	BRUCE	SGH-3015	ECH	325.40	66.14	4.92
643	BRUCE	SGH-4012	ECH	347.10	88.19	3.94
644	BRUCE	SGH-4212	ECH	364.45	92.59	3.94
645	BRUCE	SGH-5012	ECH	433.87	110.23	3.94
650	Twinwood	V20B	ECH	35.58	9.04	3.94
651	Twinwood	V100D	ECH	87.66	22.27	3.94
652	Twinwood	V160B	ECH	140.58	35.71	3.94
653	Twinwood	V400A	ECH	263.84	67.02	3.94
656	Pilemast	24-750	ECH	1.50	0.75	2.00
657	Pilemast	24-900	ECH	1.80	0.90	2.00
658	Pilemast	24-2000	ECH	4.00	2.00	2.00
659	Pilemast	24-2500	ECH	5.00	2.50	2.00
660	Pilemast	36-3000	ECH	9.00	3.00	3.00
661	Pilemast	36-5000	ECH	15.00	5.00	3.00
669	MVE	M-12	OED	30.21	2.82	10.71
670	MVE	M-19	OED	49.38	4.02	12.30

Type	Hammer Make	Hammer Model	Hammer Type	Rated Energy kip-feet	Ram Weight kips	Stroke feet
671	MVE	M-30	OED	83.35	6.62	12.60
801	DKH	PH-5	ECH	43.40	11.02	3.94
802	DKH	PH-7	ECH	60.75	15.43	3.94
803	DKH	PH-7S	ECH	60.75	15.43	3.94
804	DKH	PH-10	ECH	86.79	22.05	3.94
805	DKH	PH-13	ECH	112.83	28.66	3.94
806	DKH	PH-20	ECH	216.98	44.09	4.92
807	DKH	PH-30	ECH	325.47	66.14	4.92
808	DKH	PH-40	ECH	433.96	88.18	4.92
809	DKH	DKH-713	ECH	112.92	28.66	3.94
850	PILECO	D8-22	OED	18.66	1.76	10.60
851	PILECO	D12-42	OED	29.89	2.82	10.60
852	PILECO	D19-42	OED	42.51	4.01	10.60
853	PILECO	D25-32	OED	58.41	5.51	10.60
854	PILECO	D30-32	OED	70.07	6.61	10.60
855	PILECO	D36-32	OED	84.16	7.94	10.60
856	PILECO	D46-32	OED	107.48	10.14	10.60
857	PILECO	D62-22	OED	161.31	13.67	11.80
858	PILECO	D80-23	OED	197.57	17.64	11.20
859	PILECO	D100-13	OED	246.85	22.04	11.20
860	PILECO	D125-32	OED	308.67	27.56	11.20
861	PILECO	D225-22	OED	555.34	49.58	11.20
862	PILECO	D250-22	OED	617.06	55.09	11.20
863	PILECO	D138-32	OED	340.61	30.41	11.20
864	PILECO	D180-32	OED	444.27	39.67	11.20
865	PILECO	D280-22	OED	688.55	61.73	11.16
866	PILECO	D160-32	OED	395.08	35.28	11.20
867	PILECO	D400-12	OED	810.10	88.15	9.19
868	PILECO	D600-12	OED	1215.10	132.22	9.19
869	PILECO	D800-22	OED	1620.20	176.30	9.19
921	BRUCE	SGH-0212	ECH	17.34	4.40	3.94
922	BRUCE	SGH-0715	ECH	75.77	15.40	4.92
923	BRUCE	SGH-1015	ECH	108.47	22.05	4.92
924	BRUCE	SGH-1215	ECH	130.16	26.46	4.92
925	BRUCE	SGH-2512	ECH	216.94	55.12	3.94
926	BRUCE	SGH-2515	ECH	271.17	55.12	4.92
927	BRUCE	SGH-3512	ECH	303.71	77.16	3.94
928	BRUCE	SGH-3515	ECH	379.64	77.16	4.92
929	BRUCE	SGH-4015	ECH	433.87	88.19	4.92
930	BRUCE	SGH-4215	ECH	455.56	92.59	4.92
931	BRUCE	SGH-4512	ECH	390.48	99.21	3.94
932	BRUCE	SGH-4515	ECH	488.10	99.21	4.92
933	BRUCE	SGH-4712	ECH	407.84	103.62	3.94

Type	Hammer Make	Hammer Model	Hammer Type	Rated Energy kip-feet	Ram Weight kips	Stroke feet
934	BRUCE	SGH-4715	ECH	509.80	103.62	4.92
935	BRUCE	SGH-4719	ECH	645.74	103.62	6.23
936	BRUCE	SGH-5015	ECH	542.34	110.23	4.92
937	BRUCE	SGH-5715	ECH	618.26	125.66	4.92
938	BRUCE	SGH-6015	ECH	650.80	132.28	4.92
939	BRUCE	SGH-7015	ECH	759.27	154.32	4.92
940	BRUCE	SGH-8015	ECH	867.74	176.37	4.92
949	JUNTTAN	HHK10S	ECH	108.49	22.05	4.92
950	JUNTTAN	HHK28S	ECH	303.78	61.73	4.92
951	JUNTTAN	HHK5S	ECH	54.27	11.03	4.92
952	JUNTTAN	HHK7S	ECH	75.97	15.44	4.92
953	JUNTTAN	HHK9S	ECH	97.68	19.85	4.92
954	JUNTTAN	HHK12S	ECH	130.24	26.47	4.92
955	JUNTTAN	HHK14S	ECH	151.95	30.88	4.92
956	JUNTTAN	HHK16S	ECH	173.65	35.29	4.92
957	JUNTTAN	HHK18S	ECH	195.36	39.70	4.92
958	JUNTTAN	HHK20S	ECH	217.07	44.11	4.92
959	JUNTTAN	HHK25S	ECH	271.22	55.11	4.92
960	JUNTTAN	HHK36S	ECH	390.56	79.36	4.92
961	JUNTTAN	HHU5A	ECH	54.27	11.03	4.92
962	JUNTTAN	HHU7A	ECH	75.94	15.43	4.92
963	JUNTTAN	HHU9A	ECH	97.64	19.84	4.92
964	JUNTTAN	HHU12A	ECH	130.19	26.45	4.92
965	JUNTTAN	HHU14A	ECH	151.88	30.86	4.92
966	JUNTTAN	HHU16A	ECH	173.58	35.27	4.92
968	JUNTTAN	SHK100-3	ECH	26.91	6.61	4.07
969	JUNTTAN	SHK100-3	ECH	35.89	8.82	4.07
970	JUNTTAN	SHK100-3	ECH	44.84	11.02	4.07
971	JUNTTAN	SHK100-3	ECH	53.82	13.23	4.07
972	JUNTTAN	SHK110-5	ECH	44.98	11.02	4.08
973	JUNTTAN	SHK110-5	ECH	53.82	13.23	4.07
974	JUNTTAN	SHK110-5	ECH	65.62	15.43	4.25
975	JUNTTAN	SHK110-5	ECH	77.42	17.64	4.39
976	JUNTTAN	SHK110-5	ECH	87.74	19.84	4.42
977	JUNTTAN	SHK100-5	ECH	44.84	11.02	4.07
978	JUNTTAN	SHK100-5	ECH	53.82	13.23	4.07
979	JUNTTAN	SHK110-7	ECH	65.63	15.43	4.25
980	JUNTTAN	SHK110-7	ECH	77.43	17.64	4.39
981	JUNTTAN	SHK110-7	ECH	87.74	19.84	4.42
998	HYPOTHET	EX 4	OED	23.38	2.75	8.50
999	SELF	Drop/10t	ECH	300.00	20.00	15.00
1001	DFI-Corp	HHA250-4	ECH	25.18	5.51	4.57
1002	DFI-Corp	HHA300-4	ECH	28.75	6.61	4.35

Type	Hammer Make	Hammer Model	Hammer Type	Rated Energy kip-feet	Ram Weight kips	Stroke feet
1003	DFI-Corp	HHA325-4	ECH	30.36	7.16	4.24
1004	DFI-Corp	HHA350-4	ECH	31.80	7.70	4.13
1005	DFI-Corp	HHA400-6	ECH	51.92	8.80	5.90
1006	DFI-Corp	HHA450-6	ECH	57.04	9.92	5.75
1007	DFI-Corp	HHB500-6	ECH	66.66	11.00	6.06
1008	DFI-Corp	HHB600-6	ECH	77.88	13.20	5.90
1020	J&M	70B HIH	ECH	21.00	7.00	3.00
1021	J&M	82 HIH	ECH	32.80	8.20	4.00
1022	J&M	115 HIH	ECH	46.00	11.50	4.00
1023	J&M	160 HIH	ECH	64.00	16.00	4.00
1024	J&M	220 HIH	ECH	88.00	22.00	4.00
1025	J&M	275 HIH	ECH	110.00	27.50	4.00
1026	J&M	345 HIH	ECH	138.00	34.50	4.00
1134	Pilemer	DKH-3U	ECH	26.00	6.60	3.94
1135	Pilemer	DKH 10L	ECH	86.79	22.05	3.94
1201	Liebherr	H 50/3	ECH	28.97	6.60	4.39
1202	Liebherr	H 50/4	ECH	35.02	8.80	3.98
1203	Liebherr	H 85/5	ECH	43.34	11.00	3.94
1204	Liebherr	H 85/7	ECH	60.16	15.43	3.90
1205	Liebherr	H 110/7	ECH	60.16	15.43	3.90
1206	Liebherr	H 110/9	ECH	78.01	19.85	3.93
1251	ICE	I-30 V2	OED	71.71	6.62	10.84
1261	APE	D 19-52	OED	47.13	4.19	11.25
1262	APE	D 16-32	OED	39.69	3.53	11.25
1263	APE	D 19-32	OED	47.13	4.19	11.25
1264	APE	D 25-32	OED	62.01	5.51	11.25
1265	APE	D 30-32	OED	74.42	6.62	11.25
1266	APE	D 36-32	OED	89.30	7.94	11.25
1267	APE	D 46-32	OED	114.11	10.14	11.25
1268	APE	D 62-22	OED	153.80	13.67	11.25
1269	APE	D 80-23	OED	198.45	17.64	11.25
1270	APE	D 100-32	OED	248.06	22.05	11.25
1271	APE	D 120-32	OED	349.69	27.60	12.67
1272	APE	D 70-42	OED	173.64	15.44	11.25
1273	APE	D 25-52	OED	62.01	5.51	11.25
1274	APE	D 30-52	OED	74.42	6.62	11.25
1275	APE	D 36-52	OED	89.30	7.94	11.25
1276	APE	D 46-52	OED	114.11	10.14	11.25
1277	APE	D 50-52	OED	124.03	11.03	11.25
1278	APE	D 62-52	OED	153.80	13.67	11.25
1279	APE	D 70-52	OED	173.64	15.44	11.25
1280	APE	7.5a	ECH	24.00	12.00	2.00
1281	APE	7.5b	ECH	20.40	10.20	2.00

Type	Hammer Make	Hammer Model	Hammer Type	Rated Energy kip-feet	Ram Weight kips	Stroke feet
1282	APE	7.5c	ECH	15.20	7.60	2.00
1283	APE	9.5a	ECH	50.66	16.00	3.17
1284	APE	9.5b	ECH	44.32	14.00	3.17
1285	APE	7-3	ECH	42.00	14.00	3.00
1286	APE	8-3	ECH	48.00	16.00	3.00
1287	APE	8	ECH	16.00	8.00	2.00
1288	APE	8a	ECH	24.00	12.00	2.00
1289	APE	10-4	ECH	80.00	20.00	4.00
1321	MENCK	MHU 240U	ECH	221.20	35.73	6.19
1322	MENCK	MHU 440S	ECH	324.37	52.45	6.18
1323	MENCK	MHU 360U	ECH	324.37	52.45	6.18
1324	MENCK	MHU 550S	ECH	404.06	65.96	6.13
1325	MENCK	MHU 450U	ECH	404.06	65.96	6.13
1326	MENCK	MHU 660S	ECH	485.17	80.39	6.04
1327	MENCK	MHU 540U	ECH	485.17	80.39	6.04
1328	MENCK	MHU 720T	ECH	588.19	99.93	5.89
1329	MENCK	MHU 650U	ECH	588.19	99.93	5.89
1330	MENCK	MHU1000S	ECH	736.48	126.98	5.80
1331	MENCK	MHU 900T	ECH	736.48	126.98	5.80
1332	MENCK	MHU 810U	ECH	736.48	126.98	5.80
1333	MENCK	MHU1700S	ECH	1272.95	207.15	6.15
1334	MENCK	MHU2100S	ECH	1573.92	257.18	6.12
1335	MENCK	MHU3000S	ECH	2216.56	370.23	5.99
1336	MENCK	MHU1400B	ECH	1032.08	145.71	7.08
1337	MENCK	MHU3500S	ECH	2582.43	385.85	6.69
1371	IHC	S-3000	ECH	2211.93	332.44	6.65
1372	IHC	S-4000	ECH	2948.91	444.30	6.64
1401	FAMBO	HR250	ECH	1.81	0.55	3.28
1402	FAMBO	HR500akk	ECH	3.62	1.10	3.28
1403	FAMBO	HR500	ECH	4.34	1.10	3.94
1404	FAMBO	HR1000	ECH	8.68	2.20	3.94
1405	FAMBO	HR1500	ECH	13.02	3.31	3.94
1406	FAMBO	HR2000	ECH	17.36	4.41	3.94
1407	FAMBO	HR2750	ECH	23.87	6.06	3.94
1408	FAMBO	HR3000	ECH	26.04	6.61	3.94
1409	FAMBO	HR4000	ECH	34.72	8.82	3.94
1410	FAMBO	HR5000	ECH	43.40	11.02	3.94
1411	FAMBO	HR7000	ECH	60.75	15.43	3.94
1412	FAMBO	HR8000	ECH	69.45	17.64	3.94
1413	FAMBO	HR10000	ECH	86.79	22.05	3.94
1501	ICE	I-12v2	OED	29.63	2.82	10.50
1502	ICE	I-8v2	OED	18.69	1.76	10.60
1503	ICE	I-19v2	OED	46.14	4.01	11.50

Type	Hammer Make	Hammer Model	Hammer Type	Rated Energy kip-feet	Ram Weight kips	Stroke feet
1504	ICE	I-30v2	OED	76.05	6.61	11.50
1505	ICE	I-36v2	OED	93.73	7.94	11.81
1506	ICE	I-46v2	OED	119.77	10.14	11.81
1507	ICE	I-62v2	OED	172.37	14.59	11.81
1508	ICE	I-80v2	OED	208.30	17.64	11.81
1509	ICE	I-100v2	OED	260.37	22.05	11.81
1510	ICE	I-125v2	OED	310.10	27.56	11.25
1511	ICE	I-160v2	OED	393.45	35.27	11.16
1512	ICE	IP-2	ECH	17.36	4.41	3.94
1513	ICE	IP-3	ECH	26.04	6.61	3.94
1514	ICE	IP-5	ECH	43.40	11.02	3.94
1515	ICE	IP-7	ECH	60.75	15.43	3.94
1516	ICE	IP-10	ECH	86.78	22.04	3.94
1517	ICE	IP-13	ECH	112.83	28.66	3.94
1520	ICE	I-138v2	OED	328.62	30.40	10.81
1531	SPI	D 19-42	OED	42.61	4.02	10.60
1532	SPI	D 30-32	OED	72.08	6.80	10.60
1601	DELMAG	D 2	OED	1.78	0.49	3.61
1602	DELMAG	D 4	OED	3.60	0.84	4.30
1603	DELMAG	D 8-12	OED	20.10	1.76	11.42
1604	DELMAG	D 12-52	OED	33.98	2.82	12.05
1605	DELMAG	D 16-52	OED	40.20	3.52	11.42
1606	DELMAG	D 25-52	OED	66.34	5.51	12.04
1607	DELMAG	D 30-52	OED	75.44	6.60	11.43
1611	DELMAG	D138-32	OED	339.51	30.44	11.16
1612	DELMAG	D180-32	OED	442.64	39.68	11.16
1613	DELMAG	D300-32	OED	737.73	66.14	11.16
1614	DELMAG	D400-32	OED	983.64	88.18	11.16
1620	HMC	TD19	OED	46.09	4.01	11.49
1621	HMC	TD30	OED	69.87	6.61	10.57

Type	Hammer Make	Hammer Model	Hammer Type	Rated Power kW	Ecc. Mass kips	Frequency Hz
620	MAIT	34	VIB	227.00	1.23	33.30
621	MAIT	42	VIB	309.00	1.52	33.30
622	MAIT	54	VIB	450.00	0.98	33.30
623	MAIT	68	VIB	531.00	1.23	33.30
624	MAIT	120	VIB	674.00	1.74	30.00
698	ICE	50B	VIB	432.00	10.42	26.70
699	ICE	3117	VIB	235.00	1.12	28.30
700	ICE	23-28	VIB	21.00	0.10	26.70
701	ICE	216	VIB	130.00	0.46	26.70
702	ICE	216E	VIB	130.00	0.46	26.70
703	ICE	11-23	VIB	164.00	0.46	31.70
704	ICE	223	VIB	242.00	0.46	38.30
705	ICE	416L	VIB	242.00	0.92	26.70
706	ICE	812	VIB	375.00	1.82	26.70
707	ICE	815	VIB	375.00	1.84	26.70
708	ICE	44-30	VIB	242.00	1.30	20.00
709	ICE	44-50	VIB	377.00	1.30	26.70
710	ICE	44-65	VIB	485.00	1.30	27.50
711	ICE	66-65	VIB	485.00	1.95	21.70
712	ICE	66-80	VIB	597.00	1.95	26.70
713	ICE	1412B	VIB	597.00	2.04	21.00
714	ICE	1412C	VIB	470.00	2.02	23.00
715	ICE	V125	VIB	984.00	1.04	25.80
716	ICE	14RF	VIB	242.00	1.01	38.30
717	ICE	14-23	VIB	164.00	1.17	35.00
718	ICE	22-23V	VIB	164.00	0.92	26.90
719	ICE	22-30	VIB	250.00	0.92	26.90
720	HMC	3+28	VIB	21.00	0.11	26.80
721	HMC	3+75	VIB	56.00	0.11	36.10
722	HMC	13+200	VIB	149.00	0.35	26.70
723	HMC	13S+200	VIB	149.00	0.35	26.70
724	HMC	13H+200	VIB	164.00	0.35	29.80
725	HMC	25+220	VIB	164.00	0.61	20.90
726	HMC	26+335	VIB	242.00	0.71	25.60
727	HMC	26S+335	VIB	242.00	0.71	25.60
728	HMC	51+335	VIB	242.00	1.21	19.50
729	HMC	51+535	VIB	377.00	1.21	26.40
730	HMC	51S+535	VIB	377.00	1.21	26.40
731	HMC	51+740	VIB	485.00	1.21	27.50
732	HMC	76+740	VIB	485.00	1.82	21.70
733	HMC	76+800	VIB	597.00	1.82	26.10
734	HMC	115+800	VIB	597.00	1.35	20.40
735	HMC	230+1600	VIB	1193.00	2.69	20.40

Type	Hammer Make	Hammer Model	Hammer Type	Rated Power kW	Ecc. Mass kips	Frequency Hz
750	MKT	V-2B	VIB	52.00	0.15	30.00
751	MKT	V-5C	VIB	138.00	0.43	28.33
752	MKT	V-20B	VIB	242.00	0.20	28.33
753	MKT	V-30	VIB	448.00	1.47	28.33
754	MKT	V-35	VIB	485.00	1.60	28.33
755	MKT	V-140	VIB	1341.00	1.17	23.33
770	APE	3	VIB	10.58	0.00	38.30
771	APE	6	VIB	10.58	0.01	38.30
772	APE	15	VIB	59.67	0.11	30.00
773	APE	20	VIB	59.67	0.15	38.30
774	APE	20E	VIB	59.67	0.15	38.30
775	APE	50	VIB	194.00	0.23	30.00
776	APE	50E	VIB	194.00	0.23	30.00
777	APE	100	VIB	194.00	0.32	30.00
778	APE	100E	VIB	194.00	0.14	30.00
779	APE	100HF	VIB	260.00	0.14	43.00
780	APE	150	VIB	260.00	0.14	30.00
781	APE	150T	VIB	260.00	0.17	30.00
782	APE	150HF	VIB	466.00	0.32	43.00
783	APE	200	VIB	466.00	0.29	30.00
784	APE	200T	VIB	466.00	0.34	30.83
785	APE	200T HF	VIB	738.00	0.34	43.00
786	APE	300	VIB	738.00	0.34	25.00
787	APE	400B	VIB	738.00	0.78	23.33
788	APE	600	VIB	800.00	1.05	23.30
789	APE	Tan 400	VIB	1476.00	1.37	23.33
790	APE	Tan 600	VIB	1800.00	2.11	23.30
791	APE	200-6	VIB	470.00	0.43	30.00
811	MGF	RBH 80	VIB	50.00	0.60	30.00
812	MGF	RBH 140	VIB	85.00	1.04	26.67
813	MGF	RBH 200	VIB	125.00	0.74	26.67
814	MGF	RBH 320	VIB	200.00	0.79	26.67
815	MGF	RBH 460	VIB	255.00	1.13	26.67
816	MGF	RBH 1050	VIB	460.00	1.55	22.50
817	MGF	RBH 1575	VIB	700.00	1.16	22.50
818	MGF	RBH 2400	VIB	975.00	1.77	23.50
880	ICE	23RF	VIB	384.00	0.83	38.30
881	ICE	1412BT	VIB	1193.00	1.67	21.70
882	ICE	23-40	VIB	30.00	0.19	31.80
883	ICE	28-35	VIB	261.00	1.16	27.30
884	ICE	28RF-35	VIB	261.00	1.16	27.30
885	ICE	V360	VIB	783.00	0.94	25.00
886	ICE	V360 T	VIB	1566.00	1.88	25.00

Type	Hammer Make	Hammer Model	Hammer Type	Rated Power kW	Ecc. Mass kips	Frequency Hz
887	ICE	44-30V	VIB	250.00	0.92	26.00
888	ICE	44-70	VIB	585.00	0.92	28.10
889	ICE	66-70	VIB	585.00	0.92	23.00
890	ICE	7RF	VIB	154.00	0.51	38.30
891	ICE	66-70HS	VIB	585.00	0.92	26.70
892	ICE	66-80HS	VIB	597.00	0.92	29.20
893	ICE	100c-Tdm	VIB	1774.00	1.83	26.67
894	ICE	423	VIB	377.00	0.92	38.30
895	ICE	32RF	VIB	391.00	1.16	33.30
896	ICE	36RF	VIB	431.00	1.30	33.30
897	ICE	46RF	VIB	678.00	1.66	38.30
898	ICE	64RF	VIB	663.00	1.16	32.50
899	ICE	44B	VIB	595.00	1.30	30.00
900	Mueller	MS16HF	VIB	219.00	1.16	39.20
901	Mueller	MS25H2	VIB	218.00	0.90	28.00
902	Mueller	MS25H3	VIB	218.00	0.90	28.00
903	Mueller	MS50H2	VIB	419.00	1.20	27.00
904	Mueller	MS50H3	VIB	419.00	1.20	27.00
905	Mueller	MS25HHF	VIB	274.00	0.58	27.30
906	Mueller	MS50HHF	VIB	562.00	1.17	27.30
907	Mueller	MS100HHF	VIB	750.00	2.33	24.90
908	Mueller	MS120HHF	VIB	895.00	2.30	25.60
909	Mueller	MS200HHF	VIB	837.00	4.25	22.90
910	Mueller	MS-10HFV	VIB	203.00	0.39	39.30
911	Mueller	MS-16HFV	VIB	294.00	0.53	39.20
912	Mueller	MS-24HFV	VIB	720.00	0.85	39.20
913	Mueller	MS-32HFV	VIB	551.00	1.05	39.60
914	Mueller	MS-48HFV	VIB	823.00	1.69	39.20
915	Mueller	MS-62HFV	VIB	735.00	1.82	35.00
1039	J&M	11-23	VIB	164.00	0.92	31.70
1040	J&M	1412	VIB	559.00	1.67	21.70
1041	J&M	1412T	VIB	1119.00	1.67	21.70
1042	J&M	216	VIB	149.00	0.92	26.70
1044	J&M	22-23	VIB	164.00	0.92	20.80
1045	J&M	22-30	VIB	261.00	0.92	27.50
1050	J&M	28-35	VIB	261.00	1.17	27.50
1051	J&M	360	VIB	783.00	0.94	21.70
1052	J&M	416	VIB	250.00	0.92	26.70
1053	J&M	416B	VIB	261.00	0.92	26.70
1054	J&M	416S	VIB	250.00	0.92	26.70
1055	J&M	815	VIB	429.00	0.92	26.70
1056	J&M	44-30	VIB	250.00	0.92	20.00
1057	J&M	44-50	VIB	399.00	0.92	26.70

Type	Hammer Make	Hammer Model	Hammer Type	Rated Power kW	Ecc. Mass kips	Frequency Hz
1058	J&M	44-65	VIB	552.00	0.92	27.50
1060	J&M	66-65	VIB	552.00	0.92	21.70
1061	J&M	66-80	VIB	559.00	0.92	26.70
1100	PVE	14M	VIB	190.00	1.01	28.30
1101	PVE	23M	VIB	234.00	1.66	27.50
1102	PVE	25M	VIB	294.00	0.98	28.30
1103	PVE	27M	VIB	294.00	0.98	28.30
1104	PVE	38M	VIB	392.00	0.92	28.30
1105	PVE	50M	VIB	440.00	1.20	28.30
1106	PVE	52M	VIB	564.00	0.75	28.30
1107	PVE	105M	VIB	784.00	1.52	22.50
1108	PVE	110M	VIB	784.00	0.80	22.50
1109	PVE	200M	VIB	1130.00	1.45	23.30
1110	PVE	2307	VIB	190.00	0.47	38.30
1111	PVE	1420	VIB	190.00	1.01	33.30
1112	PVE	2315	VIB	234.00	1.09	38.30
1113	PVE	2520	VIB	294.00	1.81	33.30
1114	PVE	2310VM	VIB	190.00	0.72	38.30
1115	PVE	2315VM	VIB	234.00	1.09	38.30
1116	PVE	2316VM	VIB	294.00	1.16	38.30
1117	PVE	2319VM	VIB	392.00	1.37	38.30
1118	PVE	2323VM	VIB	392.00	0.83	38.30
1119	PVE	2332VM	VIB	564.00	1.16	38.30
1120	PVE	2335VM	VIB	784.00	1.27	38.30
1121	PVE	40VM	VIB	564.00	1.45	33.30
1122	PVE	50VM	VIB	564.00	1.20	30.00
1123	PVE	55M	VIB	403.00	1.17	28.33
1124	PVE	82M	VIB	565.00	1.76	28.33
1125	PVE	300M	VIB	1796.00	6.21	23.33
1126	PVE	16VM	VIB	335.00	0.35	38.33
1127	PVE	20VM	VIB	395.00	0.41	38.33
1128	PVE	24VM	VIB	395.00	0.52	38.33
1129	PVE	28VM	VIB	403.00	0.61	38.33
1130	PVE	2070VM	VIB	1130.00	1.52	33.33
1131	PVE	2312VM	VIB	252.00	0.26	38.33
1132	PVE	2350VM	VIB	790.00	1.09	38.33
1142	PTC	30HP	VIB	196.00	0.87	27.00
1143	PTC	40HD	VIB	269.00	0.87	28.00
1144	PTC	50HD1	VIB	255.00	0.87	25.00
1145	PTC	50HD2	VIB	290.00	0.87	25.00
1146	PTC	65HD	VIB	305.00	0.87	26.00
1147	PTC	60HD	VIB	305.00	0.87	28.00
1148	PTC	75HD	VIB	410.00	0.87	25.00

Type	Hammer Make	Hammer Model	Hammer Type	Rated Power kW	Ecc. Mass kips	Frequency Hz
1149	PTC	100HD	VIB	451.00	0.87	23.00
1150	PTC	100HDS	VIB	564.00	0.87	23.00
1151	PTC	175HD	VIB	611.00	0.87	23.00
1152	PTC	240HD	VIB	988.00	0.87	23.00
1153	PTC	240HDS	VIB	988.00	0.87	30.00
1154	PTC	120HD	VIB	410.00	0.87	23.00
1155	PTC	130HD	VIB	564.00	0.87	23.00
1156	PTC	200HD	VIB	710.00	0.87	23.00
1157	PTC	265HD	VIB	1080.00	0.87	24.00
1340	H&M	H-150	VIB	94.00	0.11	28.30
1341	H&M	H-1700	VIB	165.00	0.20	20.00
1431	BRUCE	SGV-80	VIB	112.20	0.13	33.33
1432	BRUCE	SGV-100	VIB	142.60	0.18	30.00
1433	BRUCE	SGV-200	VIB	184.80	0.31	28.83
1434	BRUCE	SGV-300	VIB	211.20	0.35	27.50
1435	BRUCE	SGV-400	VIB	286.00	0.44	26.67
1436	BRUCE	SGV-450	VIB	323.40	0.48	26.67
1437	BRUCE	SGV-600	VIB	451.50	0.72	26.67
1438	BRUCE	SGV-1000	VIB	569.10	1.03	25.00
1630	LBFoster	4150	VIB	335.00	0.53	25.00

U.S. Department of Transportation
Federal Highway Administration

Publication No. FHWA-NHI-16-010
FHWA GEC 012 – Volume II
September 2016

NHI Courses No. 132021 and 132022

Design and Construction of Driven Pile Foundations – Volume II

Developed following:

AASHTO LRFD Bridge Design Specifications, 7th Edition, 2014, with 2015 Interim.

and

AASHTO LRFD Bridge Construction Specifications, 3rd Edition, 2010, with '11, '12, '13, '14, and '15 Interims.

NATIONAL HIGHWAY INSTITUTE
Training Solutions for Transportation Excellence

NOTICE

The contents of this report reflect the views of the authors, who are responsible for the facts and accuracy of the data presented herein. The contents do not necessarily reflect policy of the Department of Transportation. This report does not constitute a standard, specification, or regulation. The United States Government does not endorse products or manufacturers. Trade or manufacturers′ names appear herein only to illustrate methods and procedures, and are considered essential to the objective of this document.

Technical Report Documentation Page

1. REPORT NO.	2. GOVERNMENT ACCESSION NO.	3. RECIPIENT'S CATALOG NO.
FHWA-NHI-16-010		

4. TITLE AND SUBTITLE	5. REPORT DATE
Geotechnical Engineering Circular No. 12 – Volume II Design and Construction of Driven Pile Foundations	September 2016
	6. PERFORMING ORGANIZATION CODE

7. AUTHOR(S)	8. PERFORMING ORGANIZATION REPORT NO.
Patrick J. Hannigan, PE, Frank Rausche, PhD, PE, Garland E. Likins, PE, Brent R. Robinson, PE, and Matthew L. Becker, EI.	

9. PERFORMING ORGANIZATION NAME AND ADDRESS	10. WORK UNIT NO.
Ryan R. Berg & Associates, Inc. 2190 Leyland Alcove Woodbury, MN 55125	11. CONTRACT OR GRANT NO. DTFH61-11-D-00049

12. SPONSORING AGENCY NAME AND ADDRESS	13. TYPE OF REPORT & PERIOD COVERED
National Highway Institute U.S. Department of Transportation Federal Highway Administration, Washington, DC 20590	Final Report
	14. SPONSORING AGENCY CODE

15. SUPPLEMENTARY NOTES

FHWA COTR: Heather Shelsta

FHWA Technical Working Group: Naser Abu-Hejleh, PhD, PE; Scott Anderson, PhD, PE; and Silas Nichols, PE

16. ABSTRACT

This document presents information on the analysis, design, and construction of driven pile foundations for highway structures. This document updates and replaces FHWA NHI-05-042 and FHWA NHI-05-043 as the primary FHWA guidance and reference document on driven pile foundations. The manual addresses design aspects including subsurface exploration, laboratory testing, pile selection, aspects of geotechnical and structural limit states, as well as technical specifications. Construction aspects including static load tests, dynamic tests, rapid load tests, wave equation analyses, dynamic formulas and development of driving criteria, as well as pile driving equipment, pile driving accessories, and monitoring of pile installation inspection are also covered. Step by step procedures are included for most analysis procedures and design examples.

17. KEY WORDS	18. DISTRIBUTION STATEMENT
Driven pile foundations, foundation economics, site characterization, geomaterial properties, axial compression resistance, axial tension resistance, lateral resistance, pile groups, specifications, nominal resistance determination tests, construction monitoring and quality assurance.	No restrictions.

19. SECURITY CLASSIF.	20. SECURITY CLASSIF.	21. NO. OF PAGES	22. PRICE
Unclassified	Unclassified	541	

CONVERSION FACTORS

Approximate Conversions to SI Units			Approximate Conversions from SI Units		
When You Know	**Multiply By**	**To Find**	**When You Know**	**Multiply By**	**To Find**
(a) Length					
inch (in.)	25.4	millimeter (mm)	millimeter (mm)	0.039	inch (in.)
foot (ft)	0.305	meter (m)	meter (m)	3.28	foot (ft)
yard (yd)	0.914	meter (m)	meter (m)	1.09	yard (yd)
mile (mi)	1.61	kilometer (km)	kilometer (km)	0.621	mile (mi)
(b) Area					
square inches (in^2)	645.2	square millimeters (mm^2)	square millimeters (mm^2)	0.0016	square inches (in^2)
square feet (ft^2)	0.093	square meters (m^2)	square meters (m^2)	10.764	square feet (ft^2)
Acres (ac)	0.405	hectares (ha)	hectares (ha)	2.47	Acres (ac)
square miles (mi^2)	2.59	square kilometers (km^2)	square kilometers (km^2)	0.386	square miles (mi^2)
square inches (in^2)	645.2	square millimeters (mm^2)	square millimeters (mm^2)	0.0016	square inches (in^2)
(c) Volume					
fluid ounces (oz)	29.57	milliliters (mL)	milliliters (mL)	0.034	fluid ounces (oz)
Gallons (gal)	3.785	liters (L)	liters (L)	0.264	Gallons (gal)
cubic feet (ft^3)	0.028	cubic meters (m^3)	cubic meters (m^3)	35.32	cubic feet (ft^3)
cubic yards (yd^3)	0.765	cubic meters (m^3)	cubic meters (m^3)	1.308	cubic yards (yd^3)
(d) Mass					
ounces (oz)	28.35	grams (g)	grams (g)	0.035	ounces
pounds (lb)	0.454	kilograms (kg)	kilograms (kg)	2.205	pounds
short tons (2000 lb) (T)	0.907	megagrams (tonne) (Mg)	megagrams (tonne) (Mg)	1.102	short tons (2000 lb)
(e) Force					
pound (lb)	4.448	Newton (N)	Newton (N)	0.2248	pound (lb)
(f) Pressure, Stress, Modulus of Elasticity					
pounds per square foot (psf)	47.88	Pascals (Pa)	Pascals (Pa)	0.021	pounds per square foot (psf)
pounds per square inch (psi)	6.895	kiloPascals (kPa)	kiloPascals (kPa)	0.145	pounds per square inch (psi)
(g) Density					
pounds per cubic foot (pcf)	16.019	kilograms per cubic meter (kgm^3)	kilograms per cubic meter (kgm^3)	0.0624	pounds per cubic feet (pcf)
(h) Temperature					
Fahrenheit temperature (^oF)	5/9(^oF- 32)	Celsius temperature (^oC)	Celsius temperature (^oC)	9/5(^oC)+ 32	Fahrenheit temperature (^oF)

Notes:

1) The primary metric (SI) units used in civil engineering are meter (m), kilogram (kg), second (s), Newton (N), and Pascal ($Pa=N/m^2$).

2) In a "soft" conversion, an English measurement is mathematically converted to its exact metric equivalent.

3) In a "hard" conversion, a new rounded metric number is created that is convenient to work with and remember.

PREFACE

The purpose of this manual is to provide updated, state-of-the-practice information for the design and construction of driven pile foundations in accordance with the Load and Resistance Factor Design (LRFD) platform. Engineers and contractors have been designing and installing pile foundations for many years. During the past three decades, the industry has experienced several major improvements including newer and more accurate methods of predicting and measuring geotechnical resistance, vast improvements in design software, highly specialized and sophisticated equipment for pile driving, and improved methods of construction control. Previous editions of the FHWA Design and Construction of Driven Pile Foundations manual were published 1985, 1996, and 2006 and chronical the many changes in design and construction practice over the past 30 years. This two volume edition, GEC-12, serves as the FHWA reference document for highway projects involving driven pile foundations.

Volume I, FHWA-NHI-16-009, covers the foundation selection process, site characterization, geotechnical design parameters and reporting, selection of pile type, geotechnical aspects of limit state design, and structural aspects of limits state design. Volume II, FHWA-NHI-16-010, addresses static load tests, dynamic testing and signal matching, rapid load testing, wave equation analysis, dynamic formulas, contract documents, pile driving equipment, pile accessories, driving criteria, and construction monitoring. Comprehensive design examples are presented in publication FHWA-NHI-16-064.

Throughout this manual, numerous references will be made to the names of software or technology that are proprietary to a specific manufacturer or vendor. Please note that the FHWA does not endorse or approve commercially available products, and is very sensitive to the perceptions of endorsement or preferred approval of commercially available products used in transportation applications. Our goal with this development is to provide recommended technical guidance for the safe design and construction of driven pile foundations that reflects the current state of practice and provides information on advances and innovations in the industry. To accomplish this, it is necessary to illustrate methods and procedures for design and construction of driven pile foundations. Where proprietary products are described in text or figures, it is only for this purpose.

The primary audience for this document is: agency and consulting engineers specialized in geotechnical and structural design of highway structures; engineering geologists and consulting engineers providing technical reviews, or who are engaged in the design, procurement, and construction of driven pile foundations This document is also intended for management, specification and contracting specialists, as well as for construction engineers interested in design and contracting aspects of driven pile systems.

This document draws material from the three earlier FHWA publications in this field; FHWA-DP-66-1 by Vanikar (1985), FHWA HI 97-013 and FHWA HI 97-014 by Hannigan et al. (1998), and FHWA NHI-05-042 and FHWA NHI-05-043 by Hannigan et al. (2006). Photographs without specific acknowledgement in this two volume document are from these previous editions, their associated training courses, or from the consulting practice of GRL Engineers, Inc.

The following individuals were part of the Ryan R. Berg & Associates internal peer review team and are acknowledged for their technical advice and contributions to this version of the document:

Mr. Jerry DiMaggio – Applied Research Associates, Inc.
Mr. Van Komurka – Wagner Komurka Geotechnical Group, Inc.
Mr. Billy Camp – S&ME, Inc.
Dr. Brian Anderson – Auburn University

TABLE OF CONTENTS

LIST OF TABLES

LIST OF FIGURES

LIST OF SYMBOLS

A	-	Pile cross sectional area (9.2) (9.5) (10.4) (10.5) (10.6) (12.8); Slope of tangent modulus line (9.5).
A_c	-	Cross sectional area of concrete (9.5).
a	-	Acceleration of pile (11.4).
a(t)	-	Acceleration measured at the gage location (10.4).
B	-	Y-intercept of the tangent modulus line (9.5).
b	-	Pile width or diameter (9.2);
bpm	-	Blow per minute (15.13) (18.7).
C	-	Wave speed of pile material (10.5) (10.6) (11.3) (12.8).
C_4	-	Damping constant for Statnamic test (11.4).
D	-	Pile width for WEAP quake calculation(12.5);
D_w	-	Wave length (11.3).
E	-	Elastic modulus of pile material (9.2) (9.5) (10.4) (10.5) (10.6) (12.8).
E_c	-	Elastic modulus of concrete (9.5).
E_d	-	Developed hammer energy (13.3).
E_p	-	Energy computed at the gage location (10.6).
E_{sm}	-	Secant modulus (9.5).
E_{st}	-	Elastic modulus of steel (9.5).
F	-	Axial force in plane of gage (9.5); Force (10.5).
$F(t)$	-	Force computed at gage location (10.4) (10.6).
F_a	-	Statnamic inertia load (11.4).
F_{eff}	-	Hammer efficiency factor (13.3).
F_{max}	-	Maximum measured force applied during testing (11.4).
F_p	-	Statnamic pore water pressure force (11.4).
F_{stn}	-	Statnamic induced load (11.4).
F_t	-	Force measured on pile head (11.4).
F_u	-	Statnamic static soil resistance force (11.4).
F_v	-	Statnamic dynamic soil resistance force (11.4).
f'_c	-	Concrete compressive strength at 28 days (14.2).
f_{pe}	-	Effective prestress in concrete (14.2).
g	-	Acceleration due to gravity (15.8).
h	-	Ram stroke (13.1) (15.8) (15.13) (18.7).
J	-	Dimensionless damping factor based on soil type (10.6).
KE	-	Kinetic Energy (15.8).

L	-	Total pile length (10.5) (10.6) (11.3); Pile length below dial gages or gage location (9.2) (10.6); Length of pile between two measuring points under no load condition (9.5).
M_t	-	Tangent modulus (9.5).
m	-	Mass of pile (11.4); Ram mass (15.8).
N_b	-	Pile penetration resistance with units of (blows/inch) (13.3).
N_{ft}	-	Pile penetration resistance with units of (blows/foot) (13.3).
N_t	-	Toe bearing capacity coefficient (12.7).
N_w	-	Wave number (11.3).
Q	-	Test load (9.2) (9.5).
Q_{avg}	-	Average load in the pile between two points (9.5).
Q_f	-	Failure load (9.2) (9.3).
RSP	-	Case method static nominal resistance (10.6).
RTL	-	Total static and dynamic resistance on pile during driving (10.6).
R_n	-	Nominal resistance (11.4) (13.1)
R_{ndr}	-	Nominal driving resistance (13.3).
R_p	-	Nominal toe resistance (9.5).
R_1	-	Deflection reading at upper measurement location (9.5).
R_2	-	Deflection reading at lower measurement location (9.5).
s_b	-	Set per blow (13.1); Permanent pile set (13.3).
s_f	-	Measured pile head movement at failure (9.2) (9.3).
t_L	-	Load duration (11.4).
t_{umax}	-	Time of maximum displacement for Statnamic test (11.4).
t_1	-	Time of initial impact (10.6).
t_2	-	Time of reflection of initial impact from pile toe (t_1+2L/C) (10.6).
t_4	-	Time at beginning of Stage 4 for Statnamic test (11.4).
V	-	Velocity of pile (11.4).
$V(t)$	-	Velocity measured at gage location (10.4).
V_i	-	Impact velocity (15.8).
V_o	-	Normalizing constant (11.4).
V_{static}	-	Velocity used to determine parameters α and β for Sheffield Method (11.4).
W	-	Ram weight (13.1).
$WD(t)$	-	Downward traveling wave, wave down (10.6).
WD_m	-	Wave down, measured (10.6).
$WU(t)$	-	Upward traveling wave, wave up (10.6).
WU_c	-	Wave up, computed (10.6).
WU_m	-	Wave up, measured (10.6).

α	-	Sheffield Method rate parameter (11.4).
β	-	Sheffield Method rate parameter (11.4).
ξ	-	Loading rate reduction factor (11.4).
Δ	-	Elastic deformation of pile (9.2).
$\Delta\varepsilon$	-	Change of strain from one load increment to the next (9.5).
$\Delta\sigma$	-	Change of stress from one load increment to the next (9.5).
ε	-	Strain measured in gage (9.5).
$\varepsilon(t)$	-	Measured strain at time, t (10.4).
σ	-	Normal stress (pressure) on plane of failure, stress (9.5).
ϕ_{dyn}	-	Resistance factor (based on the construction control method) (13.2).

LIST OF ACRONYMNS

AASHTO	-	American Association of State Highway and Transportation Officials
ASTM	-	American Society for Testing and Materials
BL	-	Blast load
BOR	-	Beginning of Restrike
BR	-	Vehicular braking force
CD	-	Consolidated Drained triaxial test
CE	-	Vehicular centrifugal force
CED	-	Closed End Diesel hammer
CEP	-	Closed End Pipe
COR	-	Coefficient of Restitution
CPT	-	Cone Penetration Test
CPTu	-	Piezo Cone Penetration Test
CR	-	Force effects due to creep
CT	-	Vehicular collision force
CU	-	Consolidated Undrained triaxial test
CV	-	Vessel collision force
DA	-	Design Angular Distortion
DC	-	Dead load components and attachments
DD	-	Downdrag
DMT	-	Dilatometer test
DW	-	Wearing surface and utilities
DWT	-	Deadweight tonnage
EH	-	Horizontal earth pressure
EL	-	Locked-in stress
EOD	-	End of Drive
EQ	-	Earthquake load
ER	-	SPT hammer efficiency as determined by energy measurements
ES	-	Earth surcharge
EV	-	Vertical earth pressure
FHWA	-	Federal Highway Administration
FR	-	Friction load
I.D.	-	Inner diameter
IC	-	Ice load
IM	-	Vehicular dynamic load allowance
KE	-	Kinetic Energy

LL	-	Liquid Limit; Vehicular Live Load
LS	-	Live Load Surcharge
LVDT	-	Linear Variable Differential Transformer
MUP	-	Modified Unloading Point Method
NHI	-	National Highway Institute
O.D.	-	Outer Diameter
OED	-	Open Ended Diesel hammer
OEP	-	Open Ended Pipe
PE	-	Potential Energy
PGA	-	Peak Ground Acceleration coefficient
PI	-	Plasticity Index
PL	-	Plastic Limit; Pedestrian Live Load
PS	-	Secondary forces from post-tensioning
RSA	-	Residual Stress Analysis
SE	-	Force effect due to settlement
SH	-	Force effects due to shrinkage
SPT	-	Standard Penetration Test
SRD	-	Soil Resistance to Driving
SUP	-	Segmental Unloading Point Method
TG	-	Force effect due to temperature gradient
TU	-	Force effect due to uniform temperature
UPM	-	Unloading Point Method
UU	-	Unconsolidated Undrained triaxial test
VST	-	Vane shear test
WA	-	Water load and steam pressure
WD	-	Downward traveling wave, Wave Down
WEAP	-	Wave Equation Analysis Program
WL	-	Wind on live load
WS	-	Wind load on structure
WU	-	Upward traveling wave, Wave Up

CHAPTER 9

STATIC LOAD TESTING

9.1 GENERAL

Static load testing of piles is the most accurate method of determining load capacity. Depending upon the size of the project and other project variables, static load tests may be performed either during the design stage or construction stage. Conventional load test types include the axial compression, axial tension and lateral load tests.

The purpose of this chapter is to provide an overview of static testing and its importance as well as to describe the basic test methods and interpretation techniques. For additional details on static load testing, reference should be made to publications listed at the end of this chapter including the most recent ASTM test standards as well as the NYSDOT Static Pile Load Test Manual, GCP-18 (2007).

9.1.1 Reasons and Prerequisites for a Static Load Test Program

Static load testing provides the engineer with valuable design verification information on the nominal resistance and deformation response of test or production piles. Reasons to perform static load tests include the following:

1. Provide information for design verification or design refinement as well as information for construction verification or construction procedure modification based on measured load-deflection or measured load-transfer data.

2. Confirm the ability of the subsurface materials to provide the nominal geotechnical resistance.

3. Determine or calibrate resistance factors for new static design methods, local or regional geologic conditions, or dynamic or rapid load test analysis methods or procedures.

4. Determine p-y response of laterally loaded piles.

Static load test program development and oversight should be performed by an experienced foundation engineer. Static load tests are frequently used to establish a comparison baseline for design, testing, and construction techniques. The quality of static load tests is always important, but should be of utmost importance when performing research or updating current LRFD resistance factors. Poorly performed tests or analyses can result in unsafe or grossly uneconomical foundations.

In order to adequately plan and implement a static load testing program, the following information should first be obtained or developed.

1. A detailed subsurface exploration program at the test location. A load test is not a substitute for a subsurface exploration program.

2. Well defined subsurface stratigraphy including engineering parameters of geomaterials and identification of groundwater conditions.

3. Static analyses to economically select appropriate pile type(s) and length(s) as well as to select appropriate location(s) for load test(s).

9.1.2 Developing a Static Load Test Program

The goal and objectives of a static load test program should be clearly established, while the type and frequency of tests should be selected to provide the required knowledge for final design purposes or for construction verification. A significantly different level of effort and instrumentation is required if the goal of the load test program is simply to confirm the nominal geotechnical resistance or if detailed load-transfer information is desired for final design or improvement of design efficiency. The following items should be considered during the test program planning so that the program provides the desired information.

1. The capacity of the loading apparatus (reaction system and jack) should be specified so that the test pile(s) may be loaded to the geotechnical nominal resistance. A loading apparatus designed to load a pile to only to the anticipated nominal resistance is usually insufficient to obtain geotechnical failure. Hence, the true nominal geotechnical resistance cannot be determined, and the full benefit from performing a static load test to improve design efficiency is not realized. The jack capacity should be between 120% and 150% of the anticipated maximum load to be applied.

2. Specifications should require the use of a load cell and spherical bearing plate as well as linear variable displacement transducers (LVDT's) or dial gages with sufficient travel to allow accurate measurements of load and movement at the pile head. LVDT's or dial gages with insufficient travel that must be shimmed and reset during the test should be prohibited. Where possible, deformation measurements should also be made at the pile toe and at intermediate points to allow for an evaluation of shaft and toe resistances. The load cell capacity should be between 120% and 150% of the anticipated maximum load to be applied.

3. The load test program should be supervised by a foundation engineer experienced in this field of work.

4. A test pile installation record should be maintained with installation details appropriately noted. Too often, only the hammer model and driving resistance are recorded on a test pile log. Additional items such as hammer stroke (particularly at final driving), fuel/energy setting, hammer cushion materials and dimensions, pile cushion material and cushion thickness when new and replaced, accurately determined final set, details on any installation aids used such as predrilling and their depths, start and ending driving times, stopping depths and associated time durations for splicing, equipment maintenance, etc., should be recorded.

5. Use of dynamic monitoring on the load test pile is recommended for estimates of the nominal resistance at the time of driving including the soil resistance distribution, evaluation of drive system performance, calculation of driving stresses, and refinement of wave equation input parameters.

9.1.3 When and Where to Load Test

Static load testing during either the design or construction phase should be performed to achieve a desired goal. This usually involves determining the nominal geotechnical resistance or load-transfer information at a representative site location. The number of load tests needed and their location should be selected based on the site variability. The AASHTO resistance factor for determination of the nominal resistance by static load testing is based on performing one load test per site condition. Site variability is discussed in Section 5.5.3 and in AASHTO (2014).

The following criteria, adapted from FHWA-SA-91-042 by Kyfor et al. (1992), summarize conditions when static pile load testing can be effectively utilized:

1. When substantial cost savings can be realized. This is often the case on large projects involving either friction piles (to determine that estimated pile lengths can be reduced) or end bearing piles (to determine that a higher nominal resistance can be used).

2. When the nominal geotechnical resistance is uncertain due to limitations of an engineer's experience base, or due to unusual site or project conditions.

3. When subsurface conditions vary considerably across the project, but can be delineated into zones of similar conditions. Static tests can then be performed in representative areas to delineate foundation variation.

4. When a significantly higher nominal geotechnical resistance is contemplated relative to typical practice.

5. When significant time dependent changes in nominal resistance are anticipated as a result of soil setup or relaxation.

6. When a reliable assessment of axial tension resistance or lateral deflection is important.

7. Verification of new design or testing methods.

8. When new pile types, large diameter open end pipe piles, and/or pile installation procedures are utilized.

9. When existing piles will be reused to support a new structure with heavier loads.

10. When, during construction, the estimated nominal resistance using dynamic formulas or dynamic analysis methods differs significantly from the estimated resistance at that depth determined by static analysis. For example, H-piles that "run" when driven into loose to medium dense sands and gravels.

11. When developing LRFD calibration based on local and regional geologic conditions.

9.1.4 Effective Use of Load Test Information

9.1.4.1 Design Stage

The best information for design of a pile foundation is provided by the results of a load testing program conducted during the design phase. The number of static tests, types of piles to be tested, method of driving and test load requirements should be selected by the geotechnical and structural engineers responsible for design. A cooperative effort between the two disciplines is necessary. The following are the advantages of load testing during the design stage.

a. Allows load testing of several different pile types, pile sections, and lengths resulting in the design selection of the most economical pile foundation.

b. Confirm drivability to minimum penetration requirements and suitability of nominal geotechnical resistance at the estimated pile penetration depths.

c. Establishes preliminary driving criteria for production piles.

d. The availability of pile driving information to construction project bidders should reduce their bid "contingency."

e. Reduces potential for contract disputes related to pile driving problems.

f. Allows the results of load test program to be reflected in the final design and specifications.

9.1.4.2 Construction Stage

Load testing at the start of construction may be the only practical time for testing on some projects that cannot justify the cost of a design stage program. Construction stage static load tests are invaluable to confirm that the design loads are appropriate, to establish the final design lengths for production piles, and to assure that the pile installation procedure is satisfactory. Perhaps most importantly, these results can be used to refine the estimated pile lengths shown on the plans and establish minimum pile penetration requirements.

9.1.4.3 Load Test Databases

As mentioned in Paikowsky (2004) and Abu-Hejleh (2015), load test databases are needed for design method reliability calibrations and to improve the geotechnical design of production foundations. High quality, complete, load test databases offer the ability to compare design and construction verification methods with full scale load test results. The information may allow the increase of the resistance factor for a specific design method, or provide designers with preferable foundation alternatives and construction methods given similar site conditions.

One such study was performed in 2010 by the Oregon Department of Transportation (DOT), where they evaluated driven pile resistance factors based upon wave equation analyses (Smith et al. 2011). At that time, the AASHTO recommended resistance factor, φ_{dyn}, for wave equation analysis was 0.40. This resistance factor resulted in increased pile foundation costs within the LRFD framework. Therefore, the Oregon DOT performed a calibration study to assess the reliability of a higher resistance factor for wave equation analysis. After reviewing several databases, the study recommended a wave equation analysis resistance factor of 0.55 for initial driving and 0.40 for restrikes. As a result of this research and other efforts, the recommended resistance factor for wave equation analysis in the AASHTO (2010) design specifications was changed from φ_{dyn} =0.40 to φ_{dyn} =0.50.

The FHWA Deep Foundation Load Test Database (DFLTD) contains data from several state highway agencies, FHWA offices and international sources. Although it is no longer updated, the DFLTD is available upon request by contacting the FHWA and contains approximately 1300 load test results from 1985 to 2003. Additional load test databases have been developed by several state transportation agencies.

It is recommended that load test results and accompanying geotechnical and pile installation information be stored in databases. The respective report section of the ASTM standard for axial compression, axial tension, and lateral load tests identifies the complete site, installation, and load test details that should maintained in a database. Maintaining this information allows the database to be effective for development and calibration of new design or construction control methods.

9.1.5 Resistance Factors for Static Load Testing

Resistance factors applicable to the nominal axial geotechnical resistance determined from a static load test are provided in Table 9-1. The resistance factor varies depending on whether the load test is in axial compression or tension as well as whether dynamic testing is performed. A resistance factor is not provided for lateral load testing as this is generally controlled by deformation criteria in the service limit state rather than by the strength limit state.

Table 9-1 Resistance Factors Based on Static Load Testing of Driven Piles (modified from AASHTO 2014)

Condition	Resistance Determination Method	Resistance Factor
Nominal Axial Compression Resistance of Single Pile, ϕ_{dyn}	Driving criteria established by successful static load test of at least one pile per site condition and dynamic testing of at least two piles per site condition, but no less than 2% of the production piles.	0.80
Nominal Axial Compression Resistance of Single Pile, ϕ_{dyn}	Driving criteria established by successful static load test of at least one pile per site condition without dynamic testing.	0.75
Nominal Axial Tension Resistance of Single Pile, ϕ_{up}	Static load test.	0.60

9.2 AXIAL COMPRESSION LOAD TEST

Piles are most frequently tested in axial compression. However, they can also be tested in axial tension as well as for their lateral resistance. Figure 9-1 illustrates the basic mechanism of performing an axial compression load test. This mechanism normally includes the following steps:

1. The pile is loaded incrementally from the pile head using some predetermined loading sequence, or it can be loaded at a continuous, constant rate.

2. During the test, readings are recorded of the time, applied load, and pile head movement. Strain measurements at other points along the pile shaft can be obtained concurrently to yield load transfer details and unit shaft resistances.

3. A load movement curve is plotted.

4. The geotechnical nominal resistance and the movement at the nominal resistance are determined by one of the several methods of interpretation.

5. Movement is usually measured only at the pile head. However, the pile can also be instrumented with telltales to determine movement anywhere along the pile. Telltales (solid rods protected by tubes) are shown in Figure 9-1.

6. Telltales can be used to determine the strain between telltale locations. Strain gages, attached to, or embedded within the pile can be used to determine the strain at discrete locations along the pile length. Both of these strain measurements can be used to estimate load transfer along the pile shaft.

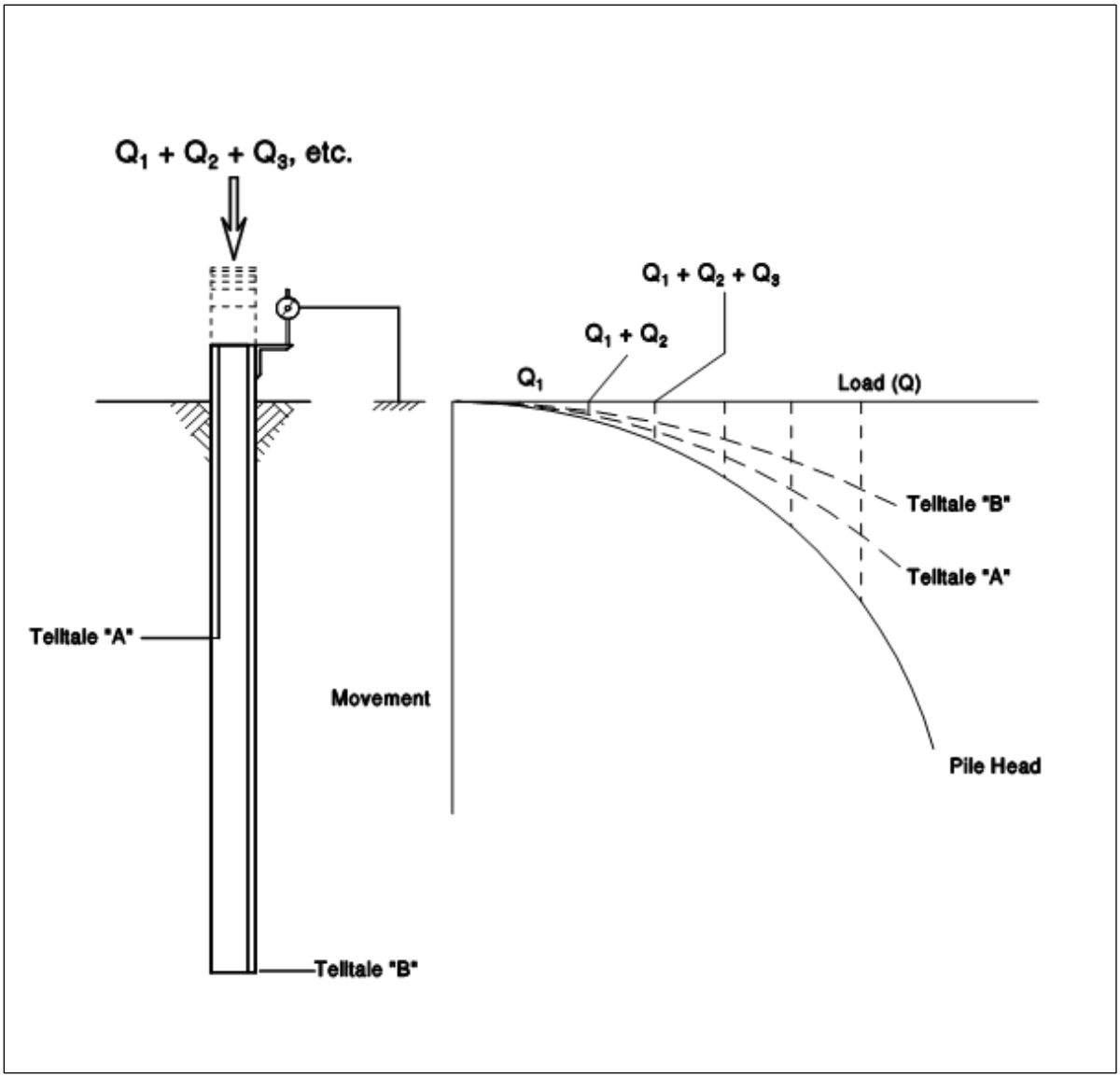

Figure 9-1 Axial compression static load test diagram.

9.2.1 Compression Load Test Equipment

ASTM D1143-07 (re-approved 2013) recommends several alternative systems for (1) applying compression load to the pile, and (2) measuring movements. Most often, compression loads are applied by hydraulically jacking against a beam that is anchored by piles or ground anchors, or by jacking against a weighted platform. The primary means of measuring the load applied to the pile should be with a calibrated load cell. The jack pressure from a calibrated pressure gage should also be recorded and be used as a secondary means of calculating the load applied to the pile. To minimize eccentricities in the applied load, a spherical bearing plate should be included in the load application arrangement.

Axial pile head movements are usually measured by LVDT's or dial gages that measure movement between the pile head and independently supported reference beam. The ASTM standard requires dial gages or LVDT's to have a minimum of 2 inches of travel and a precision of at least 0.01 inches. However, it is preferable and highly recommended to have gages with a minimum travel of 4 inches particularly for long piles with large elastic deformations under load and with a precision of 0.001 inches. A minimum of two dial gages or LVDT's mounted equidistant from the pile head, equidistant from the center of the pile, and diametrically opposite should be used. In many instances, four dial gages or LVDT’s mounted in diametrically opposite pairs may be advantageous.

A redundant backup system consisting of a scale, mirror, and wire system should be provided with a scale precision of 0.01 inches. The backup system should also be mounted on two diametrically opposite pile faces. Both the reference beams and backup wire system are to be independently supported with a clear distance of at least 5 times the pile diameter and not less than 8 feet between their supports and the test pile or reaction piles. A remote backup system consisting of a survey level should also be used in case reference beams or wire systems are disturbed during the test. The survey level can also monitor reaction pile movement where reaction piles are used.

ASTM D1143 specifies that the clear distance between a test pile and reaction piles be at least 5 times the maximum diameter of the reaction pile or test pile (whichever has the greater diameter if not the same pile type) but not less than 8 feet. If a weighted platform is used, the clear distance between cribbing supporting the weighted platform and the test pile should exceed 5 feet.

A schematic of a typical compression load test setup is presented in Figure 9-2. Photographs of the typical load application and movement monitoring components are presented in Figures 9-3 and 9-4. To improve the accuracy of the load cell readings, the loading arrangement shown in Figure 9-3 should include steel bearing plates between the hydraulic jack ram and the load cell, and between the load cell and spherical bearing plates. These bearing plates are included in the loading arrangement shown in Figure 9-5, and are discussed in greater detail in Section 9.6. The MnDOT mobile load frame attached to reaction piles is shown in Figure 9-5 with the load test being setup enclosed in a temporary heated structure for winter weather control. Wood reference beams are used to minimize temperature fluctuations on the reference beams.

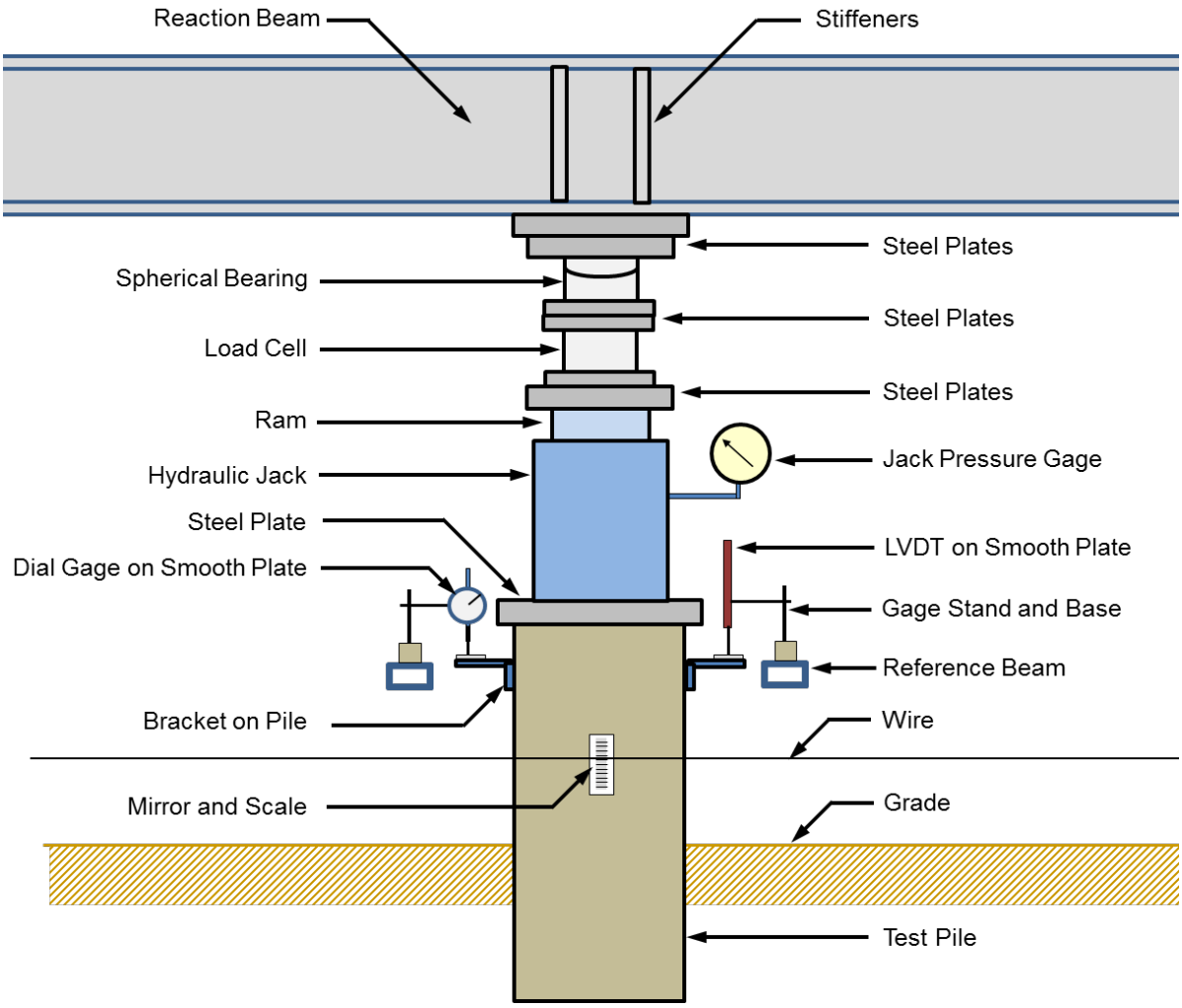

Figure 9-2 Static load test setup diagram.

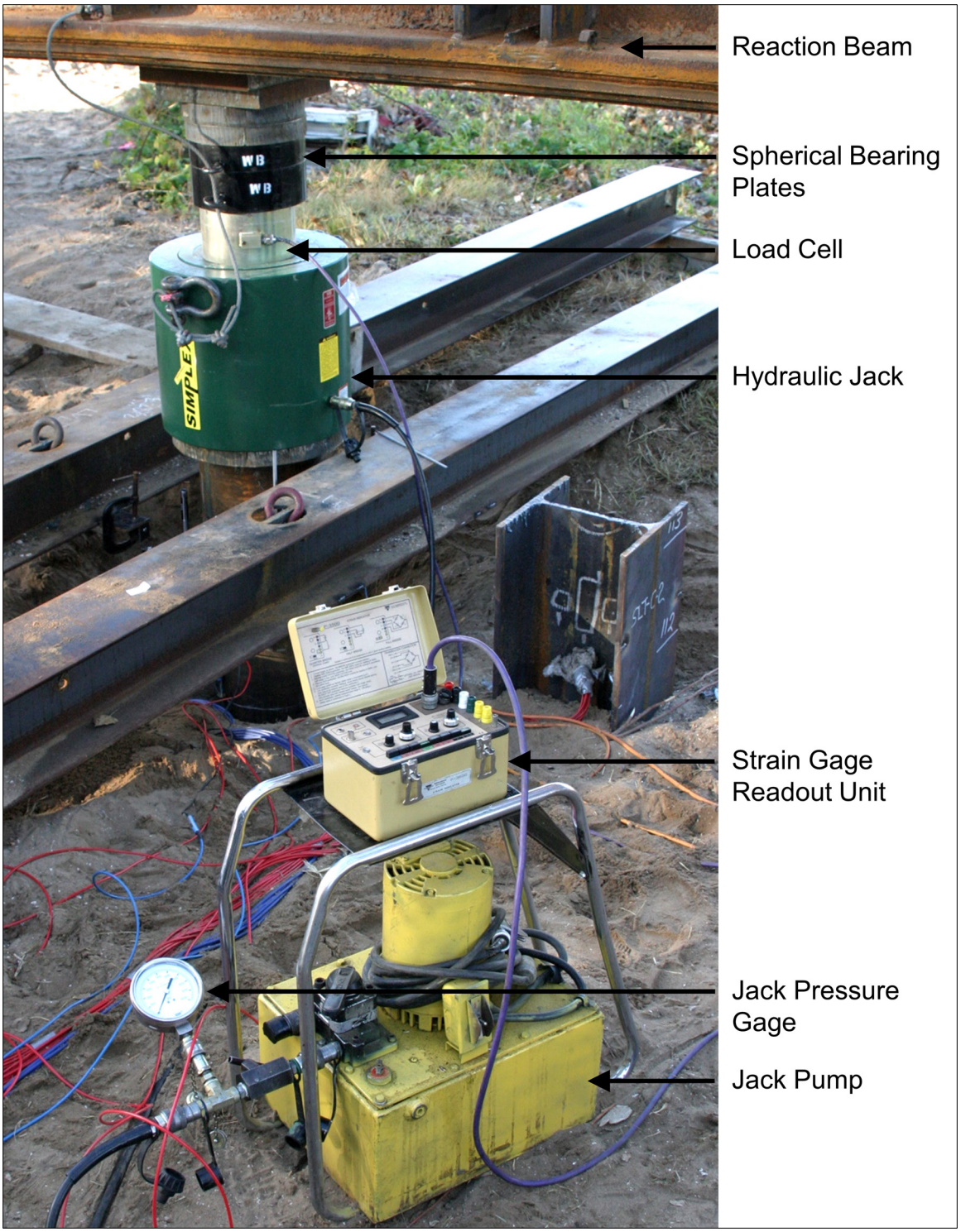

Figure 9-3 Load test application and monitoring system.

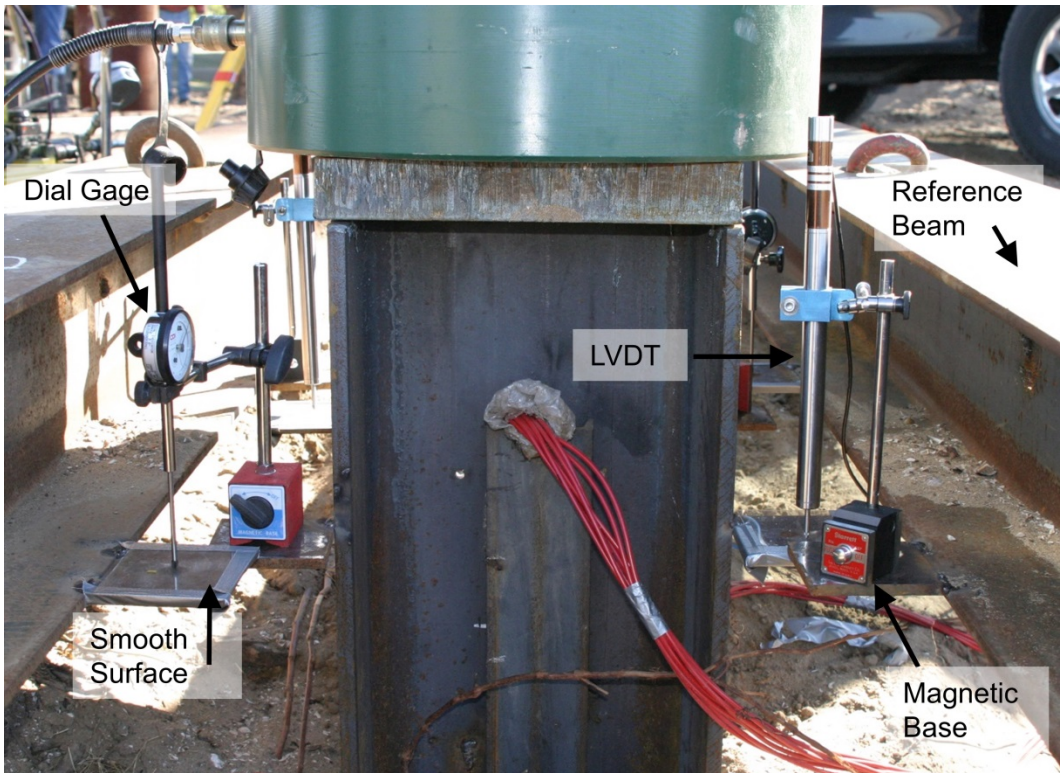

Figure 9-4 Load test movement monitoring components.

Figure 9-5 MnDOT reaction beam and load test setup (courtesy MnDOT).

A typical compression load test arrangement using reaction piles is presented in Figure 9-6 and a weighted platform arrangement is shown in Figure 9-7. It is recommended that load and movement measurements be recorded remotely using electronic instrumentation so that personnel are a significant distance from the load application / reaction system. Additional details on load application as well as pile head load and movement measurements may be found in ASTM D1143.

9.2.2 Recommended Axial Compression Test Loading Method

It is essential that standardized load testing procedures be followed. Several loading procedures are detailed in ASTM D1143, Standard Test Method for Deep Foundations Under Static Axial Compressive Load. The quick load test procedure is recommended by AASHTO (2014). This procedure is recommended because the load test can typically be performed in 2 to 4 hours thereby reducing construction delays and load test costs. However, alternative test procedures are also provided in ASTM D1143.

In the quick test procedure, the load is applied in increments of 5% of the anticipated nominal geotechnical resistance. This loading increment should produce on the order of 20 data points being recorded before reaching the geotechnical nominal resistance load thus allowing a detailed load-movement curve to be plotted.

Load increments should be held no more than 15 minutes and no less than 4 minutes, using the same time interval for all load increments. Readings of load and gross movement are to be recorded at 0.5, 1, 2, and 4 minutes after the load increment increase, with 8 and 15 minute readings if longer load increments have been selected. This procedure is to continue until the geotechnical nominal resistance or jack capacity is reached within the safe structural design limitations of the pile and reaction system. ASTM D1143 states that a longer hold time may be considered at the geotechnical nominal resistance to access creep. Note that this is not feasible if plunging movement under the applied load has occurred. If plunging movement occurs, the pump pressure should be locked off and the system should be allowed to come to equilibrium under the maximum resisted load. Upon reaching and holding the maximum load or reaching the load where plunging movement occurred, the pile is unloaded in 5 to 10 equal decrements which are each held for no more than 15 minutes and no less than 4 minutes. Readings of load and gross movement are to be recorded at 0.5, 1, 2, and 4 minutes (as well as 8 and 15 minutes) after each load reduction, including the zero load, which can be held longer to assess rebound.

Figure 9-6 4000-Ton mobile load test frame (courtesy Caltrans).

Figure 9-7 Static load test setup using weighted platform.

9.2.3 Presentation and Interpretation of Axial Compression Test Results

The results of axial compression load tests should be presented in a report conforming to the requirements of ASTM D1143. A load-movement curve similar to the one shown in Figure 9-8 should be plotted for interpretation of load test results.

The literature abounds with different methods of defining the nominal geotechnical resistance from static load tests. Methods of interpretation based on maximum allowable gross movements which do not take into account the elastic deformation of the pile are not recommended. These methods overestimate the nominal resistance of short piles and underestimate the nominal resistance of long piles. Methods which account for elastic deformation and are based on failure criterion provide a better understanding of pile performance and provide more accurate results.

AASHTO (2014) design specifications Article 10.7.3.8.2 provides three interpretation criteria of axial compression test results based on pile size. All of the methods include consideration of the elastic deformation of the pile. For uniform presentation and interpretation of the axial compression load test results, the load and movement scales are selected so that the line representing the elastic deformation, Δ, of the pile is inclined at an angle of about 20° from the load axis.

The elastic deformation, Δ, for a pile of uniform cross section is computed from:

$$\Delta = \frac{QL}{AE} \qquad \text{Eq. 9-1}$$

Where:

- Δ = elastic deformation of pile (inches).
- Q = test load (kips).
- L = pile length below dial gage or LVDT measurement location (inches).
- A = pile cross sectional area (in^2).
- E = elastic modulus of pile material (ksi).

AASHTO (2014) axial compression load test interpretation methods are based on an offset limit method as proposed by Davisson (1972). An offset limit line parallel to the elastic deformation line is plotted as shown in Figure 9-8. The point at which the observed load movement curve intersects the offset limit line is by definition the nominal geotechnical resistance or failure load. Note that this is a limiting deformation based criteria. In Figure 9-8, geotechnical plunging failure was not

achieved, and additional geotechnical resistance develops beyond the defined failure load with additional pile head movement. If the load-movement curve does not intersect the offset limit line, the pile has a nominal geotechnical resistance in excess of the maximum applied test load.

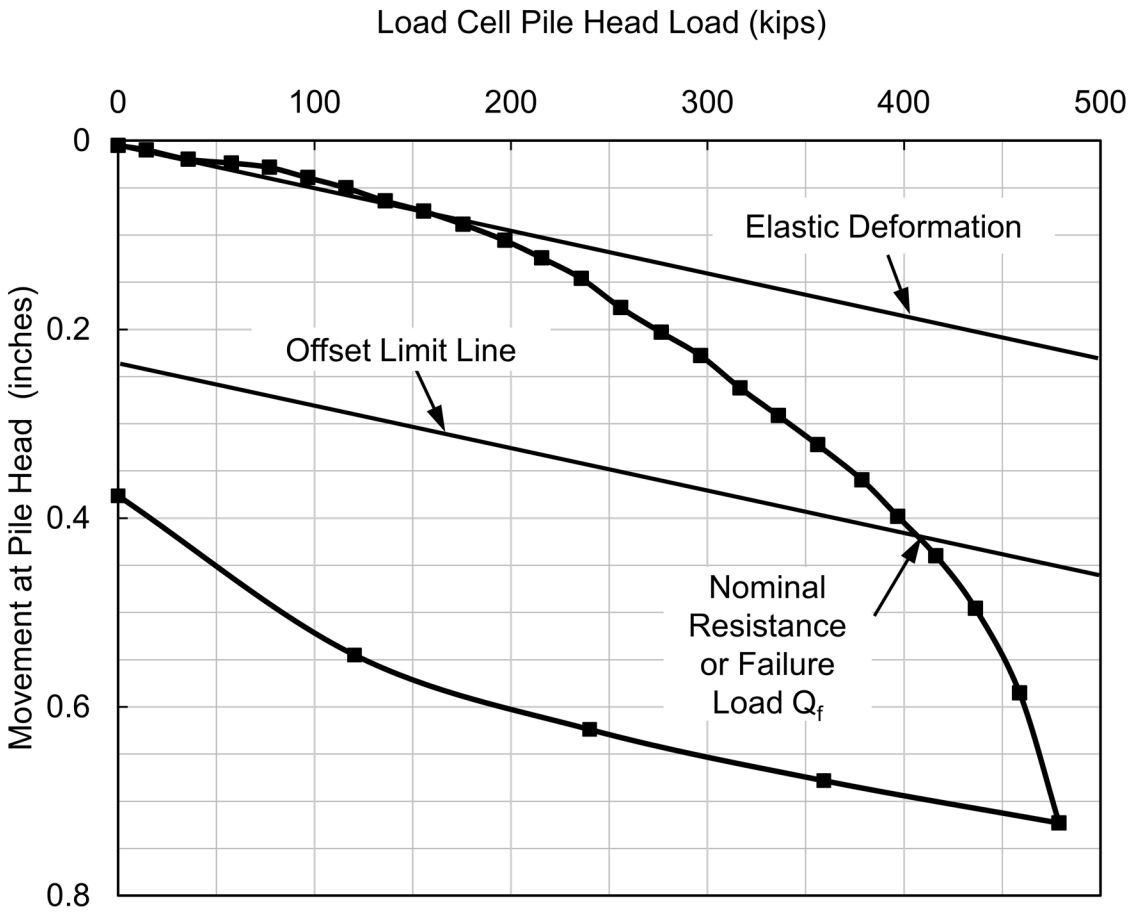

Figure 9-8 Typical load-movement curve for axial compression load test.

For piles 24 inches or less in diameter, the nominal geotechnical resistance, or failure load Q_f, is that load which produces a movement of the pile head equal to:

$$s_f = \Delta + \left(0.15 + \frac{b}{120}\right) \qquad \text{Eq. 9-2}$$

Where:

s_f = measured pile head movement at the nominal resistance (inches).

Δ = elastic deformation of pile per Equation 9-1 (inches).

b = pile width or diameter (inches).

For piles larger than 36 inches in diameter, additional pile toe movement is necessary to develop the toe resistance. For these larger diameter piles, the nominal geotechnical resistance, or failure load, can be defined as the load which produces at movement at the pile head equal to:

$$s_f = \Delta + \mathrm{b}/30 \qquad \text{Eq. 9-3}$$

Where:

s_f = measured pile head movement at the nominal resistance (inches).
Δ = elastic deformation of pile per Equation 9-1 (inches).
b = pile width or diameter (inches).

For piles greater than 24 inches but less than 36 inches in diameter, linear interpolation should be performed between Eq. 9-2 and Eq. 9-3.

The pile diameter, *b*, used in Eq. 9-2 and Eq. 9-3 is defined by AASHTO as the pile diameter or width of side for square piles. However, for H-piles the value for b is not defined. For consistency with AASHTO treatment of square piles, it is recommended that the flange width be chosen for b.

It should be noted that the Davisson method is applicable for load tests in which the increment of load is held for not more than 1 hour. It is not applicable to load tests with long load holds and will underestimate the nominal geotechnical resistance in those cases due to the additional pile head movement that occurs during the extended load holds.

As discussed in Section 9.2.1, the load applied to the pile head is measured with a primary (load cell) and back-up (jack pressure) system. The applied load determined from both the primary and secondary system should be in general agreement, and should be compared to each other throughout the test to detect any major errors or discrepancies. If during initial loading increments, large discrepancies are observed between the applied load indicated by the primary and secondary systems, the test should be stopped, and the cause of the large discrepancy evaluated. Strain gage instrumentation above the ground surface can oftentimes quickly determine whether the load measured by the primary system or backup system is correct, and therefore which system should be used to control the test. If a load test is performed with large unresolved discrepancies, safety issues and/or later controversies may arise. If the lower value of applied load is used, and the actual applied load is the higher value, a safety issues can occur during the test by operating the jack beyond its intended range, or by exceeding the nominal

structural resistance of the test pile or reaction system. If the higher value of applied load is used, and the actual applied load is the lower value, the test may be terminated prematurely or the nominal resistance determined from the test lower than anticipated. This may require the entire load test to be repeated, the use of longer pile lengths than necessary, a foundation redesign because of the lower load, or revisions to the driving criterion. Therefore whenever large discrepancies occur, the applied load should be removed from the test pile (unloaded), the cause of the discrepancy identified and corrected, and the load test restarted.

The factored compression resistance is 0.75 to 0.80 of the nominal resistance defined by the failure load. This range in the factored compression resistance depends on whether the driving criteria is developed solely from the static load test results (ϕ_{dyn} = 0.75), or if static load test results and dynamic testing with signal matching (ϕ_{dyn} = 0.80) is used.

An axial compression load test will not provide detailed load-transfer information in the penetrated geomaterials solely from the pile head load-movement results. Additional instrumentation as described in Section 9.5 is required if load-transfer information along the pile shaft or the delineation of shaft and toe resistances is desired.

9.2.4 Limitations of Axial Compression Tests

Compression load tests can provide a wealth of information for design and construction of pile foundations and are the most accurate method of determining nominal resistance. However, static load test results cannot be used to account for long-term settlement, downdrag from consolidating and settling soils, or to adequately represent pile group action. Other shortcomings of static load tests include test cost, the time required to setup and complete a test, and the minimal information obtained on driving stresses or extent of pile damage (if any). Static load test results can also be misleading on projects with highly variable soil conditions. If detailed load-transfer assessments are desired, the pile must have additional strain gage instrumentation attached or embedded in the pile, which can add significant cost.

9.3 TENSION LOAD TEST

Tension load tests are performed to determine axial tension (uplift) resistance of piles. The uplift resistance is often a significant factor in determining minimum pile penetration requirements for pile groups subject to large uplift loading demand including cofferdam seals that create large buoyancy forces, cantilever segmental bridge construction, as well as seismic, vessel impact, or debris loading. The basic mechanics of a tension test are similar to compression load testing, except the pile is loaded in tension. Tension load tests are often economical since they can frequently be performed by jacking against a reaction beam supported by crane mats rather than reaction piles.

9.3.1 Tension Load Test Equipment

ASTM D3689-07 (re-approved 2013) describes The Standard Method of Testing Deep Foundations Under Static Axial Tensile Load. Several alternative systems for applying tension load to the pile and measuring movements are provided in this standard. Most often, tension loads are applied by centering a hydraulic jack on reaction beams supported by reaction piles or by mats and cribbing supported by the ground. The jack can be a center hole jack allowing a rod embedded in the pile to pass in between the reaction beams and through the jack. This is a common arrangement for concrete piles with relatively low tension loads. Alternatively, a yoke type of connection can be used to transfer the tension load to the pile. In this arrangement, steel rods pass on either side of the reaction beam(s). The rods are connected to the pile and to a beam on top of the jack. This is a common arrangement for steel piles. The primary means of measuring the load applied to the pile should be from a calibrated load cell with the jack load recorded from a calibrated pressure gage as backup. A spherical bearing plate should be included in the load application arrangement.

Axial pile head movements are usually measured by dial gages or LVDT's that measure movement between the pile head and an independently supported reference beam. For tension testing, ASTM requires that the dial gages or LVDT's have a minimum of 2 inches of travel and a precision of at least 0.01 inches. While not required, gages with 4 inches of travel are recommended. A minimum of two dial gages or LVDT's mounted equidistant from the point of load application, equidistant from the center of the pile, and diametrically opposite should be used. A redundant backup system consisting of a scale, mirror, and wire system should be provided with a scale precision of 0.01 inches. The backup system should also be mounted on two diametrically opposite pile faces. Both the reference beams and

backup wire system are to be independently supported with a clear distance of at least 5 times the pile diameter and not less than 8 feet between supports and the test pile or reaction piles. A remote backup system consisting of a survey level should also be used in case reference beams or wire systems are disturbed during the test. Additional details on load application, and pile head load and movement measurements may be found in ASTM D3689.

Photographs of tension load test arrangements are presented in Figure 9-9 and 9-10. In Figure 9-9, a tension load test arrangement for a nearshore situation using a reaction beam and reaction piles is presented. In Figure 9-10, a tension load test arrangement for a land situation using a reaction beam supported by crane mats and timber cribbing is illustrated.

9.3.2 Tension Test Loading Methods

Several loading procedures are detailed in ASTM D3689. The Quick Test method where load is applied in increments of 5% of the anticipated nominal geotechnical tension resistance is recommended. This loading increment should produce on the order of 20 data points being recorded before reaching the nominal geotechnical resistance thus allowing a detailed load-movement curve to be plotted. All load increments should be held for the same time interval of no more than 15 minutes and no less than 4 minutes.

Readings of load and gross movement are to be recorded at 0.5, 1, 2, and 4 minutes after the load increment increase, with 8 and 15 minute readings for longer hold times. This procedure is to continue until the nominal geotechnical resistance or jack capacity is reached within the safe structural design limitations of the pile and reaction system. Upon reaching and holding the maximum load or reaching the load where geotechnical pullout failure occurred, the pile is unloaded in 5 to 10 equal decrements which are each held for no more than 15 minutes and no less than 4 minutes. Load and gross movement are to be recorded at 0.5, 1, 2, and 4 minutes (as well as 8 and 15 minutes if applicable) after each load reduction, including the zero load. Additional optional loading procedures are detailed in ASTM D3689.

It is generally desirable to test a pile in tension loading to geotechnical pullout failure, particularly during a design stage test program. If construction stage tension tests are performed on production piles, the piles should be redriven to the original pile toe elevation and the previous driving resistance upon completion of the load testing.

Figure 9-9 Tension test on pipe pile using reaction piles (courtesy of Besix).

Figure 9-10 Tension test on H-pile using mats and cribbing (courtesy of WKG[2]).

9.3.3 Presentation and Interpretation of Tension Test Results

The results of tension load tests should be presented in a report conforming to the requirements of ASTM D3689. A load movement curve similar to the one shown in Figure 9-11 should be plotted for interpretation of tension load test results.

A widely accepted method for determining the nominal geotechnical resistance in tension loading has not been published. Fuller (1983) reported that acceptance criteria for tension tests have included a limit on the gross or net upward movement of the pile head, the slope of the load movement curve, or an offset limit method that accounts for the elastic lengthening of the pile plus an offset.

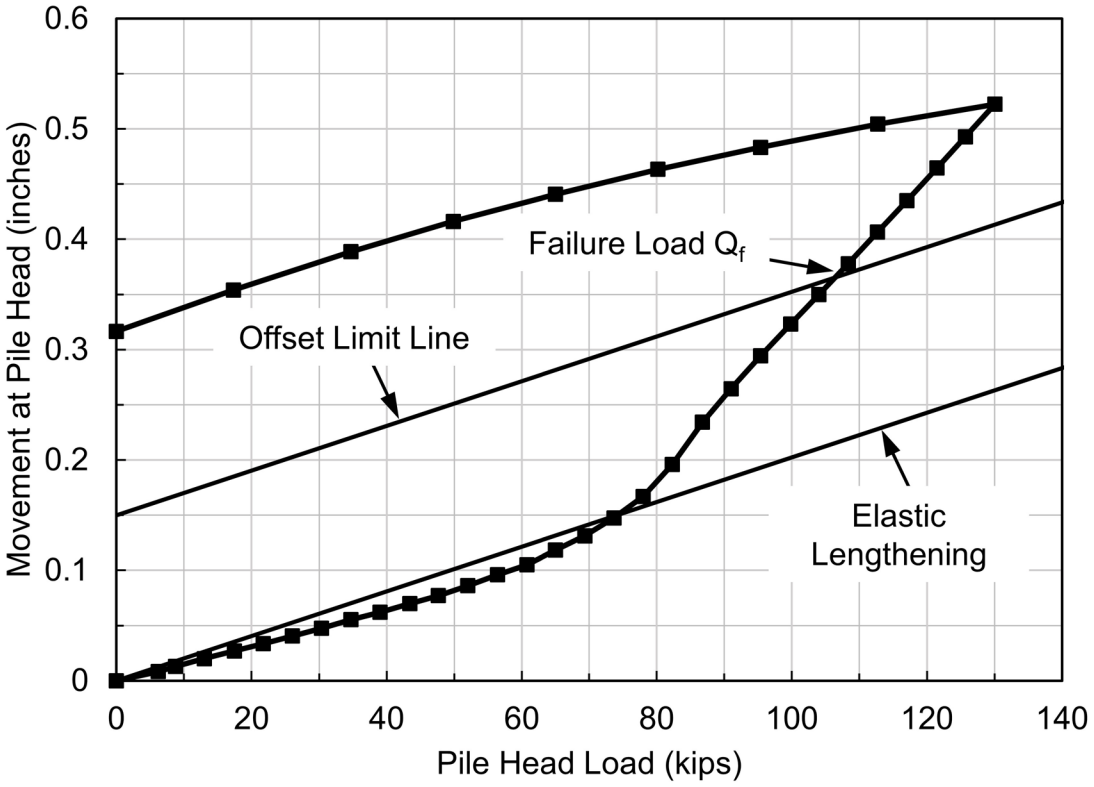

Figure 9-11 Typical tension load test load-movement curve.

AASHTO (2014) design specifications recommend tension load tests be evaluated using a modified Davisson Method that considers the elastic lengthening of the pile plus an offset limit. For tension loading, the suggested offset is 0.15 inches. Hence, the load at which the load movement curve intersects the elastic lengthening plus 0.15 inches is then defined as the nominal tension resistance or failure load. The factored tension resistance is then 0.60 of the nominal tension resistance defined by the failure load.

9.4 LATERAL LOAD TEST

Lateral load tests are performed on projects where piles are subjected to significant lateral loads. The importance of determining pile response to lateral loading has greatly increased, particularly with regard to extreme event limit states consideration such as seismic and vessel impact. Lateral load testing has also increased due to the greater use of noise walls and large overhead signs. Most lateral load tests are performed on a single pile with a free head condition. In service, most piles are installed in groups having a fixed head condition. Hence, lateral load test results on a single pile with a free head pile condition may not be directly applicable to design. Accordingly, the primary purpose of lateral load testing is to determine the p-y curves modelling soil behavior to be used in the design or to verify the appropriateness of the p-y curves on which the design is based. Lateral load tests are often economical since they can frequently be performed by jacking or pulling between two piles. For design stage tests, the two piles can be different pile types or pile sections enabling lateral deformation behavior for two pile types to be assessed with one lateral load test.

9.4.1 Lateral Load Test Equipment

ASTM D3966-07 (re-approved 2013) describes The Standard Method of Testing Deep Foundations Under Lateral Load. Several alternative systems for applying the lateral load to the pile and measuring movements are provided in this standard. Most often, lateral loads are applied by a hydraulic jack acting against a reaction system (e.g. piles, deadman, or weighted platform), or by a hydraulic jack acting between two piles. When jacking between two piles, pulling the piles toward one another is the preferred arrangement as the system comprises a two-force member and so alignment is naturally maintained. However, with this arrangement ASTM requires a significant distance between the test piles clear distance of not less than 20 feet or 20 pile diameters. The primary means of measuring the load applied to the pile(s) should be from a calibrated load cell with the jack load recorded from a calibrated pressure gage as backup. ASTM D3966 requires a spherical bearing plate(s) be included in the load application arrangement unless the load is applied by pulling.

Lateral pile head movements are usually measured by dial gages or LVDT's that measure movement between the pile head and an independently supported reference beam mounted perpendicular to the direction of movement. For lateral load testing, ASTM requires the dial gages or LVDT's have a minimum of 3 inches of travel and a precision of at least 0.01 inches. For tests on a single pile, one dial

gage or LVDT is mounted on the side of the test pile opposite the point of load application. A backup system consisting of a scale, mirror, and wire system should be provided with a scale precision of 0.01 inches. The backup system is mounted on the top center of the test pile or on a bracket mounted along the line of load application.

It is strongly recommended that lateral deflection measurements versus depth also be obtained during a lateral load test. This can be accomplished either by installing an inclinometer casing on or in the test pile to the depth where it is reasonable certain that no lateral movement will occur and recording inclinometer readings immediately after application or removal of a load increment held for a duration of 30 minutes or longer. Alternatively, a Shape Accel Array (SSA) can be embedded in or attached to the test pile. Kyfor et al. (1992) noted that lateral load tests in which only the lateral deflection of the pile head is measured are seldom justifiable. Additional details on load application, and pile head load and movement measurements may be found in ASTM D3966 and FHWA-SA-91-042 (Kyfor et al. 1992).

A photograph of a typical lateral load test arrangement is presented in Figure 9-12. This figure shows a 14 and a 16 inch O.D. concrete filled pipe pile being pushed apart. The jack is located adjacent to the right pile and the load cell and spherical bearing plate are located adjacent to the left pile. Figures 9-13 and 9-14 present close-ups of these devices. Both piles were also equipped with a string of in-place inclinometers for prompt readout of the deflected pile shape with each load increment. A photograph of the multiple inclinometer string components is presented in Figure 9-15.

As an alternative means to measure horizontal deflection, a Shape Accel Array (SSA) can be embedded in or placed along the pile length (Rollins et al. 2009). These triaxial accelerometers are typically installed in 1 inch diameter PVC casing, are recoverable and reusable, and can output displacements for both static and dynamic loads (Measureand 2015). SSAs are currently produced in 12 inch segments and therefore provide a more detailed assessment of deflections as compared with typical inclinometers. Figure 9-16 shows a typical SSA.

In cases where it is not feasible to acquire lateral deflection measurements versus depth, it may be useful to measure pile head rotation during the lateral load test. The pile head rotation can be obtained by measuring the lateral pile deflection at two different elevations above the point of load application or by attaching an inclinometer probe or tiltmeter to the pile head. The measured pile head rotation may be used to assess appropriate p-y modelling.

Figure 9-12 Lateral load test on 14 inch and 16 inch O.D. concrete filled pipe piles (courtesy of WKG[2]).

Figure 9-13 Jack for lateral load test (courtesy of WKG[2]).

Figure 9-14 Spherical bearing plate and load cell for lateral load test (courtesy of WKG[2]).

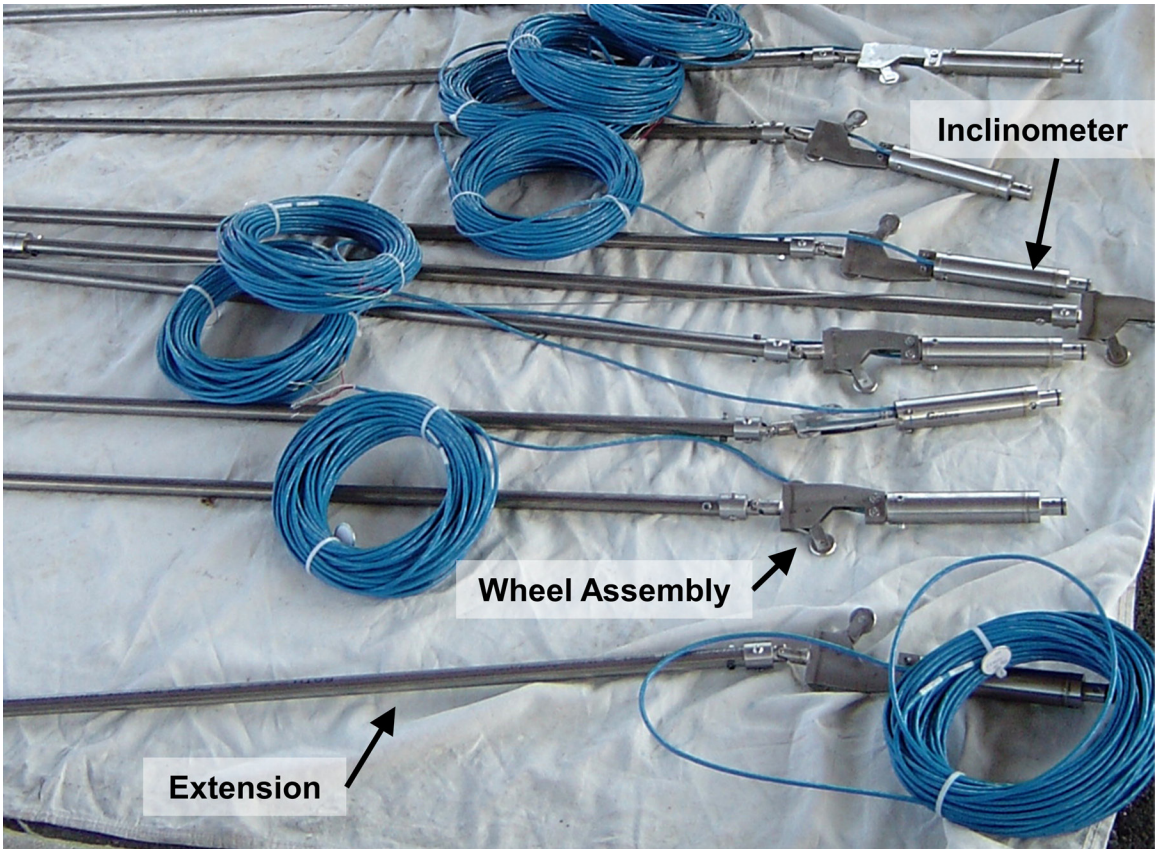

Figure 9-15 Multiple inclinometer string components for lateral load test (courtesy of WKG[2]).

Figure 9-16 Typical Shape Accel Array (SSA) (courtesy of Measurand).

9.4.2 Lateral Test Loading Methods

Several loading procedures are detailed in ASTM D3966. The Standard Loading procedure requires that the total test load be 200% of the proposed lateral design load. Variable load increments are applied with the magnitude of load increment decreasing with applied load. The load duration is also variable, increasing from 10 minutes early in the test to 60 minutes at the maximum load. Upon completing the maximum test load, the pile is unloaded in four load decrements equal to 50% of the maximum load, with 10 minute holds between load decrements. This loading schedule is shown in Table 9-2.

Table 9-2 Standard Loading Schedule (after ASTM D3966)

Percent of Design Load	Load Duration, minutes
0	-
25	10
50	10
75	15
100	20
125	20
150	20
170	20
180	20
190	20
200	60
150	10
100	10
50	10
0	30

Readings of load and gross movement are recorded immediately before and after each change in load, with additional readings taken at 5 minute intervals between load increments. Upon load removal, readings should be taken at 15 and 30 minutes.

9.4.3 Presentation and Interpretation of Lateral Test Results

The results of lateral load tests should be presented in a report conforming to the requirements of ASTM D3966. The interpretation and analysis of lateral load test results is much more complicated than those for compression and tension load tests. Figure 9-17 presents a typical pile head load-movement curve from a lateral load test. A lateral deflection versus depth curve similar to the one shown in Figure 9-18 should also be reported for lateral load tests that include lateral deflection measurements versus depth. The measured lateral deflection behavior versus depth should also be plotted and compared to design analysis results from p-y computer software as indicated in Figure 9-19. Based upon the comparison of measured and predicted results, the p-y curves to be used for design (design stage tests), or the validity of the p-y curves on which the design was based (construction stage tests) can be determined.

Refer to FHWA IP 84 11, Handbook on Design of Piles and Drilled Shafts Under Lateral Load by Reese (1984) as well as FHWA-SA-91-042, Static Testing of Deep Foundation by Kyfor et al. (1992) for additional information on methods of analysis and interpretation of lateral load test results.

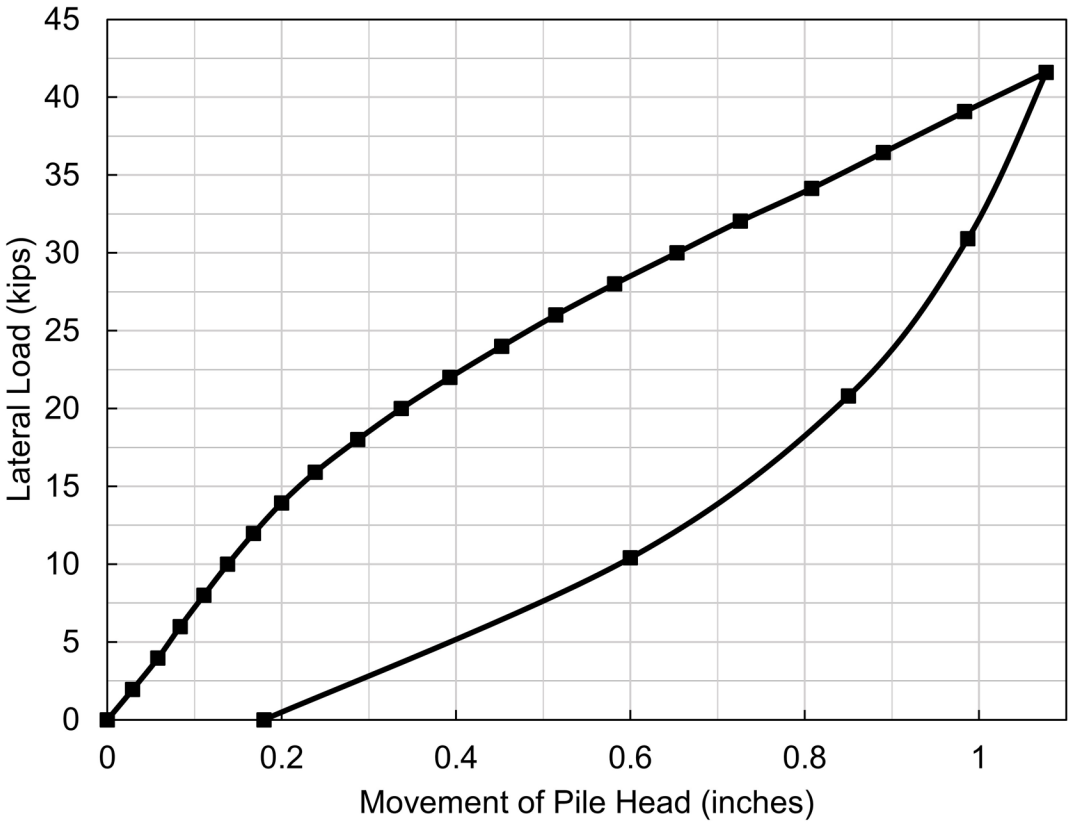

Figure 9-17 Typical lateral load test, pile head load-deflection curve.

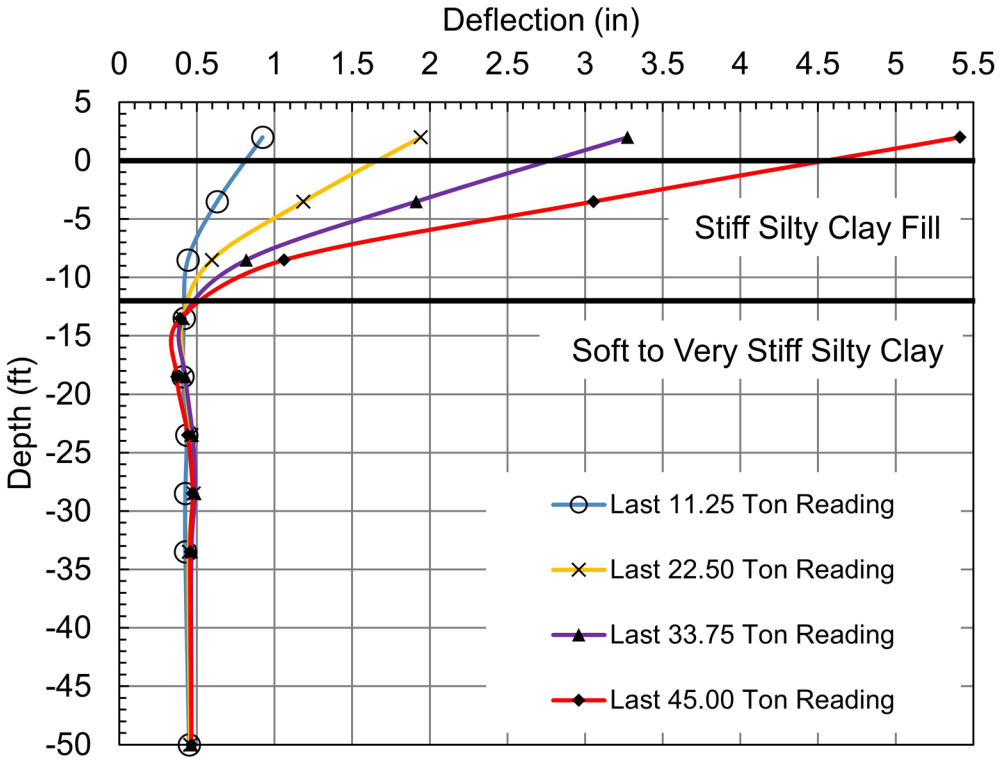

Figure 9-18 Plot of lateral load test measured deflected shape versus depth.

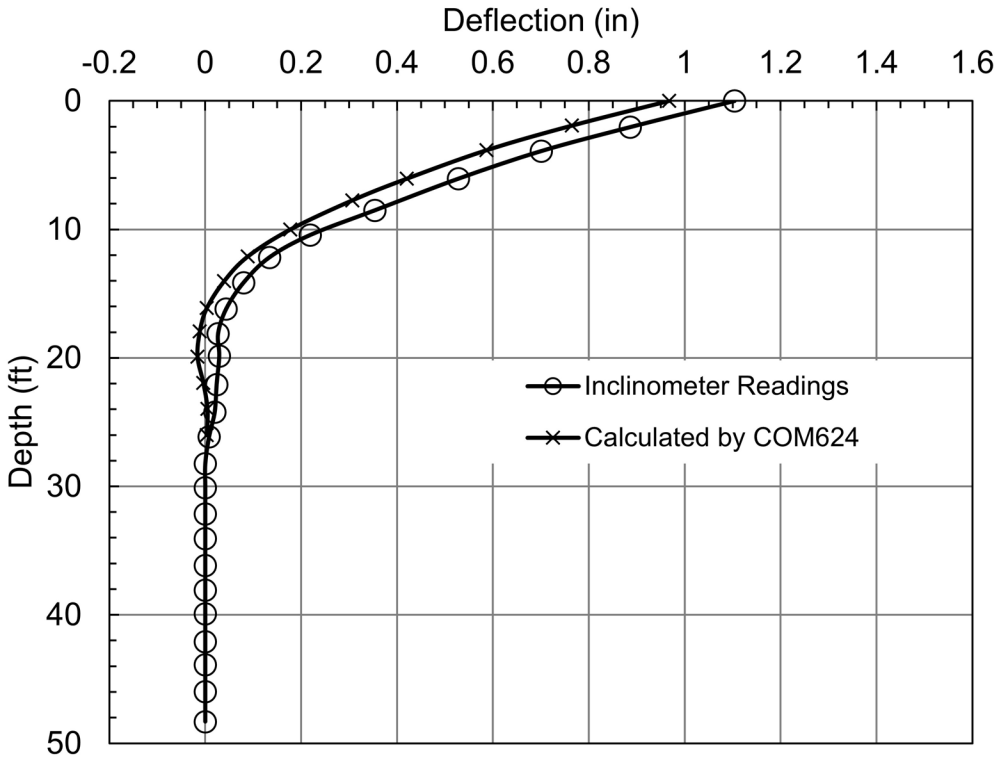

Figure 9-19 Comparison of measured and COM624P predicted load deflection behavior versus depth (after Kyfor et al. 1992).

9.5 LOAD TRANSFER EVALUATIONS

The magnitude of shaft and toe resistances or the unit shaft resistance values can be determined though instrumented static load tests. Load transfer evaluation along the pile shaft may be determined through the use of telltale rods (extensometers) or through surface mounted or embedded strain gages. Details on the use of telltales or strain gages for load transfer determinations are discussed in the following sections.

9.5.1 Use of Telltales

Telltales are thin steel rods that extend from the pile head to a selected point in the pile. The rods are encased within a slightly larger tube. A schematic of telltale rod placement within a load test is shown in Figure 9-20. The NYSDOT Static Pile Load Test Manual, GCP-18 (2007) provides telltale details for pipe piles, H-piles, and timber piles.

LVDT's or dial gages attached to the top of the telltale rod measure the relative movement between the rod attachment locations on the pile and other points such as the independent reference beam or the pile head. When using multiple rods, the deflection difference between the rod attachment points can provide the load transfer between those fixed locations. According to Kyfor et al. (1992), the average load in the pile, Q_{avg}, between two measuring points can be determined as follows:

$$\mathrm{Q}_{avg} = A\ E\ \frac{R_1 - R_2}{L} \qquad \text{Eq. 9-4}$$

Where:

Q_{avg} = average load in pile between two points (kips).
A = pile cross sectional area (in^2).
E = elastic modulus of pile material (ksi).
R_1 = deflection reading at upper measurement location (inches).
R_2 = deflection reading at lower measurement location (inches).
L = length of pile between two measuring points under no load condition.

If the R_1 and R_2 readings correspond to the pile head and the pile toe respectively, then an estimate of the shaft and toe resistances may be computed. For a pile with an assumed constant soil resistance distribution (uniform), Fellenius (1990) states

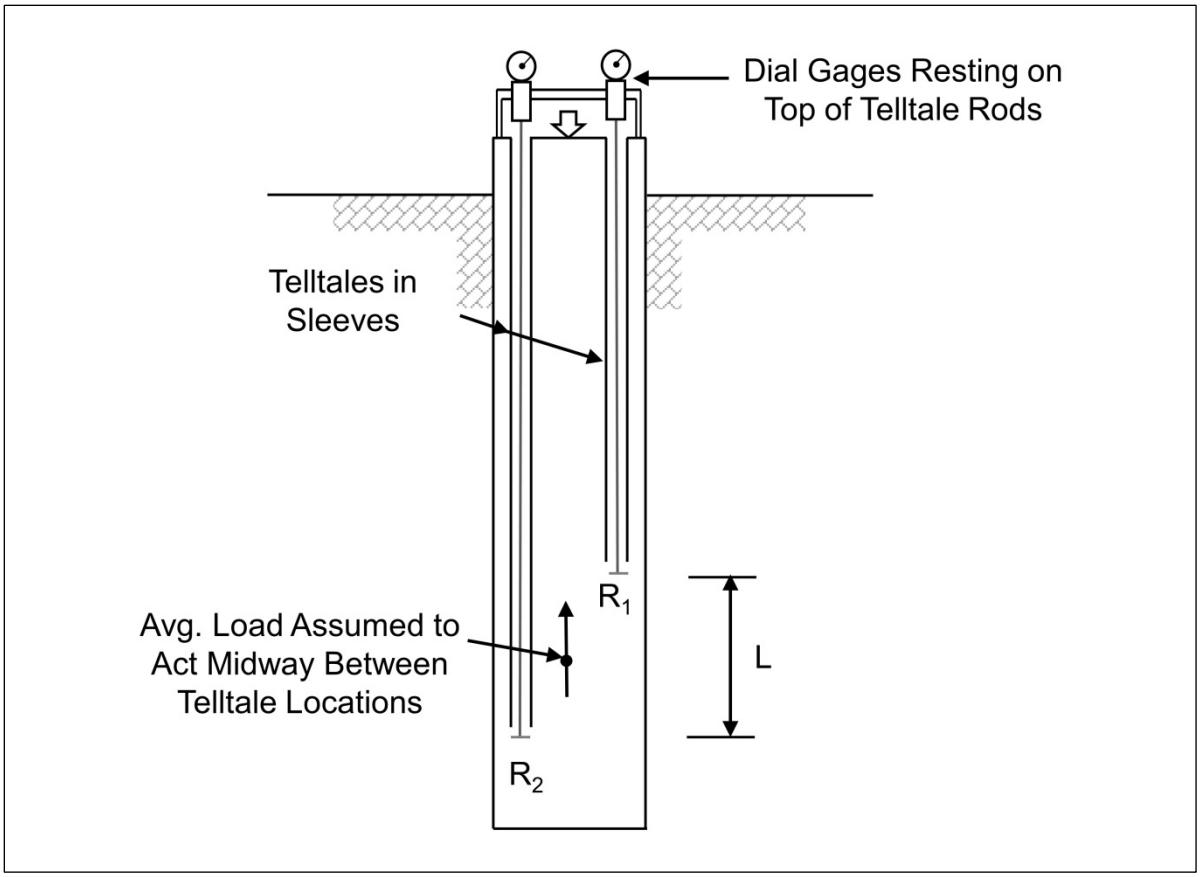

Figure 9-20 Diagram of telltale rods installed on pile
(modified from Kyfor et al. 1992).

that an estimate of the toe resistance, R_p, can be computed from the applied pile test load, Q. The applied pile head load, Q, is chosen as close to the nominal resistance or failure load as possible.

$$R_p = 2\,Q_{avg} - Q \qquad \text{Eq. 9-5}$$

Where:

R_p = nominal toe resistance (kips).
Q_{avg} = average load in pile between two points (kips).
Q = test load, applied at the pile head (kips).

For a pile with an assumed linearly increasing soil resistance distribution (triangular), the estimated toe resistance may be calculated using:

$$R_p = 3\,Q_{avg} - 2\,Q \qquad \text{Eq. 9-6}$$

Where:

R_p = nominal toe resistance (kips).

Q_{avg} = average load in pile between two points (kips).

Q = test load, applied at the pile head (kips).

The estimated shaft resistance can then be calculated from the applied pile head load minus the toe resistance.

9.5.2 Use of Strain Gages

When detailed load transfer data is desired, telltale measurements alone are insufficient, due to the presence of unaccounted for residual load. Dunnicliff (1988) suggests that weldable vibrating wire strain gages be used on steel piles and sister bars with vibrating wire strain gages be embedded in concrete piles for detailed load transfer evaluations. Other gage types may also be used if load transfer measurements under both static and dynamic conditions are desired. A geotechnical instrumentation specialist should be used to select the appropriate instrumentation for the application, to select instrumentation that can withstand pile handling and pile driving, to determine the needed instrumentation redundancy, and to determine the appropriate data acquisition system for the program.

A sister bar vibrating wire strain gage is presented in Figure 9-21. The protective cover has been removed from the top gage in the box. Sister bar gages are often cast into prestressed concrete piles or embedded in concrete filled pipe piles during concrete placement. The sister bars are tied to the longitudinal rebar in the casting yard for prestressed concrete piles or attached to centralized steel bar or pipe when cast into a concrete filled pipe pile.

An arc-weldable vibrating wire strain gage attached to a steel H-pile is shown in Figure 9-22. The gage attachment blocks are welded to the pile and then the vibrating wire gage positioned between the mounting blocks.

Piles can also be instrumented with resistance type strain gages. These gages can be used for both static load-transfer and dynamic measurements on the pile. A bolt-on, waterproof, foil resistance strain gage attached to the side of a steel pipe pile is shown in Figure 9-23. The gages and instrumentation cables are covered and protected by a steel channel as the pile is driven below grade. Resistance type strain gages mounted on sister bars are shown in Figure 9-24. These gages are being cast into a prestressed concrete pile. The center sister bar also includes an accelerometer for dynamic testing purposes.

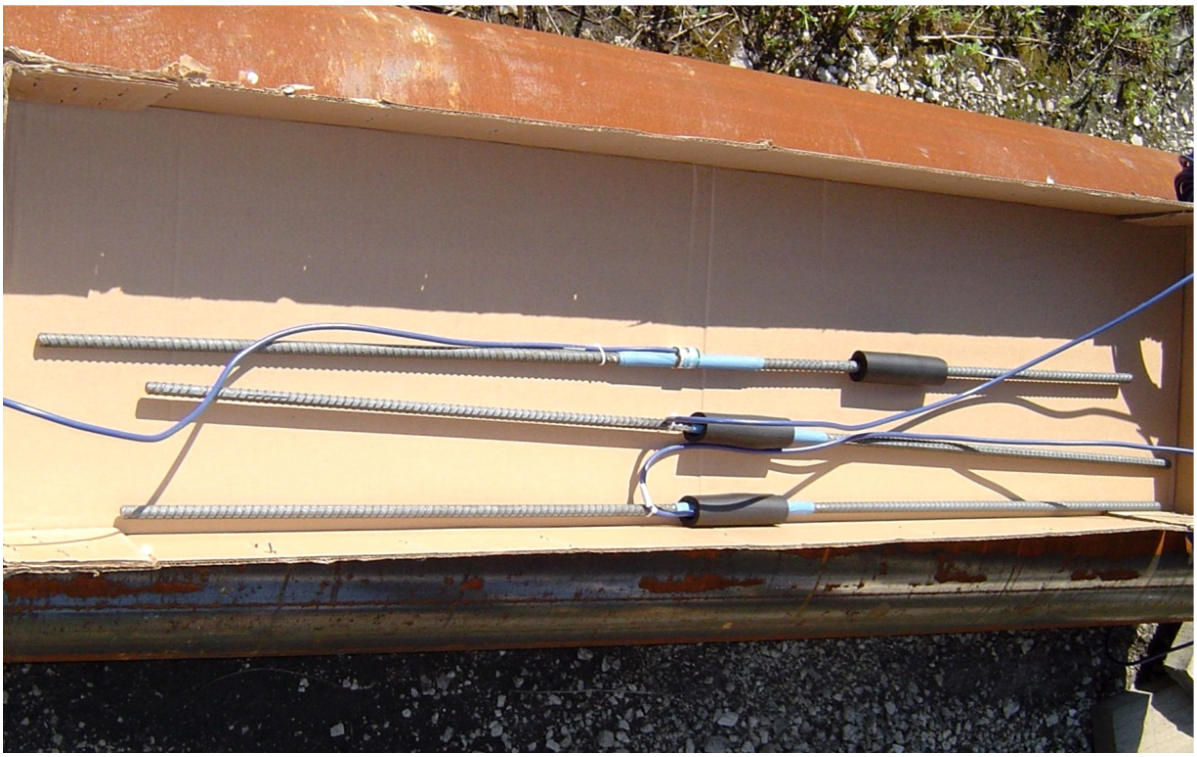

Figure 9-21 Vibrating wire strain gage sister bars for concrete embedment.

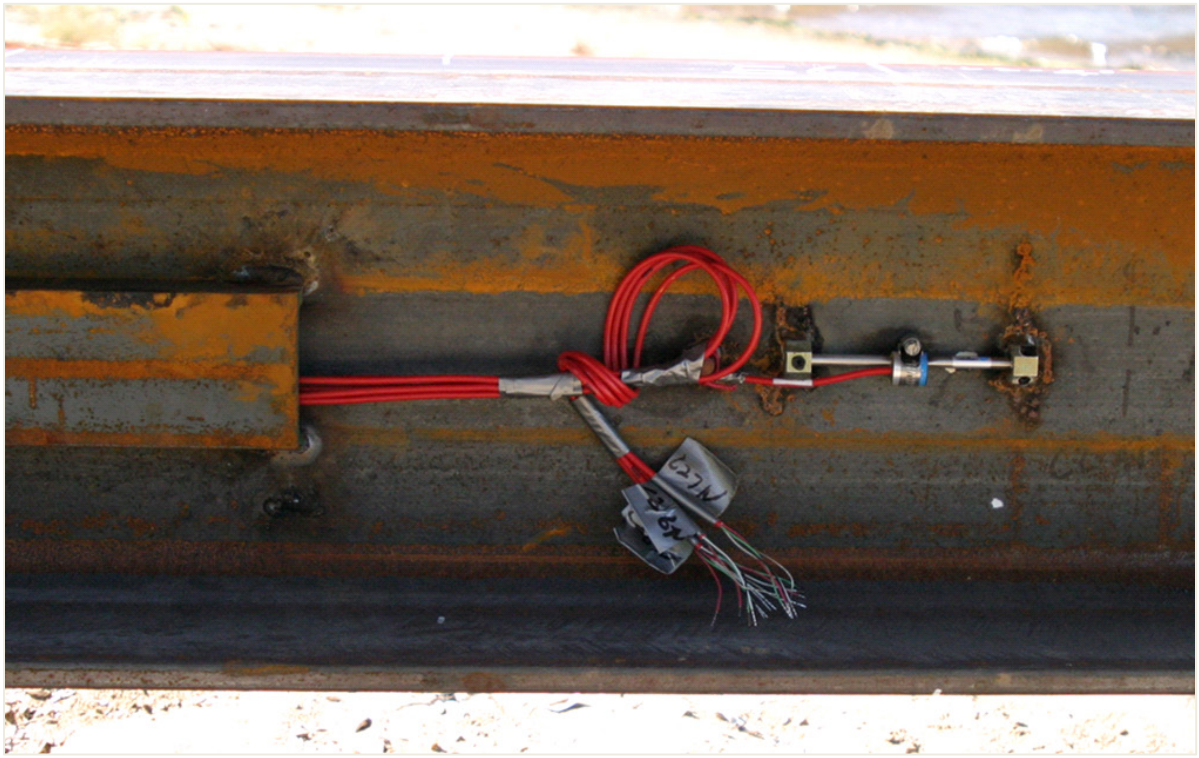

Figure 9-22 Vibrating wire strain gage with welded anchor blocks and protective channel.

Figure 9-23 Waterproof electrical resistance strain gage bolted on pipe pile with protective channel (courtesy of Besix).

Figure 9-24 Electrical resistance strain gage on sister bars in concrete pile casting bed.

Moisture is one of the leading causes of resistance strain gage failure. Therefore, all lead wires should be carefully checked for any nicks or abrasion and sealed as appropriate in these instrumentation situations. A multiple channel data acquisition system is also required as part of the instrumentation system.

Strain gages are generally attached at pre-selected points along the pile length to determine load-transfer and unit shaft resistances in specific strata or at prescribed locations. The closest soil boring to the load test location should be reviewed as part of the load-transfer instrumentation program planning so that the desired unit shaft resistance values for the selected geomaterials are determined. Additional gages can be distributed based upon the Engineer's experience, the need for instrumentation redundancy, site specific conditions, and project requirements. Cost effective designs can be finalized based on the determined geomaterial resistances.

The uppermost gage location should be below the pile head in an area where shaft resistance does not act on the pile. Dunnicliff (1988) recommends three undamaged pile diameters be left above the ground surface to simulate an unconfined compression specimen. At a minimum, the pile head strain gages should be at least two pile diameters below the pile head to allow for full load development across the pile section. At this location, a modulus determination can be made while a comparison of internal and external strain readings can indicate composite section action for concrete filled pipe piles (Sellers 1995; Komurka 2015). As depicted in Figure 9-25, it is also prudent to mitigate bending effects by using multiple external gage pairs equidistant from the head and center of the pile, or centralizers on single embedded gages.

Komurka (2015) also recommended another gage location; two pile diameters above the pile toe to be used for load transfer evaluation near the pile toe. He reported load transfer can be extrapolated from this location over the remainder of the pile to estimate the pile toe resistance. Sister bars near the pile toe should not rest on the toe when cast into concrete filled pipe piles but should instead be supported from the pile head during the concrete curing process.

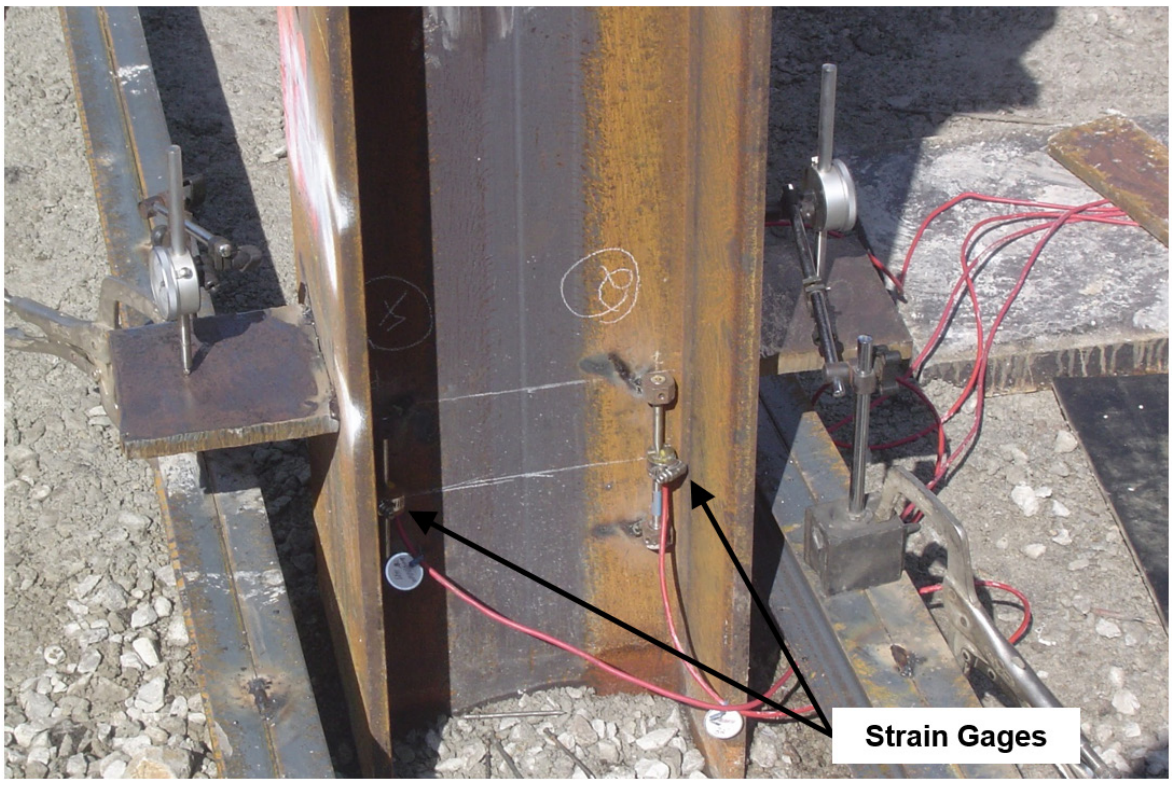

Figure 9-25 Multiple externally mounted strain gages (2 on each web face) located in soil resistance free area during static load test (courtesy WKG[2]).

Following strain gage attachment and pile installation, the axial force in the plane of the gage can be determined using Eq. 9-7.

$$F = \varepsilon\, E\, A \qquad \text{Eq. 9-7}$$

Where:

- F = axial force in plane of gage (kips).
- ε = strain measured in gage.
- E = elastic modulus of pile material (ksi).
- A = pile cross sectional area (in^2).

The modulus of elasticity for steel is well defined. However, for concrete filled steel piles, a composite modulus of the concrete and steel section must be calculated using Eq. 9-8.

$$\mathrm{E} = \frac{\mathrm{E}_{st}\,\mathrm{A}_{st} + \mathrm{E}_c\,\mathrm{A}_c}{\mathrm{A}_{st} + \mathrm{A}_c} \qquad \text{Eq. 9-8}$$

Where:

E = elastic modulus of pile material (ksi).
E_{st} = elastic modulus of steel (ksi).
A_{st} = cross sectional area of steel (in^2).
$\mathrm{E_c}$ = elastic modulus of concrete (ksi).
A_c = cross sectional area of concrete (in^2).

The modulus of elasticity of concrete also decreases with increasing strain, and this value should vary over the pile length due to load-transfer. Fellenius (2001), recommended the Tangent Modulus Method be used to determine a secant modulus, E_{sm}, for load transfer evaluations of concrete piles. The tangent modulus versus measured microstrain is plotted for all strain gage levels and all load increments. As shown in Figure 9-26, a best fit line through the data determines the slope, *A*, and y-axis intercept, *B*. Following determination of the tangent modulus line from Eq. 9-9, integration is used to calculate stress in Eq. 9-10.

$$\mathrm{M}_t = \left(\frac{\Delta\sigma}{\Delta\varepsilon}\right) = A\varepsilon + B \qquad \text{Eq. 9-9}$$

$$\sigma = \left(\frac{\mathrm{A}}{2}\right)\varepsilon^2 + B\varepsilon \qquad \text{Eq. 9-10}$$

Where:

M_t = tangent modulus (ksi).
$\Delta\sigma$ = change of stress from one load increment to the next (ksi).
$\Delta\varepsilon$ = change of strain from one load increment to the next.
A = slope of tangent modulus line.
ε = strain measured in gage.
B = Y-intercept of the tangent modulus line.
σ = stress (ksi).

Through the use of Hooke's law, the secant modulus is related to stress and strain in Eq. 9-11. By substituting terms from Eq. 9-10, the secant modulus can be expressed as shown in Eq. 9-12.

$$\sigma = \mathrm{E}_{sm}\varepsilon \qquad \text{Eq. 9-11}$$

$$\mathrm{E}_{sm} = 0.5\,A\,\varepsilon + B \qquad \text{Eq. 9-12}$$

Where:

σ = stress (ksi).
E_{sm} = secant modulus (ksi).
ε = strain measured in gage.
A = Slope of tangent modulus line.
B = Y-intercept of the tangent modulus line.

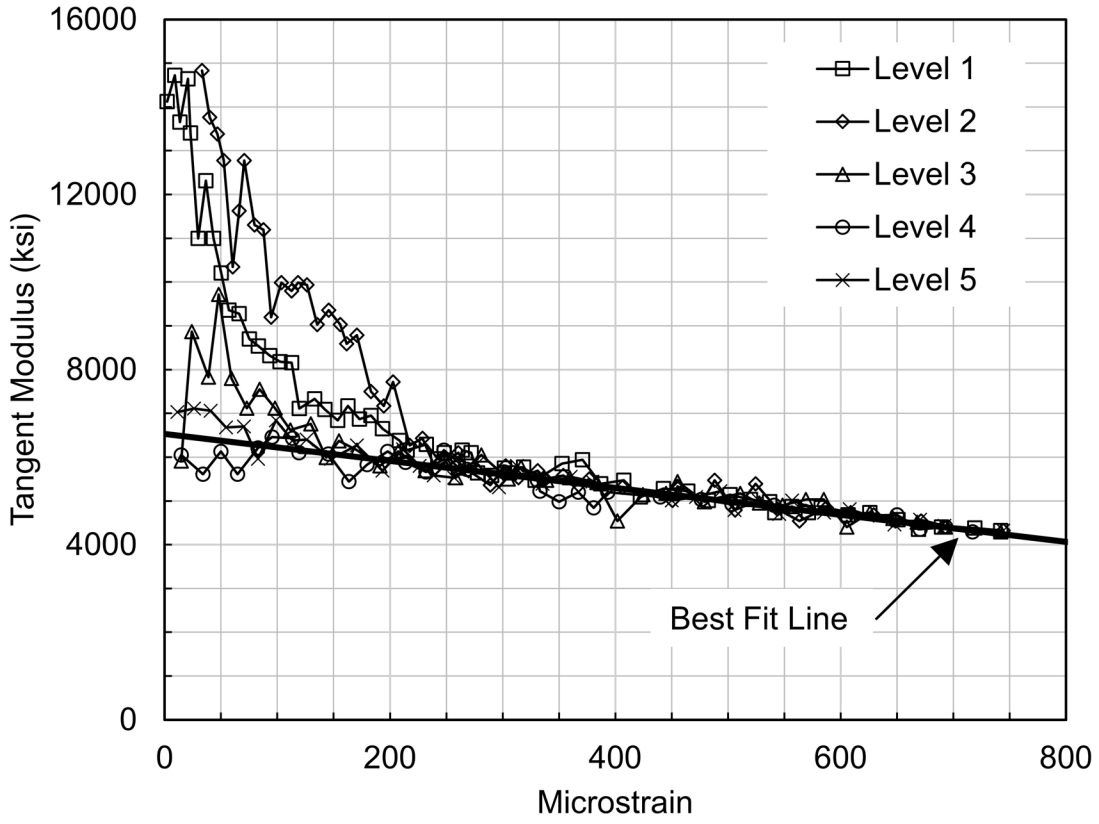

Figure 9-26 Tangent modulus method for determining elastic modulus (modified from Fellenius 2001).

Once the modulus for the pile material is determined, Eq. 9-7 can be used to determine the force or load at a given depth. A plot of axial load versus elevation from a static load test is presented in Figure 9-27. In this figure, seven embedded gages were installed to provide a detailed load transfer evaluation for a 14 inch diameter, concrete filled, steel pipe pile. The load transferred to the soil can be calculated from the difference in force between selected measurement locations. For example, when utilizing the final load increment, 16.3 tons of load (e.g. 53.9 tons - 37.6 tons equals 16.3 tons) is transferred to the soil between the strain gages located at elevations EL 549.7 and EL 537.4. The pile in Figure 9-27 is 3.67 feet in

circumference, and because the final two strain gages are located 12.3 feet apart, the unit shaft resistance over this interval is 16.3 tons divided by 45.1 ft^2 (12.3 feet times 3.67 feet) or 0.36 tsf. It should be noted that this computation did not consider the effects of any residual load in the pile which is discussed in Section 9.5.3.

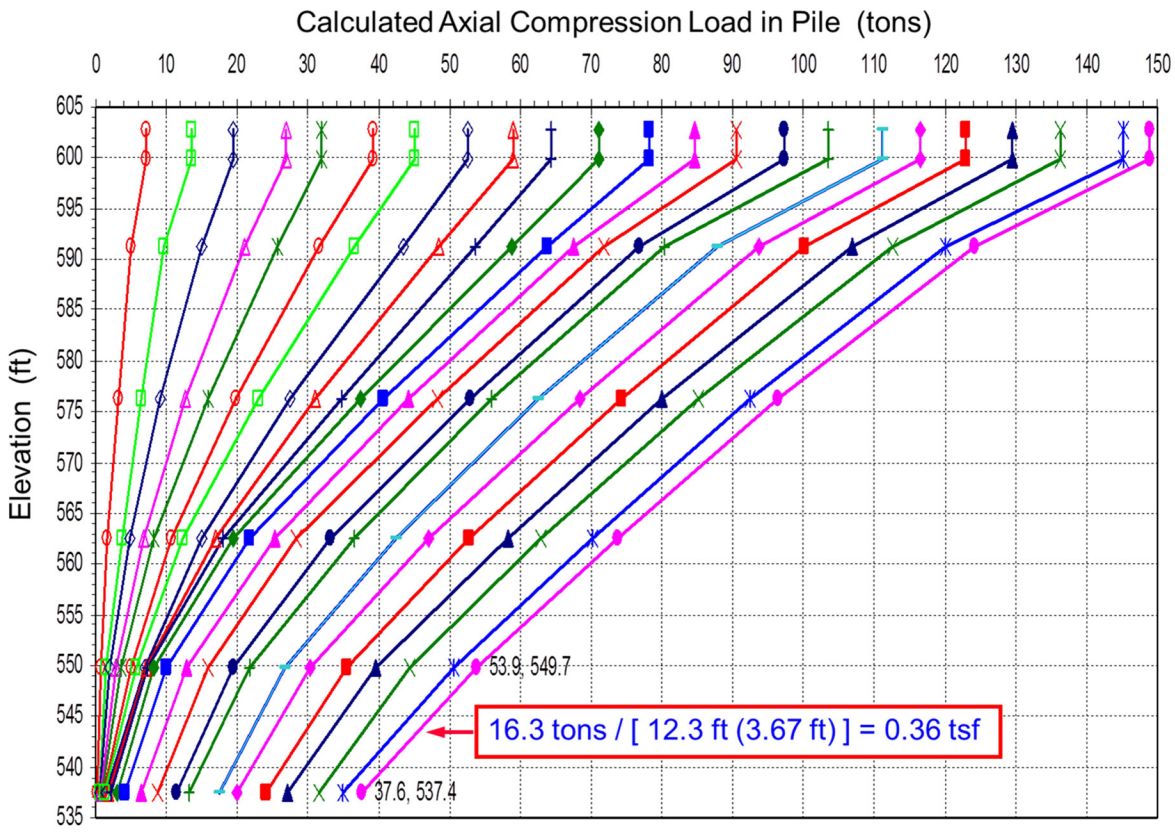

Figure 9-27 Plot of axial load versus strain gage elevation for load transfer assessment.

Unit shaft resistance values can be used to evaluate nominal resistances of other similar size and type of piles (e.g. 12 inch or 16 inch O.D. in the above case) or to refine the pile penetration depth for the required nominal resistance. When performed in the design phase, foundation design can be optimized through a more complete understanding of load transfer mechanisms in the geomaterials.

9.5.3 Determination of Residual Load

During driving, residual loads can be locked into a pile that does not completely rebound after a hammer blow (i.e. return to a condition of zero stress along its entire length). This is particularly true for flexible piles, piles with large shaft resistances, and piles with large toe quakes. Load transfer evaluations using telltale measurements described above assume that no residual loads are locked in the pile

during driving. Therefore, the load distribution calculated from Eq. 9-5 to 9-7 would not include residual loads. If measuring points R_1 and R_2 in Figure 9-20 correspond to the pile head and pile toe of a pile that has locked-in residual loads, the calculated average pile load would also include the residual loads. This would result in a lower toe resistance being calculated than actually exists as depicted in Figure 9-28.

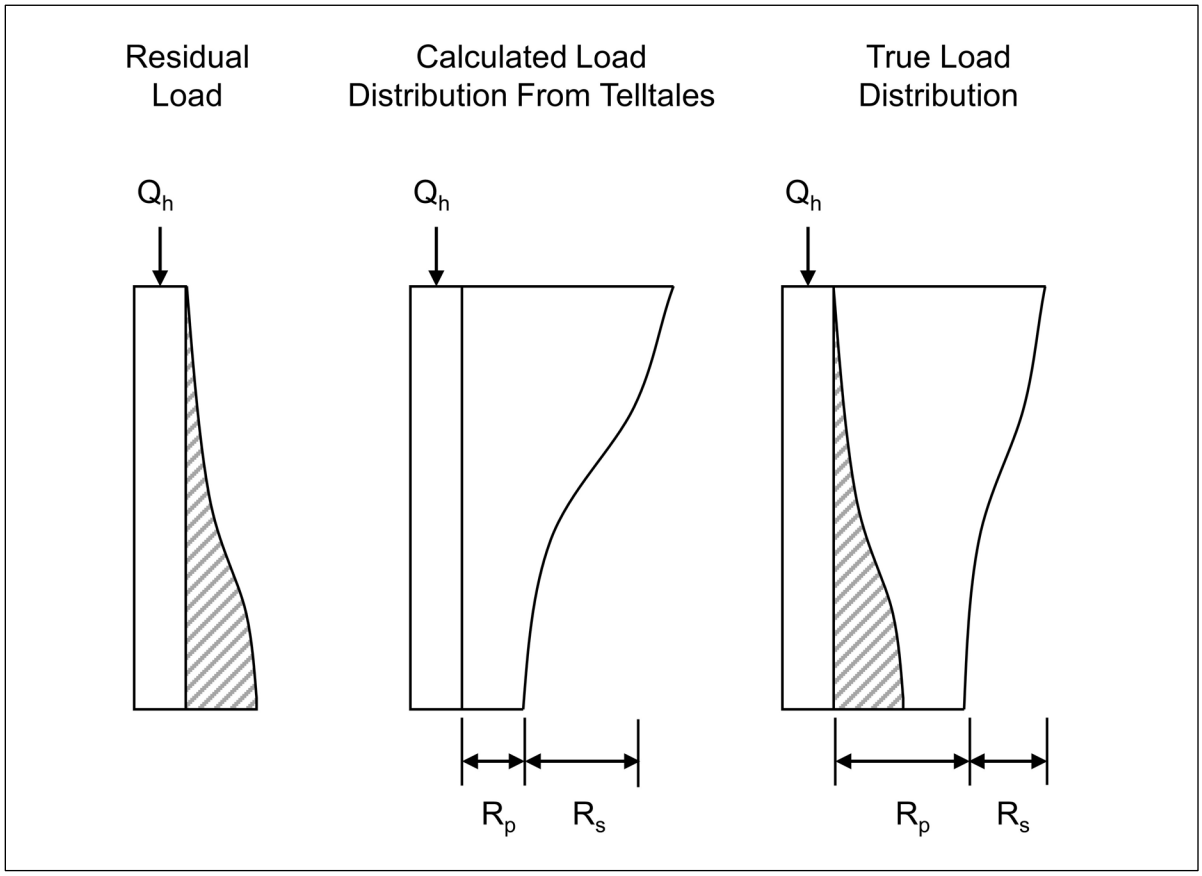

Figure 9-28 Example of residual load effects on load transfer evaluation.

In a static load test performed on a pile with residual loads, negative shaft resistance will be present along the upper portion of the pile. Figure 9-28 illustrates the minimal residual load in the upper portion of the pile which must be overcome before the true shaft resistance from the applied load can be measured. Moreover, residual loads are present along the pile shaft and at the pile toe before the static load test begins. This concept is illustrated for mobilized shaft resistance in Figure 9-29, Fellenius (2014). If no residual loads acted upon the pile prior to static load testing, Path O-B-C would represent the developed shaft resistance. However when residual loads are present, Point D is the origin of the residual load, which initially loads the pile along Path D-A. Thus, when applying load during the static load test, shaft resistance develops along Path A-O-B-C. If residual load is not accounted for, the

loading path will be thought to move through Path A-B-C, and a shaft resistance twice as large as the true shaft resistance will be measured, Fellenius (2014).

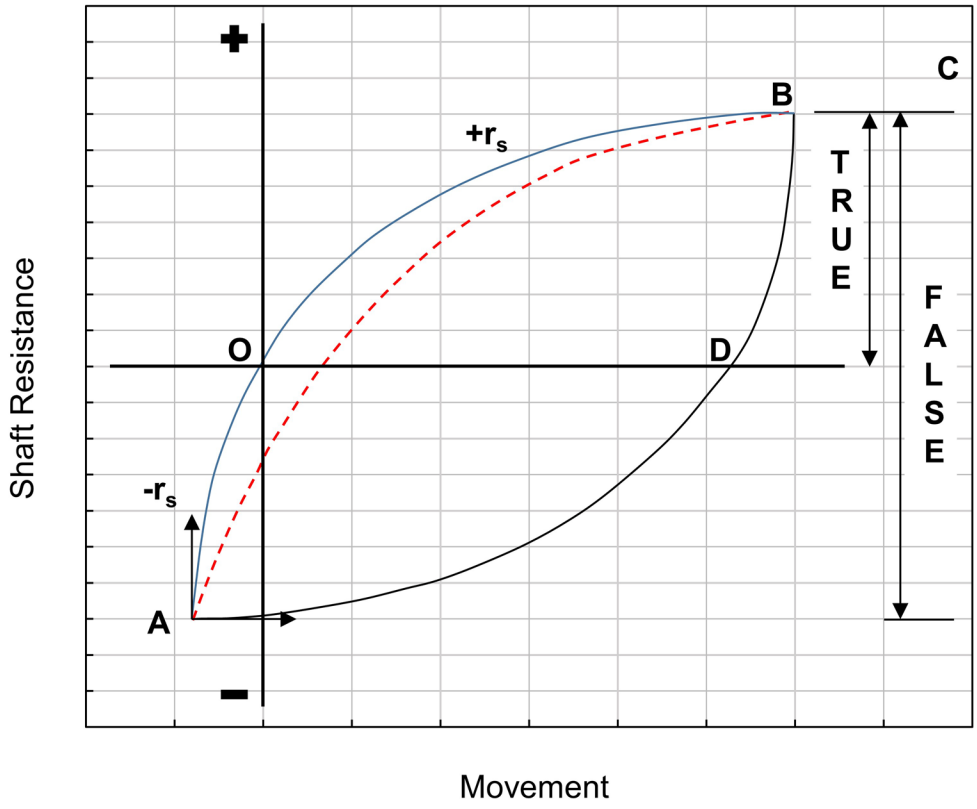

Figure 9-29 Mobilized shaft resistance hysteresis loop for pile during static load test (after Fellenius 2014).

Residual load can also develop at the pile toe. In Figure 9-30, Fellenius (2014), presents paths for toe resistance mobilization. Without the presence of residual load, toe resistance is developed along Path O-B-C. However when residual load exists within the pile, load develops along Path A-D-B-C. Toe resistance therefore develops prior to applying load during the static load test. In the above mentioned case of unloading, toe resistance is unloaded following the hysteresis loop of Path B-D'-A (when starting at Point B), where subsequent loading follows Path A-D-B-C. In summation, the residual load can result in underestimating the developed toe resistance.

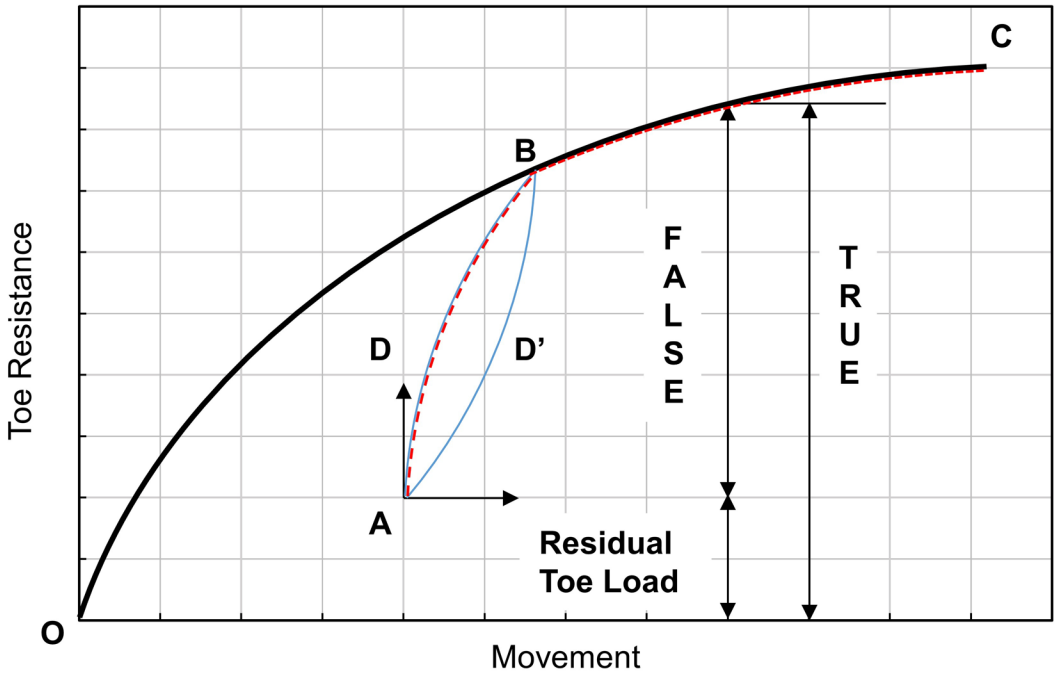

Figure 9-30 Mobilized toe resistance for pile during static load test. (after Fellenius 2014).

It is apparent from the above discussion that residual load locked into a pile can affect the apparent resistance distribution determined from a static load test. While the geotechnical nominal resistance is unaffected, the computed shaft and toe resistances are altered. Therefore, additional measures should be taken to determine the true resistance distribution and unit resistance values. This is particularly important when uplift resistance is being assessed from the shaft resistance determined in an instrumented compression load test or where unit resistance values are being used for design decisions.

Fellenius (2002b) presented a case where residual loads were evaluated from a strain gage instrumented static load test in conjunction with subsurface exploration results. When using strain gages for load-transfer in a static load test, it is important that the" zero reading" be made prior to pile installation (and for sister bars, the factory reading) such that no load exists in the pile. Fellenius et al. (2003) noted that a lower bound estimate of residual load may be obtained from the difference in strain measured just before commencement of the load test and at the true no load condition. This calculation of the residual load may however be an underestimate, in particular, when thermal strains occur in hydrating concrete.

Figure 9-31 presents strain gage instrumented static load test results for a prestressed concrete pile driven 48 feet into a loose to medium dense uniform sand. Reference should be made to Altaee et al. (1992) and Fellenius (2002b) for further details on the static load test or subsurface conditions. The “measured load” at a given depth is calculated using Eq. 9-7 and then that load subtracted from the applied pile head load to obtain the “measured load” versus depth.

In Figure 9-31 the measured load curve has an inflection point near a depth of 23 feet, and progresses downwards with increasing slope. This should not be the case in a uniform subsurface profile as it would require the unit shaft resistance to be smaller in the bottom third of the pile than in the middle portion of the pile. Therefore, residual load is likely to have influenced the true load distribution.

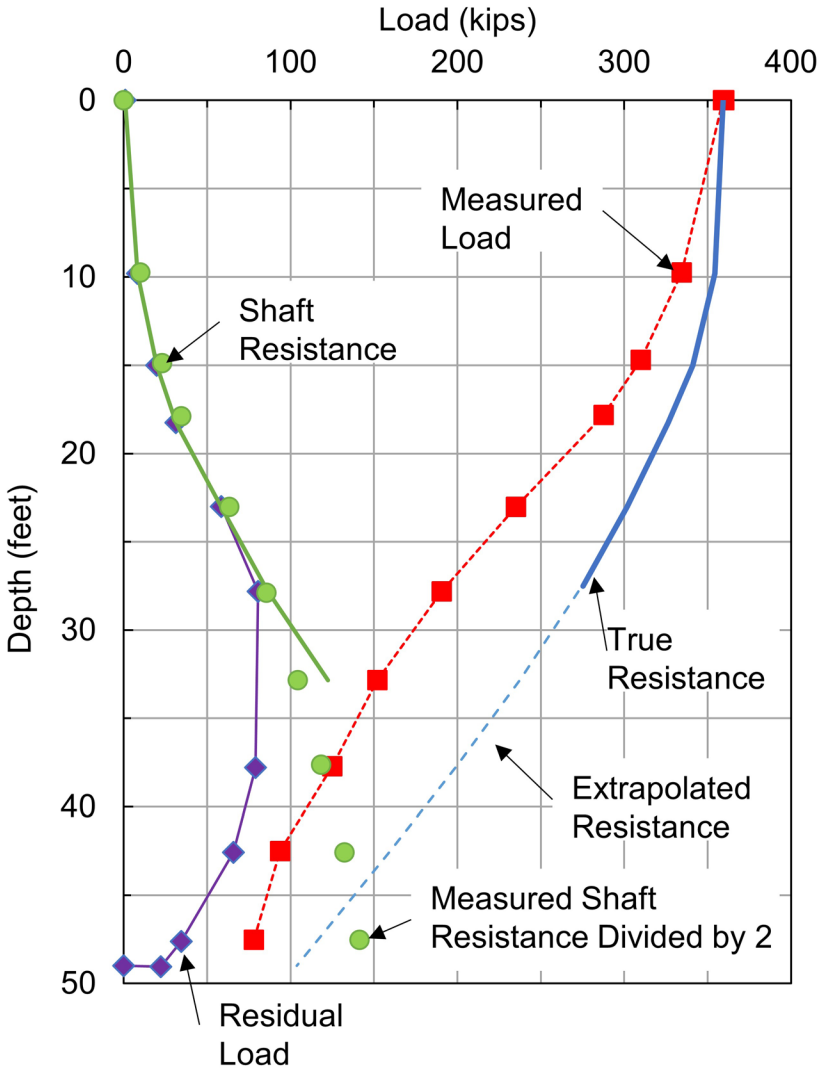

Figure 9-31 Instrumented static load test results and soil resistance distribution (modified from Fellenius 2002b with data from Altaee et al. 1992).

After plotting the measured load and calculating unit resistances along the pile, the measured shaft resistance divided by 2 (from the Measured Load) versus depth is added to the Figure 9-31 graph. The curve for the True Resistance then follows down to the inflection level (calculated as the difference in load applied at the pile head and the Measured Resistance divided by 2). Below this point, and because the uniform soil should exhibit similar shear strengths, the True Resistance curve may be extrapolated downward. In effect, it is assumed that the remaining unit shaft resistance is equal to that in the length just above this inflection, and does not follow the "false" measured values that indicate otherwise. The residual load is plotted as the difference of the True Resistance (with the extrapolated portion) and Measured Load. Engineering judgement and careful interpretation of the subsurface profile and load test results is necessary when determining residual load.

9.6 PRACTICAL ISSUES AND CONSIDERATIONS

Static load tests are the most reliable and most expensive method for determination of nominal geotechnical resistance or lateral deformation. Static load tests are sometimes avoided because of cost concerns or potential time delays in design or construction. While the economic benefits of performing a static load test should be carefully considered, cost alone should not be the deciding factor. Load transfer information from axial tests or deflected shape versus depth behavior in lateral load tests is extremely valuable when performed and evaluated by knowledgeable instrumentation specialists who should be involved in static load test program development and implementation.

Delays to a project in the design or construction stage usually occur when the decision to perform static load tests is added late in the project. During a design stage program, delays can be minimized by determining early in the project whether a static load test program should be performed. In the construction stage, delays can be minimized by clearly specifying the number and locations of static load test to be performed as well as the time necessary for the engineer to review the results. In addition, the specifications should state that the static load test must be performed prior to ordering pile lengths or commencing production driving. In this way, the test results are available to the design and construction engineer early in the project so that the maximum benefits can be obtained. At the same time the contractor is also aware of the test requirements and analysis duration and can schedule the project accordingly.

Fellenius (1984) reported on a static load test where the initial test was performed with the load determined from a load cell and jack pressure gage. In this test, the

load determined from the load cell exceeded the load from the jack pressure gage and the accuracy of the test was in question. A second load test was performed after replacing the load cell and recalibrating the jack and load cell system. A comparison of the load from the jack and load cell in the second test is shown in Figure 9-32. The load determined from the jack pressure gage exceeded the load determined by the load cell by 10 to 20% in loading and underestimated the load by 5% in unloading. When load cell and jack pressure readings do not agree, the source of the discrepancy should be determined and the load test rerun if needed.

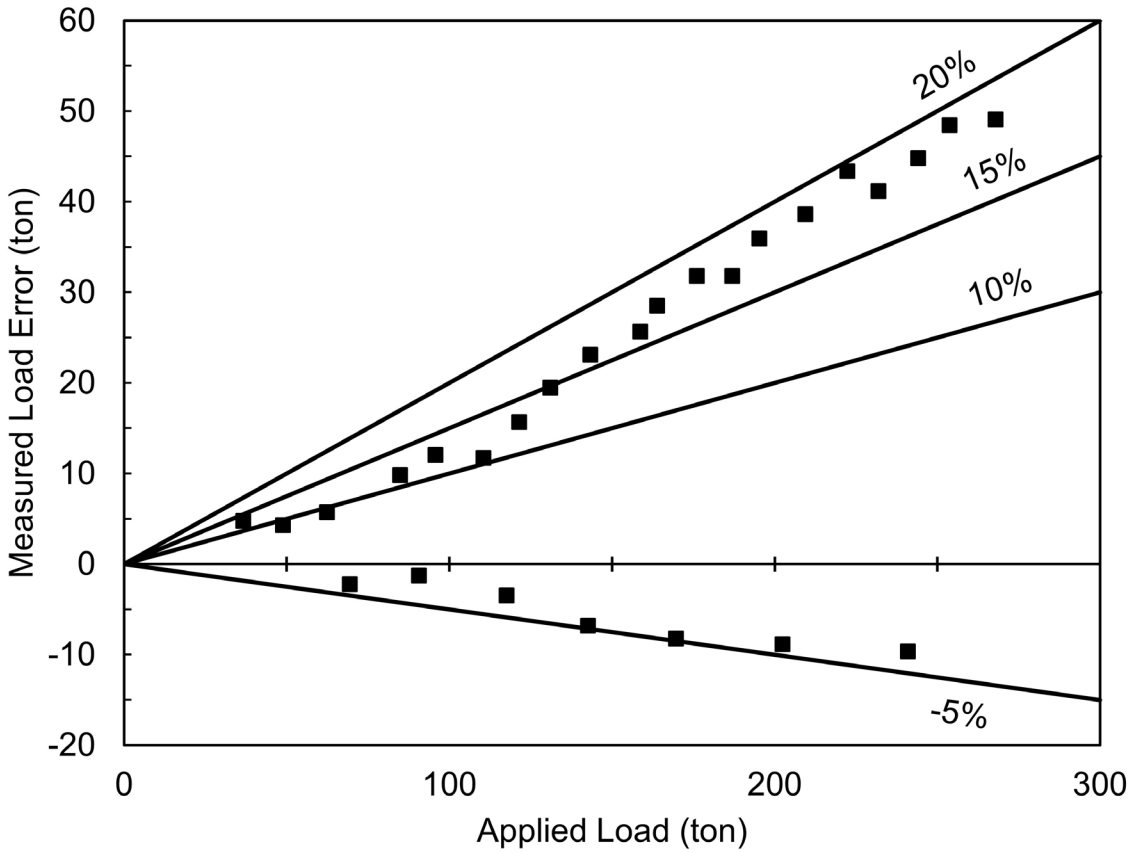

Figure 9-32 Variation between applied pile head load determined from load cell and jack pressure gage (after Fellenius 1984).

Load cells and jacks should also be properly sized to reduce measurement errors in the applied load. Geokon (2013) noted load cell error typically occurs if the load cell and hydraulic jack piston are not equal in diameter. The thickness of the bearing plates can further compound loading error, especially if the plate(s) is not sufficiently thick to reduce bending effects. In the Geokon study, three jack piston sizes were used while retaining the same load cell of size 4 inch I.D., 5-3/4 inch O.D with a maximum load of 300 kips. Furthermore, electrical resistance strain gages were bonded to the load cell's middle outside circumference, Sellers (2015). Jack A had

dimensions of 2 inch I.D., 4 inch O.D., Jack B had dimensions of 4 inch I.D., 5-3/4 inch O.D., and Jack C had dimensions of 6 inch I.D, 8 inch O.D. Figure 9-33 summarizes size effects for the jack and bearing plate to the load cell response.

Jack		Load Cell response to applied load (100%)	
		1" thick plate	2" thick plate
A (smaller)	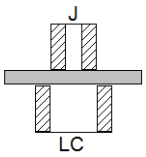	108%	102%
B (same size)	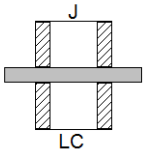	100%	100%
C (bigger)	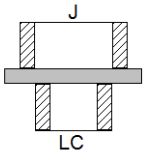	96%	98%

Figure 9-33 Load cell response based on jack and bearing plate size (after Geokon 2013).

9.7 ADVANTAGES, DISADVANTAGES, AND LIMITATIONS

The advantages of performing static load tests are summarized below.

1. A static load test allows a more rational design. Confirmation of geomaterial resistance through static load testing is considerably more reliable than resistance estimates from static analyses and dynamic formulas.

2. An improved knowledge of pile-soil behavior is obtained that may allow a reduction in pile lengths or an increase in the factored pile load, either of which may result in potential savings in foundation costs.

3. With the improved knowledge of pile-soil behavior, a higher resistance factor may be used on the determined nominal resistance. Resistance factors between 0.75 and 0.80 are recommended when static load tests are utilized, as compared to a resistance factor of 0.40 when using the Modified Gates dynamic formula. Hence, a cost savings potential again exists.

4. The nominal resistance determined from load testing allows confirmation that the factored load may be adequately supported at the planned pile penetration depth.

Disadvantages include the load test cost, the time required to setup and perform a test, as well as the time required for complete result interpretation (particularly for tests with load transfer data). In addition, minimal information is obtained on driving stress levels or on the extent of pile damage (if any). Static load test results can also be misleading on projects with highly variable soil conditions. Site size and variability should therefore be considered when relying upon results for a single test pile.

As for limitations, static load test results cannot be used to account for long-term settlement, downdrag from consolidating and settling soils, or to adequately represent pile group action.

REFERENCES

Abu-Hejleh, N., DiMaggio, J.A., Kramer, W.M., Anderson, S., and Nichols, S. (2010). Implementation of LRFD Geotechnical Design for Bridge Foundations: Reference Manual. FHWA-NHI-10-039. National Highway Institute, Federal Highway Administration, Washington, D.C., 82 p.

Abu-Hejleh, N., Abu-Farsakh, M., Suleiman, M.T., Tsai, C. (2015). State Practices in Databases for Deep Foundation Load Tests. GSP 256: Proceedings of the International Foundations Conference and Equipment Exposition 2015. San Antonio, TX, pp. 237-246.

Altaee, A., Fellenius, B.H., and Evgin E. (1992). Axial Load Transfer for Piles in Sand. I: Tests on an Instrumented Precast Pile. Canadian Geotechnical Journal, Vol. 29, No. 1, pp. 11-20.

American Association of State Highway and Transportation Officials (AASHTO). (2014). AASHTO LRFD Bridge Design Specifications, US Customary Units, Seventh Edition, with 2015 Interim Revisions. American Association of State Highway and Transportation Officials, Washington, D.C., 1960 p.

ASTM D1143-07. (2014). Standard Test Methods for Deep Foundations Under Static Axial Compressive Load. Book of ASTM Standards, Vol. 4.08, ASTM International, West Conshohocken, PA, 15 p.

ASTM D3689-07. (2014). Standard Test Methods for Deep Foundations Under Static Axial Tensile Load. Book of ASTM Standards, Vol. 4.08, ASTM International, West Conshohocken, PA, 13 p.

ASTM D3966-07. (2014). Standard Test Methods Deep Foundation Under Lateral Load. Book of ASTM Standards, Vol. 4.08, ASTM International, West Conshohocken, PA, 18 p.

Cheney, R.S. and Chassie, R.G. (2000). Soils and Foundations Workshop Reference Manual. FHWA HI-00-045, U.S. Department of Transportation, National Highway Institute, Federal Highway Administration, Washington, D.C., 358 p.

Crowther, C.L. (1988). Load Testing of Deep Foundations: the Planning, Design, and Conduct of Pile Load Tests. John Wiley & Sons, New York, NY, 233 p.

Davisson, M.T. (1972). High Capacity Piles. Proceedings, Soil Mechanics Lecture Series on Innovations in Foundation Construction, American Society of Civil Engineers, ASCE, Illinois Section, Chicago, IL, pp. 81-112.

Dunnicliff, J. (1988). Geotechnical Instrumentation for Monitoring Field Performance. John Wiley & Sons, New York, NY, pp. 467-479.

Fellenius, B.H. (1984). Ignorance is Bliss – and That is Why We Sleep so Well. Geotechnical News Magazine, Vol. 2, No. 4, pp. 14-15.

Fellenius, B.H. (1990). Guidelines for the Interpretation of the Static Loading Test. Deep Foundations Institute Short Course Text, First Edition, 44 p.

Fellenius, B.H. (2001). From Strain Measurements to Load in an Instrumented Pile. Geotechnical News Magazine, Vol. 19, No. 1, pp. 35-38.

Fellenius, B.H. (2002a). Determining the Resistance Distribution in Piles. Part 1: Notes on Shift of No-Load Reading and Residual Load. Geotechnical News Magazine, Vol. 20, No. 2, pp. 35-38.

Fellenius, B.H. (2002b). Determining the Resistance Distribution in Piles. Part 2: Method for Determining the Residual Load. Geotechnical News Magazine, Vol. 20, No. 3, pp. 25-29.

Fellenius, B.H., Harris, D., and Anderson, D.G. (2003). Static Loading Test on a 45 m Long Pipe Pile in Sandpoint, Idaho. Canadian Geotechnical Journal, Vol.41, No. 4, pp. 613-628.

Fellenius, B.H. (2014). Basics of Foundation Design. Electronic Edition. www.Fellenius.net, 410 p.

Fuller, F.M. (1983). Engineering of Pile Installations. McGraw-Hill, New York, NY, 286 p.

Geokon (2013) Load Cell Instruction Manual, Appendix C, Load Cell Calibrations – Effects of Bearing Plate Warping, Lebanon, NH, pp. 18-20.

Komurka, V.E. (2015). Personal communication.

Kyfor, Z.G., Schnore, A.S., Carlo, T.A. and Bailey, P.F. (1992). Static Testing of Deep Foundations. Report No. FHWA-SA-91-042, U.S. Department of Transportation, Federal Highway Administration, Office of Technology Applications, Washington, D.C., 174 p.

New York State Department of Transportation (NYSDOT). (2007). Static Pile Load Test Manual, Geotechnical Engineering Bureau, GCP-18, Revision #3, www.dot.ny.gov, 55 p.

Paikowsky, S.G. (2004), with contributions from Birgisson, B., McVay, M., Nguyen, T., Kuo, C., Baecher, G., Ayyub, B., Stenersen, K., O.Malley, K., Chernauskas, L., and O'Neill, M., Load and Resistance Factor Design (LRFD) for Deep Foundations, NCHRP Report 507. Transportation Research Board, Washington, D.C., 76 p.

Reese, L.C. (1984). Handbook on Design of Piles and Drilled Shafts Under Lateral Load. Report No. FHWA-IP-84-11, U.S. Department of Transportation, Federal Highway Administration, Office of Implementation, McLean, VA, 386 p.

Rollins, K., Gerber, T., and Cummins, C. (2009). Monitoring Displacement vs. Depth in Lateral Pile Load Tests with Shape Accelerometer Arrays, Proceedings of the Seventeenth International Conference on Soil Mechanics & Geotechnical Engineering, Alexandria, Egypt, Oct. 5-9, 2009. Vol.3, pp. 2016-2019.

Sellers, B. (2015). Personal communication.

Smith, T., Banas, A., Gummer, M., and Jin, J. (2011). Recalibration of the GRLWEAP LRFD Resistance Factor for Oregon DOT. Publication No. OR-RD-98-00, Oregon Department of Transportation, Research Unit, Salem, OR, 82 p.

CHAPTER 10

DYNAMIC TESTING AND SIGNAL MATCHING ANALYSIS

Dynamic test methods use measurements of strain and acceleration taken near the pile head as a pile is driven or restruck with a pile driving hammer. These dynamic measurements can be used to determine the performance of the pile driving system, calculate pile installation stresses, assess pile integrity, and evaluate the nominal geotechnical resistance.

Dynamic test results should be further evaluated using signal matching techniques to determine the relative soil resistance distribution on the pile, as well as dynamic soil properties for use in wave equation analyses. This chapter provides a brief discussion of dynamic test equipment and analysis methods.

10.1 BACKGROUND

Work on the development of the dynamic pile testing techniques that have become known as the Case Method started with a Master thesis project at Case Institute of Technology. This work was done by Eiber (1958) at the suggestion and under the direction of Professor H.R. Nara. In this first project, a laboratory study was performed in which a rod was driven into dry sand. The Ohio Department of Transportation (ODOT) and the Federal Highway Administration subsequently funded a project with HPR funds at Case Institute of Technology beginning in 1964. This project was directed by Professors R.H. Scanlan and G.G. Goble. The research work under the direction of Professor Goble continued to be funded by ODOT and FHWA, as well as several other public and private organizations until 1976.

Four principal directions were explored during the 12 year period that the funded research project was active. There was a continuous effort to develop improved transducers for the measurement of force and acceleration during pile driving. Field equipment for recording and data processing was also continually improved. Model piles were driven and tested both statically and dynamically at sites in Ohio. Full scale piles driven and statically tested by ODOT, and later other transportation agencies, were also tested dynamically to obtain nominal resistance correlations. Finally, analysis method improvements were developed, including both field

solutions (Case Method) in the Pile Driving Analyzer system (PDA) and an associated signal matching technique (CAse Pile Wave Analysis Program or CAPWAP). Additional information on the research project and its results may be found in Goble and Rausche (1970), Rausche et al. (1972), and Goble et al. (1975).

ODOT began to apply the results of this research to their construction projects in about 1968. Commercial use of the methods began in 1972 when the test equipment and analysis methods became practical for use in routine field testing by a trained engineer. Further implementation of dynamic testing methods in the 1980's resulted from FHWA Demonstration Project 66, in which additional correlation data was collected, and method benefits were demonstrated on transportation projects throughout the US.

Dynamic testing equipment and signal matching software have continued to be improved and enhanced over the 40 years since its original development. Other dynamic testing and analysis systems have also developed during that time period, primarily in Europe. One of the early European systems was advanced by the Netherlands Organization for Applied Scientific Research (TNO). This group developed the FPDS equipment and its associated signal matching technique, TNOWAVE, Reiding et al. (1988). Additional dynamic testing and analysis systems have also emerged over time including the Embedded Data Collector (EDC), Hererra et al. (2009), as well as the PDR dynamic testing system and Allwave-DLT signal matching software, Middendorp and Verbeek (2010).

10.2 APPLICATIONS FOR DYNAMIC TESTING METHODS

Samtani and Nowatzki (2006) note that dynamic testing costs much less and requires less time than static pile load testing. They also note that important information can be obtained regarding the behavior of the pile driving system and pile-soil response that is not available from a static pile load test. Determination of driving stresses and pile integrity with dynamic test methods has resulted in fewer, higher nominal resistance piles in foundation designs due to better pile installation control. Some of the applications for dynamic testing methods are discussed below.

10.2.1 Nominal Resistance

a. Assessments of nominal geotechnical resistance versus pile penetration depth can be obtained by testing from the start to the end of driving. This can

be helpful in profiling the depth to the bearing stratum and thus the required production pile lengths.

b. Evaluation of the nominal geotechnical resistance at the time of testing. Soil setup or relaxation potential can be assessed by restrike testing several piles and comparing nominal resistance at restrike with that at end-of-initial driving.

c. Signal matching analysis provides refined estimates of nominal resistance, the soil resistance distribution, as well as insight into soil quake and damping parameter selection for wave equation analyses. Signal matching and wave equation analysis programs have different pile and soil models. Therefore, signal matching determined dynamic soil parameters may require adjustment, as described in Section 12.6.9, for input in wave equation analysis programs.

10.2.2 Hammer and Driving System Performance

a. Calculation of energy transferred to the pile for comparison with the manufacturer's rated energy and/or wave equation predictions of hammer and drive system performance. Energy transfer can also be used to determine the effect of changes in hammer cushion or pile cushion materials on the pile penetration resistance or blow count.

b. Determination of drive system performance under different hammer strokes, operating pressures, batter angles, or changes in hammer maintenance by comparative testing of hammers, or of a single hammer over an extended period of use.

c. Identification of hammer performance issues, such as pre-ignition problems with diesel hammers or preadmission in air/steam hammers.

d. Determination of whether soil behavior or hammer performance is responsible for changes in the observed penetration resistance or blow count.

10.2.3 Driving Stresses and Pile Integrity

a. Calculation of compression and tension driving stresses. In cases with driving stress problems, this information can be helpful when evaluating adjustments to pile installation procedures. Calculated stresses can also be compared to specified driving stress limits.

b. Determination of the extent and location of pile structural damage, Rausche and Goble (1979). Thus, costly extraction may not be necessary to confirm or quantify damage suspected from driving records.

c. Compression and tension stress distribution throughout the pile obtained from signal matching.

10.3 RESISTANCE FACTORS FOR DYNAMIC TESTING

AASHTO (2014) design specifications provide resistance factors for dynamic pile testing with signal matching. When the driving criteria is established by dynamic testing with signal matching on two piles per site condition, but no less than 2% of the production piles, the AASHTO specified resistance factor is 0.65. When the driving criteria is established by dynamically testing with signal matching on 100% of the production piles, the AASHTO specified resistance factor is 0.75. The AASHTO resistance factor is 0.80 when the driving criteria is established by a successful static load test of one pile per site condition in conjunction with dynamic testing with signal matching on two piles per site condition but no less than 2% of the production piles. When a dynamic test with signal matching is used for determination of the nominal resistance in axial tension, the AASHTO specified resistance factor is 0.50.

AASHTO resistance factors for dynamic testing with signal matching were originally developed from data presented in NCHRP Report 507, Load and Resistance Factor Design (LRFD) for Deep Foundations, Paikowsky (2004). The database used to develop the recommended resistance factors defined the nominal resistance determined by a static load test as the load where the static load test load-deflection curve exceeded the Davisson offset limit. Similarly, the nominal resistance from dynamic testing with signal matching was defined as the nominal resistance during restrike determined by the CAPWAP signal matching program. If a different static load test interpretation criterion or a different signal matching analysis method is used, modification or local calibration of the resistance factor should be considered.

The Florida Department of Transportation sponsored a research effort by McVay and Wasman (2015) to determine the resistance factor for dynamic tests performed with the Embedded Data Collector (EDC) system. Resistance factors were calculated using First Order Second Moment (FOSM) principles, and using the UF and the Tran methods. The research study recommended that the calculated resistance values be considered as preliminary due to the limited size of the database.

10.4 DYNAMIC TESTING

A typical dynamic testing system consists of a minimum of two strain transducers and two accelerometers. The reusable gages are externally bolted to diametrically opposite sides of the pile at a location two to three diameters below the pile head. These gages measure strain and acceleration, and account for non-uniform hammer impacts and pile bending.

Two diametrically opposite mounted strain transducers are required for a valid dynamic test to average out and compensate for the influence of non-uniform impacts and bending. All driven pile types (prestressed concrete piles; steel pipe, H, Monotube, and Tapertube piles; timber piles; and composite piles) can be easily tested using external gages with the pile preparation and gage attachment procedures varying slightly for each pile type.

Figure 10-1 illustrates the typical pile preparation procedures required for dynamic testing using a reusable external gage system. In Figure 10-1(a), a prestressed concrete pile is being prepared for external gage attachment using a hammer drill to create holes in the concrete. The holes for the strain transducers are drilled through a template to maintain location tolerance. Concrete anchors are then set into the drilled holes and the gages are bolted to the concrete anchors. Removal of the concrete dust remaining in the drilled holes prior to setting the concrete anchors improves anchor bond with the concrete. For steel pipe, Monotube, and Tapertube piles, diametrically opposite holes are drilled into the steel as shown in Figure 10-1(b) and tapped. External gages are then attached using high strength bolts inserted in the threaded holes. For steel H-piles, holes are drilled holes through the web as shown in Figure 10-1(c) and bolts are used to attach gages on both opposite web faces. Wood lag screws are used to attach external gages on timber piles.

Pile preparation and gage attachment typically requires 15 to 20 minutes for each pile to be tested. After the gages are attached, the pile driving or restrike process continues following usual procedures. For restrike tests, the pile can be drilled and gages attached at any convenient location 2 or more diameters below the pile head. Drilling near the pile head or reusing the original gage holes at that location is not necessary. Most restrike tests are typically on the order of 20 blows or less.

Figure 10-1 Pile preparation for dynamic testing.

A photograph of an externally mounted accelerometer, strain transducer, and Wi-Fi transmitter bolted to a steel H-pile is shown in Figure 10-2(a). Signals can be transmitted from these gages either via the Wi-Fi transmitter shown, or by a splitter cable and main cable that collects and transfers signals from the individual gages. System manufacturers also offer a combined strain transducer and accelerometer as shown mounted on a pipe pile in Figure 10-2(b). The transmitter or signal collection cable is not visible in the photograph. Dynamic test records from either gage arrangement are acquired for every hammer blow and transmitted wirelessly or by main cable to the data acquisition system.

On concrete piles, dynamic testing can be performed using either reusable external gages or embedded gages. An embedded gage set typically consists of one strain transducer and one accelerometer cast into the pile at a distance of two to three diameters below the pile head. Only one strain transducer and one accelerometer is required in this situation, provided the embedded gage set is located on the central

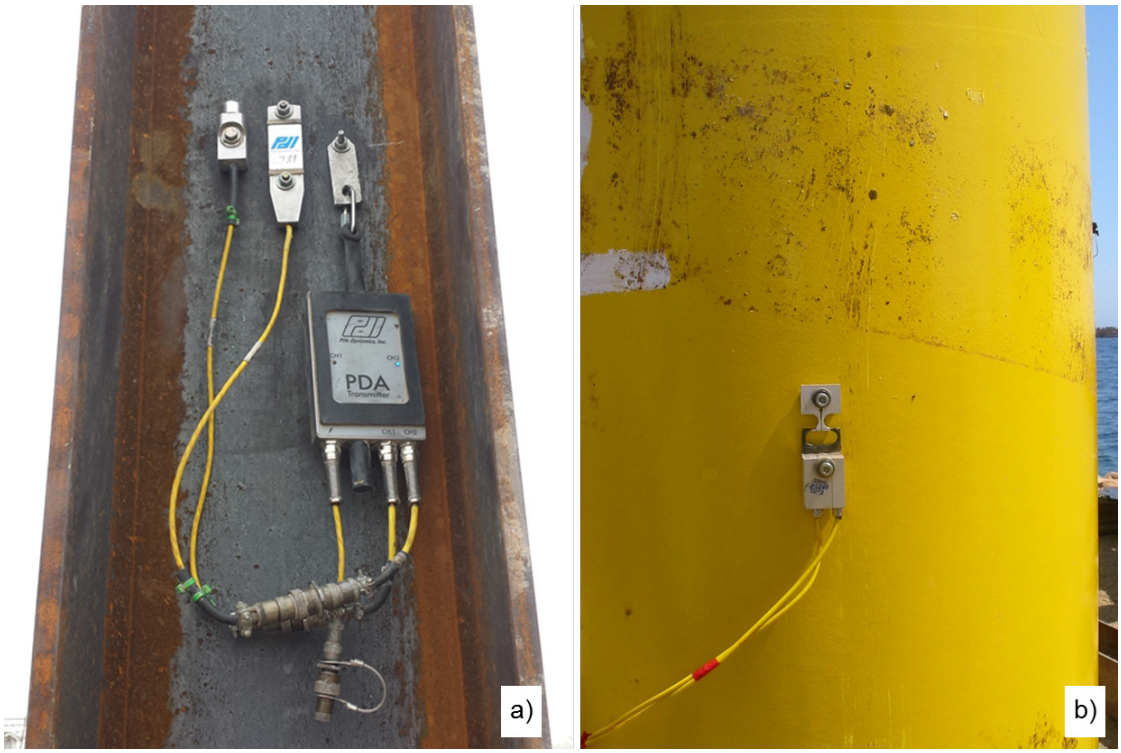

Figure 10-2 a) Accelerometer, strain gage, and WiFi transmitter (courtesy Pile Dynamics) and b) combined strain gage and accelerometer (courtesy Allnamics).

axis of the pile, such that bending and non-uniform impacts are eliminated. Non-uniform concrete piles, such as those with voided center sections, complicate use of embedded gages if the change in cross section occurs near the embedded gage location. Embedded gages should be located at least one diameter from the cross sectional change. An external gage system with the gages placed on the voided section below the cross section change is recommended in this situation and for concrete cylinder piles where a central axis gage location is not possible.

An embedded gage system consisting of a strain transducer and accelerometer being cast into a concrete pile is shown in Figure 10-3. The object on the right side sitting atop the casting bed houses the transmitter which will be cast flush mounted into the pile surface. The wire on the left side connects the transmitter to a second embedded gage set cast into the pile near the pile toe.

Figure 10-4 illustrates another embedded gage arrangement consisting of a sister bar mounted strain gage and accelerometer being cast into a concrete pile. Two diametrically opposite sister bar mounted strain gages are also shown in the figure. The additional diametrically opposite sister bar strain gages are not standard and were installed for measurement comparison with the center mounted gage.

Figure 10-3 Embedded strain gage and accelerometer unit being cast into concrete pile (courtesy Radise International).

Figure 10-4 Embedded resistance strain gage and accelerometer mounted on sister bar being cast into concrete pile (courtesy of Pile Dynamics, Inc.).

Embedded gages can also be cast into concrete piles at locations other than near the pile head. These additional embedded gages can be monitored during driving concurrently with gages located near the pile head for further insight into driving stresses, load transfer, or potential pile toe damage.

Depending on the dynamic testing system, data can be wirelessly sent from the pile to the processing unit using a reusable transmitter as shown in Figure 10-2(a), or using a transmitter cast into a concrete pile with the embedded gages.

The data acquisition system conditions and converts the measured strain and acceleration signals to force and velocity records versus time. The force is computed from the measured strain, ε, times the product of the pile elastic modulus, *E*, and cross sectional area, *A*, using Equation 10-1.

$$F(t) = E\,A\,\varepsilon(t) \qquad \text{Eq. 10-1}$$

Where:

$F(t)$ = force computed at the gage location at time t (kips).
E = elastic modulus of pile material (ksi).
A = pile cross sectional area (in^2).
$\varepsilon(t)$ = measured strain at time t.

The velocity is obtained by integrating the measured acceleration record over time using Equation 10-2.

$$V(t) = \int a(t)dt \qquad \text{Eq. 10-2}$$

Where:

$V(t)$ = velocity computed at gage location at time t (ft/s).
$a(t)$ = measured acceleration at gage location at time t (ft/s^2).

In most dynamic testing systems, all components for processing, storing, and displaying dynamic test signals are combined into either a dedicated field processing unit such as the Pile Driving Analyzer (PDA) shown in Figure 10-5 or a laptop computer such as the Embedded Data Collector (EDC) shown in Figure 10-6.

During driving, these systems perform integrations and all other required computations to analyze the acquired dynamic records for transferred energy, driving stresses, structural integrity, and nominal geotechnical resistance. Numerical results for user selected dynamic quantities are also displayed with each blow in real time. Basic force and velocity records as well as other results can be viewed on the system screen during the test. Processed test records are digitally stored and then used for subsequent signal matching analysis performed on-site or in the office as well as for graphical and numeric output summaries.

Figure 10-5 Pile Driving Analyzer processing unit (courtesy of Pile Dynamics, Inc.).

Figure 10-6 Embedded Data Collector system (courtesy of Radise International).

10.5 BASIC WAVE MECHANICS

This section is intended to summarize basic wave mechanics principles applicable to pile driving. Through this general overview, an understanding of dynamic testing concepts and how dynamic test results can be qualitatively interpreted can be obtained.

When a uniform elastic rod of cross sectional area, *A*, elastic modulus, *E*, and wave speed, *C*, is struck by a mass, then a force, *F*, is generated at the impact surface of the rod. This force compresses the adjacent part of the rod. Since the adjacent material is compressed, it also experiences an acceleration and attains a particle velocity, *V*. As long as there are no resistance effects on the uniform rod, the force in the rod will be equal to the particle velocity times the rod impedance, *EA/C*.

Figure 10-7(a) illustrates a uniform rod of length, *L*, with no resistance effects, that is struck at one end by a mass. Force and velocity (particle velocity) waves will be created in the rod, as shown in Figure 10-7(b). These waves will then travel down the rod at the material wave speed, *C*. At time L/C, the waves will arrive at the end of the rod, as shown in Figures 10-7(c) and 10-7(d). Since there are no resistance effects acting on the rod, a free end condition exists. A tensile wave reflection occurs at a free end which doubles the pile velocity at the free end and the net force becomes zero. The wave then travels up the rod with force of the same magnitude as the initial input, except in tension, and the velocity of the same magnitude and same sign.

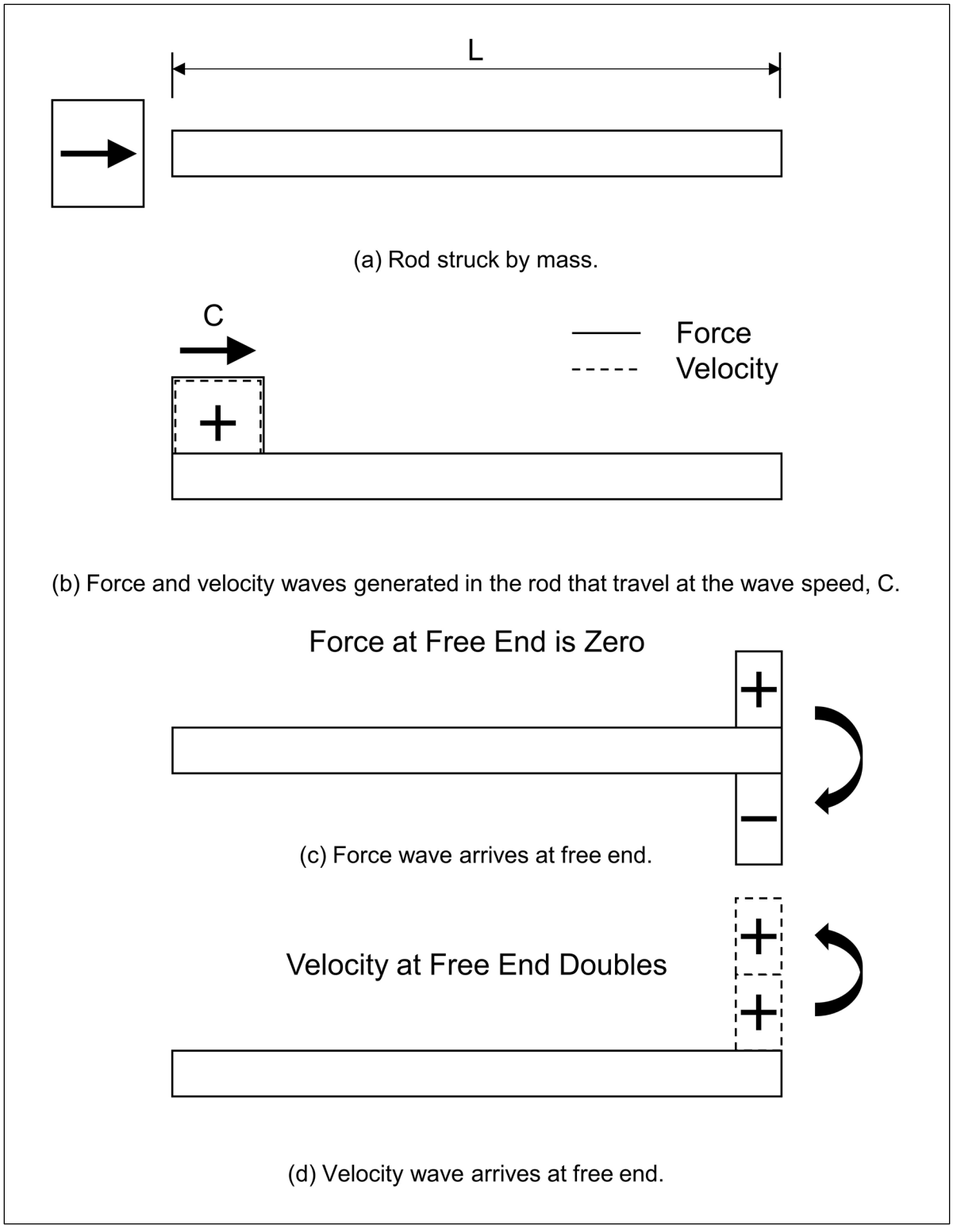

Figure 10-7 Free end wave mechanics.

Consider now that the rod is a pile with no resistance effects, and that force and velocity records are obtained from measurements made near the pile head. A typical force and velocity record versus time for this "free end" condition is presented in Figure 10-8.

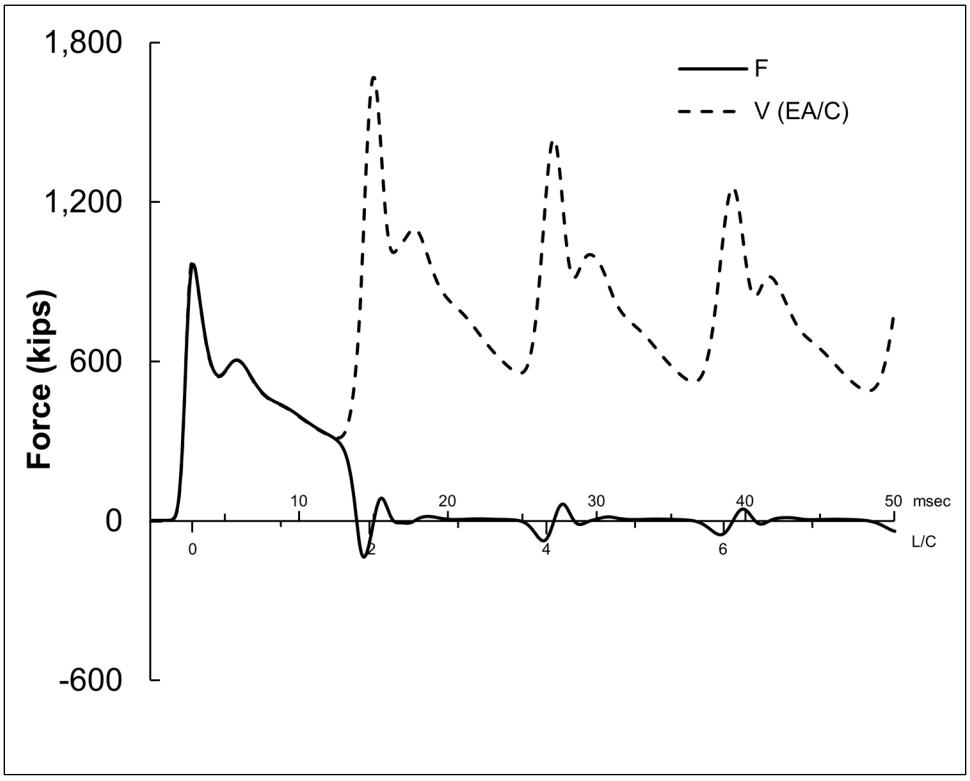

Figure 10-8 Force and velocity times (EA/C) records versus time for free end.

The toe response in the records occurs at time 2L/C. This is the time required for the waves to travel to the pile toe and back to the measurement location, divided by the wave speed. Since there are no resistance effects acting on the pile shaft, the force and velocity records are equal until the reflection from the free end condition arrives at the measurement location. At time 2L/C, the force wave goes to zero and the velocity wave doubles in magnitude. Note the repetitive pattern in the records at 2L/C intervals generated as the waves continue to travel down and up the pile. This illustration is typical of an easy driving situation where the pile "runs" under the hammer blow.

Figure 10-9(a) illustrates a uniform rod of length, *L*, struck by a mass. Again there are no resistance effects along the rod length, but the pile end is fixed, i.e., it is prevented by some mechanism from moving in such a manner that the particle velocity must be zero material wave speed, *C*. At time L/C, the waves will arrive at

the end of the rod as shown in Figures 10-9(c) and 10-9(d). There the fixed end condition will cause a compression wave reflection and therefore the force at the fixed end doubles in magnitude and the pile velocity becomes zero. A compression wave then travels up the rod.

Consider now that the rod is a pile with a fixed end condition and that force and velocity records are again obtained from measurements made near the pile head. The force and velocity records versus time for this condition are presented in Figure 10-10. Since there are no resistance effects acting on the pile shaft, the force and velocity records are equal until the reflection from the fixed end condition arrives at the measurement location. At time 2L/C, the force wave increases in magnitude and the velocity wave goes to zero. This illustration is typical of a hard driving situation where the pile is driven to rock.

As discussed above, the force and velocity records versus time are equal or proportional at impact and remain proportional thereafter until affected by soil resistance or cross sectional changes. Reflections from either effect will arrive at the measurement location at time 2X/C where X is the distance to the soil resistance or cross section change. Both soil resistance effects and cross sectional increases will cause an increase in the force record and a proportional decrease in the velocity record. Conversely, cross sectional reductions, such as those caused by pile damage, will cause a decrease in the force record and an increase in the velocity record.

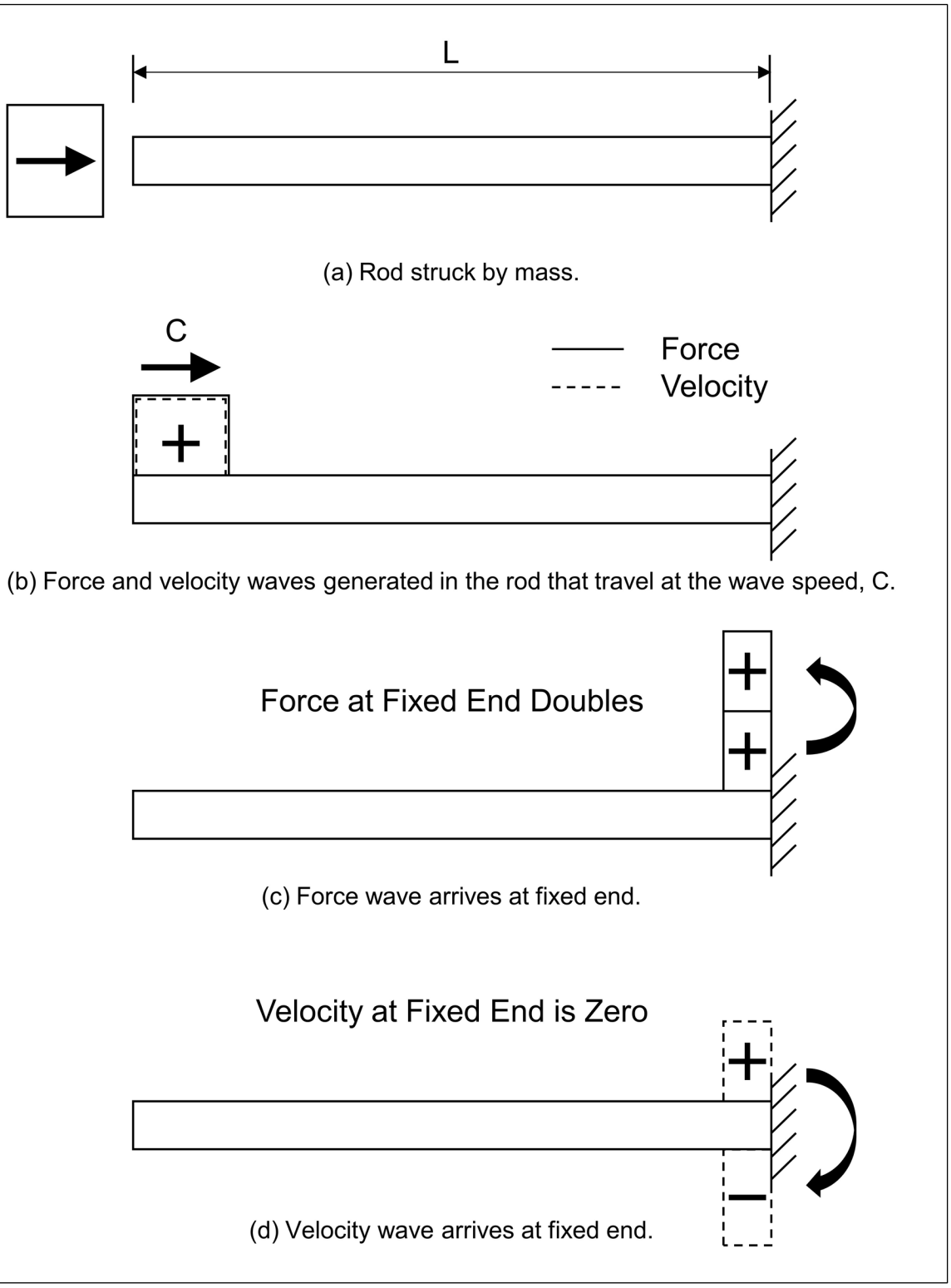

Figure 10-9 Fixed end wave mechanics.

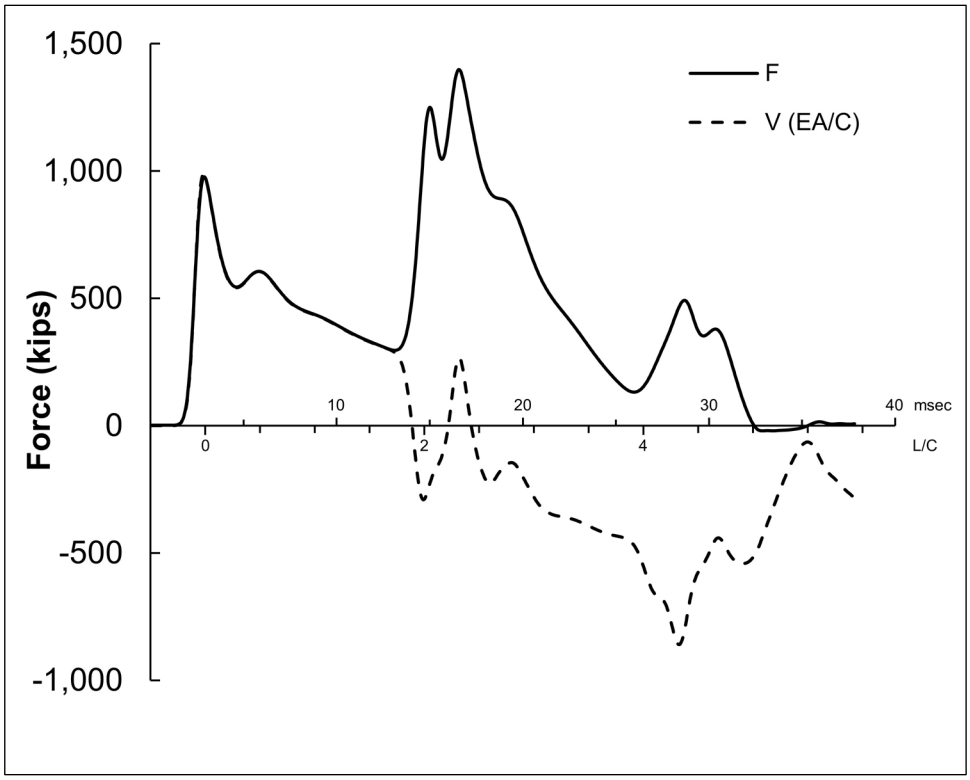

Figure 10-10 Force and velocity times (EA/C) records versus time for fixed end.

The concept of soil resistance effects on force and velocity records can be further understood by reviewing the theoretical soil resistance example presented in Figure 10-11. In this case, the soil resistance on a pile consists only of a small resistance located at a depth, A, below the measurement location, and a larger soil resistance at depth B. No other soil resistance effects act on the pile, so a free end condition is present at the pile toe.

The force and velocity records versus time for this example are presented in the lower portion of the figure. The onset of impact occurs when the force and velocity records rise together prior to time 0. The time interval from the onset of impact until the peak impact velocity is referred to as the rise time. The force and velocity records remain proportional or equal until one rise time before time 2A/C. At that time, the reflection from the small soil resistance effect begins to arrive at the measurement location. This soil resistance reflection causes the small increase in the force record and the small decrease in the velocity record at time 2A/C.

No additional soil resistance effects act on the pile between time 2A/C and time 2B/C. Therefore, the force and velocity records will remain parallel over this time interval with no additional separation. At one rise time prior to time 2B/C, the

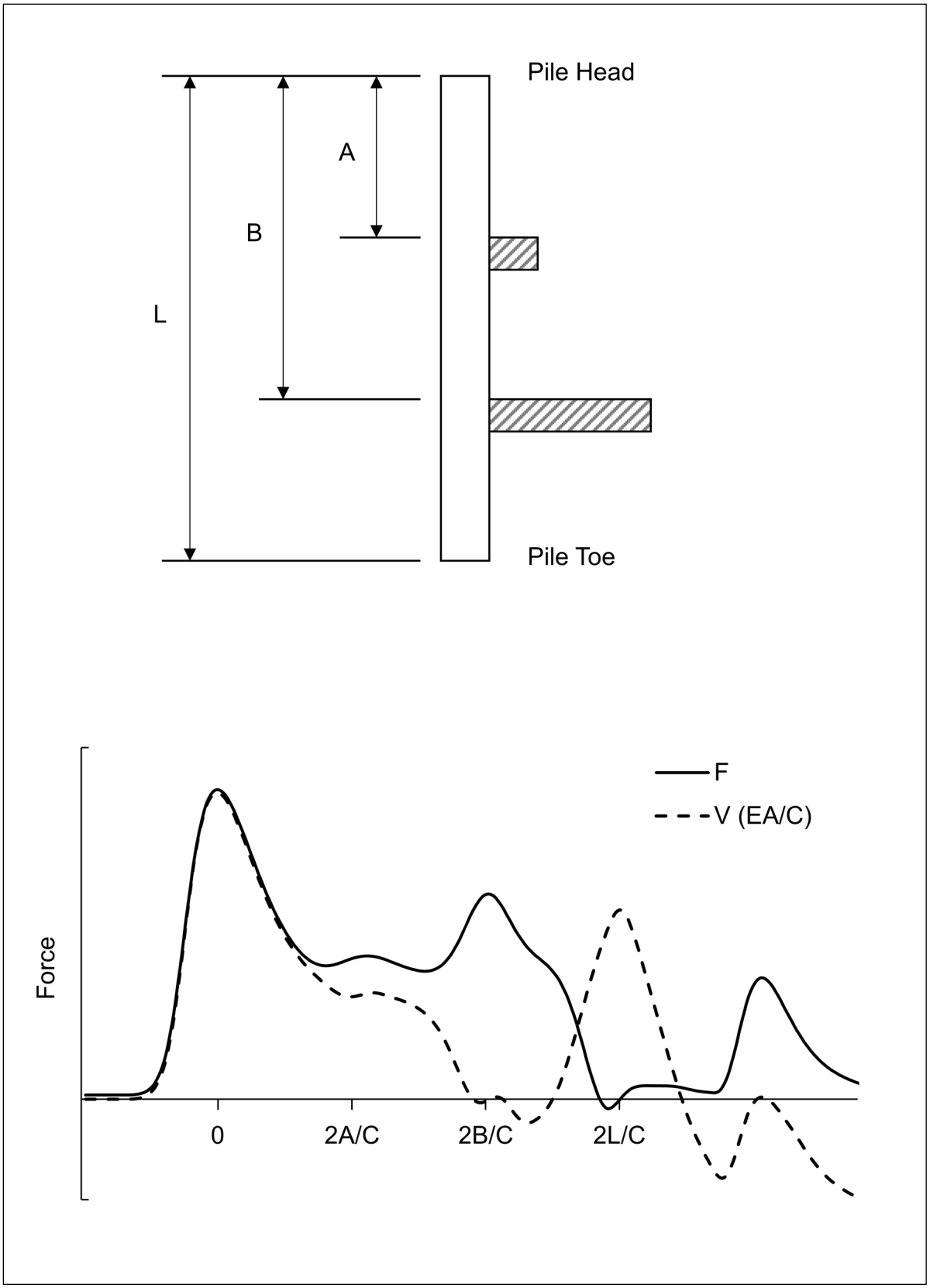

Figure 10-11 Soil resistance effects on force and velocity records (after Hannigan 1990).

reflection from the large soil resistance effect will begin to arrive at the measurement location. This large soil resistance reflection then causes the large increase in the force record and the large decrease in the velocity record at time 2B/C. No additional soil resistance effects act on the pile between time 2B/C and time 2L/C. Therefore, the force and velocity records exhibit no additional separation over this time interval.

At one rise time before time 2L/C, the reflection from the pile toe will arrive at the measurement location. Since no resistance is present at the pile toe, a free end condition exists, and a tensile wave is reflected. Hence, an increase in the velocity record and a decrease in the force record occurs.

These basic interpretation concepts of force and velocity records versus time can be used to qualitatively evaluate the soil resistance effects on a pile. In Figure 10-12(a), minimal separation occurs between the force and velocity records between time 0, or the time of impact, and time 2L/C. In addition, a large increase in the velocity record and corresponding decrease in the force record occurs at time 2L/C. Hence, this record indicates minimal shaft and minimal toe resistance on the pile.

In Figure 10-12(b), minimal separation again occurs between the force and velocity records between time 0 and time 2L/C. However in this example, a large increase in the force record and corresponding decrease in the velocity record occurs at time 2L/C. Therefore, this force and velocity record indicates minimal shaft and a large toe resistance on the pile.

In Figure 10-12(c), a large separation between the force and velocity records occurs between time 0 and time 2L/C. This force and velocity record indicates a large shaft resistance on the pile.

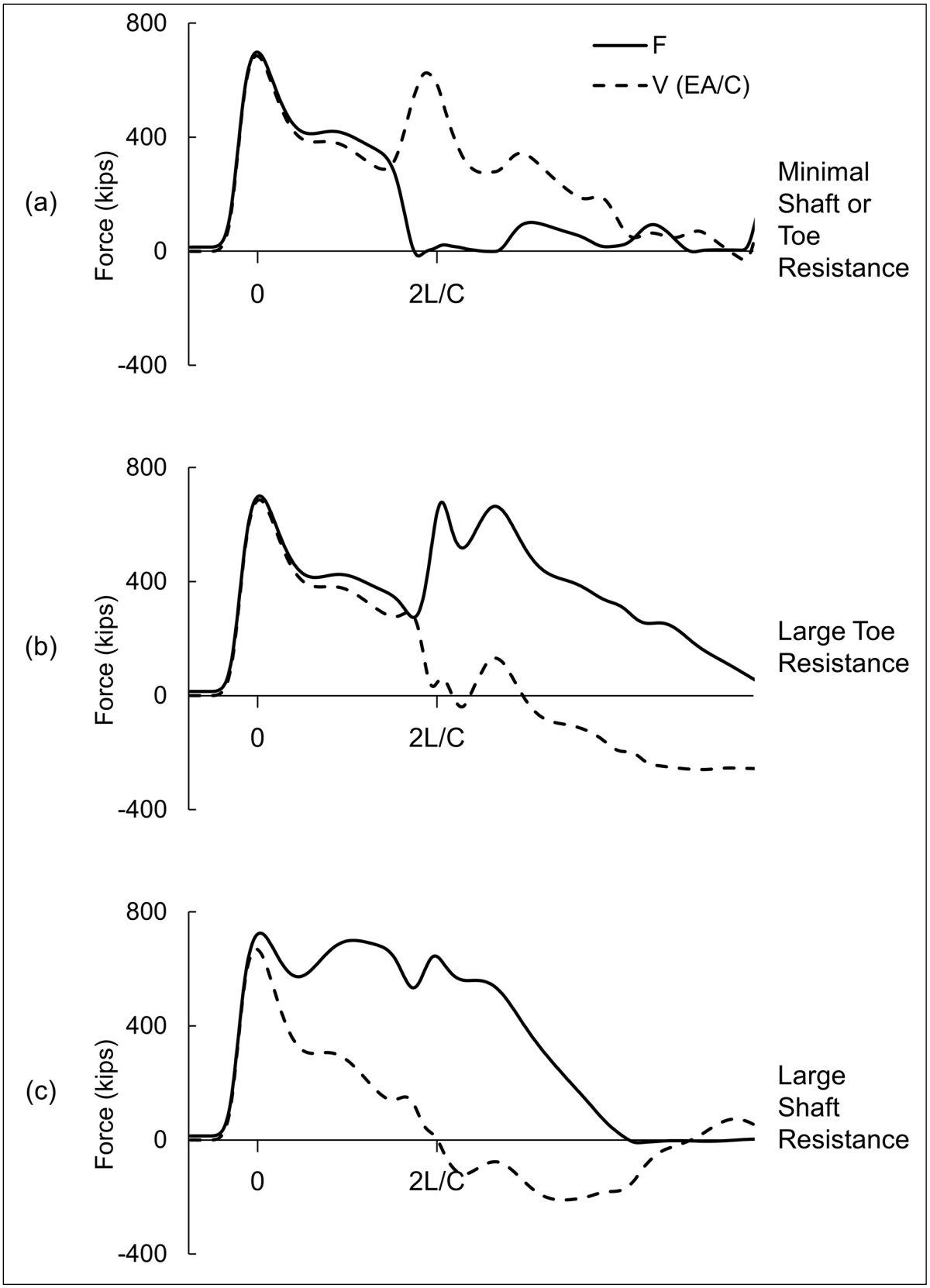

Figure 10-12 Typical force and velocity records for various soil resistance conditions.

10.6 DYNAMIC TESTING METHODOLOGY

As introduced in Section 10.1, simple field solutions such as the Case Method, and more rigorous numerical modeling or signal matching methods such as CAPWAP have been developed for analyzing dynamic measurement data. These dynamic test methods are sometimes confused with wave equation analysis described in Chapter 12, so it is useful to briefly review dynamic test and analysis methods as well as their application.

The wave equation is a computer program that is typically performed prior to field work. During the design stage, a wave equation drivability analysis is performed to check the suitability of potential pile types and sections. During the construction phase, the wave equation is used to check the suitability of the contractor's proposed equipment to satisfy nominal resistance and penetration requirements. In either application, the program inputs require the engineer to make assumptions on the hammer performance and static and dynamic soil response. Following test pile installation, a refined wave equation analysis may also be performed. In a refined analysis, the engineer uses hammer performance and soil response information from dynamic measurements and signal matching results to "calibrate" the wave equation to the field conditions. This process is described in Section 12.6.9. The wave equation provides a relationship between the nominal geotechnical resistance and the pile penetration resistance or blow count. It is therefore often used in establishing the driving criteria or in assessing the nominal geotechnical resistance of a pile based on its observed pile penetration resistance.

During test pile or production driving, dynamic measurements are made for estimates of the nominal geotechnical resistance. During driving, Case Method results for nominal resistance are calculated in real time from the measured force and velocity records obtained for each hammer blow. The Case Method equations for nominal resistance are described in detail in Section 10.6.1. While these simple field methods are useful for assessing the nominal resistance, AASHTO (2014) requires the nominal resistance be determined through signal matching analysis. Additional Case Method equations are used for calculation of driving stresses and pile integrity, as well as computation of transferred hammer energy. These additional Case Method equations are also described later in this chapter.

Signal matching is a more rigorous numerical analysis procedure that uses the measured force and velocity records from one hammer blow. Signal matching programs use the dynamic measurement data along with wave equation type pile and soil modeling to calculate the nominal geotechnical resistance, the relative soil

resistance distribution, the dynamic soil properties of quake and damping, and compression and tension stresses throughout the pile. The nominal resistance determined by signal matching is a more accurate assessment of the nominal resistance than Case Method results. Signal matching determined soil information along with the dynamic test data on driving system performance are often used in the development of a refined wave equation analysis. This is the best use of all the three methods for driving criteria determination. Signal matching analysis is described in greater detail in Section 10.6.6.

10.6.1 Nominal Resistance Determination by Case Method

Research conducted at Case Western Reserve University in Cleveland, Ohio resulted in a method which uses electronic measurements taken during pile driving to predict nominal resistance. Assuming the pile is linearly elastic and has constant cross section, the total static and dynamic resistance on a pile during driving, *RTL*, can be expressed using the following equation, which was derived from a closed form solution to the one dimensional wave propagation theory:

$$RTL = \frac{1}{2}[F(t_1) + F(t_2)] + \frac{1}{2}[V(t_1) - V(t_2)](\frac{EA}{C}) \qquad \text{Eq. 10-3}$$

Where:

RTL= total static and dynamic resistance on pile during driving (kips).
$F(t)$ = force measured at gage location at time t (kips).
$V(t)$ = velocity measured at gage location at time t (ft/s).
t_1 = time of first peak input.
t_2 = time of reflection of first peak input from pile toe $(t_1 + 2L/C)$.
L = pile length below gage location (feet).
E = elastic modulus of pile material (ksi).
A = pile cross sectional area (in^2).
C = wave speed of pile material (ft/s).

To obtain the static nominal resistance, the dynamic resistance (damping) must be subtracted from the above equation. Goble et al. (1975) found that the dynamic resistance component could be approximated as a linear function of a damping factor times the pile toe velocity, and that the pile toe velocity could be estimated from dynamic measurements at the pile head. This led to the standard Case Method nominal resistance equation, *RSP*, expressed as follows:

$$RSP = RTL - J\left[V(t_1)\left(\frac{EA}{C}\right) + F(t_1) - RTL\right] \qquad \text{Eq. 10-4}$$

Where:

RSP= standard Case Method equation for static nominal resistance (kips).
RTL= total static and dynamic resistance on pile during driving (kips).
J = Case damping factor based on soil type near the pile toe (unit less).
$F(t)$ = force measured at gage location at time t (kips).
$V(t)$ = velocity measured at gage location at time t (ft/s).
t_1 = time of first peak input.
E = elastic modulus of pile material (ksi).
A = pile cross sectional area (in^2).
C = wave speed of pile material (ft/s).

Typical damping factors versus soil type at the pile toe were determined by finding the range in the Case damping factor, *J*, for a soil type that provided a correlation of the RSP static nominal resistance within 20% of the static load test failure load, determined using the Davisson (1972) offset limit method. The original range in Case damping factor versus soil type from this correlation study, Goble et al. (1975), as well as typical ranges in Case damping factor for the RSP equation based on subsequent experience, Pile Dynamics, Inc. (2015), are presented in Table 10-1. While use of these values may provide good initial estimates of the nominal resistance, site specific damping correlations should be developed based upon signal matching analysis or static load test results. It should also be noted that Case damping is a non-dimensional damping factor and is not the same as the Smith damping discussed in Chapter 12 for wave equation analysis.

The RSP or standard Case Method equation is best used to evaluate the nominal resistance of low displacement piles, and piles with large shaft resistances. For displacement piles driven in soils with large toe quakes and for piles with large toe resistances, the maximum toe resistance is often delayed in time. This condition can be identified from the force and velocity records. In these instances, the standard Case Method equation may indicate a relatively low nominal resistance and the maximum Case Method equation, RMX, should be used. The maximum Case Method equation searches for the t_1 time in the force and velocity records which results in the maximum nominal resistance. An example of this technique is presented in Figure 10-13. When using the maximum Case Method equation, experience has shown that the Case damping factor should be at least 0.4, and on the order of 0.2 to 0.4 higher than that used for the standard Case Method equation for nominal resistance, RSP. Typical ranges in Case damping factor for the RMX equation are also presented in Table 10-1.

Table 10-1 Summary of Case Damping Factors for RSP and RMX Equations

Soil Type at Pile Toe	Original Case Damping Correlation Range Goble et al. (1975)	Recommended Range in Case Damping Constant for RSP Equation Pile Dynamics (2015)	Recommended Range in Case Damping Constant for RMX Equation Pile Dynamics (2015)
Clean Sands	0.05 to 0.20	0.10 to 0.15	0.40 to 0.50
Silty Sands	0.15 to 0.30	0.15 to 0.25	0.50 to 0.70
Silts	0.20 to 0.45	0.25 to 0.40	0.60 to 0.80
Silty Clays	0.40 to 0.70	0.40 to 0.70	0.70 to 0.90
Clay	0.60 to 1.10	0.70 or higher	0.90 or higher

The RMX and RSP Case Method equations are the two most commonly used solutions for field evaluation of pile nominal resistance. Additional automatic Case Method solutions are available that do not require selection of a Case damping factor. These automatic methods, referred to as RAU and RA2, search for the time when the pile toe velocity is zero and hence damping is minimal. The RAU method may be applicable for piles with minimal shaft resistance, and the RA2 method may be applicable to piles with toe resistance plus moderate shaft resistance. These automatic methods in their appropriate condition are often helpful supplemental indicators of the nominal resistance with the more traditional maximum or standard Case Method equations.

While the above Case Method equations are valuable for a quick field assessment of the nominal resistance, AASHTO (2014) does not provide a resistance factor for these or any other simple direct methods. Signal matching analysis on the collected dynamic test data is required for all nominal resistance assessments to be in compliance with AASHTO specifications.

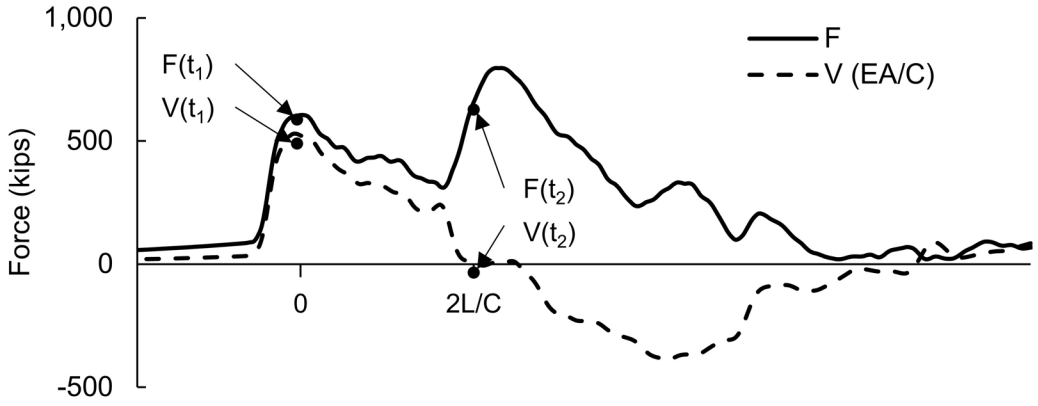

TOTAL RESISTANCE

RTL = ½ [$F(t_1)$ +$F(t_2)$] + ½ [$V(t_1)$ –$V(t_2)$] (EA/C)
= ½ [599 + 587] + ½ [13.6 – 0.3] 38.9
= 593 + 259 = 852 kips

STATIC RESISTANCE

RSP = RTL – J [$V(t_1)$*(EA/C) + $F(t_1)$ – RTL]
= 852 – 0.4 [13.6 * 38.9 + 599 – 852]
= 852 – 110 = 742 kips

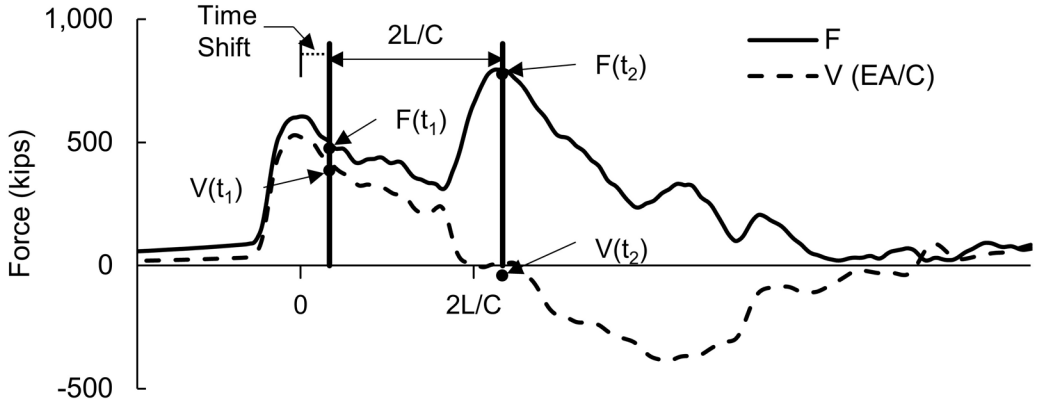

TOTAL RESISTANCE

RTL = ½ [$F(t_1)$ +$F(t_2)$] + ½ [$V(t_1)$ – $V(t_2)$] (EA/C)
= ½ [529 + 795] + ½ [11.7 – 0.1] 38.9
= 662 + 226 = 888 kips

STATIC RESISTANCE

RMX = RTL – J [$V(t_1)$*(EA/C) + $F(t_1)$ – RTL]
= 888 – 0.7 [11.7 * 38.9 + 529 – 888]
= 888 – 67 = 821 kips

Figure 10-13 Examples of standard Case Method, RSP, and maximum Case Method, RMX, calculations for estimates of nominal resistance.

10.6.2 Soil Resistance Distributions

As noted in Section 10.6, soil resistance effects can be assessed from dynamic test records. The relative magnitude of the soil resistance can be evaluated from the difference between the force record and velocity times impedance records at a given time during the 2L/C time interval following impact. The depth of the soil resistance below the gage location can be determined from the reflection time, 2X/C where X is the depth and C is the pile wave speed. While relative soil resistance distribution effects can be evaluated in this manner, the magnitude of the soil resistance at a given depth should be determined from more rigorous signal matching analysis as described in Section 10.6.6.

For piles with externally mounted or embedded strain gages that are dynamically monitored during driving, the pile forces calculated by measurements at the monitored locations can be compared to the calculated forces at those depths in signal matching results. However, the presence of residual forces from pile casting and/or pile driving greatly complicate any simple closed form solution of the soil resistance distribution from externally mounted or embedded instrumentation.

10.6.3 Energy Transfer

The energy transferred to the pile head can be computed from the strain and acceleration measurements. As described in Section 10.3, the acceleration signal is integrated to obtain velocity, and the strain measurement is converted to force. Transferred energy is equal to the work done which can be computed from the integral of the force and velocity records over time as given below:

$$E_p(t) \int_0^t F(t)\, V(t)\, dt \qquad \text{Eq. 10-5}$$

Where:

$E_p(t)$ = energy computed at the gage location at time t (ft-kips).
$F(t)$ = force measured at gage location at time t (kips).
$V(t)$ = velocity measured at gage location at time t (ft/s).

This procedure is illustrated in Figure 10-14. The maximum energy transferred to the pile head corresponds to the maximum value of $E_p(t)$. The output quantity EMX is the maximum value of $E_p(t)$ and can be used to evaluate the performance of the hammer and driving system as described in Section 10.7.

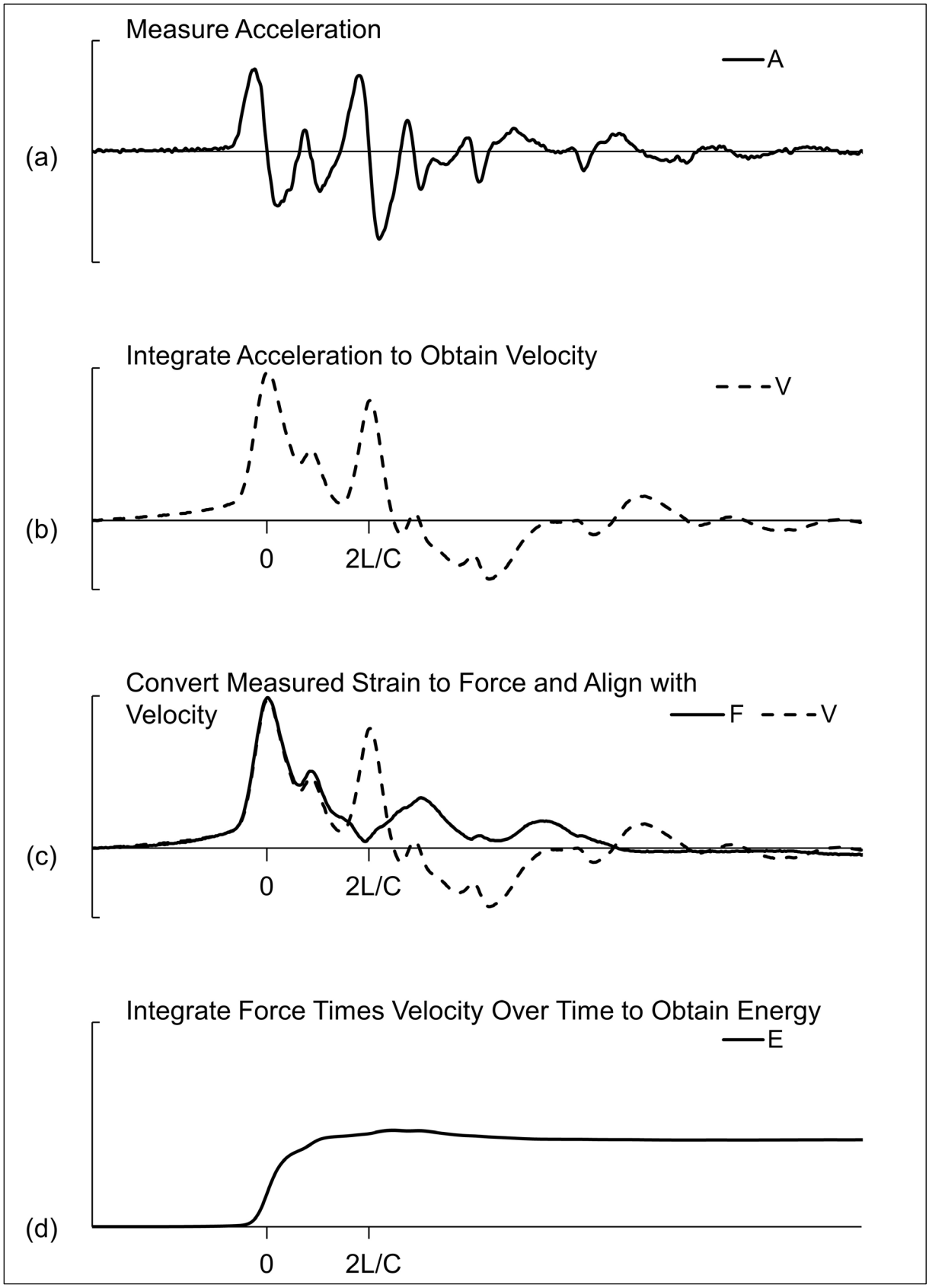

Figure 10-14 Energy transfer computation.

10.6.4 Driving Stresses

The compression stress at the gage location can be calculated using the measured strain and pile modulus of elasticity. However, the maximum compression stress in the pile may be greater than the compression stress calculated at the gage location, such as in the case of a pile driven through soft soils to rock. In these cases, signal matching or wave equation analysis may be used to evaluate the maximum compression stress elsewhere in the pile. Figure 10-15 illustrates the computation process for compression and tension stresses. Force and velocity records for an 18 inch square prestressed concrete pile with a large toe resistance are presented in the top half of the figure. The penetration resistance associated with this record is 29 blows per inch. The vertical scale between the zero axis and the top of the window box is identified as 1500 kips. Point A identifies the maximum compression force at the gage location of 795 kips. The maximum compression stress at the gage location, CSX, is then this force of 795 kips divided by the pile cross section area of 324 in^2 or 2.45 ksi.

Computed tension stresses are based upon the superposition of the upward and downward traveling waves. The downward traveling wave, wave down identified as WD, and the upward traveling wave, wave up identified as WU, are presented in the lower half of Figure 10-15. The vertical scale between the zero axis and the top of the lower box is once again 1500 kips. The value of wave down, WD, at time (t) is computed from the measured force and velocity records according to:

$$WD\ (t) = \frac{1}{2}\left[F(t) + V(t)\left(\frac{EA}{C}\right)\right] \qquad \text{Eq. 10-6}$$

Where:

$WD(t)$	=	downward traveling wave, wave down, at time t (kips).
$F(t)$	=	force measured at gage location at time t (kips).
$V(t)$	=	velocity measured at gage location at time t (ft/s).
E	=	elastic modulus of pile material (ksi).
A	=	pile cross sectional area (in^2).
C	=	wave speed of pile material (ft/s).

The value of wave up, WU, at time (t) is computed from the measured force and velocity records according to:

$$WU\ (t) = \frac{1}{2}\left[F(t) - V(t)\left(\frac{EA}{C}\right)\right] \qquad \text{Eq. 10-7}$$

Where:

$WU(t)$	=	upward traveling wave, wave up, at time t (kips).
$F(t)$	=	force measured at gage location at time t (kips).
$V(t)$	=	velocity measured at gage location at time t (ft/s).
E	=	elastic modulus of pile material (ksi).
A	=	pile cross sectional area (in^2).
C	=	wave speed of pile material (ft/s).

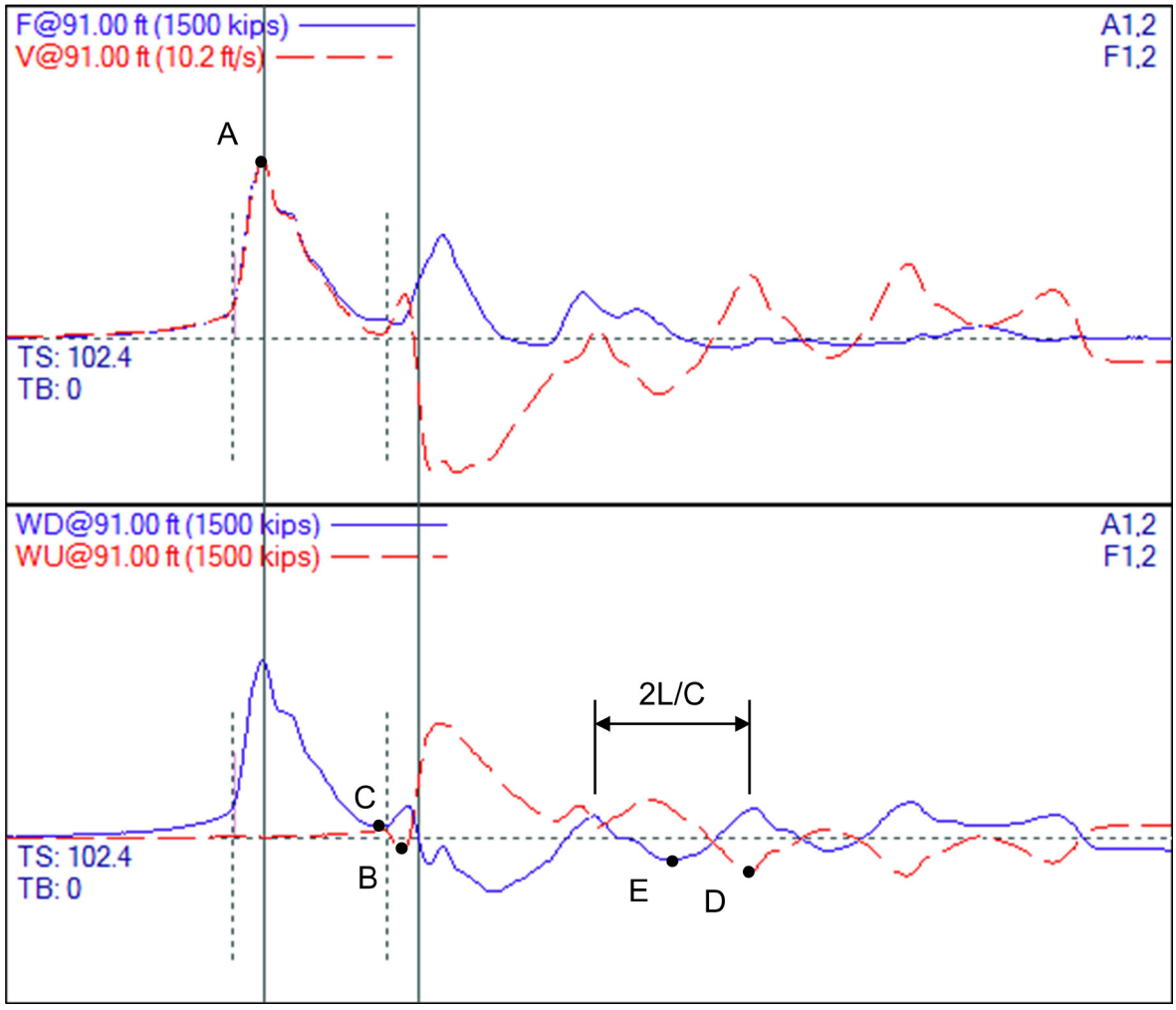

Figure 10-15 Example compression and tension stress calculation.

In Figure 10-15, the tension in the pile is computed from the superposition of the maximum upward tension force in wave up at time 2L/C +/- 20% identified by point B, and the minimum downward compression force in wave down between time 0 and time *2L/C* identified by point *C*. For the example presented, these values are -62 kips for point B and 45 kips for point *C*. The computed net tension force, CTN, is -17 kips. This corresponds to a computed tension stress maxima within the first

2L/C, TSN, of 0.05 ksi. This low tension stress in the upward traveling wave agrees with the hard driving conditions depicted by the force and velocity records and reported blow count.

The maximum tension stress can also occur later in the blow. Therefore, the full record length is searched for the minimum net tension force occurring from the upward travelling tension wave and the minimum value of the downward travelling wave in the previous 2L/C interval. In the example given, the minimum tension force occurs as a result of the tension in wave up of -154 kips identified by point D and the minimum force in the wave down in the preceding 2L/C interval of -105 kips identified by point E. The computed tension force of -259 kips corresponds to a computed tension stress, TSX, of 0.80 ksi. Hence, high tension stresses can occur in hard driving cases due to the downward traveling wave. This occurs when the reflected compression wave from a fixed toe condition reaches the free end at the pile head and reflects down the pile as a tension wave.

10.6.5 Pile Integrity

The basic concepts of wave mechanics were presented in Section 10.4. Convergence between the force and velocity records prior to the rise time before the toe response at time 2L/C indicates a reduction in pile impedance, *EA/C*. For uniform cross section piles, an impedance reduction is therefore pile damage.

The Beta Method, developed by Rausche and Goble (1979), is used to assess the relative severity of any damage along the pile shaft based on the convergence between the force and velocity records. If damage is detected, the relative severity of the damage is quantified and assigned a BTA value indicating the approximate reduction in pile impedance at the damage location. Rausche and Goble (1979) proposed the guidelines in Table 10-2 as in indication of the severity of pile damage. Piles with BTA values below 80% correspond to damaged or broken piles.

Table 10-2 Pile Damage Guidelines (after Rausche and Goble 1979)

BTA	Severity of Damage
1.0	Undamaged
0.8 – 1.0	Slightly Damaged
0.6 – 0.8	Damaged
Below 0.6	Broken

A method to assess pile toe damage solely for concrete piles driven using the EDC system with an embedded strain gage and accelerometer at both the pile head and pile toe was proposed by Verbeek and Middendorp (2011). This method uses a change in the prestress strain level in the top or bottom strain gage to assess damage in that portion of the pile. A change in the prestress level by more than 50 microstrains over 10 consecutive blows was recommended as identifying pile damage. This method will detect damage occurring due to a change in the prestress level but not damage due to concrete tension cracks.

One limitation of the original Beta method was its ability to detect damage near the pile toe when high toe resistances and/or stress wave reflections occur. Likins and Rausche (2014) revisited the original Beta method based on improvements in signal processing since 1979. For concrete piles, the wave speed must be determined from an early blow. They proposed near toe damage can then be assessed by looking for a reflection occurring too early for the correct 2L/C time. The PDA performs this computation and automatically identifies an early toe reflection by a BTT value that changes from 100% to 1% thereby highlighting the early toe reflection for further study and evaluation by the test engineer. The BTA and BTT methods can be used for pile damage assessments on all pile types.

10.6.6 Signal Matching

Once dynamic test data is acquired, it is routinely analyzed with a signal matching software program at select events such as the end of initial driving and beginning of restrike, or at key pile penetration depths such as the estimated pile toe elevation. Signal matching software programs include CAPWAP, iCAP, TNOWAVE, and All-Wave DLT. The pile and soil models used in these programs vary. Hence, both the analyst and the end user should fully understand the models contained within a specific program as well as that programs performance and limitations under a given set of conditions.

Signal matching programs allow a more rigorous evaluation of nominal geotechnical resistance, the relative resistance distribution, as well as insight into the soil quake and soil damping. Signal matching analyses are typically performed on an individual hammer blow selected from the end of driving or beginning of restrike. As such, a signal matching analysis refines the field dynamic test results at a particular penetration depth or time.

The AASHTO resistance factor for a dynamic test with signal matching was based on restrike dynamic test data analyzed with the CAPWAP program. Therefore, the

discussion and examples presented in the remainder of this signal matching section will use the analysis procedures and output from that program for illustrative purposes.

The CAPWAP signal matching program uses wave equation type pile and soil models with the measured force and velocity records from the dynamic test replacing the hammer model. In this method, depicted in Figure 10-16, the pile is modeled by a series of continuous pile segments and static and dynamic soil resistances are modeled by elasto-plastic springs and dashpots, respectively. The dynamic test data is used to quantify pile force and pile motion, which are two of the three unknowns. The remaining unknown is the boundary conditions, which are defined by the soil model.

First, reasonable estimates of the soil resistance distribution, soil quakes, and soil damping parameters are made. Then, the measured wave down is used to set the pile model in motion. The program then computes the equilibrium wave up, which can be compared to the measured wave up. Initially, the computed and measured wave up will not agree with each other. Adjustments are made to the soil model and the calculation process repeated.

The ability to match the measured and computed waves at various times is controlled by different factors. Figure 10-17 presents an initial trial in the signal matching process where the measured and computed records do not agree. This figure identifies the factors that most influence the signal match quality over a particular zone. The assumed shaft resistance distribution has the dominant influence on match quality beginning with the rise of the record at time t_r before impact and continuing for a time duration of 2L/C thereafter. This is identified as Zone 1 in Figure 10-17.

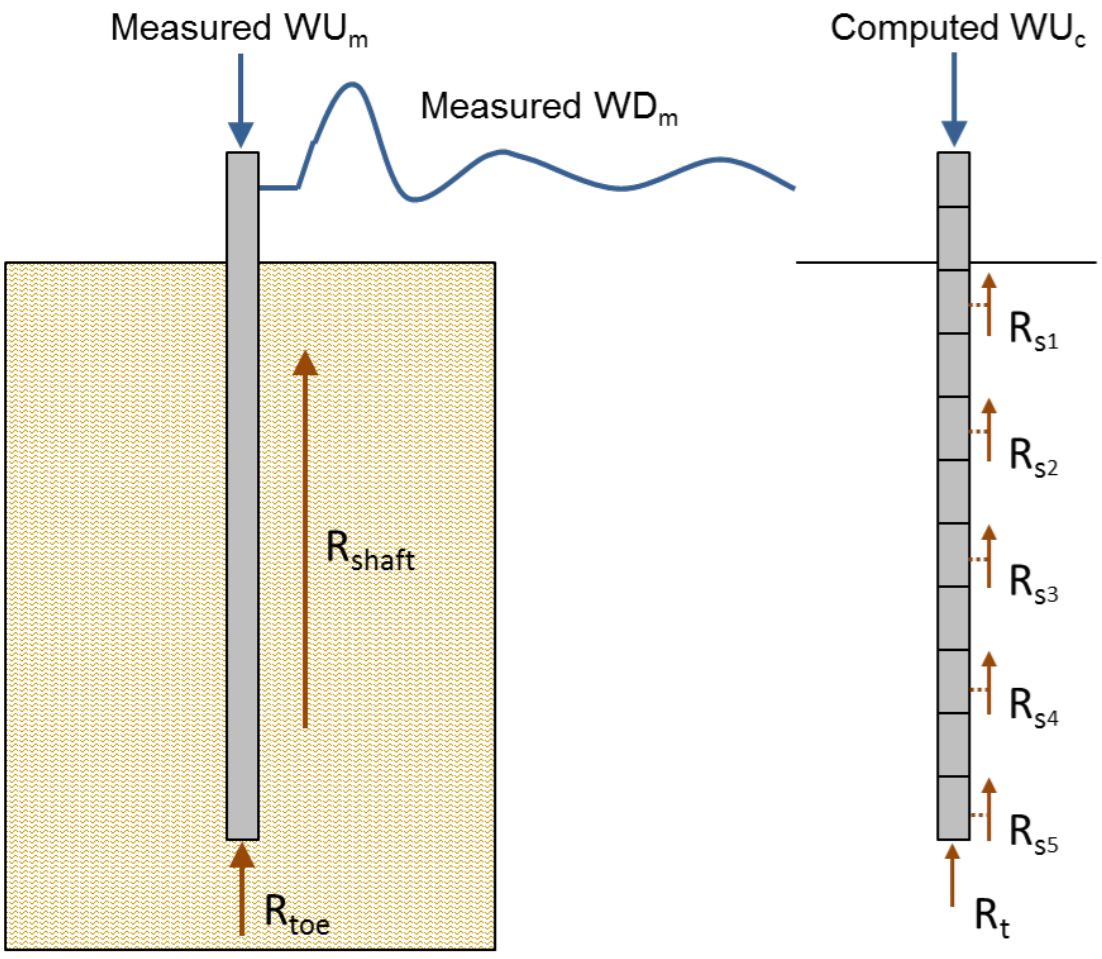

1. Set up pile and soil model. Assume R_{shaft}, R_{toe}, and $R_{nominal}$.
2. Apply measured wave down, WD_m, to model at pile head and compute wave up, WU_c.
3. Compare computed wave up, WU_c, with measured wave up, WU_m.
4. Adjust R_{shaft}, R_{toe}, $R_{nominal}$, quake, and damping.
5. Return to step 2 and iterate until satisfactory match is obtained.

Figure 10-16 Schematic of CAPWAP signal matching method.

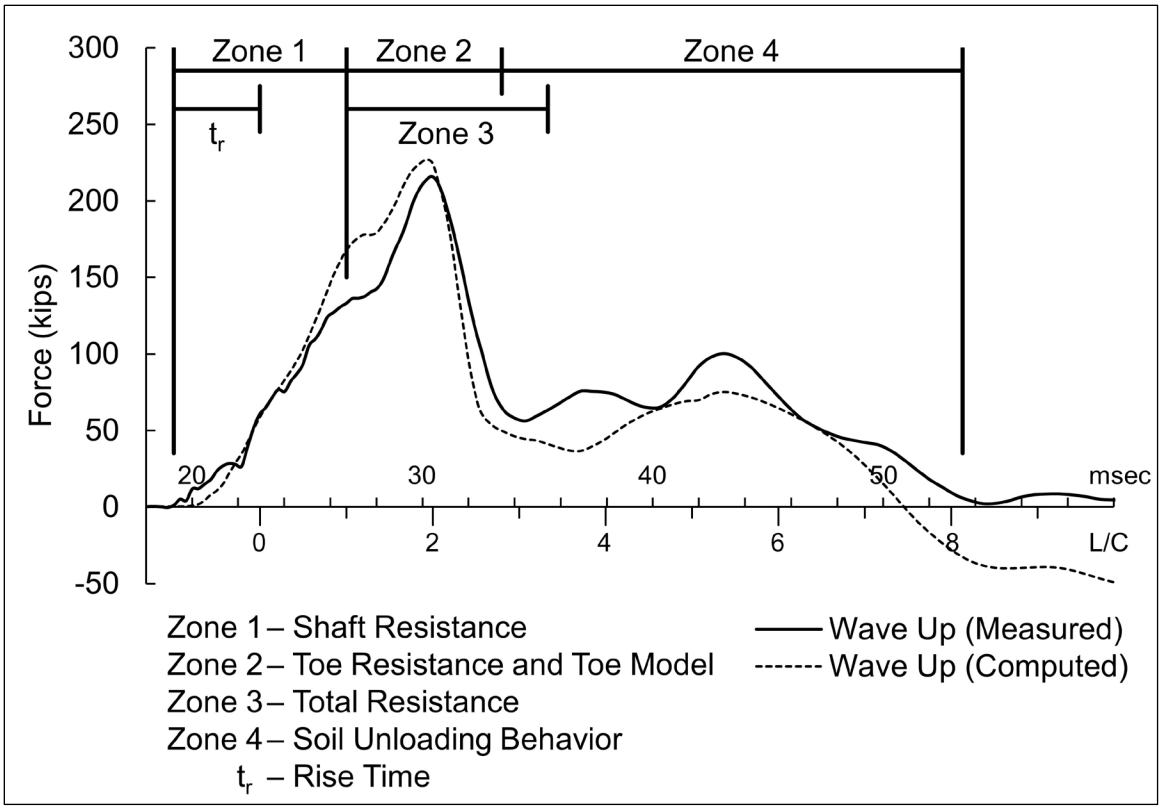

Figure 10-17 Factors most influencing signal matching analysis.

In Zone 2, the toe resistance and toe model (toe damping, toe quake, and toe gap) most influence the wave match. Zone 2 begins where Zone 1 ends and continues for a time duration equal to the rise time, t_r plus 3 ms. During Zone 3, which begins where Zone 1 ends and continues for a time duration of the rise time t_r plus 5 ms, the overall nominal resistance controls the match quality. A good wave match in Zone 3 is essential for accurate nominal resistance assessments. Zone 4 begins at the end of Zone 2 and continues for a duration of 20 ms. The unloading behavior of the soil most influences match quality in this zone.

With each analysis, the program evaluates the match quality by summing the absolute values of the relative differences between the measured and computed waves. The program computes a match quality number for each analysis that is the sum of the individual match quality numbers for each of these four zones. An illustration of the iteration process is presented in Figure 10-18.

Throughout the iteration process, adjustments are made to the soil model until no further improvement can be obtained between the measured and computed wave up. The resulting soil model from signal matching is then considered the best estimate of the nominal resistance, including the soil resistance distribution, the soil quakes, and the soil damping characteristics.

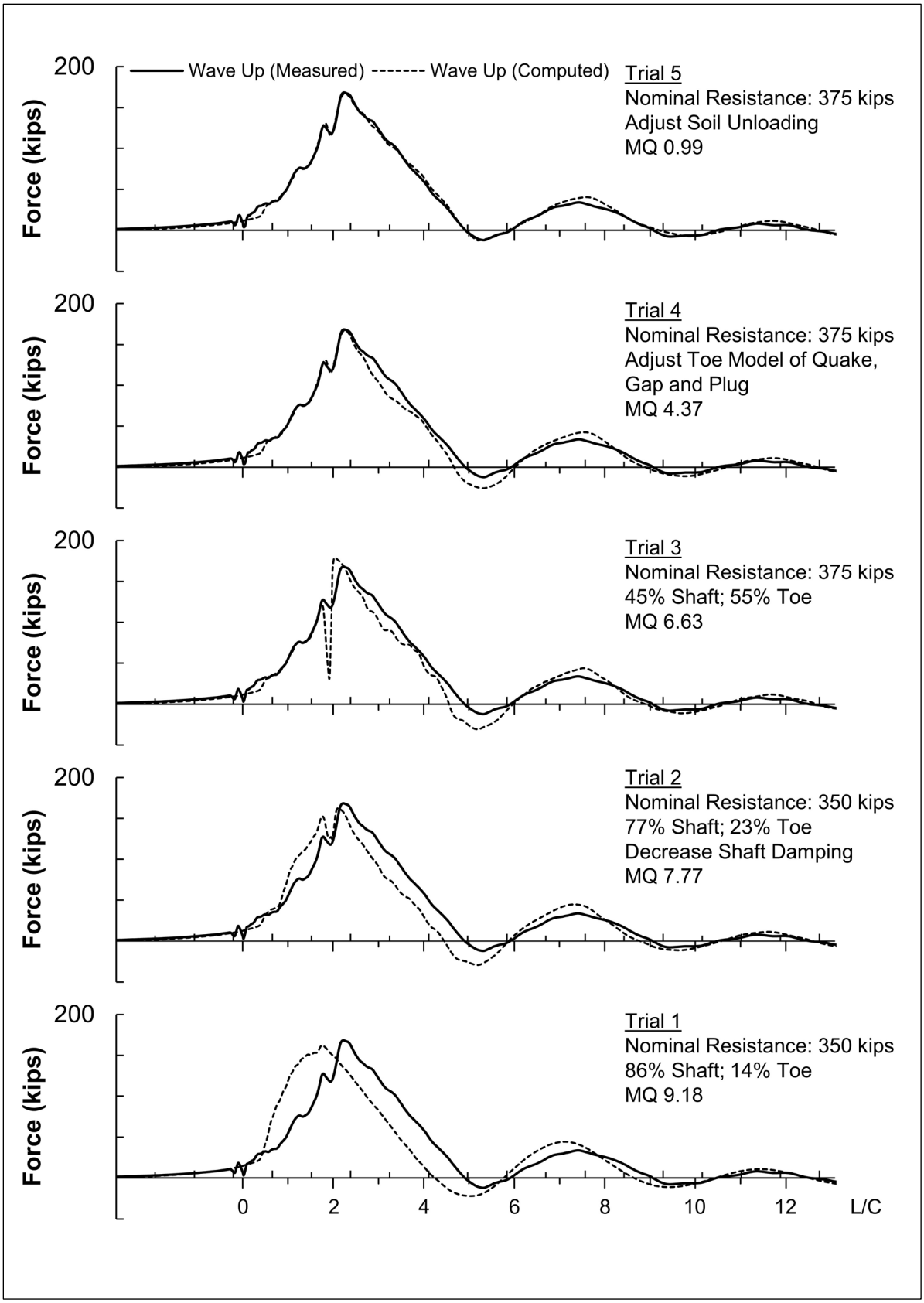

Figure 10-18 Example of signal matching iteration matching process.

The final graphical results from a signal matching analysis are presented in Figure 10-19. Four plots are included in the graphical output. While wave up matching was performed for the analysis, the “final match” plot in the upper left hand corners is typically presented in terms of the measured and computed force waves versus time. The force and velocity record versus time for the analyzed hammer blow are presented in the upper right hand plot. In the lower right hand corner, the shaft resistance magnitude on each soil segment in kips/ft is plotted above the load transfer diagram in kips. Important numerical results are presented immediately to the right of these plots including the analyzed pile properties, the final match quality number, maximum compression and tension stresses, as well as dynamic soil properties. The final plot, in the lower left hand corner, includes simulated static load test result. The pile model along with the soil resistance and quake values are used to develop these pile top and pile toe load versus displacement plots.

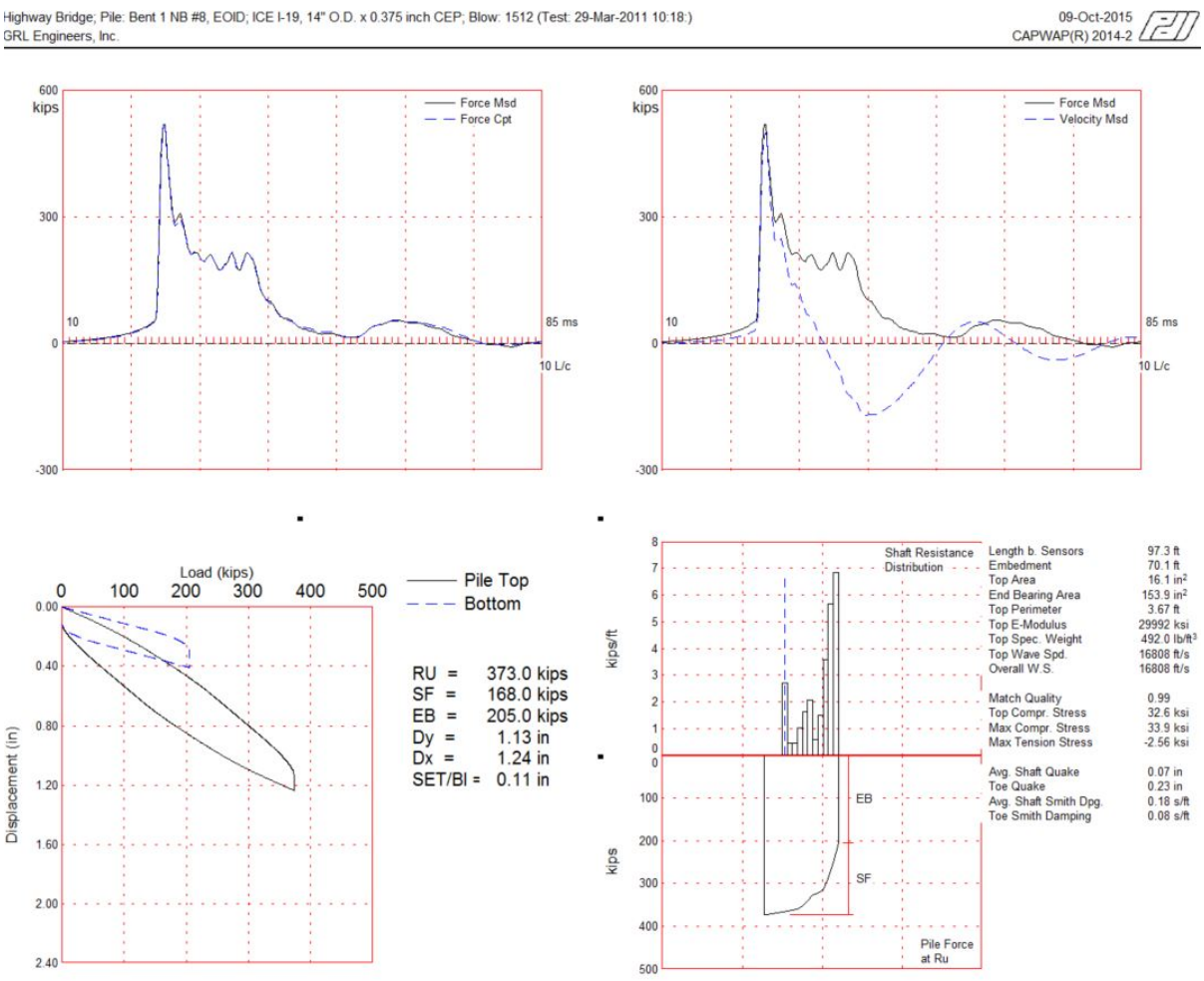

Figure 10-19 Example of signal matching graphical output.

An example of a signal matching final result summary is presented in Figure 10-20. For each soil segment, this table lists the depth below grade and the corresponding static soil resistance, Ru. Unit shaft resistance values are also provided in the far right hand column and can be compared to expected values from static analyses. The shaft and toe quake and damping values are summarized in the "Soil Model Parameters / Extensions" table beneath the soil resistance output. The match quality number, pile penetration resistance, compression and tension stresses, and transferred energy are summarized in the bottom section.

The "EXTREMA TABLE", presented in Figure 10-21, summarizes the stress distribution throughout the pile. This table is important because it indicates if higher compression stresses are present elsewhere in the pile below the gage location at pile segment number 1. In the example provided, the maximum compression stresses is 33.9 ksi and it occurs at a distance of 30.2 feet below the gage location. Similarly, the maximum tension stress of 2.56 ksi occurs at a location 77.2 feet below the gage location.

Figure 10-22 presents the "CASE METHOD" summary table. This output table can be used to determine which Case Method nominal resistance equation and damping factor correlates best with the nominal resistance from the more rigorous signal matching analysis. Hence, this table helps determine which Case Method equation and what damping factor should be used for any similar piles that will not be analyzed by signal matching. For the results summarized in Figure 10-22, the RMX Case Method equation with a damping factor of 1.45 would likely be selected based on correlation with the nominal resistance from the signal matching analysis.

The final output table from signal matching analysis is the "PILE PROFILE AND PILE MODEL" table presented in Figure 10-23. For the uniform closed-end pipe pile in the analysis example, no significant changes in the pile cross section area, elastic modulus, unit weight, or perimeter were entered. For non-uniform pile types of differing materials, tapered piles, or open end piles with added impedance due to a soil plug, a more complex pile profile would be reported.

CAPWAP SUMMARY RESULTS

Total CAPWAP Capacity: 373.0; along Shaft 168.0; at Toe 205.0 kips

Soil Sgmnt No.	Dist. Below Gages ft	Depth Below Grade ft	Ru kips	Force in Pile kips	Sum of Ru kips	Unit Resist. (Depth) kips/ft	Unit Resist. (Area) ksf
				373.0			
1	30.2	3.0	8.0	365.0	8.0	2.70	0.74
2	36.9	9.7	3.0	362.0	11.0	0.45	0.12
3	43.6	16.4	3.0	359.0	14.0	0.45	0.12
4	50.3	23.1	7.0	352.0	21.0	1.04	0.28
5	57.0	29.8	11.0	341.0	32.0	1.64	0.45
6	63.7	36.5	14.0	327.0	46.0	2.09	0.57
7	70.5	43.2	4.0	323.0	50.0	0.60	0.16
8	77.2	49.9	10.0	313.0	60.0	1.49	0.41
9	83.9	56.6	24.0	289.0	84.0	3.58	0.98
10	90.6	63.4	38.0	251.0	122.0	5.66	1.55
11	97.3	70.1	46.0	205.0	168.0	6.86	1.87
Avg. Shaft			15.3			2.40	0.65
Toe			205.0				191.77

Soil Model Parameters/Extensions		Shaft	Toe
Smith Damping Factor		0.18	0.08
Quake	(in)	0.07	0.23
Case Damping Factor		1.06	0.57
Damping Type		Viscous	Viscous
Unloading Quake	(% of loading quake)	52	49
Reloading Level	(% of Ru)	100	100
Unloading Level	(% of Ru)	9	
Resistance Gap (included in Toe Quake)	(in)		0.07
Soil Plug Weight	(kips)		0.027

CAPWAP match quality = 0.99 (Wave Up Match) ; RSA = 0
Observed: Final Set = 0.11 in; Blow Count = 108 b/ft
Computed: Final Set = 0.10 in; Blow Count = 118 b/ft

max. Top Comp. Stress = 32.6 ksi (T= 26.3 ms, max= 1.042 x Top)
max. Comp. Stress = 33.9 ksi (Z= 30.2 ft, T= 27.9 ms)
max. Tens. Stress = -2.56 ksi (Z= 77.2 ft, T= 51.7 ms)
max. Energy (EMX) = 22.4 kip-ft; max. Measured Top Displ. (DMX)= 0.86 in

Figure 10-20 Example signal matching output “Summary Results” table.

Highway Bridge; Pile: Bent 1 NB #8, EOID — Test: 29-Mar-2011 10:18
ICE I-19, 14" O.D. x 0.375 inch CEP; Blow: 1512 — CAPWAP(R) 2014-2
GRL Engineers, Inc.

EXTREMA TABLE

Pile Sgmnt No.	Dist. Below Gages ft	max. Force kips	min. Force kips	max. Comp. Stress ksi	max. Tens. Stress ksi	max. Trnsfd. Energy kip-ft	max. Veloc. ft/s	max. Displ. in
1	3.4	523.2	-11.2	32.6	-0.70	22.4	17.4	0.87
2	6.7	524.0	-11.8	32.6	-0.74	22.2	17.4	0.85
4	13.4	525.8	-13.0	32.7	-0.81	21.9	17.3	0.82
6	20.1	528.7	-14.3	32.9	-0.89	21.6	17.2	0.78
8	26.8	541.2	-15.3	33.7	-0.95	21.1	16.8	0.74
10	33.6	516.4	-18.4	32.2	-1.15	19.5	16.5	0.70
12	40.3	511.7	-25.2	31.9	-1.57	18.6	16.3	0.66
14	47.0	512.8	-31.6	31.9	-1.97	17.7	15.8	0.61
16	53.7	504.5	-35.9	31.4	-2.24	16.4	15.2	0.57
17	57.0	514.7	-39.0	32.1	-2.43	16.1	14.8	0.54
18	60.4	485.5	-38.7	30.2	-2.41	14.6	14.4	0.52
19	63.7	490.2	-40.6	30.5	-2.53	14.3	14.2	0.49
20	67.1	445.4	-38.9	27.7	-2.42	12.6	14.1	0.47
21	70.5	452.4	-40.2	28.2	-2.51	12.3	13.8	0.45
22	73.8	448.0	-40.2	27.9	-2.50	11.6	13.5	0.42
23	77.2	461.9	-41.1	28.8	-2.56	11.3	13.0	0.40
24	80.5	446.7	-38.9	27.8	-2.43	10.2	12.4	0.37
25	83.9	466.9	-39.0	29.1	-2.43	9.9	11.7	0.34
26	87.2	415.9	-33.5	25.9	-2.09	8.2	10.9	0.32
27	90.6	422.7	-33.6	26.3	-2.09	7.9	10.7	0.30
28	93.9	309.3	-24.8	19.3	-1.55	5.8	10.9	0.28
29	97.3	334.4	-24.7	20.8	-1.54	4.0	10.4	0.25
Absolute	30.2			33.9			(T =	27.9 ms)
	77.2				-2.56		(T =	51.7 ms)

Figure 10-21 Example signal matching output “Extrema” table.

Highway Bridge; Pile: Bent 1 NB #8, EOID — Test: 29-Mar-2011 10:18
ICE I-19, 14" O.D. x 0.375 inch CEP; Blow: 1512 — CAPWAP(R) 2014-2
GRL Engineers, Inc.

CASE METHOD

J =	0.0	0.2	0.4	0.6	0.8	1.0	1.2	1.4	1.6	1.8
RP	630.3	593.0	555.7	518.4	481.1	443.8	406.4	369.1	331.8	294.5
RX	630.3	593.0	555.7	518.4	481.1	443.8	406.4	376.7	362.8	351.3
RU	660.0	587.6	515.1	442.7	370.3	297.8	225.4	152.9	80.5	8.1

RAU = 124.9 (kips); RA2 = 340.0 (kips)

Current CAPWAP Ru = 373.0 (kips); Corresponding J(RP)= 1.38; J(RX) = 1.45

VMX ft/s	TVP ms	VT1*Z kips	FT1 kips	FMX kips	DMX in	DFN in	SET in	EMX kip-ft	QUS kips	KEB kips/in
17.5	26.15	501.8	520.4	520.6	0.86	0.11	0.11	22.4	552.7	1296

Figure 10-22 Example signal matching output “Case Method” table.

Highway Bridge; Pile: Bent 1 NB #8, EOID Test: 29-Mar-2011 10:18
ICE I-19, 14" O.D. x 0.375 inch CEP; Blow: 1512 CAPWAP(R) 2014-2
GRL Engineers, Inc.

PILE PROFILE AND PILE MODEL

Depth ft	Area in^2	E-Modulus ksi	Spec. Weight lb/ft^3	Perim. ft
0.0	16.1	29992.4	492.000	3.67
97.3	16.1	29992.4	492.000	3.67

Toe Area 153.9 in^2

Top Segment Length 3.36 ft, Top Impedance 29 kips/ft/s

Wave Speed: Pile Top 16807.9, Elastic 16807.9, Overall 16807.9 ft/s
Pile Damping 1.00 %, Time Incr 0.200 ms, 2L/c 11.6 ms
Total volume: 10.846 ft^3; Volume ratio considering added impedance: 1.000

Figure 10-23 Example signal matching output “Pile Profile and Pile Model” table.

10.7 CONSIDERATIONS IN TEST SPECIFICATION AND IMPLEMENTATION

Dynamic testing is specified in many ways depending upon the information desired or purpose of the testing. For example, a number of test piles driven at preselected locations may be specified. In this application, the test piles are usually driven in advance of, or at the start of, production driving so that the information obtained can be used to establish driving criteria and/or pile order lengths for each substructure unit. Alternatively, or in addition to a test pile program, dynamic tests on a specified percentage of the production pile quantity per site condition may be performed. Production pile testing is usually performed for quality assurance checks on nominal resistance, hammer performance, driving stress compliance, pile integrity, and for site variability considerations. Lastly, dynamic testing can be used where it was not specified to troubleshoot problems that arise during construction such as differing penetration depths or unusual driving records.

The number of piles that should be dynamically tested on the project depends upon the project size, variability of the subsurface conditions, the availability of static load test information, and the reasons for performing the dynamic tests. For example, it may be desirable to test a higher percentage of piles where there are difficult subsurface conditions with an increased risk of pile damage, or where time dependent soil strength changes are being relied upon for a significant portion of the nominal resistance.

On smaller projects, AASHTO specifications suggest a minimum of two dynamic tests per site condition, but no less than 2% of the production piles. On larger projects and small projects with anticipated installation difficulties or significant time

dependent nominal resistance issues, a greater number of piles should be tested. Dynamically testing one or two piles per substructure location is not unusual in these situations. Regardless of the project size, the design or construction engineer should be able to adjust the number and locations of dynamically tested piles based on design or construction issues that arise. For example, a change to 100% dynamic testing and the resulting higher resistance factor may benefit a project having pile length overruns if the cost of testing and associated construction time is less than the cost of the pile length overrun.

Restrike dynamic tests should be performed whenever pile nominal resistance is being evaluated by dynamic test methods. Restrikes are often specified 24 hours after initial driving. However, in fine grained soils, longer time periods are generally required for the full time dependent nominal resistance changes to occur. Therefore, longer restrike times should be specified in these soil conditions whenever possible. On small projects, long restrike durations can present significant construction sequencing problems. Even so, at least one longer term restrike should be performed in these cases. Longer term restrike should be specified 2 to 6 days after the initial 24 hour restrike, depending upon the soil type. A warmed up hammer (from driving or restriking a non-test pile) should be used for any restrike test.

In soils that exhibit a large increase in resistance from soil setup, it may not be possible to activate all the resistance during restrike with the pile hammer used for the pile installation. In this situation, a drop hammer system such as the one shown in Figure 10-24 can be used to determine the nominal resistances during restrike. Typically, a ram weight of approximately 2% of the desired nominal geotechnical resistance is required for resistance mobilization in a high strain dynamic test.

When dynamic testing is performed by a consultant, the requirements for signal matching analysis should be clearly addressed in the dynamic testing specification including the signal matching method. The AASHTO resistance factor of 0.65 is based on signal matching on restrike dynamic test data with the CAPWAP analysis method. A modified or locally calibrated resistance factor may be appropriate for other signal matching methods. This includes the simplified automatic signal matching program, iCAP, that shares some but not all of the soil and pile modeling and analysis capabilities of the CAPWAP program.

On design-build projects, it is common for the dynamic testing to be performed under the design-build team with independent verification tests or test reviews performed by the owner. On conventional design-bid-build projects, it is also sometimes contractually convenient to specify that the general contractor retain the services of

Figure 10-24 APPLE drop weight system.

the dynamic testing firm. However, this can create potential problems since the contractor is then responsible for the owner's quality assurance program. Some agencies have contracted directly with a dynamic testing firm to avoid this potential conflict. Other large public owners have acquired dynamic test equipment and perform these tests with their in-house staff.

Knowledgeable dynamic testing personnel who properly acquire and interpret dynamic test records are important for correct implementation of dynamic test results on a project. Therefore, specifications should require that dynamic testing personnel attain an appropriate level of expertise on the Pile Driving Contractors Association (PDCA) sponsored "Dynamic Measurement and Analysis Proficiency Test" for providers of high strain dynamic testing services. The test was designed to reflect the knowledge and ability of dynamic test providers which is then indicated in a "Certificate of Proficiency." The exam results categorize the six levels of proficiency as provisional, basic, intermediate, advanced, master, or expert. This allows agencies to specify the level of expertise required for their standard practice or for a given project. Additional details on the exam can be found on the PDCA website, www.piledrivers.org.

10.8 PRESENTATION AND INTERPRETATION OF DYNAMIC TEST RESULTS

The results of dynamic pile tests should be summarized in a formal report that is sent to both the construction engineer and foundation designer. The construction engineer should understand the information available from the dynamic testing and its role in the project construction. As discussed in Chapter 7, numerous factors are considered in a pile foundation design. Therefore, the foundation designer should review the test results since many considerations; (downdrag, scour, uplift, lateral loads, settlement, etc.) may affect the overall design and construction requirements.

10.8.1 Field Results

Construction personnel are often presented with dynamic testing results with minimal guidance on how to use or interpret the information. Therefore, it may be helpful to both construction personnel and foundation designers to familiarize themselves with a typical screen display and the information available in the field during a dynamic test. Figure 10-25 presents a typical dynamic test screen display from the Pile Driving Analyzer 8G system.

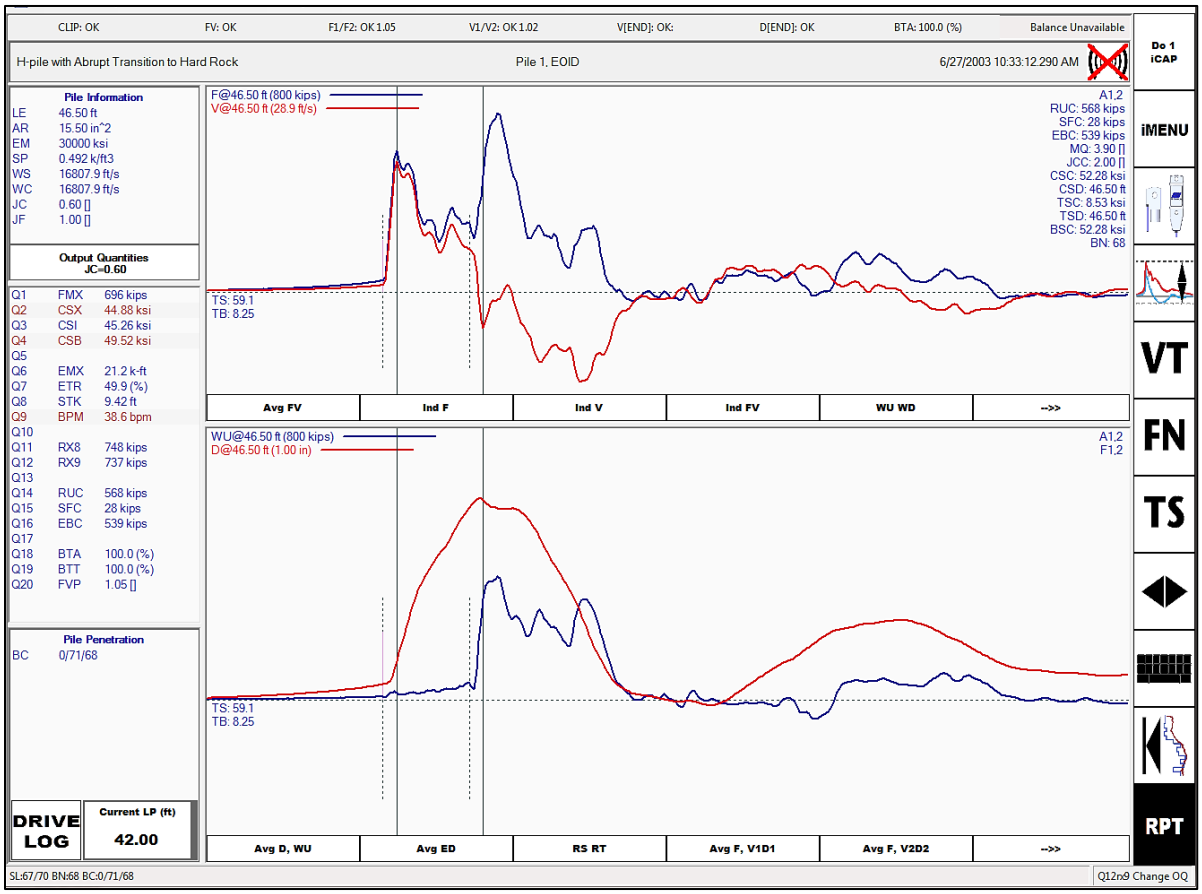

Figure 10-25 Typical dynamic test display from Pile Driving Analyzer.

The main pile information input quantities are displayed near the upper left corner of the screen and include the pile length below gages, LE; the pile cross sectional area at the gages, AR; the pile elastic modulus, EM; the unit weight of the pile material, SP; the pile wave speed, WS; as well as the Case damping factor, JC.

The graphic portion of the screen is typically divided into two displays as illustrated above in Figure 10-25. The upper graphic display presents the force and velocity records versus time plotted proportionally. The lower display presents the upward travelling wave, WU, and the displacement at the gage location versus time. Both displays will change for each hammer blow. The first full height solid vertical line represents time t_1 in the Case Method calculations and corresponds to the time of impact (i.e., the first input peak, as the waves pass the gage location near the pile head). The second full height solid vertical line represents time t_2 in the Case Method calculations and corresponds to the time when the input waves have traveled to the pile toe and returned to the gage location at time 2L/C. The partial height, dotted, vertical lines preceding the full height lines note the start of the impact event or start of the toe reflection, respectively.

An experienced test engineer can visually interpret these signals for data quality, soil resistance distribution, and pile integrity. As discussed earlier, soil resistance forces cause a relative increase in the force wave and a corresponding relative decrease in the velocity wave. Therefore on a pile with a uniform cross section, the separation between the force and velocity records between times t_1 and t_2 indicates the shaft resistance. The magnitude of separation is also indicative of the magnitude of the total soil resistance above that depth. Toe resistance is indicated by the separation between these records beginning at the rise time marker prior to time t_2.

A search for convergence between the force and velocity records is performed beginning at the time of the sharp rise in the records prior to time t_1 and continuing for a time interval of 2L/C thereafter. If convergence between the force and velocity records occurs prior to the rise in the velocity record preceding time t_2, a cross sectional reduction or pile damage is indicated. The degree of convergence between the force and velocity records is expressed by the BTA integrity value as a percentage of the approximate reduced cross sectional area. As discussed in Section 10.6.5, an early reflection prior to 2L/C is also evaluated and, if noted, a BTT value of 1% will highlight the need for record review for toe damage by the engineer.

The results of Case Method numerical computations are identified by three letter codes displayed on the left hand side of the screen. A summary of the most

commonly computed quantities and their corresponding three letter code is presented in Table 10-3.

Table 10-3 Description of Typical Dynamic Test Output Codes

PDA Output Code	Output Quantity Description
CSX	Maximum compression stress at the gage location.
CSI	Maximum compression stress from an individual strain transducer.
CSB	Maximum computed compression stress at pile toe.
TSX	Maximum computed tension stress.
BTA	Pile integrity factor.
BTT	Integrity indicator for early toe reflection.
LTD	Length to pile damage.
EMX	Maximum energy transferred to the gage location.
ETR	Energy transfer ratio (EMX / E rated).
STK	Computed hammer stroke.
BPM	Hammer operating rate.
RMX	Maximum Case Method (requires damping factor, J).
RSP	Standard Case Method (requires damping factor, J).
RSU	Case Method with unloading correction (requires damping factor, J).
RAU	Automatic Case Method - toe bearing. No shaft resistance.
RA2	Automatic Case Method - Moderate shaft resistance.
RUC*	iCAP nominal resistance.
SFC*	iCAP shaft resistance.
EBC*	iCAP toe resistance.
CSC*	iCAP computed maximum compression stress.
CBC*	iCAP computed compression stress at pile toe.
TSC*	iCAP computed tension stress.

* - requires additional iCAP automated signal matching software.

In the example given in Figure 10-25, the first four output quantities Q1, Q2, Q3, and Q4 provide information on the maximum force and associated driving stresses. The maximum average force at the pile head, FMX, is 696 kips. This corresponds to an average compression stress at the gage location, CSX, of 44.9 ksi. The maximum compression stress from an individual strain transducer, CSI, is 45.3 ksi, and the

maximum computed compression stress at the pile toe, CSB, is 49.5 ksi. Hence, driving stress levels are quite high and are above AASHTO recommended limits.

As noted earlier, the compression stress levels exceed the driving stress limits as well as the guaranteed minimum yield strength for H-piles made from A572, Grade 50 steel. Hence, the potential for pile toe damage is high. The pile integrity, BTA, is calculated as 100%, indicating that no detected damage. The integrity near the pile toe is also assessed and a BTT of 100% is calculated despite the very high driving stresses resulting from the abrupt refusal driving on hard rock.

An assessment of the performance of the single acting diesel hammer is made from output quantities Q5 through Q9. The average energy transferred to the gage location, EMX, is 21.2 ft-kips. As indicated by Q6, this corresponds to an energy transfer ratio, ETR, of 49.9% (EMX / manufacturer's rated hammer energy of 42.4 ft-kips). The hammer stroke, STK is 9.42 feet and the hammer operating rate, BPM, is 38.6 blows per minute.

Output quantities Q11 and Q12 display the nominal resistance as evaluated by the maximum Case Method, RMX, with a damping factor of 0.80 and 0.90. These nominal resistance computations are 748 and 737 kips, respectively and are reported as RX8 and RX9.

Output quantities Q14 to Q16 present the results of automated signal matching analysis using the iCAP method. The iCAP results indicate a nominal resistance, RUC, of 568 kips with 28 kips of shaft resistance, SFC, and 539 kips of toe resistance, EBC. Complete automated signal matching results are presented in the upper right corner of the graphical screen and include the match quality, MQ, of 3.90 along with the maximum computed compression stress, CSC, of 52.3 ksi which occurs at the pile toe. It should be emphasized that iCAP automated signal matching is only applicable to uniform piles. It cannot accurately analyze non-uniform piles, piles with splice gaps, damaged piles, concrete piles with minor cracking, or piles with uncertain properties. iCAP should also not be used for large diameter open-end pipe piles (due to internal plug movements) or on piles in unusual soil conditions.

Construction personnel should review the dynamic test results and check that the calculated driving stresses, CSX and TSX, are maintained within specification limits. Drive system performance indicated by the transferred energy, EMX, should be within a reasonable range of that predicted by wave equation analysis or recorded on previous tests at the site. If significant variations in energy are noted, the

reasons for the discrepancy should be evaluated. The recorded hammer speed should be compared to the manufacturer's specifications. Nominal resistance estimates should be compared with the required nominal resistance. In soils with time dependent soil strength changes, this comparison of nominal resistance should be based on restrike tests and not end of initial driving results.

10.8.2 Evaluation of Hammer and Drive System Performance

The performance of a hammer and driving system can be evaluated from a driving system's energy transfer ratio, which is defined as the energy transferred to the pile head divided by the manufacturer's rated hammer energy. The energy transfer ratio should not be misinterpreted as the hammer efficiency as the energy transfer ratio includes all energy losses in the driving system. Numerous factors affect the transferred energy and hence the energy transfer ratio. These include the hammer stroke, fuel setting, helmet weight, hammer and pile cushions, pile impedance, pile length, soil resistance, dynamic soil properties, as well as the hammer efficiency.

Figure 10-26 presents energy transfer ratios for selected hammer and pile type combinations expressed as a percentile. In this graph, the average transfer efficiency for a given hammer-pile combination can be found by noting where that graph intersects the 50th percentile. Depending upon the hammer-pile combination, average transferred energies as a percentage of the rated energy range from about 26% for a diesel hammer on a concrete pile to 69% for a hydraulic hammer on a steel pile.

Histograms of the energy transfer ratios for all diesel, single acting (SA) air/steam, and single acting (SA) hydraulic hammer on steel or concrete and timber piles are presented in Figures 10-27, 10-28, and 10-29, respectively. The histograms may be useful in assessing drive system performance as they provided the distribution and standard deviation of drive system performance for a given hammer-pile combination at the end of drive condition.

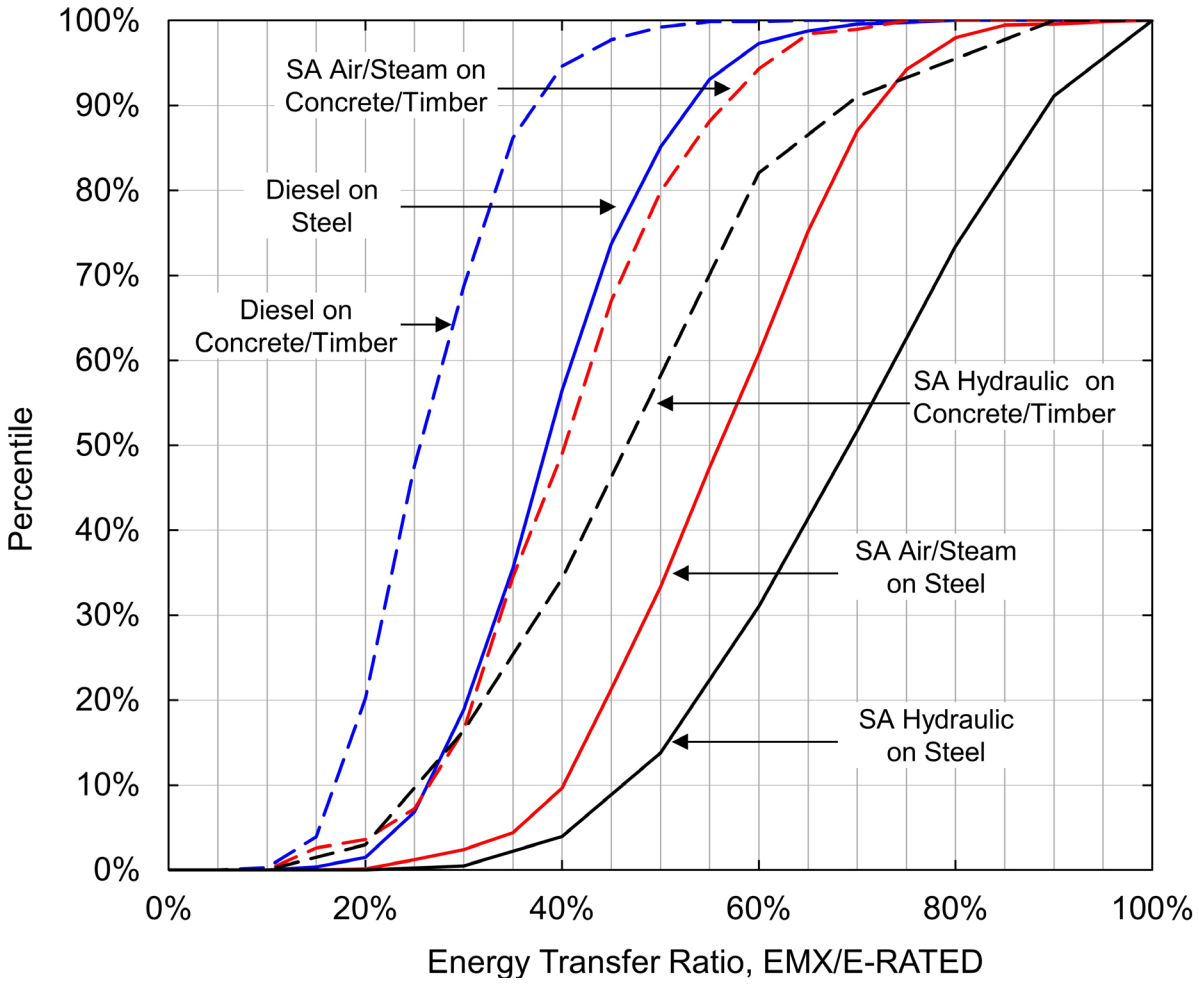

Figure 10-26 Energy transfer ratios for select hammer and pile combinations.

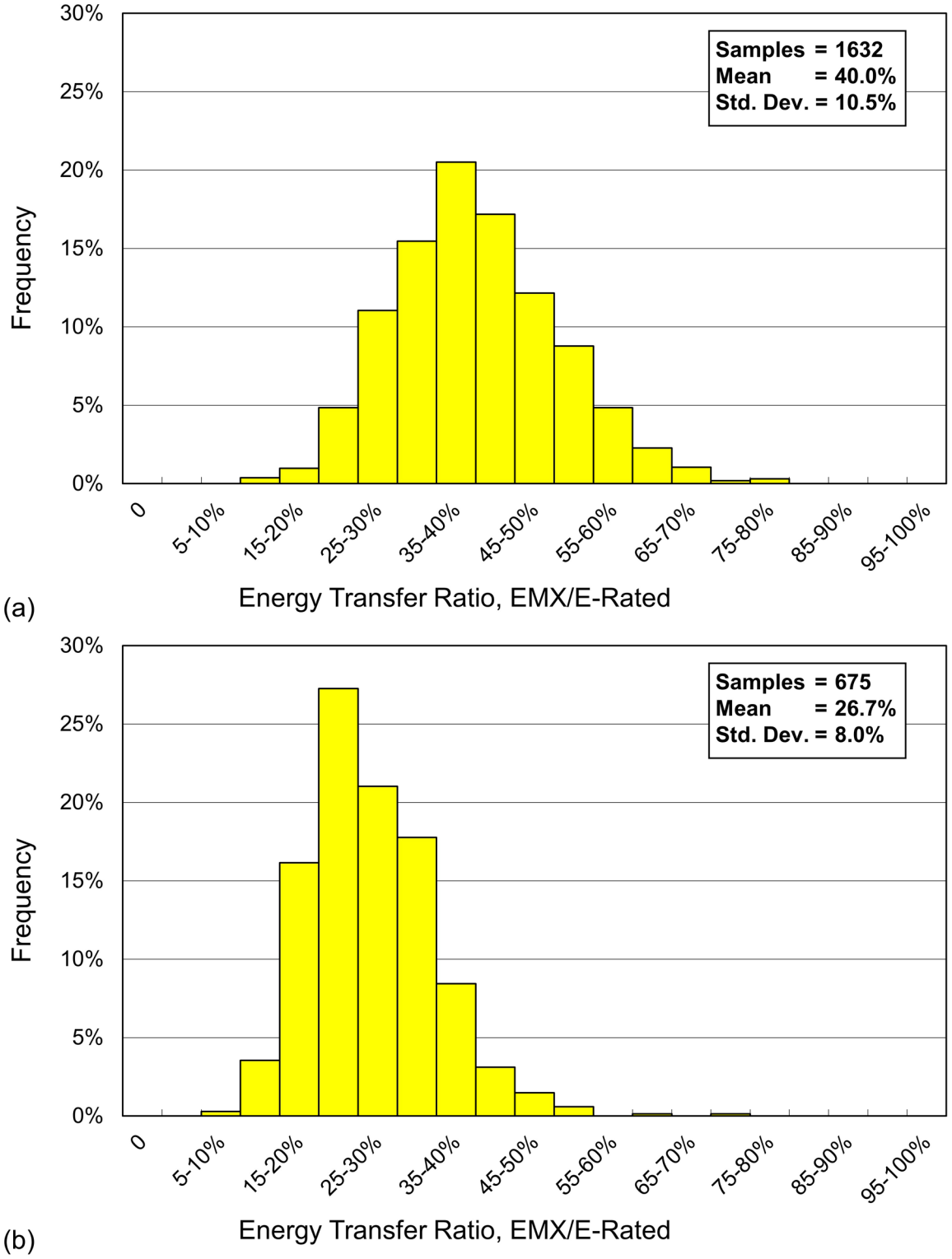

Figure 10-27 Histograms of energy transfer ratio for diesel hammers on (a) steel piles and (b) concrete/timber piles.

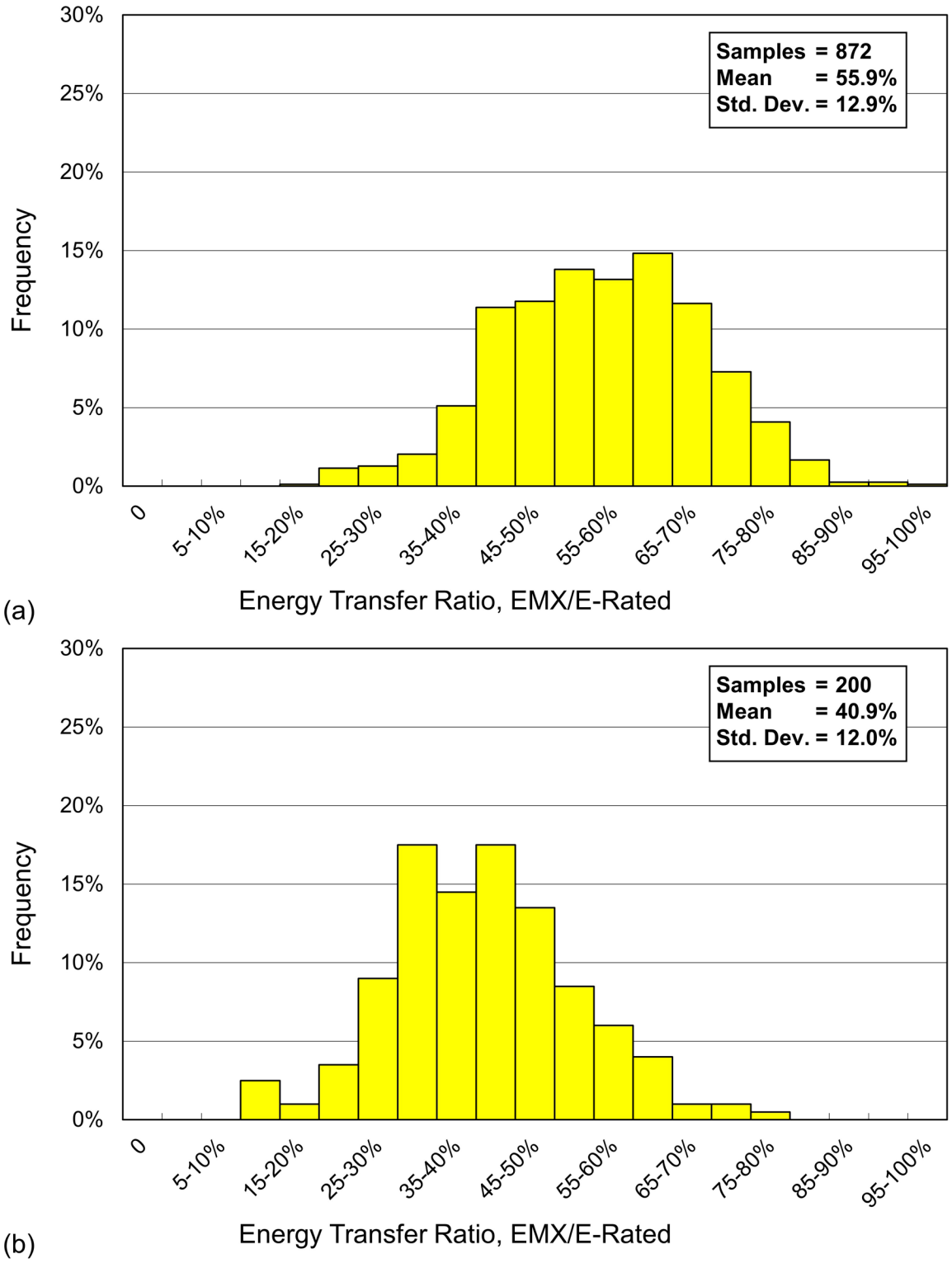

Figure 10-28 Histograms of energy transfer ratio for single acting air/steam hammers on (a) steel piles and (b) concrete/timber piles.

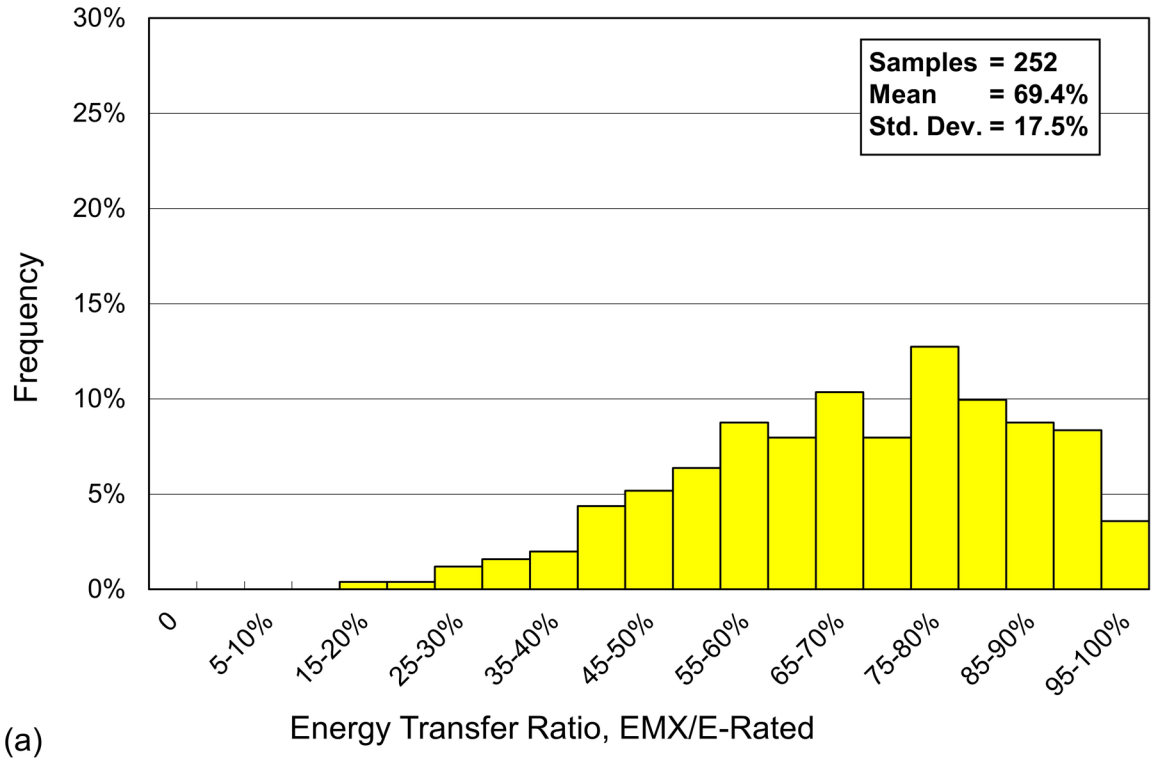

(a)

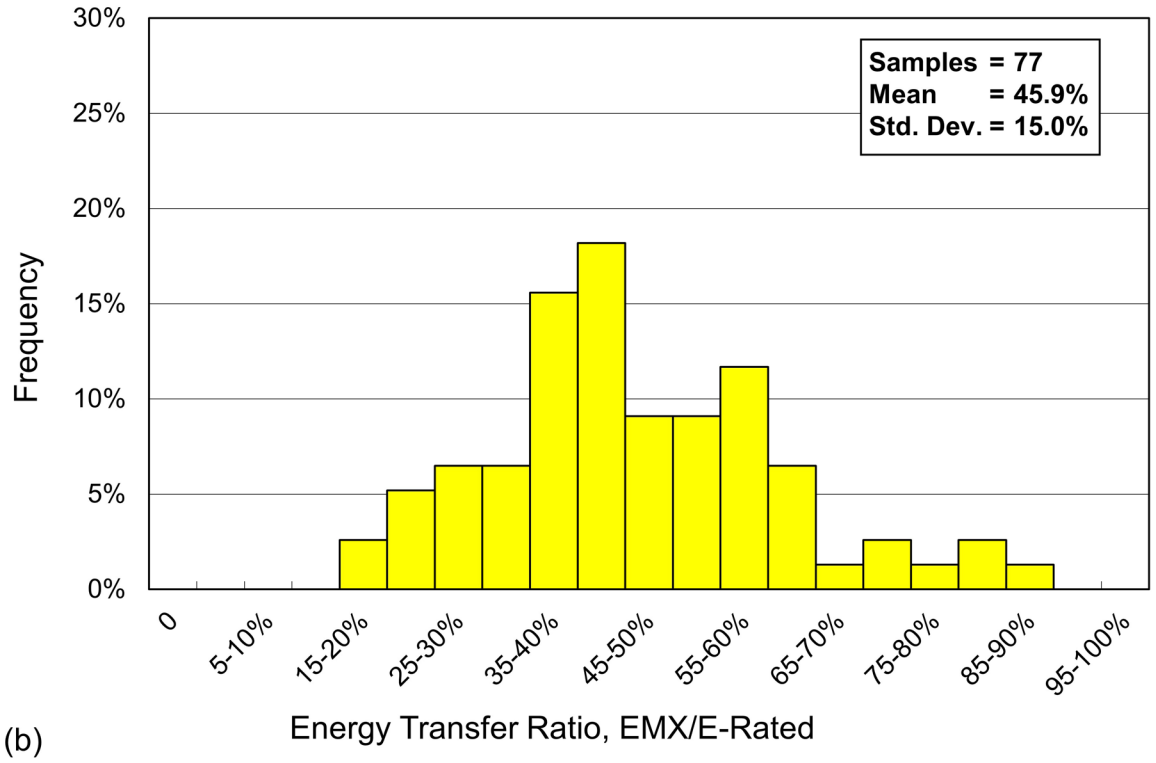

(b)

Figure 10-29 Histograms of energy transfer ratio for single acting hydraulic hammers on (a) steel piles and (b) concrete/timber piles.

10.8.3 Test Record Illustrating Problematic Hammer Performance

Records for a single acting diesel hammer exhibiting diesel fuel pre-ignition are presented in Figure 10-30. On this project, the diesel hammer had been operated relatively continuously all day with minimal down time. Note the magnitude of the force record during the pre-compression phase prior to impact, and compare that to a more typical diesel hammer record in Figure 10-31. In the presented pre-ignition data for Blow 986, the hammer stroke is 7.49 feet, the impact force is 383 kips, the transferred energy is 20.6 ft-kips, and the energy transfer ratio is 29.4% which is 10% less than the mean value for a diesel hammer on a steel pile. In Figure 10-26, an energy transfer ratio of 29.4% for a single acting diesel hammer on a steel pile falls near the 18th percentile which is also clearly indicative of a problem. For comparison, Blow 2 of the same drive sequence had a similar hammer stroke of 7.53 feet when the diesel fuel was not pre-igniting. However, in Blow 2, the hammer had an impact force of 481 kips, a transferred energy of 34.2 ft-kips, and an energy transfer ratio of 48.8%.

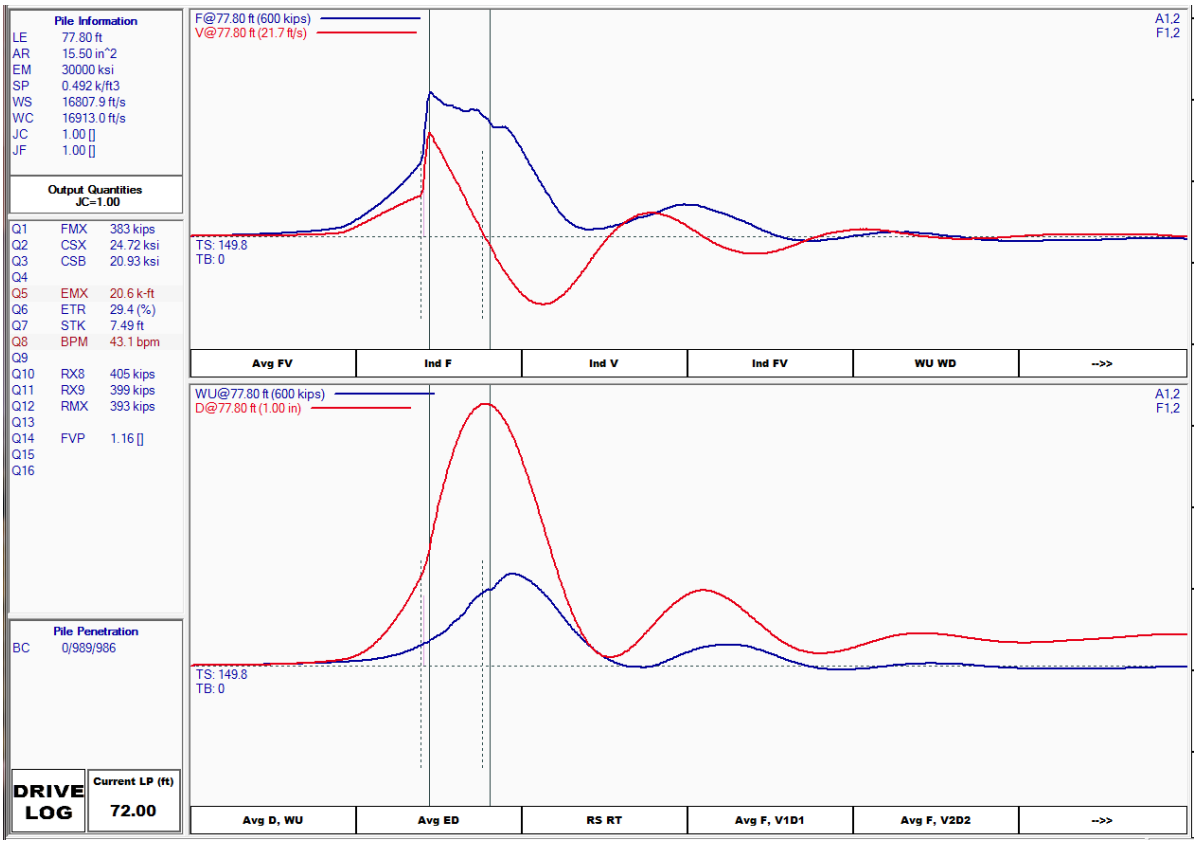

Figure 10-30 Example dynamic test records on pre-igniting diesel hammer.

Note the magnitude of the force record in Figure 10-30 during the pre-compression phase prior to impact. The pre-compression force on the pile is almost 50% of the

impact force. This reduces the effectiveness of the hammer blow on the pile because it takes more energy to compress the combustion gases in the combustion chamber prior to the ram impacting the impact block. The reduced transferred energy to the pile results in a greater blow count occurring at a shallower pile penetration depth. Hence, if pre-ignition was not detected, pile driving would be terminated prematurely at a nominal resistance less than the required resistance.

10.8.4 Test Record Illustrating Pile Damage

Force and velocity records are presented in the upper graph of Figure 10-31 for a HP 14x117 H-pile driven with a single acting diesel hammer. The lower graph presents the wave up and displacement records. The pile information section of the screen in the left hand corner indicates the H-pile has a length of 88.3 feet below the gages. A visual interpretation of the force and velocity record suggests the pile has developed moderate shaft resistance over the lower portion of the pile with a significant amount of the nominal resistance due to toe resistance. Note that a full height, dash and dotted vertical line has also appeared between the two solid vertical lines corresponding to the pile head, t_1, and pile toe, t_2. Convergence between the force and velocity records before time 2L/C, as noted by the dash and dotted line, indicates a pile impedance reduction or damage.

The BTA warning box near the top of the screen has also turned black and indicates a calculated BTA value of 82%. For the example shown, damage was occurring at a depth of 83.2 feet below gages due to the H-pile buckling and bending at this location. The integrity near the pile toe has been assessed and a BTT of 1% is reported highlighting the occurrence of near toe damage. The pile was extracted to confirm the indicated damage 5 feet above the pile toe. Photographs of the extracted pile are presented in Figure 10-32.

10.8.5 Test Records Illustrating Soil Setup

Test records for a 14 inch O.D. x 0.50 inch wall closed end pipe pile driven with a single acting diesel hammer are presented in Figures 10-33 and 10-34. Dynamic testing on this test pile was performed during initial driving and again during restrike 3 days after initial driving. The required nominal resistance was 765 kips based on resistance verification using dynamic testing with signal matching. At this test pile location, a minimum penetration depth of 90 feet was also specified to satisfy lateral loading requirements. Soil conditions consist of predominantly stiff to very stiff silty clays with interbedded medium dense to dense silty sand and sandy silt layers.

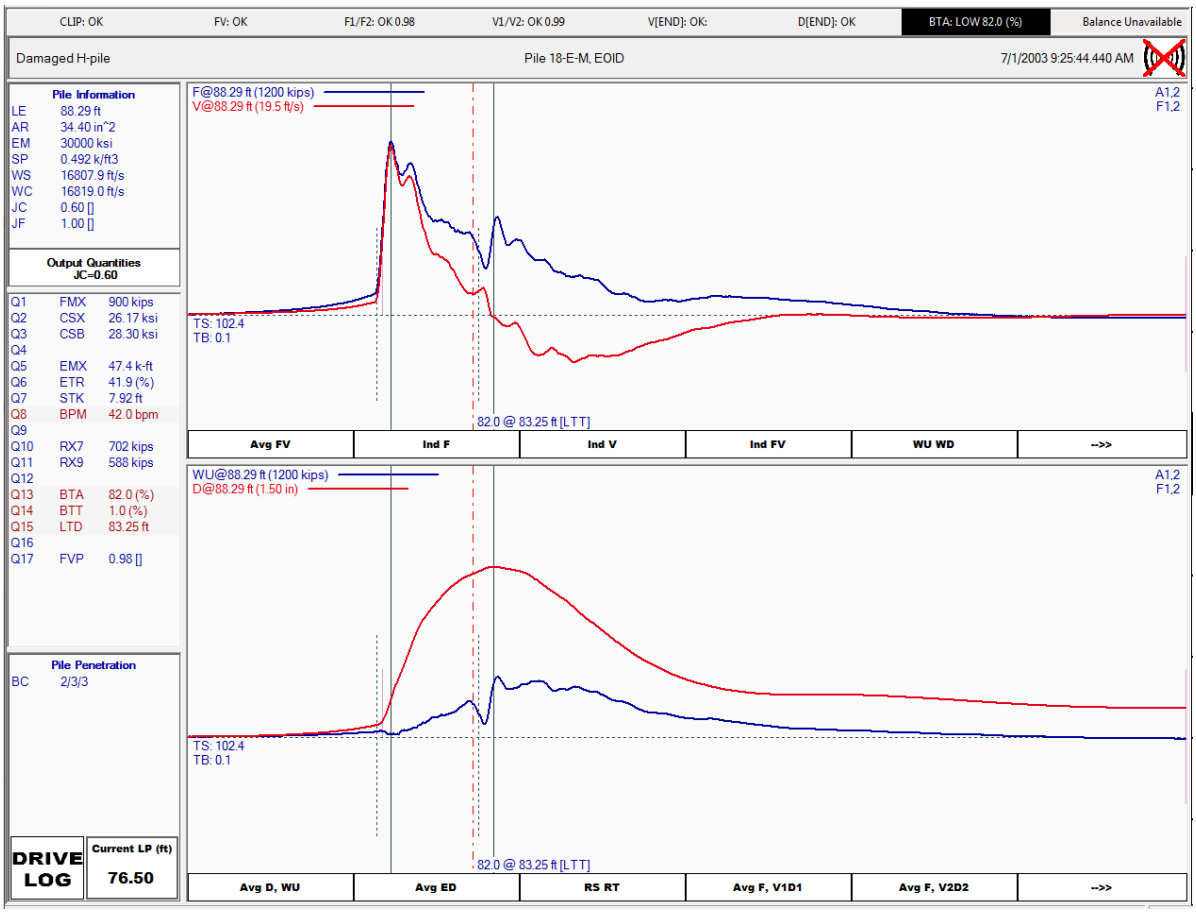

Figure 10-31 Example dynamic test records indicating pile damage.

Figure 10-32 Photographs of extracted pile showing damage.

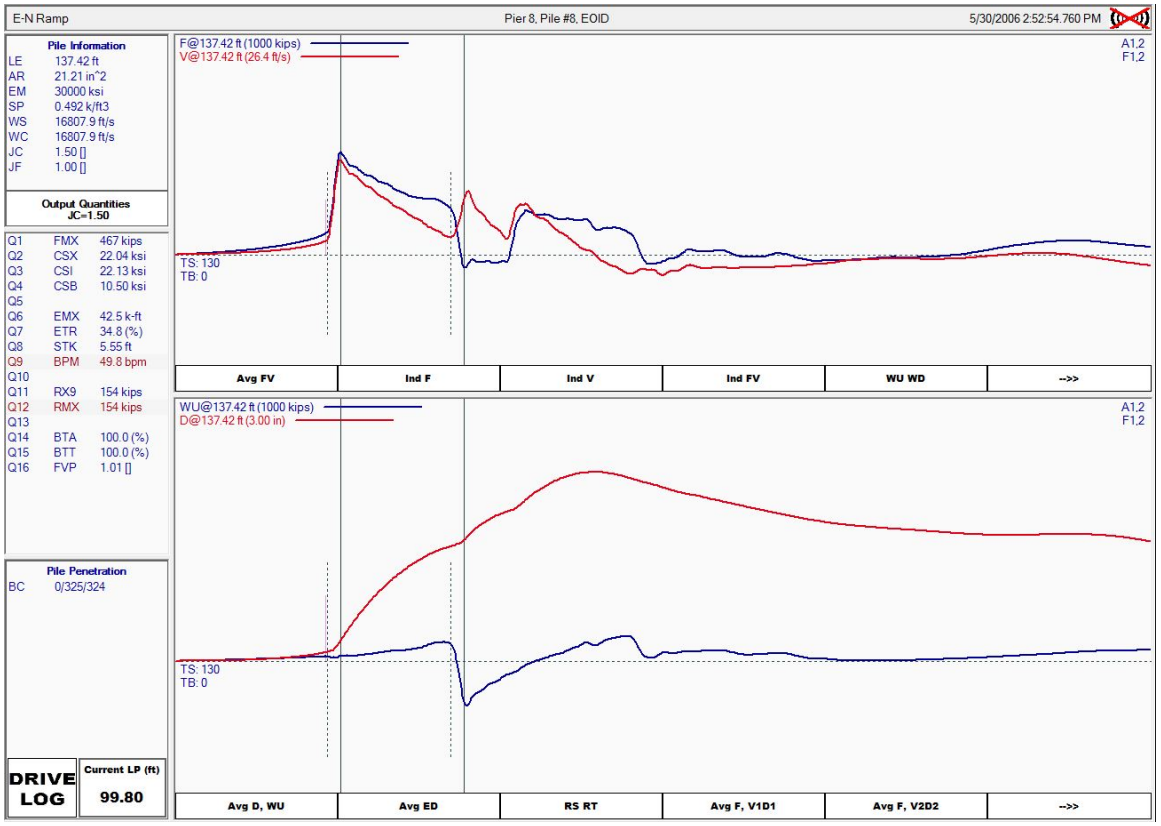

Figure 10-33 Example test record illustrating soil setup - end of initial driving data.

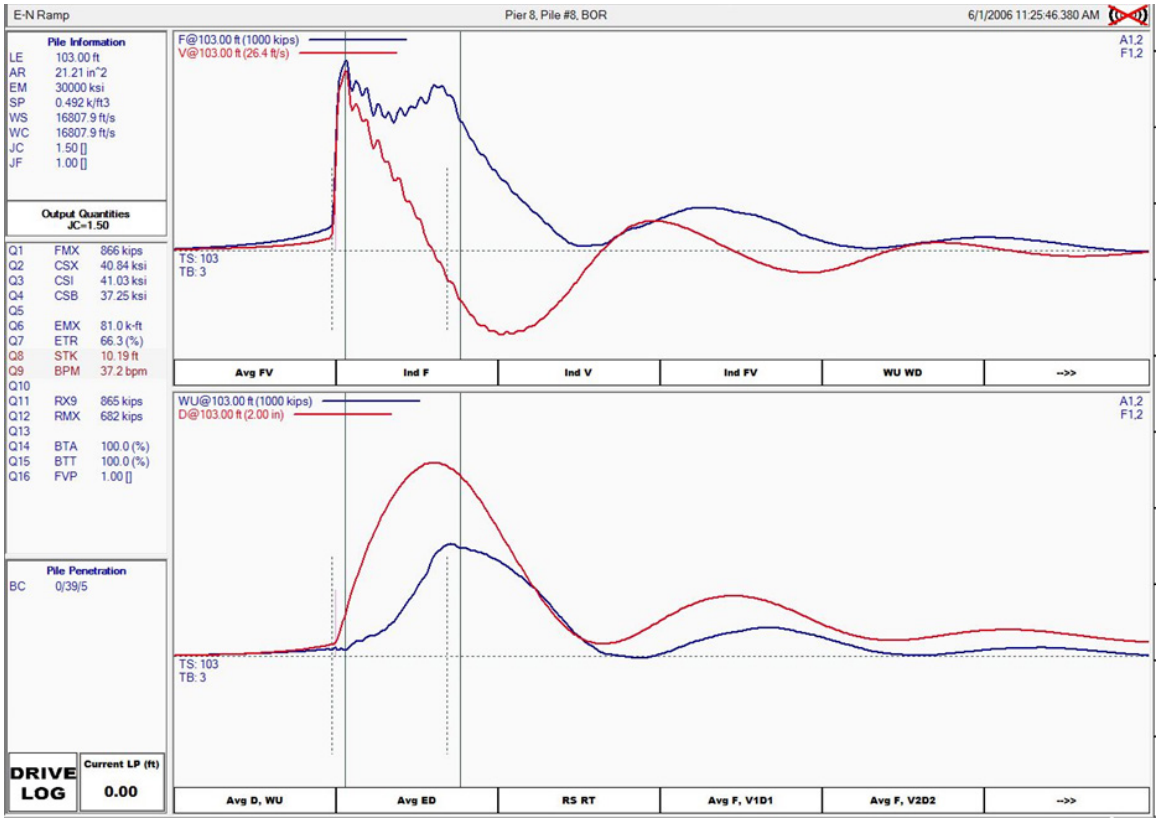

Figure 10-34 Example test record illustrating soil setup - beginning of restrike data.

Figure 10-33 presents a representative dynamic test record obtained near final driving. The pile penetration resistance or blow count at the end of initial driving was 9 blows per foot at an average hammer stroke of 5.8 feet. For the presented hammer blow, the impact force was 467 kips, the transferred energy was 42.5 ft-kips, and the energy transfer ratio was 34.8%. The nominal resistance based on the Case Method solution was 154 kips which was well below the 765 kips required. This was substantiated by signal matching analysis which indicated a nominal resistance of 129 kips, with 75 kips of the resistance carried by shaft resistance and 54 kips through toe resistance.

Figure 10-34 presents a representative dynamic test record obtained near the beginning of restrike 3 days later. The blow count at the beginning of restrike was 8 blows per inch at an average hammer stroke of 10.1 feet. Hence, both the restrike blow count and hammer stroke were significantly higher. For the blow presented, the impact force was 866 kips, the transferred energy was 81.0 ft-kips, and the energy transfer ratio is 66.5%. The nominal resistance based on the Case Method solution was 682 kips, or roughly 4.4 times the nominal resistance at the end of driving. A nominal resistance of 737 kips with 472 kips of shaft resistance and 265 kips of toe resistance was determined by signal matching. Long term restrike tests showed that, with additional time, the 765 kip nominal resistance would be obtained.

The increased nominal resistance during restrike is visually apparent when comparing the end of initial driving and beginning of restrike test records. The separation between the force and velocity records between time 0 and time 2L/C is substantially greater in the restrike test data compared to the end of initial driving data. This is also apparent in the restrike wave up record which has a much greater magnitude as well as significantly steeper slope compared to the end of driving wave up record.

The magnitude of the separation between the force and velocity records in the restrike data substantially increases beginning near the midpoint between time 0 and time 2L/C. This is also apparent in the wave up graph which has a significant change in slope occurring at the same time. These records indicate that the much larger shaft resistance present during restrike developed primarily over the lower half of the pile.

A dramatic change in the test records also occurs at, and immediately, after 2L/C. This indicates a change in the toe resistance and dynamic toe response. Signal matching analysis indicated an increase in the toe resistance, an increase in both the shaft and toe damping, and a reduction in the soil quake at the pile toe.

10.8.6 Test Records Illustrating Relaxation

Test records for HP 12 x 74 H-pile was driven into very dense, clayey silt with a single acting diesel hammer are presented in Figures 10-35 and10-36. SPT N values in the clayey silt deposit ranged from 37 to 100 blows per foot with a SPT N value of 87 blows per foot closest to the pile toe elevation. Dynamic testing was performed on the pile during initial driving and 3 days later during restrike. A nominal resistance of 408 kips was required based on resistance verification using dynamic testing with signal matching.

Figure 10-35 presents a representative dynamic test record obtained near final driving. The pile penetration resistance or blow count at the end of initial driving was 26 blows per foot at an average hammer stroke of 9.1 feet. For the presented hammer blow, the impact force was 738 kips, the transferred energy was 38.6 ft-kips, and the energy transfer ratio was 55.0%. The nominal resistance based on the Case Method solution was 456 kips, exceeding the 408 kips required. This was substantiated by signal matching analysis which indicated a nominal resistance of 471 kips, with 216 kips of the resistance carried by shaft resistance and 255 kips through toe resistance.

Figure 10-36 presents a representative dynamic test record obtained near the beginning of restrike. The blow count at the beginning of restrike was 3 blows per inch at an average hammer stroke of 8.3 feet. Hence, the restrike blow count was slightly higher, but the hammer stroke was reduced. For the blow presented, the impact force was 646 kips, the transferred energy was 27.0 ft-kips, and the energy transfer ratio was 38.5%. The nominal resistance based on the Case Method solution was 351 kips, or roughly 100 kips less than at the end of driving. Signal matching analysis indicated a nominal resistance at the beginning of restrike of 330 kips with 235 kips of shaft resistance and 95 kips of toe resistance.

The reduced nominal resistance during restrike is evident when comparing the end of initial driving and beginning of restrike records. The force and velocity records in the top portion of both figures exhibit less separation between force at velocity records at, and immediately after, the 2L/C marker. This is also apparent in the wave up graphs in the lower portion of both figures. The restrike record has a lower magnitude resistance occurring after the 2L/C marker as well as having a flatter slope.

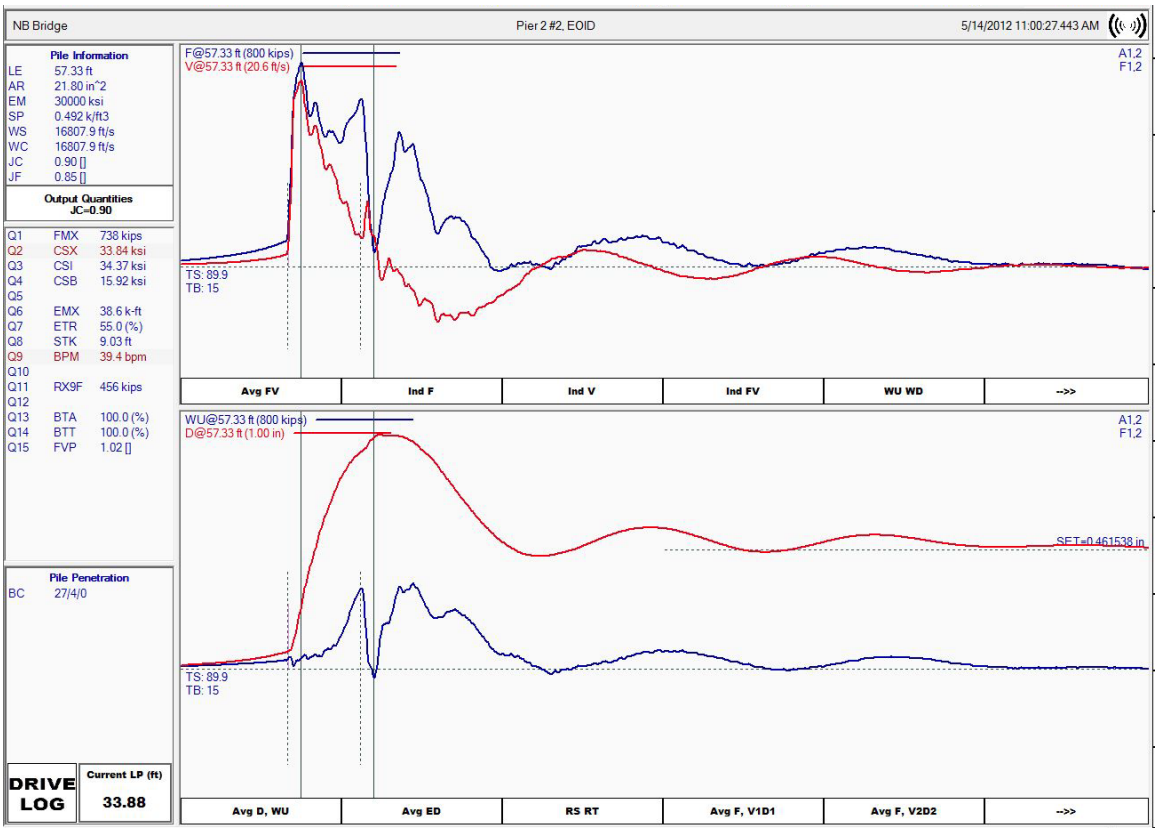

Figure 10-35 Example test record illustrating relaxation - end of initial driving data.

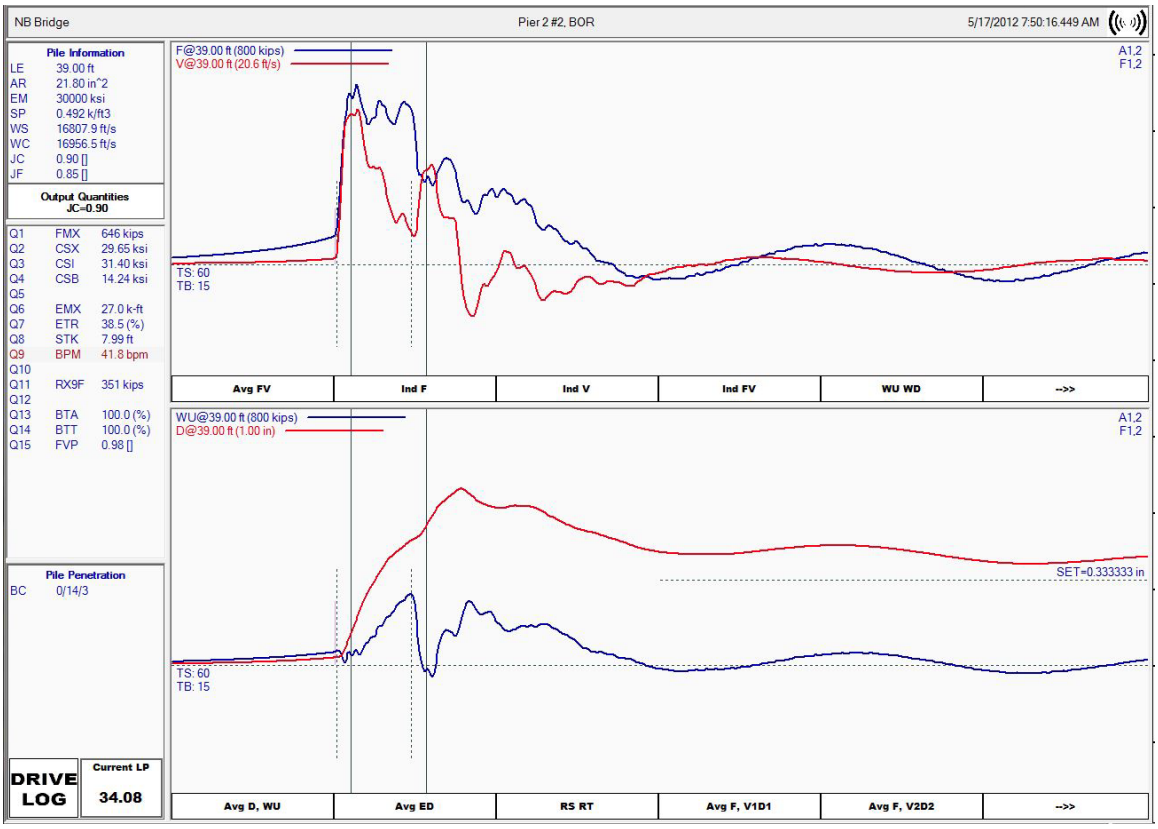

Figure 10-36 Example test record illustrating relaxation - beginning of restrike data.

10.8.7 Reporting of Dynamic Test Results

Additional insight into the pile and soil behavior during driving can be obtained by comparing the dynamic test numerical results versus pile penetration depth and corresponding driving resistance. Dynamic testing systems typically assign a sequential blow number to each hammer blow. By comparing the pile driving log with these blow numbers, numerical and graphical summaries of the dynamic testing results versus pile penetration depth and pile penetration resistance can be prepared.

An example of a numerical summary of dynamic testing results versus depth for a 24 inch square prestressed concrete pile driven with an APE D62-22 diesel hammer is presented in Figure 10-37. The test pile has a required nominal resistance of 1000 kips. Compression and tension stresses are limited to 3.80 ksi and 1.50 ksi, respectively. The accompanying graphical results are presented in Figure 10-38. Specification should require that the dynamic test data for each pile tested be processed versus pile penetration depth with the corresponding blow count in a similar manner. These numerical and graphical results can easily be compared to project requirements by construction personnel.

The effects of fuel setting adjustments as well as pile cushion changes are readily apparent in these graphical and numerical results. Near 43 feet, the diesel hammer fuel setting was increased from fuel setting 1 to 2. Dynamic test results at this depth illustrate an increase in both the compression and tension driving stresses, an increase in the hammer stroke, and an increase in transferred energy. A decrease in the pile penetration resistance also occurs as a result of the fuel setting adjustment even though a small increase in the nominal resistance occurs. Near 68 feet, the fuel setting is once again increased, this time from fuel setting 2 to 3. At that depth and time, the pile cushion is also replaced. When driving is resumed, both compression and tension driving stresses increase, the hammer stroke increases, and the transferred energy increases. The pile penetration resistance decreases as a result of the fuel setting adjustment even though a small increase in the nominal resistance once again occurs. Driving is temporarily stopped at the estimated pile penetration depth of 76 feet and a one hour restrike performed. Unfortunately, the nominal resistance slightly decreases during restrike requiring the test pile to subsequently be driven deeper for the required nominal resistance. The compression and tension driving stresses were maintained within specification limits throughout the test pile installation process.

GRL Engineers, Inc. Page 1
Case Method & iCAP® Results PDIPLOT2 2015.1.51.2 - Printed 30-September-2015

PDA Plot Example - 24" Prestressed Concrete Pile APE D62-22
OP: MLB Date: 26-June-2013

AR: 576.00 in² SP: 0.150 k/ft³
LE: 118.00 ft EM: 6,346 ksi
WS: 14,000.0 f/s JC: 0.70 []

CSX: Max Measured Compr. Stress STK: O.E. Diesel Hammer Stroke
CSB: Compression Stress at Bottom EMX: Max Transferred Energy
TSX: Tension Stress Maximum RMX: Max Case Method Capacity

BL#	Depth	BLC	TYPE	CSX	CSB	TSX	STK	EMX	RMX
	ft	blows/ft		ksi	ksi	ksi	ft	k-ft	kips
8	21	8	AV5	1.93	0.54	1.37	6.16	28.1	218
18	22	10	AV10	1.93	0.58	1.36	5.94	26.9	231
25	23	7	AV7	1.97	0.60	1.38	6.01	27.9	235
34	24	9	AV9	1.96	0.61	1.37	5.95	27.0	248
44	25	10	AV9	1.99	0.62	1.40	6.00	27.5	259
57	26	13	AV13	2.00	0.68	1.36	6.04	27.2	287
68	27	11	AV11	2.03	0.69	1.41	6.10	28.0	287
81	28	13	AV10	2.04	0.75	1.37	6.10	27.7	300
94	29	13	AV13	2.01	0.73	1.36	6.05	27.0	297
104	30	10	AV8	2.02	0.73	1.39	6.04	27.3	287
115	31	11	AV11	1.94	0.62	1.39	5.86	26.2	268
124	32	9	AV9	2.01	0.67	1.39	6.01	27.3	264
134	33	10	AV10	2.03	0.64	1.42	6.03	27.9	244
142	34	8	AV8	2.07	0.64	1.46	6.15	29.2	227
150	35	8	AV8	1.96	0.55	1.42	5.88	27.2	208
159	36	9	AV9	1.92	0.54	1.38	5.84	26.1	207
171	37	12	AV11	2.07	0.66	1.40	6.18	28.5	241
189	38	18	AV18	2.11	0.79	1.32	6.32	28.4	339
218	39	29	AV29	2.16	1.00	1.19	6.50	27.7	447
255	40	37	AV37	2.23	1.16	1.10	6.67	28.7	526
304	41	49	AV49	2.25	1.23	1.03	6.68	29.0	566
356	42	52	AV52	2.24	1.24	0.95	6.63	28.7	572
412	43	56	AV56	2.20	1.25	0.87	6.51	27.4	564
457	44	45	AV45	2.44	1.36	1.02	7.26	33.4	585
497	45	40	AV40	2.64	1.44	1.14	7.85	38.5	601
536	46	39	AV39	2.70	1.44	1.17	8.02	40.0	595
571	47	35	AV35	2.77	1.45	1.20	8.29	42.4	592
605	48	34	AV34	2.85	1.50	1.25	8.46	44.5	599
642	49	37	AV37	2.86	1.52	1.22	8.43	44.3	606
679	50	37	AV37	2.87	1.55	1.20	8.39	44.7	611
719	51	40	AV40	2.88	1.56	1.20	8.38	45.0	613
754	52	35	AV35	2.90	1.57	1.19	8.36	45.3	603
791	53	37	AV37	2.92	1.57	1.22	8.34	45.5	595
830	54	39	AV38	2.99	1.60	1.21	8.48	47.1	602
864	55	34	AV34	3.04	1.66	1.23	8.54	48.4	616
907	56	43	AV43	3.06	1.74	1.22	8.58	48.9	647
954	57	47	AV47	3.07	1.83	1.16	8.58	49.0	664
1004	58	50	AV50	3.13	1.90	1.14	8.71	50.5	675
1053	59	49	AV44	3.11	1.96	1.08	8.58	49.2	680
1106	60	53	AV53	3.13	1.99	1.07	8.61	49.5	684
1155	61	49	AV49	3.11	2.02	1.02	8.57	48.7	669
1208	62	53	AV53	3.11	2.02	1.02	8.55	48.5	658
1258	63	50	AV50	3.05	1.98	1.00	8.41	47.3	639
1308	64	50	AV50	2.94	1.92	0.96	8.21	44.7	602
1354	65	46	AV46	2.88	1.91	0.91	8.19	43.9	570
1404	66	50	AV50	2.82	1.91	0.83	8.14	43.0	549
1452	67	48	AV48	2.80	1.93	0.77	8.17	42.6	545
1501	68	49	AV49	2.80	1.94	0.74	8.26	42.6	542
1549	69	48	AV41	2.90	2.02	0.75	8.73	45.3	600
1593	70	44	AV44	3.18	2.15	0.88	8.83	49.0	594
1638	71	45	AV45	3.16	2.18	0.82	8.80	48.4	600
1687	72	49	AV49	3.13	2.20	0.76	8.86	47.9	627
1740	73	53	AV53	3.09	2.21	0.70	8.99	48.3	665
1798	74	58	AV52	3.02	2.22	0.63	8.91	47.2	706
1855	75	57	AV57	2.99	2.23	0.59	9.09	47.8	743
1904	76	49	AV47	3.09	2.20	0.78	9.02	49.6	735
1955	77	51	AV51	3.25	2.22	0.88	8.95	52.9	711
1995	78	48	AV40	3.15	2.18	0.80	8.96	50.7	694
2018	79	48	AV23	3.24	2.22	0.86	8.93	51.8	710
2065	80	47	AV47	3.34	2.34	0.83	8.96	54.3	761
2119	81	54	AV54	3.31	2.40	0.74	9.06	53.8	847
2182	82	63	AV63	3.24	2.47	0.60	9.10	51.9	938
2258	83	76	AV76	3.13	2.55	0.47	9.08	49.6	1,011
2367	84	109	AV109	3.15	2.57	0.50	9.21	50.7	1,028
2462	85	95	AV95	3.20	2.45	0.58	9.32	51.7	1,006

Figure 10-37 Typical tabular presentation of dynamic test results.

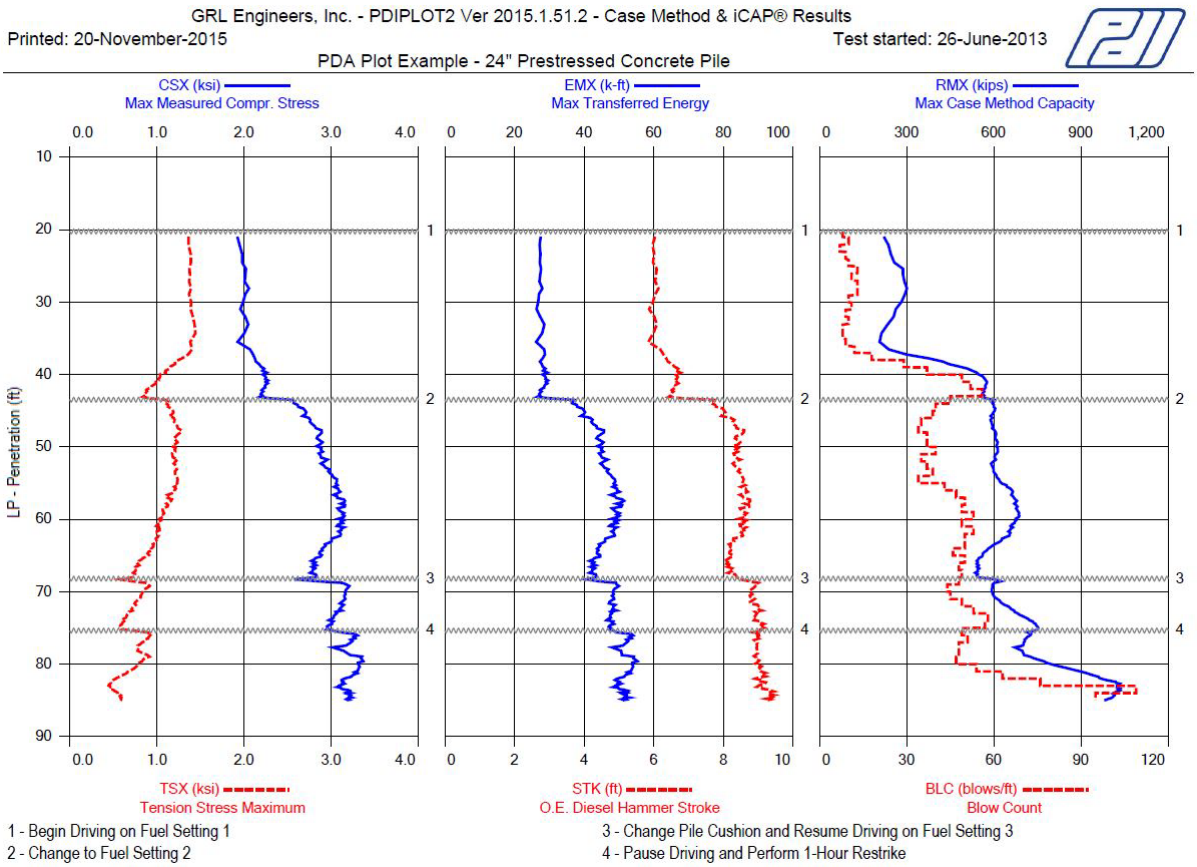

Figure 10-38 Typical graphical presentation of dynamic test results versus depth.

10.9 CASE HISTORY

The following case history illustrates how dynamic pile testing and analysis was used on a small single span bridge constructed in a remote area. The subsurface exploration for the project found a 98 foot thick deposit of moderately clean, medium dense to dense sands with SPT N values ranging from 10 to 50. Based upon these conditions, the foundation report recommended 12.75 inch O.D. closed end pipe piles be used for the bridge abutment foundations. The pipe piles had an estimated length of 39 feet for a nominal resistance of 326 kips. The foundation report recommended wave equation analysis be used for construction control. Dynamic testing of one test pile at each abutment was also specified with the test pile information to be used by the engineer to provide the contractor pile order lengths.

The Case Method was used to evaluate pile nominal resistance versus penetration depth during the test pile driving. More rigorous signal matching analyses were also performed on the dynamic test data to check the Case Method results at selected

pile penetration depths. During initial driving at Abutment 1, the 12.75 inch pipe pile drove beyond the estimated pile penetration depth without developing the required nominal resistance. The pile was driven to a depth of 75 feet and had an end of drive nominal resistance of 235 kips. A restrike dynamic test performed one day after initial driving indicated the nominal resistance increased slightly to 245 kips.

While the test pile information from Abutment 1 was being evaluated, three additional test piles were driven at Abutment 2. First, dynamic testing of a 16 inch O.D. closed end pipe pile was performed to determine if a larger diameter pipe pile could develop the required nominal resistance and, if so what pile penetration depth was necessary. The 16 inch pile was driven to a depth of 89 feet and had an end of drive nominal resistance of 222 kips. A one day restrike test on this pile indicated a nominal resistance of 280 kips. The 16 inch pile was driven deeper following the restrike test to a final penetration depth of 112 feet. With the additional driving, the nominal resistance at the end of redrive decreased to 240 kips.

Approximately two weeks later, a 12.75 O.D. closed end pipe pile and a 14 inch diameter Monotube pile with a 25 foot tapered lower section were driven at Abutment 2. The 12.75 inch pipe pile was driven to a penetration depth of 95 feet with an end of drive nominal resistance of 105 kips. The Monotube pile was driven to a depth of 43 feet and had an end of drive nominal resistance of 190 kips. One day restrike tests on both piles indicated a slight increase in nominal resistance to 180 kips and 205 kips, respectively. During this same site visit, a 16 day restrike test was performed on the 16 inch pipe pile. The long term restrike nominal resistance for the 16 inch pipe pile was 400 kips.

The dynamic testing results from both abutments indicated that the required nominal resistance could not be obtained at or near the estimated pile penetration depth with the 12.75 inch pipe piles. However, two foundation solutions were indicated by the dynamic testing results. If a reduced nominal resistance were chosen, the test results indicated a Monotube pile driven to a significantly shorter penetration depth could develop about the same nominal resistance as could be developed by the 12.75 inch pipe piles. Alternatively, if the original nominal resistance was desired, 16 inch pipe piles could be driven on the order of 92 feet below grade.

Although not originally planned, two static load tests were performed to confirm the nominal resistance that could be achieved at the site. The 12.75 inch pipe and the 14 inch Monotube piles at Abutment 2 were selected for testing. The static load test results indicated the 12.75 inch pipe pile with a pile penetration depth of 95 feet had a nominal resistance of 230 kips and the Monotube pile with a pile penetration

depth of 43 feet had a nominal resistance of 220 kips. The dynamic test nominal resistances determined during restrike were in good agreement with these static load tests results particularly when the additional time between the dynamic restrike tests and static load tests is considered.

Based on the required pile lengths and the nominal resistances determined from the dynamic and static load testing, a cost evaluation of the foundation alternatives was performed. The cost analysis indicated that the Monotube piles would be the most economical pile foundation type. This case study illustrates how the routine application of dynamic testing on a small project helped facilitate the solution to an unexpected foundation problem.

10.10 ADVANTAGES, DISADVANTAGES, AND LIMITATIONS

An advantage of dynamic testing over other methods of nominal resistance verification is the additional information gained on the pile installation process. In addition to providing estimates of nominal resistance during driving and during restrike, dynamic test data can be used to check hammer and drive system performance, to monitor driving stresses, and to assess pile structural integrity.

Many piles can also be dynamically tested during initial driving or during restrike in one day. This makes dynamic testing an economical and quick testing method. Results are generally available immediately after each hammer blow.

On large projects, dynamic testing can be used to supplement static pile load tests or reduce the overall number of static tests to be performed. Since dynamic tests are more economical than static tests, additional coverage can also be obtained across a project at reduced costs. On small projects where static load tests may be difficult to justify economically, dynamic tests offer a viable construction control method.

Dynamic tests can provide information on pile nominal resistance versus depth, nominal resistance variations between locations, and nominal resistance variations with time after installation through restrike tests. This information can be helpful in augmenting the foundation design, when available from design stage test pile programs, or in optimizing pile lengths when used early in construction test programs.

When used as a construction monitoring and quality control tool, dynamic testing can assist in early detection of pile installation problems such as poor hammer performance or high driving stresses. Test results can then facilitate the evaluation and solution of these installation problems.

On projects where dynamic testing was not specified and unexpected or erratic driving behavior or pile damage problems develop, dynamic testing offers a quick and economical method of troubleshooting.

Results from dynamic testing and signal matching analysis can be used to develop pile driving criterion. A procedure describing the use of dynamic test results to refine wave equation input parameters and wave equation analysis results is described in Section 12.6.9.

A disadvantage with dynamic testing for determining the nominal resistance can be the pile driving system. The pile hammer must be capable of mobilizing all the soil resistance acting on the pile. Shaft resistance can generally be mobilized at a fraction of the movement required to mobilize the toe resistance. However, when pile penetration resistances approach 10 blows per inch, the soil resistance may not be fully mobilized at and near the pile toe. In these circumstances, dynamic test capacities tend to produce lower bound estimates of the nominal resistance. If available, a larger pile hammer or higher hammer stroke can be used to increase the net pile penetration per blow and thereby mobilize more resistance, if present.

Dynamic testing estimates of nominal resistance also indicate the nominal resistance at the time of testing. Since increases and decreases in the pile nominal resistance with time typically occur due to soil setup/relaxation, restrike tests after an appropriate waiting period are usually required for a better indication of long term pile nominal resistance. This may require an additional move of the pile driving rig for restrike testing.

A limitation of dynamic testing can be the geotechnical failure mechanism. Large diameter open ended pipe piles or H-piles which do not bear on rock may behave differently under dynamic and static loading conditions. This is particularly true if a soil plug does not form during driving. In these cases, limited toe resistance develops during the dynamic test. However, under slower static loading conditions, these open section piles may develop a soil plug and therefore a higher pile nominal resistance under static loading conditions. Interpretation of test results by experienced personnel is important in these situations.

10.11 PRACTICAL ISSUES AND CONSIDERATIONS

Several practical issues and considerations should be clearly understood by the parties responsible for analyzing and reviewing dynamic test results. Some of the more common issues encountered include:

- Understanding that specifying “a dynamic test” does not implicitly require the dynamic test personnel to furnish driving criteria.

  Like any other engineering service, dynamic test results should be analyzed and reviewed. While it is often desirable to continue driving production piles immediately after the dynamic test is complete, time should be allocated for analysis and reporting of test results. If the driving criteria is to be determined from the dynamic test results, that should be clearly identified in the project specifications as well as when the driving criteria is to be furnished to the owner or contractor.

- Understanding the limitations of dynamic tests in easy driving and hard driving situations.

  At pile penetration resistances less than 24 blows per foot and above 120 blows per foot, dynamic test and analysis methods can overpredict and underpredict the nominal resistance, respectively. At low blow counts (high set per blow), it is difficult for dynamic methods to easily separate the static and dynamic soil resistance effects resulting in a tendency to overpredict the static resistance. Use of a reduced hammer stroke or lower fuel setting can help improve the accuracy of dynamic methods in low blow count situations. At very high blow counts (low set per blow), dynamic test methods tend to produce lower bound nominal resistance estimates as not all of the resistance (particularly at and near the toe) is fully activated. In these high blow count situations, use of a larger hammer stroke, higher fuel setting, pile hammer with a greater rated energy, or variable stroke drop hammer can help improve dynamic method accuracy.

- Understanding that a dynamic test provides the mobilized nominal resistance at the time of testing.

  The nominal resistance determined in a dynamic test is the mobilized resistance at that particular time. The nominal resistance of a pile typically changes over time. It may increase (soil setup) or decrease (relaxation).

Dynamic tests must be performed at both the end of initial driving and during restrike at a later time in order to quantify time dependent changes in nominal resistance.

- Knowing how to perform and evaluate restrike dynamic test results.

  Ideally, the hammer stroke or fuel setting is selected such that the penetration resistance at the beginning of restrike falls between 3 and 10 blows per inch. In this situation, the test record to select for signal matching analysis is readily apparent. An early, high energy blow, with good data quality should be selected and analyzed for the nominal resistance. The restrike blow count should be carefully recorded over the full restrike event as the rate by which the blow count decreases from inch to inch can be helpful. When the restrike blow count is less than 24 blows per foot, a lower energy restrike blow should be chosen for signal matching analysis to reduce the potential for overpredicting the nominal resistance.

  In more difficult situations, limited pile movement may occur during restrike and several records may need to be analyzed with signal matching. Superposition of the activated shaft resistances under various restrike hammer blows may be used to assess the nominal pile resistance. In initial restrike blows, the shaft resistance may be mobilized along the upper portion of the pile shaft. Later restrike blows may indicate more shaft resistance on the lower portion of the pile once the upper shaft resistance has started to breakdown. The toe resistance and shaft resistance on the lower portion of the pile from the end of drive analysis should also be reviewed and, if appropriate, used in a superposition case. When using the toe resistance from an end of drive situation, the analyst should be confident that relaxation in the toe bearing layer is not a consideration or overestimation of the nominal resistance could result by using superposition.

- Difficulty to accept that, in some cases, dynamic measurements may provide conservative predictions of the true geotechnical resistance and correlations and extrapolation between dynamic and static load test results are necessary.

  Dynamic methods can yield conservative estimates of the true geotechnical resistance in some situations. Open ended pipe piles or H-piles which do not bear on rock may behave differently under dynamic and static loading conditions. Under dynamic loading conditions, the soil inside a pipe pile or between H-pile flanges may slip and produce internal shaft resistances.

Under static loading conditions, this soil may plug and move with the pile resulting in toe resistance over the full pile cross section. Hence both shaft and toe resistances may be different in open profile pile sections under static and dynamic loading conditions. Plugging behavior can also vary in different geomaterials. Careful interpretation and extrapolation of dynamic results is required in these situations.

- Understanding modeling uncertainties in signal matching analysis that can affect the reported soil resistance distribution.

  A portion of the soil resistance calculated on an individual soil segment in a signal matching analysis can usually be shifted up or down the shaft one soil segment without significantly altering the overall match quality. Similarly, it may be possible to shift a portion of the soil resistance from the last shaft segment to the pile toe or vis versa without significantly altering match quality. Therefore, use of the signal matching determined soil resistance distribution for uplift, scour, drag force, and other geotechnical considerations should be made with an understanding of these analysis limitations.

REFERENCES

American Association of State Highway and Transportation Officials (AASHTO). (2014). AASHTO LRFD Bridge Design Specifications, US Customary Units, Seventh Edition, with 2015 Interim Revisions. American Association of State Highway and Transportation Officials, Washington, D.C., 1960 p.

Abu-Hejleh, N., Kramer, W.M., Mohamed, K., Long, J.H., and Zaheer, M.A. (2013). Implementation of AASHTO LRFD Design Specifications for Driven Piles, FHWA-RC-13-001. U.S. Dept. of Transportation, Federal Highway Administration, Washington, D.C., 71 p.

ASTM D4945-12. (2014). Standard Test Method for High-Strain Dynamic Testing of Piles. Book of ASTM Standards, Vol. 4.08, ASTM International, West Conshohocken, PA, 9 p.

Davisson, M.T. (1972). High Capacity Piles. Proceedings, Soil Mechanics Lecture Series on Innovations in Foundation Construction, American Society of Civil Engineers, ASCE, Illinois Section, Chicago, IL, pp. 81-112.

Eiber, R.J. (1958). A Preliminary Laboratory Investigation of the Prediction of Static Pile Resistances in Sand. Master's Thesis, Department of Civil Engineering, Case Institute of Technology, Cleveland, OH.

Goble, G.G., Likins, G.E. and Rausche, F. (1975). Bearing Capacity of Piles from Dynamic Measurements. Final Report, Department of Civil Engineering, Case Western Reserve University, Cleveland, OH, 37 p.

Goble, G.G. and Rausche, F. (1970). Pile Load Test by Impact Driving. Highway Research Record, Highway Research Board, No. 333, Washington, D.C., pp.123-129.

Goble, G.G., Rausche, F. and Likins, G.E. (1980). The Analysis of Pile Driving - A State-of-the-Art. Proceedings of the 1st International Seminar on the Application of Stress-Wave Theory on Piles, Stockholm, H. Bredenberg, Editor, A.A. Balkema Publishers, pp.131-161.

Likins, G. E., and Rausche, F. (2014). Pile Damage Prevention and Assessment Using Dynamic Monitoring and the Beta Method, From Soil Behavior Fundamentals to Innovations in Geotechnical Engineering, ASCE Geo-Institute Geotechnical Special Publication No. 233, Reston, VA, pp. 428-442.

Hannigan, P.J. (1990). Dynamic Monitoring and Analysis of Pile Foundation Installations. Deep Foundations Institute Short Course Text, First Edition, 69 p.

Herrera, R., Jones, L., and Lai, P. (2009). Driven Concrete Pile Foundation Monitoring with Embedded Data Collector System. Contemporary Topics in Deep Foundations, pp. 621-628.

McVay M.C., and Wasman, S.J. (2015). Embedded Data Collector (EDC) Phase II Load and Resistance Factor Design (LRFD), FDOT Contract BDV31-977-13, Florida Department of Transportation, Tallahassee, FL, 139 p.

Paikowsky, S.G. (2004), with contributions from Birgisson, B., McVay, M., Nguyen, T., Kuo, C., Baecher, G., Ayyub, B., Stenersen, K., O.Malley, K., Chernauskas, L., and O'Neill, M., Load and Resistance Factor Design (LRFD) for Deep Foundations, NCHRP Report 507. Transportation Research Board, Washington, D.C., 76 p.

Pile Dynamics, Inc. (2015). Pile Driving Analyzer Manual; Model 8G, Cleveland, OH.

Rausche, F., Goble, G.G., and Likins, G.E. (1985b). Dynamic Determination of Pile Capacity. American Society of Civil Engineers, ASCE, Journal of the Geotechnical Engineering Division, Vol. 111, No. 3, pp. 367-383.

Rausche, F. and Goble, G.G. (1979). Determination of Pile Damage by Top Measurements. Behavior of Deep Foundations. American Society for Testing and Materials, ASTM STP 670, R. Lundgren, Editor, pp. 500-506.

Rausche, F., Likins, G.E., Goble, G.G. and Miner, R. (1985a). The Performance of Pile Driving Systems. Main Report, U.S. Department of Transportation, Federal Highway Administration, Office of Research and Development, Washington, D.C., Volumes I-IV.

Rausche, F., Moses, F., and Goble, G.G. (1972). Soil Resistance Predictions from Pile Dynamics. Journal of the Soil Mechanics and Foundations Division, ASCE, Vol. 98, No. 9, pp. 367-383.

Reiding, F.J., Middendorp, P., Schoenmaker, R.P., Middendorp, F.M. and Bielefeld, M.W. (1988). FPDS-2, A New Generation of Foundation Diagnostic Equipment, Proceeding of the 3rd International Conference on the Application of Stress Wave Theory to Piles, Ottawa, B.H. Fellenius, Editor, BiTech Publishers, pp. 123-134.

Verbeek, G. and Middendorp, P. (2011). Determination of Pile Damage in Concrete Piles. Deep Foundations Institute Journal, Vol. 6, No. 2, pp. 44-50.

CHAPTER 11

RAPID LOAD TESTING

The nominal resistance of driven pile foundations in axial compression can be evaluated by rapid load test methods. Rapid load tests methods can be applied to all driven pile types on land or over water. The test methods can provide time and cost savings where high loads are required or access is difficult. ASTM D7383, Standard Test Methods for Axial Compressive Force Pulse (Rapid) Testing of Deep Foundations, provides additional details on rapid load test methods and procedures.

11.1 REQUIREMENTS FOR RAPID LOAD TESTS

In general, the previously stated reasons and prerequisites for a static load test program described in Section 9.1.1 are valid for rapid load test programs. Rapid load tests can be used to provide verification or refinement of the foundation design, confirm the nominal geotechnical resistance, and, in some instances, quantify the p-y response of laterally loaded piles. Knowledge of the subsurface stratigraphy including the engineering parameters of the geomaterials should be known prior to performing a rapid load test.

Rapid Load Tests procedures are standardized in ASTM D7383 (2010). In this method, a loading apparatus generates a force pulse that will result in an applied pile head force versus time plot as shown in Figure 11-1. A target peak force is determined that should exceed the nominal geotechnical resistance plus the dynamic soil resistance. The target peak force is based on soil types, pile type and other project requirements. The applied force should exceed 50% of the actual peak force for a time duration of 4L/C or four times the pile length, L, divided by the pile material wave speed, C. The force applied must also exceed the static weight applied to the pile head due to the apparatus prior to the test, known as the pre-load force, for a time duration of at least 12L/C. Shorter time durations than 12L/C can be acceptable if additional force or movement measurement devices are used along the pile length at a distance described in the ASTM standard.

The force pulse should be measured by a calibrated force transducer placed between the loading apparatus and the pile head with the rated transducer capacity

being at least 10% higher than the target peak force. The resulting pile head displacement should be measured by one or more calibrated displacement transducers. The ASTM standard also allows the Engineer to approve secondary pile head displacement measurement devices including redundant displacement transducers or accelerometers. As noted above, additional devices to measure force or displacement can be used along the pile's length when the force pulse duration is less than 12L/C. All force and displacement measurements should be recorded versus time on an appropriate recording device with an appropriate sampling frequency and signal conditioning.

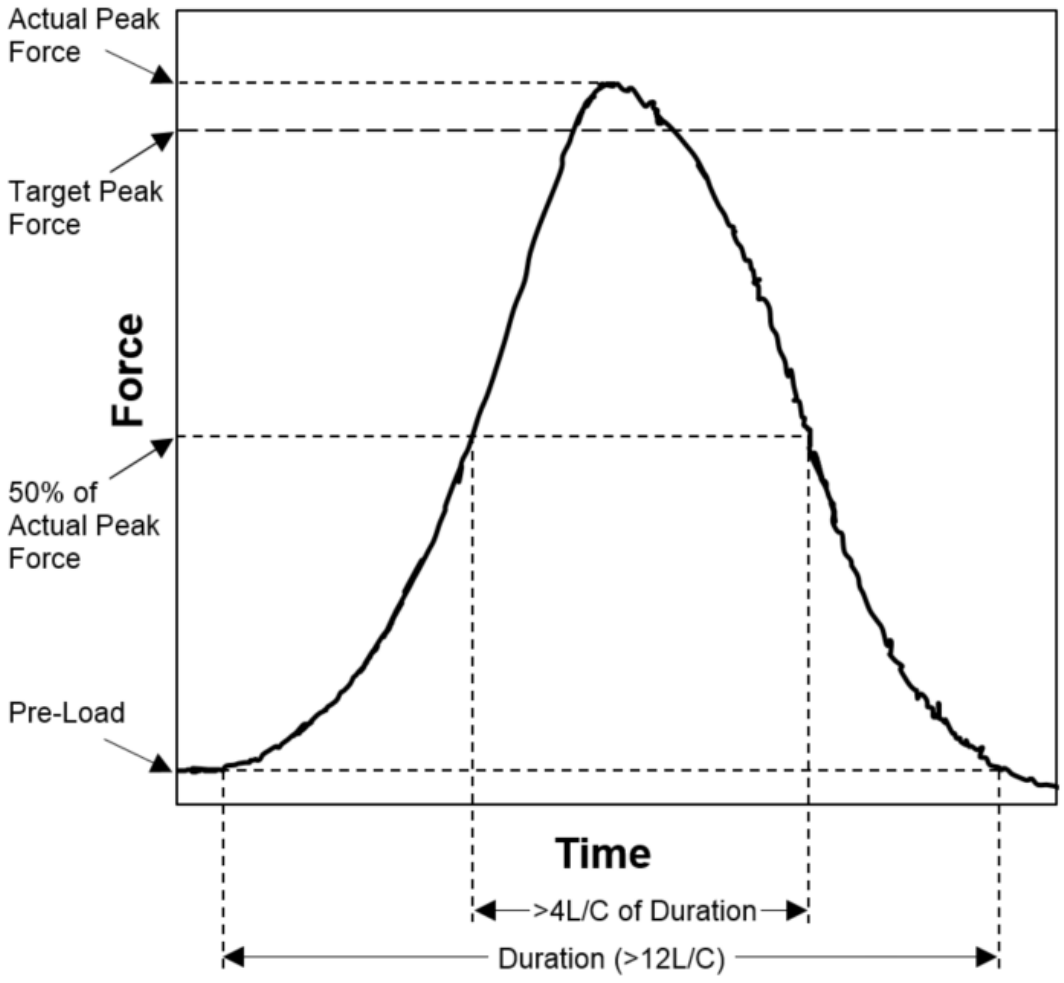

Figure 11-1 Typical axial compressive force pulse (after ASTM D7383).

11.2 BACKGROUND ON RAPID LOAD TEST METHODS

Rapid load testing can be performed using a combustion gas and a reaction mass or with a cushioned drop weight system. These methods will be described in subsequent sections.

11.2.1 Combustion Gas and Reaction Mass Apparatus (Statnamic)

The Statnamic testing method was developed in 1988 by Berminghammer Foundation Equipment and TNO, the Dutch governmental organization for applied scientific research. Bermingham and Janes (1989) described the method which uses solid fuel burned within a pressure chamber to rapidly accelerate upward the reaction mass positioned on top of the pile head. As the gas pressure increases, an upward force is exerted on the reaction mass, while an equal and opposite force pushes downward on the pile. Loading increases to a maximum and then unloads by a venting of the gas pressure. A load cell and accelerometers measure load and acceleration. Typically, the reaction mass weighs a minimum of 5% of the target peak force. The Statnamic test method is licensed to a single source in the US.

Statnamic tests for evaluation of static pile capacity have been performed on steel, concrete and timber piles. At present, individual piles, or pile groups with a combined static and dynamic resistance less than 9,000 kips can be tested. Axial compression tests have been conducted on both vertical and battered piles. The test method has been used on land and over water.

The principles of Statnamic can be described by Newton's Laws of Motion:

1. A body will continue in a state of rest or uniform motion unless compelled to change by an external force.

2. A body subjected to an external force accelerates in the direction of the external force and the acceleration is proportional to the force magnitude ($F = ma$).

3. For every action there is an opposite and equal reaction ($F_{12} = -F_{21}$).

In the Statnamic test, a reaction mass is placed on top of the pile to be tested. The ignition and burning of the solid fuel creates a gas pressure force, F, that causes the reaction mass, m, to be propelled upward so that the acceleration amounts to about

20 g's (F=ma). An equivalent downward force is applied to the foundation element, ($F_{12} = -F_{21}$). The Statnamic concept is illustrated in Figure 11-2.

Development began in 1988 with a Statnamic device capable of a 22 kip test load. From 1988 through 1992, the test load capability was incrementally increased to 3600 kips. In 1994, a 6800 kip testing device was introduced. In 1998, a hydraulic catch mechanism was developed. The maximum test capacity was increased to 9000 kips in 2005.

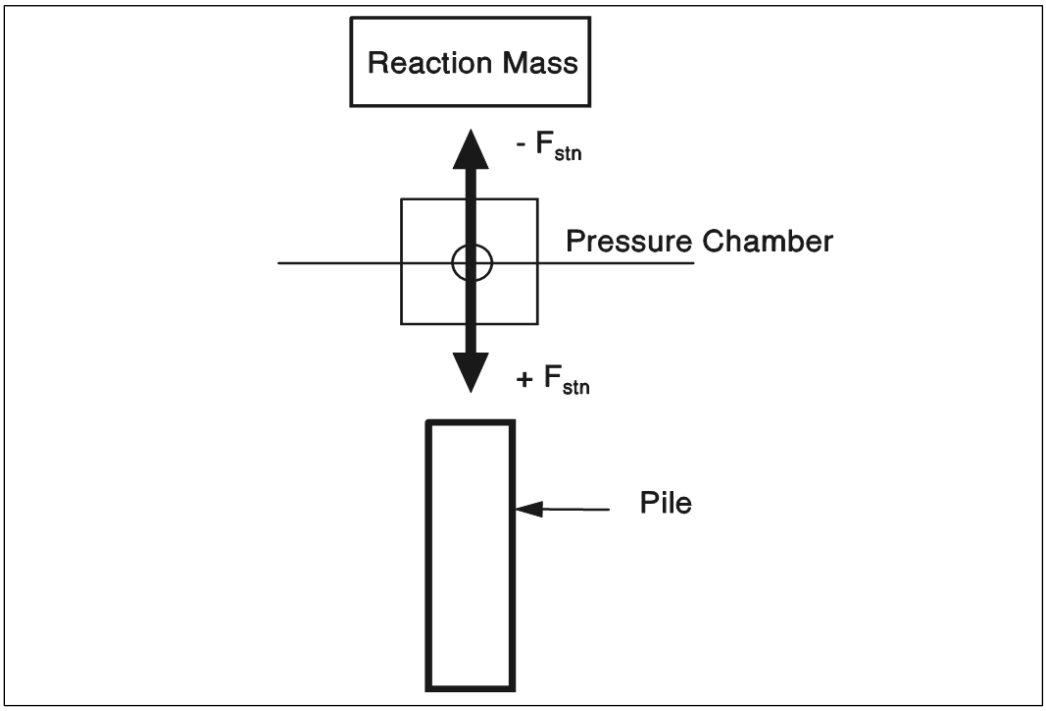

Figure 11-2 Statnamic concept (courtesy of Berminghammer Foundation Equipment).

A base plate is attached to the pile head. The load cell, accelerometer, and piston base are positioned on top of the base plate. Next, the launching cylinder is placed on top of the piston base, thus enclosing the pressure chamber and propellant material. The segmental reaction mass is then stacked on the launching cylinder and a catching mechanism is placed around the reaction mass.

Depending upon the test load, a hydraulic catch, mechanical catch, or gravel retention structure is used to catch the reaction mass. The hydraulic catch system shown in Figure 11-3 is used for test loads of 1000 kips. A mechanical catch system is used for test loads of up to 4,400 kips and a gravel retention structure as shown in Figure 11-4 is used for loads of up to 9,000 kips. For the gravel retention structure, gravel backfill is placed in the annulus between the reaction mass and the

retention structure. After propellant ignition and reaction mass launch, the granular backfill slumps into the remaining void to cushion the reaction mass fall.

The magnitude and duration of the applied load and the loading rate are controlled by the selection of piston and cylinder size, the fuel mass, the fuel type, the reaction mass, and the gas venting technique. The force applied to the pile is measured by the load cell. The acceleration of the pile head is monitored by the accelerometer and is integrated once to obtain pile head velocity and again to obtain displacement. Load and displacement data from the load cell and accelerometers are recorded, digitized, and displayed immediately in the field. Typical raw signals of the load and displacement records are given in Figure 11-5. These signals can then be converted into a raw load - displacement curve as given in Figure 11-6, which requires interpretation to derive the static pile capacity.

Figure 11-3 1000 kip hydraulic catch device on prestressed concrete pile (courtesy of Applied Foundation Testing).

Figure 11-4 Statnamic test in progress with gravel catch mechanism - 9,000 kip device (courtesy of Applied Foundation Testing).

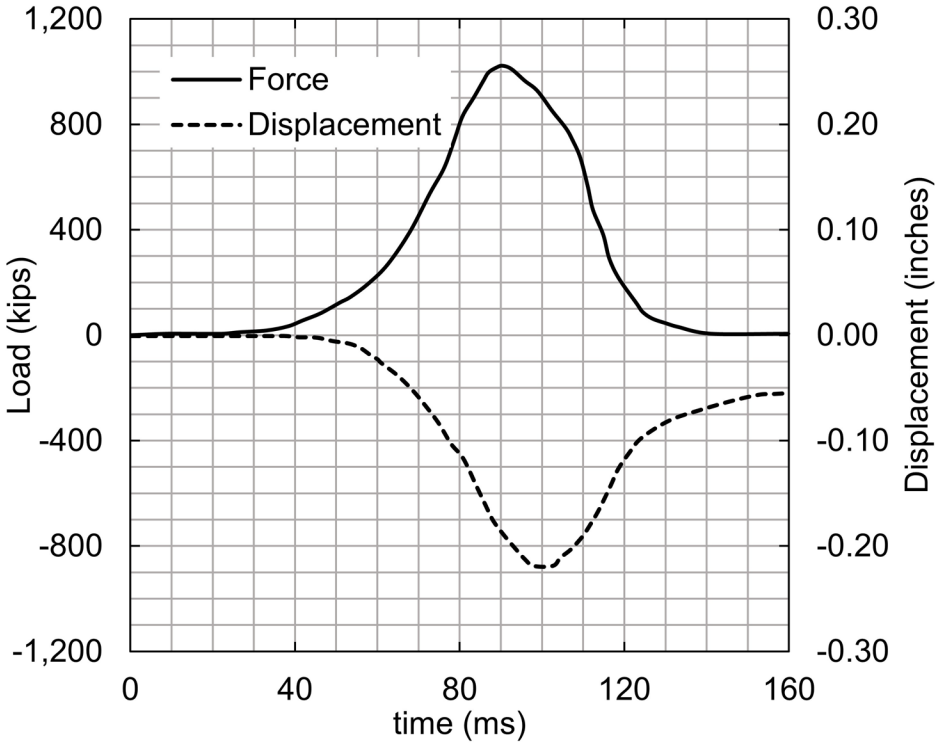

Figure 11-5 Statnamic raw force and displacement measurements versus time (courtesy of Berminghammer Foundation Equipment).

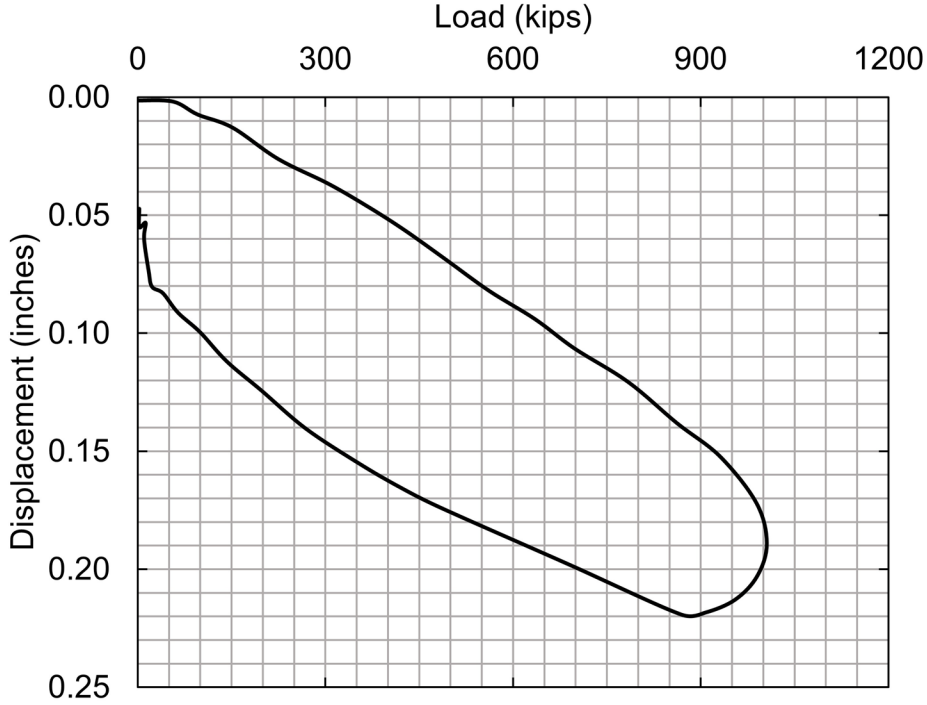

Figure 11-6 Statnamic load versus displacement (courtesy of Berminghammer Foundation Equipment).

11.2.2 Cushioned Drop Weight Systems

Rapid load tests can also be performed using cushioned drop weight systems that can generate the required peak force and force pulse duration. A drop weight, typically weighing between 5 and 15% of the target peak force, is mobilized to the site. A system (a crane, jack or some other mechanism) capable of lifting the drop weight to the required drop height and guiding it to strike the pile on center is also required. A load cell is once again located atop the pile head. However, in the cushioned drop weight systems, a spring system or a package of cushioning material is placed between the drop weight and the load cell. The springs or cushions lengthen the duration of the force pulse imparted to the pile. Some systems also include a clamping or catching mechanism to catch the rebounding drop mass after the force pulse has been applied. The catch mechanism prevents the application of additional force and improves the measurement of the pile head displacement from the main impact event.

The Pseudo Static Pile Load Tester, developed by Fundex (Schellingerhout and Revoort 1996), is a system with a clamp. This device, shown in Figure 11-7a, typically applies a series of drops from increasing release heights. Gradually, higher peak forces are applied and greater nominal resistances are mobilized, if present. The data acquisition and processing equipment is also shown in the photograph. Williams (2014) reported the system can achieve test loads up to 800 kips.

A large cushioned drop weight system for rapid load testing has also been reported by Miyasaka et al. (2009). In this system, named Hybridnamic, a modular ram of up to 85 tons is dropped on a cushion product specially developed to lengthen the force pulse duration. Other cushion materials, such as wood, are also viable. The drop height, drop weight and cushion thickness can be simulated with wave equation analysis. Drop weights of up to 170 kips are available, mobilizing nominal resistances of on the order of 1700 kips. A photograph of the Hybridnamic system is presented in Figure 11-7b.

Another drop weight system that can be used for rapid load testing is the APPLE system (Rausche et al. 2008). This system, shown in Figure 11-8, can be configured with a ram weight of up to 160 kips. The system is capable of mobilizing nominal resistances of on the order of 1600 kips using rapid load test procedures.

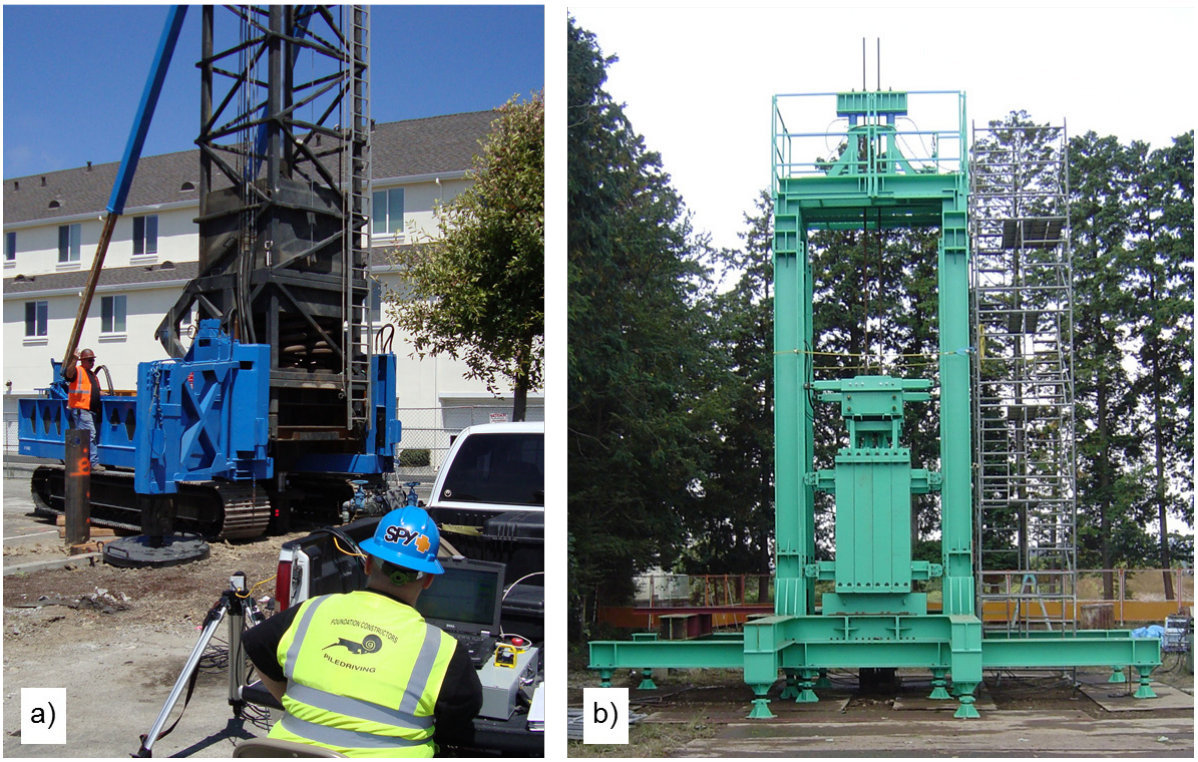

Figure 11-7 Drop weight rapid load test systems: (a) Fundex system (courtesy Foundation Constructors Inc.) and (b) Hybridnamic system.

Figure 11-8 APPLE 32 ton modular rapid load test system with transducer.

11.3 RAPID LOAD TEST APPLICATIONS

Rapid load tests are primarily used to determine the nominal axial compressive resistance. A variety of pile types and sizes from small diameter timber, steel, and concrete piles up to large diameter open end steel pipes and concrete cylinder piles have been tested using rapid load tests. Internal and external strain gage instrumentation has also been used on rapid load tested piles for both nominal resistance interpretation as described in Section 11.4 and for load transfer assessments.

Rapid load tests are attractive for testing large diameter open end pipe piles for two reasons. First, large diameter open end pipe piles often have high nominal resistances which are difficult to statically load test economically. Second, the longer duration, lower acceleration force pulse generated by a rapid load test, sometimes reduces slippage of the internal soil plug under the dynamic loading event.

Rapid load testing with a combustion gas apparatus has also been used for lateral load testing of piles and pile groups.

11.4 RAPID LOAD TEST INTERPRETATION METHODS

Initial correlations of Statnamic rapid load test results with static load tests for projects with toe bearing piles founded in till and rock showed good agreement without adjustment of the load - displacement results (Janes et al. 1991). However, in later tests, Statnamic rapid load test results overestimated the nominal resistance in some soils due to the dynamic loading rate effects (Janes and Campanella 1994). Several analysis procedures depending on pile length and pile response, as well as adjustment factors based on loading rate have subsequently been developed to derive the nominal resistance from Statnamic rapid load test results. These analysis procedures include the Unloading Point Method (UPM), the Modified Unloading Point Method (MUP), the Segmental Unloading Point Method (SUP), the Fully Mobilized UPM, and for cohesive soils the Sheffield Method. These methods are described in sections 11.4.1 through 11.4.5. Recommended loading rate reduction factors from NCHRP 21-08 by Paikowsky (2006) on Innovative Load Testing Systems for results analyzed with these rapid load test methods are discussed in Section 11.4.6.

In addition to selecting the appropriate interpretation method and applying an appropriate loading rate reduction factor, rapid load tested piles should have sufficient maximum displacement of the pile head. Miyasaka et al. (2009) noted that rapid load tests using the unloading point method with a maximum displacement of 1 to 3% of the equivalent pile diameter potentially overpredicted the nominal resistance compared to static load tests. Therefore, Miyasaka recommended running rapid load tests to a sufficiently large permanent displacement, on the order of 3% or more of the pile diameter. Holscher et al. (2012) recommended the maximum displacement of the pile head during the test be larger than 5% of the equivalent pile diameter to achieve geotechnical failure. Geotechnical failure is needed so that the dynamic soil resistance can be properly assessed and subtracted from the nominal resistance.

Middendorp and Bielefeld (1995) proposed the wave number, N_w, as a guide for determining whether the Statnamic test was influenced by stress wave behavior and to determine the analysis procedure to be used. The wave number considers the foundation length, the wave speed of the pile material, and the duration of loading and is calculated from:

$$N_w = \frac{D_w}{L} = \frac{C\ t_L}{L} \qquad \text{Eq. 11-1}$$

Where:

N_w = wave number (unit less).
D_w = wave length (feet).
L = total pile length (feet).
C = wave speed of pile material (ft/s).
t_L = load duration (seconds).

11.4.1 Unloading Point Method (UPM)

The first widely used analysis method to adjust the raw Statnamic load - displacement results for dynamic loading rate effects was the Unloading Point Method (UPM) proposed by Middendorp et al. (1992).

In the UPM, all elements of the pile are assumed to move in the same direction and with almost the same velocity. According to the developers, this allows the pile to be treated as a rigid body undergoing translation as long as the pile has a wave number, N_w, greater than 12. The forces acting on the pile during a Statnamic test include the Statnamic induced load, F_{stn}, the pile inertia force, F_a, and the soil resistance forces which include the static soil resistance, F_u, the dynamic soil

resistance, F_v, and the resistance from pore water pressure, F_p. A free body diagram of the forces acting on a pile during a Statnamic test is presented in Figure 11-9. The soil resistance forces shown in the free body diagram are distributed along the pile shaft as well as at the pile toe.

In mathematical terms, the force equilibrium on the pile may be described as follows:

$$F_{stn}(\mathrm{t}) = F_a(\mathrm{t}) + F_u(\mathrm{t}) + F_v(\mathrm{t}) + F_p(\mathrm{t}) \qquad \text{Eq. 11-2}$$

Where:

F_{stn} = Statnamic induced load (kips).
F_a = pile inertia force (kips).
F_u = static soil resistance (kips).
F_v = dynamic soil resistance (kips).
F_p = resistance from pore pressure (kips).

This equation may be rewritten in terms of static soil resistance as follows:

$$F_u(\mathrm{t}) = F_{stn}(\mathrm{t}) - F_a(\mathrm{t}) - F_v(\mathrm{t}) - F_p(\mathrm{t}) \qquad \text{Eq. 11-3}$$

A simplifying assumption is made that the pore water pressure resistance, F_p, can be treated as part of the dynamic resistance, F_v. This simplifies the above equation to:

$$F_u(\mathrm{t}) = F_{stn}(\mathrm{t}) - F_a(\mathrm{t}) - F_v(\mathrm{t}) \qquad \text{Eq. 11-4}$$

Consider the Statnamic load - displacement data presented in Figure 11-10. The Statnamic load - displacement data can be separated into five stages. Stage 1 includes the assembling of the Statnamic piston and reaction mass and thus is a static loading phase. The reaction mass is launched and Stage 2 therefore provides the initial loading of the dynamic event. The soil resistance is treated as linearly elastic. Pile acceleration and velocity are small, resulting in low inertia and damping forces on the pile.

Stage 3 is the basic load application portion of the cycle with fuel burning and pressure in the combustion chamber. In Stage 3, significant nonlinear soil behavior occurs as the pile and soil experience high acceleration and velocity. Thus the highest inertia and damping forces are generated in this stage. The maximum Statnamic applied load is reached at the end of Stage 3.

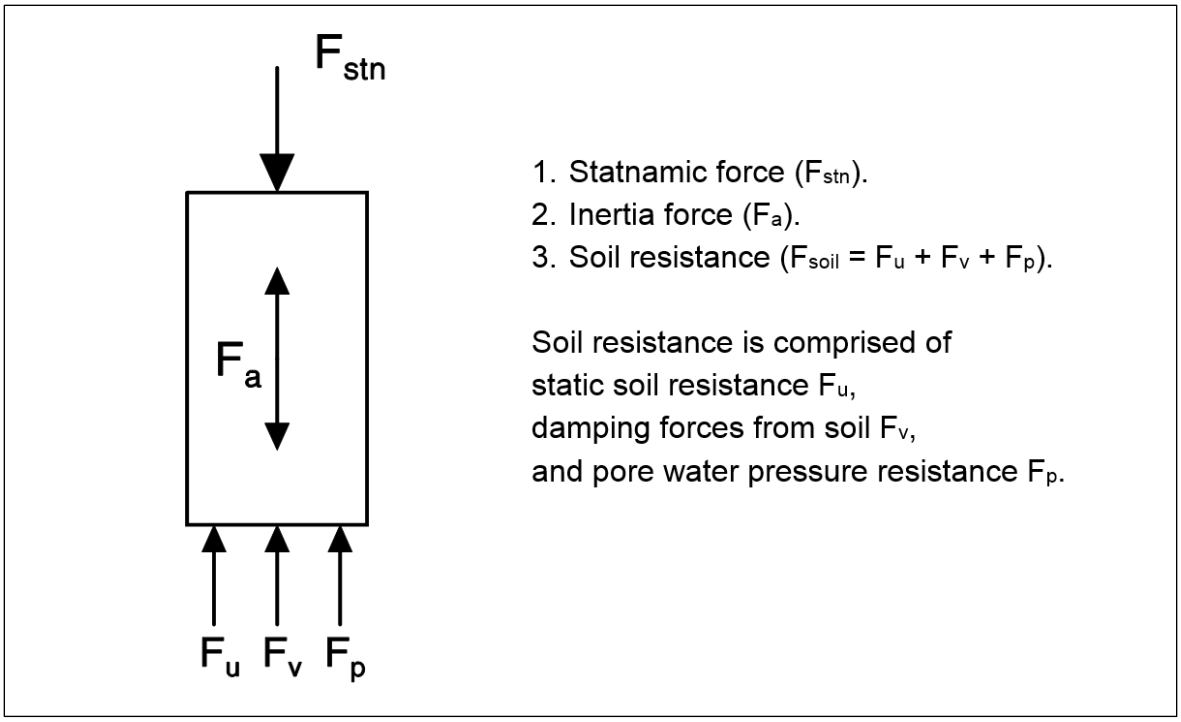

Figure 11-9 Free body diagram of pile forces in a Statnamic test (after Middendorp et al. 1992).

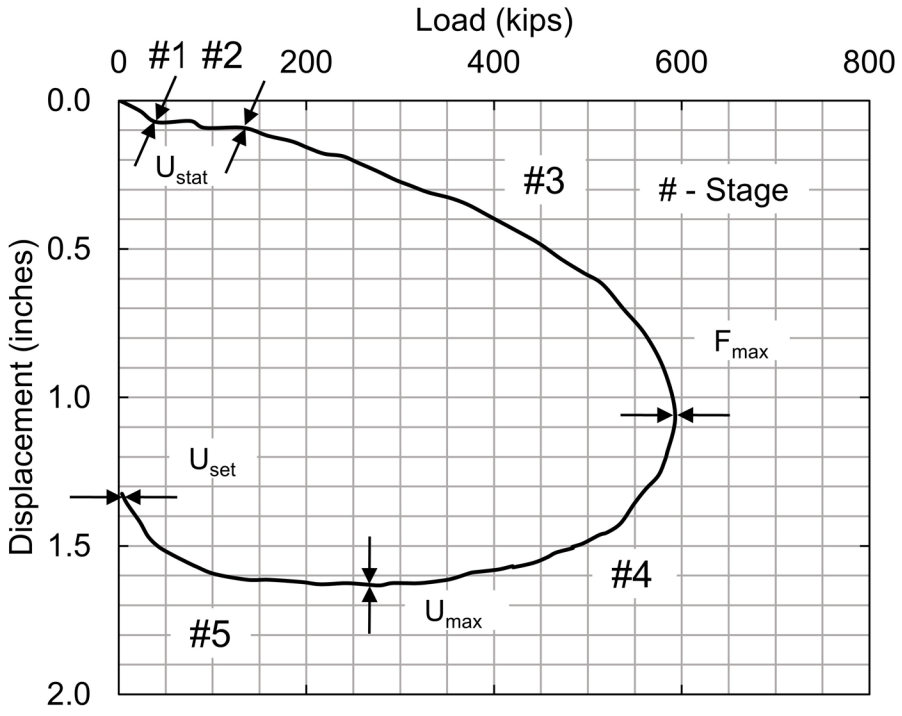

Figure 11-10 Five stages of a Statnamic test (after Middendorp et al. 1992).

In Stage 4, pressure in the combustion chamber is allowed to vent. Pile downward velocity and displacement continue but decrease throughout Stage 4. While the maximum Statnamic load is reached at the end of Stage 3, the maximum displacement occurs at the end of Stage 4. This is often due to the pile inertia force or significant dynamic resistance forces, $F_v(t)$, but may also occur in soils with strain softening (the residual soil resistance is significantly lower than the peak resistance). Since the pile velocity is zero at the point of maximum displacement, t_{umax}, the viscous damping, $F_v(t)$, on the pile is also zero at the end of Stage 4 and the static pile capacity may be expressed only at that time as:

$$F_u(t_{umax}) = F_{stn}(t_{umax}) - F_a(t_{umax}) \qquad \text{Eq. 11-5}$$

In Stage 5, the soil rebounds from the loading event and to achieve final equilibrium the pile unloads and rebounds as load and movement cease. The displacement at the end of Stage 5 is the permanent displacement or set experienced under the test event.

The data processing system records the applied Statnamic load and pile head acceleration and displacement throughout the test. The nominal static soil resistance, F_u, can then be calculated from the Statnamic load at the point of maximum displacement, $F_{stn}(t_{umax})$, minus the pile inertia force. This nominal static soil resistance yields one point on the derived static load - displacement curve and may occur at a large displacement. If a limiting movement criterion such as described in Chapter 9 is used for load test interpretation, the nominal resistance may be less than this nominal static soil resistance.

To obtain the remaining points on the derived static load - displacement curve, the damping resistance, F_v, at other load - displacement points must be determined. Assuming all damping is viscous (e.g. linear), then the damping resistance force can be expressed in terms of a damping constant, C_4, times the pile velocity at the corresponding time, $v(t)$. The pile velocity is obtained by differentiating the measured pile head displacement.

If the maximum applied Statnamic load is greater than the nominal resistance, then the soil resistance at the beginning of Stage 4 through the point of maximum displacement at the end of Stage 4 will be a constant and will be equal to $F_u(t_{max})$, assuming the soil is perfectly plastic and does not exhibit strain hardening. The damping constant, C_4, may be calculated from the maximum Statnamic load at the beginning of Stage 4, t_4. This may be expressed as:

$$C_4 = \frac{F_{stn}(\mathrm{t}_4) - F_u(\mathrm{t}_{umax}) - \mathrm{ma}(\mathrm{t}_4)}{V(\mathrm{t}_4)} \qquad \text{Eq. 11-6}$$

Where:

C_4	=	damping constant.
F_{stn}	=	Statnamic induced load.
F_u	=	static soil resistance.
m	=	mass of pile.
a	=	acceleration of pile.
V	=	velocity of pile.
t_4	=	time at beginning of Stage 4 (see Figure 11-10).
t_{umax}	=	time at maximum displacement (see Figure 11-10).

Assuming the damping constant, C_4, is constant throughout the Statnamic loading event, the derived static load may be calculated at any point in time from:

$$F_u(\mathrm{t}) = F_{stn}(\mathrm{t}) - \mathrm{ma}(\mathrm{t}) - \mathrm{C}_4\mathrm{V}(\mathrm{t}) \qquad \text{Eq. 11-7}$$

Where:

F_u	=	static soil resistance.
F_{stn}	=	Statnamic induced load.
m	=	mass of pile.
a	=	acceleration of pile.
C_4	=	damping constant.
V	=	velocity of pile.

The derived Statnamic load - displacement curve is then constructed using the above equation and corresponding pile head displacement. An example of the derived load-displacement curve with the Unloading Point Method illustrating how the dynamic rate effects are subtracted from the Statnamic results is presented in Figure 11-11.

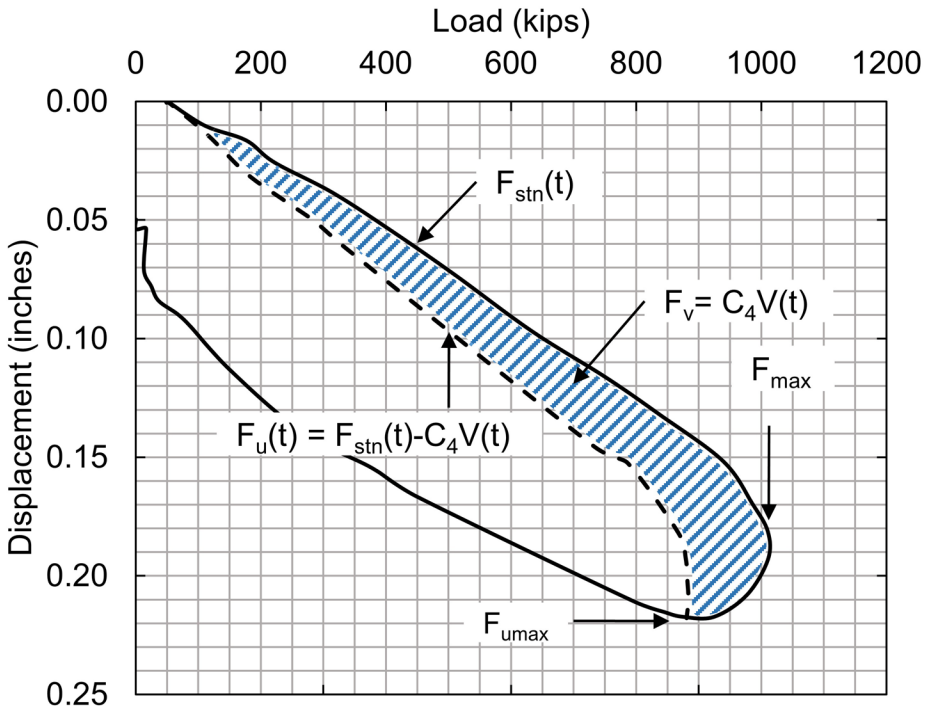

Figure 11-11 Derived Statnamic load displacement curve with rate effects (courtesy of Berminghammer Foundation Equipment).

11.4.2 Modified Unloading Point Method (MUP)

The Unloading Point Method rigid body assumption is not applicable for piles with a high toe resistance. On these piles, the pile head response (acceleration, velocity, and displacement) is significantly different than that at the pile toe. Because of the shortcomings of the UPM in this condition, the Modified Unloading Point Method (MUP) was developed by Justason (1997). The MUP method requires adding an additional accelerometer at the pile toe to define the toe behavior. The MUP method still assumes the pile to be a single mass but the acceleration of the mass is defined from the average of the pile head and toe displacement. The MUP method then uses the previously described UPM analysis procedure using the applied Statnamic force and the average accelerations and velocities.

11.4.3 Segmental Unloading Point Method (SUP)

Analytical studies by Brown (1995) have shown that the rigid body assumption used in the Unloading Point Method can result in overprediction of the nominal resistance and is not appropriate for long slender piles. Analysis of relatively long piles with a wave number, N_w, less than 10 was also problematic with the averaging techniques

used in the Modified Unloading Point Method because of the time delay between the movement of the pile head and the movement of the pile toe and the resulting phase shift of the signals. To address this condition, the Segmental Unloading Point (SUP) Method was developed, and is described in Mullins et al. (2002). The SUP method separates the pile into discrete segments of shorter length where strain gages and accelerometers are used to calculate the force, acceleration, velocity and displacement of each segment. Details of the computation procedures may be found in Mullins et al. (2002), and in NCHRP 21-08, Paikowsky (2006).

The maximum number of segments is generally controlled by the number of strain gages. However, each strain gage level does not constitute a segment. Strain gage placement is usually determined by soil stratigraphy considerations. Multiple strain gages can be placed in a segment. The segment length is selected independent of gage location and must produce a wave number greater than 12.

The SUP method performs MUP analyses for each segment. The pile head derived static resistance is then calculated by summing the derived static response of each pile segment.

11.4.4 Fully Mobilized UPM

Miyasaka et al. (2009) proposed a modification to the unloading point method to avoid overprediction of the nominal resistance in cases where limited axial movement occurs. A case study was presented for a statically and rapidly load tested steel sheet pile installed in a mixed profile consisting of 9.5 feet of medium sand (SPT N=10), 8.9 feet of very loose silt (N=0), 16.4 feet of gravelly sand (N = 10 to 20), and 3.9 feet of stiff, gravelly clay, underlain by fine dense sand (N = 50+). UPM results indicated an overprediction by as much as 1.43 times the nominal resistance if sufficient maximum and net pile head movement were not achieved. A comparison of the UPM results for each load cycle with the static load test result is presented in Figure 11-12. The drop height for rapid load tests range from 0.6 feet to 4.9 feet. Note the UPM and static load test results agree reasonable well once a maximum nominalized displacement exceeding 2.8% and a normalized net displacement in excess of 1.5% are achieved. Thus, for full mobilization of the geotechnical resistance using UPM results, Miyasaka proposed obtaining a minimum net permanent displacement of at least 3% of the pile diameter. ASTM D7383 also cautions on possible overprediction of the nominal resistance in rapid load test analysis cases with insufficient axial movement.

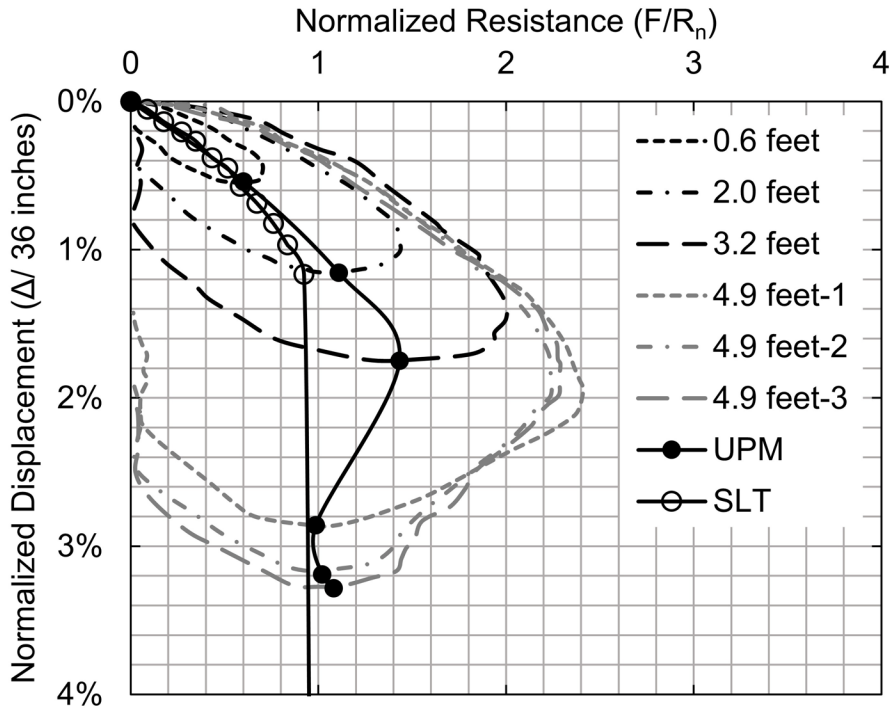

Figure 11-12 Normalized resistance versus normalized displacement (after Miyasaka et al. 2009).

11.4.5 Sheffield Method for Cohesive Soils

Brown (2004), as well as Brown and Hyde (2006), describe an analysis method that incorporates loading rate effects in cohesive soils. Details of this method, the Sheffield Method, can be found in Holscher et al. (2012) Appendix D. The Sheffield Method incorporates the rate effect variation with pile settlement, and does not include rate reduction factors from Paikowsky (2006). It is applicable for piles installed in clay and assumes the majority of the nominal resistance is derived from shaft resistance. Holscher et al. (2012) cautioned strongly that this method not be used in sands or rock. The Sheffield Method depends on specific rate parameters, denoted α and β. It is preferable that the parameters α and β be determined from triaxial tests performed at variable displacement rates. However, if laboratory test data is not available, published literature values may be used. Rule of thumb values for α have also been empirically correlated to soil index tests from a relatively small data set, predominantly from cohesive soils from Europe, and $\beta = 0.2$. The Sheffield Method is show in Equation 11-8.

$$F_u(\mathrm{t}) = \frac{F_t(\mathrm{t}) - \mathrm{ma(t)}}{1 + \frac{F_t(\mathrm{t})}{F_{max}}\alpha\left[\left(\frac{\mathrm{V(t)}}{V_o}\right)^{\beta} - \left(\frac{V_{static}}{V_o}\right)^{\beta}\right]} \qquad \text{Eq. 11-8}$$

In which:

$$\alpha = 0.031\,\mathrm{PI} + 0.46 \qquad \text{Eq. 11-9}$$

Where:

F_u	=	static soil resistance.
F_t	=	force measured on pile head.
F_{max}	=	maximum measured force applied during testing.
m	=	mass of pile.
a	=	acceleration of pile.
V	=	velocity of pile.
V_{static}	=	velocity used to determine parameters α and β.
V_o	=	normalizing constant.
α	=	material dependent parameter 1.
β	=	material dependent parameter 2.
PI	=	Plasticity Index.

11.4.6 Loading Rate Reduction Factors

In NCHRP 21-08, Innovative load Testing Systems, Paikowsky (2006) reported the correlation of 34 Statnamic rapid load test results with static load test results. The correlation database included driven H-piles, pipe piles and concrete piles as well as drilled shafts. Based on the correlation results, a loading rate reduction factor was recommended depending on the site soil or rock conditions. The loading rate reduction factor is to be applied to the derived static load-movement curve to account for overpredictions of the nominal resistance. Loading rate reduction factors of 0.96, 0.91, 0.69, and 0.65 were recommended for rock, sand, silt, and clay, respectively. Paikowsky recommended these loading rate reduction factors be applied to UPM, MUP, and SUP analyses of Statnamic test results.

Weaver and Rollins (2010) reviewed a different limited database of static load test and rapid load test results for drilled shafts with cohesive soils along the shaft and beneath the toe. That review indicated an average loading rate reduction factor of 0.47 with a range of plus or minus 0.14 when used with the UPM. While not measured on driven piles, the results suggest a lower loading rate reduction factor should be considered when evaluating rapid load test results in cohesive deposits. This is particularly true if the pile head displacement is less than the 5% of the equivalent pile diameter needed to achieve geotechnical failure.

Brown and Powell (2013) reviewed the correlation between published static load tests and rapid load test results evaluated by UPM analysis. Based on this review, they proposed the loading rate reduction factor, ξ, for UPM analysis be selected based on the liquid limit, LL, of the clay soil in accordance with Equation 11-10.

$$\xi = -0.0033\,\mathrm{LL} + 0.69 \qquad \text{Eq. 11-10}$$

Where: LL = Liquid Limit (%)

Their compilation of correlation results is presented in Figure 11-13 .

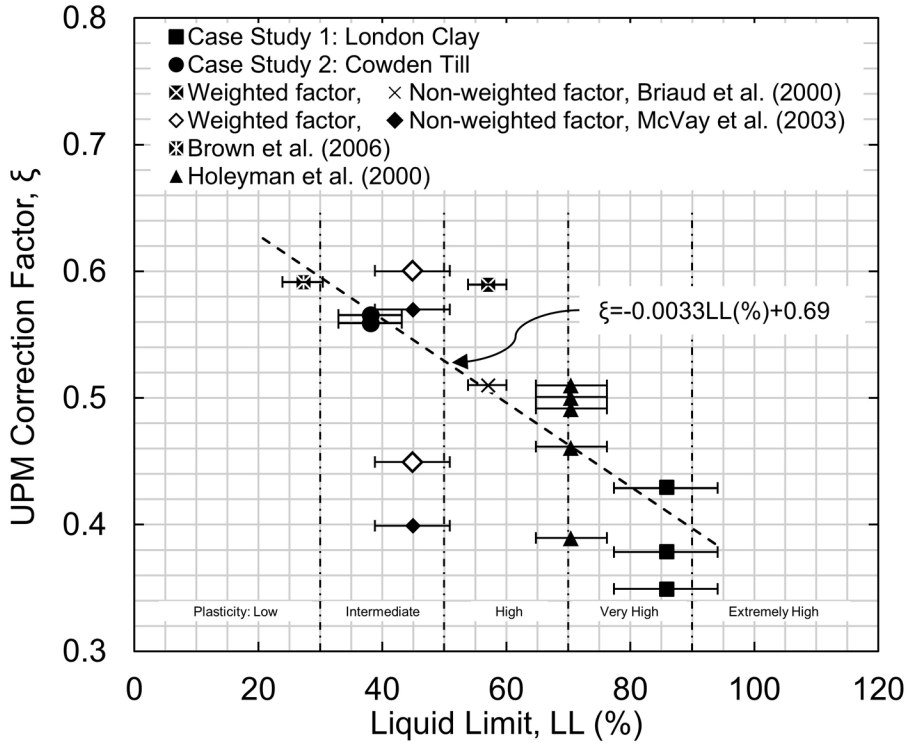

Figure 11-13 Variation of the UPM loading rate reduction factor versus the soil liquid limit (after Brown and Powell 2013).

Correlations of rapid load test results with cushioned drop weight systems using the UPM, MUP or SUP analysis procedure with static load test results on driven piles in clays have not been reported in the literature. However, UPM, MUP or SUP analyses from cushioned drop weight systems would be subject to similar loading rate considerations.

11.4.7 Resistance Factors

AASHTO (2014) does not address resistance factors for rapid load test results analyzed with any of the previously described interpretation methods. Some agencies have stated resistance factor guidance or have sponsored research efforts to determined resistance factors for nominal resistance determined by rapid load test methods.

For redundant piles, the South Carolina Department of Transportation's Geotechnical Design Manual, Version 1.1 (2010) suggests strength limit state resistance factors of 0.70 for a rapid load test result on a toe bearing pile in rock or very dense sand, and 0.65 for the nominal resistance determined by a rapid load test on a friction pile. For non-redundant piles, a reduced resistance factor of 0.55 is recommended for either end bearing or friction piles. These resistance factors for redundant and non-redundant piles are applicable to piles tested in axial compression with either the Statnamic rapid load test method or by high strain dynamic monitoring. The SCDOT manual notes that no increase in resistance factor is allowed on sites with multiple Statnamic tests unless the Statnamic rapid load test results are calibrated to a static load test.

A Florida Department of Transportation sponsored research project for determination of the resistance factor for rapid load tests was performed by McVay et al. (2003). The developed database was described as "small for statistical analysis purposes" and McVay calculated resistance factors using the FOSM approach to a reliability index, β, of 2.5. The calibration was performed using only the UPM analysis method with the loading rate reduction factors proposed by Mullins (2002), and summarized by Paikowsky (2006). The database used by McVay included 34 driven pile cases. Fifteen of the cases consisted of steel pipe piles ranging from 36 to 126 feet in length and 13 to 31 inches in diameter. Another 15 of the driven pile cases consisted of prestressed concrete piles ranging from 23 to 177 feet in length and 16 to 36 inches in diameter. The data sets were from project sites in the United States, Canada, and Japan.

Due to the limited size of the correlation database, McVay recommended a resistance factor of 0.70 for the nominal axial resistance determined by a rapid load test on redundant driven piles in rock and non-cohesive soils, and a resistance factor of 0.60 for redundant driven piles in sands-clays-rocks mixed layers. For non-redundant driven piles, McVay recommended resistance factors of 0.60 and 0.50 for these soils conditions, respectively. For driven piles embedded primarily in clays, the Statnamic rapid load test method was not recommended by McVay without a

calibrated static load test. This reflects the variability of the loading rate reduction factors described in the previous section. It should also be noted these resistance factors were developed using the unloading point method (UPM) of analysis, and that modified or segmental unloading point methods were not used in the calibration.

Cushioned drop mass apparatus testing has very little written in terms of rapid load tests calibrated to static load tests. Presumably, if signal matching is used on the rapid load test results as calibrated for high strain dynamic testing, the resistance factor for high strain dynamic testing with signal matching could be used. In all cases, the designer must decide on appropriate resistance factors considering redundancy of the foundation elements, number of tests, and the required reliability index prior to proceeding with a rapid load test program.

11.5 LATERAL LOADING APPLICATION

The use of the Statnamic test for lateral load application was also studied in NCHRP Report 461, Static and Dynamic Lateral Loading of Pile Groups by Brown et al. (2001). A lateral Statnamic test on a nine pile group is shown in Figure 11-14. The maximum lateral load applied to date in a Statnamic test is 2,700 kips. However, this is not a limit of the Statnamic test device but rather of the pile group response.

Figure 11-14 Lateral Statnamic test on nine pile group
(courtesy of Utah State University).

11.6 CASE HISTORY

In 2004, a Statnamic rapid load test was conducted on a 42 inch O.D. x 0.75 inch thick wall, open end pipe pile. This 111 foot long pile was driven into a mixed soil profile. The soil conditions at the site were generally described as 46 feet of clay with interbedded layers of sands and silts over the upper 46 feet. This layer was underlain by sands to a depth of 95 feet, and then interbedded layers of sands and clayey silts from 95 to 118 feet. The rapid load test was performed on the open end pipe pile approximately 7 months after installation. The load-displacement plot for this test is presented in Figure 11-15.

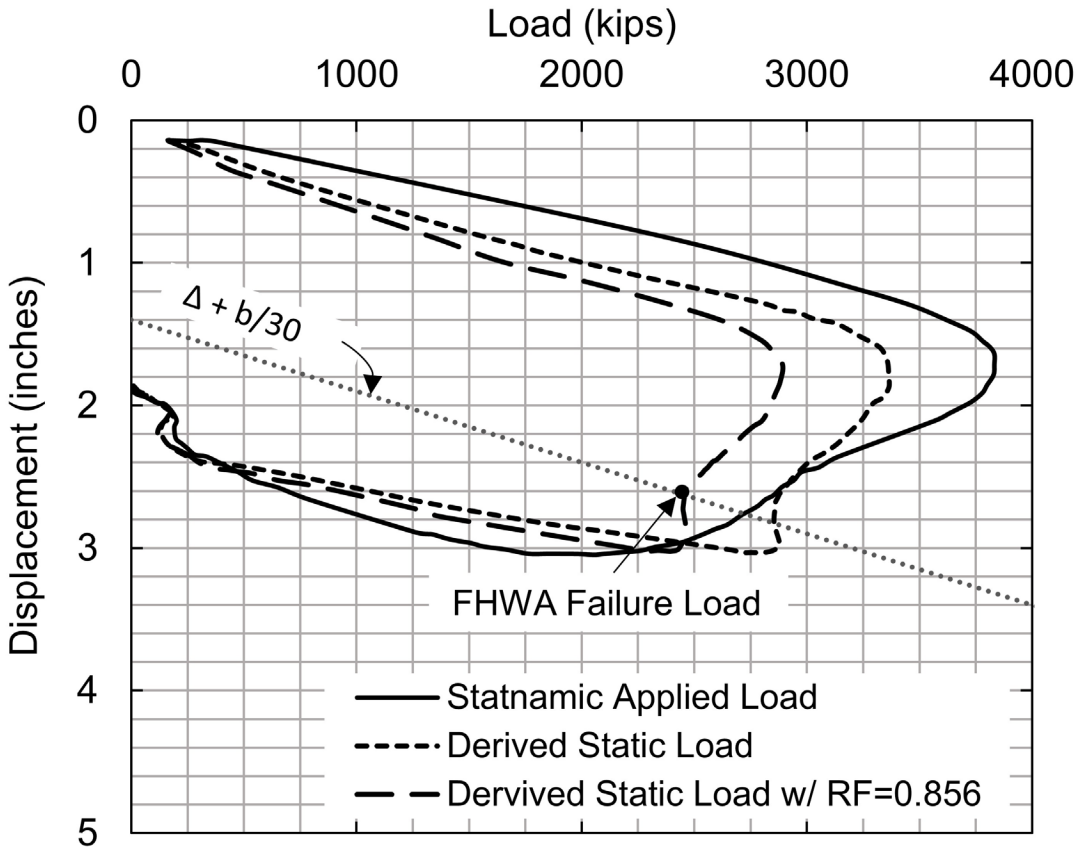

Figure 11-15 Statnamic test result (courtesy Minnesota DOT).

The Statnamic test apparatus had a maximum capacity of 4270 kips and applied a load of 3840 kips. The Modified Unloading Point (MUP) Method was used to evaluate the Statnamic test result. The pile was originally driven without anticipating that a Statnamic test would be later conducted. Therefore, the pile was not equipped with a pile toe accelerometer. The testing firm assumed that the pile toe acceleration was one half of the measured pile head acceleration, and the average of the measured and assumed acceleration was then used to conduct the MUP

analysis. A loading rate reduction factor of 0.856 (weighted for the site stratigraphy) was also applied to the test result. The Statnamic derived static load-displacement curve was then evaluated according to the FHWA recommended static load test interpretation criterion for large piles in use at that time. That criterion defined failure as the sum of the elastic deflection plus the ratio of the pile diameter over 30. The assigned failure load following this approach was 2,480 kips.

11.7 ADVANTAGES, DISADVANTAGES, AND LIMITATIONS

Advantages of rapid load testing relative to static testing include lower cost, shorter time required for test setup, and on-site mobility. The cost of a rapid load test can be on the order of one quarter to one half the cost of an equivalent static load test. The range in the cost of a rapid load test relative to a static load test depends upon the magnitude of the required load, the location of the site, and labor costs.

Cost savings may increase for rapid load tests when multiple tests are performed at the same site, or when rapid load tests are performed on piles having higher nominal resistances. Once a rapid load test apparatus is mobilized to a site, one or two rapid load tests can typically be performed in one day using the gravel catch structure. A greater number of rapid load tests per day can typically be performed using either the hydraulic catch device with the combustion gas and reaction mass apparatus or the cushioned drop weight systems.

The segmental reaction mass design for rapid load testing systems is advantageous as it allows assembly with relatively small hoisting equipment. In addition, since the reaction mass is typically 5 to 10 percent of the applied load, movement around a site for multiple tests is easier than for a static test.

Another advantage of a rapid load test is the mobilization of the soil resistance due to soil plugging in open ended sections. The slower loading rate in a rapid load test can be helpful in maintaining plugged behavior compared to a high strain dynamic test where the plug may slip under higher accelerations. Hence, plug behavior in a rapid load test may more closely resemble soil plug response in a static load test.

Rapid load tests do not require reaction piles. The smaller footprint associated with a rapid load test can be an advantage on sites with limited work areas.

Rapid load tests also have disadvantages. Rapid load test results must include both the influence of and correction for loading rate effects in all soil types. Correlations with conventional static tests are still being obtained to further address this issue as well as for calibration of rapid load test resistance factors.

The applied force pulse in a rapid load test necessary to mobilize the nominal resistance must be larger than the combined static and dynamic soil resistances. This disadvantage can be problematic in soils with high dynamic resistances. The pile in the presented rapid load test case history was driven into a mixed soil profile with low dynamic resistance based on the applied loading rate reduction factor of 0.856. The Statnamic test applied load in this soil was 55% greater than the derived nominal resistance. The Statnamic applied pile stress was 40.3 ksi, or roughly 90% of the guaranteed yield strength of the pile material. The applied stress would have been larger to achieve this same nominal resistance in a soil profile having higher dynamic resistance.

A maximum net pile head displacement of at least 3% of the pile diameter is required for full mobilization of the soil resistance with the UPM analysis technique to obtain geotechnical failure. Miyasaka et al. (2009) demonstrated that normalized pile head displacements less than 3% can result in overprediction of the nominal resistance.

Due to the limited number of rapid load tests systems and their locations, the mobilization cost for a rapid load test can be high. This is particularly true if the project requires only a single rapid load test, or if the test equipment must be mobilized from a distant location.

A limitation of a rapid load test can be instrumentation redundancy. Rapid load tests conducted without pile strain gage information lack the redundant check available in a conventional static load test (load cell and pressure gage) to check the calibration accuracy of the applied load.

11.8 PRACTICAL ISSUES AND CONSIDERATIONS

In a conventional static load test, a conservative estimate of the nominal geotechnical resistance is obtained when limited pile head movement occurs under the applied static loads. However, this is not necessarily the case in a rapid load test. When a rapid load test exhibits load-displacement behavior with a limited maximum displacement and permanent set, the nominal resistance may be either

underpredicted or overpredicted. For piles driven into a dense granular deposit or on hard rock, a pile exhibiting a small permanent set likely indicates the nominal resistance has been underpredicted. However, in other soils and soft rock, the nominal resistance may be overpredicted as the force pulse is insufficient to cause geotechnical failure of the soil or soft rock and allow separation of the static and dynamic soil resistance effects. Rapid load tests in soils or soft rock should therefore have a permanent displacement of at least 3% of the pile diameter.

In layered soil profiles, a weighted loading rate reduction factor, ξ, must be determined and applied. The weighted loading rate reduction factor should be estimated based on the percentage of nominal resistance carried in a given layer and the appropriate loading rate reduction factor for the corresponding soil. Using the NCHRP 21-08 loading rate reduction factors described in Section 11.4.6, the loading rate reduction factor for a pile obtaining 50% of its nominal resistance in sand, $\xi = 0.91$, and 50% in clay, $\xi = 0.65$, would be 0.78. Similarly if 75% of the nominal resistance is obtained from the clay layer and 25% from the sand layer, the loading rate reduction factor would be 0.71.

In soils with high dynamic resistances, pile stresses should also be considered when selecting a rapid load test for nominal resistance verification. Pile stresses should be kept below the driving stress limits of the strength limit state when performing a rapid load test.

REFERENCES

ASTM D7383-10 (2010). Standard Test Methods for Axial Compressive Force Pulse (Rapid) Testing of Deep Foundations. Annual Book of ASTM Standards, Vol. 4.08, ASTM International, West Conshohocken, PA, 9 p.

Bermingham, P. and Janes, M. (1989). An Innovative Approach to Load Testing of High Capacity Piles. Proceedings of the International Conference on Piling and Deep Foundations, London, England, Rotterdam Publishers, Vol. 1, pp. 409-413.

Brown, D.A. (1995). Closure – Evaluation of Static Capacity of Deep Foundations from Statnamic Testing. American Society of Testing and Materials (ASTM), Geotechnical Testing Journal, Vol. 18, No. 4, pp. 495-498.

Brown, D.A., O'Neill, M.W., Hoit, M., McVay, M., El Naggar, M.H., and Chakraborty, S. (2001). Static and Dynamic Lateral Loading of Pile Groups, NCHRP Report 461. Transportation Research Board – National Research Council, Washington, D.C., 50 p.

Brown, M.J. (2004). The Rapid Load Testing of Piles in Fine Grained Soils, Ph.D. Thesis, University of Sheffield, Sheffield, UK, 274 p.

Brown, M.J., Hyde, A.F.L., and Anderson, W.F. (2006). Analysis of a Rapid Load Test on an Instrumented Bored Pile in Clay, Geotechnique, Vol 56, Issue 9, pp. 627-638.

Brown M.J. and Powell, J.J.M. (2013). Comparison of Rapid Load Test Analysis Techniques in Clay Soils, Journal of Geotechnical and Geoenvironmental Engineering, Vol 139, No. 1, American Society of Civil Engineers, pp. 152-161.

Holscher, P., Brassinga, H., Brown, M., Middendorp, P., Profittlich, M., and Tol, F. (2012). Rapid Load Testing on Piles – Interpretation Guidelines, CRC Press/ Baalkema, Leiden, 104 p.

Janes, M., Sy, A. and Campanella, R.G. (1994). A Comparison of Statnamic and Static Load Tests on Steel Pipe Piles in the Fraser Delta. Deep Foundations. Proceedings of the 8th Annual Vancouver Geotechnical Society Symposium, Vancouver, Canada, pp. 1-17.

Justason, M.D. (1997). Report of Load Testing at the Taipei Municiapl Incinerator Expansion Project, Taipei City, Taiwan.

McVay, M.C., Kuo, C.L., and Guisinger, A.L., (2003). Calibrating Resistance Factor in the Load and Resistance Factor Design of Statnamic Loading Test, University of Florida Project No. 4910450482312, Final Report, 129 p.

Middendorp, P., Bermingham, P. and Kuiper, B. (1992). Statnamic Load Testing of Foundation Piles. Proceedings of the Fourth International Conference on the Application of Stresswave Theory to Piles, Balkema Publishers, A.A., The Hague, The Netherlands, pp. 581-588.

Middendorp, P., and Bielefeld, M.W. (1995). Statnamic Load Testing and the Influence of Stress Wave Phenomena, Proceedings of the First International Statnamic Seminar, Vancouver, Canada, pp. 207-220.

Mullins, G., Lewis, C., and Justason, M. (2002). Advancements in Statnamic Data Regression Techniques. Deep Foundations 2002: An International Perspective on Theory, Design, Construction, and Performance, American Society of Civil Engineers (ASCE), Geo Institute, GSP No.116, Vol. 2, pp. 915-930.

Miyasaka T., Likins, G.E., Kuwabara, F., Rausche, F., and Hyodo, M. (2009). Improved Methods for Rapid Load Tests of Deep Foundations, Contemporary Topics in Deep Foundations, GSP 185, pp. 629-636.

Paikowsky, S. (2006). Innovative Load Testing Systems, NCHRP 21-08. National Cooperative Highway Research Program, Transportation Research Program, Washington, D.C., 148 p.

Rausche, F., Likins, G., Miyasaka, T., and Bulluck, P. (2008). The Effect of Ram Mass on Pile Stresses and Pile Penetration, Proceedings of the 8th International Conference on the Application of Stress Wave Theory to Piles, IOS Press, Lisbon, Portugal, pp. 389-394.

SCDOT Geotechnical Design Manual Version 1.1 (2010). South Carolina Department of Transportation, Chapter 9, 7 p.

Schellingerhout, A.J.G., and Revoort, E., (1996). Pseudo Static Pile Load Tester, Proceeding of the 5th International Conference on the Application of Stress-Wave Theory to Piles, University of Florida, Gainesville, FL, pp. 1031-1037.

Weaver T.J., and Rollins, K.M. (2010). Reduction Factor for the Unloading Point Method at Clay Sites, Journal of Geotechnical and Geoenvironmental Engineering, Vol 136, No. 4, American Society of Civil Engineers, pp. 643-646.

Williams, B. (2014). Rapid Load Testing course notes, Pile Load Testing Options Course, Pile Driving Contractors Association, Sacramento, CA.

CHAPTER 12

WAVE EQUATION ANALYSIS

12.1 WAVE EQUATION ANALYSIS INTRODUCTION

As discussed in AASHTO (2014) Article C10.7.3.8.5 as well as in Chapter 13 of this manual, dynamic formulas, together with observed penetration resistances, do not yield acceptably accurate predictions of actual nominal pile resistances. Moreover, they do not provide information on stresses in the piles during driving. The so-called "wave equation analysis" of pile driving has eliminated many shortcomings associated with dynamic formulas by realistically simulating the hammer impacts and pile penetration process. For most engineers, the term wave equation refers to a partial differential equation. However, for the foundation specialist, it means a complete approach to the mathematical representation of a system consisting of hammer, cushions, helmet, pile, and soil along with an associated computer program for the convenient calculation of the dynamic motions and forces in this system after ram impact.

The approach was developed by E.A.L. Smith (1960), and after the rationality of the approach had been recognized, several researchers developed a number of computer programs. For example, the Texas Department of Highways supported research at the Texas Transportation Institute (TTI) in an attempt to determine driving stresses and reduce concrete pile damage using a realistic analysis method. FHWA sponsored the development of both the TTI program (Hirsch et al. 1976) and the WEAP program (Goble and Rausche 1976). FHWA supported the WEAP development to obtain analysis results backed by measurements taken on construction piles during installation for a variety of hammer models. The WEAP program was updated several times under FHWA sponsorship, until 1986 (Goble and Rausche 1986). Later, additional options, improved data files, refined mathematical representations and modern user conveniences were added to this program on a proprietary basis, and the program is now known as GRLWEAP, (Pile Dynamics, Inc. 2010). Similar computer programs have been developed, such as PDPWAVE (Bielefeld and Middendorp 1992), that are based on the method of characteristics, a mathematical model that differs from Smith's lumped mass model.

The wave equation approach has been subjected to a number of checks and correlation studies. Studies on WEAP performance of have produced publications demonstrating that program's performance and utility (e.g., Blendy 1979; Soares et al. 1984; Rausche et al. 2004). Documentation of the most recent version of this program, GRLWEAP 2010, has been prepared by Pile Dynamics, Inc. (2010).

AASHTO (2014) design specifications recommend a resistance factor of 0.50 when wave equation analysis is used for the determination of the nominal resistance without the benefit of dynamic measurements or load test results but with field confirmation of hammer performance. The wave equation database used for LRFD calibration consisted of nominal resistance predictions determined using the GRLWEAP program and its associated pile and soil models.

This chapter explains what a wave equation analysis is, how it works, and what problems it can solve. Example problems, highlighting wave equation program applications, are demonstrated. Basic wave equation program input and output are presented for demonstration purposes using the GRLWEAP software. However, this should not be construed as a promotion or endorsement of this particular software product by the FHWA.

12.2 WAVE PROPAGATION

Input preparation for wave equation analyses is often very simple, requiring only very basic driving system and pile parameters in addition to a few soil parameters for which standard recommendations are given. Thus, a wave equation program can be run with minimal specialized knowledge. However, interpretation of calculated results is facilitated, and errors in result application may be avoided, by knowledge of the mechanics of stress wave propagation and familiarity with the particular project’s design requirements and constraints.

In the first moment, after a hammer has struck the pile top, only the pile particles near the ram-pile interface are compressed. This compressed zone, or force pulse, as shown in Figure 12-1, expands into the pile toward the pile toe at a constant wave speed, C, which depends on the pile's elastic modulus and mass density (or specific weight). When the force pulse reaches the embedded portion of the pile, its amplitude is reduced by the action of static and dynamic soil resistance forces. Depending on the magnitude of the soil resistances along the pile shaft and at the pile toe, the force pulse will reflect from the pile toe either as a tension or a compression force pulse, which travels back to the pile head. Both incident and

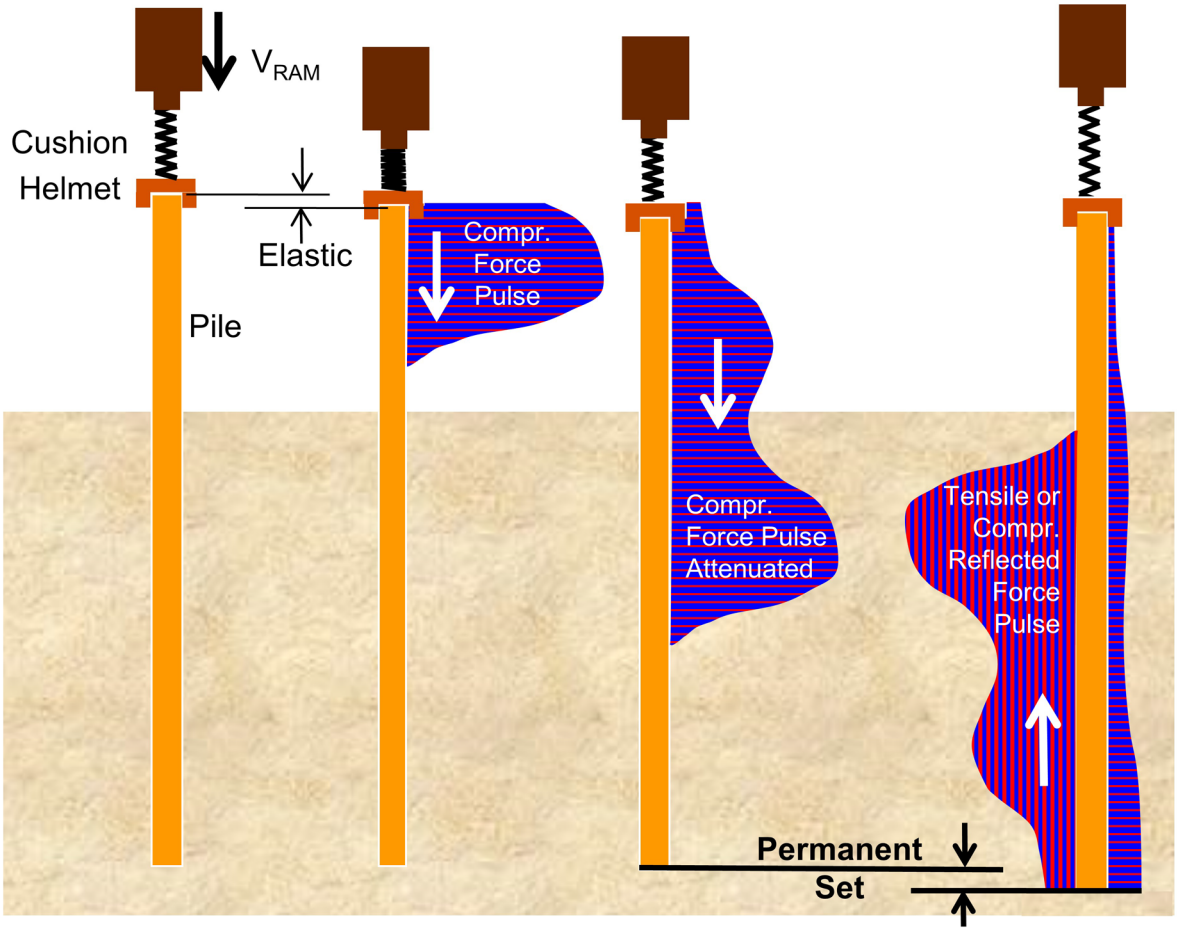

Figure 12-1 Wave propagation in a pile (adapted from Cheney and Chassie 2000).

reflected force pulses will cause a pile toe motion and produce a permanent pile set if their combined energy and force are sufficient to overcome the static and dynamic resistance effects of the soil.

12.3 WAVE EQUATION METHODOLOGY

In a Smith-type wave equation analysis, the hammer, helmet, and pile are modeled by a series of segments each consisting of a concentrated mass and a weightless spring. The hammer and pile segments are approximately one meter in length. Shorter segments occasionally improve the accuracy of the numerical solution at the expense of longer computer run times (Rausche et al. 2004). Spring stiffness and mass values are calculated from the cross sectional area, modulus of elasticity, and specific weight of the corresponding pile section. Hammer and pile cushions are represented by additional springs whose stiffness are calculated from area, modulus of elasticity, and thickness of the cushion materials. In addition, coefficients of

restitution (COR) are usually specified to model energy losses in cushion materials, and in all segments, which can separate from their neighboring segments by a certain slack distance. The COR is equal to 1.0 for a perfectly elastic collision which preserves all energy, and is equal to 0.0 for a perfectly plastic condition which loses all deformation energy. The usual condition of partially elastic collisions is modeled with an intermediate COR value. For example, the default value for the COR of wood is 0.50. However, when a softwood cushion is badly worn, a value of 0.25 may be more appropriate and can be entered into the wave equation input together with other cushion properties.

The soil resistance along the embedded portion of the pile and at the pile toe is represented by both static and dynamic components. Therefore, both a static soil resistance force which is pile displacement related, and a dynamic soil resistance forces which is pile velocity related act on every embedded pile segment. The static soil resistance forces are modeled by elasto-plastic springs and the dynamic soil resistance by dashpots. The displacement at which the static soil resistance changes from elastic to plastic behavior is referred to as the soil "quake". In the Smith damping model, the dynamic soil resistance is proportional to a damping factor times the pile velocity times the temporary static soil resistance. Additional discussion on quake and damping factors is presented in Section 12.6.7. A schematic of the wave equation hammer-pile-soil model is presented in Figure 12-2.

As the analysis commences, a calculated or assumed nominal resistance (ultimate capacity, R_{ut}) from user specified values is distributed along the shaft and toe according to user input or program calculation among the elasto-plastic springs. Similarly, user specified damping factors are assigned to shaft and toe to represent the dynamic soil resistance. The analysis then proceeds by calculating a ram velocity based on hammer efficiency and stroke inputs. The ram movement causes displacements of helmet and pile head springs, and therefore compressions (or extensions) and related forces acting at the top and bottom of the segments. Furthermore, the movement of a pile segment causes both static and dynamic soil resistance forces. A summation of all forces acting on a segment, divided by its mass, yields the acceleration of the segment. The product of acceleration and time step summed over time is the segment velocity. The velocity multiplied by the time step yields a change of segment displacement which then results in new spring forces. These spring forces divided by the pile cross sectional area at the corresponding section equal the stress at that point.

Similar calculations are made for each segment until the accelerations, velocities and displacements of all segments have been calculated during the time step. The

analysis then repeats for the next time step using the updated motion variables, velocity and displacement, of the segments from the previous time step. From this process, the accelerations, velocities, displacements, forces, and stresses of each segment are computed over time. Additional time steps are analyzed until the pile toe begins to rebound.

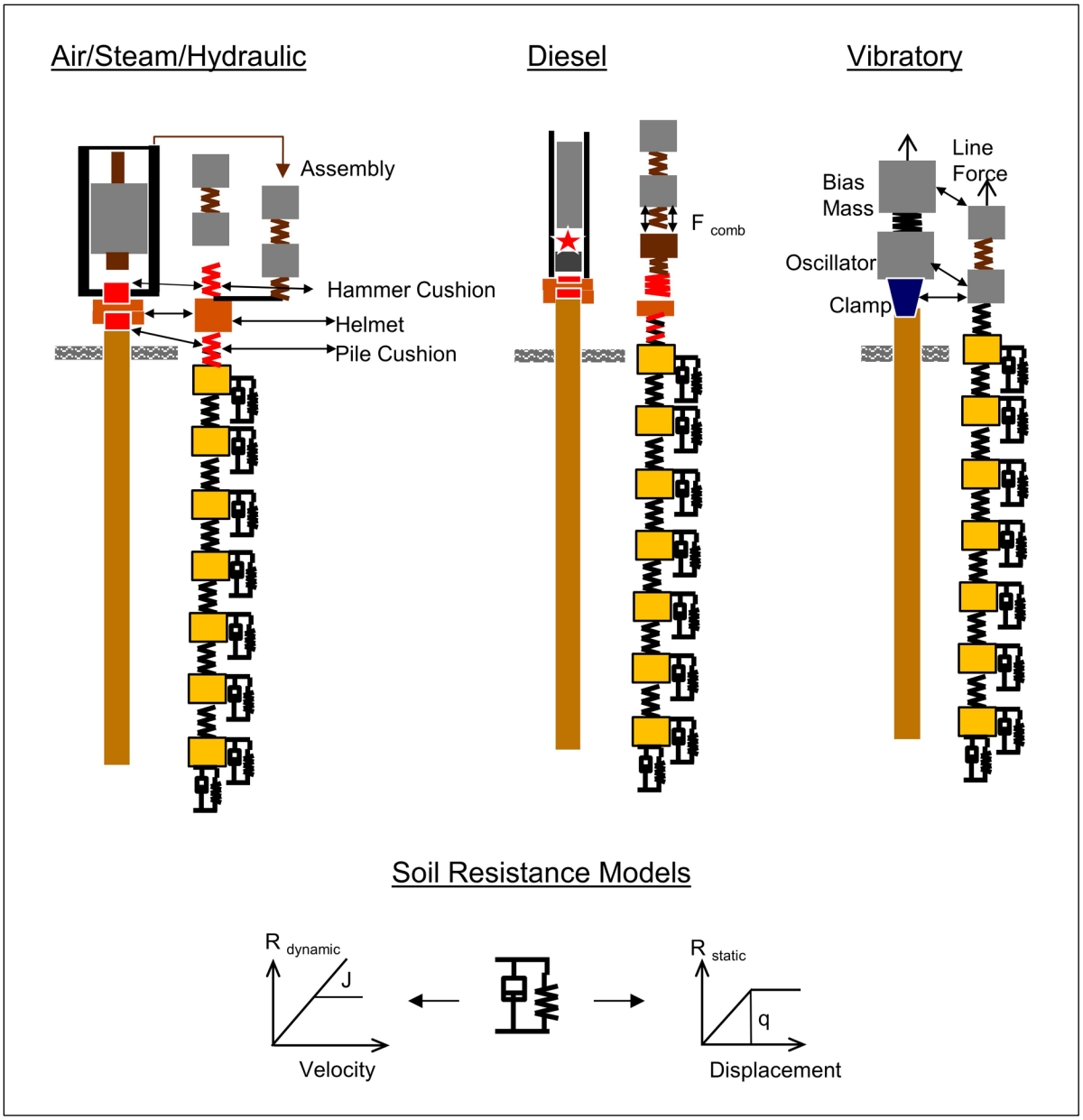

Figure 12-2 Typical wave equation pile and soil models.

The permanent set in inches of the pile toe is calculated by subtracting a weighted average of the shaft and toe quakes from the maximum pile toe displacement. An alternation calculation option available in the GRLWEAP program is called Residual Stress Analysis (RSA) which analyzes several hammer blows in sequence and then determines the permanent set from the pile top displacements of consecutive blows. However, to date, this more accurate approach has only been adopted for and checked against records from fluted and tapered piles. The inverse of the permanent set is the penetration resistance (blow count) in blows per foot or blows per inch that corresponds to the input nominal resistance. By performing wave equation analyses over a wide range of nominal resistances a curve or "bearing graph" can be plotted which relates nominal resistances to the pile penetration resistance or blow count.

A wave equation bearing graph is substantially different from a similar graph generated from a dynamic formula. The wave equation bearing graph is associated with a single driving system, hammer stroke, pile type, soil profile, and a particular pile length. If any one of the above items is changed, the bearing graph will also change. Furthermore, wave equation bearing graphs also include the maximum calculated compression and tension stresses.

In addition to the bearing graph, wave equation analysis can provide two alternative results, the constant capacity analysis, or "inspector's chart", and the “drivability analysis.” The inspector's chart establishes a relationship between variable hammer energy or stroke and pile penetration resistance for one particular, user specified, nominal resistance (ultimate capacity) value. Associated stress maxima are also included in the chart, enabling the user to select a practical hammer energy or stroke range both for reasonable penetration resistances and driving stress control. This analysis option is described in greater detail in Section 12.5.2.

The drivability analysis calculates penetration resistances and stresses from user input shaft and toe resistance values at up to 100 user selected pile penetrations. The calculated results can then be plotted together with the nominal resistance values versus pile penetration. The resulting plot would depict those pile penetrations where refusal might be expected or where dangerously high driving stress levels could develop. In addition, a crude estimate of pure driving time (not counting interruptions) is provided by this analysis option. The drivability option is described in greater detail in Section 12.5.3.

12.4 WAVE EQUATION APPLICATIONS

A bearing graph provides the wave equation analyst with two types of information:

1. It establishes a relationship between nominal resistance and pile penetration resistance or blow count. From the user's input data of the resistance values along shaft and at the toe, the wave equation analysis estimates the permanent set in inches under one hammer blow. Specifying up to ten nominal resistance (ultimate capacity) values yields a relationship between nominal resistance and penetration resistance in blows per foot or blows per inch.

2. The analysis also relates driving stresses in the pile to the pile penetration resistance.

3. The analysis also relates hammer stroke or hammer energy to the pile penetration resistance for a given nominal resistance.

The user typically develops a bearing graph or an inspector's chart for different pile lengths and uses these graphs in the field, with the observed penetration resistance, to determine when the pile has been driven to the required nominal resistance.

In the design stage, the foundation engineer should select typical pile types and driving equipment known to be locally available. Then by performing the wave equation analysis with various equipment and pile size combinations, it becomes possible to rationally:

1. Design the pile section for drivability to the required depth and/or nominal resistance.

For example, design considerations such as scour or consolidation settlements due to lower soft layers may make it necessary to drive a pile through a hard layer whose penetration resistance exceeds the resistance expected at final penetration. A thin walled pipe pile may have been initially chosen during design. However, when this section is checked for drivability, the wave equation analysis may indicate that even the largest hammers will not be able to drive the pipe pile to the required depth, because it is too flexible (its impedance is too low). Therefore, a wall thickness greater than necessary to carry the factored load has to be chosen for drivability considerations. (Switching to an H-pile or predrilling may be other alternatives).

2. Aid in the selection of pile material properties to be specified based on probable driving stresses in reaching penetration and/or nominal resistance requirements.

Suppose that it would be possible to drive a thinner walled pipe pile or lower weight H-pile section to the desired depth, but with excessive driving stresses. More cushioning or reduced hammer energy would lower the stresses, but would result in a refusal penetration resistance. Choosing a high strength steel grade for the pipe or H-section could solve this problem. For concrete piles, higher concrete strength and/or higher prestress levels may provide acceptable solutions.

3. Support the decision for a new penetration depth, factored load, and/or different number of piles.

In the above example, after it has been determined that the pile section or its material strength had to be increased to satisfy pile penetration requirements, it may have become feasible to increase the design load of each pile and to reduce the total number of piles. Obviously, these considerations would require revisiting geotechnical and/or structural considerations.

Once the project has reached the construction stage, additional wave equation analyses should be performed on the actual driving equipment by:

1. Construction engineers – for hammer approval and cushion design.

Once the pile type, material, and pile penetration requirements have been selected by the foundation designer, the hammer size and hammer type must be selected. These parameters may have a decisive influence on driving stresses. For example, a hammer with adjustable stroke or fuel pump setting may have the ability to drive a concrete pile through a hard layer while allowing for reduced stroke heights and increased tension stress control when penetrating soft soil layers.

Cushions are often chosen to reduce driving stresses. However, softer cushions absorb and dissipate greater amounts of energy thereby increasing the penetration resistance. Since it is both safer (reducing fatigue effects) and more economical to limit the number of blows applied to a pile, softer cushions cannot always be chosen to maintain acceptable driving stresses. Also, experience has shown that the addition of hammer cushion material is relatively ineffective for limiting driving stresses.

Hammer size, energy setting, and cushion materials should always be chosen such that the maximum expected penetration resistance is less than 120 blows/ft. One exception to this upper limit is piles driven through soft soils that transition abruptly to hard rock. In this unique case, piles are often final seated on the hard rock at 5 blows per ¼ inch (240 blows/foot equivalent) and the use of a larger hammer may result in driving stress concerns.

For most situations where wave equation simulation is used for hammer selection, it is prudent to select a hammer that can achieve the required nominal resistance at a blow count not exceeding 100 blows/ft. The blow count should also be greater than 30 blows/t for reasonably accurate construction control. This is required, because (a) the relative error of an inaccurate blow count measurement is greater for lower penetration resistances and (b) the dynamic methods of nominal resistance assessment tend to over-predict when driving is very easy. Of course, adjustable hammers may be accepted based on their lower energy settings. Exceptions should also be made when the accuracy of the blow count measurement is irrelevant. Such situations arise when the pile has to be driven to depth at expected capacities above the required minimum or because a large component of the nominal resistance is derived from soil setup.

2. Contractors – to select an economical driving system to minimize installation cost.

While the construction engineer is interested in a safe pile installation method, contractors would like to minimize equipment size and driving time for cost considerations. Light weight, simple, and rugged hammers which have a high blow rate are obviously preferred. The wave equation analysis can be used to roughly estimate the anticipated number of hammer blows and the time of driving. This information is particularly useful for a relative evaluation of the economy of driving systems.

For concrete piles, additional considerations might include the cost of pile cushions, which are usually discarded after a pile has been installed. Thus, thick plywood pile cushions may result in a considerable cost.

Near refusal penetration resistances are particularly time-consuming. Since it is known that stiffer piles drive faster with lower risk of damage, the contractor may choose to upgrade the wall thickness of a pipe pile or the section of an H-pile for improved overall economy.

12.5 WAVE EQUATION EXAMPLES

This section presents several examples that illustrate the application of the wave equation analysis for the solution of design and construction problems. The resistance factor applied to the nominal resistance in the following examples is 0.80 unless otherwise stated in the example. This assumes that a static pile load test was performed in addition to and to calibrate the wave equation result. As noted in Chapter 7, a resistance factor of 0.65 should be applied to the nominal resistance if dynamic testing with signal matching would be performed on the project instead of a static load test. If only wave equation analyses were used for resistance verification, then a resistance factor of 0.50 would be applicable. Furthermore, the nominal resistance times the resistance factor in a wave equation analysis should be greater than the sum of the critical factored loads plus resistances from any overlying layers unsuitable for or not present during long term support. Note that the nominal resistance (Chapter 7) corresponds to ultimate capacity in the literature. Hence, input or output for wave equation analysis programs often identify the nominal resistance as ultimate capacity or R_n.

12.5.1 Example 1 – General Bearing Graph

One of the primary applications of a wave equation analysis is to develop a bearing graph relating the nominal resistance to the pile penetration resistance or blow count. A bearing graph is often used to develop the driving criterion. For a desired nominal resistance, the required blow count can be obtained from the bearing graph.

Consider the soil profile in Figure 12-3. In this example, the foundation designer has estimated that a 65 foot long, 14 inch by 0.312 inch wall, closed end pipe pile with a steel yield strength of 35 ksi will be driven 62 feet into a deep deposit of medium sands. The foundation designer anticipates that the pile would achieve a nominal resistance of 350 kips at that depth. Using only wave equation analysis for the field verification method, the AASHTO resistance factor is 0.50. This would allow a maximum factored load of 0.50 times 350 kips or 175 kips. The designer also anticipated that the resistance on the shaft (pile toe) would be 52% (48%) of the total nominal resistance and that it would be triangularly distributed. Note that the calculated resistance is the expected long term nominal resistance and because the soil type is sand it can be expected that the resistance during driving will be essentially the same. Also, based on program recommendations for this displacement pile driven into a medium sand, the toe quake is input as the pile diameter divided by 60 (0.23 inches) while the shaft damping in these cohesionless soils is set to 0.05 s/ft. Shaft quake and toe damping are generally left at the

defaults of 0.10 inches and 0.15 s/ft, respectively. These recommendations have, on the average, yielded satisfactory agreement with field observation and dynamic testing results. However, once piles have been driven at specific sites, load tests may indicate that different parameters may be more appropriate. Figure 12-3 summarizes the input quantities.

The contractor selected a Delmag D12-42 single acting diesel hammer for driving the pipe piles. The contractor's hammer submittal indicates that the hammer cushion will consist of 1 inch of aluminum and 1 inch of Conbest with a cross sectional area of 227 in^2 and an averaged (Conbest and aluminum) elastic modulus of 530 ksi. A helmet weight of 1.7 kips is reported.

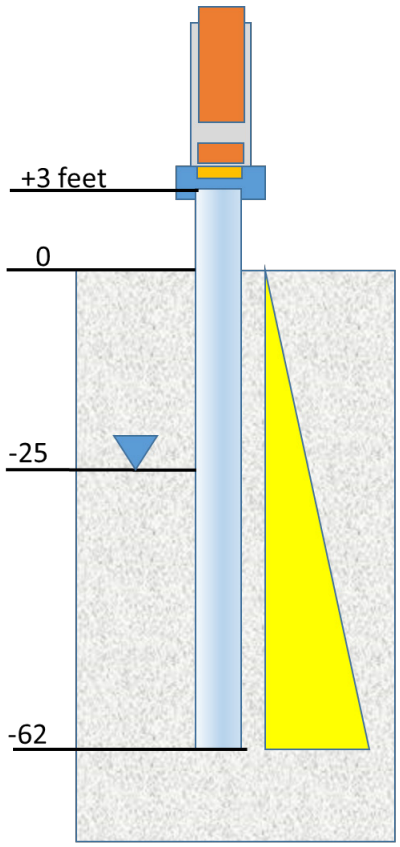

Hammer	DELMAG D12-42
Rated energy	34 ft-kips
Hammer cushion	1 inch Conbest + 1 inch aluminum
	A = 227 in^2; E = 530 ksi; COR = 0.8
Helmet Weight	1.7 kips
Pile Size	14 in. O.D. x 0.312 in. wall
Pile Type	closed ended pipe
Pile Yield strength	35 ksi
Pile Length	65 ft
Penetration	62 ft
Soil Type	medium dense sand
Water table	25 ft below grade
Shaft/toe quakes	0.10 / 0.23 inch
Shaft/toe damping	0.05 / 0.15 s/ft
Shaft resistance	52% - triangular
Toe resistance	48%

Figure 12-3 Example 1 – Problem profile.

Based on this information, a wave equation analysis can be performed. The nominal resistance of 350 kips is input along with selected additional values for which the wave equation analysis calculates the net permanent displacement and, inversely, the penetration resistance in blows/foot. By plotting calculated penetration resistances versus the corresponding input nominal resistance values, a bearing graph is developed. The results of the example analysis are shown in Table 12-1 and in Figure 12-4.

In the bottom half of the bearing graph, the nominal resistance versus penetration resistance in blows/foot is represented by the solid line. This graph shows that for a nominal resistance (ultimate capacity) of 350 kips, a penetration resistance of 99 blows/foot is required. This is less than the AASHTO recommended limit of 120 blows/foot. Although this is a relatively high blow count, it will neither require an excessive pile driving effort nor would it be too low to be inaccurate as far as construction control is concerned.

Table 12-1 Bearing Graph Numerical Results

Nominal Resistance kips	Maximum Compression Stress ksi	Maximum Tension Stress ksi	Penetration Resistance (Blow Count) bl/ft	Hammer Stroke ft	Transferred Energy ft-kips
50	19.15	1.19	5.1	5.70	17.3
100	22.40	0.58	11.8	6.54	15.8
150	24.52	1.57	20.7	7.21	15.6
200	25.82	1.52	29.9	7.64	15.7
250	27.17	2.05	42.5	8.16	16.3
300	28.14	2.21	63.4	8.52	16.9
350	28.89	2.18	98.8	8.82	17.3
400	29.34	2.11	169.6	8.99	17.4
450	29.97	2.11	279.9	9.24	17.7
500	30.34	2.08	631.3	9.41	17.9

Also in the bottom half of the bearing graph, the corresponding hammer stroke versus penetration resistance is represented by the dashed line. This curve is important for variable stroke hammers as a check on hammer performance when the driving criterion is applied. In this case, the penetration resistance of 99 blows/foot for 350 kip nominal resistance is based upon the hammer operating at a hammer stroke of 8.8 feet. Should field observations indicate significantly (say more than 10% difference) higher or lower strokes, then a lower or higher penetration resistance would be necessary for the same nominal resistance, because the hammer force and/or energy would be higher or lower. Hammer stroke information is therefore essential for field evaluation and control of the pile installation process.

An inspector's chart analysis (see Example 2) provides this information determining required blow count as a function of hammer stroke. For significantly differing hammer field performance, a new wave equation analyses would be necessary with a modified maximum combustion pressure or a fixed input stroke.

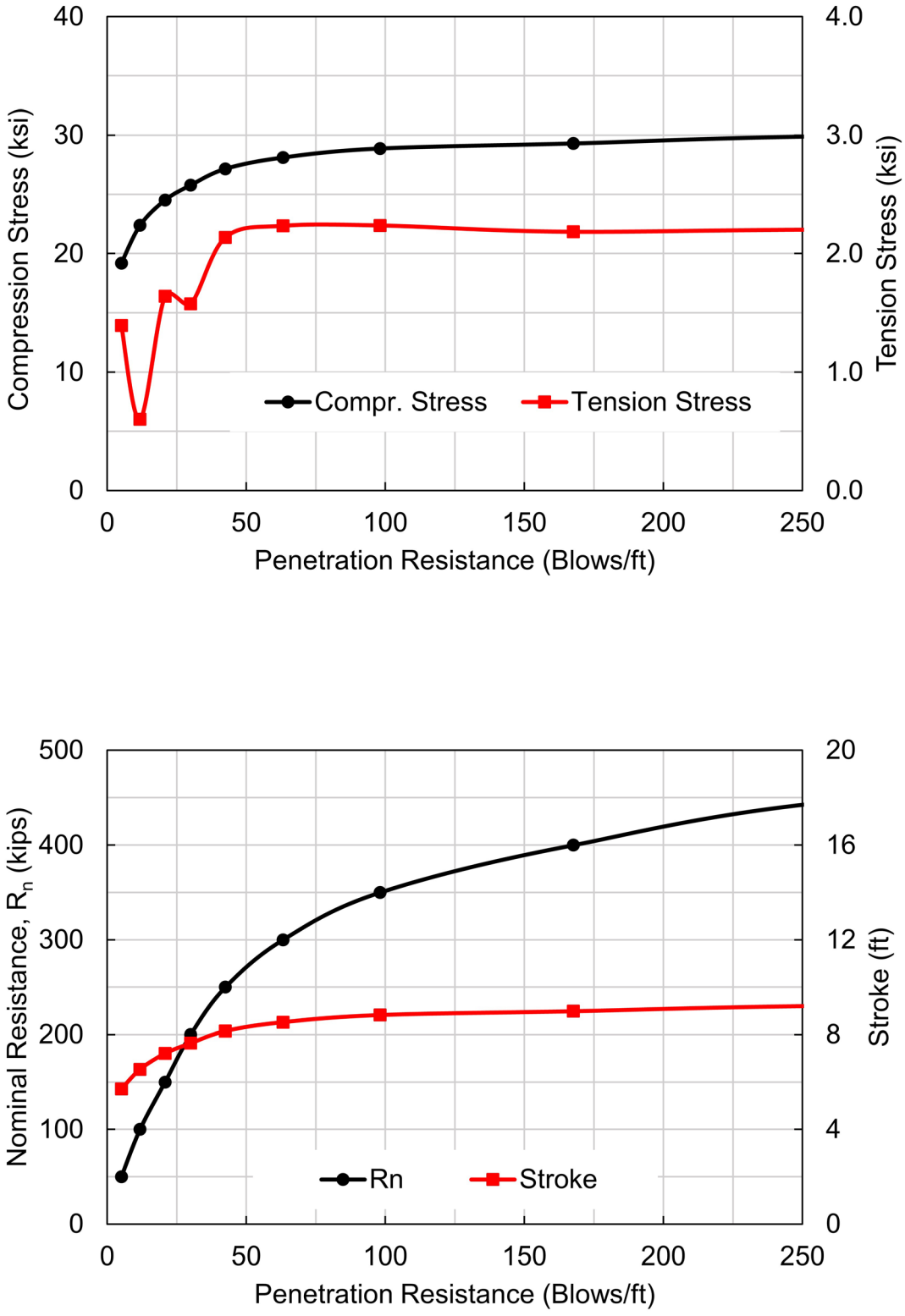

Figure 12-4 Typical wave equation bearing graph. Top plot – driving stresses; bottom plot – nominal resistance and diesel hammer stroke.

In the upper half of Figure 12-4, maximum compression and tension driving stresses are plotted as a function of penetration resistance. Of primary interest for a steel pile is the compression driving stress, which is represented by the solid black line. This plot shows that, at 99 blows/foot (and at the required nominal resistance), the maximum compression stress calculated in the pile is almost 29 ksi. This is less than 90% of the yield strength of 35 ksi or 31.5 ksi. This compression stress level is acceptable according to Article 10.7.8 of AASHTO (2014) design specifications and as discussed further in Chapter 8. However, any non-uniform stress components (e.g. bending caused by poor hammer-pile alignment or pile-toe contact with sloping rock) are not included in the wave equation results and would be additional. In any case, the 90% yield limit applies to the stress averaged over the pile cross section.

Though the analysis was conducted for an estimated penetration of 62 feet, in the field the required penetration resistance may be reached at a lesser or greater depth. The static analysis only serves as an initial estimate of the required penetration depth. The actual driving behavior and construction monitoring will confirm whether or not the static calculation was adequate. If the actual driving behavior is significantly different from the analyzed situation (say the required blow count is already reached at 50 feet of penetration), an additional analysis should be performed to better match field observations. In general, the nominal resistance versus pile penetration resistance relationship is relatively insensitive to changes in the penetration depth and, therefore, to the distribution of the resistance along the pile unless there is a significant change in the soil profile. Of course, if unexpected changes in hammer performance, driving system components, or soil properties appear to cause the difference, then it would be prudent to check the equipment performance and soil resistance by dynamic measurements. Higher penetration resistances from penetrating embankment fills or scour susceptible material, etc., should also be considered in this assessment.

12.5.2 Example 2 – Constant Capacity / Variable Stroke Option

The hammer-pile-soil information used in Example 1 will be reused for a constant capacity (or inspector's chart) analysis in Example 2. In this example, the penetration resistance required for the 350-kip nominal resistance is evaluated over a range of hammer strokes. The resulting inspector's chart would be helpful for field personnel in determining when pile driving can be terminated if the field observed hammer stroke varies from that originally predicted by the wave equation bearing graph analysis. Figure 12-5 shows the resulting inspector's chart. The lower half of Figure 12-5 presents the hammer stroke versus penetration resistance plot for the required nominal resistance of 350 kips. Where the point of intersection of the observed stroke and penetration resistance plots below the curve, the nominal resistance has not been obtained. Any combination of stroke and penetration resistance plotting above the curve indicates that the required resistance level has been reached. For example, any stroke greater than 8.2 feet at a penetration resistance of 90 blows/foot is acceptable. The upper half of either graph shows the stress maxima associated with a particular driving resistance. Hence, the inspector's chart analysis aids the inspection personnel in field control.

12.5.3 Example 3 – Drivability Studies

Scour and seismic design considerations often result in increased pile penetration requirements. Therefore, the ability of a given pile to be driven to the required penetration depth should be evaluated in the design stage in a wave equation drivability study, as presented in this example.

Figure 12-6 illustrates the installation conditions at an interior bridge pier in a river. A cofferdam will be required for pier construction. The interior of the cofferdam will be excavated 16.5 feet below riverbed prior to pile installation. The excavated layer consists of loose silt. Below the silt, a 13.5 foot thick layer of extremely dense sand and gravel layer with some clay was noted which in turn overlies a medium dense sand layer. Bedrock was encountered approximately 70 feet below riverbed.

The contractor has selected a Conmaco C 160 air hammer which has a ram weight of 16.25 kips, a rated stroke of 3.0 feet for a rated energy of 48.75 ft-kips. The hammer cushion consists of Nylon, the helmet weight is 4.07 kips and the pile cushion was chosen as 10 inches of plywood. A new pile cushion is to be used for every pile. For that reason the elastic modulus of 30 ksi for "new plywood" is used at

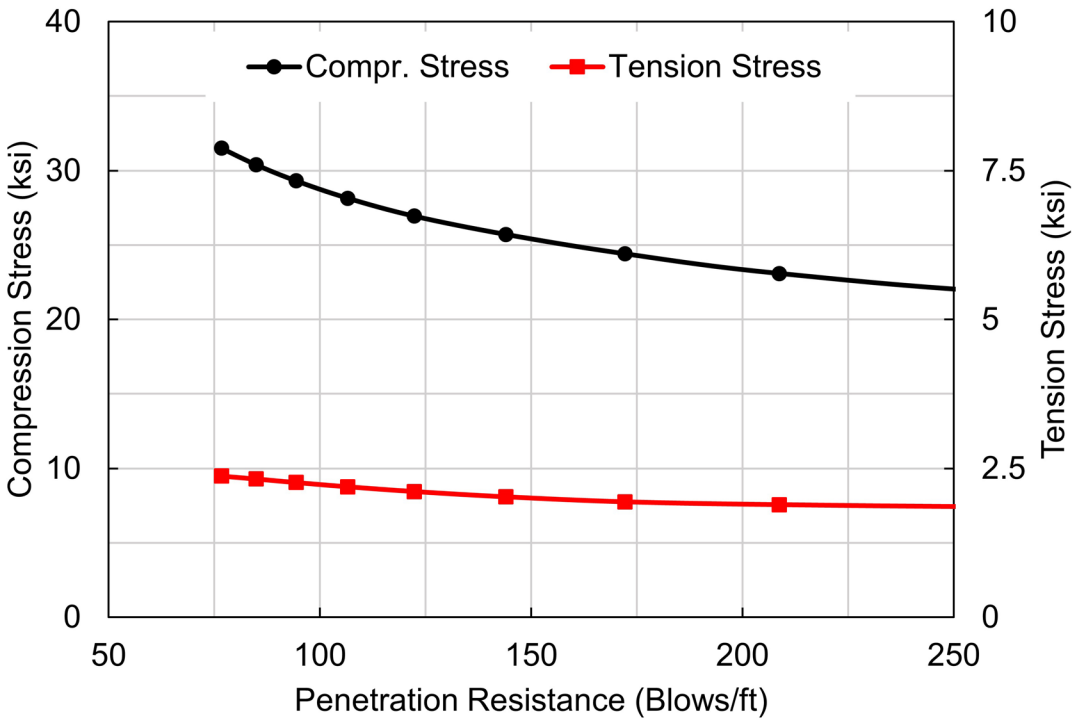

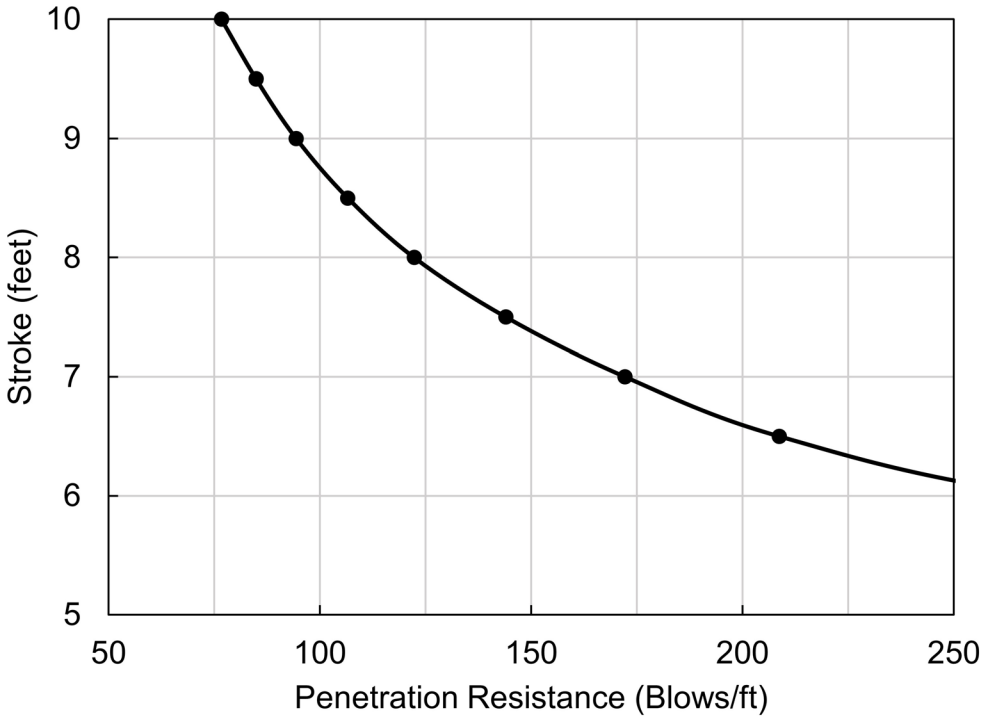

Figure 12-5 Constant capacity analysis (inspector's chart).

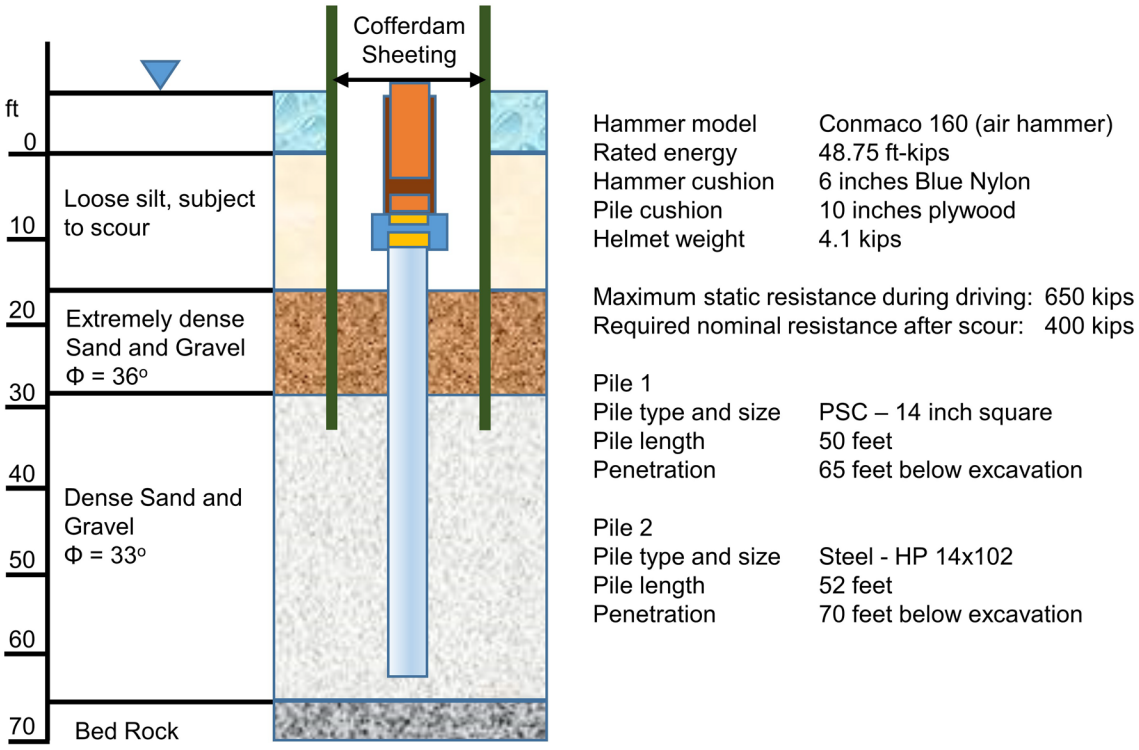

Figure 12-6 Example 3 – Problem profile.

the beginning of driving. However, as the plywood compresses during driving and gets harder, a “used plywood cushion” elastic modulus of 75 ksi should be chosen to reflect the associated higher stiffness of the harder cushion at end of driving. This recommendation is based on correlation studies (Rausche et al. 2004) which indicated that the stiffness of plywood cushions at the end of driving are typically 2.5 times higher than in their new condition (for oak boards the factor is 1.5). Note that for the correctly effecting the stiffness increase, only the elastic modulus should be modified while the cushion thickness is always entered as the nominal thickness in the “new” cushion conditions.

The extremely dense sand and gravel layer was estimated to have a soil friction angle $\phi = 43^{\circ}$. This friction angle was used in the static calculations of toe resistance. However, the friction angle was limited to 36° for the hard angular gravel when calculating shaft resistance. The friction angle for the medium dense sand layer was estimated to be $\phi = 33^{\circ}$.

During construction, the silt soils will be removed from within the cofferdam area. However, the silt soils outside the cofferdam will still be present at the time of construction. Therefore, the soil resistance to pile driving should be calculated with consideration for the overburden pressure from these materials. However, hydraulic

experts predict that the 16.5 feet of loose silt may erode completely due to channel degradation scour. Thus, for long term pile nominal resistance, static calculations should ignore the effective weight of the silt layer. As a result, a higher soil resistance than required to meet the static load requirements must be anticipated during pile installation.

Initial static analysis indicates that a 14 inch square prestressed concrete pile would develop the required nominal resistance of 400 kips, primarily through end bearing, at a depth of 10 feet below the cofferdam excavation level (26.5 feet below river bed). However, when considering the reduction in the effective overburden pressure from the scouring of the silt layer, the pile would have an nominal resistance of only 241 kips at a penetration depth of 10 feet below cofferdam excavation level and 318 kips immediately above the dense sand where the end bearing would be unreliable. Additional static nominal resistance calculations were performed at increased pile penetration depths for the pre-scour profile. These analyses show that when punching through the upper, extremely dense sand layer the nominal resistance would at first be lower in the dense sand and gravel but would again reach a 400 kip nominal resistance at a depth of 49 feet below cofferdam excavation level (65.5 feet below river bed).

For the installation condition, a pre-scour analysis indicates that the nominal resistance at a depth of 49 feet would be 472 kips and this is the soil resistance that must be overcome at the end of driving. (An almost identical driving resistance exists at a depth of 13 feet depth below excavation (29.5 feet below river bed)).

Next, nominal unit resistance values for both shaft and toe resistance versus depth with consideration of the silt overburden stress were calculated by static analysis and input into a wave equation program. The soil profile consists primarily of sandy materials. Significant soil setup or relaxation in these materials is not considered likely and therefore no gain or loss factors due to driving had to be considered in the drivability analysis (gain/loss factors for both shaft and toe were set to 1.0). Since the study is conducted in the design stage, the use of a locally available single acting air hammer driving system was assumed.

The following additional input considerations should be mentioned:

1. The concrete pile is a displacement pile. For that reason, the toe quake for the extremely dense sand and gravel was set to the pile width, D, divided by 120 (0.12 inches).

2. For the dense sand the toe quake was set to D/60 – 0.23 inches.

3. The pile cushion becomes stiffer (elastic modulus increases and thickness decreases) during pile installation. GRLWEAP Help (Rausche et al. 2004), recommends using a pile cushion stiffness for the end of driving which is 2.5 times the initial stiffness which is based on an elastic modulus of 30 ksi. This correction factor includes both the effect of the cushion reduction in thickness as well as the increase in elastic modulus. Thus for the various depths analyzed, the cushion stiffness was gradually increased between the initial and final driving depths.

The drivability analysis result (Figure 12-7) indicated that the 14 inch concrete pile would encounter a maximum penetration resistance of 158 blows/foot in the upper extremely dense sand and gravel deposit just before breaking through to the dense sand layer. For the final depth of 49 feet (65.5 feet below river bed) a penetration resistance of 60 blows/foot was calculated. Since the high blow count in the extremely dense sand layer is only present for a short distance, it could be concluded that the 14 inch concrete pile could be driven to the required penetration depth of 49 feet. This might be an erroneous conclusion. Although the static analysis would likely provide an adequate assessment of soil resistance for the first pile driven, an increase in the friction angle from group densification could significantly affect the resistance to driving of additional displacement piles, particularly within the tight confinement of the cofferdam. Also, dense deposits tend to develop negative pore pressures during shear, resulting in temporary increases in soil resistance which may later dissipate. If it is assumed that these factors cause a 30% increase in both shaft and toe resistances during the driving of subsequent piles, a second drivability analysis for the densified condition would indicate that the later piles essentially refuse (blow count greater than 240 blows/foot) at a depth of 11 feet below excavation (27.5 feet below river bed). The nominal resistance at that depth is 579 kips. Maximum calculated driving stresses were 3.7 ksi discouraging the use of a larger hammer, unless a sufficiently high concrete strength would be chosen. If displacement piles were indeed used, predrilling or jetting would likely be required to advance the piles through the upper stratum.

A low displacement pile such as an H-pile or open end pipe pile, which would cause a lower or no densification, presents a more attractive foundation solution. Thus, the analysis was repeated for a 55 feet long, HP 14x102 H-pile which would allow the pile to reach bedrock at 53.5 feet depth (70 feet below river bed). Note that it is common practice to analyze H-pile drivability with a toe resistance as though the H-pile would be plugging while at the same time assuming a toe quake of only 0.10 inches as for a non-displacement pile. In other words it is tacitly assumed that the

pile is only partially plugging or that the plug slips during driving. This also means that there is no major densification effect when driving the H-pile.

The drivability results, shown in Figure 12-7, include the pile penetration resistance, maximum compression stresses and transferred energy for the normal (first pile) and later (densified) conditions. The concrete pile results are also shown in Figure 12-8. Along with the wave equation drivability results for the low displacement HP 14x102 H-pile. Figure 12-8 allows for a comparison of penetration resistance and transferred energy and shows that the low displacement steel pile will drive with a significantly lower penetration resistance though the extremely dense sand and gravel layer.

Note that the penetration depth in these figures corresponds to the depth below cofferdam excavation level. The maximum penetration resistance calculated for the H-pile to penetrate the extremely dense sand and gravel stratum is only 45 blows blows/foot. Corresponding compression driving stresses do not exceed 32 ksi and are within driving stress limit. The nominal resistance increases significantly at deeper pile penetration depths. However, the penetration resistance increases to only 44 blows/foot before quickly transitioning to refusal conditions when the pile reaches rock. The results indicate that the H-pile could be driven to bedrock allowing for a possible higher factored load, reduced number of piles and a more cost effective design.

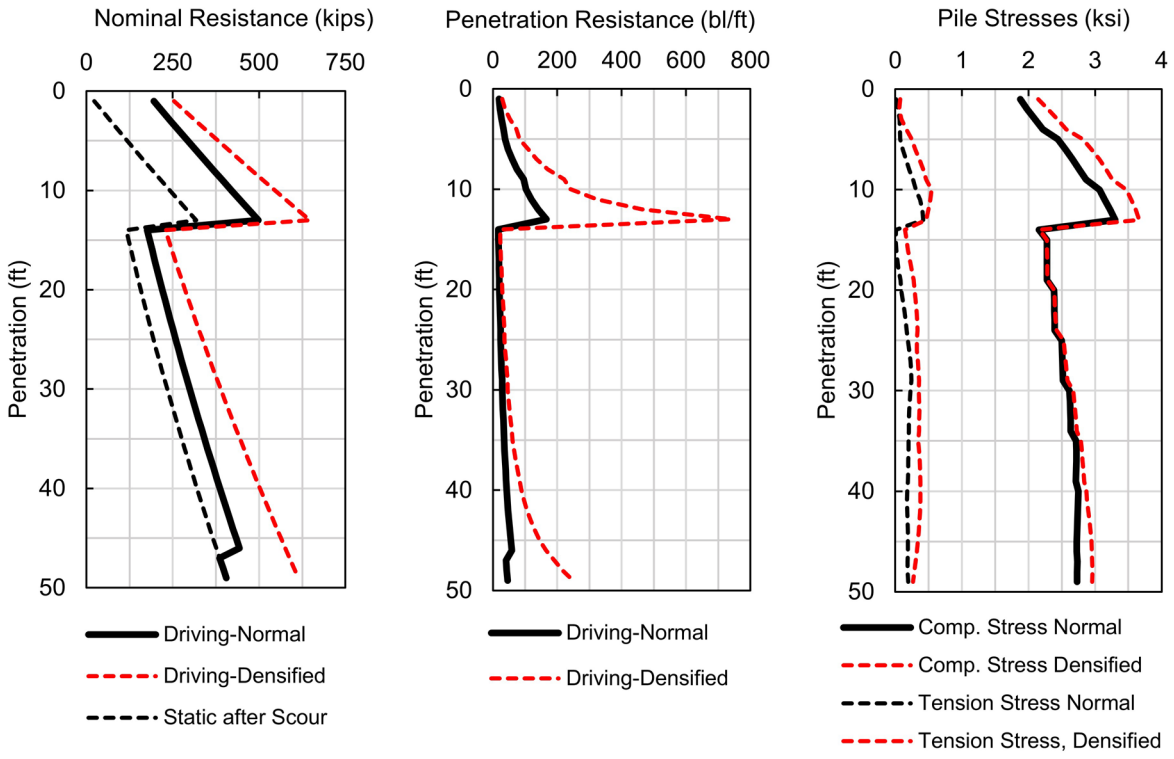

Figure 12-7 Nominal resistance, calculated blow count and stresses for before and after densification and nominal resistance for the after scour condition.

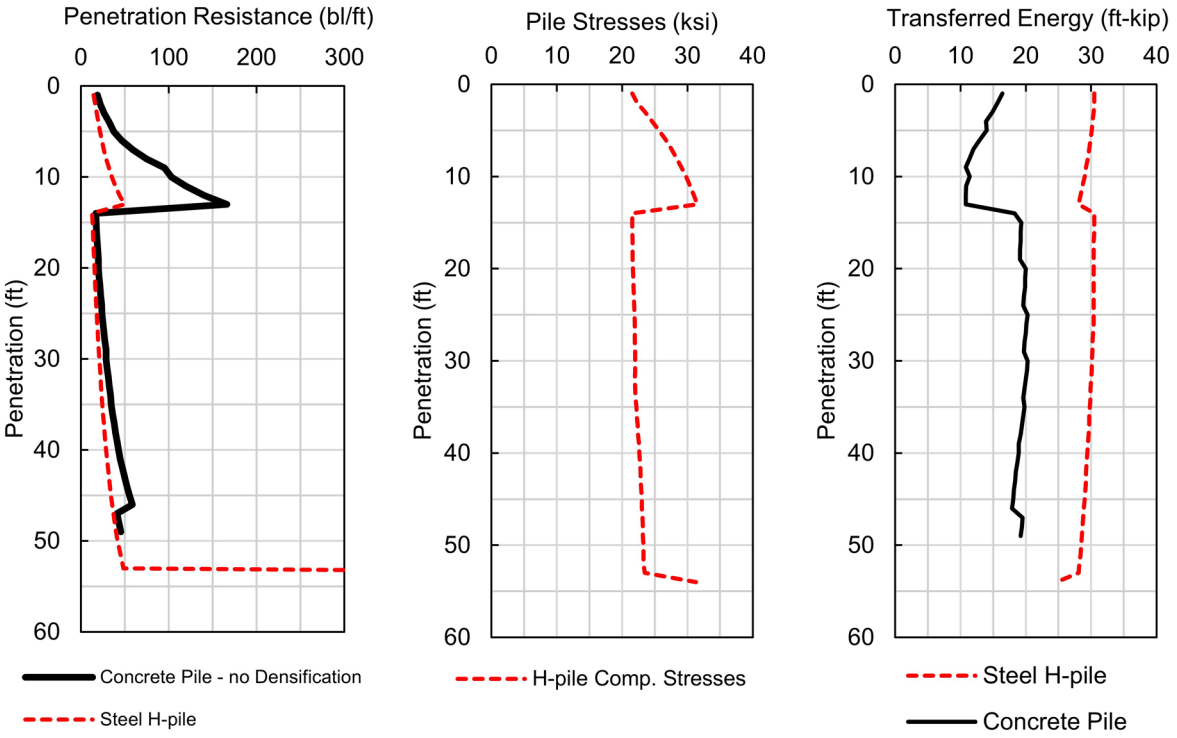

Figure 12-8 Drivability results for H-pile with corresponding concrete pile results.

12.5.4 Example 4 – Tension and Compression Stress Control

Example 4 illustrates the use of the wave equation for the control of tension stresses in a 60 feet long concrete pile. Static calculations indicate a 14-inch square, prestressed concrete pile driven through 20 feet of loose silty fine sand, 35 feet of medium dense sandy silt, and 3 feet into a dense sand and gravel deposit could develop a required nominal resistance of 400 kips. The static analysis also indicates that the nominal resistance is distributed as 55% shaft resistance and 45% toe resistance with a variable shaft resistance distribution along the pile shaft as shown in Figure 12-9.

The contractor selected a Junttan HHK 3A hydraulic hammer for driving the prestressed concrete piles. This hammer has a ram weight of 6.6 kips and a rated energy of 26 ft-kips. The contractor's hammer submittal indicates that the hammer cushion will consist of 8 inches of a material that has an elastic modulus of 360 ksi and a coefficient of restitution of 0.90 and a cross sectional area of 250 in^2. A helmet weighing 1.0 kip is also planned for the driving system.

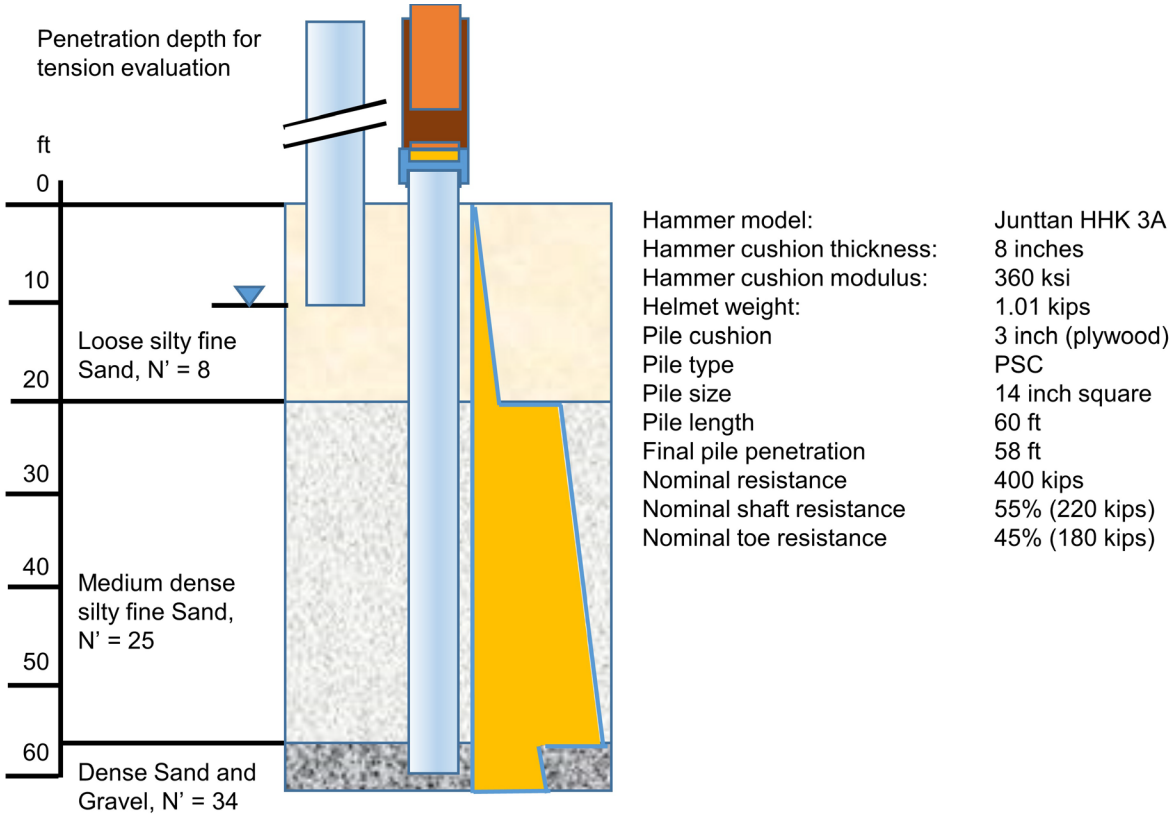

Figure 12-9 Example 4 – Problem profile.

The concrete pile will have a compression strength of 5.5 ksi and an effective prestress after losses of 0.70 ksi. Using the AASHTO (2014) driving stress recommendations, discussed in Chapter 8, results in maximum recommended driving stresses of 4.1 ksi in compression and 0.92 ksi in tension.

One of the main concerns with the drivability of concrete piles is the possibility of developing high tension stresses during easy driving conditions when the soil provides little or no toe resistance. Therefore, the wave equation should be used to evaluate the contractor's proposed driving system during both low and high resistance conditions.

First, an evaluation of tension stresses during easy driving is presented. The weight of the pile and driving system is anticipated to be on the order of 20 kips. Hence, the pile penetration depth for the wave equation analysis should be selected below the depth to which the pile will likely penetrate or "run" under the weight of the pile and driving system, or approximately 10 feet. At this depth, the pile is still within the loose silty fine sand stratum and tension driving stresses are anticipated to be near their peak. Although not strictly correct, for the first low resistance analysis of 20 kips it is accurate enough to assume the same shaft resistance percentage (55%) as for the final penetration of 58 feet. For a complete bearing graph not only the 20-kip nominal resistance, but also other higher values are input and analyzed.

The contractor submitted a plywood pile cushion design comprised of four 3/4 inch sheets with a total thickness of 3 inches. Pile cushion stiffness significantly affects tension driving stresses. Therefore, it is necessary to determine whether or not the contractor's proposed pile cushion thickness is sufficient to maintain tension stress levels below specified limits. In the first trial, the 3 inch pile cushion is assumed to possess the properties of new plywood. Thus, the original pile cushion thickness of 3 inches and the new cushion elastic modulus of 30 ksi are input. Based on this information, the wave equation analysis indicates for the 20-kip nominal resistance a maximum tension stress of 1.47 ksi. The magnitude of the calculated tension stress exceeds the allowable driving stress limitation of 0.92 ksi.

A second wave equation analysis was therefore performed with an increased pile cushion thickness of 6 inches. By using the thicker pile cushion, the maximum tension stress was reduced from 1.47 ksi to 0.89 ksi which was less than the specified driving stress limit. The original and second wave equation analysis results for the easy driving condition at a pile penetration depth of 10 feet are presented in Figure 12-10.

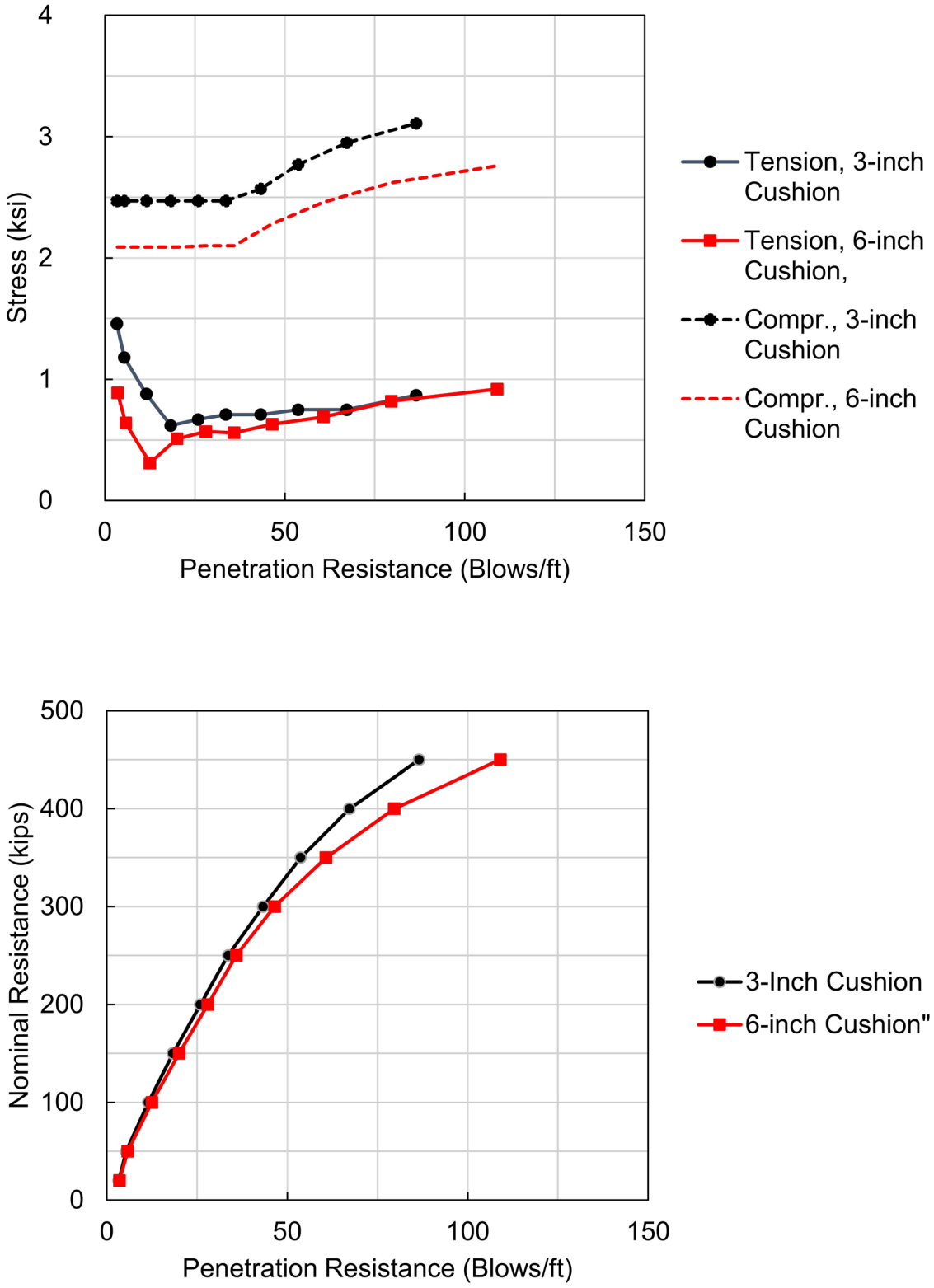

Figure 12-10 Bearing graphs for easy driving condition, two pile cushion thicknesses.

The Junttan HHK 3A hydraulic hammer has an adjustable stroke height (or energy level). In the previous two analyses, it was assumed that the hammer would be run at the maximum rated energy of 26 ft-kips which corresponds to an equivalent stroke of 3.94 feet. To reduce pile cushion costs, the contractor suggested piles be driven with a reduced stroke and thinner less costly pile cushion. The wave equation analysis was therefore repeated for a 3 inch cushion and a 1.75 foot hammer stroke, corresponding to a potential energy of 11.6 ft-kips. For this configuration, the calculated maximum tension stress was 0.90 ksi at the 20-kip nominal resistance.

If the hammer would only be operated at the reduced 1.75 foot stroke, then the blow count would be at refusal (greater than 240 blow/foot) for the required 400 kip nominal resistance. Therefore, an additional analysis was performed for the final penetration depth of 58 feet using the full hammer stroke and rated energy and a used 3 inch thick pile cushion. The cushion was modeled with an elastic modulus of 75 ksi which considers that the cushion thickness is also reduced. Obviously, in this case it is not necessary to analyze the 20 kip nominal resistance value.

The wave equation analysis results for the final driving condition are shown in Figure 12-11. They indicate a penetration resistance of 56 blows/foot for the 400 kip required nominal resistance. The associated tension and compression stresses are 0.58 and 3.32 ksi which are less than the maximum recommended driving stresses of 0.92 and 4.15 ksi, respectively.

Figure 12-11 also indicates that the tension stresses for the full stroke driving would be excessive, greater than 0.92 ksi, if full stroke driving were used with the 3-inch cushion at a nominal resistance of 250 kips or less. For this resistance value, on the other hand, the reduced stroke analysis indicates a penetration resistance of 85 blows/foot. Based on these findings the following recommendation would be made to the contractor:

- Use a fresh 3-inch thick plywood cushion for every pile.
- Operate the hammer at a reduced equivalent stroke of 1.75 ft.
- Once the penetration resistance reaches 85 blow/foot, increase the equivalent stroke to the full rated stroke of 3.94 feet.
- Drive the pile to a minimum driving resistance of 56 blows/foot at the full rated stroke condition.

Note that it may be quicker, simpler, and possibly more cost effective to use the 6 inch pile cushion and full hammer energy for the complete driving sequence.

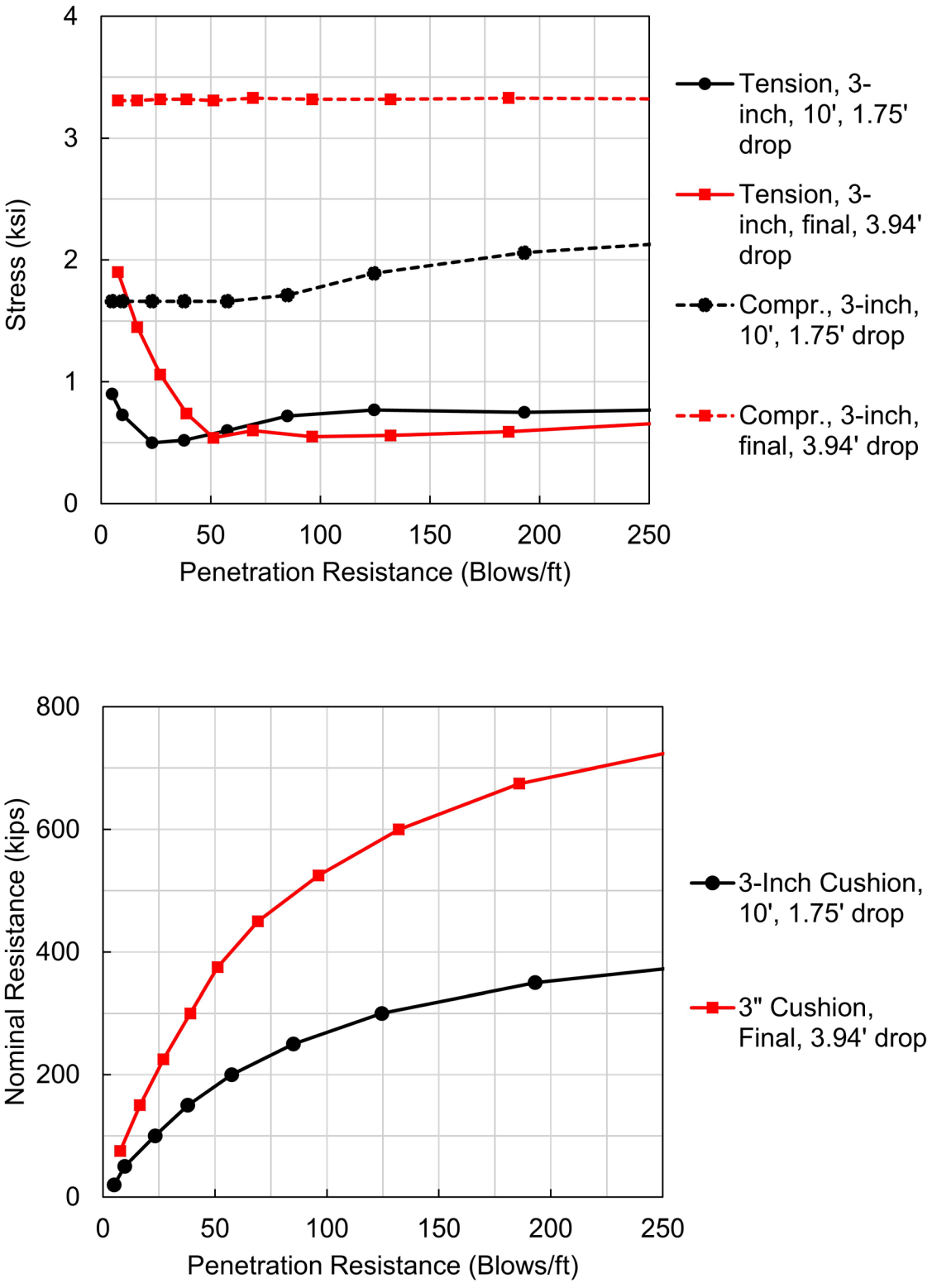

Figure 12-11 Bearing graphs for early low energy and end of driving high energy driving condition.

12.5.5 Example 5 – Use of Soil Setup

Consider the soil profile in Figure 12-12. In this example, a 12 inch square, prestressed concrete pile is to be driven into a thick deposit of stiff clay. The stiff clay has an average shear strength of 1.5 ksf. Based on field vane shear tests, it is estimated that the remolded shear strength at the time of driving will be 1.1 ksf, resulting in an expected soil setup factor of 1.36. A static analysis indicates that a nominal resistance of 300 kips after setup can be obtained for the proposed pile type at a penetration depth of 50 feet. The static analysis also indicates that the nominal resistance is distributed as 92% uniform shaft resistance and 8% toe resistance.

The contractor selected a Vulcan 08 single acting air hammer for driving the prestressed concrete piles. The contractor's hammer submittal indicates that the hammer cushion will consist of 8.5 inch of Hammortex with a cross sectional area of 148 in^2. The pile cushion will consist of plywood with a total thickness of 6 inches. It is anticipated that the pile cushion will compress and stiffen during driving similar to that described in Example 4. For an easy driving analysis, the assumption of a new pile cushion with the elastic modulus of 30 ksi would apply. For the late driving scenario, a compressed cushion modulus of 75 ksi should be considered. As mentioned earlier, using this 2.5 times higher modulus will not only account for the stiffening of the material but also for its thickness decrease. The contractor's submittal indicates that the helmet weighs 2.6 kips.

Based upon the reported soil type and setup behavior, a 36% increase in nominal resistance with time is expected at this site. Therefore, piles could be driven to a reduced nominal resistance, or static resistance to driving (SRD), of 225 kips instead of the required value of 300 kips with the remaining 75 kips expected from soil setup. As noted earlier in this chapter, a static load test will be performed on the project to confirm the expected resistance gain.

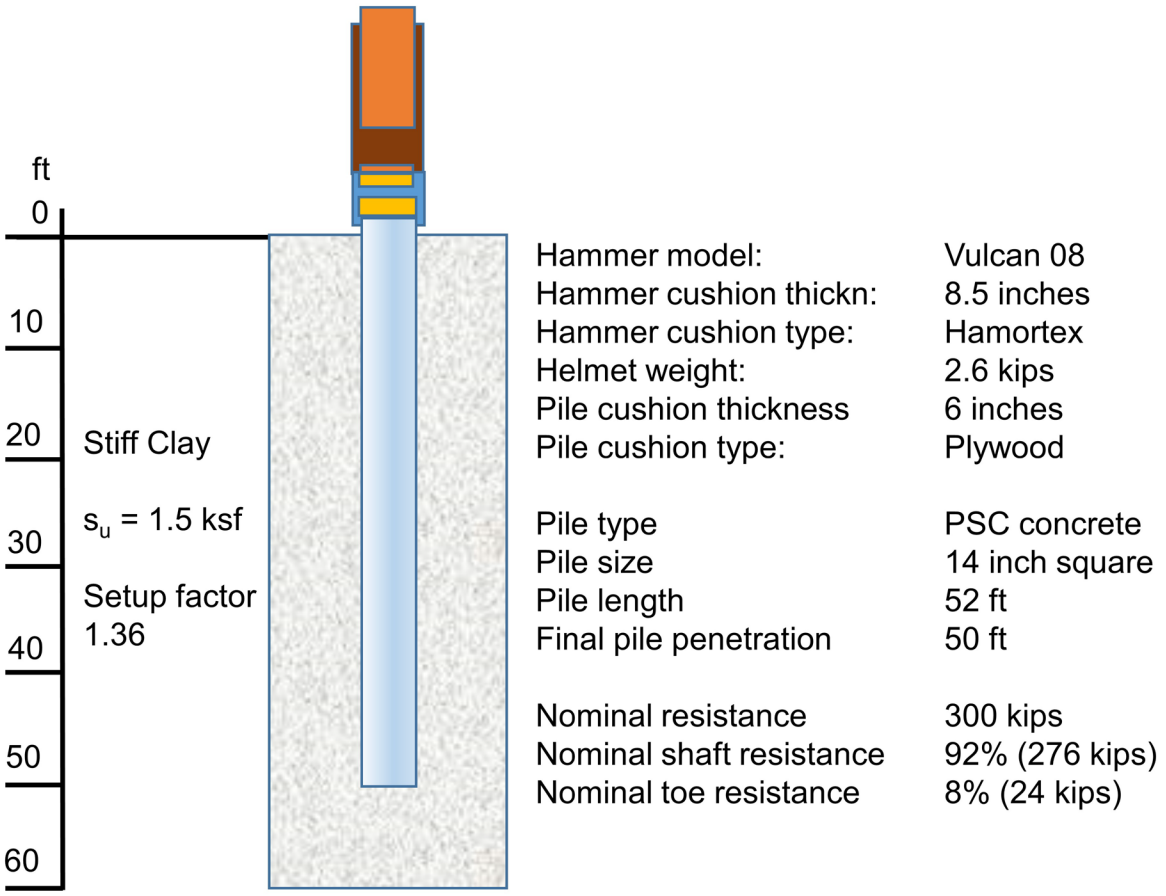

Figure 12-12 Example 5 –- Problem profile.

The wave equation results presented in Figure 12-13 indicate a final penetration resistance of 43 blows/foot could be used as the driving criteria for a 225 kip SRD or end of driving nominal resistance. This is significantly less than the 89 blows/foot required for a nominal resistance of 300 kips. Hence, significant pile length and driving effort may be saved by driving the piles to the lower resistance. However, this approach requires a restrike test or a static load test sometime after pile installation; the waiting time period is soil type dependent as discussed in Section 7.2.4.

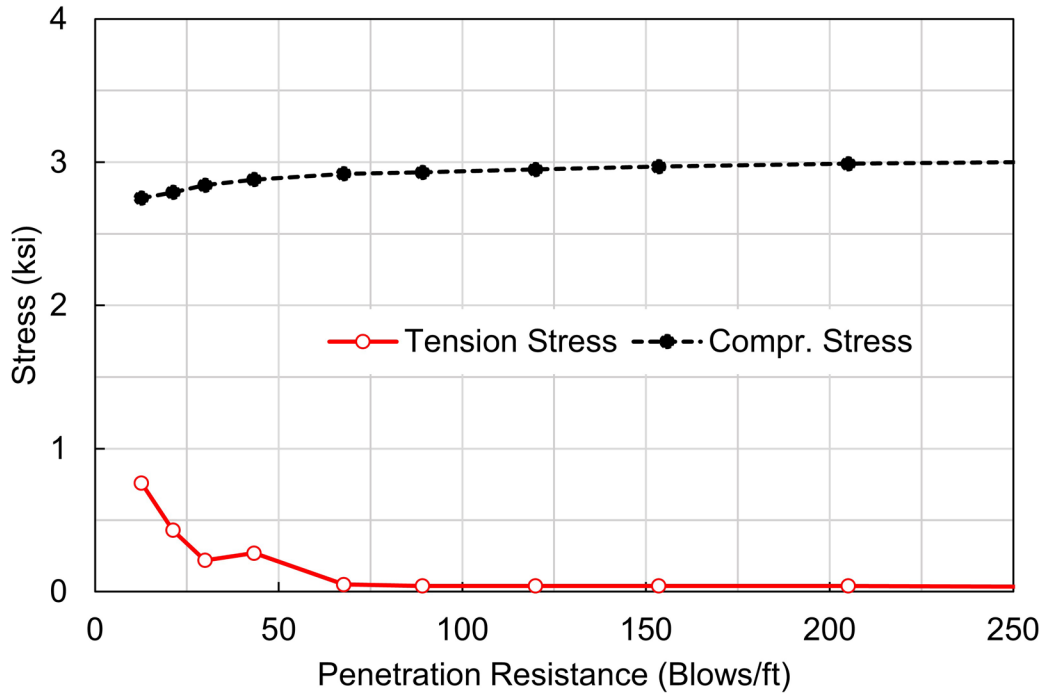

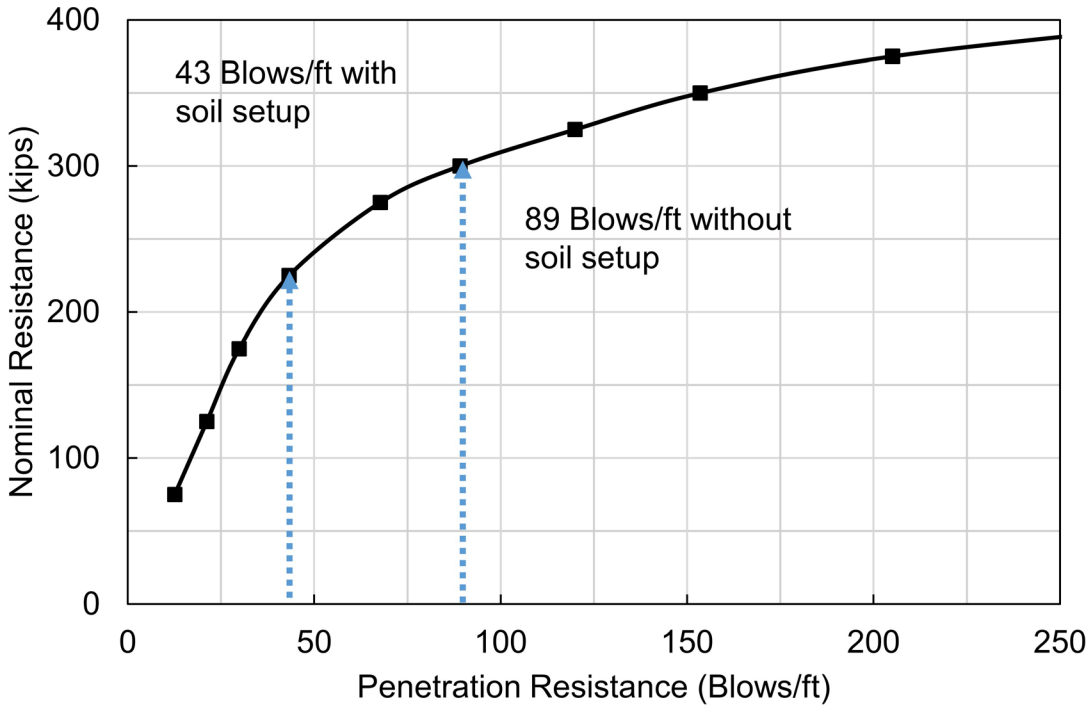

Figure 12-13 Using a bearing graph with soil setup.

12.5.6 Example 6 – Driving System Characteristics

Example 6 presents a wave equation comparison of two hammers having the same potential energy. Dynamic formulas such as the Modified Gates formula consider only the potential energy of the driving system. Therefore, the penetration resistance required for a specific nominal resistance by this and most other dynamic formulas would be the same for two hammers provided that the hammers had the same potential energy. In this example, the penetration resistances predicted by the wave equation for these two hammers in the same pile-soil condition is, however, quite different.

In this example, a 14 inch O.D. x 0.375 inch wall, closed end pipe pile is to be driven to a nominal resistance of 400 kips. The pile has a furnished length of 66 feet and an embedded length of 52.5 feet. A static analysis indicates that the soil resistance distribution will be 30% shaft resistance and 70% toe resistance. The shaft resistance will be distributed triangularly along the embedded portion of the pile shaft. The example problem's soil profile is presented in Figure 12-14. With a very dense, dry soil at the pile toe, the normal program recommendation for the quake at the pile toe is D/120 or 0.12 inch. However, experience with the bearing layer from previous dynamic measurements showed that the silty fine sand at this site is highly elastic and has a larger than normal toe quake of 0.40 inch.

The contractor is considering using either a Vulcan 014 air hammer or an ICE 42-S open end diesel hammer to drive the piles. Both hammers have the same manufacturer’s rated hammer energy of 42 ft-kips. However, the ram of the Vulcan 014 is roughly 3.5 times heavier than the ram of the ICE hammer. Details of these hammers and their associated proposed driving systems are summarized in Table 12-2.

Wave equation results for the two hammers are plotted on the same bearing graph in Figure 12-15. For the high toe quake case (0.40 inches), wave equation analysis calculates a penetration resistance of 94 blows/ft to achieve a 400 kip nominal resistance with the heavy ram air hammer whereas the lighter ram diesel hammer requires a penetration resistance of 209 blows/ft. For the standard toe quake case (0.12 inches), the heavy ram air hammer requires a penetration resistance of 56 blows/ft while the light ram diesel hammer requires 99 blows/ft. Hence, even though both hammers have the same potential energy, the required penetration resistance for the 400 kip nominal resistance is quite different.

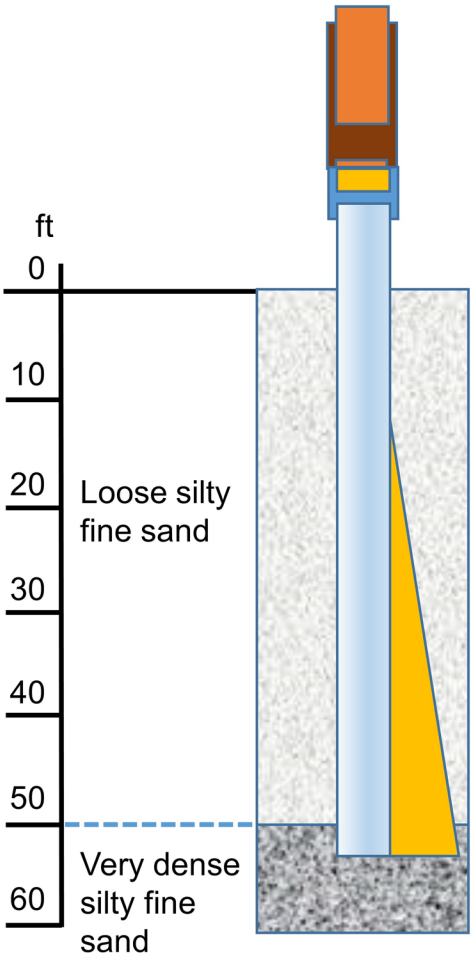

First hammer model:	ICE 42-S
Rated energy:	42 ft-kips
Second hammer model:	Vulcan 014
Rated energy:	42 ft-kips
Hammer cushion	varies
Helmet weight:	varies
Pile type:	Closed End Pipe
Pile diameter:	14 inches
Pile wall thickness:	0.375 inches
Pile length:	66 ft
Final pile penetration:	52.5 ft
Nominal resistance:	400 kips
Nominal shaft resistance:	30% (120 kips)
Nominal toe resistance:	70% (280 kips)
Toe quake:	0.4 inches

Figure 12-14 Example 6 – Problem profile.

Table 12-2 Example 6: Proposed Hammer and Driving Systems

Hammer Model	Vulcan 014	ICE 42S
Ram Weight, kips	14	4.09
Rated Energy, ft-kips	42	42
Rated Stroke, ft	3.0	10.3
Helmet Weight, kips	1.67	2.05
H. Cushion Material	Nycast	Blue Nylon
H. Cushion E-Mod, ksi	208	175
H. Cushion Area, in^2	234	398
H. Cushion Thickness, in	6.0	2.0
H. Cushion COR	0.91	0.92

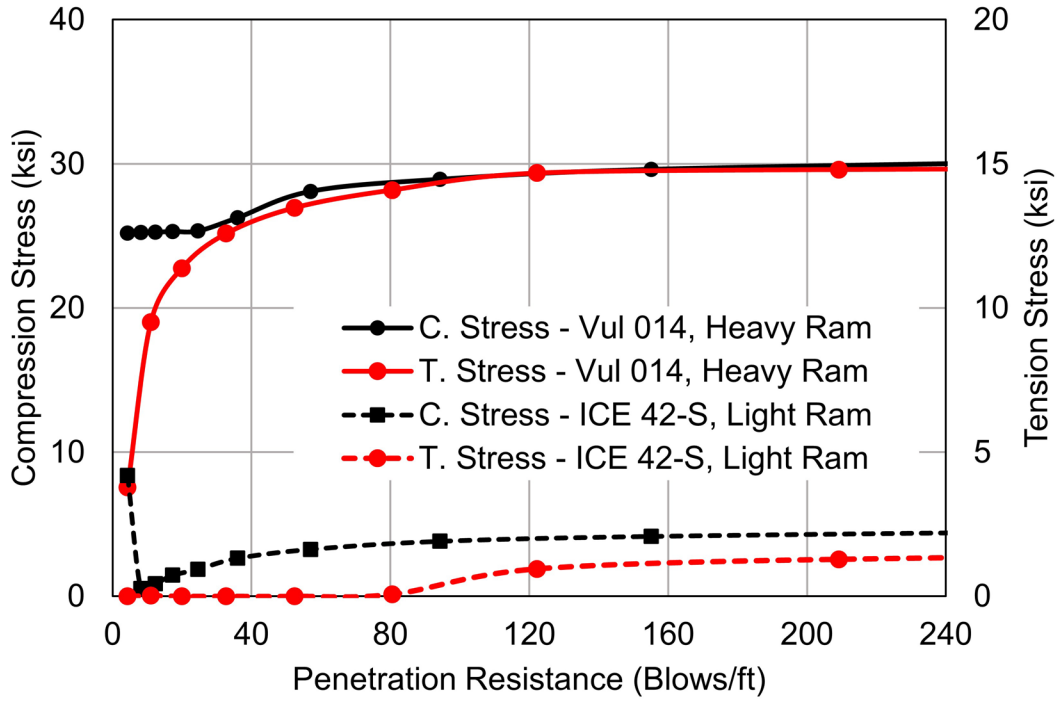

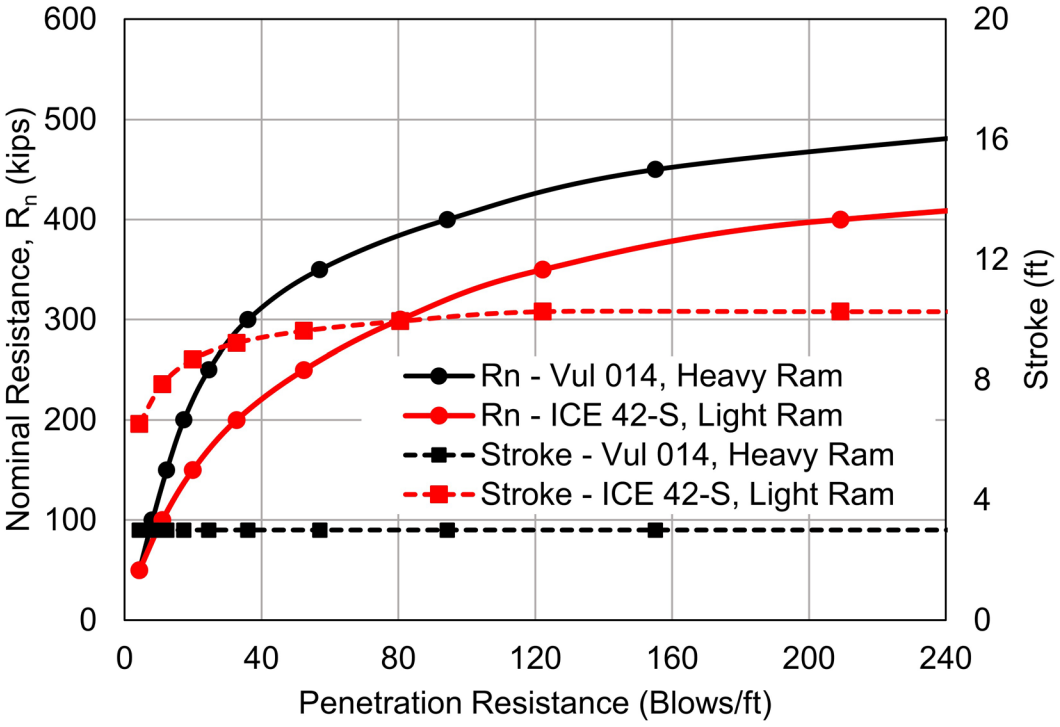

Figure 12-15 Bearing graph – for two hammers with equivalent potential energy and large toe quake.

Even though the Vulcan 014 requires a lower penetration resistance (blow count) for the same nominal resistance and has a lower efficiency (0.67 vs. 0.80 for the diesel hammer), it transfers roughly 20% more energy into the pile. This is because, first, the diesel hammer uses part of its energy to compress the gasses prior to impact. Second, the lower impact velocity of the heavy hammer is associated with lower energy losses. And lastly, the duration of the air hammer's impact is longer and consequently more effective at driving into a highly elastic soil with a large quake.

It is, however, interesting to note that for the smaller normal quake case in Figure 12-16, the lighter ram's blow counts improve relative to the heavier hammer at high nominal resistances and blow counts. This phenomenon can be explained with the diesel hammer's higher stroke and, therefore, higher impact force during harder driving. At the higher penetration resistance levels, energy is not as important as force to overcome the soil resistance.

This example illustrates the dynamic complexities of hammer-pile-soil interaction. Clearly, the potential energy alone, which is the sole hammer input in dynamic formulas, does not adequately assess pile drivability.

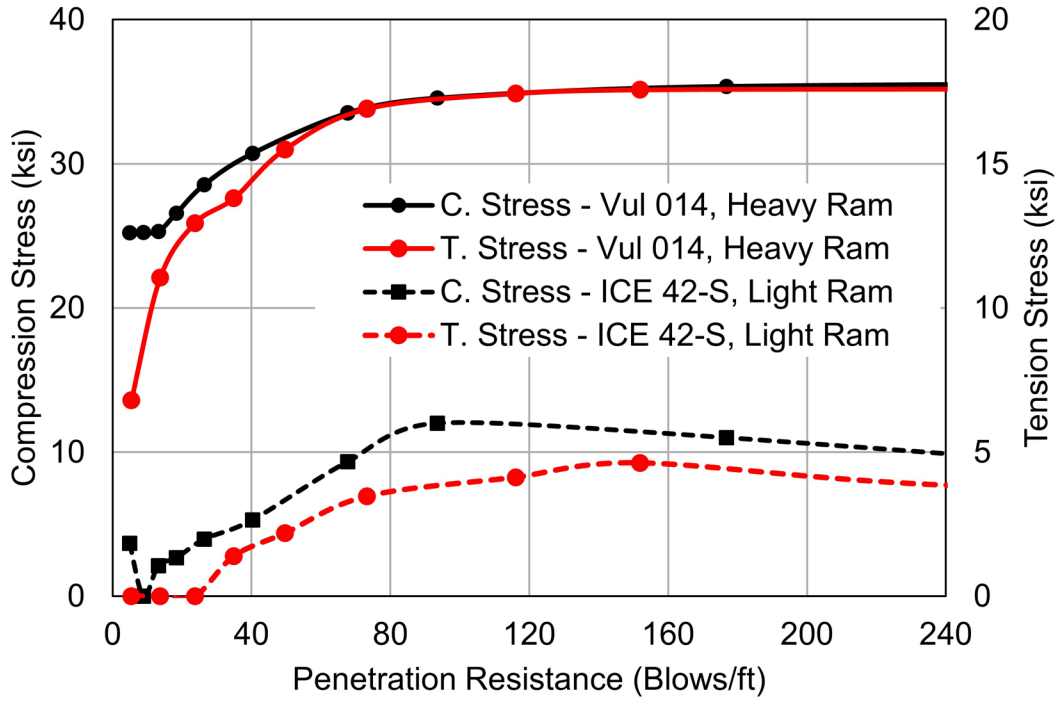

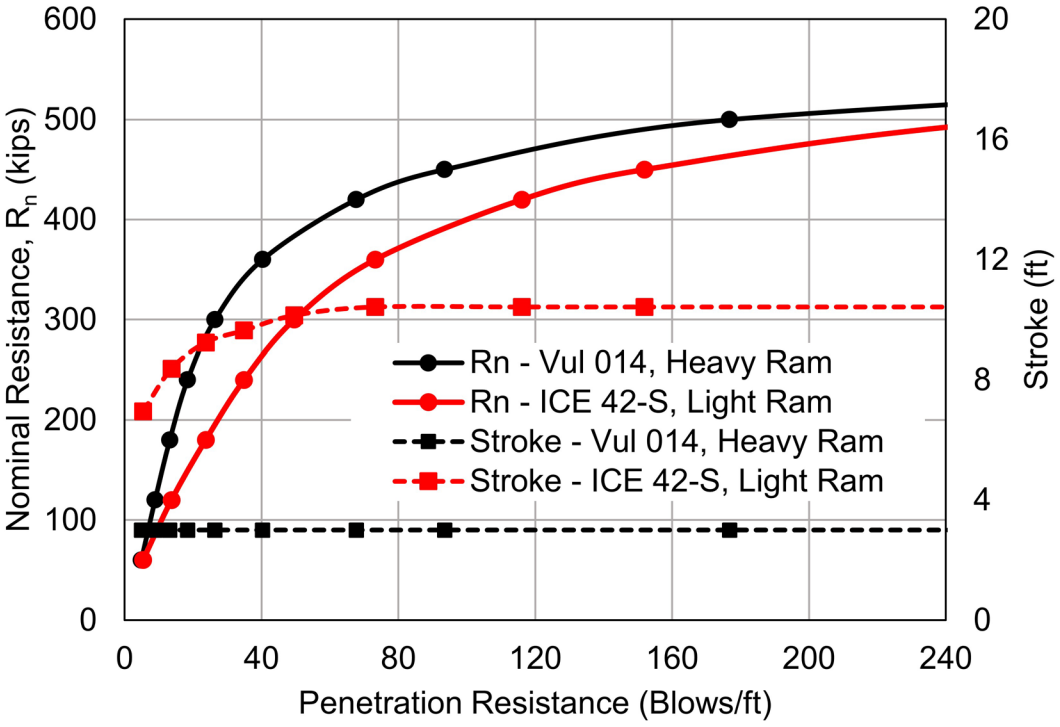

Figure 12-16 Bearing graph – for two hammers with equivalent potential energy and normal toe quake.

12.5.7 Example 7 – Assessment of Pile Damage

Another pile driving construction concern is pile damage. Although it is frequently assumed that steel H-piles can be driven through boulders and fill materials containing numerous obstructions, pile installation reviews reveal that this assumption is invalid. H-piles without commercially manufactured pile toe reinforcement present one of the most commonly damaged pile types. The damage occurs because of the ease with which flanges can be curled, rolled, and torn. Because deforming a pile plastically or otherwise non-elastically requires a significant amount of energy, pile damage has a detrimental effects on both penetration resistance and, therefore, nominal resistance activation (the blow count will be higher at the same resistance).

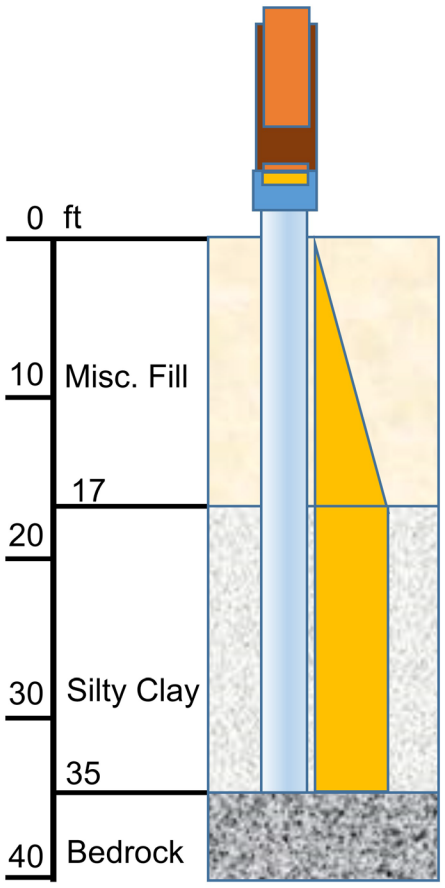

Hammer model:	Pileco D12-42
Rated energy:	29.9 ft-kips
Hammer cushion:	
Type:	Aluminum-Micarta
Thickness:	2 inches
Helmet Weight:	1.3 kips
Pile type:	Steel H-pile
Pile size:	HP 12x53
Pile length:	40 ft
Final pile penetration:	35 ft
Nominal resistance:	380 kips
Nominal shaft resistance:	20% (76 kips)
Nominal toe resistance:	80% (304 kips)

Figure 12-17 Example 7 –- Problem profile.

This example illustrates how the wave equation can be used to obtain insight into a driving situation involving pile damage. The project conditions are shown in Figure 12-17. The HP 12x53 H-piles are 40 feet in length with a factored load of 304 kips and a nominal resistance of 380 kips based on confirmation with a static load test.

The soil profile consisted of 15 to 17 feet of miscellaneous fill, including some bricks and concrete. Below the fill, 15 feet of silty clay overlay bedrock which was encountered at a depth of about 35 feet. The design called for driving the piles to bedrock.

The contractor selected a Pileco D12-42 single acting diesel hammer with a rated energy of 29.9 ft-kips to drive the piles. Using the FHWA modified Gates formula specified in the contract documents, the required penetration resistance was 46 blows/ft with this hammer for a nominal resistance of 380 kips.

Figure 12-18 presents the wave equation results indicating a nominal resistance of 245 kips at the Gates blow count of 46 blows/ft, well below the required 380 kip nominal resistance. On the other hand, the wave equation also showed that the maximum compression stresses at the pile toe would reach 40 ksi when the required nominal resistance was reached at 104 blows/foot and even 43 ksi at refusal. Most H-pile sections are now made of steel with a 50 ksi yield strength. However, in this example case, the yield strength was only 36 ksi and the compression driving stress limit only 32.4 ksi (90% of the yield strength).

In accordance with the contract requirement, several static load tests were conducted. In all cases, the piles failed to carry the 380 kip nominal resistance in spite of the fact that several of the piles were eventually driven to a penetration resistance exceeding 240 blows/ft with no indication of damage at the pile head. Because of the high penetration resistances to which several piles were driven, it was apparent that even harder driving would not result in a higher nominal resistance. Consequently, the contractor was requested to pull several of the piles to check for possible damage. Upon extraction, it was noted that the piles were severely damaged at the pile toe. The flanges were separated and rolled up from the web. While the damage probably occurred as the unprotected piles were driven through the miscellaneous rubble fill, it is also obvious from Figure 12-18 that the refusal blow count would generate dynamic steel pile stresses in excess of 40 ksi, and therefore in excess of the driving stress limit. The highest stresses would occur at the pile toe according to the numerical wave equation results while the stresses at the pile top were significantly lower (thus no damage at the pile head). Tables 12-3 and 12-4 show the maximum values of forces, stresses, and other variables calculated by wave equation analysis for both the required nominal resistance of 380 kips and the refusal driving situation (penetration at or in excess of 240 blows/ft) respectively.

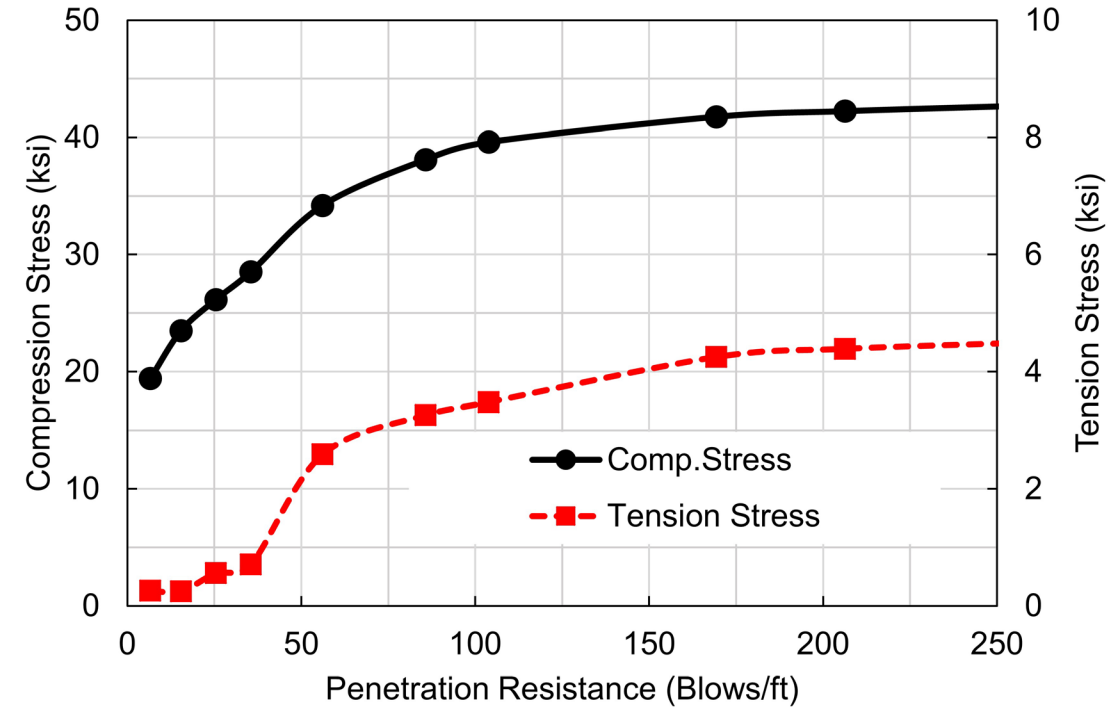

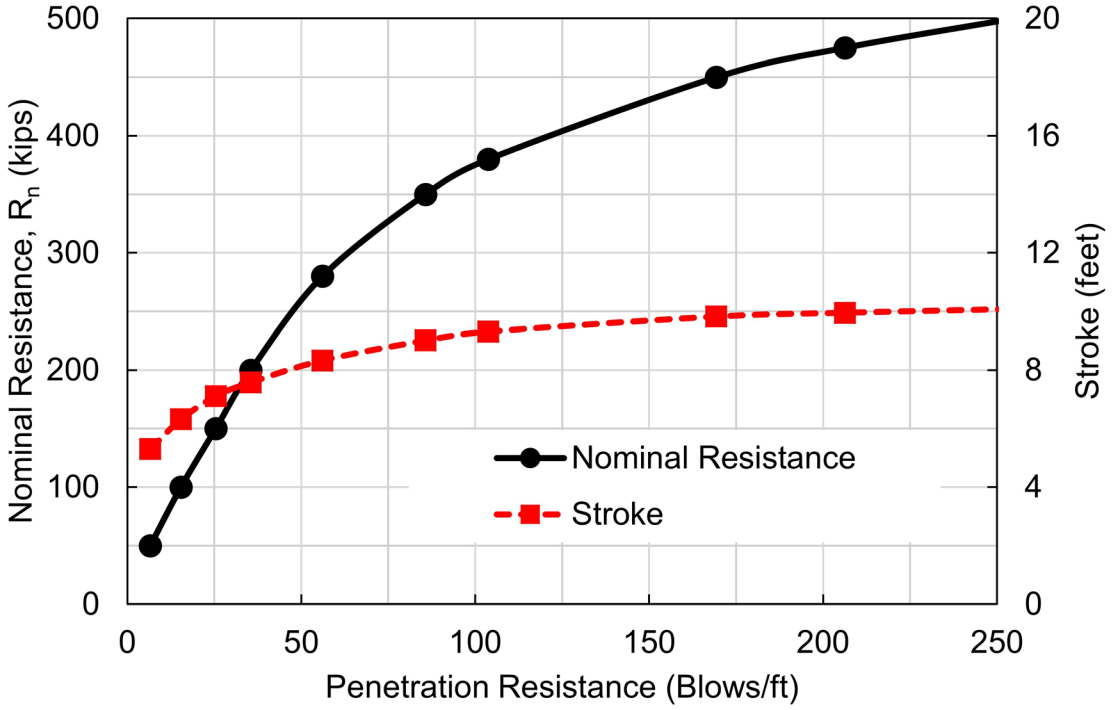

Figure 12-18 Wave equation bearing graph for proposed driving system.

Table 12-3 Example 7 – Maxima of Forces, Stresses and Other Variables for Required Nominal Resistance of 380 kips

Segment No.	Max Tension Force kips	Max Compr. Force kips	Max Tension Stress ksi	Max Compr. Stress ksi	Max Velocity ft/s	Max Displacement inches	Max Transfer Energy kip-ft
Top = 1	0.0	502.2	0.00	32.40	16.49	0.584	15.99
2	-18.9	492.1	-1.22	31.75	16.60	0.556	15.61
3	-35.7	498.7	-2.31	32.17	16.56	0.524	15.07
4	-49.1	501.2	-3.17	32.34	16.49	0.490	14.35
5	-54.0	502.4	-3.48	32.41	16.29	0.454	13.46
6	-53.9	499.6	-3.48	32.23	16.06	0.415	12.42
7	-50.7	495.6	-3.27	31.98	15.77	0.374	11.23
8	-39.6	502.7	-2.56	32.43	15.43	0.335	10.13
9	-31.3	523.0	-2.02	33.74	15.17	0.301	9.24
10	-27.6	537.3	-1.78	34.66	15.02	0.272	8.57
11	-21.7	556.4	-1.40	35.90	14.01	0.244	7.96
Toe = 12	-12.2	613.9	-0.79	39.61	9.58	0.216	7.46

Table 12-4 Example 7 – Maxima of Forces, Stresses and Other Variables for at Refusal Driving Condition (Nominal Resistance of 500 kips)

Segment No.	Max Tension Force kips	Max Compr. Force kips	Max Tension Stress ksi	Max Compr. Stress ksi	Max Velocity ft/s	Max Displacement inches	Max Transfer Energy kip-ft
Top = 1	0.0	586	0.00	37.80	17.51	0.590	17.39
2	-23.6	539.2	-1.52	34.79	17.63	0.559	16.94
3	-40.7	530.5	-2.63	34.23	17.61	0.526	16.32
4	-59.3	532.2	-3.82	34.33	17.46	0.490	15.48
5	-69.1	532.5	-4.46	34.36	17.22	0.452	14.43
6	-69.6	540.2	-4.49	34.85	16.90	0.411	13.19
7	-57.0	552.2	-3.68	35.62	16.50	0.367	11.77
8	-53.0	566.0	-3.42	36.52	16.09	0.320	10.23
9	-50.2	582.3	-3.24	37.57	15.69	0.271	8.65
10	-40.8	591.6	-2.63	38.17	15.33	0.224	7.27
11	-23.6	613.5	-1.52	39.58	13.79	0.184	6.23
Toe = 12	-13.3	661.6	-0.86	42.68	8.57	0.147	5.48

The effect of the damage on the pile drivability can also be evaluated with a wave equation analysis. Since static load tests indicate that piles driven as hard as 240 blows/foot did not support the 380-kip load, one pair of nominal resistance and penetration resistance values is available as a reference point on the wave equation bearing graph. For the damaged pile scenario, a bearing graph may be calculated for the pile with damaged toe by a simply reducing the elastic modulus of the lowest pile segment until results agree with the penetration resistance and nominal resistance observations. In the present case, the reduced toe segment stiffness was found to be approximately 10% of the normal value.

Figure 12-19 presents wave equation results for both the undamaged and the damaged pile toe scenarios. The results indicate that the nominal resistance of 380 kips could not be obtained for the damaged pile, regardless of the penetration resistance. Essentially, the damaged pile section "cushioned" the hammer blow at the pile toe and attenuated the hammer energy. Once damaged, the soil resistance at the pile toe could not be overcome, and therefore, the pile toe would not advance. The above illustrates that not only blow counts but also driving stresses also may limit the drivability of a pile to the required nominal resistance.

The potential for pile damage on this project could have been greatly reduced if a wave equation had been performed during the design stage or had been specified for construction control. As pointed out earlier, the wave equation bearing graph in Figure 12-19 illustrates that the nominal resistance of 380 kips could only be obtained by the contractor's driving system at a penetration resistance of 104 blows/foot or more with an associated pile toe stress of 40 ksi, a stress in excess of the steel yield strength of 36 ksi and recommended limit driving stress of 32.4 ksi.

Considering that the stresses calculated by the wave equation are averages over the cross section, a non-uniform distribution of the soil or rock resistance could have added significant additional bending stresses in the steel pile near its toe. Hence, the potential damage would have been clearly apparent at the time of the contractor's hammer submittal had a wave equation analysis been performed. Additional wave equation analyses of the contractor's driving system could have been performed at the same time to determine if driving stress levels could be acceptably reduced by using reduced fuel settings or shorter hammer strokes. If driving stresses could not be controlled in this manner, as is most likely in the present case, approval of the proposed driving system should not have been obtained, and either alternate hammers should have been evaluated or a higher steel yield strength required.

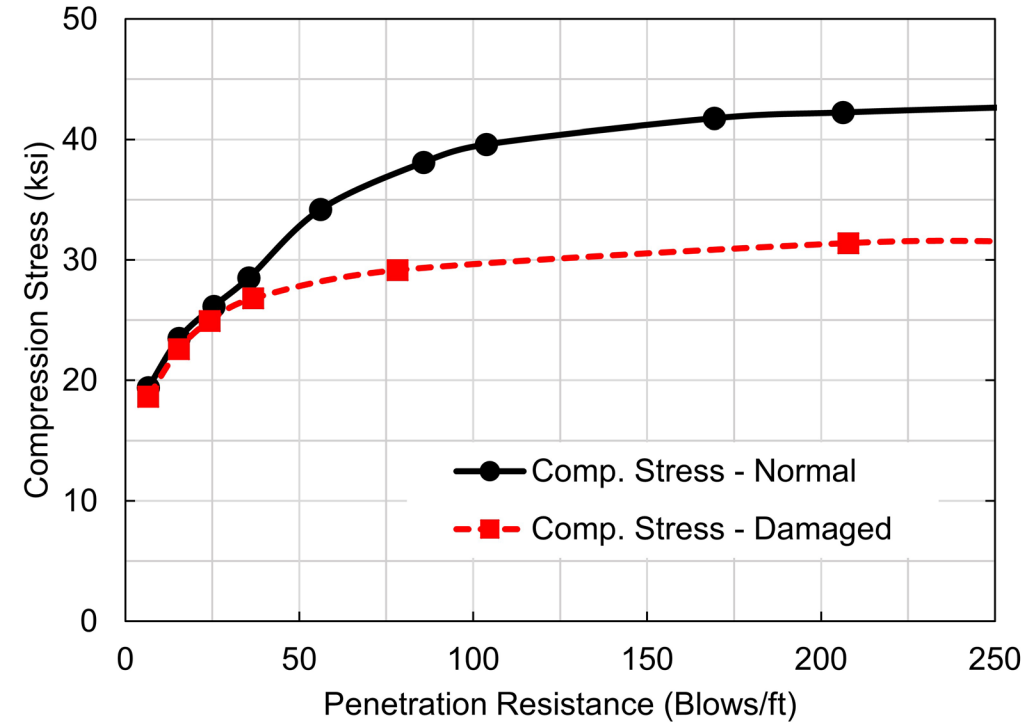

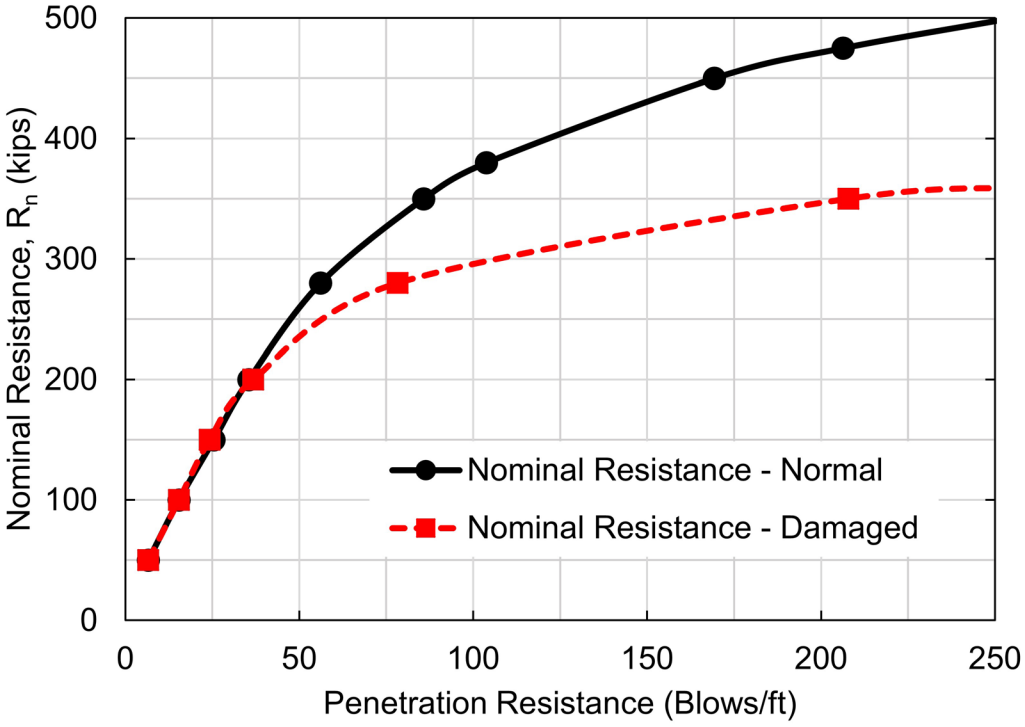

Figure 12-19 Wave equation bearing graphs for damaged and undamaged pile.

In any event, where H-piles have to be driven through materials that could include obstructions or where piles have to be driven to hard rock, it is always strongly recommended to protect the pile toe with a so-called driving shoe. Driving shoes are discussed in Chapter 16 and consist of steel castings which can be welded to the pile toe. Driving shoes tend to centralize the toe resistance force and/or reinforce the flanges.

12.5.8 Example 8 – Selection of Wall Thickness

This wave equation example demonstrates the selection process for the required wall thickness of a pipe pile. Consider the soil and problem profile presented in Figure 12-20. The foundation details are based on a bridge construction situation where a major bridge was built over a lake with a water depth of 85 feet. The piles extended 25 feet above the water level. Based upon static soils analysis the piles were to be driven through 25 feet of granular overburden, 5 feet of overconsolidated glacial till, and then to a hard bedrock. Thus total pile length was 140 feet. The piles had to be designed for a factored load of 1600 kips; a resistance factor of 0.80 (static load testing was required) yielded a required nominal resistance of 2000 kips. Structural considerations called for a minimum wall thickness of 0.50 inches. However, as a drivability check, wave equation analyses were performed for the 48 inch outside diameter pipe pile with four different wall thicknesses of 0.50, 0.75, 1.00, and 1.25 inches. The analyses were based on the following assumptions:

1. A Berminghammer 6005 open end diesel hammer would be available. This hammer has a ram weight of 13.6 kips and a rated energy of 161 ft-kips.

2. The pile is driven open ended and because of its relatively shallow penetration, it will not plug.

3. The toe resistance will develop against only the steel toe area on the hard rock. The toe resistance is estimated to be 1600 kips or 80% of nominal resistance for all four pile types regardless of wall thickness.

4. Because the pile is a low-displacement type driven to hard rock, the program recommended toe quake is 0.04 inches. (For moderately hard rock the standard 0.10 inch quake could be assumed.)

5. Average shaft damping was assumed to be 0.10 s/ft.

6. During driving, open end pipe piles with diameters greater than 30 inches usually do not plug and for moderate penetrations (say less than 10 diameters) it may be assumed for the dynamic analysis that at least partial internal friction occurs. The shaft resistance in the present case was assumed to act equally on the inside and outside surfaces of the pile and amount to 20% of the total nominal resistance. For greater pile penetration depths, it would be less likely that so much internal friction occurs during driving because the effective stresses acting inside the pipe and, therefore, the unit shaft resistance inside the pipe would be less than for the outside shaft resistance. For that reason, the internal friction is often only assumed to be either 0 or 50% of the outside friction. In wave equation analysis modeling, a 50% inside friction could be simulated by a 50% increase in the pile perimeter while the unit shaft resistance would remain as calculated for the outside pile wall.

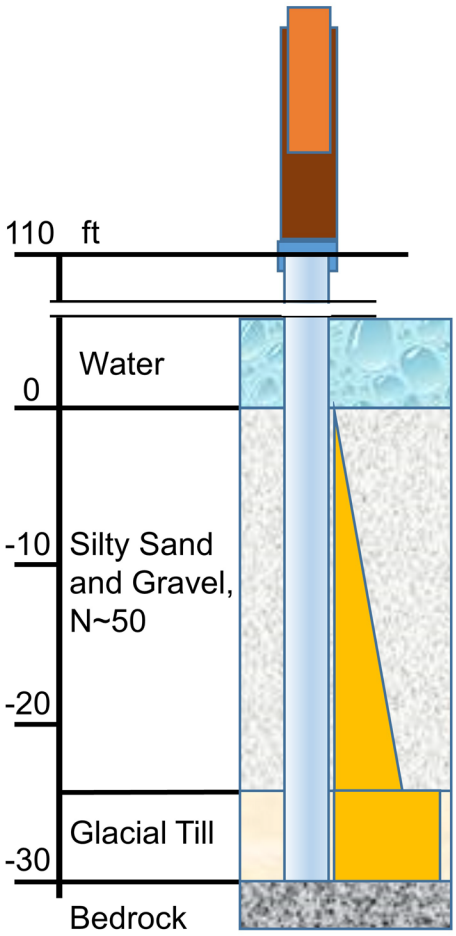

Hammer Model:	Berminghammer 6005
Rated energy:	161 ft-kips
Hammer cushion type:	None - Direct Drive
Helmet weight:	6 kips
Pile type:	Open End Pipe Pile
Pile size:	48 inches
Pile length:	140 ft
Final pile penetration:	30 ft
Nominal resistance:	2000 kips
Nominal shaft resistance:	20% (400 kips)
Nominal toe resistance:	80% (1600 kips)

Figure 12-20 Example 8 – Problem profile.

Figure 12-21 presents the results of these analyses in the form of bearing graphs and Table 12-5 summarizes calculated stresses, blow counts, stroke and transferred energy for the required 2000 kip nominal resistance.

Calculated maximum driving stresses are not more than 43 ksi for the 0.50 inch wall pipe and less than 35 ksi for the other thicker wall pile sections. Assuming that the pipe piles would be manufactured from Grade 3 pipe with yield strength of 45 ksi, the driving stress limit would be 40.5 ksi. Therefore, all except the 0.5 inch wall piles should withstand the driving stresses. However, uneven or sloping rock would cause higher localized stress concentrations. It would, therefore, be wise to choose a greater wall thickness for which the driving stresses allow for an additional margin of safety.

Table 12-5 Example 8 – Wave Equation Results for Four Potential Pipe Pile Wall Thicknesses at 2000 kip Nominal Resistance

Wall Thickness inches	Stroke feet	Transferred Energy ft-kips	Compression Stress ksi	Blow Count blows/ft
0.50	9.1	93	42.8	127
0.75	8.7	79	34.2	100
1.00	8.5	71	29.1	90
1.25	8.6	68	25.4	88

For hammer approval, AASHTO (2010) LRFD Bridge Construction Specification require the wave equation penetration resistance to be between 24 and 120 blows/foot. The wave equation analysis results indicate that the 0.50 inch thick wall pipe would require too high a blow count while the 0.75 inch wall thickness would have an acceptable penetration resistance. Use of the 1.00 or 1.25 inch wall thickness would help little with either drivability or driving stresses and be much more costly. Table 12-5 also shows that while hammer strokes were nearly the same, the transferred energies varied significantly with the more flexible piles accepting more energy. However, this energy was needed to elastically compress the very long piles and was therefore not available for actual work to overcome the soil resistance.

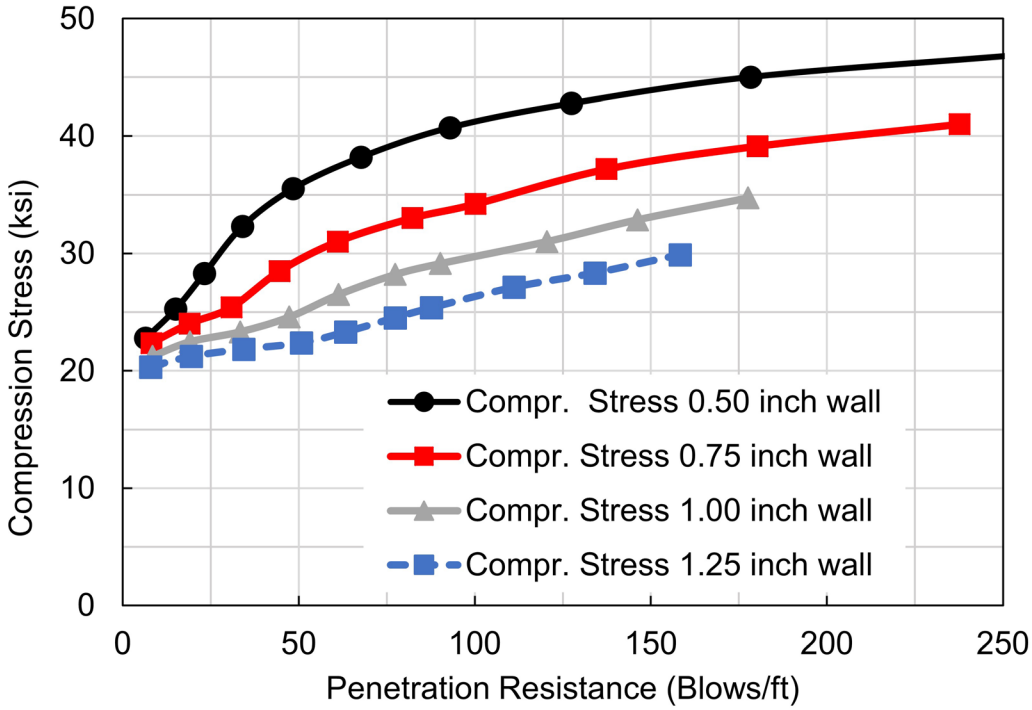

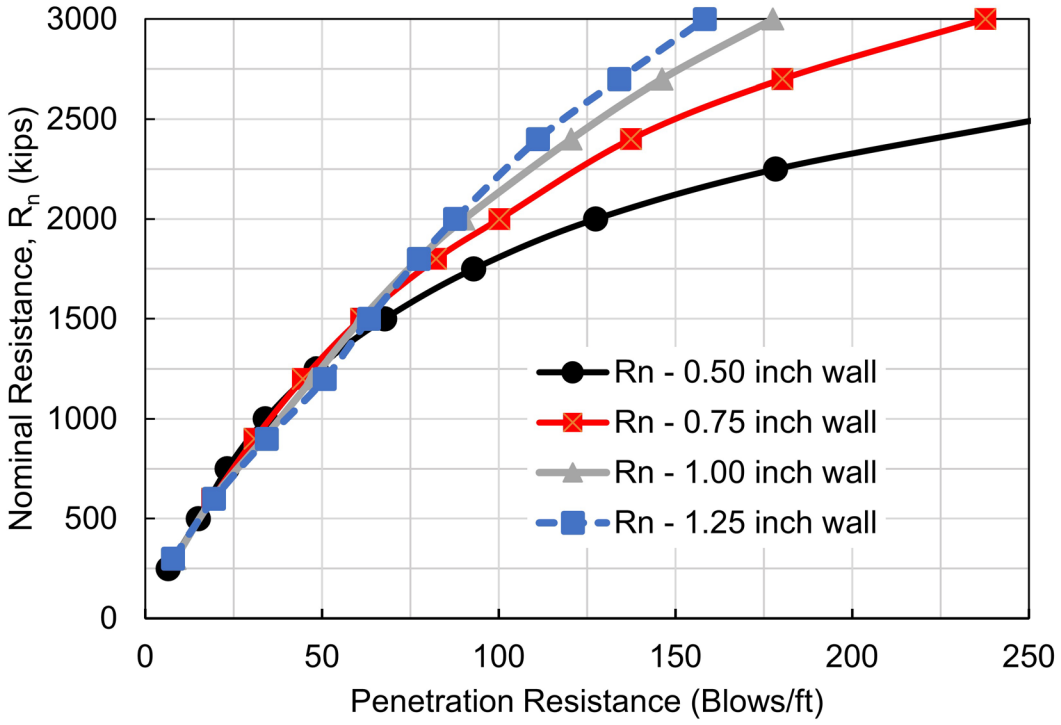

Figure 12-21 Bearing graphs for open end pipe piles with wall thicknesses of 0.50, 0.75, 1.00, and 1.25 inches.

The actual project which was used as a guide in setting up this example was successfully completed with the 0.75 inch wall thickness. Reportedly, the static load test did not fail under a 2000-kip proof test. While this project was successfully completed, a caution about driving and analyzing large diameter open end pipe piles should be added. When driving to dense soil layers, large pipes may not plug during driving and they may plug under static loading conditions. Pile driving may therefore be much easier than predicted by the wave equation if the analysis were made on the assumption of a plugged pile which behaves like a displacement pile with high toe resistance and a large toe quake. The situation may also be different at the end of driving and during a restrike. It is recommended to perform wave equation analyses with upper and lower bound soil resistance values to assess hammer sizing.

It is also important to remember that a driving criterion for a pile driven to hard rock should not be specified in terms of blows per unit penetration, but rather as a maximum penetration for a certain number of hammer blows. In the present case, for the pile with the ¾ inch wall (a required blow count of 100 blows per foot was calculated for the ¾ inch wall pile) it would be reasonable to require that the pile be accepted when its penetration under 10 consecutive hammer blows is less than 0.5 inches while the hammer stroke is between 8.5 and 9.0 ft. Specifying that the pile would have to penetrate a certain distance into a hard rock to qualify for having achieved the nominal resistance would most probably lead to pile toe damage. Even when driving into moderately hard rock, overdriving the piles should be done cautiously. This is sometimes problematic, since some shales or weathered rock materials exhibit relaxation after driving and it is desirable to drive piles in those formations to a capacity in excess of the required nominal resistance. Wave equation results should indicate that the higher resistance can be achieved within material stress limits if overdriving is required.

12.5.9 Example 9 – Evaluation of Vibratory Driving

This example illustrates the use of a wave equation analysis for evaluating vibratory hammer installation of the sheet piles required for the cofferdam construction. The situation is depicted in Figure 12-22 and is similar to Example 3. The sheet piles must be installed using a vibratory hammer. The contractor has an ICE 815 hammer available and intends to drive pairs of AZ18 sheet piles whose combined cross sectional area is 29.5 in^2. These are Z-section sheets, each with a width of 24.8 inches, a depth of 15 inches and a thickness of 0.37 inches. At the time of sheet pile installation, the soil within the cofferdam is not excavated. The 50 foot long sheet piles are vibrated from mudline to an estimated depth of 35 feet below mudline.

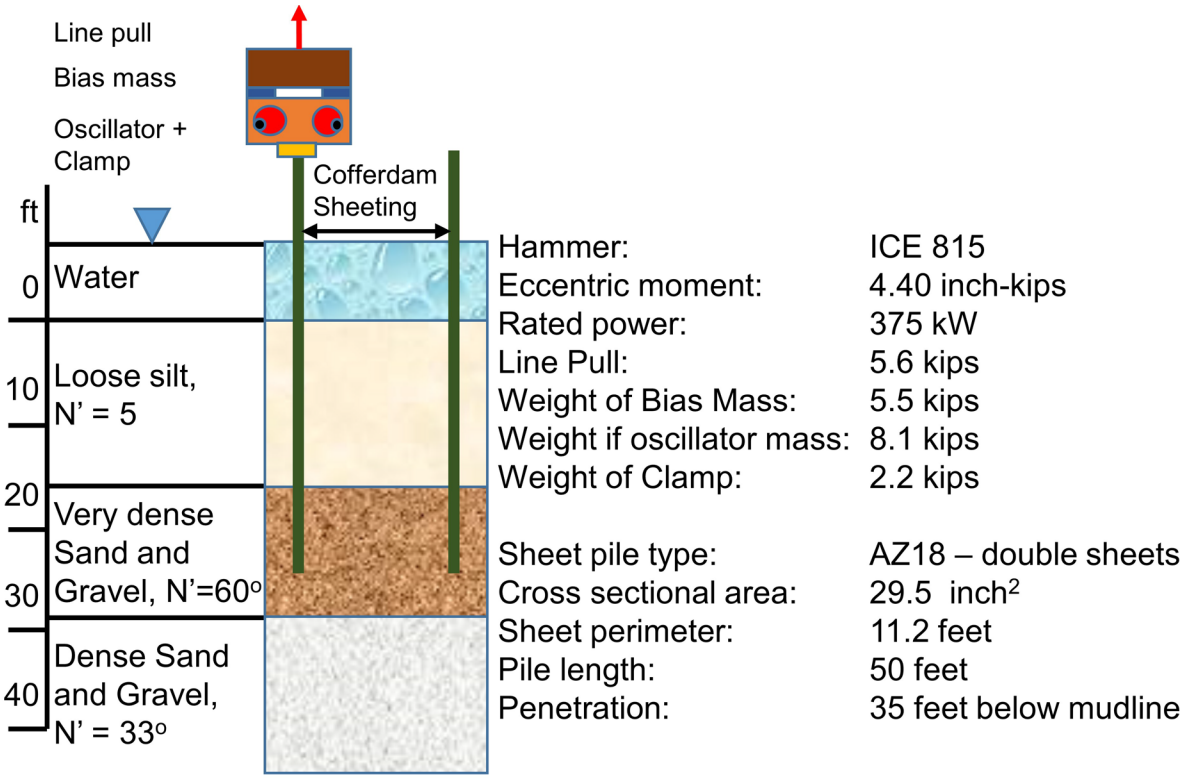

Figure 12-22 Example 9 – Problem profile.

For the non-excavated condition, the sheet piles must first penetrate a 16.5 foot thick layer of soft silt, followed by very dense sand and gravel, and then dense sand and gravel layers. The static resistance values were calculated based on corrected SPT values of 5 for the silt, 110 for the very dense sand and gravel, and 33 for the dense sand and gravel. As is reasonable for submerged coarse grained soils subjected to vibratory driving, a shaft resistance loss of 75% of the long term resistance was assumed while no loss of resistance was assumed for the silt, which was considered cohesive. This situation is modeled with respective setup factors for silt and sand layers of 1.0 and 4.0. The associated gain/loss factor was, therefore, set to 0.25 which produces an SRD in the sands which is 25% of the long term resistance while the silt is assumed having an SRD equal to the long term resistance. (Note: it is not recommended to use these setup and gain/loss factors for drivability analyses of impact pile driving). For the toe resistance it was conservatively assumed that the full long term resistance would be present during the vibratory driving (gain/loss factor equal to 1.0).

As per program recommendations, damping factors were set to twice the values assumed for impact driving, i.e., a shaft damping of 0.30 s/ft in the silt (assumed to behave cohesive) and 0.10 s/ft in the sand and gravel layers. Toe damping was

input as 0.30 s/ft for all layers. Also the damping type was switched from Smith to Smith-viscous per program recommendations. In addition, program recommendations are that only quakes should be doubled for cohesive soils but not non-cohesive soils. This guidance was followed for the silt layer while quakes were left at their 0.10 inch default values in the sands and gravels. The calculated unit soil resistance values and the associated dynamic soil parameters are shown in Table 12-6.

Table 12-6 Soil Information for Vibratory Sheet Pile Driving in Example 9

Depth feet	Unit Shaft Resist ksf	Unit Toe Resist. ksf	Skin Quake inch	Toe Quake inch	Skin Damping s/ft	Toe Damping s/ft
0.0	0.0	0.0	0.20	0.20	0.30	0.30
16.5	0.283	22.7	0.20	0.20	0.30	0.30
16.5	0.465	250.6	0.10	0.10	0.10	0.30
29.0	1.272	250.6	0.10	0.10	0.10	0.30
29.0	0.274	137.8	0.10	0.10	0.10	0.30
43.0	0.453	137.8	0.10	0.10	0.10	0.30

The pertinent information needed for the hammer model is shown in Figure 12-22, i.e., bias mass of 5.5 kips and an oscillator mass of 8.1 kips of the ICE 815 hammer. The clamp weight of 2.2 kips is added to the oscillator mass in the analysis. The two main masses are connected by elastomers which are modeled with very soft springs so as to isolate the crane line from the oscillator vibrations while at the same time adding crowd force to the driving system. The eccentric moment, represented in the program by a mass and a radius, is 4.4 inch-kips for the ICE 815 hammer. With a rated frequency of 26.7 Hz (1600 rpm) the centrifugal force of this unit is 320 kips. However, for conservatism, it is assumed that the hammer will only be run at 20 Hz which yields a centrifugal force of 180 kips. Efficiency and start-up time (the time necessary for the hammer to reach full frequency) are left at their respective 1.0 and 0.0 default values. Another input is a 7-kip line pull, or upward directed crane force, which may be needed to maintain hammer-pile system stability. Oftentimes after the pile has sufficient embedment for stability, the operator will let the line slacken which will allow for a greater downward force and therefore an increase in the speed of pile penetration. An upward directed (positive) line force is therefore a conservative input.

Figure 12-23 shows the drivability results in graphic form and Table 12-7 shows the results in numerical form. For the first analyzed depth of 6 feet, the SRD is less than all of the applied weights (hammer weight plus clamp weight plus pile weight minus line pull) causing the sheet pile to “run” as indicated in the final results by the zero (0) penetration time. After the pile penetrates into the very dense sand layer, the required penetration time sharply increases to values up to almost 20 s/ft, but reduces to much more comfortable values as the sheet pile toe enters the dense sand and gravel. The final foot of penetration requires less than 5 s/ft. At that point, the SRD ranges between 85 and 90 kips with 28 kips acting at the sheet pile toe (the steel area of the pile). The calculated compression and tension stress maxima are rather small varying between 2 and 5 ksi. These stresses are typical for vibratory pile driving, by it should be remembered that these stresses are averaged over the pile cross sectional area. Local stress concentrations of much higher magnitudes must be expected, for example in the areas surrounding the pile clamp.

Vibratory hammer refusal has occasionally been specified as low as 1 inch/min corresponding to a very high penetration time of 720 s/ft, and the results, therefore, suggest that the sheet pile installation should be possible with the 815 hammer. However, the accuracy of the wave equation prediction strongly depends on the realism of the relatively crudely estimated static resistance to driving (SRD). Furthermore, a good alignment of the sheet piles and thus no excessive interlock friction is another condition for a successful installation.

It should be emphasized that the drivability analysis of vibratory pile driving is a reasonably reliable tool for equipment selection. On the other hand driving time estimates can widely fluctuate (even from pile to pile on the same) since they are extremely sensitive to soil resistance variations, particularly at the pile toe. Even greater uncertainty exists when attempting to relate SRD and even more so, long term resistance to penetration time. While research in this area has been and is occasionally being done, no really reliable methods have yet been established that would allow for a nominal resistance calculation from vibratory driving observations.

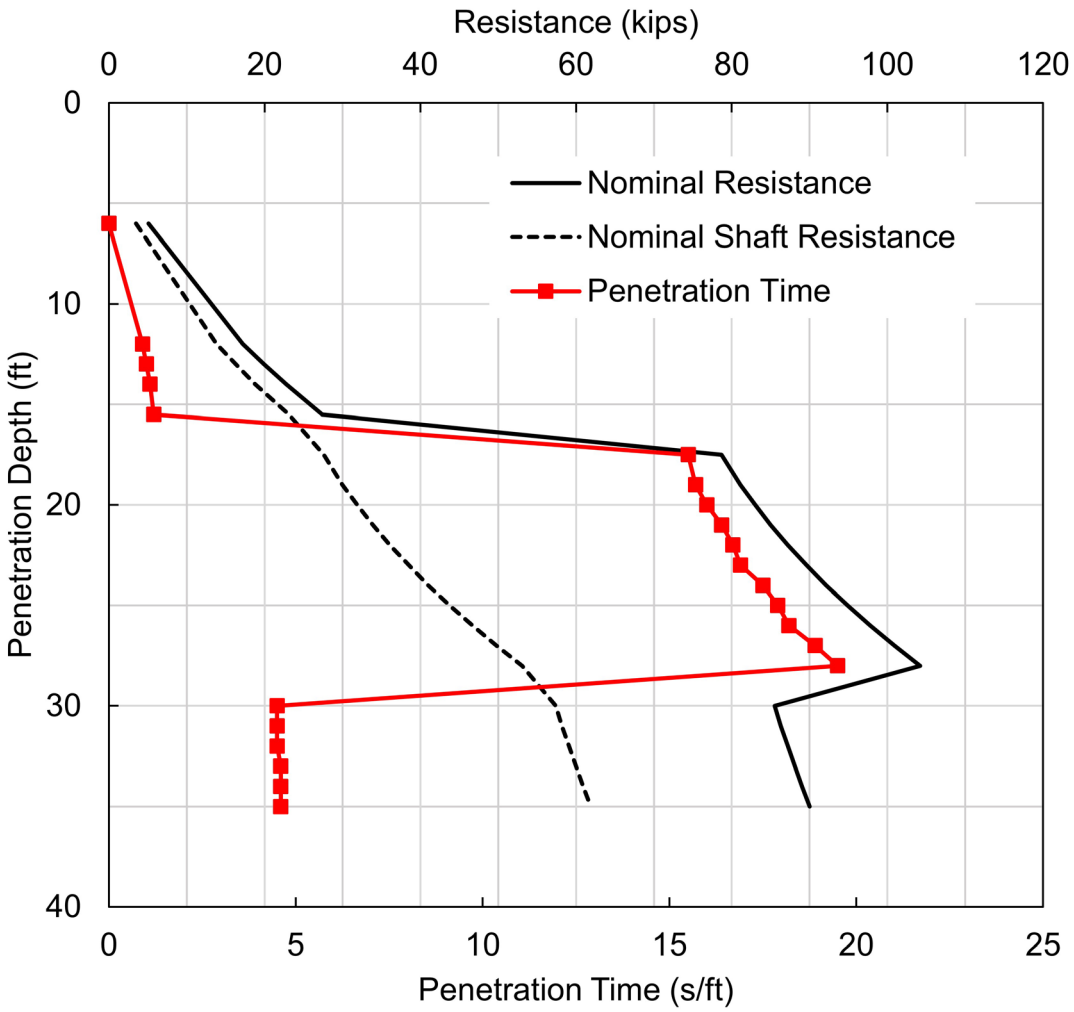

Figure 12-23 Nominal resistance and wave equation calculated penetration time for vibratory drivability analysis.

Table 12-7 Nominal Resistance and Wave Equation Calculated Results for Vibratory Drivability Analysis. Total Drive Time – 4 Minutes

Depth feet	Nominal Resist. kips	Shaft Resist. kips	Toe Resist. kips	Pen. Time s/ft	Comp. Stress ksi	Tension Stress ksi
6.0	5.1	3.5	1.7	0.0	0.0	0.0
12.0	17.2	13.8	3.4	0.9	2.4	-1.6
13.0	19.9	16.3	3.6	1.0	2.5	-1.5
14.0	22.8	18.8	3.9	1.1	1.9	-1.4
15.5	27.4	23.1	4.3	1.2	1.9	-1.3
17.5	78.7	27.6	51.1	15.5	3.1	-3.4
19.0	81.1	30.0	51.1	15.7	3.2	-3.5
20.0	83.0	31.9	51.1	16.0	3.3	-3.6
21.0	85.0	33.9	51.1	16.4	3.4	-3.7
22.0	87.2	36.1	51.1	16.7	3.5	-3.8
23.0	89.6	38.5	51.1	16.9	3.6	-3.9
24.0	92.1	41.0	51.1	17.5	3.8	-4.0
25.0	94.9	43.8	51.1	17.9	4.0	-4.2
26.0	97.8	46.7	51.1	18.2	4.1	-4.3
27.0	100.9	49.8	51.1	18.9	4.3	-4.5
28.0	104.2	53.1	51.1	19.5	4.5	-4.7
30.0	85.5	57.4	28.1	4.5	4.3	-4.0
31.0	86.3	58.2	28.1	4.5	4.3	-4.1
32.0	87.2	59.1	28.1	4.5	4.4	-4.2
33.0	88.1	60.0	28.1	4.6	4.4	-4.2
34.0	89.0	60.9	28.1	4.6	4.5	-4.3
35.0	90.0	61.9	28.1	4.6	4.6	-4.4

12.6 ANALYSIS DECISIONS FOR WAVE EQUATION MODELING

A wave equation analysis offers the engineer a variety of input and analysis options. Choosing just one of these options may limit what can be learned from the simulations. For example, it may be helpful to calculate both a bearing graph and drivability plot or investigate pile stress extrema and blow counts for both a diesel hammer and a hydraulic one. The two hammer types would be different as far as energy transfer and driving resistance even if the hammers are identically rated. The drivability analysis would show certain potential driving problems such as start-up problems for the diesel in easy driving or refusal in dense intermediate soil layers. The following sections aim at helping the analyst to understand why certain options were made available and how they can help achieve an optimal pile installation.

12.6.1 Selecting the Proper Approach

Even though the wave equation analysis is an invaluable tool for the pile design process, it should not be confused with a static geotechnical analysis. Some wave equation programs, provide a simplified static analysis for resistance distribution purposes. However, the basic wave equation approach does not determine the nominal resistance of a pile based on soil boring data. The wave equation calculates a penetration resistance for an assumed nominal resistance (ultimate capacity), or conversely, it assigns an estimated nominal resistance (ultimate capacity) to a pile based on a field observed penetration resistance. It is one thing to perform a wave equation bearing graph for an expected nominal resistance at a particular pile penetration and a totally different matter to actually realize that nominal resistance at that depth. Significant cost overruns can occur when pile lengths required during construction vary significantly from those estimated during design by a static analysis. To avoid such occurrences, it is imperative that a static analysis, as described in Chapter 7, precede the wave equation analysis. The static analysis will yield an approximate pile penetration for a desired nominal resistance or a nominal resistance for a certain depth. The static analysis can also generate a plot of estimated pile nominal resistance as a function of depth. As a preparation for the wave equation analysis, it is important that the static analysis evaluates the soil resistance in the driving situation (e.g., remolded soil strength, before excavation, before scour, before fill placement, etc.). For the assessment of long term static conditions, the static analysis must consider the influence of soil setup or relaxation, additional change due to excavation, water table variations, and scour, etc.

After completion of the static analysis, a wave equation analysis should be performed, leading to either a bearing graph as illustrated in Example 1, or a

drivability analysis of penetration resistances and stresses versus depth as presented in Example 3. Sometimes both analyses are performed. The validity of the bearing graph depends on the proximity of the analyzed soil profile and the site variability of the soil properties. The drivability analysis calculates penetration resistances and stresses for a number of penetration depths and, therefore, provides a more complete result. However, there is a very basic difference between these two approaches. The bearing graph approach allows the engineer to assess the nominal resistance of a pile given a penetration resistance at a certain depth and to formulate a driving criterion for a required nominal resistance. The drivability analysis points out certain problems that might occur during driving prior to reaching the target penetration. If the pile actually drives differently from the wave equation predictions, a reanalysis with different soil resistance parameters would be needed to match the observed behavior.

Even if an accurate static analysis and a wave equation analysis have been performed with realistic soil parameters, the experienced foundation engineer would not be surprised if the penetration resistance during pile installation were to differ substantially from the predicted one. Most likely, the observed penetration resistance would be lower than calculated. As an example, suppose that a pile had to be driven into a clay for a factored load of 182 kips. With a resistance factor of 0.65 (dynamic testing of at least 2% of the piles would be specified), the required nominal resistance would be 280 kips. The static soil analysis indicates that the pile should penetrate to a depth of 82 feet to meet this nominal resistance requirement. There would be negligible toe resistance, and based upon remolded soil strength parameters, the soil may exhibit only 50% of its long term strength during driving (soil setup factor = 2). It is therefore only necessary to drive the pile to a nominal resistance of 140 kips, which should be achieved at the 82 foot depth. The expected end of installation penetration resistance would then correspond to 140 kips. A restrike test, performed 7 days after installation, would include soil setup effects and might show the required 280-kip nominal resistance and a much higher penetration resistance than at the end of driving.

The above discussion points out one major reason for differences between analysis and reality. However, as with all mathematical simulations of complex situations, agreement of wave equation results with actual pile performance depends on the realism of the method itself and on the accuracy of the model parameters. The accuracy of the wave equation analysis will be poor when either soil model or soil parameters inaccurately reflect the actual soil behavior and when the driving system parameters do not represent the state of maintenance of hammer or cushions. The

pile behavior is satisfactorily represented by the wave equation approach in the majority of cases. A review of potential wave equation error sources follows.

12.6.2 External Combustion Hammer Consideration

For external combustion hammers (e.g., air or hydraulically powered hammers) one of the most important wave equation input quantity is the hammer efficiency. It is defined as that portion of the potential ram energy that is available in the form of kinetic ram energy immediately proceeding the time of impact. Many sources of energy loss are usually lumped into this one number. If the hammer efficiency is set too high, an optimistically low penetration resistance would be predicted. This in turn could lead to a dangerous overprediction of nominal resistance. If the efficiency is set very low, for conservative pile nominal resistance assessments, the stresses may be underpredicted, leading to possible pile damage during installation.

Hammer efficiency and hammer stroke should be reduced for inclined (battered) pile driving. These reductions depend on the hammer type and batter angle. For hammers with internal ram energy measurements, no reductions are required to cover losses due to inclined pile driving. Modern hydraulic hammers often allow for a continuously adjustable ram kinetic energy which is measured and displayed on the control panel. In this case, the hammer efficiency need not cover friction losses of the descending ram but only losses that occur during the impact (e.g., due to improper ram-pile alignment), and it may therefore be relatively high (say 0.95). For such hammers, the wave equation analysis can select the proper energy level for control of driving stresses and economical penetration resistances by trying various energy (equivalent stroke) values that are lower than the rated value.

Similarly, a number of air/steam hammers can be fitted with equipment that allows for variable strokes. The wave equation analysis can help to find the penetration resistance at which the stroke can be safely increased to maximum. It is important, however, to realize that in fact the reduced stroke is often exceeded and the maximum stroke not fully reached. Corresponding increases and decreases of efficiency to cover the uncertainty of the actual equivalent stroke, may, therefore, be investigated.

12.6.3 Diesel Hammer Considerations

The diesel hammer stroke increases when the soil resistance, and therefore penetration resistance, increases. Certain wave equation programs simulate this behavior by trying a down stroke and, when the calculated up stroke is different, repeating the analysis with the new value for the down stroke until the strokes converge. The accuracy of the resulting stroke is therefore dependent on the realism of the complete hammer-pile-soil model and should be checked in the field by comparison with the actual stroke. The consequences of an inaccurate stroke could be varied. For example, an optimistic assumption of combustion pressure could lead to high stroke predictions and, therefore, non-conservative predictions of nominal resistance while stress estimates would be conservatively high (which may lead to a hammer rejection).

Stroke and energy transferred into the pile appear to be closely related, and large differences (say more than 10%) between stroke predictions and observations should be explained. Unfortunately, higher strokes do not always mean higher transferred energy values. When a diesel hammer preignites, probably because of poor maintenance, the gases combusting before impact slow the speed of the descending ram and cushion its impact. As a result, only a small part of the ram energy is transferred to the pile. A larger part of the ram energy remains in the hammer producing a high stroke. If, in this case, the combustion pressure would be calculated by matching the computed with the observed stroke under the assumption of a normally performing hammer, the calculated transferred energy would be much higher than the measured one, and the calculated penetration resistances (blow counts) would be non-conservatively low. It is, therefore, recommended that hammer problems are corrected as soon as detected on the construction site. If this is not possible, several diesel stroke or pressure options should be tried when matching wave equation results with field observations and the most conservative results should be selected. Section 12.8 discusses the available diesel hammer stroke options in greater detail.

Generally the hammer data file of wave equation programs contain reduced combustion pressures for those hammers which have stepwise adjustable fuel pumps. Note that decreasing combustion pressures may be associated with program input fuel pump settings that also have decreasing numbers. (For example, Delmag, APE D-Series, Pileco, ICE I-Series and other makes have fuel pump settings with 4 (maximum), 3, 2, and 1 (minimum), roughly correspond to combustion pressures of 100, 90, 81 and 73 percent of that associated with the hammer's rated energy.) Other diesel hammers may have continuously adjustable

fuel pumps; for stroke control of such diesel hammers, a reduced combustion pressure may be chosen as a percentage of the data file value which corresponds to the hammer's rated energy. However, for construction control, the hammer stroke has to be measured, e.g., calculating it from the hammer's speed of operation in blows per minute using a so-called Saximeter, and adjustments of the fuel amount have to be made by the operator until the desired, analyzed stroke is achieved.

12.6.4 Vibratory Hammer Considerations

Vibratory hammers come in a variety of models, among them high frequency hammers and resonance free hammers. For the high frequency hammers, as they are approaching the natural frequency of the piles, it will be difficult to make accurate predictions of drivability and or stresses because of the uncertainty of the hammer, pile and soil response. Resonance free hammers have a variable eccentric moment which would require different hammer data file values for eccentric moments that differ from the rated one, should the hammer be run on a reduced setting. However, in general, the reduced eccentric moments are only used during the starting and stopping cycle so as to reduce the danger of low frequency soil resonance while the maximum one is used for the production driving situation.

Vibratory hammers usually perform at 100% efficiency, with the greatest uncertainty the actual frequency. Note that often reduced driving times can be achieved with lower frequencies than maximum depending on the mass and stiffness of the combined soil-pile system.

As pointed out in Example 9, there is a great difference in how the soil responds to a vibratory hammer and an impact hammer. In granular, submerged soils the shaft resistance may almost complete vanish due to a liquefaction type effect. In cohesive soils, if they are sensitive to vibration a similar very pronounced loss of resistance may occur during driving. However, in soils where the bond between pile surface and soil is not broken, possibly because the hammer amplitude is too small, the resistance of the soil attached to pile may lead to refusal. In any event, where the vibratory excitation of the soil-pile interface leads to great losses of resistance, the relationship between speed of pile penetration rate and soil resistance is virtually meaningless while for those soil where the soil-pile bond is not broken, the full soil resistance is also not mobilized.

12.6.5 Batter Pile Considerations

Pile top bending due to poor hammer alignment is more likely to occur in battered than in vertical driving because of difficulties with maintaining a good hammer–pile alignment. The problem is aggravated during restrike, because realigning hammer and pile is then even more difficult than maintaining alignment during initial driving.

Inclined pile driving also causes, sometimes unexpected, bending stress problems if the piles are not properly supported and guided by the hammer leads. In fact, for offshore leads where the pile supports the non-axial weight component of pile, leads and hammer, these bending stresses are predictable. Offshore versions of wave equation programs have been developed for those situations that include a routine for calculating these bending stresses which are then superimposed to the dynamic stresses. However, for piles supported by fixed, swinging or semi-fixed leads it is assumed that the piles are supported in such a way that no significant bending stresses result along the length of the pile that is supported by the leads. This must be confirmed on site by a thorough inspection.

It has been mentioned that external combustion hammers (primarily air or hydraulic hammers) possibly do not reach the full effective stroke during inclined or batter pile driving, because of limitations of the effective (vertical) ram travel. This should be modeled by a reduced stroke. It must be expected that the full rated hammer energy will not be available even if the hammer efficiency is satisfactory. The increased friction in the hammer due to the pile batter can be estimated under consideration of a friction coefficient and batter angle. The wave equation software's Help section should provide some helpful values. For instrumented hammers, the friction loss is generally internally measured and/or compensated for. As the pile is driven, energy measurements whether in the hammer or by pile top measurements, will be able to assess the actual hammer energy transferred from the hammer to the pile.

For open end diesel hammers, also called internal combustion hammers, the ram travel is unlimited and it is likely that the actual, inclined ram travel is greater than the vertical ram travel under similar pile and soil conditions. However, friction effects should be accounted for by a reduced efficiency value as discussed for the external combustion hammers.

12.6.6 Hammer and Pile Cushion Considerations

Hammer cushions are primarily used to protect the hammer while pile cushions protect concrete pile tops. Direct Drive hammers use no cushioning material and are sometimes used for steel pile driving situations.

Cushion materials are subjected to destructive stresses during their service and, therefore, continuously change properties. For hammer cushions, a variety of man-made materials (e.g., Micarta, Conbest, and Nylon among others) are acceptable while wood chips as a hammer cushion are totally unpredictable and therefore should never be allowed. Frequently, hammer cushions are engineered as sandwiches of aluminum plates (to extract heat) and softer cushioning materials. The input values for the combined stiffness of two cushion materials can be easily calculated from the individual material properties by remembering that the inverse of the combined stiffness, k_c, of two springs in series is the sum of the inverse of the two individual springs ($1/k_c = 1/k_1 + 1/k_2$). However, for most commonly used cushions the Help section of the wave equation software contains extensive material property tables. Wood chips or softwood with the grain parallel to the pile axis as a hammer cushion have totally unpredictable material properties and therefore should not be allowed.

It has been explained in Example 4 that pile cushions experience a particularly pronounced increase in their stiffness during driving, because they are generally made of soft wood with its grain perpendicular to the load. Typically, the effectiveness of wood cushions in transferring energy increases until they begin to burn and quickly deteriorate. This typically happens after approximately 1500 hammer blows. For conservative stress predictions, the harder, used cushion could be modeled by an increased elastic modulus and reduced thickness. In the United States two types of pile cushions are most frequently encountered. The most common pile cushion consists of plywood sheets and the second most common pile cushion is made of oak boards. Improved agreement with measurements can be achieved if new and used plywood cushions are analyzed with elastic moduli of 30 and 75 ksi, respectively (Rausche et al. 2004). For oak board pile cushions, the respective recommended values for new and used cushions are 60 and 90 ksi. These elastic modulus values should always be used with the nominal (uncompressed) thickness. For conservative nominal resistance predictions, a less effective pile cushion may be modeled using by a somewhat lower, maybe 50% lower than normally recommended, input for both elastic modulus and coefficient of restitution.

Uncushioned or direct-drive diesel and hydraulic hammers are also frequently encountered when steel piles are driven. The advantage of these hammers is obvious: their energy transfer to the pile is not subject to varying cushion properties. For the wave equation analysis, the stiffness of the spring between hammer and helmet is derived from the elastic properties of either ram or impact block (diesels) since there is no hammer cushion. (This stiffness is very high, much higher than the stiffness values of most other components within the system, and for numerical reasons, may lead to inaccurate stress predictions. Analyses with different numbers of pile segments (the automatically selected number of pile segments is the pile length divided by 3.3 feet) would show the sensitivity of the numerical solution. In general, the greater the number of pile segments, the more accurate the stress calculation). Choosing 1 foot long segments (the number of pile segments then equals the pile length in feet) would generate a much more detailed pile model than is standard.

12.6.7 Selection of Soil and Rock Parameters

The greatest errors in nominal resistance predictions are usually observed when the soil resistance has been improperly considered. A very common error is the confusion of factored design loads with the wave equation's nominal resistance (usually called ultimate capacity in the wave equation documentations). Note that the wave equation nominal resistance always must be multiplied by a resistance factor which depends on the nominal resistance verification method and this product has to be greater than the factored load. In the past, and that is still the way the wave equation documentation describes the approach, the ultimate capacity was divided by a factor of safety to yield the allowable design load. Resistance factors suggested by FHWA and AASHTO are discussed in Chapter 7.

Since the soil is disturbed at the end of driving, it then often has a lower nominal resistance (occasionally also a higher one) than at a later time. For this reason, a restrike test should be conducted to assess the nominal resistance after time dependent soil strength changes have occurred. However, restrike testing is not always easy. The hammer is often not warmed up and only slowly starts to deliver the expected energy while at the same time the nominal resistance of the soil deteriorates. Depending on the sensitivity of the soil, the penetration resistance may be taken from the first 3 inches of pile penetration even though this may be conservative for some sensitive soils. For high penetration resistances (e.g., more than 10 blows/inch) smaller than 3-inch penetrations should be considered or the penetration for ten blows should be accurately measured. For sensitive soils with quickly lost soil setup resistance, measuring the penetrations of individual blows in

the beginning of a restrike should be attempted if possible. Of course, this information then has to be used together with the energy transferred to the pile head for each blow during the early restrike.

For construction control, rather than restrike testing many piles, it is more reasonable to develop a site specific setup factor in a pre-construction test program. As long as the hammer is powerful enough to move the pile during restrike and mobilize the soil resistance, restrike tests with dynamic measurements are an excellent tool to calculate setup factors. For the production pile installation criterion, the required end of driving resistance is then the required nominal resistance divided by the setup factor. From the wave equation calculated bearing graph and with the reduced end of driving nominal resistance, the required end of driving penetration resistance is found.

Although the proper consideration of static resistance at the time of driving or restriking is of major importance for accurate results, dynamic soil resistance parameters sometimes play an equally important role. In general, shaft damping factors on the order of 0.05 s/ft for non-cohesive soils, 0.10 s/ft for silty sands, clayey sands, and sandy silts, 0.15 s/ft for cohesive silts and sandy clays, and 0.20 s/ft for cohesive soils are typical. For most soils, the toe damping factor is about 0.15 s/ft. The above values are general recommendations for initial driving conditions. Damping factors have been observed to vary with waiting times after driving. Thus, damping factors higher than recommended above and in the GRLWEAP Manual (say twice as high) may have to be chosen for analyses modeling restrike situations. Studies on this subject are still continuing. In any event, damping factors are not a constant for a given soil type. For soft soils, damping factors may be much higher than recommended, and on hard rock they may be much lower. However, choosing too low a damping factor may produce non-conservative nominal resistance predictions. The program recommendations for damping factors are averages which work reasonable well as a first assumption (see input description in Section 12.7). After piles have been driven and dynamically tested, appropriate site specific values should be available.

Shaft quakes are usually satisfactory as recommended at 0.10 inch. However, for displacement piles, toe quakes can vary widely and reach values well in excess of the program recommended range of 1/60 and 1/120 of pile diameter or pile width, particularly when the soil is saturated and/or rather sensitive to dynamic effects. Only dynamic measurements can reveal more accurate soil quakes. However, short of such measurements, conservative assumptions must sometimes be made to protect against unforeseen problems. Fortunately, toe quakes have a relatively

insignificant effect on the wave equation results of piles having most of their resistance acting along the shaft. For piles achieving their nominal resistance primarily through toe resistance, large toe quakes often develop during driving in saturated soils causing the toe resistance to build up only very slowly during the hammer blow. As a consequence, at the first instant of stress wave arrival at the pile toe, little resistance exists and damaging tension stress reflections can develop in concrete piles even if the penetration resistance is high. At the same time, large toe quakes dissipate an unusually large amount of energy and therefore cause high penetration resistances. Thus, more cushioning or lower hammer strokes may not be a possible alternative for stress reductions. Instead, in extreme cases, hammers with heavier rams and lower strokes should be chosen to reduce the detrimental effects of large toe quakes. Example 6 in Section 12.5.6 illustrates the effect of a large toe quake.

Stress predictions, particularly tension stresses, are also sensitive to the input of the resistance distribution and to the percentage of toe resistance. If the soil resistance distribution is based on a static analysis, chances are that the shaft resistance is set too high because of the loss of shaft resistance during driving. It is therefore recommended that drivability analyses be performed with shaft resistances reduced by estimated setup factors, which will adjust the statically calculated nominal resistance to match the conditions occurring during driving.

Soft rock is generally modeled like a soil with quakes and damping values chosen as for the underlying material (e.g. clay for a claystone or shale). However, pile toe compression stresses can be damaging when the piles are driven to a hard rock. Since piles generally do not penetrate into a hard rock and since the plastic stage cannot be reached, the main concern is not with the nominal resistance but with the pile toe stresses. The resistance mobilized is usually a lower bound conservative value. Hence, to be conservative it is recommended to analyze these hard rock cases with a toe quake of 0.04 inches. A lower than the normal 0.15 s/ft damping value may also be used (e.g., 0.05 s/ft).

Residual stress wave equation analyses are superior to normal analyses in basic concept and probably also in results. Unfortunately, because of lack of correlation work, no empirically determined dynamic soil constants (quake and damping values) can be recommended for use with residual stress analyses. Experience exists for fluted and tapered piles which supports using the residual stress analysis with commonly used damping factors. Residual stress analyses should be performed (maybe in addition to standard analyses for long slender piles with significant shaft resistance components,) to assess potentially damaging stress conditions and the

possibility of nominal resistance values which could be much higher than indicated by the standard wave equation analysis. Note that residual stress analyses may not be meaningful for representation of early restrike situations in which energies increase from blow to blow while, in sensitive soils, capacities successively decrease. The residual stress analysis assumes that hammer energy and pile nominal resistance are constant under several hammer blows. For further information please see also Section 12.7.1 and the background information of the wave equation computer program.

12.6.8 Pile Modeling Considerations

In general, the pile is represented more accurately and reliably than other parts of the wave equation model. Of course, unit weight and elastic modulus have to be well known which is sometimes challenging for concrete and timber. Note that for concrete and timber there is a significant difference between the static elastic modulus and the dynamic one, the latter usually being significantly higher than the static one. Since approximately 2012, it has also been observed that even the steel elastic modulus can be higher by up to 7% for large diameter pipe piles than normally assumed. Plastic piles are also some times analyzed and because of the large variety of materials and their basically non-elastic behavior, dynamic testing is needed to determine the material properties prior to performing the analysis.

Modern wave equation programs automatically generate a pile model which is generally satisfactory for most commonly encountered situations. However, there are differences in the basic approach between different software products and the user should be aware of any limitations of these products in certain situations.

For the Smith-type programs which use mass and stiffness to represent the elastic properties of the hammer, driving system and pile, non-linear system components like cushions or splices with slacks are relatively easily and quite realistically represented. In addition, the default 3.3 foot long pile sections are generally adequate although smaller segments can lead to an improved program performance. Situations where smaller pile segments or also smaller computational time increments are helpful may be highly non-uniform piles or uncushioned driving systems. Like the length of the pile segments, computational time increments are normally set by the computer program, but can be modified with a factor which E.A.L. Smith called a safety factor against numerical instability. This factor is normally 1.6 in GRLWEAP and may be increased to 3 or even 5 if unusual situations cause the program to give a numerical instability warning.

For programs which use the characteristics approach to solving the underlying differential equation (e.g. Middendorp 2004) the computational time increment must be equal to the wave travel time of every segment. This leads to segments of different lengths when the pile consists of different materials such as a concrete pile with steel stinger. While the characteristics solution has the advantage of truthfully modeling ideal elastic situations, such as a square input pulse without degradation, there is a natural tendency for waves propagating along materials to maintain lower frequency components and shed higher frequency ones. This leads to a smoothing of the pulse traveling along the pile which is similar to the degradation observed when analyzing with a lumped mass model. Modeling piles with slacks in splices is also more difficult with the characteristics method than using the more forgiving Smith approach.

Unusual situations which require special attention are: installations which include followers, particularly when a soft cushion separates a steel follower from a concrete pile, mandrel driven piles, and composite piles such as a concrete pile with a steel stinger. These conditions require modeling using splices with compression and tension slacks, parallel piles and more than one toe model. Examples of these more complex situations are available in the help section of the GRLWEAP software.

Another problem frequently encountered is the uncertainty on how to model open end pipe piles. Very large diameters (say greater than 120 inches diameter) will never plug during driving and may experience some internal friction. This can be modeled by using an increased perimeter as discussed in Section 12.5.8. Smaller diameter (say 30 inches or less) open ended pipe piles, will generally plug once driven a sufficient, diameter dependent distance into a dense or very dense material. Intermediate pile sizes may or may not plug and then behave either like the piles with larger or the smaller diameters. The pile model may have to include a consideration of the mass effect and soil model needs to address the effective toe area over which toe resistance acts. While this is primarily a soil model problem, it potentially affects the mass properties of the pile model over the plug length. As noted in Chapter 7, Holloway and Beddard (1995) also reported that hammer blow intensity (impact force and energy) influenced plug formation and slippage. Brown and Thompson (2015) published a Synthesis of the current practice of design and analysis of large open ended pipe piles which provides further insight on this issue.

When the pile model to be analyzed is unusual in its complexity, it is recommended to perform sensitivity studies by comparing results with different numbers of pile segments and/or reduced time increments and possible maximum and minimum values of pile properties.

12.6.9 Comparison with Dynamic Measurements

Often, wave equation predicted stresses and nominal resistance values initially appear to agree quite well with results from field dynamic measurements, described in Chapter 10. However, there are additional observations and measurements that should be compared, such as stroke or bounce chamber pressure and transferred energy. Often transferred energy values are somewhat lower than calculated, and adjustment of hammer efficiency alone may improve energy agreement but produce problems with driving stress and nominal resistance agreement. Thus, instead of adjusting hammer efficiency, the cushion stiffness or coefficient of restitution may require reduction. Sometimes matching of measured values can be very frustrating and difficult, and the task should be done with reason. Matching stresses and transferred energies within 10% of the observed or measured quantities may be accurate enough.

Note: The wave equation maximum stresses in the final summary table can occur anywhere along the length of the pile and therefore at a location different from where the field measurements were taken. It is therefore important to check the maximum driving stresses in the Extrema Tables for the pile segment that corresponds to the measurement location when comparing wave equation calculation and field measurement results.

Matching wave equation results to field observations and measurements is often referred to as a Refined Wave Equation Analysis (Rausche et al. 2009). The following procedure requires that wave equation input parameters for hammer, driving system, and soil resistance are adjusted and then wave equation analyses are performed for the field verified nominal resistance. The following data preparation steps and successive input parameter adjustments generally lead to an acceptable solution. As noted in Section 12.6.8, multiple wave equation software programs exist and some use different models. The correlation procedure below is specifically based on the hammer, pile, and soil models used in GRLWEAP and CAPWAP. Procedures for other wave equation and/or signal matching programs may differ depending upon the hammer, pile, and soil models used in those programs.

a. Set up a table with the observed stroke or bounce chamber pressure for diesel hammers, and measured values of compression stresses and transferred energy, both at the measurement location. Include in this table for concrete piles the PDA calculated maximum tension stresses. These values should be averages over several consistent blows of pile installation or the

earliest consistent blows of restrike testing. Additional matching quantities are the CAPWAP calculated nominal resistance and penetration resistance.

b. Set up the GRLWEAP wave equation model to run bearing graphs for the actual hammer, pile, and driving system with total nominal resistance, resistance distribution, quake, and damping obtained from dynamic field measurements and by signal matching.

c. Perform wave equation analyses and compare results with table values from step a. Adjust hammer efficiency (for diesel hammers, also maximum combustion pressure) until agreement between measured and wave equation computed compression stress and transferred energy (for diesel hammers, also stroke) is within 10%. For steel piles modifications of the hammer cushion stiffness and/or its coefficient of restitution and for concrete piles adjustments of the pile cushion stiffness and/or its coefficient of restitution may also be needed.

d. After an initial agreement has been achieved for transferred energy and pile top compression stress, compare calculated penetration resistance for CAPWAP nominal resistance and associated maximum tension stresses. For steel piles, adjust hammer cushion stiffness and coefficient of restitution, and for concrete piles, adjust the equivalent pile cushion parameters, together with efficiency, to improve agreement of penetration resistance and tension stresses within the 10% tolerance.

e. Adjust the hammer efficiency to values not greater than 0.95 and not less than 50% of the standard recommended hammer efficiency values for that hammer type. The exceptions are hammers whose stroke input is based on measured impact velocity, therefore efficiency values greater than 0.95 are possible. Adjust cushion coefficients of restitution between 0.10 and 1.0.

f. If penetration resistance and stresses cannot be simultaneously matched by adjusting hammer and driving system parameters, change the shaft and toe damping and the toe quake simultaneously and proportionately to achieve agreement between measured and computed penetration resistance. Under certain conditions, it may also be necessary to change the wave equation damping model from Smith to Smith-Viscous.

Perfect agreement should not be expected between wave equation results and quantities derived from field measurements. The reason is primarily a difference between the measured pile top force and velocity and the corresponding quantities obtained by the wave equation driving system model. Also, there may be some differences in the pile model and soil models between the different analyses programs used for wave equation and signal matching. Plots of wave equation calculated and dynamic test measurements such as force and velocity can be easily generated and can sometimes explain the differences between observed or measured and calculated values.

12.7 WAVE EQUATION ANALYSIS INPUT

As described in the previous sections, the input for a wave equation analysis consists of information about the soil, pile, hammer, cushions, helmet, splices, and any other devices which participate in the transfer of energy from hammer to soil. This input information is usually gathered from contract plans, the contractor's completed Pile and Driving Equipment Data Form (Figure 12-24), soil boring, and a static pile nominal resistance analysis. In a case where the contractor proposes using a follower as part of the driving system, detailed drawings of the follower should also be obtained. Helpful information can also be found in the "Help" display of the wave equation program. These tables are correct only for ideal situations but may yield valuable data before a specific driving system has been identified. In general, contractors tend to assemble equipment from a variety of sources, not all of them of a standard type. It is therefore important to check and confirm the equipment that the contractor has actually included in the driving system on the project.

Contract No.:_____ Structure Name and/or No.:_____

Project:_____

_____

Pile Driving Contractor or Subcontractor:_____

County:_____

(Piles driven by)

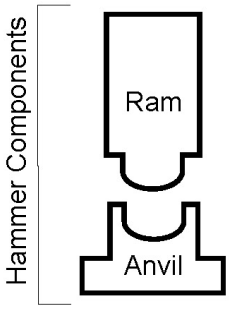

Hammer

Manufacturer:_____ Model No.:_____

Hammer Type:_____ Serial No.: _____

Manufacturers Maximum Rated Energy:_____(ft-lbs)

Stroke at Maximum Rated Energy:_____(ft)

Range in Operating Energy:_____to_____(ft-lbs)

Range in Operating Stroke:_____to_____(ft)

Ram Weight:_____(kips)

Modifications:_____

_____

_____

Striker Plate

Weight:_____(kips) Diameter:_____(in)

Thickness:_____(in)

Hammer Cushion

Material #1	Material #2 (Composite Cushion)
Name:_____	Name:_____
Area:_____(in^2)	Area:_____(in^2)
Thickness/Plate:_____(in)	Thickness/Plate:_____(in)
No. of Plates:_____	No. of Plates:_____

Total Thickness of Hammer Cushion:_____(in)

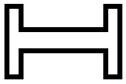

Helmet

Weight:_____(kips)

Insert (If Any)

Weight:_____(kips)

Total Weight of Helmet and Insert:_____(kips)

Pile Cushion

Material:_____

Area:_____(in^2) Thickness/Sheet:_____(in^2)

No. of Sheets:_____

Total Thickness of Pile Cushion:_____(in)

Maximum Thickness Accommodated by Helmet :_____(in)

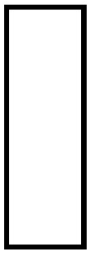

Pile

Pile Type:_____

Wall Thickness:_____(in) Taper:_____

Cross Sectional Area:_____(in^2) Weight/ft:_____

Ordered Length:_____(ft)

Factored Resistance:_____(kips)

Nominal Resistance:_____(kips)

Description of Splice:_____

_____

Driving Shoe/Closure Plate Description:_____

_____

Submitted By:_____ Date:_____

Telephone No.:_____ Email:_____

Figure 12-24 Pile driving and equipment data form.

The following sections explain the most important input quantities needed to run the GRLWEAP program. For a more detailed explanation of input quantities, reference is made to the program's Help Section (function key F1 or F3 or click on Help).

The (second topic) of the Help Menu (F1 or click on Help) explains the Main Input screen and all of its menus, data entry fields, and information indicators. Figure 12-25 shows this Help Window as it first appears and subdivides the Main Input screen into 10 major sections:

A Standard Window Menus
B Icons for standard Windows Operations
C Icons for GRLWEAP displays and operations
D GRLWEAP Drop-Down Menus
E Input fields for Title and Hammer Selection
F Hammer Parameters and Pile Material Selection
G Hammer and Pile Cushion Input
H Pile Data Input
I Ultimate Capacity (Nominal Resistance) Input or Gain/Loss Factors
J Soil Parameters

Although a simple bearing graph analysis only requires input in the GRLWEAP Main Input Screen, it is recommended to utilize the step-by-step input requests generated after clicking on the “New Document” icon (or New in the File Menu).

The Job Information window shown in Figure 12-26 will display first, accepting input of a title of up to 40 characters and the assignment of a file name and directory. Browse may be used to navigate the user’s computer and assign the desired directory.

Clicking on Next will open up the Select Hammer window shown in Figure 12-27. The GRLWEAP program includes a hammer data file in which the major mechanical properties of approximately 1000 hammers are stored. By selecting an identification number (ID) and/or corresponding hammer name in the List of Hammers window, the user prompts the program to automatically input the selected hammer’s properties. Note that the automatic hammer input assumes use of a well maintained and unmodified hammer.

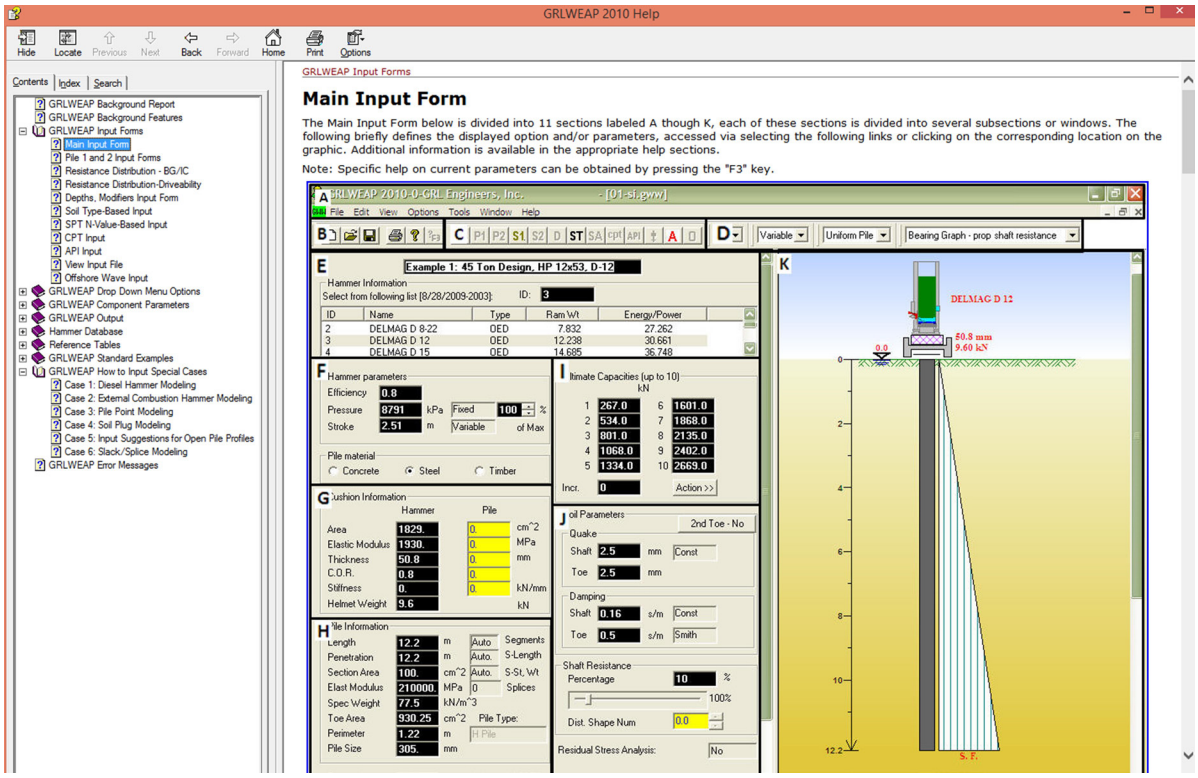

Figure 12-25 GRLWEAP help window for main input form.

While initially all hammers are displayed in the order of hammer **ID** number, the display may be reorganized by certain hammer types or manufacturers. Hammer types are OED (Open End Diesels), CED (Closed End Diesels), ECH (External Combustion Hammers, including the air, steam, hydraulic and drop hammer categories), and VIB (Vibratory Hammers). The user can also organize the contents in the List of Hammers window by hammer **Name**, **Type**, **Ram Weight** or **Rated Energy** by clicking on the column heading.

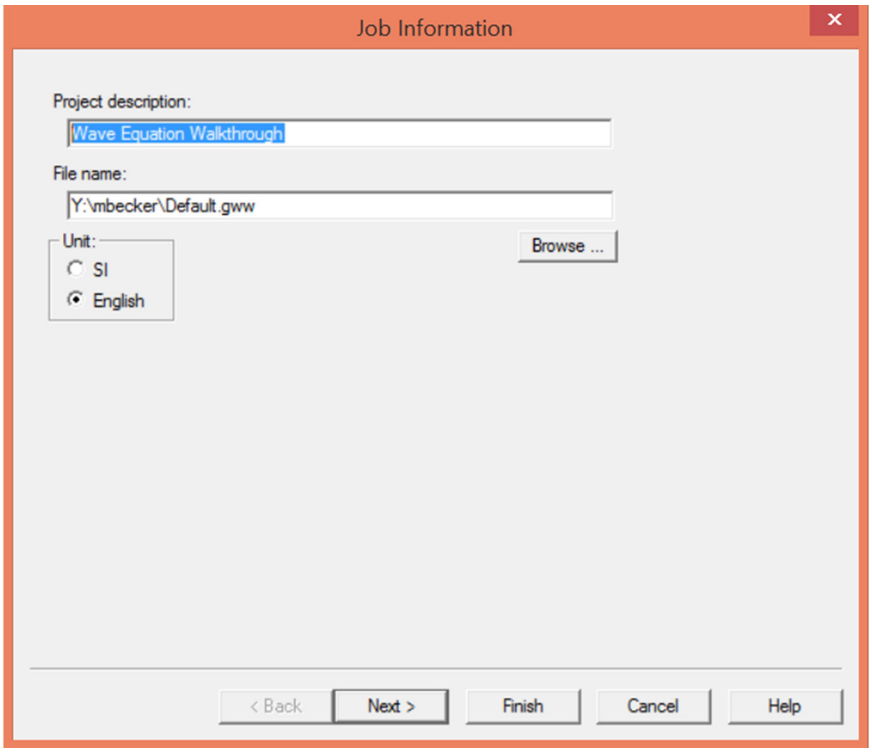

Figure 12-26 Job information window.

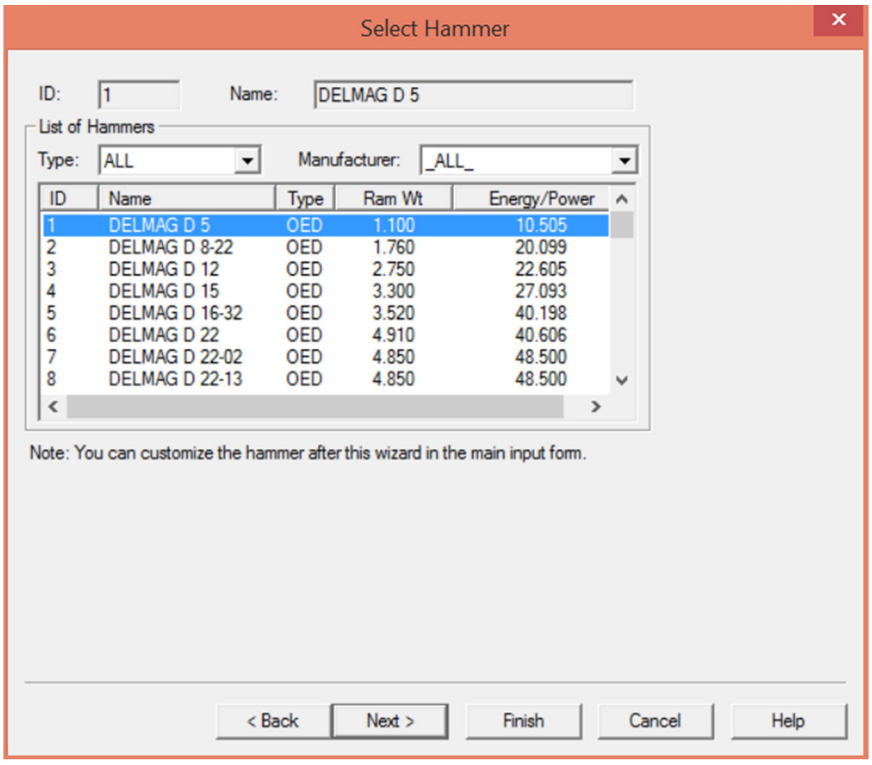

Figure 12-27 Select hammer window.

The next section involves the **Analysis Type** window, displayed in Figure 12-28. For a simple **Bearing Graph**, the **Proportional Shaft Resistance** option is the default. It assumes constant percentages of shaft resistance and end bearing for all nominal resistance values to be analyzed. The alternate bearing graph options analyze the various nominal resistance values either assuming a **Constant Shaft Resistance** or a **Constant End Bearing**.

A modified Bearing Graph approach, the **Inspector's Chart** provides the possibility of analysis with an increasing stroke (or hammer energy values) for a single nominal resistance value. This option is useful for diesel hammers, whose stroke can vary and/or be adjusted by different fuel settings, and for hydraulic hammers, whose energy level can be selected on the hammers' control panel.

The user may also choose the **Drivability** option. It requires as an input the unit shaft resistance and unit toe resistance as a function of pile penetration and, therefore, requires an accurate static soil analysis. The resulting output will show the corresponding nominal resistance values together with calculated penetration resistance (blow count), pile stress maxima, and other quantities and, thus, indicates the complete, expected driving behavior.

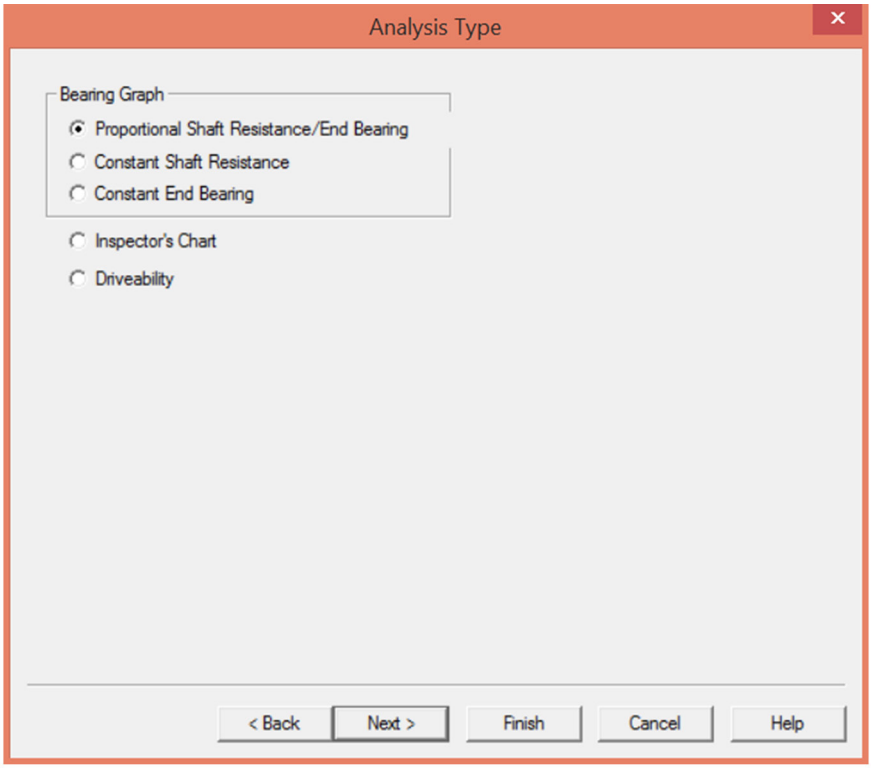

Figure 12-28 Analysis type window.

Clicking on **Next** brings up the **Pile Input** window, illustrated in Figure 12-29. After selection of the pile material, i.e., **Concrete**, **Steel**, or **Timber**, the program inputs default values for pile top elastic modulus, coefficient of restitution, and specific weight in the corresponding fields and also, for concrete pile material, activates the pile cushion input section. As with the hammer cushion, described below, the user may utilize the **Area Calculator** and the **Cushion Material Properties** Help by pressing the **F3** function key or directly input a stiffness. Additionally, selection of the pile material will automatically select the pile damping parameter which is accessible through **Options**, **General Options**, **Damping**. The user may adjust the aforementioned defaults but must enter the initial inputs for the Pile Length and cross Section Area. For the latter, the user may again employ the **Area Calculator**, shown in Figure 12-30, which also provides the Pile Size, Perimeter and Toe Area based on pile type and pile dimensional information. These quantities are particularly important for the drivability analysis when calculating the nominal resistance from the unit resistance values.

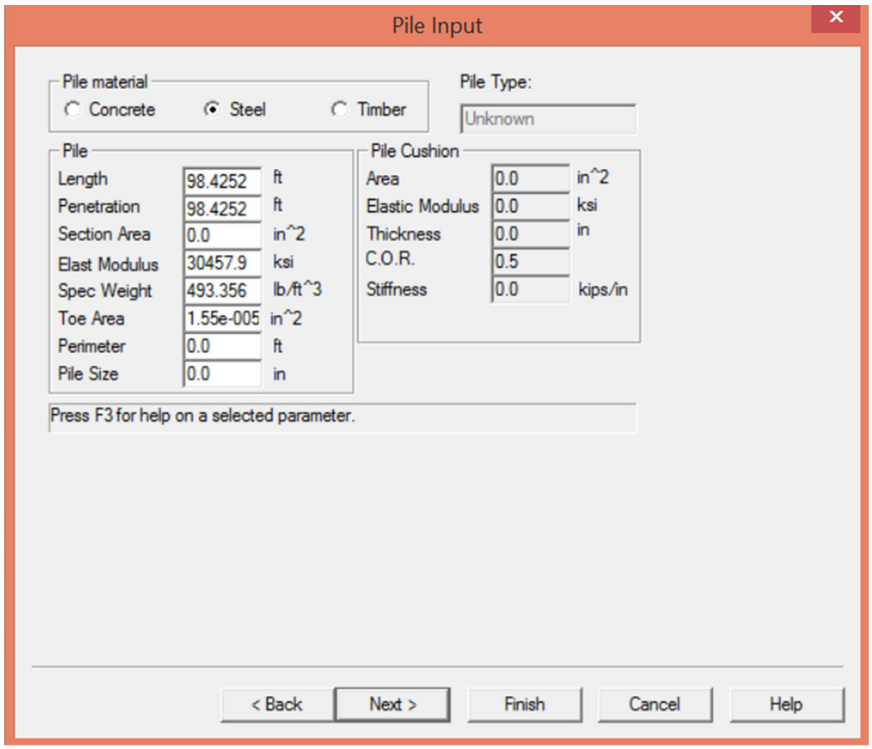

Figure 12-29 Pile input window.

It is important to note that for non-uniform piles the input quantities of Cross **Sectional Area**, **Elastic Modulus**, **Spe**cific **Weight** and **Perimeter**, in this window only refer to the pile top. Also **Toe Area** and **Pile Size** may need correction for non-uniform piles, the latter because it is used for calculating a recommended toe quake.

Once the data entry wizard has been finished, the non-uniform quantities must be entered in the P1 window, accessible after clicking on the pile type drop-down menu. As form most default values, those automatically chosen for pile elastic modulus and specific weight may or may not be correct and must be reviewed by the program user. For example, for concrete or timber piles, measurements could indicate other values. Pressing **F3** with the cursor on the Elastic Modulus or Specific Weight input field brings up added Help information. The following information is required information.

Length is the total pile length in the leads in feet. For example, if plans require a pile of 50 feet in length but the contractor is driving 60 long piles, the proper analysis length would be the full 60 feet. If pile sections are spliced together to form a longer pile, an analysis before and after splicing may be of interest. In such cases, the Length may be either the length of a single section before splicing or the combined length after splicing.

Penetration refers to the analyzed pile toe penetration below grade in feet for Bearing Graph or Inspector's Chart and final penetration for Drivability Analyses. This measurement must use the same soil grade reference as that of the soil resistance distribution.

Section Area is the pile cross section area at the pile head in $inch^2$.

Elastic Modulus is the elastic modulus of the pile material at the pile head in ksi.

Spec Weight is the weight per unit volume of the pile material at the pile head in lbs/ft^3. This value is used for calculating the mass of the pile material by division with 32.17 ft/s^2. The program provides for a modification of the pile's weight component by modification of the gravity acceleration value in Options/General Options/Numeric to reflect, for example, the effect of buoyancy or pile inclination on the pile weight on the soil.

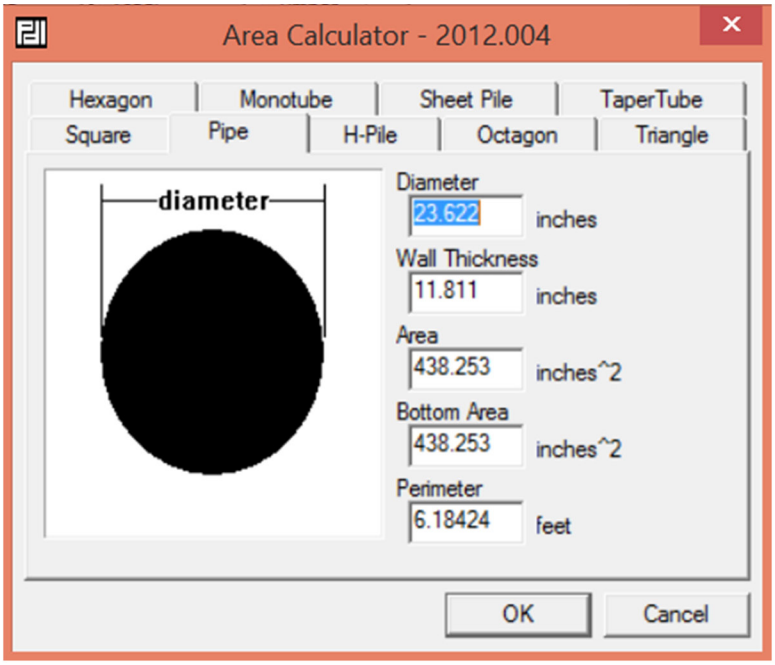

Figure 12-30 Area calculator window

After the pile input is done, clicking on **Next** will open up the Hammer Cushion window, as shown in Figure 12-31. GRLWEAP offers an extensive data file for those situations in which the contractor's available equipment is unknown. The data file has been made possible courtesy of the various manufacturers and dealers whose products are listed. Please note that this file is neither complete nor necessarily appropriate for all situations, as the contractor may not follow the manufacturer's recommendations. The required information consists of:

Area is the area of the hammer cushion perpendicular to the load in inch^2.

Elastic Modulus is the elastic modulus of the hammer cushion material in ksi.

Thickness of the hammer cushion. For sandwiched cushions, this is the thickness of the cushion material that corresponds to the elastic modulus in inches. If the entire stack thickness is entered, the combined elastic modulus of the sandwich and the striker plate is not included. If no hammer cushion exists, leave this value and the stiffness value at zero.

C.O.R. is the Coefficient of Restitution of the hammer cushion material.

Stiffness of the hammer cushion in kips/inch. Use of this optional input will override the inputs for area, elastic modulus, and thickness.

Helmet Weight, consisting of the combined weight of the helmet, hammer cushion, striker plate, inserts, and all other components located between the hammer and pile in kips. The input may be zero if there is no helmet mass.

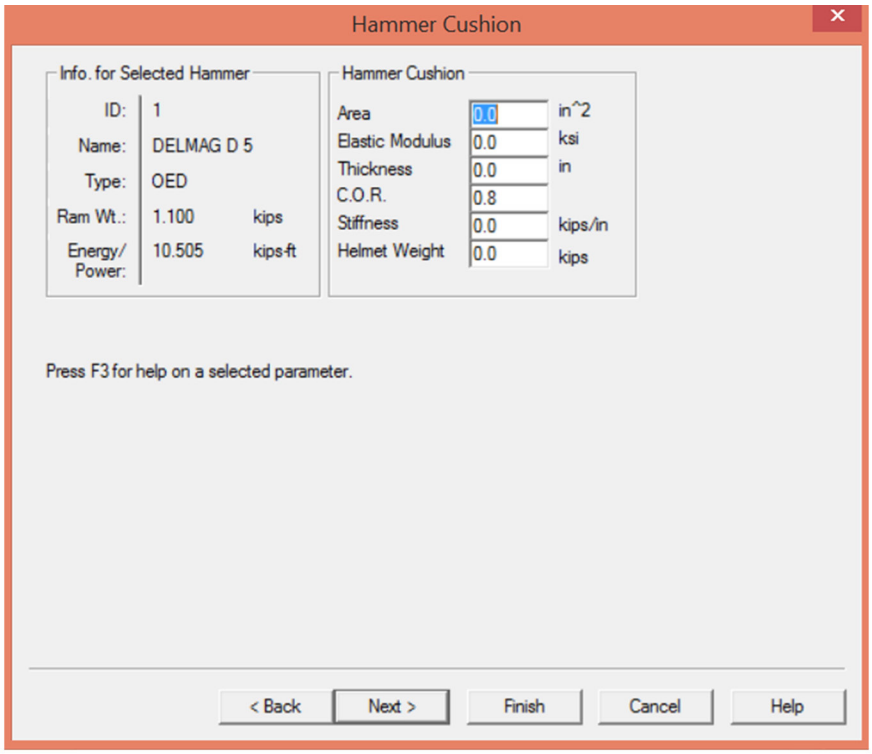

Figure 12-31 Hammer cushion window.

Ideally, the contractor would provide the above drive system data for his actual hammer system. However, if not available, the required hammer cushion data may be selected using one of three different methods:

1. The hammer cushion Stiffness and Coefficient of Restitution may be known from other analyses and can be input directly into the appropriate fields. In such cases, hammer cushion area, elastic modulus, and thickness are not needed.

2. If some or all of the driving system data is to be retrieved from the program data file, merely pressing F3 while the cursor is on one of the associated input fields and then clicking on Manufacturer's Recommended Driving System opens a listing of the recommended input. The user may transfer the suggestions in whole or part to the input sheet.

3. If the cushion material area, thickness, and type are known but modulus of elasticity and Coefficient of Restitution are not, pressing F3 while the cursor is

on the elastic modulus field and then selecting Cushion Material Properties brings up a list of frequently used cushion materials and their properties. These values can be transferred directly to the hammer cushion data input fields.

The **Next** input sections for bearing graph or inspector's chart analyses may be done in the dynamic soil parameters window on the **Main Input Form** or **Soil Profile Input** window, displayed in Figure 12-32. (For Drivability analyses, the **S1 Form** is opened as later discussed.) The most convenient input is through the **ST** analysis in the **Soil Profile Input** window. There, the user first specifies the:

Number of Soil Layers. It is recommended to divide the soil into layers of not more than 10 feet in thickness for improved accuracy.

Final Penetration Depth is the distance from grade to that depth to which data is to be given in feet. The window will at first display the value entered under the pile information. However, it may be changed here with the exception that it cannot be greater than the pile length.

Water Table is the distance from grade in feet where the water table begins. If grade is underwater, enter zero or a negative value; the later will show on the Main Screen graphics the water depth. As far as buoyancy is concerned both zero and negative values give the same result.

Effective Overburden at Grade is the intensity of any overburden pressure in ksf. For example, in the case of an excavation of limited extent (trench), the depth of excavation times the soil unit weight equals the effective overburden.

For each layer, the analyst then enters:

Either the **Layer Bottom Depth** or the **Layer Thickness** in feet.

The layer soil type as either **Granular** (non-cohesive soil for primarily sandy or other coarse grained soils) or **Cohesive** (for clays and silts) and selects as sub types the density or consistency of the layer. For intermediate soil types or non-cohesive silts, it may be conservative to choose "cohesive", since soil damping is then assigned a higher value. However, under all circumstances, the analyst should review the results obtained from this very simplified analysis.

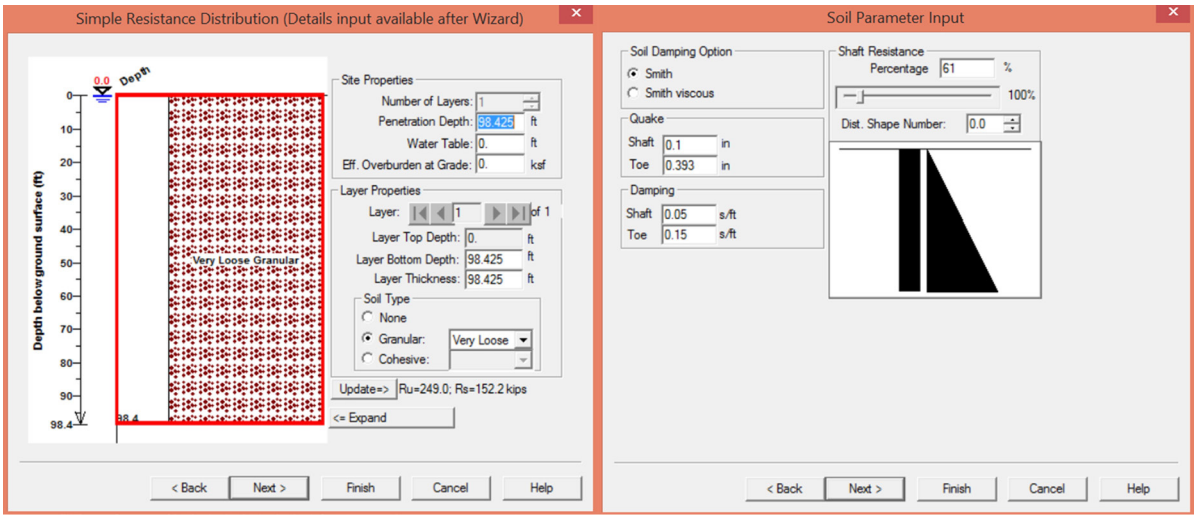

Figure 12-32 (a) Soil profile input window for soil type based static soil analysis and (b) Soil parameter input window for bearing graph analysis.

After clicking **Update**, the program will display a nominal resistance ($\mathbf{R_u}$) and a nominal shaft resistance ($\mathbf{R_s}$) value. These two results pertain to the **Final** penetration **Depth**, where the ratio $\mathbf{R_s/R_u}$ is the percentage of shaft resistance and one of the soil resistance inputs generated by the routine. Under no circumstances should these values be used for pile design purposes. The results are based on the following two methods:

For Non-Cohesive Soils

Using the Effective Stress Method, the unit shaft resistance is $f_s = \beta\ \sigma'_v$, with β being the Bjerrum-Burland beta coefficient as tabulated in Table 12-8 and σ'_v being the effective vertical stress at the midpoint of a given soil layer. The unit toe resistance is $q_p = N_t\ \sigma'_{vt}$, where N_t is a toe bearing capacity coefficient (see Table 12-8) and σ_{vt} is the effective overburden pressure at the pile toe. Both $\mathbf{f_s}$ and $\mathbf{q_p}$ are subjected to certain specified limits.

For Cohesive Soils

For cohesive soils, **ST** applies a modified α-method, also called the total stress method, and relies on the unconfined compression strength (q_u) of the soil layer. The q_u-value and, based on it, the unit shaft and unit toe resistance values are shown as a function of both soil type and a representative N-value in Table 12-9.

Table 12-8 Soil Parameters in ST Analysis for Granular Soil Types

Soil Type	SPT N	Friction Angle ϕ	Unit Weight pcf	β	N_t	Max. Unit Shaft Res. ksf	Max. Unit End Bearing ksf
Very Loose	2	25 - 30	86	0.203	12.1	0.5	50
Loose	7	27 - 32	102	0.242	18.1	1.0	100
Medium	20	30 - 35	118	0.313	33.2	1.5	150
Dense	40	35 - 40	125	0.483	86.0	2.0	200
Very Dense	50+	38 - 43	141	0.627	147.0	4.o	400

Table 12-9 Soil Parameters in ST Analysis for Cohesive Soil Types

Soil Type	SPT N	Unconfined Compression Strength ksf	Unit Weight pcf	Max. Unit Shaft Res. ksf	Max. Unit End Bearing ksf
Very Soft	1	0.25	111	0.07	1.1
Soft	3	0.75	111	0.23	3.3
Medium	6	1.50	118	0.40	6.7
Stiff	12	3.00	131	0.81	14.0
Very Stiff	24	6.00	131	1.30	27.0
Hard	32+	8.00+	121-140	1.60	36.0

After the soil types of all layers have been entered, the program computes the percentage and distribution of shaft resistance, the average shaft damping parameter, and the toe quake. These wave equation input values are based on pile penetration, water table depth, pile size, pile perimeter, and pile toe area. Damping and quake values are adjusted considering soil and pile type. Again, the analyst is responsible for checking these values and should be aware that this analysis is not applicable to non-uniform piles.

It is very important that the user carefully reviews the wave equation input parameters resulting from this very simplified static soil analysis, possible in the **Soil Parameters Input** window (see Figure 12-32b). Particular attention should be paid to the pile toe area because the shaft resistance percentage and toe quake directly depend on its magnitude. Also, it is recommended to perform comparative analyses, for example, when the soil type does not clearly fall into either the cohesive or granular categories. In such cases, results for both soil types should be

obtained and compared. The ST generated input parameters should be reviewed once the input wizard has been finished and the main screen is displayed.

Help pertaining to both soil type input and soil quakes and damping appears in the program Help Menu under GRLWEAP Input Forms, Soil Type-Based Input Form and GRLWEAP Component Parameters, Soil Parameters, respectively. It is also recommended that the user carefully review both the PDI (2010) Background Report and the program Help.

For Bearing Graphs or Inspector's Charts, the user must input between one and ten nominal resistance values in the **Ultimate Capacity** window shown in Figure 12-33. Several options are available including values spaced at constant increments (Incr.), generated by pressing "Interpolate" to interpolate between the first and last entries, and **Automatic Capacities**, based on the pile cross section properties. It is recommended to analyze nominal resistance values that will provide a meaningful bearing graph for both easy and hard driving conditions. The input wizard is now finished. The completed **Main Input** screen should resemble that shown in Figure 12-39. To perform a more complex analysis, additional inputs may be made by specifying a Non Uniform Pile or a more detailed soil resistance distribution in Variable Resistance Distribution.

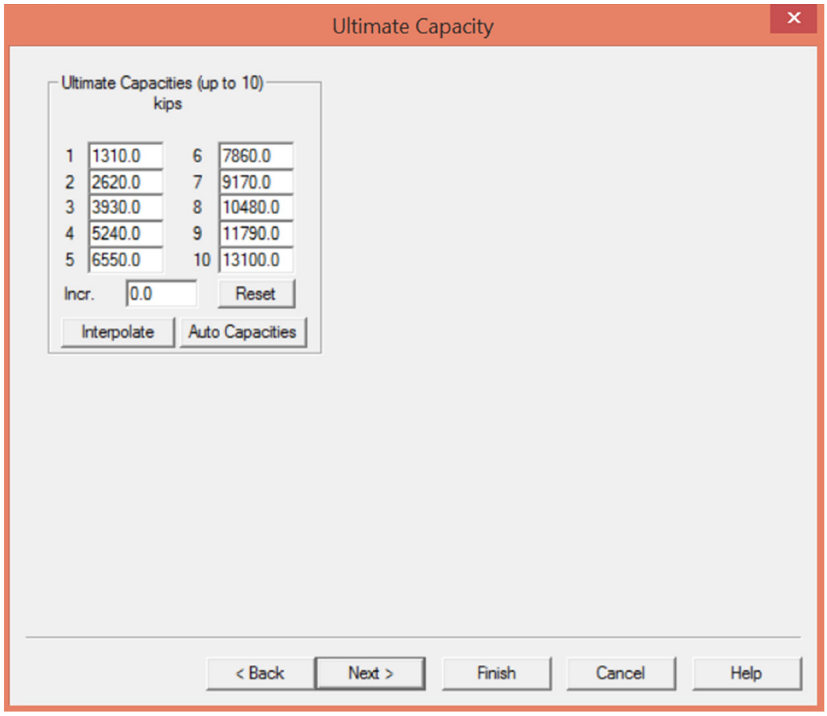

Figure 12-33 Window for entering up to 10 nominal resistance values for bearing graph and inspector's chart analyses.

For Drivability, instead of nominal resistance values, the analyst must input **Resistance Gain/Loss Factors**. Figure 12-34 shows the related window. The analyst may perform at most 5 analyses at each specified depth and provide at most five associated gain/loss factors for both the pile shaft and toe. These factors are related to the soil resistance parameters to be entered in the S1 Form (Figure 12-35) discussed below. A factor of 1.0 implies no change in soil strength during driving and thus that no resistance gain or loss will be analyzed. A factor less than 1.0 proportionally reduces the resistance values under consideration of their relative setup factors and thus reflects that the soil resistance is lower during driving and increases after pile installation, i.e., soil setup. A factor greater than 1.0 proportionally increases the resistance values and thus reflects the soil relaxation scenario, i.e., where the soil resistance is greatest during driving. In most cases, it is sufficient to enter two values for the shaft analysis. The first shaft value, marked 1, would be the inverse of the highest soil setup factor entered in the S1 Form and would represent the greatest resistance loss during driving along the shaft. The associated toe resistance factor, Toe 1, would be set to 1.0 to indicate neither gain nor loss of toe resistance during driving. For the second analysis, Shaft 2 and the associated factor Toe 2 would be set to 1.0. This latter input then reflects the absence of both gain and loss during driving at each depth analyzed (see Figure 12-34).

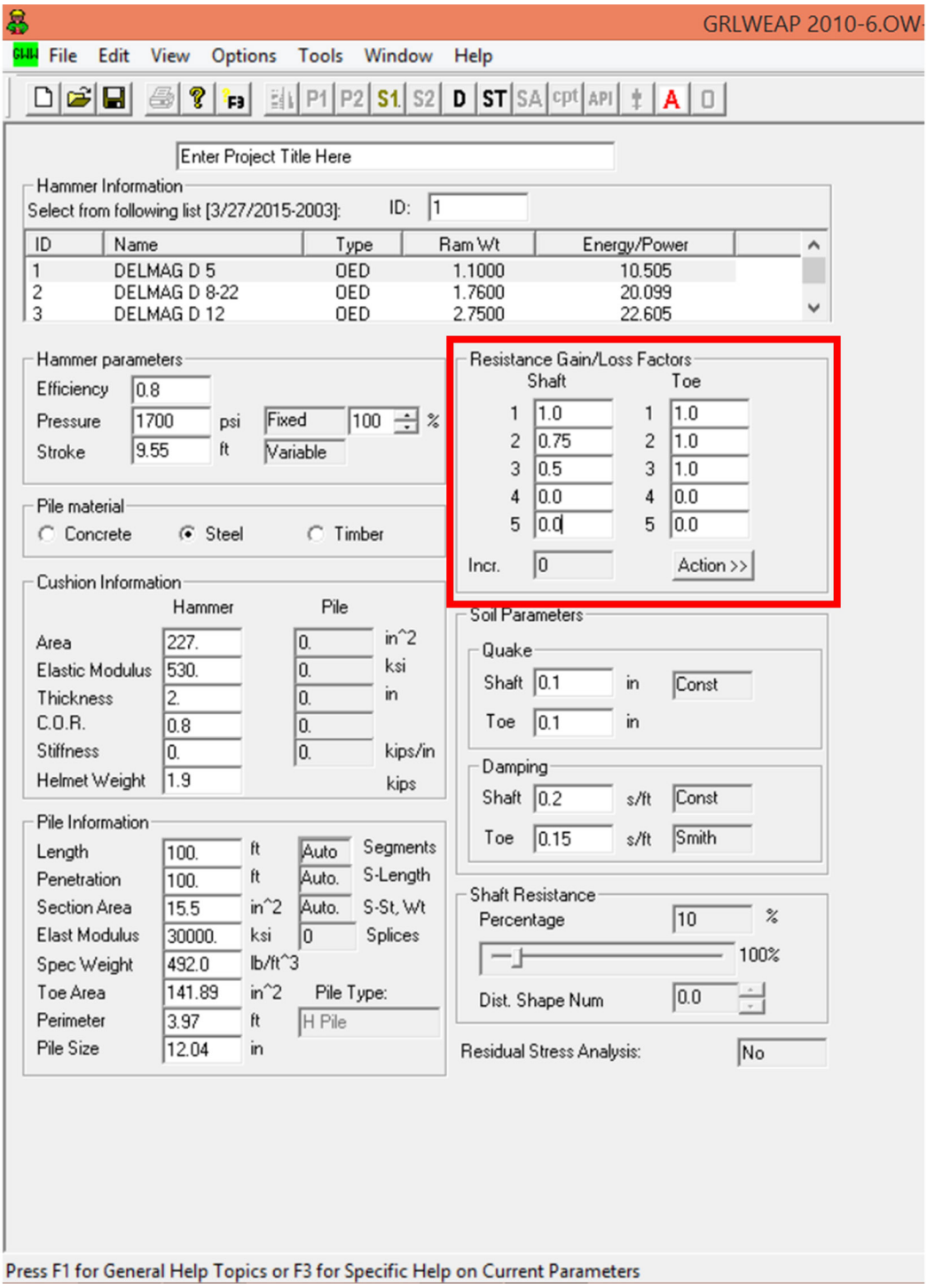

Figure 12-34 Resistance gain/loss factors in main input form for drivability analysis.

Next for Drivability analyses, the GRLWEAP program requires input in the S1 Form (Figure 12-35). Important inputs for each soil layer are (refer also to descriptions for the equivalent bearing graph inputs):

Depth is the soil layer distance below grade or mudline in feet.

Nominal Unit Shaft Resistance in ksf is determined by a static geotechnical analysis (e.g., the GRLWEAP SA routine). GRLWEAP multiplies this input by the pile perimeter, the segment length, and a soil layer specific gain/loss factor to yield the shaft resistance at the segment.

Nominal Unit Toe Resistance in ksf equals the unit toe resistance determined by a static geotechnical analysis.

Skin quake is the shaft quake in inch, usually left at the default value of 0.10 inch.

Toe quake in inch is per the Soil Parameter Help.

Skin damping is the shaft damping in s/ft as per the Soil Parameter Help.

Toe damping in s/ft, usually left at the default value of 0.15 s/ft.

Setup factor is based on site specific knowledge and, in conjunction with the resistance gain/loss factor, determines for each soil layer the soil resistance to driving.

The parameters of Limit Distance and Setup Time allow for a qualitative evaluation of soil strength change during driving interruptions, providing for more detailed analyses of splice time interruptions. These parameters have no influence on results as long as entered **Wait Times** in the **Depths**, **Modifiers Input Form** (see Figure 12-38) are zero.

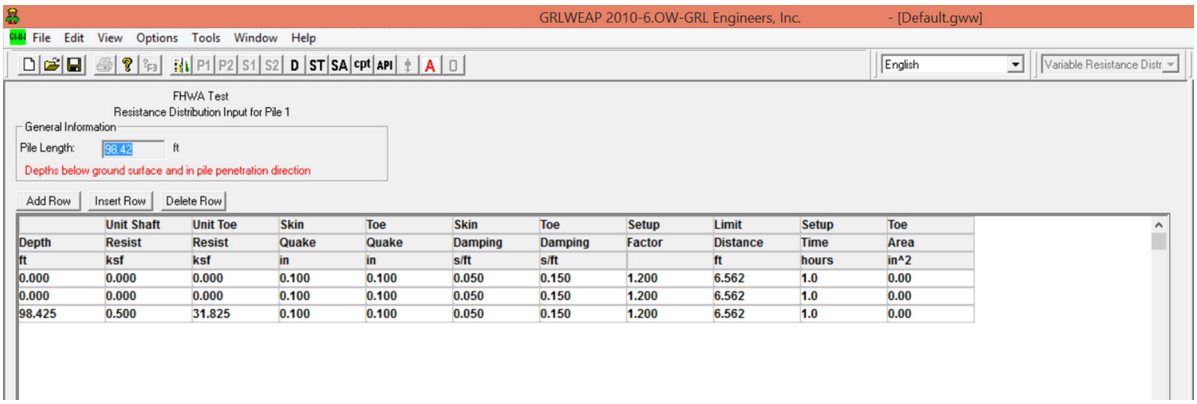

Depth	Unit Shaft Resist	Unit Toe Resist	Skin Quake	Toe Quake	Skin Damping	Toe Damping	Setup Factor	Limit Distance	Setup Time	Toe Area
ft	ksf	ksf	in	in	s/ft	s/ft		ft	hours	in^2
0.000	0.000	0.000	0.100	0.100	0.050	0.150	1.200	6.562	1.0	0.00
0.000	0.000	0.000	0.100	0.100	0.050	0.150	1.200	6.562	1.0	0.00
98.425	0.500	31.825	0.100	0.100	0.050	0.150	1.200	6.562	1.0	0.00

Figure 12-35 S1 form for soil resistance vs. depth input.

Should the user utilize the static analysis (SA) routine that is built into the GRLWEAP program to complete the S1 Form, clicking the SA icon will open the Figure 12-36 window. First, selection of Profile and New allows specification of the following quantities in the Static Analysis General Information window (refer to Figure 12-36):

The **Total Number of Soil Layers** to be included between grade and a depth equal to the total pile length in feet.

The depth of the **Water Table** in feet.

Overburden Pressure in ksf; see also ST above for an explanation of these inputs.

After closing the **Profile** window, the soil layer specific input can be made in the **SA** window. The following information should be provided (see Figure 12-37):

Layer Bottom Depth or **Layer Thickness** is in ft.

If the SPT N-value is known, choose from Gravel, Sand (with sub types indicating Grading and Grain Size), Silt, Clay, or Rock. Then enter the SPT N-value (not greater than 60), and the program will calculate a unit resistance and a unit weight for the soil layer.

If the SPT N-value is unknown, choose Other and either Cohesive or Cohesionless and then provide the Unit Weight in kips/ft^3 and the Unit Shaft Resistance and Unit Toe Resistance, both in ksf. The program will reduce the input unit weight value below the water table to yield an effective overburden.

Upon user request, the SA routine will also fill in the Other Parameters, i.e., the input values for quake, damping, setup factor, limit distance and setup time columns. Oftentimes these values do not differ from the default values specified earlier and then can be left at zero. Again, the user should carefully review the automatically generated input values prior to performing the actual wave equation analysis.

The SA routine is basically an effective stress method with different approaches for sand, silt and clay. This method is described in detail in the Background Report of the GRLWEAP program (PDI, 2010) and that

description should be reviewed prior to using this approach. It applies very conservative limits on the unit resistance values which may be non-conservative as far as drivability analyses is concerned (calculated driving resistances and stresses may be low). Also the method is only applicable to piles with straight sections (not applicable to tapered piles) and should never serve as the sole static soil analysis method for a pile design. In fact, it is always prudent to compare several static analysis methods for an assessment of the range of possible results.

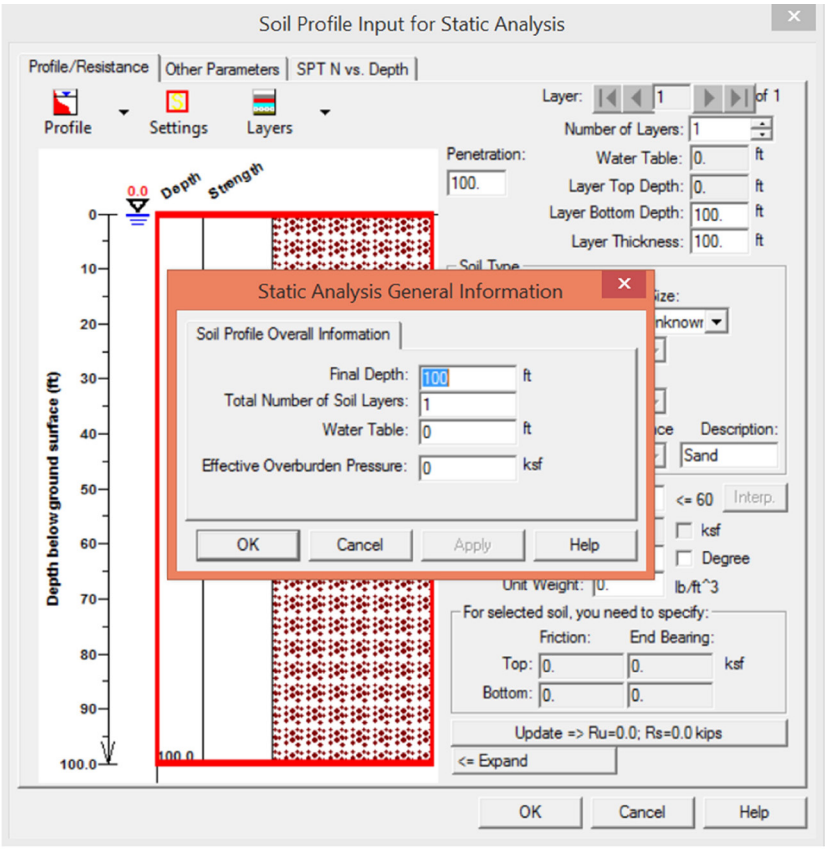

Figure 12-36 New profile window for the SA static analysis.

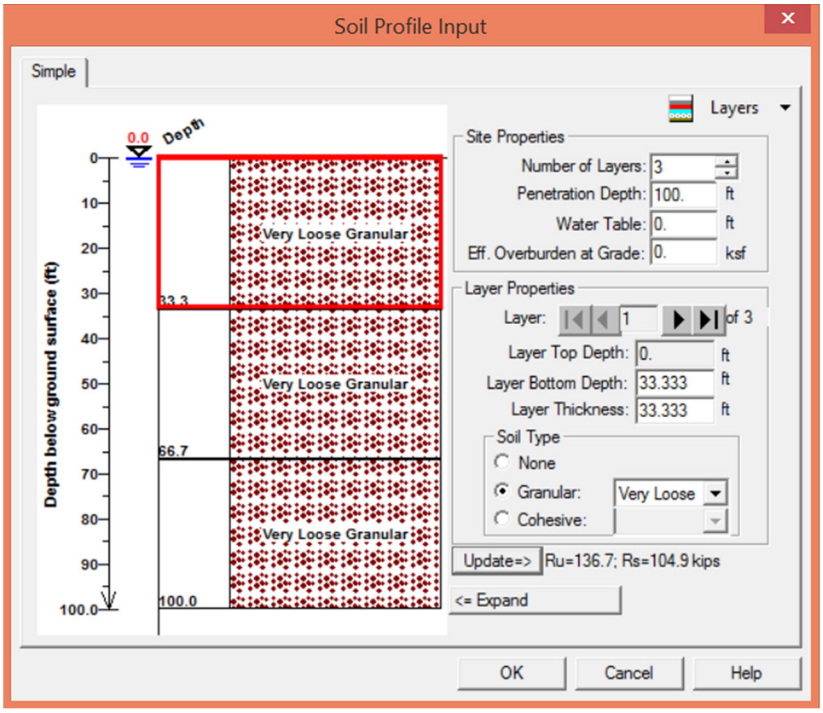

Figure 12-37 Soil property input window for the SA static analysis.

In a Drivability analysis, another required input is found in the **Depths**, **Modifiers Input Form**, accessible after clicking the **D** icon (see Figure 12-38). This form provides for the input of:

Depth to be analyzed in feet is a required input for at least two different depth values.

The pile **Temporary Length** in feet may be less than or equal to the length value given as the final length input and allows for consideration of a reduced pile length prior to splicing.

Wait Time in hours, which would be applicable if driving were to be interrupted, for example, for splicing operations. This input is only useful for a qualitative assessment of setup effects during the driving interruption, which, in turn, is a function of the Limit Distance and the Setup Time. Also it only applies to the first gain/loss factor. (As mentioned, this is rarely needed for highway construction projects.)

Stroke and **Efficiency** allow for variation of these hammer parameters as a function of depth. If not specified, the values input previously will be considered.

Diesel Pressure input allows for a modification of the hammer setting and/or stroke.

Pile Cushion Coefficient Of Restitution (**COR**) or **Stiffness Factor** can also be varied as a function of depth. For example, and considering the recommendations for new and used pile cushion parameters, the Stiffness Factor may be gradually increased from 1.0 to 2.5 if the cushion elastic modulus was specified earlier with the “New” elastic modulus.

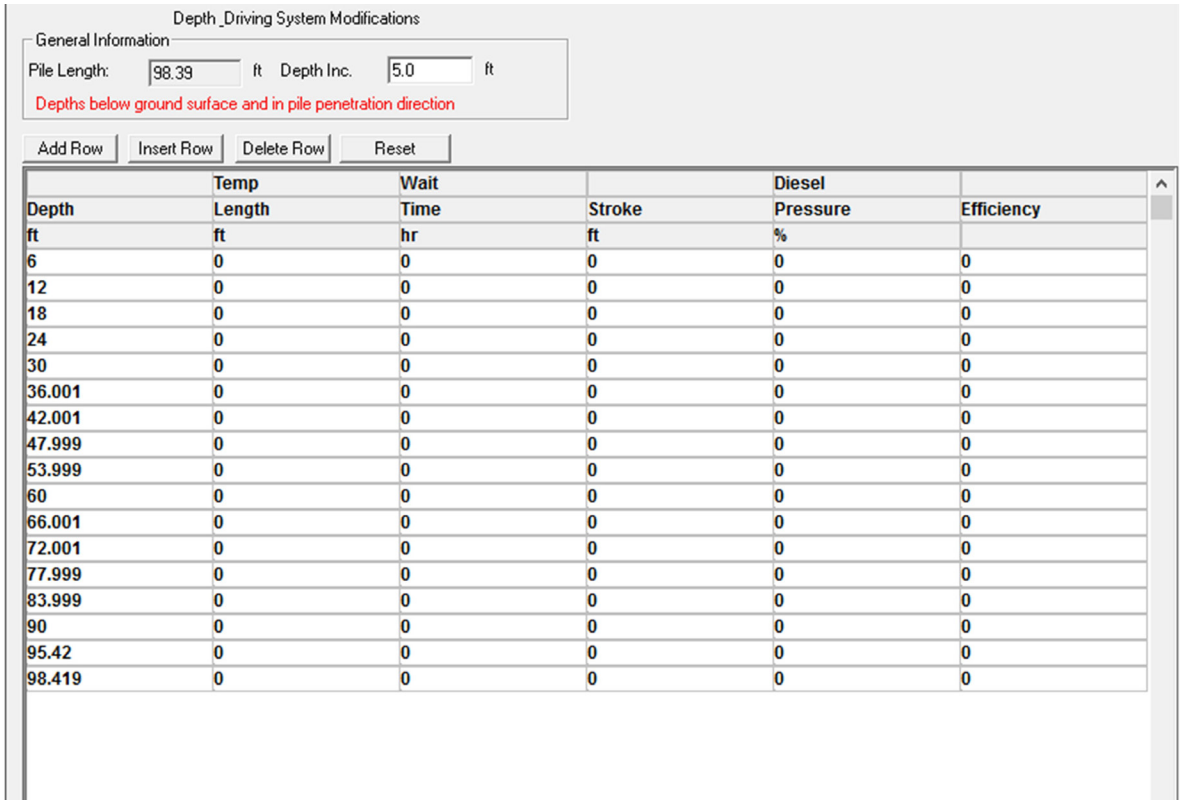

	Temp	Wait		Diesel	
Depth	Length	Time	Stroke	Pressure	Efficiency
ft	ft	hr	ft	%	
6	0	0	0	0	0
12	0	0	0	0	0
18	0	0	0	0	0
24	0	0	0	0	0
30	0	0	0	0	0
36.001	0	0	0	0	0
42.001	0	0	0	0	0
47.999	0	0	0	0	0
53.999	0	0	0	0	0
60	0	0	0	0	0
66.001	0	0	0	0	0
72.001	0	0	0	0	0
77.999	0	0	0	0	0
83.999	0	0	0	0	0
90	0	0	0	0	0
95.42	0	0	0	0	0
98.419	0	0	0	0	0

Figure 12-38 Depths, modifiers input form.

12.7.1 Other Analysis Options

A variety of options exist in the GRLWEAP program for non-standard input, analyses, and output. The setting of important options is indicated on the Main Input screen (see Figure 12-39). Please refer to the program Help Menu for additional, less frequently used options.

Important options pertain to the modification of certain hammer parameter, pile model, and soil resistance input. These options are generally accessible by clicking

Options/General Options, or Hammer Parameters, or Pile Parameters, or Soil Parameters. For proper hammer modeling, the Efficiency and Stroke values contained in the hammer data file must often be modified. This modification can be done on the Main Input screen below the Hammer Information window. Alternatively, these and other hammer details may be modified by clicking on Options, Hammer Parameters. Relevant quantities are explained in the Help Menu and will not be further discussed here.

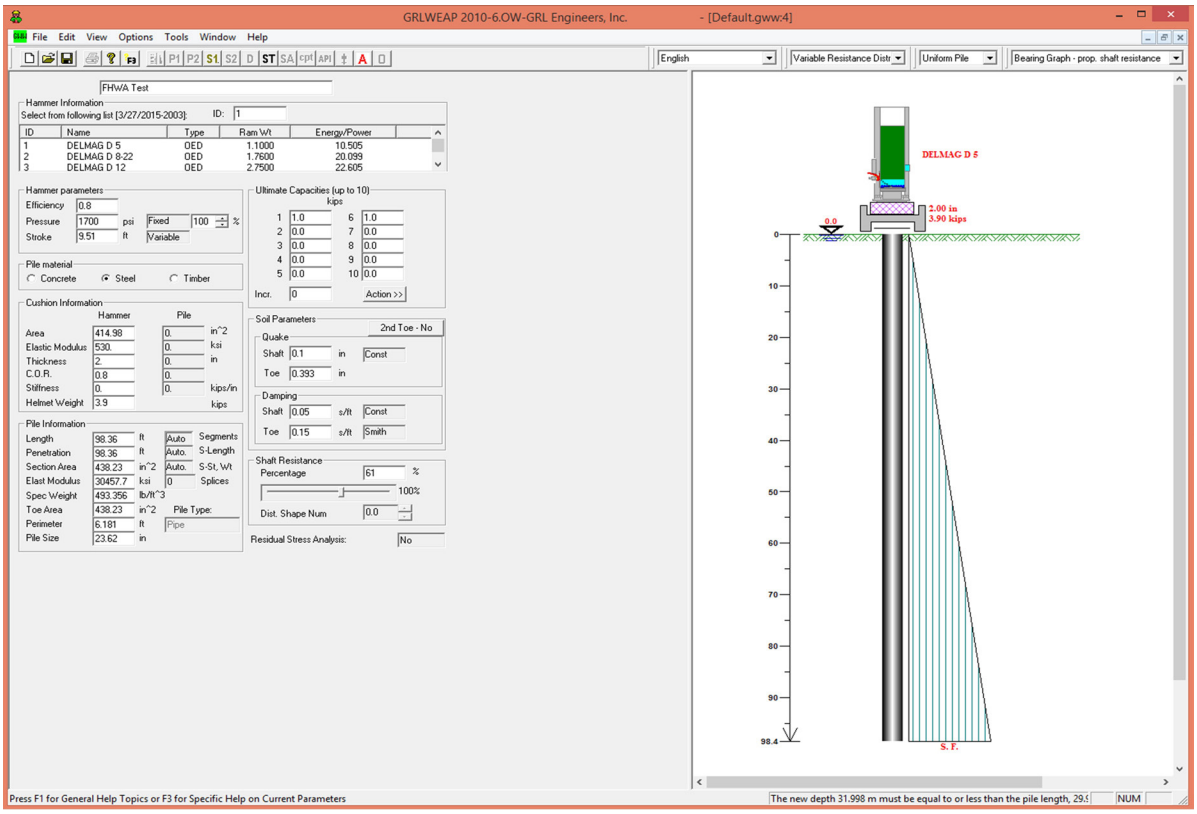

Figure 12-39 Completed main input for a simple bearing graph.

As mentioned, efficiency is a very important hammer parameter. The efficiency values in the hammer data file were selected according to the observed average behavior of all hammers of the same type. However, depending on a particular hammer's make or state of maintenance, the hammer may perform differently than assumed, and its parameters should be adjusted accordingly. Furthermore, because of uncertainties in actual hammer performance, greater and lesser efficiency values should be analyzed for conservative stresses and blow counts, respectively. Finally, efficiency should be adjusted for an inclined or batter pile which is simplified in the Options/Pile Parameters/Batter Inclination Input Window shown in Figure 12-40. Refer to the Help Menu for recommended efficiency reductions and further guidance for inclined pile driving.

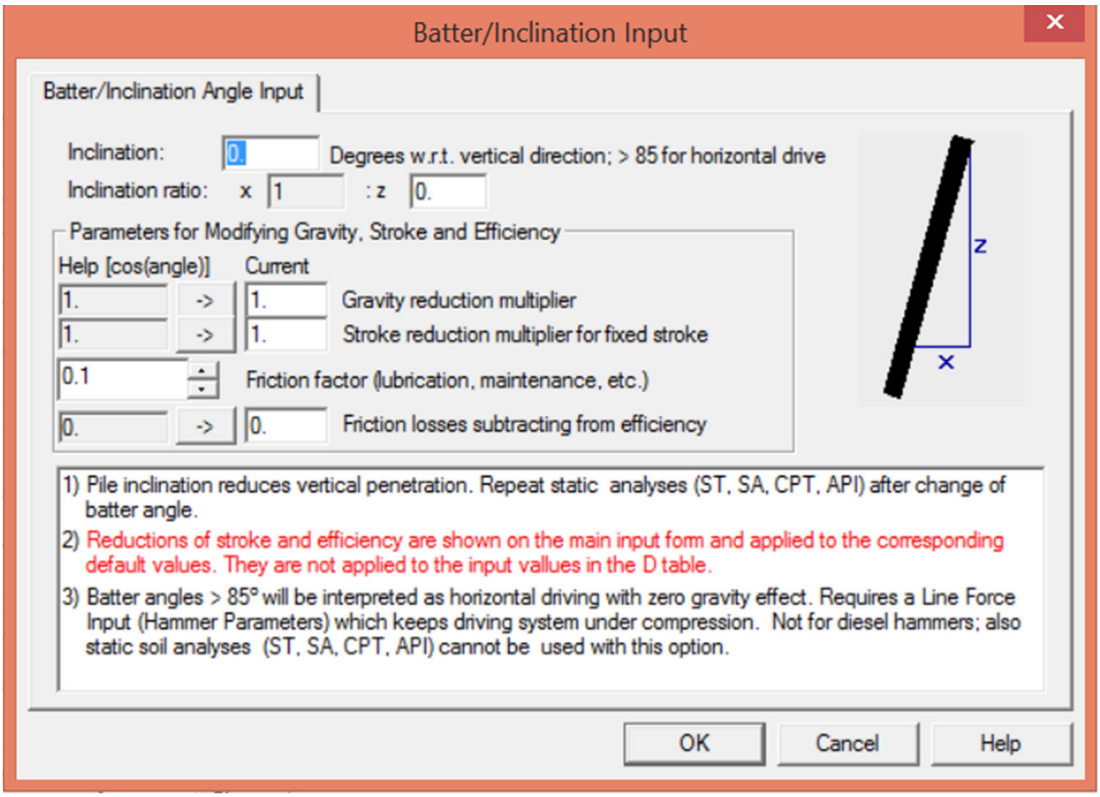

Figure 12-40 Batter/Inclination input window.

Stroke in feet is a useful performance parameter for single acting diesel hammers whose ram is visible and whose stroke is not equal to the rated value. For other hammers, energy level may be known, but since stroke is equal to energy divided by ram weight, stroke serves as an input for an adjusted hammer energy setting.

Pressure in psi is important for diesel hammers when the calculated and observed hammer strokes differ. A new pressure value may be tried for better agreement. Also, if the hammer is physically run at a reduced fuel setting, the pressure value should be reduced in the program accordingly.

Several options for **Pile Parameters** are available in GRLWEAP primarily for the purpose of flexibility in pile model generation. The status of many of these options is indicated under the Pile top Information on the Main Input Form.

The **Number of Pile Segments** may either be automatically set based on segment lengths of 3.3 feet, or the user may use a different number by clicking on **Options**, **Pile Parameters**, **Pile Segment Option**. Usually the program default of 3.3 feet segment lengths yields satisfactory accuracy. To avoid loss of this computational accuracy, only segments smaller than the default value should be entered. In the Pile Segment Option, the user can also modify the relative length of the segments

(the information field marked S-Length would then be set to Man. for manual) and enter the segment stiffness and mass values. In the latter case, the information field marked S-ST, W_t would be set to manual.

Some piles are spliced with devices that allow for slippage during extension or compression. In Options/Pile Parameters/Splices, the user can choose the Number of Splices to be modeled and, after clicking on Update, edit the entry fields shown in Figure 12-41. For each splice, the user enters the Distance in feet of the splice location referenced from the pile head, the Tension Slack in feet, i.e. the distance that the splice can extend without transmitting a tension force, the C.O.R. or coefficient of restitution for the spring representing the spliced section, and the Compression Slack in feet, i.e., the distance that the splice can compress with a spring stiffness which increases linearly from zero to its loading value. The Main Input Form indicates the selected number of splices; the graphic of the hammer, driving system, pile, and soil model on the Main Input Form also indicates a splice with a slight gap in the pile representation. Note that neither an uncracked welded splice of a steel pile nor a well performing epoxy splice of a concrete pile requires slack modeling. These splices do not allow for slippage and, therefore, should be modeled as a uniform pile section and not as a splice with a slack.

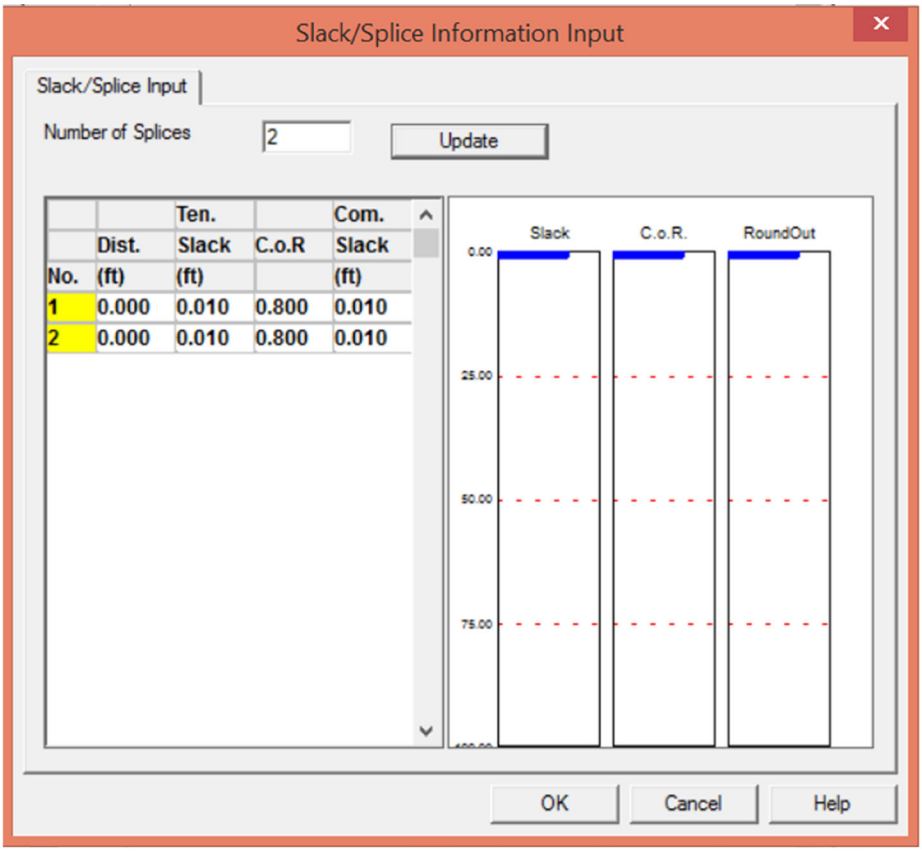

Figure 12-41 Slack/Splice information input window.

Non-uniform pile properties are modeled by selecting Non-Uniform Pile from the Pile Type drop-down menu which activates the P1 window. The user should complete the necessary information by specifying pile variations and adding the necessary number of rows immediately above and below a change of cross sectional area (**X-Area**), elastic modulus (**E. Modulus**), specific weight (**Spec. Wt.**), **Perimeter**, and Critical Index (**Crtcl. Index**) (see Figure 12-42). Note that Perimeter is needed for the computation of total shaft resistance in Drivability analyses. The Critical Index input is needed for the listing of critical rather than absolute maximum stresses in the result summary for piles consisting of materials of different strengths (for example, for a concrete pile with steel stinger, the concrete section may be more important to investigate for stresses then the steel stinger, even though the steel stinger may have stresses which are 10 times higher than the concrete stresses). Pile sections for which the Critical Index is set 1 are included in the search for a maximum tension and compression stresses for final output.

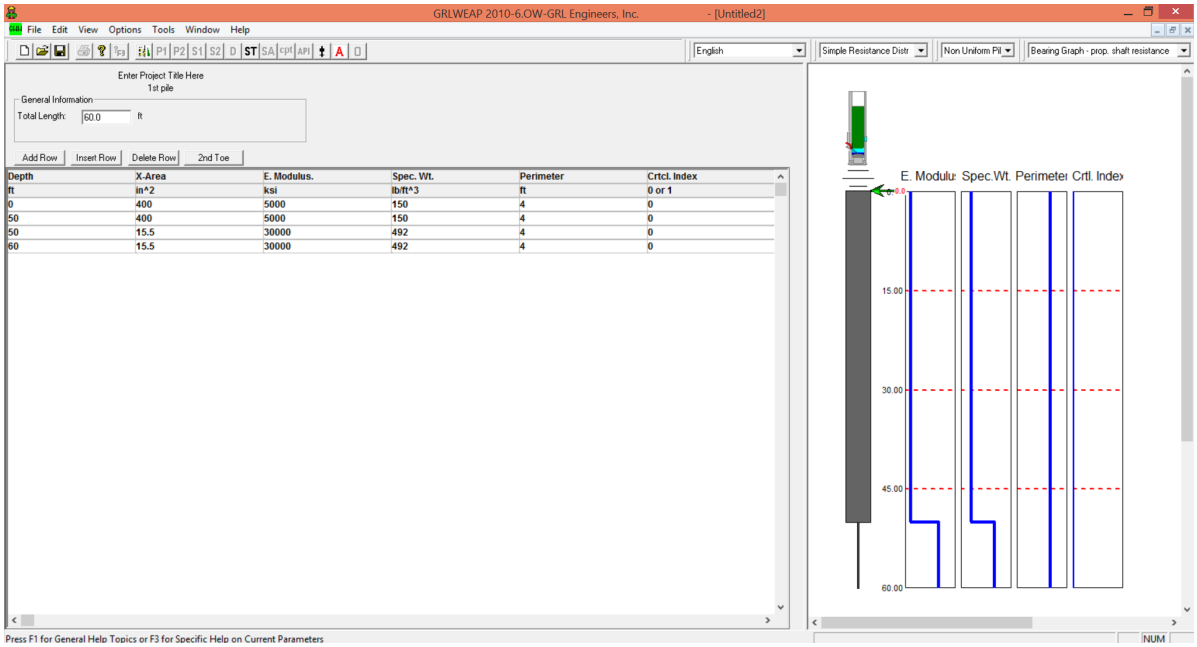

Figure 12-42 Data entry screen for non-uniform piles.

Several infrequently used options concerning primarily the pile model can be accessed in Options/General Options/Numeric (see Figure 12-43). An important but somewhat different pile option leading to an alternate type of analysis is the Residual Stress Analysis (RSA). The input number indicates the maximum number of repeat analyses (or blows) allowed, with a “1” representing the absolute limit of 100 cycles. Potentially important for large piles is the input of an adjusted Hammer and Pile Gravity. The default gravitational constant is 32.17 ft/s^2. The default value would represent a vertically driven pile above the water table. If the static weight is less

due to either pile inclination or buoyancy, this value should be reduced using Options/General Options/Numeric. Note that the hammer and pile mass magnitudes will not be affected by this change of their gravitational constant.

Soil parameter options, like pile options, allow for increased input flexibility. Under Options/Soil Parameters, it is possible to enter individual nominal resistance values, damping, and quake values for each pile segment. Use of these options causes the corresponding field labels in the soil input section of the Main Input Form to read "Variable."

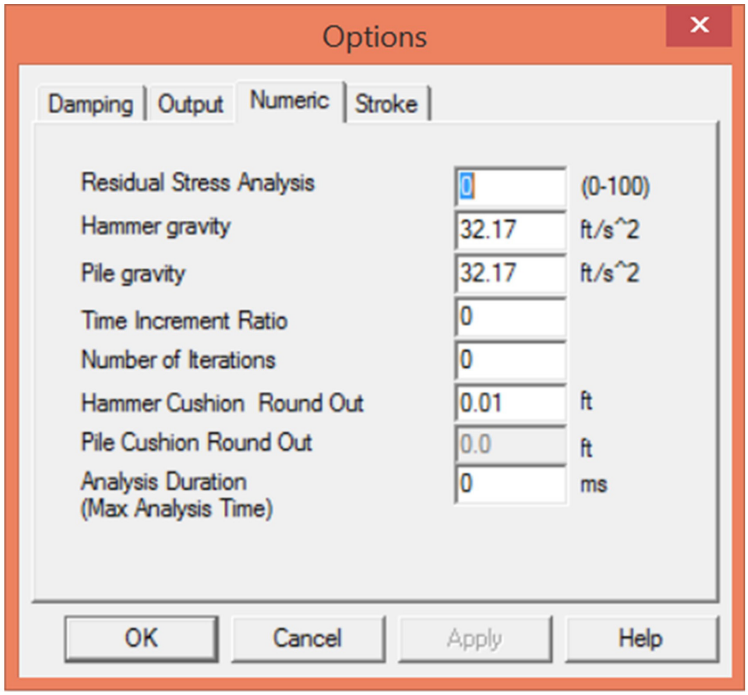

Figure 12-43 Numeric options window.

The **Damping Option**, accessible in Options/General Options/Damping (Figure 12-44), is rarely used for routine applications and is more useful for the researcher. In most instances, the Soil Damping is set to Smith damping. If the Residual Stress Analysis is performed or a vibratory hammer is analyzed then the Smith viscous damping option should be selected. Also Refined Wave Equation analyses sometimes have to done with Smith viscous damping for a good match. Hammer Damping and Pile Damping Options have been preset to a percentage of the impedance of the ram and hammer cushion and the pile, respectively, though the preset values may be replaced with small non-negative integers. Given a negative input, the program will read a zero value. For the pile material, the program automatically chooses values of 1, 2 and 5 for steel, concrete and wood, respectively. Another pile material (e.g., plastic piles) may require other, possibly

higher inputs. While not enough is known about these parameters, their effect on the computed results is relatively insignificant.

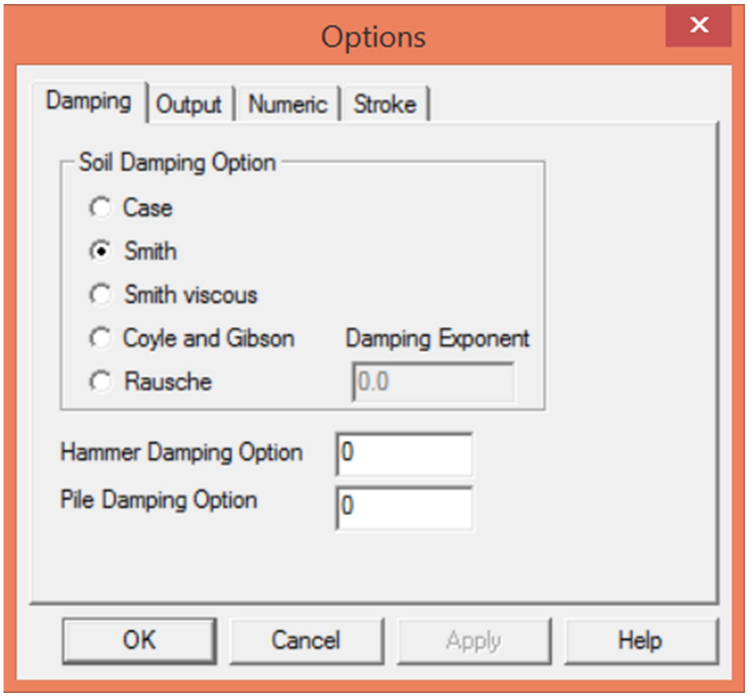

Figure 12-44 Damping options window.

The **Stroke Option**, important for diesel hammers, is accessible in Options/General Options/Stroke (see Figure 12-45). For any diesel hammer, the stroke is a function of fuel settings, pile mass and stiffness, and soil resistance. The stroke option allows the user to control whether the program will analyze a fixed stroke or calculate the stroke (default) based on the combustion pressure provided in either the hammer database or the user modified input. A fixed stroke can either be analyzed with an iteratively adjusted combustion pressure, such that upstroke equals down stroke, or with a single impact whose upstroke is then potentially different from its down stroke. On the Main Input Form below the Hammer Information window, this selected stroke option is identified. The selection of the Stroke Option is particularly important for Inspector's Chart analyses, and the reading of the associated Help is strongly recommended.

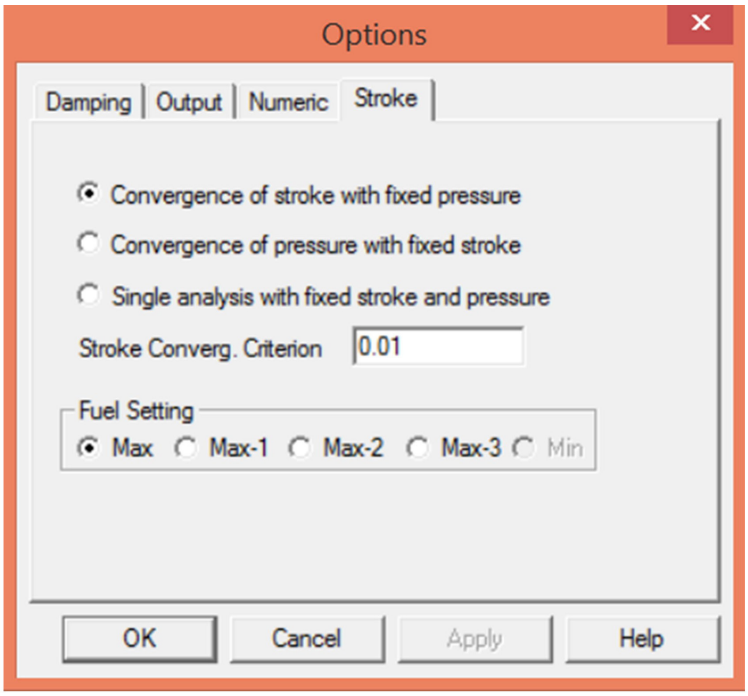

Figure 12-45 Stroke options window for diesel hammers.

The Stroke Options window also allows for a selection of Fuel Settings for those diesel hammers that have stepwise adjustable fuel pumps. Alternatively, the corresponding fractions of the maximum combustion pressures can be selected on the Main Input Form. As noted in Section 12.6.3, analyzing a hammer with a high combustion pressure, even if the high stroke is the result of pre-ignition, may lead to high calculated transferred energies and, therefore, non-conservative nominal resistance predictions and conservative stress predictions. On the other hand, if the observed hammer stroke is relatively low and friction (which should be modeled with a reduced hammer efficiency) has been eliminated as a reason for the low stroke, a reduced combustion pressure presents a reasonable analysis option. Because of the potential for an overprediction of nominal resistance due to excessive pressure adjustment, the Inspector's Chart option does not increase the combustion pressure above the value in the hammer data file despite the presence of any values for high stroke analyses in the "**Convergence of pressure with fixed stroke**."

12.8 WAVE EQUATION ANALYSIS OUTPUT AND INTERPRETATION

The GRLWEAP program offers several output options that may be invoked or modified using Options, General Options, Output as displayed in Figure 12-46. The box labeled Type allows for selection of certain variables (e.g., force, velocity, stress) at a number of different segments. The user may opt to plot these variables as a function of time or create a table for transfer to other programs. Of particular interest is the plotting of pile top force and proportional velocity vs. time for comparison with dynamic measurements.

The Numerical box underneath allows for the control of the numerical output in one of three means. Choosing Minimum (default for drivability analyses) will exclude the extrema tables that are included in the Normal output selection. The extrema tables are very helpful when investigating the location of maximum stress values, and even though they may make the output very long, it is often desirable to revert to the Normal option, even for drivability analyses. Another worthy candidate for the normal output is the multi-material pile. The final numerical option, Debug generates so much numerical output that it is rarely needed for real applications.

After an analysis has been run, clicking the **O** (**Output**) icon transfers control to the output program in which several output modes (depending on output and analysis options) of the Project Summary (containing several important parameters and title components) become available: **Bearing Graph** or **Drivability**, **Variables vs. Time** and **Numeric results**.

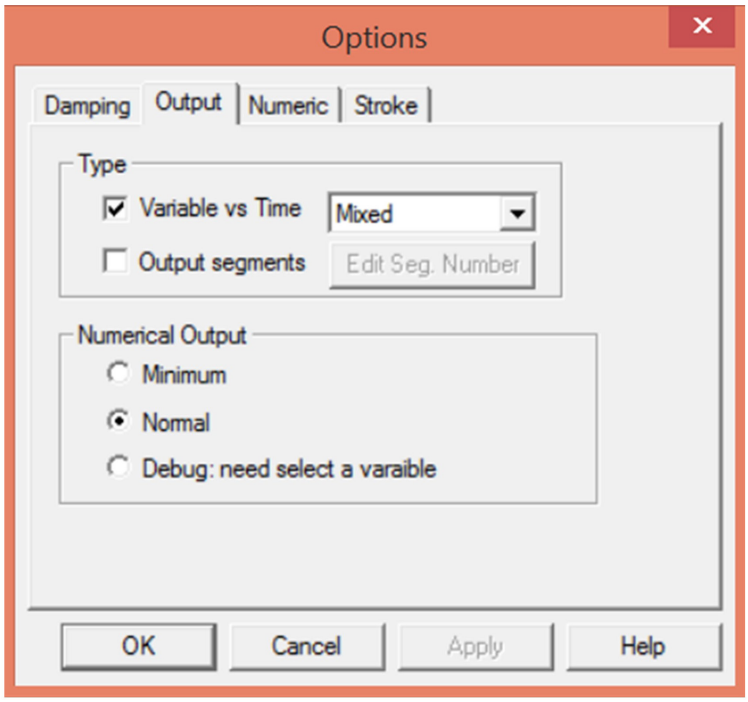

Figure 12-46 Output options window.

The Numerical GRLWEAP Output, or Numeric results, is the most important output. It begins with a listing of file names used for input and the input file (*.GWW). There follows a disclaimer pointing out some of the uncertainties associated with wave equation analyses. The user is urged to check that the correct data file is used and consider the disclaimer when drawing conclusions from analysis results.

The first page of output, shown in Figure 12-47, lists the hammer and drive system components used in the analysis. Hence hammer model, stroke, and efficiency, helmet weight, and hammer and pile cushion properties including thickness, area, elastic modulus, and coefficient of restitution are but a few of the input details printed on this page.

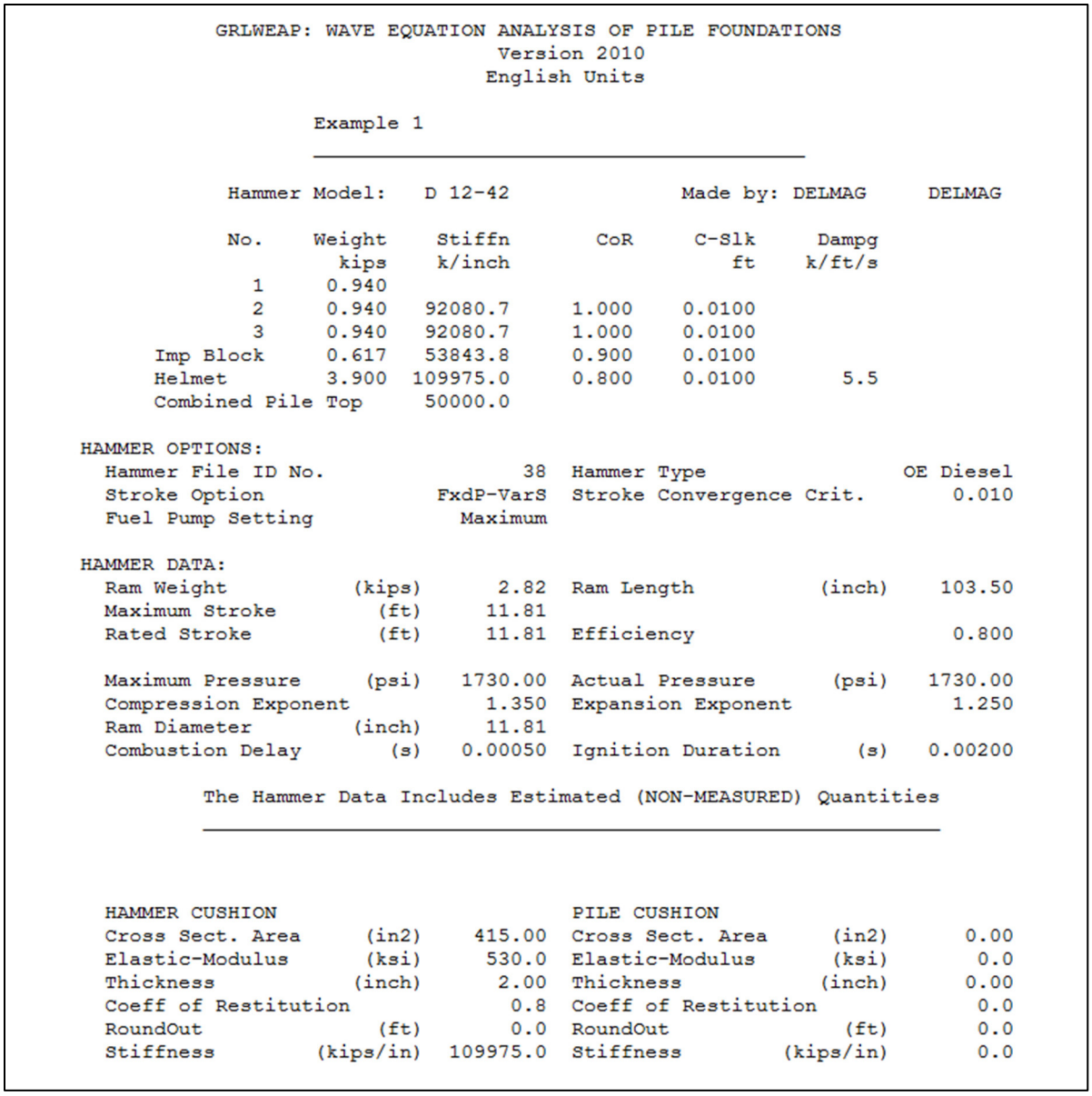

```
            GRLWEAP: WAVE EQUATION ANALYSIS OF PILE FOUNDATIONS
                                 Version 2010
                               English Units

                        Example 1
                        _________________________________________

            Hammer Model:   D 12-42              Made by: DELMAG     DELMAG

            No.     Weight     Stiffn       CoR      C-Slk      Dampg
                      kips     k/inch                   ft     k/ft/s
              1      0.940
              2      0.940    92080.7     1.000     0.0100
              3      0.940    92080.7     1.000     0.0100
      Imp Block      0.617    53843.8     0.900     0.0100
      Helmet         3.900   109975.0     0.800     0.0100        5.5
      Combined Pile Top      50000.0

HAMMER OPTIONS:
  Hammer File ID No.                 38  Hammer Type                  OE Diesel
  Stroke Option               FxdP-VarS  Stroke Convergence Crit.         0.010
  Fuel Pump Setting             Maximum

HAMMER DATA:
  Ram Weight           (kips)      2.82  Ram Length           (inch)     103.50
  Maximum Stroke         (ft)     11.81
  Rated Stroke           (ft)     11.81  Efficiency                      0.800

  Maximum Pressure      (psi)   1730.00  Actual Pressure       (psi)    1730.00
  Compression Exponent            1.350  Expansion Exponent               1.250
  Ram Diameter         (inch)     11.81
  Combustion Delay       (s)   0.00050  Ignition Duration       (s)    0.00200

          The Hammer Data Includes Estimated (NON-MEASURED) Quantities
          ____________________________________________________________


  HAMMER CUSHION                       PILE CUSHION
  Cross Sect. Area      (in2)    415.00  Cross Sect. Area      (in2)        0.00
  Elastic-Modulus       (ksi)    530.0   Elastic-Modulus       (ksi)        0.0
  Thickness            (inch)     2.00  Thickness            (inch)       0.00
  Coeff of Restitution              0.8  Coeff of Restitution                0.0
  RoundOut               (ft)       0.0  RoundOut               (ft)        0.0
  Stiffness         (kips/in)  109975.0  Stiffness         (kips/in)        0.0
```

Figure 12-47 Hammer model, hammer options, and driving system output.

The second page of output, presented in Figure 12-48, summarizes the pile and soil model used in the analysis. A brief summary of the pile profile is provided at the top of the page and includes the pile length, area, modulus of elasticity, specific weight, perimeter, material strength (normally 0 for uniform piles), wave speed, and pile impedance (EA/C). A detailed summary of the pile and soil model follows the pile profile. The detailed pile model includes the number of pile segments, their weight and stiffness, and any compression slacks (C-Slk) or tension slacks (T-Slk) with associated coefficient of restitution (C.O.R.). The listing also shows segment bottom depth (LbTop) and the averages of both segment circumference and cross sectional area. The summarized soil model includes the soil static soil resistance distribution (Soil-S), the soil damping parameters (Soil-D) along the shaft and at the pile toe, as

well as the soil quakes along the shaft and at the pile toe. Additional pile and soil modeling options, including the percent shaft resistance, are summarized below in Figure 12-48.

On the third page, shown in Figure 12-49, an extrema table is printed for each pile segment number. This extrema output (Table 12-10) is printed for each analyzed nominal resistance and includes:

Table 12-10 GRLWEAP Extrema Output

Abbreviation	Description
No	Pile segment number
mxTForce	Maximum tension (negative) force in kips
mxCForce	Maximum compression force in kips
mxTStrss	Maximum tension (negative) stress in ksi
mxCStrss	Maximum compression stress in ksi
max V	Maximum velocity in ft/s
max D	Maximum displacement in inches
max Et	Maximum transferred energy in kip-ft

The "t" values following the extreme values are times in milliseconds relative to hammer impact. Note that tension is shown as a negative in these tables. For the analysis of diesel hammers, the iteration on hammer stroke is indicated beneath the extrema table information followed by the maximum combustion pressure analyzed in psi.

For bearing graph analyses, GRLWEAP concludes by printing a summary table for all input nominal resistances (ultimate capacities) after the extrema table listing. The summary table is illustrated in Figure 12-50 and includes the analyzed nominal resistance (ultimate capacity, R_{ut}) and corresponding penetration resistance (Bl Ct) for blow count, analyzed hammer stroke (for diesel hammers, both the down stroke and the rebound stroke), maximum tension stress (negative, Ten Str), maximum compression stress (Comp Str), maximum transferred energy (ENTHRU), and, for diesel hammers, hammer operating speed (Bl Rt). The indicators "i t" locate where (pile segment number) and when (time after impact in m/s) the extreme stress values occur.

Example 1 07/21/2015
GRLWEAP Version 2010

PILE PROFILE:

Toe Area	(in2)	438.250	Pile Type		Pipe
Pile Size	(inch)	23.620			

L b Top ft	Area in2	E-Mod ksi	Spec Wt lb/ft3	Perim ft	C Index	Wave Sp ft/s	EA/c k/ft/s
0.0	400.00	5000.	150.0	6.7	1	12426.	160.9
50.0	400.00	5000.	150.0	6.7	1	12426.	160.9
50.0	53.00	30000.	492.0	4.0	0	16807.	94.6
60.0	53.00	30000.	492.0	4.0	0	16807.	94.6

Wave Travel Time 2L/c (ms) 9.237

	Pile and Soil Model				Total Capacity Rut (kips)			1310.0		
No.	Weight kips	Stiffn k/in	C-Slk ft	T-Slk ft	CoR	Soil-S kips	Soil-D s/ft	Quake inch	LbTop ft	Perim ft	Area in2
1	1.389	50000	0.010	0.000	0.85	2.5	0.050	0.100	3.33	6.7	400.0
2	1.389	50000	0.000	0.000	1.00	7.4	0.050	0.100	6.67	6.7	400.0
3	1.389	50000	0.000	0.000	1.00	12.3	0.050	0.100	10.00	6.7	400.0
4	1.389	50000	0.000	0.000	1.00	17.3	0.050	0.100	13.33	6.7	400.0
5	1.389	50000	0.000	0.000	1.00	22.2	0.050	0.100	16.67	6.7	400.0
6	1.389	50000	0.000	0.000	1.00	27.1	0.050	0.100	20.00	6.7	400.0
7	1.389	50000	0.000	0.000	1.00	32.1	0.050	0.100	23.33	6.7	400.0
8	1.389	50000	0.000	0.000	1.00	37.0	0.050	0.100	26.67	6.7	400.0
9	1.389	50000	0.000	0.000	1.00	41.9	0.050	0.100	30.00	6.7	400.0
10	1.389	50000	0.000	0.000	1.00	46.9	0.050	0.100	33.33	6.7	400.0
11	1.389	50000	0.000	0.000	1.00	51.8	0.050	0.100	36.67	6.7	400.0
12	1.389	50000	0.000	0.000	1.00	56.7	0.050	0.100	40.00	6.7	400.0
13	1.389	50000	0.000	0.000	1.00	61.7	0.050	0.100	43.33	6.7	400.0
14	1.389	50000	0.000	0.000	1.00	66.6	0.050	0.100	46.67	6.7	400.0
15	1.389	50000	0.000	0.000	1.00	71.5	0.050	0.100	50.00	6.7	400.0
16	0.604	39750	0.000	0.000	1.00	76.5	0.050	0.100	53.33	4.0	53.0
17	0.604	39750	0.000	0.000	1.00	81.4	0.050	0.100	56.67	4.0	53.0
18	0.604	39750	0.000	0.000	1.00	86.3	0.050	0.100	60.00	4.0	53.0
Toe						510.9	0.150	0.393			

22.644 kips total unreduced pile weight (g= 32.17 ft/s2)
22.644 kips total reduced pile weight (g= 32.17 ft/s2)

PILE, SOIL, ANALYSIS OPTIONS:

Non-uniform pile		Pile Segments: Automatic	
No. of Slacks/Splices	2	Pile Damping (%)	1
Pile Penetration (ft)	100.00	Pile Damping Fact.(k/ft/s)	3.219
% Shaft Resistance	61		
Soil Damping Option	Smith		
Max No Analysis Iterations	0	Time Increment/Critical	160
Output Time Interval	2	Analysis Time-Input (ms)	0
Output Level: Variable vs Time			

Figure 12-48 Pile, soil, and analysis options.

Example 1 07/21/2015
GRLWEAP Version 2010

Rut= 1310.0, Rtoe = 510.9 kips, Time Inc. =0.060 ms

No	mxTForce kips	mxCForce kips	mxTStrss ksi	mxCStrss ksi	max V ft/s	max D inch	max Et kip-ft
1	0.0	1483.8	0.00	3.71	9.01	0.186	13.31
2	-149.2	1477.7	-0.37	3.69	8.95	0.182	13.21
3	-210.2	1473.1	-0.53	3.68	8.87	0.178	13.03
4	-210.1	1466.5	-0.53	3.67	8.79	0.174	12.80
5	-229.3	1454.5	-0.57	3.64	8.69	0.170	12.50
6	-248.2	1440.8	-0.62	3.60	8.56	0.165	12.15
7	-257.0	1424.4	-0.64	3.56	8.44	0.160	11.74
8	-276.0	1402.0	-0.69	3.50	8.28	0.157	11.30
9	-291.3	1381.2	-0.73	3.45	8.13	0.158	10.83
10	-318.5	1354.3	-0.80	3.39	7.94	0.160	10.36
11	-325.8	1327.0	-0.81	3.32	7.77	0.162	9.86
12	-332.8	1295.1	-0.83	3.24	7.58	0.164	9.27
13	-345.0	1256.7	-0.86	3.14	7.50	0.167	8.60
14	-328.4	1179.9	-0.82	2.95	7.85	0.169	7.84
15	-287.4	1010.2	-0.72	2.53	8.74	0.169	6.87
16	-311.8	789.1	-5.88	14.89	9.36	0.166	5.82
17	-248.1	629.8	-4.68	11.88	10.46	0.166	4.74
18	-107.0	422.3	-2.02	7.97	10.78	0.164	4.19

Activated Capacity 1012.2 k
(Eq) Strokes Analyzed and Last Return (ft):
11.81 10.43 10.42

Max. Combustion Pressure 1730.0 psi

Figure 12-49 Extrema table output.

Example 1 07/21/2015
GRLWEAP Version 2010

Rut kips	Bl Ct b/ft	Stroke (ft) down	Stroke (ft) up	Ten Str ksi	i	t	Comp Str ksi	i	t	ENTHRU kip-ft	Bl Rt b/min
655.0	1209.6	9.76	9.75	-1.21	4	22	3.51	1	2	12.4	38.2
1310.0	9999.0	10.43	10.42	-0.86	0	0	3.71	0	0	13.3	36.9

Figure 12-50 Final summary for bearing graph analysis.

Review of the "printed output" can be accomplished on the computer screen before printing. This review is extremely important as it can point out inadvertent omissions or erroneous input data. The reviewer should carefully check ram weight, stroke, efficiency, cushion stiffness, pile mass and stiffness values, soil parameters, etc. Furthermore, any error messages or warnings issued by the program should be checked for relevance to the results.

12.9 PLOTTING OF WAVE EQUATION RESULTS

The summary table results are usually presented in the form of a bearing graph relating the nominal resistance (ultimate capacity) to the pile penetration resistance. Plotting can be done by program built-in plotting routines or by saving the copying Numerical Output data to the clipboard and then pasting it in some other plotting program. The GRLWEAP program provides for the plotting of:

- one or two bearing graphs in the same plot,
- an Inspector's Chart,
- drivability results (e.g., blow count, nominal resistance, stresses, stroke, and transferred energy vs. depth) for one or two gain/loss factors, and
- the plotting of selected variables vs. time (e.g., forces, velocities, displacements etc.)

The wave equation bearing graph or inspector's chart should be provided for the resident construction engineer, pile inspector, and the contractor.

12.10 SUGGESTIONS FOR PROBLEM SOLVING

Table 12-11 summarizes some of the field problems that can be solved through use of wave equation analysis. Field problems may arise due to soil, hammer, driving system, and pile conditions that are not as anticipated or unknown. Of course, all possibilities cannot be treated in this summary. Sometimes, the performance of the wave equation program may produce an unexpected or apparently useless result and a corrective action may be required. A number of such problems together with suggested solutions are listed in Table 12-12. Further information may also be found in PDI (2010) and in the program's Help Menu.

Table 12-11 Suggested Use of the Wave Equation to Solve Field Problems

Problem	Solution
Concrete pile spalling or slabbing near pile head.	Perform wave equation analysis; find pile head stress for observed blow count and compare with allowable stresses. If high calculated stress, add pile cushioning. If low calculated stress, investigate pile quality, hammer performance, hammer-pile alignment.
Concrete piles develop complete horizontal cracks in easy driving.	Perform wave equation analysis; check tension stresses along pile (extrema tables) for observed blow counts. If high calculated tension stresses, add cushioning or reduce stroke. If low calculated tension stresses, check hammer performance and/or perform measurements.
Concrete piles develop complete horizontal cracks in hard driving.	Perform wave equation analysis; check tension stresses along pile (extrema table). If high calculated tension stresses, consider heavier ram. If low calculated tension stresses, take measurements and determine quakes, which may be higher than anticipated.
Concrete piles develop partial horizontal cracks in easy driving.	Check hammer-pile alignment since bending may be the problem. If alignment appears to be normal, tension and bending combined may be too high; solution as for complete cracks.
Steel pile head deforms or timber pile top mushrooms.	Check helmet size/shape; check steel strength; check evenness of pile head, banding of timber pile head. If okay, perform wave equation and determine pile head stress. If calculated stress is high, reduce hammer energy (stroke) for low blow counts; for high blow counts different hammer or pile type may be required.
Unexpectedly low blow counts during pile driving.	Investigate soil borings; if soil borings do not indicate soft layers, pile may be damaged below grade. Perform wave equation and investigate both tension stresses along pile and compression stresses at toe. If calculated stresses are acceptable, investigate possibility of obstructions / uneven toe contact on hard layer or other reasons for pile toe damage.

Table 12-11 Suggested Use of the Wave Equation to Solve Field Problems (Continued)

Problem	Solution
Higher blow count than expected.	Review wave equation analysis and check that all parameters were reasonably considered. Check hammer and driving system. If no obvious defects are found in driving system, field measurements should be taken. Problem could be pre-ignition, preadmission, low hammer efficiency, soft cushion, large quakes, high damping, greater soil strengths, or temporarily increased soil resistance with later relaxation (perform restrike tests to check).
Lower blow count than expected.	Probably soil resistance is lower than anticipated. Perform wave equation and assess soil resistance. Perform restrike testing (soil resistance may have been lost due to pile driving), establish setup factor and drive to lower nominal resistance. Hammer performance may also be better than anticipated, check by measurement.
Diesel hammer stroke (bounce chamber pressure) is higher than calculated.	The field observed stroke exceeds the wave equation calculated stroke by more than 10%. Check that hammer was set to correct setting. Compare calculated and observed blow counts. If observed are higher, soil resistance is probably higher than anticipated. If blow counts are comparable, reanalyze with higher combustion pressure to match observed stroke and assure that pre-ignition is not a problem, *e.g.*, by measurements.
Diesel hammer stroke (bounce chamber pressure) is lower than calculated.	The field observed stroke is less than 90% of the stroke calculated by the wave equation. Check that hammer was set to correct setting. Check that ram friction is not a problem (ram surface should have well lubricated appearance). Compare calculated and observed blow count. If observed one is lower, soil resistance is probably lower than anticipated. If blow counts are comparable, reanalyze with lower combustion pressure to match observed hammer stroke.

Table 12-12 Wave Equation Analysis Problems

Problem	Solution
Cannot find hammer in data file.	Contact the hammer manufacturer or the author(s) of the wave equation program. Pile Dynamics, Inc., for example, regularly updates and posts its hammer data file on its web page. Alternatively, the user may utilize a hammer of same type and of similar ram weight and energy rating and modify its data to match the unlisted hammer's specifications as closely as possible.
Cannot find an acceptable hammer to drive pile within driving stress and penetration resistance limits.	Both calculated stresses and blow counts are too high. Increase pile impedance or material strength or redesign for lower capacities. Alternatively, check whether soil has potential for setup. If soil is fine grained or known to exhibit setup gains after driving, then end of driving nominal resistance may be chosen lower than required. Nominal resistance should be confirmed by restrike testing or static load testing.
Diesel hammer analysis with low or zero transferred energies.	Probably soil resistance too low for hammer to run. Try higher capacities.
Unknown hammer energy setting.	Perform analyses until the cushion thickness/hammer energy setting combination yields acceptable stresses with minimum cushion thickness. Specify that the corresponding cushion thickness and hammer fuel setting be used in the field and their effectiveness verified by measurements.
Cannot find a suggested set of driving system data.	Contact contractor, equipment manufacturer, or use data for similar systems.
Unknown pile cushion thickness.	Perform analyses until cushion thickness/hammer energy setting combination is found that yields acceptable stresses with minimum cushion thickness. Specify that this thickness be used in the field and its effectiveness verified by measurements.
Calculated pile cushion thickness is uneconomical.	In order to limit stresses, an unusually thick pile cushion was needed for pile protection. Try to analyze with reduced energy settings. For tension stress problems, energy settings often can be increased after pile reaches sufficient soil resistance.

Table 12-12 Wave Equation Analysis Problems (Continued)

Problem	Solution
Calculated driving times are unrealistically high or low.	The calculation of driving times is very sensitive, particularly at high blow counts. Use extreme caution when using these results for cost estimation. Also, no interruption times are included and the estimate is only applicable to non-refusal driving.
Wave equation calculated energy and/or forces are difficult to match with field measurements.	In general, it is often difficult to make all measured quantities agree with their calculated equivalents. A 10% agreement should be sufficient. Parameters to be varied include hammer efficiency, diesel hammer combustion pressure, external combustion hammer stroke, coefficients of restitution, hammer cushion properties for steel piles, pile cushion properties for concrete piles, and pile top properties for timber piles. Resistance distribution also may affect the pile top forces.

12.11 ADVANTAGES, DISADVANTAGES, AND LIMITATIONS

One of the primary advantages of wave equation analysis is the ability to evaluate the drivability and suitability of a pile foundation design early in the design process. This allows economic evaluations on pile section selection to be easily and rationally decided based on predicted driving stresses and penetration resistances. For the contractor, wave equation analysis provides one of the best methods for equipment selection, determining the need for pile installation aids, and selecting pile cushion thickness. For the engineer, wave equation analysis provides the best method for hammer approval. No other computational tool for the simulation of the dynamic pile driving event is able to match the convenience and realism of this approach. Once the necessary information for program input is in hand, (closest boring, proposed driving system, and foundation details), a wave equation analysis can be performed relatively quickly.

A disadvantage of wave equation analysis is the information needed on the soil conditions, pile and foundation details, and hammer system for the analyst to make informed program input selections. A dynamic formula is simpler and quicker, albeit also less accurate, as the only input information needed for formula use is generally the hammer energy. The program user should have knowledge of the software

program, soil mechanics, and pile design and construction to understand and correctly apply results in unique and specific applications.
Wave equation limitations include, in some soil conditions, conservative estimates of the nominal resistance. Open end pipe piles or H-piles in granular profiles often behave differently under dynamic and static loading conditions. Under dynamic conditions, a plug may slip and produce additional shaft resistance. However under static loading, a plug may form over the full cross section resulting in soil resistance developing on a larger toe area. The wave equation model in this scenario may suitably predict the static behavior. The nominal resistance determined from wave equation analysis can be unconservative at low blow counts (less than 30 blows per foot) and overly conservative at very high blow counts (greater than 120 blows per foot).

12.12 PRACTICAL ISSUES AND CONSIDERATIONS

When confronted with the task of performing drivability analyses for a major bridge project, the question is often how many different analyses have to be performed to adequately represent the various pile, nominal resistance and soil conditions. Performing too many different analyses is not only time consuming it also may lead to confusions.

Nominal resistance determination by wave equation analysis or dynamic testing in soils with unknown long term behavior requires restrike testing. However, if a restrike test is performed, then it would add little cost to do dynamic testing at the same time and take advantage of a higher resistance factor. Thus wave equation based nominal resistance determination is only practical for small jobs where experience with similar conditions exist so that no restrike testing is necessary. In that case the use of the Inspector's Chart is a valuable tool. For open end diesel hammers, this would, however, require that the hammer stroke is accurately monitored. Also in that case, care should be taken to check whether or not there are unusual changes in stroke and/or blow count vs. depth behavior which could, for example, be indications of an overheating hammer.

When analyzing the driving long concrete piles with a large number of hammer blows, it is important to consider that pile cushion replacement should be done after approximately 1500 hammer blows. A drivability analysis has to properly reflect the pile cushion replacement by a change of stiffness. It is not advisable to schedule such a cushion change shortly before the end of driving where a new cushion would cause a low energy transfer and therefore an inflated blow count.

When specifying a blow count criterion two considerations are important: if the end of penetration resistance is low because of a large hammer, check to see if the hammer energy can be sufficiently reduced to provide a driving criterion above 30 blows/ft. Considering soil setup and allowing for a criterion with reduced nominal resistance may lead to a situation where the pile driving hammer is incapable to producing a blow count less than 120 blows/ft during a restrike. If nominal resistance verification by dynamic methods is important, then a larger hammer (e.g., a drop hammer) should be provided for the restrike test. Alternatively, the pile driving hammer has to be chosen large enough to produce restrike blow counts below 120 blows/ft.

When driving to a hard rock surface it would be unwise to specify the required penetration resistance in blows/foot. Instead it is recommended to specify a maximum pile penetration under a certain number of blows, for example, not more than ½ inch under 10 hammer blows. Bearing graphs and Inspector's Charts can be provided with this alternative penetration resistance measurement.

REFERENCES

American Association of State Highway and Transportation Officials (AASHTO). (2014). AASHTO LRFD Bridge Design Specifications, US Customary Units, Seventh Edition, with 2015 Interim Revisions. American Association of State Highway and Transportation Officials, Washington, D.C., 1960 p.

Bielefeld, M.W. and Middendorp, P. (1992). Improved Pile Driving Prediction for Impact and Vibratory Hammers. Proceedings of the Fourth International Conference on the Application of Stresswave Theory to Piles, Balkema Publishers, A.A. The Hague, The Netherlands, pp. 395-399.

Blendy, M.M. (1979). Rational Approach to Pile Foundations. Symposium on Deep Foundations, ASCE National Convention.

Brown, D.A., and Thompson, W.R. (2015). Design and Load Testing of Large Diameter Open-Ended Driven Piles. A Synthesis of Highway Practice. NCHRP Synthesis 478, Transportation Research Board, Washington, D.C., 2015.

Cheney, R.S. and Chassie, R.G. (2000). Soils and Foundations Workshop Reference Manual. FHWA HI-00-045, U.S. Department of Transportation, National Highway Institute, Federal Highway Administration, Washington, D.C., 358 p.

Goble, G.G. and Rausche, F. (1976). Wave Equation Analysis of Pile Driving – WEAP Program, FHWA IP-76-14.3., U.S. Department of Transportation, Federal Highway Administration, Office of Research and Development, Washington, D.C., Volumes I-IV.

Goble, G.G. and Rausche, F. (1986). Wave Equation Analysis of Pile Driving - WEAP86 Program. U.S. Department of Transportation, Federal Highway Administration, Implementation Division, McLean, VA, Volumes I-IV.

Hirsch, T.J., Carr, L. and Lowery, L.L. (1976). Pile Driving Analysis, TTI Program, IP-76-13. U.S. Department of Transportation, Federal Highway Administration, Offices of Research and Development, Washington, D.C., 308 p.

Holloway, D.M. and Beddard, D.L. (1995). Dynamic Testing Results Indicator Pile Test Program – I-880. Proceedings of the 20th Annual Members Conference of the Deep Foundations Institute. Charleston, SC, pp. 105-126.

Middendorp, P. (2004). Thirty Years of Experience with the Wave Equation Solution Based on the Method of Characteristics. Proceedings of the Seventh International Conference on the Application of Stresswave Theory to Piles, Selangor, Kuala Lumpur, Malaysia, pp. 95-106.

PDI, Pile Dynamics, Inc. (2010). GRLWEAP Background Report, Version 2010. Cleveland, OH, 149 p.

Rausche, F., Liang, L., Allin, R., and Rancman, D. (2004). Applications and Correlations of the Wave Equation Analysis Program GRLWEAP. Proceedings of the Seventh International Conference on the Application of Stresswave Theory to Piles, Selangor, Kuala Lumpur, Malaysia, pp. 107-123.

Rausche, F., Nagy, M., Webster, S., and Liang, I.L. (2009). CAPWAP and Refined Wave Equation Analyses for Drivability Predictions and Capacity Assessment of Offshore Pile Installations. Proceedings of the ASME Twenty Eighth International Conference on Ocean and Arctic Engineering, Paper No. OMAE2009-80163, Honolulu, HI, pp. 375-383.

Reiding, F.J., Middendorp, P., Schoenmaker, R.P., Middendorp, F.M., and Bielefeld, M.W. (1988). The FPDS-2, A New Generation of Foundation Diagnostic Equipment. Proceedings of the Third International Conference on the Application of Stress Wave Theory to Piles, Ottawa, Canada, BiTech Publishers, pp. 123-134.

Smith, E.A.L. (1960). Pile Driving Analysis by the Wave Equation. American Society of Civil Engineers (ASCE), Journal of the Soil Mechanics and Foundations Division, Vol. 86, No. 4, pp. 35-61.

Soares, M., de Mello, J., and de Matos, S. (1984). Pile Drivability Studies, Pile Driving Measurements. Proceedings of the Second International Conference

on the Application of Stress-Wave Theory to Piles, Balkema Publishers, A.A., Stockholm, Sweden, pp. 64-71.

U.S. Army Corps of Engineers, (1991). Design of Pile Foundations, Engineering Manual EM 1110-2-2906. U.S. Department of the Army, Washington, D.C., 184 p.

CHAPTER 13

DYNAMIC FORMULAS

13.1 BACKGROUND

Engineers have attempted to find rational methods to determine the geotechnical resistance of a driven pile as long as they have been used for structure foundations. Initially, prediction methods were proposed using pile penetration observations made during driving. However, the only realistic measurement that could be obtained during driving was the pile set per blow. Thus energy concepts equating the potential energy of the hammer to the penetration resistance of the pile (set per blow) as it is driven through the soil were developed to estimate the geotechnical capacity or nominal pile resistance. In equation form this can be expressed as:

$$\mathrm{W\,h} = R_n\, s_b \qquad \text{Eq. 13-1}$$

Where:

- W = ram weight.
- h = ram stroke.
- R_n = nominal resistance.
- s_b = set per blow.

These types of expressions are known as dynamic formulas. Because of their simplicity, dynamic formulas have been widely used for many years. Numerous dynamic formulas have also been proposed over time and some include consideration of pile weight, energy losses in drive system components, pile temporary compression, and other factors. Whether simple or more complex dynamic formulas are used, the nominal resistances determined by dynamic formulas have generally shown poor correlations and wide scatter when statistically compared with the nominal resistances determined by static load test results.

AASHTO (2014) LRFD Bridge Design Specifications include two dynamic formulas; the FHWA modified Gates formula, discussed herein in Section 13.3.1, and an AASHTO modified version of the Engineering News formula, discussed further in Section 13.3.2. Both the AASHTO design and construction specifications state a dynamic formula should not be used when the nominal resistance exceeds 600 kips.

13.1.1 Historical Accuracy of Dynamic Formulas

Wellington proposed the popular Engineering News formula in 1892. It was developed for evaluating the nominal resistance or capacity of timber piles driven primarily by drop hammers in sand. Concrete and steel piles were unknown at that time, as were many of the pile hammer types and hammer sizes used today. Therefore, it should be of little surprise that the formula performs poorly in predicting the capacity or nominal resistance of the pile foundations used today.

The inadequacies of dynamic formulas have been known for a long time. In 1941, an ASCE committee on pile foundations assembled the results of numerous static load tests along with the predicted capacities from several dynamic formulas, including the Engineering News, Hiley, and Pacific Coast formulas. The mean failure load of the load test database was 91 tons. After reviewing the database, Peck (1942) proposed that a new and simple dynamic formula could be used that stated the capacity of every pile was 91 tons. Peck concluded that the use of this new formula would result in a prediction statistically closer to the actual pile capacity than that obtained by using any of the dynamic formulas contained in the 1941 study. A more detailed discussion of both the 1941 ASCE debate as well as the inadequacies of dynamic formulas can be found in Likins et al. (2012).

Chellis (1961) noted that the actual factor of safety obtained by using the Engineering News formula varied from as low as ½ to as high as 16. Sowers (1979) reported that the safety factor from the Engineering News formula varied from as low as 2/3 to as high as 20. Fragasny et al. (1988) in the Washington State DOT study entitled "Comparison of Methods for Estimating Pile Capacity" found that the Hiley, Gates, Janbu, and Pacific Coast Uniform Building code formulas all provide relatively more dependable results than the Engineering News formula.

As part of a FHWA research project, Rausche et al. (1996) compiled a database of static load test piles that included pile capacity predictions using the FHWA recommended static analysis methods, preconstruction and refined wave equations, as well as dynamic measurements coupled with CAPWAP signal matching analysis. The reliability of the various capacity prediction methods were then compared with the results of the static loading tests. The results of these comparisons are presented in Figure 13-1 in the form of probability density function curves versus the ratio of predicted load over the static load test result. The mean values and coefficients of variation for the methods studied are presented in Table 13-1. The closer the mean value of the ratio of the predicted/static load test result is to 1.0 and the smaller the coefficient of variation (COV) the more reliable the method.

Prediction method performance using driving observations of blow count and hammer stroke are identified as EOD for end of driving observations or BOR for beginning of restrike.

In the 1998 version of the FHWA pile manual, the database compiled by Rausche et al. (1996) was modified to include resistance predictions from the allowable load version of the Engineering News as well as the FHWA Modified Gates dynamic formulas at both the end of driving and beginning of restrike. The database for the dynamic formulas was also expanded and included additional data sets. The allowable load determined using the Engineering News formula in this study was compared to one half of the nominal resistance determined from the static load test, while the nominal resistance from the Modified Gates formula was compared directly to the nominal resistance determined from the static load test. The correlation results of the dynamic formulas are included in Table 13-1.

Based on the end of driving data, the Engineering News formula had a mean value of 1.22 and a coefficient of variation of 0.74, while the Modified Gates had a mean value of 0.96 with a coefficient of variation of 0.41. The coefficient of variation is the standard deviation divided by the mean value. Hence, the greater a method's mean value is from 1.0 the lower the accuracy of the method, and the larger the coefficient of variation the less reliable the method. Table 13-1 clearly shows the Engineering News formula has a tendency to overpredict capacity. The higher coefficient of variation also suggests that the Engineering News formula is significantly less reliable than the Modified Gates formula.

Table 13-1 also illustrates that evaluation of pile capacity, by either Gates or Engineering News dynamic formula from restrike set and energy observations, has a significant tendency to overpredict capacity. The Engineering News formula capacity results, from restrike observations, had a mean value of 1.89 and a coefficient of variation of 0.46. The Modified Gates formula capacity results, from restrike observations, had a mean value of 1.33 and a coefficient of variations of 0.48.

If the static load test failure loads are divided by the Engineering News allowable design loads, the database indicates an average factor of safety of 2.3 as compared to the factor of safety of 6.0 theoretically included in the allowable load version of the formula. More important, the actual factor of safety from the Engineering News formula ranged from 0.6 to 13.1. This lack of reliability causes the Engineering News formula to be ineffective as a tool for estimating capacity. The fact that 12% of the database has a factor of safety of 1.0 or less is also significant. However,

complete failure of a bridge due to inadequate geotechnical resistance determined by Engineering News formula is unusual. The problem usually is indicated by long term damaging settlements which occur after construction.

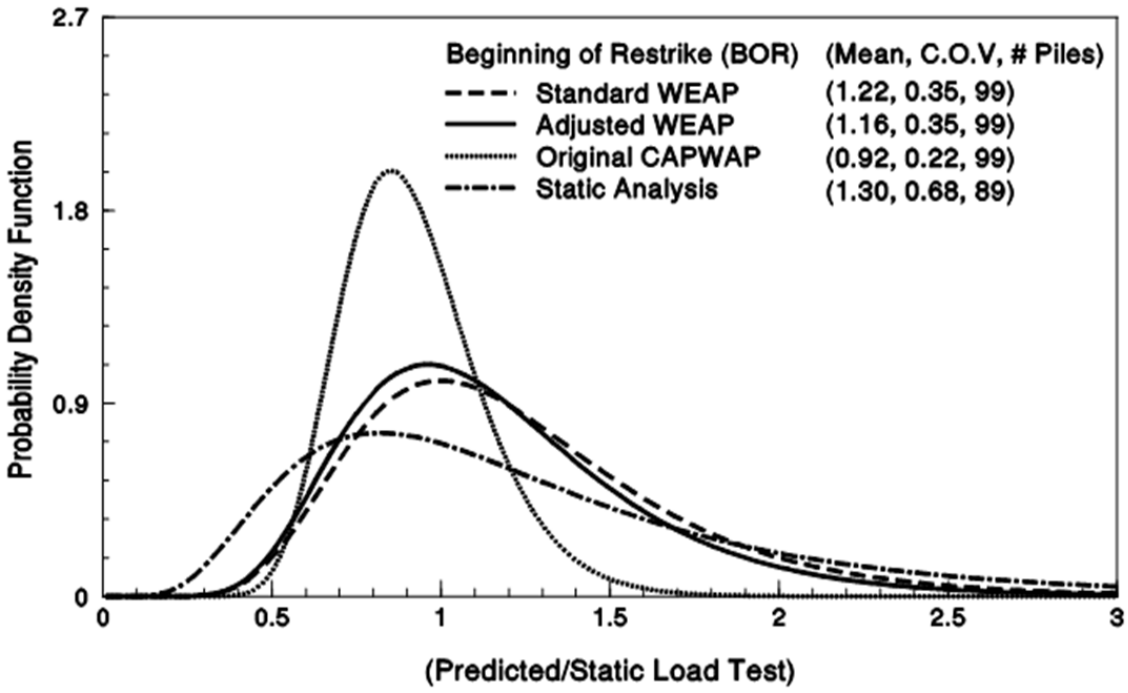

Figure 13-1 Log normal probability density function for four resistance predictions (after Rausche et al. 1996).

Dynamic formulas were historically used on small projects where conservative design load estimates, greater foundation redundancy, and resultant reserve foundation capacity helped mitigate some foundation performance problems. This hidden reserve resistance has been largely reduced in LRFD designs that utilize fewer, larger size piles, with higher nominal resistances.

The version of the Engineering News formula in the AASHTO (2014) LRFD Bridge Design Specifications is a modified from the historical allowable load version and calculates an ultimate capacity or nominal resistance. However, inherent problems with dynamic formulas remain as discussed in Section 13.1.2.

Table 13-1 Mean Values and Coefficients of Variation for Various Methods

Prediction Method	Status	Mean	C.O.V.	# Piles
Standard WEAP*	BOR	1.22	0.35	99
Hammer Performance Adjusted WEAP*	BOR	1.16	0.35	99
CAPWAP*	BOR	0.92	0.22	99
Static Analysis*	-	1.30	0.68	89
Engineering News Formula	EOD	1.22	0.74	139
Engineering News Formula	BOR	1.89	0.46	122
Modified Gates Formula	EOD	0.96	0.41	139
Modified Gates Formula	BOR	1.33	0.48	122

* From Rausche et al. (1996)
EOD = End of Driving, BOR = Beginning of Restrike

13.1.2 Basic Limitations with Dynamic Formulas

Dynamic formulas have limitations, and are therefore less reliable than other field methods for nominal resistance verification. The basic limitations associated with pile driving formulas can be traced to the modeling of each component within the pile driving process: the driving system, the pile, and the soil. Dynamic formulas poorly represent the driving system and the energy losses of drive system components. Dynamic formulas also assume a rigid pile, thus neglecting pile axial stiffness effects on drivability, and further assume that the soil resistance is constant and instantaneous to the impact force. A more detailed discussion of these limitations is presented below.

The derivation of most formulas is not based on a realistic treatment of the driving system. Most formulas only consider the potential energy of the driving system. The variability of equipment performance is typically not considered. Driving systems include many elements in addition to the ram, such as the anvil for a diesel hammer, the helmet, the hammer cushion, and for a concrete pile, the pile cushion. These components affect the distribution of the hammer energy with time, both at and after impact, which influences the magnitude and duration of peak force. The peak force and its duration determine the ability of the driving system to advance the pile into the soil.

Dynamic formulas also assume that the pile is rigid and its length is not considered. This assumption completely neglects the pile's flexibility, which affects its ability to penetrate the soil. The energy delivered by the hammer sets up time-dependent stresses and displacements in the helmet, in the pile, and in the surrounding soil. In addition, the pile behaves, not as a concentrated mass, but as a long elastic rod in which stresses travel longitudinally as waves. Compression waves which travel to the pile toe are responsible for advancing the pile into the ground.

The soil resistance is also very crudely treated by assuming that it is a constant force. This assumption neglects the characteristics of real soil behavior. The dynamic soil resistance is the resistance of the soil to rapid pile penetration produced by a hammer blow. This resistance is in no way similar to the static soil resistance. However, most dynamic formulas consider the resistance during driving equal to the nominal resistance or capacity, and do not consider the dynamic behavior of the soil during pile penetration. The rapid penetration of the pile into the soil during driving is resisted not only by static friction and cohesion, but also by the soil viscosity, which is comparable to the viscous resistance of liquids against rapid displacement under an applied force. The net effect is that the driving process creates dynamic soil resistance forces along the pile shaft and at the pile toe, due to the high shear rate. The soil resistance during driving, from the combination of dynamic soil resistance and available static soil resistance, is generally not equal to the static soil resistance under static loads.

13.2 RESISTANCE FACTORS FOR DYNAMIC FORMULAS

Resistance factors applicable to the nominal axial geotechnical resistance determined from select dynamic formulas are provided in Table 13-2. The resistance factor varies depending on the dynamic formula and, in some cases, pile type. Only the FHWA modified Gates formula and AASHTO modified Engineering News formula have resistance factors in AASHTO. If a dynamic formula is used to establish driving criterion, AASHTO (2010) LRFD Bridge Construction Specifications Article 4.4.4.5 recommends use of the FHWA modified Gates formula. If a dynamic formula other than the FHWA modified Gates formula or AASHTO modified Engineering News formula is used, AASHTO specifications state that it should be calibrated based on measured static load test results to obtain an appropriate resistance factor.

The lower reliability of dynamic formulas is supported by the resistance factors for dynamic formulas contained in the AASHTO (2014) LRFD Bridge Design

Specifications. The AASHTO resistance factor for nominal resistances determined by dynamic formula is 0.40 for the FHWA modified Gates formula and 0.10 for the AASHTO modified Engineering News Formula. For non-redundant foundations consisting of 4 piles or less, the resistance factor associated with a given dynamic formula should be further reduced by 20%.

Table 13-2 Resistance Factors for Dynamic Formulas
(modified from AASHTO 2014)

Formula	Resistance Determination Method	AASHTO (2014) Resistance Factor
FHWA Modified Gates Formula, ϕ_{dyn}	Nominal resistance determined using FHWA Modified Gates Formula at end of driving condition only. See Section 13.3.1.	0.40
AASHTO Modified Engineering News Formula, ϕ_{dyn}	Nominal resistance determined using AASHTO Modified Engineering News Formula at end of driving condition only. See Section 13.3.2.	0.10
WSDOT Dynamic Formula, ϕ_{dyn}	Nominal resistance determined using WSDOT Dynamic Formula at end of driving condition only. See Section 13.3.3.1.	Not in AASHTO See discussion in text.
MnDOT Dynamic Formula, ϕ_{dyn}	Nominal resistance determined using MnDOT Dynamic Formula. See Section 13.3.3.2.	Not in AASHTO See discussion in text.

13.3 DYNAMIC FORMULAS

13.3.1 FHWA Modified Gates Formula

For small projects where a dynamic formula is used, AASHTO states that the FHWA Modified Gates formula is preferable, since it correlates better with static load test results. The FHWA Modified Gates formula below has been revised to reflect the nominal resistance in kips and includes the 80 percent efficiency factor on the rated energy, E_d, recommended by Gates. The specified units below must be used.

$$R_{ndr} = 1.75\sqrt{E_d}\log_{10}(10\,N_b) - 100 \qquad \text{Eq. 13-2}$$

Where:

R_{ndr} = nominal driving resistance (kips).

E_d = developed hammer energy (ft-lbs). If ram velocity is not measured, it may be assumed equal to the potential energy of the ram in the form of ram weight, W, (lbs) times stroke height, h (ft).

N_b = pile penetration resistance (blows/inch).

It is often desirable for construction inspection personnel or contractors to know the number of hammer blows per foot of pile penetration which will be required to obtain the specified nominal resistance. The FHWA modified Gates formula for this purpose can be re-written as follows:

$$N_{ft} = 12\,(10^x) \qquad \text{Eq. 13-3}$$

In which:

$$x = [(R_{ndr} + 100)\,/\,1.75\sqrt{E_d})] \qquad \text{Eq. 13-4}$$

Where:

N_{ft} = pile penetration resistance (blows/foot).

x = exponent defined by Equation 13-4 and terms per Equation 13-2.

All dynamic formulas are empirically developed based the resistance predicted using end of drive blow count observations with the resistance determined from static load test results performed at a later time. The FHWA modified Gates formula therefore inherently includes time dependent resistance changes due to soil setup or relaxation. AASHTO (2014) recommends a resistance factor, φ_{dyn}, of 0.40 for the FHWA Modified Gates formula, and that the formula be used only for end of drive conditions.

13.3.2 AASHTO Modified Engineering News Formula

The Engineering News formula was developed to provide an estimated nominal resistance based upon hammer energy and the observed pile set. The formula uses the pile set during driving to empirically estimate the long term nominal resistance. Therefore, this dynamic formula also incorporates any time dependent soil resistance changes as a result of the empirical procedure. For this reason, restrike set observation should not be used to calculate the nominal resistance.

The AASHTO modified version for nominal resistance calculations based on end of driving conditions is presented in Equation 13-5. The specified units for energy and set must be used.

$$R_{ndr} = \frac{12\ E_d}{s_b + 0.1} \qquad \text{Eq. 13-5}$$

Where:

R_{ndr} = nominal driving resistance (kips).
E_d = developed hammer energy (ft-kips).
s_b = permanent pile set (inches).

As noted in Section 13.1.1, the Engineering News formula has long been recognized to be one of the least accurate and least consistent of the dynamic formulas. AASHTO specifications (2014) reflect this by assigning a resistance factor of 0.10 to the Engineering News formula and recommending that the formula be applied to only end of drive conditions.

13.3.3 Other Dynamic Formulas

A few state transportation agencies have developed their own dynamic formulas and associated resistance factors through calibration with static load test databases. Hammer type, pile type and size, as well as geologic conditions were considered in the dynamic formulas developed by the Washington State DOT and Minnesota DOT.

13.3.3.1 Washington State DOT Pile Driving Formula

The Washington State DOT utilized a database of 141 static pile load results from Paikowsky et al. (2004) to evaluate nominal resistance predictions made by the FHWA Modified Gates formula relative to the static load test results. The original WSDOT intent was to slightly modify and improve the FHWA modified Gates

formula. However, enough changes were made that a new dynamic formula was developed and named the WSDOT pile driving formula. The formula is presented in Equation 13-6 and the associated research study is presented in Allen (2005).

$$R_{ndr} = 6.6\mathrm{F}_{eff}E_d \ \ln(10N_b) \qquad \text{Eq. 13-6}$$

Where:

R_{ndr} = nominal pile resistance measured during driving (kips).

F_{eff} = Hammer efficiency factor.
- 0.55 for air/steam hammers on all pile types.
- 0.35 for closed end diesel hammers on all pile type.
- 0.47 for open end diesel hammers on steel piles.
- 0.37 for open end diesel hammers on timber or concrete piles.
- 0.58 for hydraulic hammers on all pile types.
- 0.28 for drop hammers on all pile types.

E_d = developed energy, equal to W * h (ft-kips).

W = ram weight (kips).

h = observed ram stroke (feet).

N_b = number of blows for 1.0 inch of pile permanent set, averaged over the last four inches of driving.

Table 13-3 summarizes the pile types, the range in pile section size, the range in load test failure load, and the number of data sets for a given pile type in the correlation database. Based on the database used to develop the formula, Allen estimated the average amount of resistance from soil setup included in the formula resistance prediction is about 30 to 70%. Hence, the formula should not be used for nominal resistance assessments using restrike observations since setup is already included in the dynamic formula correlation calibration.

Monte Carlo simulations were used for reliability analyses to estimate the reliability index, β, and the resistance factor needed to achieve a target reliability index value of 2.3 or 3.0, Allen (2005). Based on a target β of 2.3, WSDOT recommended a resistance factor, φ_{dyn}, of 0.55 be used with this formula for redundant foundations. For non-redundant foundations, defined as 4 piles or less, the WSDOT recommended resistance factor is 0.45 based on a target β of 3.0. The WSDOT dynamic formula, either as presented in Equation 13-6 or in a slightly modified version, has been adopted by the state transportation agencies in Washington, New Mexico, and Illinois.

Table 13-3 Pile Types and Sizes Contained in WSDOT Formula Database

Pile Type	Range in Pile Size	Range in Static Load Test Failure Load for Pile Type (kips)	Number of Datasets
Precast Concrete	12 to 36 inch	308 to 1797	49
Closed End Pipe	10 to 48 inch O.D.	237 to 1300	46
H-pile	10 to 14 inch	214 to 1239	29
Open End Pipe	24 to 60 inch O.D.	586 to 1984	9
Concrete Cylinder	20 to 54 inch O.D.	324 to 1452	5
Monotube	N/A	227 to 463	2
Timber	N/A	200	1

13.3.3.2 Minnesota Pile Formula 2012 (MPF12)

Paikowsky et al. (2009) combined pipe pile and H-pile load test information from Database PD/LT 2000, developed for the NCHRP Report 507 LRFD calibration study, with additional pipe and H-pile correlation data gathered from MnDOT practice. The original MnDOT/LT 2008 database included 40 H-pile, 65 closed end pipe pile, and 12 open end pipe pile data sets typical of the pile types, sizes, and soil conditions encountered in MnDOT practice. With time, additional datasets were added to the database. The expanded database was used for development and calibration of a new dynamic formula named the Minnesota Pile Formula 2012 (MPF12).

In using the formula, it was recommended that the hammer energy (W)(h) be limited to 85% of the hammer manufacturer's maximum rated energy in cases where the hammer energy exceeded the 85% value. The Minnesota Pile Formula 2012 (MPF12) for use on steel and concrete piles is presented in Equation 13-7.

$$R_{ndr} = 40\sqrt{\frac{W\,h}{1000}}\log\left(\frac{10}{s_b}\right) \qquad \text{Eq. 13-7}$$

Where:

R_{ndr} = nominal driving resistance (kips).
W = ram weight (lbs).
h = observed ram stroke (feet).
s_b = permanent set of last hammer blow (inches).
Wh = not to exceed 85% of manufacturer's maximum rated energy (ft-lbs).

The first order second moment method (FOSM) procedure and Monte Carlo simulations were used for reliability analyses to estimate a target reliability index value of 2.33 for redundant foundations. Based on these procedures, Paikowsky et al. (2014), recommended resistance factors, φ_{dyn}, of 0.50 for pipe piles, 0.60 for H-piles, 0.50 for non-voided, prestressed concrete piles up to 24 inch in size, and 0.80 for voided prestressed concrete piles 20 inch to 54 inch in size. It was recommended that the MPF12 formula be further modified as part of a later research study for the large, voided, concrete piles. All of the resistance factors recommended in the study were also based on the pile penetration resistance falling between 2 and 15 blows per inch.

The MPF12 dynamic formula was also evaluated for timber piles. It was noted that a modifier of 0.5 should be applied to the formula for timber piles due to the increased energy loss. The hammer energy (W)(h) should be limited to 85% of the hammer manufacturer's maximum rated energy in cases where the hammer energy exceeds the 85% value. The resulting modified form of MPF12 for timber piles is as follows:

$$R_{ndr} = 20\sqrt{\frac{W\,h}{1000}}\log\left(\frac{10}{s_b}\right) \qquad \text{Eq. 13-8}$$

Where:

R_{ndr} = nominal driving resistance (kips).
W = ram weight (lbs).
h = observed ram stroke (feet).
s_b = permanent set of last hammer blow (inches).
Wh = not to exceed 85% of manufacturer's maximum rated energy (ft-lbs).

Paikowsky et al. (2014) recommended a resistance factor, φ_{dyn}, of 0.60 be used for the nominal resistance determined with Equation 13-8 for timber piles. This resistance factor was also based on a pile penetration resistance of between 2 and 15 blows per inch.

The research study proposed that the MPF12 dynamic formulas could be used for either end of driving or restrike conditions with no change in the resistance factor or formula. This is somewhat unusual as most dynamic formulas are limited to only end of drive applications since they are empirically correlated to load test results and therefore inherently include time dependent changes in the nominal geotechnical resistance.

13.4 DYNAMIC FORMULA CASE HISTORY

To illustrate the variable performance of dynamic formulas compared to more reliable methods, a case history will be briefly discussed. A 50 feet long, 24 inch square, prestressed concrete pile was driven 45 feet below grade with an ICE I-46 single acting diesel hammer. The factored load to be supported by the pile was 380 kips. Soil conditions consisted of 30 feet of loose to medium dense sand overlying a 5 feet thick layer of medium dense cemented sand and limestone. The cemented sand was underlain by the intended bearing layer of medium dense to dense sand.

At the end of driving the test pile had a penetration resistance of 49 blows per foot at an average hammer stroke of 8.14 feet. The test pile was restruck 5 days after initial driving and had restrike penetration resistances of 4, 2, 2, and 2 blows per inch. The corresponding average hammer stroke at the beginning and end of this restrike was 8.05 and 8.55 feet, respectively. An axial compression load test was performed on this pile one week after initial driving (3 days after the restrike). Following the static load test, the pile was again restruck. The penetration resistances per inch of the second restrike were 4, 3, 3, 3, 3, 3, 3, and 4 blows per inch. The average hammer stroke at the beginning of this second restrike was 7.21 feet.

Nominal resistance estimates from dynamic formulas as well as from wave equation analysis, dynamic testing with signal matching, and static load testing are summarized in Table 13-4. The wave equation nominal resistance predictions were obtained from a fixed stroke bearing graph analysis with the soil model determined using default values from the GRLWEAP ST soil model. Dynamic testing signal matching results are based on CAPWAP results. The static load test failure load was determined using the Davisson Offset limit criteria.

For the presented case, the MnDOT dynamic formula provided the closest nominal resistance prediction to the static load test result based on inputting end of initial driving penetration resistance and stroke values into the four dynamic formulas. Overall the closest correlation to the static load test determined nominal resistance

was achieved from wave equation analysis (1% underprediction) and dynamic testing with signal matching (4% underprediction). A comparison of the maximum factored resistance that could be supported based on the results from a given method is presented in Table 13-5. The factored dynamic test results with signal matching on beginning of restrike data correlated best to the maximum factored resistance determined from the static load test.

Table 13-4 Case History – Comparison of Calculated Nominal Resistances

Nominal Resistance Method	Test Condition	Resistance Factor for Test Method φ_{dyn}	Nominal Resistance (kips)	Difference Relative to Static Load Test Resistance (%)
AASHTO EN Formula	EOD	0.10	2872	+ 463
AASHTO EN Formula	BOR-1	- - -	2799 (2)	+ 449
AASHTO EN Formula	EOR-1	- - -	1734 (2)	+ 240
AASHTO EN Formula	BOR-2	- - -	2507 (2)	+ 391
FHWA Modified Gates Formula	EOD	0.40	710	+ 39
FHWA Modified Gates Formula	BOR-1	- - -	701 (2)	+ 37
FHWA Modified Gates Formula	EOR-1	- - -	570 (2)	+ 12
FHWA Modified Gates Formula	BOR-2	- - -	658 (2)	+ 29
WSDOT Formula	EOD	0.55 (1)	950	+ 86
WSDOT Formula	BOR-1	- - -	934 (2)	+ 83
WSDOT Formula	EOR-1	- - -	806 (2)	+ 58
WSDOT Formula	BOR-2	- - -	837 (2)	+ 64
MNDOT Formula	EOD	0.50 (1)	585	+ 15
MNDOT Formula	BOR-1	0.50 (1)	579	+ 14
MNDOT Formula	EOR-1	0.50 (1)	485	- 5
MNDOT Formula	BOR-2	0.50 (1)	548	+ 7
Wave Equation Analysis	EOD	0.50	560	+ 10
Wave Equation Analysis	BOR-1	0.50	560	+ 10
Wave Equation Analysis	EOR-1	0.50	440	- 14
Wave Equation Analysis	BOR-2	0.50	505	- 1
Dynamic Test & Signal Matching	EOD	0.65	600	+ 18
Dynamic Test & Signal Matching	BOR-1	0.65	523	+ 3
Dynamic Test & Signal Matching	EOR-1	0.65	460	- 10
Dynamic Test & Signal Matching	BOR-2	0.65	490	- 4
Static Load Test	- - -	- - -	510	- - -

Notes: (1) – Resistance factor not in AASHTO.

(2) – Method not recommended to be used in restrike condition by AASHTO or formula developer.

Table 13-5 Case History – Comparison of Factored Resistance

Nominal Resistance Method	Test Condition	Resistance Factor for Test Method φ_{dyn}	Maximum Factored Resistance From Method (kips)	Difference Relative to Load Test Determined Factored Resistance (%)
AASHTO EN Formula	EOD	0.10	287	- 13
AASHTO EN Formula	BOR-1	- - -	280 (2)	- 16
AASHTO EN Formula	EOR-1	- - -	173 (2)	- 48
AASHTO EN Formula	BOR-2	- - -	251 (2)	- 24
FHWA Modified Gates Formula	EOD	0.40	284	- 14
FHWA Modified Gates Formula	BOR-1	- - -	280 (2)	- 15
FHWA Modified Gates Formula	EOR-1	- - -	228 (2)	- 31
FHWA Modified Gates Formula	BOR-2	- - -	263 (2)	- 21
WSDOT Formula	EOD	0.55 (1)	522	+ 58
WSDOT Formula	BOR-1	- - -	514 (2)	+ 55
WSDOT Formula	EOR-1	- - -	443 (2)	+ 34
WSDOT Formula	BOR-2	- - -	460 (2)	+ 39
MNDOT Formula	EOD	0.50 (1)	293	- 12
MNDOT Formula	BOR-1	0.50 (1)	289	- 13
MNDOT Formula	EOR-1	0.50 (1)	242	- 27
MNDOT Formula	BOR-2	0.50 (1)	274	- 17
Wave Equation Analysis	EOD	0.50	280	- 16
Wave Equation Analysis	BOR-1	0.50	280	- 16
Wave Equation Analysis	EOR-1	0.50	220	- 34
Wave Equation Analysis	BOR-2	0.50	253	- 24
Dynamic Test & Signal Matching	EOD	0.65	390	+ 18
Dynamic Test & Signal Matching	BOR-1	0.65	340	+ 3
Dynamic Test & Signal Matching	EOR-1	0.65	299	- 10
Dynamic Test & Signal Matching	BOR-2	0.65	319	- 4
Static Load Test	- - -	0.75	332	- - -

Notes: (1) – Resistance factor not in AASHTO.

(2) – Method not recommended to be used in restrike condition by AASHTO or formula developer.

13.5 ADVANTAGES, DISADVANTAGES, AND LIMITATIONS

Dynamic formulas offer a method to quickly estimate nominal resistance during driving. Because of the simple inputs such as hammer energy and pile set, relatively little engineering judgement is needed to perform the calculations. The primary advantages of dynamic formula use are the immediate availability of the driving criterion and the minimal delay to pile driving operations.

Conversely, dynamic formulas have several disadvantages. They do not consider the entire driving system (i.e. hammer, pile, and soil), variation in hammer performance, nor energy losses due to pile stiffness. However, the primary disadvantages are formula accuracy and reliability. Most shortcomings of dynamic formulas can be overcome by a more realistic analysis of the pile driving process, such a wave equation analysis. Dynamic testing and analysis is another tool which is superior to use of dynamic formulas.

AASHTO limits dynamic formula use to piles with a nominal resistance of 600 kips or less. This nominal resistance value is well beyond the typical nominal resistance values in historical databases evaluating dynamic formula performance. Other codes such as the International Building Code limit formula use to 160 kips because of their limitations. Dynamic formulas are based on Newtonian impact theory which is invalidated by the use of hammer and pile cushions.

13.6 PRACTICAL ISSUES AND CONSIDERATIONS

Use of a dynamic formula is often “justified” because of the small number of piles on a project or the presence of a consistent and hard bearing layer such as bedrock. On small projects with a limited number of piles, the cost of the extra pile length resulting from use of a less reliable nominal resistance verification method may be more economical than the testing cost or test method impact on the construction schedule. Similarly when piles are driven to a hard bearing layer, little additional pile length may be necessary to achieve the higher nominal resistance required by a dynamic formula and more reliable resistance verification methods may not be economically justified. However, driving stresses and their control must be considered in this situation and this assessment cannot be made using a dynamic formula.

The Indiana Department of Transportation evaluated installation costs on driven pile foundations for state bridge projects installed from 2009 to 2014. The pile foundations were installed using either the FHWA modified Gates dynamic formula or dynamic testing with signal matching. On the dynamic testing controlled projects, each test pile was dynamically monitored during both initial driving and during restrike with the restrike test conducted between 1 and 7 days after initial driving depending on the subsurface conditions. The cost per lineal foot of pile and the cost per kip of load support for pile foundation projects controlled by dynamic formula or dynamic testing with signal matching as reported by Zaheer et al. (2015) is summarized in Table 13-6.

Table 13-6 INDOT Dynamic Formula and Dynamic Testing Comparison

Details	FHWA Modified Gates Formula	Dynamic Testing with Signal Matching	Totals
Plan Contract Length (ft)	246,052	995,100	1,241,152
Paid Pile Length (ft)	216,664	937,873	1,154,517
Pile Length underrun or {overrun} (lf)	29,408	57,227	86,638
Pile Length underrun or {overrun} (%)	13.6%	6.1%	7.5%
Cost Paid to Contractor	$11,653,634	$46,178,800	$57,832,434
Average Unit Cost (per lf)	$ 53.79	$ 49.24	$ 50.09

Zaheer et al. (2015) determined that the use of a simple dynamic formula has several economic drawbacks. Their review also concluded the factored load carried by a dynamic formula controlled pile was 21% less than the factored load carried by a dynamically tested pile. For the same factored load, pile lengths determined through use of a dynamic formula were 10 to 20% greater than the length determined from dynamic testing. The cost per kip of supported structure load for a dynamic formula pile was 39% higher than that of a dynamically tested pile. Overall, the average unit cost per linear foot of dynamic formula installed pile was 9.2% more than the cost per foot of dynamic test with signal matching installed pile.

REFERENCES

Allen, T.M. (2005). Development of the WSDOT Pile Driving Formula and Its Calibration for Load and Resistance Factor Design (LRFD), WA-RD 610.1, Research Office, Washington State Department of Transportation, Olympia, WA, 45 p.

American Association of State Highway and Transportation Officials (AASHTO). (2014). AASHTO LRFD Bridge Design Specifications, US Customary Units, Seventh Edition, with 2015 Interim Revisions. American Association of State Highway and Transportation Officials, Washington, D.C., 1960 p.

Chellis R.D. (1961). Pile Foundations. Second Edition, McGraw-Hill Book Company, New York, NY, pp. 21-23.

Fragasny, R.J., Higgins, J.D. and Argo, D.E. (1988). Comparison of Methods for Estimating Pile Capacity, WA-RD 163.1, Washington State Department of Transportation, Olympia, WA, 62 p.

Paikowsky, S.G. (2004). with contributions from Birgisson, B., McVay, M., Nguyen, T., Kuo, C., Baecher, G., Ayyub, B., Stenersen, K., O.Malley, K., Chernauskas, L., and O'Neill, M., Load and Resistance Factor Design (LRFD) for Deep Foundations, NCHRP Report 507. Transportation Research Board, Washington, D.C., 76 p.

Paikowsky, S.G., Marchionda, C.M., O'Hearn, C.M., and Canniff, M.C. (2009). Developing a Resistance Factor for Mn/DOT's Pile Driving Formula, MN/RC 2009-37. Minnesota Department of Transportation, St. Paul, MN, 294 p.

Paikowsky, S.G., Canniff, M., Robertson, S., and Budge, A.S. (2014). Load and Resistance Factor Design (LRFD) Pile Driving Project – Phase II Study, MN/RC 2014-16. Minnesota Department of Transportation, St. Paul, MN, 514 p.

Peck, R.B. (1942). Discussion: Pile Driving Formulas. Proceedings of the American Society of Civil Engineers, Vol. 68, No. 2, pp. 905-909.

Rausche, F., Thendean, G., Abou-matar, H., Likins, G.E. and Goble, G.G. (1996). Determination of Pile Drivability and Capacity from Penetration Tests, DTFH61-91-C-00047, Final Report. U.S. Department of Transportation, Federal Highway Administration, McLean, VA, 432 p.

Sowers, G.F. (1979). Introductory Soil Mechanics and Foundations. Fourth Edition, Macmillan Publishing Co., Inc., New York, NY, pp. 531-533.

Wellington, A. (1892). Discussion of “The Iron Wharf at Fort Monroe, VA by J.B. Chucklee.” American Society of Civil Engineers (ASCE), Transactions, Vol. 27, No. 543, pp. 129-172.

Zaheer, M., Salgado, R., Prezzi, M., and Han, F. (2015). INDOT/Purdue Pile Driving Method for Estimation of Axial Capacity. Presentation at 2015 Purdue Road School Transportation Conference and Expo.

CHAPTER 14

CONTRACT DOCUMENTS

14.1 OVERVIEW OF PLAN AND SPECIFICATION REQUIREMENTS

Pile foundations generally cannot be inspected after installation. Therefore, construction specifications and monitoring are of prime importance for a successful pile foundation. Preparation of the contract plans, plan details, and specifications related to piling issues are the responsibility of the foundation designer in cooperation with materials and construction personnel. Project plans should include:

- Location of piles.
- Pile numbering system to clearly identify each pile in group or bent.
- Pile type, section, and estimated length.
- Pile toe details, driving shoe, closure plate, etc.
- Pile splicing details.
- Pile cut off elevation.
- Pile cap connection details.
- Estimated pile toe elevation.
- Minimum pile toe elevation, if needed.
- Required pile batter and direction.
- Orientation of H-piles.
- Factored resistance, R_r.
- Nominal resistance, R_n.
- Nominal driving resistance, R_{ndr}.
- Location of subsurface borings.
- Results of subsurface exploration.

It is the designer's responsibility to confirm that plans and specifications have been prepared using compatible language. This is particularly true in defining the required nominal driving resistance, which is an important component of any driven pile specification. Problems can arise when plans provide only the factored resistance, the nominal resistance, or the nominal driving resistance without other details such as the resistance factor associated with the construction control method or anticipated losses in resistance due to scour, liquefaction, or relaxation. For

example, plan statements such as "piles shall have a resistance of 300 kips," provide an unclear description of the contract requirements as the resistance could be interpreted as the factored resistance, nominal resistance, or nominal driving resistance. Plans should therefore clearly indicate the factored resistance, the resistance factor, the nominal resistance, the additional resistance from any unsuitable layers (scour, liquefaction and their elevations), resistance changes following driving (setup or relaxation effects) and the resulting nominal driving resistance.

This chapter includes a generic pile specification for highway projects that was originally developed with input from State and Federal bridge and geotechnical engineers and released in FHWA Geotechnical Guideline 13. It has been updated over time as necessary and modified from an ASD to LRFD specification. AASHTO LRFD Bridge Construction specifications (2010) provide a similar document with additional commentary. A good driven pile specification should include the basic components in Table 14-1.

The intent of the attached generic specification is to provide highway designers and transportation agencies with a comprehensive driven pile specification. However, this specification is not intended to be used directly for project application without review and modification by the foundation designer and transportation agency. Commentary sections are included where appropriate to assist the foundation designer in tailoring the generic specification to project requirements. The commentary sections explain the reasons behind development of particular sections of the specification and the relationship of the specification requirements to necessary pile design or construction activities.

Note that only driven piles are addressed in the specification. Other deep foundation types such as drilled shafts require completely different construction controls and are therefore not appropriate for inclusion in this generic pile specification.

In conventional design-bid-build contracts, agency standard specifications are used. The agency warrants to the contractor that the drawings and prescriptive specifications are complete and free from error (agency takes the risk). In design-build contracts, specifications are performance based which allows the design-builder to use their design and construction expertise to satisfy project requirements. The design-builder warrants to the agency that it will produce design documents that are complete and free from error (design-builder takes the risk). Standard specifications are used In CM/GC contract documents.

Table 14-1 Items to Include in a Driven Pile Specification

Category	Item
Pile Materials	Material type, grade, and strength. Coating details. Transportation and handling.
Driving System and Equipment	Hammer. Hammer and pile cushions. Helmet and inserts. Pile leads. Followers. Predrilling equipment. Jetting equipment. Spudding equipment.
Installation Issues	Driving sequence. Pile location tolerances. Pile alignment tolerances. Pile shoe or toe protection requirement. Pile splices. Pile cutoff. Pile cap connection. Pile heave. Pile rejection criteria.
Resistance Verification	Static load testing. Dynamic testing. Rapid load testing. Wave equation analysis. Dynamic formulas.
Basis of Payment	Method of measurement. Payment items.

14.2 GENERIC DRIVEN PILE SPECIFICATION

14.2.1 SECTION X.01 DESCRIPTION

This item shall consist of furnishing and driving foundation piles of the type and dimensions designated, including cutting off or building up foundation piles when required. Piling shall conform to and be installed in accordance with these specifications, and at the location, and to the elevation, penetration depth and/or nominal resistance shown on the plans, or as directed by the Engineer.

Except when test piles are required, the Contractor shall furnish the piles in accordance with the dimensions shown in the contract documents. When test piles are required, the pile lengths shown on the plans are for estimating purposes only and the actual lengths to be furnished for production piles will be determined by the Engineer after the test piles have been driven and tested. The lengths given in the order list will be based on the lengths which are assumed after cutoff to remain in the completed structure. The Contractor shall, without added compensation, increase the lengths to provide for fresh heading and for such additional length as may be necessary to suit the Contractor's method of operation.

Where required by the contract documents, the Contractor shall perform the static and/or dynamic and/or rapid load tests of the type and quantity specified at the locations indicated on the plans.

Commentary:

The objective of this specification is to provide criteria by which the Owner can assure that designated piles are properly installed and the Contractor can expect equitable compensation for work performed. The Owner's responsibility is to estimate the pile lengths required for the nominal resistances. Pile lengths should be estimated based on subsurface explorations, testing and analysis which are completed during the design phase, and expected variability in the subsurface conditions. Pile contractors who enter contractual agreements to install piles for an owner should not be held accountable or indirectly penalized for inaccuracies in estimated lengths. The Contractor's responsibility is to provide and install designated piles, undamaged, to the length specified by the Owner. This work is usually accomplished within an established framework of restrictions necessary to insure a "good" pile foundation. The price bid for this item of work will reflect the Contractor's estimate of both actual cost to perform the work and perceived risk.

14.2.2 SECTION X.02 SUBMITTALS AND APPROVALS

A) Pile Installation Plan:

A Pile Driving Installation Plan shall be prepared by the Contractor and submitted to the Engineer no later than 30 days before driving the first pile. The Pile Driving Installation Plan shall include the following:

1. List and size of proposed equipment including cranes, barges, pile driving equipment, jetting equipment, compressors, and predrilling equipment. Manufacturer's data sheets on hammers should be included.

2. Methods to determine hammer energy in the field for determination of nominal resistance. Include in the submittal necessary charts and recent calibrations for any pressure measuring equipment.

3. Detailed drawings of any proposed followers.

4. Detailed drawings of any templates.

5. Details of proposed load test equipment, all load test instrumentation, and load test procedures. Submitted load test program information should also include the details and arranged of the reaction frame and reaction piles as well as recent calibrations of jacks, required load cells and all monitoring equipment.

6. Sequence of driving of piles for each different configuration of pile layout.

7. Proposed schedule for test pile program and production pile driving.

8. Details of proposed means and procedures to document the preconstruction condition of existing nearby structures and utilities as well as proposed procedures for their protection and monitoring during the contract period.

9. Required shop drawings for piles, cofferdams, etc.

10. Methods and equipment proposed to prevent movement of piles during placement and compaction of fill within 15 feet of the piles.

11. Proposed method for placing steel reinforcement and concrete in concrete filled pipe piles.

12 Methods to prevent deflection of battered piles due to their own weight and to maintain their as-driven position until casting of the pile cap is complete.

13. Proposed pile splice locations and details of any mechanical or proprietary splices to be used.

B) Pile Driving Equipment Approval by Wave Equation:

All pile driving equipment furnished by the Contractor shall be subject to the approval of the Engineer. All pile driving equipment should be sized such that the project piles can be driven with reasonable effort to the estimated contract lengths without damage. Approval of pile driving equipment by the Engineer will be based on wave equation analysis unless a dynamic formula has been specified for nominal resistance verification in the field. In no case shall the driving equipment be transported to the project site until approval of the Engineer is received in writing. The Contractor shall submit a completed Pile Driving and Equipment Data Form (shown in Figure 14-1) to the Engineer for approval as part of the pile installation plan at least 30 days prior to the start of pile driving. If a follower is to be used, detailed drawings of the follower shall be included as part of this submittal.

Commentary:

Use of wave equation analysis for approval of driving equipment can substantially reduce pile driving costs and pile driving claims by checking that the equipment mobilized to the project can drive the pile to the required penetration depth without damage. Agencies should encourage Contractors to use wave equation analysis to select the optimum hammer for each project. In cases where disputes arise over rejection of pile driving equipment, the Engineer should request the Contractor to submit proof of the adequacy of the pile driving equipment. Proof should consist of, but not be limited to, a wave equation analysis of the proposed driving equipment performed by a registered professional engineer. All costs of this submission shall be the responsibility of the Contractor. The Pile and Driving Equipment Data Form should be submitted for approval even if wave equation analysis will not be used for hammer approval. The approved form should be used by

Contract No.:_____ Structure Name and/or No.:_____

Project:_____

_____

Pile Driving Contractor or Subcontractor:_____

County:_____

(Piles driven by)

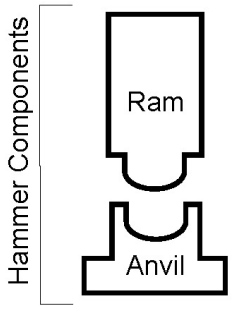

Hammer

Manufacturer:_____ Model No.:_____

Hammer Type:_____ Serial No.: _____

Manufacturers Maximum Rated Energy:_____(ft-lbs)

Stroke at Maximum Rated Energy:_____(ft)

Range in Operating Energy:_____to_____(ft-lbs)

Range in Operating Stroke:_____to_____(ft)

Ram Weight:_____(kips)

Modifications:_____

_____

_____

Striker Plate

Weight:_____(kips) Diameter:_____(in)

Thickness:_____(in)

Hammer Cushion

Material #1	Material #2 (Composite Cushion)
Name:_____	Name:_____
Area:_____(in^2)	Area:_____(in^2)
Thickness/Plate:_____(in)	Thickness/Plate:_____(in)
No. of Plates:_____	No. of Plates:_____

Total Thickness of Hammer Cushion:_____(in)

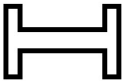

Helmet

Weight:_____(kips)

Insert (If Any)

Weight:_____(kips)

Total Weight of Helmet and Insert:_____(kips)

Pile Cushion

Material:_____

Area:_____(in^2) Thickness/Sheet:_____(in^2)

No. of Sheets:_____

Total Thickness of Pile Cushion:_____(in)

Maximum Thickness Accommodated by Helmet :_____(in)

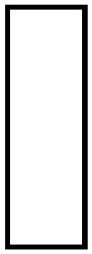

Pile

Pile Type:_____

Wall Thickness:_____(in) Taper:_____

Cross Sectional Area:_____(in^2) Weight/ft:_____

Ordered Length:_____(ft)

Factored Resistance:_____(kips)

Nominal Resistance:_____(kips)

Description of Splice:_____

_____

Driving Shoe/Closure Plate Description:_____

_____

Submitted By:_____ Date:_____

Telephone No.:_____ Email:_____

Figure 14-1 Drive system submittal form.

the pile inspector to check the proposed hammer and drive system components are as furnished and are maintained during the driving operation.

The criteria, which the Engineer will use to evaluate the pile driving equipment from the wave equation results, consists of both the required number of hammer blows per foot of penetration as well as the pile driving stresses at the required nominal resistance. The required penetration resistance (blow count) indicated by the wave equation at the required nominal resistance shall be between 30 and 96 blows per foot for the driving equipment to be acceptable.

Commentary:

Practical refusal is defined later in this generic specification as 10 blows per inch. Therefore, the upper limit of the penetration resistance for hammer approval should be less than the criteria for practical refusal. Otherwise, slight variations in assumed soil behavior or hammer performance will result in refusal driving conditions occurring prior to achieving the nominal resistance with an approved driving system.

In addition, the pile driving stresses indicated by the wave equation analysis of the proposed driving equipment shall not exceed material specific limits for the driving system to be acceptable. The AASHTO (2014) resistance factor for driven pile drivability analysis, φ_{da}, is 1.0 for all pile types with the exception of timber piles where it is 1.15. For steel piles, maximum compressive driving stresses shall not exceed the resistance factor, φ_{da}, times 90 percent of the minimum yield strength of the pile material. For prestressed concrete piles in normal environments, tensile stresses shall not exceed φ_{da} times 0.095 multiplied by the square root of the concrete compressive strength, f'_c, plus the effective prestress value, f_{pe} (with both f'_c and f_{pe} in ksi). For prestressed concrete piles in severe corrosive environments, tensile stresses shall not exceed φ_{da} times f_{pe}. Compressive stresses for prestressed concrete piles shall not exceed φ_{da} times 85 percent of the compressive strength minus the effective prestress value, (i.e. $0.85\ f'_c - f_{pe}$). For timber piles, the compressive driving stress shall not exceed φ_{da} times the reference design value of wood in compression parallel to the grain, F_{co}, as listed on the plans or provided in AASHTO (2014) Table 8.4.1.1-1.

The Contractor will be notified of the acceptance or rejection of the driving system within 14 calendar days of the Engineer's receipt of the Pile and Driving Equipment Data Form. If the wave equation analyses show that either pile damage or inability to drive the pile with a reasonable driving resistance to the desired nominal

resistance will result from the Contractor's proposed equipment or methods, the Contractor shall modify or replace the proposed methods or equipment at his expense until subsequent wave equation analyses indicate the piles can be reasonably driven to the desired nominal resistance, without damage. The Engineer will notify the Contractor of the acceptance or rejection of the revised driving system within 7 calendar days of receipt of a revised Pile and Driving Equipment Data Form.

During pile driving operations, the Contractor shall use the approved system. No variations in the driving system will be permitted without the Engineer's written approval. Any change in the driving system will only be considered after the Contractor has submitted the necessary information for a revised wave equation analysis. The Contractor will be notified of the acceptance or rejection of the driving system changes within 7 calendar days of the Engineer's receipt of the requested change. The time required for submission, review, and approval of a revised driving system shall not constitute the basis for a contract time extension to the Contractor.

Commentary:

The nominal driving resistance, R_{ndr}, is the soil resistance which must be overcome (including resistance from unsuitable layers, liquefiable soils, and scour zone soils) to reach the pile penetration depth where the factored resistance can be achieved with an appropriate resistance factor based on the nominal resistance verification method used in the field. The resistance factor depends on the reliability of the resistance determination method as well as, for some methods, the number of tests performed. Table 14-2 provides a summary of the resistance determination methods and their associated resistance factors. AASHTO does not provide a recommended resistance factor for rapid load test methods as discussed in Section 11.4.7.

The nominal driving resistance is affected by:

1. *The resistance in unsuitable soil support layers overlying suitable support layers.*

2. *Minimum penetration requirements.*

3. *Temporary loss or increase in soil strength due to driving operations.*

4. *Pile installation methods which alter the in place soil resistance such as jetting, predrilling, etc.*

The designer must estimate the nominal driving resistance. Only on the most routine pile projects will the nominal driving resistance be equal to nominal resistance (i.e. the nominal resistance is the factored resistance divided by the resistance factor). More typically, piles are used to penetrate upper soil layers which are unsuitable for load support due to either poor soil characteristics, or future loss of load support by scour or liquefaction. In such cases, resistance in the unsuitable layers is not considered in determining the pile penetration necessary to support the factored resistance. However, the estimated nominal driving resistance must include the resistance encountered in penetrating those unsuitable support layers, in addition to the nominal resistance.

The nominal driving resistance must be shown on the contract documents to permit the Contractor to properly size the driving equipment and the Engineer to judge the acceptability of the Contractor's driving equipment. Optimum pile installation generally occurs when the nominal driving resistance is obtained with a driving effort below the point of maximum curvature (typically around 84 to 96 blows per foot) of the wave equation bearing graph. Larger penetration resistance result in negligible pile penetration per blow and generally inefficient driving conditions. Excessive driving resistances can also result in damage to the pile or the driving system.

Table 14-2 Resistance Factors for Field Determination Methods (after AASHTO 2014)

Condition	*Resistance Determination Method*	*AASHTO Resistance Factor*
Nominal Resistance of Single Pile in Compression	*Driving criteria established by successful static load test of at least one pile per site condition and dynamic testing with signal matching of at least two piles per site condition, but no less than 2% of the production piles.*	*0.80*
Dynamic Analysis and Static Load Test Methods, ϕ_{dyn}	*Driving criteria established by successful static load test of at least one pile per site condition without dynamic testing.*	*0.75*
	Driving criteria established by dynamic testing with signal matching conducted on 100% of production piles.	*0.75*
	Driving criteria established by dynamic testing with signal matching of at least two piles per site condition, but no less than 2% of the production piles.	*0.65*
	Wave equation analysis, without pile dynamic measurements or load test, at end of drive conditions only.	*0.50*
	FHWA Modified Gates dynamic pile formula (End of Drive condition only).	*0.40*
	Engineering News dynamic pile formula (End of Drive condition only).	*0.10*
Nominal Resistance of Single Pile in Tension	*Static load test.*	*0.60*
Dynamic Analysis and Static Load Test Methods, ϕ_{up}	*Dynamic testing with signal matching.*	*0.50*

C) Pile Driving Equipment Approval by Alternate Method:

An alternate method of driving equipment approval will be used when the contract documents state that nominal resistance verification in the field will be determined from a dynamic formula. The alternate approval method requires that the energy of the driving equipment be rated by the manufacturer at or above the appropriate minimum energy level in Table 14-3 corresponding to the nominal resistance shown on the plans. The penetration resistance required by the dynamic formula for the submitted hammer and required nominal resistance should not exceed 10 blows per inch.

During pile driving operations, the Contractor shall use the approved system. If the Engineer determines the Contractor's hammer is unable to transfer sufficient energy to the pile, the hammer shall be removed from service until repaired to the satisfaction of the Engineer. No variations in the driving system will be permitted without the Engineer's written approval. Any changes in the driving system will be considered only after the Contractor has submitted a new Pile and Driving Equipment Data form. The Contractor will be notified of the acceptance or rejection of the proposed change in driving equipment within 7 calendar days of the Engineer's receipt of the form.

Table 14-3 Alternate Approval Method Minimum Pile Hammer Requirements

Nominal Resistance (kips)	Minimum Manufacturers Rated Hammer Energy (ft-lbs) *
180 and under	-----
181 to 300	-----
301 to 420	-----
421 to 540	-----
541 to 600	-----
Over 600	-----

* See commentary.

Commentary:

A table of the minimum rated hammer energy vs. nominal resistance should be developed using wave equation analyses of commonly available driving systems for the pile types, pile lengths, and pile loads routinely used by the specific agency. These analyses should model the typical soil and pile

installation conditions. The wave equation results should be evaluated for driving stress levels and penetration resistance (blow count) to determine which hammer energies are too large (driving stress problems or penetration resistance at nominal resistance less than 30 blows/ft) and which energies are too small (penetration resistance at nominal resistance greater than practical refusal value of 120 blows /ft).

Once the specific table of energy values has been developed, it should only be considered for routine projects in uniform soil conditions. Projects involving long piles or large nominal resistances relative to the factored load (such as piles subject to significant scour depths or piles to be driven through embankments) should use project specific wave equation analyses to establish minimum driving equipment requirements. Piles to soft and hard rock should also be evaluated by wave equation analysis to reduce the risk of pile damage from too large a hammer.

14.2.3 SECTION X.03 MATERIALS

Materials shall meet the requirements in the following Subsections of Section X.03 Materials:

Portland Cement Concrete
Reinforcing Steel
Prestressing Strands / Post-Tensioning Tendons
Structural Steel
Castings for Pile Shoes
Steel Shells for Cast in Place Piles
Timber Piles
Timber Preservative and Treatment
Protective Coatings

Commentary:

The appropriate sections of each agency's standard specifications should be included under the X.03 Materials. A generic materials section cannot be provided herein, considering the vast combinations of materials used in piling operations and the varying control methods used by individual agencies. The above list contains the common material components. Additions or deletions may be required to this list based on the content of individual agency

standard specifications and the pile type specified. The 3rd Edition of the AASHTO LRFD Bridge Construction Specifications contains additional text and commentary on pile material topics which should be reviewed and used to update agency standard specifications as appropriate.

14.2.4 SECTION X.04 DRIVING EQUIPMENT AND APPURTENANCES

A) Pile Hammers:

Piles may be driven with air, steam, diesel, or hydraulic hammers. Drop hammers, if specifically permitted in the contract, shall not be used for concrete piles or for piles whose required nominal resistance exceeds 120 kips. When drop hammers are permitted, the ram shall have a weight not less than 2.0 kips and the height of the drop shall not exceed 12.0 feet. In no case shall the ram weight of the drop hammer be less than the combined weight of helmet and pile. All drop hammers shall be equipped with hammer guides to insure concentric impact on the helmet.

Air/steam hammers shall be operated and maintained within the manufacturer's specified ranges. The plant and equipment furnished for air/steam hammers shall have sufficient capacity to maintain at the hammer, under working conditions, the volume and pressure specified by the manufacturer. The hose connecting the compressor or boiler with the hammer shall be at least the minimum size recommended by the hammer manufacturer. The plant and equipment shall be equipped with accurate pressure gauges which are easily accessible to the Engineer. The weight of the striking parts of air/steam hammers shall not be less than one third the weight of helmet and pile being driven, and in no case shall the striking parts weigh less than 2.75 kips. If a wave equation analysis is used for hammer approval the minimum ram weight requirements shall not apply.

Open end (single acting) diesel hammers shall be equipped with a device such as rings on the ram to permit the Engineer to visually determine hammer stroke at all times during pile driving operations. Also, the Contractor shall provide the Engineer a chart from the hammer manufacturer equating stroke and blows per minute for the open end diesel hammer to be used. For open end diesel hammers, the contractor shall provide and maintain in working order for the Engineer's use, an approved device to automatically determine and display ram stroke.

Closed end (double acting) diesel hammers shall be equipped with a bounce chamber pressure gauge, in good working order, mounted near ground level so as

to be easily read by the Engineer. Also, the Contractor shall provide the Engineer a chart, calibrated to actual hammer performance within 60 days of use, equating bounce chamber pressure to either equivalent energy or stroke for the closed end diesel hammer to be used.

Hydraulic hammers shall be equipped with a system for measuring and immediately displaying in the field, the kinetic energy or ram impact velocity. The system shall be maintained in good working order and operational at all times piles are driven.

Vibratory hammers, when permitted for installing production piles, shall be used only after the pile toe elevation for the nominal resistance is established by load testing and/or from test piles restruck with an impact hammer. The Contractor shall perform, at his cost, the load tests and/or extra work required by the Engineer as needed for approval of the vibratory hammer use. Installation of production piles with vibratory hammers shall be controlled according to power consumption, rate of penetration, specified toe elevation, or other means acceptable to the Engineer which assures the nominal resistance equals or exceeds the nominal resistance of the test pile. In addition, the first of every 10 piles installed with a vibratory hammer shall be restruck with an impact hammer of suitable energy to verify the nominal resistance before driving the remaining piles.

Commentary:

Pile inspectors frequently do not possess adequate knowledge or technical information concerning even the most basic details of the Contractor's hammer. Chapters 15 and 18 provide information on driving equipment and monitoring. Agencies and contractors should also provide pile “inspectors” with basic manuals such as FHWA/RD 86/160 "The Performance of Pile Driving Systems: "Inspections Manual" or "Inspectors Manual for Pile Foundations" and "A Pile Inspectors Guide to Hammers, Second Edition" available from the Deep Foundation Institute, 120 Charlotte Place, Englewood Cliffs, NJ 07632.

On large projects or on projects requiring large pile resistances, specifications should consider requiring kinetic energy readout devices for hammers as described in Section 15.19 of Chapter 15. Several manufacturers can equip their hammers with these devices when requested. Any existing hammer can also be retrofitted with a kinetic energy readout device. These devices allow improved quality assurance and can detect changes in hammer performance over time that may necessitate adjustment to the pile installation criterion.

At present no formula exists to reliably predict the nominal resistance of piles driven with vibratory hammers. Until reliable procedures are developed for vibratory installation, special precautions must be taken to insure foundation piles installed with vibratory hammers have both adequate nominal resistance and structural integrity. As discussed in Section 7.10.5, the use of vibratory hammers may also affect the shaft resistance that develops on the pile. On critical projects, "owners" should consider the use of dynamic testing during restrike to substantiate pile nominal resistance and integrity.

B) Drive System Components and Accessories:

1. Hammer Cushion: Impact pile driving equipment designed to be used with a hammer cushion shall be equipped with a suitable thickness of hammer cushion material to prevent damage to the hammer or pile and to insure uniform driving behavior. Hammer cushions shall be made of durable manufactured materials, provided in accordance with the hammer manufacturer's guidelines. Wood, wire rope, and asbestos hammer cushions are specifically disallowed and shall not be used. A striker plate, as recommended by the hammer manufacturer, shall be placed directly above the hammer cushion to insure uniform compression of the cushion material. The hammer cushion shall be removed from the helmet and inspected in the presence of the Engineer when beginning pile driving at each structure or after each 100 hours of pile driving, whichever is less. Any reduction of hammer cushion thickness exceeding 25 percent of the original thickness shall be replaced by the Contractor before driving is permitted to continue.

Commentary:

For hammers requiring cushion material, mandatory use of a durable hammer cushion material that will retain uniform properties during driving is necessary to accurately relate penetration resistance (blow count) to nominal pile resistance. Non-durable materials which deteriorate during driving cause erratic estimates of nominal resistance and, if allowed to dissolve, result in damage to the pile or driving system.

2. Helmet: Piles driven with impact hammers require an adequate helmet or drive head to distribute the hammer blow to the pile head. The surface of the helmet in contact with the pile shall be plane and smooth and shall be aligned parallel with the hammer base and the pile head. The helmet shall be guided by the leads and not be free swinging. The helmet shall fit around the pile head in such a manner as to prevent transfer of torsional forces during driving, while maintaining proper alignment

of hammer and pile. An insert may be used with a helmet to adapt the helmet to different types or sizes of piles.

For steel and timber piling, the pile heads shall be cut squarely and a helmet, as recommended by the hammer manufacturer, shall be provided to hold the axis of the pile in line with the axis of the hammer.

For timber piles, the least inside helmet or hammer base horizontal dimension shall not exceed the pile head diameter by more than 2.0 inches. If the timber pile diameter slightly exceeds the least helmet or hammer base dimension, the pile head shall be trimmed to fit the helmet.

For precast concrete and prestressed concrete piles, the pile head shall be plane and perpendicular to the longitudinal axis of the pile to prevent eccentric impacts from the helmet.

For special types of piles, appropriate helmets, mandrels or other devices shall be provided in accordance with the manufacturer's recommendations so that the piles may be driven without damage.

3. Pile Cushion: The heads of concrete piles shall each be protected by a pile cushion having the same cross sectional area as the pile top. Pile cushions shall be made of plywood, hardwood, or composite plywood and hardwood materials.

The minimum pile cushion thickness placed on the pile head prior to driving shall be determined by wave equation analysis so that driving stress limits are not exceeded. If a dynamic formula is used, the minimum pile cushion thickness shall be at least 4 inches.

A new pile cushion shall be provided for each pile. In addition, the pile cushion shall be replaced during the driving of any pile if the cushion is compressed more than one-half the original thickness or it begins to burn. Pile cushions shall be protected from the weather, and kept dry prior to use. Pile cushion shall not be soaked in any liquid unless approved by the Engineer. The use of manufactured pile cushion materials in lieu of a wood pile cushion shall be evaluated on a case by case basis.

A used pile cushion in good condition shall be used for restrike tests. The used pile cushion shall be the same cushion from the end of initial driving unless that pile cushion condition has deteriorated. If the original pile cushion has deteriorated,

another used pile cushion of similar thickness as the original cushion at the end of drive shall be used.

Commentary:

A pile cushion is only needed for the protection of concrete piles. If the wave equation analysis of the Contractor's hammer indicates tension stresses exceed specification limits, the pile cushion may need to be substantially thicker than 4 inches. Pile cushion thicknesses greater than 18 inches have been used to mitigate tension stresses. Compressive stresses at the pile head can generally be controlled with a relatively thin pile cushion. However, wood pile cushions may become overly compressed and hard after about 1000 to 1500 hammer blows. Conversely, cushions exposed to less than 50 blows are generally not suitable for restrikes.

4. Leads: Piles shall be supported in line and position with leads while being driven. Pile driver leads shall be constructed in a manner that affords freedom of movement of the hammer while maintaining alignment of the hammer and the pile to insure concentric impact for each blow.

Leads may be either fixed or swinging type. Swinging leads shall be adequately embedded in the ground or the pile constrained in a structural frame such as a template to maintain alignment and location tolerances. Swinging leads shall be fitted with a pile gate at the bottom of the leads unless used with a template. Leads shall be of sufficient length to make the use of a follower unnecessary. Leads used for driving batter piles shall be designed to permit and maintain proper alignment of the batter pile. A horizontal brace may be required between the crane and base of leads to maintain alignment and location tolerances in some batter pile installation conditions.

5. Followers: Followers shall only be used when approved in writing by the Engineer, or when specifically stated in the contract documents. When a follower is proposed, a wave equation analysis shall be used to evaluate the suitability of the proposed driving system. As a general guide, the cross sectional area of a steel follower when driving concrete piles should be at least 20 percent of the cross sectional area of the concrete pile. When driving steel or timber piles, the cross sectional area of the steel follower should have an impedance between 50 percent and 200 percent of the pile impedance.

The follower and pile shall be held and maintained in equal and proper alignment during driving. The follower shall be of such material and dimensions to permit the piles to be driven to the penetration depth determined necessary from the driving of the full length piles. The follower shall be designed with guides adapted to the leads that maintain the hammer, follower and pile in alignment during driving. The lower end of the follower shall be equipped with a helmet or follower-pile connection suitable for the pile type being driven.

The final position and alignment of the first two piles installed with followers in each substructure unit shall be verified to be in accordance with the location and alignment tolerances in Section X.06 C) 4 before additional piles are installed.

Commentary:

The use of a follower often causes substantial and erratic reductions in the hammer energy transmitted to the pile due to the follower flexibility, poor connection to the pile head, frequent misalignment, etc. Reliable correlations of penetration resistance with nominal resistance are very difficult when followers are used. Therefore, the nominal resistance of select follower driven piles should be checked with either a static load test or dynamic testing with signal matching. Severe problems with pile alignment and location frequently occur when driving batter piles with a follower in a cofferdam unless a multi-tier template is used.

6. Jets: Jetting shall only be permitted if approved in writing by the Engineer or when specifically stated in the contract documents. The contractor shall determine the number of jets and the volume and pressure of water at the jet nozzles to freely erode the material adjacent to the pile without affecting the lateral stability of the final in place pile.

The Contractor shall control and dispose of all jet water in a manner satisfactory to the engineer or as specified in the contract documents. If jetting is specified or approved by the engineer and the jetting is performed as specified or approved, the contractor shall not be held responsible for any damage to the site caused by the jetting operations. If jetting is performed for the contractor's convenience, the contractor shall be responsible for all damage to the site caused by jetting operations.

Jet pipes shall be removed when the bottom of the jet pipe is 5 feet above the minimum or prescribed toe elevation unless otherwise indicated by the contract

documents or the Engineer. Following jet removal, the jetted pile shall be driven to the required nominal resistance with an impact hammer. If the required nominal resistance is not achieved at the prescribed toe elevation, the pile may be allowed to setup and the required nominal resistance determined through restriking. The jetting procedures should be reviewed by the Engineer and adjustments made if applicable so that the required nominal resistance can be achieved without restrike verifications.

When jetting is used, the Contractor shall submit details of the proposed jetting and pile driving plan. Where practical, all piles in a pile group shall be jetted to the required penetration depth before beginning pile driving. When large pile groups or pile spacing and batter make this impractical, restrike tests on a select number of previously driven piles shall be performed to check nominal resistance after jetting operations are completed.

7. Predrilling Equipment: When stated in the contract documents, the Contractor shall provide predrilling equipment to drill holes at pile locations of the size specified and to the depths shown in the contract documents or as approved in writing by the Engineer. If subsurface obstructions, such as boulders or rock layers are encountered, the diameter of the predrilled hole may be increased with Engineers approval to the least dimension adequate for pile installation.

Commentary:

The appropriate diameter of the predrilled hole depends on the purpose of the predrilled hole. If predrilling is performed to minimize problems with maintaining alignment tolerances, or to mitigate heave or vibrations, predrilled holes are typically smaller than the diameter or diagonal of the pile. When predrilling is performed to penetrate through an embankment or to bypass obstructions, a larger predrilled hole with a diameter not more than the largest dimension of the pile plus 6 inches may be acceptable. In either case, the excavated zone surrounding the pile is generally backfilled with an approved material of sand, pea gravel, or grout after the pile is driven depending on design requirements.

8. Spuds: When stated in the contract documents or approved by the Engineer, the Contractor shall provide spudding equipment to displace obstructions, debris, or unsuitable materials at pile locations. The spudding equipment shall create an opening through the material of the size specified and to the depths shown in the contract documents or as approved by the Engineer in writing.

14.2.5 SECTION X.05 DETERMINATION OF NOMINAL RESISTANCE

A) Axial Compression Resistance:

The nominal resistance of piles in axial compression shall be determined by the Engineer based on one of the methods listed below.

1. Static Load Tests: Compression load tests shall be performed by procedures set forth in ASTM D1143 using the quick load test method, except that the test shall be taken to geotechnical plunging failure or the capacity of the loading system. Testing equipment and measuring systems shall conform to ASTM D1143, except that the loading system shall be capable of applying 150 percent of the nominal resistance. A load cell and spherical bearing plate shall be used.

The Contractor shall submit to the Engineer for approval detailed plans prepared by a licensed professional engineer of the proposed loading apparatus. The submittal shall include calibrations for the hydraulic jack, load cell, and pressure gage conducted within 30 days of the load test. If requested by the Engineer, the jack, load cell, and pressure gage shall be recalibrated after the load test.

The loading apparatus shall be constructed to allow the various increments of the load to be placed gradually, without causing vibration to the test pile. When the approved method requires the use of reaction piles, the reaction piles shall be of the same type and diameter as the production piles. Reaction piles shall be surveyed and monitored for upward movement during the load test. Reaction piles driven at production pile locations that have a permanent upward movement of 0.25 inches or more upon completion of the load test shall be redriven. Timber or tapered piles installed in permanent locations shall not be used as reaction piles.

While performing the load test, the contractor shall provide safety equipment and employ adequate safety procedures. Adequate support for the load test plates, jack, and ancillary devices shall be provided to prevent them from falling in the event of a release of load due to hydraulic failure, test pile failure, or other cause.

The nominal geotechnical resistance or failure load of a pile statically tested in axial compression is defined by the pile head movement under load. For piles 24 inches or less in diameter or width, the failure load is the pile head load which produces a measured movement of the pile head equal to:

$$s_f = \Delta + \left(0.15 + \frac{\mathrm{b}}{120}\right) \qquad \text{Eq. 14-1}$$

Where:

s_f = pile head movement at failure (inches).
Δ = elastic deformation of total pile length (inches).
b = pile diameter or width of side for square piles (inches).

For piles larger than 36 inches in diameter, additional pile toe movement is necessary to develop the toe resistance. For these larger diameter piles, the nominal geotechnical resistance or failure load can be defined as the load which produces movement at the pile head equal to:

$$s_f = \Delta + b/30 \qquad \text{Eq. 14-2}$$

Where:

s_f = pile head movement at failure (inches).
Δ = elastic deformation of total pile length (inches).
b = pile diameter or width of side for square piles (inches).

For piles greater than 24 inches in diameter but less than 36 inches in diameter, linear interpolation should be performed between Eq. 14-1 and 14-2.

The top elevation of the test pile shall be determined immediately after driving and again just before load testing to check for heave. If more than ¼ inch of heave occurs the load test pile may require re-driving before the load test is performed.

Unless otherwise specified in the contract documents or by the Engineer, the static load test shall not be performed sooner than 5 days after the test pile or any reaction piles were driven.

On completion of the load testing, any test or reaction piling not a part of the finished structure shall be removed or cut off at least 1 foot below either the bottom of footing or the finished ground elevation, if not located within the footing area.

Commentary:

The nominal resistance may increase (soil setup) or decrease (relaxation) after the end of driving. Therefore, it is essential that static load testing be performed after equilibrium conditions in the soil have re-established. Static load tests performed before equilibrium conditions have re-established will underestimate the long term nominal resistance in soil setup conditions and overestimate the long term nominal resistance in relaxation cases. For piles

in clays, specifications should require at least 2 weeks or longer to elapse between driving and load testing. In sandy silts and sands, 5 days to a week is usually sufficient. Load testing of piles driven into shales should also be delayed for at least 2 weeks after driving. Additional discussion on time dependent changes in nominal resistance may be found in Section 7.2.4.

Each static load test pile should determine the load transferred to the pile toe. Instrumentation commonly consists of strain gages and/or telltale rods mounted at varying depths above the pile toe. Also, a load cell and spherical bearing plate should be mounted between the load frame and the pile head to verify the readings from the hydraulic jack pressure gauge. Due to jack ram friction, loads indicated by a jack pressure gauge are commonly 10 percent to 20 percent higher than the actual load imposed on the pile.

If the static load tests are to be performed by an independent firm retained by the Contractor and not by the Engineer, an additional specification section detailing the complete load test instrumentation monitoring requirements as well as the report submission requirements for the load test results and result interpretation must be added. A corresponding pay item must then be added to this specification for load test reporting. Alternatively, the report requirements can be described herein and then included as part of the static load test pay item.

When static load tests are used to control production pile driving, the time required to analyze and/or review the load test results as well as to establish driving criteria should be specified so that the delay time is clearly identified. Static load testing is discussed in greater detail in Chapter 9 of this manual.

2. Dynamic Testing with Signal Matching: Dynamic measurements shall be obtained using dynamic test processing equipment, calibrated transducers, and procedures set forth in ASTM D4945. The measurements will be taken by a qualified engineer during the driving of piles designated as dynamic test piles. Signal matching analysis shall be performed on representative data collected at the end of initial driving and at the beginning of each restrike events. Additional signal matching analysis may be performed as determined by the Engineer.

Commentary:

This section on dynamic testing covers only the Contractor's activities as they relate to the dynamic tests. If the dynamic tests are to be performed by an

independent firm retained by the Contractor and not by the Engineer, an additional specification section detailing the dynamic test analysis and reporting requirements must be added. Merely referencing the ASTM D4945 standard is insufficient. ASTM D4945 does not specify signal matching requirements or their frequency; it does not specify if, how, and by whom, driving criteria are established; nor does it identify what substructure locations are covered by the criteria.

Dynamic testing personnel should have attained an appropriate level of expertise (Expert, Master, Advanced, Intermediate, Basic, or Provisional) on the "Dynamic Measurement and Analysis Proficiency Test" sponsored by the Pile Driving Contractors Association (PDCA) and Pile Dynamics, Inc. (PDI) for providers of dynamic testing services. Dynamic testing methods are discussed in Chapter 10.

Whenever static load tests are specified, dynamic tests are recommended to be performed on at least half the reaction piles prior to driving the static load test pile as well as on the static load test pile when it is driven. The dynamic test results are used both to confirm that the desired nominal resistance can be attained at the estimated static load test pile penetration depth and to fine tune the dynamic test procedures for site soil conditions. Dynamic monitoring of the static load test pile during restrike after completion of the static load test is also highly recommended. This restrike test allows correlation of static test results with dynamic test results. Signal matching analysis of dynamic test data is required for nominal resistance determination per AASHTO (2014) and also assists in quantifying the dynamic soil parameters, soil quake and damping, for the site.

When dynamic tests are specified on production piles, the first pile driven in each substructure foundation is typically tested. The total number of dynamic tests performed will vary from two piles per site condition, but not less than 2% of production piles, to 100% of the production piles. The number of dynamic tests required per AASHTO depends on the variability of the site conditions as well as the resistance factor selected for design verification. Additional discussion on the number of piles dynamically tested and the associated resistance factor can be found in Section 10.3.

Prior to placement in the leads, the Contractor shall make diametrically opposite faces of each pile to be dynamically tested available for predrilling the instrumentation attachment holes. The dynamic testing engineer will furnish the

equipment, materials, and labor necessary for drilling holes in the piles for mounting the instrumentation. The instruments will typically be attached 2 to 3 pile diameters below the head of the pile with bolts placed in masonry anchors for the concrete piles, or through drilled holes on the steel piles, or with wood screws for timber piles.

The Contractor shall provide the dynamic testing engineer reasonable means of access to the pile for attaching instruments after the pile is placed in the leads. A manlift or platform with minimum size of 4 feet x 4 feet designed to be raised to the top of the pile while the pile is located in the leads shall be provided and operated by the Contractor. Alternatively, Contractor's personnel following the dynamic testing engineer's instructions can attach the instruments to the pile after it is placed in the leads. For some pile types and project conditions, the dynamic testing engineer may also recommend instrument attachment to the pile prior to lifting. It is estimated that approximately 1 hour per pile will be needed for instrument attachment and removal.

If requested, the Contractor shall furnish electric power for the dynamic test equipment. The power supply at the outlet shall be 10 amp, 115 volt, 55-60 cycle, A.C. only. Field generators used as the power source shall be equipped with functioning meters for monitoring voltage and frequency levels.

For dynamic testing conducted from a barge or other difficult to access sites, the Contractor shall furnish a shelter to protect the dynamic test equipment from the elements. The shelter shall have a minimum floor size of 8 feet x 8 feet and minimum roof height of 6.5 feet. The inside temperature of the shelter shall be between 45 and 95 degrees and be located within 50 feet of the pile location.

With the dynamic testing equipment attached, the Contractor shall drive the pile to the design penetration depth or to a depth determined by the Engineer. The Engineer will use the nominal resistance estimates at the time of driving and/or restriking from dynamic test methods to determine the required pile penetration depth for the nominal resistance. The stresses in the piles will be monitored during driving so that the measured stresses do not exceed the specified material values in Section X.02 B). If necessary, the Contractor shall reduce the driving energy transmitted to the pile by using additional cushions or reducing the energy output of the hammer in order to maintain stresses below the values in Section X.02 B). If non axial driving is indicated by dynamic test equipment measurements, the Contractor shall immediately realign the driving system.

The Contractor shall wait up to 24 hours (or a longer duration per Table 14-4 if specified in the contract documents) and restrike the dynamic load test pile with the

dynamic testing instruments attached. It is estimated that the Engineer will require approximately 30 minutes to reattach the instruments. A cold hammer shall not be used for the restrike. The hammer shall be warmed up before restrike begins by applying at least 20 blows to another pile or to timber mats placed on the ground. The maximum amount of penetration required during restrike shall be 3 inches, or the maximum total number of hammer blows required will be 20, whichever occurs first. After restriking, the Engineer will either provide the cutoff elevation or specify additional pile penetration and testing.

Commentary:

A dynamic test often includes monitoring during both initial driving and during one restrike event within a specified time period. Alternatively, the initial driving and restrike test events can be individual items. Any long term restrike tests after the initial restrike should be paid as a separate item unless the restrike schedule is specifically stated in the dynamic test specification.

The restrike time and frequency should be clearly stated in the specifications and should be based on the time dependent strength change characteristics of the soil. Table 14-4 provides restrike durations commonly used for various soil types.

Table 14-4 Common Time Delay for Restrike Based Upon Soil Type

Soil Type	Time Delay Until Restrike
Clean Sands	1 Day
Silty Sands	2 Days
Sandy Silts	3-5 Days
Silty Clays	7-14 Days*
Shales	10-14 Days*

* Longer times sometimes required.

The restrike time interval is particularly important when dynamic testing is used for construction control. Specifying too short of a restrike time for friction piles in fine grained deposits may result in pile length overruns. However, it is sometimes difficult for long term restrikes to be accommodated in the construction schedule. In these cases, multiple restrikes are often specified on selected piles with shorter term restrikes at other locations.

The time necessary to analyze the dynamic test results and provide driving criteria to the contractor once restrikes are completed should also be stated in the specifications. This is important when the testing is done by agency personnel or their consultants as well as when the testing firm is retained by the contractor. In cases where the testing is retained by the contractor, the time required for agency review of the test results and to provide driving criteria should be specified relative to the agency's receiving the test results.

3. Rapid Load Tests: The nominal resistance shall be determined by a rapid load test performed in accordance with the procedures set forth in ASTM D7383. The rapid load test may be performed using either a combustion gas and reaction mass system or with a cushioned drop weight system. The peak force shall exceed the targeted nominal geotechnical resistance plus the dynamic soil resistance. The applied force pulse shall exceed 50% of the actual peak force for a time duration of 4L/C and the static pre-load force for a time duration of at least 12L/C where L is the pile length in feet and C is the pile wave speed in ft/s. A time duration of less than 12L/C is acceptable if additional force and movement measurements devices are used along the pile length in accordance with ASTM D7383.

The Contractor shall trim the head of the test pile flat, level, and perpendicular to the pile axis at the elevation directed by the rapid load testing agency. The area surrounding the test pile shall also be prepared in accordance with the requirements necessary to support the rapid load test device and conduct the test. Depending on the site conditions, this may necessitate site grading, use of crane pads, constructing a support frame, and/or other measures for positioning and supporting the rapid load test device.

The force shall be measured using a calibrated force transducer or load cell placed between the loading apparatus and the pile head. The load capacity of the transducer shall be at least 10% greater than the targeted peak force. The pile head movement shall be measured by one or more calibrated displacement transducers.

The nominal geotechnical resistance determined by a rapid load test shall be assessed by an approved interpretation procedure. The procedure shall identify the loading rate reduction factor used with the analysis method.

Commentary:

Section 11.4.1 through 11.4.5 describes nominal resistance interpretation methods for rapid load tests. The pile length and soil conditions are primary

factors in selecting the interpretation method. If additional force and movement devices are necessary for the interpretation method, time must be allotted for obtaining and installing this instrumentation in or on the test pile. A significant permanent pile head displacement is also needed for nominal resistance determination. The loading rate in a rapid load test also affects the nominal resistance and must be considered.

AASHTO (2014) does not include a resistance factor for rapid load tests. Hence, this must be stipulated by the designer whenever rapid load tests are specified. A discussion of resistance factors currently in use with rapid load tests is provided in Section 11.4.7. All rapid load tests are performed by independent testing firms. Therefore, the time required for agency review of the rapid load test results should be specified relative to when the agency's receives the rapid load test results. A detailed discussion of rapid load test methods is provided in Chapter 11.

Unless otherwise specified in the contract documents or by the Engineer, the rapid load test shall not be performed sooner than 5 days after driving the test pile.

Commentary:

This specification addresses only the Contractor's activities as they relate to performing a rapid load test. If the rapid load tests are to be performed by an independent testing firm retained by the Contractor and not retained by the Engineer, an additional specification section detailing the complete rapid load test instrumentation monitoring requirements as well as the report submission requirements for the rapid load test results and result interpretation must be added. A corresponding pay item must then be added to this specification for rapid load test reporting. Alternatively, the report requirements can be described herein and then included as part of the rapid load test pay item.

The Contractor's independent testing firm shall submit to the Engineer, for approval, detailed plans of the rapid load test equipment arrangement, proposed test procedure, and nominal resistance interpretation method. The submittal shall also include calibrations for the transducer or load cells and all additional instrumentation. All calibrations shall be within the calibration period specified within ASTM D7383.

4. Wave Equation: The nominal resistance shall be determined by the Engineer based on a wave equation analysis. Piles shall be driven with the approved driving equipment to the ordered length or other lengths necessary to obtain the required nominal resistance. Jetting, predrilling, or other methods to facilitate pile penetration shall be modeled in the analysis if proposed and allowed by the contract documents. Adequate pile penetration depth for the nominal resistance shall be considered obtained when the wave equation penetration resistance is achieved within 5 feet of the estimated pile toe elevation. Piles not achieving the penetration resistance within this limit shall be driven to penetration depths established by the Engineer.

5. Dynamic Formula: The nominal resistance shall be determined by dynamic formula if the contract documents contain a provision that dynamic formula be used to establish driving criteria. Dynamic formulas should not be used if the required nominal resistance is greater than 600 kips. Formula results should not be considered applicable when the pile head is crushed, broomed, or damaged, or when a follower is used.

If a dynamic formula is used to establish driving criteria, piles shall be driven to a penetration depth necessary to obtain the nominal resistance according to the Modified Gates formula with specified units as follows:

$$R_{ndr} = 1.75\sqrt{E_d}\log_{10}(10\,N_b) - 100 \qquad \text{Eq. 14-3}$$

Where:

R_{ndr} = nominal driving resistance (kips).
E_d = developed hammer energy, (W)(h), during the observed set (ft-lbs).
W = ram weight (lbs).
h = average hammer stroke during set observation (ft).
N_b = number of hammer blows per inch (blows/in).

The number of hammer blows per foot of pile penetration required to obtain the nominal resistance shall be calculated as follows:

$$N_{ft} = 12\,(10^x) \qquad \text{Eq. 14-4}$$

In which:

$$x = \left[\frac{R_{ndr}+100}{1.75\sqrt{E_d}}\right] - 1 \qquad \text{Eq. 14-5}$$

Where:

N_{ft} = number of hammer blows for final foot of driving (blows/ft).
R_{ndr} = nominal driving resistance (kips).
E_d = developed hammer energy, (W)(h), during the observed set (ft-lbs).
W = ram weight (lbs).
h = average hammer stroke during set observation (ft).

Commentary:

Additional dynamic formulas besides the FHWA Modified Gates formula were presented in Chapter 13. Other dynamic formulas may be used based on agency practice and local calibrations.

Driven piles should be monitored in terms of their nominal driving resistance. The nominal driving resistance at a given pile penetration depth reflects the total resistance mobilized by the pile. This may include resistance in soil deposits unsuited for long term load support, as well as suitable layers. Therefore, the penetration resistance (blow count) should be established for the nominal driving resistance that must be overcome in order to reach anticipated pile penetration depth. These nominal driving resistances are determined by static analysis procedures.

In the case of piles to be driven to a specified minimum pile toe elevation, the nominal driving resistance must be computed by static analysis to include the resistance of all soil layers penetrated by the pile above the minimum pile toe elevation as well as the toe resistance at that depth. The minimum pile toe elevation may have been specified for reasons other than axial compression resistance in order to meet lateral, uplift, or serviceability requirements. The nominal driving resistance is directly related to the maximum pile driving stress during installation. The driving stress is more critical than the stress imparted after installation by the factored design load.

Good piling practices dictate use of the wave equation in place of dynamic formulas. AASHTO design specifications require a wave equation drivability analysis be performed during the foundation design stage. The soil profile used in this design stage wave equation analysis can be easily re-used along with details on the Contractors proposed driving system to obtain a construction stage wave equation analysis that includes the penetration resistance and maximum pile stresses for the required nominal driving

resistance. FHWA recommends that all agencies use wave equation analysis with a goal of minimizing use of dynamic formulas on all pile projects. Wave equation analysis is discussed in greater detail in Chapter 12 of this manual.

B) Axial Tension Resistance:

The nominal resistance of piles in axial tension shall be determined by the Engineer based on one of the methods listed below.

1. Static Load Tests: Tension load tests shall be performed by procedures set forth in ASTM D3689 using the quick load test method, except that the test shall be taken to plunging failure or the capacity of the loading system. Testing equipment and measuring systems shall conform to ASTM D3689, except that the loading system shall be capable of applying 150 percent of the anticipated nominal resistance.

The Contractor shall submit to the Engineer for approval detailed plans prepared by a licensed professional engineer of the proposed loading apparatus. The submittal shall also include calibrations for the hydraulic jack, load cell, and pressure gage conducted within 30 days of the load test. If requested by the Engineer, the jack, load cell, and pressure gage shall be recalibrated after the load test.

The loading apparatus shall be constructed to allow the various increments of the load to be placed gradually, without causing vibration to the test pile.

When the approved method requires the use of reaction piles, the reaction piles shall be of the same type and diameter as the production piles. Reaction piles shall be surveyed and monitored for movement during the load test. Reaction piles driven at production pile locations that have a permanent upward displacement greater than 0.25 inch shall be redriven upon completion of the static load test. Timber or tapered piles installed in permanent locations shall not be used as reaction piles.

While performing the load test, the contractor shall provide safety equipment and employ adequate safety procedures. Adequate support for the load test plates, jack, and ancillary devices shall be provided to prevent them from falling in the event of a release of load due to hydraulic failure, test pile failure, or other cause.

The nominal geotechnical resistance or failure load of a pile statically tested in axial tension is defined by the pile head movement under load. The failure load is the pile head load which produces a measured upward movement of the pile head equal to:

$$s_f = \Delta + (0.15) \qquad \text{Eq. 14-6}$$

Where:

s_f = pile head upward movement at failure (inches).

Δ = elastic lengthening of the total pile length (inches).

The maximum factored resistance under tension loading is the tension load test failure load determined using Equation 14-6 multiplied by the resistance factor, ϕ_{up}, for a static load test in axial tension from Table 14-2.

Unless otherwise specified in the contract documents or by the Engineer, the static load test shall not be performed sooner than 5 days after the test pile or any anchor piles were driven.

On completion of the load testing, any test or anchor piling not a part of the finished structure shall be removed or cut off at least 1 foot below either the bottom of footing or the finished ground elevation, if not located within the footing area.

Commentary:

If the static load tests are to be performed by an independent firm retained by the Contractor and not by the Engineer, an additional specification section detailing the complete load test instrumentation monitoring requirements as well as the report submission requirements for the load test results and result interpretation must be added. A corresponding pay item must then be added to this specification for load test reporting. Alternatively, the report requirements can be described herein and then included as part of the static load test pay item.

It is essential that static load testing be performed after equilibrium conditions in the soil have re-established as discussed in the commentary of Section 14.2.5.1 A. The time required to analyze and/or review the load test results should be specified so that the delay time is clearly identified. Static load testing is discussed in greater detail in Chapter 9 of this manual.

2. Dynamic Testing with Signal Matching: Dynamic measurements following procedures set forth in ASTM D4945 will be taken by the Engineer during the driving of piles designated as dynamic test piles. Signal matching analysis should be performed on representative data collected at the end of initial driving and at the beginning of all restrike events. Additional signal matching analysis may be

performed as determined by the Engineer. The maximum factored resistance for tension loading can be taken as the signal matching determined shaft resistance value multiplied by the resistance factor, ϕ_{up}, for dynamic testing in Table 14-2. Signal matching results from restrike tests should be used in this evaluation.

Commentary:

The commentary provided under the dynamic testing section for determination of the nominal axial compression resistance is applicable and should be reviewed for additional guidance.

C) Lateral Resistance:

The resistance and movement of piles subject to lateral loads shall be determined by the Engineer based on the following method.

1. Static Load Tests: Lateral load tests shall be performed by procedures set forth in ASTM D3966. Unless otherwise specified, the lateral load shall be applied incrementally following the standard loading procedure up to maximum applied load of 200% of the design lateral load. The lateral load shall be applied by a hydraulic jack acting between two piles, or between one pile and a reaction system. Testing equipment and measuring systems shall conform to ASTM D3966. A load cell and spherical bearing plate shall be used with the loading apparatus.

The Contractor shall submit to the Engineer for approval, detailed plans of the proposed loading apparatus prepared by a licensed professional engineer. The submittal shall also include calibrations for the hydraulic jack, load cell, and pressure gage conducted within 30 days of the load test. If requested by the Engineer, the jack, load cell, and pressure gage shall be recalibrated after the load test. The loading apparatus shall be constructed to allow the various increments of the load to be placed gradually, without causing vibration to the test pile.

Commentary:

ASTM D3966 provides a standard and 7 optional lateral load test procedures. All of the procedures have different loading schedules. Therefore, the loading procedure should be clearly identified so that the time required to conduct the lateral test is a function of the procedure.

If the lateral load tests are to be performed by an independent firm retained by the Contractor and not by the Engineer, an additional specification section detailing the complete lateral load test instrumentation monitoring requirements as well as the report submission requirements for the load test results and result interpretation must be added. A corresponding pay item must then be added to this specification for lateral load test reporting. Alternatively, the report requirements can be described herein and then included as part of the lateral load test pay item.

Unless otherwise specified or directed by the Engineer, lateral pile deflection measurements versus depth shall be obtained for each lateral load increment applied during the test using a string of in-place inclinometers, a Shape Accel Array, or other approved measure.

While performing the lateral load test, the contractor shall provide safety equipment and employ adequate safety procedures. The load test plates, jack, and ancillary devices shall be restrained to limit movement in the event of a sudden release of load due to hydraulic failure, test pile failure, or other cause.

14.2.6 SECTION X.06 PREPARATION AND DRIVING

A) Site Work:

1. Excavation and Fill Placement: Where practical, the site grade in the immediate work area shall be excavated to the specified elevation before the piles are driven. Material forced up between and adjacent to driven piles within the cap area shall be removed to the required elevation prior to pile cap concrete placement.

At bridge abutments and other locations directly adjacent to fill placement, fill material shall be placed and the fill settlement complete to the magnitude specified by the foundation designer before driving piles.

Commentary:

When approved by the Engineer, piles may be installed prior to embankment construction when minimal settlement or lateral displacement is expected in the soils beneath the embankment.

2. Predrilling for Driving: When required by the contract documents, the Contractor shall predrill holes of a size specified, at pile locations, and to the depths shown in the contract documents or approved in writing by the Engineer. After pile placement in the predrilled hole, the pile shall be driven with an impact hammer to the driving criteria specified by the Engineer. Any void space remaining around the pile in the predrilled zone after completion of driving shall be filled with sand or other approved material unless specifically prohibited or otherwise directed by contract documents. Material resulting from the drilled holes shall be disposed of as approved by the Engineer. The use of spuds shall not be permitted in lieu of predrilling, unless specifically approved in writing by the Engineer.

Commentary:

Except for end bearing piles, predrilling shall be stopped at least 5 feet above the plan pile toe elevation and the pile shall be driven with an impact hammer to a penetration resistance criteria specified by the Engineer. Where piles are to be end bearing on rock or hardpan, predrilling may be carried to the surface of the rock or hardpan.

If the Engineer determines that predrilling has disturbed the nominal resistance of previously installed piles, those piles that have been disturbed shall be restored to conditions meeting the requirements of this specification by redriving or by other methods acceptable to the Engineer. Redriving or other remedial measures shall be instituted after the predrilling operations in the area have been completed. The Contractor shall be responsible for the costs of any necessary remedial measures, unless the predrilling method was specifically included in the contract documents and properly executed by the Contractor.

Commentary:

Augering, wet rotary drilling, or other methods of predrilling shall be used only when approved by the Engineer or in the same manner as used for any indicator piles or load test piles. When permitted, such procedures shall be carried out in a manner which will not impair the nominal resistance already in place or the safety of existing adjacent structures.

3. Predrilling through Embankments: If required by contract documents, predrilled holes extending to natural ground shall be used where piles are to be driven through compacted fill or embankments greater than 5 feet in thickness. The predrilled hole shall have a diameter not more than the greatest dimension of the

pile cross section plus 6 inches unless a different predrilled hole diameter is specified. Material resulting from the drilled holes shall be disposed of as approved by the Engineer.

B) Preparation of Piles for Driving:

1. Pile Heads: The heads of all piles shall be plane and perpendicular to the longitudinal axis of the pile before the helmet is attached. Precast concrete pile heads shall be flat, smooth, and perpendicular to the longitudinal axis to prevent eccentric impact from the helmet. Prestressing strands shall be cutoff below the surface of the end of the pile. The heads of all concrete piles shall be protected with a suitably thick pile cushion during driving as described in Section X.04 B) 3. For concrete and timber piles, the pile head shall be chamfered on all sides.

2. Collars and Bands: Timber pile heads shall be equipped with collars, bands, or other devices to protect against splitting and brooming of the pile head when timber piles are to be driven to a nominal resistance in excess of 200 kips or when driving conditions require them.

3. Pile Shoes and Closure Plates: Pile shoes and closure plates of the type and dimensions specified shall be provided and installed on piles when designated on the contract plans or specifications. Pile shoes for H-piles and open end pipe piles shall be fabricated from cast steel conforming to ASTM A148/A148M (Grade 90-60). End closure plates for closed end pipe piles shall be made of ASTM A36/A36M steel or better. The closure plate diameter and thickness shall be as specified by the Engineer. Shoes for timber piles shall be steel and shall be fastened securely to the pile. Timber pile toes shall be carefully shaped to secure an even uniform bearing on the pile shoe.

Commentary:

H pile shoes composed of steel plates welded to the flanges and webs are not recommended because this reinforcement provides neither protection nor increased strength at the critical area of the flange to web connection. The designer should select and detail on the plans the proper pile shoe to suit the application. Additional information on pile shoes is presented in Chapter 16 of this manual.

4. Pile Marking for Prior to Driving: The Contractor shall mark the piles in 1 foot increments beginning at the pile toe and continuing to the pile head. The cumulative

distance from the pile toe shall be marked on the pile at 5 foot intervals from the pile toe. These cumulative distances shall be noted just above the corresponding foot marker. Prior to driving, the Contractor shall, if necessary, add inch marks between the 1 foot markers over a 10 foot length of pile as directed by the Engineer.

C) Pile Driving:

1. Test, Probe, and Indicator Piles: Test, probe, or indicator piles (hereafter referred to collectively as test piles), shall be driven before other piles are ordered. These piles shall be driven at the locations shown on the plans and to the penetration depths, penetration resistances (blow count) or nominal resistances as directed by the Engineer. In general, the specified length of test piles will be slightly greater than the estimated length of production piles in order to provide for variation in soil conditions. The driving equipment used for driving test piles shall be the approved system that the Contractor proposes to use on the production piling. Approval of driving equipment shall follow the requirements of in Section X.02 of these Specifications. The Contractor shall excavate the ground at each test pile location to the elevation of the bottom of the footing before the test pile is driven.

Test piles which do not attain the nominal driving resistance before reaching a distance of 1 foot above the estimated pile toe elevation on the plans shall be allowed to "set up" for 12 to 24 hours, or as directed by the Engineer, before being redriven. A cold hammer shall not be used for redrive. The hammer shall be warmed up before driving begins by applying at least 20 blows to another pile. If the specified nominal driving resistance is not attained on redriving, the Engineer may direct the Contractor to drive a portion or all of the remaining test pile length and repeat the "set up" redrive procedure. Test piles that have not achieved the required nominal driving resistance during redrive shall be spliced, if necessary, and driven until the required nominal driving resistance is obtained or as directed by the Engineer.

A record of driving of the test pile will be prepared by the Engineer, including the number of hammer blows per 1 foot intervals over the entire driven length, the as-driven length of the test pile, cutoff elevation, penetration in ground, and any other pertinent information. Near the end of initial driving, the Engineer may record the number of hammer blows per 1 inch of pile movement. If a redrive is necessary, the Engineer will record the number of hammer blows per 1 inch of pile movement for the first 1 foot of redrive. The Contractor shall not order piling to be used in the permanent structure until test pile data has been reviewed and pile order lengths are determined by the Engineer. The Engineer will provide the pile order list within 7

calendar days after completion of all test pile driving specified in the contract documents.

Commentary:

Test piles are recommended on projects where: 1) large quantities or long lengths of friction piling are estimated, even if load tests are to be used at adjacent footings; 2) large nominal soil resistance is expected in relation to the factored load and, 3) concrete piles are used.

The pile order lengths based on the test pile results should consider the anticipated variation in subsurface conditions. This is a particularly important consideration for concrete or timber piles which are both problematic if ordered shorter than required.

2. Production Piles: Production piles shall be driven by the Contractor to either the required nominal resistance, or the required nominal resistance and minimum pile toe elevation (if specified), or to a designated pile toe elevation. The pile penetration resistance (blow count) and the associated pertinent hammer performance observation for the hammer type (hammer stroke, impact velocity, hammer blow rate) should be documented during all driving sequences. Pile penetration resistance and the corresponding hammer performance documentation are required to evaluate the nominal resistance of impact driven piles.

Jetting or other methods shall not be used to facilitate pile penetration unless specifically permitted in the contract plans or in writing by the Engineer. The nominal resistance of jetted piles shall be based on the penetration resistances recorded during impact driving after the jet pipes have been removed. Jetted piles not attaining the nominal resistance at the ordered length shall be spliced, as required, at the Contractor's cost, and driven with an impact hammer until the nominal resistance is achieved using the approved driving criteria.

The nominal resistance of piles driven with followers shall be considered acceptable when the follower driven piles satisfy the driving criteria established by wave equation analysis and the criteria is either substantiated or modified based on a static load test or dynamic testing with signal matching.

The nominal resistance of piles driven with vibratory hammers shall be based on the penetration resistance recorded during impact driving after the vibratory equipment has been removed from the first pile in each group of ten piles. Vibratory installed

piles not attaining the nominal resistance at the estimated pile toe elevation shall be spliced, at the Contractor's cost, and driven with an impact hammer until the nominal resistance is achieved. When the nominal resistance is attained, the remaining 9 piles shall be installed to similar pile toe elevation with similar vibratory hammer power consumption and rate of penetration as the first pile.

Approval of a pile hammer relative to material driving stress levels shall not relieve the Contractor of responsibility for piles damaged because of misalignment of the leads, deterioration of cushion materials, failure of splices, malfunctioning of the pile hammer, or other improper construction methods. Piles damaged for such reasons shall be rejected and replaced at the Contractor's expense when the Engineer determines that the damage impairs the strength of the pile.

3. Driving Stress: Compression and tension stresses occurring in the pile material during driving shall not exceed the maximum stress levels defined in Section X.02 B) unless otherwise specified in the contract documents or by the Engineer.

4. Installation Sequence: The order of placing and final driving of individual piles within pile groups shall be either starting from the center of the group and proceeding outwards in both directions or starting at the outside row and proceeding progressively across the group.

5. Pile Location, Alignment, and Cutoff Tolerance: Piles shall be driven with a variation of not more than 0.25 inches/foot (1:50) from the vertical or not more than 0.5 inches /foot (1:25) from the batter shown in the contract documents. Piles for trestle bents shall also be driven so that the bent cap may be placed in its proper location without adversely affecting the resistance of the piles.

The pile head location after driving shall be within 6 inches of plan location for all piles capped below final grade, and shall be within 3 inches of plan location for bents supported by piles.

No pile shall be closer than 4 inches from any edge of the pile cap. Any increase in pile cap dimensions or added reinforcing steel caused by out-of-tolerance or out-of-position piles shall be at the Contractor’s expense.

The final cutoff elevation of the pile head shall be no more than 1.5 inches above or more than 4 inches below the cutoff elevation shown in the plans. In addition, the pile shall have a minimum embedment into the pile cap of at least 8 inches.

If the location and/or tolerances specified in the preceding paragraphs are exceeded, the extent of overloading shall be evaluated by the Engineer. The cost of redesign shall be at the Contractor's expense.

Commentary:

Conditions exist, such as soft overburden soils directly overlying a sloping bedrock, where final pile location and/or alignment may be beyond the contractor's control. These cases should be identified during the design stage with specifications tailored to meet the site and project requirements. Tight tolerances of 3 inches or less are not practical.

6. Heaved Piles: Level readings to check for pile heave after driving shall be made by the Engineer at the start of pile driving operations and shall continue periodically until the Engineer determines that such checking is no longer required. If pile heave is observed, accurate level readings referenced to a fixed datum shall be undertaken by the Engineer on all piles immediately after installation and periodically thereafter as adjacent piles are driven to determine the magnitude of the pile heave. Piles that derive their nominal resistance predominant through end bearing shall be redriven if more than 0.25 inch of heave is measured. Piles that achieve their nominal resistance primarily through shaft resistance shall be redriven if more than 1.5 inches of heave is measured. If pile heave is detected on any piles that have been concrete filled, the piles shall be redriven to original position after the concrete has obtained sufficient strength. Redriving shall be done using a hammer-pile cushion system satisfactory to the Engineer. The Contractor shall be paid for all work performed in conjunction with redriving piles because of pile heave provided the initial driving was done in accordance with the specified installation sequence and approved pile installation plan.

7. Obstructions: If piles encounter unforeseeable, isolated obstructions, the Contractor shall be paid for the cost of obstruction removal and for all remedial design or construction measures caused by the obstruction. Obstruction removal is only practical when obstructions are located near the ground surface.

8. Practical and Absolute Refusal: Practical refusal is defined as a pile penetration resistance (blow count) of 10 blows per inch for a maximum of 3 consecutive inches of pile penetration. Absolute refusal is defined as 20 blows for one inch or less of pile penetration. Driving should terminate immediately if either of these criteria are achieved. In the case of hard rock, an absolute refusal criterion of 5 blows per ¼ inch or 10 blows per ½ inch may be preferred to reduce the risk of pile

toe or driving equipment damage. The practical and absolute refusal definitions are based on the approved hammer system operating at its maximum fuel or stroke setting unless approval was established on hammer operation at a reduced fuel or stroke setting. When the required pile penetration depth cannot be achieved by driving without exceeding practical or absolute refusal with the approved hammer, use of other penetration aids such as predrilling or jetting should be evaluated.

Commentary:

Clear definitions for practical and absolute refusal are problematic. Factors such as the site soil profile, the characteristics of the bearing layer, pile type, hammer type, and hammer manufacturer limitations to prevent hammer damage all influence what is considered an acceptable refusal criteria. Many hammer manufacturers state that the hammer warranty is voided when pile penetration resistance (blow count) exceed 10 blows per inch for 6 to 12 consecutive inches of driving or 20 blows per inch for more than 1 inch.

When driving is easy until final driving, a high penetration resistance may be satisfactory. However, penetration resistances greater than 10 blows per inch should be used with care, particularly for concrete or timber piles. Extended driving at a penetration resistance greater than 10 blows per inch with a properly operating hammer should be avoided.

9. Pile Splices: Full length piles shall always be used wherever practical. Where splices are unavoidable for steel or concrete piles, their number, locations and details shall be subject to approval of the Engineer. In no case shall timber piles be spliced.

When splicing of steel piles is permitted, the method of splicing piles shall be in accordance with ANSI/AWS D1.1 or as approved by the Engineer. Either shielded arc or submerged arc welding should be used when splicing steel piles. Only certified welders shall perform welding. Mechanical splices that are not welded may be used only for compression piles.

Where splicing concrete piles is permitted, the concrete pile splice details shall conform to contract documents or as approved by the Engineer. Mechanical splices may be used if they satisfy all compression, tension, and bending resistance requirements of the design.

10. Pile Cutoff: The pile head of all permanent piles and pile casings shall be cutoff to a true plane at the required elevation and anchored to the structure as shown on the contract documents. All cutoff lengths shall become the property of the Contractor, and shall be removed from the site and disposed of properly.

For treated timber piles, a liberal application of copper naphthenate shall be given to the cut area immediately after cutoff. The copper naphthenate solution shall have a minimum of 2 percent copper metal and should be applied until visible evidence of further penetration has ceased.

Treated timber piles for marine applications exposed to weather shall be capped with a permanently fixed coating such as epoxy or with conical or other caps attached to the piles.

Commentary:

Additional structural details for timber, steel, concrete and cast in place piles should be included by each agency in this driven pile specification, either directly or by reference to appropriate sections of the individual agency's standard specification. Typical items include: timber pile butt treatment and preservative treatment; precast concrete pile reinforcement, forming, casting, curing, and handling; steel pile field painting; cast in place pile details for shell piles, interior reinforcement and concrete.

11. Unsatisfactory Piles: The methods used in transportation, handling, and driving piles shall not subject the piles to excessive stresses or abuse producing cracking, crushing or spalling of concrete piles; splitting, splintering, or brooming of the timber piles; or deformation of steel piles. A concrete pile will be considered defective if a visible crack, or cracks, appears around the entire periphery of the pile, or if any defect is observed which, as determined by the Engineer, affects the strength or service life of the pile. Misaligned piles shall not be forced into proper position. Any pile damaged during driving by reason of internal defects, or by improper driving, or by defective splicing, or driven out of its proper location, or driven below the designated cutoff elevation, shall be corrected by the Contractor, without added compensation, by a method approved by the Engineer.

Commentary:

Defective piles can often be remediated by:

- *withdrawing the defective pile and replacing it with a new and, when necessary, longer pile. In removing piles, jets may be used in conjunction with jacks or other devices for pulling in an effort to remove the whole pile, or*

- *driving a second pile adjacent to the defective pile.*

Piles driven past their specified top of pile elevation can:

- *be spliced or built up as otherwise provided herein, or*

- *have a sufficient portion of the footing extended down to properly embed the overdriven pile.*

Piles driven out of location can be remediated by:

- *driving one or more replacement piles adjacent to the out of position piles, or*

- *extending the footing laterally to incorporate the out of location pile, or*

- *redesigning and adding more reinforcing steel to the pile cap.*

14.2.7 SECTION X.07 METHOD OF MEASUREMENT

A) Mobilization of Pile Driving Equipment:

Payment for mobilization will be made at the lump sum price bid for this item as follows: Seventy five percent (75 percent) of the amount bid will be paid when the equipment for driving piles is mobilized, assembled, and driving of satisfactory piles has commenced. The remaining 25 percent will be paid when the work of driving piles is completed. The lump sum price bid shall include the cost of furnishing all labor, materials and equipment necessary for transporting, erecting, maintaining, replacing any ordered equipment, dismantling and removing of the entire pile driving equipment.

The cost of all labor, including the manipulation of the pile driving equipment and materials in connection with driving piles, shall be included in the unit price bid for the piles to be driven.

B) Piles Furnished:

The quantity of piles furnished will be measured for payment using the number of piles furnished (per linear foot or each) in accordance with the contract documents and shall include full compensation for all costs involved with furnishing and delivering piles to the project site in the unit price bid for furnished piles.

When pile build-ups or extensions are necessary, the extension length, approved by the Engineer, will be included in the total length of piling furnished.

No allowance will be made for that length of piles furnished by the Contractor to replace piles which were previously accepted by the Engineer, but were subsequently damaged by the Contractor prior to completion of the contract.

C) Piles Driven:

The quantity of piles driven will be measured for payment using the number of piles driven (per linear foot or each) in accordance with the contract documents and shall include full compensation of all costs involved in the actual driving of the piles as well as all related pile costs for which compensation is not identified as a specific pay item. These related pile costs shall include furnishing all labor, equipment, and materials necessary to install and complete the pile. All costs shall be included in the unit price bid for the piles driven.

D) Test Piles Furnished:

The quantity of test piles furnished will be measured for payment using the number test piles furnished (per linear foot or each) in accordance with the contract documents and shall include full compensation of all costs involved with furnishing and delivering test piles to the project site in the unit price bid for furnished test piles.

E) Test Piles Driven:

The quantity of test piles driven will be measured for payment using the number of test piles driven (per linear foot or each) in accordance with the contract documents and shall include full compensation of all costs involved in the actual driving of test piles as well as all related test pile costs for which compensation is not identified as a specific pay item. These related test pile costs shall include furnishing all labor, equipment, and materials necessary to install and complete the test pile. All costs shall be included in the unit price bid for the test piles driven.

F) Static Pile Load Test:

The quantity of static load tests for payment will be measured by the number of load tests completed and accepted. This pay item shall include all labor, equipment, and materials needed to construct and perform the static pile load test in accordance with contract documents.

Reaction and test piling which are not a part of the permanent structure will be included in the unit price bid for each load test. Reaction and test piling, which are a part of the permanent structure, will be paid for under the appropriate pay item.

Static load tests performed at the option of the Contractor will not be included in the quantity measured for payment.

G) Dynamic Pile Load Test:

The quantity of dynamic pile tests for payment will be measured by the number of dynamic pile tests completed and accepted in accordance with the contract documents. The pay item for dynamic pile test (during driving), or dynamic pile test (during restrike) shall include full compensation for furnishing all labor, equipment, and materials necessary to perform the dynamic pile test as specified in the contract documents. If the dynamic test is performed at a test pile location (non-production location), the unit price for test piles furnished and test piles driven will be paid in addition to the unit price for the dynamic pile test (during driving), or dynamic pile test (during restrike). If the dynamic test is performed at a production pile location, the unit price for piles furnished and piles driven will be paid in addition to the unit price for the dynamic pile test (during driving), or dynamic pile test (during restrike).

If an unspecified dynamic pile test requires substantial repositioning, delay, or downtime of the pile driving rig (such as may occur for a second longer term restrike on a test pile conducted at the owner’s request), additional compensation shall be paid at the unit price per hour for the out of sequence move, delay, or downtime in addition to the applicable unit bid prices for dynamic pile test, test piles, or piles.

H) Rapid Pile Load Test:

The quantity of rapid load tests for payment will be measured by the number of load tests completed and accepted. This pay item shall include all labor, equipment, and materials needed to prepare the site for the test, construct and perform the test per the contract documents.

I) Lateral Load Test:

The quantity of lateral load tests for payment will be measured by the number of lateral load tests completed and accepted. When contract documents stipulate that two piles are to be laterally load tested by pushing apart or pulling together two piles, the lateral load test pay quantity shall comprise the lateral load testing of both piles. This pay item shall include all labor, equipment, and materials needed to prepare the site for the test, construct and perform the lateral load test per the contract documents.

J) Splices:

The quantity of splices measured for payment shall be only those splices actually made that were required to drive the piles in excess of the plan estimated and approved pile lengths as accepted for payment by the Engineer. The unit price bid per splice shall comprise full compensation for procurement, delivery, and attachment of the splice including all labor, equipment, and ancillary materials.

K) Pile Shoes:

The quantity of pile shoes measured for payment shall be those shoes actually installed on piles and accepted for payment by the Engineer. The unit price bid per pile shoe shall comprise full compensation for procurement, delivery, and attachment of the shoes including all labor, equipment, and ancillary materials.

Commentary

Pile shoes can be alternatively be included in the furnished pile price if clearly stated on the plans and in the contract documents.

L) Predrilling:

The quantity of predrilling measured for payment shall be taken to include full compensation for providing all labor, equipment, and materials necessary to perform the predrilling work in accordance with the contract documents.

M) Jetting

The quantity of jetting measured for payment shall be taken to include full compensation for providing all labor, equipment, and materials necessary to perform jetting work in accordance with the contract documents.

N) Pile Cutoff

The quantity of pile cutoffs measured for payment shall be taken to include full compensation for providing all labor and equipment needed to provide a plane and level pile head surface at the required cutoff elevation as specified by the contract documents. The contract unit price also includes full compensation for proper disposal of the cutoff material.

O) Spudding

The quantity of spudding measured for payment shall be taken to include full compensation for providing all labor, equipment, and materials necessary to perform the spudding work in accordance with the contract documents.

P) Delays, Downtime, Rig Moves

The quantity of time measured for payment for delays, downtime, or out of sequence pile driving rig moves caused by the owner, agents, or subcontractors not otherwise compensated in contract pay items shall be recorded for each claimed occurrence and shall be taken to include full compensation for all labor and equipment.

14.2.8 SECTION X.08 BASIS OF PAYMENT

The accepted quantities, determined as described above, will be paid for at the respective contract document price per unit of measurement for each of the general pay items listed below. Payment will be made for each size and type of pile shown in the contract documents. Prices and payment will be full compensation for the work prescribed by the contract documents. Pay item and pay units are described below in Table 14-5.

Table 14-5 Basis of Payment

Pay Item	Pay Unit
Mobilization and Demobilization	Lump sum
Piles Furnished	Linear foot or each
Piles Driven	Linear foot or each
Test Pile Furnished	Linear foot or each
Test Pile Driven	Linear foot or each
Static Load Test	Each
Dynamic Pile Test (during driving)	Each
Dynamic Pile Test (during restrike)	Each
Rapid Load Test	Each
Lateral Load Test	Each
Pile Splices	Each
Pile Shoes	Each
Predrilling	Linear foot or Each
Jetting	Linear foot or Each
Pile Cut-off (over 5 ft lengths only)	Each
Spudding (Punching)	Per hour
Delays, Downtime, or Out-of-Sequence Moves	Per hour

Commentary:

The pile payment items in Table 14-5 have been chosen to separate the major fixed costs from the variable costs. Many agencies oversimplify pile payment by including all costs associated with the driving operation in the price per foot of pile installed. Contractors bidding such "simple" items need to break down the total cost of the mobilization, splices, shoes, etc., to a price per linear foot based on the total estimated quantity. If that quantity underruns, the contractor does not recover the full cost of mobilization, splices, shoes, etc. If that quantity overruns, the agency pays an unfair price for the overrun quantity. The use of separate items for operations of major fixed cost such as mobilization can substantially mitigate the inequitable impact of length variations. Similarly, the ordered pile length is the agency's responsibility. Separate payment for furnishing piles and driving piles compensates the contractor for actual materials used and installation costs, even when modest overruns or underruns occur.

REFERENCES

American Association of State Highway and Transportation Officials (AASHTO). (2010). AASHTO LRFD Bridge Construction Specifications, US Customary Units, Third Edition, with 2011, 2012, 2013, 2014, and 2015 Interim Revisions. American Association of State Highway and Transportation Officials, Washington, D.C., 680 p.

American Association of State Highway and Transportation Officials (AASHTO). (2014). AASHTO LRFD Bridge Design Specifications, US Customary Units, Seventh Edition, with 2015 Interim Revisions. American Association of State Highway and Transportation Officials, Washington, D.C., 1960 p.

ASTM D1143-07. (2014). Standard Test Methods for Deep Foundations Under Static Axial Compressive Load. Book of ASTM Standards, Vol. 4.08, ASTM International, West Conshohocken, PA, 15 p.

ASTM D3689-07. (2014). Standard Test Methods for Deep Foundations Under Static Axial Tensile Load. Book of ASTM Standards, Vol. 4.08, ASTM International, West Conshohocken, PA, 13 p.

ASTM D4945-12. (2014). Standard Test Method for High-Strain Dynamic Testing of Piles. Book of ASTM Standards, Vol. 4.08, ASTM International, West Conshohocken, PA, 9 p.

Deep Foundations Institute (DFI). (1995). A Pile Inspector's Guide to Hammers, Second Edition, Deep Foundations Institute, Englewood Cliffs, NJ, pp. 71.

Deep Foundations Institute (DFI). (1997). Inspectors Manual for Driven Pile Foundations, Second Edition, Deep Foundations Institute, Englewood Cliffs, NJ, pp. 69.

Geotechnical Guideline 13 (1985). Geotechnical Engineering Notebook, U.S. Department of Transportation. Federal Highway Administration, Washington, D.C., 37 p.

Rausche, F., Likins, G.E., Goble, G.G., Hussien, M. (1986). The Performance of Pile Driving Systems; Inspector's Manual. U.S. Department of Transportation, Federal Highway Administration, Washington, D.C., 92 p.

CHAPTER 15

PILE DRIVING EQUIPMENT

The task of successfully installing piles involves selecting the most cost effective equipment to drive each pile to its specified depth without damage in the least amount of time. The pile driving system is also used as a measuring instrument to evaluate a pile's nominal geotechnical resistance. Therefore, the challenge to both the engineer and the pile contractor becomes one of knowing, or learning about, the most suitable equipment for a given set of site conditions, and then confirming that the driving system is operating properly.

The crane, leads, hammer, and helmet are the primary components of any driving system. Followers and equipment for jetting, predrilling, and spudding may be permitted under certain circumstances. This chapter presents a basic description of each component of a driving system. For additional guidance, readers are referred to pile driving equipment manufacturers and suppliers. Unless otherwise noted, photographs are provided courtesy of GRL Engineers, Inc.

15.1 CRANES

The most common crane used for pile driving has historically been the crawler crane. Crawler cranes have very good mobility for most site conditions, good stability due to their wide base, and typically require minimal effort when walked and repositioned on the job site. A hydraulic power pack unit or air compressor may be mounted as a crane counterweight to facilitate pile driving operations. Crawler cranes also have a 360 degree hoisting radius. Crawler cranes must be trucked to the job site in pieces and assembled by another crane. Firm ground conditions are required for movement and operation. In soft ground conditions, the use of crane mats may be required. A photograph of a typical crawler crane set up for pile driving is presented in Figure 15-1.

Truck or mobile cranes are also used as pile driving rigs. Mobile cranes have good mobility on many job sites and can travel to the job under their own power. Setup and breakdown are relatively simple. However, mobile cranes cannot walk with heavy loads. Therefore, mobile crane movement between substructure locations

Figure 15-1 Crawler crane pile driving rig with lattice boom and swinging leads.

usually requires laying down and un-attaching the hammer and leads, moving the crane, and then re-attaching the hammer and lead system. Outriggers are used on mobile cranes for stability and leveling. The power pack unit or air compressor cannot be crane mounted. Mobile cranes also have restricted side lifting capabilities. A photograph of a mobile crane set up for pile driving is presented in Figure 15-2.

Figure 15-2 Truck crane pile driving rig with lattice boom and swinging leads.

Rough terrain cranes can also be used for pile driving. They can be set up fast and easily on a job site, they can be relocated and releveled relatively quickly, and can walk in some cases with loads over the front. When on location, outriggers are used for stability and leveling. Rough terrain cranes have greater mobility than truck cranes in difficult terrain. However, they have very restricted side lifting capabilities and a hammer power source cannot be crane mounted. A photograph of a rough terrain crane set up for pile driving is presented in Figure 15-3.

Figure 15-3 Rough terrain pile driving rig with telescoping boom and offshore leads.

15.2 DEDICATED AND UNIVERSAL RIGS

In recent years, use of dedicated and universal rigs has increased on pile driving projects. These specialty pile driving rigs or universal rigs include an attached telescoping leader that can be quickly transitioned from their horizontal transport position to the vertical driving position using hydraulically operated support arms. Hence, system setup is relatively fast without the need of additional heavy equipment. These systems include winch lines that can be used to offload piles as

well as loft piles into position beneath the hammer prior to pile driving. A dedicated pile driving system equipped with a hydraulic pile hammer is presented in Figure 15-4, while a universal rig setup for driving piles with a diesel pile hammer is shown in Figure 15-5.

Figure 15-4 Dedicated pile driving system.

Figure 15-5 Universal rig setup for pile driving (courtesy Bauer-Pileco).

15.3 LEADS

Lead systems are used with crawler, truck, and rough terrain pile driving rigs. The function of a set of leads is to maintain alignment of the hammer-pile system so that a truly concentric blow is delivered to the pile for each impact. Typical lead types are illustrated in Figure 15-6. The most common lead type is the box lead. Leads can be configured for use with the pile driving rig as a swinging lead, fixed lead, semi-fixed or vertical travel lead, or as an offshore lead. The most widely used lead configuration is a swinging lead depicted in Figure 15-7. Swinging leads are widely used because of their simplicity, lightness and low cost. Leads can be hung from

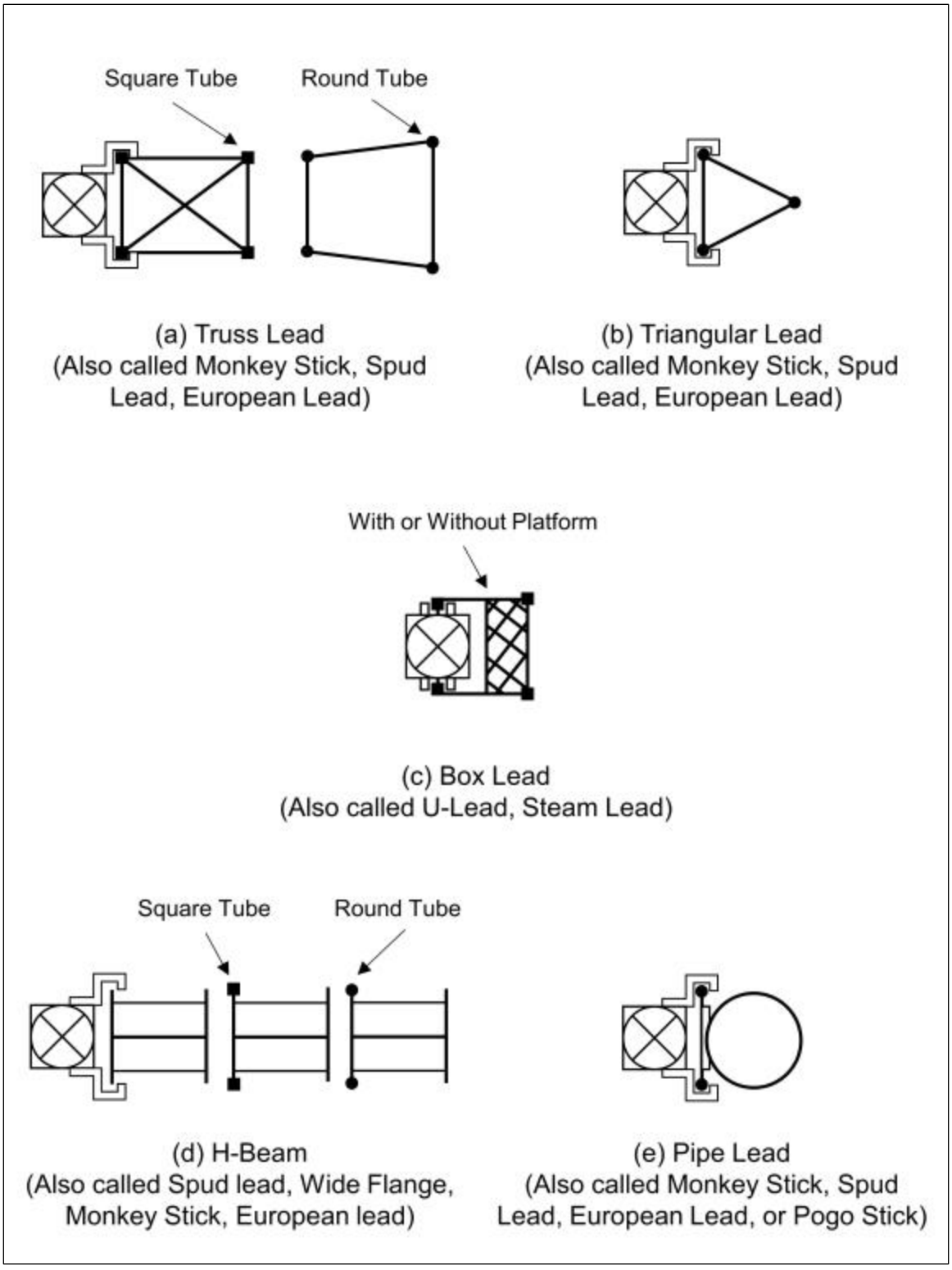

Figure 15-6 Typical lead types (after DFI Publication 1981).

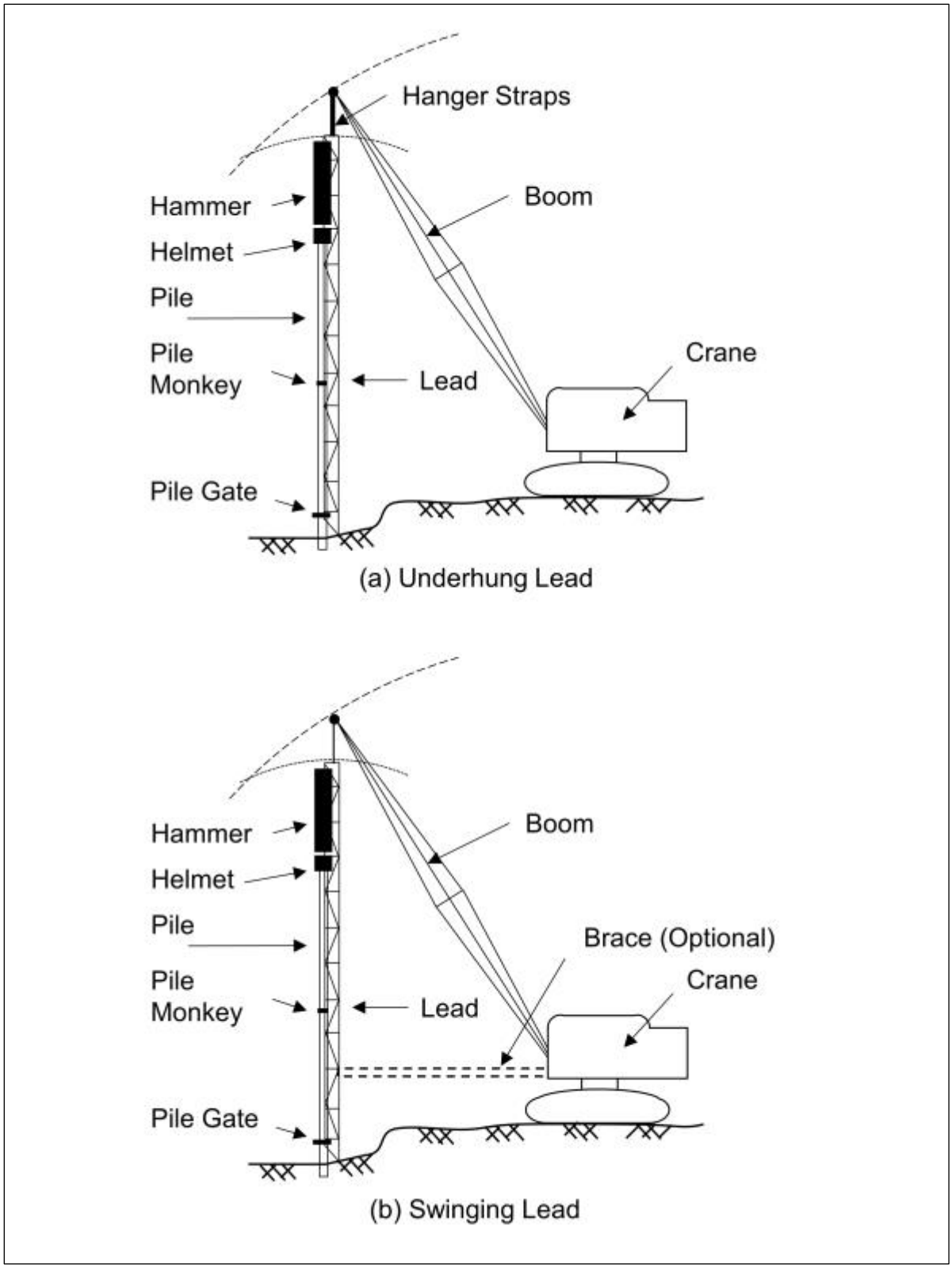

Figure 15-7 Swinging lead systems (after DFI Publication 1981).

the boom with hanger straps as illustrated in Figure 15-7(a) with the hammer held by a crane line. The most common arrangement however, is shown in Figure 15-7(b) where the leads and hammer are held by separate crane lines. Swinging leads are free to rotate sufficiently to align the hammer and the head of the pile without precise alignment of the crane with the pile head. Because the weight of the leads is low, this type of lead generally permits the largest crane operating radius, providing more site coverage from one crane position.

Photographs of swinging lead arrangements on pile driving rigs were previously presented in Figure 15-1 and 15-2. A stabbing guide is located at the bottom of a swinging lead system as illustrated in Figure 15-8. Pile location and alignment are controlled by positioning the lead system over the pile location, lifting the leads, and then dropping the leads so that the stabbing guide at the bottom of the leads penetrates into the ground. The crane boom is then manipulated until the specified verticality or batter angle is achieved.

Pile driving specifications have historically penalized or prohibited swinging leads. This general attitude is not justified based on currently available equipment. There are many cases where swinging leads are more desirable than fixed leads. For example, swinging leads are preferable for pile installation in excavations or over water. As noted earlier, the function of a lead is to hold the pile in good alignment with the driving system in order to prevent pile damage, and to hold the pile in its proper position for driving. If a swinging lead is long enough so that the bottom is firmly embedded in the ground, and if the bottom of the lead is equipped with a gate then bottom alignment of the pile will be maintained (Figure 15-9). In this situation, if the pile begins to move out of position during driving, it must move the bottom of the lead with it. Swinging leads should be of sufficient length so that the free line between the boom tip and the top of the leads is short, thus holding the top of the lead in good alignment. When batter piles are driven, pile alignment is more difficult to set with swinging leads. This problem is accentuated for diesel hammers since the hammer starting operation will tend to pull the pile out of line.

Fixed leads are connected to the boom point and to the crane frame using a spotter or brace that runs from the bottom of the leads to the crane. A schematic of a typical fixed lead system is depicted in Figure 15-10(a) and a photograph is presented in Figure 15-11. A fixed lead system attempts to hold the pile in true alignment while driving but may require more time for rig repositioning prior to driving.

Figure 15-8 Stabbing guide at bottom of box leads.

Figure 15-9 Pile gate with latch for use on truss lead (courtesy Berminghammer).

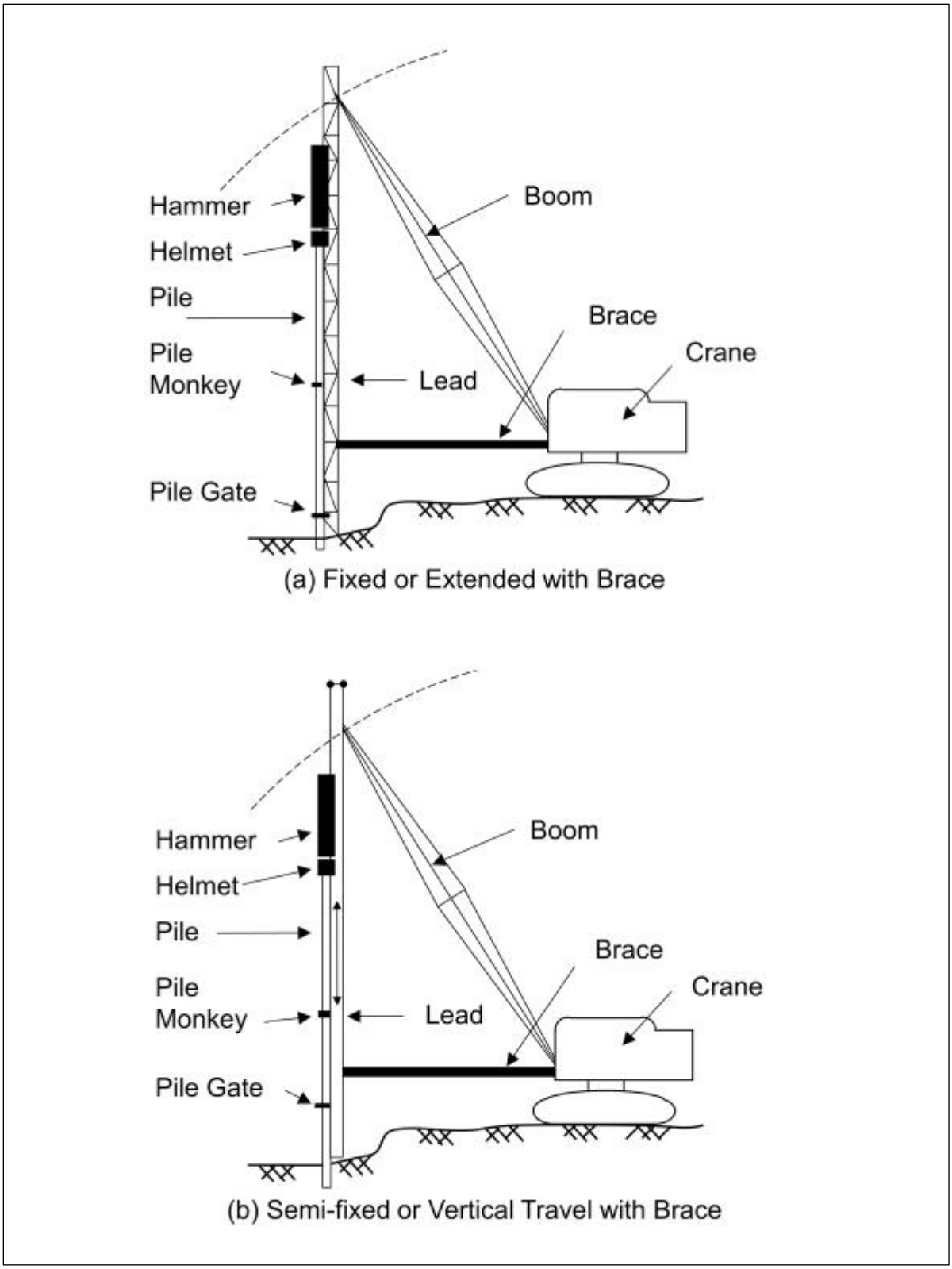

Figure 15-10 Fixed lead systems (after DFI Publication 1981).

Figure 15-11 Fixed lead system with air compressor mounted as counterweight (courtesy FHWA Demo 66).

As an alternative to a fixed lead system, a semi-fixed or vertical travel lead may be used. A semi-fixed lead, as shown in Figure 15-12, allows vertical lead movement at the lead connection points to the boom and brace which the standard fixed lead system does not.

Figure 15-12 Vertical travel lead system (courtesy Berminghammer).

Figure 15-13(a) illustrates that a fixed lead is limited to plumb piles or batter piles in line with the leads and crane boom. To drive side batter piles, a moonbeam must be attached at the end of the spotter or brace as depicted in Figure 15-13(b).

Offshore leads are similar to swinging leads in that they are free to rotate sufficiently to align the hammer and pile head, however they do not require precise alignment of the crane with the pile head, and they generally consist of only a short lead section with a pile guide at the base. An offshore lead schematic is depicted in Figure 15-14. The short lead section is intended only to hold and axially align the hammer with the pile head, and does not provide support for batter or full pile alignment during the driving process. When offshore leads are used, a template is constructed to hold the pile in position during driving. Section 15.3 provides a further discussion on templates. A photograph of an offshore lead with guide is shown in Figure 15-15 and of an offshore lead system in use with a rough terrain crane in Figure 15-3.

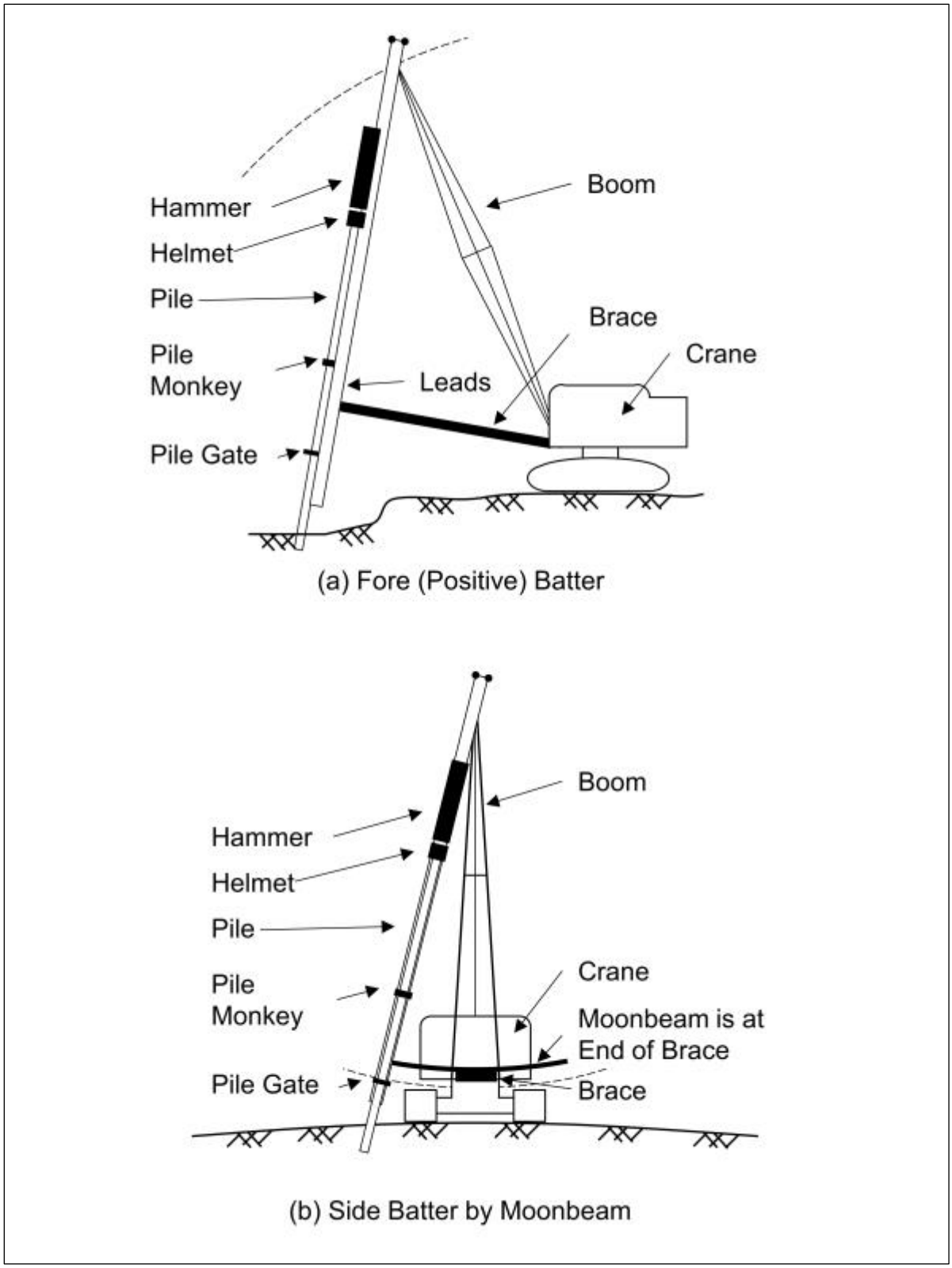

Figure 15-13 Lead configuration for batter piles (after DFI publication 1981).

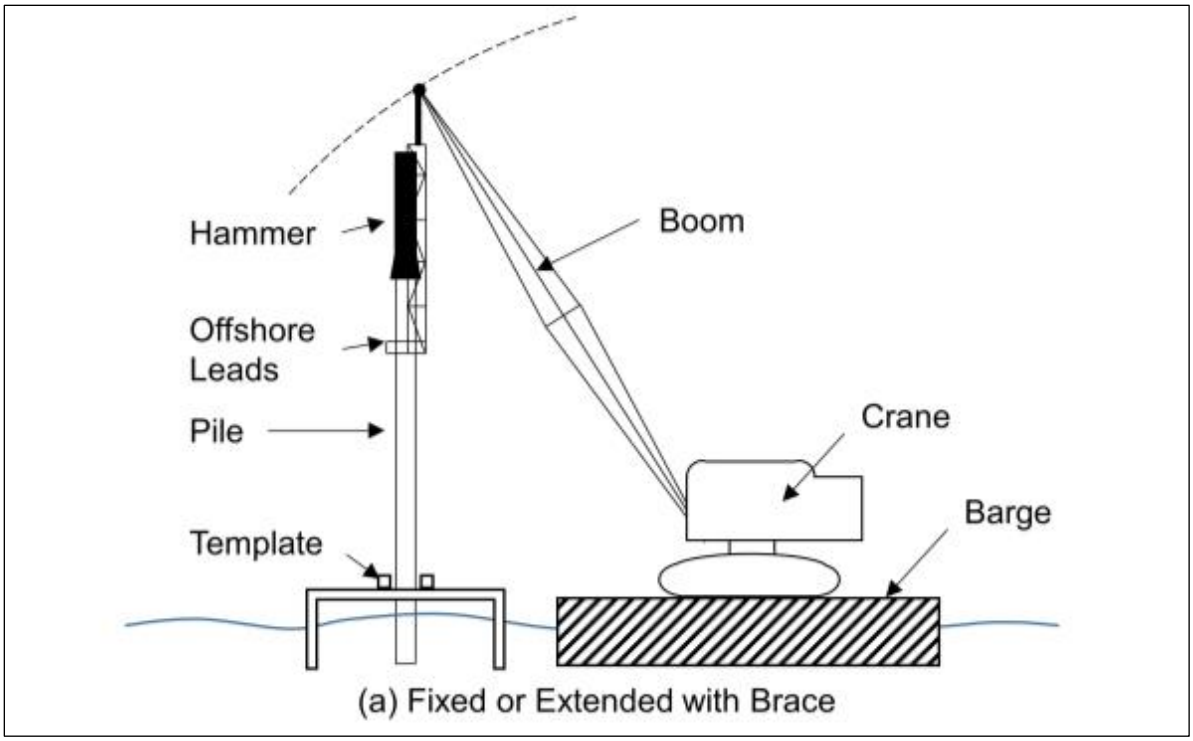

Figure 15-14 Typical offshore lead configuration.

Figure 15-15 Offshore lead and pile guide (left) with pipe pile helmet (right) (courtesy Berminghammer).

Regardless of lead type chosen, the pile must be kept in good alignment with the hammer to avoid eccentric impacts which can cause local stress concentrations and pile damage. The hammer and helmet, centered in the leads and on the pile head, keep the pile head in alignment. A pile gate at the bottom of the leads should be used to keep the lower portion of the pile centered in the leads.

15.4 TEMPLATES

Templates are required to hold piles in proper position and alignment when an offshore or swinging lead system is used over water or excavations. The top of the template should be located within 5 feet of the pile cutoff elevation or the water elevation, whichever is lower. The preferred elevation of the template is at or below the pile cutoff elevation so that final driving can occur without stopping for template removal. A photograph of a typical template is presented in Figure 15-16. When templates include batter piles, it must be remembered that the correct location for the batter piles in the template arrangement will vary depending upon the template elevation relative to the pile cutoff elevation. For example, consider a template located 5 feet above pile cutoff elevation. If the plan pile locations at cutoff are used at the template elevation, a 1H:4V batter pile would be 15 inches out of location at the pile cutoff elevation. This problem is illustrated in Figure 15-17. Template construction should also allow the pile to pass freely through the template without binding. Templates with rollers are preferable, particularly for batter piles.

Figure 15-16 Template system.

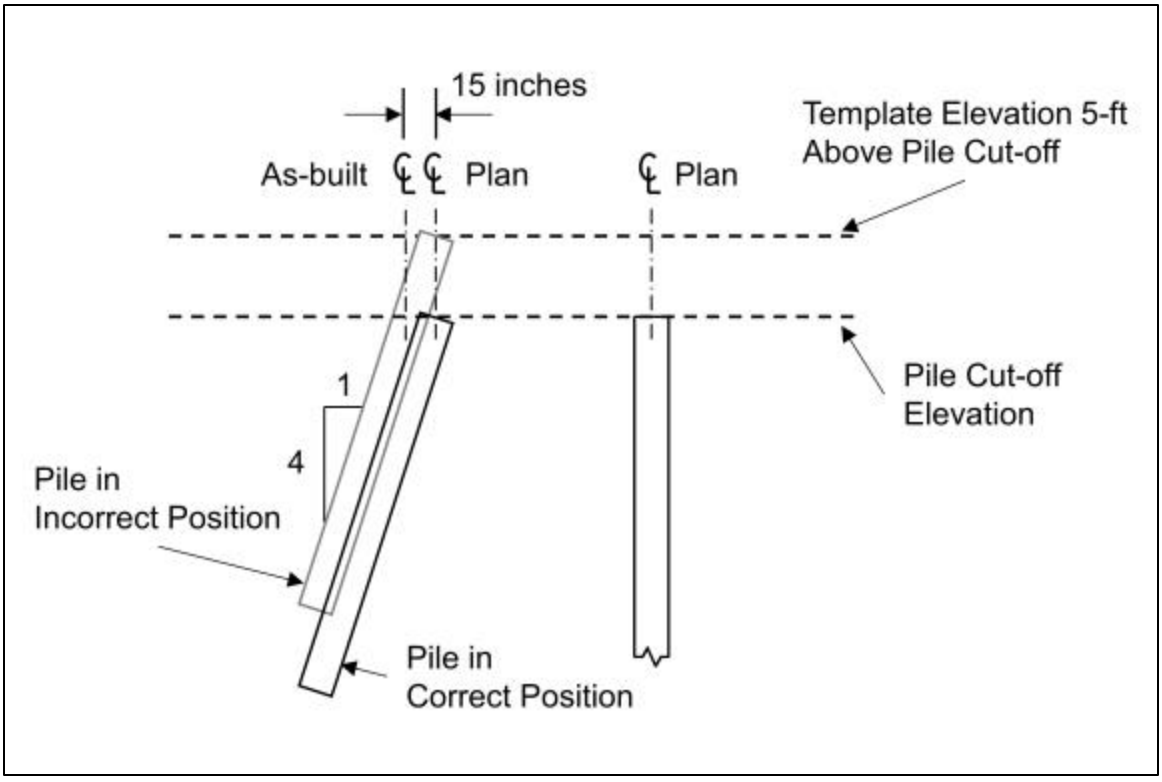

Figure 15-17 Template elevation effects on batter piles (after Passe 1994).

15.5 HELMETS

Figure 15-18 shows the components of a typical helmet and the nomenclature used for associated components. The helmet configuration and size used depends upon the lead type, pile type and the type of hammer used for driving. Helmets may be a one piece unit manufactured for driving a specific pile type and size, or may consist of two pieces consisting of a base helmet with an insert to accommodate various pile types and sizes. Details on the proper helmet for a particular hammer can be obtained from hammer manufacturers, suppliers and contractors. To avoid the transmission of torsion or bending forces, the helmet or insert should fit loosely, but not so loosely as to prevent the proper alignment of hammer and pile. Helmets or inserts should be approximately 0.1 to 0.2 inches larger than the pile diameter. Proper hammer-pile alignment is particularly critical for precast concrete piles.

In Figure 15-19 a photograph of a helmet that cracked during driving provides a unique cross sectional view illustrating a typical striker plate, hammer cushion (consisting of two aluminum plates and one micarta plate), and helmet configuration. Photographs of one piece helmets for a concrete pile and pipe pile are presented in Figure 15-20(a) and 15-20(b), respectively.

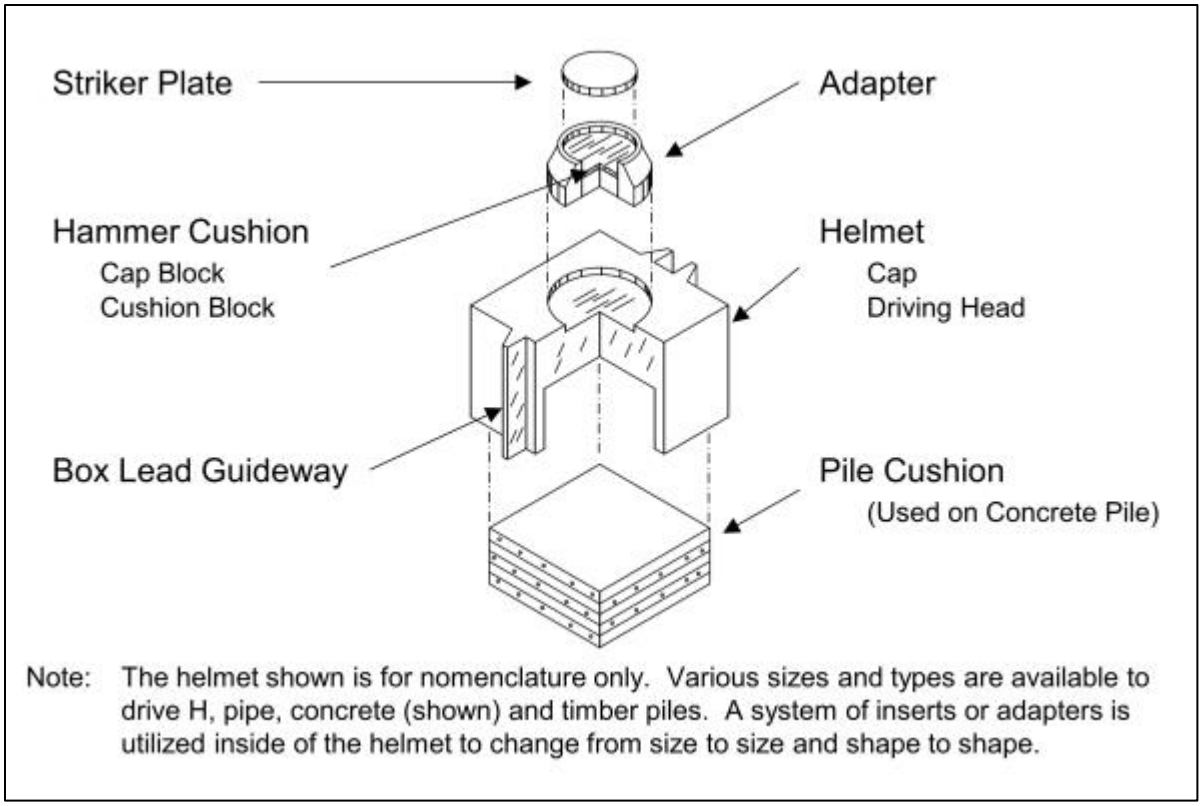

Figure 15-18 Helmet components (after DFI Publication 1981).

Figure 15-19 Cross section of cracked helmet with striker plate and aluminum and micarta hammer cushion (courtesy of WKG[2]).

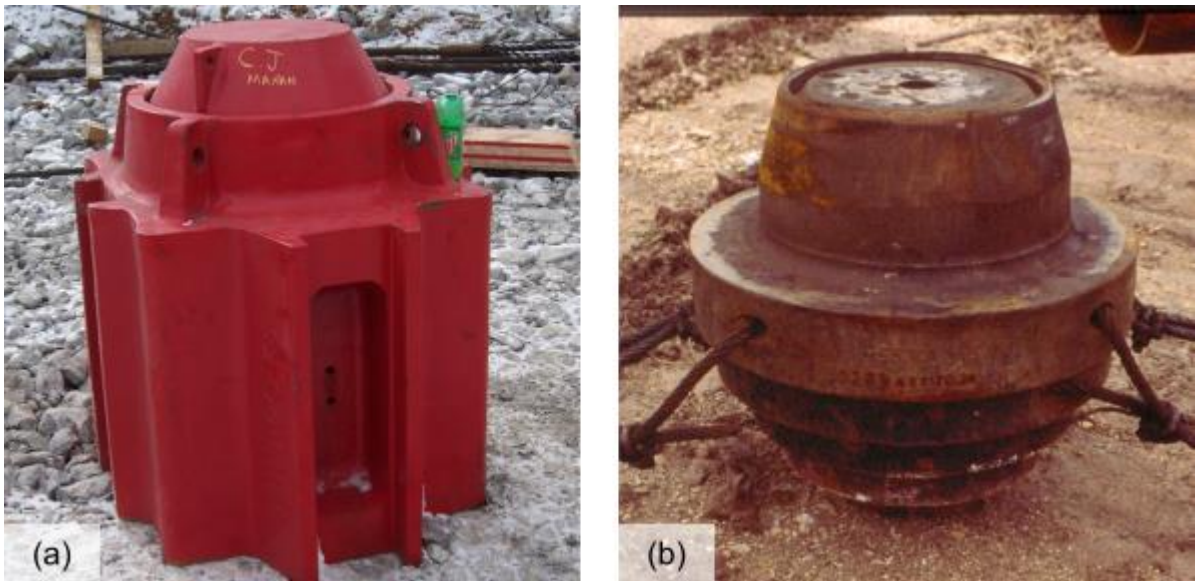

Figure 15-20 One piece helmets for (a) concrete pile and (b) pipe pile.

A two piece system consisting of a base or primary helmet and an insert can also be used to adapt a base helmet for driving different pile types. A base helmet with an insert for driving H-piles is presented in Figure 15-21(a) and a photograph showing several pipe pile inserts to accommodate different pipe pile diameters and wall thickness on the same project is presented in Figure 15-21(b).

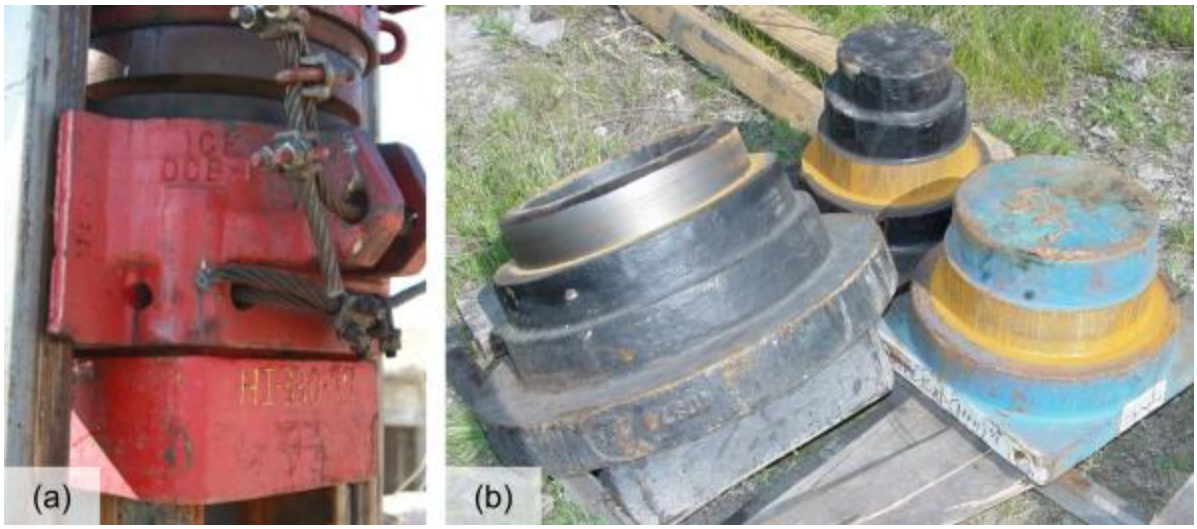

Figure 15-21 Inserts for (a) H-pile and (b) varying pipe pile diameter and wall thickness.

15.6 HAMMER CUSHIONS

Most hammers use a hammer cushion between the hammer and the helmet to relieve the impact shock, thus protecting the pile hammer. However, some hammer models exist that do not require a hammer cushion, or utilize a direct drive option where the hammer cushion is replaced by a steel striker plate. Ineffective hammer cushions can cause damage to hammer striking parts, anvil, helmet or pile. Hammer cushion materials are usually proprietary man-made materials such as micarta, nylon, urethane or other durable polymers. Over time, hammer cushion materials become compressed and stiffen as additional hammer impacts are applied. Therefore, hammer cushions eventually become ineffective, or may result in significant reduction in transferred energy or increased bending stress. Proprietary hammer cushions may last for up to 200 hours of driving.

In the past, a commonly used hammer cushion was made of hardwood (one piece), approximately 6 inches thick, with the wood grain parallel to the pile axis. This type of cushioning has the disadvantage of quickly becoming crushed and burned as well as having variable elastic properties during driving. With the widespread availability of hammer cushions from durable man-made materials, hammer cushions consisting of hardwood, small pieces of wood, wire rope, or other highly elastic material should not be permitted. Cushion materials containing asbestos are not acceptable because of health hazards. All of these hammer cushion materials are prohibited by AASHTO LRFD Bridge Construction Specifications.

Proprietary man-made hammer cushion materials have better energy transmission characteristics than a hardwood block, maintain more nearly constant elastic properties, and have a relatively long life. Their use results in more consistent transmission of hammer energy to the pile and more uniform driving. Since proprietary hammer cushion materials last up to 200 hours, it is often sufficient on smaller projects to inspect the cushion material only once before the start of pile driving operation. Periodic inspections of hammer cushion wear and thickness should be performed on larger projects. Many hammers require a specific cushion thickness for proper hammer timing. In these hammers, improper cushion thickness will result in poor hammer performance. Some man-made hammer cushions are laminated sandwiches of aluminum and another material such as micarta. The aluminum is used to transfer the heat generated during impact out of the cushion, thus prolonging its useful life. Some common proprietary hammer cushion materials are shown in Figure 15-22 and include Conbest and aluminum (top left), Blue Nylon (right), and aluminum and Micarta (lower left).

Figure 15-22 Typical hammer cushion materials.

15.7 PILE CUSHIONS

To avoid damage to the head of a concrete pile as a result of direct impact from the helmet, a pile cushion should be placed between the helmet and the pile head. Typical pile cushions are made of compressible material such as plywood, hardwood, plywood and hardwood composites or other man made materials. Wood pile cushions should have a minimum thickness of 4 inches. Pile cushions should be checked periodically for damage and replaced before excessive compression or charring takes place. After replacing a cushion during driving, the blow count from the first 100 blows should not be used for pile acceptance as the cushion is still rapidly absorbing energy. The blow count will only be reliable after 100 blows of full energy application. The total number of blows which can be applied to a wood cushion is generally between 1000 and 2000. For wood pile cushions, it is recommended that a new, dry cushion be used for each pile. Old or water soaked cushions do not have good energy transfer, and will often deteriorate quickly. A

photograph of plywood pile cushions is presented in Figure 15-23. An unused cushion is shown on the right, while a used and compressed cushion is shown on the left.

Figure 15-23 Plywood pile cushions: (left) used and (right) new.

15.8 HAMMERS

Pile hammers can be categorized in three main types: impact hammers, vibratory ahammers, and resonant hammers. Impact hammer are the primary hammer type used to install foundation piles. There are numerous types of impact hammers having variations in the types of power source, configurations, and rated energies. Figure 15-24 shows a classification of hammers based on motivation and configuration factors. Table 15-1 presents characteristics and uses of several types of hammers. A detailed discussion of various types of hammers follows later in this chapter. Discussion on the key inspection issues associated with each hammer type is provided in Chapter 18. Additional hammer guidance may be found in The Performance of Pile Driving Systems by Rausche et al. (1986), as well as in the Deep Foundation Institute Pile Inspector's Guide to Hammers (1995).

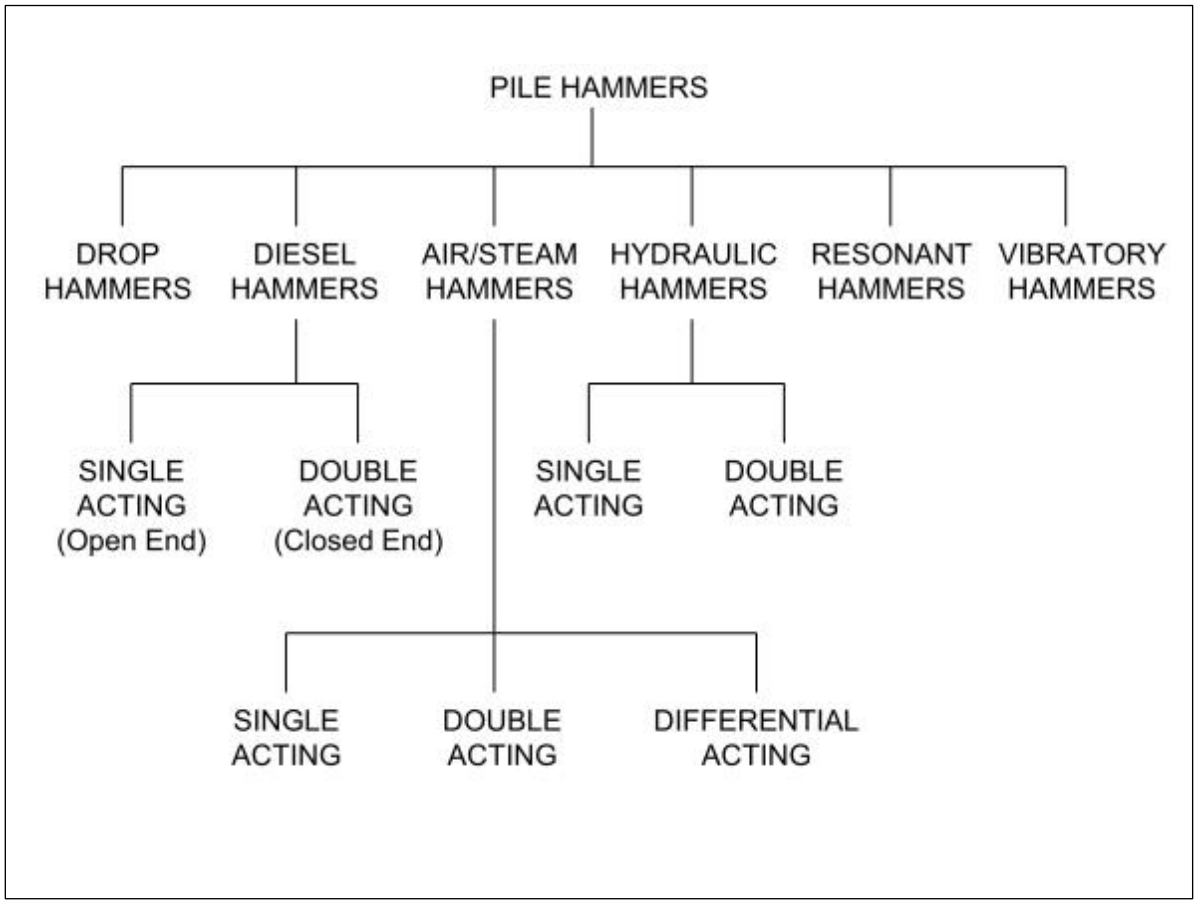

Figure 15-24 Pile hammer classification.

Table 15-1 Typical Pile Hammer Characteristics and Uses

Hammer Type	Single Acting Air / Steam	Double Acting Air / Steam	Differential Acting Air / Steam	Single Acting Diesel (open end)	Double Acting Diesel (closed end)
Rated energy (ft-kips)	7 to 1800	1 to 21	15 to 50	9 to 1620	5 to 73
Impact velocity (ft/sec)	8 to 16.5	15 to 20	13 to 15	10 to 16.5	8 to 16.5
Blow Rate (blows/minute)	35 to 60	95 to 300	98 to 300	40 to 60	80 to 105
Energy (per blow)	Ram weight x stroke.	(Ram weight + effective piston head area x effective fluid pressure) x stroke.	(Ram weight + effective piston head area x effective fluid pressure) x stroke.	Ram weight x stroke.	(Ram weight + bounce chamber pressure) x stroke.
Lifting power	Air or steam.	Air or steam.	Air or steam.	Provided by the combustion of injected diesel fluid.	Provided by the combustion of injected diesel fluid.
Maintenance	More complex than for drop hammer.	More complex than for single acting.	More complex than for single acting.	More complex than most air impact hammers.	More complex than most air impact hammers.
Hammer suitability for types of piles	Versatile for any pile, particularly large concrete and steel pipe.	Timber, steel H and pipe piles.	Timber, steel H and pipe piles.	All types of piles.	All types of piles.
Major advantages	Relatively simple and moderate cost.	More productive than single acting. Some double acting fully enclosed and can be used underwater.	More productive than single acting. Differential air hammer uses less volume of air or steam than double acting and has lower impact velocity.	Carry their own fuel from which power is internally generated. Stroke is a function of pile resistance.	Carry their own fuel from which power is internally generated. Stroke is a function of pile resistance.
Major disadvantages	Need air compressor or steam plant. Heavy compared with most diesel hammers.	Costs more than single acting. Need air compressor or steam plant.	Costs more than single acting. Need air compressor or steam plant. Heavy compared to diesel hammer.	Pollution from diesel exhaust. Higher cost hammer. Low blows per minute at higher strokes for single acting.	Pollution from diesel exhaust. Higher cost hammer. Hammer lift off in hard driving conditions.
Remarks	Commonly available hammer type.	Ram accelerates downward under pressure.	Ram accelerates downward under pressure.	Most commonly used hammer type. Variable stroke.	Limited availability and use in practice.

Table 15-1 Typical Pile Hammer Characteristics and Uses (Continued)

Hammer Type	Drop	Single Acting Hydraulic	Double Acting Hydraulic	Vibratory	Resonant
Rated energy (ft-kips)	7 to 60	25 to 2162	25 to 2581	----	----
Impact velocity (ft/sec)	23 to 33	5 to 18	5 to 23	----	----
Blow Rate (blows/minute)	4 to 8	30 to 50	40 to 90	750 to 2,400 vibrations/minute	up to 10,800 vibrations/minute
Energy (per blow)	Ram weight x height of fall.	Ram weight x stroke.	(Ram weight + effective piston head area x effective fluid pressure) x stroke.	----	----
Lifting power	Provided by hoisting engine or a crane.	Hydraulic	Hydraulic	Hydraulic or electric power.	Hydraulic
Maintenance	Simple	More complex than other impact hammers.	More complex than other impact hammers.	Highest maintenance cost.	More complex than other hammer types
Hammer suitability for types of piles	All types except concrete piles	All types of piles.	All types of piles.	End bearing steel H and pipe piles. Very effective in granular soils.	Steel H piles and pipe piles.
Major advantages	Lowest initial cost equipment.	Fully variable energy can be delivered.	Energy is variable over a wide range. Can be used for underwater driving.	Can be used for pulling or driving. Fast operating pile installation tool.	Fast pile installation. Very low ground vibrations. Reduced noise.
Major disadvantages	Very high dynamic forces and danger of pile damage. Lowest pile productivity.	High initial cost. Energy readout device recommended to monitor performance.	High initial cost. Fully enclosed, need energy readout device to monitor performance.	High investment and maintenance. Not recommend for friction pile installations.	Limited availability at present.
Remarks	Generally obsolete.	Commonly available hammer type.	Commonly available hammer type.	Variable moment hammers can help control construction vibrations.	Newer hammer type and may require additional field inspection and/or testing.

Note: Vibratory and resonant hammer rated based on power, not energy.

15.8.1 Hammer Energy Concepts

Before the advent of computers and the availability of the wave equation to evaluate pile driving, driving criteria for a given nominal resistance was evaluated by concepts of work or energy. Work is done when the hammer forces the pile into the ground a certain distance. The hammer energy was equated with the work required, defined as the nominal geotechnical resistance times the final set. This simple idea led engineers to calculate energy ratings for pile hammers and resulted in numerous dynamic formulas which ranged from very simple to very complex. Dynamic formulas have generally been replaced by more reliable methods of resistance determination. However, the energy rating legacy for pile hammers remains.

The energy rating of hammers operating by gravity principles only (drop, single acting air/steam or hydraulic hammers) was assigned based on their potential energy at full stroke (ram weight, w, times stroke, h). Although single acting (open end) diesel hammers could also be rated this way, some manufacturers used other principles for energy rating. Historically, these hammers have usually been rated by the manufacturer's rating, while the actual observed stroke was often ignored in using the dynamic formula. In current practice, the stroke is often measured electronically from the blow rate, which is an improvement over past practice. In the case of all double acting hammers (air/steam, hydraulic, or diesel), the net effect of the downward pressure on the ram during the downstroke is to increase the equivalent stroke and reduce time required per blow cycle. The equivalent stroke is defined as the stroke of the equivalent single acting hammer yielding the same impact velocity. The manufacturers generally calculate the potential energy equivalent for double acting hammers.

Ideally, the impact velocity, V_i, could be directly computed using basic laws of physics from the equivalent maximum stroke as shown in Equation 15-1.

$$V_i = \sqrt{2\,g\,h} \qquad \text{Eq. 15-1}$$

Where:

V_i = impact velocity (ft/s).
g = acceleration due to gravity (32.17 ft/s^2).
h = ram stroke (feet).

The kinetic energy could be computed from Equation 15-2.

$$KE = \frac{1}{2}\,m\,V_i^{\,2} \qquad \text{Eq. 15-2}$$

Where:

KE = kinetic energy (ft-lbs).
V_i = impact velocity (ft/s).
m = ram mass (slugs/kips).

If there were no losses, the kinetic energy would equal the potential energy. In reality however, energy losses occur due to a variety of factors (friction, residual air pressures, preadmission, gas compression in the diesel combustion cylinder, pre-ignition, etc.) which result in the kinetic energy being less than the potential energy. It is the inspector's task to identify these losses when possible, and the contractor's task to correct situations where losses are excessive. Some hammers, such as modern hydraulic hammers, measure the velocity near impact and hence can calculate the actual kinetic energy available.

Further losses occur in the transmission of energy to the pile. The hammer cushion, helmet, and pile cushion all have kinetic energy and store some strain energy, while the pile head also has inelastic collision losses. Energy is transferred to the pile with time and therefore the energy delivered to the pile can be calculated from the work done as the integral of the product of force and velocity with time. This is referred to as the transferred energy or ENTHRU.

Pile length, stiffness and resistance influence the energy delivered to the pile. The actual stroke (or potential energy) of diesel hammers depends on the pile resistance and the net transferred energy, which can vary. The stroke of single acting air/steam hammers is somewhat dependent upon the pile resistance and rebound while the stroke of all double acting hammers is even more dependent on pile resistance due to lift-off considerations. In reality, transferred energy increases only when both the force and velocity are positive (compression forces; downward velocity). As resistance increases and/or for shorter pile lengths, the rebound or upward velocity occurs earlier, and the pile then transfers energy back to the driving system. In fact, the energy returning to the hammer may occur before all the energy has been transferred into the pile.

15.9 DROP HAMMERS

The most rudimentary pile hammer still in use today is the drop hammer as shown in Figure 15-25. These hammers consist of a hoisting engine having a friction clutch, a hoist line, and a drop weight. The hammer stroke is widely variable and often not very precisely controlled. Operation proceeds by engaging the hoist clutch to raise the drop weight or ram. The hoist clutch is then disengaged, allowing the drop

weight to fall as the hoist line pays out. Efficiency of the fall is low since the ram is attached by a cable to the hoist and must overcome the rotational inertia of the hoist. Ideally, the crane operator engages the clutch immediately after impact to prevent excessive cable spooling. If the operator prematurely engages the clutch, or it is partially engaged during spooling, the fall efficiency and impact energy is reduced.

The hammer operating speed (blows per minute) depends upon the skill of the operator and the height of fall being used, but is generally very slow. One of the greatest risks in using a drop hammer is overstressing and damaging the pile. Pile stresses are generally increased with an increase in the impact velocity (hammer stroke) of the striking weight. Therefore, the maximum stroke should be limited to those strokes where pile damage is not expected to occur. In general, drop hammers are not as efficient as other impact hammers but are inexpensive and simple to operate and maintain. Current use of these hammers is generally limited to sheet pile installations where pile resistance is not an issue. Drop hammers are not recommended for foundation pile installations.

Figure 15-25 Typical drop hammer.

15.10 SINGLE ACTING AIR/STEAM HAMMERS

Single acting air/steam hammers are essentially gravity, or drop hammers, for which the hoist line has been replaced by a pressurized medium, being either steam or air. While originally developed for steam power, the vast majority of these hammers today operate on compressed air. To lift the ram weight with motive pressure, a simple one cylinder steam engine principle is used. The ram consists of a compact block with a so called ram point attached at its base. The ram point strikes against a striker plate as illustrated in Figure 15-26. A photograph of a typical single acting air/steam hammer is presented in Figure 15-27(a).

During the upstroke cycle, the ram is raised by externally produced air or steam pressure acting against a piston housed in the hammer cylinder. The piston in turn is connected to the ram by a rod. Once the ram is raised a certain distance, a valve is activated and the pressure in the chamber is released. At that time, the ram has some remaining upward velocity that depends upon the pile rebound, inlet air pressure, and volume of air within the hammer cylinder. Against the action of gravity and friction, the ram then "coasts" up to the maximum height (stroke). The maximum stroke, and hence hammer potential energy, is therefore not constant and depends upon the pressure and volume of air or steam supplied, as well as the amount of pile rebound due to soil resistance effects. During the downstroke cycle, the ram falls by gravity (less friction) to impact the striker plate and hammer cushion. Just before impact, the pressure valve is activated and pressure again enters the cylinder. This occurs approximately 2 inches before impact, but depends on having the correct hammer cushion thickness. If the hammer cushion height is too low, then the pressure is introduced too early, reducing the impact energy of the ram. This condition is referred to as "preadmission."

The dynamic forces exerted on a pile by a single acting air/steam hammer are of the same short time duration as those exerted by a drop hammer. Because operating strokes are generally shorter, the accelerations generated by single acting air/steam hammers do not reach the magnitude of drop hammers. Some hammers may be equipped with two nominal strokes, one full stroke and another of lesser height. The hammer operator can switch between the two to better match the driving conditions and limit driving resistance or control tension driving stresses as needed. The maximum stroke of single acting air/steam hammers generally ranges from 3 to 5 feet. The weights of single acting air/steam hammer rams are usually considerably higher than drop hammer weights. Single acting air/steam hammers have the advantages of moderate cost and relatively simple operation and maintenance. They can be used for many pile types, particularly large concrete and steel piles.

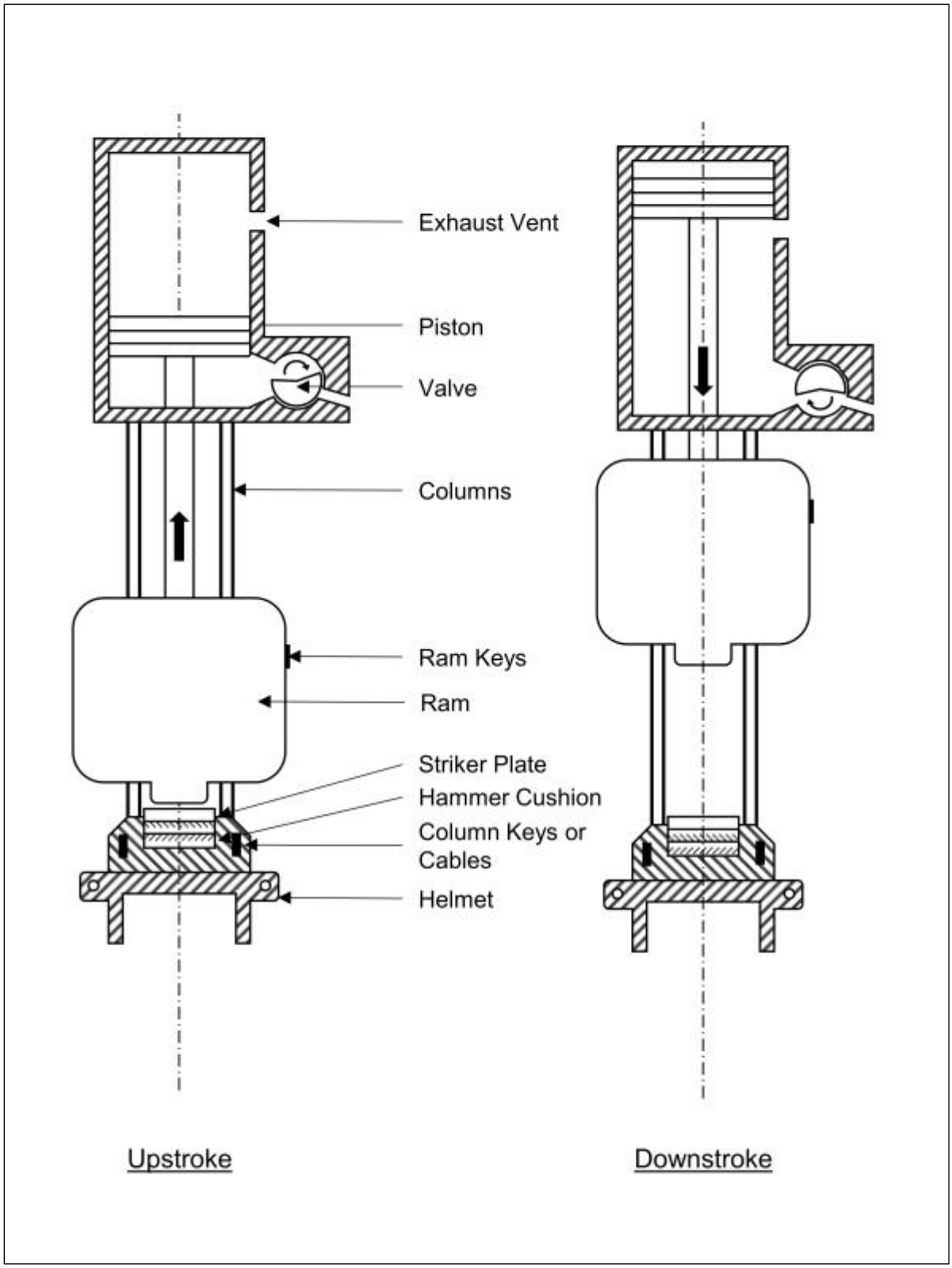

Figure 15-26 Schematic of a single acting air/steam hammer.

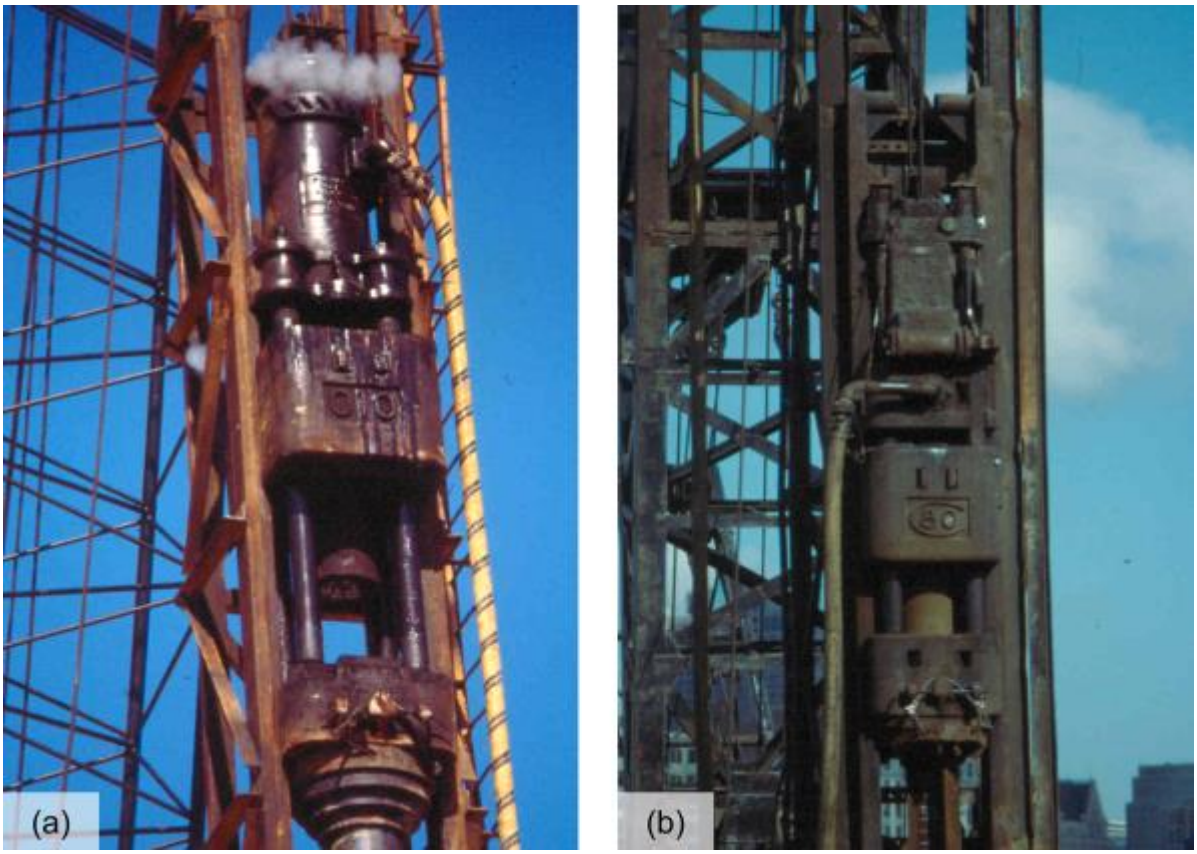

Figure 15-27 (a) Single acting air, and (b) differential acting air hammers.

15.11 DOUBLE ACTING AIR/STEAM HAMMERS

The working principle of a double acting air/steam hammer is illustrated in Figure 15-28. For a double acting hammer, the ram is raised by pressurized air or steam during the upstroke. As the ram nears the maximum up stroke, the lower air valve opens, allowing the lower cylinder chamber to release the pressurized air. Once the ram reaches full stroke, the upper valve changes to admit pressurized air or steam to the upper cylinder. Gravity and the upper cylinder pressure accelerate the ram through its downward fall. As with the single acting hammer, the stroke is again not constant, due to variable lift pressure and volume as well as differing pile rebound. During hard driving with high pile rebound, the pressure may need to be reduced to prevent lift off, the hammer actually lifting up and away from the pile head. Since the maximum stroke is limited and the same pressure is applied during downstroke, a reduction in the operating pressure due to lift off may cause the kinetic energy at impact to be reduced during these hard driving situations. Just before impact, the valve positions are reversed and the cycle repeats.

The correct cushion thickness is extremely important for the proper operation of the hammer. If the hammer timing is off significantly, it is possible for the hammer to run with the ram moving properly, but with little or no impact force delivered to the pile. The kinetic energy of the ram at impact depends on the ram weight and stroke as well as the motive pressure effects. The overall result is that a properly operating double acting hammer with its shorter stroke delivers comparable impact energy per blow at up to about two times the blow rate of a single acting hammer of the same ram weight.

Some double acting air/steam hammers are fully enclosed and can be operated underwater. They may be more productive than single acting hammers, but are more dependent upon the air pressure. Experience has shown that on average, they are slightly less efficient than equivalently rated single acting hammers. Double acting hammers generally cost more than single acting hammers and require additional maintenance. Similar to single acting air/steam hammers, they require an air compressor or a steam plant. However, double acting air/steam hammers consume more air and require greater air pressures than equivalent single acting hammers. The use of double acting air/steam hammers has diminished and they are infrequently encountered in practice.

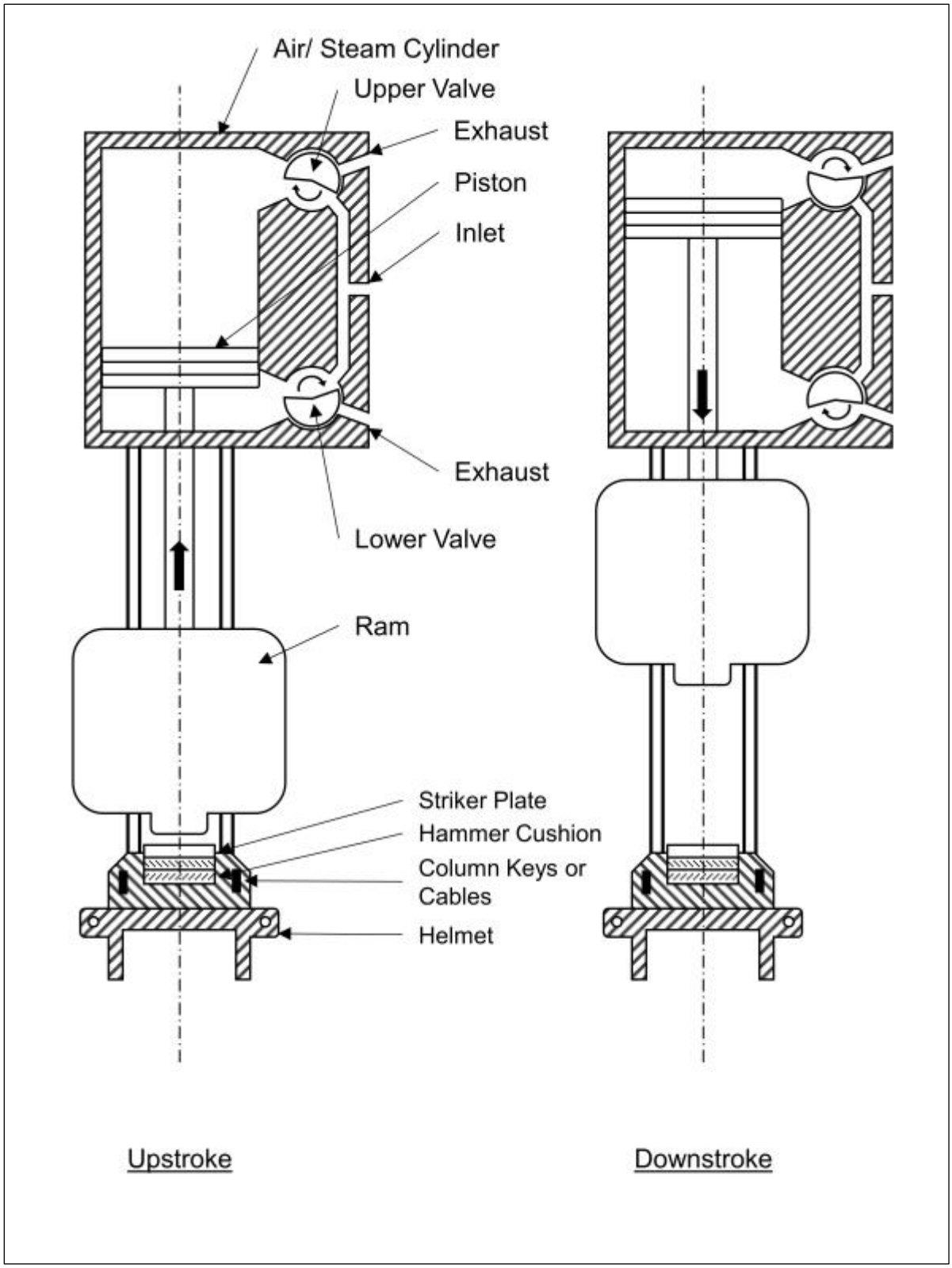

Figure 15-28 Schematic of a double acting air/steam hammer.

15.12 DIFFERENTIAL ACTING AIR/STEAM HAMMERS

The differential acting air/steam hammer is another type of double acting hammer with relatively short stroke and fast blow rates. A photograph of a differential acting air hammer is presented in Figure 15-27(b), while the working principle is illustrated in Figure 15-29. Operation is achieved by pressure acting on two different diameter pistons connected to the ram. At the start of the cycle, the single valve is positioned so that the upper chamber is open to atmospheric pressure only and the lower chamber is pressurized with the motive fluid. The pressure between the two pistons has a net upward effect due to the differing areas, thus raising the ram. The ram has an upward velocity when the valve position changes and applies air pressure into the upper chamber, causing the net force to change to the downward direction. Thus air pressure along with gravity and friction slows the ram, and after attaining the maximum stroke of the cycle, assists gravity during the downstroke to speed the ram.

As with the double acting hammers, the kinetic energy at impact may need to be reduced during hard driving since the pressure, which assists gravity during downstroke, must be reduced to prevent hammer lift-off. As with the other air/steam hammers, when the ram attains its maximum kinetic energy just before impact, the valve position is reversed and the cycle begins again. Therefore, the hammer cushion must be of the proper thickness to prevent preadmission which could cause reduced transferred energy. Very high air pressures between 120 and 140 psi at the hammer inlet are required for proper operation. However, most air compressors only produce pressures of about 120 to 130 psi at the compressor. As with the double acting hammer, the efficiency of a differential hammer is somewhat lower than the equivalent single acting air/steam hammer. The heavier ram of the differential acting hammer is lifted and driven downward with a lower volume of air or steam than is used by a double acting hammer. The use of differential acting air/steam hammers has also diminished and they too are infrequently encountered in practice.

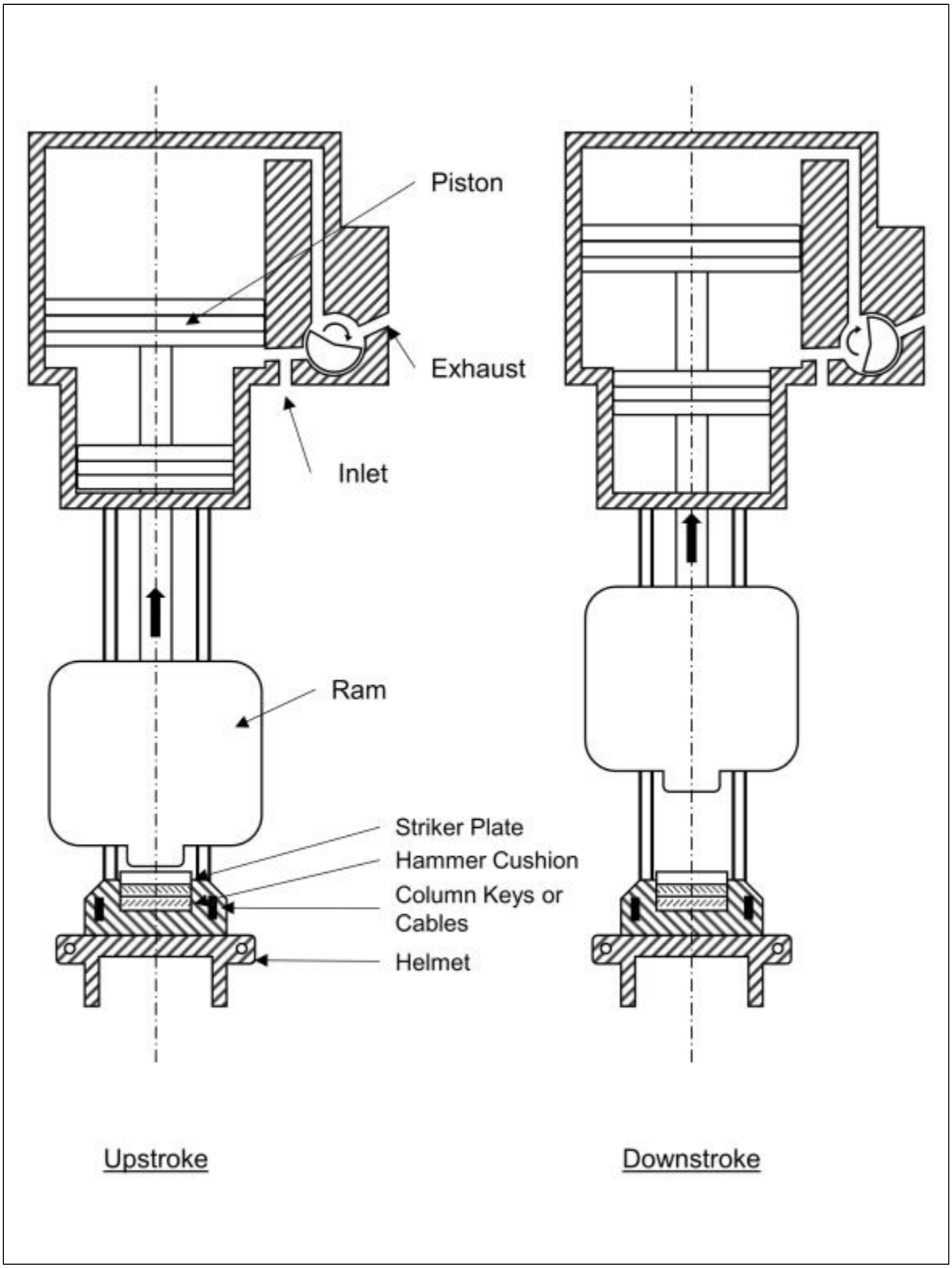

Figure 15-29 Schematic of a differential acting air/steam hammer.

15.13 SINGLE ACTING (OPEN END) DIESEL HAMMERS

The basic distinction between all diesel hammers and all air/steam hammers is that, whereas air/steam hammers are one cylinder engines requiring motive power from an external source, diesel hammers carry their own fuel from which they generate power internally. Figure 15-30 shows the working principle of a single acting diesel hammer. The initial power to lift the ram must be furnished by a hoist line or other source to lift the ram upward on a trip block. After the trip mechanism is released, the ram guided by the outer hammer cylinder falls under gravity. As the ram falls, diesel fuel is injected into the cylinder below the air/exhaust ports. Once the ram passes the air/exhaust ports the diesel fuel is compressed and heats the entrapped air. As the ram impacts the anvil the fuel explodes, increasing the gas pressure. In some hammers the fuel is injected in liquid form as shown in Figure 15-30(b), while in other hammers the fuel is atomized and injected later in the cycle and just prior to impact. In either case, the combination of ram impact and fuel explosion drives the pile downward, and the gas pressure and pile rebound propels the ram upward in the cylinder. On the upstroke, the ram passes the air ports and the spent gases are exhausted. Since the ram has a velocity at that time, the ram continues upward against gravity, and fresh air is pulled into the cylinder. The cycle then repeats until the fuel input is interrupted.

There is no consensus by the various hammer manufacturers on how a single acting diesel hammer should be rated. Many manufacturers use the maximum potential energy computed simply from maximum stroke times the ram weight. The actual hammer stroke achieved is a function of fuel charge, condition of piston rings containing the compressed gases, recoil dampener thickness, driving resistance, and pile length and stiffness. Therefore, the hammer stroke cannot be fully controlled. A set of conditions will generate a certain stroke which can only be adjusted within a certain range by the fuel charge. It may not be possible to achieve the manufacturer's maximum rated stroke under all conditions. In normal conditions, part of the available potential energy is used to compress the gases as the ram proceeds downward after passing the air ports. The gases ignite when they attain a certain combination of pressure and temperature. Under continued operation, when the hammer's temperature increases due to the burning of the gases, the hammer fuel may ignite prematurely. This condition, called "pre-ignition", reduces the effectiveness of the hammer, as the pressure increases dramatically before impact, causing the ram to do more work compressing the gases and leaving less energy available to be transferred into the pile.

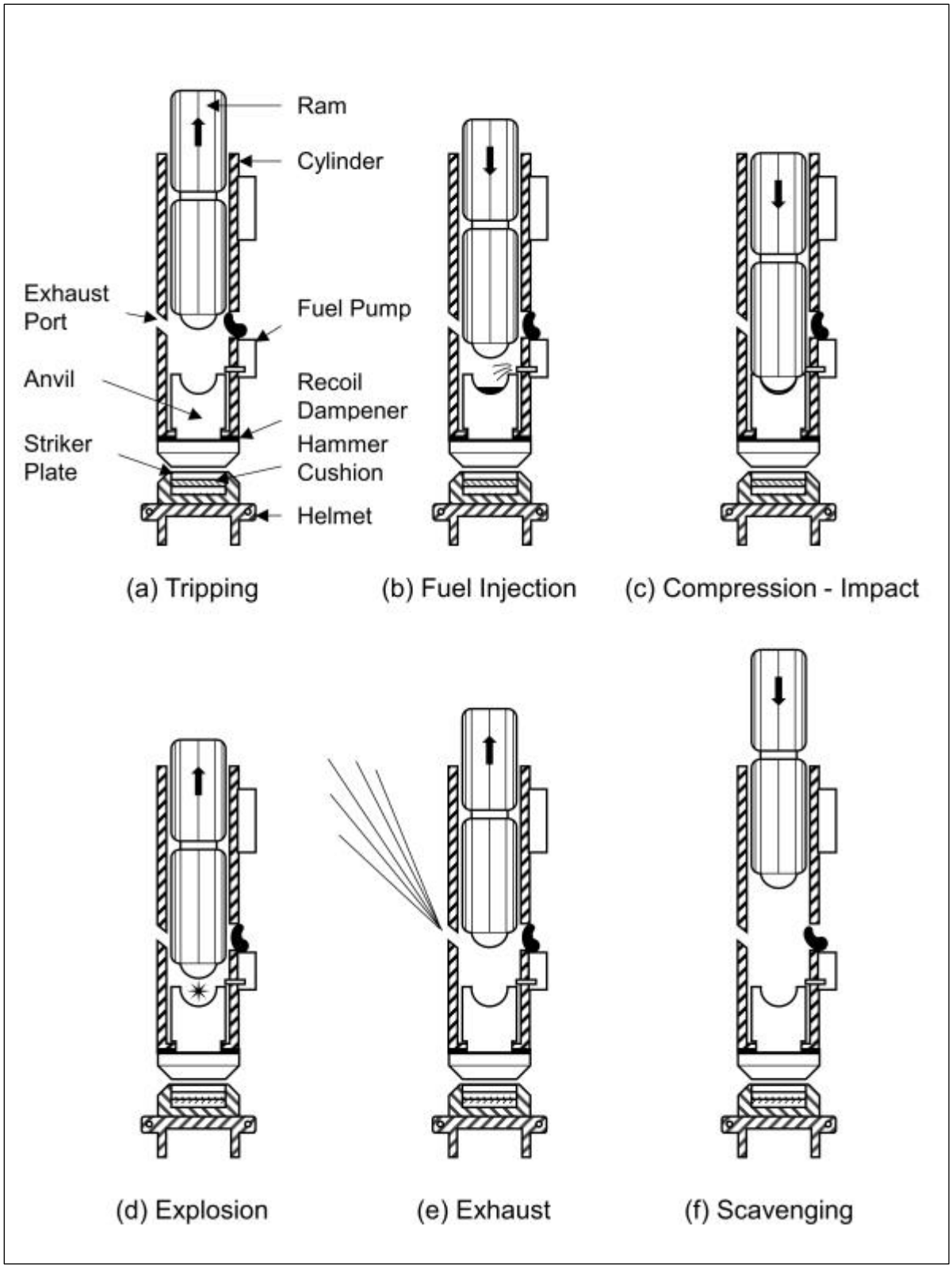

Figure 15-30 Schematic of a single acting diesel hammer.

When driving resistance is very low, the upward ram stroke may be insufficient to scavenge (or suction) the air into the cylinder and the hammer may not continue to operate. Thus, the ram must be manually lifted repeatedly until resistance increases. The stroke can be reduced for most hammers by reducing the amount of fuel injected. Some hammers have stepped fuel settings while others have continuously variable throttles. Other hammers use pressure to maintain fuel flow by connecting a hand operated fuel pump to the hammer, which is operated at the ground. By adjusting the fuel pump pressure, hammer strokes may be reduced. Using the hammer on reduced fuel can be useful for limiting driving stresses. For single acting diesel hammers, the stroke is also a function of pile resistance, which also helps in limiting driving stresses. This feature is very useful in controlling tensile stresses in concrete piles during easy driving conditions. The actual stroke can and should be monitored. The stroke of a single acting diesel hammer can be calculated from the following formula:

$$h = 4.01\left(\frac{60}{bpm}\right)^2 - 0.3 \qquad \text{Eq. 15-3}$$

Where:

h = ram stroke (feet).
bpm = blows per minute.

Note: This formula is only applicable for calculating the stroke of single acting diesel hammers and not correct for other hammer types.

Diesel hammers may be expensive and their maintenance more complex. Concerns over air pollution from the hammer exhaust have also arisen, causing some areas to require a switch to kerosene fuel. However, it should be noted that diesel hammers burn far less fuel to operate than the air compressor required for an air/steam hammer. To address environmental concerns, some diesel hammers can be operated using biodiesel fuel and non-petroleum lubricants. One manufacturer has also developed a smokeless diesel hammer. Diesel hammers are also considerably lighter than air/steam hammers with similar energy ratings, allowing a larger crane operating radius and/or a lighter crane to be used. A photograph of a typical single acting diesel hammer is shown in Figure 15-31(a).

15.14 DOUBLE ACTING (CLOSED END) DIESEL HAMMERS

The double acting diesel hammer works very much in principle like the single acting diesel hammer. The main change consists of a closed cylinder top. When the ram moves upward, air is being compressed at the top of the ram in the so called "bounce chamber" which causes a shorter stroke and therefore a higher blow rate. A photograph of a typical double acting diesel hammer is provided in Figure 15-31(b).

Figure 15-31 (a) Single acting diesel and, (b) double acting diesel hammers.

The bounce chamber has ports so that atmospheric pressure exists as long as the ram top is below these ports, as shown in Figure 15-32. Operationally, as the ram passes the bounce chamber port and moves toward the cylinder top, it creates a pressure which effectively reduces the stroke and stores energy, which in turn will be used on the downstroke. Like the single acting hammer, the actual stroke depends on fuel charge, pile length and stiffness, soil resistance, and condition of piston rings. As the stroke increases, the chamber pressure also increases until the total upward force is in balance with the weight of the cylinder itself. Further compression beyond this maximum stroke is not possible, and if the ram still has an upward

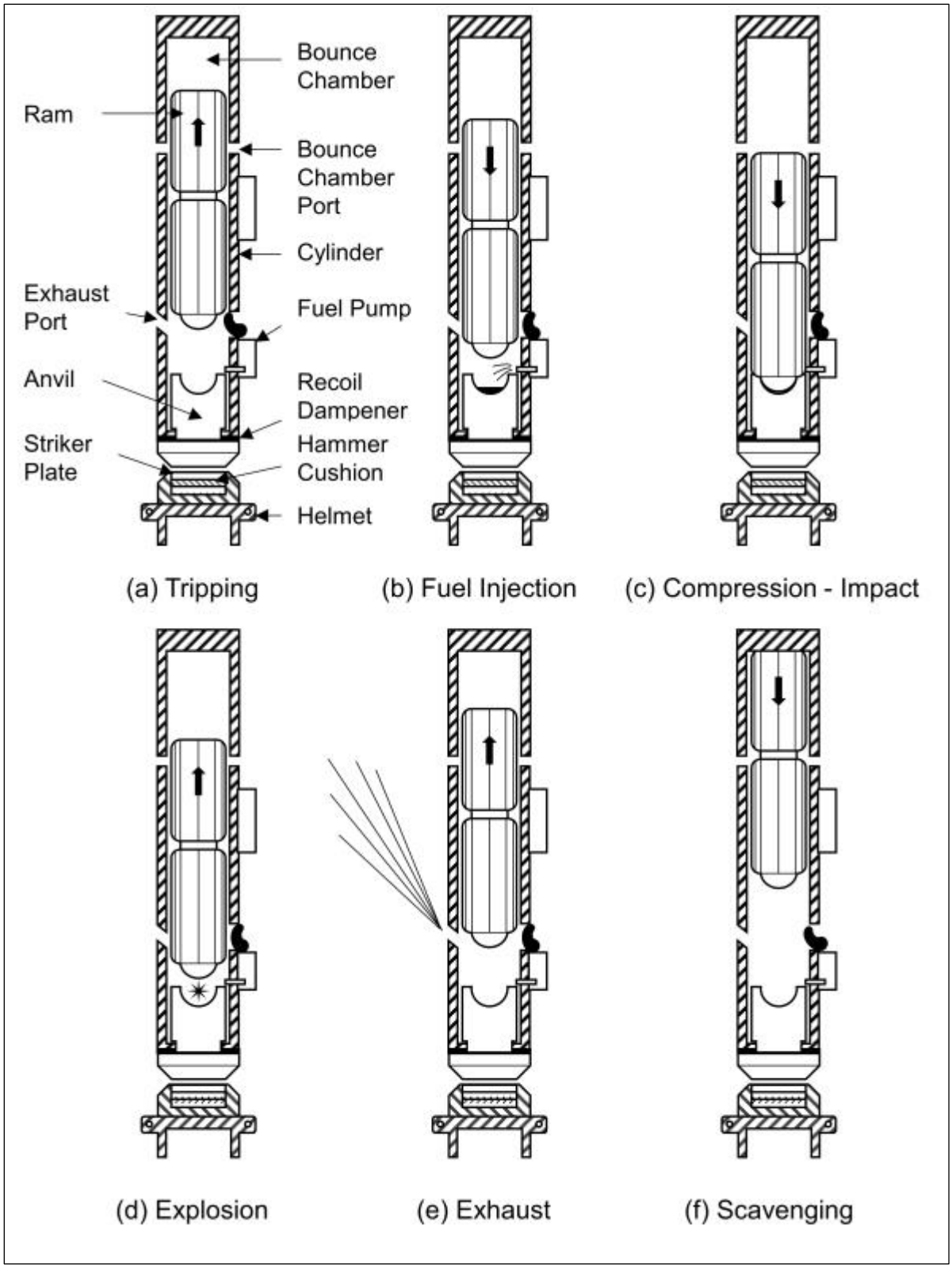

Figure 15-32 Schematic of a double acting diesel hammer.

velocity, uplift of the hammer will result. This uplift should be avoided as it can lead both to an unstable driving condition and to hammer damage. For this reason, the fuel amount, and hence maximum combustion chamber pressure, should be reduced so that there is only a very slight lift-off, or none at all. Most of these hammers have hand held fuel pumps connected by rubber hose to control the fuel flow. Hammer strokes, and therefore hammer energy, may be increased or decreased by the fuel pump pressure.

To determine the energy provided by the hammer, the peak bounce chamber pressure in the hammer is read from a bounce chamber pressure gage. The hammer manufacturer should supply a chart which correlates the bounce chamber pressure gage reading as a function of hose length with the energy provided by the hammer. The use of double acting diesel hammers is limited and they are infrequently encountered in practice.

15.15 SINGLE ACTING HYDRAULIC HAMMERS

Single acting hydraulic hammers use an external hydraulic power source to lift the ram. They can be perhaps thought of as a modern, although more complicated, version of air/steam hammers in that the ram weights and maximum strokes are similar in size and the ram is lifted by an external power source. Low headroom models exist that can be mounted on an excavator while larger models can be mounted on specialty / universal rigs or in conventional leads. During operation, hydraulic actuators lift the ram which then retracts quickly at predetermined height. This fully releases the ram, which falls under gravity, impacting the striker plate and hammer cushion located in the helmet. The hydraulic cylinder then lifts the ram again and the cycle is repeated. Single acting hammers are classified as such because of dependence upon gravity alone to perform the work. Some hammer models include hydraulic accumulators that can provide a relatively small double acting component. A schematic of a single acting hydraulic hammer is illustrated in Figure 15-33(a), while a photograph of a single acting hydraulic hammer is presented in Figure 15-34(a).

Most single acting hydraulic hammers allow the ram stroke, blow rate, and dwell time (duration ram remains on top of pile following impact) to be continuously varied and controlled using a pendant attached to the hydraulic power pack. Very short strokes may be used during easy driving to prevent pile run or to minimize tension stresses in concrete piles. Higher strokes are available for hard driving conditions.

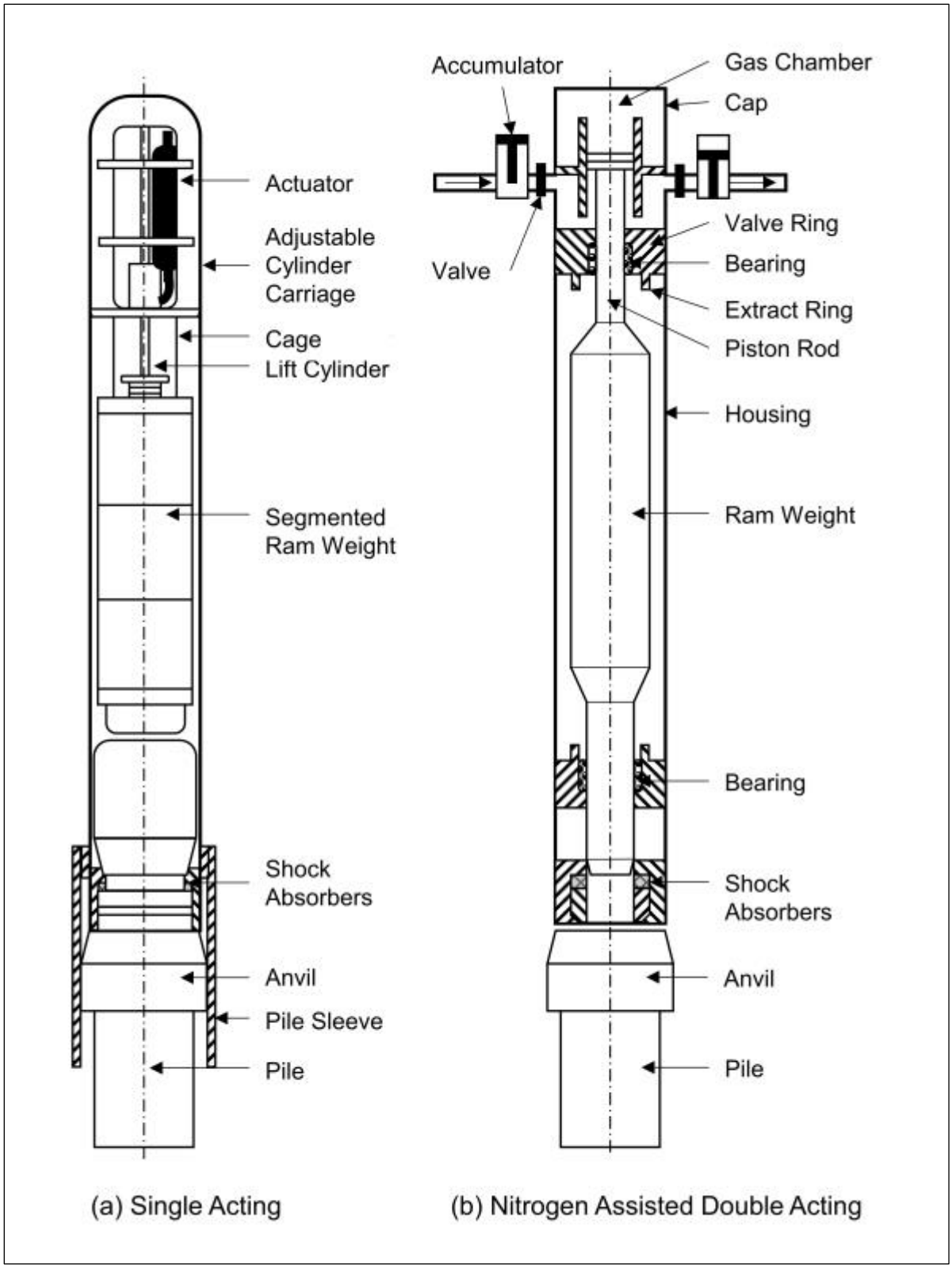

Figure 15-33 Schematic of hydraulic hammers:
(a) single acting and (b) double acting.

Figure 15-34 (a) Single acting hydraulic, and (b) double acting hydraulic hammers.

On many single acting hydraulic hammers, such as the one illustrated in Figure 15-33a, the stroke can be easily be visually estimated. Most newer hydraulic hammers include a built-in monitoring system which determines the ram velocity just before impact. The ram velocity can be converted to kinetic energy or equivalent stroke. Because of the variability of stroke, this hammer monitor should be required as part of the hammer system. The monitor results should be observed during pile driving with appropriate hammer performance notes recorded on the driving log. Hydraulic hammers require a dedicated hydraulic power pack, and can be more complex to operate and maintain compared to other hammers.

15.16 DOUBLE ACTING HYDRAULIC HAMMERS

Double acting hydraulic hammers cover the same range of manufacturer's rated energy as the single acting hydraulic hammers but can also be significantly larger. Figure 15-33(b) presents a schematic of a double acting hydraulic hammer. Double acing hammer consist of a ram attached to a piston rod which are entirely enclosed within the hammer housing and an external hydraulic source supplies the power to the hammer. Oil flows through a supply valve into the hammer and out through a

return valve to the power pack. During hammer operation, the return valve closes, which causes the piston to rise. When the piston reaches a predetermined height, the supply valve closes and the return valve opens. Pressure is relieved and the ram begins its downward stroke accelerated by hydraulic pressure or compressed nitrogen gas. The ram then strikes the anvil, which in turn contacts the pile. Steel on steel impact occurs between these two parts which results in a relatively high energy transfer.

Similar to single acting hydraulic hammers, the ram stroke can be controlled to adapt to the driving conditions. However because of the enclosed housing, the stroke cannot be visually estimated. Built-in monitoring systems are therefore essential on double acting hammers to document hammer performance. A photograph of a double acting hydraulic hammer is included in Figure 15-34(b). A significant advantage of the fully enclosed double acting hydraulic hammers is that they can operate underwater. This allows piles to be driven without using a follower or extra length pile. Most double acting hydraulic hammers do not have conventional hammer cushions and thus generate steel to steel impacts with high efficiency. Some models can also be used to drive piles horizontally.

15.17 VIBRATORY HAMMERS

Vibratory hammers use paired counter-rotating eccentric weights to impart a sinusoidal vibrating axial force to the pile (the horizontal components of the paired eccentric weights cancel). A schematic of a vibratory hammer is presented in Figure 15-35 and a photograph is included in Figure 15-36. Several types of vibratory hammers exist, variable moment vibratory hammers, high frequency vibratory hammers, standard vibratory hammers and low frequency vibratory hammers. Variable moment and high frequency hammers typically operate at up to 2300 to 2400 vibrations per minute or 40 Hz. Standard vibratory hammers operate at up to a maximum of 1600 vibrations per minute or 26 Hz and low frequency vibratory hammers operate up to about 1200 vibrations per minute or 20 Hz.. The lower the operating rate (vibrations per minute) of the vibratory hammer the greater the effect on the soil and structure. Hence, hammer start up and shut down often produce the most construction vibration concerns. Variable moment vibratory hammers are attractive in these situations as the hammer can be brought to full operating speed with the eccentric moments in neutral thus avoiding critical frequencies for potential vibration damage.

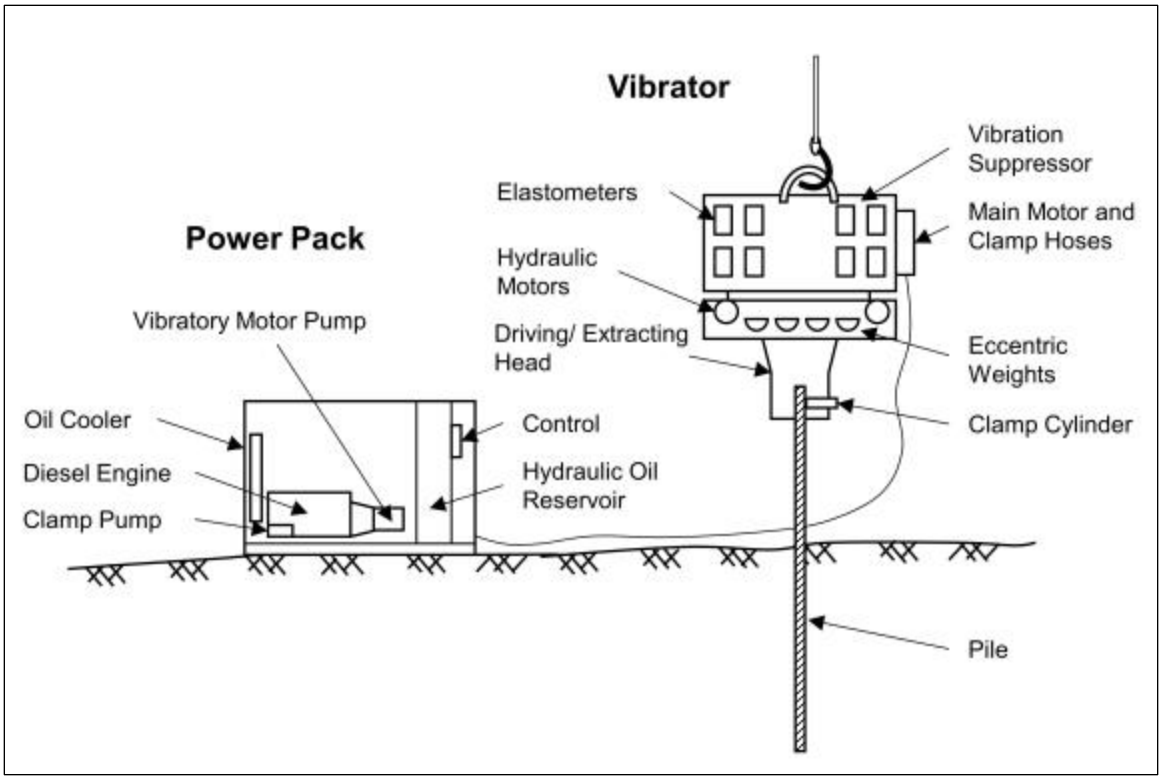

Figure 15-35 Schematic of a vibratory hammer.

Figure 15-36 Vibratory hammer installing an H-pile (courtesy ICE).

Vibratory hammers are rigidly connected by hydraulic clamps to the pile head and may be used for either pile installation or extraction. Vibratory hammers typically do not require leads, although templates are often required for sheet pile cells. These hammers are not rated by impact energy delivered per blow, but instead are classified by energy developed per second and/or by the driving force they deliver to the pile. The power source to operate a vibratory hammer is usually a hydraulic power pack.

Vibratory hammers are commonly used for driving/extracting sheet piles and can also be used for installing non-displacement H-piles and open end pipe piles. However, it is often difficult to install closed end pipes and other displacement piles due to difficulty in displacing the soil laterally at the toe. Vibratory hammers should not be used for precast concrete piles because of possible pile damage due to tensile and bending stress considerations. Vibratory hammers are most effective in granular soils, particularly if submerged. They also may work in silty or softer clays, but most experience suggests they are less effective in stiff to hard clays.

Some wave equation analysis programs can simulate vibratory driving. Dynamic measurements have also been made on vibratory hammer installed piles. However, a reliable technique for estimating nominal resistance during vibratory hammer installation has not yet been developed. If a vibratory hammer is used for pile installation, confirmation of the nominal resistance by other means is still necessary.

15.18 RESONANT HAMMERS

Resonant pile hammers use a hydraulic piston-cylinder design to generate a high magnitude, high frequency, oscillating force. The amplitude and magnitude of the force is controlled through a valve that rapidly switches hydraulic oil to alternating sides of the piston that oscillates at up to 180 Hz (10,800 vibrations per minute). Piles are advanced into the soil using the high frequency vibration and resonance. A proprietary algorithm automatically adjusts and optimizes the frequency to maintain resonance. Janes (2009) summarized projects where resonant hammers have been used to install steel H-piles and pipe piles.

Advantages of the resonant hammer include fast pile installation, very low ground vibrations, and reduced noise levels compared to conventional equipment. Typical cranes and hydraulic power packs can be used on resonant pile hammer projects. Similar to vibratory installed piles, a disadvantage of resonant hammer use is nominal resistance verification. A reliable technique for determining the nominal

resistance is not available. Therefore, a conventional impact hammer and associated standard nominal resistance verification methods must be employed after resonant hammer pile installation is completed. A photograph of a resonant hammer is shown in Figure 15-37.

Figure 15-37 Resonant hammer installing an H-pile (courtesy of Resonance Technology).

15.19 IMPACT HAMMER SIZE SELECTION

It is important that the contractor and the engineer choose the proper hammer for efficient use on a given project. An impact hammer which is too small may not be able to drive the pile to the required resistance, or may require an excessive number of blows. On the other hand, an impact hammer which is too large may damage the pile. The use of empirical dynamic pile formulas to select hammer energy and size is not recommended as this approach incorrectly assumes these formulas result in the desired nominal resistance. Results from these formulas become progressively worse as both the complexity of the hammers and the required nominal pile resistance increase.

A wave equation analysis, which considers the hammer cushion pile soil system, is the recommended method to determine the optimum hammer size. In general, a hammer having a ram weight of 1 to 2% of the required nominal resistance or nominal driving resistance, whichever is greater, often yields a good first estimate of the necessary hammer size. Table 15-2 also provides approximate minimum hammer energy sizes for preliminary equipment evaluation based on ranges of nominal resistances. These are generalizations of equipment size requirements that should be modified based on pile type, pile loads, pile lengths, and local soil conditions. In some cases, such as short piles to rock, a smaller hammer than indicated may be more suitable to control driving stresses. This generalized table should not be used in a specification. Guidance on developing a minimum energy table for use in a specification is provided in Chapter 14.

Table 15-2 Preliminary Hammer Energy Requirements

Nominal Resistance (kips)	Minimum Manufacturer's Rated Energy (ft-lbs)
180 and under	12,000
181 to 300	21,000
301 to 415	28,800
416 to 540	37,600
540 to 600	42,000

15.20 HAMMER KINETIC ENERGY MONITORING

Several pile driving hammers are available from their manufacturers with kinetic energy readout devices. These devices typical monitor hard wired proximity switches built into the hammer body. The impact velocity and hammer kinetic energy are calculated based on the time it takes the ram to travel the distance between the proximity switches. These devices also typically provide the hammer blow rate, and for open end diesel hammers, the hammer stroke. Examples of hammer manufacturer provided devices are presented in Figure 15-38 for an IHC hydraulic hammer and Figure 15-39 and Figure 15-40 for a Berminghammer diesel hammer.

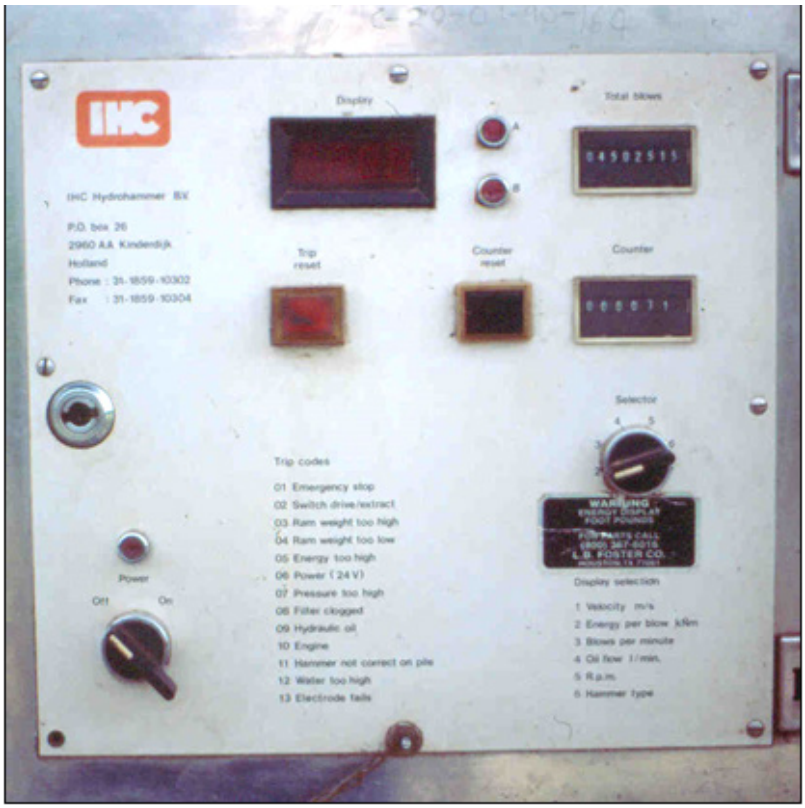

Figure 15-38 IHC hydraulic hammer kinetic energy readout panel.

Any existing hammer can also be retrofitted for these measurements by attaching proximity switches to the hammer body. Attachment procedures vary depending upon the hammer model. For a diesel hammer, proximity switches are set into two 1.2 inch diameter smooth bore drill holes in the cylinder wall above the combustion chamber. For air/steam or single acting hydraulic hammers, the proximity switches are attached to the hammer body. The proximity switches are connected to a transmitter mounted on the hammer that sends the impact velocity and kinetic energy to a wireless hand held unit. This hand held unit, called an E-Saximeter, can also be used to keep a pile driving log if the inspector presses the enter key with each passing pile penetration increment. For single acting diesel hammers, the hammer stroke can also be calculated and displayed. A photograph of a diesel hammer retrofitted for kinetic energy measurements is presented in Figure 15-41 and the readout device is in Figure 15-42.

Hammers equipped with kinetic energy readout devices provide improved quality control and are particularly attractive on large projects or with piles that require a large nominal resistance. These devices can detect changes in hammer performance over time that may necessitate adjustment to the pile installation criterion.

Figure 15-39 Proximity switch attachment for Berminghammer diesel hammer (courtesy Berminghammer).

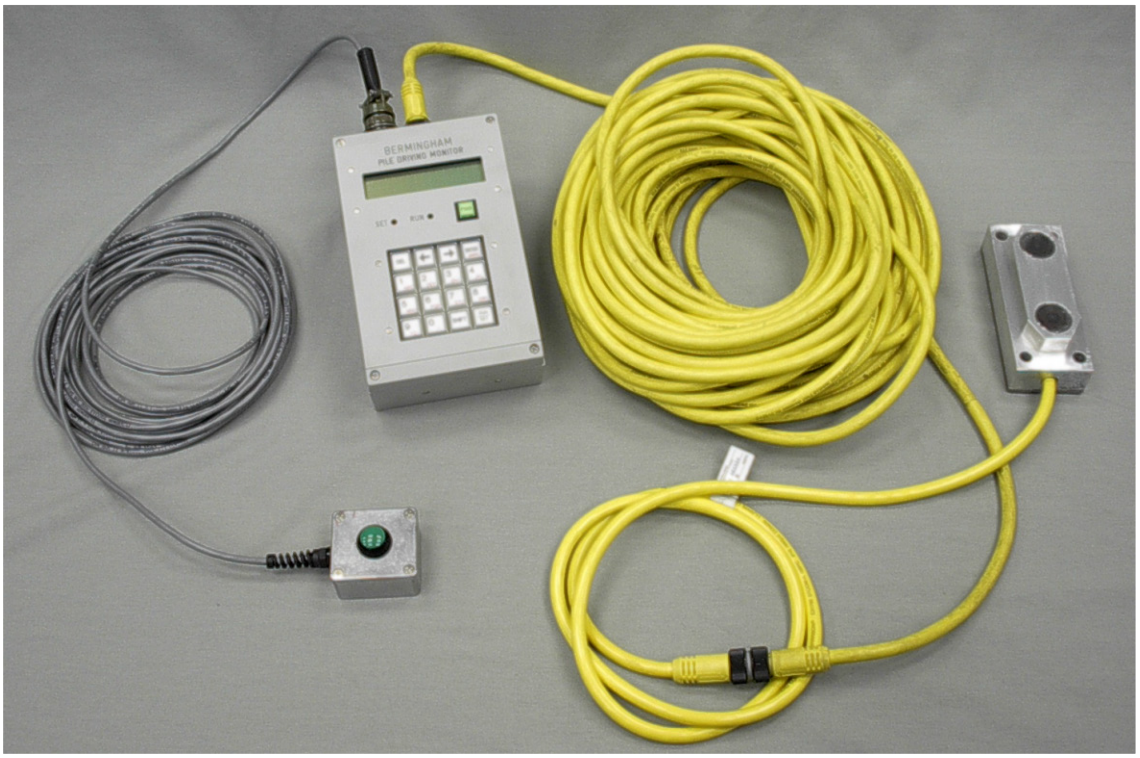

Figure 15-40 Proximity switches, readout device and driving log trigger switch for Berminghammer diesel hammer (courtesy Berminghammer).

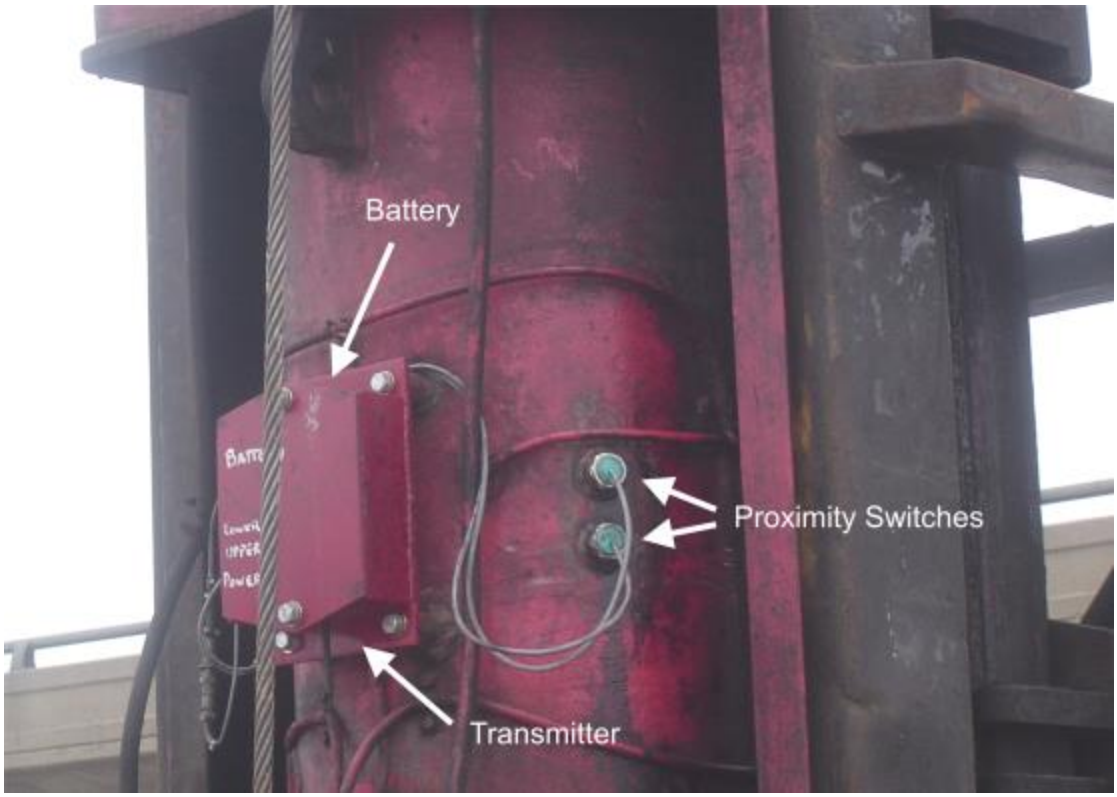

Figure 15-41 Proximity switches and transmitter on retrofitted diesel hammer.

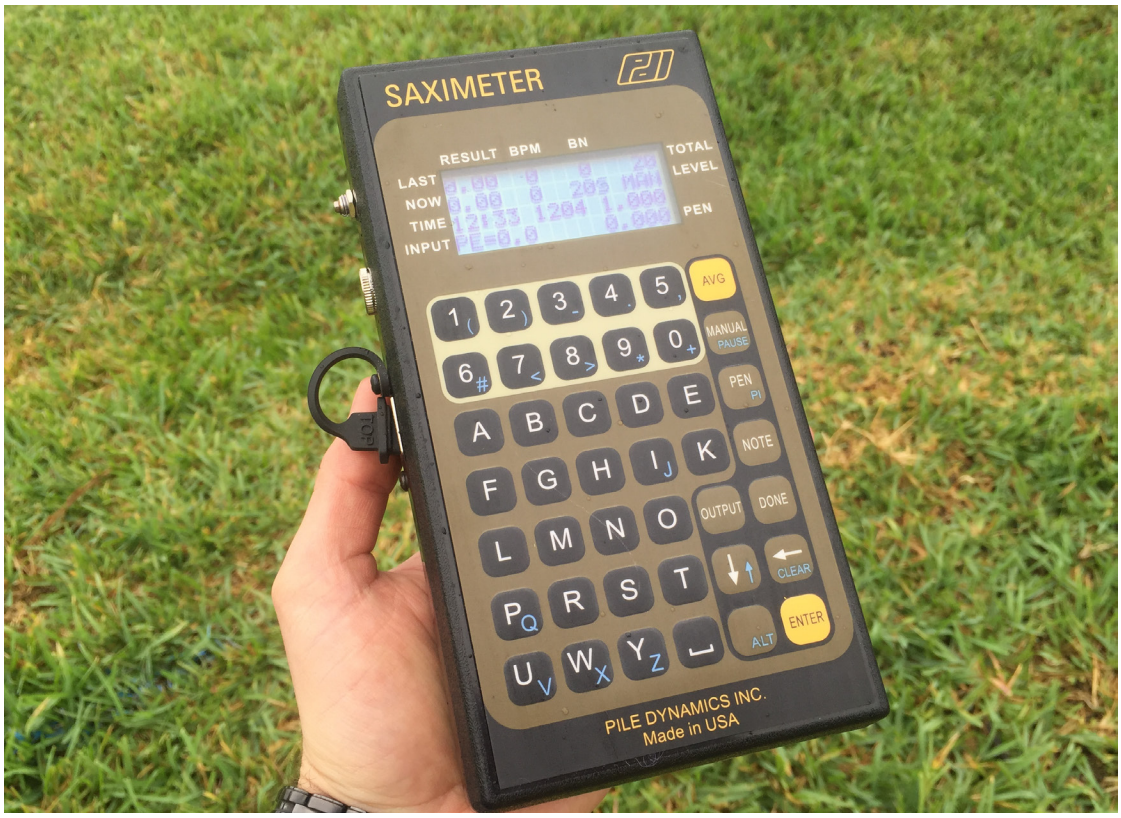

Figure 15-42 E-Saximeter wireless kinetic energy readout device.

15.21 NOISE SUPPRESION EQUIPMENT

Depending upon the hammer and pile type used, noise from impact pile driving operations can range from around 80 to 130 dBa. Local ordinances or specification may place limits on noise levels that may influence equipment selection or may dictate that pile driving noise shrouds be used in order to meet the specified noise limits. Manufacturers of a few diesel and hydraulic hammers can provide optional noise suppression devices that may reduce the pile driving generated noise by about 10 dBa. An example of a noise shroud produced by a hammer manufacturer is presented in Figure 15-43.

Greater reductions in pile driving noise have been obtained by combining noise abatement techniques on a project. A 20 to 25 dBa reduction was obtained through the combined use of shock absorbing cushion material, a hammer exhaust noise shroud, application of damping compound to the steel piles, and use of a noise shroud around the hammer-pile impact area. Hammer and pile type selection can also influence the pile driving generated noise and should be considered in the design stage of projects in noise sensitive areas.

Figure 15-43 Noise shroud for IHC hydraulic hammer.

15.22 UNDERWATER NOISE SUPPRESSION EQUIPMENT

Bubble curtains are sometimes required when driving piles through water to reduce underwater sound waves, shock waves, and overpressures that impact marine mammals and fish. In general, overpressure levels greater than 4.4 psi have been found to be detrimental. However, the detrimental overpressure level will vary depending upon the species of fish, their size, and their maturity level.

Bubble curtain devices use air bubbles to attenuate the pile driving induced pressure wave. Bubble curtains can be categorized as bubble rings or bubble walls. A bubble ring is typically used around a single pile and typically consists of a high volume air compressor a primary feed line, a primary distribution manifold, medium volume secondary feed lines, and secondary distribution manifolds. Bubble walls combine the features of bubble rings with a sound damping curtain that encapsulates the air bubbles. Bubble walls are typically placed around a complete substructure location rather than an individual pile.

For a bubble curtain to be effective, the bubble curtain must completely surround the pile driving activity. This can sometimes be difficult to accomplish with a bubble ring in areas with tides and currents, or when the foundation design includes batter piles. Bubble rings are sometimes used in conjunction with containment devices such as a large diameter pile sleeve, a turbidity curtain, or a cofferdam in these situations. A bubble wall system may be more attractive in areas where a bubble ring system requires containment devices. A photograph of a pile driven inside bubble ring used in conjunction with a containment device is presented in Figure 15-44. Longmuir and Lively (2001) presented a case history where use of a bubble ring reduced overpressures during pile driving from in excess of 22 psi with no mitigation to less than 3 psi.

The WSDOT and FHWA sponsored a full scale test of new underwater noise suppression technology developed by the University of Washington and Marine Construction Technologies, PBC. The research study developed a patented solution for mandrel bottom driving a steel pipe pile, trademarked a Reinwall pile. In the full scale field study where 30 inch pipe piles were driven, Reinwall et al. (2014) determined that the air gap between the mandrel and conventional steel pipe resulted in a 21 to 23 dBa reduction in underwater noise compared to the 3 to 6 dBa reduction achieved with a typical bubble curtain.

Figure 15-44 Bubble ring with containment device (courtesy of WSDOT).

15.23 FOLLOWERS

A follower is a structural member interposed between the pile hammer and the pile, to transmit hammer blows to the pile head when the pile head is below the reach of the hammer. This occurs when the pile head is below the bottom of leads. Followers are sometimes used for driving piles below the deck of existing bridges, for driving piles underwater, or for driving the pile head below grade. A photograph of a follower for driving steel H-piles underwater is presented in Figure 15-45(a).

Maintaining pile alignment, particularly for batter piles, is a problem when a follower is used while driving below the bottom of the leads. The use of a follower is accompanied by a loss of effective energy delivered to the pile due to compression of the follower and losses in the connection. This loss of effective energy delivered to the pile affects the blow count to obtain the required nominal resistance. These losses can be estimated by an extensive and thorough wave equation analysis, or field evaluated by dynamic measurements. In Figure 15-45(b), the hammer-follower-pile alignment issues are apparent for the H-pile being driven on a batter.

A properly designed follower should have about the same stiffness (per unit length) as the equivalent length of pile to be driven. Followers with significantly less

stiffness should be avoided. Followers often require considerable maintenance. In view of the difficulties that can be associated with followers, their use should be avoided when possible. For piles to be driven underwater, one alternative is to use a hammer suitable for underwater driving.

Figure 15-45 (a) Follower and (b) follower in use drving H-piles.

15.24 JETTING

Jetting is the use of water or air to facilitate pile penetration by displacing the soil. In some cases, a high pressure air jet may be used in combination with water. Jets may be used to create a pilot hole prior to or simultaneously with pile placement. Jetting pipes may be located either inside or outside the pile. Jetting is usually most effective in loose to medium dense granular soils.

Jetting is not recommended for friction piles because the frictional resistance is reduced by jetting. Jetting should also be avoided if the piles are designed to provide substantial lateral resistance. For end bearing piles, the final required resistance must be obtained by driving (without jetting). Backfilling should be required if the jetted hole remains open after the pile installation. A separate pay item for jetting should be included in the contract documents when jetting is anticipated. Alternatives to jetting include predrilling and spudding.

The use of jetting has been greatly reduced due to environmental restrictions. Hence, jetting is rarely used unless containment of the jetted materials can be provided. Photographs of a dual jet system mounted on a concrete pile and a jet/punch system are presented in Figures 15-46 and Figure 15-47, respectively.

Figure 15-46 Dual jet system mounted on concrete pile (courtesy of Florida DOT).

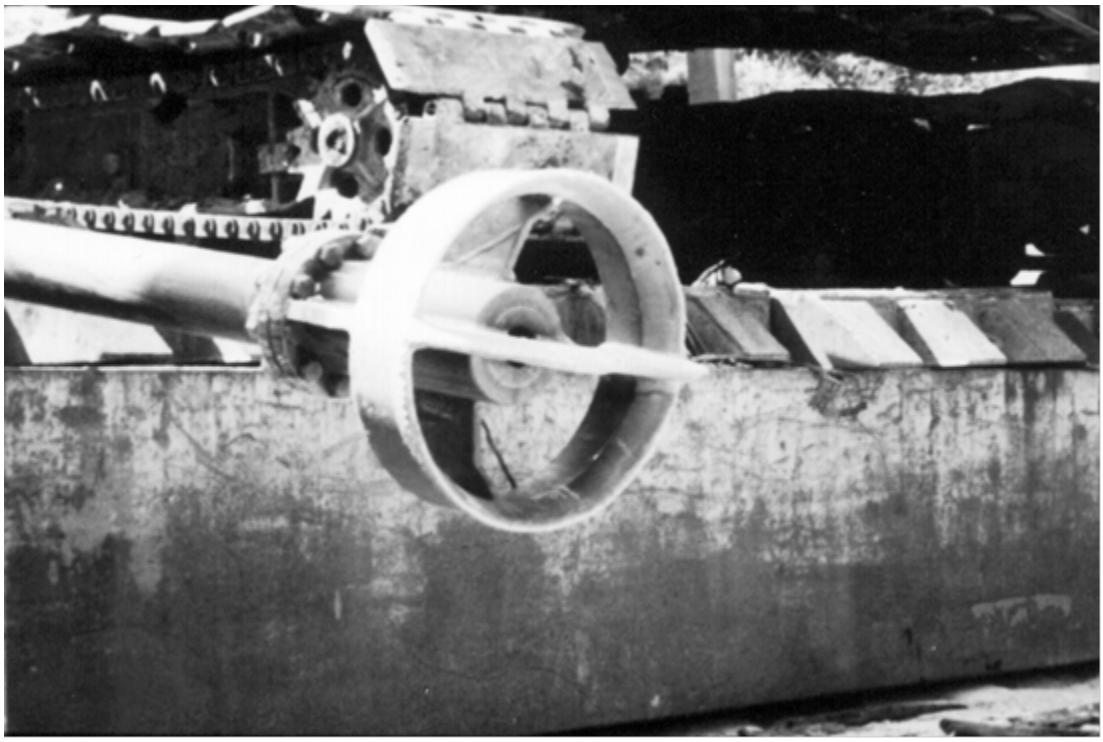

Figure 15-47 Jet/Punch system (courtesy of Florida DOT).

15.25 PREDRILLING

Soil augers or rotary drills may sometimes be used to facilitate driving or limit vibrations. Predrilling is sometimes necessary to install a pile through soils with obstructions, such as old timbers, boulders, and riprap. Predrilling is also frequently used for pile placement through soil embankments and may be helpful to reduce pile heave when displacement piles are driven at close spacing.

The predrilled hole diameter depends upon the size and shape of the pile, and soil conditions. The hole should be large enough to permit driving but small enough so the pile will be supported against lateral movement. The hole size and depth should be noted in the contract documents. In most situations, the predrilled hole diameter should be 4 inches less than the diagonal of square or steel H-piles, and 1 inch less than the diameter of round piling. Where piles must penetrate into or through very hard material, it is usually necessary to use a diameter equal to the diagonal width or diameter of the piling. When predrilled holes are used in embankments, a hole of up to 6 inches larger than the greatest pile cross sectional dimension is sometimes used. A separate pay item for predrilling should be included in the contract documents when predrilling is anticipated. A photograph of a solid flight auger predrilling system is presented in Figure 15-48.

Figure 15-48 Solid flight auger predrilling system.

15.26 SPUDDING

Spudding is the act of opening a hole through dense material by driving or dropping a short and strong member and then removing it. The contractor may resort to spudding in lieu of jetting or predrilling when the upper soils consist of miscellaneous fill and debris. A potential difficulty of spudding is that a spud may not be able to be pulled when driven too deep. However, an advantage of spudding is that soil cuttings and groundwater are not brought to the ground surface, which could then require disposal due to environmental concerns. Two spudding devices are shown in Figure 15-49. The spud in Figure 15-49(a) consists of a thick walled pipe section with a conical tip formed from steel plates. The spud in Figure 15-49(b) was made by adding a wedge shaped tip and plates to a H-pile section.

15.27 EQUIPMENT SUBMITTALS

The Contractor should provide an equipment submittal of all proposed equipment as well as the proposed procedures for equipment use to the Engineer prior to pile

Figure 15-49 (a) Pipe pile and (b) H-pile spuds.

driving operation. In addition, a Pile Installation Plan should be prepared and followed throughout the project. This allows the Engineer to evaluate the proposed equipment, perform a wave equation analysis with appropriately modeled soil conditions, and provide preliminary or final driving criteria. Figure 15-50 presents a drive system submittal form covering hammer components and hammer accessories as well as pile type, pile section, pile splicing and pile toe details. Additional information on any jetting, predrilling, or spudding equipment should be submitted in conjunction with this hammer submittal form. Reference can be made to Section 14.2.1 and 14.2.3 of Chapter 14 respectively for specifications regarding the Pile Installation Plan and equipment used for driving.

By submitting technical information related to the pile driving equipment, the Engineer can evaluate the suitability and expected performance of the proposed system. Without the specific installation system details, the accuracy of any wave equation modeling and resulting driving criteria or drivability assessment is reduced. An in depth discussion of wave equation analyses is provided in Chapter 12 of this manual.

Contract No.:_____ Structure Name and/or No.:_____

Project:_____

_____ Pile Driving Contractor or Subcontractor:_____

County:_____

(Piles driven by)

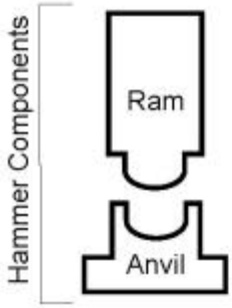

Hammer

Manufacturer:_____ Model No.:_____

Hammer Type:_____ Serial No.:_____

Manufacturers Maximum Rated Energy:_____(ft-lbs)

Stroke at Maximum Rated Energy:_____(ft)

Range in Operating Energy:_____to_____(ft-lbs)

Range in Operating Stroke:_____to_____(ft)

Ram Weight:_____(kips)

Modifications:_____

_____

_____

Striker Plate

Weight:_____(kips) Diameter:_____(in)

Thickness:_____(in)

Hammer Cushion

Material #1	Material #2 (Composite Cushion)
Name:_____	Name:_____
Area:_____(in^2)	Area:_____(in^2)
Thickness/Plate:_____(in)	Thickness/Plate:_____(in)
No. of Plates:_____	No. of Plates:_____

Total Thickness of Hammer Cushion:_____(in)

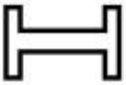

Helmet

Weight:_____(kips)

Insert (If Any)

Weight:_____(kips)

Total Weight of Helmet and Insert:_____(kips)

Pile Cushion

Material:_____

Area:_____(in^2) Thickness/Sheet:_____(in^2)

No. of Sheets:_____

Total Thickness of Pile Cushion:_____(in)

Maximum Thickness Accommodated by Helmet :_____(in)

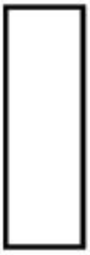

Pile

Pile Type:_____

Wall Thickness:_____(in) Taper:_____

Cross Sectional Area:_____(in^2) Weight/ft:_____

Ordered Length:_____(ft)

Factored Resistance:_____(kips)

Nominal Resistance:_____(kips)

Description of Splice:_____

_____

Driving Shoe/Closure Plate Description:_____

_____

Submitted By:_____ Date:_____

Telephone No.:_____ Email:_____

Figure 15-50 Drive system submittal form.

REFERENCES

Deep Foundations Institute (1981). A Pile Inspector's Guide to Hammers, First Edition, Deep Foundations Institute, Englewood Cliffs, NJ.

Deep Foundations Institute (1995). A Pile Inspector's Guide to Hammers. Second Edition, Deep Foundations Institute, Englewood Cliffs, NJ.

Janes, M. (2009). Sonic Pile Driving. The History and the Resurrection of Vibration-Free Pile Driving. Piledriver Magazine, Q1, Vol. 6, No. 1, pp. 61-67.

Longmuir, C. and Lively, T. (2001). Bubble Curtain Systems Help Protect the Marine Environment. Pile Driving Contractors Association Summer Newsletter, pp. 11-16, www.piledrivers.org.

Passe, Paul D. (1994). Pile Driving Inspector's Manual. State of Florida Department of Transportation.

Rausche, F., Likins, G.E., Goble, G.G. and Hussein, M. (1986). The Performance of Pile Driving Systems. Inspection Report, FHWA/RD-86/160, U.S. Department of Transportation, Federal Highway Administration, Office of Research and Development, Washington, D.C., 92 p.

Reinhall, P.G., Dahl, P.H., and Dardis (2014). Attenuation of Noise from Impact Pile Driving Using an Acoustic Shield, Journal of the Acoustical Society of America, Vol. 135, No. 4, 2388.

CHAPTER 16

PILE ACCESSORIES

Pile accessories are frequently used for pile toe protection or to facilitate pile splicing. Accessories are available for driven piles that can make pile installation easier and faster. They can also reduce the possibility of pile damage and help provide a more dependable and permanent support for any structure. Heavier foundation loads, pile installations to sloping rock surfaces or into soils with obstructions, and longer pile lengths, are project situations where the use of pile toe attachments and splice accessories are often cost effective and sometimes necessary for a successful installation. However, pile accessories may add significant cost to the project and should not be used unless specifically needed. Pile toe attachments and splices for timber, steel, concrete and composite piles are discussed in this chapter. During driving and under all applicable loading conditions, pile toe attachments and splices should develop the required structural resistance.

16.1 TIMBER PILES

Potential problems associated with driving timber piles include splitting and brooming of the pile toe and/or pile head, splitting or bowing of the pile body, and breaking of the pile during driving. Protective attachments at the pile toe and at the pile head can minimize these problems.

16.1.1 Pile Toe Attachments

Timber pile toe protection devices include steel boots or points. The trend toward larger pile hammers and higher nominal resistances may result in greater risk of damage for timber piles if obstructions are encountered. Figure 16-1 shows two types of commonly use pile toe attachments. Timber pile boots are designed to cover the entire pile toe without the need for trimming. Timber pile points involve trimming the pile toe to fit the point. Both toe protection devices can be secured quickly in the field. The toe protection device is the device over the pile toe and then nailing the shoe straps to the pile toe and anchoring the attachment. Figure 16-2 shows a pile boot attached to a timber pile.

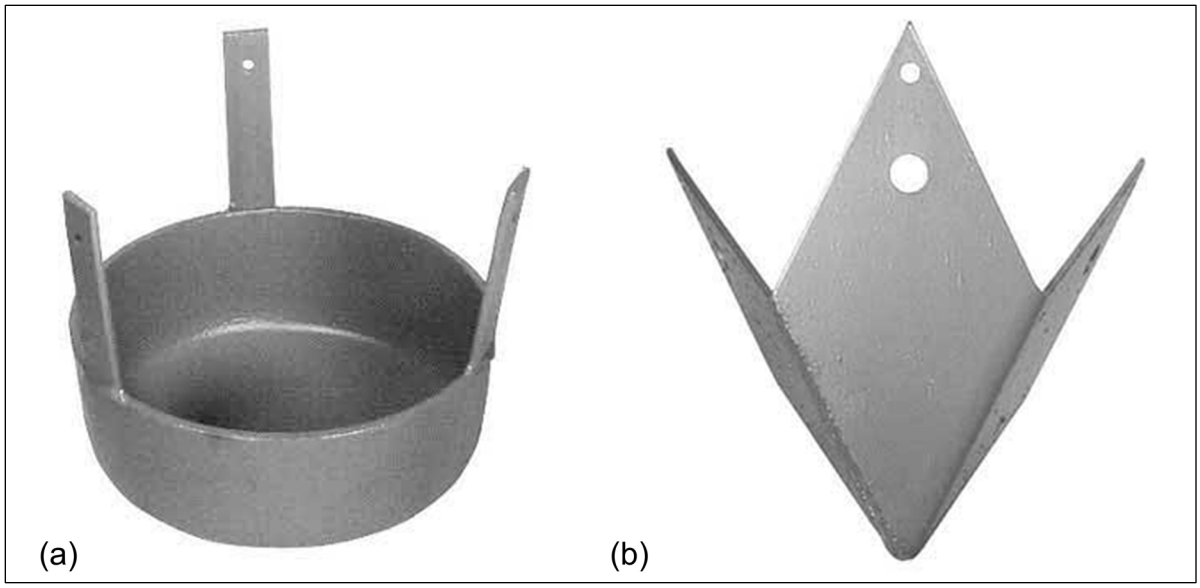

Figure 16-1 Timber pile toe attachments: (a) Pile boot and (b) Pile point (courtesy Skyline Steel).

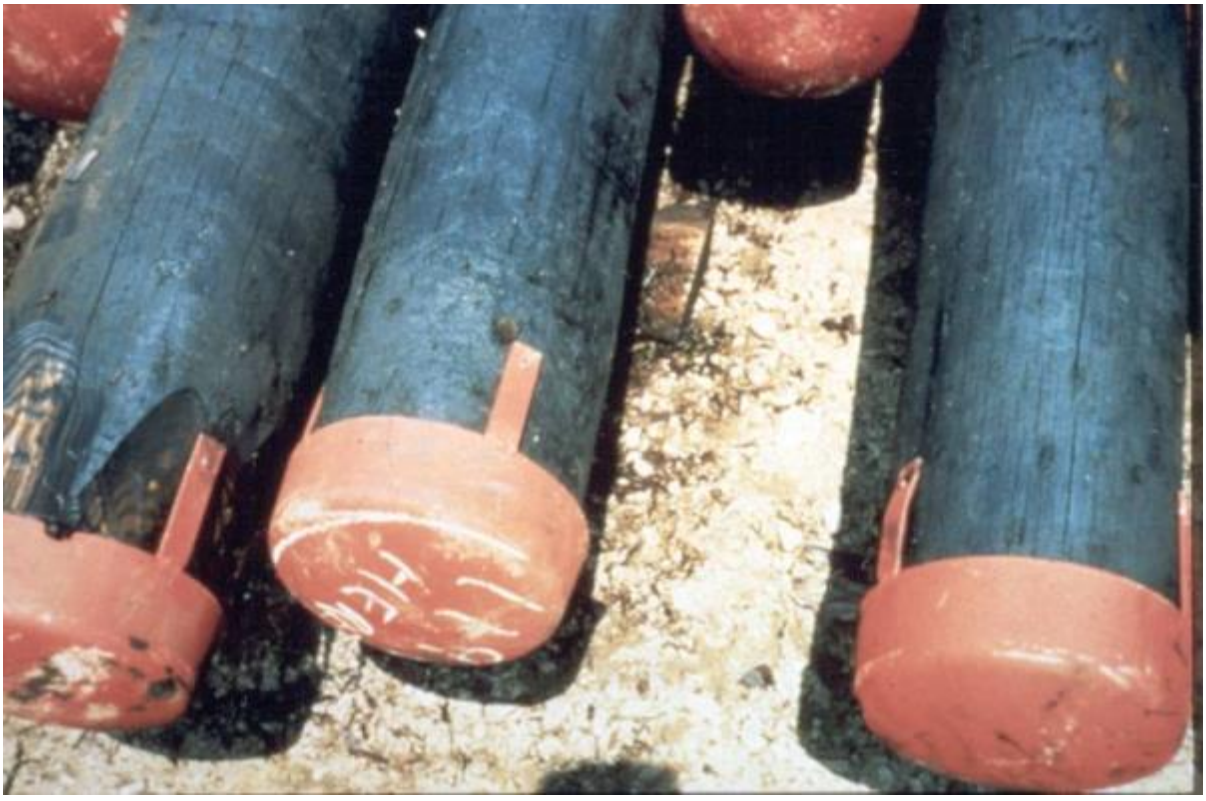

Figure 16-2 Timber pile with pile boot attached.

16.1.2 Attachments at Pile Head

The American Wood Preservers Institute (Collin 2012), recommends banding timber piles with heavy metal strapping at the pile head prior to driving to prevent splitting. AASHTO (2010) requires collars, bands, or other devices to prevent splitting and brooming when the required nominal driving resistance is more than 200 kips on a timber pile. A photograph of a banded timber pile head is shown in Figure 16-3.

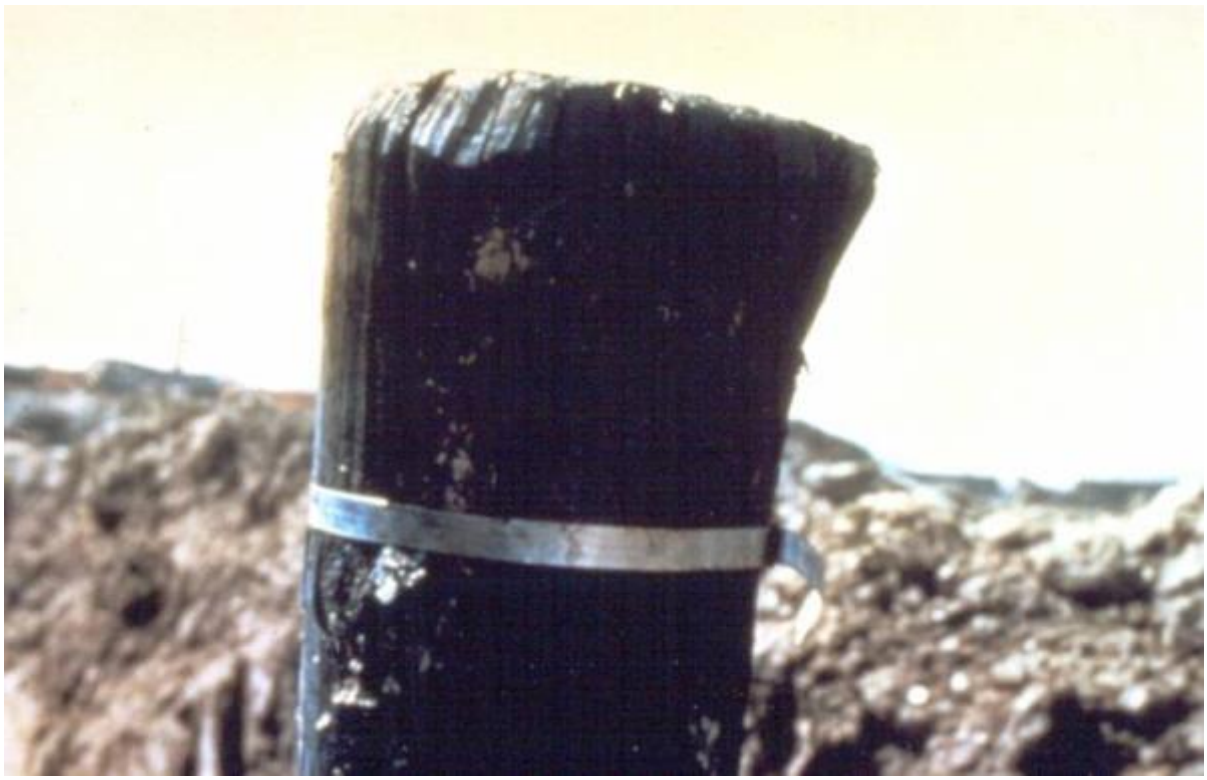

Figure 16-3 Banded timber pile head.

16.1.3 Splices

Timber pile splices are undesirable. It is virtually impossible to develop the full bending strength of a spliced timber pile. AASHTO (2010) states that timber piles should not be spliced unless specified in the contract documents or in writing by the engineer. When timber pile lengths prove insufficient for the required nominal resistance, longer piles should be ordered, or the foundation should be redesigned using additional piles of the furnished length.

16.2 STEEL H-PILES

Steel H-piles are often used to penetrate through hard or problematic upper soil layers and terminate in a very dense or hard bearing layer such as rock. The bearing layer can be at a depth that requires single or multiple H-pile splices. Depending on the nature of the surficial materials, pile toe attachments may also be needed to prevent or reduce pile toe damage. Pile toe attachments are discussed in detail in Section 16.2.1. Splicing methods for H-piles are described in Section 16.2.2. The importance of proper welding procedures and weld inspection are discussed in Section 16.5.

16.2.1 Pile Toe Attachments

Steel H-piles are generally easy to install due to the non-displacement character of the pile. Problems can arise when driving H-piles through man-made fills, very dense gravel, or deposits containing boulders. If left unprotected under these conditions, the pile toe may deform to an unacceptable extent and separation of the H-pile flanges and web may occur. Figure 16-4(a) and 16-4(b) show an extracted H-pile that was driven without a pile shoe through a deposit containing boulders. In Figure 16-4(a), the pile has just been extracted after dynamic test records indicated pile toe damage. The extracted H-pile has a boulder wedged between the flanges. In Figure 16-4(b), the H-pile has been laid on the ground and the extent of the toe damage is apparent including separation of the flange and web.

Commercially manufactured pile shoes can help minimize or prevent toe damage problems. Pile shoes are also desirable for H-piles driven to hard rock to facilitate distributing high localized contact stresses over a greater cross sectional area. This is particularly helpful when piles are to be driven onto sloping rock surfaces. Pile toe reinforcement consisting of steel plates welded to the flanges and web are not recommended because the reinforcement provides neither protection nor increased strength at the critical area of the flange-to-web connection.

Several manufactured H-pile shoes are available in various shapes and styles as shown in Figure 16-5 (a through c). Pile shoes should be fabricated from cast steel conforming to ASTM A148/A148M (Grade 90-60). These shoes are attached to the H piles with fillet welds along the outside of each flange as illustrated in Figure 16-6. Most agencies have a standard detail for shoe attachment. In general, the lower portion of the H-pile flanges are beveled and a 5/16 inch fillet weld or greater depending on flange thickness used to attach the shoe.

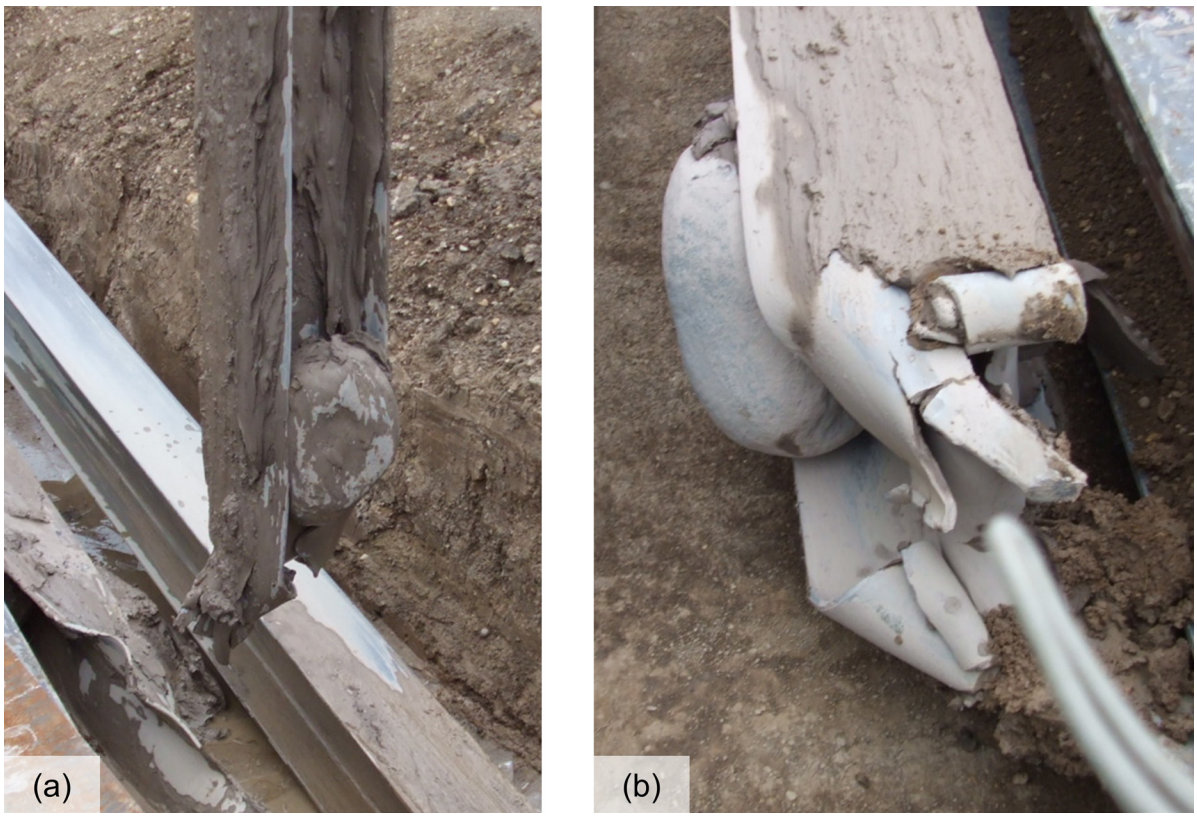

Figure 16-4 Damaged H-pile driven without pile toe protection (courtesy Wisconsin DOT).

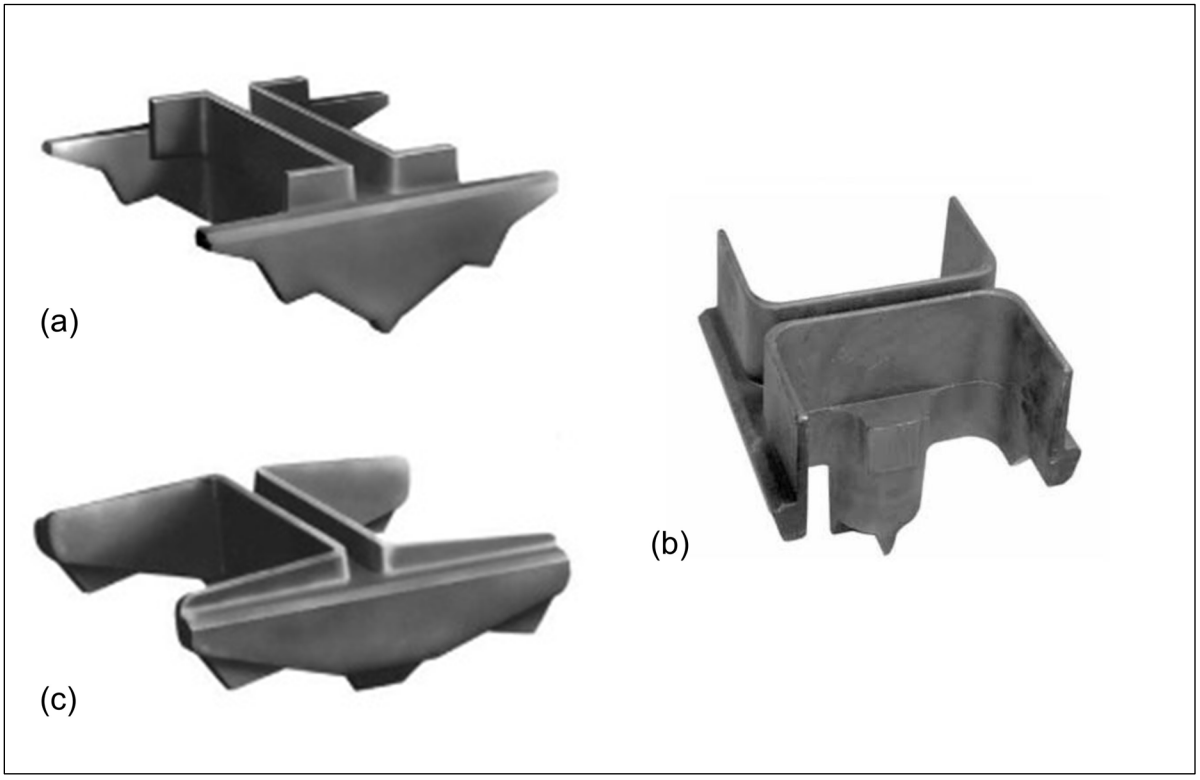

Figure 16-5 Styles of H-pile driving shoes (courtesy Skyline Steel).

Figure 16-6 Pile shoe welded to pile toe using fillet welds along exterior flanges.

Manufacturers recommend different shoe shapes for various applications. It is recommended that for a given set of subsurface conditions, pile shoes from different manufacturers should be considered as equivalent provided they are manufactured from similar strength materials using similar fabrication techniques. Minor variations in configuration should be given minimum importance, except in specific subsurface conditions where a certain shape would give a definite advantage.

16.2.2 Splices

H-pile splices are routinely made by using a full penetration groove weld along the web and both flanges as shown in Figure 16-7. Commercially manufactured H-pile splicers as shown in Figure 16-8 are also used. Some agencies also utilize a welded square or diamond backer plate detail in conjunction with a welded splice. H-pile splices must satisfy all the pile structural resistance requirements in axial compression, tension, and bending demanded by the foundation loading conditions. The appropriate splice details; a full penetration weld or an H-pile splicer, will be determined by the foundation loading conditions. Welded splice

Figure 16-7 Full penetration groove weld with backer bars.

Figure 16-8 H-pile splicer.

strength, beyond that required to survive pile driving induced stresses, is necessary for piles subjected to bending stresses and cyclic loading. Hence, it is essential that H-pile splices be performed by certified welders following approved procedures. Further discussion on field welds is discussed in Section 16.5.

For the manufactured H-pile splicer, a notch is cut into the web of the driven pile section and the splicer is slipped over that pile. A 5/16 inch fillet weld extending vertically from the four corner of the H-pile splicer is then made between the edge of the H-pile splicer and the H-pile flanges. The length of each fillet weld is typically on the order of 2.5 to 4 inches. The flanges on the add-on H-pile section are chamfered at 45 degrees to facilitate flange welding. Typically the add-on section of pile is positioned, aligned, and held while a 5/16 inch fillet weld is made between the edge of the H-pile splicer plate and the H-pile flanges. The length of each fillet weld is again on the order of 2.5 to 4 inches. After completion of the upper welds, either a full penetration or partial penetration groove weld (depending on design) is made along both flanges. A partially completed splice is shown in Figure 16-9.

Figure 16-9 Partially completed splice using H-pile splicer.

Most H-piles produced today are typically made from ASTM A-572, Grade 50 steel or higher. When H-pile splicers are used they should also be made from the same high strength steel as the H-pile.

16.3 STEEL PIPE PILES

Steel pipe piles can be designed to be driven either closed end or open end. Pile toe attachments are designed for both installation situations. Toe attachments can be used to minimize the potential for toe damage in difficult subsurface conditions as well as to help limit pile deflection. Steel pipe piles lengths can be easily increased in the field using welded or friction splices. Pile toe attachments are discussed in detail in Section 16.3.1. Splicing methods for pipe piles are described in Section 16.3.2. The importance of proper welding procedures and weld inspection are discussed in Section 16.5.

16.3.1 Pile Toe Attachments

Pile toe attachments on pipe piles are used to reduce the possibilities of pile toe damage and limit pile deflection. Problems during installation of closed end pipe piles may arise when driving through materials containing obstructions. In this case, piles may deflect and deviate from their design alignment to an unacceptable extent. When driving open end pipe piles through or into very dense materials, the toe of the pile may be deformed.

Closed end pipe piles are most frequently installed with a flat plate welded to the pile toe as shown in Figure 16-10. The flat plate thickness typically ranges from 0.75 to 1.0 inch thick for closed end pipe piles having an outside diameter of 18 inches or less. A thicker closure plate may be required by the engineer for larger diameter piles. The diameter of the closure plate is typically 5/8 inch larger in diameter than the outside diameter of the pipe pile in order to allow a 5/16 inch fillet weld to attach the closure plate to the pile toe. The closure plate can also be the same diameter as the pile in which case either the pile toe or the closure plate must be beveled so that a partial penetration weld can be made. End plates should be made of ASTM A36/A36M steel or better.

A conical toe attachment can also be used as a pile toe closure device for closed end pipe piles. Conical toe attachments can have a rounded shape as shown in Figure 16-11(a) or a 60 degree point as shown in Figure 16-11(b). These conical

Figure 16-10 Closure plate typical of closed end steel pipe pile.

attachments generally cost more than flat closure plate devices. In addition, flat closure plates generally develop a higher unit toe resistance. In the same soil profile, a closed end pipe pile with a conical toe attachment may drive slightly longer than a pipe with a flat closure plate for the same nominal resistance. A conical toe attachment is typically welded to the pile toe using a full or partial penetration groove weld. Conical toe attachments should be made from cast steel conforming to ASTM A148/A148M (Grade 90-60). A photograph of a conical toe attachment welded to a pipe pile is presented in Figure 16-12.

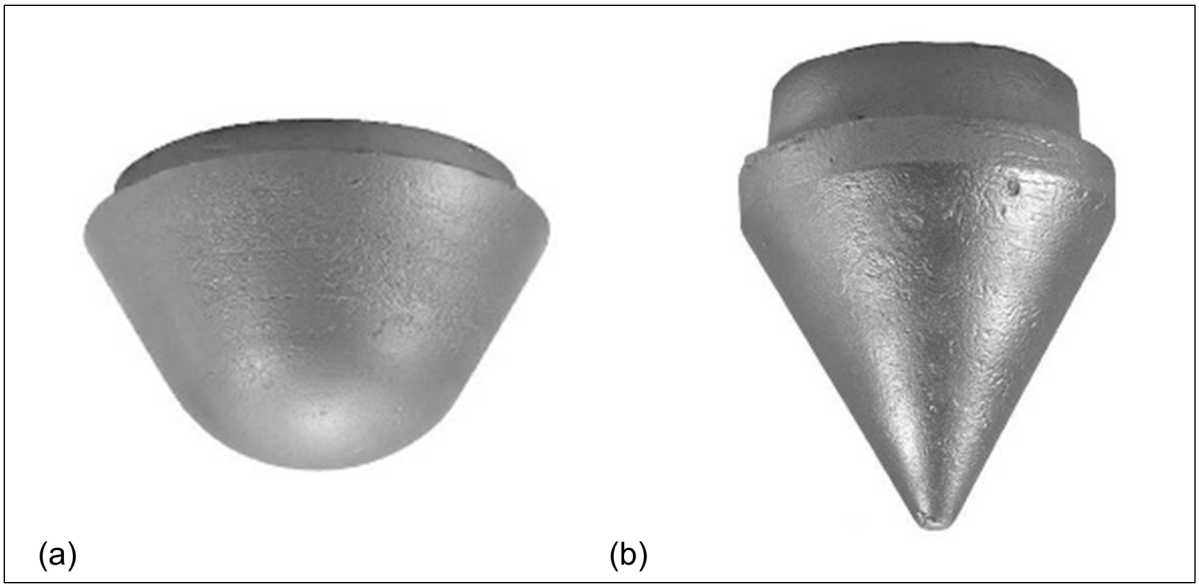

Figure 16-11 Conical toe attachments for closed end pipe piles: (a) Rounded (b) Pointed conical tip (courtesy Skyline Steel).

Figure 16-12 Conical toe attachment welded on a closed end steel pipe pile.

A “rock crusher” driving shoe is a preferred pipe pile closure device where sloping bedrock is encountered. This pile toe attachment consists of a thick flat plate with

heavy steel plates forming a 45 degree point. A photograph of the rock crusher toe protection device is included in Figure 16-13.

Figure 16-13 Rock crusher driving shoe welded on a closed end steel pipe pile.

When installing open end pipe piles in dense gravel or to rock, the use of cutting shoes will help protect the piles and distribute high localized contact stresses over a larger pile area. Cutting shoes are made from cast steel conforming to ASTM A148/A148M (Grade 90-60). Both inside flange and external flange cutting shoe designs are available as shown in Figure 16-14.

Both cutting shoes have a bearing ring where the open end pipe pile sits on the cutting shoe. Cutting shoes with an outside flange can make drilling through the pile toe easier, if needed. However, the shoe perimeter is larger in diameter than the pile section and can therefore reduce shaft resistance. Both inside and outside flange cutting shoes can be welded to pile toe, however, the outside flange is sometimes used with only a friction fit. Photographs of inside flange and outside flange cutting shoes on open end pipe piles are presented in 16-15 and 16-16 respectively.

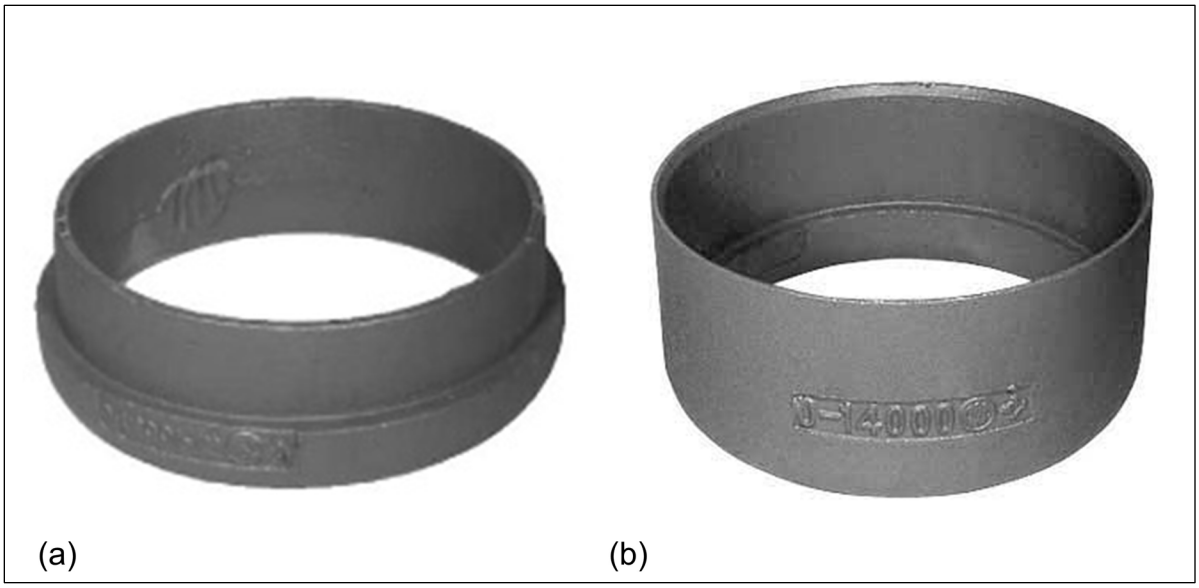

Figure 16-14 Cutting shoes for open end pipe piles:
(a) Inside flange and (b) Outside flange (courtesy Skyline Steel).

Figure 16-15 Inside flange cutting shoe welded to open end steel pipe pile.

Figure 16-16 Outside flange cutting shoe on open end steel pipe pile.

Large diameter open end pipe piles, 36 inches in diameter or greater, are frequently used in heavily loaded foundations having a limited number of piles. In these situations, use of a thicker wall bottom section over the lower two pile diameters is the preferred toe protection mechanism. The thicker wall toe section functions as an inside cutting shoe by having the same outside diameter as the design pile section. The thicker wall section helps distribute localized stresses and reduce the potential for pile toe damage that may otherwise develop due to partial pile toe contact with boulders, sloping bedrock, or on batter pile installations.

16.3.2 Splices

Steel pipe pile sections can be spliced by full penetration welding, or by using a mechanical drive-fit or friction splicer. Full penetration groove welds are depicted in Figure 16-17(a). A schematic of a friction splicer is shown in Figure 16-17(b). When a friction splicer is used in cases where the full bending strength of the pile is needed, fillet welds are required. However, the friction splicer must be fully seated into both top and bottom pile sections before performing the fillet weld to avoid subsequent cracking of the weld. Therefore, a full penetration weld is preferred in cases where the full bending strength is required.

For the full penetration weld, a backing ring, shown in Figure 16-18, is designed to sit between both pile sections and aides in pile alignment. Pins extending from the

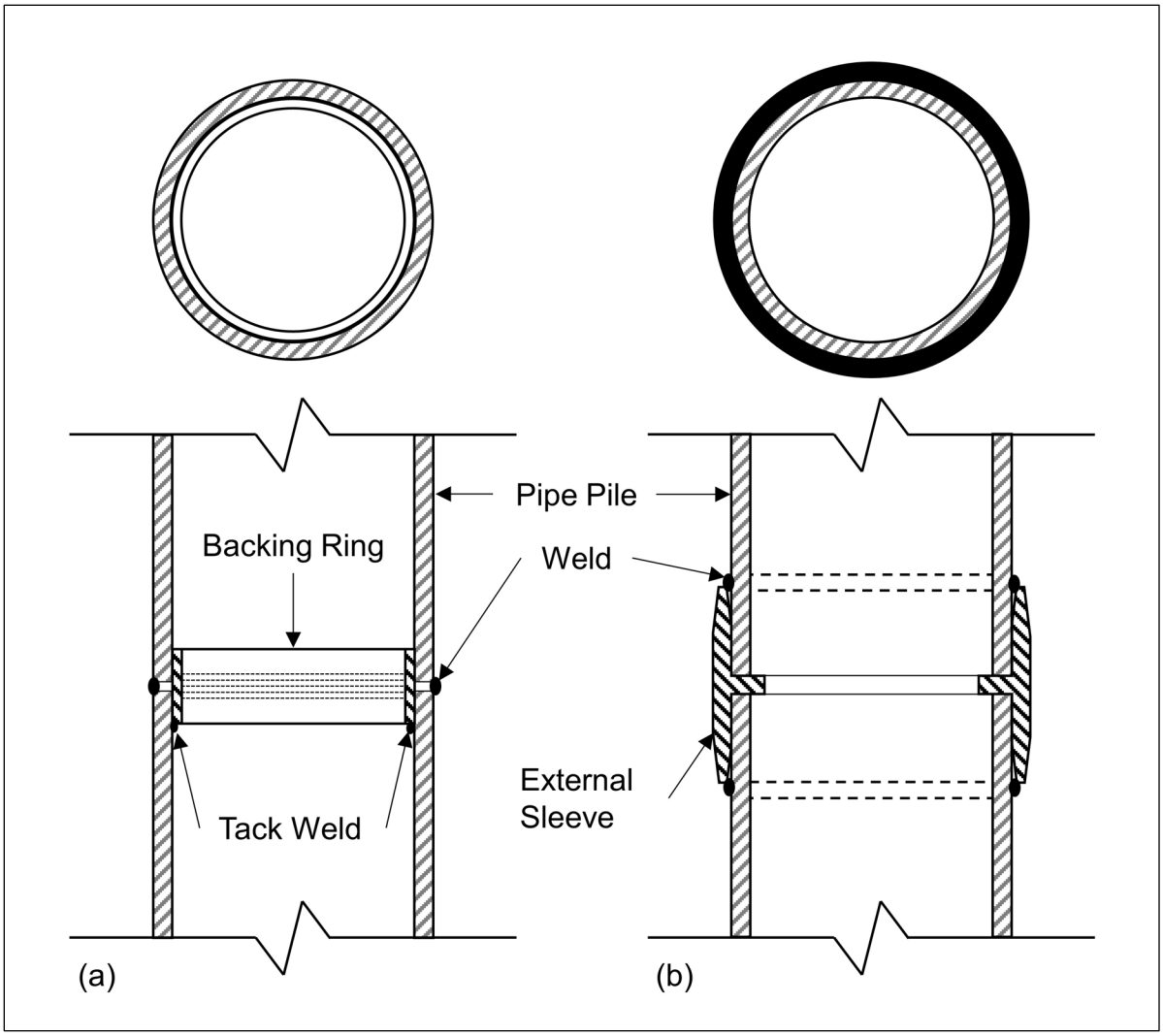

Figure 16-17 Splices for pipe piles.

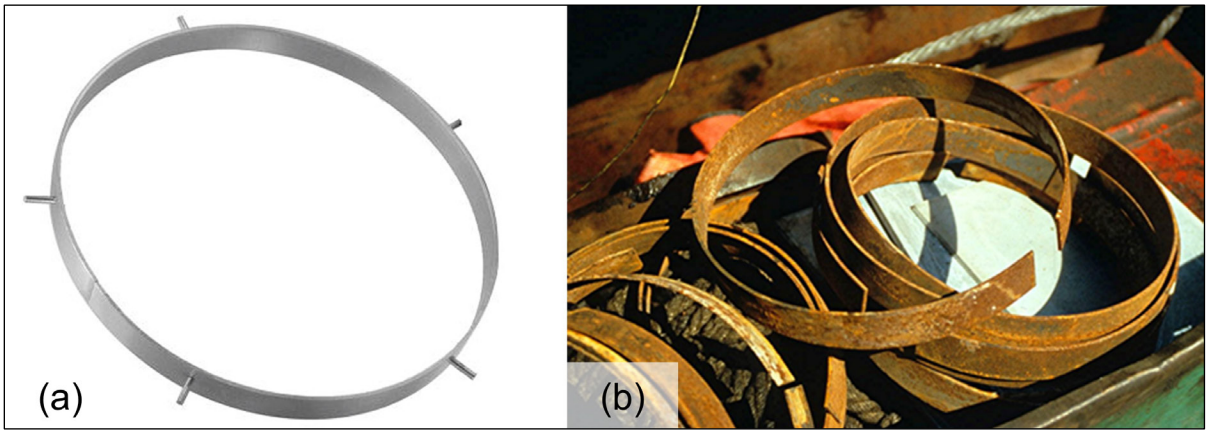

Figure 16-18 Backing rings for pipe pile splicing
(a) with pins (courtesy Skyline Steel) and (b) without.

backing ring provide a gap to facilitate welding the root pass. A photograph of the backup ring in place on a lower pile section is shown in Figure 16-19. Following completion of the root pass, additional passes are made around the splice to complete the full penetration weld and connect the pipe pile sections. Figure 16-20 shows a completed splice.

Figure 16-19 Backing ring tack welded to bottom pile.

Figure 16-20 Welded pipe pile sections.

In applicable situations, pipe piles can also be spliced with manufactured drive-fit or friction splicers similar to the one shown in Figure 16-21. These splicers are typically cast from ASTM A27 (Grade 65-35) or ASTM A148/A148M (Grade 90-60) steel and are designed with a taper for a frictional connection to eliminate the need for welding. A 3/8 inch bearing is located at the midpoint of the friction splicer for load transfer from the top pipe section to lower pile section. Little advanced preparation is required for this splice; however the adjoining pile sections must be square. If the initial pile section has some pile top damage following driving, the damaged section must be cut off and made square for a suitable friction connection with the drive-fit splicer. Unless a friction splicer is fillet welded to the top and bottom pile sections, the full pile strength in bending will not be provided. The suitability and location of friction splicers on piles subject to uplift loads should also be determined by the design engineer. If friction splicers are used on spiral welded pipe piles, fillet welds are also often necessary to provide a barrier to prevent ground water from leaking into the pile. A completed splice using the drive-fit friction splicer is shown in Figure 16-22.

Figure 16-21 Drive-fit mechanical friction splicer for pipe pile (courtesy Skyline Steel).

Figure 16-22 Drive-fit mechanical friction splicer on pipe pile.

16.3.3 Constrictor Plates

As discussed in Section 6.4.2 and Section 7.10 7, large diameter open ended pipe (LDOEP) piles can “core” or remain unplugged during driving. To facilitate plugging at a targeted depth in the soil stratigraphy, a constrictor plate is sometimes designed and welded inside the pile. Figure 16-23 shows the top surface of a constrictor plate with stiffeners welded inside a 60 inch O.D. pipe pile. A different constrictor plate detail is presented in Figure 6-14 of Section 6.4.2. Constrictor plates are often used inside large diameter open end pipe piles to force plugged behavior and a larger nominal resistance. Research on LDOEP pile design including constrictor plates is ongoing.

Figure 16-23 Constrictor plate installed inside pipe pile.

16.4 PRECAST CONCRETE PILES

16.4.1 Pile Toe Attachment

The toe of precast concrete piles may be damaged in compression under hard driving. In hard driving conditions and for toe bearing piles on rock, special cast steel toe attachments can be added to the pile during casting. However, toe attachments are not routinely used for concrete piles.

When necessary, a flat cast steel shoe as shown in Figure 16-24(a), or an "Oslo Point" or “Rock Injector Point” as shown in Figure 16-24(b), can be cast into a concrete pile for toe protection. The characteristics of Oslo or Rock Injector points are such that the pile can be “chiseled into” most rock types to ensure proper seating. These points generally have a 3.5 inch diameter hardened steel point housed in the steel casting attached to the concrete pile. All toe attachments for precast concrete piles must be attached during casting of the piles and not in the field. A photograph of an Oslo point with and without the hardened steel point in the housing is presented in Figure 16-25.

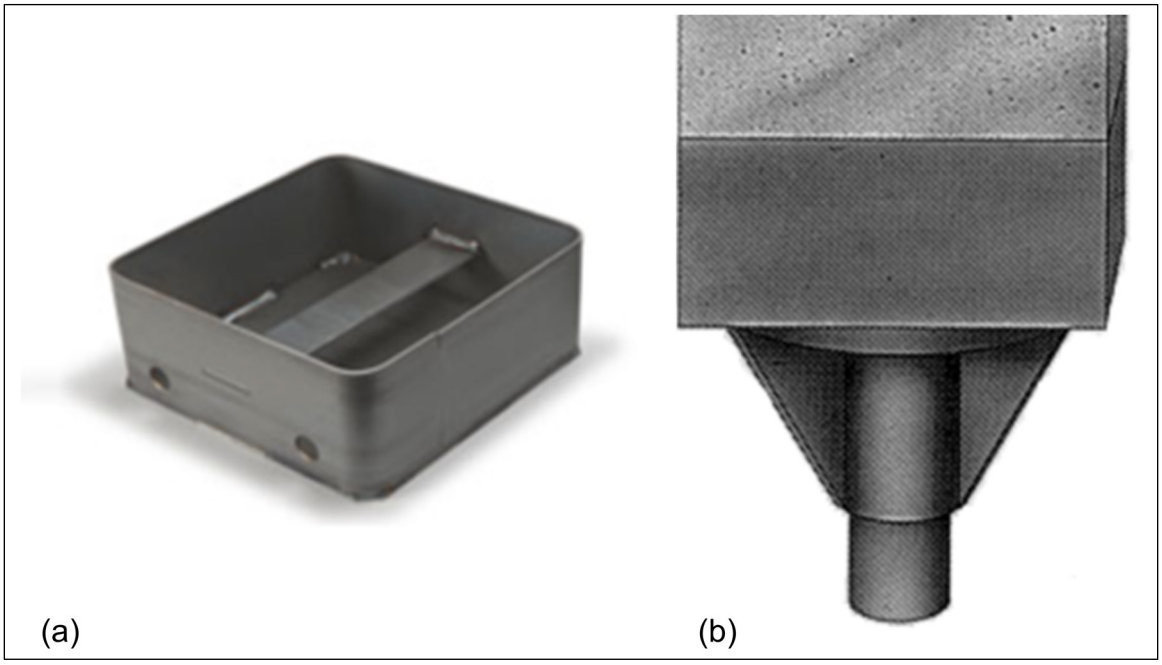

Figure 16-24 Pile toe attachments on concrete pile:
(a) Flat shoe (courtesy Titus Steel) and (b) Oslo point.

Figure 16-25 Oslo point for concrete pile.

Another toe attachment sometimes used with a prestressed concrete pile is an H-pile or pipe pile section cast into the pile toe. These devices are not typically used for toe protection but more to facilitate overall pile penetration depths in very dense or hard materials where it may be difficult to achieve the required pile penetration depth with a displacement pile. Depending on the characteristics of the materials to be penetrated, the embedded steel sections may or may not be equipped with its' own toe protection attachment. A photograph of a square prestressed concrete pile section with an embedded H-pile section at the pile toe is presented in Figure 16-26. In this situation the steel section must be appropriately sized for the concrete section, foundation loading conditions, and subsurface conditions to prevent overstressing.

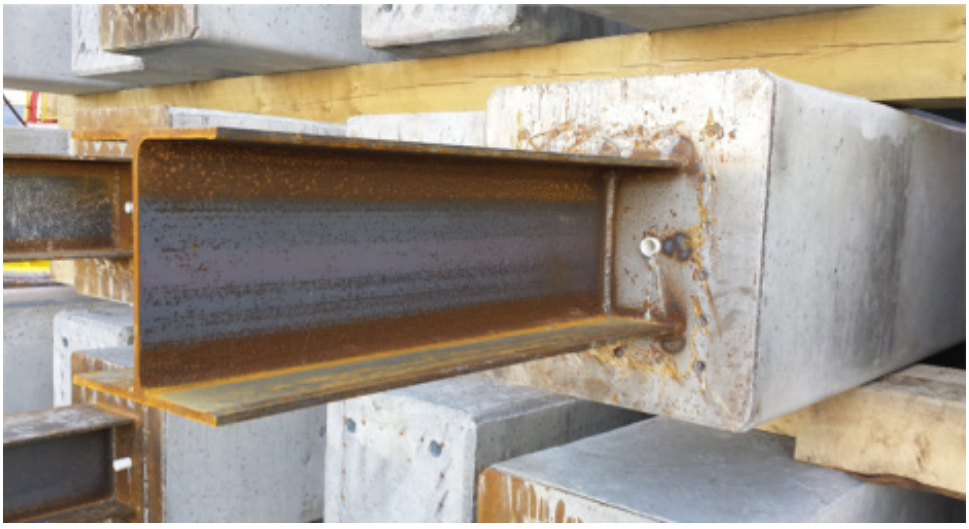

Figure 16-26 Steel H-pile cast into toe of prestressed concrete pile.

16.4.2 Splices

Virtually all concrete piles driven in the United States are prestressed to minimize potential problems associated with handling and tension stresses during driving. However, the ends of prestressed concrete piles are not effectively prestressed due to development length, and thus special precautions must be taken when splicing prestressed concrete piles. Whenever possible, concrete piles should be ordered with sufficient length to avoid splicing. However, if splicing is required, the splices available can be divided into four types: Dowel, Welded, Mechanical, and Sleeve. Illustrations of these splice types are provided in Figure 16-27. The wedge and pinned connectors can be classified as mechanical splices while the connector ring is a sleeve splice.

As part of a FDOT research effort on development of a new post tensioned concrete pile splice, Mullins and Sen (2015) summarized the available splicing systems for prestressed concrete piles including the capacity, failure type, durability, installation, and production aspects. The results of this summary are presented in Table 16-1.

Table 16-1 Summary of Precast Concrete Pile Splices (after Mullins and Sen 2015)

Name of Splice	Type	Capacity	Failure Type	Durability	Installation	U.S. Produced
Epoxy Dowel	Dowel	Poor	Ductile	Good	Moderate / Poor	Yes
Kie-Lock	Mechanical	Good	Ductile	Moderate	Good	No
ICP	Welded	Good	Brittle	Moderate	Moderate	No
NU Chuck	Bolted	Good	Brittle	Moderate	Untested / Moderate	Yes
UF Tube	Grouted Tube	Good	Ductile	Good	Poor	Yes
GYA	Mechanical	Good	Ductile	Moderate	Good	No
Macalloy	Post Tensioned	Good	Ductile	Good	Moderate / Poor	No

In the above table, capacity was defined as how well the splice met the flexural and tensile strength requirements for driving forces and pile loads. The failure type identified how the splice fails. Ductile failure is preferable to brittle failure. Durability noted the splice resistance to reinforcement and strand corrosion. Installation identified the time and labor requirements to complete the splice and U.S. produced

identifies whether the splice is made in the U.S. Foreign made splices require special exceptions on some Federal funded projects. Some splices are only applicable for a specific pile type such as the UF Tube which is designed for voided concrete piles.

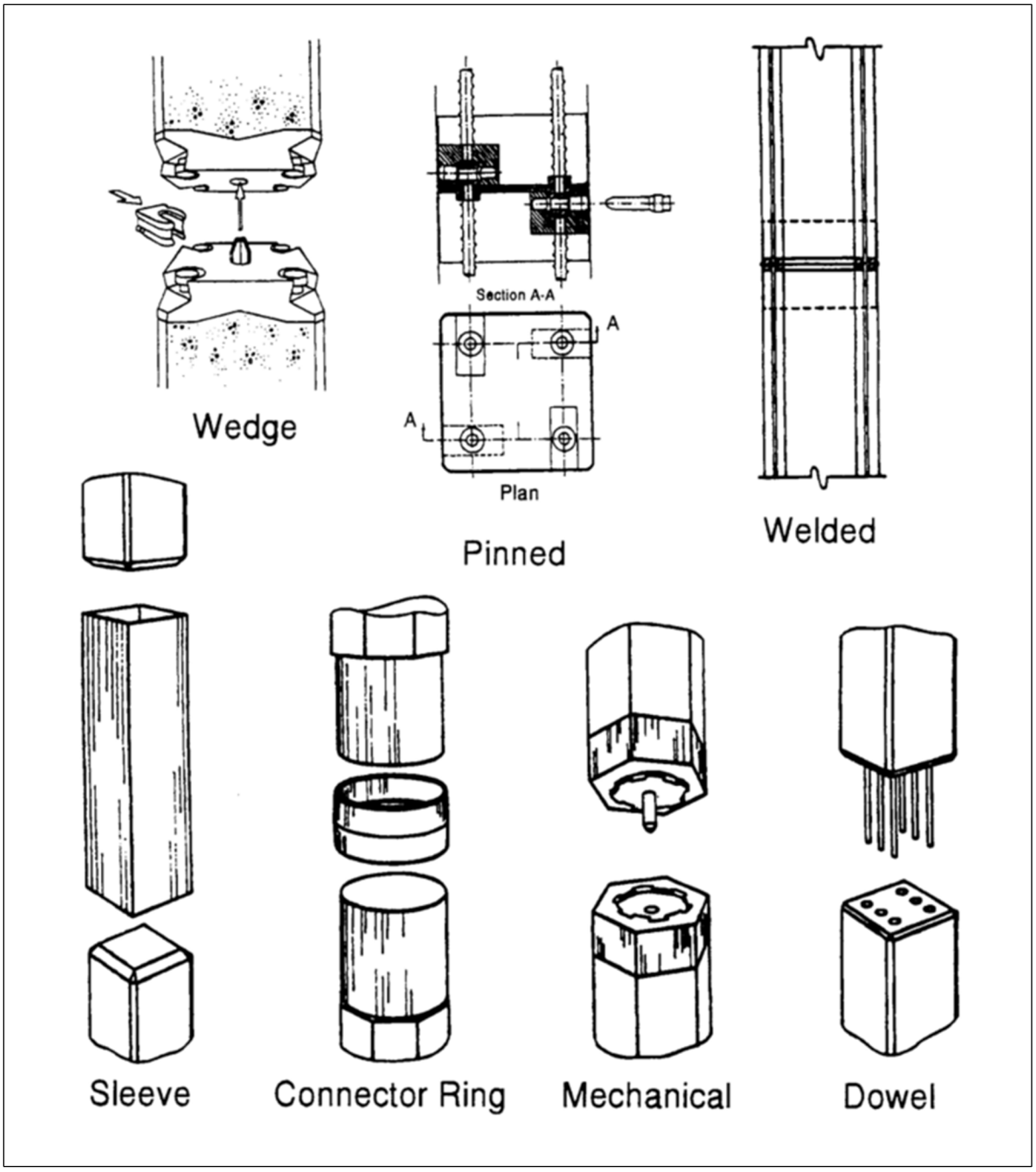

Figure 16-27 Commonly used prestressed concrete pile splices (after PCI 1993).

A schematic of an epoxy dowel splice for prestressed concrete pile is presented in Figure 16-28 while photographs of the splice in progress are presented in Figure 16-29(a) and 16-29(b). The bottom pile section to be spliced requires holes to receive the dowels. These holes may be cast into the pile when splicing is planned, or drilled in the field when splicing is needed, but was unexpected. The bottom section is driven with no special consideration and the top section is cast with the dowel bars in the end of the pile. When spliced together in the field, the top section with the protruding dowels is guided and set in position and a thin sheet metal form is placed around the splice. Epoxy is then poured, filling the holes of the bottom section and the small space between the piles. Pile driving can typically resume on epoxy dowel splices one to two days after epoxy placement. Epoxy dowel splices can be time consuming but are comparatively inexpensive. These splices have been reliable if dowel bars are of sufficient length and strength, and if proper application of the epoxy is provided. The number, length, and location of the dowel holes, as well as the dowel bar size, must be designed. As noted by Mullins and Sen (2015), the splice has limitations meeting all the flexural and tensile strength requirements for driving forces and foundation loads.

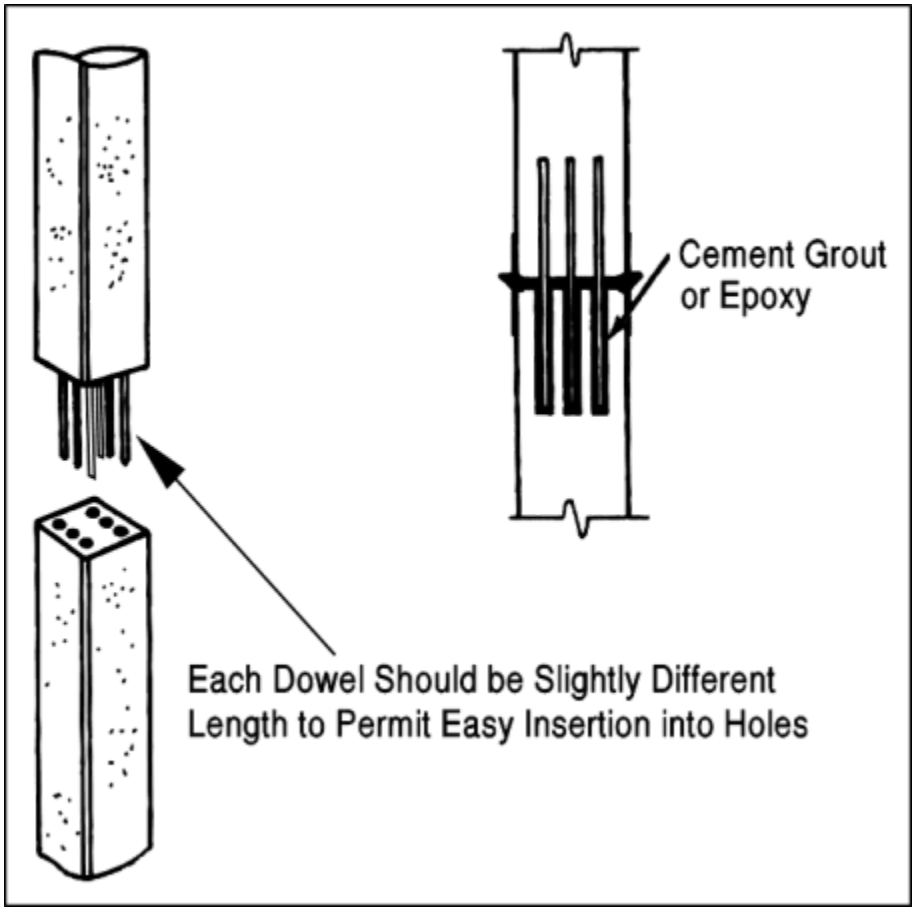

Figure 16-28 Cement/Epoxy-dowel splice (after Bruce and Herbert 1974).

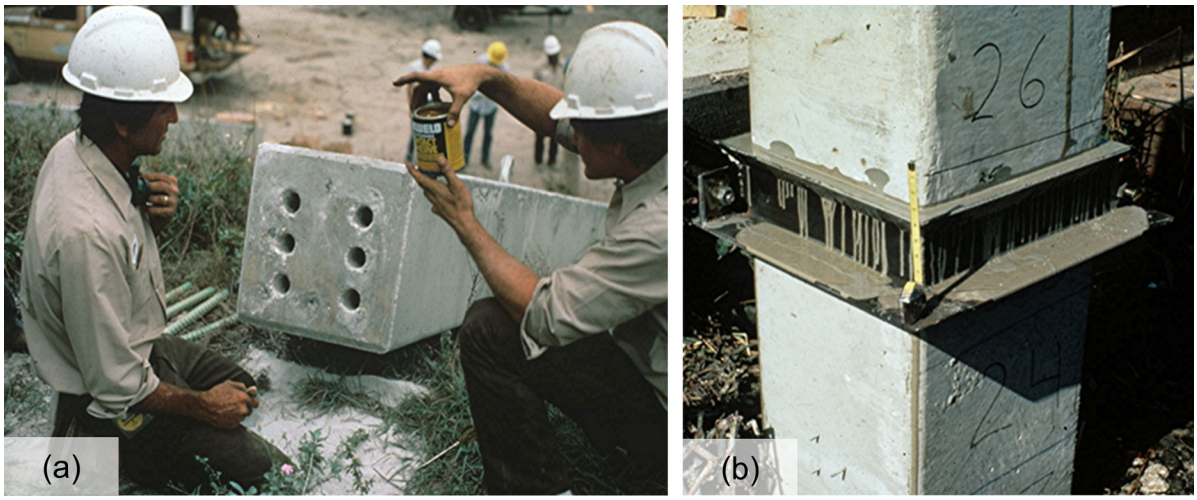

Figure 16-29 Epoxy-dowel splice: (a) pile with core holes and (b) splice in progress.

Welded splices require having steel fittings cast into the end sections of the concrete pile when manufactured. Sections are welded around the entire perimeter. Figure 16-30(a) shows the beveled steel fitting at the head of the driven pile section and Figure 16-30(b) shows the completed ICP pile welded splice.

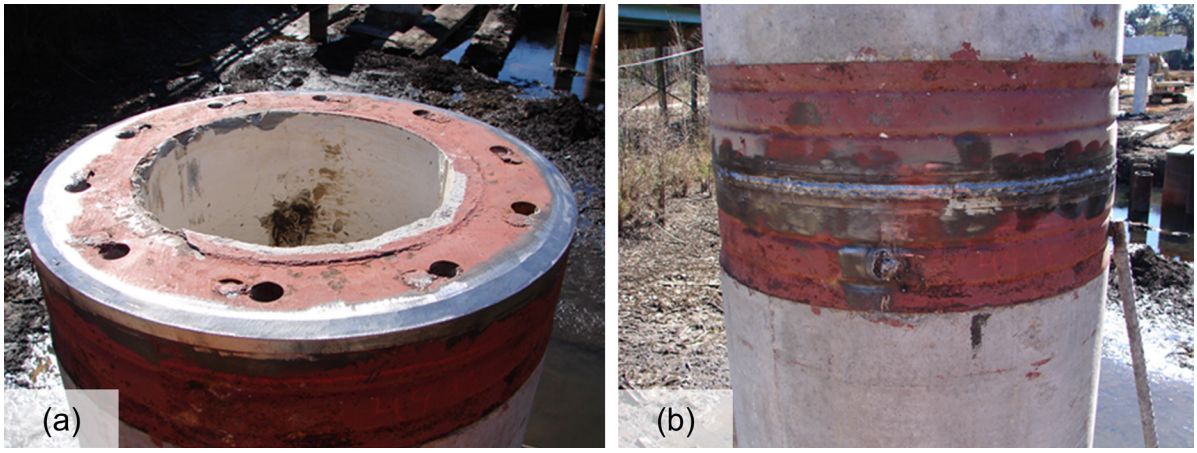

Figure 16-30 Welded ICP splice: (a) beveled steel fitting and (b) welded splice.

Most mechanical splices for prestressed concrete piles, such as the Kie-Lock, Herkules, and ABB, among others, are made of steel castings and are available for square, octagonal, hexagonal, and/or round sectional shapes. The steel castings are installed in the formwork of a prestressed concrete pile prior to concrete placement. The Kie-Lock (Figure 16-31) and Hercules splices require mating both male and female castings, while most other mechanical splices are gender neutral. All mechanical splices are then locked by inserting bars, wedges, pins, keys, or other mechanical connections after aligning the sections. Although mechanical splices can be expensive, they do save considerable time and they have been designed to properly account for all loading conditions, including tension.

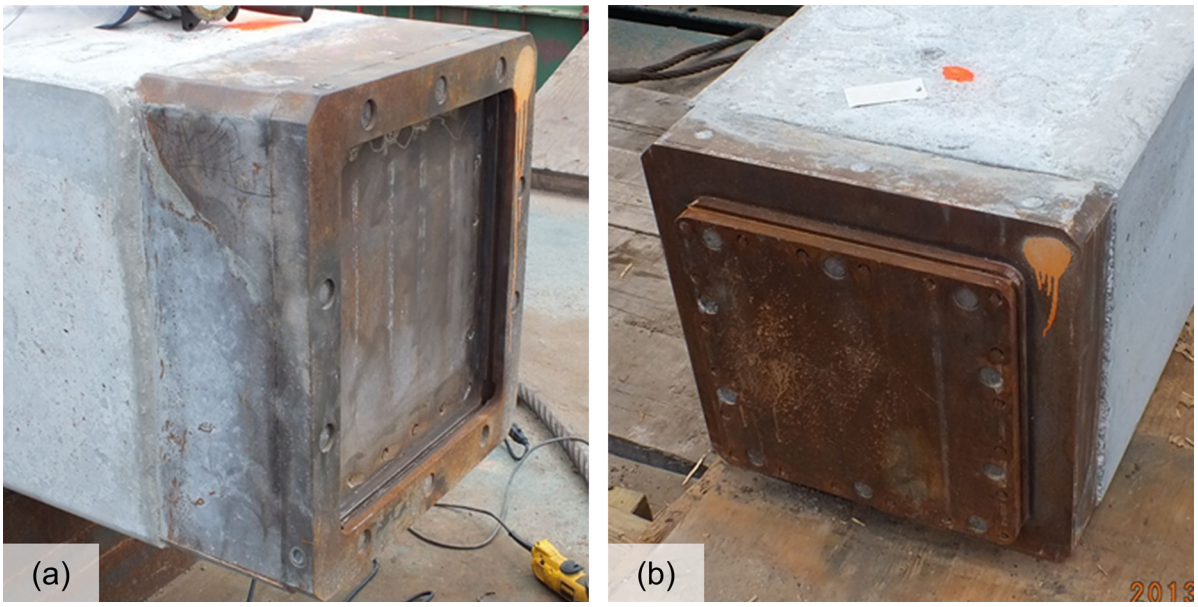

Figure 16-31 Kie-Lock splice.

A new concrete pile splice is under development for the Florida DOT in research by Mullins and Sen (2015). The splice is shown in a horizontal position in Figure 16-32. The splice is post-tensioned after joining the two concrete pile sections with the full prestress level restored across the splice and adjacent pile sections. For this splice, anchorages for the strands are cast into the lower section and open ducts are cast into the upper pile section. Steel strands are then locked into the lower anchor blocks and inserted though the upper pile section. After the two pile sections are mated, the steel strands are post-tensioned and the remaining duct voids grouted.

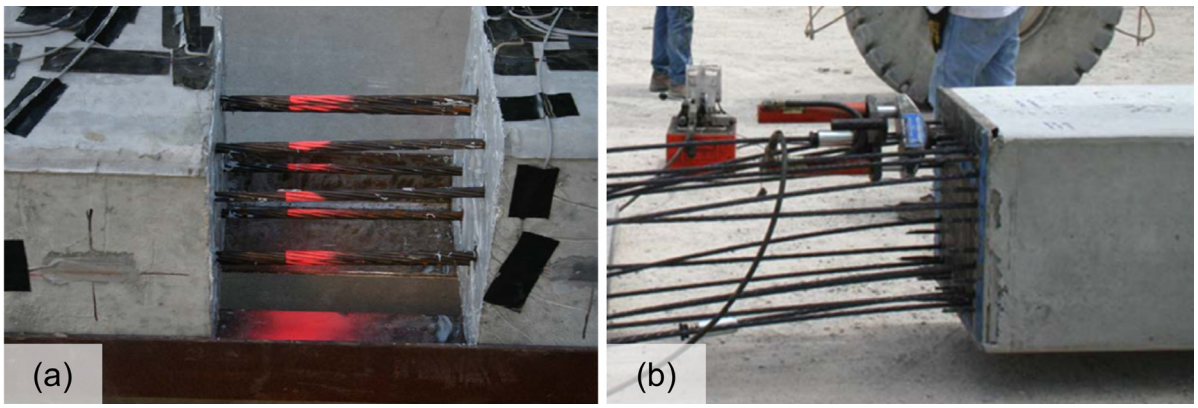

Figure 16-32 Post-tensioned splice (a) splice joint and (b) post tensioning strands in upper section (courtesy University of South Florida).

Sleeve type concrete splices are illustrated in Figure 16-33. These concrete pile splices can be rapidly applied and are very effective in reducing tension driving stresses. However, they cannot be used where static uplift loading will be required.

A Hawaiian can sleeve splice is shown in Figure 16-33(a). The sleeve must have sufficient length and strength if lateral or bending loads are anticipated. A Bruns connector ring splice is shown in Figure 16-33(b). The Bruns splice requires steel castings at the ends of the concrete piles. The shorter connector ring design has limited tensile and flexural strength and is therefore not recommended for designs with those loading considerations.

Figure 16-33 Sleeve splices: (a) Hawaiian can and (b) Bruns splice.

If a specific splice is specified based on previous experience, then an option for substituting some other concrete splice should not be allowed unless the substitute splicer is field tested. The alternative splice should be required to have equivalent compressive, tensile and flexural strength to the originally specified splice. The substitute splicer can be tested by driving a number of spliced test piles and observing the performance.

16.5 WELDED SPLICES AND TOE ATTACHMENTS

Field welding is required on many pile splices and pile toe attachments. Weld quality is paramount in maintaining the full pile material strength. Due to the importance of field welding quality, the Michigan Department of Transportation developed a detailed document “Field Manual for Pile Welding” (2012). The New York State Department of Transportation also devoted twelve pages in their “Pile Driving Inspection Manual” (2012) to pile splicing and toe attachments. The NYSDOT document includes minimum splice times for weld preparation and welding as a function of pile section and splice type.

If not performed properly, welds at splice locations can crack or break during driving. Examples of welded pile splices that failed during driving are presented in Figures 16-34 and 16-35. The pipe pile weld in Figure 16-34 cracked as a result of bending stresses occurring during hammer-pile alignment. The weld shown in Figure 16-35 broke a few hammer blows following splicing. The H-pile splice had been completed in low temperatures without properly preheating the pile metal. The main sources of welded splice problems, when they occur, can be traced to poor pile surface preparation, insufficient bevel or root opening, or general non-compliance with approved welding procedures or splice details.

Figure 16-34 Cracked weld on pipe pile splice.

Figure 16-35 Broken weld on H-pile splice.

16.5.1 Welding Surface Preparation

Prior to commencing welding, the pile joint to be welded must be properly cleaned. If the ambient temperature is below 32 degrees Fahrenheit the weld area must also be preheated. Figure 16-36 illustrates a steel pipe pile head which has been properly cut and beveled at the required angle to accommodate a welded splice. Without the appropriate bevel, weld penetration will be reduced, and it will not be possible to complete a full penetration groove weld. In Figure 16-37, a grinder is being used to prepare the pile head surface for welding. Typically, the add on H-pile section will have a 45 degree bevel with a 1/8 or 1/4 inch root opening to complete a full penetration weld. In Figure 16-38, two H-pile sections have been positioned for splicing. The specified splice detail required a full penetration weld. However, a full penetration weld is clearly impossible given the lack of a root opening and bevel shown in the figure.

Figure 16-36 Beveled edges on pipe pile in preparation for weld.

Figure 16-37 Grinding edges of web and flange in preparation for weld.

Figure 16-38 H-pile splice preparation without adequate root opening or bevel.

Proper pile section alignment is required prior to splicing. Figure 16-39 illustrates poor section alignment, a poor quality groove weld on the flange, and poor quality and insufficient fillet weld lengths on a splice with an H-pile splicer. When H-pile splicers are used, section alignment and root opening should be checked prior to welding. Figure 16-40 shows an extracted H-pile from the same project where dynamic testing indicated a cracked weld during driving. The H-pile was extracted after driving; however only the upper pile section returned. The pile separated at the poorly welded splice with the H-pile splicer and lower pile section lost below ground.

Figure 16-39 Misalignment between pile sections and poor quality weld.

Figure 16-40 Extracted H-pile upper section. Weld cracked during driving and extracted section retrieved without H-pile splicer or lower pile section.

16.5.2 Temperature Requirements During Welding and Splicing

In colder climates where the ambient air temperature is below 32 degrees Fahrenheit, the steel in the vicinity of the splice should be preheated to a minimum temperature of 70 degrees Fahrenheit within 3 inches of the weld immediately prior to welding and maintained at a minimum of 50 degrees Fahrenheit until the welding is complete. No welding should be performed when the ambient air temperature is below 0 degrees Fahrenheit. Figure 16-41 illustrates an H-pile being preheated at the splice location prior to welding.

Figure 16-41 Heating pile splice location prior to welding.

16.5.3 Welding Pile Toe Accessories

Pile toe attachments should be welded to the toes of H-piles and pipe piles following the approved welding procedure by approved welders. In Figure 16-42, small spot welds; one on the web and one at the corner of each flange have been used to attach the driving shoe to the pile toe. The limited welding can facilitate the loss of the driving shoe when difficult driving conditions are encountered. A partial penetration groove weld along the full length of the H-pile flange is shown attaching the driving shoe to the H-pile in Figure 16-43. This detail greatly reduces the possibility of driving shoe loss or the shoe not performing as intended when cobbles or bedrock is encountered.

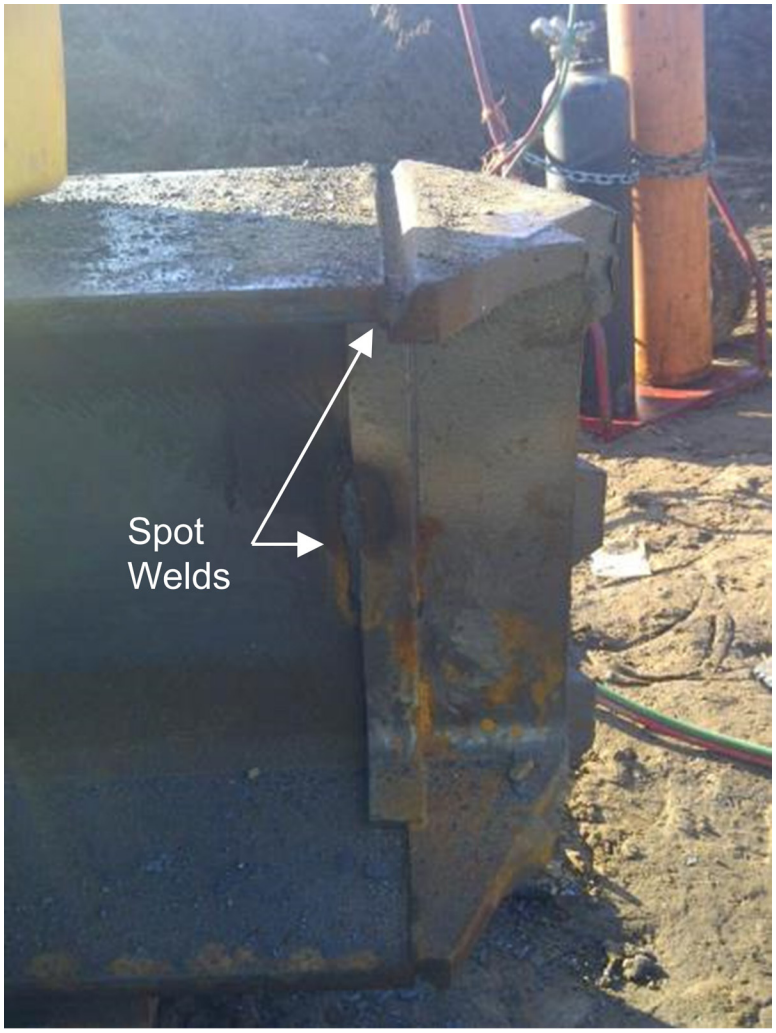

Figure 16-42 Unsatisfactory spot welds used for shoe attachment.

Figure 16-43 Full groove weld between pile and toe attachment.

16.5.4 Welded Splice Checklist

The following checklist is from the Michigan Department of Transportation Field Manual for Pile Welding (2012). It highlights several key items to be addressed for successful field welded splices.

16.5.4.1 Preparation

- Welders should be certified by an authorized agency to perform the type of work, and produce the type of weld to be used.
- A Weld Procedure Specification (WPS) should be developed and approved prior to work commencement.
- Joint preparation, pile alignment, root openings, bevels and fit up should be completed according to contract plans.
- Weld surfaces should be ground and cleaned. Coatings, oil, grease, rust, dirt, moisture and other contaminants within the weld zone should be removed.
- When ambient air temperature is below 32 degrees Fahrenheit, the pile splice area should be preheated, and maintained at 70 degrees. Welding should not be performed when ambient temperature is below 0 degrees Fahrenheit. Heating and housing may be approved by an engineer.
- The contractor should have an approved quality control plan, and perform welding with respect to the established quality control plan.

16.5.4.2 During Welding

- Electrodes should be properly stored. This includes:
    - Electrodes should be stored in a hermetically sealed container or hot box with a minimum temperature of 250 degrees Fahrenheit.
    - One exposed to the atmosphere, electrodes should be either used within two-hours, or redried for two hours at a minimum of 500 degrees.
    - Electrodes that become wet should be discarded and not used.
    - Electrodes should be discarded if they are dropped on the ground, exposed to rain or not properly stored.
- Tack welds used during fit up should not be part of the final weld.
- The welder(s) should follow the approved WPS, contractor quality control plan and should inspect his/her own work.
- The welder(s) should clean between passes, removing all slag and repairing discontinuities between passes.
- The welder(s) should back gouge to sound metal for full penetration groove welds before welding the backside (if applicable).

16.5.4.3 Final Weld Inspection

- All slag, spatter, and debris should be removed from weld surface.
- The weld size, length and profile should meet project requirements.
- Arc strikes should be ground smooth.
- A final inspection for cracks or other discontinuities, porosity, undercut, underfill, overlap, lack of penetration, or lack of fusion should be performed before accepting the weld.
- Repairs or replacement of weld should be performed before accepting the weld.

REFERENCES

American Association of State Highway and Transportation Officials (AASHTO). (2014). AASHTO LRFD Bridge Design Specifications, US Customary Units, Seventh Edition, with 2015 Interim Revisions. American Association of State Highway and Transportation Officials, Washington, D.C., 1960 p.

ASTM A148-14. (2014). Standard Specification for Steel Castings, High Strength, for Structural Applications. Book of ASTM Standards, Vol. 1.02, ASTM International, West Conshohocken, PA, 4 p.

ASTM A27-13. (2014). Standard Specification for Steel Castings, Carbon, for General Application. Book of ASTM Standards, Vol. 1.02, ASTM International, West Conshohocken, PA, 4 p.

ASTM A572-15. (2015). Standard Specification for High-Strength Low-Alloy Columbium-Vanadium Structural Steel. Book of ASTM Standards, Vol. 1.04, ASTM International, West Conshohocken, PA, 4 p.

Collin, J.G. (2002), Timber Pile Design and Construction Manual. American Wood Preservers Institute (AWPI), 122 p.

Michigan Department of Transportation (MDOT). (2012). Field Manual for Pile Welding. Division of Bridge Field Services, First Edition, MI, 35 p.

Mullins, G., and Sen, R. (2015). Investigation and Development of an Effective, Economical and Efficient Concrete Pile Splice. Florida Department of Transportation, Tallahassee, FL, 270 p.

New York Department of Transportation (NYDOT). (2012). Pile Driving Inspection Manual, GEM-26, pp. 13-25.

Precast/Prestressed Concrete Institute (PCI). (1993). Precast/Prestressed Concrete Institute Journal. Vol. 38, No. 2, pp.14-41.

Washington State Department of Transportation (WSDOT). (2012). Standard Specifications for Road, Bridge and Municipal Construction. WS, 974 p.

CHAPTER 17

DRIVING CRITERIA

Pile foundations must be installed to meet limit state requirements for compressive, tensile, and lateral resistances as well as to satisfy serviceability requirements. Driven pile foundations are therefore used to satisfy nominal resistance requirements, pile penetration requirements, or both. As the pile is driven into the soil or rock, observations of the pile penetration resistance or blow count provide an indication of the nominal geotechnical resistance. Several methods have been developed that correlate the observed blow count and the associated hammer operational performance with the nominal geotechnical resistance achieved.

Driven pile foundations are generally installed using a driving criterion that equates the blow count and hammer stroke to the nominal geotechnical resistance. A minimum pile penetration depth may often be included in the driving criterion in cases when scour, foundation settlement, uplift or lateral loading demands impact design performance. The correlation of the observed blow count and hammer stroke to the nominal geotechnical resistance can be established from one or a combination of two of the following methods: static load test (Chapter 9), dynamic testing with signal matching (Chapter 10), rapid load testing (Chapter 11), wave equation analysis (Chapter 12) or dynamic formulas (Chapter 13).

17.1 DEVELOPMENT OF THE PILE DRIVING CRITERIA

The foundation designer should specify the method to be used for determination of the driving criteria. Furthermore, construction personnel should clearly understand the method being used and its proper implementation on the project.

Brown and Thompson (2011) summarized current state transportation agency practices on driving criteria in the NCHRP Synthesis 418, “Developing Production Pile Driving Criteria from Test Pile Data.” This report surveyed 42 transportation agencies covering a wide range of pile types and sections, hammer types and sizes, project sizes, as well as soil and rock conditions. The agencies reported their predominant method of establishing driving criteria were, from most frequent to least frequent:

- Drive piles to a blow count determined from another pile that had previously been subjected to dynamic testing and analysis.
- Drive piles to a blow count determined from a dynamic formula.
- Drive piles to a blow count determined from a wave equation analysis.
- Drive piles to practical refusal.
- Drive piles to a specified tip elevation.
- Drive piles to a blow count determined from another pile that had previously been statically load tested.

The resistance verification methods mentioned above each have their own resistance factor in AASHTO (2014). Hence, a change in the resistance verification method during construction will necessitate driving production piles to either a higher or lower nominal resistance than shown on the original contract documents. For example, a change from dynamic testing with signal matching (ϕ_{dyn} = 0.65) to the FHWA modified Gates formula (ϕ_{dyn} = 0.40) will result in a 63% increase in the required nominal resistance. This can create problems if the pile driving system was not originally sized for the higher nominal resistance. Conversely, a switch from the FHWA modified Gates formula (ϕ_{dyn} = 0.40) to either a static load test (ϕ_{dyn} = 0.75) on one pile, or to 100% dynamic testing with signal matching will result in an 87% reduction in the required nominal resistance. In this scenario, reduced nominal resistance piles may allow the use of a smaller pile hammer, or may solve a problematic pile installation condition such as avoiding a damage causing boulder layer since piles with a reduced nominal resistance may terminate at a higher, and therefore, safer installation elevation.

When developing driving criteria, consideration should also be given to the effect of time dependent changes in the nominal geotechnical resistance. In conditions exhibiting soil setup, pile penetration resistances at the end of driving less than that required for the nominal resistance may be acceptable when setup is confirmed by later restrikes. Conversely in geomaterials that exhibit relaxation, pile penetration resistances at the end of driving should be greater than those needed for the required nominal resistance to account for the future loss of nominal resistance.

Restrike tests are typically performed in soils with time dependent soil strength changes to confirm the expected change in nominal resistance. Restrike tests are also performed on projects in the event unexpected changes in nominal resistance occur with time. In cases where time dependent soil strength changes are anticipated, static or dynamic restrike tests should be delayed by an appropriate waiting period until the anticipated soil strength changes have occurred. Additional

information on time dependent soil resistance effects is presented in Section 7.2.4 and approximate waiting periods for various soil types is noted in Section 14.5.2.1. When time dependent soil strength changes occur, care has to be taken to assess the driving criterion for the soil condition at the end of driving. For example, if soil setup results in a 50% increase of nominal resistance from the end of driving to the time of an acceptable setup period, then piles may be driven to a blow count that produces the required nominal resistance divided by 1.5. Obviously, this reduced driving criterion may result in substantial savings compared to driving the piles to the full nominal resistance. Restrike tests should be performed on a representative percentage of production piles to substantiate that the anticipated soil setup occurs over the site. A contingency plan should also be in place in the event restrike results indicate less than required nominal resistance, such as performing a second longer term restrike or driving piles to a greater penetration depth.

17.2 PRACTICAL AND ABSOLUTE REFUSAL

As noted above, agencies sometimes use practical refusal as a driving criteria. Definitions for practical and absolute refusal are based on an approved hammer system operating properly at its maximum fuel or stroke setting unless hammer approval was established based on hammer operation at a reduced fuel or stroke setting. If refusal driving conditions develop in combination with suspect hammer performance, further evaluation of hammer energy transfer and the source of the refusal driving conditions are appropriate.

Practical refusal is defined as a pile penetration resistance (blow count) of 10 blows per inch for a maximum of 3 consecutive inches of pile penetration. Practical refusal is often used as a criterion for piles driven to a consistent and hard bearing layer. Blow counts greater than 10 blows per inch should be used with care for concrete piles and should be avoided for timber piles. Absolute refusal is defined as 20 blows for one inch or less of pile penetration. Driving should terminate immediately once either criteria are achieved with a properly sized and properly working hammer.

Practical and absolute refusal criteria should be used to avoid driving for an extended duration at excessively high and unreasonable blow count requirements. When seating a pile on hard rock, an absolute refusal criterion of 5 blows per ¼ inch or 10 blows per ½ inch may be preferred to 20 blows per inch to reduce the risk of pile toe or driving equipment damage.

When the required pile penetration depths cannot be achieved by driving without exceeding practical or absolute refusal criteria with the approved hammer, use of other pile penetration aids should be evaluated. Predrilling, jetting, and spudding equipment are discussed in Chapter 15.

17.3 PRACTICAL ISSUES AND CONSIDERATIONS

Prior to the onset of test pile or production pile driving, numerous practical issues and considerations should be clearly understood by the parties responsible for developing the driving criteria, approving a submitted criteria, or responsible for implementing the criteria in the field. Some of the more common issues encountered include:

- The lack of, or an incomplete or conflicting definition of, pile driving acceptance criteria within contract documents.

  Specifications should clearly identify the pile acceptance requirements (nominal resistance requirements in compression or uplift; required minimum pile penetration depth, if any, to meet lateral resistance or serviceability requirements, to avoid premature pile acceptance in competent layers overlying compressible ones, or due to high driving resistance caused by obstructions or poor hammer performance, etc.) as well as the resistance verification method.

- Clear identification of who determines when driving is terminated on test or production piles.

  On test pile projects, numerous parties may be present on the job site each with different responsibilities. A pile “inspector” will likely be present for the agency or for the DB team to record the pile penetration resistance or blow count as well as the associated hammer performance during test pile installation. The agency’s project engineer or its design consultant may be present to observe test pile driving, another agency or contractor retained engineer may be present performing a dynamic pile test during driving, and the contractor’s foreman may be documenting pile installation. Who and what (resistance verification method) determines when test pile driving is terminated should be clearly established in the contract documents and revisited prior to test pile installation. A detailed, manually recorded, pile driving log should always be maintained as part of a test pile installation.

During production driving, the pile inspector often serves as the agencies lone representative during driving and determines when the driving criteria established from the test pile program or by other means is achieved.

- Definition, or lack thereof, of time considerations in pile acceptance criterion.

  Pile acceptance criteria are based on achieving a nominal resistance at a specific time. Therefore, the pile acceptance criterion must clearly state when the criterion is to be applied such as at the end of initial driving or at the beginning of restrike. If based on restrike conditions, the time window when restrike tests are to be performed must be incorporated into the criterion. Oftentimes a time dependent nominal resistance correlation is established that requires restrike tests within a set time period. Restrike tests performed too early or too late may invalidate this correlation. Restrike tests on piles having limited drivability in soil setup environments may also need to be performed within a set time window to avoid refusal condition during restrike.

- Definition, or lack thereof, of driving criteria applicability and refinement as necessary to various substructure locations, subsurface conditions, or nominal resistance demands.

  Contract documents should identify test pile locations, the substructure units covered by those test pile locations, and that the resultant driving criterion is applicable to those substructure units. In some cases developing an appropriate driving criterion may necessitate the extrapolation of the test pile results to higher or lower nominal resistances, shorter or longer pile lengths, different batter angles, or slightly variable soil stratigraphy within the identified substructure locations by using refined and then modified wave equation analysis.

- The purpose of specifying and achieving a minimum pile penetration depth or required pile toe elevation.

  Minimum pile penetration requirements may be specified due to the depth of scour, the compressibility of soil layers, the presence of liquefaction susceptible layers, satisfying lateral or uplift loading demands, and other factors besides the nominal geotechnical resistance in axial compression. A minimum penetration depth should generally not be specified only to achieve an axial compression resistance.

- The difference between estimated and minimum pile toe elevations and when a minimum pile toe elevation should be specified.

  The estimated pile toe elevation defines the estimated pile length needed to achieve the nominal geotechnical resistance in axial compression. It is used to establish contract length estimates for bidding purposes. A minimum pile toe elevation is used to satisfy performance requirements.

- The difference between the required nominal geotechnical resistance based on design requirements and the resistance required to be overcome during initial driving (greater or lesser) based on unsuitable layers or time dependent changes in soil resistance.

  The required nominal driving resistance, R_{ndr}, is the soil resistance that must be overcome at the time of pile driving in order to provide the nominal geotechnical resistance, R_n, needed to satisfy loading and performance requirements. The nominal driving resistance can be significantly greater than the nominal resistance in cases where scourable, liquefiable, highly compressible, or otherwise unsuitable soil layers must be penetrated and/or where toe resistance may decrease after initial driving due to relaxation. The nominal driving resistance can also be less than the nominal resistance in cases where these conditions are not present and/or the suitable support layers exhibit soil setup.

- Unreasonable definitions of practical and absolute refusal criteria in terms of either an excessive driving resistance (blow count) or a hard to achieve minimum pile penetration length.

  Definitions of practical and absolute refusal with regard to blow count aspects were provided in Section 17.2. These criteria should be reviewed to avoid excessively high and unreasonable blow count requirements. When piles must penetrate into very hard geomaterials, weathered bedrock, or hard bedrock to satisfy any pile penetration depth requirements, predrilled holes may be required as it may not be possible to achieve the required penetration depth through driving alone.

- Pile termination and acceptance criteria in soft and hard rock.

Oftentimes piles can be driven into soft rock at considerable distances with a gradual buildup of both the pile penetration resistance as well as the nominal geotechnical resistance. In general, this condition is not too problematic unless the driving occurs at high blow counts for an extended duration of driving resulting in a reduction in hammer performance. In the case of hard rock, driving should be terminated relatively quickly once hard rock is encountered to reduce the risk of pile toe or hammer damage as discussed in Section 17.2.

- Understanding the limitations of dynamic tests and wave equation analyses in easy driving (less than 24 blows per foot) and hard driving (more than 120 blows per foot) situations.

  At pile penetration resistances less than 24 blows per foot and above 120 blows per foot, dynamic test and analysis methods can overpredict and underpredict the nominal resistance, respectively. At low blow counts (high set per blow), it is difficult for dynamic methods to easily separate the static and dynamic soil resistance effects resulting in a tendency to overpredict the static resistance. Use of a reduced hammer stroke or lower fuel setting can help improve the accuracy of dynamic methods in low blow count situations. At very high blow counts (low set per blow), dynamic test methods tend to produce lower bound nominal resistance estimates as not all of the resistance (particularly at and near the toe) is fully activated. In these high blow count situations, use of a larger hammer stroke, higher fuel setting, pile hammer with a greater rated energy, or variable stroke drop hammer can help improve dynamic method accuracy.

- Understanding that static load testing, dynamic testing with signal matching, wave equation analysis results, and dynamic formula results will give different values of the nominal resistance on the same pile.

  All of the above methods for nominal resistance verification have a different resistance factor, indicating they all differ in reliability. Therefore, it should be surprising if an identical nominal resistance were determined from each method. Driving criteria should be developed using the most reliable of the resistance verification methods available provided that the results from that resistance verification method are checked and appear reasonable.

  In the case of a static load test, the correlating data is only the pile penetration depth, blow count at end of driving, and the associated hammer

stroke. Other tools must therefore be used to determine what other stroke and blow count combinations (the load test stroke and blow count values) are suitable for the required nominal resistance at the same penetration depth (accomplished by refined wave equation analysis) or if the same blow count and stroke are suitable for the nominal resistance at other locations and pile penetration depths (accomplished by a review of subsurface conditions and static analysis). A procedure for calibrating wave equation generated driving criteria to the dynamic testing signal matching results was described in Section 12.6.9. A similar approach may be used to calibrate wave equation based driving criteria to the static load test as described in Section 17.4.

- An understanding of how to perform and evaluate restrike dynamic test results.

  Ideally, the hammer stroke or fuel setting is selected such that the penetration resistance at the beginning of restrike falls between 2 to 3 and 10 blows per inch. In this situation, the test record to select for signal matching analysis is readily apparent. An early, high energy blow, with good data quality should be selected and analyzed for the nominal resistance. The restrike blow count should be carefully recorded over the full restrike event as the rate by which the blow count decreases from inch to inch can be helpful. When the restrike blow count is near or less than 24 blows per foot, a lower energy restrike blow should be chosen for signal matching analysis to reduce the potential for overpredicting the nominal resistance.

  In more difficult situations, limited pile movement may occur during restrike and several records may need to be analyzed with signal matching. Superposition of the activated shaft resistances under various restrike hammer blows may be used to assess the nominal geotechnical resistance. Initial restrike blows may mobilize the shaft resistance along the upper portion of the pile shaft. Later restrike blows may indicate more shaft resistance on the lower portion of the pile once the upper shaft resistance has started to breakdown. The toe resistance and shaft resistance on the lower portion of the pile from the end of drive analysis should also be reviewed and, if appropriate, used in a superposition case. When using the toe resistance from an end of drive situation, the analyst should be confident that relaxation in the bearing layer is not a consideration or overestimation of the nominal resistance could result by using superposition.

- Failure to make timely decision regarding the acceptance of production piles during installation.

The acceptability of production piles must be determined in a timely manner following completion of driving. Delay claims can result if decisions to splice and drive deeper, the need to add piles, or the need to drive replacement piles, cannot be made in a reasonable amount of time.

- Difficulty to accept that, in some cases, dynamic methods of estimating nominal resistance (dynamic formulas, wave equation and dynamic measurements) may yield conservative predictions of the true geotechnical resistance and thus, correlations and extrapolation between dynamic and static load test results are necessary.

  Dynamic methods can yield conservative estimates of the true geotechnical resistance in some situations. For example, an undersized hammer will not be able to mobilize the full soil resistance. Occasionally also, open ended pipe piles or H-piles which do not bear on rock may behave differently under dynamic and static loading conditions. Under dynamic loading conditions, the soil inside a pipe pile or between H-pile flanges may slip and produce internal shaft resistances. Under static loading conditions, this soil may plug and move with the pile resulting in toe resistance over the full pile cross section. Hence both shaft and toe resistances may be different in open profile pile sections under static and dynamic loading conditions. Plugging behavior can also vary in different geomaterials. Careful interpretation and extrapolation of dynamic results is required in these situations. Additional commentary on pile driving of open pile sections is provided in Section 7.10.7.

17.4 EXAMPLES FOR ESTABLISHING DRIVING CRITERIA

The following simplified examples illustrate the considerations necessary to establish both economical and safe installation criteria (a) for 2% dynamic testing or (b) for one static test plus 2% dynamic testing. Various other ways of determining a driving criterion could be envisioned. For example, based on initial testing results, a refined wave equation bearing graph could be established, providing required blow counts for different nominal resistance values. Another example would be performing restrike dynamic testing after all piles had been installed to a wave equation calculated required blow count. That approach may be satisfactory if the bearing layer would be well documented and competent. However, if the final restrike tests would indicate insufficient nominal resistance, the piles would have to be redriven to a greater depth, or additional piles would be necessary, or 100% testing may be

necessary. The latter remedy would then allow for an increased resistance factor and, hopefully make the reduced nominal resistance values acceptable.

17.4.1 Driving Criterion – Example 1

For a small bridge project with less than 100 piles, the foundation designer determined that dynamic testing with signal matching should be used for the nominal resistance verification method and driving criteria. Therefore dynamic testing with signal matching was specified on 2% of the production piles using the AASHTO resistance factor, ϕ_{dyn}, of 0.65. The bridge project involved pile driving at three pier and two abutment locations. Soil borings indicated a relatively uniform site consisting of sandy soils.

All dynamic tests were performed prior to production pile driving began at each substructure location. One pile at each abutment or pier was tested for a total of five test piles. This quantity exceeded the requirement of a minimum of two test piles for the uniform site condition. The factored loads were 117 kips at the abutments and 150 kips at the piers. This meant the required nominal resistance per pile was 117kips / 0.65 or 180 kips at the abutments and 150 kips / 0.65 or 230 kips at the piers. Piles were dynamically tested during initial driving and again during restrike the next day as applicable for the sandy soil conditions. Signal matching was performed on the dynamic test data acquired at the end-of-driving and beginning of restrike for each of the five test piles. A summary of the test results is presented in Table 17-1.

Table 17-1 Example 1 Summary of Requirements and Results

Test Pile Location	Factored Load (kips)	Required Nominal Resistance (kips)	Test Pile Blow Count (bl/ft)	Nominal Resistance from Signal Matching at EOD (kips)	Nominal Resistance from Signal Matching at BOR (kips)	Soil Setup Factor
N Abut.	117	180	40	185	215	1.16
Pier 1	150	230	47	235	275	1.17
Pier 2	150	230	49	240	290	1.21
Pier 3	150	230	50	245	290	1.18
S Abut.	117	180	42	188	215	1.14

At the abutments, the average test pile nominal resistances from signal matching at the end of driving and restrike were 187 and 215 kips respectively; the average

setup factor was, therefore, 1.15. The average driving resistance at the end of driving varied between 40 and 42 blows/ft.

Using the nominal resistances calculated by signal matching, it was conservatively decided that for the production piles, the EOD nominal resistances could be 10% less than the required nominal resistance of 180 kips. The associated required penetration resistance, i.e., the driving criterion, was determined through refined wave equation analysis to be 36 blows/ft. This yielded a 164 kip nominal resistance at end of driving which with setup provided the 180 kip nominal resistance.

At the piers, the average test pile capacity from signal matching at the end of driving and restrike were 240 and 285 kips respectively; the average setup factor was, therefore, 1.19. The average driving resistance at the end of driving varied between 47 and 50 blows/ft.

Using the nominal resistances calculated by signal matching, it was once again conservatively decided that for the production piles, the EOD nominal resistances could be 10% less than the required nominal resistance of 230 kips. The associated required penetration resistance was determined through refined wave equation analysis to be 43 blows/ft. This yielded a 209 kip nominal resistance at end of driving which with setup provided the 230 kip nominal resistance.

Note: The test piles were driven to nominal resistance values in excess of those required, and were, therefore, acceptable as production piles.

17.4.2 Driving Criterion – Example 2

For a relatively small bridge project with two abutments, three piers and less than 120 piles, the foundation designer determined that static load testing and dynamic testing of 2% of the production piles (AASHTO resistance factor ϕ_{dyn}, of 0.80) should be used for the nominal resistance verification method and driving criteria. Therefore a static load test was planned at one pier along with dynamic testing and signal matching on 2% of the production piles. The bridge project involved pile driving at three pier and 2 abutment locations. Subsurface conditions are relatively uniform across the bridge site and consist primarily of medium dense fine sands.

Based on factored loads of 144 kips at the abutments and 184 kips at the piers, the required nominal resistances per pile were 180 kips at the abutments and 230 kips at the piers. The static load test frame and reaction system was set up at a pier

location for a target loading capacity of 230 kips, but with a maximum test load capability of 350 kips.

The static test loading was preceded by dynamically monitoring the installation of first the reaction piles and then the static load test pile. The reaction piles were driven to a penetration depth determined by static analysis as required for their uplift load (350 kips/number of reaction piles) and to a corresponding driving resistance determined by wave equation analysis. The static load test pile was driven to a depth determined by static analysis for the required 230-kip nominal resistance and this was achieved at a final penetration resistance of 60 blows/ft. The load test frame was then constructed and one week after installation, the static load test was performed. This was followed by dynamic restrike tests of the static load test pile and all reaction piles.

The signal matching result at the end of driving on the load test pile indicated a nominal resistance of 220 kips. The static load test evaluated by the Davisson Criterion, failed at a nominal resistance of 260 kips. Signal matching on the restrike dynamic test data indicated a nominal resistance of 290 kips. While this 30 kip difference in nominal resistance between the dynamic test restrike and static load test was likely caused by the preloading of the granular soils by the static load test performed before the restrike, the geotechnical engineer attributed it to a systemic difference between the test methods. For conservatism, a correlation factor of 260 kips / 290 kips or 0.9 was recommended to be applied to all dynamic test results. For the load test pile this meant that the agreed upon EOD nominal resistance was 90% of 220 kips or 198 kips which yielded a soil setup factor of 260 kips / 198 kips or 1.31. The geotechnical engineer also recommended a conservative soil setup factor of 1.2 be used across the relatively uniform site which then required that the piles be driven to EOD nominal resistances confirmed by signal matching of 167 kips (180 kips / (1.2* 0.9) = 167 kips) at the abutments and 212 kips (230 kips / (1.2*0.9) = 212 kips) at the piers.

One production pile in each pier or abutment location was then dynamically tested and analyzed in this manner. When the test pile reached the required EOD nominal resistance, the associated penetration resistance or blow count was established as the driving criterion for the remainder of the production piles at that pier or abutment.

REFERENCES

American Association of State Highway and Transportation Officials (AASHTO). (2014). AASHTO LRFD Bridge Design Specifications, US Customary Units, Seventh Edition, with 2015 Interim Revisions. American Association of State Highway and Transportation Officials, Washington, D.C., 1960 p.

Brown, D.A., and Thompson, W.R. (2011). Developing Production Pile Criteria from Test Pile Data. National Cooperative Highway Research Program (NCHRP) Synthesis 418, Washington, D.C., 54 p.

CHAPTER 18

CONSTRUCTION MONITORING OF PILE INSTALLATION

Knowledgeable construction monitoring and inspection play a critical role in the proper installation of pile foundations. The general trend in cost effective pile foundation design is to use fewer piles each with a higher nominal resistance. This often requires the use of larger pile sections and bigger installation equipment. The construction monitoring of these pile installations becomes critical because of less redundancy (fewer piles required), smaller tolerances, and higher resistance factors.

Construction monitoring is only as good as the knowledge, experience and qualifications of the “inspector”. The role and duties of inspection personnel will vary depending upon the contract delivery method. However, pile inspection is still required for foundation acceptance regardless of how the necessary tasks are contractually assigned. Inspection personnel must understand their role on the project as well as the operation of the hammer and its accessories, the pile behavior, the soil conditions, and how these components interact. Most pile installation problems are avoidable if the inspector uses systematic inspection procedures coupled with good communication and cooperation with the contractor.

The inspector must be more than just a "blow counter". The inspector is the "eyes and ears" for the owner and engineer. Timely observations, suggestions, reporting, and correction advice can ultimately assure the success of the project. The earlier a problem or unusual condition is detected and reported by the inspector, the earlier a solution or correction in procedures can be applied, and hence a potentially negative situation can be limited to a manageable size. If the same problem is left unattended, the number of piles affected increases, as do the cost of remediation and the potential for claims or project delays. Thus, early detection and reporting of any problem may be critical to keep the project on schedule and within budget.

An outline of construction monitoring procedures and maintenance of pile driving records is provided in this chapter. Further details on the inspection of piles and pile driving systems may be found in the Deep Foundations Institute (1995); (1997), provided at the end of the chapter. The FHWA document “Performance of Pile Driving Systems” by Rausche et al. (1986), as well as hammer and equipment manufacturer’s literature are also good sources for information and details on

hammer operation. The Florida Department of Transportation also developed and continues to update an excellent inspection manual for driven pile foundations as part of their inspector training program, Passe (1994). The pile installation monitoring procedures and record keeping methods presented herein should be refined as needed based on the project delivery method and agency practice.

18.1 MONITORING NEEDS BASED ON THE PROJECT DELIVERY METHOD

Transportation projects have historically been designed and constructed using the design-bid-build (DBB) delivery method. Design-Build (DB) and Construction Manager / General Contractor (CMGC) project delivery methods are increasingly being used due to the reduced project development and delivery time associated with these methods. An overview of the key construction monitoring items on driven pile foundations projects and how the typical duties associated with that item vary depending on DBB or DB contract delivery is summarized in Table 18-1. Construction monitoring duties for the driven pile foundations items noted in Table 18-1 for CMGC project delivery contracts may fall under either DBB or DB depending on the individual project.

18.2 ITEMS TO BE MONITORED

Regardless of the project delivery method there are several items to be monitored by the “inspector” on every pile foundation project. These include test piles driven to establish order lengths or for load testing, as well as for production piles. Items to be inspected can be grouped under one of the following areas:

1. Review of the foundation design report, project plans and specifications prior to the arrival at the project site.

2. Inspection of piles prior to installation.

3. Review contractor’s pile installation plan.

4. Inspection of pile driving equipment both before and during operation.

5. Inspection of test or indicator piles installation.

6. Inspection during production pile driving and maintenance of driving records.

Table 18-1 Overview of Key Construction Monitoring and Inspection Items and Agency Inspection Duties on Design-Bid-Build and Design Build Contracts.

Item	Design-Bid-Build	Design-Build
Pile Installation Plan including Hammer Submittal	Review pile installation plan. Perform or review required analyses for hammer approval if hammer approval performed.	Submit DB team pile installation plan to Engineer for conformance check with contract documents and requirements.
Test Pile Installation	Inspect piles, hammer and appurtenances before driving. Inspect and record test pile driving, pile splices, pile alignment, location, and reference elevation.	Observe test pile installation and documentation by others. Communicate any concerns to Engineer.
Nominal Resistance Verification	Perform resistance verification observations (blow count and stroke) or tests (static, dynamic).	Review results of resistance verification method test.
Driving Criteria and Production Pile Order Lengths	Analyze test pile and resistance verification results. Establish driving criteria and determine order lengths.	Review driving criteria established by design-build team.
Production Pile Installation	Inspect piles, inspect pile splices, inspect and record production pile driving, document final alignment, location, and elevations.	Check all piles met the established driving criteria and associated plan requirements.
Foundation Certification	Required documentation completed as part of overall inspection process.	Review foundation certification package from design-build team with Engineer.
Verification Testing	Not applicable.	Select piles for verification testing in coordination with Engineer.
Piling Problems and Resolution	Identify, document, and evaluate any piling problems. Coordinate problem resolution with Engineer, Designer, and Contractor.	Document resolution of any noted deficiencies.

A flow chart identifying the key components of the pile inspection process is presented in Figure 18-1. On DBB projects the Contact Engineer corresponds to the agency engineer. On DB projects, the Contact Engineer is the design-build team foundation engineer of record.

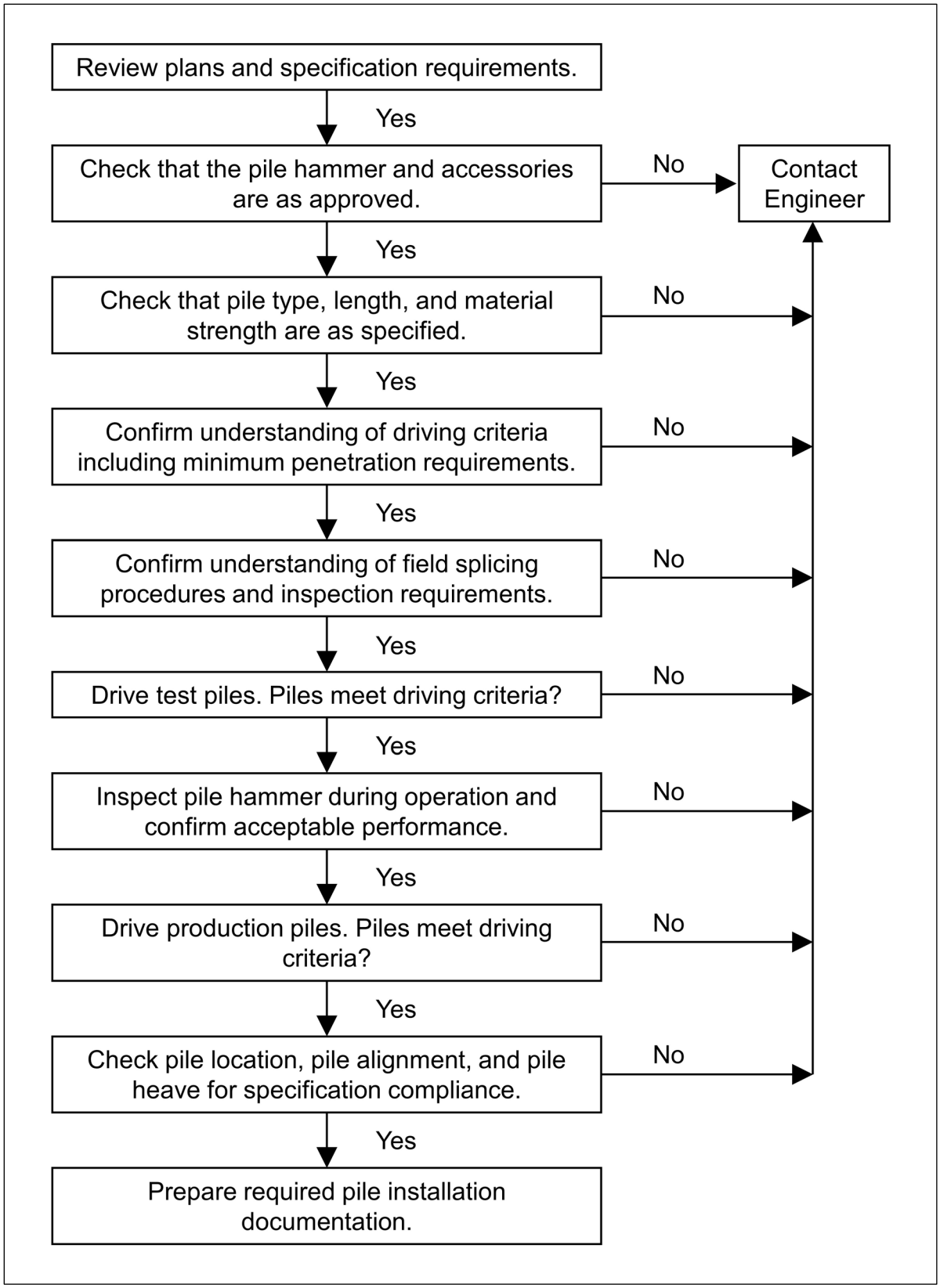

Figure 18-1 Key components of the pile installation inspection process.

18.3 REVIEW OF PROJECT PLANS AND SPECIFICATIONS

The first task in construction monitoring or inspection is to thoroughly review the project plans and specifications as they pertain to pile foundations. All equipment and procedures specified, including any indicator or test program of static and/or dynamic testing, should be clearly understood. If questions arise, clarification should be obtained from the originator of the specifications. The preliminary driving criteria should be known, as well as methods for using the test program results to adjust the criteria to site specific hammer performance and soil conditions. The pile inspector should fully understand the responsibility of his/her organization in the DB or DBB project and should have answers to the following questions:

1. Is the inspector on the project in an observational capacity reporting to the foundation designer?, or

2. Does his/her organization have the direct responsibility to make decisions during driving of the test pile(s) and/or the production piles?

The inspector should also know:

1. Whom to contact if something goes wrong, and/or where to seek advice.

2. Whom to send copies of driving records and daily inspection reports.

3. What is required in the construction monitoring reports during pile driving activities and upon completion of the project.

4. How to inform contractor when work deviates from contract documents without directing contractor's work.

18.4 INSPECTORS TOOLS

The checklist shown in Figure 18-2 is modified from Williams Earth Science (1995) and summarizes the tools a pile inspector should have readily available to perform their job.

Approved Job Information

- ☐ Project Plans and Specifications with Revisions
- ☐ Special Provisions
- ☐ Pile Installation Plan
- ☐ Driving Criteria
- ☐ Casting/Ordered Lengths
- ☐ Approved Splice Detail

Daily Essentials

- ☐ Hard Hat
- ☐ Boots
- ☐ Ear Protection
- ☐ Pen/Pencil (and spare)
- ☐ Scale
- ☐ Measuring Tape
- ☐ Builder's Square
- ☐ Level
- ☐ Watch
- ☐ Calculator
- ☐ Camera

Indexed Notebook of Driven Piles

- ☐ Test Pile Program
- ☐ Production
- ☐ Construction Daily

Blank Forms

- ☐ Pile Driving Log
- ☐ Daily Inspection Reports
- ☐ Personal Diary

References

- ☐ State Standard Specifications
- ☐ Design and Construction of Driven Pile Foundations (FHWA GEC-12)
- ☐ Performance of Pile Driving Systems Inspectors Manual (FHWA/RD-86/160)

Figure 18-2 Key components of the pile installation process (modified from Williams Earth Science 1995).

18.5 INSPECTION OF PILES PRIOR TO AND DURING INSTALLATION

The inspection check list will be different for each type of pile, but some items will be the same. A certificate of compliance for the piles is generally required by the specifications. The inspector should obtain this certificate from the contractor and compare the specification requirements with the information provided on the certificate. The following sections contain specific guidance for each major pile type. Section 18.7 provides similar sections for each major hammer type. A detailed pile driving inspection list for a project can be obtained by combining the check list for that projects pile type in Section 18.5, and hammer type in Section 18.7.

18.5.1 Timber Piles

Physical details for round timber piles are sometimes referred to in the ASTM pile specification, ASTM D25. Regardless of the referenced specifications, the following items should be checked for compliance:

a. The timber should be of the specified species.

b. The piles should have the specified minimum length, and have the correct pile toe and butt sizes. The pile butt must be cut squarely with the pile axis.

c. The twist of spiral grain and the number and distribution of knots should be acceptable.

d. The piles should be acceptably straight.

e. The piles must be pressure treated as specified.

f. The pile butts and/or toe may require banding as detailed in Chapter 16.

g. Steel shoes which may be specified must be properly attached. Details are provided in Chapter 16.

h. Pile splices, if allowed by plans and specifications, must meet the project requirements.

18.5.2 Precast Concrete Piles

On many projects, inspection and supervision of casting operations for precast concrete piles is provided by the transportation agency. Frequently, in lieu of this inspection, a certificate of compliance is required from the contractor. The following checklist provides items to be inspected at the casting yard (when applicable):

a. Geometry and other characteristics of the forms.

b. Dimensions, quantity, and quality of spiral reinforcing and prestressing steel strands, including a certificate indicating that the prestressing steel meets specifications.

c. If the pile is to have mechanical or welded splices, or embedded toe protection, the splice or toe protection connection details including number, size and lengths of dowel bars should be checked for compliance with the approved details and for the required alignment tolerance. They should be cast within tolerance of the true axial alignment.

d. Quality of the concrete (mix, slump, strength, etc.) and curing conditions.

e. Prestressing forces and procedures, including time of tension release, which is related to concrete strength at time of transfer.

f. Handling and storage procedures, including minimum curing time for concrete strength before removal of piles from forms.

The following is a list of items for prestressed concrete piles to be inspected at the construction site:

a. The piles should be of the specified length and section. Many specifications require a minimum waiting period after casting before driving is allowed. Alternatively, the inspector must be assured that a minimum concrete strength has been obtained. If the piles are to be spliced on the site, the splices should meet the specified requirements (type, alignment, etc.).

b. There should be no evidence that any pile has been damaged during shipping to the site, or during unloading of piles at the site. Lifting hooks are generally cast into the piling at pick up points. Piles should be unloaded by properly sized and tensioned slings attached to each lifting hook. Piles should be inspected for cracks or spalling.

c. The piles should be stored properly. When piles are being placed in storage, they should be stored above ground on adequate blocking in a manner which keeps them straight and prevents undue bending stresses.

d. The contractor should lift the piles into the leads properly and safely. Cables looped around the pile are satisfactory for lifting. Chain slings should never be permitted. Cables should be of sufficient strength and be in good condition. Frayed cables are unacceptable and should be replaced. For shorter piles, a single pick-up point may be acceptable. The pick-up point locations should be as specified by the casting yard. For longer piles, two or more pick up points at designated locations may be required.

e. The pile should be free to twist and move laterally in the helmet.

f. Piles should have no noticeable cracks when placed in leads or during installation. Spalling of the concrete at the top or near splices should not be evident.

18.5.3 Steel H-Piles

The following should be inspected at the construction site:

a. The piles should be of the specified steel grade, length, or section/weight.

b. Pile shoes, if required for pile toe protection, should be as specified. Pile shoe details are provided in Chapter 16.

c. Splices should be either proprietary splices or full penetration groove welds as specified. The top and bottom pile sections should be in good alignment before splicing. Pile splice details are discussed in Chapter 16.

d. Pile splices and pile toe attachments must be welded properly.

e. The piles being driven must be oriented with flanges in the correct direction as shown on the plans. Because the lateral resistance to bending of H-piles is considerably more in the direction perpendicular to flanges, the correct orientation of H-piles is very important.

f. There should be no observable pile damage, including deformations at the pile head.

18.5.4 Steel Pipe Piles

The following should be inspected at the construction site:

a. The piles should be of specified steel grade, length, and minimum section/weight (wall thickness) and either seamless or spiral welded as specified.

b. Piles should be driven either open ended or closed ended. Closed-ended pipe piles should have bottom closure plates or conical points of the correct size (diameter and thickness) and be welded on properly, as specified. Open end pipe piles should have cutting shoes that are welded on properly.

c. The top and bottom pile sections should be in good alignment before splicing. Splices or full penetration groove welds should be installed as specified. Pile splice details are discussed in Chapter 16.

d. There should be no observable pile damage, including deformations at the pile head. After installation, closed-end pipes should be visually inspected for damage or water prior to filling with concrete.

18.6 INSPECTION OF DRIVING EQUIPMENT

A typical driving system consists of crane, leads, hammer, hammer cushion, helmet, and in the case of concrete piles, a pile cushion. As discussed in Chapter 15, each component of the drive system has a specific function and plays an important role in the pile installation. The project plans and specifications may specify or restrict certain items of driving equipment. The inspector must check the contractor's driving equipment and obtain necessary information to determine conformity with the plans and specifications prior to the commencement of installation operations.

The following checklist will be useful in the inspection of pile driving equipment before driving:

1. The pile hammer should be the approved make and model as submitted or should meet specification requirements if no submittal is required.

Usually the specifications require certain hammer types and/or specify minimum and/or maximum energy ratings. The inspector should make sure for single acting air/steam hammers that the contractor uses the proper size external power source and that, for adjustable stroke hammers, the stroke necessary for the required energy be obtained. For double acting or differential air/steam, the contractor must again obtain the proper size external power source and the operating pressure and volume must meet the hammer manufacturer's specification. For open end diesel hammers, the inspector should obtain a chart for determining stroke from visual observation, or alternatively have available a device for electronically estimating the stroke from the blow rate. For closed end diesel hammers, the contractor should supply the inspector with a calibration certificate for the bounce chamber pressure gauge and a chart which correlates the bounce chamber pressure with the energy developed by the hammer. The bounce chamber pressure gauge should be provided by the contractor. For single acting and double acting hydraulic hammers, the contractor should supply a system for measuring and displaying the hammer energy or impact velocity.

2. The hammer cushion being used should be checked to confirm it is of the approved material type, size and thickness.

The main function of the hammer cushion is to protect the hammer itself from fatigue and high frequency accelerations which would result from steel to steel impact with the helmet and/or pile. The hammer cushion should have the proper material and same shape/area to snugly fit inside the helmet (drive cap). If the cushion diameter is too small, the cushion will break or badly deform during hammer blows and become ineffective. The hammer cushion must not be excessively deformed or compressed. Some air/steam hammers rely upon a certain total thickness (of cushion plus striker plate) for proper valve timing. Hammers with incorrect hammer cushion thickness may not operate, or will have improper kinetic energy at impact. Since it is difficult to inspect this item once the driving operation begins, it should be checked before the contractor starts pile driving on a project as well as periodically during production driving on larger projects. A photograph of a hammer cushion ready for inspection prior to insertion into the helmet is presented in Figure 18-3. The Blue Nylon hammer cushion disks are shown in the lower right corner of the photograph. The hammer cushion thickness and diameter, the diameter of the helmet cushion pot, as well as the dimensions of the striker plate should all be measured by the inspector during a hammer cushion inspection. A damaged aluminum plate, found during a cushion check of an aluminum and micarta hammer cushion, is displayed on the left hand side of Figure 18-4.

3. The helmet (drive cap) should properly fit the pile.

The purpose of the helmet is to hold the pile head in alignment and transfer the impact concentrically from the hammer to the pile. The helmet also houses the hammer cushion, and must accommodate the pile cushion thickness for concrete piles. The helmet should fit loosely to avoid transmission of torsion or bending forces, but not so loosely as to prevent the proper alignment of hammer and pile. Helmets should ideally be of roughly similar size to the pile diameter. Although generally discouraged, spacers may be used to adapt an oversize helmet, provided the pile will still be held concentrically with the hammer. A properly fitting helmet is important for all pile types, but is particularly critical for precast concrete piles. A poorly fitting helmet often results in pile head damage. Check and record the helmet weight for conformance to wave equation analysis or for future wave equation analysis. Larger weights will reduce the energy transfer to the pile.

Figure 18-3 Check of Blue Nylon hammer cushion material before use.

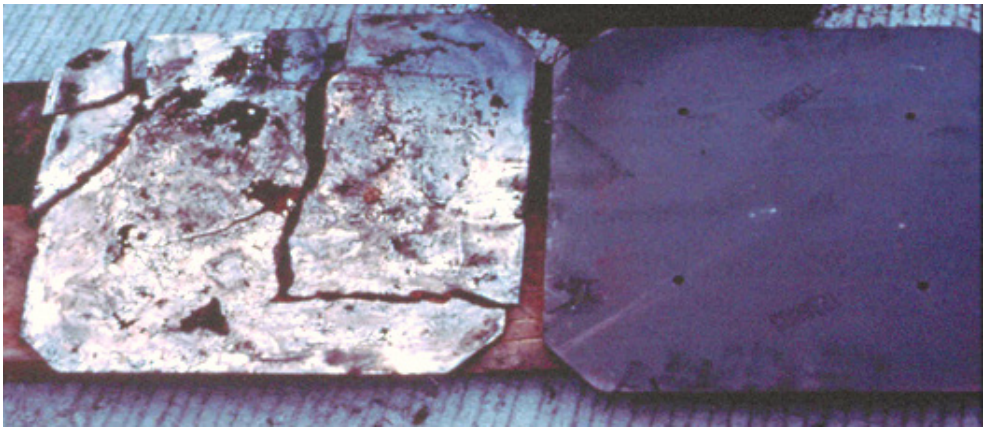

Figure 18-4 Damaged aluminum and micarta hammer cushion.

4. The pile cushion should be of correct type material and thickness for concrete piles.

The purpose of the pile cushion is to reduce high compression stresses, to evenly distribute the applied forces to protect the concrete pile head from damage, and to reduce the tension stresses in easy driving. Pile cushions for concrete piles should have the required thickness determined from a wave equation analysis but not less than 4 inches. A new plywood, hardwood, or composite wood pile cushion, which is not water soaked, should be used for every pile. In Figure 18-5, a new, 22 inch thick plywood pile cushion is being inserted into a helmet. The helmet with pile cushion inserted is shown in Figure 18-6. Note that after cushion insertion, minimal depth remains in the helmet to accommodate and adequately restrain the pile head.

Figure 18-5 New pile cushion being inserted into helmet.

Figure 18-6 Helmet with new pile cushion installed.

The cushion material should be checked periodically for damage and replaced before excessive compression (more than half the original thickness), burning, or charring occurs. Wood cushions may take only about 1,000 to 2,000 blows before they deteriorate. During hard driving, more than one cushion may be necessary for a single pile. Longer piles or piles driven with larger hammers may require thicker pile cushions.

5. Predrilling, jetting or spudding equipment, if specified or permitted, should be available for use and meet the requirements.

The depth of predrilling, jetting or spudding should be very carefully controlled so that it does not exceed the allowable limits. Predrilling, jetting, or spudding below the allowed depths will generally result in a reduced nominal geotechnical resistance, and the pile acceptance may become questionable. Additional details on predrilling, jetting, and spudding equipment are presented in Chapter 15.

6. The lead system being used must conform to the requirements, if any, in the specifications. Lead system details are discussed in detail in Chapter 15.

The leads perform the very important function of holding the hammer and pile in good alignment with each other. Poor alignment reduces energy transfer as some energy is then imparted into horizontal motion. Poor alignment also generally results in higher bending stresses and higher local contact stresses which can cause pile damage. This is particularly important at end of driving when blow counts are highest and driving stresses are generally increased. Sometimes the specifications do not allow certain lead systems or may require a certain type system. A pile gate at the lead bottom which properly centers the pile should be required, as it helps maintain good alignment.

Note: On many projects, a wave equation analysis is used to determine preliminary driving criteria for design and/or construction control. The contractor is usually required to provide a pile and driving equipment data form similar to Figure 15-50 and obtain prior approval from the agency. Even if wave equation analysis is not required, this form should be included in the project files so a wave equation analysis could be performed in the future. This form can also function as a check list for the inspector to compare the proposed equipment with the actual equipment on-site.

18.7 INSPECTION OF DRIVING EQUIPMENT DURING INSTALLATION

The main purpose of construction monitoring and inspection is to assure that piles are installed so that they meet the driving criteria and are undamaged. Driving criteria are often defined, in part, by a minimum pile penetration resistance or blow count that is measured in blows per foot or blows per inch. Driving criteria assure that piles have the required nominal resistance. The blow count, however, is dependent upon the performance of the pile driving hammer. The blow count will generally be lower when the hammer imparts higher energy and force to the pile, while the blow count will be higher if the hammer imparts lower energy and force to the pile. High blow counts can be due either to soil resistance or to a poorly

performing hammer. Thus, the inspector must evaluate if the hammer is performing properly to assure that the driving criteria has been met and therefore the nominal resistance is achieved.

Each hammer has its own operating characteristics; the inspector should not blindly assume that the hammer on the project is in good working condition. Two different types of hammers with identical manufacturer's rated energy will not drive the same pile in the same soil with the same blow count. In fact, two supposedly identical hammers (same make and model) may not have similar driving capability due to several factors including differing friction losses, valve timing, air supply hose type-length-condition, fuel type and intake amount, ring condition, and other maintenance status items. The inspector should become familiar with the proper operation of the hammer(s) used on site. The inspector may wish to contact the hammer manufacturer or supplier who generally will welcome the opportunity to supply further information. The inspector should review the operating characteristics for the hammer which are included in Chapter 15. The following checklists briefly summarize key hammer inspection issues.

18.7.1 Drop Hammers

a. Determine/confirm the ram weight. Ram weight can be calculated from the ram volume and steel density of 492 lb/ft^3 if necessary.

b. The leads should have sufficient tolerance and/or the guides greased to allow the ram to fall without obstruction or binding.

c. Make sure the desired stroke is maintained. Low strokes will reduce energy. Excessively high strokes increase pile stresses and could cause pile damage.

d. Make sure the helmet stays properly seated on the pile and that the hammer and pile maintain alignment during operation.

e. Make sure the hammer hoist line is spooling out freely during the drop and at impact. If the hoist line drags, less energy will be delivered. If the crane operator catches the ram too early, not only is less energy delivered, but energy is transmitted into the hoist line, crane boom, and hoist, which could cause maintenance and/or safety problems.

18.7.2 Single Acting Air/Steam Hammers

a. Determine/confirm the ram weight. Ram weight can be calculated from the ram volume and steel density of 492 lb/ft^3 if necessary. Check for and record any identifying labels as to hammer make, model and serial number.

b. Check the air or steam supply and confirm it is of adequate capacity to provide the required pressure and flow volume. Also check the number, length, diameter, and condition of the air/steam hoses. Manufacturers provide guidelines for proper compressors and supply hoses. Air should be blown through the hose before attaching it to the hammer. The motive fluid lubricator should occasionally be filled with the appropriate lubricant as specified by the manufacturer. During operation, check that the pressure at the compressor or boiler is equal to the rated pressure plus hose losses. The pressure should not vary significantly during driving. The photograph of an air compressor display panel in Figure 18-7 illustrates the discharge pressure dial that should be checked.

c. Visually inspect the slide bar and its cams for excessive wear. Some hammers can be equipped with a slide bar with dual set of cams to offer two different strokes. The stroke can be changed with a valve, usually operated from the ground. Measure the stroke being attained and confirm it meets specification.

d. Check that the columns or ram guides, piston rod, and slide bar are well greased.

e. For most air/steam hammers, the total thickness of hammer cushion and striker plate must match the hammer manufacturer's recommendation and the hammer cushion cavity in the helmet for proper valve timing and hammer operation. This thickness must be maintained and should be checked before placing the helmet into the leads, and thereafter by comparison of cam to valve position and/or gap between ram and hammer base when the ram is at rest on the pile top.

Figure 18-7 Air compressor display panel.

f. Make sure the helmet stays properly seated on the pile and that the hammer and pile maintain alignment during operation.

g. The ram and column keys used to fasten together hammer components should all be tight.

h. The hammer hoist line should always be slack, with the hammer's weight fully carried by the pile. Excessive tension in the hammer hoist line is a safety hazard and will reduce energy to the pile. Leads should always be used.

i. Compare the observed hammer speed in blows per minute near end of driving with the manufacturer's specifications. Blows per minute can be timed with a stopwatch or a saximeter. Slower operating rates may imply a short stroke (from inadequate pressure or volume, restricted or undersized hose, or inadequate lubrication) or improper valve timing (possibly from incorrect cushion thickness or worn parts). Erratic hammer operation, such as skipping

blows, can result from improper cushion thickness, poor lubrication, foreign material in a valve, faulty valve/cam system, or loose hammer fasteners or keys.

j. As the blow count increases, the ram stroke may also increase, causing it to strike the upper hammer assembly and lifting the hammer ("racking") from the pile. If this behavior is detected, the air pressure flow should be reduced gradually until racking stops. The flow should not be overly restricted so that the stroke is reduced.

k. Some manufacturers void their warranty if the hammer is consistently operated above 10 blows per inch of penetration beyond short periods such as required when toe bearing piles are driven to rock. Therefore, in prolonged hard driving situations, it may be more desirable to use a larger hammer or stiffer pile section.

l. Common problems and problem indicators for air/steam hammers are summarized in Table 18-2.

An inspection form for single and differential acting air/steam hammers is provided in Figure 18-8. The primary feature of this form is the three column area in the middle of the form. The left column illustrates the key objects of the driving system. The middle column contains the manufacturer's requirements for key objects and the right column is used to record the observed condition of those objects. This format allows the inspector to quickly identify potential problems and an immediate correction may be possible. The hammer inspection form is intended to be used periodically during the course of the project as a complement to the pile driving log.

The bottom portion of the hammer inspection form contains an area where observations at final driving should be recorded. This information may be particularly interesting to an engineer who has performed a wave equation analysis as the actual situation can then be compared to the analyzed one. Therefore, it is recommended that a copy of the completed hammer inspection form be provided to appropriate design and construction personnel.

Table 18-2 Common Problems and Indicators for Air/Steam Hammers
(after Williams Earth Sciences 1995)

Common Problems	Indicators
Air trip mechanism on hammer malfunctioning.	Erratic operation rates or air valve sticking open or close.
Cushion stack height not correct (affects timing of trip mechanism air valve).	Erratic operation rates.
Compressor not supplying correct pressure and volume of air to hammer.	Blows per minute rate is varying either faster or slower than the manufacturer specified.
Air supply line kinked or tangled in leads, boom or other.	Visually evident.
Moisture in air ices up hammer.	Ice crystals exiting exhaust ports of hammer.
Lack of lubricant in air supply lines.	Erratic operation rates.
Packing around air chest worn, allowing air blow by.	Ram raises slowly - blows per minute rate slower than manufacturer specifications - air leaking around piston shaft and air chest.
Nylon slide bar worn.	Visually evident.
Ram columns not sufficiently greased.	Visually evident.

Project/Pile: _____ Hammer Name _____

Date: _____ Serial No. _____

Conditions: _____

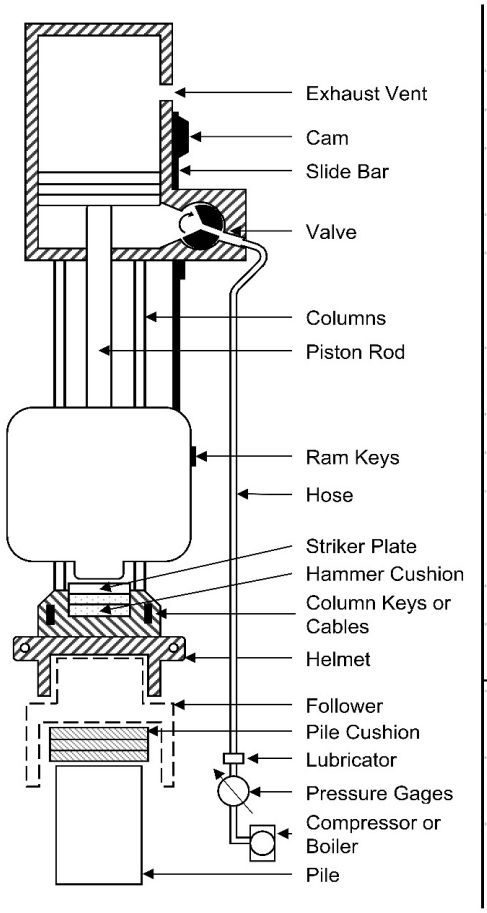

Object	Requirements	Observations
	Slide Bars/ Cams Greased? Tight?	Yes / No Remarks _____
	Columns Greased?	Yes / No
	Ram Keys Tight?	Yes / No
	Hose	I.D. Size _____ Length _____ Leaks? _____ Obstructions? _____
	Striker Plate	t= _____ D= _____
	Hammer Cushion	t= _____ D= _____ Material _____ How long in use? _____
	Column Keys or Cables Tight?	Yes / No
	Helmet	Type or Weight? _____
	Follower?	Yes / No Type? _____
	Pile Cushion	Material _____ t= _____ Size _____ How long in use? _____
	Lubricator Filled	Yes / No
	Pressure at Hammer _____ psi	Measured _____ psi at _____ feet from Hammer
	Fluctuating During Driving?	Yes / No How much? _____
	Check Compressor and Boiler?	Size _____ ft^3/min Make _____
	Pile	Material _____ Length _____ Size _____ Batter _____

Manufacturer's Hammer Data

Ram Weight _____

Max Stroke _____

Rated Energy _____

Blows/min in Hard Driving _____

Attached Saximeter Printout

Observation when Bearing is Confirmed

Full Ram Stroke _____ Yes/No _____ %

Blows/min _____ Blows/ft _____

High Pile Rebound? Yes/No

Pile Whipping? Yes/No

Pile- Hammer Alignment Front/Back ___ Sides ___

Crane Size and Make _____

Lead Type _____

Hammer Lead Guides Lubricated Yes/No

Piston Rod Lubricated _____

Exhaust Description _____

Freezing? Condensing?

Lubricant Apparent?

Figure 18-8 Inspector's form for single and differential acting air/steam hammers.

18.7.3 Double Acting or Differential Air/ Steam Hammers

a. Determine/confirm the ram weight. Ram weight can be calculated from the ram volume and steel density of 492 lbs/ft^3 if necessary. Check for and record any identifying labels as to hammer make, model and serial number.

b. Check the air or steam supply and confirm it is of adequate capacity to provide the required pressure and flow volume. This is extremely important since approximately half the rated energy comes from the pressure on the ram during the downstroke. Check also the number, length, diameter, and condition of the air/steam hoses. Manufacturers provide guidelines for proper compressors and supply hoses. Air should be blown through the hose before attaching it to the hammer. The motive fluid lubricator should occasionally be filled with the appropriate lubricant as specified by the manufacturer. During operation, check that the pressure at the compressor or boiler is equal to the rated pressure plus hose losses. The pressure should not vary significantly during driving. Record the pressure at the beginning of driving.

c. Visually inspect the slide bar and its cams for excessive wear. Measure the stroke being attained and confirm that it meets specification.

d. Check that the columns or ram guides, piston rod, and slide bar are well greased.

e. For most air/steam hammers, the total thickness of hammer cushion and striker plate must match the hammer manufacturer's recommendation and the hammer cushion cavity in the helmet for proper valve timing and hammer operation. This thickness must be maintained, and can be checked before assembly of the helmet into the leads, and thereafter by comparison of cam to valve position and/or gap between ram and hammer base when the ram is at rest on the pile.

f. Make sure the helmet stays properly seated on the pile and that the hammer and pile maintain alignment during operation.

g. The ram and column keys used to fasten together hammer components should all be tight.

h. The hammer hoist line should always be slack with the hammer's weight and be fully carried by the pile. Excessive tension in the hammer hoist line is a

safety hazard and will reduce energy to the pile. Leads should always be used.

i. Compare the observed hammer speed in blows per minute near end of driving with the manufacturer's specifications. Blows per minute can be timed with a stopwatch or a saximeter. Slower operating rates may imply a short stroke (from inadequate pressure or volume, restricted or undersized hose, or inadequate lubrication) or improper valve timing (possibly from incorrect cushion thickness or worn parts). Erratic hammer operation, such as skipping blows, can result from improper cushion thickness, poor lubrication, foreign material in a valve, faulty valve/cam system, or loose hammer fasteners or keys.

j. As the penetration resistance increases, the ram stroke may also increase, causing it to strike the upper hammer assembly and lifting the hammer (racking) from the pile. If this behavior is detected, the pressure flow should be reduced gradually until racking stops. This will result in a reduction in energy since the pressure also acts during the downstroke, thereby contributing to the rated energy. Record the final pressure. The flow should not be overly restricted so that the stroke is also reduced, causing a further reduction in energy. For optimum performance, the pressure flow should be kept as full as possible so that the hammer lift-off is imminent.

k. Some manufacturers void their warranty if the hammer is consistently operated above 10 blows per inch of penetration beyond short periods such as required when toe bearing piles are driven to rock. Therefore, in prolonged hard driving situations, it may be more desirable to use a larger hammer or stiffer pile section.

l. Record the final pressure and compare with manufacturer's energy rating at this pressure.

m. Common problems and problem indicators for air/steam hammers are summarized in Table 18-2.

An inspection form for enclosed double acting air/steam hammers is provided in Figure 18-9. The primary feature of this form is the three column area in the middle of the form. The left column identifies key objects of the driving system. The middle column contains the manufacturer's requirements for key objects and the right column is used to record the observed condition of those objects. This format allows

Project/Pile: _____ Hammer Name _____

Date: _____ Serial No. _____

Conditions: _____

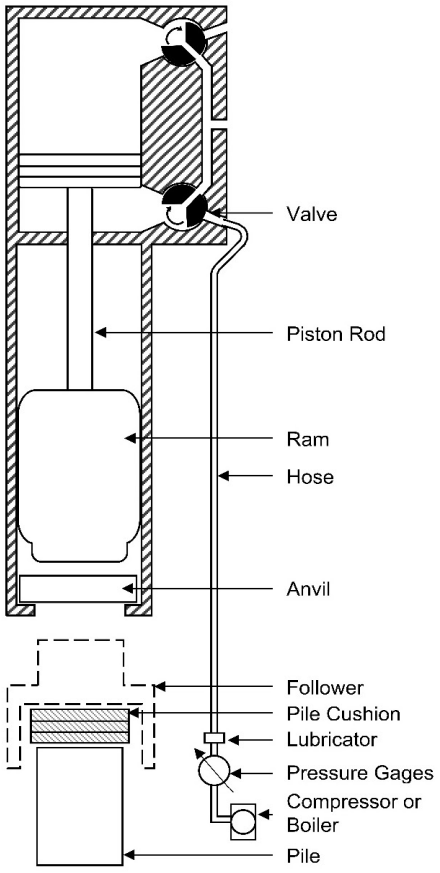

Object	Requirements	Observations
	Striker Plate	t= _____ D= _____
	Hammer Cushion	t= _____ D= _____ Material _____ How long in use? _____
	Helmet	Type or Weight? _____
	Follower	Yes / No Type? _____
	Pile Cushion	Material _____ t= _____ Size _____ How long in use? _____
	Hose	I.D. Size _____ Length _____ Leaks? Obstructions?
	Lubricator Filled	Yes / No
	Pressure at Hammer _____ psi	Measured _____ psi at _____ feet from Hammer
	Fluctuating During Driving?	Yes / No How much? _____
	Check Compressor and Boiler?	Size _____ ft^3/min Make _____
	Pile	Material _____ Length _____ Size _____ Batter _____

Manufacturer's Hammer Data

Ram Weight _____

Max Stroke _____

Rated Energy _____

Blows/min in Hard Driving _____

Attached Saximeter Printout

Observation when Bearing is Confirmed

Full Ram Stroke Yes/No _____ %

Blows/min _____ Blows/ft _____

High Pile Rebound? Yes/No Pile Whipping? Yes/No

Pile- Hammer Alignment Front/Back ___ Sides ___

Crane Size and Make _____

Lead Type _____

Hammer Lead Guides Lubricated Yes/No

Piston Rod Lubricated _____

Exhaust Description Freezing? Condensing?

Lubricant Apparent?

Figure 18-9 Inspector's form for enclosed double acting air/steam hammers.

the inspector to quickly identify potential problems and an immediate correction may be possible. The hammer inspection form is intended to be used periodically during the course of a project as a complement to the pile driving log.

The bottom portion of the hammer inspection form contains an area where observations at final driving should be recorded. This information may be particularly interesting to an engineer who has performed a wave equation analysis as the actual situation can then be compared to the analyzed one. Therefore, it is recommended that a copy of the completed hammer inspection form be provided to appropriate design and construction personnel.

18.7.4 Single Acting Diesel Hammers

a. Determine/confirm that the hammer is the correct make and model. Check for and record any identifying labels as to hammer make, model and serial number.

b. Make sure all exhaust ports are open with all plugs removed.

c. Inspect the recoil dampener for condition and thickness. If this is excessively worn or of an improper thickness (consult manufacturer) it should be replaced. If the recoil dampener is too thin, the stroke will be reduced. Conversely, if it is too thick, or if cylinder does not rest on the dampener between blows, the ram could blow out the hammer top and become a safety hazard.

d. Check that lubrication of all grease nipples is regularly made. Most manufacturers recommend the impact block be greased every half hour of operation.

e. As the ram is visible between blows, check the ram for signs of uniform lubrication and ram rotation. Poor lubrication will increase friction and reduce energy to the pile.

f. Determine the hammer stroke, especially at end of driving or beginning of restrike. A "jump stick" attached to the cylinder is a safety hazard and should not be used. The stroke can be determined by a saximeter which measures the time between blows and then calculates the stroke. The ram stroke

height, h, can also be calculated from this formula using the number of blows per minute (bpm) recorded:

$$h = 4.01\left(\frac{60}{bpm}\right)^2 - 0.3 \qquad \text{Eq. 18-1}$$

Where:

h = ram stroke (feet).

bpm = blow per minute (dimensionless).

The calculated stroke may require correction for batter or inclined piles. The inspector should always observe the ram rings and visually estimate the stroke using the manufacturer's chart.

g. As the blow count increases, the stroke should also increase. At the end of driving, if the ram fails to achieve the correct stroke (part of the driving criteria from a wave equation analysis), the cause could be lack of fuel. Most hammers have adjustable fuel pumps. Some have distinct fuel settings as shown in Figure 18-10(a), others are continuously variable as shown in Figure 18-10(b), and some use a pressure pump as shown in Figure 18-11. Make sure the pump is on the correct fuel setting or pressure necessary to develop the required stroke. The fuel and fuel line should be free of dirt or other contaminants. A clogged or defective fuel injector will also reduce the stroke and should be replaced if needed.

h. Low strokes could be due to poor compression caused by worn or defective piston or anvil rings. Check compression by raising the ram, and with the fuel turned off, allowing the ram to fall. The ram should bounce several times if the piston and anvil rings are satisfactory.

i. Watch for signs of pre-ignition. When a hammer preignites, the fuel burns before impact, requiring extra energy to compress gas and leaving less energy to transfer to the pile. In long sustained periods of driving, or if the wrong fuel with a low flash point is used, the hammer could overheat and preignite. When pre-ignition occurs, less energy is transferred and the blow count rises, giving a false indication of high nominal resistance. If piles driven with a cold hammer drive deeper or with less hammer blows, or if the blow count decreases after short breaks, pre-ignition could be the cause and should be investigated. Dynamic testing is the preferable method to check for pre-ignition.

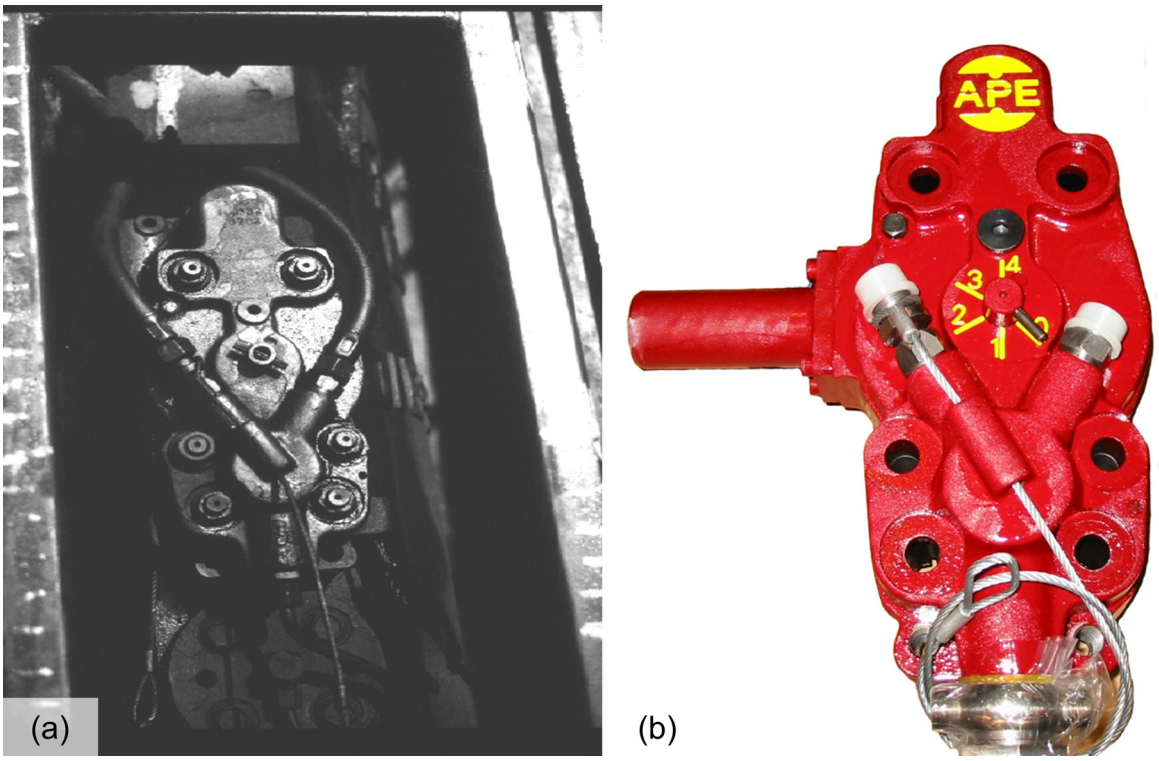

Figure 18-10 Fuel Pumps: (a) fixed four step pump and (b) variable fuel pump.

Figure 18-11 Hydraulic pump for fuel pump adjustments.

j. For some diesel hammers, the total thickness of hammer cushion and striker plate must match the hammer manufacturer's recommendation and the hammer cushion cavity in the helmet for proper fuel injection and hammer operation. This total thickness must be maintained.

k. Make sure the helmet stays properly seated on the pile and that the hammer and pile maintain alignment during operation.

l. The hammer hoist line should always be slack, with the hammer's weight fully carried by the pile. Excessive tension in the hammer hoist line is a safety hazard and will reduce energy to the pile. Leads should always be used.

m. Some manufacturers void their warranty if the hammer is consistently operated above 10 blows per inch of penetration beyond short periods, such as those required when toe bearing piles are driven to rock. Therefore, in prolonged hard driving situations, it may be more desirable to use a larger hammer or stiffer pile section.

n. Common problems and problem indicators for single acting diesel hammers are presented in Table 18-3.

An inspection form for single acting diesel hammers is provided in Figure 18-12. The primary feature of this form is the three column area in the middle of the form. The left column identifies key objects of the driving system, the middle column contains the manufacturer's requirements for that object and the right column is used to record the observed condition of that object. This format allows the inspector to quickly identify potential problems and an immediate correction may be possible. The hammer inspection form is intended to be used periodically during the course of a project as a complement to the pile driving log.

The bottom portion of the hammer inspection form contains an area where observations at final driving should be recorded. This information may be particularly interesting to an engineer who has performed a wave equation analysis as the actual situation can then be compared to the analyzed one. Therefore, it is recommended that a copy of the completed hammer inspection form be provided to appropriate design and construction personnel.

Project/Pile: _____ Hammer Name _____

Date: _____ Serial No. _____

Conditions: _____

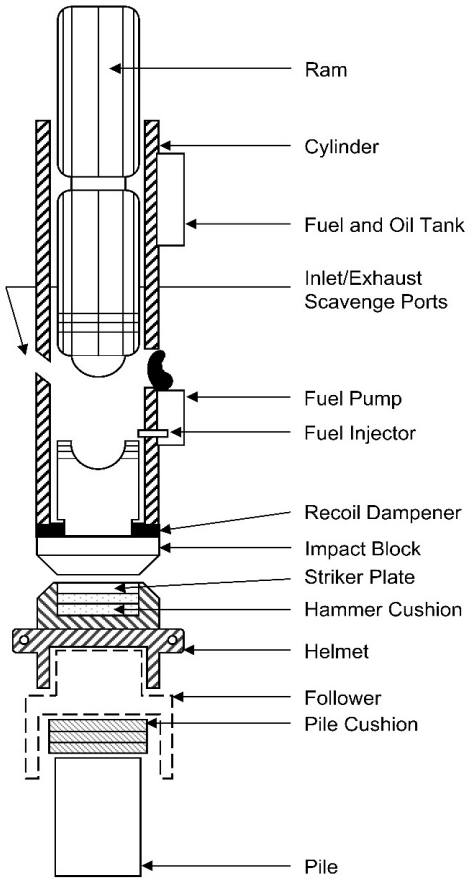

Object	Requirements	Observations
	Ram Lubricated	Yes / No
	Fuel Tank Filled with Type II Diesel?	Yes / No Type _____
	Exhaust Ports Open?	Yes / No
	Fuel Pump	Hammer Setting _____
	Recoil Dampener Undamaged?	Yes / No
	Impact Block Lubricated?	Yes / No
	Striker Plate	t= _____ D= _____
	Hammer Cushion	t= _____ D= _____ Material _____ How long in use? _____
	Helmet	Type or Weight? _____
	Follower?	Yes / No Type? _____
	Pile Cushion	Material _____ t= _____ Size _____ How long in use? _____
	Pile	Material _____ Length _____ Size _____ Batter _____

Manufacturer's Hammer Data

Ram Weight _____

Hammer Setting	Rated Energy ft-kips	Rated Stroke, feet
min		
max		

Attached Saximeter Printout

Observation when Bearing is Confirmed

Excessive Cylinder Rebound? Yes/No

High Pile Rebound? Yes/No

Pile Whipping? Yes/No

Pile- Hammer Alignment Front/Back _____ Sides _____

Crane Size and Make _____

Lead Type _____

Hammer Lead Guides Lubricated? Yes/No

Color of Smoke _____

Steel to Steel Impact Sound _____

Figure 18-12 Inspector's form for single acting diesel hammers.

Table 18-3 Common Problems and Indicators for Single Acting Diesel Hammers (after Williams Earth Sciences 1995)

Common Problems	Indicators
Water in fuel.	Hollow sound, white smoke.
Fuel lines clogged.	No smoke or little gray smoke.
Fuel pump malfunctioning.	Inconsistent ram strokes, little gray smoke or black smoke.
Fuel injectors malfunctioning.	Inconsistent ram strokes, little gray smoke or black smoke.
Oil low.	Blows per minute rate is lower than specified.
Oil pump malfunctioning.	Blows per minute rate is lower than specified.
Water in combustion chamber.	Hollow sound, white smoke.
Piston rings worn.	Low strokes.
Tripping device broken.	Pawl or pin used to lift piston does not engage piston. Pawl engages but does not lift piston.
Over heating.	Paint and oil on cooling fins start to burn/sound changes.

18.7.5 Double Acting Diesel Hammers

a. Determine/confirm that the hammer is the correct make and model. Check for and record any identifying labels as to hammer make, model and serial number.

b. Make sure all exhaust ports are open with all plugs removed.

c. Inspect the recoil dampener for condition and thickness. If excessively worn or of improper thickness (consult manufacturer), it should be replaced. If it is too thin, the stroke will be reduced. If it is too thick or if cylinder does not rest on dampener between blows, the ram will cause hammer lift-off.

d. Check that lubrication of all grease nipples is regularly made. Most manufacturers recommend the impact block be greased every half hour of operation.

e. After the hammer is stopped, check the ram for signs of lubrication by looking into the exhaust port or trip slot. Poor lubrication increases friction, thus reducing energy to the pile.

f. Always measure the bounce chamber pressure, especially at end of driving or restrike. This indirectly measures the equivalent stroke or energy. All double acting diesels have a gauge. On most hammers an external gauge is connected by a hose to the bounce chamber. A photograph of a typical external bounce chamber pressure gauge is presented in Figure 18-13. The manufacturer should supply a chart relating the bounce chamber pressure for a specific hose size/length to the rated energy. The inspector should compare measured bounce chamber pressure with the manufacturer's chart to estimate the energy. The bounce chamber pressure measured may require correction for batter or inclined piles.

g. As the penetration resistance increases, the stroke and bounce chamber pressure should also increase. If the ram fails to achieve the correct stroke or bounce chamber pressure (part of the driving criteria from a wave equation analysis) at final driving, the cause could be lack of fuel. All these hammers have continuously variable fuel pumps. Check that the fuel pump is on the correct fuel setting. The fuel should be free of dirt or other contaminants. A clogged or defective fuel injector reduces the stroke.

h. In hard driving, high strokes cause high bounce chamber pressures. If the cylinder weight cannot balance the bounce chamber pressure, the hammer will lift-off of the pile and the operator must reduce the fuel to prevent this unstable racking behavior. Ideally it is set and maintained so that lift-off is imminent. The bounce chamber pressure gauge reading should correspond to the hammer's maximum bounce chamber pressure for the hose length used when lift-off is imminent. If not, then the bounce chamber pressure gauge is out of calibration and should be replaced, or the bounce chamber pressure tank needs to be drained.

i. Low strokes indicated by a low bounce chamber pressure could be due to poor compression caused by worn or defective piston or anvil rings. Check compression with the fuel turned off by allowing the ram to fall. The ram should bounce several times if the piston and anvil rings are satisfactory.

Figure 18-13 Typical external bounce chamber pressure gauge.

j. Watch for pre-ignition. When a hammer preignites, the fuel burns before impact requiring extra energy to compress the gas and reducing energy transferred to the pile. When pre-ignition occurs, the blow count increases giving a false indication of high nominal resistance. In long sustained periods of driving or if low flash point fuel is used, the hammer could overheat and preignite. If piles driven with a cold hammer drive deeper or with fewer hammer blows, or if the blow count decreases after short breaks, investigate for pre-ignition, preferably with dynamic testing.

k. For some diesel hammers, the total thickness of the hammer cushion and striker plate must match the manufacturer's recommendation for proper fuel injection timing and hammer operation. This total thickness must be maintained.

l. Make sure the helmet stays properly seated on the pile and that the hammer and pile maintain alignment during operation.

m. The hammer hoist line should always be slack, with the hammer's weight fully carried by the pile. Excessive tension in the hammer hoist line is a safety hazard and will reduce energy to the pile. Leads should always be used.

n. Some manufacturers void their warranty if the hammer is consistently operated above 10 blows per inch of penetration beyond short periods such as those required when toe bearing piles are driven to rock. Therefore, in prolonged hard driving situations, it may be more desirable to use a larger hammer or stiffer pile section.

o. Common problems and problem indicators for double acting diesel hammers are presented in Table 18-4.

An inspection form for double acting diesel hammers is provided in Figure 18-14. The primary feature of this form is the three column area in the middle of the form. The left column identifies key objects of the driving system, the middle column contains the manufacturer's requirements for that object and the right column is used to record the observed condition of that object. This format allows the inspector to quickly identify potential problems and an immediate correction may be possible. The hammer inspection form is intended to be used periodically during the course of a project as a complement to the pile driving log.

The bottom portion of the hammer inspection form contains an area where observations at final driving should be recorded. This information may be particularly interesting to an engineer who has performed a wave equation analysis as the actual situation can then be compared to the analyzed one. Therefore, it is recommended that a copy of the completed hammer inspection form be provided to appropriate design and construction personnel.

Table 18-4 Common Problems and Indicators for Double Acting Diesel Hammers (after Williams Earth Sciences 1995)

Common Problems	Indicators
Water in fuel.	Hollow sound, white smoke.
Fuel lines clogged.	No smoke or little gray smoke.
Fuel pump malfunctioning.	Inconsistent ram strokes, little gray smoke or black smoke.
Fuel injectors malfunctioning.	Inconsistent ram strokes, little gray smoke or black smoke.
Oil low.	Blows per minute rate is lower than specified.
Oil pump malfunctioning.	Blows per minute rate is lower than specified.
Build-up of oil in bounce chamber.	Not visible from exterior.
Water in combustion chamber.	Hollow sound, white smoke.
Piston rings worn.	Low strokes.
Tripping device broken.	Pawl or pin used to lift piston does not engage piston. Pawl engages but does not lift piston.
Over heating.	Paint and oil on cooling fins start to burn/ sound changes.

Project/Pile: _____ Hammer Name _____

Date: _____ Serial No. _____

Conditions: _____

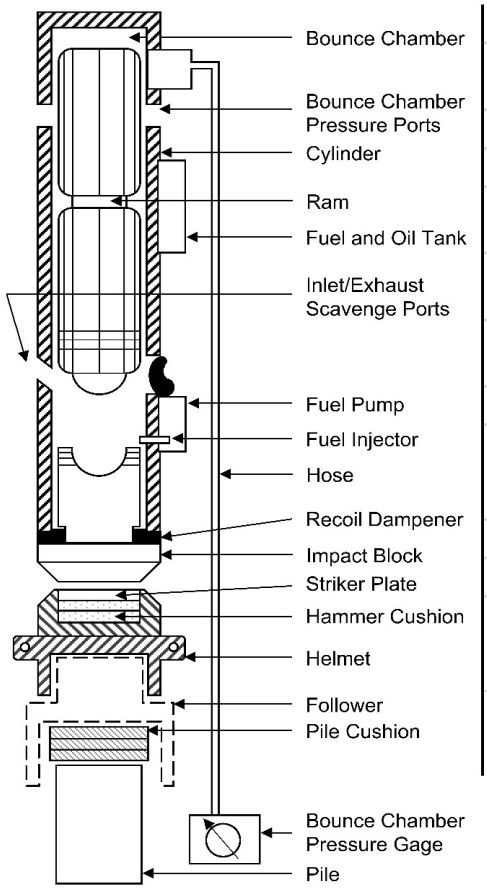

Object	Requirements	Observations
	Ram Lubricated?	Yes / No
	Fuel Tank Filled with Type II Diesel?	Yes / No Type _____
	Exhaust Ports Open?	Yes / No
	Fuel Pump	Hammer Setting _____
	Recoil Dampener Undamaged?	Yes / No
	Impact Block Lubricated?	Yes / No
	Bounce Chamber Hose	Length _____
	Striker Plate	t= _____ D= _____
	Hammer Cushion	t= _____ D= _____ Material _____ How long in use? _____
	Helmet	Type or Weight? _____
	Follower?	Yes / No Type? _____
	Pile Cushion	Material _____ t= _____ Size _____ How long in use? _____
	Pile	Material _____ Length _____ Size _____ Batter _____

Manufacturer's Hammer Data

Ram Weight _____

Max Stroke _____

Rated Energy

Bounce Chamber Pressure, psi	Rated Energy ft-kips

Attached Saximeter Printout

Observation when Bearing is Confirmed

Bouce Chamber Pressure _____

Cylinder Lift-off Type or Depth _____

Excessive Cylinder Rebound? Yes/No

High Pile Rebound? Yes/No

Pile Whipping? Yes/No

Pile- Hammer Alignment Front/Back _____ Sides _____

Crane Size and Make _____

Lead Type _____

Hammer Lead Guides Lubricated? Yes/No

Color of Smoke _____

Steel to Steel Impact Sound _____

Figure 18-14 Inspector's form for double acting diesel hammers.

18.7.6 Single Acting Hydraulic Hammers

a. Determine/confirm the ram weight. If necessary, the ram weight can be calculated from the ram volume and steel density of 492 lbs/ft^3 although some rams may be hollow or filled with lead. There may also be identifying labels as to hammer make, model, and serial number which should be recorded.

b. Check the power supply and confirm it has adequate capacity to provide the required pressure and flow volume. Also, check the number, length, diameter, and condition of the hoses (no leaks in hoses or connections). Manufacturers provide guidelines for power supplies and supply hoses. Hoses bent to a radius less than recommended could adversely affect hammer operation or cause hose failure.

c. Hydraulic hammers must be kept clean and free from dirt and water. Check the hydraulic filter for blocked elements. Most units have a built in warning or diagnostic system.

d. Check that the hydraulic power supply is operating at the correct speed and pressure. Allow the hammer to warm up before operation, and do not turn off power pack immediately after driving.

f. For single acting hydraulic hammers with observable rams, measure the stroke being attained and confirm that it meets specification. For hammers with enclosed rams, it is impossible to observe the ram and estimate the stroke.

g. Check that the ram guides and piston rod are well greased.

h. Where applicable, the total thickness of hammer cushion and striker plate must be maintained to match the manufacturer's recommendation for proper valve timing and hammer operation.

i. Make sure the helmet stays properly seated on the pile and that the hammer and pile maintain alignment during operation.

j. The hammer hoist line should always be slack, with the hammer's weight fully carried by the pile. Excessive tension in the hammer hoist line is a safety hazard and will reduce energy to the pile. Leads should always be used.

k. Compare the observed hammer speed in blows per minute from near end of driving with the manufacturer's specifications. Blows per minute can be timed with a stopwatch or a saximeter. Slower operating rates at full stroke may imply excessive friction, or incorrect hydraulic power supply.

l. As the penetration resistance increases, the ram stroke may also increase, causing the ram to strike the upper hammer assembly and lifting the hammer from the pile (racking). If this behavior is detected, the pressure flow should be reduced gradually until racking stops. Many of these hammers have sensors, and if they detect this condition, the hammer will automatically shut down. The flow should not be overly restricted so that the correct stroke is maintained.

m. Some manufacturers void their warranty if the hammer is consistently operated above 10 blows per inch of penetration beyond short periods such as those required when toe bearing piles are driven to rock. Therefore, in prolonged hard driving situations, it may be more desirable to use a larger hammer or stiffer pile section.

n. Common problems and problem indicators for hydraulic hammers are summarized in Table 18-5.

Table 18-5 Common Problems and Indicators for Single Acting Hydraulic Hammers (after Williams Earth Sciences 1995)

Common Problems	Indicators
Hoses getting caught in leads.	Visually evident.
Fittings leaking.	Hydraulic fluid dripping.
Electrical connections.	Erratic performance.
Sensors.	Erratic performance.

Project/Pile: _____ Hammer Name _____

Date: _____ Serial No. _____

Conditions: _____

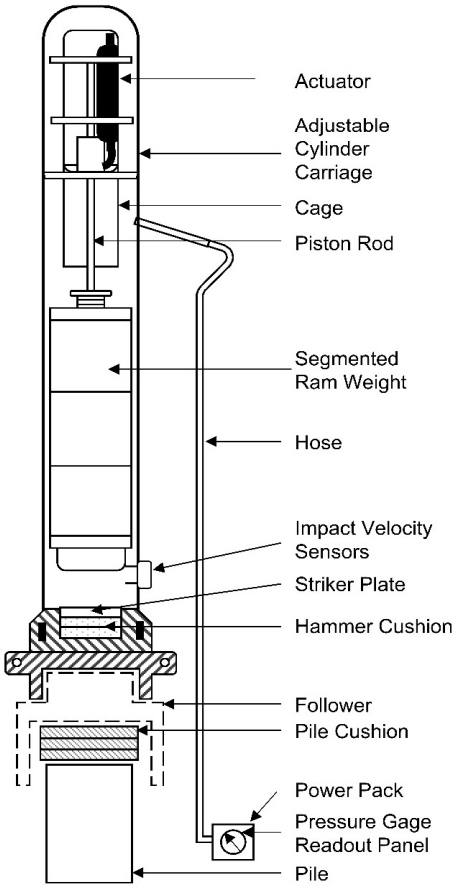

Object	Requirements	Observations
	Ram Visible	Yes / No
		Observed Ram Stoke _____ ft
	Ram Downward Pressure Provided?	Yes / No
		Hyd. Pressure Rated _____ psi
		Hyd. Pressure Actual _____ psi
	Impact Velocity Measurement?	Yes / No
	If No, then	Freefall? Yes / No
		Observed Fall Height _____ ft
		Pressure under ram during fall _____
		Preadmission Possible? Yes / No
	Striker Plate	t= D=
	Hammer Cushion	t= _____ D= _____
		Material _____
		How long in use? _____
	Helmet	Type or Weight? _____
	Power Pack	Make _____
		Model _____
	Pressure Gage?	Yes / No Reading _____
	Computer Readout?	Yes / No Reading _____
	Follower	Yes / No Type? _____
	Pile Cushion	Material _____
		t= _____ Size _____
		How long in use? _____
	Pile	Material _____
		Length _____ Size _____
		Batter _____

Manufacturer's Hammer Data

Ram Weight _____

Max Stroke _____

Min Stroke _____

Max Energy _____

Min Energy _____

Attached Saximeter Printout

Observation when Bearing is Confirmed

Hammer Uplifting? Yes/No

Reduced Pressure? Yes/No _____ %

Blows/min _____ Blows/ft _____

High Pile Rebound? Yes/No

Pile Whipping? Yes/No

Pile- Hammer Alignment Front/Back ___ Sides ___

Crane Size and Make _____

Lead Type _____

Hammer Lead Guides Lubricated Yes/No

Figure 18-15 Inspector's form for single acting hydraulic hammers.

18.7.7 Double Acting Hydraulic Hammers

a. Determine/confirm the ram weight. There may also be identifying labels as to hammer make, model, and serial number which should be recorded.

b. Check the power supply and confirm it has adequate capacity to provide the required pressure and flow volume. Also, check the number, length, diameter, and condition of the hoses (no leaks in hoses or connections). Manufacturers provide guidelines for power supplies and supply hoses. Hoses bent to a radius less than recommended could adversely affect hammer operation or cause hose failure.

c. Hydraulic hammers must be kept clean and free from dirt and water. Check the hydraulic filter for blocked elements. Most units have a built in warning or diagnostic system.

d. Check that the hydraulic power supply is operating at the correct speed and pressure. Check and record the pre-charge pressures or accumulators. Allow the hammer to warm up before operation, and do not turn off power pack immediately after driving.

e. Most double acting hydraulic hammers have built in sensors to determine the ram velocity just prior to impact. This result may be converted to kinetic energy or equivalent stroke. The inspector should verify that the correct ram weight is entered in the hammer's "computer". This monitored velocity, stroke, or energy result should be constantly monitored and recorded. Some hammers have, or can be equipped with, a printout device to record that particular hammer's performance information with pile penetration depth and/or blow count. This is the most important hammer check that the inspector can and should make for these hammers. A photograph of a hydraulic hammer readout panel mounted on the power pack is presented in Figure 18-16. Hand held displays are also available on some hammers.

f. Most double acting hydraulic hammers are fully enclosed and therefore do not have observable rams. On these hammers it is impossible to measure the stroke being attained and confirm that it meets specification. Properly working energy readout devices are therefore mandatory for inspection.

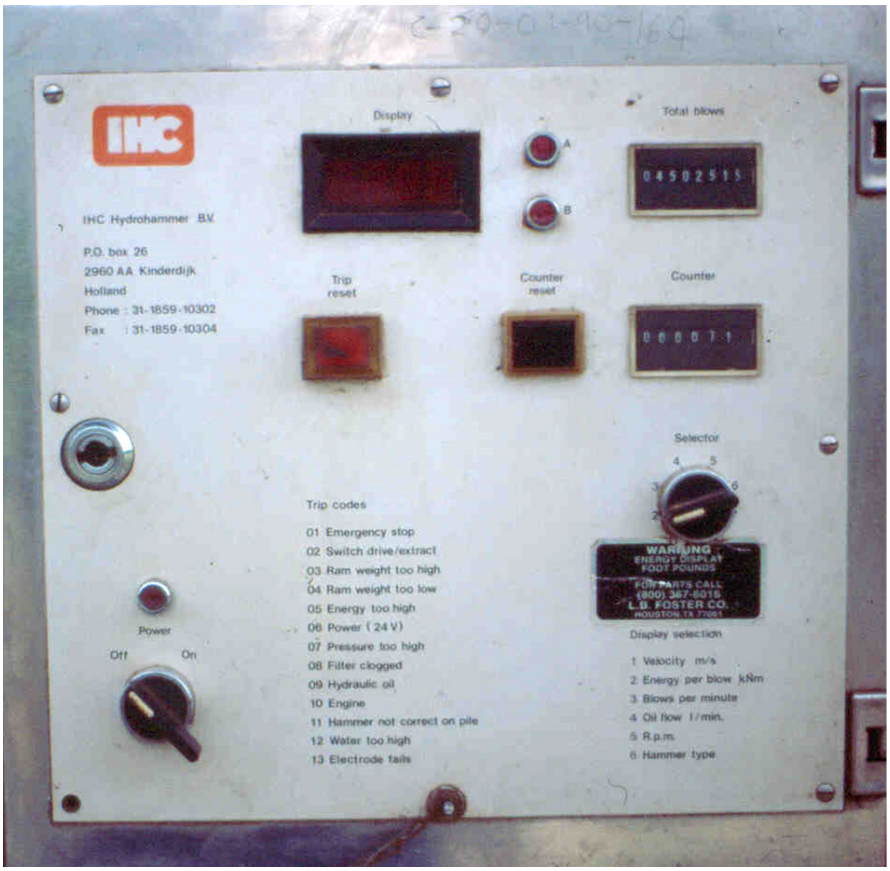

Figure 18-16 IHC hydraulic hammer read-out panel.

g. Most double acting hydraulic hammers are steel ram on steel anvil impact and do not use a striker plate or hammer cushion. One manufacturer uses an aluminum stack for a hammer cushion. Double acting hydraulic hammer models designed for use on concrete piles have a synthetic anvil block instead of a steel one. Document the anvil or cushioning mechanism, dimensions used in the double acting hammer model.

i. Make sure the helmet stays properly seated on the pile and that the hammer and pile maintain alignment during operation.

j. The hammer hoist line should always be slack, with the hammer's weight fully carried by the pile. Excessive tension in the hammer hoist line is a safety hazard and will reduce energy to the pile. Leads should always be used.

k. Compare the observed hammer speed in blows per minute from near end of driving with the manufacturer's specifications. Blows per minute can be timed with a stopwatch or a saximeter. Slower operating rates at full stroke may imply excessive friction, or incorrect hydraulic power supply.

l. As the penetration resistance increases, the ram stroke may also increase, causing the ram to strike the upper hammer assembly and lifting the hammer from the pile (racking). If this behavior is detected, the pressure flow should be reduced gradually until racking stops. Many of these hammers have sensors, and if they detect this condition, the hammer will automatically shut down. The flow should not be overly restricted so that the correct stroke is maintained.

m. Some manufacturers void their warranty if the hammer is consistently operated above 10 blows per inch of penetration beyond short periods such as those required when toe bearing piles are driven to rock. Therefore, in prolonged hard driving situations, it may be more desirable to use a larger hammer or stiffer pile section.

n. Common problems and problem indicators for double acting hydraulic hammers with nitrogen caps are summarized in Table 18-6.

Table 18-6 Common Problems and Indicators for Double Acting Hydraulic Hammers

Common Problems	Indicators
Hydraulic hoses crossed.	Jumping hydraulic hoses.
Incorrect pressure in accumulators.	Jumping hydraulic hoses.
Cap pressure too high.	Hammer jumping on pile.
Low oil supply.	Erratic hammer operation.
Pressure or return valve malfunctioning.	Erratic or no hammer operation.
Hammer inoperable.	Control cable not connected.
Hammer inoperable.	Bulb A or B not lit on control panel.
Hoses getting caught in leads.	Visually evident.
Fittings leaking.	Hydraulic fluid dripping.
Electrical connections.	Erratic performance.
Sensors.	Erratic performance.

Project/Pile: _____ Hammer Name _____

Date: _____ Serial No. _____

Conditions: _____

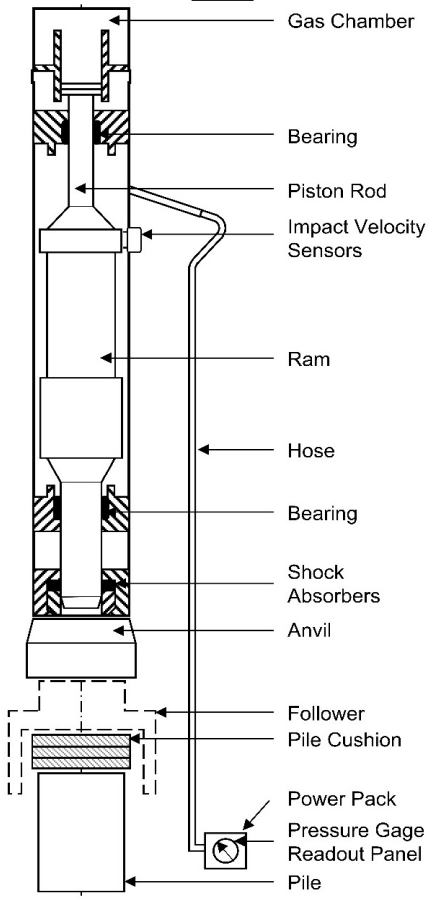

Object	Requirements	Observations
	Ram Visible	Yes / No
		Observed Ram Stoke _____ ft
	Ram Downward Pressure	Hyd. Pressure Rated _____ psi
		Hyd. Pressure Actual _____ psi
	Impact Velocity Measurement	Measured Impact Velocity _____ ft/s
		Fall _____ ft
	Anvil	Type or Weight? _____
	Power Pack	Make _____
		Model _____
	Pressure Gage?	Yes / No Reading _____
	Follower	Yes / No Type? _____
	Pile Cushion	Material _____
		t= _____ Size _____
		How long in use? _____
	Pile	Material _____
		Length _____ Size _____
		Batter _____

Manufacturer's Hammer Data

Ram Weight _____

Max Stroke _____

Min Stroke _____

Max Energy _____

Min Energy _____

Attached Saximeter Printout

Observation when Bearing is Confirmed

Hammer Uplifting? Yes/No

Reduced Pressure? Yes/No _____ %

Blows/min _____ Blows/ft _____

High Pile Rebound? Yes/No

Pile Whipping? Yes/No

Pile- Hammer Alignment Front/Back ____ Sides ____

Crane Size and Make _____

Lead Type _____

Hammer Lead Guides Lubricated Yes/No

Figure 18-17 Inspector's form for hydraulic hammers.

18.7.8 Resonant Hammers

a. Confirm that the hammer make and model meets specifications. There may also be identifying labels as to hammer make, model and serial number which should be recorded.

b. Check the power supply to confirm adequate capacity to provide the required pressure and flow volume. Check also the number, length, diameter, and condition of the hoses (no leaks in hoses or connections). Manufacturers provide guidelines for proper power supplies and supply hoses. Hoses bent to a smaller radius than recommended could affect hammer operation or cause hose failure.

c. Resonant hammers must be kept clean and free from dirt and water. Check the hydraulic filter for blocked elements. Most units have a built in warning or diagnostic system.

d. Check and record that the hydraulic power supply is operating at the correct speed and pressure. Allow the hammer to warm up before operation, and do not turn off the power pack immediately after driving.

e. Record the resonant vibrating frequency.

f. Make sure the hydraulic clamps for attachment to the pile are in good working order and effective.

g. The hammer hoist line should always be slack enough to allow penetration with the hammer's weight primarily carried by the pile. Excessive tension in the hammer hoist line will retard penetration. If used for extraction, the hoist line should be tight at all times. Leads may or may not be used.

18.7.9 Vibratory Hammers

a. Confirm that the hammer make and model meets specifications. There may also be identifying labels as to hammer make, model and serial number which should be recorded.

b. Check the power supply to confirm adequate capacity to provide the required pressure and flow volume. Check also the number, length, diameter, and condition of the hoses (no leaks in hoses or connections). Manufacturers

provide guidelines for proper power supplies and supply hoses. Hoses bent to a smaller radius than recommended could affect hammer operation or cause hose failure.

c. Vibratory hammers must be kept clean and free from dirt and water. Check the hydraulic filter for blocked elements. Most units have a built in warning or diagnostic system.

d. Check and record that the hydraulic power supply is operating at the correct speed and pressure. Allow the hammer to warm up before operation, and do not turn off the power pack immediately after driving.

e. Record, if available, the vibrating frequency.

f. Make sure the hydraulic clamps for attachment to the pile are in good working order and effective.

g. The hammer hoist line should always be slack enough to allow penetration with the hammer's weight primarily carried by the pile. Excessive tension in the hammer hoist line will retard penetration. If used for extraction, the hoist line should be tight at all times. Leads are rarely used.

18.8 INSPECTION OF TEST OR INDICATOR PILES

Most pile foundation projects required verification of the foundation design and nominal resistance through the testing of some selected piles. The size of the foundation and relative costs of testing often dictate the type and number, if any, of verification tests performed. The inspector may be responsible for coordinating the test pile program with the contractor, other state personnel, and/or outside testing agencies.

Small foundations with few piles may be designed conservatively with low resistance factors and greater pile lengths. On these projects, test piles for verification testing are frequently not required. All piles are then production piles, and the entire pile foundation is usually installed in one or two days. Information on the piles, hammers, and other observations are recorded by the inspector and appropriately passed on or filed. Inspection should be thorough as it is the only assurance of a good foundation. If any problems are observed, such as very low blow counts, refusal driving above scour depths, or excessive pile lengths, the problems and all

pertinent observations must be reported quickly so that immediate corrective action can be taken.

On most projects, some level of verification testing is specified. Small to mid-size projects may have only a single static test (Chapter 9) on one pile at a specific depth, or there may be a few dynamic test piles (Chapter 10). The dynamic tests may include either testing during driving to assess hammer performance and driving stresses, or testing during restrike to assess nominal resistance, or both. The static or dynamic tests should be performed and reviewed by personnel having appropriate knowledge of the test method and proper procedures. Generally, tests are done on some of the first piles driven to verify or adjust the driving criteria which will then be used for subsequent production piles. This further verification provides rational basis for changes to the driving criteria, if necessary, which should be applied to subsequent production pile driving.

On larger projects, multiple test piles distributed across the site are often required to verify or adjust the driving criteria as conditions warrant. The goal is to determine driving criteria which will lead to a safe and economical foundation. Such tests could be primarily done at one time at the beginning of the construction. For example, so-called indicator piles are driven in selected locations across the project site to establish order lengths for concrete piles. Selected piles are generally statically and/or dynamically tested. Alternatively, testing could be performed as the construction progresses with some test(s) establishing the driving criteria for piles in close proximity to the test pile(s), followed by production pile driving, and then repeating the process in stages across the site.

The test piles are often the most critical part of the foundation installation. The procedures and driving criteria established during this phase will be applied to all subsequent production piles. The largest savings are often found at this time. For example, test results may determine that the design pile length results in a greater nominal resistance than required and that the piles could be made substantially shorter. Alternatively, problems with the test piles are usually followed by the same problems with production piles. Since problems are in themselves costly, and if left unresolved may eventually escalate, determination of the best solution as quickly as possible should be accomplished. It is the inspector's responsibility to be observant and communicate significant observations precisely and in a timely manner to the appropriate agency, design, or construction personnel.

The answers to the following questions should be known before driving test piles. It is often beneficial to have a preconstruction pile driving meeting between the contractor, project administrator, and the inspector to clarify these items.

1. Who determines test pile locations?

2. Who determines the test pile driving criteria?

3. Who stops the driving when the driving criterion is met?

4. Who decides at what depth to stop the indicator/test piles?

5. Who checks cutoff elevations?

6. Who checks for heave?

7. Who determines if static test and/or dynamic test results indicate an acceptable test pile?

8. Who determines if additional tests are required?

9. Who determines if modifications to procedures or equipment are required?

10. What documentation is required from test pile installations (test pile driving record, dynamic test results, static test report) and who produces what documentation?

11. Who produces the production pile driving criteria and how quickly will it be available?

12. Who has authority to allow production pile installation to begin?

13. When is the authorization to proceed to production pile driving given relative to test pile driving?

14. Can production piles (initial pile section or entire piles) be driven in advance of the production pile driving criteria and if so at whose risk?

18.9 INSPECTION OF PRODUCTION PILES

During the production pile driving operations, the inspector's function is to apply the knowledge gained from the test program to each and every production pile. Quality assurance measures for the pile quality and pile splices; hammer operation and cushion replacement; overall evaluation of pile integrity; procedures for completing the piles (e.g. filling pipe piles with concrete); and unusual or unexpected occurrences need to be addressed. Complete documentation for each and every pile must be obtained, and then passed on to the appropriate authorities in a timely manner.

The following items should be checked frequently (e.g. for each production pile):

1. Is the pile the specified type, size, length, and strength?

2. Is the pile installed in the correct location, within acceptable tolerances, and with the correct orientation?

3. Are splices, if applicable, made to specification?

4. Is pile toe protection required and properly attached?

5. Is the pile acceptably plumb?

6. Is the hammer working correctly?

7. Is the hammer cushion the correct type and thickness?

8. Is the pile cushion the correct type and thickness? Is it being replaced regularly?

9. Did the pile meet the driving criteria as expected?

10. Did the pile have unusual driving conditions and therefore potential problems?

11. Is there any indication of pile heave?

12. Is the pile cutoff at the correct elevation?

13. Is there any visual damage?

14. Have all pipe piles been visually inspected prior to concrete filling? Has it been filled with the specified strength concrete? Were concrete samples taken?

15. Are piles which are to be filled with concrete, such as open ended pipes and prestressed concrete piles with center voids, being cleaned properly after driving is completed?

16. If there is any question about pile integrity, has the issue been resolved? Is the pile acceptable, or does it need remediation or replacement?

17. Is the documentation for this pile complete, including driving log? Has it been submitted on a timely basis to the appropriate authority?

Previous sections of this chapter provide material which relate to inspection of production piles and offer detailed answers to the questions raised above. Although the inspector has now had the experience of test pile installation, a few additional details and concerns are perhaps appropriate.

Counting the number of hammer blows per minute and comparing it to the manufacturer's specification will provide a good indication of whether or not the hammer is working properly. The stroke of the hammer for most single and double acting air/steam hammers can be observed. Check the stroke of a single acting diesel hammer with a saximeter or by computation from the blows per minute using Equation 18-1. Check and record the bounce chamber pressure for double acting diesel hammers. The stroke of most single acting hydraulic hammers can be observed. Record the energy from the built-in energy monitor in addition to hammer stroke for each pile. Double hydraulic hammers must have a built-in energy monitor, and this information should be recorded for each pile. The hammer inspection form presented earlier in this chapter should be completed for the hammer type used.

A hammer cushion of manufactured material usually lasts for many hours of pile driving, (as much as 200 hours for some manufactured materials) so it is usually sufficient to check before the pile driving begins and periodically thereafter. Pile cushions (usually made of plywood) need frequent changing because of excessive compression or charring and have a typical life of about 1000 to 2000 hammer blows. Pile cushions should preferably be replaced as soon as they compress to one half of the original thickness, or if they begin to burn. No changes to the pile cushion thickness should be permitted near final driving. The required pile

penetration resistance or blow count for nominal resistance verification should only be determined following the first 100 blows after cushion replacement. A new pile cushion reduces energy transfer and therefore produces an inflated blow count compared to a used cushion.

Inspection of pile splices is important to assure pile integrity. Poorly made splices are a potential source of problems and possible pile damage during driving. In some cases damage may be detected from the blow count records. Dynamic pile testing can be useful in questionable cases.

Pile driving stresses should be kept within specified limits. If dynamic monitoring equipment was used during test pile driving, the developed driving criteria should keep driving stresses within specified limits. If periodic dynamic tests are made, a check that the driving stresses remain within the specified limits can be provided. Adjustments of the ram stroke for all hammer types may be necessary to avoid pile damage. For concrete piles, cushion thicknesses or driving procedures may need adjustment to control tension and compression stresses. If dynamic testing is not used, a wave equation analysis is essential to evaluate the anticipated driving stresses.

Driving of piles at high blow counts, above 10 blows per inch, should be avoided by matching the driving system with the pile type, length and subsurface conditions. This should have been accomplished in the design phase by performing wave equation analysis. However, conditions can change across the project due to site variability.

All piles should be checked for damage after driving is completed. The driving records for all pile types can be compared with adjacent piles for unusual records or vastly different penetrations. Piles suspected of damage (including timber, H, and solid concrete piles) could be tested to confirm integrity and/or determine extent and location of damage using high strain dynamic pile testing, or for concrete piles, low strain integrity testing methods. These methods are discussed in Chapter 10. Alternatively, the pile could be replaced or repaired, if possible.

Check for water leakage and soil inflow into closed end pipe piles before placing concrete. The concrete mix should have a high slump and small aggregate. A pipe pile can be easily checked for damage and sweep by lowering a light source inside the pile. A mirror can also be used to reflect sunlight inside a pipe pile for internal inspection.

The driving sequence of piles in a pier or bent can be important. The driving sequence can affect the way piles drive as well as the influence the new construction has on adjacent structures. This is especially true for displacement piles. For non-displacement piles, the driving sequence is generally not as critical.

The driving sequence of displacement pile groups should be from the center of the group outward or from one side to the other side. The preferred driving sequence of the displacement pile group shown in Figure 18-18 would be (a) by the pile number shown, (sequence 1), (b) by driving each row starting in the center and working outward (sequence 2), or (c) by driving each row starting on one side of the group and working to the other side (sequence 3).

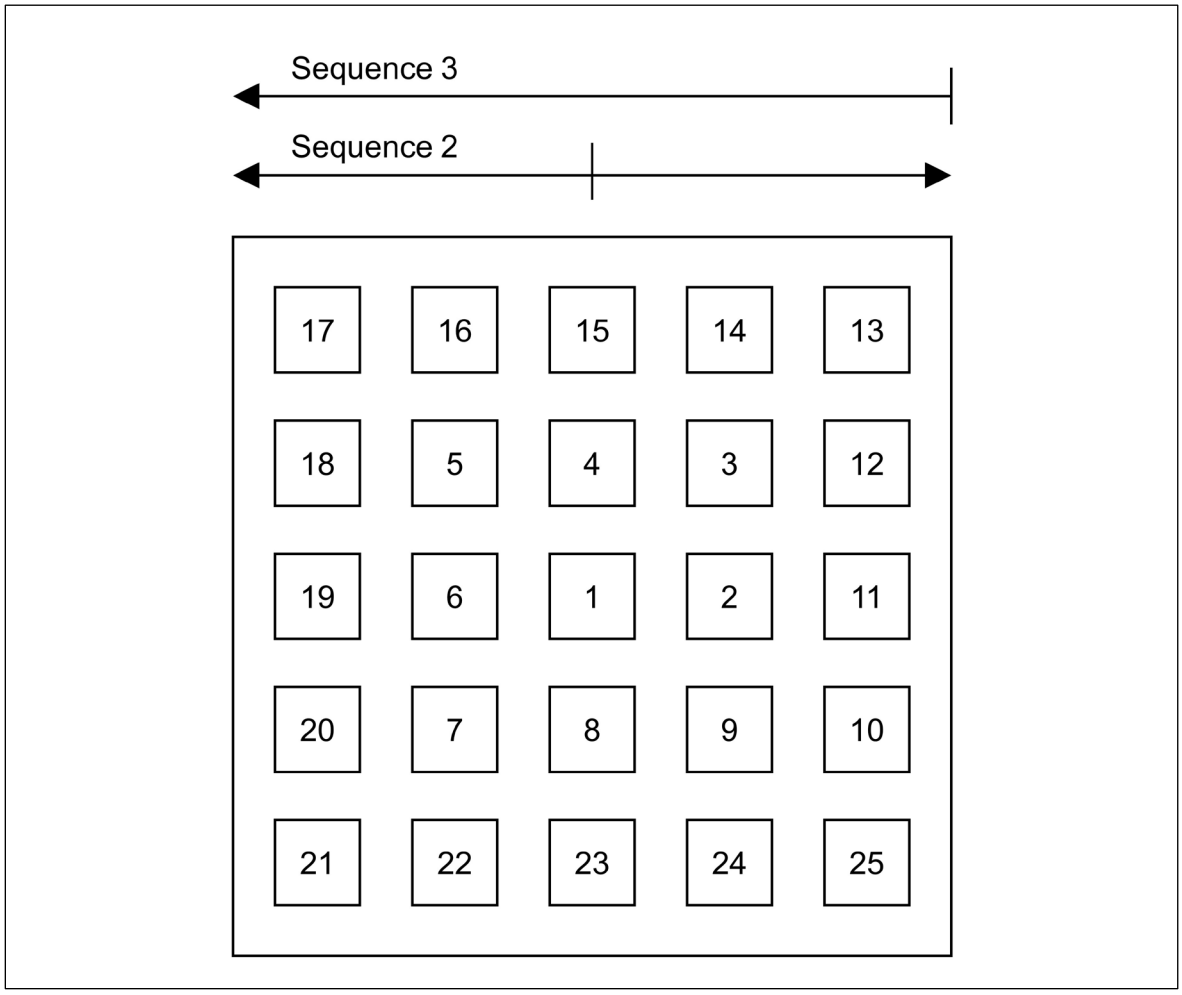

Figure 18-18 Driving sequence of displacement pile groups (after Passe 1994).

Pile groups should not be driven from the outside to the center (the reverse of sequences 1 or 2). If groups are driven in that order, displaced soils becomes trapped and compacted in the center of the pile group. This can cause problems

with driving the piles in the center of the group and prevent those piles from meeting minimum pile penetration depths for scour.

When driving close to an existing structure or utility, it is generally preferable to drive the piles nearest the existing structure or utility first and work away. For example, if a structure was located on the right side of the pile group shown in Figure 18-18, the piles should be driven by sequence 3. This reduces the amount of soil displaced toward the existing structure. The displacement of soil toward an existing structure has caused problems before. It can be especially critical next to a bascule bridge where, very small movements can prevent the locking mechanism from locking.

On some projects, vibration measurements may be required to ascertain if pile driving vibrations are within acceptable and/or specified maximum levels. Woods (1997) noted that vibration damage is relatively uncommon at a distance of one pile length away from driving. However, damage from vibration induced settlement of loose, clean sands can be a problem up to 1300 feet away from driving. Prior to the start of construction, a survey of structures and utilities within 400 feet of pile driving activities is often performed to document their existing condition. Some specifications tie the preconstruction survey limits to the hammer energy and require a preconstruction survey of all structures located within a distance in feet of 0.25 times the square root of the hammer energy in foot-pounds. The preconstruction survey generally consists of photographing or videotaping existing damage, as well as affixing crack gages to existing cracks in some cases.

Woods (1997) noted that damage to freshly placed concrete from pile driving vibrations may not be a risk but further research on the setting and curing of concrete may be warranted.

A cold hammer should not be used when restriking piles after a setup period. Twenty hammer blows are usually sufficient to warm up most hammers. Also be sure to record the restrike penetration resistance for each 1 inch interval during the restrike.

A summary of common pile installation problems and possible solutions is presented in Table 18-7.

Table 18-7 Common Pile Installation Problems and Possible Solutions

Common Problems	Possible Solutions
Piles encountering refusal blow count above minimum pile penetration requirements.	Have wave equation analysis performed and check that pile has sufficient drivability and that the driving system is matched to the pile. If the pile and driving system are suitably matched, check driving system operation for compliance with manufacturer's guidelines. If no obvious problems are found, dynamic measurements should be made to determine if the problem is driving system or soil behavior related. Driving system problems could include pre-ignition, preadmission, low hammer efficiency, or soft cushion. Soil problems could include greater soil strength than anticipated, temporarily increased soil resistance with later relaxation (requires restrike to check), large soil quakes, or high soil damping.
Piles driving significantly deeper than estimated pile penetration depths.	Soil resistance at the time of driving probably is lower than anticipated or driving system performance is better than anticipated. Have wave equation analysis performed to assess nominal resistance based on the blow count at the time of driving. Perform restrike tests after an appropriate waiting period to evaluate soil strength changes with time. If the nominal resistance based on restrike blow count is still low, check drive system performance and restrike pile with dynamic measurements. If drive system performance is as assumed and restrike nominal resistance low, the soil conditions are weaker than anticipated. Foundation piles will probably need to be driven deeper than originally estimated or additional piles will be required to support the load. Contact the structural engineer/designer for recommended change.

Table 18-7 Common Pile Installation Problems and Possible Solutions (Continued)

Common Problems	Possible Solutions
Abrupt change or decrease in blow count for bearing piles.	If borings do not indicate weathered profile above bedrock/bearing layer then pile toe damage is likely. Have wave equation analysis performed and evaluate pile toe stress. If calculated toe stress is high and blow counts are low, a reduced hammer energy (stroke) and higher blow count could be used to achieve nominal resistance with a lower toe stress. If calculated toe stress is high at high blow counts, a different hammer or pile section may be required. For piles that allow internal inspection, reflect light to the pile toe and tape the length inside the pile for indications of toe damage. For piles that cannot be internally inspected, dynamic measurements could be made to evaluate problem or pile extraction could be considered for confirmation of a damage problem.
Blow count significantly lower than expected during driving.	Review soil borings. If soil borings do not indicate soft layers, pile may be damaged below grade. Have wave equation analysis performed and investigate both tensile stresses along pile and compressive stresses at toe. If calculated stresses are within allowable limits, investigate possibility of obstructions / uneven toe contact on hard layer or other reasons for pile toe damage. If pile was spliced, re-evaluate splice detail and field splicing procedures for possible splice failure.
Vertical (heave) or lateral movement of previously installed piles when driving new piles.	Pile movements likely due to soil displacement from adjacent pile driving. Contact geotechnical engineer for recommended action. Possible solutions include redriving of installed piles, change in sequence of pile installation, or predrilling of pile locations to reduce ground movements. Lateral pile movements could also result from adjacent slope failure in applicable conditions.

Table 18-7 Common Pile Installation Problems and Possible Solutions (Continued)

Common Problems	Possible Solutions
Piles driving out of alignment tolerance.	Piles may be moving out of alignment tolerance due to hammer-pile alignment control or due to soil conditions. If due to poor hammer-pile alignment control, a pile gate, template or fixed lead system may improve the ability to maintain alignment tolerance. Soil conditions such as near surface obstructions (see subsequent section) or steeply sloping bedrock having minimal overburden material (pile point detail is important) may prevent tolerances from being met even with good alignment control. In these cases, survey the as-built condition and contact the structural engineer for recommended action.
Piles driving out of location tolerance.	Piles may be moving out of location tolerance due to hammer-pile alignment control or due to soil conditions. If due to poor hammer-pile alignment control, a pile gate, template or fixed lead system may improve the ability to maintain location tolerance. Soil conditions such as near surface obstructions (see subsequent section) or steeply sloping bedrock having minimal overburden material (pile point detail is important) may prevent tolerances from being met even with good alignment control. In these cases, survey the as-built condition and contact the structural engineer for recommended action.
Piles encountering shallow obstructions.	If obstructions are within 10 feet of working grade, obstruction excavation and removal is probably feasible. If obstructions are at deeper depth, are below the water table, or the soil is contaminated, excavation may not be feasible. Spudding or predrilling of pile locations may provide a solution with method selection based on the type of obstructions and soil conditions.

Table 18-7 Common Pile Installation Problems and Possible Solutions (Continued)

Common Problems	Possible Solutions
Piles encountering obstructions at depth.	If deep obstructions are encountered that prevent reaching the desired pile penetration depth, contact the structural engineer/designer for remedial design. Nominal resistance of piles hitting obstructions should be reduced based upon pile damage potential and soil matrix support characteristics. Additional foundation piles may be necessary.
Concrete piles develop complete horizontal cracks in easy driving.	Have wave equation analysis performed and check tension stresses along pile (extrema tables) for the observed blow counts. If the calculated tension stresses are high, add cushioning or reduce stroke. If calculated tension stresses are low, check hammer performance and/or perform dynamic measurements.
Concrete piles develop complete horizontal cracks in hard driving.	Have wave equation analysis performed and check tension stresses along pile (extrema table). If the calculated tension stresses are high, consider a hammer with a heavier ram. If the calculated tension stresses are low, perform dynamic measurements and evaluate soil quakes which are probably higher than anticipated.
Concrete piles develop partial horizontal cracks in easy driving.	Check hammer-pile alignment since bending may be causing the problem. If the alignment appears to be normal, tension and bending combined may be too high. The possible solution is as above with complete cracks.
Concrete pile spalling or slabbing near pile head.	Have wave equation analysis performed. Determine the pile head stress at the observed blow count and compare predicted stress with material stress limits. If the calculated stress is high, increase the pile cushioning. If the calculated stress is low, investigate pile quality, hammer performance, and hammer-pile alignment.

Table 18-7 Common Pile Installation Problems and Possible Solutions (Continued)

Common Problems	Possible Solutions
Steel pile head deforms.	Check helmet size/shape, steel yield strength, and evenness of the pile head. If all seem acceptable, have wave equation analysis performed and determine the pile head stress. If the calculated stress is high and blow counts are low, use reduced hammer energy (stroke) and higher blow count to achieve nominal resistance. If the calculated stress is high at high blow counts, a different hammer or pile type may be required. Nominal resistance determination should not be made using blow counts obtained when driving with a deformed pile head.
Timber pile head mushrooms.	Check helmet size/shape, the evenness of the pile head, and banding of the timber pile head. If all seem acceptable, have wave equation analysis performed and determine the pile head stress. If the calculated stress is high and blow counts are low, use reduced hammer energy (stroke) and higher blow count to achieve nominal resistance. Nominal resistance determination should not be made using blow counts obtained when driving with a mushroomed pile head.

18.10 DRIVING RECORDS AND REPORTS

Pile driving records vary depending upon the organization performing the monitoring or inspection service. A typical pile driving record is presented in Figure 18-19. The following is a list of items that appear on most pile driving records:

1. Project identification number.

2. Project name and location.

3. Structure identification number.

4. Date and time of driving (start, stop, and interruptions).

5. Name of the contractor.

6. Hammer make, model, ram weight, energy rating. The actual stroke and operating speed should also be recorded whenever it is changed.

7. Hammer cushion description, size and thickness, and helmet weight.

8. Pile cushion description, size and thickness, depth where changed.

9. Pile location, type, size and length.

10. Pile number or designation matching pile layout plans.

11. Pile ground surface, cut off, and final penetration elevations and embedded length.

12. Penetration resistance data in blows per foot with the final 1 foot normally recorded in blows per inch.

13. Graphical presentation of driving data (optional).

14. Cut off length, length in ground and order length.

15. Comments or unusual observations, including reasons for all interruptions.

16. Signature and title of the inspector.

The importance of maintaining detailed pile driving records cannot be overemphasized. The driving records form a basis for payment and for making engineering decisions regarding the adequacy of the foundation to support the design loads. Great importance is given to driving records in litigations involving claims. Sloppy, inaccurate, or incomplete records encourage claims and result in higher cost foundations. The better the pile driving is documented, the lower the foundation cost will probably be and the more likely it will be completed on schedule.

In addition to the driving records, the inspector should be required to prepare a daily inspection report. The daily inspection report should include information on equipment working at the site, description of construction work accomplished, and the progress of work. Figure 18-20 shows an example of a daily inspection report.

PROJECT NO.: _____ DATE: _____

JOB LOCATION: _____ BENT / PIER NO.: _____ PILE NO.: _____

PILE TYPE: _____ LENGTH: _____ COATING: _____ NOMINAL RESISTANCE: _____

HAMMER: _____ RATED ENERGY: _____ OPERATING RATE: _____ HELMET WT.: _____

HAMMER CUSHION TYPE: _____ t= _____ PILE CUSHION TYPE: _____ t= _____

REF. ELEV.: _____ MIN TOE ELEV.: _____ FINAL TOE ELEV.: _____ CUTOFF ELEV.: _____

WEATHER: _____ TEMP.: _____ START TIME: _____ END TIME: _____

FEET	BLOWS	STROKE / PRESSURE	REMARKS	FEET	BLOWS	STROKE / PRESSURE	REMARKS
0 to 1				35 to 36			
1 to 2				36 to 37			
2 to 3				37 to 38			
3 to 4				38 to 39			
4 to 5				39 to 40			
5 to 6				40 to 41			
6 to 7				41 to 42			
7 to 8				42 to 43			
8 to 9				43 to 44			
9 to 10				44 to 45			
10 to 11				45 to 46			
11 to 12				46 to 47			
12 to 13				47 to 48			
13 to 14				48 to 49			
14 to 15				49 to 50			
15 to 16				50 to 51			
16 to 17				51 to 52			
17 to 18				52 to 53			
18 to 19				53 to 54			
19 to 20				54 to 55			
20 to 21				55 to 56			
21 to 22				56 to 57			
22 to 23				57 to 58			
23 to 24				58 to 59			
24 to 25				59 to 60			
25 to 26				60 to 61			
26 to 27				61 to 62			
27 to 28				62 to 63			
28 to 29				63 to 64			
29 to 30				64 to 65			
30 to 31				65 to 66			
31 to 32				66 to 67			
32 to 33				67 to 68			
33 to 34				68 to 69			
34 to 35				69 to 70			

PILE SUPPLIER: _____ PILE CAST OR ROLLING DATE: _____

PILE TOE ATTACHMENTS: _____ FINAL PILE HEAD CONDITION: _____

FINAL ALIGNMENT: _____ FINAL PLUMBNESS: _____ INTERNAL INSPECTION: _____

INSPECTORS SIGNATURE: _____

Figure 18-19 Pile driving log.

Daily Inspection Report

Project No.: _____
Date: _____

Project: _____

Weather Conditions: _____

Contractor: _____

Contractor's Presonnel Present: _____

Equipment Working: _____

Description of Work: _____

Special Person's Visiting Job: _____

Test Performed: _____

Special Coments: _____

Inspector's Signature: _____

Figure 18-20 Daily inspection report.

18.11 SAFETY

Pile driving involves the use of heavy equipment and heavy loads. The pile driving inspector should be cognizant of these activities and position his or herself accordingly. One of the more dangerous operations during pile driving is the lifting of the pile and the positioning of it under the hammer for driving. The inspector should remember that a 100 feet pile can fall 100 feet from the pile location during positioning. It is better to have a planned escape route prior to pile positioning rather than attempt to quickly determine one should difficulties arise during the pile lifting and positioning process.

The area beneath a suspended load should be avoided. If the hoisting device fails or slips, serious injury could occur. The inspector should also avoid the area behind the crane and be cognizant whenever the crane is moving or swinging.

The inspector should select a position to maintain the pile driving record that is a sufficient distance away from the pile location during driving. The area immediately in front of the pile should be avoided. Heavy pieces sometimes fall from a pile hammer or helmet during operation that could cause serious injury if the inspector were positioned under or near the hammer. All pile types can be also damaged during driving. Concrete and timber piles can break suddenly, and long steel piles can buckle. A sudden pile break or buckling can make the area around the pile location quite dangerous due to the broken or buckled section. A sudden loss of resistance beneath an operating pile hammer can also overload the hammer line causing it to break and the hammer to fall. Damage to the head of a concrete pile during driving can also result in heavy concrete pieces falling due to hammer-pile alignment problems or due to pile cushion deterioration. Standing beneath the hammer and monitoring the final pile penetration resistance by placing marks on the pile every 10 or 20 hammer blows should be avoided for the above reasons. The final blow count can be determined instead by marking the pile prior to driving with 1 inch marks over the anticipated final penetration depth.

Safety devices such as a hard hat, ear protection, steel toed work boots, eye protection, safety vest, fall protection harness, and life jacket should be worn as job conditions dictate. Additional site specific, state, or federal safety rules may also apply and these should be reviewed.

REFERENCES

Deep Foundations Institute (DFI). (1995). A Pile Inspector's Guide to Hammers, Second Edition, Deep Foundations Institute, Englewood Cliffs, NJ, 71 p.

Deep Foundations Institute (DFI). (1997). Inspectors Manual for Driven Pile Foundations, Second Edition, Deep Foundations Institute, Englewood Cliffs, NJ, 69 p.

Passe, Paul D. (1994). Pile Driving Inspector's Manual. State of Florida Department of Transportation.

Rausche, F., Likins, G.E., Goble, G.G., Hussein, M. (1986). The Performance of Pile Driving Systems; Inspector's Manual. U.S. Department of Transportation, Federal Highway Administration, Washington, D.C., 92 p.

Williams Earth Sciences (1995). Inspector's Qualification Program for Pile Driving Inspection Manual. State of Florida Department of Transportation.

Woods, R.D. (1997). Dynamic Effects of Pile Installations on Adjacent Structures. NCHRP Synthesis 253, National Cooperative Highway Research Program, Transportation Research Board, Washington, D.C., 85 p.

Appendix A

LIST OF FHWA/ NHI RESOURCES RELEVANT TO DEEP FOUNDATIONS

Abu-Hejleh, N., DiMaggio, J.A., Kramer, W.M., Anderson, S., and Nichols, S. (2010). Implementation of LRFD Geotechnical Design for Bridge Foundations: Reference Manual. FHWA-NHI-10-039. National Highway Institute, Federal Highway Administration, Washington, D.C.

Abu-Hejleh, N., Kramer, W.M., Mohamed, K., Long, J.H., and Zaheer, M.A. (2013). Implementation of AASHTO LRFD Design Specifications for Driven Piles, FHWA-RC-13-001. U.S. Dept. of Transportation, Federal Highway Administration, Washington, D.C., 71 p.

Arneson, L.A., Zevenbergen, L.W., Lagasse, P.F., and Clopper, P.E. (2012). Evaluating Scour at Bridges, Fifth Edition, FHWA-HIF-12-003, Hydraulic Engineering Circular (HEC) No. 18. U.S. Dept. of Transportation, Federal Highway Administration, 340 p.

Azizinamini, A., Power, E.H., Myers, G.F., and Ozyildirim, H.C. (2014). Bridges for Service Life Beyond 100 Years, Innovative Systems Subsystems, and Components, S2-R19A-RW-1 Strategic Highway Research Program 2 (SHRP), Transportation Research Board, Washington, D.C., 248 p.

Briaud J-L. and Miran, J. (1992). The Cone Penetration Test, FHWA-SA-91-043. U.S. Department of Transportation, Federal Highway Administration, Office of Technology Applications, Washington, D.C., 161 p.

Brown, D.A., and Thompson, W.R. (2011). Developing Production Pile Criteria from Test Pile Data. National Cooperative Highway Research Program (NCHRP) Synthesis 418, Washington, D.C., 54 p.

Brown, D. A., Turner, J.P. and Castelli R.J. (2010). Drilled Shafts: Construction Procedures and LRFD Design Methods, FHWA-NHI-10-016, Geotechnical Engineering Circular (GEC) No. 10. U.S. Dept. of Transportation, Federal Highway Administration, 970 p.

Brown, D.A., Dapp, S.D., Thompson, W.R., and Lazarte, C.A. (2007). Design and Construction of Continuous Flight Auger (CFA) Piles. FHWA-HIF-07-03, Geotechnical Engineering Circular (GEC) No.08. U.S. Dept. of Transportation, Federal Highway Administration, 289 p.

Cheney, R.S. and Chassie, R.G. (2000). Soils and Foundations Workshop Reference Manual. FHWA HI-00-045, U.S. Department of Transportation, National Highway Institute, Federal Highway Administration, Washington, D.C., 358 p.

Elias, V., Welsh, J.P., Warren, J., Lukas, R.G., Collin J.G., and Berg, R.R. (2006). Ground Improvement Methods Volumes I and II, FHWA-NHI-06-019 and FHWA NHI-06-020. National Highway Institute, Federal Highway Administration, U.S. Department of Transportation, Washington D.C.

Federal Highway Administration (FHWA). (1996). Geotechnical Engineering Notebook DT-15. Differing Site Conditions. U.S. Dept. of Transportation, Federal Highway Administration, Washington, D.C., 36 p.

Federal Highway Administration (FHWA). (2002a). Life-Cycle Cost Analysis Primer, IF-02-047. Federal Highway Administration, U.S. Department of Transportation. Washington, D.C., 24 p.

Geotechnical Guideline 13 (1985). Geotechnical Engineering Notebook, U.S. Department of Transportation. Federal Highway Administration, Washington, D.C., 37 p.

Ghosn, M., Moses, F., and Wang, J. (2003). Design of Highway Bridges for Extreme Events, NCHRP Report 489. National Cooperative Highway Research Program. Transportation Research Board, Washington, D.C., 174 p.

Goble, G.G. and Rausche, F. (1976). Wave Equation Analysis of Pile Driving – WEAP Program, FHWA IP-76-14.3., U.S. Department of Transportation, Federal Highway Administration, Office of Research and Development, Washington, D.C., Volumes I-IV.

Goble, G.G. and Rausche, F. (1986). Wave Equation Analysis of Pile Driving - WEAP86 Program. U.S. Department of Transportation, Federal Highway Administration, Implementation Division, McLean, VA, Volumes I-IV.

Hawk, H. (2003). Bridge Life-Cycle Cost Analysis, NCHRP483. Transportation Research Board of the National Academies, Washington, D.C., 96 p.

Kavazanjian, E., Wan, J-N. J., Martin, G.R., Shamsabadi, A., Lam, I., Dickenson, S.E., and Hung, C.J. (2011). LRFD Seismic Analysis and Design of Transportation Geotechnical Features and Structural Foundations, FHWA-NHI-11-032, Geotechnical Engineering Circular (GEC) No. 3. U.S. Dept. of Transportation, Federal Highway Administration, Washington, D.C., 592 p.

Kimmerling, R.E. (2002). Shallow Foundations, FHWA-IF-02-054, Geotechnical Engineering Circular (GEC) No. 6. U.S. Dept. of Transportation, Federal Highway Administration, Washington, D.C., 310 p.

Kyfor, Z.G., Schnore, A.R., Carlo, T.A. and Bailey, P.F. (1992). Static Testing of Deep Foundations, FHWA-SA-91-042. U.S. Department of Transportation, Federal Highway Administration, Office of Technology Applications, Washington, D.C., 174 p.

Lam, I.P. and Martin, G.R. (1986). Seismic Design of Highway Bridge Foundations. Volume II - Design Procedures and Guidelines, FHWA-RD-86-102. U.S. Department of Transportation, Federal Highway Administration, Office of Engineering and Highway Operations, McLean, VA, 167p.

Long, J., and Anderson, A. (2014). Improved of Driven Pile Installation and Design in Illinois: Phase 2, FHWA-ICT-14-019. Illinois Department of Transportation, Bureau of Material and Physical Research, Springfield, IL, 84 p.

Marsh, M.L., Buckle, I.G., and Kavazanjian Jr, E. (2014). LRFD Seismic Analysis and Design of Bridges, FHWA-NHI-15-004. National Highway Institute, U.S. Dept. of Transportation, Federal Highway Administration, Washington, D.C., 608 p.

Mayne, P.W., Christopher, B., Berg, R., and DeJong, J. (2001). Manual on Subsurface Investigations, FHWA NHI-01-031, U.S. Dept. of Transportation, National Highway Institute, Federal Highway Administration, Washington, D.C., 301 p.

Munfakh, G., Arman, A., Collin, J.G., Hung, J.C.-J., and Brouillette, R.P. (2001). Shallow Foundations Reference Manual, FHWA-NHI-01-023. National Highway Institute, Federal Highway Administration, Washington, D.C., 222 p.

Rausche, F., Likins, G.E., Goble, G.G., Hussien, M. (1986). The Performance of Pile Driving Systems; Inspector's Manual. U.S. Department of Transportation, Federal Highway Administration, Washington, D.C., 92 p.

Rausche, F., Thendean, G., Abou-matar, H., Likins, G.E. and Goble, G.G. (1996). Determination of Pile Drivability and Capacity from Penetration Tests, DTFH61-91-C-00047, Final Report. U.S. Department of Transportation, Federal Highway Administration, McLean, VA, 432 p.

Reese, L.C. (1984). Handbook on Design of Piles and Drilled Shafts Under Lateral Load. Report No. FHWA-IP-84-11, U.S. Department of Transportation, Federal Highway Administration, Office of Implementation, McLean, VA, 386 p.

Reese, L.C. (1986). Behavior of Piles and Pile Groups Under Lateral Load, FHWA-RD-85-106. U.S. Department of Transportation, Federal Highway Administration, Office of Engineering and Highway Operations Research and Development, Washington, D.C., 311 p.

Rixner, J.J., Kraemer, S.R. and Smith, A.D. (1986). Prefabricated Vertical Drains Volume I, Engineering Guidelines, FHWA-RD-86-168. U.S. Department of Transportation, Federal Highway Administration, Office of Engineering and Highway Operations Research and Development, McLean, VA, 117 p.

Sabatini, P. J., Elias, V., Schmertmann, G. R., and Bonaparte, R. (1997). Earth Retaining Systems FHWA-SA-96-038, Geotechnical Engineering Circular (GEC) No. 2. U.S. Department of Transportation, Federal Highway Administration, Washington, D.C.

Sabatini, P.J., Tanyu, B., Armour., P., Groneck, P., and Keeley, J. (2005). Micropile Design and Construction, FHWA-NHI-05-039. National Highway Institute, U.S. Dept. of Transportation, Federal Highway Administration, Washington, D.C., 436 p.

Samtani, N.C. and Nowatzki, E.A. (2006). Soils and Foundations: Reference Manual, Vol. 1, FHWA-NHI-06-088, U.S. Dept. of Transportation, National Highway Institute, Federal Highway Administration, Washington, D.C., 462 p.

Samtani, N.C., Nowatzki, E.A., and Mertz, D.R. (2010). Selection of Spread Footings on Soils to Support Highway Bridge Structures, FHWA-RC TD-10-001. U.S. Department of Transportation, Federal Highway Administration, Washington, D.C., 98 p.

Schmertmann, J.H. (1978). Guidelines For Cone Penetration Test, Performance, and Design, FHWA-TS-78-209. U.S. Department of Transportation, Federal Highway Administration, Washington, D.C., 145 p.

Tanyu B.F., Sabatini, P. J., and Berg, R.R. (2008). Earth Retaining Structures, FHWA-NHI-07-07. U.S. Department of Transportation, Federal Highway Administration, Washington, D.C., 792 p.

Wightman, W., Jalinoos, F., Sirles., and Hanna, K. (2003), Applications of Geophysical Methods to Related Highway Problems. U.S. Dept. of Transportation, Federal Highway Administration, 716 p.

Wilson, K.E., Kimmerling, R.E., Goble, G.C., Sabatini, P.J., Zang, S.D., Zhou, J.Y. Amrhein, W.A., Bouscher, J.W. and Danaovich, L.J. (2006). LRFD for Highway Bridge Substructures and Earth Retaining Structures Reference Manual, FHWA NHI-05-094. U.S. Dept. of Transportation, Federal Highway Administration, Washington, D.C., 1730 p.

Appendix B

LIST OF ASTM AND AASHTO PILE DESIGN AND TESTING SPECIFICATIONS

American Association of State Highway and Transportation Offices (AASHTO). Standard Method of Test for High Strain Dynamic Testing of Piles, AASHTO Designation T-298-33.

American Association of State Highway and Transportation Officials (AASHTO). (1978). Manual on Foundation Investigations Second Edition.. AASHTO Highway Subcommittee on Bridges and Structures, Washington, D.C., 196 p.

American Association of State Highway and Transportation Officials (AASHTO). (2001). Standard Recommended Practice for Assessment of Corrosion of Steel Piling for Non-Marine Applications. AASHTO Standard Specifications for Transportation Materials and Methods of Sampling and Testing, Part 1B: Specifications, 24th Edition,. 13 p.

American Association of State Highway and Transportation Officials (AASHTO). (2011) Guide Specifications for LRFD Seismic Bridge Design, 2nd Edition, with 2012, 2014, and 2015 Interim Revisions. American Association of State Highway and Transportation Officials, Washington, D.C., 331 p.

American Association of State Highway and Transportation Officials (AASHTO). (2014). AASHTO LRFD Bridge Design Specifications, US Customary Units, Seventh Edition, with 2015 Interim Revisions. American Association of State Highway and Transportation Officials, Washington, D.C., 1960 p.

ASTM A27-13. (2014). Standard Specification for Steel Castings, Carbon, for General Application. Book of ASTM Standards, Vol. 1.02, ASTM International, West Conshohocken, PA, 4 p.

ASTM A572-15. (2015). Standard Specification for High-Strength Low-Alloy Columbium-Vanadium Structural Steel. Book of ASTM Standards, Vol. 1.04, ASTM International, West Conshohocken, PA, 4 p.

ASTM D1143-07. (2014). Standard Test Methods for Deep Foundations Under Static Axial Compressive Load. Book of ASTM Standards, Vol. 4.08, ASTM International, West Conshohocken, PA, 15 p.

ASTM D1452-09. (2014). Standard Practice for Soil Exploration and Sampling by Auger Borings. Annual Book of ASTM Standards, Vol. 4.08, ASTM International, West Conshohocken, PA, 6 p.

ASTM D1586-11. (2014). Standard Test Method for Standard Penetration Test (SPT) and Split-Barrel Sampling of Soils. Annual Book of ASTM Standards, Vol. 4.08, ASTM International, West Conshohocken, PA, 9 p.

ASTM D1587-12. (2014). Standard Practice for Thin-Walled Tube Sampling of Soils for Geotechnical Purposes. Annual Book of ASTM Standards, Vol. 4.08, ASTM International, West Conshohocken, PA, 4 p.

ASTM D2113-14. (2014). Standard Practice for Rock Core Drilling and Sampling of Rock for Site Investigation. Annual Book of ASTM Standards, Vol. 4.08, ASTM International, West Conshohocken, PA, 20 p.

ASTM D2573-08. (2012). Standard Test Method for Field Vane Shear Test in Cohesive Soil. Annual Book of ASTM Standards, Vol. 4.08, ASTM International, West Conshohocken, PA, 8 p.

ASTM D3689-07. (2014). Standard Test Methods for Deep Foundations Under Static Axial Tensile Load. Book of ASTM Standards, Vol. 4.08, ASTM International, West Conshohocken, PA, 13 p.

ASTM D4633-10. (2014). Standard Test Method for Energy Measurement for Dynamic Penetrometer. Book of ASTM Standards, Vol. 4.08, ASTM International, West Conshohocken, PA, 7 p.

ASTM D4719-07. (2014). Standard Test Methods for Prebored Pressuremeter Testing in Soils Annual. Book of ASTM Standards, Vol. 4.08, ASTM International, West Conshohocken, PA, 10 p.

ASTM D4945-12. (2014). Standard Test Method for High-Strain Dynamic Testing of Piles. Book of ASTM Standards, Vol. 4.08, ASTM International, West Conshohocken, PA, 9 p.

ASTM D4971-02. (2014). Standard Test Method for Determining the In Situ Modulus of Deformation of Rock Using the Diametrically Loaded 76-mm (3-in.) Borehole Jack. Book of ASTM Standards, Vol. 4.08, ASTM International, West Conshohocken, PA, 7 p.

ASTM D5778-12. (2014). Standard Test Method for Electronic Friction Cone and Piezocone Penetration Testing of Soils. Book of ASTM Standards, Vol. 4.08, ASTM International, West Conshohocken, PA, 20 p.

ASTM D5882-07. (2013). Standard Test Method for Low-Strain Dynamic Testing of Piles Annual Book of ASTM Standards, Vol. 4.09, ASTM International, West Conshohocken, PA, 6 p.

ASTM D6032-08. (2014). Standard Test Method for Determining Rock Quality Designation (RQD) of Rock Core. Annual Book of ASTM Standards, Vol. 4.09, ASTM International, West Conshohocken, PA, 5 p.

ASTM D6635-07. (2014). Standard Test Method for Performing the Flat Dilatometer. Book of ASTM Standards, Vol. 4.09, ASTM International, West Conshohocken, PA, 16 p.

ASTM D7012-14. (2014). Standard Tests Method for Compressive Strength and Elastic Moduli of Intact Rock Core Specimens under Varying States of Stress and Temperatures. Annual Book of ASTM Standards, Vol. 4.09, ASTM International, West Conshohocken, PA, 9 p.

ASTM D7383-10 (2010). Standard Test Methods for Axial Compressive Force Pulse (Rapid) Testing of Deep Foundations. Annual Book of ASTM Standards, Vol. 4.08, ASTM International, West Conshohocken, PA, 9 p.

ASTM Vol 4.08. (2014). Soil and Rock I, Vol. 4.08, ASTM International, West Conshohocken, PA, 1826 p.

ASTM Vol 4.09. (2014). Soil and Rock II, Vol. 4.09, ASTM International, West Conshohocken, PA, 1754 p.

Appendix C

PILE HAMMER INFORMATION

Type	Hammer Make	Hammer Model	Hammer Type	Rated Energy kip-feet	Ram Weight kips	Stroke feet
1	DELMAG	D 5	OED	10.51	1.10	9.55
2	DELMAG	D 8-22	OED	20.10	1.76	11.42
3	DELMAG	D 12	OED	22.61	2.75	8.22
4	DELMAG	D 15	OED	27.09	3.30	8.21
5	DELMAG	D 16-32	OED	40.20	3.52	11.42
6	DELMAG	D 22	OED	40.61	4.91	8.27
7	DELMAG	D 22-02	OED	48.50	4.85	10.00
8	DELMAG	D 22-13	OED	48.50	4.85	10.00
9	DELMAG	D 22-23	OED	51.22	4.85	10.56
10	DELMAG	D 25-32	OED	66.34	5.51	12.04
11	DELMAG	D 30	OED	59.73	6.60	9.05
12	DELMAG	D 30-02	OED	66.20	6.60	10.03
13	DELMAG	D 30-13	OED	66.20	6.60	10.03
14	DELMAG	D 30-23	OED	73.79	6.60	11.18
15	DELMAG	D 30-32	OED	75.44	6.60	11.43
16	DELMAG	D 36	OED	83.82	7.93	10.57
17	DELMAG	D 36-02	OED	83.82	7.93	10.57
18	DELMAG	D 36-13	OED	83.82	7.93	10.57
19	DELMAG	D 36-23	OED	88.50	7.93	11.16
20	DELMAG	D 36-32	OED	90.56	7.93	11.42
21	DELMAG	D 44	OED	90.16	9.50	9.49
22	DELMAG	D 46	OED	107.08	10.14	10.56
23	DELMAG	D 46-02	OED	107.08	10.14	10.56
24	DELMAG	D 46-13	OED	96.53	10.14	9.52
25	DELMAG	D 46-23	OED	107.08	10.14	10.56
26	DELMAG	D 46-32	OED	122.19	10.14	12.05
27	DELMAG	D 55	OED	125.00	11.86	10.54
28	DELMAG	D 62-02	OED	152.45	13.66	11.16
29	DELMAG	D 62-12	OED	152.45	13.66	11.16
30	DELMAG	D 62-22	OED	164.60	13.66	12.05
31	DELMAG	D 80-12	OED	186.24	17.62	10.57
32	DELMAG	D 80-23	OED	212.50	17.62	12.06
33	DELMAG	D100-13	OED	265.68	22.07	12.04
35	DELMAG	D 19-52	OED	43.20	4.00	10.80
36	DELMAG	D 6-32	OED	13.52	1.32	10.23

Type	Hammer Make	Hammer Model	Hammer Type	Rated Energy kip-feet	Ram Weight kips	Stroke feet
37	DELMAG	D 12-32	OED	31.33	2.82	11.11
38	DELMAG	D 12-42	OED	33.30	2.82	11.81
39	DELMAG	D 14-42	OED	34.50	3.09	11.18
40	DELMAG	D 19-32	OED	42.44	4.00	10.61
41	DELMAG	D 19-42	OED	43.24	4.00	10.81
42	DELMAG	D200-42	OED	492.04	44.09	11.16
43	DELMAG	D120-42	OED	301.79	26.45	11.41
44	DELMAG	D150-42	OED	377.33	33.07	11.41
45	DELMAG	D125-42	OED	313.63	27.56	11.38
46	DELMAG	D 21-42	OED	55.75	4.63	12.04
47	DELMAG	D 5-42	OED	10.56	1.10	9.60
48	DELMAG	D160-32	OED	393.45	35.27	11.16
49	DELMAG	D260-32	OED	639.36	57.32	11.16
50	FEC	1200	OED	22.50	2.75	8.18
51	FEC	1500	OED	27.09	3.30	8.21
52	FEC	2500	OED	50.00	5.50	9.09
53	FEC	2800	OED	55.99	6.16	9.09
54	FEC	3000	OED	63.03	6.60	9.55
55	FEC	3400	OED	73.01	7.48	9.76
56	FEC	D-18	OED	39.70	3.97	10.00
61	MITSUBIS	M 14	OED	25.25	2.97	8.50
62	MITSUBIS	MH 15	OED	28.14	3.31	8.50
63	MITSUBIS	M 23	OED	43.01	5.06	8.50
64	MITSUBIS	MH 25	OED	46.84	5.51	8.50
65	MITSUBIS	M 33	OED	61.71	7.26	8.50
66	MITSUBIS	MH 35	OED	65.62	7.72	8.50
67	MITSUBIS	M 43	OED	80.41	9.46	8.50
68	MITSUBIS	MH 45	OED	85.43	10.05	8.50
70	MITSUBIS	MH 72B	OED	135.15	15.90	8.50
71	MITSUBIS	MH 80B	OED	149.60	17.60	8.50
81	LINKBELT	LB 180	CED	8.10	1.73	4.68
82	LINKBELT	LB 312	CED	15.02	3.86	3.89
83	LINKBELT	LB 440	CED	18.20	4.00	4.55
84	LINKBELT	LB 520	CED	26.31	5.07	5.19
85	LINKBELT	LB 660	CED	51.63	7.57	6.82
90	HITACHI	HNC65	ECH	56.42	14.33	3.94
91	HITACHI	HNC80	ECH	69.43	17.64	3.94
92	HITACHI	HNC100	ECH	86.79	22.05	3.94
93	HITACHI	HNC125	ECH	108.49	27.56	3.94
101	KOBE	K 13	OED	25.43	2.87	8.86
103	KOBE	K22-Est	OED	45.35	4.85	9.35
104	KOBE	K 25	OED	51.52	5.51	9.35
107	KOBE	K 35	OED	72.18	7.72	9.35

Type	Hammer Make	Hammer Model	Hammer Type	Rated Energy kip-feet	Ram Weight kips	Stroke feet
110	KOBE	K 45	OED	92.75	9.92	9.35
112	KOBE	KB 60	OED	130.18	13.23	9.84
113	KOBE	KB 80	OED	173.58	17.64	9.84
120	ICE	180	CED	8.13	1.73	4.70
121	ICE	422	CED	23.12	4.00	5.78
122	ICE	440	CED	18.56	4.00	4.64
123	ICE	520	CED	30.37	5.07	5.99
124	ICE	640	CED	40.62	6.00	6.77
125	ICE	660	CED	51.63	7.57	6.82
126	ICE	1070	CED	72.60	10.00	7.26
127	ICE	30-S	OED	22.50	3.00	7.50
128	ICE	40-S	OED	40.00	4.00	10.00
129	ICE	42-S	OED	42.00	4.09	10.27
130	ICE	60-S	OED	59.99	7.00	8.57
131	ICE	70-S	OED	70.00	7.00	10.00
132	ICE	80-S	OED	80.00	8.00	10.00
133	ICE	90-S	OED	90.00	9.00	10.00
134	ICE	100-S	OED	100.00	10.00	10.00
135	ICE	120-S	OED	120.00	12.00	10.00
136	ICE	200-S	OED	100.00	20.00	5.00
137	ICE	205-S	OED	170.00	20.00	8.50
139	ICE	32-S	OED	26.01	3.00	8.67
140	ICE	120S-15	OED	132.45	15.00	8.83
142	MKT	DE-20C	OED	20.00	2.00	10.00
143	MKT	DE-30C	OED	28.00	2.80	10.00
144	MKT	DE-33C	OED	33.00	3.30	10.00
145	MKT	DE333020	OED	40.00	4.00	10.00
146	MKT	DE 10	OED	8.80	1.10	8.00
147	MKT	DE 20	OED	16.00	2.00	8.00
148	MKT	DE 30	OED	22.40	2.80	8.00
149	MKT	DA35B SA	OED	23.80	2.80	8.50
150	MKT	DE 30B	OED	23.80	2.80	8.50
151	MKT	DA 35B	CED	21.00	2.80	7.50
152	MKT	DA 45	CED	30.72	4.00	7.68
153	MKT	DE 40	OED	32.00	4.00	8.00
154	MKT	DE 35	OED	35.00	3.50	10.00
155	MKT	DE 42	OED	42.00	4.20	10.00
157	MKT	DE 50C	OED	50.00	5.00	10.00
158	MKT	DE 70C	OED	70.00	7.00	10.00
159	MKT	DE 50B	OED	42.50	5.00	8.50
160	MKT	DA55B SA	OED	40.00	5.00	8.00
161	MKT	DA 55B	CED	38.20	5.00	7.64
162	MKT	DE 70B	OED	59.50	7.00	8.50

Type	Hammer Make	Hammer Model	Hammer Type	Rated Energy kip-feet	Ram Weight kips	Stroke feet
163	MKT	DE-50B	OED	50.00	5.00	10.00
164	MKT	DE-70B	OED	70.00	7.00	10.00
165	MKT	DE-110C	OED	110.00	11.00	10.00
166	MKT	DE-150C	OED	150.00	15.00	10.00
167	MKT	DA 35C	CED	21.00	2.80	7.50
168	MKT	DA 55C	CED	38.20	5.00	7.64
171	CONMACO	C 50	ECH	15.00	5.00	3.00
172	CONMACO	C 65	ECH	19.50	6.50	3.00
173	CONMACO	C 550	ECH	25.00	5.00	5.00
174	CONMACO	C 565	ECH	32.50	6.50	5.00
175	CONMACO	C 80	ECH	26.00	8.00	3.25
176	CONMACO	C 100	ECH	32.50	10.00	3.25
177	CONMACO	C 115	ECH	37.38	11.50	3.25
178	CONMACO	C 80E5	ECH	40.00	8.00	5.00
179	CONMACO	C 100E5	ECH	50.00	10.00	5.00
180	CONMACO	C 115E5	ECH	57.50	11.50	5.00
181	CONMACO	C 125E5	ECH	62.50	12.50	5.00
182	CONMACO	C 140	ECH	42.00	14.00	3.00
183	CONMACO	C 160	ECH	48.75	16.25	3.00
184	CONMACO	C 200	ECH	60.00	20.00	3.00
185	CONMACO	C 300	ECH	90.00	30.00	3.00
186	CONMACO	C 5200	ECH	100.00	20.00	5.00
187	CONMACO	C 5300	ECH	150.00	30.00	5.00
188	CONMACO	C 5450	ECH	225.00	45.00	5.00
189	CONMACO	C 5700	ECH	350.00	70.00	5.00
190	CONMACO	C 6850	ECH	510.00	85.00	6.00
191	CONMACO	C 160 **	ECH	51.78	17.26	3.00
192	CONMACO	C 50E5	ECH	25.00	5.00	5.00
193	CONMACO	C 65E5	ECH	32.50	6.50	5.00
194	CONMACO	C 200E5	ECH	100.00	20.00	5.00
195	CONMACO	C 300E5	ECH	150.00	30.00	5.00
196	CONMACO	C 1750	ECH	1050.00	175.00	6.00
204	VULCAN	VUL 01	ECH	15.00	5.00	3.00
205	VULCAN	VUL 02	ECH	7.26	3.00	2.42
206	VULCAN	VUL 06	ECH	19.50	6.50	3.00
207	VULCAN	VUL 08	ECH	26.00	8.00	3.25
208	VULCAN	VUL 010	ECH	32.50	10.00	3.25
209	VULCAN	VUL 012	ECH	39.00	12.00	3.25
210	VULCAN	VUL 014	ECH	42.00	14.00	3.00
211	VULCAN	VUL 016	ECH	48.75	16.25	3.00
212	VULCAN	VUL 020	ECH	60.00	20.00	3.00
213	VULCAN	VUL 030	ECH	90.00	30.00	3.00
214	VULCAN	VUL 040	ECH	120.00	40.00	3.00

Type	Hammer Make	Hammer Model	Hammer Type	Rated Energy kip-feet	Ram Weight kips	Stroke feet
215	VULCAN	VUL 060	ECH	180.00	60.00	3.00
220	VULCAN	VUL 30C	ECH	7.26	3.00	2.42
221	VULCAN	VUL 50C	ECH	15.10	5.00	3.02
222	VULCAN	VUL 65C	ECH	19.18	6.50	2.95
223	VULCAN	VUL 65CA	ECH	19.57	6.50	3.01
224	VULCAN	VUL 80C	ECH	24.48	8.00	3.06
225	VULCAN	VUL 85C	ECH	25.99	8.52	3.05
226	VULCAN	VUL 100C	ECH	32.90	10.00	3.29
227	VULCAN	VUL 140C	ECH	35.98	14.00	2.57
228	VULCAN	VUL 200C	ECH	50.20	20.00	2.51
229	VULCAN	VUL 400C	ECH	113.60	40.00	2.84
230	VULCAN	VUL 600C	ECH	179.16	60.00	2.99
231	VULCAN	VUL 320	ECH	60.00	20.00	3.00
232	VULCAN	VUL 330	ECH	90.00	30.00	3.00
233	VULCAN	VUL 340	ECH	120.00	40.00	3.00
234	VULCAN	VUL 360	ECH	180.00	60.00	3.00
235	VULCAN	VUL 505	ECH	25.00	5.00	5.00
236	VULCAN	VUL 506	ECH	32.50	6.50	5.00
237	VULCAN	VUL 508	ECH	40.00	8.00	5.00
238	VULCAN	VUL 510	ECH	50.00	10.00	5.00
239	VULCAN	VUL 512	ECH	60.00	12.00	5.00
240	VULCAN	VUL 520	ECH	100.00	20.00	5.00
241	VULCAN	VUL 530	ECH	150.00	30.00	5.00
242	VULCAN	VUL 540	ECH	200.00	40.90	4.89
243	VULCAN	VUL 560	ECH	300.00	62.50	4.80
245	VULCAN	VUL 3100	ECH	300.00	100.00	3.00
246	VULCAN	VUL 5100	ECH	500.00	100.00	5.00
247	VULCAN	VUL 5150	ECH	750.00	150.00	5.00
248	VULCAN	VUL 6300	ECH	1800.00	300.00	6.00
251	RAYMOND	R 1	ECH	15.00	5.00	3.00
252	RAYMOND	R 1S	ECH	19.50	6.50	3.00
253	RAYMOND	R 65C	ECH	19.50	6.50	3.00
254	RAYMOND	R 65CH	ECH	19.50	6.50	3.00
255	RAYMOND	R 0	ECH	24.38	7.50	3.25
256	RAYMOND	R 80C	ECH	24.48	8.00	3.06
257	RAYMOND	R 80CH	ECH	24.48	8.00	3.06
258	RAYMOND	R 2/0	ECH	32.50	10.00	3.25
259	RAYMOND	R 3/0	ECH	40.63	12.50	3.25
260	RAYMOND	R 150C	ECH	48.75	15.00	3.25
261	RAYMOND	R 4/0	ECH	48.75	15.00	3.25
262	RAYMOND	R 5/0	ECH	56.88	17.50	3.25
263	RAYMOND	R 30X	ECH	75.00	30.00	2.50
264	RAYMOND	R 8/0	ECH	81.25	25.00	3.25

Type	Hammer Make	Hammer Model	Hammer Type	Rated Energy kip-feet	Ram Weight kips	Stroke feet
265	RAYMOND	R 40X	ECH	100.00	40.00	2.50
266	RAYMOND	R 60X	ECH	150.00	60.00	2.50
270	MENCK	MHU 100C	ECH	73.71	11.10	6.64
271	MENCK	MH 68	ECH	49.18	7.72	6.37
272	MENCK	MH 96	ECH	69.43	11.02	6.30
273	MENCK	MH 145	ECH	104.80	16.53	6.34
274	MENCK	MHU 195	ECH	143.74	21.36	6.73
275	MENCK	MHU 220	ECH	162.17	24.84	6.53
276	MENCK	MHU 400	ECH	294.82	51.09	5.77
277	MENCK	MHU 600	ECH	442.28	75.52	5.86
278	MENCK	MHU 1000	ECH	737.38	126.98	5.81
279	MENCK	MHU 1700	ECH	1253.24	207.15	6.05
280	MENCK	MHU 2100	ECH	1548.29	257.18	6.02
281	MENCK	MHU 3000	ECH	2211.90	370.23	5.97
282	MENCK	MRBS 500	ECH	45.07	11.02	4.09
283	MENCK	MRBS 750	ECH	67.77	16.53	4.10
285	MENCK	MRBS 850	ECH	93.28	18.96	4.92
286	MENCK	MRBS1100	ECH	123.43	24.25	5.09
287	MENCK	MRBS1502	ECH	135.59	33.07	4.10
288	MENCK	MRBS1800	ECH	189.81	38.58	4.92
289	MENCK	MRBS2500	ECH	262.11	63.93	4.10
290	MENCK	MRBS2502	ECH	225.95	55.11	4.10
291	MENCK	MRBS2504	ECH	225.95	55.11	4.10
292	MENCK	MRBS3000	ECH	325.36	66.13	4.92
293	MENCK	MRBS3900	ECH	513.34	86.86	5.91
294	MENCK	MRBS4600	ECH	498.94	101.41	4.92
295	MENCK	MRBS5000	ECH	542.33	110.23	4.92
296	MENCK	MRBS6000	ECH	759.23	132.27	5.74
297	MENCK	MRBS7000	ECH	631.40	154.00	4.10
298	MENCK	MRBS8000	ECH	867.74	176.37	4.92
299	MENCK	MRBS8800	ECH	954.53	194.01	4.92
300	MENCK	MBS12500	ECH	1581.83	275.58	5.74
301	MKT	No. 5	ECH	1.00	0.20	5.00
302	MKT	No. 6	ECH	2.50	0.40	6.25
303	MKT	No. 7	ECH	4.15	0.80	5.19
304	MKT	9B3	ECH	8.75	1.60	5.47
305	MKT	10B3	ECH	13.11	3.00	4.37
306	MKT	C5-Air	ECH	14.20	5.00	2.84
307	MKT	C5-Steam	ECH	16.20	5.00	3.24
308	MKT	S-5	ECH	16.25	5.00	3.25
309	MKT	11B3	ECH	19.15	5.00	3.83
310	MKT	C826 Stm	ECH	24.40	8.00	3.05
311	MKT	C826 Air	ECH	21.20	8.00	2.65

Type	Hammer Make	Hammer Model	Hammer Type	Rated Energy kip-feet	Ram Weight kips	Stroke feet
312	MKT	S-8	ECH	26.00	8.00	3.25
313	MKT	MS-350	ECH	30.80	7.72	3.99
314	MKT	S 10	ECH	32.50	10.00	3.25
315	MKT	S 14	ECH	37.52	14.00	2.68
316	MKT	MS 500	ECH	44.00	11.00	4.00
317	MKT	S 20	ECH	60.00	20.00	3.00
318	IHC	S-30	ECH	21.70	3.53	6.15
319	IHC	S-40	ECH	28.93	4.85	5.97
320	IHC	S-35	ECH	25.53	6.63	3.85
321	IHC	S-70	ECH	51.25	7.73	6.63
322	IHC	S-90	ECH	65.90	9.94	6.63
323	IHC	S-120	ECH	89.37	13.48	6.63
324	IHC	S-150	ECH	110.06	16.60	6.63
325	IHC	S-200	ECH	145.64	22.00	6.62
326	IHC	S-280	ECH	205.31	30.06	6.83
327	IHC	S-400	ECH	292.60	44.20	6.62
328	IHC	S-500	ECH	366.09	55.30	6.62
329	IHC	S-600	ECH	443.54	67.00	6.62
330	IHC	S-900	ECH	658.36	99.45	6.62
331	IHC	S-1200	ECH	891.05	134.60	6.62
332	IHC	S-1800-L	ECH	1170.39	166.00	7.05
333	IHC	S-2300	ECH	1681.48	254.00	6.62
334	IHC	S-2000	ECH	1473.97	222.65	6.62
335	IHC	SC-30	ECH	21.81	3.76	5.80
336	IHC	SC-40	ECH	29.86	5.51	5.42
337	IHC	SC-50	ECH	36.82	7.29	5.05
338	IHC	SC-60	ECH	44.95	13.30	3.38
339	IHC	SC-75	ECH	54.80	12.15	4.51
340	IHC	SC-110	ECH	81.89	17.46	4.69
341	IHC	SC-150	ECH	109.35	24.30	4.50
342	IHC	SC-200	ECH	152.51	30.20	5.05
343	IHC	SC-250	ECH	179.80	37.26	4.83
344	IHC	S-750	ECH	550.79	83.11	6.63
345	IHC	S-800	ECH	589.97	88.15	6.69
346	IHC	S-1400	ECH	1033.84	147.94	6.99
347	IHC	S-1800	ECH	1340.21	195.64	6.85
348	IHC	S-2500	ECH	1843.16	275.80	6.68
349	HERA	1900	OED	44.41	4.19	10.60
350	HERA	1250	OED	24.85	2.76	9.02
351	HERA	1500	OED	29.81	3.31	9.02
352	HERA	2500	OED	49.70	5.51	9.02
353	HERA	2800	OED	55.70	6.18	9.02
354	HERA	3500	OED	69.59	7.72	9.02

Type	Hammer Make	Hammer Model	Hammer Type	Rated Energy kip-feet	Ram Weight kips	Stroke feet
355	HERA	5000	OED	99.45	11.03	9.02
356	HERA	5700	OED	113.38	12.57	9.02
357	HERA	6200	OED	123.30	13.67	9.02
358	HERA	7500	OED	149.19	16.54	9.02
359	HERA	8800	OED	174.99	19.40	9.02
360	ICE	I-12obs	OED	30.21	2.82	10.71
361	ICE	I-19obs	OED	43.24	4.02	10.77
362	ICE	I-30obs	OED	71.45	6.62	10.80
363	ICE	I-36obs	OED	90.68	7.94	11.42
364	ICE	I-46obs	OED	107.74	10.15	10.62
365	ICE	I-62obs	OED	164.98	14.60	11.30
366	ICE	I-80obs	OED	212.40	17.70	12.00
367	ICE	I-8v2obs	OED	17.60	1.76	10.00
368	ICE	I-100obs	OED	264.45	23.61	11.20
369	BSP	SL20	ECH	14.11	3.31	4.27
370	BSP	SL30	ECH	21.69	5.51	3.94
371	FAIRCHLD	F-45	ECH	45.00	15.00	3.00
372	FAIRCHLD	F-32	ECH	32.55	10.85	3.00
374	BSP	CX40	ECH	28.21	6.61	4.27
375	BSP	CX50	ECH	37.61	8.82	4.27
376	BSP	CX60	ECH	47.01	11.02	4.27
377	BSP	CX75	ECH	52.08	13.23	3.94
378	BSP	CX85	ECH	60.75	15.43	3.94
379	BSP	CX110	ECH	78.11	19.84	3.94
381	BSP	HH3	ECH	26.02	6.61	3.94
382	BSP	HH5	ECH	43.38	11.02	3.94
383	BSP	HH7	ECH	60.78	15.43	3.94
384	BSP	HH8	ECH	69.50	17.64	3.94
385	BSP	HH9	ECH	78.17	19.84	3.94
386	BSP	HH11-1.2	ECH	95.55	24.25	3.94
387	BSP	HH14-1.2	ECH	121.59	30.86	3.94
388	BSP	HH16-1.2	ECH	138.87	35.27	3.94
391	BSP	HA30	ECH	260.37	66.14	3.94
392	BSP	HA40	ECH	347.16	88.18	3.94
393	BSP	HH11-1.5	ECH	119.31	24.25	4.92
394	BSP	HH14-1.5	ECH	151.83	30.86	4.92
395	BSP	HH16-1.5	ECH	173.54	35.27	4.92
396	BSP	CG180	ECH	131.92	26.45	4.99
397	BSP	CG210	ECH	153.91	30.86	4.99
398	BSP	CG240	ECH	175.90	35.27	4.99
399	BSP	CG270	ECH	197.88	39.68	4.99
400	BSP	CG300	ECH	219.87	44.09	4.99
401	BERMINGH	B23	CED	22.99	2.80	8.21

Type	Hammer Make	Hammer Model	Hammer Type	Rated Energy kip-feet	Ram Weight kips	Stroke feet
402	BERMINGH	B200	OED	18.00	2.00	9.00
403	BERMINGH	B225	OED	29.25	3.00	9.75
404	BERMINGH	B300	OED	40.31	3.75	10.75
405	BERMINGH	B400	OED	53.75	5.00	10.75
406	BERMINGH	B-21	OED	53.25	4.63	11.50
410	BERMINGH	B300 M	OED	40.31	3.75	10.75
411	BERMINGH	B400 M	OED	53.75	5.00	10.75
412	BERMINGH	B400 4.8	OED	43.20	4.80	9.00
413	BERMINGH	B400 5.0	OED	45.00	5.00	9.00
414	BERMINGH	B23 5	CED	22.99	2.80	8.21
415	BERMINGH	B250 5	OED	26.25	2.50	10.50
416	BERMINGH	B3505	OED	47.20	4.00	11.80
417	BERMINGH	B4005	OED	59.00	5.00	11.80
418	BERMINGH	B4505	OED	77.88	6.60	11.80
419	BERMINGH	B5005	OED	92.04	7.80	11.80
420	BERMINGH	B5505	OED	108.56	9.20	11.80
421	BERMINGH	B550 C	OED	88.00	11.00	8.00
422	BERMINGH	B2005	OED	18.00	2.00	9.00
424	BERMINGH	B2505	OED	35.40	3.00	11.80
425	BERMINGH	B3005	OED	35.40	3.00	11.80
431	BERMINGH	B6005	OED	160.95	13.64	11.80
432	BERMINGH	B6505 C	OED	253.00	22.00	11.50
433	BERMINGH	B6505	OED	202.86	17.64	11.50
434	BERMINGH	B-9	OED	21.00	2.00	10.50
435	BERMINGH	B-32	OED	81.08	7.05	11.50
436	BERMINGH	B-64	OED	166.50	14.11	11.80
437	BERMINGH	B-6505HD	OED	220.50	22.05	10.00
441	MENCK	MHF5-5	ECH	38.69	11.02	3.51
442	MENCK	MHF5-6	ECH	46.43	13.23	3.51
443	MENCK	MHF5-7	ECH	54.17	15.43	3.51
444	MENCK	MHF5-8	ECH	61.91	17.64	3.51
445	MENCK	MHF5-9	ECH	69.65	19.84	3.51
446	MENCK	MHF5-10	ECH	77.39	22.05	3.51
447	MENCK	MHF5-11	ECH	85.13	24.25	3.51
448	MENCK	MHF5-12	ECH	92.87	26.45	3.51
449	MENCK	MHF3-3	ECH	24.76	7.05	3.51
450	MENCK	MHF3-4	ECH	30.96	8.82	3.51
451	MENCK	MHF3-5	ECH	38.69	11.02	3.51
452	MENCK	MHF3-6	ECH	46.43	13.23	3.51
453	MENCK	MHF3-7	ECH	54.17	15.43	3.51
454	MENCK	MHF10-15	ECH	124.73	33.06	3.77
455	MENCK	MHF10-20	ECH	166.28	44.07	3.77
456	MENCK	MHF 5-14	ECH	108.34	30.86	3.51

Type	Hammer Make	Hammer Model	Hammer Type	Rated Energy kip-feet	Ram Weight kips	Stroke feet
457	MENCK	MHU135T*	ECH	110.59	17.99	6.15
458	MENCK	MHU500T*	ECH	368.74	65.96	5.59
459	MENCK	MHU 300S	ECH	221.20	35.73	6.19
460	MENCK	MHU 270T	ECH	221.20	35.73	6.19
461	MENCK	MHU 200T	ECH	162.24	26.75	6.07
462	MENCK	MHU 400T	ECH	324.37	52.45	6.18
463	MENCK	MHU 500T	ECH	405.53	65.96	6.15
464	MENCK	MHU 700T	ECH	567.72	92.88	6.11
465	MENCK	MHU 840S	ECH	619.22	92.88	6.67
466	MENCK	MHU 600B	ECH	457.03	65.96	6.93
467	MENCK	MHU 600T	ECH	486.63	80.39	6.05
468	MENCK	MHU 800S	ECH	604.57	99.93	6.05
469	MENCK	MHU1200S	ECH	884.84	145.71	6.07
470	MENCK	MHU1500S	ECH	1106.07	178.94	6.18
471	MENCK	MHU1700T	ECH	1400.86	227.36	6.16
472	MENCK	MHU1900S	ECH	1400.86	227.36	6.16
473	MENCK	MHU 150S	ECH	110.59	17.99	6.15
474	MENCK	MHU2700S	ECH	1990.19	318.77	6.24
475	MENCK	MHU 135T	ECH	110.59	17.99	6.15
476	MENCK	MHU 750T	ECH	604.57	99.93	6.05
477	MENCK	MHU1100T	ECH	899.66	145.71	6.18
478	MENCK	MHU150S*	ECH	110.59	17.99	6.15
479	MENCK	MHU600B*	ECH	457.03	65.96	6.93
481	JUNTTAN	HHK3A	ECH	26.05	6.62	3.94
482	JUNTTAN	HHK4A	ECH	34.73	8.82	3.94
483	JUNTTAN	HHK5A	ECH	43.41	11.03	3.94
484	JUNTTAN	HHK6A	ECH	52.10	13.23	3.94
485	JUNTTAN	HHK7A	ECH	60.75	15.43	3.94
486	JUNTTAN	HHK10A	ECH	86.83	22.05	3.94
487	JUNTTAN	HHK12A	ECH	104.19	26.47	3.94
488	JUNTTAN	HHK14A	ECH	121.56	30.88	3.94
491	JUNTTAN	HHK9A	ECH	78.14	19.85	3.94
494	JUNTTAN	HHK16A	ECH	138.92	35.29	3.94
495	JUNTTAN	HHK18A	ECH	156.29	39.70	3.94
496	JUNTTAN	HHK20A	ECH	173.65	44.11	3.94
497	JUNTTAN	HHK4SL	ECH	43.40	8.82	4.92
498	JUNTTAN	HHK3AL	ECH	17.37	6.62	2.63
499	JUNTTAN	HHK4AL	ECH	23.15	8.82	2.63
500	JUNTTAN	HHK5AL	ECH	28.94	11.03	2.63
501	HPSI	110	ECH	44.00	11.00	4.00
502	HPSI	150	ECH	60.00	15.00	4.00
503	HPSI	154	ECH	61.60	15.40	4.00
504	HPSI	200	ECH	80.00	20.00	4.00

Type	Hammer Make	Hammer Model	Hammer Type	Rated Energy kip-feet	Ram Weight kips	Stroke feet
505	HPSI	225	ECH	90.00	22.50	4.00
506	HPSI	650	ECH	32.50	6.50	5.00
507	HPSI	1000	ECH	50.00	10.00	5.00
508	HPSI	1605	ECH	83.00	16.60	5.00
509	HPSI	2005	ECH	95.10	19.02	5.00
510	HPSI	3005	ECH	154.33	30.87	5.00
511	HPSI	3505	ECH	176.33	35.27	5.00
512	HPSI	2000	ECH	80.00	20.00	4.00
514	UDDCOMB	H2H	ECH	16.62	4.40	3.77
515	UDDCOMB	H3H	ECH	24.88	6.60	3.77
516	UDDCOMB	H4H	ECH	33.18	8.80	3.77
517	UDDCOMB	H5H	ECH	41.47	11.00	3.77
518	UDDCOMB	H6H	ECH	49.76	13.20	3.77
519	UDDCOMB	H8H	ECH	82.19	17.60	4.67
520	UDDCOMB	H10H	ECH	86.88	22.05	3.94
521	DAWSON	HPH1200	ECH	8.72	2.30	3.79
522	DAWSON	HPH1800	ECH	13.72	3.30	4.16
523	DAWSON	HPH2400	ECH	17.32	4.19	4.13
524	DAWSON	HPH6500	ECH	46.98	10.25	4.58
525	DAWSON	HPH4500	ECH	32.56	7.72	4.22
526	DAWSON	HPH9000	ECH	66.30	10.47	6.33
530	BRUCE	SGH-0312	ECH	26.00	6.60	3.94
531	BRUCE	SGH-0512	ECH	43.34	11.00	3.94
532	BRUCE	SGH-0712	ECH	60.68	15.40	3.94
533	BRUCE	SGH-1012	ECH	86.77	22.05	3.94
534	BRUCE	SGH-0412	ECH	34.67	8.80	3.94
535	BANUT	S3000	ECH	26.04	6.62	3.94
536	BANUT	S4000	ECH	34.72	8.82	3.94
537	BANUT	S5000	ECH	43.41	11.03	3.94
538	BANUT	S6000	ECH	52.09	13.23	3.94
539	BANUT	S8000	ECH	69.45	17.64	3.94
540	BANUT	S10000	ECH	86.81	22.05	3.94
541	BANUT	3 Tonnes	ECH	17.35	6.61	2.62
542	BANUT	4 Tonnes	ECH	23.14	8.82	2.62
543	BANUT	5 Tonnes	ECH	28.92	11.02	2.62
544	BANUT	6 Tonnes	ECH	34.72	13.23	2.62
545	BANUT	7 Tonnes	ECH	40.49	15.43	2.62
550	ICE	70	ECH	21.00	7.00	3.00
551	ICE	75	ECH	30.00	7.50	4.00
552	ICE	110-SH	ECH	37.72	11.50	3.28
553	ICE	115-SH	ECH	37.95	11.50	3.30
554	ICE	115	ECH	46.00	11.50	4.00
555	ICE	160-SH	ECH	64.00	16.00	4.00

Type	Hammer Make	Hammer Model	Hammer Type	Rated Energy kip-feet	Ram Weight kips	Stroke feet
556	ICE	160	ECH	64.00	16.00	4.00
557	ICE	220	ECH	88.00	22.00	4.00
558	ICE	275	ECH	110.00	27.50	4.00
559	ICE	DKH-3U	ECH	26.00	6.60	3.94
560	HMC	28A	ECH	28.00	7.00	4.00
561	HMC	28B	ECH	21.00	7.00	3.00
562	HMC	62	ECH	46.00	11.50	4.00
563	HMC	86	ECH	64.00	16.00	4.00
564	HMC	119	ECH	88.00	22.00	4.00
565	HMC	149	ECH	110.00	27.50	4.00
566	HMC	187	ECH	138.00	34.50	4.00
567	HMC	19D	ECH	14.00	3.50	4.00
568	HMC	38D	ECH	28.00	7.00	4.00
569	APE	D 8-42	OED	19.80	1.76	11.25
570	APE	D 1-42	OED	1.32	0.21	6.33
571	APE	D 19-42	OED	47.13	4.19	11.25
572	APE	D 30-42	OED	74.42	6.62	11.25
573	APE	D 36-42	OED	89.30	7.94	11.25
574	APE	D 46-42	OED	114.11	10.14	11.25
575	APE	D 62-42	OED	153.80	13.67	11.25
576	APE	D 80-42	OED	198.45	17.64	11.25
577	APE	D 100-42	OED	248.06	22.05	11.25
579	APE	D 16-42	OED	39.69	3.53	11.25
580	APE	D 16-52	OED	39.69	3.53	11.25
581	APE	D 25-42	OED	62.01	5.51	11.25
582	APE	D 125-42	OED	310.08	27.56	11.25
583	APE	D 50-42	OED	124.03	11.03	11.25
584	APE	D 12-42	OED	29.77	2.65	11.25
585	APE	D 36-26	OED	89.30	7.94	11.25
586	APE	D 128-42	OED	317.25	28.20	11.25
587	APE	D 138-42	OED	342.00	30.40	11.25
588	APE	D 160-42	OED	396.90	35.28	11.25
589	APE	D 180-42	OED	446.51	39.69	11.25
590	APE	D 225-42	OED	558.00	49.60	11.25
591	APE	5.4mT	ECH	26.00	12.00	2.17
592	APE	7.2mT	ECH	51.30	16.20	3.17
593	APE	D 220-42	OED	540.81	48.46	11.16
594	APE	15-60	ECH	150.00	30.00	5.00
595	APE	10-60	ECH	100.00	20.00	5.00
596	APE	400U	ECH	400.00	80.00	5.00
598	APE	750U	ECH	750.00	120.00	6.25
599	APE	D 100-13	OED	300.04	23.70	12.66
600	BSP	DX20	ECH	14.11	3.31	4.27

Type	Hammer Make	Hammer Model	Hammer Type	Rated Energy kip-feet	Ram Weight kips	Stroke feet
601	BSP	DX25	ECH	18.09	4.41	4.10
602	BSP	DX30	ECH	21.71	5.51	3.94
603	BSP	LX2.5-SA	ECH	14.47	5.51	2.63
604	BSP	LX4-SA	ECH	23.15	8.82	2.63
605	BSP	LX5-SA	ECH	28.94	11.03	2.63
606	BSP	CGL370	ECH	271.22	55.11	4.92
607	BSP	CGL440	ECH	325.47	66.14	4.92
608	BSP	CGL520	ECH	379.71	77.16	4.92
609	BSP	CGL590	ECH	433.96	88.18	4.92
610	BSP	LX7-SA	ECH	40.52	15.44	2.63
625	BRUCE	SGH-1212	ECH	104.13	26.46	3.94
626	BRUCE	SGH-1312	ECH	112.81	28.66	3.94
627	BRUCE	SGH-1315	ECH	141.01	28.66	4.92
628	BRUCE	SGH-1412	ECH	121.48	30.87	3.94
629	BRUCE	SGH-1415	ECH	151.85	30.87	4.92
630	BRUCE	SGH-1612	ECH	138.84	35.27	3.94
631	BRUCE	SGH-1615	ECH	173.55	35.27	4.92
632	BRUCE	SGH-1618	ECH	208.26	35.27	5.90
633	BRUCE	SGH-1619	ECH	219.83	35.27	6.23
634	BRUCE	SGH-1812	ECH	156.19	39.68	3.94
635	BRUCE	SGH-1815	ECH	195.24	39.68	4.92
636	BRUCE	SGH-2012	ECH	173.55	44.09	3.94
637	BRUCE	SGH-2015	ECH	216.94	44.09	4.92
638	BRUCE	SGH-2312	ECH	199.58	50.71	3.94
639	BRUCE	SGH-2315	ECH	249.48	50.71	4.92
640	BRUCE	SGH-3012	ECH	260.32	66.14	3.94
641	BRUCE	SGH-3013	ECH	282.02	66.14	4.26
642	BRUCE	SGH-3015	ECH	325.40	66.14	4.92
643	BRUCE	SGH-4012	ECH	347.10	88.19	3.94
644	BRUCE	SGH-4212	ECH	364.45	92.59	3.94
645	BRUCE	SGH-5012	ECH	433.87	110.23	3.94
650	Twinwood	V20B	ECH	35.58	9.04	3.94
651	Twinwood	V100D	ECH	87.66	22.27	3.94
652	Twinwood	V160B	ECH	140.58	35.71	3.94
653	Twinwood	V400A	ECH	263.84	67.02	3.94
656	Pilemast	24-750	ECH	1.50	0.75	2.00
657	Pilemast	24-900	ECH	1.80	0.90	2.00
658	Pilemast	24-2000	ECH	4.00	2.00	2.00
659	Pilemast	24-2500	ECH	5.00	2.50	2.00
660	Pilemast	36-3000	ECH	9.00	3.00	3.00
661	Pilemast	36-5000	ECH	15.00	5.00	3.00
669	MVE	M-12	OED	30.21	2.82	10.71
670	MVE	M-19	OED	49.38	4.02	12.30

Type	Hammer Make	Hammer Model	Hammer Type	Rated Energy kip-feet	Ram Weight kips	Stroke feet
671	MVE	M-30	OED	83.35	6.62	12.60
801	DKH	PH-5	ECH	43.40	11.02	3.94
802	DKH	PH-7	ECH	60.75	15.43	3.94
803	DKH	PH-7S	ECH	60.75	15.43	3.94
804	DKH	PH-10	ECH	86.79	22.05	3.94
805	DKH	PH-13	ECH	112.83	28.66	3.94
806	DKH	PH-20	ECH	216.98	44.09	4.92
807	DKH	PH-30	ECH	325.47	66.14	4.92
808	DKH	PH-40	ECH	433.96	88.18	4.92
809	DKH	DKH-713	ECH	112.92	28.66	3.94
850	PILECO	D8-22	OED	18.66	1.76	10.60
851	PILECO	D12-42	OED	29.89	2.82	10.60
852	PILECO	D19-42	OED	42.51	4.01	10.60
853	PILECO	D25-32	OED	58.41	5.51	10.60
854	PILECO	D30-32	OED	70.07	6.61	10.60
855	PILECO	D36-32	OED	84.16	7.94	10.60
856	PILECO	D46-32	OED	107.48	10.14	10.60
857	PILECO	D62-22	OED	161.31	13.67	11.80
858	PILECO	D80-23	OED	197.57	17.64	11.20
859	PILECO	D100-13	OED	246.85	22.04	11.20
860	PILECO	D125-32	OED	308.67	27.56	11.20
861	PILECO	D225-22	OED	555.34	49.58	11.20
862	PILECO	D250-22	OED	617.06	55.09	11.20
863	PILECO	D138-32	OED	340.61	30.41	11.20
864	PILECO	D180-32	OED	444.27	39.67	11.20
865	PILECO	D280-22	OED	688.55	61.73	11.16
866	PILECO	D160-32	OED	395.08	35.28	11.20
867	PILECO	D400-12	OED	810.10	88.15	9.19
868	PILECO	D600-12	OED	1215.10	132.22	9.19
869	PILECO	D800-22	OED	1620.20	176.30	9.19
921	BRUCE	SGH-0212	ECH	17.34	4.40	3.94
922	BRUCE	SGH-0715	ECH	75.77	15.40	4.92
923	BRUCE	SGH-1015	ECH	108.47	22.05	4.92
924	BRUCE	SGH-1215	ECH	130.16	26.46	4.92
925	BRUCE	SGH-2512	ECH	216.94	55.12	3.94
926	BRUCE	SGH-2515	ECH	271.17	55.12	4.92
927	BRUCE	SGH-3512	ECH	303.71	77.16	3.94
928	BRUCE	SGH-3515	ECH	379.64	77.16	4.92
929	BRUCE	SGH-4015	ECH	433.87	88.19	4.92
930	BRUCE	SGH-4215	ECH	455.56	92.59	4.92
931	BRUCE	SGH-4512	ECH	390.48	99.21	3.94
932	BRUCE	SGH-4515	ECH	488.10	99.21	4.92
933	BRUCE	SGH-4712	ECH	407.84	103.62	3.94

Type	Hammer Make	Hammer Model	Hammer Type	Rated Energy kip-feet	Ram Weight kips	Stroke feet
934	BRUCE	SGH-4715	ECH	509.80	103.62	4.92
935	BRUCE	SGH-4719	ECH	645.74	103.62	6.23
936	BRUCE	SGH-5015	ECH	542.34	110.23	4.92
937	BRUCE	SGH-5715	ECH	618.26	125.66	4.92
938	BRUCE	SGH-6015	ECH	650.80	132.28	4.92
939	BRUCE	SGH-7015	ECH	759.27	154.32	4.92
940	BRUCE	SGH-8015	ECH	867.74	176.37	4.92
949	JUNTTAN	HHK10S	ECH	108.49	22.05	4.92
950	JUNTTAN	HHK28S	ECH	303.78	61.73	4.92
951	JUNTTAN	HHK5S	ECH	54.27	11.03	4.92
952	JUNTTAN	HHK7S	ECH	75.97	15.44	4.92
953	JUNTTAN	HHK9S	ECH	97.68	19.85	4.92
954	JUNTTAN	HHK12S	ECH	130.24	26.47	4.92
955	JUNTTAN	HHK14S	ECH	151.95	30.88	4.92
956	JUNTTAN	HHK16S	ECH	173.65	35.29	4.92
957	JUNTTAN	HHK18S	ECH	195.36	39.70	4.92
958	JUNTTAN	HHK20S	ECH	217.07	44.11	4.92
959	JUNTTAN	HHK25S	ECH	271.22	55.11	4.92
960	JUNTTAN	HHK36S	ECH	390.56	79.36	4.92
961	JUNTTAN	HHU5A	ECH	54.27	11.03	4.92
962	JUNTTAN	HHU7A	ECH	75.94	15.43	4.92
963	JUNTTAN	HHU9A	ECH	97.64	19.84	4.92
964	JUNTTAN	HHU12A	ECH	130.19	26.45	4.92
965	JUNTTAN	HHU14A	ECH	151.88	30.86	4.92
966	JUNTTAN	HHU16A	ECH	173.58	35.27	4.92
968	JUNTTAN	SHK100-3	ECH	26.91	6.61	4.07
969	JUNTTAN	SHK100-3	ECH	35.89	8.82	4.07
970	JUNTTAN	SHK100-3	ECH	44.84	11.02	4.07
971	JUNTTAN	SHK100-3	ECH	53.82	13.23	4.07
972	JUNTTAN	SHK110-5	ECH	44.98	11.02	4.08
973	JUNTTAN	SHK110-5	ECH	53.82	13.23	4.07
974	JUNTTAN	SHK110-5	ECH	65.62	15.43	4.25
975	JUNTTAN	SHK110-5	ECH	77.42	17.64	4.39
976	JUNTTAN	SHK110-5	ECH	87.74	19.84	4.42
977	JUNTTAN	SHK100-5	ECH	44.84	11.02	4.07
978	JUNTTAN	SHK100-5	ECH	53.82	13.23	4.07
979	JUNTTAN	SHK110-7	ECH	65.63	15.43	4.25
980	JUNTTAN	SHK110-7	ECH	77.43	17.64	4.39
981	JUNTTAN	SHK110-7	ECH	87.74	19.84	4.42
998	HYPOTHET	EX 4	OED	23.38	2.75	8.50
999	SELF	Drop/10t	ECH	300.00	20.00	15.00
1001	DFI-Corp	HHA250-4	ECH	25.18	5.51	4.57
1002	DFI-Corp	HHA300-4	ECH	28.75	6.61	4.35

Type	Hammer Make	Hammer Model	Hammer Type	Rated Energy kip-feet	Ram Weight kips	Stroke feet
1003	DFI-Corp	HHA325-4	ECH	30.36	7.16	4.24
1004	DFI-Corp	HHA350-4	ECH	31.80	7.70	4.13
1005	DFI-Corp	HHA400-6	ECH	51.92	8.80	5.90
1006	DFI-Corp	HHA450-6	ECH	57.04	9.92	5.75
1007	DFI-Corp	HHB500-6	ECH	66.66	11.00	6.06
1008	DFI-Corp	HHB600-6	ECH	77.88	13.20	5.90
1020	J&M	70B HIH	ECH	21.00	7.00	3.00
1021	J&M	82 HIH	ECH	32.80	8.20	4.00
1022	J&M	115 HIH	ECH	46.00	11.50	4.00
1023	J&M	160 HIH	ECH	64.00	16.00	4.00
1024	J&M	220 HIH	ECH	88.00	22.00	4.00
1025	J&M	275 HIH	ECH	110.00	27.50	4.00
1026	J&M	345 HIH	ECH	138.00	34.50	4.00
1134	Pilemer	DKH-3U	ECH	26.00	6.60	3.94
1135	Pilemer	DKH 10L	ECH	86.79	22.05	3.94
1201	Liebherr	H 50/3	ECH	28.97	6.60	4.39
1202	Liebherr	H 50/4	ECH	35.02	8.80	3.98
1203	Liebherr	H 85/5	ECH	43.34	11.00	3.94
1204	Liebherr	H 85/7	ECH	60.16	15.43	3.90
1205	Liebherr	H 110/7	ECH	60.16	15.43	3.90
1206	Liebherr	H 110/9	ECH	78.01	19.85	3.93
1251	ICE	I-30 V2	OED	71.71	6.62	10.84
1261	APE	D 19-52	OED	47.13	4.19	11.25
1262	APE	D 16-32	OED	39.69	3.53	11.25
1263	APE	D 19-32	OED	47.13	4.19	11.25
1264	APE	D 25-32	OED	62.01	5.51	11.25
1265	APE	D 30-32	OED	74.42	6.62	11.25
1266	APE	D 36-32	OED	89.30	7.94	11.25
1267	APE	D 46-32	OED	114.11	10.14	11.25
1268	APE	D 62-22	OED	153.80	13.67	11.25
1269	APE	D 80-23	OED	198.45	17.64	11.25
1270	APE	D 100-32	OED	248.06	22.05	11.25
1271	APE	D 120-32	OED	349.69	27.60	12.67
1272	APE	D 70-42	OED	173.64	15.44	11.25
1273	APE	D 25-52	OED	62.01	5.51	11.25
1274	APE	D 30-52	OED	74.42	6.62	11.25
1275	APE	D 36-52	OED	89.30	7.94	11.25
1276	APE	D 46-52	OED	114.11	10.14	11.25
1277	APE	D 50-52	OED	124.03	11.03	11.25
1278	APE	D 62-52	OED	153.80	13.67	11.25
1279	APE	D 70-52	OED	173.64	15.44	11.25
1280	APE	7.5a	ECH	24.00	12.00	2.00
1281	APE	7.5b	ECH	20.40	10.20	2.00

Type	Hammer Make	Hammer Model	Hammer Type	Rated Energy kip-feet	Ram Weight kips	Stroke feet
1282	APE	7.5c	ECH	15.20	7.60	2.00
1283	APE	9.5a	ECH	50.66	16.00	3.17
1284	APE	9.5b	ECH	44.32	14.00	3.17
1285	APE	7-3	ECH	42.00	14.00	3.00
1286	APE	8-3	ECH	48.00	16.00	3.00
1287	APE	8	ECH	16.00	8.00	2.00
1288	APE	8a	ECH	24.00	12.00	2.00
1289	APE	10-4	ECH	80.00	20.00	4.00
1321	MENCK	MHU 240U	ECH	221.20	35.73	6.19
1322	MENCK	MHU 440S	ECH	324.37	52.45	6.18
1323	MENCK	MHU 360U	ECH	324.37	52.45	6.18
1324	MENCK	MHU 550S	ECH	404.06	65.96	6.13
1325	MENCK	MHU 450U	ECH	404.06	65.96	6.13
1326	MENCK	MHU 660S	ECH	485.17	80.39	6.04
1327	MENCK	MHU 540U	ECH	485.17	80.39	6.04
1328	MENCK	MHU 720T	ECH	588.19	99.93	5.89
1329	MENCK	MHU 650U	ECH	588.19	99.93	5.89
1330	MENCK	MHU1000S	ECH	736.48	126.98	5.80
1331	MENCK	MHU 900T	ECH	736.48	126.98	5.80
1332	MENCK	MHU 810U	ECH	736.48	126.98	5.80
1333	MENCK	MHU1700S	ECH	1272.95	207.15	6.15
1334	MENCK	MHU2100S	ECH	1573.92	257.18	6.12
1335	MENCK	MHU3000S	ECH	2216.56	370.23	5.99
1336	MENCK	MHU1400B	ECH	1032.08	145.71	7.08
1337	MENCK	MHU3500S	ECH	2582.43	385.85	6.69
1371	IHC	S-3000	ECH	2211.93	332.44	6.65
1372	IHC	S-4000	ECH	2948.91	444.30	6.64
1401	FAMBO	HR250	ECH	1.81	0.55	3.28
1402	FAMBO	HR500akk	ECH	3.62	1.10	3.28
1403	FAMBO	HR500	ECH	4.34	1.10	3.94
1404	FAMBO	HR1000	ECH	8.68	2.20	3.94
1405	FAMBO	HR1500	ECH	13.02	3.31	3.94
1406	FAMBO	HR2000	ECH	17.36	4.41	3.94
1407	FAMBO	HR2750	ECH	23.87	6.06	3.94
1408	FAMBO	HR3000	ECH	26.04	6.61	3.94
1409	FAMBO	HR4000	ECH	34.72	8.82	3.94
1410	FAMBO	HR5000	ECH	43.40	11.02	3.94
1411	FAMBO	HR7000	ECH	60.75	15.43	3.94
1412	FAMBO	HR8000	ECH	69.45	17.64	3.94
1413	FAMBO	HR10000	ECH	86.79	22.05	3.94
1501	ICE	I-12v2	OED	29.63	2.82	10.50
1502	ICE	I-8v2	OED	18.69	1.76	10.60
1503	ICE	I-19v2	OED	46.14	4.01	11.50

Type	Hammer Make	Hammer Model	Hammer Type	Rated Energy kip-feet	Ram Weight kips	Stroke feet
1504	ICE	I-30v2	OED	76.05	6.61	11.50
1505	ICE	I-36v2	OED	93.73	7.94	11.81
1506	ICE	I-46v2	OED	119.77	10.14	11.81
1507	ICE	I-62v2	OED	172.37	14.59	11.81
1508	ICE	I-80v2	OED	208.30	17.64	11.81
1509	ICE	I-100v2	OED	260.37	22.05	11.81
1510	ICE	I-125v2	OED	310.10	27.56	11.25
1511	ICE	I-160v2	OED	393.45	35.27	11.16
1512	ICE	IP-2	ECH	17.36	4.41	3.94
1513	ICE	IP-3	ECH	26.04	6.61	3.94
1514	ICE	IP-5	ECH	43.40	11.02	3.94
1515	ICE	IP-7	ECH	60.75	15.43	3.94
1516	ICE	IP-10	ECH	86.78	22.04	3.94
1517	ICE	IP-13	ECH	112.83	28.66	3.94
1520	ICE	I-138v2	OED	328.62	30.40	10.81
1531	SPI	D 19-42	OED	42.61	4.02	10.60
1532	SPI	D 30-32	OED	72.08	6.80	10.60
1601	DELMAG	D 2	OED	1.78	0.49	3.61
1602	DELMAG	D 4	OED	3.60	0.84	4.30
1603	DELMAG	D 8-12	OED	20.10	1.76	11.42
1604	DELMAG	D 12-52	OED	33.98	2.82	12.05
1605	DELMAG	D 16-52	OED	40.20	3.52	11.42
1606	DELMAG	D 25-52	OED	66.34	5.51	12.04
1607	DELMAG	D 30-52	OED	75.44	6.60	11.43
1611	DELMAG	D138-32	OED	339.51	30.44	11.16
1612	DELMAG	D180-32	OED	442.64	39.68	11.16
1613	DELMAG	D300-32	OED	737.73	66.14	11.16
1614	DELMAG	D400-32	OED	983.64	88.18	11.16
1620	HMC	TD19	OED	46.09	4.01	11.49
1621	HMC	TD30	OED	69.87	6.61	10.57

Type	Hammer Make	Hammer Model	Hammer Type	Rated Power kW	Ecc. Mass kips	Frequency Hz
620	MAIT	34	VIB	227.00	1.23	33.30
621	MAIT	42	VIB	309.00	1.52	33.30
622	MAIT	54	VIB	450.00	0.98	33.30
623	MAIT	68	VIB	531.00	1.23	33.30
624	MAIT	120	VIB	674.00	1.74	30.00
698	ICE	50B	VIB	432.00	10.42	26.70
699	ICE	3117	VIB	235.00	1.12	28.30
700	ICE	23-28	VIB	21.00	0.10	26.70
701	ICE	216	VIB	130.00	0.46	26.70
702	ICE	216E	VIB	130.00	0.46	26.70
703	ICE	23-Nov	VIB	164.00	0.46	31.70
704	ICE	223	VIB	242.00	0.46	38.30
705	ICE	416L	VIB	242.00	0.92	26.70
706	ICE	812	VIB	375.00	1.82	26.70
707	ICE	815	VIB	375.00	1.84	26.70
708	ICE	44-30	VIB	242.00	1.30	20.00
709	ICE	44-50	VIB	377.00	1.30	26.70
710	ICE	44-65	VIB	485.00	1.30	27.50
711	ICE	66-65	VIB	485.00	1.95	21.70
712	ICE	66-80	VIB	597.00	1.95	26.70
713	ICE	1412B	VIB	597.00	2.04	21.00
714	ICE	1412C	VIB	470.00	2.02	23.00
715	ICE	V125	VIB	984.00	1.04	25.80
716	ICE	14RF	VIB	242.00	1.01	38.30
717	ICE	14-23	VIB	164.00	1.17	35.00
718	ICE	22-23V	VIB	164.00	0.92	26.90
719	ICE	22-30	VIB	250.00	0.92	26.90
720	HMC	3+28	VIB	21.00	0.11	26.80
721	HMC	3+75	VIB	56.00	0.11	36.10
722	HMC	13+200	VIB	149.00	0.35	26.70
723	HMC	13S+200	VIB	149.00	0.35	26.70
724	HMC	13H+200	VIB	164.00	0.35	29.80
725	HMC	25+220	VIB	164.00	0.61	20.90
726	HMC	26+335	VIB	242.00	0.71	25.60
727	HMC	26S+335	VIB	242.00	0.71	25.60
728	HMC	51+335	VIB	242.00	1.21	19.50
729	HMC	51+535	VIB	377.00	1.21	26.40
730	HMC	51S+535	VIB	377.00	1.21	26.40
731	HMC	51+740	VIB	485.00	1.21	27.50
732	HMC	76+740	VIB	485.00	1.82	21.70
733	HMC	76+800	VIB	597.00	1.82	26.10
734	HMC	115+800	VIB	597.00	1.35	20.40
735	HMC	230+1600	VIB	1193.00	2.69	20.40

Type	Hammer Make	Hammer Model	Hammer Type	Rated Power kW	Ecc. Mass kips	Frequency Hz
750	MKT	V-2B	VIB	52.00	0.15	30.00
751	MKT	V-5C	VIB	138.00	0.43	28.33
752	MKT	V-20B	VIB	242.00	0.20	28.33
753	MKT	V-30	VIB	448.00	1.47	28.33
754	MKT	V-35	VIB	485.00	1.60	28.33
755	MKT	V-140	VIB	1341.00	1.17	23.33
770	APE	3	VIB	10.58	0.00	38.30
771	APE	6	VIB	10.58	0.01	38.30
772	APE	15	VIB	59.67	0.11	30.00
773	APE	20	VIB	59.67	0.15	38.30
774	APE	20E	VIB	59.67	0.15	38.30
775	APE	50	VIB	194.00	0.23	30.00
776	APE	50E	VIB	194.00	0.23	30.00
777	APE	100	VIB	194.00	0.32	30.00
778	APE	100E	VIB	194.00	0.14	30.00
779	APE	100HF	VIB	260.00	0.14	43.00
780	APE	150	VIB	260.00	0.14	30.00
781	APE	150T	VIB	260.00	0.17	30.00
782	APE	150HF	VIB	466.00	0.32	43.00
783	APE	200	VIB	466.00	0.29	30.00
784	APE	200T	VIB	466.00	0.34	30.83
785	APE	200T HF	VIB	738.00	0.34	43.00
786	APE	300	VIB	738.00	0.34	25.00
787	APE	400B	VIB	738.00	0.78	23.33
788	APE	600	VIB	800.00	1.05	23.30
789	APE	Tan 400	VIB	1476.00	1.37	23.33
790	APE	Tan 600	VIB	1800.00	2.11	23.30
791	APE	200-6	VIB	470.00	0.43	30.00
811	MGF	RBH 80	VIB	50.00	0.60	30.00
812	MGF	RBH 140	VIB	85.00	1.04	26.67
813	MGF	RBH 200	VIB	125.00	0.74	26.67
814	MGF	RBH 320	VIB	200.00	0.79	26.67
815	MGF	RBH 460	VIB	255.00	1.13	26.67
816	MGF	RBH 1050	VIB	460.00	1.55	22.50
817	MGF	RBH 1575	VIB	700.00	1.16	22.50
818	MGF	RBH 2400	VIB	975.00	1.77	23.50
880	ICE	23RF	VIB	384.00	0.83	38.30
881	ICE	1412BT	VIB	1193.00	1.67	21.70
882	ICE	23-40	VIB	30.00	0.19	31.80
883	ICE	28-35	VIB	261.00	1.16	27.30
884	ICE	28RF-35	VIB	261.00	1.16	27.30
885	ICE	V360	VIB	783.00	0.94	25.00
886	ICE	V360 T	VIB	1566.00	1.88	25.00

Type	Hammer Make	Hammer Model	Hammer Type	Rated Power kW	Ecc. Mass kips	Frequency Hz
887	ICE	44-30V	VIB	250.00	0.92	26.00
888	ICE	44-70	VIB	585.00	0.92	28.10
889	ICE	66-70	VIB	585.00	0.92	23.00
890	ICE	7RF	VIB	154.00	0.51	38.30
891	ICE	66-70HS	VIB	585.00	0.92	26.70
892	ICE	66-80HS	VIB	597.00	0.92	29.20
893	ICE	100c-Tdm	VIB	1774.00	1.83	26.67
894	ICE	423	VIB	377.00	0.92	38.30
895	ICE	32RF	VIB	391.00	1.16	33.30
896	ICE	36RF	VIB	431.00	1.30	33.30
897	ICE	46RF	VIB	678.00	1.66	38.30
898	ICE	64RF	VIB	663.00	1.16	32.50
899	ICE	44B	VIB	595.00	1.30	30.00
900	Mueller	MS16HF	VIB	219.00	1.16	39.20
901	Mueller	MS25H2	VIB	218.00	0.90	28.00
902	Mueller	MS25H3	VIB	218.00	0.90	28.00
903	Mueller	MS50H2	VIB	419.00	1.20	27.00
904	Mueller	MS50H3	VIB	419.00	1.20	27.00
905	Mueller	MS25HHF	VIB	274.00	0.58	27.30
906	Mueller	MS50HHF	VIB	562.00	1.17	27.30
907	Mueller	MS100HHF	VIB	750.00	2.33	24.90
908	Mueller	MS120HHF	VIB	895.00	2.30	25.60
909	Mueller	MS200HHF	VIB	837.00	4.25	22.90
910	Mueller	MS-10HFV	VIB	203.00	0.39	39.30
911	Mueller	MS-16HFV	VIB	294.00	0.53	39.20
912	Mueller	MS-24HFV	VIB	720.00	0.85	39.20
913	Mueller	MS-32HFV	VIB	551.00	1.05	39.60
914	Mueller	MS-48HFV	VIB	823.00	1.69	39.20
915	Mueller	MS-62HFV	VIB	735.00	1.82	35.00
1039	J&M	11-23	VIB	164.00	0.92	31.70
1040	J&M	1412	VIB	559.00	1.67	21.70
1041	J&M	1412T	VIB	1119.00	1.67	21.70
1042	J&M	216	VIB	149.00	0.92	26.70
1044	J&M	22-23	VIB	164.00	0.92	20.80
1045	J&M	22-30	VIB	261.00	0.92	27.50
1050	J&M	28-35	VIB	261.00	1.17	27.50
1051	J&M	360	VIB	783.00	0.94	21.70
1052	J&M	416	VIB	250.00	0.92	26.70
1053	J&M	416B	VIB	261.00	0.92	26.70
1054	J&M	416S	VIB	250.00	0.92	26.70
1055	J&M	815	VIB	429.00	0.92	26.70
1056	J&M	44-30	VIB	250.00	0.92	20.00
1057	J&M	44-50	VIB	399.00	0.92	26.70

Type	Hammer Make	Hammer Model	Hammer Type	Rated Power kW	Ecc. Mass kips	Frequency Hz
1058	J&M	44-65	VIB	552.00	0.92	27.50
1060	J&M	66-65	VIB	552.00	0.92	21.70
1061	J&M	66-80	VIB	559.00	0.92	26.70
1100	PVE	14M	VIB	190.00	1.01	28.30
1101	PVE	23M	VIB	234.00	1.66	27.50
1102	PVE	25M	VIB	294.00	0.98	28.30
1103	PVE	27M	VIB	294.00	0.98	28.30
1104	PVE	38M	VIB	392.00	0.92	28.30
1105	PVE	50M	VIB	440.00	1.20	28.30
1106	PVE	52M	VIB	564.00	0.75	28.30
1107	PVE	105M	VIB	784.00	1.52	22.50
1108	PVE	110M	VIB	784.00	0.80	22.50
1109	PVE	200M	VIB	1130.00	1.45	23.30
1110	PVE	2307	VIB	190.00	0.47	38.30
1111	PVE	1420	VIB	190.00	1.01	33.30
1112	PVE	2315	VIB	234.00	1.09	38.30
1113	PVE	2520	VIB	294.00	1.81	33.30
1114	PVE	2310VM	VIB	190.00	0.72	38.30
1115	PVE	2315VM	VIB	234.00	1.09	38.30
1116	PVE	2316VM	VIB	294.00	1.16	38.30
1117	PVE	2319VM	VIB	392.00	1.37	38.30
1118	PVE	2323VM	VIB	392.00	0.83	38.30
1119	PVE	2332VM	VIB	564.00	1.16	38.30
1120	PVE	2335VM	VIB	784.00	1.27	38.30
1121	PVE	40VM	VIB	564.00	1.45	33.30
1122	PVE	50VM	VIB	564.00	1.20	30.00
1123	PVE	55M	VIB	403.00	1.17	28.33
1124	PVE	82M	VIB	565.00	1.76	28.33
1125	PVE	300M	VIB	1796.00	6.21	23.33
1126	PVE	16VM	VIB	335.00	0.35	38.33
1127	PVE	20VM	VIB	395.00	0.41	38.33
1128	PVE	24VM	VIB	395.00	0.52	38.33
1129	PVE	28VM	VIB	403.00	0.61	38.33
1130	PVE	2070VM	VIB	1130.00	1.52	33.33
1131	PVE	2312VM	VIB	252.00	0.26	38.33
1132	PVE	2350VM	VIB	790.00	1.09	38.33
1142	PTC	30HP	VIB	196.00	0.87	27.00
1143	PTC	40HD	VIB	269.00	0.87	28.00
1144	PTC	50HD1	VIB	255.00	0.87	25.00
1145	PTC	50HD2	VIB	290.00	0.87	25.00
1146	PTC	65HD	VIB	305.00	0.87	26.00
1147	PTC	60HD	VIB	305.00	0.87	28.00
1148	PTC	75HD	VIB	410.00	0.87	25.00

Type	Hammer Make	Hammer Model	Hammer Type	Rated Power kW	Ecc. Mass kips	Frequency Hz
1149	PTC	100HD	VIB	451.00	0.87	23.00
1150	PTC	100HDS	VIB	564.00	0.87	23.00
1151	PTC	175HD	VIB	611.00	0.87	23.00
1152	PTC	240HD	VIB	988.00	0.87	23.00
1153	PTC	240HDS	VIB	988.00	0.87	30.00
1154	PTC	120HD	VIB	410.00	0.87	23.00
1155	PTC	130HD	VIB	564.00	0.87	23.00
1156	PTC	200HD	VIB	710.00	0.87	23.00
1157	PTC	265HD	VIB	1080.00	0.87	24.00
1340	H&M	H-150	VIB	94.00	0.11	28.30
1341	H&M	H-1700	VIB	165.00	0.20	20.00
1431	BRUCE	SGV-80	VIB	112.20	0.13	33.33
1432	BRUCE	SGV-100	VIB	142.60	0.18	30.00
1433	BRUCE	SGV-200	VIB	184.80	0.31	28.83
1434	BRUCE	SGV-300	VIB	211.20	0.35	27.50
1435	BRUCE	SGV-400	VIB	286.00	0.44	26.67
1436	BRUCE	SGV-450	VIB	323.40	0.48	26.67
1437	BRUCE	SGV-600	VIB	451.50	0.72	26.67
1438	BRUCE	SGV-1000	VIB	569.10	1.03	25.00
1630	LBFoster	4150	VIB	335.00	0.53	25.00

U.S. Department of Transportation
Federal Highway Administration

Publication No. FHWA-NHI-16-064
FHWA GEC 012
September 2016

NHI Courses No. 132021 and 132022

Design and Construction of Driven Pile Foundations – Comprehensive Design Examples

Developed following:

AASHTO LRFD Bridge Design Specifications, 7th Edition, 2014, with 2015 Interim.

and

AASHTO LRFD Bridge Construction Specifications, 3rd Edition, 2010, with '11, '12, '13, '14, and '15 Interims.

NATIONAL HIGHWAY INSTITUTE
Training Solutions for Transportation Excellence

NOTICE

The contents of this report reflect the views of the authors, who are responsible for the facts and accuracy of the data presented herein. The contents do not necessarily reflect policy of the Department of Transportation. This report does not constitute a standard, specification, or regulation. The United States Government does not endorse products or manufacturers. Trade or manufacturers′ names appear herein only to illustrate methods and procedures, and are considered essential to the objective of this document.

Technical Report Documentation Page

1. REPORT NO.	2. GOVERNMENT ACCESSION NO.	3. RECIPIENT'S CATALOG NO.
FHWA-NHI-16-064		

4. TITLE AND SUBTITLE	5. REPORT DATE
Geotechnical Engineering Circular No. 12 Design and Construction of Driven Pile Foundations - Comprehensive Design Examples	September 2016
	6. PERFORMING ORGANIZATION CODE
7. AUTHOR(S) Patrick J. Hannigan, PE, Frank Rausche, PhD, PE, Garland E. Likins, PE, Brent R. Robinson, PE, and Matthew L. Becker, EI.	8. PERFORMING ORGANIZATION REPORT NO.
9. PERFORMING ORGANIZATION NAME AND ADDRESS Ryan R. Berg & Associates, Inc. 2190 Leyland Alcove Woodbury, MN 55125	10. WORK UNIT NO.
	11. CONTRACT OR GRANT NO. DTFH61-11-D-00049
12. SPONSORING AGENCY NAME AND ADDRESS National Highway Institute U.S. Department of Transportation Federal Highway Administration, Washington, DC 20590	13. TYPE OF REPORT & PERIOD COVERED Final Report
	14. SPONSORING AGENCY CODE

15. SUPPLEMENTARY NOTES

FHWA COTR: Heather Shelsta

FHWA Technical Working Group: Naser Abu-Hejleh, PhD, PE; Scott Anderson, PhD, PE; and Silas Nichols, PE

16. ABSTRACT

This document presents comprehensive design examples for driven pile foundations on highway structures. The worked design examples supplement the material presented in FHWA-NHI-16-009 and FHWA-NHI-16-010, the primary FHWA guidance documents on driven pile foundations. The worked LRFD design examples address strength, service and extreme limit state considerations for a two span bridge structure in highly variable subsurface conditions. Pile foundation design examples in cohesionless, cohesive, and layered soil profiles are presented as well as pile design on hard rock. The worked examples follow the step by step design and construction process outlined in Chapter 2 of FHWA-NHI-16-009.

17. KEY WORDS	18. DISTRIBUTION STATEMENT		
Driven pile foundations, foundation economics, site characterization, geomaterial properties, axial compression resistance, axial tension resistance, lateral resistance, pile groups, nominal resistance determination tests, construction monitoring and quality assurance.	No restrictions.		
19. SECURITY CLASSIF. Unclassified	20. SECURITY CLASSIF. Unclassified	21. NO. OF PAGES 265	22. PRICE

CONVERSION FACTORS

Approximate Conversions to SI Units			Approximate Conversions from SI Units		
When You Know	**Multiply By**	**To Find**	**When You Know**	**Multiply By**	**To Find**
(a) Length					
inch (in.)	25.4	millimeter (mm)	millimeter (mm)	0.039	inch (in.)
foot (ft)	0.305	meter (m)	meter (m)	3.28	foot (ft)
yard (yd)	0.914	meter (m)	meter (m)	1.09	yard (yd)
mile (mi)	1.61	kilometer (km)	kilometer (km)	0.621	mile (mi)
(b) Area					
square inches (in^2)	645.2	square millimeters (mm^2)	square millimeters (mm^2)	0.0016	square inches (in^2)
square feet (ft^2)	0.093	square meters (m^2)	square meters (m^2)	10.764	square feet (ft^2)
Acres (ac)	0.405	hectares (ha)	hectares (ha)	2.47	Acres (ac)
square miles (mi^2)	2.59	square kilometers (km^2)	square kilometers (km^2)	0.386	square miles (mi^2)
square inches (in^2)	645.2	square millimeters (mm^2)	square millimeters (mm^2)	0.0016	square inches (in^2)
(c) Volume					
fluid ounces (oz)	29.57	milliliters (mL)	milliliters (mL)	0.034	fluid ounces (oz)
Gallons (gal)	3.785	liters (L)	liters (L)	0.264	Gallons (gal)
cubic feet (ft^3)	0.028	cubic meters (m^3)	cubic meters (m^3)	35.32	cubic feet (ft^3)
cubic yards (yd^3)	0.765	cubic meters (m^3)	cubic meters (m^3)	1.308	cubic yards (yd^3)
(d) Mass					
ounces (oz)	28.35	grams (g)	grams (g)	0.035	ounces
pounds (lb)	0.454	kilograms (kg)	kilograms (kg)	2.205	pounds
short tons (2000 lb) (T)	0.907	megagrams (tonne) (Mg)	megagrams (tonne) (Mg)	1.102	short tons (2000 lb)
(e) Force					
pound (lb)	4.448	Newton (N)	Newton (N)	0.2248	pound (lb)
(f) Pressure, Stress, Modulus of Elasticity					
pounds per square foot (psf)	47.88	Pascals (Pa)	Pascals (Pa)	0.021	pounds per square foot (psf)
pounds per square inch (psi)	6.895	kiloPascals (kPa)	kiloPascals (kPa)	0.145	pounds per square inch (psi)
(g) Density					
pounds per cubic foot (pcf)	16.019	kilograms per cubic meter (kgm^3)	kilograms per cubic meter (kgm^3)	0.0624	pounds per cubic feet (pcf)
(h) Temperature					
Fahrenheit temperature (^oF)	5/9(^oF- 32)	Celsius temperature (^oC)	Celsius temperature (^oC)	9/5(^oC)+ 32	Fahrenheit temperature (^oF)

Notes:

1) The primary metric (SI) units used in civil engineering are meter (m), kilogram (kg), second (s), Newton (N), and Pascal ($Pa=N/m^2$).

2) In a "soft" conversion, an English measurement is mathematically converted to its exact metric equivalent.

3) In a "hard" conversion, a new rounded metric number is created that is convenient to work with and remember.

PREFACE

The purpose of this manual is to provide updated, state-of-the-practice information for the design and construction of driven pile foundations in accordance with the Load and Resistance Factor Design (LRFD) platform. Engineers and contractors have been designing and installing pile foundations for many years. During the past three decades, the industry has experienced several major improvements including newer and more accurate methods of predicting and measuring geotechnical resistance, vast improvements in design software, highly specialized and sophisticated equipment for pile driving, and improved methods of construction control. Previous editions of the FHWA Design and Construction of Driven Pile Foundations manual were published 1985, 1996, and 2006 and chronical the many changes in design and construction practice over the past 30 years. This two volume edition, GEC-12, serves as the FHWA reference document for highway projects involving driven pile foundations.

Volume I, FHWA-NHI-16-009, covers the foundation selection process, site characterization, geotechnical design parameters and reporting, selection of pile type, geotechnical aspects of limit state design, and structural aspects of limits state design. Volume II, FHWA-NHI-16-010, addresses static load tests, dynamic testing and signal matching, rapid load testing, wave equation analysis, dynamic formulas, contract documents, pile driving equipment, pile accessories, driving criteria, and construction monitoring. Comprehensive design examples are presented in publication FHWA-NHI-16-064.

Throughout this manual, numerous references will be made to the names of software or technology that are proprietary to a specific manufacturer or vendor. Please note that the FHWA does not endorse or approve commercially available products, and is very sensitive to the perceptions of endorsement or preferred approval of commercially available products used in transportation applications. Our goal with this development is to provide recommended technical guidance for the safe design and construction of driven pile foundations that reflects the current state of practice and provides information on advances and innovations in the industry. To accomplish this, it is necessary to illustrate methods and procedures for design and construction of driven pile foundations. Where proprietary products are described in text or figures, it is only for this purpose.

The primary audience for this document is: agency and consulting engineers specialized in geotechnical and structural design of highway structures; engineering geologists and consulting engineers providing technical reviews, or who are engaged in the design, procurement, and construction of driven pile foundations This document is also intended for management, specification and contracting specialists, as well as for construction engineers interested in design and contracting aspects of driven pile systems.

This document draws material from the three earlier FHWA publications in this field; FHWA-DP-66-1 by Vanikar (1985), FHWA HI 97-013 and FHWA HI 97-014 by Hannigan et al. (1998), and FHWA NHI-05-042 and FHWA NHI-05-043 by Hannigan et al. (2006). Photographs without specific acknowledgement in this two volume document are from these previous editions, their associated training courses, or from the consulting practice of GRL Engineers, Inc.

The following individuals were part of the Ryan R. Berg & Associates internal peer review team and are acknowledged for their technical advice and contributions to this version of the document:

Mr. Jerry DiMaggio - Applied Research Associates, Inc.
Mr. Van E. Komurka – Wagner Komurka Geotechnical Group, Inc.
Mr. Billy Camp – S&ME, Inc.
Dr. Brian Anderson – Auburn University

TABLE OF CONTENTS

LIST OF TABLES

LIST OF FIGURES

LIST OF SYMBOLS

A - Pile cross sectional area.
A_d - Angular distortion.
A_p - Pile toe area.
A_s - Pile shaft surface area.
B - Width of pile group.
b - Pile width or diameter, Width/ Height of square.
b_f - Flange width of pile section.
bpm - Blow per minute.
C - Wave speed of pile material.
C' - Dimensionless bearing capacity index, determined from average corrected SPT N value, for layer with consideration of SPT hammer type.
C_a - Pile adhesion.
C_c - Compression index.
C_d - Pile perimeter at depth d.
C_F - Correction factor for K_δ when $\delta \neq \phi$.
C_n - Correction factor for SPT N value.
C_r - Recompression index.
C_s - Swell index.
c' - Effective cohesion.
D - Pile embedded length; Pile width for WEAP quake calculation.
D_B - Pile embedded length into bearing stratum.
D_{np} - Depth from reference to neutral plane.
d_w - Web depth of pile section.
E - Elastic modulus of pile material.
E_m - Rock Mass Modulus.
E_n - Rated hammer energy.
ER - SPT Hammer efficiency as determined by energy measurements in accordance with ASTM D4633.
E_s - Elastic modulus of soil.
e_o - Initial soil layer void ratio.
F_y - Yield stress of steel.
g - Acceleration due to gravity.
H - Soil layer thickness.

H_o - Initial soil layer thickness.
h - Ram stroke.
h_i - Thickness of soil strata.
h_w - Height of water (pressure head) for calculation of pore water pressure.
k_c - Modulus of subgrade reaction for cyclic lateral loading.
L - Total pile length.
N_t - Toe bearing capacity coefficient.
M_{n} - Nominal flexural resistance (structural).
M_p - Plastic moment about the weak axis.
M_{r} - Factored flexural resistance (structural).
M_{rx} - Factored flexural resistance about x-axis.
M_{ry} - Factored flexural resistance about y-axis.
M_u - Factored moment load (structural).
M_{ux} - Factored moment about x-axis.
M_{uy} - Factored moment about y-axis.
m_n - Dimensionless modulus number.
m_{nr} - Dimensionless recompression modulus number.
N_c - Dimensionless bearing capacity factor.
N_q - Dimensionless bearing capacity factor.
N_{60} - SPT N value corrected for 60% energy transfer.
$(N_1)_{60}$ - SPT N value corrected for energy and overburden stress.
N_γ - Bearing capacity factor.
n - Number of piles in pile group.
P_m - P-multiplier for p-y curve.
P_n - Nominal structural resistance in axial compression.
P_r - Factored structural resistance in axial compression.
P_u - Factored axial load (structural).
P_{ui} - Maximum single pile axial load.
p_a - Atmospheric pressure.
p_f - Design foundation pressure.
Q - Factored Axial Load; Unfactored Axial Load.
Q_d - Dead or sustained load on a pile.
Q_{max} - Maximum axial compressive force in the pile.
q - Surcharge.
q_u - Unconfined compressive strength.
R_n - Nominal resistance.
R_{ndr} - Nominal driving resistance.
R_{ng} - Nominal resistance of pile group.
R_p - Nominal toe resistance.

R_r - Factored resistance.
R_{relax} - Resistance loss from relaxation.
R_{rg} - Factored resistance of the pile group.
R_s - Nominal shaft resistance.
R_{scour} - Resistance loss from scour.
R_{ug} - Nominal uplift resistance of the pile group.
S - Settlement.
S_d - Differential settlement of the foundation.
S_c - Settlement from primary consolidation.
S_h - Horizontal abutment movement.
s_u - Undrained shear strength.
t - Pipe pile wall thickness.
t_{cap} - Thickness of pile cap (8.9).
t_f - Flange thickness of pile section (8.2) (8.5).
t_{soil} - Thickness of compressible soil beneath neutral plane.
t_w - Web thickness of pile section.
V_n - Nominal shear resistance (structural).
V_r - Factored shear resistance (structural).
V_u - Factored shear load (structural).
W - Ram weight.
W_c - Estimated weight of pile cap.
W_g - Effective weight of the pile/soil block including pile cap weight.
W_s - Estimated weight of soil above pile cap.
w - Moisture content.
x - Distance along x-axis from the center of the column to each pile center.
Y_o - Pile head deflection.
y - Distance along y-axis from the center of the column to each pile center.
Z - Length of pile group .
Δ - Elastic deformation of pile.
$\Delta\varepsilon$ - Change of strain.
Δσ - Change of stress.
ε - Strain.
ε_{50} - Strain at one half the maximum principal stress.
η_g - Pile group efficiency.
γ - Total unit weight of soil.
γ' - Buoyant unit weight of soil.
γ_d - Dead Load Factor.
γ_f - Unit weight of embankment fill.

γ_i - Unit weight of soil strata for calculation of in-situ stress.
γ_l - Load factor for force effect due to live loads.
γ_p - Load factor for force effect due to permanent loads.
γ_w - Unit weight of water.
σ - Normal stress (pressure) on plane of failure, stress.
σ′ - Effective normal stress (pressure) on plane of failure (σ – u).
σ'_d - Vertical effective stress at the center of depth increment d.
σ_{dr} - Driving stress.
σ'_o - Effective stress prior to stress increase.
σ_p - Preconsolidation pressure or stress.
σ_r - Reference stress for settlement with Janbu Tangent Modulus.
σ'_v - Vertical effective stress.
σ'_{vo} - Vertical effective stress at the sample depth.
σ'_1 - Effective stress after stress increase.
ϕ - Resistance factor, statistically based multiplier on nominal resistance.
ϕ' - Effective Stress Friction Angle.
ϕ_c - Resistance factor (pile structural resistance in compression).
ϕ_{da} - Resistance factor (pile structural resistance during driving).
ϕ_{dyn} - Resistance factor (based on the construction control method).
ϕ_f - Resistance factor (pile structural resistance in flexure).
ϕ_{stat} - Resistance factor (based on the static analysis method).
ϕ_{ug} - Resistance factor for group uplift (based on the uplift analysis method).
ϕ_{up} - Resistance factor (based on the uplift analysis method).
ϕ_v - Resistance factor (pile structural resistance in shear).

LIST OF ACRONYMNS

AASHTO	-	American Association of State Highway and Transportation Officials
ASTM	-	American Society for Testing and Materials
BOR	-	Beginning of Restrike
CED	-	Closed End Diesel hammer
CEP	-	Closed End Pipe
CFA	-	Continuous Flight Auger
DA	-	Design Angular Distortion
DD	-	Downdrag
DF	-	Drag Force
DLT	-	Dynamic Load Test
EOD	-	End of Drive
ER	-	SPT hammer efficiency as determined by energy measurements
FHWA	-	Federal Highway Administration
I.D.	-	Inner diameter
NHI	-	National Highway Institute
O.D.	-	Outer Diameter
OEP	-	Open Ended Pipe
SA	-	Static Analysis
SPT	-	Standard Penetration Test
SLT	-	Static Load Test
WE	-	Wave Equation
WEAP	-	Wave Equation Analysis Program

APPENDIX D

COMPREHENSIVE DESIGN EXAMPLES

This appendix presents comprehensive design examples for a driven pile foundation project. The worked design examples supplement the material presented in publications FHWA-NHI-16-009 and FHWA-NHI-16-010, the primary FHWA guidance documents on driven pile foundations. The worked LRFD design examples address strength, service, and extreme limit state considerations for a bridge structure in highly variable subsurface conditions. Worked design examples in cohesionless, cohesive, and layered soil profiles are presented as well as pile design on hard rock. All limit states considerations are addressed as applicable in the worked design examples.

The bridge dimensions and superstructure loads were provided by a transportation agency, while the bridge structure is supported at two abutments and a pier. The soil profile for the worked design examples was developed to illustrate use of the manual's design methods and procedures in a variety of subsurface conditions. Each substructure location presents a different subsurface condition. A cohesionless soil profile is presented at the North Abutment. At the pier, worked examples in a layered subsurface profile are presented. At the South Abutment, worked examples for a cohesive soil profile underlain by a hard bedrock are presented. Strength, service, and extreme limit states are addressed at each substructure location as appropriate. An economic evaluation of candidate pile types is also included at each substructure location.

The worked design examples follow the step by step design and construction process outlined in Chapter 2 of FHWA-NHI-16-009. The design process flow chart introduced in Chapter 2 is followed in the worked design examples and is presented herein as Figure D-1.

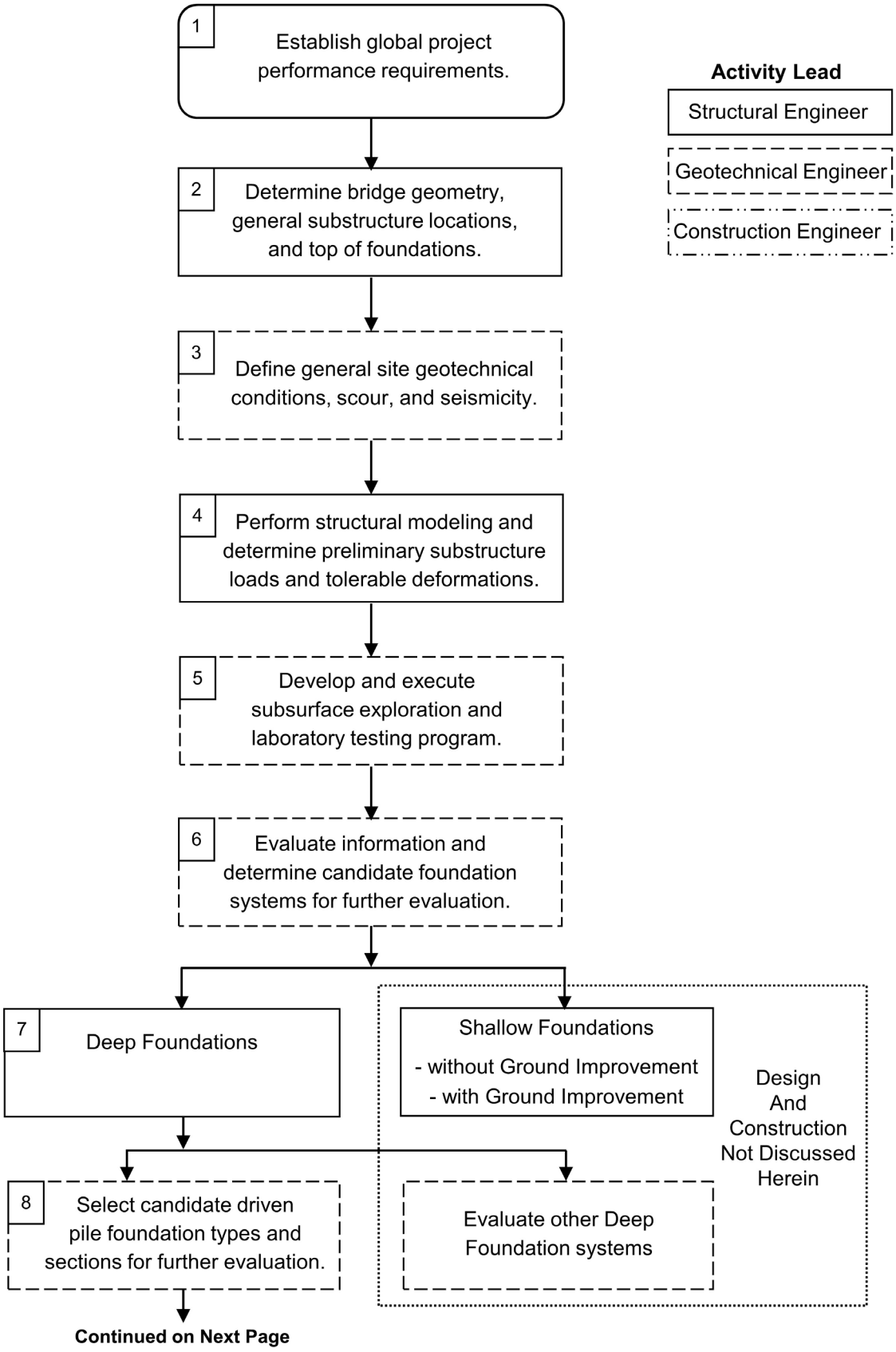

Figure D-1 Design process flow chart.

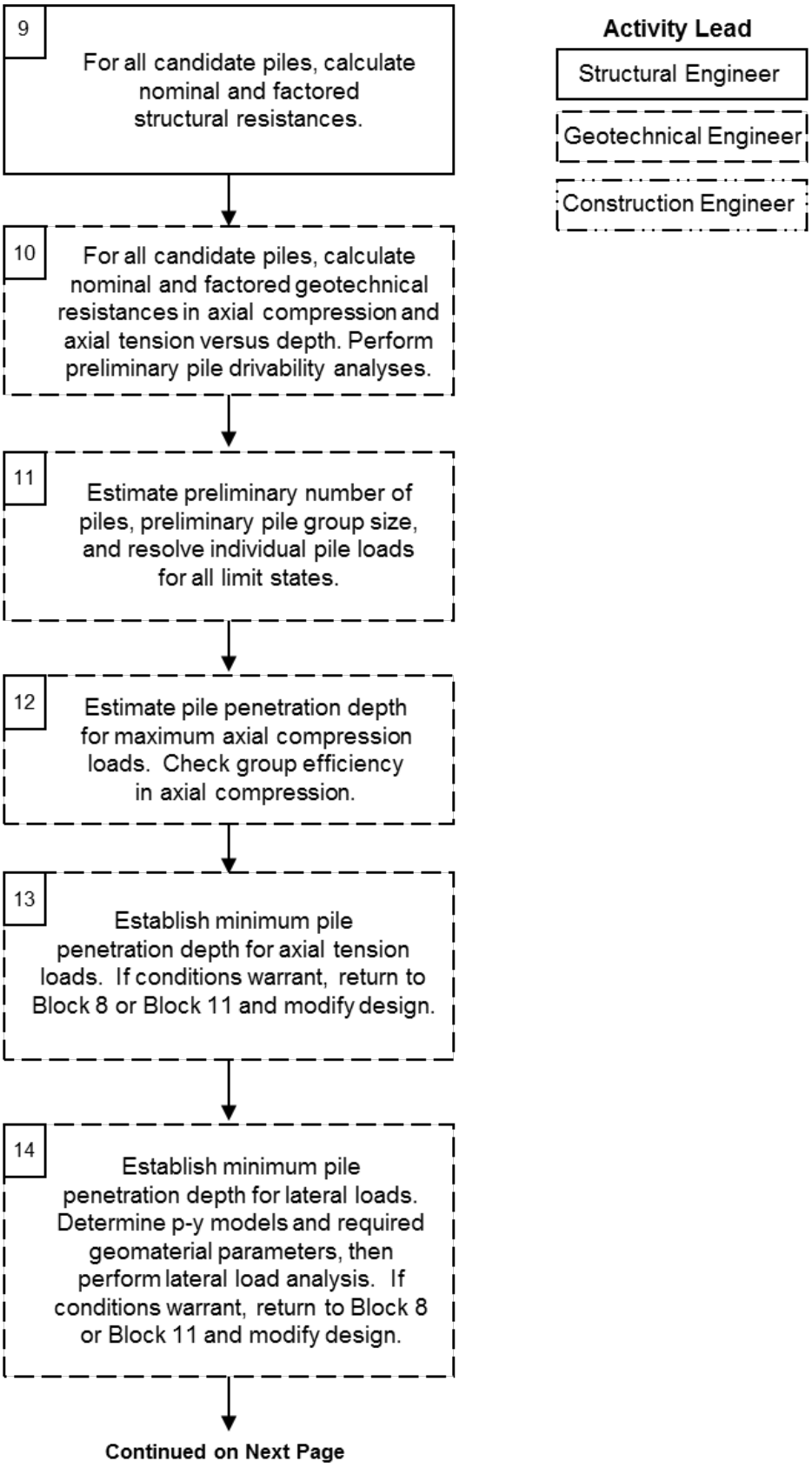

Figure D-1 Design process flow chart (continued).

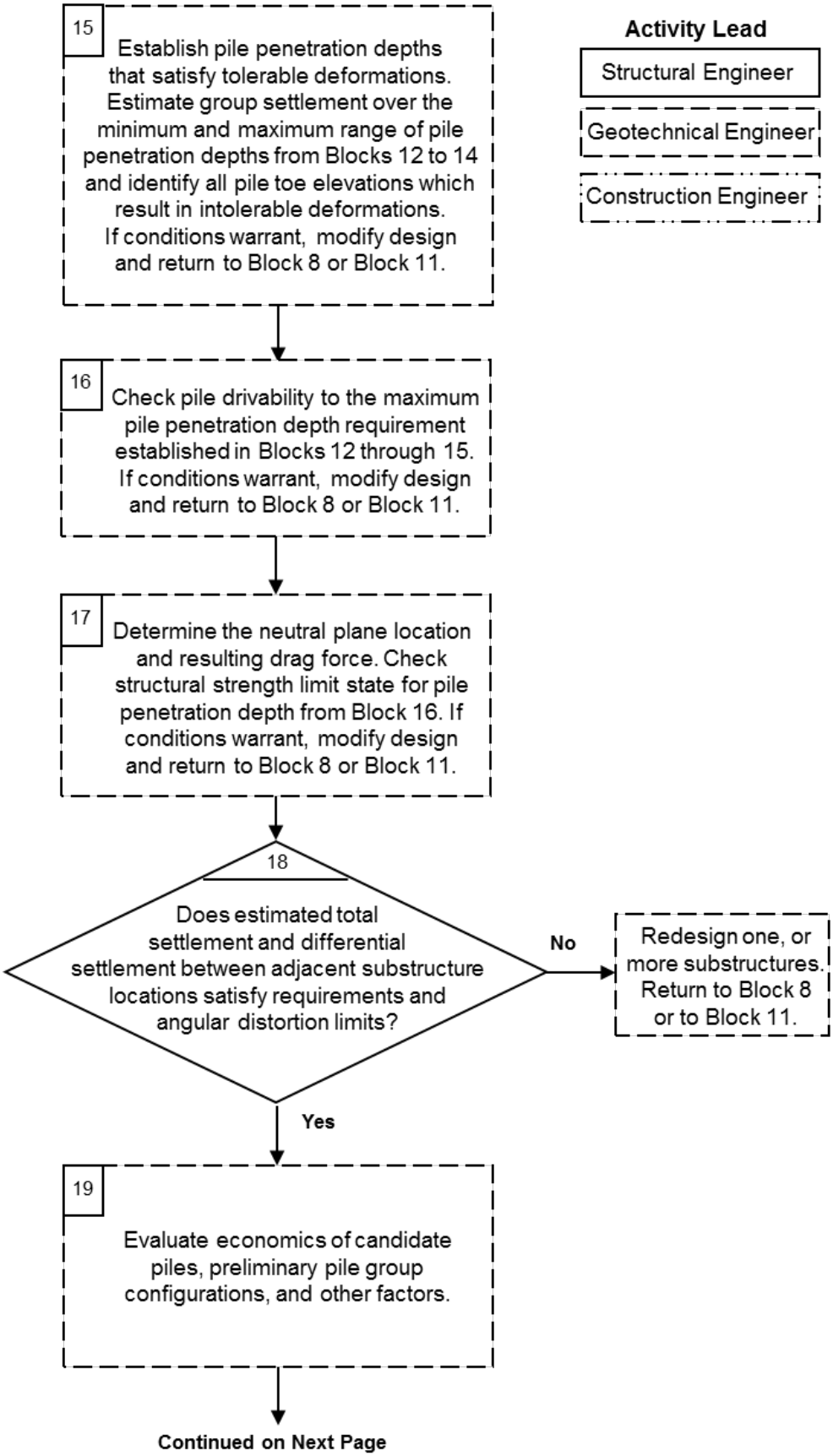

Figure D-1 Design process flow chart (continued).

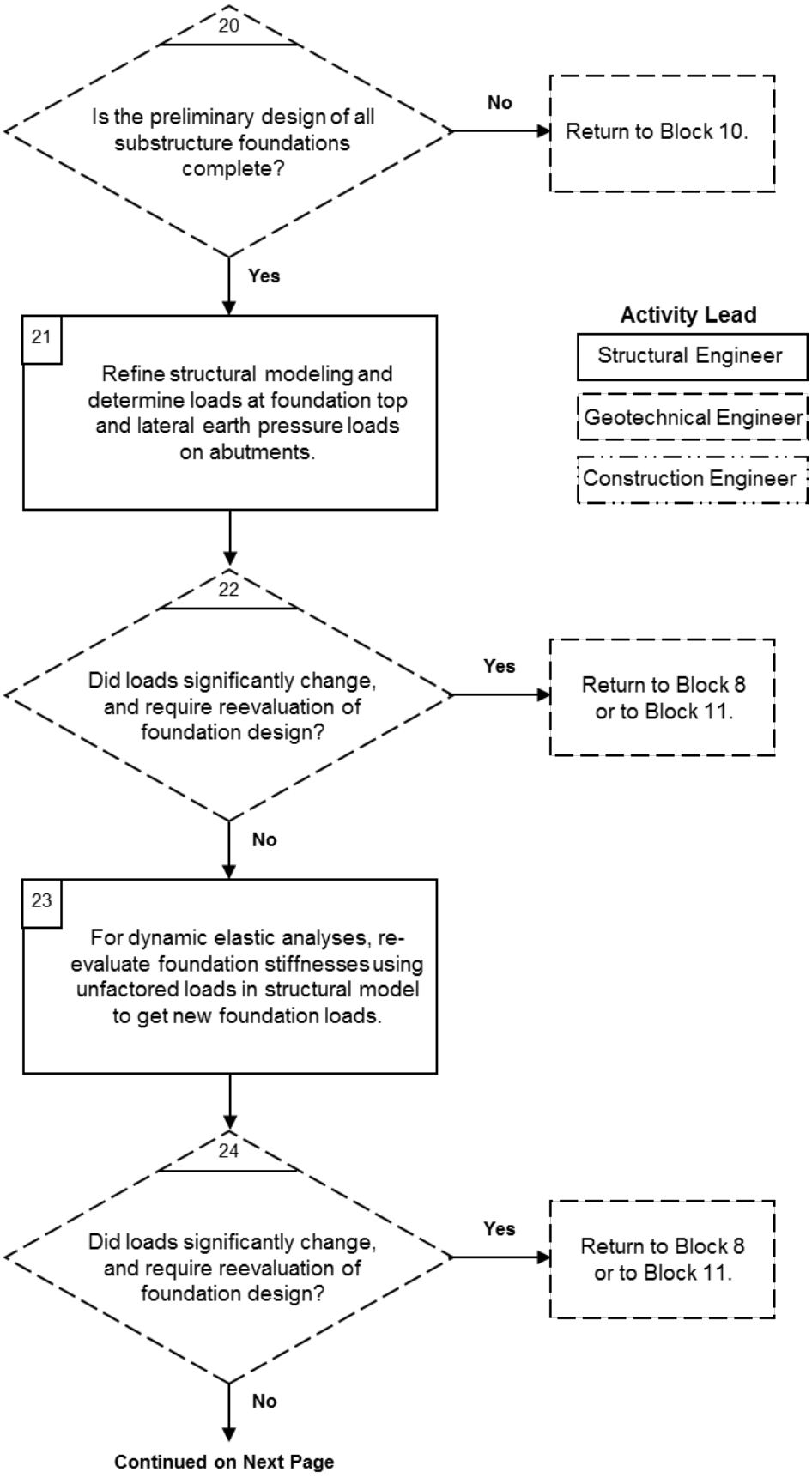

Figure D-1 Design process flow chart (continued).

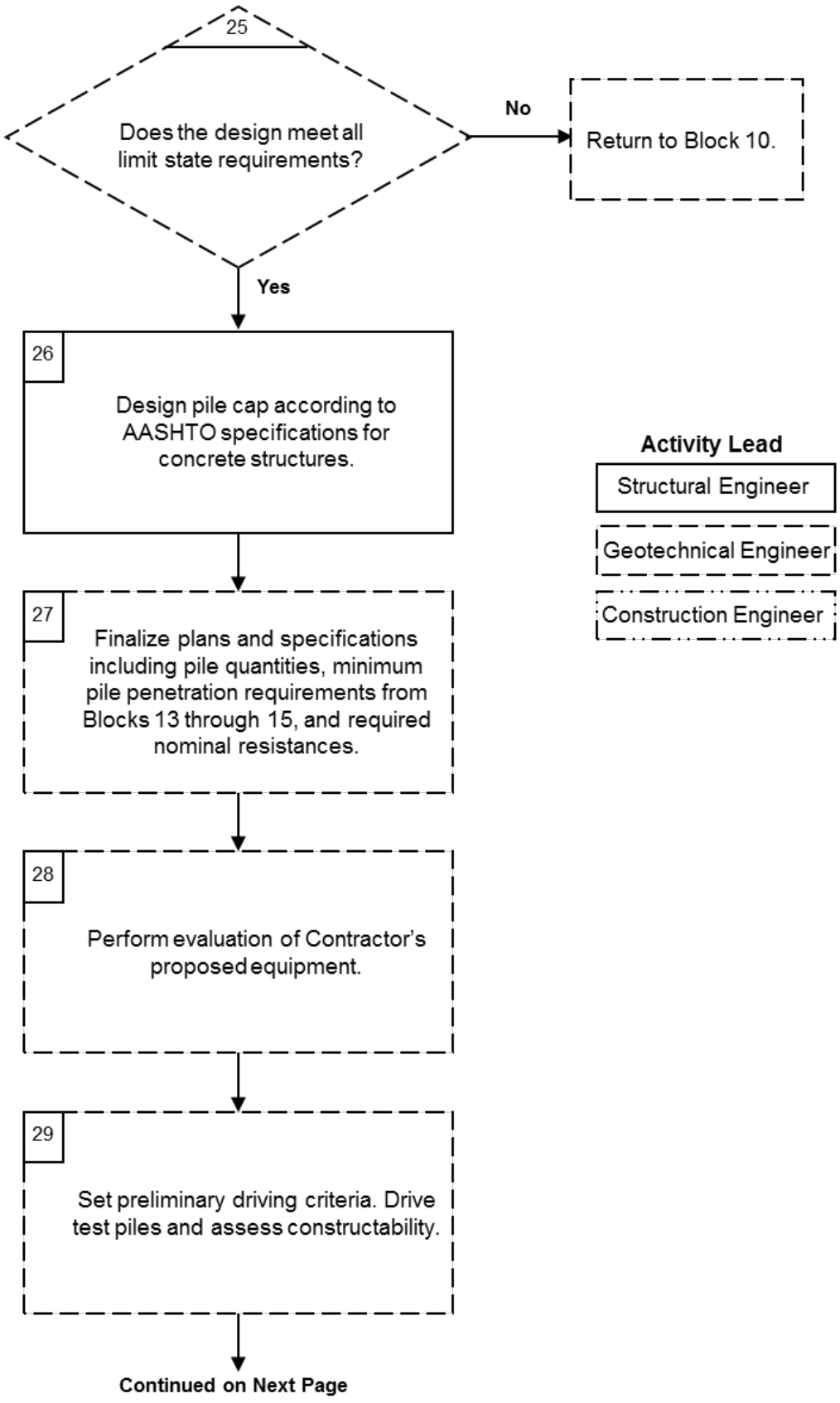

Figure D-1 Design process flow chart (continued).

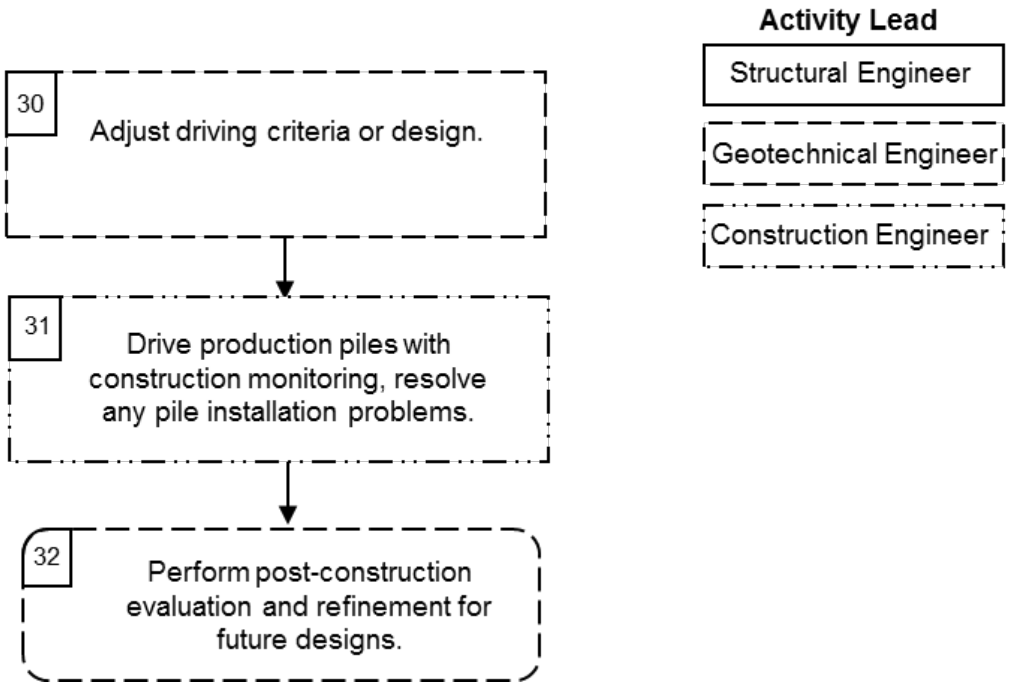

Figure D-1 Design process flow chart (continued).

D.1 Block 1: Establish Global Project Performance Requirements

The general structure requirements have been determined and are summarized below.

1. The project will consist of new twin river bridges, one for northbound traffic and one for southbound traffic. Both bridges will be designed for three travel lanes.

2. The project will be constructed at one time.

3. The general structure layout and approximate substructure locations are known but approach grades have yet to be established.

4. The foundation engineer has visited the site. During normal flow, the river is approximately 80 feet wide and 5 feet deep at the proposed bridge location. The north side of the river has a bank approximately 20 feet high consisting of silty sand. The ground surface on the south side of the river has a slightly more gradual slope with surficial soils consisting of silty clay. The new bridges will be approximately 200 feet long with a higher approach embankment required on the south side.5. Based on other bridge structures similar to those contemplated for this project, limit state axial compression loads are anticipated to be on the order of 2000 to 2500 kips at the abutments and 2500 to 3500 kips at the pier.

   Based on safety, drainage, and rideability considerations, a maximum total settlement at any substructure location of 1.5 inches and maximum differential settlement between substructure locations of 1 inch are desired. In addition, the lateral deformation is limited to 1 inch.

6. The new bridge structure is not subject to vessel or vehicle impact loading or seismic activity. However, substantial scour is a design consideration.

7. Lateral squeeze may or may not be a design consideration depending upon the subsurface conditions encountered.

8. No modifications appear warranted in the preliminary design such as adjustments in substructure locations or span lengths.

9. No site or surrounding environmental considerations (low headroom, utility conflicts, aggressive soil environments, limitations on noise, vibrations, etc.) need to be considered in the design.

10. There are no special factors influencing bridge span length.

D.2 Block 2: Determine Structure (Bridge) Geometry, Substructure Locations and Elevations

The general bridge geometry, probable substructure locations, and the top of foundation elevations have been established. This information is presented in Table D-1.

Table D-1 General Bridge Geometry Summary

Substructure	Substructure Station	Top of Foundation Elevation (feet)
North Abutment	1223 + 26	+ 312.0
Pier 2	1224 + 26	+ 280.0
South Abutment	1225 + 26	+ 307.0

D.3 Block 3: Define General Site Geotechnical Conditions, Scour, and Seismicity

Available foundation plans and structure performance have been collected from other projects in the vicinity. The project is located in an area known for variable subsurface conditions. Post construction issues of unsatisfactory structure performance have not been reported in the vicinity. The hydraulic engineer has been consulted to determine probable scour depths that may impact the foundation selection. Seismicity is not a design consideration.

D.4 Block 4: Perform Preliminary Structure Modeling. Determine Preliminary Substructure Loads and Tolerable Deformations

Preliminary structural analysis and modeling of the proposed bridge structure has been performed at this time. The preliminary strength, service and extreme events limit state loads and performance requirements at the foundation top have also been established. The tolerable vertical and lateral deformations previously stated in Block 1 have been confirmed by the bridge office as performance requirements.

D.5 Block 5: Develop and Execute Subsurface Exploration and Laboratory Testing Program for Feasible Foundation Systems

Prior to this stage, only the general bridge geometry, preliminary superstructure limit state loads and general site geotechnical conditions were known. The substructure locations now have been determined. A subsurface exploration and laboratory testing program has been implemented with a single boring performed at each substructure location. The soil boring logs for the southbound bridge are presented in Figures D-2 through D-4.

At each respective sample depth, the boring logs indicate the SPT N value in cohesionless soil layers, or the undisturbed Shelby tube sampling interval in cohesive layers. The results from subsequent unconfined compression tests and other index tests performed on the undisturbed samples are also provided on the boring logs at the respective sample depth. The results of the subsurface exploration and laboratory testing program are used to prepare a subsurface profile; define soil and rock parameters including strength, compressibility, parameter variation, liquefaction susceptibility, and seismic earth pressure parameters; define subsurface water conditions, as well as identify critical cross sections for design.

The results of the subsurface exploration program and laboratory test results have been used to generate a generalized soil profile which is presented in Figure D-5. This generalized soil profile is an invaluable resource as the foundation selection process proceeds. A design profile for each substructure location will be developed from the information gathered in this block and used in later blocks.

SUBSURFACE EXPLORATION LOG — BORING NO. S-1 — SHEET 1 OF 3

District	2	Hammer Fall-Casing	--	Line	Baseline
County	Sussex	Hammer Fall Sampler	--	Station	1223 + 26
Project	Sunrise Expressway	Wt. of Hammer Casing	--	Offset	20 ft Lt
Structure	Freedom Bridge	Wt. of Hammer Sampler	140 lb	Surface EL.	315.0 ft
Date Start	5/28/2011	SPT Hammer Type	Automatic	Water Table EL.	300.0 ft
Date Finish	5/28/2011	Core Barrel Type	Double Tube	Logged By	MLB
Backfill/Sealed	5/28/2011	Drill Method	Mobile B57 & HSA	Time	9:30 PM

I.D.	DEPTH ft	BLOWS /6"	N	Soil Description and Remarks	q_u tsf	γ_d pcf	w_n %
SS-1		1					
		1	4	Loose Silty Fine			
		3		Sand (SM)			
	5						
SS-2		1					
		2	4				
		2					
	10						
SS-3		2					
		2	6				
		4					
	15						
SS-4		2					
		3	6				
		3					
	20						
SS-5		2					
		3	8	Loose Silty Fine			
		5		Sand (SM)			
	25						
SS-6		3					
		6	13	Medium Dense			
		7		Coarse Sand, Little			
				Silt (SP)			
	30						
SS-7		4					
		7	15				
		8					
	35						
SS-8		3					
		5	11				
		6					
	40						

Figure D-2 Boring Log S-1, Page 1 of 3.

SUBSURFACE EXPLORATION LOG — BORING NO. S-1 — SHEET 2 OF 3

District	2	Hammer Fall-Casing	--	Line	Baseline
County	Sussex	Hammer Fall Sampler	--	Station	1223 + 26
Project	Sunrise Expressway	Wt. of Hammer Casing	--	Offset	20 ft Lt
Structure	Freedom Bridge	Wt. of Hammer Sampler	140 lb	Surface EL.	315.0 ft
Date Start	5/28/2011	SPT Hammer Type	Automatic	Water Table EL.	300.0 ft
Date Finish	5/28/2011	Core Barrel Type	Double Tube	Logged By	MLB
Backfill/Sealed	5/28/2011	Drill Method	Mobile B57 & HSA	Time	9:30 PM

I.D.	DEPTH ft	BLOWS /6"	N	Soil Description and Remarks	q_u tsf	γ_d pcf	w_n %
SS-9		6 7 8	15	Medium Dense Coarse Sand, Little Silt (SP)			
	45						
SS-10		7 9 9	18				
	50						
SS-11		18 21 19	40	Dense Gravel with Sand (GW)			
	55			Note: Occasional Cobbles 54-55 ft			
SS-12		17 19 20	39				
	60						

I.D.	DEPTH ft	BLOWS /6"	N	Soil Description and Remarks	q_u tsf	γ_d pcf	w_n %
SS-13		18 21 20	41	Dense Gravel with Sand (GW)			
	65						
SS-14		20 22 21	43				
	70			Note: Occasional Cobbles 69-70 ft			
SS-15		21 20 21	41				
	75						
SS-16		20 22 22	44				
	80						

Figure D-2 Boring Log S-1, Page 2 of 3.

SUBSURFACE EXPLORATION LOG — BORING NO. S-1 — SHEET 3 OF 3

District	2	Hammer Fall-Casing	--	Line	Baseline
County	Sussex	Hammer Fall Sampler	--	Station	1223 + 26
Project	Sunrise Expressway	Wt. of Hammer Casing	--	Offset	20 ft Lt
Structure	Freedom Bridge	Wt. of Hammer Sampler	140 lb	Surface EL.	315.0 ft
Date Start	5/28/2011	SPT Hammer Type	Automatic	Water Table EL.	300.0 ft
Date Finish	5/28/2011	Core Barrel Type	Double Tube	Logged By	MLB
Backfill/Sealed	5/28/2011	Drill Method	Mobile B57 & HSA	Time	9:30 PM

I.D.	DEPTH ft	BLOWS /6"	N	Soil Description and Remarks	q_u tsf	γ_d pcf	w_n %
SS-17		22 22 23	45	Dense Gravel with Sand (GW)			
	85						
SS-18		23 24 24	48				
	90						
SS-19		22 24 22	46				
	95						
SS-19		25 24 23	47				
RC-1				Limestone Bedrock Rock Core 1 97.0 - 102.0 ft REC = 83% RQD = 81%			
	100						

I.D.	DEPTH ft	BLOWS /6"	N	Soil Description and Remarks	q_u tsf	γ_d pcf	w_n %
	105			EOB @ 102.0 ft			
	110						
	115						
	120						

Figure D-2 Boring Log S-1, Page 3 of 3.

SUBSURFACE EXPLORATION LOG — BORING NO. S-2 — SHEET 1 OF 2

District	2	Hammer Fall-Casing	--	Line	Baseline
County	Sussex	Hammer Fall Sampler	--	Station	1224 + 26
Project	Sunrise Expressway	Wt. of Hammer Casing	--	Offset	20 ft Lt
Structure	Freedom Bridge	Wt. of Hammer Sampler	140 lb	Surface EL.	285.0 ft
Date Start	6/2/2011	SPT Hammer Type	Automatic	Water Table EL.	290.0 ft
Date Finish	6/3/2011	Core Barrel Type	Double Tube	Logged By	MLB
Backfill/Sealed	6/3/2011	Drill Method	Mobile B57 & HSA	Time	5:30 PM

I.D.	DEPTH ft	BLOWS /6"	N	Soil Description and Remarks	q_u tsf	γ_d pcf	w_n %
SS-1		1 1 2	3	Loose Silty Fine Sand (SM)			
	5						
SS-2		2 2 2	4				
SS-3		21 25 26	51	Extremely Dense Gravel (GP)			
	10						
SS-4		26 27 25	52				
	15						
SS-5		26 28 27	55				
	20						

I.D.	DEPTH ft	BLOWS /6"	N	Soil Description and Remarks	q_u tsf	γ_d pcf	w_n %
UD-1				Very Stiff Silty Clay (CL)	3.10	98	31
	25						
UD-2					3.21	104	23
	30						
UD-3					3.25	105	22
	35						
UD-4					3.30	103	24
	40						

Figure D-3 Boring Log S-2, Page 1 of 2.

SUBSURFACE EXPLORATION LOG — BORING NO. S-2 — SHEET 2 OF 2

District	2	Hammer Fall-Casing	--	Line	Baseline
County	Sussex	Hammer Fall Sampler	--	Station	1224 + 26
Project	Sunrise Expressway	Wt. of Hammer Casing	--	Offset	20 ft Lt
Structure	Freedom Bridge	Wt. of Hammer Sampler	140 lb	Surface EL.	285.0 ft
Date Start	6/2/2011	SPT Hammer Type	Automatic	Water Table EL.	290.0 ft
Date Finish	6/3/2011	Core Barrel Type	Double Tube	Logged By	MLB
Backfill/Sealed	6/3/2011	Drill Method	Mobile B57 & HSA	Time	5:30 PM

I.D.	DEPTH ft	BLOWS /6"	N	Soil Description and Remarks	q_u tsf	γ_d pcf	w_n %
UD-5				Very Stiff Silty Clay (CL)	3.34	105	22
	45						
UD-6					3.40	106	21
	50						
SS-6		18 19 19	38	Dense Gravel with Sand (GP) Note: Occasional Cobbles 52-53 ft			
	55						
SS-7		21 22 24	46				
	60						

I.D.	DEPTH ft	BLOWS /6"	N	Soil Description and Remarks	q_u tsf	γ_d pcf	w_n %
SS-8		19 19 22	41	Dense Gravel with Sand (GP)			
	65						
SS-9		21 24 26	50				
	70						
RC-1				Limestone Bedrock Rock Core 1 70.0 - 75.0 ft REC = 90% RQD =79%			
	75						
				EOB @75.0 ft			
	80						

Figure D-3 Boring Log S-2, Page 2 of 2.

SUBSURFACE EXPLORATION LOG BORING NO. S-3 SHEET 1 OF 3

District	2	Hammer Fall-Casing	--	Line	Baseline
County	Sussex	Hammer Fall Sampler	--	Station	1225 + 26
Project	Sunrise Expressway	Wt. of Hammer Casing	--	Offset	20 ft Lt
Structure	Freedom Bridge	Wt. of Hammer Sampler	140 lb	Surface EL.	310.0 ft
Date Start	6/4/2011	SPT Hammer Type	Automatic	Water Table EL.	305.0 ft
Date Finish	6/5/2011	Core Barrel Type	Double Tube	Logged By	MLB
Backfill/Sealed	6/5/2011	Drill Method	Mobile B57 & HSA	Time	5:30 PM

I.D.	DEPTH ft	BLOWS /6"	N	Soil Description and Remarks	q_u tsf	γ_d pcf	w_n %
UD-1				Medium Silty Clay (CL)	0.65	86	26
	5						
UD-2					0.66	85	29
	10						
UD-3					0.68	85	30
	15						
UD-4					0.70	84	32
	20						
UD-5				Medium Silty Clay (CL)	0.72	85	31
	25			Stiff Silty Clay (CL)			
UD-6					1.79	95	30
	30						
UD-7					1.85	97	27
	35						
UD-8					1.93	100	24
	40						

Figure D-4 Boring Log S-3, Page 1 of 3.

SUBSURFACE EXPLORATION LOG BORING NO. S-3 SHEET 2 OF 3

District	2	Hammer Fall-Casing	--	Line	Baseline
County	Sussex	Hammer Fall Sampler	--	Station	1225 + 26
Project	Sunrise Expressway	Wt. of Hammer Casing	--	Offset	20 ft Lt
Structure	Freedom Bridge	Wt. of Hammer Sampler	140 lb	Surface EL.	310.0 ft
Date Start	6/4/2011	SPT Hammer Type	Automatic	Water Table EL.	305.0 ft
Date Finish	6/5/2011	Core Barrel Type	Double Tube	Logged By	MLB
Backfill/Sealed	6/5/2011	Drill Method	Mobile B57 & HSA	Time	5:30 PM

I.D.	DEPTH ft	BLOWS /6"	N	Soil Description and Remarks	q_u tsf	γ_d pcf	w_n %
UD-9				Stiff Silty Clay (CL)	2.00	99	26
	45						
UD-10				Very Stiff Silty Clay (CL)	3.11	104	24
	50						
UD-11					3.19	103	25
	55						
UD-12					3.30	106	22
	60						
UD-13				Very Stiff Silty Clay (CL)	3.36	105	23
	65						
UD-14					3.39	106	21
	70						
UD-15					3.50	107	21
	75						
UD-16					3.55	108	20
	80						

Figure D-4 Boring Log S-3, Page 2 of 3.

SUBSURFACE EXPLORATION LOG — BORING NO. S-3 — SHEET 3 OF 3

District	2	Hammer Fall-Casing	--	Line	Baseline
County	Sussex	Hammer Fall Sampler	--	Station	1225 + 26
Project	Sunrise Expressway	Wt. of Hammer Casing	--	Offset	20 ft Lt
Structure	Freedom Bridge	Wt. of Hammer Sampler	140 lb	Surface EL.	310.0 ft
Date Start	6/4/2011	SPT Hammer Type	Automatic	Water Table EL.	305.0 ft
Date Finish	6/5/2011	Core Barrel Type	Double Tube	Logged By	MLB
Backfill/Sealed	6/5/2011	Drill Method	Mobile B57 & HSA	Time	5:30 PM

I.D.	DEPTH ft	BLOWS /6"	N	Soil Description and Remarks	q_u tsf	γ_d pcf	w_n %
UD-17				Very Stiff Silty Clay (CL)	3.58	109	19
	85						
UD-18					3.60	108	20
	90						
UD-19					3.65	110	19
	95						
UD-20					3.70	110	18
SS-1		RC-1		Limestone Bedrock Rock Core 1 96.0 - 101.0 ft REC = 93% RQD =88%			
	100						

I.D.	DEPTH ft	BLOWS /6"	N	Soil Description and Remarks	q_u tsf	γ_d pcf	w_n %
	105			EOB @101.0 ft			
	110						
	115						
	120						

Figure D-4 Boring Log S-3, Page 3 of 3.

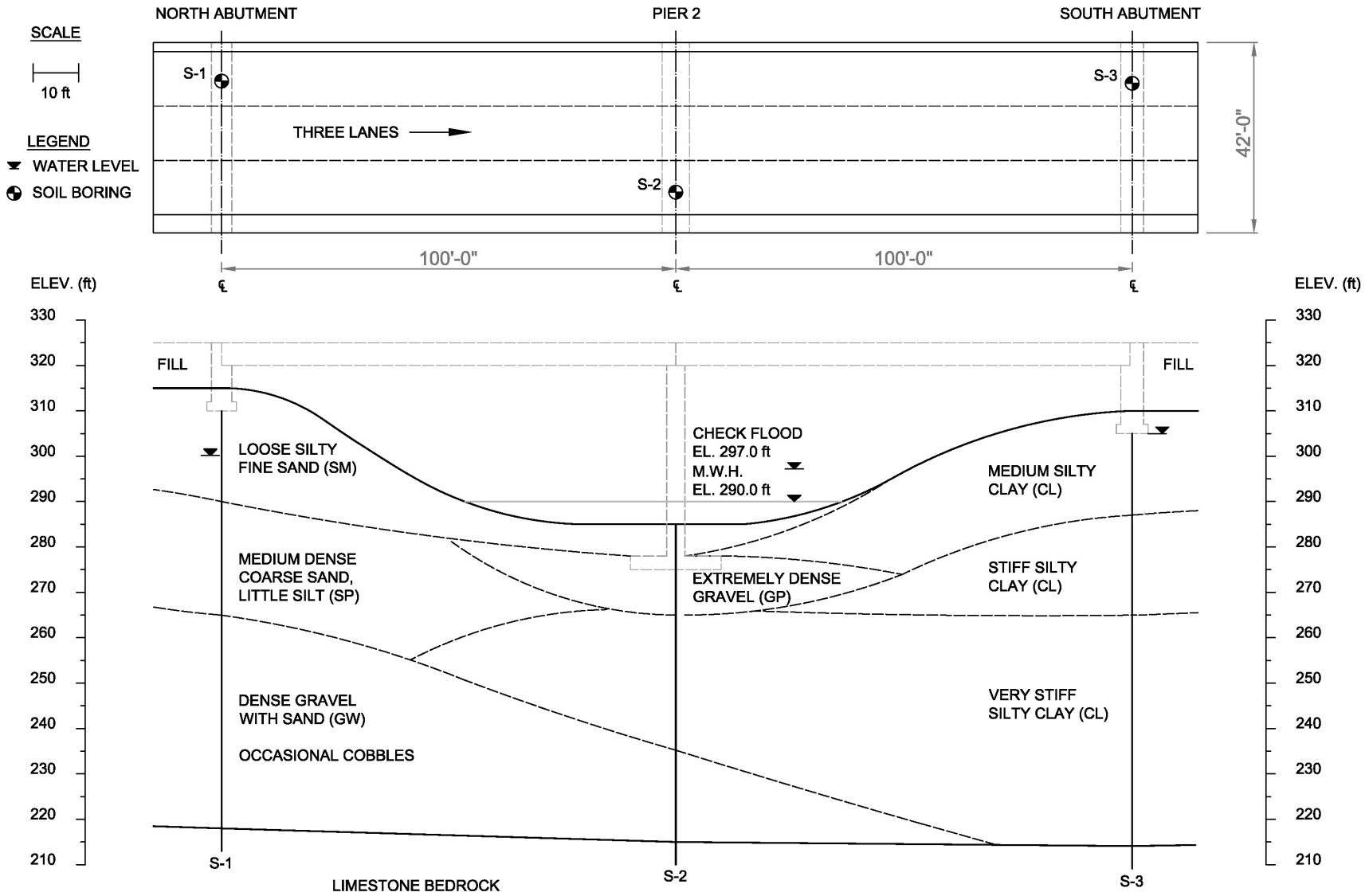

Figure D-5 Site Profile View.

D.6 Block 6: Evaluate Information and Determine Candidate Foundation Systems

The question to be answered is what candidate foundation systems are appropriate for consideration based on the site conditions. This question will be answered based primarily on the strength and compressibility of the geomaterials, the proposed loading conditions, the project deformation limits, the project schedule, and the foundation cost. The hydraulic analysis indicates the potential for substantial scour at the center pier. The selection of the appropriate foundation system including cost considerations is discussed in greater detail in Chapter 3.

D.7 Block 7: Determine if a Deep Foundation is Required

Based on the strength and compressibility of the near surface geomaterials, scour concerns, as well as the required construction timeline, it is decided that a deep foundation system is required for structure support. Driven piles and other deep foundation systems must now be evaluated. Through this process, some foundation systems become less viable as constructability and cost considerations are refined. In the final analysis, the design, construction, and testing costs associated with addressing the variable subsurface conditions at this site are prohibitive for all of the drilled deep foundation solutions. Accordingly, driven piles are selected for the structure support; and drilled shaft, micropile, CFA pile, and other drilled deep foundation systems are eliminated.

D.8 Block 8: Select Candidate Driven Pile Types and Sections

Driven pile foundation systems consisting of steel H-piles, closed-end steel pipe piles, and prestressed concrete piles are initially considered technically and economically feasible. However, due to pile drivability concerns presented by the extremely dense gravel layer at Pier 2, closed-end steel pipe piles and prestressed concrete piles are eliminated from further consideration. In this geographic region, steel H-piles are commonly used. Local contractors are familiar with H-pile installation and splicing, and H-piles are readily available from a local manufacturing facility. For these reasons, in addition to the ease with which H-piles can accommodate length variations associated with site variability, H-piles are viewed as the primary candidate pile type. Several H-pile sections are viable, and those sections will be advanced as candidate driven pile foundation systems.

Foundation loads are now closer to being finalized as are the tolerable deformation limits for the structure. At this stage in the design process, detailed analyses are required at each substructure location. Therefore, Block 9 through Block 19 will be repeated for each of the three substructure locations: North Abutment, Pier 2, and South Abutment. The design process will be presented for these blocks at a given substructure location before repeating the same steps at the next substructure location.

D.9 Block 9: North Abutment – Calculate Nominal and Factored Structural Resistances for all Candidate Piles

The nominal structural resistance is now evaluated for five candidate H-pile sections. The H-pile sections selected for evaluation include a HP 10x42, a HP 12x53, a HP 12x74, a HP 14x89, and a HP 14x117. A detailed step by step example for calculation of the nominal structural resistance was previously presented in Section 8.5.3 for an HP 14x117 H-pile section. Therefore, this process is not repeated for the five candidate pile sections. Table D-2 presents the calculated nominal structural resistances in axial compression, flexure, and shear for the five candidate sections. An unbraced length of 1 foot was assumed in these calculations.

Table D-2 Nominal Structural Resistances in Axial Compression, Flexure and Shear

H-pile Section	HP 10x42	HP 12x53	HP 12x74	HP 14x89	HP 14x117
P_n, Nominal Resistance in Axial Compression (kips)	618	767	1088	1303	1718
M_{ny}, Nominal Resistance in Weak Axis Flexure (kip-ft)	82	114	118	257	380
M_{nx}, Nominal Resistance in Strong Axis Flexure (kip-ft)	176	295	433	592	807
$V_{n,}$ Nominal Resistance in Shear (kips)	118	149	214	246	331

It is anticipated that the piles at the North Abutment will be driven into the dense gravel with sand deposit, or possibly to the underlying bedrock. The dense gravel with sand deposit contains occasional cobbles. In these conditions, pile shoes are recommended for use with the H-piles to reduce the risk of damage. Therefore, the applicable structural resistance factors, ϕ_c, are 0.5 for axial compression resistance and 0.7 for combined axial compression and flexural resistance. A resistance factor

of ϕ_v =1.0 is used for shear, and a resistance factor of ϕ_f=1.0 is applicable for flexure only. Table D-3 summarizes the calculated factored structural resistances in axial compression, combined axial compression and flexure, flexure, and shear.

Table D-3 Factored Structural Resistance in Axial Compression, Flexure and Shear

H-pile Section	HP 10x42	HP 12x53	HP 12x74	HP 14x89	HP 14x117
P_r, Factored Resistance in Axial Compression, ϕ_c = 0.5 (kips)	309	383	544	652	859
P_r, Factored Resistance in Axial Compression and Flexure, ϕ_c = 0.7 (kips)	433	537	762	912	1203
M_{ry}, Factored Resistance in Weak Axis Flexure, ϕ_f=1.0 (kip-ft)	82	114	118	257	380
M_{rx}, Factored Resistance in Strong Axis Flexure, ϕ_f=1.0 (kip-ft)	176	295	433	592	807
V_r, Factored Resistance in Shear ϕ_v =1.0 (kips)	118	149	214	246	331

D.10 Block 10: North Abutment – Calculate Nominal and Factored Geotechnical Resistances in Axial Compression and Tension Versus Depth for all Candidate Piles; Perform Preliminary Pile Drivability Analyses

The engineering properties of the subsurface materials at the North Abutment were determined in Block 5. The results of the boring program and laboratory tests are now used to develop a design profile for each substructure location. Engineering judgement was used in developing the design profile to delineate the subsurface conditions into layers with similar properties. An effective stress diagram, depicted in Figure D-6, was also constructed in association with the design profile. This diagram includes the total stress, porewater pressure, and effective stress versus depth. Figure D-6 also presents the basic soil profile for quick reference to the relevant soil layers. The effective stress diagram was computed using Equations 5-7 through 5-9 from Chapter 5. These equations are repeated below. For Figure D-6, the total stress, porewater pressure, and effective stress were calculated at 1 foot increments using a spreadsheet.

$$\sigma_{vo} = \sum_i^n (\gamma_i h_i) \quad \text{[Eq. 5-7]}$$

$$u = \gamma_w h_w \quad \text{[Eq. 5-8]}$$

$$\sigma'_{vo} = \sum_i^n (\gamma_i h_i) - \gamma_w h_w \quad \text{[Eq. 5-9]}$$

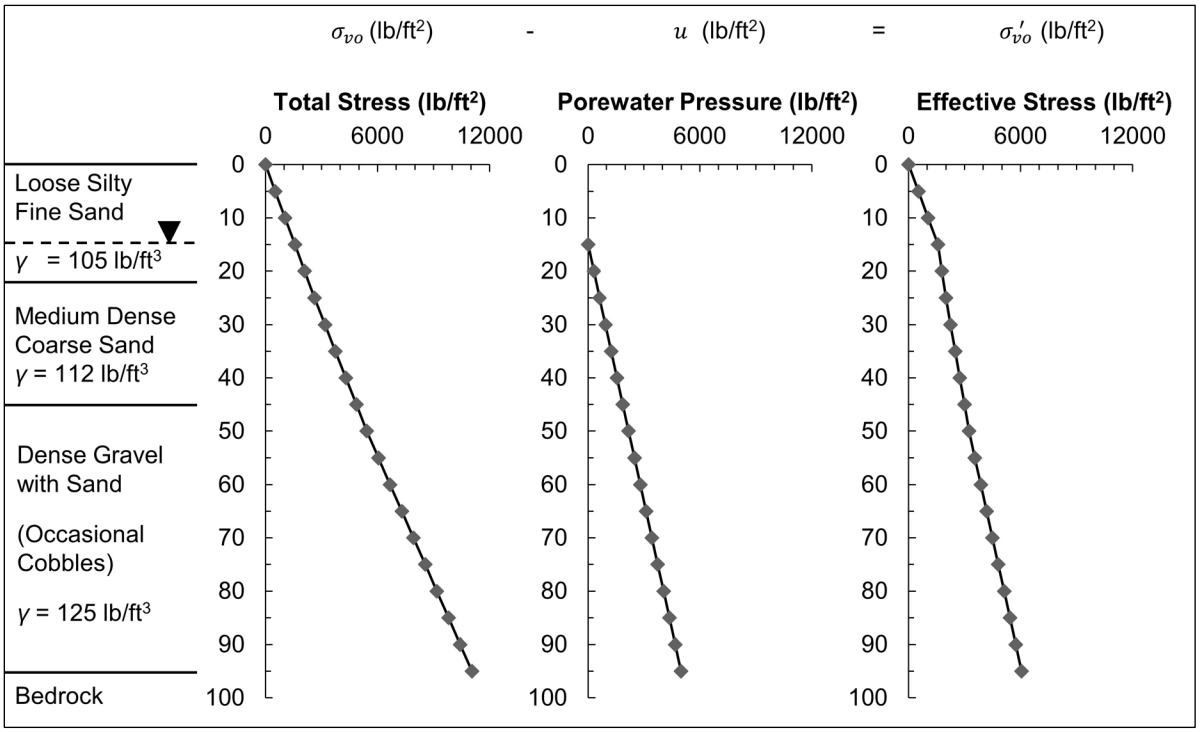

Figure D-6 Effective stress diagram for North Abutment using Boring S-1.

To continue development of an idealized design profile, field SPT N values were corrected for hammer energy transfer and vertical effective stress. The field SPT N values were first corrected for energy transfer using Equation 5-1. These results are presented in Table D-4 Typical correlations for SPT hammer type and energy transfer are provided in Section 5.1.1 (e.g., typical energy transfer of 80% for automatic hammer). The SPT hammer on the drill rig used for this project's subsurface exploration program was calibrated in accordance with ASTM D4633. Results of this calibration indicated an average energy transfer of 75%. Therefore, the *ER* value in Equation 5-1 is equal to 75.

$$N_{60} = N\left(\frac{ER}{60}\right) \quad \text{[Eq. 5-1]}$$

The SPT N value was corrected for vertical effective stress as presented in Equation 5-2, using the Peck et al. (1974) correction factor, C_n. The depth value for this calculation was taken from the middle depth of the SPT sampling event after the 6

inch seating interval (e.g., the SPT N value recorded from 0.5-1.5 feet was corrected using the vertical effective stress at a depth of 1 foot).

$$(N_1)_{60} = C_n N_{60} \quad \text{[Eq. 5-2]}$$

$$C_n = 0.77 \log \left(\frac{20}{\sigma'_{vo}}\right) \quad \text{[Eq. 5-3]}$$

Table D-4 Correction of Field SPT N Value for Energy and Vertical Effective Stress at the North Abutment using S-1

Soil Layer	Depth (ft)	σ'_{vo} (ksf)	Field N value	N_{60}	C_n	$(N_1)_{60}$
1	1	0.105	4	5	1.99	10
1	6	0.630	4	5	1.39	7
1	11	1.155	6	8	1.19	9
1	16	1.618	6	8	1.07	8
1	21	1.831	8	10	1.03	10
2	26	2.058	13	16	0.99	16
2	31	2.306	15	19	0.95	18
2	36	2.554	11	14	0.92	13
2	41	2.802	15	19	0.89	17
2	46	3.050	18	23	0.86	19
3	51	3.363	40	50	0.83	41
3	56	3.676	39	49	0.80	39
3	61	3.989	41	51	0.77	40
3	66	4.302	43	54	0.75	40
3	71	4.615	41	51	0.72	37
3	76	4.928	44	55	0.70	39
3	81	5.241	45	56	0.68	38
3	86	5.554	48	60	0.66	40
3	91	5.867	46	58	0.64	37
3	96	6.180	47	59	0.62	37

After correcting the SPT N values for energy transfer and vertical effective stress, an average corrected N value was determined for each respective layer. The N value from the first SPT sample in Layer 1 was not included in this procedure since the bottom of the footing at the North Abutment is below this sample depth.

Table D-5 presents the average $(N_1)_{60}$ value for each layer at the North Abutment, the coefficient of variation, COV, within the layer, and the effective stress friction angle, ϕ', chosen for the layer. The coefficient of variation for each layer was less than 25% indicating low variability within each of the identified layers. Therefore, separating the soil profile into additional layers was not performed, as it would have been with the existence of higher variability soil.

The $(N_1)_{60}$ values were used to estimate the effective stress friction angle of each soil layer in accordance with Table 5-5. Layer 3 consists of hard angular gravel with sand. Therefore, as discussed in Section 5.5.1 of Chapter 5, the design friction angle in this layer was limited to 36 degrees for estimating the shaft resistance while a friction angle of 40 degrees was used to estimate the toe resistance.

Table D-5 Effective Stress Friction Angle Correlations at the North Abutment

Soil Layer	Average $(N_1)_{60}$	COV	ϕ' shaft (degrees)	ϕ' toe (degrees)
1	9	14.4%	33	33
2	17	13.5%	36	36
3	39	3.7%	36	40

The design profile for the North Abutment is presented in Figure D-7, with the bottom of footing elevation 5 feet below ground surface elevation. Some soil properties in the design soil profile such as the elastic moduli, E_s, and the initial cyclic modulus of subgrade reaction, $k_{c,}$ have been selected based on published correlations in the absence of laboratory and field testing. For this particular soil profile, the elastic moduli were determined from the SPT correlation in Table 5-11 and the initial cyclic moduli of subgrade reaction were selected based on representative values shown in Table 7-22. The figure format used to summarize the design profile is used at all substructure locations and therefore includes design value placeholders for cohesive soil parameters, the undrained shear strength, s_u, and 50% strain factor, ε_{50}. However, cohesive soils are not present at the North Abutment.

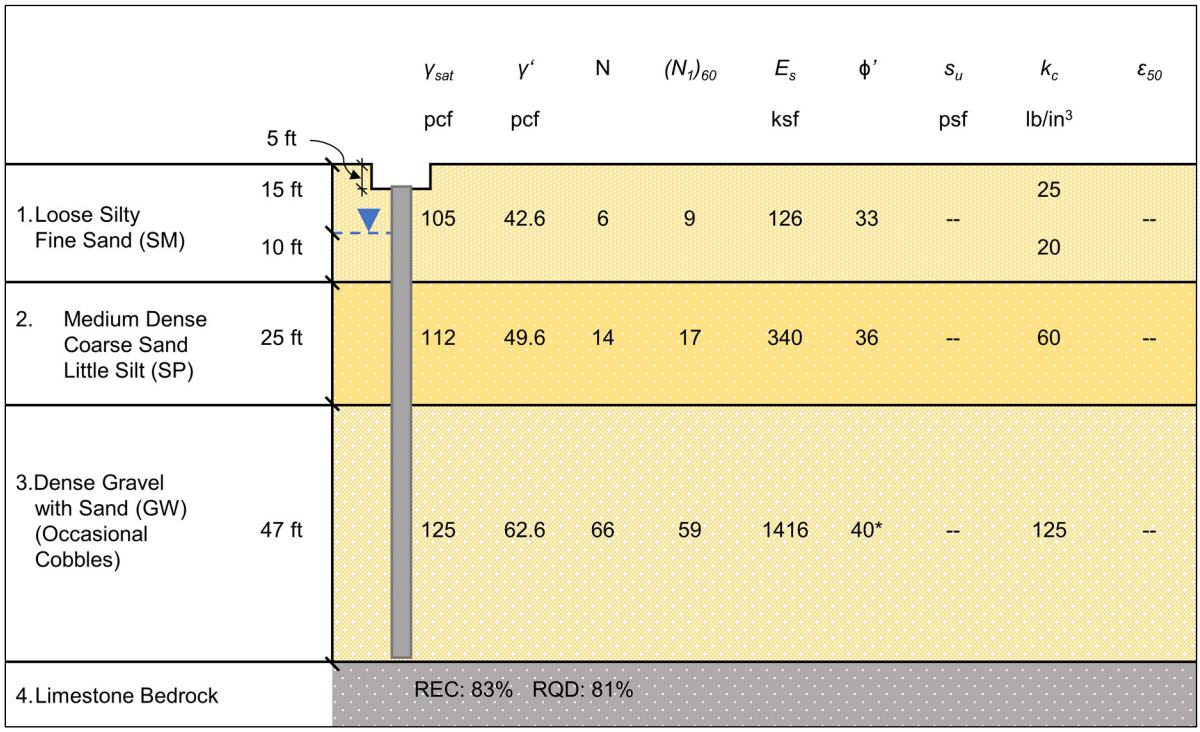

Figure D-7 Design profile at the North Abutment.

D.10.1 Geotechnical Resistance in Axial Compression

The nominal geotechnical resistance in axial compression is now determined for the selected candidate H-pile sections. The nominal geotechnical resistance can be calculated by hand or with computer software using an appropriate analysis method for cohesionless soils and the pile type. Chapter 7 describes appropriate methods for this purpose as well as computer programs available at the time of this manual's publication.

For this abutment, the DrivenPiles computer program was used to calculate the nominal resistance, shaft resistance, and toe resistance each as a function of depth for each of the five candidate H-piles. This software program was selected since it uses the FHWA recommended Nordlund method. This method is appropriate for calculating the nominal geotechnical resistance of H-piles in cohesionless soils such as those encountered in Boring S-1. The DrivenPiles program code also allows the analyst to select a different friction angle for shaft and toe resistance calculations in any layer. This option was utilized for the gravel with sand and occasional cobbles comprising Layer 3.

A summary of the shaft, toe, and nominal geotechnical resistance determined by the Nordlund static analysis method is presented for one of the candidate pile sections

in Table D-6. These results are also presented graphically in Figure D-8. The depth indicated in both Table D-6 and Figure D-8 is referenced from the bottom of footing, which is 5 feet below the original ground surface elevation. The nominal shaft, nominal toe, and nominal geotechnical resistances were calculated for all of the candidate pile sections in a similar manner. The nominal geotechnical resistances in axial compression versus pile penetration depth are presented in Figure D-9 for all candidate pile types.

Once the nominal geotechnical resistance in axial compression versus pile penetration depth has been calculated, the factored geotechnical resistance in axial compression versus pile penetration depth can be determined. The factored geotechnical resistance depends on the resistance determination method selected for the design.

If pile installation will be controlled by driving to a depth determined by static analysis method, then the factored geotechnical resistance in axial compression as a function of pile penetration depth can be determined by multiplying the calculated nominal resistance at a given depth by the resistance factor associated with the static analysis method, ϕ_{stat}. AASHTO (2014) resistance factors for static analysis methods are presented in Table 7-1 of this manual.

If the nominal resistance will be confirmed by a field determination method, the factored geotechnical resistance in axial compression as a function of pile penetration depth can be determined by multiplying the calculated nominal geotechnical resistance at a given depth by the resistance factor associated with the field determination method, ϕ_{dyn}. AASHTO (2014) resistance factors for field resistance determination methods are presented in Table 7-2.

Table D-6 Nominal Shaft, Nominal Toe and Nominal Geotechnical Resistance for HP 12x74 at the North Abutment

Depth (feet)	Nominal Shaft Resistance (kips)	Nominal Toe Resistance (kips)	Nominal Geotechnical Resistance (kips)		Depth (feet)	Nominal Shaft Resistance (kips)	Nominal Toe Resistance (kips)	Nominal Geotechnical Resistance (kips)
0.01	0.0	16.4	16.4		37	151.0	155.4	306.4
1	1.1	19.7	20.7		38	157.9	155.4	313.3
2	2.3	23.0	25.3		39	165.0	155.4	320.4
3	3.7	26.2	30.0		40	172.1	155.4	327.5
4	5.3	29.5	34.9		41	179.4	155.4	334.8
5	7.2	32.8	40.0		42	186.8	155.4	342.2
6	9.2	36.1	45.2		43	194.3	155.4	349.7
7	11.4	39.4	50.7		44	202.0	155.4	357.4
8	13.7	42.6	56.4		44.99	209.7	155.4	365.1
9	16.3	45.9	62.2		45.01	209.8	398.8	608.6
9.99	19.1	49.2	68.2		46	217.6	406.4	624.0
10.01	19.1	49.2	68.3		47	225.7	414.1	639.8
11	22.0	50.5	72.5		48	233.9	421.8	655.7
12	25.0	51.3	76.2		49	242.2	428.1	670.3
13	28.0	51.3	79.3		50	250.7	428.1	678.8
14	31.2	51.3	82.4		51	259.4	428.1	687.5
15	34.4	51.3	85.6		52	268.2	428.1	696.3
16	37.7	51.3	88.9		53	277.2	428.1	705.3
17	41.0	51.3	92.3		54	286.3	428.1	714.4
18	44.5	51.3	95.7		55	295.5	428.1	723.6
19	48.0	51.3	99.2		56	304.9	428.1	733.0
19.99	51.5	51.3	102.8		57	314.5	428.1	742.6
20.01	51.6	110.2	161.8		58	324.2	428.1	752.3
21	56.5	112.8	169.3		59	334.1	428.1	762.2
22	61.5	115.5	176.9		60	344.1	428.1	772.2
23	66.6	118.1	184.7		61	354.2	428.1	782.3
24	71.9	120.8	192.7		62	364.6	428.1	792.7
25	77.2	123.5	200.7		63	375.0	428.1	803.1
26	82.7	126.2	208.9		64	385.7	428.1	813.7
27	88.3	128.8	217.2		65	396.4	428.1	824.5
28	94.0	131.5	225.6		66	407.3	428.1	835.4
29	99.9	134.2	234.1		67	418.4	428.1	846.5
30	105.9	136.9	242.7		68	429.6	428.1	857.7
31	111.9	139.5	251.5		69	441.0	428.1	869.1
32	118.2	142.2	260.4		70	452.5	428.1	880.6
33	124.5	144.9	269.4		71	464.2	428.1	892.3
34	130.9	147.6	278.5		72	476.0	428.1	904.1
35	137.5	150.2	287.7		73	488.0	428.1	916.1
36	144.2	152.9	297.1		74	500.1	428.1	928.2

Table D-6 Nominal Shaft, Nominal Toe and Nominal Geotechnical Resistance for HP 12x74 at the North Abutment (continued)

Depth (feet)	Nominal Shaft Resistance (kips)	Nominal Toe Resistance (kips)	Nominal Geotechnical Resistance (kips)		Depth (feet)	Nominal Shaft Resistance (kips)	Nominal Toe Resistance (kips)	Nominal Geotechnical Resistance (kips)
75	512.4	428.1	940.5		84	629.8	428.1	1057.8
76	524.9	428.1	953.0		85	643.5	428.1	1071.6
77	537.4	428.1	965.5		86	657.48	428.1	1085.58
78	550.2	428.1	978.3		87	671.57	428.1	1099.67
79	563.05	428.1	991.15		88	685.82	428.1	1113.92
80	576.09	428.1	1,004.19		89	700.21	428.10	1,128.31
81	589.28	428.1	1,017.38		90	714.76	428.10	1,142.86
82	602.6	428.1	1030.7		91	729.46	428.10	1,157.56
83	616.1	428.1	1044.2		91.99	744.16	428.10	1,172.26

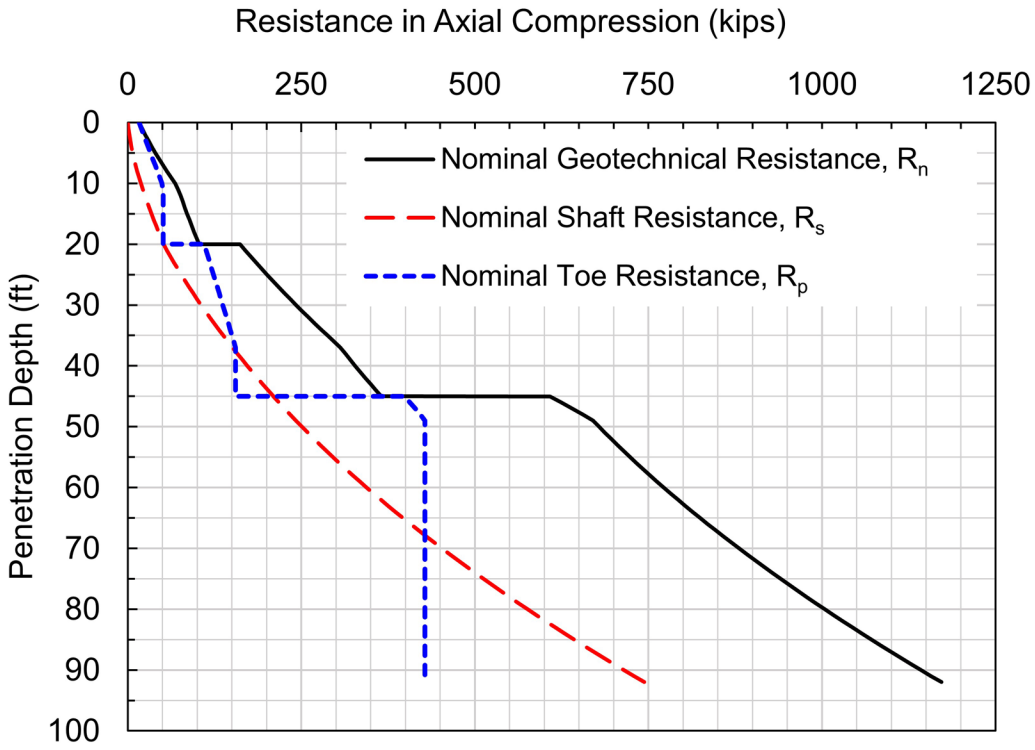

Figure D-8 Geotechnical resistance in axial compression versus pile penetration depth for HP 12x74 candidate pile section at North Abutment.

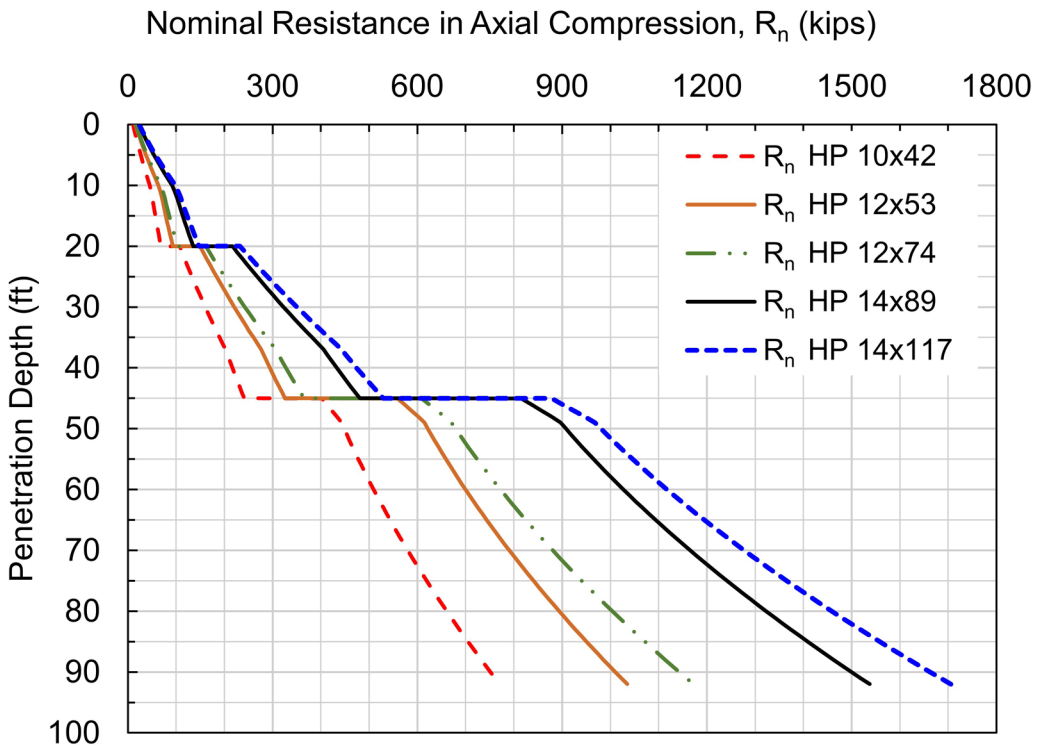

Figure D-9 Nominal geotechnical resistance in axial compression versus pile penetration depth for all candidate pile sections at the North Abutment.

Figure D-10 presents a design chart of the nominal resistance, R_n, and the factored geotechnical resistance, R_r, in axial compression versus pile penetration depth for the HP 12x74 H-pile section at the North Abutment. The design chart includes the nominal geotechnical resistance as well as a number of factored geotechnical resistances. The factored geotechnical resistances are presented for a selection of resistance determination methods. The factored geotechnical resistance versus penetration depth is plotted for resistance determination by a static load test with dynamic testing of 2% of the piles (ϕ_{dyn}=0.80), by dynamic testing of at least two piles per site condition, but no less than 2% of the production piles, with signal matching (ϕ_{dyn}=0.65), and by wave equation analysis (ϕ_{dyn}=0.50). The factored geotechnical resistance is also plotted for resistance determination by the Nordlund static analysis method (ϕ_{stat}=0.45). For a single pile section (HP 12x74), this figure illustrates the effects the various resistance determination methods have on the pile length required for a given factored resistance, the factored resistance available from a given pile section, and the potential impact of these factors on the number of piles needed to resist axial compression loads.

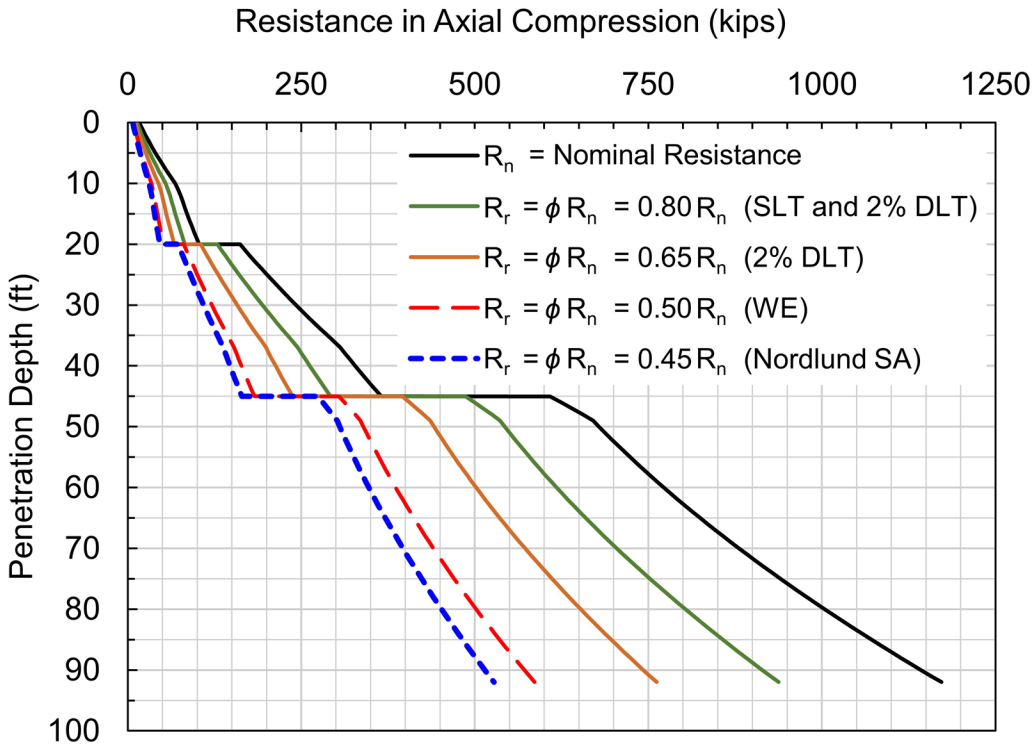

Figure D-10 Design chart of nominal and factored geotechnical resistance in axial compression versus pile penetration depth for HP 12x74 at the North Abutment.

The factored geotechnical resistance in axial compression for all candidate pile sections is presented in Figures D-11 through D-14 based on the same resistance determination methods. For all the candidate pile sections, these figures illustrate the effects the various resistance determination methods have on the pile length required for a given factored resistance, the factored resistance available from a given pile section, and the potential impact of these factors on the number of piles needed to resist axial compression loads.

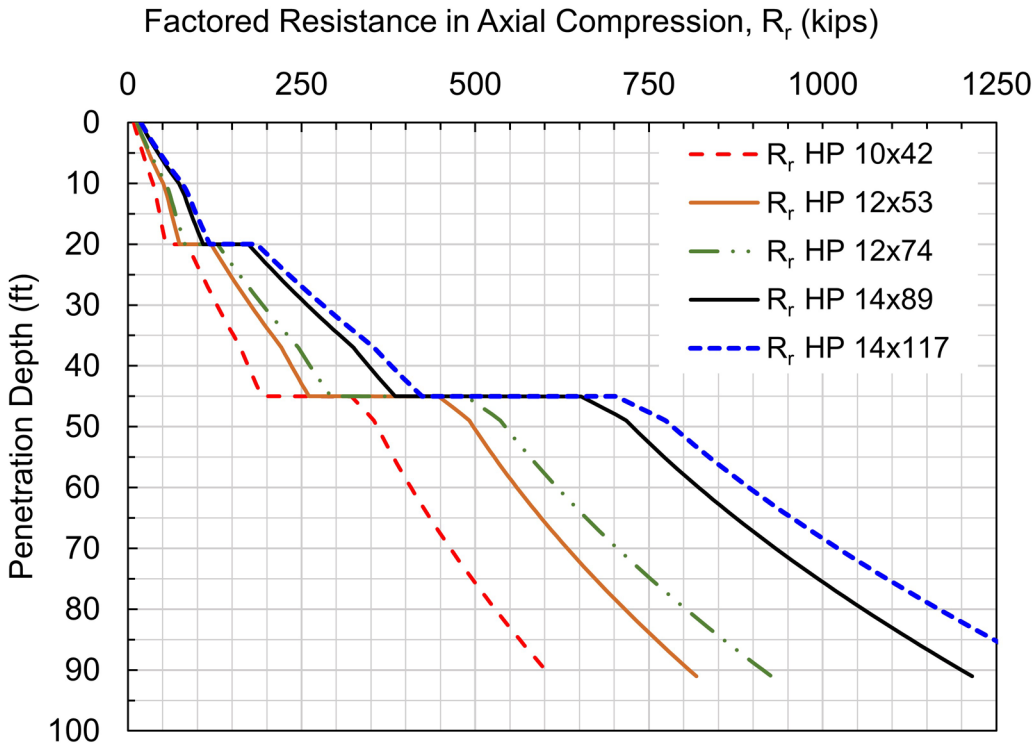

Figure D-11 Factored geotechnical resistance, R_r, in axial compression based on field determination by static load test and dynamic testing 2% of the piles, ϕ_{dyn}=0.80.

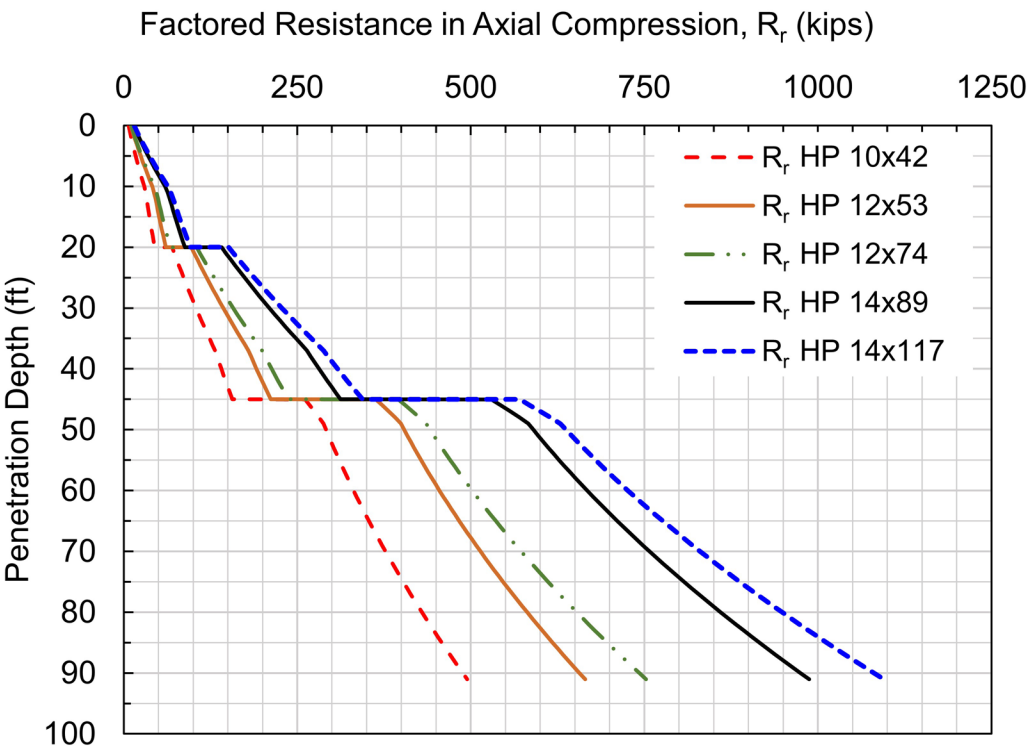

Figure D-12 Factored geotechnical resistance, R_r, in axial compression based on field determination by dynamic testing 2% of the piles, ϕ_{dyn}=0.65.

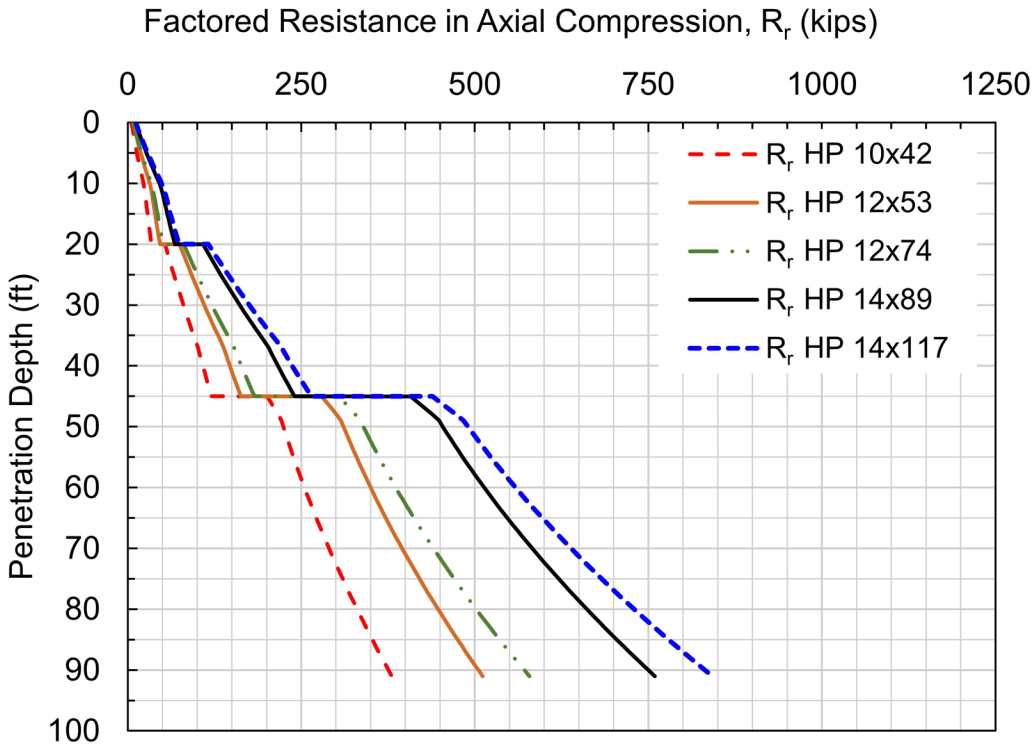

Figure D-13 Factored geotechnical resistance, R_r, in axial compression based on field determination by wave equation analysis, ϕ_{dyn}=0.50.

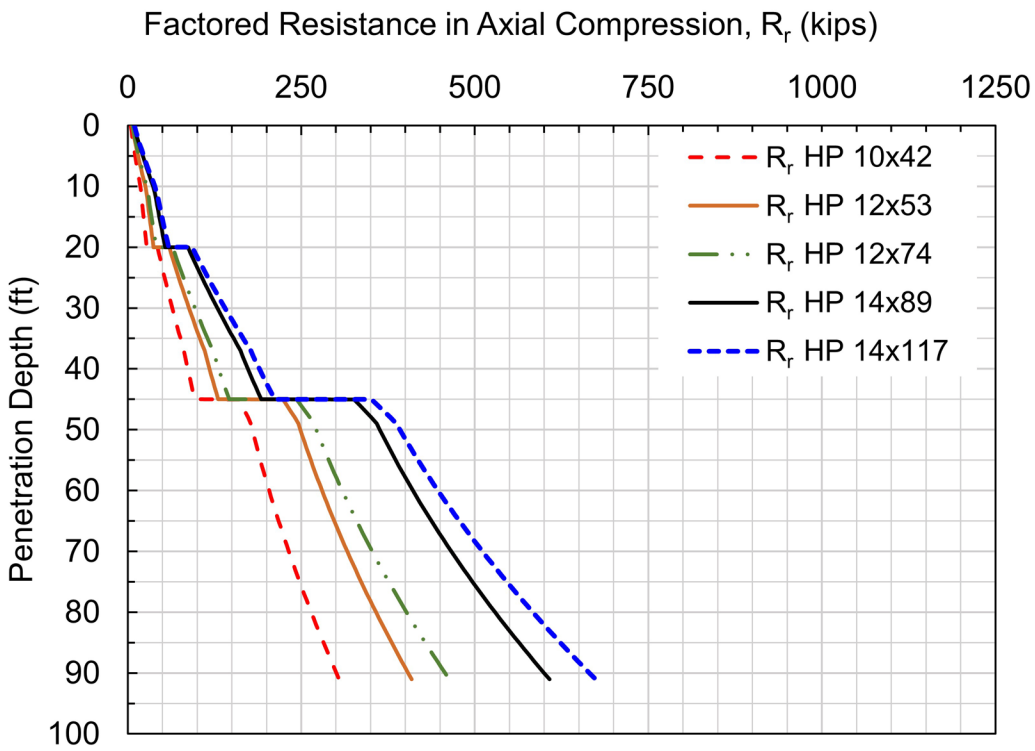

Figure D-14 Factored geotechnical resistance, R_r, in axial compression based on determination using Nordlund Method static analysis, ϕ_{stat}=0.45.

D.10.2 Geotechnical Resistance in Axial Tension

In a similar manner, the nominal and factored geotechnical resistances in axial tension (uplift) were calculated using the Nordlund method and with the DrivenPiles computer program. Figure D-15 presents the nominal shaft resistance versus penetration depth for all the candidate pile sections. As outlined in Section 7.2.3.2.1 of Chapter 7, the factored resistance in axial tension is the shaft resistance multiplied by the resistance factor, ϕ_{up}, for the resistance determination method.

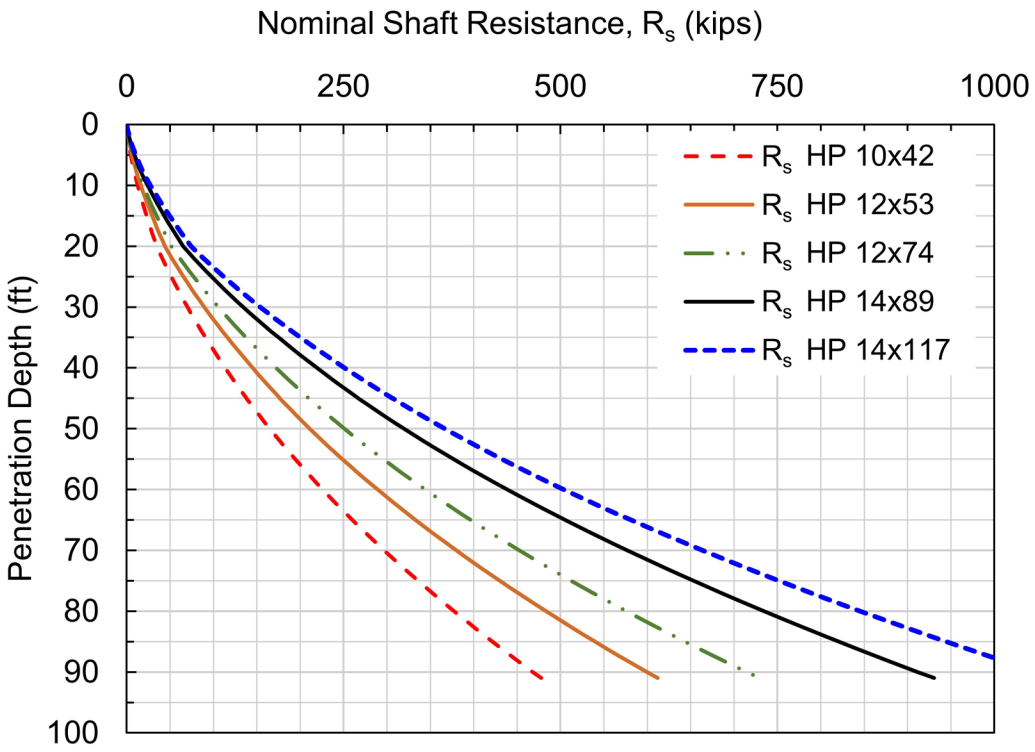

Figure D-15 Nominal shaft resistance versus penetration depth for all candidate pile sections at the North Abutment.

Figure D-16 presents a design chart of the nominal shaft resistance, R_s, and the factored geotechnical resistance, R_r, in axial tension versus pile penetration depth for the HP 12x74 H-pile section at the North Abutment. A resistance factor of 0.60 is used when the tension resistance is determined by a static load test, 0.50 when determined by a dynamic test with signal matching, and 0.35 when determined by the Nordlund static analysis method. For a single pile section (HP 12x74), this figure illustrates the effects the various resistance determination methods have on the pile length required for a given factored resistance, the factored resistance available from a given pile section, and the potential impact of these factors on the number of piles needed to resist axial tension loads.

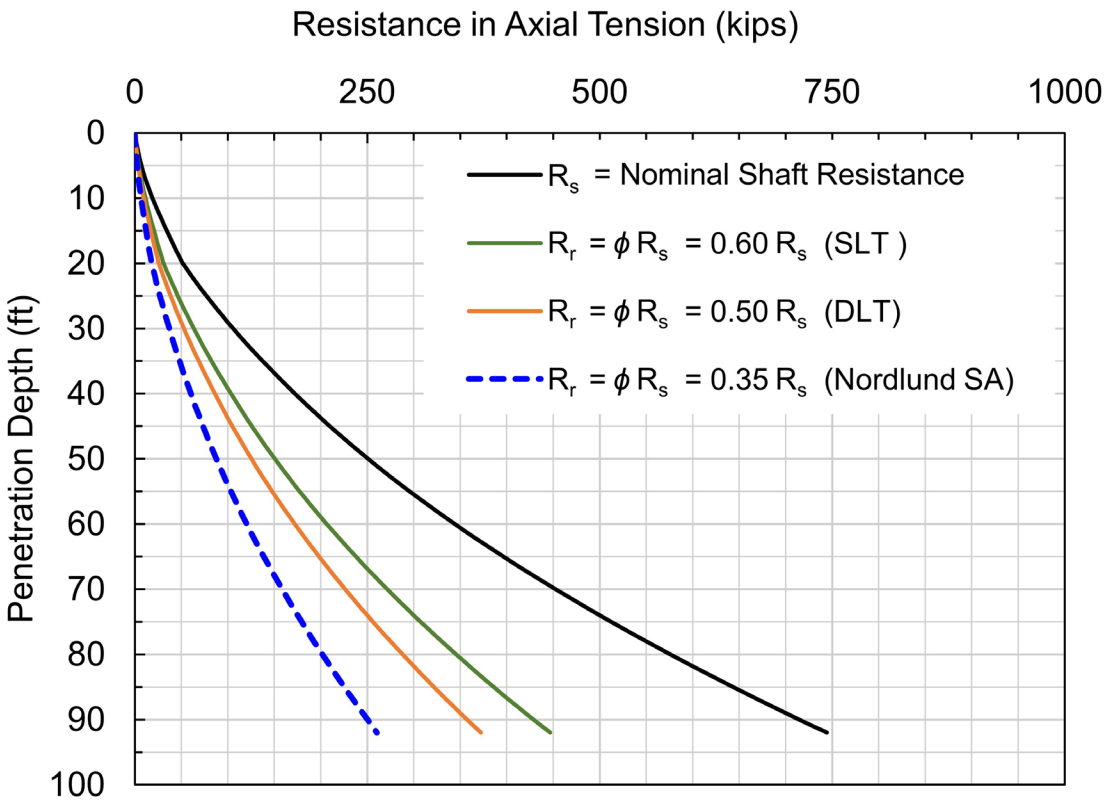

Figure D-16 Design chart of nominal and factored geotechnical resistance in axial tension for HP 12x74 at the North Abutment.

Figures D-17 to D-19 present the factored geotechnical resistance in axial tension versus penetration depth based on the field determination method for each of the candidate pile sections. For all the candidate pile sections, these figures illustrate the effects the various resistance determination methods have on the pile length required for a given factored resistance, the factored resistance available from a given pile section, and the potential impact of these factors on the number of piles needed to resist axial tension loads.

A review of the soil profile at the North Abutment indicates no unsuitable soil layers are present that should be ignored for load support. Abutment scour and liquefaction due to a seismic event are also not considerations.

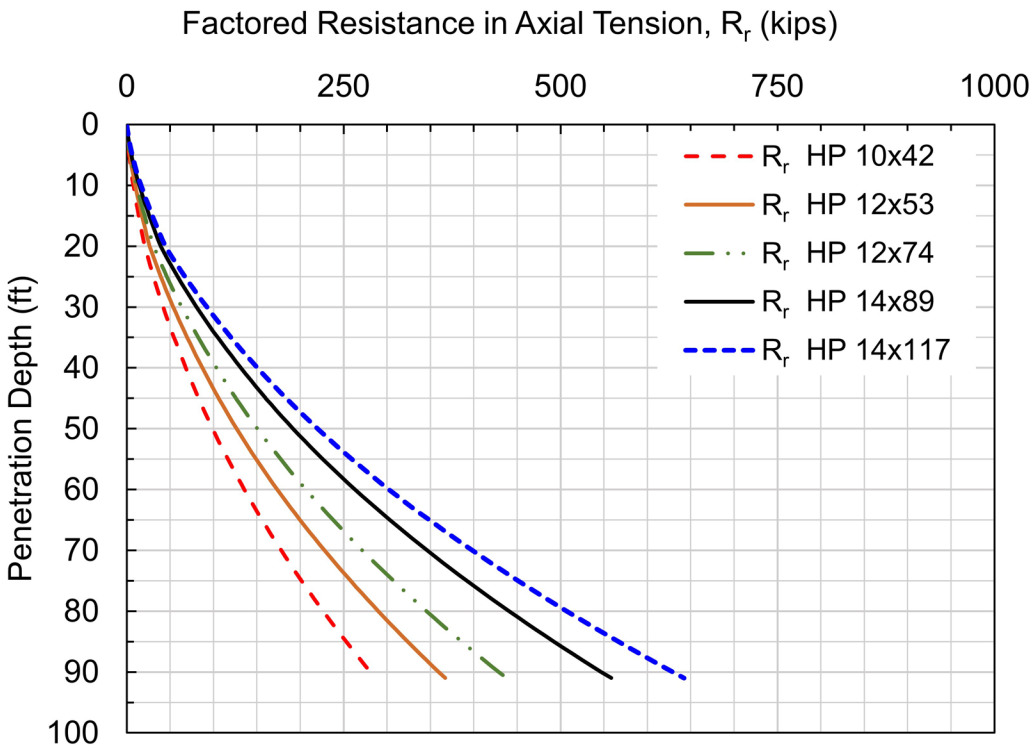

Figure D-17 Factored geotechnical resistance, R_r, in axial tension based on field determination by static load test, ϕ_{dyn}=0.60.

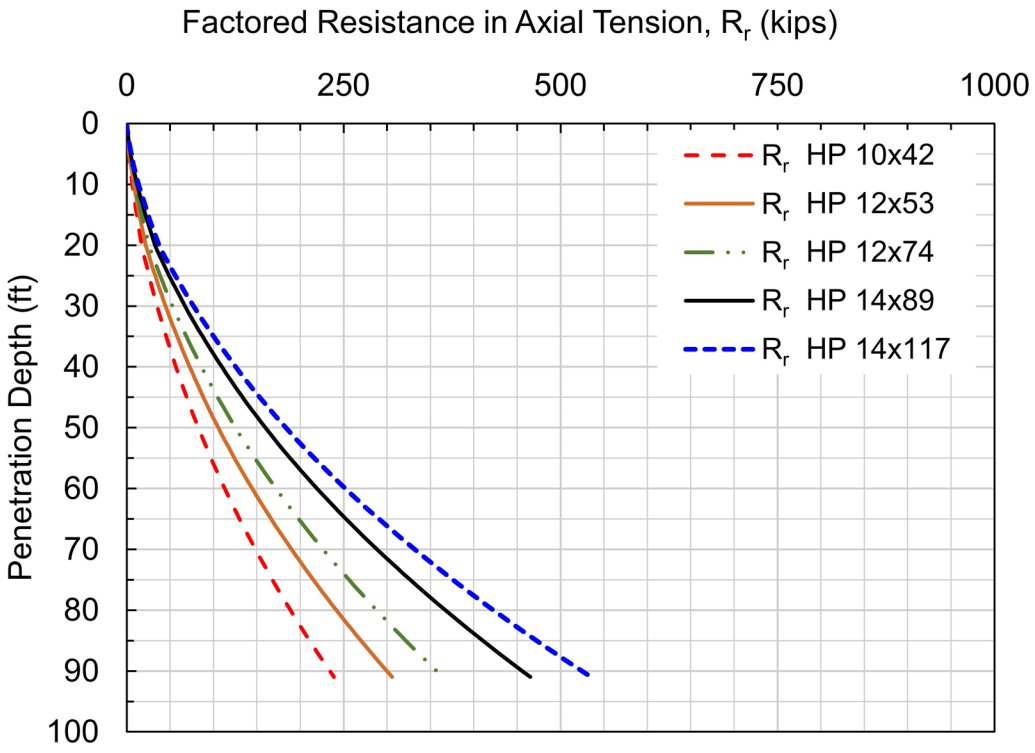

Figure D-18 Factored geotechnical resistance, R_r, in axial tension based on field determination by dynamic testing with signal matching, ϕ_{dyn}=0.50.

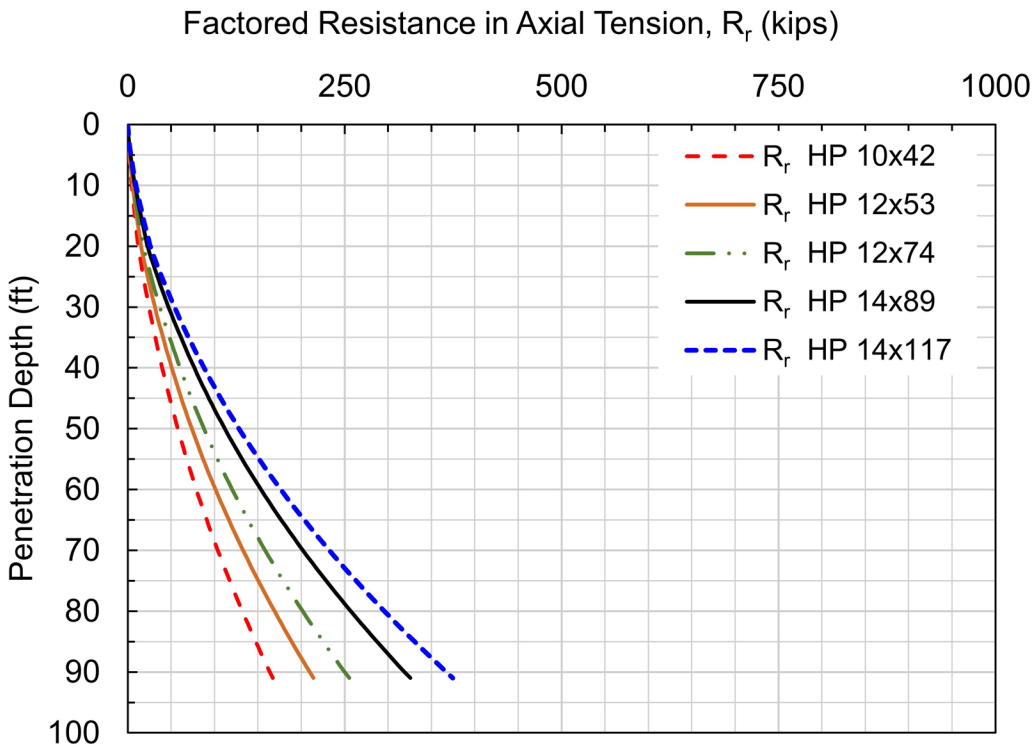

Figure D-19 Factored geotechnical resistance, R_r, in axial tension based on determination using Nordlund Method static analysis, ϕ_{stat}=0.35.

D.10.3 Preliminary Pile Drivability Assessment

A preliminary assessment of pile drivability is now performed. A check of pile drivability at this time is essential to assess the constructability of candidate pile types and/or sections and to eliminate sections with insufficient drivability. Section 12.4 provides a detailed discussion of wave equation drivability analyses and their applications.

A candidate pile section must be capable of being driven to the penetration depth necessary to achieve the nominal geotechnical resistance in axial compression and tension, and to a penetration depth necessary to satisfy lateral load demands as well as axial and lateral deformation requirements. A suitably sized pile hammer must be capable of driving the pile to this penetration depth and nominal resistance at a reasonable blow count without exceeding material stress limits. As detailed in Chapter 12, the blow count should be between 30 and 120 blows per foot at the nominal resistance. If the pile cannot be driven within these requirements, a larger pile hammer, a pile section with greater impedance, or pile installation aids such as predrilling or jetting may be required to satisfy or improve drivability.

Driving stresses during pile installation should remain below the driving stress limits associated with the pile type and material strength. For the candidate steel H-piles, compression driving stress limits are given by Equation 8-33. As per ASTM A-572 requirements, new steel H-piles are rolled with a minimum yield stress of 50 ksi.

The driving stress limit, σ_{dr}, for candidate pile sections is then calculated as follows:

$$\sigma_{dr} = \varphi_{da}\left(0.9\,F_y\right) \qquad \text{[Eq. 8-33]}$$

Where: φ_{da} = resistance factor, 1.0 for steel piles.
F_y = yield stress, 50 ksi.

Therefore, the driving stress limit, σ_{dr}, is 45 ksi.

$$\sigma_{dr} = (1.0)\big(0.9\,(50\ ksi)\big) = 45\ ksi$$

Drivability analyses were performed for all five candidate pile sections. Since the specific pile hammer is often unknown at this point in the design, a reasonably sized, commonly available single acting diesel hammer was chosen for each of the candidate pile sections. As noted in Section 15.19, a hammer having a ram weight of 1 to 2% of the larger of the required nominal resistance or required nominal driving resistance often provides a reasonable initial estimate of a trial hammer size for wave equation analysis.

Table D-7 summarizes the factored structural resistance in axial compression, P_r, and the corresponding minimum and maximum nominal driving resistance associated with full section utilization and field determination methods ranging from a static load test with dynamic testing (ϕ_{dyn}=0.80) to the FHWA modified Gates dynamic formula (ϕ_{dyn}=0.40). Given that utilization of the full structural resistance is uncommon for piles driven in soil, a reasonable initial estimate of the trial hammer size for a wave equation drivability analysis is 1 to 1.5% of the minimum R_{ndr}. Driving stresses could exceed specified limits by choosing a hammer with a ram weight significantly larger than 2% of the minimum R_{ndr}. For each pile hammer, the wave equation default values were used for the helmet weight, hammer cushion materials, and the hammer cushion material properties.

Table D-7 Summary of Pile Hammers Used in Drivability Analyses

Pile Section	Pile Cross Sectional Area (in^2)	Factored Structural Resistance, P_r (kips)	Minimum R_{ndr} ϕ_{dyn}=0.80 (kips)	Maximum R_{ndr} ϕ_{dyn}=0.40 (kips)	Ram Weight 1% of Min R_{ndr} (%)	Trial Diesel Hammer Model	Ram Weight (kips)	Rated Energy (ft-kips)
HP 10x42	12.4	309	386	773	3.86	D25-52	5.51	62.0
HP 12x53	15.5	383	478	958	4.78	D30-52	6.62	74.4
HP 12x74	21.8	544	680	1360	6.80	D36-52	7.94	89.3
HP 14x89	26.1	652	815	1630	8.15	D46-52	10.14	114.1
HP 14x117	34.4	860	1075	2150	10.07	D50-52	11.03	124.0

For the soil resistance model, the output from DrivenPiles was converted to unit shaft resistance and unit toe resistance values and then input into the wave equation program. Similar soil resistances are thereby calculated versus depth by both the static analysis and wave equation analysis programs.

The dynamic soil properties for each soil layer were chosen in accordance with wave equation program recommendations. Selection of soil quake and damping parameters is discussed in Section 12.6.7. For the North Abutment profile, some soil setup is expected in the upper silty fine sand layer and the underlying layer of medium dense sand with little silt. Therefore soil setup factors of 1.2 were selected for these two layers. No setup was expected in the dense gravel with sand of Layer 3. Soil setup is discussed in Section 7.2.4.2 and a summary of typical soil setup factors is provided in Table 7-16. A summary of the dynamic soil properties chosen for the drivability analyses are summarized in Table D-8.

In soils that exhibit setup, the long term nominal resistance may be higher than the nominal driving resistance. Therefore, a gain/loss factor of 0.833 was used to estimate the nominal driving resistance versus depth in the drivability analyses. This gain/loss factor was determined from the inverse of the highest soil setup factor within the soil model (e.g., 1 divided by 1.2 equals 0.833). A gain/loss factor of 1 would be used if it was desired to model the nominal resistance instead of the nominal driving resistance and not consider the soil strength loss during driving and any subsequent soil setup. Refer to Chapter 12 for more detailed discussion on the selection of dynamic soil properties and soil setup factors.

Table D-8 Dynamic Soil Properties for North Abutment Soil Profile

Soil Layer	Pile Section	Shaft Quake (in)	Toe Quake (in)	Shaft Damping (s/ft)	Toe Damping (s/ft)	Soil Set-Up Factor
1	HP 10 x 42	0.10	0.17	0.10	0.15	1.2
1	HP 12 x 53	0.10	0.20	0.10	0.15	1.2
1	HP 12 x 74	0.10	0.20	0.10	0.15	1.2
1	HP 14 x 89	0.10	0.23	0.10	0.15	1.2
1	HP 14 x 117	0.10	0.23	0.10	0.15	1.2
2	HP 10 x 42	0.10	0.17	0.05	0.15	1.2
2	HP 12 x 53	0.10	0.20	0.05	0.15	1.2
2	HP 12 x 74	0.10	0.20	0.05	0.15	1.2
2	HP 14 x 89	0.10	0.23	0.05	0.15	1.2
2	HP 14 x 117	0.10	0.23	0.05	0.15	1.2
3	HP 10 x 42	0.10	0.08	0.05	0.15	1.0
3	HP 12 x 53	0.10	0.10	0.05	0.15	1.0
3	HP 12 x 74	0.10	0.10	0.05	0.15	1.0
3	HP 14 x 89	0.10	0.12	0.05	0.15	1.0
3	HP 14 x 117	0.10	0.12	0.05	0.15	1.0

The DrivenPiles program calculates the nominal driving resistance which models the soil strength lost during driving as well as the geotechnical nominal resistance once setup occurs. Figure D-20 presents the nominal shaft, toe, and driving resistance versus pile penetration depth for the HP 12x74 H-pile section at the North Abutment. These nominal driving resistances are presented numerically in Table D-9. To quantify the expected soil setup at a given pile penetration depth, the values from Table D-9 can be compared against the nominal resistance previously presented in Table D-6. Figure D-21 illustrates the difference between the expected nominal driving resistance and the geotechnical nominal resistance after setup for the HP 12x74 candidate pile section. For example, at a depth of 45 feet, the expected setup from shaft resistance is 35 kips.

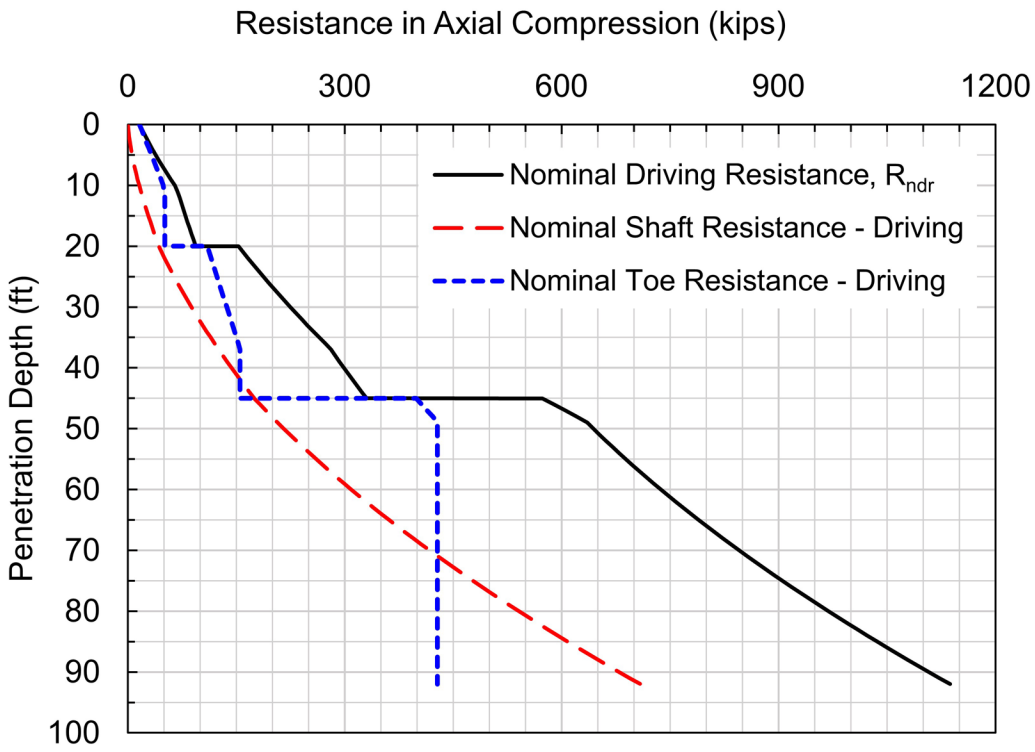

Figure D-20 Nominal driving resistance for HP 12x74 at the North Abutment.

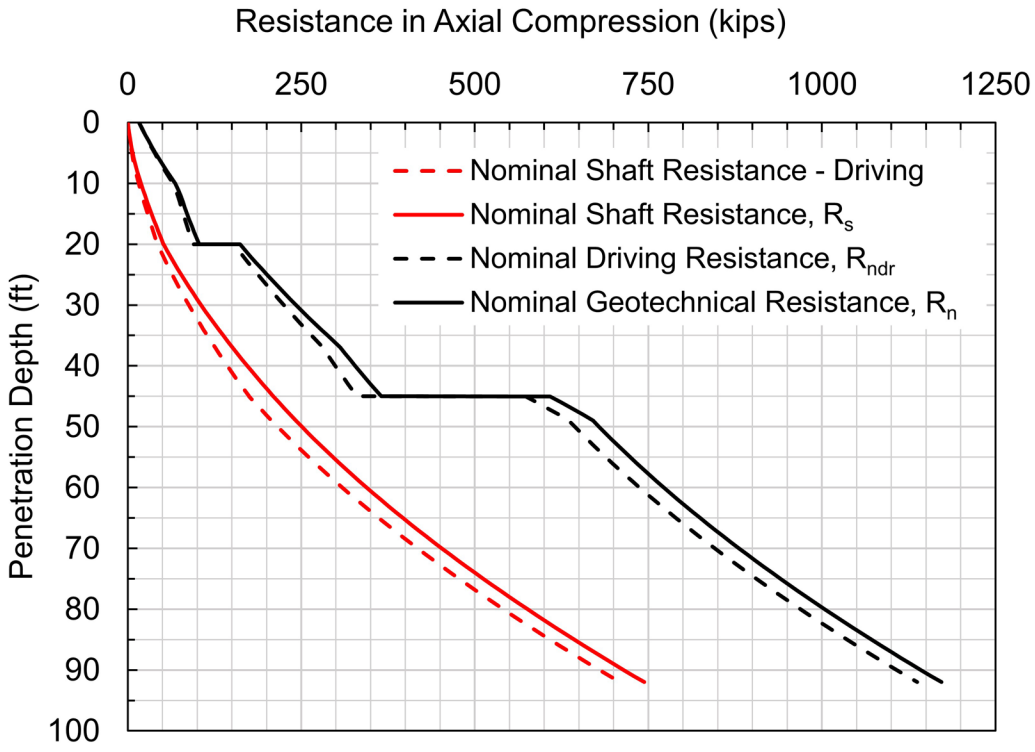

Figure D-21 Comparison of nominal driving resistance and nominal geotechnical resistance in axial compression for HP 12x74 at the North Abutment.

Table D-9 Summary of Nominal Driving Resistance Versus Pile Penetration Depth for HP 12x74 at the North Abutment

Depth (feet)	Nominal Shaft Resistance (kips)	Nominal Toe Resistance (kips)	Nominal Driving Resistance (kips)		Depth (feet)	Nominal Shaft Resistance (kips)	Nominal Toe Resistance (kips)	Nominal Driving Resistance (kips)
0.01	0.01	16.43	16.44		37	125.82	155.41	281.23
1	0.87	19.68	20.55		38	131.59	155.41	287
2	1.91	22.96	24.87		39	137.46	155.41	292.87
3	3.1	26.24	29.34		40	143.43	155.41	298.84
4	4.45	29.52	33.97		41	149.5	155.41	304.91
5	5.96	32.8	38.76		42	155.67	155.41	311.08
6	7.63	36.08	43.71		43	161.94	155.41	317.35
7	9.46	39.36	48.82		44	168.31	155.41	323.72
8	11.45	42.64	54.09		44.99	174.71	155.41	330.12
9	13.59	45.92	59.52		45.01	174.86	398.77	573.63
9.99	15.88	49.17	65.04		46	182.68	406.4	589.07
10.01	15.92	49.21	65.14		47	190.73	414.1	604.83
11	18.32	50.53	68.85		48	198.93	421.8	620.73
12	20.8	51.26	72.06		49	207.28	428.1	635.38
13	23.35	51.26	74.6		50	215.78	428.1	643.88
14	25.96	51.26	77.21		51	224.44	428.1	652.53
15	28.63	51.26	79.89		52	233.24	428.1	661.34
16	31.37	51.26	82.63		53	242.2	428.1	670.3
17	34.18	51.26	85.43		54	251.31	428.1	679.4
18	37.05	51.26	88.3		55	260.56	428.1	688.66
19	39.98	51.26	91.24		56	269.97	428.1	698.07
19.99	42.95	51.26	94.2		57	279.53	428.1	707.63
20.01	43.02	110.15	153.17		58	289.25	428.1	717.34
21	47.05	112.8	159.85		59	299.11	428.1	727.21
22	51.23	115.47	166.7		60	309.12	428.1	737.22
23	55.5	118.14	173.64		61	319.29	428.1	747.39
24	59.87	120.81	180.69		62	329.6	428.1	757.7
25	64.35	123.48	187.83		63	340.07	428.1	768.17
26	68.92	126.15	195.07		64	350.69	428.1	778.79
27	73.6	128.83	202.43		65	361.46	428.1	789.56
28	78.37	131.51	209.88		66	372.38	428.1	800.48
29	83.24	134.19	217.43		67	383.45	428.1	811.55
30	88.21	136.86	225.08		68	394.67	428.1	822.77
31	93.29	139.54	232.83		69	406.05	428.1	834.15
32	98.46	142.21	240.67		70	417.57	428.1	845.67
33	103.73	144.88	248.61		71	429.25	428.1	857.35
34	109.1	147.55	256.66		72	441.08	428.1	869.17
35	114.57	150.22	264.79		73	453.06	428.1	881.15
36	120.15	152.89	273.03		74	465.18	428.1	893.28

Table D-9 Summary of Nominal Driving Resistance Versus Pile Penetration Depth for HP 12x74 at the North Abutment (continued)

Depth (feet)	Nominal Shaft Resistance (kips)	Nominal Toe Resistance (kips)	Nominal Driving Resistance (kips)		Depth (feet)	Nominal Shaft Resistance (kips)	Nominal Toe Resistance (kips)	Nominal Driving Resistance (kips)
75	477.47	428.1	905.56		84	594.79	428.1	1022.89
76	489.9	428.1	917.99		85	608.58	428.1	1036.68
77	502.48	428.1	930.58		86	622.52	428.1	1050.62
78	515.21	428.1	943.31		87	636.62	428.1	1064.72
79	528.1	428.1	956.2		88	650.86	428.1	1078.96
80	541.13	428.1	969.23		89	665.26	428.1	1093.36
81	554.32	428.1	982.42		90	679.81	428.1	1107.9
82	567.66	428.1	995.76		91	694.5	428.1	1122.6
83	581.15	428.1	1009.25		91.99	709.2	428.1	1137.3

Graphical outputs of the preliminary drivability analyses are shown in Figure D-22. The nominal driving resistance, the blow count or pile penetration resistance, and the compression driving stress are presented versus pile penetration depth for each of the five candidate pile sections. As previously noted, the recommended blow count limit is 120 blows per foot (10 blows per inch), and the recommended driving stress limit is 45 ksi. A circular reference marker is indicated on the blow count versus penetration depth plot highlighting the depth where the blow count first exceeds 120 blows per foot. This marker is also shown at the same depth on the nominal driving resistance versus depth plot indicating the nominal driving resistance achieved when practical refusal driving conditions are encountered with the selected hammer in the modeled driving conditions. Similarly, the marker is shown at the same depth on the compression driving stress versus depth plot indicating the compression driving stress when practical refusal driving conditions are encountered.

In Figure D-22, the drivability results for the HP 12x53 section stand out from the other pile sections. The drivability results for the HP 12x53 H-pile section driven with a D30-52 driving system operated at the maximum fuel setting illustrate that refusal driving conditions of 120 blows per foot are encountered near a pile penetration depth of 52 feet. Compression driving stresses for the HP 12x53 with this hammer exceed the 45 ksi compression stress limit at a pile penetration depth of 46 feet, and reach a maximum of 45.9 ksi at a depth of 49 feet.

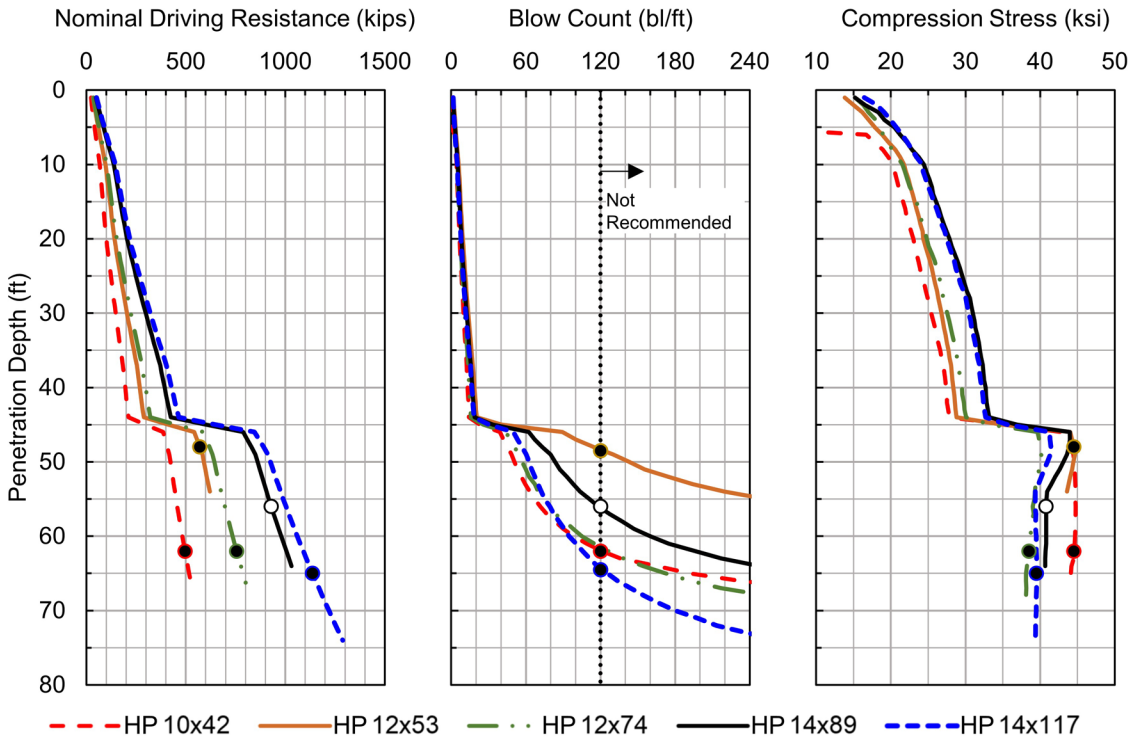

Figure D-22 Preliminary drivability results at the North Abutment.

The D30-52 hammer was also modeled at a reduced fuel setting, fuel setting 3. However, while the driving stresses can now be maintained within limits, refusal driving conditions are now encountered 4 feet shallower at a pile penetration depth of 48 feet. These results indicate the HP 12x53 pile section cannot be driven beyond 48 feet without exceeding either blow count or driving stress limits.

For the remaining candidate pile sections and selected pile hammers, the maximum pile penetration depth before achieving 120 blows per foot ranges between 57 and 64 feet. Driving stresses for some of the other candidate pile sections were close to the driving stress limit, but in all cases, the blow count limit and not the driving stress limit determined maximum drivability. A summary of the preliminary drivability results is presented in Table D-10. Once the estimated and/or minimum pile toe elevations are determined in Block 12 through Block 15 of the design process, the drivability results in Figure D-22 and Table D-10 should be reviewed to confirm that the candidate pile section can be driven to the estimated or required pile penetration depth, at reasonable blow counts, and within driving stress limits.

Table D-10 Summary of Preliminary Drivability Results at North Abutment

Pile Section	Pile Hammer	Fuel Setting	Pile Penetration Depth at Practical Refusal Limit (feet)	Nominal Driving Resistance at Practical Refusal Limit (kips)	Anticipated Nominal Resistance at Depth of Practical Refusal (kips)	Penetration Depth Exceeding Compression Driving Stress Limit (feet)	Maximum Compression Driving Stress (ksi)
HP 10x42	D25-52	4	61	489	512	> 61	43.7
HP 12x53	D30-52	4	52	605	634	46	45.9
HP 12x53	D30-52	3	48	571	600	> 48	44.5
HP 12x74	D36-52	4	61	746	780	> 61	40.1
HP 14x89	D46-52	4	57	941	985	> 57	44.5
HP 14x117	D50-52	4	64	1121	1172	> 64	41.4

As noted previously, a hammer having a ram weight of 1 to 2% of the required nominal driving resistance often provides a reasonable initial estimate of hammer size. However, if a candidate pile type does not satisfy drivability requirements with this initially selected hammer and driving stress levels are within limits, other hammers should be evaluated before eliminating the candidate pile type. For example, a D30-52 hammer was initially selected for the HP 12x74 H-pile. This driving system has a ram weight of 6.6 kips or 0.97% of the required nominal resistance, so it is slightly below the recommended trial hammer size. The blow count limit of 120 blows per foot with the D30-52 was reached at a nominal resistance of 680 kips and a pile penetration depth of 55 feet. However, compression driving stresses were 38.5 ksi or less, indicating a larger hammer could be considered.

Drivability analyses were then performed for both a D36-52 and a D46-52 pile hammer. Figure D-23 presents the drivability results for all three of these driving systems. Note that the analyses indicate that the D36-52 can drive the candidate pile section to a nominal driving resistance of 756 kips at a pile penetration depth of 62 feet before reaching the blow count limit. The maximum predicted compression driving stress of 40 ksi are also within driving stress limits. Similarly, the D46-52 can drive the same candidate pile section to a nominal driving resistance of 867 kips at a pile penetration depth of 72 feet before reaching the blow count limit. The maximum predicted compression driving stress of 44 ksi with the D46-52 is also within driving stress limits. Hence, it would have been erroneous to eliminate the HP 12x74 pile section solely based on the D30-52 drivability results. The drivability results from the two other hammers clearly indicate the candidate section can be driven to significantly higher nominal driving resistances and to greater pile penetration depths before reaching drivability limits.

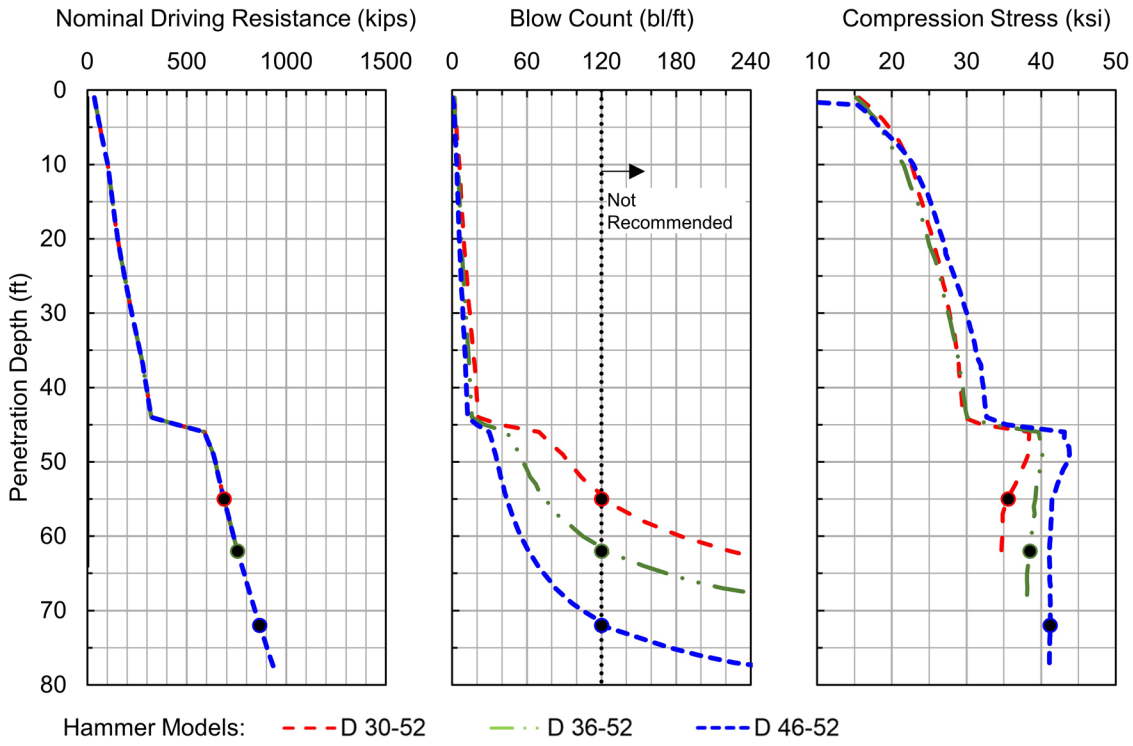

Figure D-23 Hammer size comparison to drive the HP 12x74 pile section.

At this time, the factored axial compression and tension resistances versus depth have been calculated and preliminary drivability assessments have been performed for all candidate pile sections. The factored geotechnical resistances have been evaluated for the resistance determination methods under consideration. Maximum achievable penetration depths have also been assessed with drivability analyses.

It is unreasonable to carry all possible combinations of candidate sections, resistance determination methods, and possible group configurations forward in the design process. Hence, experience, engineering judgement, and agency practice should be combined when selecting candidate pile types and sections, resistance determination methods, and potential group configurations. Otherwise, the number of possible design permutations will become unreasonable.

D.11 Block 11: North Abutment – Estimate Preliminary Number of Piles, Preliminary Pile Group Size, and Resolve Individual Pile Loads for All Limit States

The structural engineer has provided the anticipated loads for the controlling limit states at the North Abutment. These limit state loads are presented in Table D-11. The Strength I limit state loads are used to evaluate geotechnical resistance in axial

compression and tension, as well as for lateral loading. Service I limit state loads were also provided by the structural engineer without live loads. The Service I without live load (LL) includes only unfactored permanent loads such as the superstructure and wearing surface, pile cap and stem, utilities, and vertical earth pressure among others. The Service I without live load should be used for evaluating vertical deformation. There are no loads in the transverse direction at this abutment.

Table D-11 Limit State Loads on North Abutment

Limit State	Q (kips)	V_{uy} (kips)	M_{uy} (k-ft)
Strength I	2505	846	6625
Service I	1838	566	4600
Service I, without live load	1540	562	4162

Based on past experience, the agency generally utilizes 2 rows of piles at abutments with a minimum center to center pile spacing of at least 3 pile diameters. Three potential pile group configurations are therefore being considered: 2 rows of 9 piles, 2 rows of 11 piles, and 2 rows of 13 piles. These group configurations are identified as Group Configuration 1, 2, and 3, respectively in Table D-12. Because of site constraints, the pile cap length is limited to 43 feet. Furthermore, the distance from the center of any exterior pile to the pile cap edge must be at least 1.25 feet in both the transverse (x) and longitudinal (y) direction.

Table D-12 Potential Pile Group Configurations

Group Configuration	Piles per Row	Total Number of Piles	S_{bx}* (feet)	Total Footing Length (feet)	S_{by}* (feet)	Total Footing Width (feet)
1	9	18	5.0	42.5	4.0	6.5
2	11	22	4.0	42.5	4.0	6.5
3	13	26	3.0	38.5	4.0	6.5

* S_{bx} and S_{by} are illustrated in Figure D-24.

The following calculation is for the Group Configuration 1 and all applicable loads. For this configuration, 9 piles per row are used in two separate rows. Thus the transverse pile spacing, $S_{bx,}$ is 5’-0” and the total footing length is 42’-6”. The longitudinal pile spacing, $S_{by,}$ is 4’-0”. Figure D-24 shows the layout for the Group Configuration 1 pile cap.

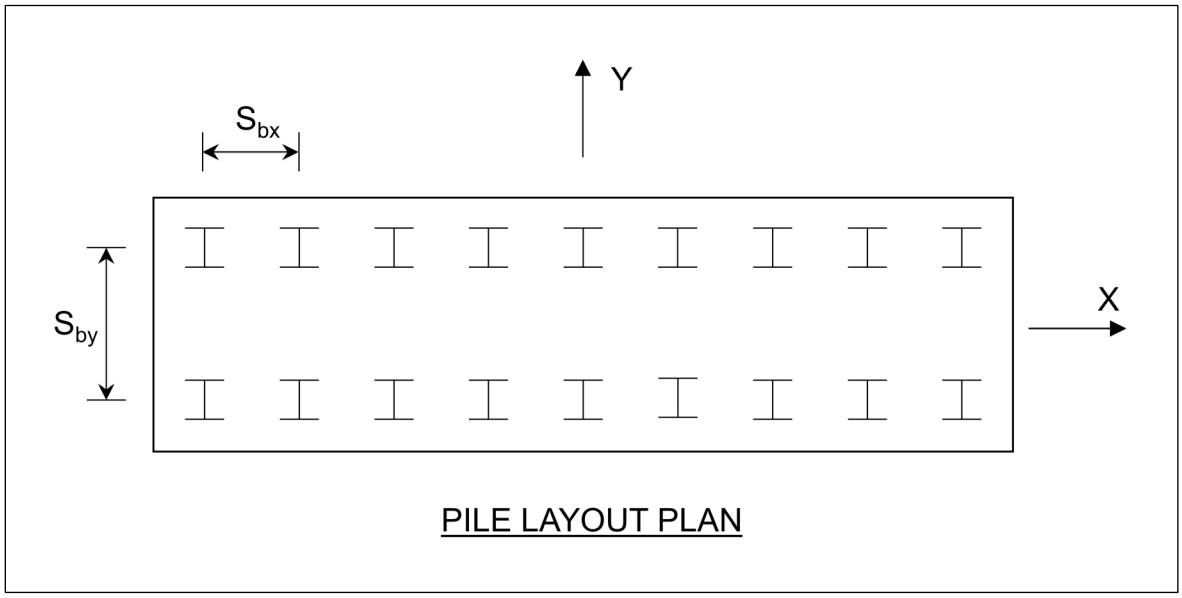

Figure D-24 Group Configuration 1 pile cap plan view.

For the established limit state loads and the trial pile group configuration depicted in Figure D-24, reactions for both the front and the back rows of piles were determined. Compression loads are taken as positive. The maximum factored load applied to each pile was subsequently calculated by dividing the reactions by the number of piles. Figure D-25 shows the free body diagram for determining the reactions and the resulting factored load per pile for both the front and the back row.

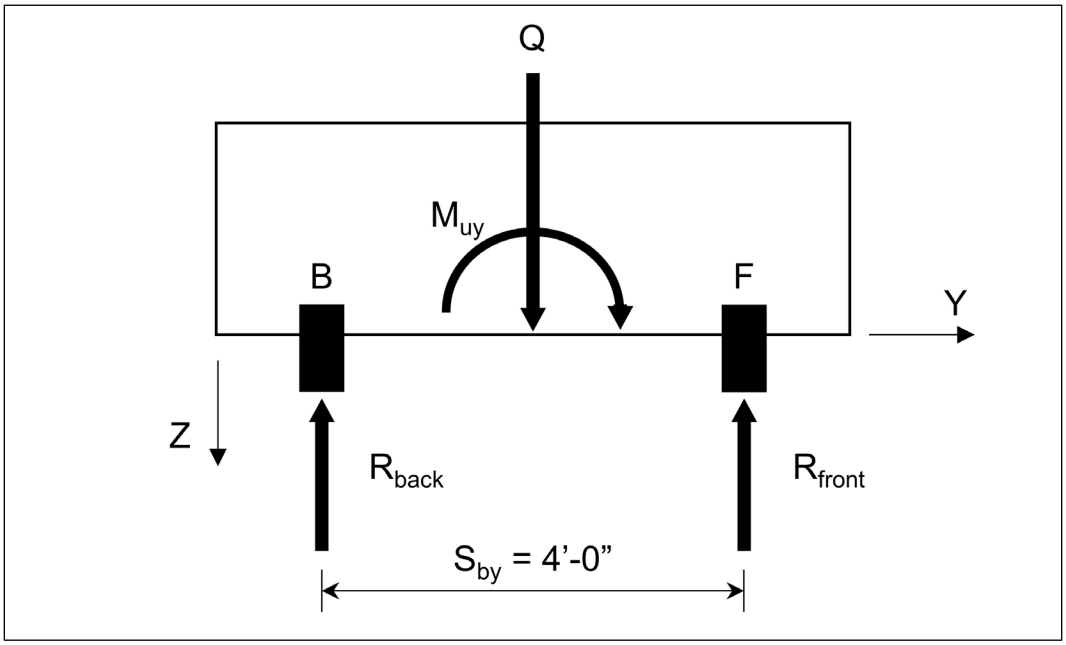

Figure D-25 Elevation view of cap free body diagram.

Table D-13 summarizes the limit state loads and the corresponding front and back row reactions. Strength I loads, Service I loads and the Service I loads without live load (LL) are provided.

Table D-13 Limit State Loads and Row Reactions for Group Configuration 1

Limit State	Q (kips)	M_{uy} (k-ft)	R_{front} (kips)	R_{back} (kips)
Strength I	2505	6625	2908	-406
Service I	1838	4600	2069	-231
Service I, without LL	1540	4162	1811	-271

Table D-14 presents the maximum factored load per pile based upon the number of piles in the group configuration. For Group Configuration 1, the Strength I limit state front-row reaction of 2908 kips divided by 9 piles yields a maximum factored load per pile of 323 kips. Table D-14 summarizes the factored load per pile for other limit states and group configurations.

Table D-14 Factored Load Per Pile for Alternative Pile Group Configurations

Group Configuration	Strength I, Q (compression) (kips)	Strength I, Q (tension) (kips)	Strength I, V_{uy} (kips)	Service I, without LL Q (kips)
1	323	-46	47	201
2	265	-37	39	165
3	224	-31	33	139

D.12 Block 12: North Abutment – Estimate Pile Penetration Depth for Maximum Axial Compression Loads; Check Group Efficiency in Axial Compression

The estimated minimum pile penetration depth necessary to obtain a factored geotechnical resistance that is equal or greater than the maximum factored load per pile is now determined. Note that the factored geotechnical resistance in axial compression and the resulting pile penetration depth is dependent upon the resistance determination method. Therefore, the influence of the field resistance determination method on the design needs to be evaluated at this point in the design process and some resistance determination methods may be eliminated from further design consideration.

The pile penetration depth necessary for the maximum factored geotechnical resistance of 323 kips on a given candidate pile section can be evaluated from Figure D-11 to Figure D-14 for the various resistance determination methods. For a factored geotechnical resistance of 323 kips in axial compression, it is estimated that pile length variation due to changes in the resistance determination method will be relatively minor. For this factored resistance, piles will also likely be driven into the gravel layer with cobbles encountered 45 feet below footing grade which increases the potential for pile damage. Therefore, it is decided that dynamic testing 2% of the production piles will be used for the resistance determination method.

Figure D-12 illustrated the factored geotechnical resistance versus penetration depth for the 5 candidate pile sections based on determination testing by dynamic testing 2% of the piles. From the static analysis results presented in this plot, the estimated penetration depth for the maximum factored geotechnical resistance of 323 kips in axial compression ranges from 43 feet for the HP 14x117 H-pile section to 59 feet for the HP 10x42 H-pile section. Similarly, the estimated pile penetration depths for all candidate pile sections and all group configurations were determined and are summarized in Table D-15.

Table D-15 Estimated Pile Penetration Depth Requirements for the Factored Geotechnical Resistance in Axial Compression at the Strength I Limit State

Group Configuration	Factored Load per Pile (kips)	HP 10x42 (feet)	HP 12x53 (feet)	HP 12x74 (feet)	HP 14x89 (feet)	HP 14x117 (feet)
1	323	59	45	45	45	43
2	265	46	45	45	38	35
3	224	45	45	43	32	30

Next, the group efficiency in axial compression is evaluated. Per Section 7.2.2.1, the nominal geotechnical resistance of a pile group in cohesionless soil, can be taken as the sum of the individual pile nominal geotechnical resistances. In a similar manner, the factored geotechnical resistance of the pile group in cohesionless soil is taken as the sum of the individual pile factored geotechnical resistances. This is recommended so long as 1) the bearing layer is not underlain by weak soil layers, 2) the piles are not installed at a pile spacing of less than 3 times the pile diameter, and 3) no special installation procedures are anticipated such as jetting or predrilling. Since all these conditions are met at the North Abutment, the nominal and factored group resistances are satisfactory.

D.13 Block 13: North Abutment – Establish Minimum Pile Penetration Depth for Axial Tension Loads; If Conditions Warrant, Modify Design and Return to Block 10

The factored geotechnical resistance in axial tension must also be evaluated as the back row of piles will be loaded in tension (Table D-13). In this case, the minimum required factored geotechnical resistance in axial tension is established using the Strength I limit state and is determined following the procedure outlined in Section 7.2.3.2. The analysis presented in this appendix slightly differs from the procedure outlined in Chapter 7 in that only a single row of piles is providing the tension resistance rather than the entire pile group. Two analyses are performed; one that considers the factored shaft resistances from individual piles, and one that considers the weight of a soil block acting with the piles. The lesser tension resistance determined from either method controls the design.

As noted in Table D-13, the Strength I limit state tension load on the back row of piles for the Group Configuration 1 is 406 kips. Therefore, the minimum factored geotechnical resistance in axial tension required from an individual pile is this factored load divided by the 9 piles in the rear row or 46 kips. In a similar manner, the minimum factored geotechnical resistance required from an individual pile in axial tension is 37 kips for Group Configuration 2, and 33 kips for Group Configuration 3.

As noted earlier, dynamic testing with signal matching will be used as the resistance determination method in the field. Therefore, the AASHTO resistance factor, ϕ_{up}, is 0.50 (Table 7-2 of Chapter 7). Figure D-18 provides plots of the factored geotechnical resistance in axial tension versus depth for all of the candidate pile types based on this resistance determination method. For each candidate section, this figure should be entered on the x-axis at the required factored axial tension resistance to determine the corresponding pile penetration depth.

Following this procedure, the estimated pile penetration depth to achieve the factored geotechnical resistance in axial tension for each candidate pile section and group configuration is summarized in Table D-16.

Table D-16 Estimated Minimum Pile Penetration Depth for Maximum Factored Geotechnical Resistance in Axial Tension at the Strength I Limit State

Group Configuration	Required Factored Resistance in Axial Tension (kips)	HP 10x42 (feet)	HP 12x53 (feet)	HP 12x74 (feet)	HP 14x89 (feet)	HP 14x117 (feet)
1	46	36	31	28	24	23
2	37	31	27	25	23	20
3	33	29	25	23	20	19

Next, the tension resistance of the pile row when considered as a soil block is calculated. For Group Configuration 1, the required factored tension resistance of the back row remains 406 kips (Table D-13) and the resistance is derived from the weight of soil as a block. The weight of soil needed in the block, W_{Block}, to resist the tension load is determined with Equation 7-39 where W_{Block} is substituted for R_{ug}.

$$R_r = \phi R_n = \phi_{ug} R_{ug} \qquad \text{Eq. [7-39]}$$

Where:

R_r = factored uplift resistance (kips).
ϕ_{ug} = resistance factor for group uplift per Table 7-1, 0.50.
R_{ug} = nominal uplift resistance of the pile group (kips).

and

$$R_{ug} = W_{Block}$$

Solving for the minimum W_{Block}:

$$W_{Block} = \frac{R_r}{\phi_{ug}} \qquad \text{Eq. [7-39 modified]}$$

$$W_{Block} = \frac{(406\ kips)}{(0.50)}$$

$$W_{Block} = 812\ kips$$

The length of the pile group will change depending upon the group configuration. For Group Configurations 1 and 2, the pile group length is 41 feet from exterior pile

edge to exterior pile edge assuming a 12 inch pile width/diameter. For Group Configuration 3, the pile group length is 37 feet using the same pile dimension. The effect of a smaller pile size on the pile group length is negligible (e.g. for HP 10x42 section, the pile group length is 40.83 feet).

The soil profile consists of three layers each with different total and effective unit weights. Therefore, the weight contribution from each soil layer was used to calculate the soil block weight at a given pile toe elevation. The following calculation is performed for Group Configuration 1 and 2 with a pile group length of 41 feet and an embedded pile length of 27 feet. Table D-17 presents a summary of the effective soil unit weight and geometry for each layer comprising the soil block. Figure D-26 provides a visual representation of the soil volume used to determine the soil block weight.

Table D-17 Geometry of Soil Block Layers for Nominal Group Tension Resistance Computation with Pile Toe at 27 Feet

Soil Block Layer	γ' (pcf)	Layer Thickness (feet)	Depth to Bottom (feet)	Z_{bottom} (feet)	Z_{top} (feet)	B_{bottom} (feet)	B_{top} (feet)
1	105.0	10.0	10.0	49.5	54.5	9.5	14.5
2	42.6	10.0	20.0	44.5	49.5	4.5	49.5
3	49.6	20.0	27.0	41.0	44.5	1.0	4.5

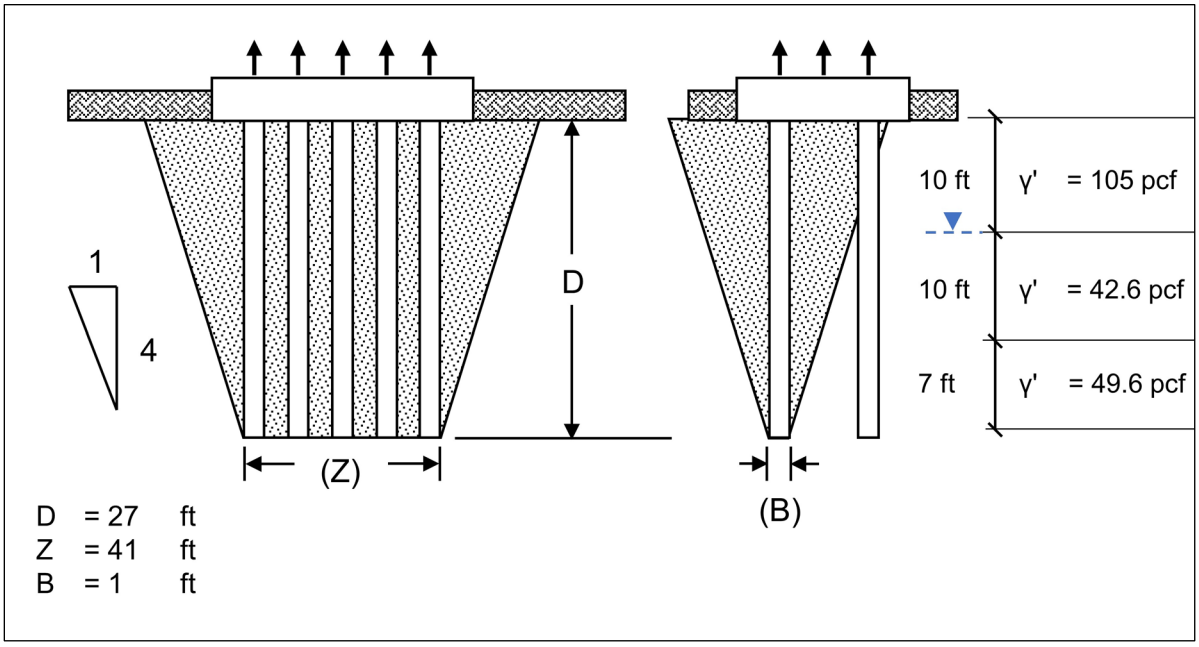

Figure D-26 Nominal tension resistance of pile group based on soil block weight.

To determine the volume of soil for each layer, the geometry presented in Table D-17 was used to calculate the volume of each layer's inverted obelisk using Equation D-1. The volume of each block layer was then multiplied by the respective soil unit weight to determine the soil block weight. All three block layers were then summed to calculate the total weight of the block. An example calculation is shown for Layer 1 of the soil block. Completed calculations are summarized in Table D-18.

Determine the volume of soil in Block Layer 1

$$\mathrm{V} = \frac{h}{6}\left[Z_{bottom}B_{top} + Z_{top}B_{bottom} + 2 * \left(Z_{top}B_{top} + Z_{bottom}B_{bottom}\right)\right] \qquad \text{Eq. D-1}$$

$$\mathrm{V} = \frac{(10\ feet)}{6}\left[(49.5\ feet) * (14.5\ feet) + (54.5\ feet) * (9.5\ feet) + 2 * \left((54.5\ feet) * (14.5\ feet) + (49.5\ feet) * (9.5\ feet)\right)\right]$$

$$\mathrm{V}_{Block\ Layer\ 1} = 6260.8\ ft^3$$

Calculate the effective soil weight in Block Layer 1

$$\mathrm{W}_{Block\ Layer\ 1} = \mathrm{V}_{Block\ Layer\ 1} * \gamma'$$

$$\mathrm{W}_{Block\ Layer\ 1} = (6260.8\ ft^3) * (105\ pcf)\ \left(\frac{1\ kip}{1000\ lbs}\right)$$

$$\mathrm{W}_{Block\ Layer\ 1} = 657.4\ kips$$

Table D-18 Calculation of Soil Volume and Soil Block Weight for Nominal Group Tension Resistance

Block Layer	Depth to Bottom (feet)	Volume of Soil (ft^3)	γ' (pcf)	Weight of Soil (lbs)	Weight of Soil (kips)
1	10	6,260.8	105.0	657,387.5	657.4
2	20	3,310.8	42.6	141,041.5	141.0
3	27	830.1	49.6	41,172.1	41.2
					839.6

The required soil block weight of 812 kips is achieved at approximately 27 feet of pile penetration. Hence any pile penetration depth of 27 feet or greater would satisfy the required nominal group tension resistance. For Group Configuration 3 with a pile group length of 37 feet, the minimum pile penetration depth to achieve a soil block weight in excess of the required nominal tension resistance of 812 kips is 28 feet.

The required minimum pile penetration depth to satisfy the nominal geotechnical resistance in axial tension is the greater depth of the above calculated individual or group resistances.

The minimum pile penetration depth necessary for the HP 12x74 section in Group Configuration 1 is determined as follows:

$D_{individual}$ = minimum penetration depth based on sum of individual pile resistance, 28 feet (Table D-16).

D_{block} = minimum penetration depth based on weight of soil block, 27 feet.

Therefore, the minimum pile penetration depth needed to satisfy the nominal geotechnical resistance in axial tension, $D_{min-tension}$, is 28 feet.

In a similar manner, this check was performed for all candidate pile sections and all group configurations. The resulting minimum pile penetration depth necessary to achieve the nominal geotechnical resistance requirements for each candidate pile section within the specified group configuration is summarized in Table D-19.

Table D-19 Established Minimum Required Pile Penetration Depth for Factored Geotechnical Resistance in Axial Tension at North Abutment

Group Configuration	HP 10x42 (feet)	HP 12x53 (feet)	HP 12x74 (feet)	HP 14x89 (feet)	HP 14x117 (feet)
1	36	31	28	27*	27*
2	31	27*	27*	27*	27*
3	29	28*	28*	28*	28*

* Indicates axial tension resistance governed by soil block weight.

D.14 Block 14: North Abutment – Establish Minimum Pile Penetration Depth for Lateral Loads. Determine p-y Models, Required Geomaterial Parameters, and Perform Lateral Load Analysis; If Conditions Warrant, Modify Design and Return to Block 10

Next, lateral analyses are performed to establish the required minimum pile penetration depth for lateral loading and to evaluate pile deflection and structural resistance for the applied limit state loads. A minimum required pile penetration depth was established to satisfy the nominal geotechnical resistance requirements in axial tension in Block 13. A deeper minimum required pile penetration depth for lateral loading can result based on the combination of factored lateral loads and structural resistances, or deflection limits. Excessive deflections and moments develop at relatively short pile lengths, where a depth to fixity is not achieved. Furthermore, the structural resistance of pile sections must be evaluated based upon the axial, lateral and moment loads. Factored structural resistances were presented in Table D-3. A lateral deformation limit of 1 inch was established as a global performance requirement in Block 1 and confirmed In Block 4 as the design progressed.

The soil profile at the North Abutment was presented in Figure D-7. For lateral load analyses, appropriate p-y models must be selected for each soil layer. The input parameters necessary for lateral load analysis using the LPILE computer program are included in the North Abutment soil profile in Figure D-7.

As discussed in Section 7.3.7.6, p-multipliers are applied to the p-y curves to model pile group behavior. The p-multipliers depend on the center to center pile spacing within the pile group. For all group configurations at the North Abutment, the pile spacing in the longitudinal direction is 4 feet. Therefore, per Section 7.3.7.6 and AASHTO (2014) design specifications, interpolation was used to determine p-multipliers for a pile spacing of 4b. In this case, the front row p-multiplier is 0.90, while the second row is 0.625.

Cyclic loading was analyzed for both rows using LPILE's Load Type 2 option, which uses Shear and Slope to model a fixed head condition. Using the limit state loads at this abutment, lateral analyses in the longitudinal (y-direction) were performed about the pile section's strong axis. Figure D-24 shows the pile orientation within the trial pile cap design.

The following calculation is presented for the HP 12x74 H-pile section using a range of factored axial and lateral loads and the Group Configuration 1. Tables D-20 and D-21 provide LPILE output summaries at the pile head for both rows considering a

pile penetration depth for lateral loading of 45 feet. The pile head is assumed to terminate at the ground surface (i.e., no stickup).

Table D-20 LPILE Summary Output at Pile Head for Front Row, p_m=0.90

Load Case	Load Type No.	Pile-Head Condition 1 V (kips)	Pile-Head Condition 2 S (rad)	Axial Load (kips)	Pile-Head Deflection (inches)	Maximum Moment in Pile (kip-ft)	Maximum Shear in Pile (kips)	Pile-Head Rotation (radians)
1	2	0	0	323	0.000	0.0	0	0
2	2	20	0	323	0.249	-95.5	20	0
3	2	30	0	323	0.396	-148.4	30	0
4	2	40	0	323	0.553	-203.1	40	0
5	2	45	0	323	0.640	-232.2	45	0
6	2	47	0	323	0.677	-244.3	47	0
7	2	50	0	323	0.736	-262.7	50	0
8	2	55	0	323	0.841	-294.5	55	0
9	2	60	0	323	0.953	-327.3	60	0

Table D-21 LPILE Summary Output at Pile Head for Second Row, p_m=0.625

Load Case	Load Type No.	Pile-Head Condition 1 V (kips)	Pile-Head Condition 2 S (rad)	Axial Load (kips)	Pile-Head Deflection (inches)	Maximum Moment in Pile (kip-ft)	Maximum Shear in Pile (kips)	Pile-Head Rotation (radians)
1	2	0	0	323	0.000	0.0	0	0
2	2	20	0	323	0.320	-104.7	20	0
3	2	30	0	323	0.508	-162.3	30	0
4	2	40	0	323	0.727	-225.1	40	0
5	2	45	0	323	0.857	-259.3	45	0
6	2	47	0	323	0.910	-273.2	47	0
7	2	50	0	323	0.998	-294.7	50	0
8	2	55	0	323	1.151	-331.4	55	0
9	2	60	0	323	1.315	-369.3	60	0

The pile group deflection can be estimated from the above LPILE's deflection results for the front and second rows. The factored load versus pile head deflection for each row is plotted in Figure D-27 along with the group average. The average lateral load per pile for a given group deflection is shown. A step by step discussion of this procedure is provided in Section 7.3.7.6.

The rigid cap method assumes piles move together, and therefore experience the same shear and lateral load. Accordingly, at the resulting factored lateral load per pile, V_y, of 47 kips (Table D-14), the estimated lateral group deflection at the pile head is determined as 0.80 inches. This lateral deflection is less than the 1 inch tolerance based upon project design requirements.

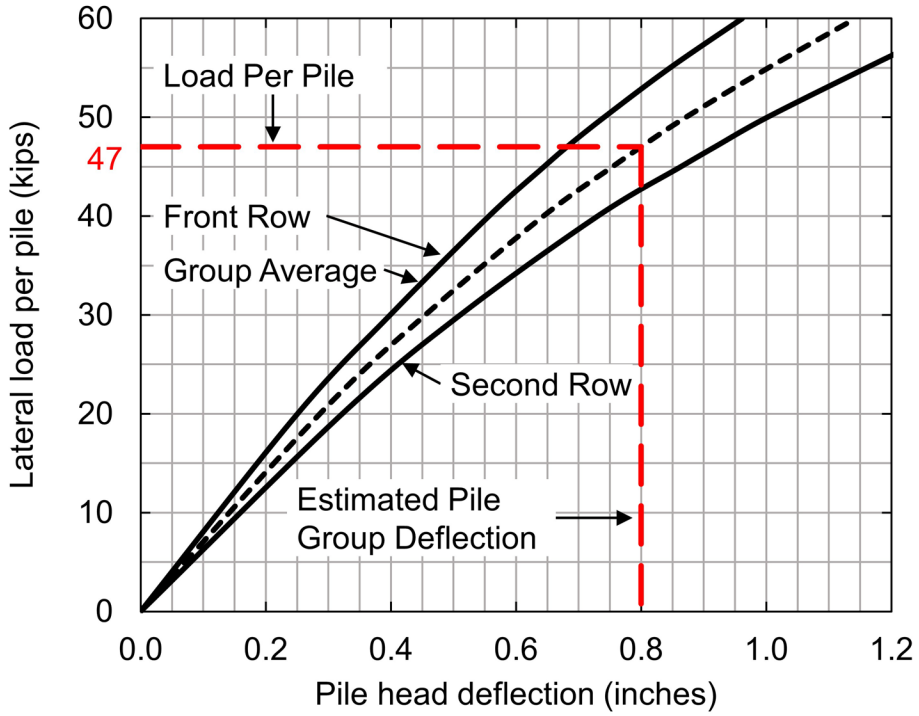

Figure D-27 Factored load versus deflection in longitudinal direction for HP 12x74 at North Abutment.

In addition to the lateral deflection limit, stresses from the resulting bending moment and shear must be evaluated to check that the pile section does not fail structurally. Using the LPILE tabular results, Figure D-28 plots the front row bending moment versus depth for the front row deflection of 0.8 inches.

Figure D-29 plots the maximum bending moment versus pile head deflection for both the front and back rows, however only the maximum bending moment for the front row is used as a “worst case” evaluation of the structural resistance in combined axial compression and flexure. As illustrated in Figure D-29, at the estimated pile head deflection of 0.80 inches, the maximum bending moment, M_{uy}, is 280 kip-ft.

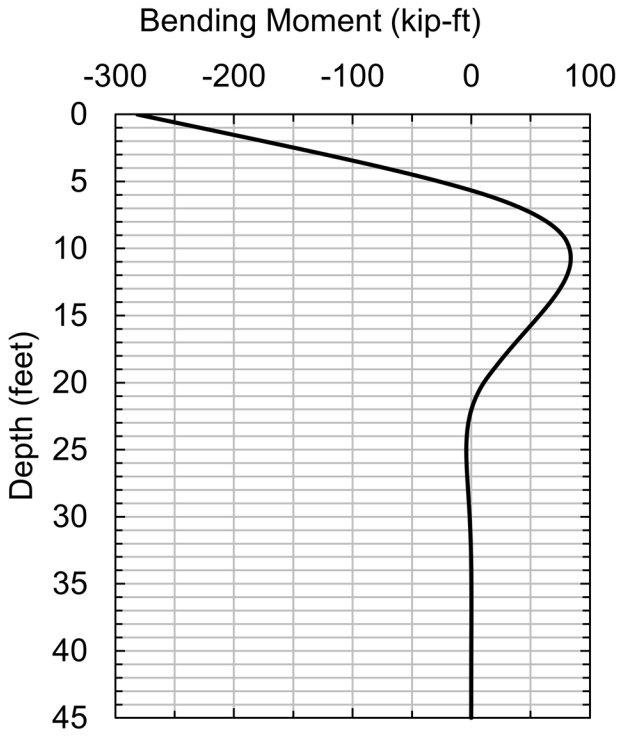

Figure D-28 Front row bending moment versus depth in longitudinal direction.

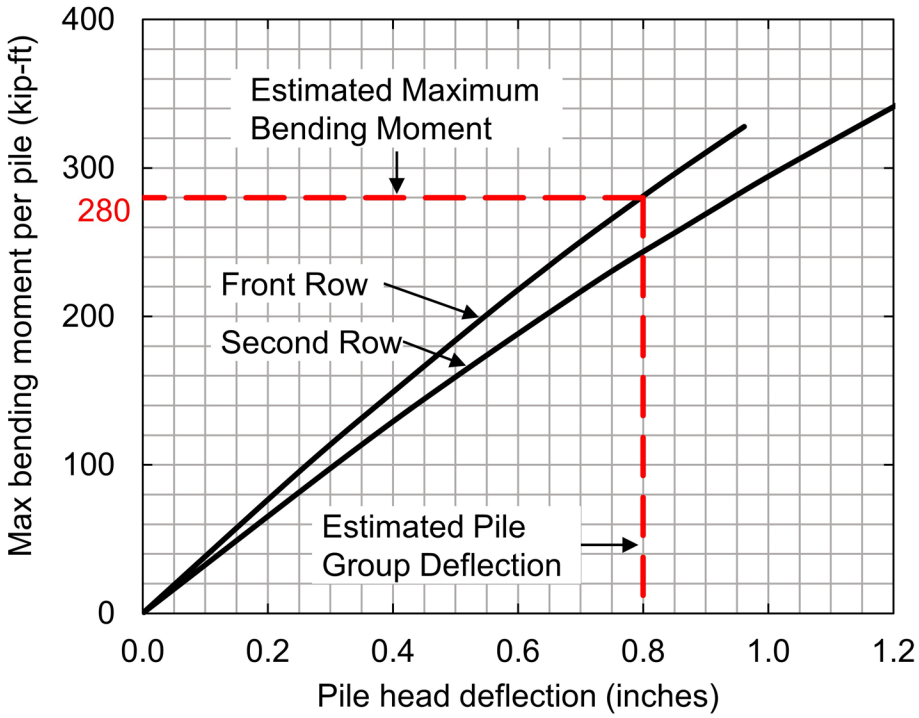

Figure D-29 Bending moment versus deflection in longitudinal direction for HP 12x74 at North Abutment.

Equation 8-58 must be satisfied for the factored axial compression load and moment in the pile. Using results of the lateral analysis, the factored structural resistance was evaluated at the pile head using the factored axial compression load and maximum bending moment (determined using factored loads). The factored structural resistances were determined and are summarized in Table D-3.

Equation 8-58 must be satisfied for the pile section to be acceptable.

P_u = factored axial load, 323 kips (TableD-14).
P_r = factored axial resistance, 762 kips (Table D-3).
M_{ux} = factored moment about x-axis, 0 kip-ft (Block 11).
M_{rx} = factored flexural resistance about x-axis, 118 kip-ft (Table D-3).
M_{uy} = factored moment about y-axis, 280 kip-ft (Figure D-29).
M_{ry} = factored flexural resistance about y-axis, 433 kip-ft (Table D-3).

$$\frac{\mathrm{P}_u}{\mathrm{P}_r}+\frac{8.0}{9.0}\left(\frac{\mathrm{M}_{ux}}{\mathrm{M}_{rx}}+\frac{\mathrm{M}_{uy}}{\mathrm{M}_{ry}}\right)\leq 1.0 \qquad \text{[Eq. 8-58]}$$

$$\frac{323\ \text{kips}}{762\ \text{kips}}+\frac{8.0}{9.0}\left(\frac{0}{118}+\frac{280}{433}\right)\leq 1.0$$

$$0.998 \leq 1.0$$

The maximum shear from factored lateral loading was then compared to the factored shear resistance from Table D-3. Based on the factored loads, the factored shear resistance is acceptable.

V_r = factored shear resistance, 214 kips (HP 12x74, Table D-3).
V_{uy} = factored shear load, 47 kips.

$$V_{uy} < V_r$$

$$47\ kips < 214\ kips$$

The lateral analysis was also performed for each candidate pile section and the deflection and factored structural resistance was subsequently evaluated considering the factored loads for the group configurations shown in Table D-14.

Pile head deflection must be limited to 1 inch, and based upon the applied loads and pile section, the factored structural resistance of the pile must also satisfy the

structural resistance interaction equation presented as Equation 8-58. Pile sections satisfying both criteria were deemed acceptable. Furthermore, as presented in Table D-22, a minimum pile penetration depth was established based on the lateral load analyses. The minimum penetration depth is identified as "- - -" for candidate pile sections not meeting the lateral deformation or structural resistance requirements.

Several of the larger pile sections provided sufficient stiffness to resist the applied loads, while smaller, less stiff sections did not (they failed the structural resistance check in Equation 8-58). Factored axial compression loads, in combination with moments caused by factored lateral loads, resulted in some sections' factored structural resistance being exceeded. As a direct result of this analysis, the HP10x42 pile section is unsuitable and eliminated as a candidate pile section for final design. However for the remainder of this example problem, this pile section will still be carried forward for illustrative purposes. Likewise, the HP 12x53 pile section is unsuitable and eliminated as a candidate pile section for Group Configurations 1 and 2.

Table D-22 Established Minimum Pile Penetration Depth Required for Lateral Loading at the North Abutment

Group Configuration	HP 10x42 (feet)	HP 12x53 (feet)	HP 12x74 (feet)	HP 14x89 (feet)	HP 14x117 (feet)
1	- - -	- - -	25	10	10
2	- - -	- - -	10	10	10
3	- - -	20	10	10	10

D.15 Block 15: North Abutment – Establish Pile Penetration Depths that Satisfy Tolerable Deformations; Estimate Group Settlement over the Minimum and Maximum Range of Pile Penetration Depths From Blocks 12 through 14 and Identify All Pile Toe Elevations Which Result in Intolerable Deformations; If Conditions Warrant, Modify Design and Return to Block 10

For the cohesionless soils at the North Abutment, pile group settlement was estimated using two methods, the Meyerhof (1976) Method and the Janbu tangent modulus method. Ideally, the settlement method chosen by the designer is one that has shown good correlation with observed results. The pile group settlement at the North Abutment was first calculated using the Meyerhof method. The Meyerhof approach is a traditional settlement estimation method for pile groups in cohesionless soils and one that is contained in the AASHTO (2014) design specifications. However, the soil conditions across the bridge substructure locations are quite variable and a settlement method that could be used at all substructure locations was also desired. Therefore, group settlement was also computed with the Janbu tangent modulus approach using an equivalent footing placed at the neutral plane.

The Meyerhof (1976) approach as presented in Section 7.3.5.2.1 was used to estimate group settlement. The settlement calculations were performed using only unfactored permanent loads. Therefore the loads from the Service I limit state without live load were used to estimate settlement (load factor of 1.0 on permanent loads). The average contact stress for the trial pile group was calculated using the vertical load, *Q*, and pile group area *Z x B*. The length of the pile group in Group Configurations 1 and 2 is 41 feet. Therefore, the following calculation is only suitable for these two group configurations. Both the group length, *Z*, and width, *B*, were calculated from exterior pile edge to exterior pile edge.

Calculate the average contact stress, p_f, from the trial pile group.

B = pile group width in longitudinal direction, 5 feet.
Z = pile group length in transverse direction, 41 feet.
Q = unfactored permanent load, 1540 kips.

$$p_f = \frac{Q}{B*Z}$$

$$p_f = \frac{1540\ kips}{(5\ feet)*(41\ feet)} = 7.512\ ksf$$

$$p_f = 7.512\ ksf$$

The group embedment influence factor, I_f, is determined based upon the pile group width and estimated pile depth using Equation 7-52.

D_B = pile embedded length into bearing stratum. In this calculation, 5 feet into dense gravel with sand (embedded length D = 50 feet).

D' = effective depth, 2/3* D_B= 3.33 feet.

$$I_f = 1 - \frac{D'}{8B} \geq 0.5 \qquad \text{[Eq. 7-52]}$$

$$I_f = 1 - \frac{3.33\ feet}{8*(5\ feet)} \geq 0.5$$

$$I_f = 0.92 \geq 0.5$$

$$I_f = 0.92$$

The total settlement is conservatively estimated using Equation 7-50.

$N_{1(60)}$ = average corrected SPT N value within a depth B below pile toe, 59 bpf.

$$S = \frac{4\ p_f\ I_f \sqrt{B}}{N_{1(60)}} \qquad \text{[Eq. 7-50]}$$

$$S = \frac{4*(7.512\ ksf)*(0.92)*\sqrt{5\ feet}}{(59\ bpf)}$$

$$S = 1.04\ inches$$

The above analysis was performed for additional pile penetration depths and for the pile group dimensions of all three group configurations. Table D-23 summarizes the analysis results for the Meyerhof (1976) estimated group settlement. The estimated group settlement depends upon the $N_{1(60)}$ value of the soil into which the pile group is embedded. In particular, at the contact of the medium dense sand and dense gravel with sand layers, this effect is magnified. This is a limitation of the Meyerhof settlement method, in which soil layers below a depth of B, the pile group width,

below the pile toe are effectively disregarded. The Engineer should consider this when assessing the minimum pile penetration depth for settlement considerations.

Table D-23 Estimated Pile Group Settlement Using Meyerhof (1976) Method For All Pile Group Configurations.

Pile Toe Elevation (feet)	Pile Penetration Depth (feet)	D_B (feet)	$N_{1(60)}$ for Bearing Stratum (bpf)	Estimated Settlement Group Configuration 1 & 2 (inches)	Estimated Settlement Group Configuration 3 (inches)
270.0	40.0	20.0	17	2.63	2.92
267.5	42.5	22.5	38	1.11	1.22
264.5	45.5	0.5	59	1.13	1.25
260.0	50.0	5.0	59	1.04	1.16
255.0	55.0	10.0	59	0.95	1.05

Note: D_B = embedded pile length into bearing stratum.

The Meyerhof (1976) approach does not include or consider the increase in vertical effective stress from embankment loading. Depending on the embankment construction and pile installation timeline, consideration of the stress increase from embankment construction on pile group settlement estimates may or may not be appropriate. Embankment loading effects were included in the second settlement computation method performed using the neutral plane method and Janbu tangent modulus. For simplification, the vertical effective stress increase is determined by treating the embankment surcharge as a strip load. Figure D-30 demonstrates this concept and defines symbols, while the change in vertical effective stress with depth is determined using Equations D-2 through D-4.

$$\Delta\sigma_v = \frac{q}{\Pi}[\beta + \sin(\beta) * \cos(\beta + 2\delta)] \qquad \text{Eq. D-2}$$

Where:

$$\beta = tan^{-1}\left(\frac{x+b}{z}\right) - tan^{-1}(\frac{x-b}{z}) \qquad \text{Eq. D-3}$$

and

$$\delta = tan^{-1}(\frac{x-b}{z}) \qquad \text{Eq. D-4}$$

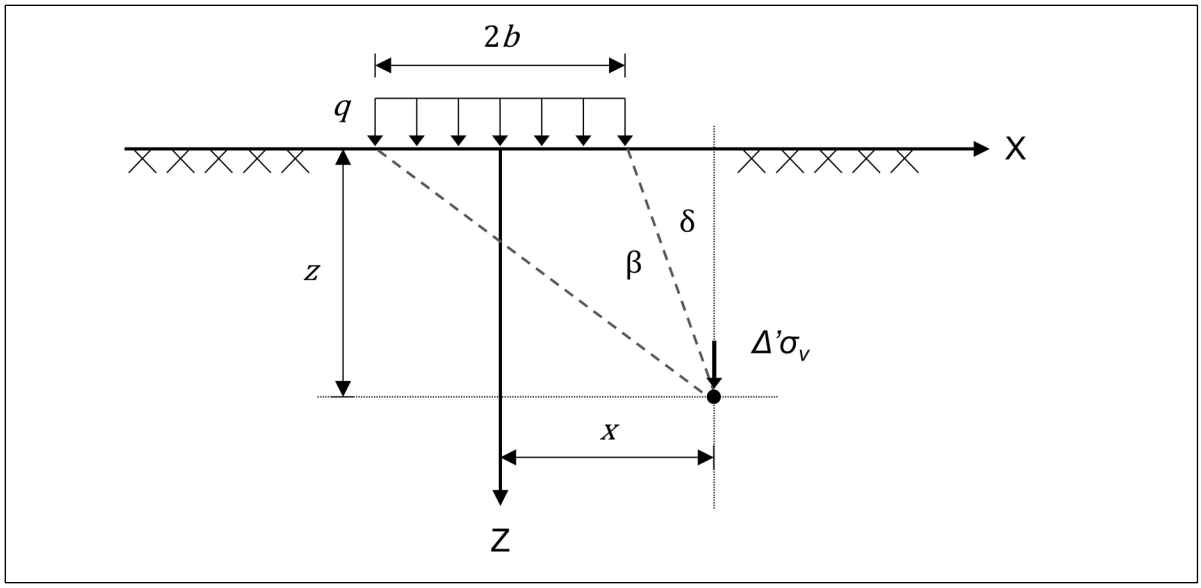

Figure D-30 Vertical effective stress increase due to strip load.

The 10 foot high embankment, with a soil unit weight 120 pcf, results in a surcharge stress at the embankment base of 1.2 ksf, and is assumed to extend 100 feet behind the abutment. Fill directly above the footing is already included in design as a permanent vertical load, EV, and therefore the embankment surcharge is assumed to act as a strip load beginning at the footing edge. The change in vertical effective stress from the embankment surcharge, $\Delta\sigma'_{v(e)}$, is determined under the footing centerline as depicted in Figure D-31.

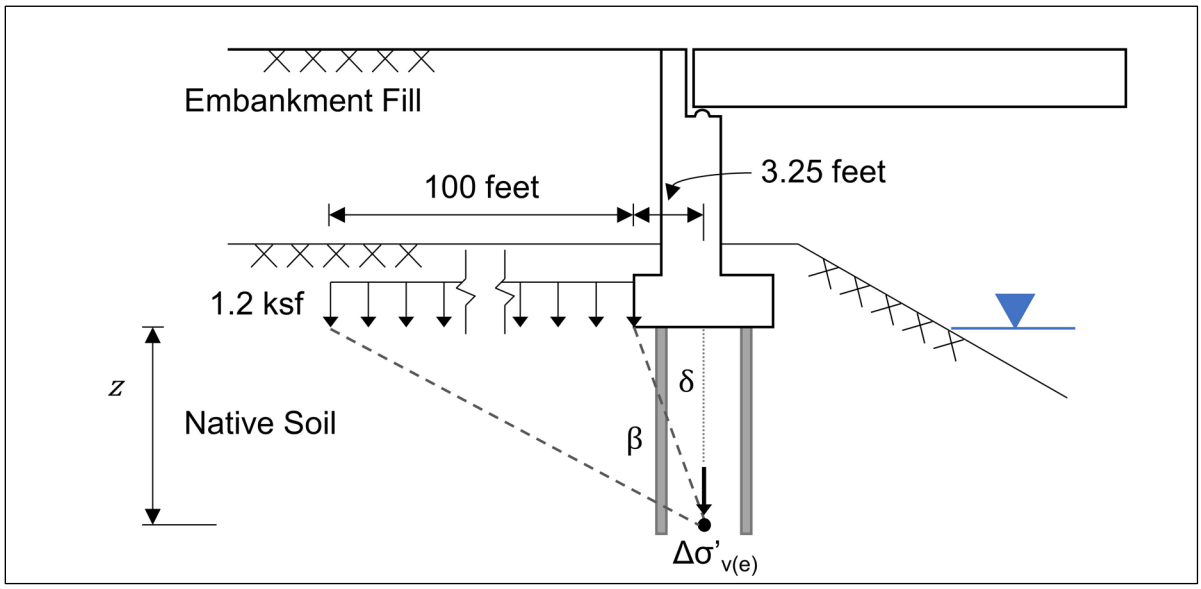

Figure D-31 Vertical effective stress increase due to embankment surcharge.

An example calculation is shown for a depth below footing, *z*, of 2.5 feet. Complete calculations were performed using a spreadsheet and are summarized in Table D-24. The bottom of the North Abutment footing is at Elevation 310 feet and therefore although the value of z in the following series of analyses may vary based upon the equivalent footing or neutral plane location. Elevation is used to provide a better comparison of effective stress change with depth.

Determine geometry of profile.

$$\mathrm{x} = 3.25\ feet + \frac{100\ feet}{2} = 53.25\ feet$$

$$\mathrm{b} = \frac{100\ feet}{2} = 50\ feet$$

Determine angle β.

$$\beta = tan^{-1}\left(\frac{x+b}{z}\right) - tan^{-1}\left(\frac{x-b}{z}\right) \qquad \text{[Eq. D-3]}$$

$$\beta = tan^{-1}\left(\frac{53.25\ feet+50\ feet}{2.1\ feet}\right) - tan^{-1}\left(\frac{53.25\ feet-50\ feet}{2.1\ feet}\right)$$

$$\beta = 0.63$$

Determine angle δ.

$$\delta = tan^{-1}\left(\frac{x-b}{z}\right) \qquad \text{[Eq. D-4]}$$

$$\delta = tan^{-1}\left(\frac{53.25\ feet-50\ feet}{2.5\ feet}\right)$$

$$\delta = 0.92$$

Calculate the change in vertical effective stress due to embankment surcharge.

q = stress per unit length, 1.2 ksf.

$$\Delta\sigma'_{v(e)} = \frac{q}{\Pi}[\beta + \sin(\beta) * \cos(\beta + 2\delta)] \qquad \text{[Eq. D-2]}$$

$$\Delta\sigma'_{v(e)} = \frac{1.2\ ksf}{\Pi}[0.63 + \sin(0.63) * \cos(0.63 + 2 * (0.92))]$$

$$\Delta\sigma'_{v(e)} = 0.07\ ksf$$

Table D-24 Vertical Effective Stress Increase from Embankment Surcharge

Elevation (feet)	Soil Layer	z (feet)	δ	β	$\Delta\sigma'_{v(e)}$ (ksf)
309.99	1	0.01	1.57	0.00	0.00
307.5	1	2.5	0.92	0.63	0.07
302.5	1	7.5	0.41	1.09	0.30
297.5	1	12.5	0.25	1.20	0.41
292.5	1	17.5	0.18	1.22	0.46
287.5	2	22.5	0.14	1.21	0.49
282.5	2	27.5	0.12	1.19	0.51
277.5	2	32.5	0.10	1.17	0.52
272.5	2	37.5	0.09	1.14	0.52
267.5	2	42.5	0.08	1.10	0.53
262.5	3	47.5	0.07	1.07	0.53
257.5	3	52.5	0.06	1.04	0.53
252.5	3	57.5	0.06	1.01	0.53
247.5	3	62.5	0.05	0.97	0.52
242.5	3	67.5	0.05	0.94	0.52
237.5	3	72.5	0.04	0.91	0.51
232.5	3	77.5	0.04	0.88	0.51
227.5	3	82.5	0.04	0.86	0.50
222.5	3	87.5	0.04	0.83	0.49
219.0	3	91.0	0.04	0.81	0.49

Note, the designer should determine if the construction schedule can accommodate the required time for embankment induced settlements to occur before the start of pile driving and superstructure construction. This example calculation assumes construction cannot be delayed, and therefore, the stress increase from embankment construction and foundations loads are applied concurrently.

Pile group settlement was calculated using the neutral plane method and Janbu tangent modulus as discussed in Section 7.3.5.6. An equivalent footing, with plan dimensions equal to those of the pile group, was evaluated at increasing pile penetration depths, and the resulting pile group settlement computed using the Janbu tangent modulus. This procedure allowed the shallowest depth of an equivalent footing to be determined that met vertical deformation requirements. The required minimum pile penetration depth was then determined by the pile toe elevation that would place the neutral plane at this same equivalent footing depth where vertical deformation requirements were satisfied.

The following example calculation is performed for an equivalent footing located at Elevation 270 feet corresponding to a pile penetration depth of 60 feet. The length of the pile group in Group Configurations 1 and 2 is 41 feet from exterior pile edge to exterior pile edge. Since Group Configuration 3 has different pile group plan dimensions, this example is suitable for only Configurations 1 and 2. Similar to the vertical effective stress increase calculations from embankment loading, the soil profile was again divided into 5 foot thick layers. The elevation shown in Table D-25 references the midpoint of each respective 5 foot thick soil layer, while z is the depth below the equivalent footing to the midpoint of each respective 5-foot-thick soil layer. Tabulated values for this analysis are recorded in Table D-25.

Considering only the unfactored permanent load acting on the superstructure, Q, calculate the change in vertical effective stress below the equivalent footing, $\Delta\sigma'_{v(\mathrm{ss})}$, at Elev. 267.5 feet.

Q = unfactored permanent load, 1540 kips (Service I, no LL, Table D-11).
B = pile group width, 5 feet.
Z = pile group length, 41 feet (Group Configurations 1 and 2 only).
z = depth below equivalent footing, 2.5 feet (Elev.267.5 feet).

$$\Delta\sigma'_{v(\mathrm{ss})} = \frac{Q}{(B+z)*(Z+z)} \qquad \text{[Eq. 7-55]}$$

$$\Delta\sigma'_{v(\mathrm{ss})} = \frac{(1540\ kips)}{((5\ feet)+(2.5\ feet))*((41 feet)+(2.5\ feet))}$$

$$\Delta\sigma'_{v(\mathrm{ss})} = 4.72\ ksf$$

Including the change in effective stress from the embankment and superstructure, calculate the new effective stress below the equivalent footing at Elev. 267.5 feet.

σ'_{vo} = initial vertical effective stress at depth z below the equivalent footing, 3.15 ksf.
$\Delta\sigma'_{v(e)}$ = change in effective stress at depth z below the equivalent footing from embankment loading, 0.53 ksf (Table D-24).
$\Delta\sigma'_{v(\mathrm{ss})}$ = change in effective stress at depth z below the equivalent footing from superstructure loading, 4.72 ksf.

$$\sigma'_{1(e+ss)} = \sigma'_{vo} + \Delta\sigma'_{v(\mathrm{ss})} + \Delta\sigma'_{v(e)}$$

$$\sigma'_{1(e+ss)} = (3.15\ ksf) + (0.53\ ksf) + (4.72\ ksf)$$

$$\sigma'_{1(e+ss)} = 8.40\ ksf$$

Determine the stress increase by comparing σ'_{vo} and $\sigma'_{1(\text{ss+e})}$.

$$Stress\ Increase = \frac{\sigma'_{1(\text{ss+e})} - \sigma'_{\text{vo}}}{\sigma'_{\text{vo}}} * 100\% \qquad \text{Eq. D-5}$$

$$Stress\ Increase = \frac{(8.40\ ksf) - (3.15\ ksf)}{(3.15\ ksf)} * 100\%$$

$$Stress\ Increase = 167\%$$

The stress increase is greater than or equal to 10%. Deformation for this depth increment should be estimated and included in the sum of all depth increments in which the stress increase is not less than 10%. A rock layer, which is considered incompressible, is located at Elev. 218 feet at this abutment, and thus it is assumed that no settlement or compression occurs below this depth.

For the dense coarse grained soil at Elev. 267.5 feet, *z* = 2.5 (stress exponent of j = 1.0), determine the strain in the layer from the increase in vertical effective stress, $\Delta\varepsilon$, with Equation 7-61.

E_s = elastic modulus of soil, 1416 ksf (Figure D-7).

σ'_{vo} = initial vertical effective stress at depth z below the equivalent footing, 3.15 ksf.

$\sigma'_{1(\text{ss+e})}$ = new vertical effective stress below the equivalent footing, 8.40 ksf.

$$\Delta\varepsilon = \frac{1}{E_s}\left[\sigma'_{1(\text{ss+e})} - \sigma'_{vo}\right] \qquad \text{[Eq. 7-61]}$$

$$\Delta\varepsilon = \frac{1}{(1416\ ksf)}[(8.40\ ksf) - (3.15\ ksf)]$$

$$\Delta\varepsilon = 0.0037$$

Calculate the layer compression denoted, *S*, with the initial height of the layer, H_o.

$$S = \Delta\varepsilon * H_o$$

$$S = 0.0037 * 5\ feet * \left(\frac{12\ inches}{1\ foot}\right)$$

$$S = 0.22\ inches$$

Table D-25 Calculation of Settlement by Janbu Tangent Modulus for Equivalent Footing at Elevation 270 feet

Elev. (feet)	z (feet)	H_o (feet)	E_s (ksf)	σ'_{vo} (ksf)	B (feet)	Z (feet)	$\Delta\sigma'_{v(ss)}$ (ksf)	$\Delta\sigma'_{v(e)}$ (ksf)	$\sigma'_{1(ss+e)}$ (ksf)	Stress Increase (%)	Δε	S (in)
267.5	2.5	5	1416	3.15	7.5	43.5	4.72	0.53	8.40	167	0.0037	0.22
262.5	7.5	5	1416	3.46	12.5	48.5	2.54	0.53	6.52	89	0.0022	0.13
257.5	12.5	5	1416	3.77	17.5	53.5	1.64	0.53	5.94	58	0.0015	0.09
252.5	17.5	5	1416	4.08	22.5	58.5	1.17	0.53	5.78	42	0.0012	0.07
247.5	22.5	5	1416	4.40	27.5	63.5	0.88	0.52	5.80	32	0.0010	0.06
242.5	27.5	5	1416	4.71	32.5	68.5	0.69	0.52	5.92	26	0.0009	0.05
237.5	32.5	5	1416	5.02	37.5	73.5	0.56	0.51	6.09	21	0.0008	0.05
232.5	37.5	5	1416	5.33	42.5	78.5	0.46	0.51	6.30	18	0.0007	0.04
227.5	42.5	5	1416	5.65	47.5	83.5	0.39	0.50	6.53	16	0.0006	0.04
222.5	47.5	5	1416	5.96	52.5	88.5	0.33	0.49	6.78	14	0.0006	0.03
219.0	51.0	2	1416	6.27	56.0	92.0	0.30	0.49	7.06	13	0.0006	0.01
											Total:	0.80

In a similar manner, the above analysis was performed for additional equivalent footing locations for all three trial group configurations. Table D-26 summarizes the results for the neutral plane method and Janbu tangent modulus estimated settlement. As established by global project performance requirements, vertical deformation (including settlement and elastic pile compression) should be limited to 1.5 inches at each substructure location. Therefore, Table D-26 indicates that this requires that the equivalent footing be located at Elevation 270 feet, a minimum of 40 feet below the bottom of pile cap (Elev. 310).

It is assumed that the equivalent footing acts at the same location as the neutral plane. Accordingly, an analysis was performed to determine the pile toe elevation

necessary to locate the neutral plane at Elev. 270.0, thereby establishing the minimum required pile penetration depth to satisfy tolerable deformations.

Table D-26 Estimated Pile Group Settlement Using Janbu Tangent Modulus with Neutral Plane Method For All Pile Group Configurations.

Equivalent Footing Elevation (feet)	Equivalent Footing Depth (feet)	Estimated Settlement Group Configurations 1 and 2 (inches)	Estimated Settlement Group Configuration 3 (inches)
285.0	25	2.30	2.46
280.0	30	1.98	2.12
275.0	35	1.54	1.65
270.0	40	0.80	0.85
265.0	45	0.76	0.81

The location of the neutral plane and the magnitude of drag force are evaluated following the procedure outlined in Section 7.3.6, using unfactored permanent loads and nominal geotechnical resistance. Because load factors for the Service limit state are 1.0, applicable loads at this limit state may be considered unfactored. The Service I, without LL limit state loads are therefore used for evaluation for the neutral plane. This example again utilizes the load for Group Configuration 1 (Q= 201 kips, Table D-14. Figure D-32 presents a graphical interpretation of the neutral plane for the HP12x74 pile driven to a penetration depth of 60 feet.

First, the sustained load plus the cumulative shaft resistance versus depth is plotted. Next, the mobilized toe resistance minus the cumulative shaft resistance versus pile penetration depth is plotted. The exact percentage of toe mobilization is unknown at this stage of design, therefore multiple toe mobilization curves should be evaluated to determine the neutral plane location. The 0% toe mobilization curve is the most conservative location to evaluate pile settlement since it locates the neutral plane at the highest elevation. The 100% toe mobilization curve should be used to check the pile section's structural strength since it results in the greatest axial force in the pile. The structural strength check is performed in Block 17.

At the North Abutment, it is expected that piles will be supported partially by toe resistance. Therefore the 0% toe mobilization curve presents an unreasonable baseline to evaluate settlement in this case. With some toe resistance likely mobilized, the 50 percent toe mobilization curve is used to evaluate settlement.

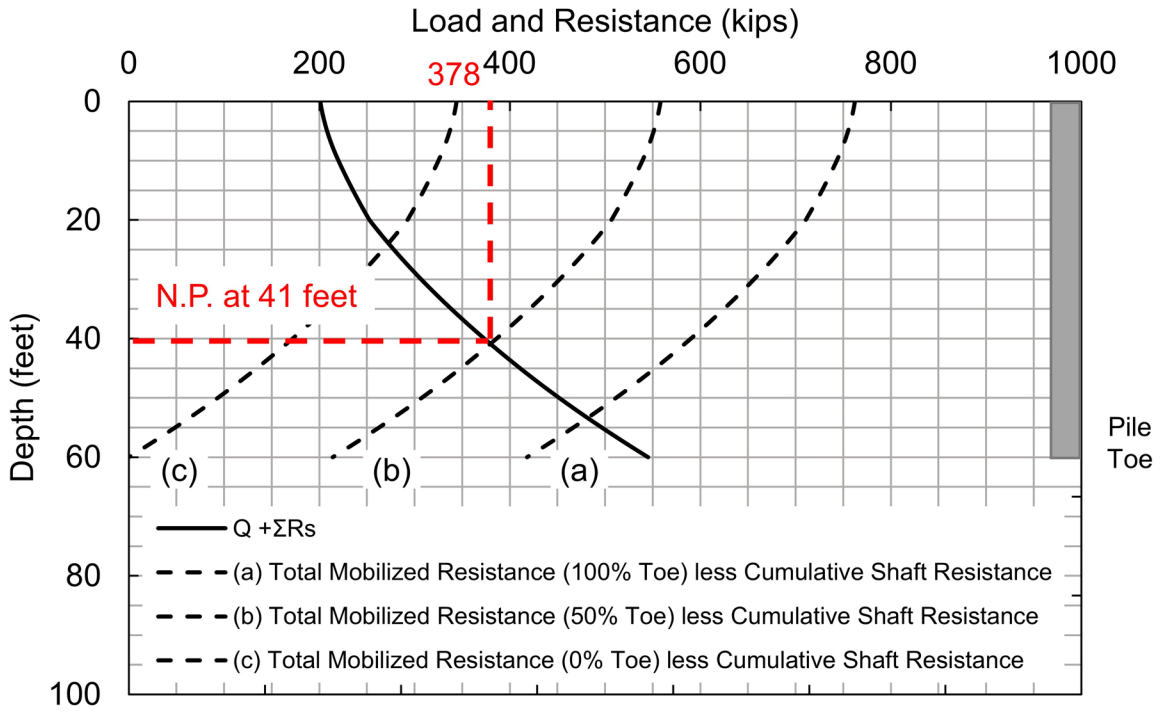

Figure D-32 Neutral plane at 50% toe mobilization for HP 12x74 at the North Abutment.

This analysis procedure was also performed for the remaining candidate pile sections and trial group configurations to determine the pile penetration depth required for the neutral plane to be located below a depth of 40 feet (Elev. 270.0 feet). Table D-27 summarizes the analysis results. The load per pile for each group configuration was previously presented in Table D-14.

Table D-27 Pile Penetration Depth Required to Locate Neutral Plane at Elev. 270.0 feet

Group Configuration	Load per Pile Q (kips)	HP 10x42 (feet)	HP 12x53 (feet)	HP 12x74 (feet)	HP 14x89 (feet)	HP 14x117 (feet)
1	201	69	60	60	54	53
2	165	64	55	55	50	50
3	139	60	52	52	48	48

A comparison of the required pile penetration depth for both settlement estimation methods yielded dissimilar results. To limit total settlement and elastic compression to less than 1.5 inches, the Meyerhof Method requires a pile penetration depth of 42.5 feet (Elev. 267.5 feet) for a HP 12x74 in Group Configuration 1. The Janbu tangent modulus approach requires a 17 foot deeper pile to satisfy the same settlement constraints with the same pile and group configuration. Table D-23 presents the minimum pile penetration depth based on group settlement estimation using the Meyerhof (1976) approach. Table D-27 presents the minimum pile penetration depth based on group settlement estimation using the Janbu Tangent modulus Method with the equivalent footing located at the neutral plane. Based on placing the neutral plane at or below EL 270, all candidate pile sections and group configurations require the piles to be driven into Soil Layer 3 (dense gravel with sand). After considering both settlement estimates, the results of the neutral plane and Janbu tangent modulus method were used to establish the minimum pile penetration depth for tolerable deformations.

A review of the soil profile at the North Abutment in Figure D-7 indicates no compressible soil layers below Soil Layer 3. Therefore, no effort is necessary to identify a maximum pile penetration depth to prevent punching through a dense layer into an unsuitable soil layer, or to causing a stress increase on a lower compressible layer causing excessive settlement. Table D-28 presents the established minimum pile penetration depths to satisfy tolerable deformations at the North Abutment using the Janbu tangent modulus approach.

Table D-28 Established Minimum Pile Penetration Depths to Satisfy Tolerable Deformations at the North Abutment

Group Configuration	HP 10x42 (feet)	HP 12x53 (feet)	HP 12x74 (feet)	HP 14x89 (feet)	HP 14x117 (feet)
1	69	60	60	54	53
2	64	55	55	50	50
3	60	52	52	48	48

Elastic shortening of the pile should be considered along with settlement. For elastic compression, the load per pile from the Service I, without LL limit state is applied at the pile head. As shown in Table D-14, this load is 201 kips.

Note that the drag force from negative shaft resistance increases the axial compression force in the pile. Negative shaft resistance above the neutral plane acts to increase axial compression force in the pile, whereas below the neutral

plane, positive shaft resistance reduces the axial compression force in the pile. This effect must be accounted for in the elastic compression calculation. Accordingly, the unfactored axial load used to compute elastic compression, Q, changes for each pile segment length, increasing equal to the unfactored permanent load plus the shaft resistance down to the neutral plane. In this example, at and below the neutral plane location of 54 feet, the unfactored axial load is equal to the resistance distribution from 100% toe mobilization. A review of Figure D-29 indicates that the maximum drag force magnitude results from 100% toe mobilization.

Equation 7-48 is used to illustrate this example for the first 12 inch increment of the HP 12x74 pile section. The average shaft resistance and average load for each respective depth interval is used to estimate the elastic compression. For each 12 inch segment, the elastic modulus remains constant, and was evaluated as 29,000 ksi. The pile cross sectional area likewise remains constant as 21.8 in^2. Remaining calculations were performed using a spreadsheet; Table D-29 summarizes the elastic compression with depth.

Determine the unfactored axial load in segment.

Q_d = unfactored permanent load, 201 kips.
R_s^- = average (negative) shaft resistance, 0.5 kips.

$$Q = Q_d + R_s^- = 201\ kips + 0.5\ kips$$

$$\mathrm{Q} = 201.5\ kips$$

Calculate elastic compression of segment with unfactored axial load from combined unfactored permanent load and negative shaft resistance.

L = segment length, 12 inches.
A = cross sectional area of pile material, 21.8 in^2.
E = elastic modulus of pile, 29,000 ksi.

$$\Delta = \frac{QL}{AE} \qquad \text{[Eq. 7-48]}$$

$$\Delta = \frac{(201.5\ kips)*(12\ inches)}{(21.8\ in^2)*(29{,}000\ ksi)}$$

$$\Delta = 0.00383\ inches$$

Table D-29 Elastic Compression Calculation

Depth Below Pile Head (feet)	Average Shaft Resistance (kips)	Average Unfactored Axial Load (kips)	Segment Compression, Δ (inches)
0	0.0	201.0	0.00000
0-1	0.5	201.5	0.00383
1-2	1.7	202.7	0.00385
2-3	3.0	204.0	0.00387
3-4	4.5	205.5	0.00390
4-5	6.3	207.3	0.00393
5-6	8.2	209.2	0.00397
6-7	10.3	211.3	0.00401
7-8	12.5	213.5	0.00405
8-9	15.0	216.0	0.00410
9-10	17.7	218.7	0.00415
10-11	20.5	221.5	0.00421
11-12	23.5	224.5	0.00426
12-13	26.5	227.5	0.00432
13-14	29.6	230.6	0.00438
14-15	32.8	233.8	0.00444
15-16	36.0	237.0	0.00450
16-17	39.3	240.3	0.00456
17-18	42.7	243.7	0.00463
18-19	46.2	247.2	0.00469
19-20	49.8	250.8	0.00476
20-21	54.0	255.0	0.00484
21-22	59.0	260.0	0.00493
22-23	64.0	265.0	0.00503
23-24	69.2	270.2	0.00513
24-25	74.5	275.5	0.00523
25-26	80.0	281.0	0.00533
26-27	85.5	286.5	0.00544
27-28	91.2	292.2	0.00555
28-29	97.0	298.0	0.00566
29-30	102.9	303.9	0.00577
30-31	108.9	309.9	0.00588
31-32	115.0	316.0	0.00600
32-33	121.3	322.3	0.00612
33-34	127.7	328.7	0.00624
34-35	134.2	335.2	0.00636
35-36	140.8	341.8	0.00649
36-37	147.6	348.6	0.00662
37-38	154.4	355.4	0.00675
38-39	161.4	362.4	0.00688

Table D-29 Elastic Compression Calculation (continued)

Depth Below Pile Head (feet)	Average Shaft Resistance (kips)	Average Unfactored Axial Load (kips)	Segment Compression, Δ (inches)
39-40	168.5	369.5	0.00701
40-41	175.8	376.8	0.00715
41-42	183.1	384.1	0.00729
42-43	190.6	391.6	0.00743
43-44	198.2	399.2	0.00758
44-45	205.9	406.9	0.00772
45-46	213.7	414.7	0.00787
46-47	221.7	422.7	0.00802
47-48	229.8	430.8	0.00818
48-49	238.1	439.1	0.00833
49-50	246.5	447.5	0.00849
50-51	255.1	456.1	0.00866
51-52	263.8	464.8	0.00882
52-53	272.7	473.7	0.00899
53-54	281.7	482.7	0.00916
54-55	290.9	482.0	0.00915
55-56	300.2	472.0	0.00896
56-57	309.7	462.5	0.00878
57-58	319.3	452.8	0.00860
58-59	329.1	443.1	0.00841
59-60	339.1	433.1	0.00822
		Total	0.37

For the pile head load of 201 kips (Group Configuration 1 loads), estimated elastic compression of the HP 12x74 pile section driven to 60 feet is 0.37 inches (pile toe at Elev. 250 feet). Combined with 0.80 inches of deformation from settlement (Table D-28), it is estimated that total vertical deformation at the North Abutment is 1.17 inches.

D.16 Block 16: North Abutment – Check pile drivability to maximum pile penetration depth requirements established in Blocks 12 through 15

Preliminary pile drivability analyses were performed for the 5 candidate pile sections in Block 10. Plots of nominal driving resistance, blow count, and compression stress versus depth were presented in Figure D-22. This figure should now be reviewed considering the established or estimated minimum pile penetration depths. A candidate pile section must be capable of being driven to the penetration depth

necessary to achieve the nominal geotechnical resistance in axial compression and tension, and to a penetration depth necessary to satisfy lateral load demands as well as axial and lateral deformation requirements. Estimated or minimum pile penetration depths were previously established in Blocks 12, 13, 14, and 15 and summarized in Tables D-15, D-19, D-22 and D-28.

Although a minimum pile penetration depth is not typically established for nominal geotechnical resistance in axial compression, the pile should also be capable of being driven reasonably close to the estimated pile penetration depth where the nominal resistance is expected to develop. If the pile cannot be driven to the required depth within driving stress limits and at reasonable blow counts, a larger pile hammer, a pile section with greater impedance, or pile installation aids such as predrilling or jetting may be required to satisfy or improve drivability. Alternatively, substructure design modifications should be considered.

For the candidate HP 12x74 H-pile section in the Group Configuration 1, the pile penetration depth for axial compression loading was estimated at 45 feet (Table D-15), the minimum penetration depth for axial tension loading was 28 feet (Table D-19), and the minimum penetration depth for lateral loading was 25 feet (Table D-22). The minimum pile penetration depth for group settlement was 60 feet (Table D-28) based on embankment and foundation loads occurring simultaneously. Accordingly, this candidate pile section must have sufficient drivability to the maximum of these depths (i.e., 60 feet).

A review of Figure D-22 indicates that the HP 12x74 pile section can be driven to 61 feet with a D36-52 hammer before encountering practical refusal. The preliminary drivability evaluation (with soil and hammer model assumptions described in Block 10), estimated that the blow count will not exceed 120 blows per foot or 10 blows per inch before this pile penetration depth. Compression driving stresses are estimated to remain below driving stress limits. Drivability results for a D46-52 pile hammer were also presented in Figure D-22 and indicated greater pile penetration depths were possible. Therefore, it is concluded that the HP 12x74 pile section can be driven to the 60 foot penetration depth.

D.17 Block 17: North Abutment – Determine the Neutral Plane Location and Resulting Drag Force; Check Structural Strength Limit State for Pile Penetration Depth From Block 16

Previously in Block 15, the neutral plane was evaluated as part of the settlement calculations. The neutral plane and resulting drag force are now evaluated to check

the structural strength limit state for candidate pile sections. Section 7.3.6 provides guidance for evaluating the neutral plane location and the magnitude of the drag force. The Service I, without live load limit state was used for the applied pile head load. This example again utilizes the load for Group Configuration 1 (Q = 201 kips, Table D-14).

At 100 percent toe mobilization, the neutral plane is at its lowest potential location, and thus the highest drag force magnitude results. Accordingly, this is the toe mobilization curve that should be used to check the pile section's structural strength. Figure D-33 presents a graphical interpretation of the neutral plane for the HP12x74 pile section driven to the estimated pile penetration depth of 60 feet. In this case the neutral plane is located 54 feet below the pile head with a resulting maximum axial compression force in the pile of 486 kips.

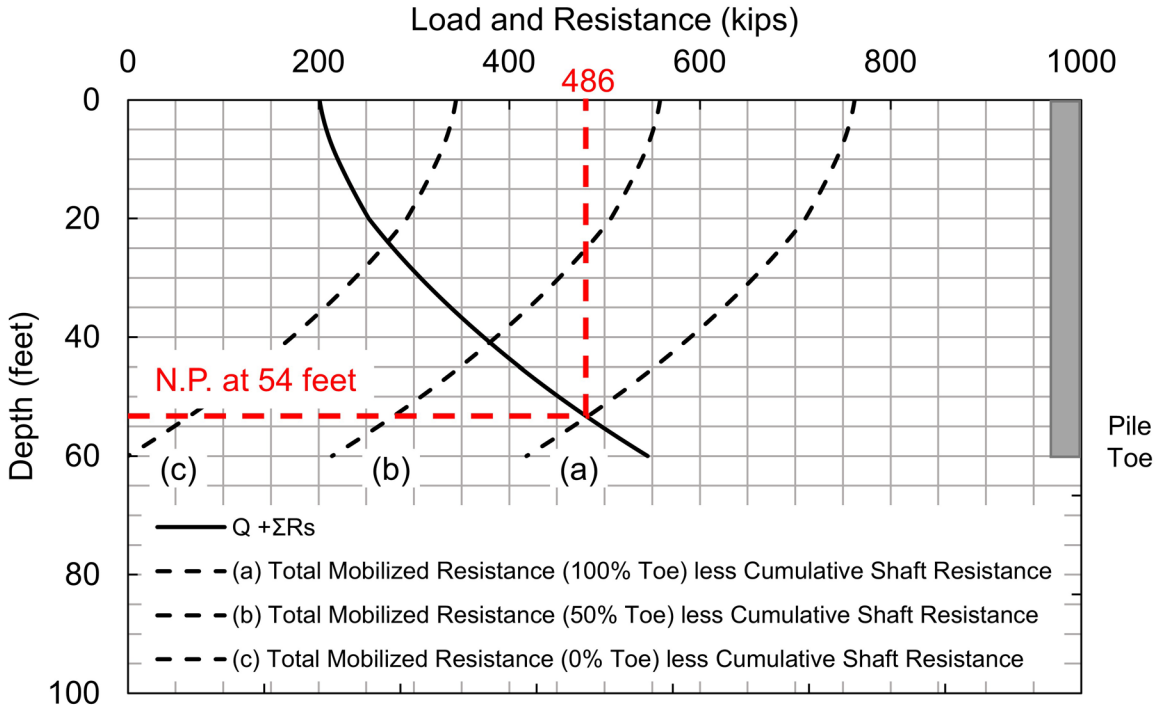

Figure D-33 Neutral plane at 100% toe mobilization for HP 12x74 at the North Abutment.

The resulting unfactored drag force, DF, is the difference between the maximum unfactored axial compression force in the pile, Q_{max}, minus the unfactored permanent load (Q). In this case, the drag force is evaluated for 100 percent toe mobilization.

$$DF = Q_{max} - Q$$

$$DF = (486\ kips) - (201\ kips) = 285\ kips$$

Following this calculation, the factored structural load was determined using Equation 7-70. As discussed in Section 7.3.6, a load factor of 1.25 is applied to the permanent load while a load factor of 1.1 is applied to the drag force. Because the pile is driven into dense gravel with cobbles, the pile toe may be subject to damage during driving, and therefore as recommended by the AASHTO (2104) code, a structural resistance factor for axial compression ϕ_c of 0.50 would be applied to the nominal structural resistance of 1088 kips (Table D-2). Accordingly, the factored structural resistance, P_r, for the HP 12x74 pile section is 544 kips.

$$1.25\ (Q) + \gamma_p(DF) < P_r \qquad \text{[Eq. 7-70[}$$

$$1.25\ (201\ kips) + 1.1(285\ kips) = 565\ kips$$

$$565\ kips > 544\ kips$$

In this case, the factored structural resistance is less than the factored loads, and therefore the pile section would be considered unacceptable. This evaluation of the structural resistance does not however consider the location of the neutral plane. In this case, the neutral plane is 6 feet above the pile toe for 100% toe mobilization, and this location on the pile may not be damaged.

The AASHTO (2014) design specifications do not specifically address drag force considerations relative to the pile structural resistance. For example, the factored structural resistance of an H-pile is the nominal structural resistance multiplied by the resistance factor for axial compression, ϕ_c. This resistance factor is 0.70 for combined axial and flexural resistance of undamaged piles, 0.60 for the axial resistance of piles in compression under good driving conditions, and 0.50 for the axial resistance of piles in compression subject to damage due to severe driving conditions. While not equivocally stated, it follows that if the neutral plane is located below the point of fixity and above the depth where H-piles are subject to potential damage during driving, then the sum of the sustained load plus drag force at the neutral plane is limited to 0.70 of the nominal structural resistance.

Hence for piles at the North Abutment, if the neutral plane is located at a depth where the pile section is likely to be straight and undamaged, a structural resistance factor for axial compression, ϕ_c, of 0.70 could be applied to the nominal structural resistance, P_n, of 1088 kips (Table D-2). Accordingly, the factored structural resistance, P_r, for the HP 12x74 pile section is 762 kips. Equation 7-68 is used to evaluate the structural resistance.

$$1.25\ (Q) + \gamma_p(DF) < P_r \qquad \text{[Eq. 7-70[}$$

$$1.25\ (201\ kips) + 1.1(285\ kips) = 565\ kips$$

$$565\ kips < 762\ kips$$

In this case, the factored structural resistance is larger than the factored load, and therefore the pile section is acceptable.

It may be beneficial to review the ratio of factored load to nominal structural resistance or, P_u / P_n. The following evaluation serves to back calculate the minimum required structural resistance factor, $\phi_{c(\min)}$, for the section to be acceptable considering the factored load.

$$\phi_{c(\min)} = \frac{P_u}{P_n}$$

$$\phi_{c(\min)} = \frac{(565\ kips)}{(1088\ kips)}$$

$$\phi_{c(\min)} = 0.52$$

To further evaluate the drag force on the HP 12x74 pile section, the ratio of factored load to nominal structural resistance or, P_u / P_n was performed at 1 foot increments over the portion of the pile. Table D-30 presents a calculation of unfactored load in the pile for 50 percent toe mobilization, the drag force, and the factored load at 1 foot increments over the lower 20 feet. The final column shows the ratio of factored load to nominal structural resistance, P_u / P_n. This comparison provides the Engineer with the minimum structural resistance factor required for the pile section to be acceptable. For example, at the pile toe (Elev. 248 feet), the pile section would be acceptable based on a structural resistance factor for axial compression, ϕ_c, of 0.50.

Table D-30 Calculation of Load in Pile, Factored Load and Comparison to Nominal Structural Resistance

Elevation (feet)	Depth on Pile (feet)	Nominal Shaft Resistance (kips)	$Q + \Sigma R_s$ (kips)	Unfactored Load in Pile (kips)	Drag Force *DF* (kips)	Factored Load P_u (kips)	P_u / P_n $\phi_{c(\min)}$
268.0	40	172	373	373	172	441	0.40
267.0	41	179	380	380	179	449	0.41
266.0	42	187	388	388	187	457	0.42
265.0	43	194	395	395	194	465	0.43
264.0	44	202	403	403	202	473	0.44
263.0	45	210	411	411	210	482	0.44
262.0	46	218	419	419	218	491	0.45
261.0	47	226	427	427	226	499	0.46
260.0	48	234	435	435	234	509	0.47
259.0	49	242	443	443	242	518	0.48
258.0	50	251	452	452	251	527	0.48
257.0	51	259	460	460	259	537	0.49
256.0	52	268	469	469	268	546	0.50
255.0	53	277	478	478	277	556	0.51
254.0	54	286	487	487	286	565	0.52
253.0	55	296	497	477	276	554	0.51
252.0	56	305	506	467	266	544	0.50
251.0	57	314	515	458	257	534	0.49
250.0	58	324	525	448	247	523	0.48
249.0	59	334	535	438	237	512	0.47
248.0	60	344	545	428	227	501	0.46

*Neutral plane located at Depth 54 feet (EL 254.0 feet) for 50 percent toe mobilization.

An analysis of the drag force was performed for each candidate pile section. The pile penetration depth utilized for the drag force structural resistance check was the required minimum penetration depth presented in Table D-28. Table D-31 presents the ratio of the factored load to nominal structural resistance, at the pile toe, for the all the candidate piles and group configurations. For H-piles which may be subject to damage during driving and require pile toe protection (i.e., as for piles driven to bedrock or through dense gravel, cobbles, etc.), the structural resistance factor in axial compression, ϕ_c, is 0.50. Considering 50 percent toe mobilization, only the HP 12x74 and HP 14x117 pile section are acceptable for all group configurations.

Table D-31 Ratio of Factored Load to Nominal Structural Resistance in Axial Compression, $\phi_{c(\min)}$, at the Pile Toe

Group Configuration	HP 10x42 $\phi_{c(\min)}$	HP 12x53 $\phi_{c(\min)}$	HP 12x74 $\phi_{c(\min)}$	HP 14x89 $\phi_{c(\min)}$	HP 14x117 $\phi_{c(\min)}$
1	0.55	0.63	0.46	0.50	0.41
2	0.54	0.63	0.46	0.43	0.35
3	0.54	0.55	0.43	0.38	0.32

The ratio of the factored load to nominal structural resistance was also evaluated at the neutral plane. In this case however, if the neutral plane was located at a depth where the pile section was assumed to be straight and undamaged, a higher resistance factor, ϕ_c, of up to 0.70 was applied. Table D-32 presents the ratio of the factored load to nominal structural resistance at the neutral plane, along with the respective neutral plane depth. For example, on the HP 12x74 pile section in Group Configuration 1, the minimum required structural resistance in axial compression $\phi_{c(\min)}$ is 0.52, at a neutral plane depth of 54 feet. This location is 6 feet above the pile toe, and is assumed undamaged, therefore the higher resistance factor of 0.70 is applied. Accordingly, the pile section is considered acceptable.

Conversely, for the HP 10x42 pile section in Group Configuration 1, the minimum required structural resistance in axial compression $\phi_{c(\min)}$ is 0.74, at a neutral plane depth of 54 feet. This location is 15 feet above the pile toe (69 feet, Table D-32), and is also assumed undamaged. After applying the higher resistance factor of 0.70, the pile section is considered unacceptable (and was also structurally unacceptable based upon the load at the pile toe, Table D-32).

Table D-32 Ratio of Factored Load to Nominal Structural Resistance in Axial Compression, $\phi_{c(\min)}$, at the Neutral Plane

Group Configuration	HP 10x42 $\phi_{c(\min)}$/ NP depth (feet)	HP 12x53 $\phi_{c(\min)}$/ NP depth (feet)	HP 12x74 $\phi_{c(\min)}$/ NP depth (feet)	HP 14x89 $\phi_{c(\min)}$/ NP depth (feet)	HP 14x117 $\phi_{c(\min)}$/ NP depth (feet)
1	0.74 / 54	0.68 / 55	0.52 / 54	0.50 / 54	0.41 / 53
2	0.67 / 54	0.63 / 55	0.47 / 53	0.43 / 50	0.35 / 50
3	0.62 / 54	0.55 / 55	0.43 / 52	0.38 / 48	0.32 / 48

Based on results of the drag force analysis, a candidate pile section may be eliminated from consideration if the factored loads are higher than the factored structural resistance. As recorded in Table D-33, the larger candidate pile sections remained acceptable considering drag force.

Table D-33 Does Candidate Pile Section Meet Structural Resistance Requirement Considering Drag Force Associated with Minimum Pile Penetration Depth?

Group Configuration	HP 10x42	HP 12x53	HP 12x74	HP 14x89	HP 14x117
1	No	No	Yes	Yes	Yes
2	No	No	Yes	Yes	Yes
3	No	No	Yes	Yes	Yes

D.18 Decision Block 18: Does Estimated Total Settlement and Differential Settlement Between Adjacent Substructure Locations Satisfy Requirements and Angular Distortion Limits?

This design step cannot yet be completed. The total settlement at the North Abutment has been estimated and it is within the established deformation limits. However, the foundation design and settlement estimates for the adjacent pier have yet to be performed. Therefore, differential settlement and angular distortion cannot be assessed at this time. This step will be revisited once design computations at the pier are performed.

D.19 Block 19: North Abutment – Evaluate Economics of Candidate Piles, Preliminary Group Configurations, and Other Factors

Until now, the design process has served to compare strength and service limits for several candidate pile types within trial group configurations. Some candidate pile types have not met all of the strength, service, or drivability requirements. It is useful to quickly review the suitable and unsuitable pile types and group configurations and then assess the cost of the viable foundation solutions.

Table D-34 summarizes the established minimum pile penetration depth based on analysis results from Blocks 12 through 15. For all candidate pile sections and group configurations at the North Abutment, the established minimum pile penetration depth was based on meeting tolerable vertical deformations.

Several candidate sections did not meet structural resistance requirements for axial loading, lateral loading or both. The candidate pile sections and/or group configurations not meeting design requirements are identified with an asterisk in Table D-34. For all three group configurations, the HP 10x42 and HP 12x52 pile sections did not meet all structural resistance requirements. These candidate pile sections and group configuration will therefore be eliminated for the final design.

Table D-34 Established Minimum Pile Penetration Depth at the North Abutment

Group Configuration	HP 10x42 (feet)	HP 12x53 (feet)	HP 12x74 (feet)	HP 14x89 (feet)	HP 14x117 (feet)
1	69*	60*	60	54	53
2	64*	55*	55	50	50
3	60*	52*	52	48	48

*Did not meet structural resistance requirement.

Table D-35 presents the estimated minimum penetration depth for each candidate section to meet the factored geotechnical resistance requirements at the Strength I limit state. The larger pile sections require less pile penetration depth than the smaller pile sections to provide the same geotechnical resistance. In addition, the factored load per pile decreases from Group Configuration 1 to Group Configuration 3. However, from the analyses in Blocks 13 through 15, the established minimum penetration depth to preclude unacceptable vertical deformation requires all piles to be driven deeper than the depth needed solely for their factored geotechnical resistance. The minimum penetration depth requirement results in the additional geotechnical resistance gained by further pile embedment to be essentially wasted and therefore uneconomical.

Table D-35 Estimated Minimum Penetration Depth for Factored Geotechnical Resistance at Strength I Limit State

Group Configuration	HP 10x42 (feet)	HP 12x53 (feet)	HP 12x74 (feet)	HP 14x89 (feet)	HP 14x117 (feet)
1	59*	45*	45**	45**	43**
2	46*	45*	45**	38**	35**
3	45*	45*	43**	32**	30**

*Did not meet structural resistance requirement.
**Must be driven deeper to meet deformation requirements (Table D-28).

The unit cost per foot of pile installed should be estimated. Past pricing information is generally the best guide. However due to fluctuations in the market price of material and other factors, pile costs are subject to change. Section 6.14 provides recent piling cost information from several state agency databases. In the calculation below, the cost of steel of $0.90 per pound is used as a baseline to determine pile cost. Equation D-5 shows the cost per linear foot calculation in which the cost is determined for the HP12x74 pile section. Table D-36 presents the cost per linear foot for each of the 5 candidate pile sections and shows reasonable agreement with the installed cost per foot of pile provided in Section 6.14.

Determine price per linear foot for HP12x74 pile section.

$\$$ = cost per pound of steel, $0.90/lb.
w = weight per linear foot of pile section, 74 lbs/ft.

$$\text{Cost} = \frac{\$}{lbs} * \frac{lbs}{ft} \qquad \text{Eq. D-6}$$

$$\text{Cost} = \left(\frac{\$0.90}{lbs}\right) * \left(\frac{74lbs}{ft}\right)$$

$$\text{Cost} = \frac{\$66.60}{ft}$$

Table D-36 Estimated Cost Per Linear Foot for 5 Candidate Pile Sections

HP 10x42 ($ / ft)	HP 12x53 ($ / ft)	HP 12x74 ($ / ft)	HP 14x89 ($ / ft)	HP 14x117 ($ / ft)
37.80	47.70	66.60	80.10	105.30

The pile cost versus pile penetration depth is plotted for each of the 5 candidate pile sections in Figure D-34. In this calculation, the cost per linear foot is multiplied by the pile length, and due to the price difference per foot, the cost difference between pile sections becomes more pronounced with depth. Table D-37 shows the price per pile at the established minimum pile penetration depth. For example, for the HP 12x 74 pile section in Group Configuration 1, the individual cost is determined by multiplying the cost per foot by the penetration depth. At its minimum pile penetration depth of 60 feet, the cost per pile is $3,996. There will be additional pile length embedded in the cap. However that length is currently undetermined, and for pile cost estimation and decision purposes, it can be considered negligible. Table D-38 shows the pile group cost reflecting the cost per pile and number of piles in the group.

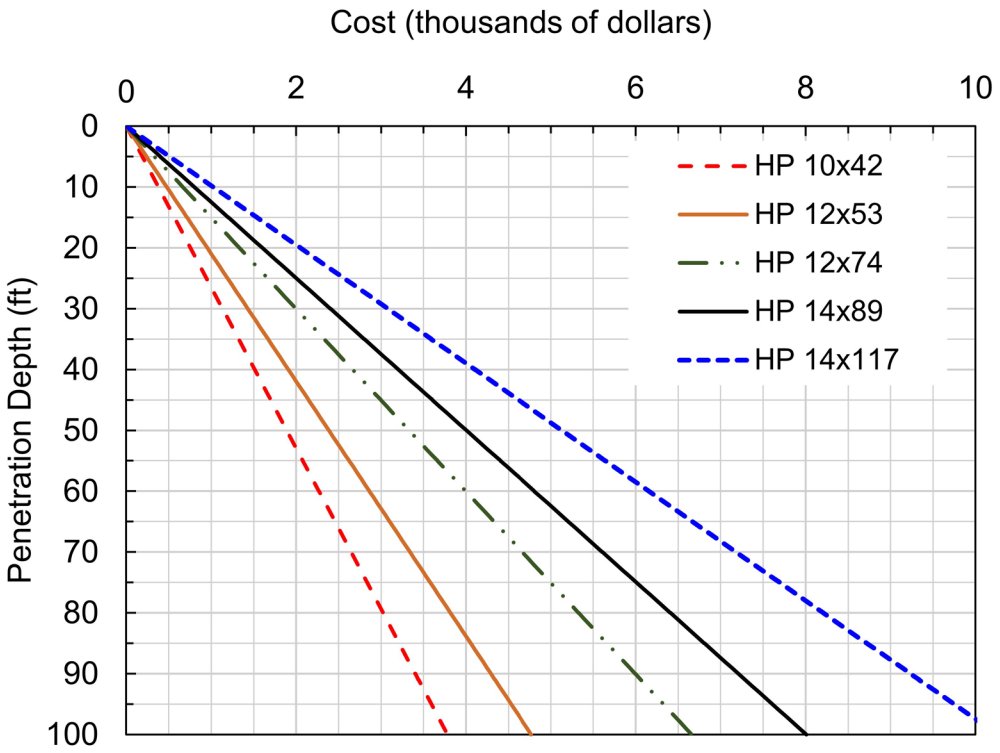

Figure D-34 Pile cost versus penetration depth.

Table D-37 Cost per Pile at Established Minimum Penetration Depth for Piles Meeting Structural Requirements

Group Configuration	HP 12x74	HP 14x89	HP 14x117
1	$3,996	$4,325	$5,438
2	3,663	4,005	5,130
3	3,463	3,845	4,925

Table D-38 Pile Group Cost at Established Minimum Penetration Depth for Piles Meeting Structural Requirements

Group Configuration	HP 12x74	HP 14x89	HP 14x117
1	$71,928	$77,857	$97,880
2	80,586	88,110	112,860
3	90,043	99,965	128,045

Based upon this comparison, the HP 14x117 pile section proves to be least economical followed by the HP 14x89 section. Conversely, the HP 12x74 pile

section in Group Configuration 1 appears to be the most economical. The cost of the pile cap must also be considered before selecting the lowest cost.

The cost of the pile cap is estimated and factored into the total foundation cost. Section 8.9 outlines a procedure to estimate the total pile cap thickness. Equation 8-80 is used along with the factored geotechnical resistance, per pile, to estimate this value. Table D-39 summarizes the factored geotechnical resistance for each pile section based upon the estimated minimum pile toe elevation.

Table D-39 Factored Geotechnical Resistance, R_r, at Estimated Minimum Pile Penetration Depth

Group Configuration	HP 12x74 (kips)	HP 14x89 (kips)	HP 14x117 (kips)
1	323	323	323
2	265	265	265
3	224	224	224

A sample calculation for determining the cap thickness is shown below for the HP 12x74 H-pile in Group Configuration 1. Table D-40 summarizes the estimated cap thickness for each pile section and pile group permutation calculated using this procedure.

Estimate the total pile cap thickness for a HP12x74 H-pile in Group Configuration 1.

P_{ui} = maximum single pile factored axial load, Q =323 kips (Table D-14).

$$t_{cap} = \frac{P_{ui}}{12} + 30 \qquad \text{[Eq. 8-80]}$$

$$t_{cap} = \frac{(323\ kips)}{12} + 30$$

$$t_{cap} = 57\ inches$$

Table D-40 Estimated Total Pile Cap Thickness

Group Configuration	HP 12x74 (inches)	HP 14x89 (inches)	HP 14x117 (inches)
1	57	57	57
2	52	52	52
3	49	49	49

Next, the volume of reinforce concrete required to construct the pile cap is determined from the estimated total pile cap thickness. The total pile cap width and length values were previously provided in Table D-12. The resulting volume of reinforced concrete in the pile cap for each pile section and pile group permutation is presented in Table D-41. Note that pile cap volume is shown in cubic yards (CY).

Table D-41 Estimated Volume of Reinforced Concrete in Pile Cap

Group Configuration	HP 12x74 (CY)	HP 14x89 (CY)	HP 14x117 (CY)
1	48.5	48.5	48.5
2	44.4	44.4	44.4
3	37.6	37.6	37.6

To estimate the pile cap cost, past pricing information is generally the best guide. However, similar to estimating the pile cost, due to fluctuations in the market price of material and other factors, pile cap costs are subject to change. The cost of the reinforced concrete pile cap, furnished and constructed, is estimated to be $500 /CY. Using this estimated value, the volumes presented in Table D-41 were used to estimate the cost of the various reinforced concrete pile caps. The pile cap cost for each candidate section and group configuration permutation is shown in Table D-42.

Table D-42 Estimated Cost of Reinforced Concrete Pile Cap

Group Configuration	HP 12x74	HP 14x89	HP 14x117
1	$24,264	$24,264	$24,264
2	22,204	22,204	22,204
3	18,794	18,794	18,795

By adding the cost of the pile cap and piles for each permutation, the estimated total foundation cost is determined as presented in Table D-43. Considering both the pile and the pile cap costs, the HP 12x74 in Group Configuration 1 is the most economical option.

With field resistance determination tests yet to be performed, only geotechnical correlations have been considered to estimate nominal resistance vs. depth relationships. Dynamic testing results may require additional (or less) pile embedment to satisfy resistance requirements. The potential for such variations between estimated and installed lengths becomes more-pronounced with friction

Table D-43 Estimated Foundation Cost Including Piles and Pile Cap at North Abutment

Group Configuration	HP 12x74	HP 14x89	HP 14x117
1	$96,192	$102,121	$122,145
2	102,790	110,314	135,064
3	108,838	118,759	146,839

piles than with end-bearing piles. To provide insight into how such potential length variations might affect costs, an additional comparison of pile cost versus depth from the estimated depth was completed for the final three candidate pile sections.

In this comparison, Table D-44 shows the cost per pile and cost per pile group for the three lowest cost permutations of group configuration and candidate sections from Table D-43 (i.e., the HP 12x74, the HP 14x89 section, and the HP14x117 section all in Group Configuration 1). Group Configuration 1 contains 18 piles. Although the pile sections have different established minimum penetration depth requirements, the depth provided in Table D-44 will be used as a baseline to evaluate the cost risk associated with pile overrun or underrun ("over/underrun") that may result from field determination testing. At the North Abutment, the established minimum pile penetration depth is greater than the estimated pile penetration depth for factored geotechnical resistance in axial compression, therefore underrun is provided for demonstration purposes only.

If the estimated soil resistance is underpredicted and the 14x89 pile section in Group Configuration 1 is determined to have sufficient factored resistance upon field determination testing at 49 feet (underrun of 5 feet), the cost per pile would be reduced by $481 and thus a reduction of $8,651 relative to the original $102,121 estimate for the total foundation cost would result. A graphical representation of this effect is presented in Figure D-35 (Underrun is shown for demonstration purposes only at the North Abutment as the established minimum pile penetration depth is 60 feet for this pile section). Conversely, if for example, the HP 12x74 section must be driven 15 feet deeper (overrun of 15 feet) to achieve sufficient factored resistance; an additional cost of $999 per pile would result. Based upon the number of piles and estimated pile cap cost, this would increase the total foundation cost by $17,982 from the original estimate of $96,192.

If it is assumed that the same pile over/underrun length will result for the pile sections after field determination testing, a cost comparison can be made for a range

of over/underrun lengths for the final candidate pile sections and group configurations. This comparison can compare the sensitivity of foundation cost to over/underrun lengths among candidate pile sections, and therefore may aid selection among the sections.

Table D-44 Comparison of Pile Over/Underrun Costs for Three Lowest Cost Alternatives at the North Abutment

Over/ Underun (feet)	HP 12x74 Change in Cost per Pile	HP 12x74 Change in Cost of Foundation	HP 14x89 Change in Cost per Pile	HP 14x89 Change in Cost of Foundation	HP 14x117 Change in Cost per Pile	HP 14x117 Change in Cost of Foundation
-5	($400)	$(7,193)	$(481)	$(8,651)	$(616)	$(11,081)
0	-	-	-	-	-	-
5	333	5,994.00	401	7,209	$513	9,234
10	666	11,98	801	14,418	1,026	18,468
15	99	17,98	1,202	21,627	1,539	27,702

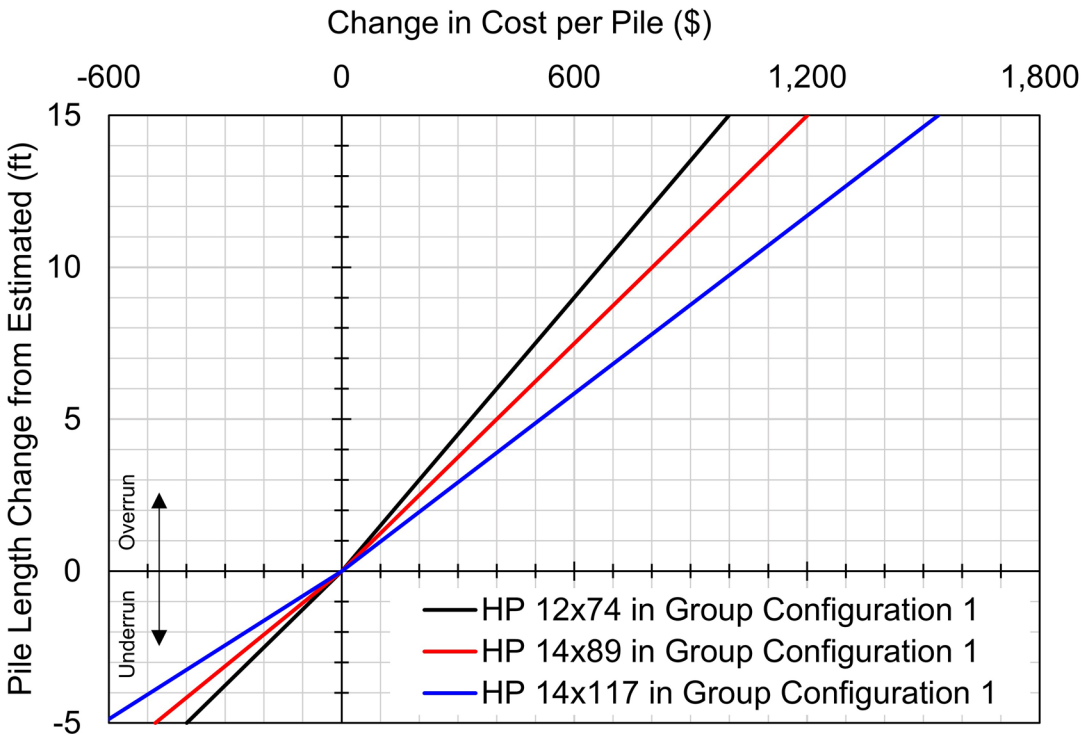

Figure D-35 Change in cost per pile from over/ underrun.

Table D-45 compares the overall foundation cost change associated with over/underrun lengths for the final thee candidate pile sections and pile group configuration permutations; graphical results of this interpretation are presented in Figure D-36 The change of foundation cost is again presented along with the relative difference based upon the same assumed pile over/underrun for the pile

sections. The difference in foundation cost is referenced from the HP12x74 pile section in Group Configuration 1. For example if 15 feet of overrun occurs for each permutation, the resulting cost difference between the HP 12x74 section in Group Configuration 1 and the HP 12x74 section in Group Configuration 1 is $17,982 minus $21,627 or -$3,645.

Table D-45 Comparison of Pile Group Over/Underrun Costs for Three Lowest Cost Alternatives at the North Abutment

Over/ Underun (feet)	HP 12x53 Change in Cost of Foundation	HP 14x89 Change in Cost of Foundation	Difference in Cost of Foundation	HP 14x117 Change in Cost of Foundation	Difference in Cost of Foundation
-5	$(7,193)	$(8,651)	$1,458	$(11,081)	$3,888
0	-	-	-	-	-
5	5,994	7,209	(1,215)	9,234	(3,240)
10	11,988	14,418	(2,430)	18,468	(6,480)
15	17,982	21,627	(3,645)	27,702	(9,720)

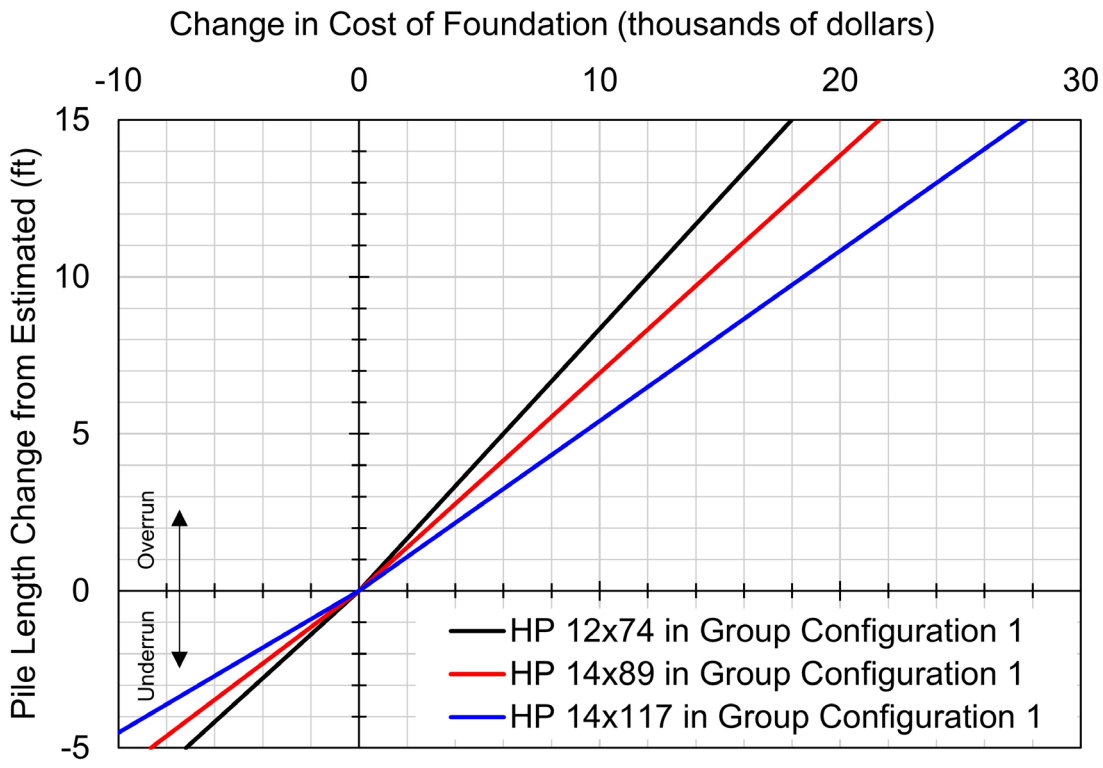

Figure D-36 Change in total cost of foundation from overrun/ underrun.

In the absence of a test pile program, a definitive cost comparison cannot be made; however, the above described cost analysis can assist to reduce the number of options and estimate the relative risk of cost overruns or savings associated with a

given candidate pile section and group configuration. At this juncture, a preliminary design of the Pier 2 and the South Abutment should be performed before making a final decision on pile type and size. This offers flexibility for the pile group design at other locations if the agency practice is to use the same pile sections at all foundation locations. If, for example, larger loads are required at Pier 2 or the South Abutment, the use of a larger pile section may be reason to further eliminate one or more of the candidate pile sections or group configurations.

D.20 Decision 20: Is the Preliminary Design of All Substructure Foundations Complete?

No. The preliminary foundation design has been completed for only the North Abutment. The preliminary design needs to be completed for the Pier and for the South Abutment. Return to Block 9 and begin the preliminary design for the next substructure location.

D.21 Block 9: Pier 2 – Calculate Nominal and Factored Structural Resistances for all Candidate Piles

The nominal structural resistance is now re-evaluated for the five candidate H-pile sections at Pier 2. The H-pile sections selected for evaluation again include a HP 10x42, a HP 12x53, a HP 12x74, a HP 14x89 and a HP 14x117. A detailed step by step example for calculation of the nominal structural resistance was previously presented in Section 8.5.3 for an HP 14x117 H-pile section. Therefore, this process is not repeated for the five candidate pile sections.

Due to channel degradation and local scour, the hydraulic engineer estimated scour depth is up to 5 feet below the bottom of pile cap for the design flood. The nominal structural resistance in axial compression must therefore account for a longer unbraced length. At the Strength limit state, the design flood event scour results in an unbraced length of 5 feet. Furthermore, for the check flood at the Extreme Event Limit State, the hydraulic engineer estimated scour potential up to 7 feet below the bottom of the pile cap. In this case, 7 feet of unbraced length is factored into the nominal structural resistance calculation. Table D-46 presents the nominal structural resistances in axial compression, flexure, and shear for the five candidate pile sections.

Table D-46 Nominal Structural Resistance in Axial Compression, Flexure and Shear

H-pile Section	HP 10x42	HP 12x53	HP 12x74	HP 14x89	HP 14x117
P_n, Nominal Resistance in Axial Compression (kips) (Strength V)	581	734	1043	1266	1670
P_n, Nominal Resistance in Axial Compression (kips) (Extreme Event II)	546	702	999	1229	1624
M_{ny}, Nominal Resistance in Weak Axis Flexure (kip-ft)	82	114	118	257	380
M_{nx}, Nominal Resistance in Strong Axis Flexure (kip-ft)	176	295	433	592	807
$V_{n,}$ Nominal Resistance in Shear (kips)	118	149	214	246	331

It is anticipated that the piles at Pier 2 will be driven into the dense gravel with sand deposit, or possibly to the underlying bedrock. The dense gravel with sand deposit contains occasional boulders. In these conditions, pile shoes are recommended for

use with the H-piles to reduce the risk of damage. Therefore, the applicable structural resistance factors, ϕ_c, are 0.5 for axial compression resistance and 0.7 for combined axial compression and flexural resistance. A resistance factor of ϕ_v =1.0 is used for shear, and a resistance factor of ϕ_f=1.0 is applicable for flexure only. Table D-47 summarizes the calculated factored structural resistances in axial compression, combined axial and flexure, flexure, and shear.

Table D-47 Factored Structural Resistance in Axial Compression, Flexure and Shear

H-pile Section	HP 10x42	HP 12x53	HP 12x74	HP 14x89	HP 14x117
P_r, Factored Resistance in Axial Compression, ϕ_c = 0.5 (kips) (Strength V)	290	367	521	633	835
P_r, Factored Axial and Flexural Resistance, ϕ_c = 0.70 (kips) (Strength V)	407	514	730	886	1169
P_n, Factored Resistance in Axial Compression, ϕ_c = 0.5 (kips) (Extreme Event II)	273	351	500	615	812
P_r, Factored Axial and Flexural Resistance, ϕ_c = 0.70 (kips) (Extreme Event II)	382	491	699	861	1137
M_{ry}, Factored Resistance in Weak Axis Flexure, ϕ_f=1.0 (kip-ft)	82	114	118	257	380
M_{rx}, Factored Resistance in Strong Axis Flexure, ϕ_f=1.0 (kip-ft)	176	295	433	592	807
V_r, Factored Resistance in Shear ϕ_v =1.0 (kips)	118	149	214	246	331

D.22 Block 10: Pier 2 – Calculate Nominal and Factored Geotechnical Resistances in Axial Compression and Tension versus Depth for all Candidate Piles; Perform Preliminary Pile Drivability Analyses

The engineering properties for the soil conditions encountered at Pier 2 were determined in Block 5. The results of the boring program and laboratory tests are now used to develop a design profile for Pier 2. Engineering judgement was used in developing the design profile to delineate the subsurface conditions into layers with similar properties. An effective stress diagram, depicted in Figure D-37, was also made for this soil profile. This diagram includes the total stress, porewater pressure and effective stress versus depth. Figure D-37 also presents the basic soil profile for quick reference to the relevant soil layers. The effective stress diagram was

computed using Equations 5-7 through 5-9 from Chapter 5. These equations are repeated below. For Figure D-37 the total stress, porewater pressure and effective stress were calculated at 1 foot increments using a spreadsheet.

$$\sigma_{vo} = \sum_i^n (\gamma_i h_i) \qquad \text{[Eq. 5-7]}$$

$$u = \gamma_w h_w \qquad \text{[Eq. 5-8]}$$

$$\sigma'_{vo} = \sum_i^n (\gamma_i h_i) - \gamma_w h_w \qquad \text{[Eq. 5-9]}$$

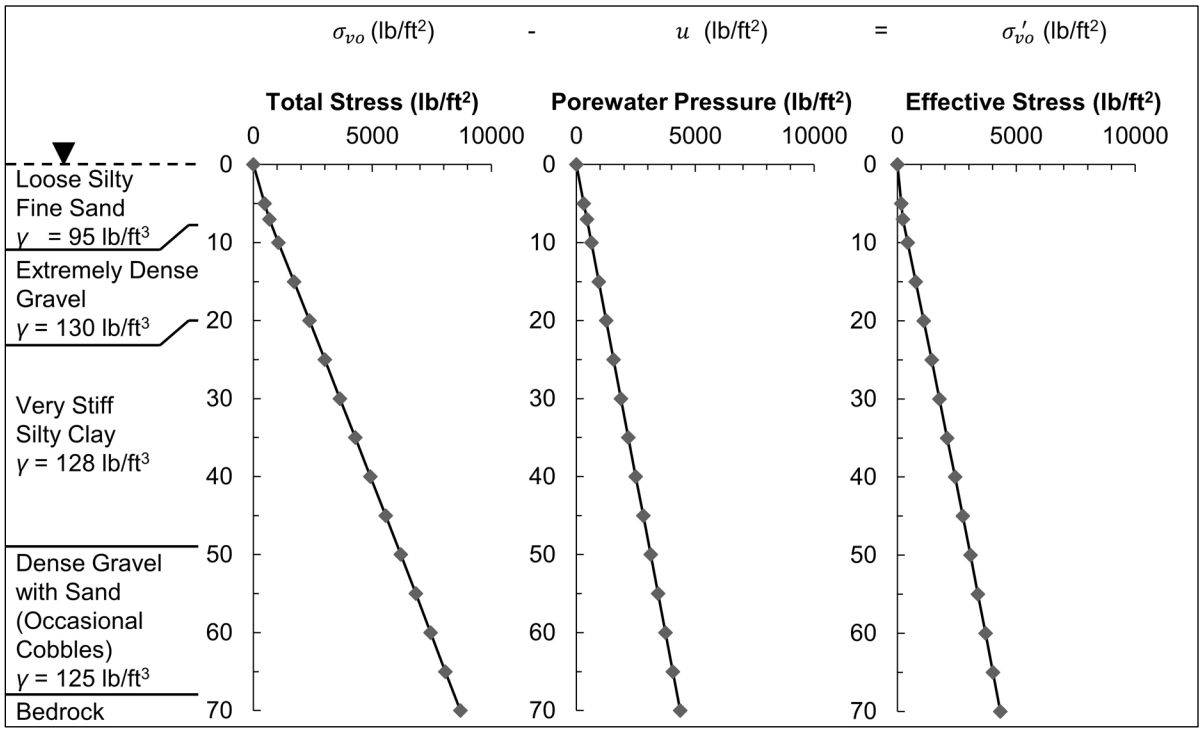

Figure D-37 Effective stress diagram for Pier 2 using Boring S-2.

To continue development of an idealized soil profile, field SPT N values were corrected for hammer energy transfer and vertical effective stress. The field SPT N values were first corrected for energy transfer using Equation 5-1. These results are presented in Table D-48. Typical correlations for SPT hammer type and energy transfer are provided in Section 5.1.1 (e.g., typical energy transfer of 80% for automatic hammer). The SPT hammer on the drill rig used for this project's soil exploration program was calibrated in accordance with ASTM D4633. Results of this calibration indicated an average energy transfer of 75%. Therefore, the *ER* value in Equation 5-1 is equal to 75.

$$N_{60} = N\left(\frac{ER}{60}\right) \qquad \text{[Eq. 5-1]}$$

The SPT N value was then corrected for vertical effective stress as presented in Equation 5-2, using the Peck et al. (1974) correction factor, C_n. The depth value for this calculation was taken from the middle depth of the SPT sampling event after the 6 inch seating interval (e.g., the SPT N value recorded from 0.5-1.5 feet was corrected using the vertical effective stress at 1 foot).

$$(N_1)_{60} = C_n N_{60} \quad \text{[Eq. 5-2]}$$

$$C_n = 0.77 \log \left(\frac{20}{\sigma'_{vo}}\right) \quad \text{[Eq. 5-3]}$$

After correcting the SPT N values for energy transfer and vertical effective stress, an average corrected N value was determined for each respective cohesionless soil layer. The N value from the first SPT sample in Layer 1 was not included in this procedure for Layer 1 since the bottom of the footing at Pier 2 is below this sample depth.

Table D-49 presents the average $(N_1)_{60}$ value for each cohesionless layer at Pier 2, the coefficient of variation, COV, within the layer, and the effective stress friction angle chosen for the layer. The coefficient of variation for each layer was less than 25% indicating low variability within each of the identified layers. Higher variability would have necessitated separating the soil profile into additional soil layers.

Table D-48 Correction of Field SPT N Value for Energy and Vertical Effective Stress at Pier 2 using Boring S-2

Soil Layer	Depth (ft)	σ'_{vo} (ksf)	Field N value	N_{60}	C_n	$(N_1)_{60}$
1	1	0.033	3	4	2.00	8
1	6	0.101	7	9	2.00	18
2	8	0.166	51	64	1.83	117
2	11	0.369	52	65	1.57	102
2	16	0.707	55	69	1.35	93
4	51	3.013	42	53	0.86	45
4	56	3.326	46	58	0.83	48
4	61	3.639	41	51	0.80	41
4	66	3.952	50	63	0.77	48

The $(N_1)_{60}$ values were used to estimate the effective stress friction angle of each soil layer in accordance with Table 5-5 of Chapter 5. These friction angle

correlations are presented in Table D-49. Layer 2 consists of extremely dense gravel and Layer 4 consists of hard angular gravel with sand. Therefore, as discussed in Section 5.5.1, a design friction angle of 36 degrees was used for estimating the shaft resistance in both of these layers while the friction angle noted in Table D-49 was used to estimate the toe resistance.

Table D-49 Soil Layer Effective Stress Friction Angle Correlations at Pier 2

Soil Layer	Average $(N_1)_{60}$	COV	ϕ' shaft (degrees)	ϕ' toe (degrees)
1	18	0.0%	32	32
2	104	9.6%	36	43
4	46	6.3%	36	38

Soil Layer 3 consists of very stiff silty clay. Unconfined compression strength tests were performed on each undisturbed cohesive soil sample. The undrained shear strength was then calculated by dividing the unconfined compression strength by 2.

Figure D-38 presents the undrained shear strength versus depth for Soil Layer 3. The undrained shear strength increases approximately linearly from 20 to 45 feet. Layer 3 was refined into 6 sublayer increments of 5 feet, each using the respective undrained shear strength value determined from laboratory testing. Table D-50 presents the shear strength values for Soil Layer 3 as well as sublayers a through f.

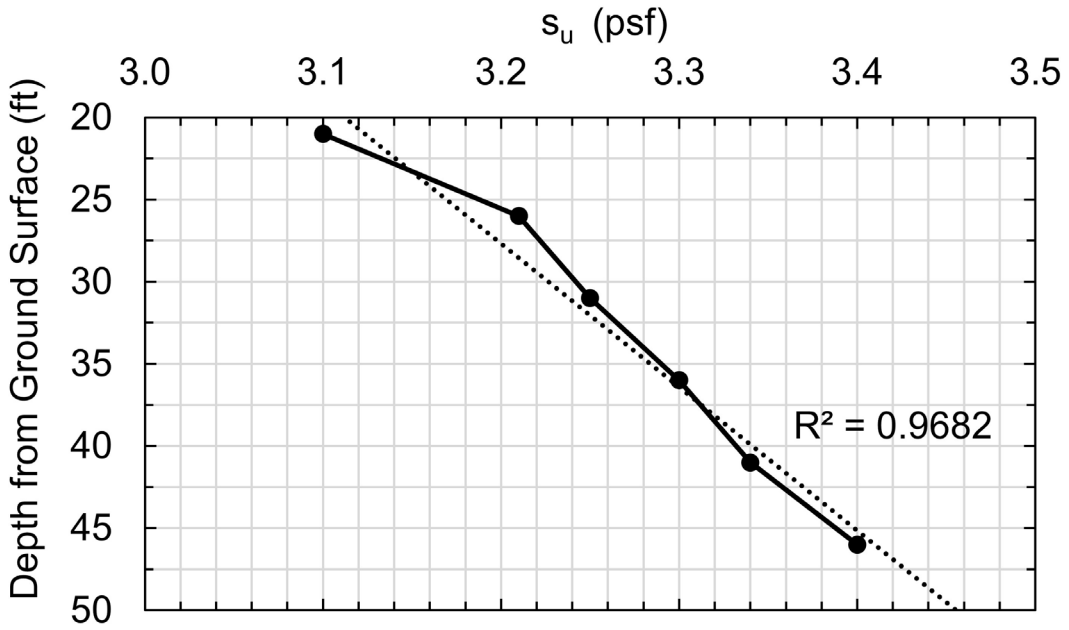

Figure D-38 Undrained shear strength, s_u, versus depth for Soil Layer 3 at Pier 2.

Table D-50 Undrained Shear Strength, s_u, for Soil Layer 3 at Pier 2

Soil Layer	Depth (ft)	σ'_{vo} (ksf)	q_u (tsf)	s_u (ksf)
3a	21	1.045	3.10	3.10
3b	26	1.373	3.21	3.21
3c	31	1.701	3.25	3.25
3d	36	2.029	3.30	3.30
3e	41	2.357	3.34	3.34
3f	46	2.685	3.40	3.40

The design soil profile for Pier 2 is presented in Figure D-39, with the bottom of footing elevation noted 10 feet below ground surface. Some soil properties in the design soil profile such as the elastic moduli, E_s, and the initial cyclic modulus of subgrade reaction, k_c, have been selected based on published correlations in the absence of laboratory and field testing. For this particular soil profile, the elastic moduli were determined from the SPT correlation in Table 5-11 and the initial cyclic moduli of subgrade reaction were selected based on representative values shown in Table 7-22. The average cohesive soil strength for Layer 3 was used to select the 50% strain factor, ε_{50}, from Table 7-21.

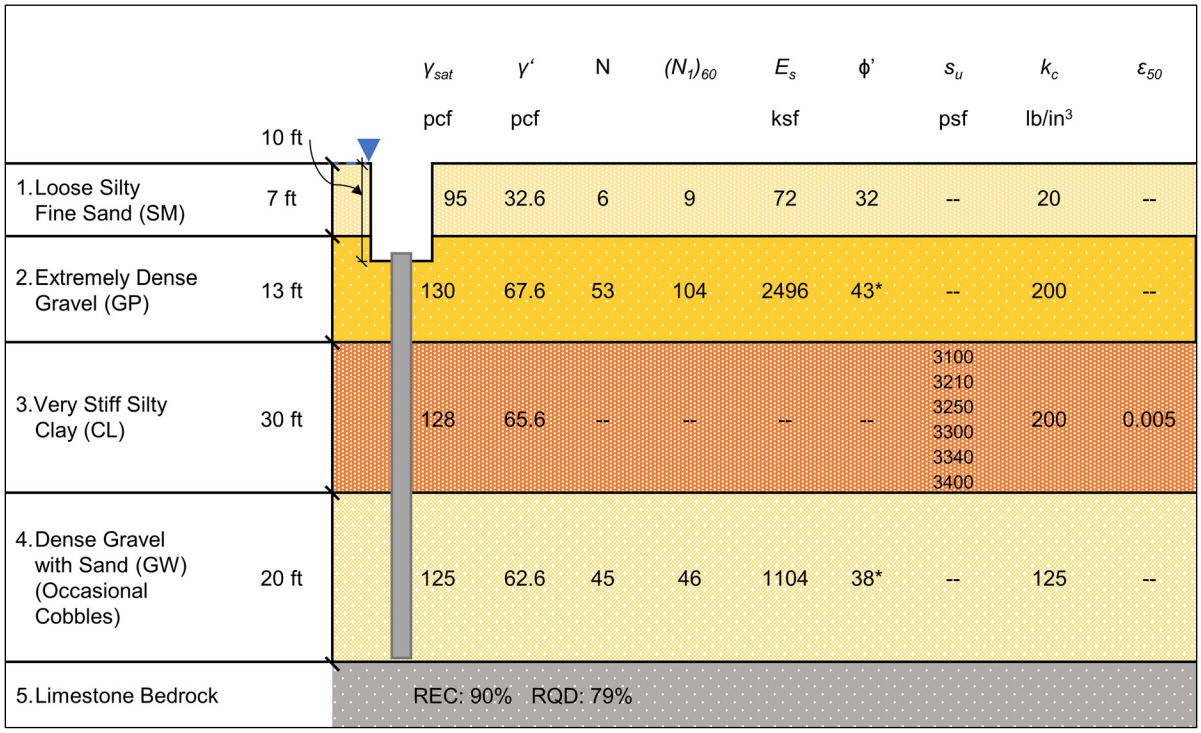

Figure D-39 Design soil profile at Pier 2.

D.22.1 Geotechnical Resistance in Axial Compression

The nominal geotechnical resistance in axial compression is now determined for the selected candidate H-pile sections. The nominal geotechnical resistance can be calculated by hand or with computer software using an appropriate analysis method based upon soil and pile type. Chapter 7 describes appropriate methods for this purpose as well as available computer programs.

For this example, the DrivenPiles computer program was used to calculate the nominal resistance, shaft resistance, and toe resistance as a function of depth for each of the five candidate H-piles. This software program was selected since it uses the FHWA recommended Nordlund method and alpha method to estimate the nominal geotechnical resistance of H-piles in cohesionless and cohesive soils, respectively. The DrivenPiles program also allows the analyst to select a different friction angle for shaft and toe resistance calculations in any layer. This option was utilized for the extremely dense gravel in Layer 2 and the gravel with sand comprising Layer 4. The computer program was also used to evaluate the nominal geotechnical resistance at Pier 2 during the design flood and at the check flood.

A summary of the nominal shaft, nominal toe, and nominal geotechnical resistance is presented for the HP 12x74 H-pile section in Table D-51. A graphical interpretation of the estimated resistance is presented in Figure D-40. The indicated pile penetration depth is referenced from the bottom of pile cap (Elev. 275.0 feet), which is 10 feet below the original ground surface (Elev. 285.0 feet).

Table D-51 Nominal Shaft, Nominal Toe and Nominal Geotechnical Resistance for HP 12x74 at Pier 2 (pre-scour)

Depth (feet)	Nominal Shaft Resistance (kips)	Nominal Toe Resistance (kips)	Nominal Geotechnical Resistance (kips)		Depth (feet)	Nominal Shaft Resistance (kips)	Nominal Toe Resistance (kips)	Nominal Geotechnical Resistance (kips)
0.01	0.0	106.5	106.5		29.99	109.9	30.5	140.4
1	1.1	123.0	124.2		30.01	110.1	30.8	140.9
2	2.4	139.7	142.1		31	115.1	30.8	145.9
3	3.9	156.4	160.2		32	120.2	30.8	151.0
4	5.5	173.1	178.5		33	125.3	30.8	156.1
4.99	7.2	189.6	196.8		34	130.4	30.8	161.2
5.01	7.3	189.9	197.2		34.99	135.5	30.8	166.3
6	9.2	206.4	215.6		35.01	135.6	31.4	166.9
7	11.3	223.1	234.4		36	140.6	31.4	172.0
8	13.5	239.8	253.3		37	145.7	31.4	177.1
9	16.0	256.5	272.4		38	150.8	31.4	182.2
9.99	18.5	273.0	291.5		39	155.9	31.4	187.3
10.01	18.6	28.6	47.2		39.99	161.0	31.4	192.3
11	22.4	28.6	51.0		40.01	161.1	251.3	412.4
12	26.3	28.6	54.9		41	168.5	256.4	424.9
13	30.4	28.6	59.0		42	176.2	261.5	437.7
14	34.6	28.6	63.2		43	184.0	266.6	450.6
14.99	38.9	28.6	67.5		44	191.9	271.7	463.7
15.01	39.0	29.6	68.6		45	200.0	275.4	475.4
16	43.1	29.6	72.8		46	208.3	275.4	483.6
17	47.4	29.6	77.0		47	216.7	275.4	492.0
18	51.8	29.6	81.4		48	225.2	275.4	500.6
19	56.4	29.6	86.0		49	234.0	275.4	509.3
19.99	61.0	29.6	90.6		50	242.8	275.4	518.2
20.01	61.1	30.0	91.1		51	251.8	275.4	527.2
21	65.5	30.0	95.5		52	261.0	275.4	536.3
22	70.1	30.0	100.1		53	270.3	275.4	545.6
23	74.8	30.0	104.8		54	279.8	275.4	555.1
24	79.7	30.0	109.7		55	289.4	275.4	564.7
24.99	84.7	30.0	114.6		56	299.1	275.4	574.5
25.01	84.7	30.5	115.2		57	309.0	275.4	584.4
26	89.5	30.5	119.9		58	319.1	275.4	594.5
27	94.4	30.5	124.9		59	329.3	275.4	604.7
28	99.5	30.5	129.9		59.99	339.6	275.4	614.9
29	104.7	30.5	135.1		60.01	339.7	1042.6	1382.3

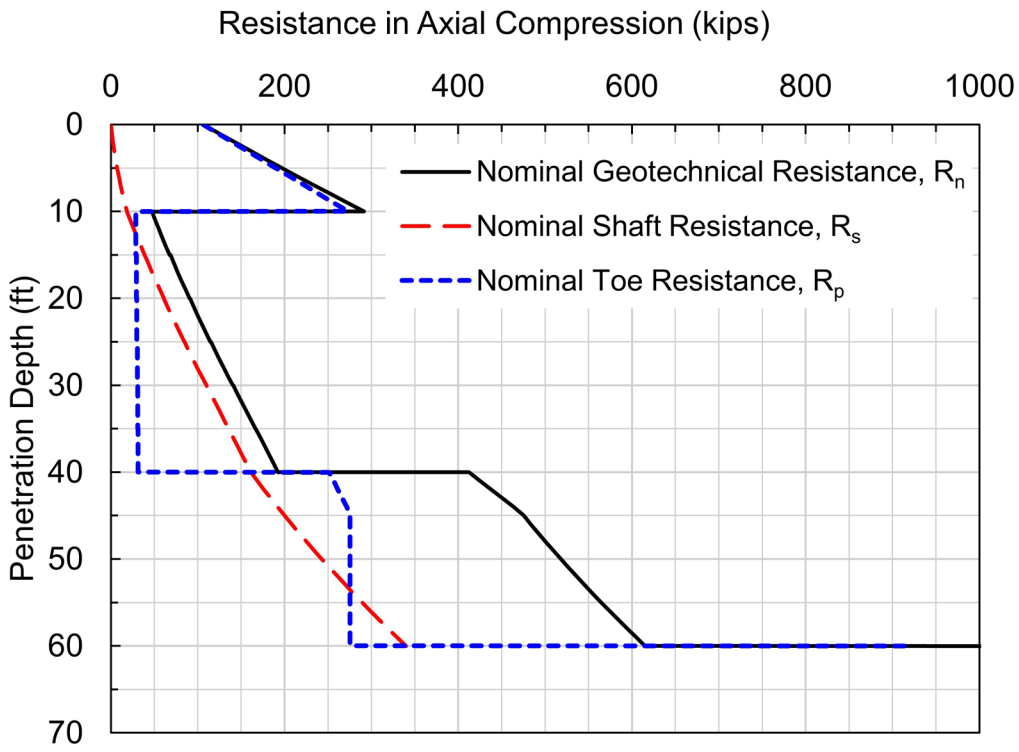

Figure D-40 Nominal geotechnical resistance in axial compression versus pile penetration depth for HP 12x74 at Pier 2 (pre scour).

D.22.1.1 Geotechnical Resistance in Axial Compression at the Design Flood

The nominal geotechnical resistance in axial compression at the design flood must also be evaluated. In the design flood, 5 feet of channel degradation scour is anticipated. The channel degradation scour results in a change in vertical effective stress from the removal of 5 feet of channel materials. The channel degradation scour occurs above the bottom of the pile cap. Hence the channel degradation scour results in no loss of nominal resistance other than that caused by the reduction in overburden stress.

In addition to the channel degradation scour, 10 feet of local scour occurs during the design flood. This 10 feet of local scour occurring below the channel degradation scour results in the loss of frictional resistance on the upper 5 feet of the pile in the design flood event. Hence, these two scour mechanisms require a more rigorous analysis of the nominal resistance beyond simple subtraction of the shaft resistance within the scour prism. Therefore, the DrivenPiles program was used to calculate the shaft, toe and nominal resistance as a function of depth for each of the five candidate H-piles in the design flood.

Figure D-41 presents plots of the nominal shaft resistance, R_s, the nominal toe resistance, R_p, and nominal resistance, R_n for the HP 12x74 pile section versus pile penetration depth. These results are also presented numerically in Table D-52. The depth indicated in both Figure D-41 and Table D-52 is referenced from the bottom of pile cap (EL 275 feet), which is 10 feet below the original ground surface elevation (EL 285 feet).

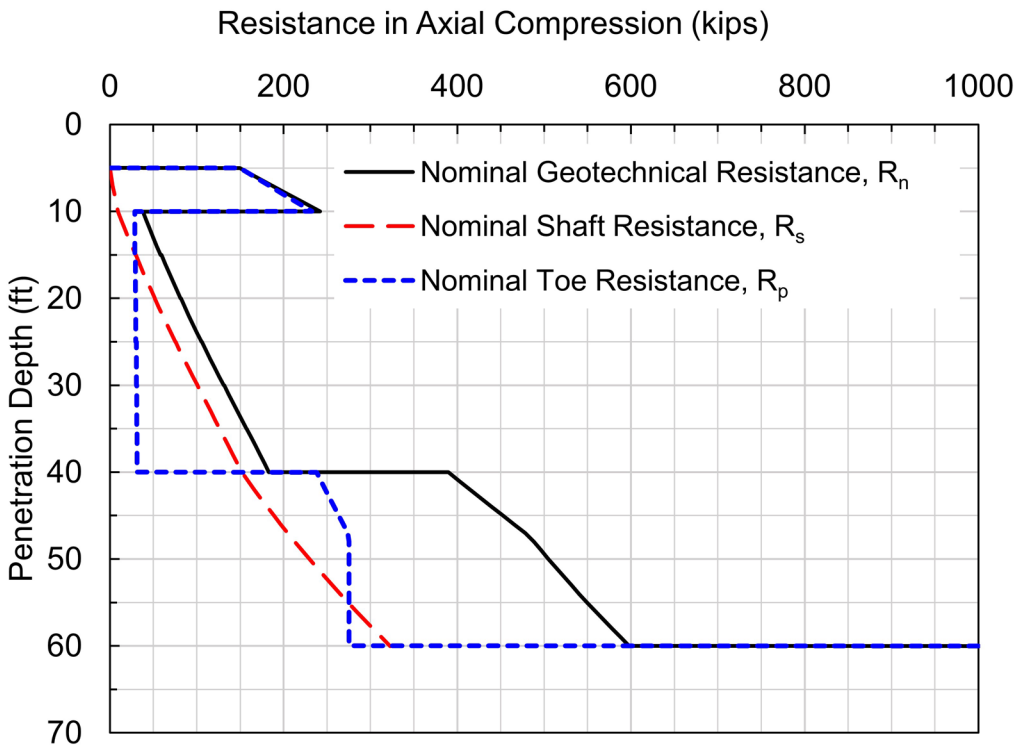

Figure D-41 Nominal geotechnical resistance in axial compression versus pile penetration depth for HP 12x74 at Pier 2 (design flood).

The nominal resistance versus depth at the design flood was calculated for all of the candidate pile sections in a similar manner. These results are presented in Figure D-42.

Table D-52 Nominal Shaft, Nominal Toe and Nominal Geotechnical Resistance for HP 12x74 at Pier 2 (design flood)

Depth (feet)	Nominal Shaft Resistance (kips)	Nominal Toe Resistance (kips)	Nominal Geotechnical Resistance (kips)		Depth (feet)	Nominal Shaft Resistance (kips)	Nominal Toe Resistance (kips)	Nominal Geotechnical Resistance (kips)
0.01	0.0	0.0	0.0		29.99	100.8	30.8	131.7
1	0.0	0.0	0.0		30.01	105.9	30.8	136.7
2	0.0	0.0	0.0		31	111.0	30.8	141.8
3	0.0	0.0	0.0		32	116.1	30.8	146.9
4	0.0	0.0	0.0		33	121.2	30.8	152.0
4.99	0.0	149.7	149.7		34	126.3	30.8	157.1
5.01	1.5	166.2	167.8		34.99	126.4	31.4	157.7
6	3.3	182.9	186.1		35.01	131.4	31.4	162.8
7	5.1	199.6	204.7		36	136.5	31.4	167.9
8	7.2	216.2	223.4		37	141.6	31.4	173.0
9	9.3	232.8	242.1		38	146.7	31.4	178.1
9.99	9.4	28.6	38.0		39	151.8	31.4	183.1
10.01	13.2	28.6	41.8		39.99	151.9	238.0	389.9
11	17.1	28.6	45.7		40.01	158.9	243.1	402.0
12	21.2	28.6	49.8		41	166.2	248.2	414.4
13	25.4	28.6	54.0		42	173.6	253.3	426.9
14	29.7	28.6	58.3		43	181.1	258.4	439.6
14.99	29.8	29.6	59.4		44	188.9	263.5	452.4
15.01	33.9	29.6	63.5		45	196.7	268.6	465.4
16	38.2	29.6	67.8		46	204.7	273.8	478.5
17	42.6	29.6	72.2		47	212.9	275.4	488.2
18	47.2	29.6	76.8		48	221.2	275.4	496.6
19	51.8	29.6	81.4		49	229.7	275.4	505.0
19.99	51.9	30.0	81.9		50	238.3	275.4	513.6
20.01	56.3	30.0	86.3		51	247.0	275.4	522.4
21	60.9	30.0	90.9		52	256.0	275.4	531.3
22	65.6	30.0	95.6		53	265.0	275.4	540.4
23	70.5	30.0	100.5		54	274.3	275.4	549.6
24	75.4	30.0	105.4		55	283.6	275.4	559.0
24.99	75.5	30.5	106.0		56	293.1	275.4	568.5
25.01	80.3	30.5	110.7		57	302.8	275.4	578.2
26	85.2	30.5	115.7		58	312.6	275.4	588.0
27	90.3	30.5	120.7		59	322.5	275.4	597.9
28	95.5	30.5	125.9		59.99	322.7	922.6	1245.3
29	100.7	30.5	131.2		60.01	327.7	1042.6	1370.3

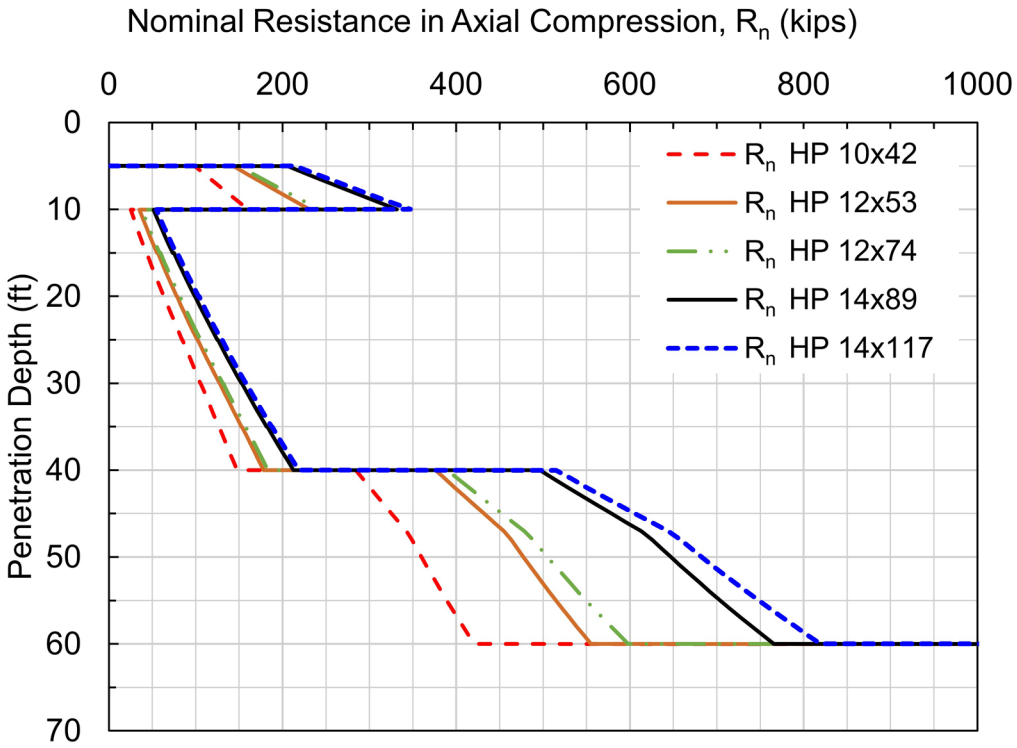

Figure D-42 Nominal geotechnical resistance in axial compression versus penetration depth for all candidate pile sections at Pier 2 (design flood).

Figure D-43 presents a design chart of the nominal and factored geotechnical resistance for the HP 12x74 pile section in axial compression during the design flood event. The design chart includes the nominal geotechnical resistance as well as the factored geotechnical resistance based on several resistance determination methods. The factored geotechnical resistance versus penetration depth is plotted for resistance determination by a static load test with dynamic testing of 2% of the piles (ϕ_{dyn}=0.80), by dynamic testing of at least two piles per site condition, but no less than 2% of the production piles, with signal matching (ϕ_{dyn}=0.65), and by wave equation analysis (ϕ_{dyn}=0.50). Also included is the factored geotechnical resistance based on the static analysis method used in this design example. For this, (ϕ_{stat}=0.45) was applied to the cohesionless soils as a result of using the Nordlund method while (ϕ_{stat}=0.35) applied to the cohesives soils as a result of using the alpha method. For a single pile section (HP 12x74), this figure illustrates the effects the various resistance determination methods have on the pile length required for a given factored resistance, the factored resistance available from a given pile section, and the potential impact of these factors on the number of piles needed to resist axial compression loads.

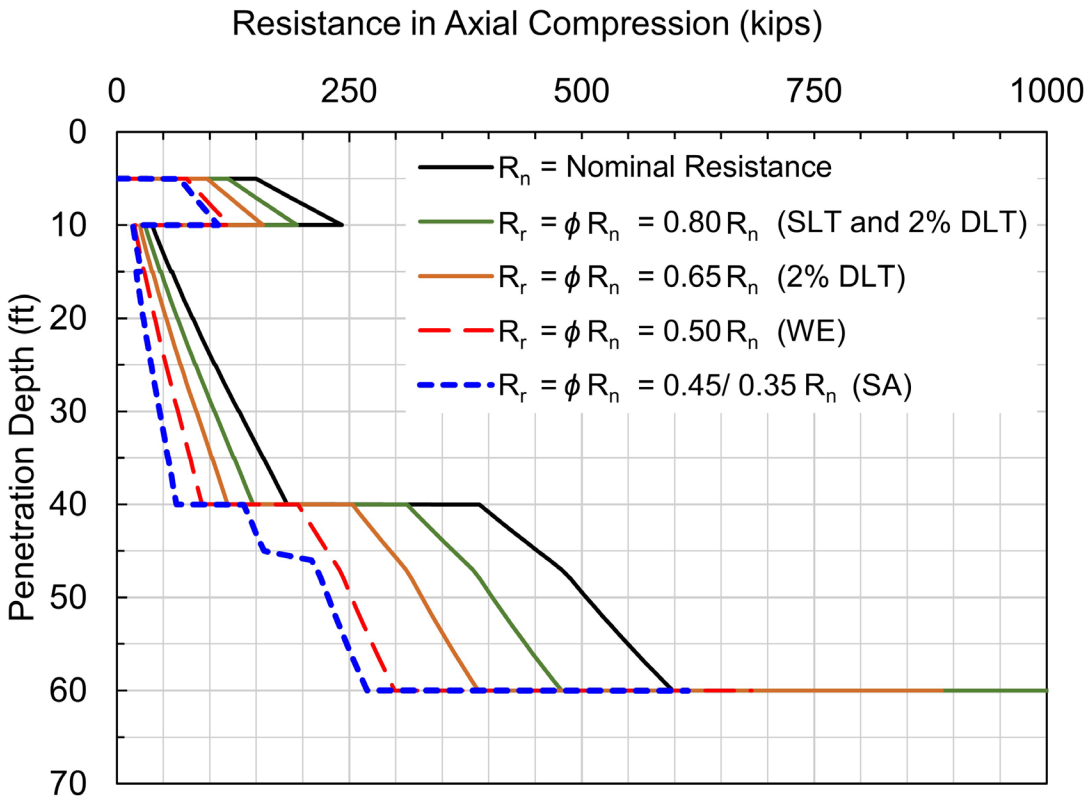

Figure D-43 Design chart of nominal and factored geotechnical resistance in axial compression versus pile penetration depth for HP 12x74 at the Pier 2 (design flood).

The factored geotechnical resistance in axial compression for all candidate pile sections is presented in Figures D-44 through D-47 during the design flood event. The presented factored geotechnical resistances are based upon on the field determination method or static analysis method used. Accordingly, these figures can be used to assess the effects of the various determination methods on pile length, pile section selection, and the required number of piles to resist axial compression loads.

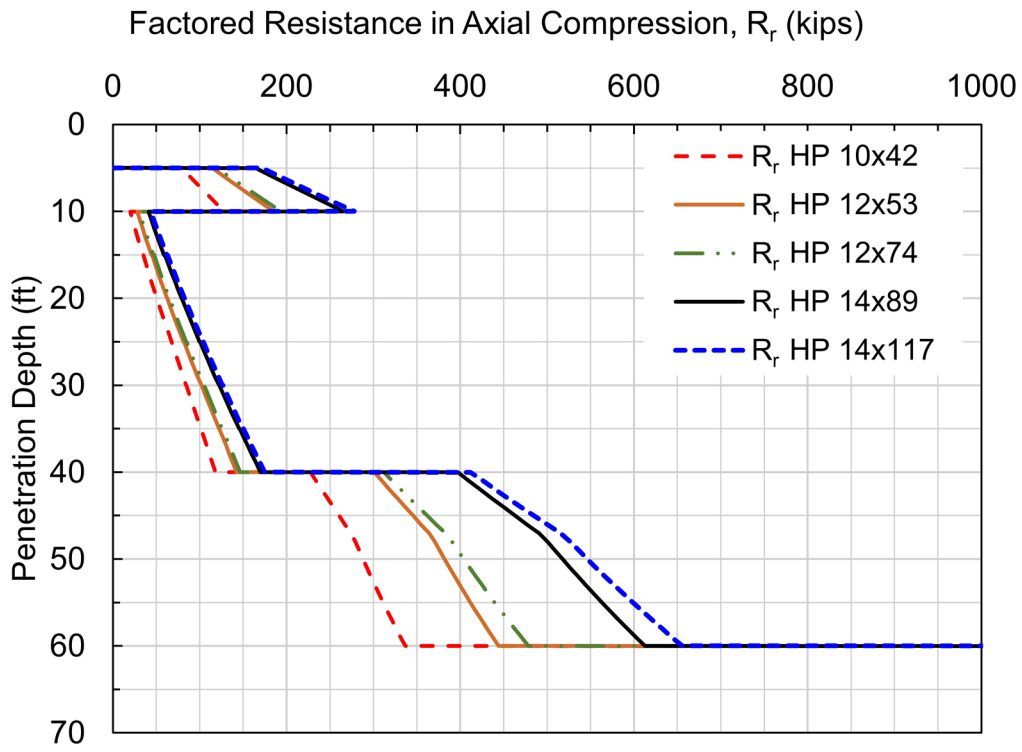

Figure D-44 Factored geotechnical resistance, R_r, in axial compression based on field determination by static load test and dynamic testing 2% of the piles, ϕ_{dyn}=0.80.

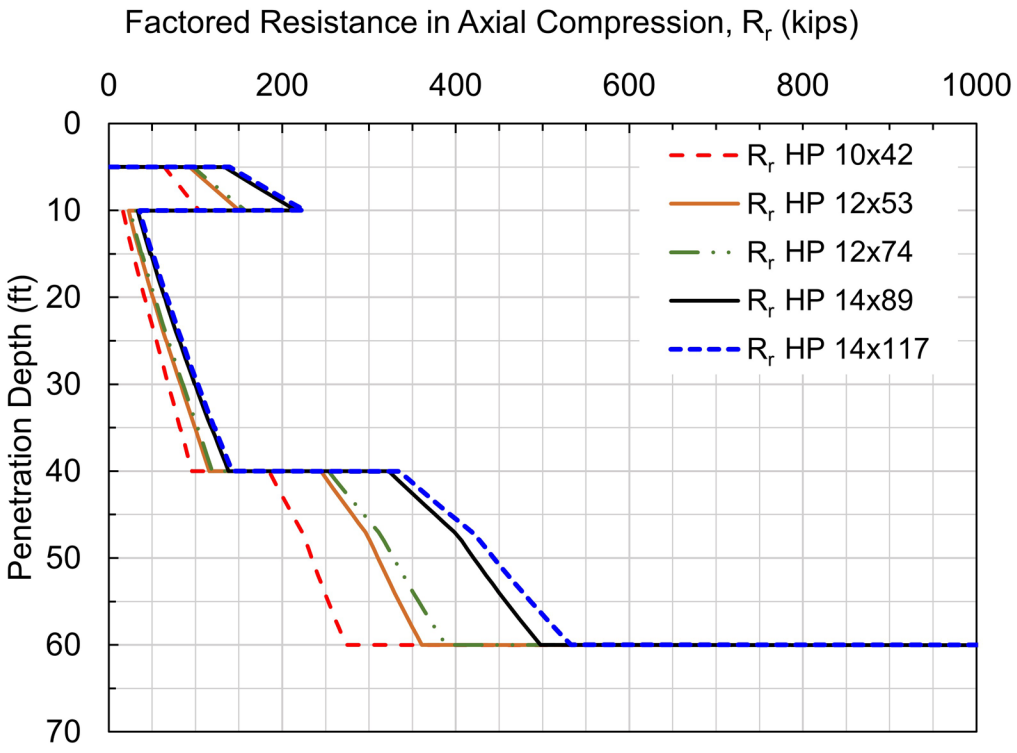

Figure D-45 Factored geotechnical resistance, R_r, in axial compression based on field determination by dynamic testing 2% of the piles, ϕ_{dyn}=0.65.

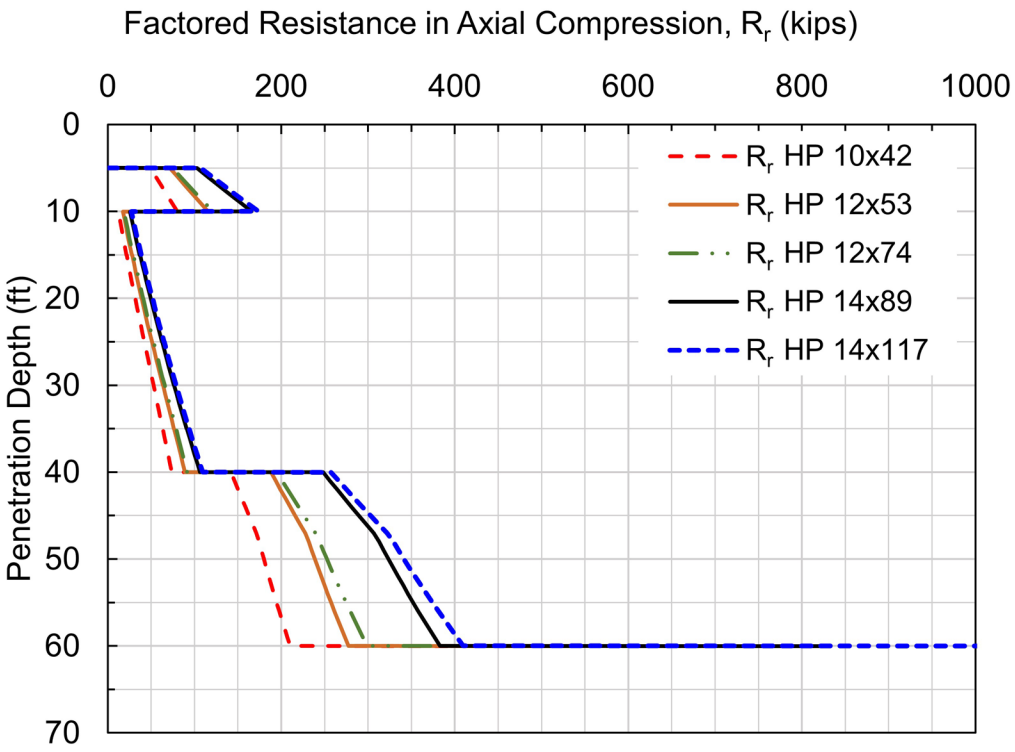

Figure D-46 Factored geotechnical resistance, R_r, in axial compression based on field determination by wave equation analysis, ϕ_{dyn}=0.50.

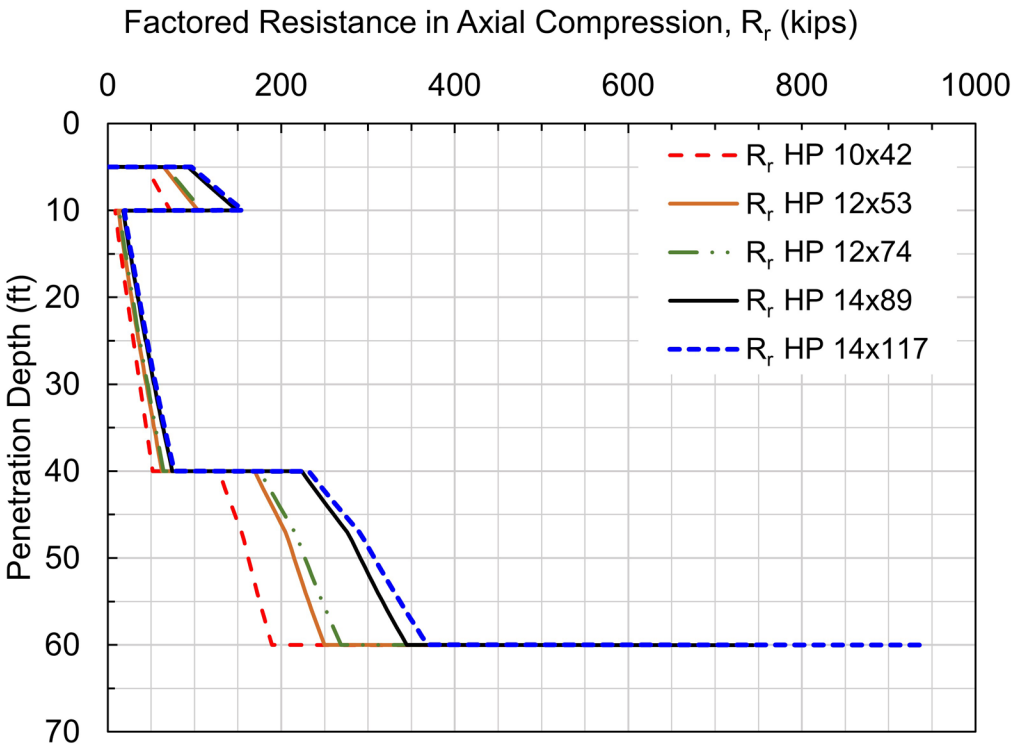

Figure D-47 Factored geotechnical resistance, R_r, in axial compression based on determination using Nordlund Method static analysis, ϕ_{stat}=0.45.

D.22.1.2 Geotechnical Resistance in Axial Compression at the Check Flood

The nominal geotechnical resistance in axial compression at the Extreme Event check flood must also be evaluated. In the check flood, 5 feet of channel degradation scour is anticipated. The channel degradation scour results in a change in vertical effective stress from the removal of 5 feet of channel materials. The channel degradation scour occurs above the bottom of the pile cap. Hence the channel degradation scour results in no loss of nominal resistance other than that caused by the reduction in overburden stress.

In addition to the channel degradation scour, 12 feet of local scour occurs during the design flood. This 12 feet of local scour occurring below the channel degradation scour results in the loss of frictional resistance on the upper 7 feet of the pile in the Extreme Event check flood. Hence, these two scour mechanisms require a more rigorous analysis of the nominal resistance beyond simple subtraction of the shaft resistance within the scour prism. The DrivenPiles program was once again used to calculate the shaft, toe and nominal resistance as a function of depth for each of the five candidate H-piles in the check flood.

Table D-53 presents a summary of the estimated nominal geotechnical resistance considering scour at the check flood for the HP 12x74 pile section. These results are also presented graphically in Figure D-48. The depth indicated in both Table D-53 and Figure D-48 is referenced from the bottom of footing (EL 275 feet), which is 10 feet below the original ground surface elevation (EL 285 feet).

The nominal shaft, nominal toe, and nominal geotechnical resistance considering scour at the check flood were calculated for all of the candidate pile sections in a similar manner. These results are presented in Figure D-49.

Table D-53 Nominal Shaft, Nominal Toe and Nominal Geotechnical Resistance for HP 12x74 at Pier 2 (check flood)

Depth (feet)	Nominal Shaft Resistance (kips)	Nominal Toe Resistance (kips)	Nominal Geotechnical Resistance (kips)		Depth (feet)	Nominal Shaft Resistance (kips)	Nominal Toe Resistance (kips)	Nominal Geotechnical Resistance (kips)
0.01	0.0	0.0	0.0		29.99	97.5	30.5	127.9
1	0.0	0.0	0.0		30.01	97.6	30.8	128.4
2	0.0	0.0	0.0		31	102.6	30.8	133.5
3	0.0	0.0	0.0		32	107.7	30.8	138.6
4	0.0	0.0	0.0		33	112.8	30.8	143.7
5	0.0	0.0	0.0		34	118.0	30.8	148.8
6	0.0	0.0	0.0		34.99	123.0	30.8	153.8
6.99	0.0	0.0	0.0		35.01	123.1	31.4	154.5
7.01	0.0	183.1	183.1		36	128.2	31.4	159.5
8	1.9	199.6	201.4		37	133.3	31.4	164.6
9	3.9	216.2	220.2		38	138.4	31.4	169.7
9.99	6.1	232.8	238.8		39	143.5	31.4	174.8
10.01	6.1	28.6	34.7		39.99	148.5	31.4	179.9
11	9.9	28.6	38.5		40.01	148.6	238.0	386.6
12	13.9	28.6	42.5		41	155.7	243.1	398.7
13	18.0	28.6	46.6		42	162.9	248.2	411.1
14	22.2	28.6	50.8		43	170.3	253.3	423.6
14.99	26.5	28.6	55.1		44	177.9	258.4	436.3
15.01	26.6	29.6	56.2		45	185.6	263.5	449.1
16	30.7	29.6	60.3		46	193.5	268.6	462.1
17	35.0	29.6	64.6		47	201.5	273.8	475.2
18	39.4	29.6	69.0		48	209.6	275.4	485.0
19	43.9	29.6	73.5		49	217.9	275.4	493.3
19.99	48.5	29.6	78.1		50	226.4	275.4	501.8
20.01	48.6	30.0	78.6		51	235.0	275.4	510.4
21	53.0	30.0	83.0		52	243.8	275.4	519.1
22	57.6	30.0	87.6		53	252.7	275.4	528.1
23	62.4	30.0	92.4		54	261.8	275.4	537.1
24	67.2	30.0	97.2		55	271.0	275.4	546.4
24.99	72.2	30.0	102.2		56	280.4	275.4	555.7
25.01	72.3	30.5	102.7		57	289.9	275.4	565.2
26	77.0	30.5	107.5		58	299.6	275.4	574.9
27	82.0	30.5	112.4		59	309.4	275.4	584.7
28	87.0	30.5	117.5		59.99	319.3	275.4	594.6
29	92.2	30.5	122.7		60.01	319.4	1042.6	1362.0

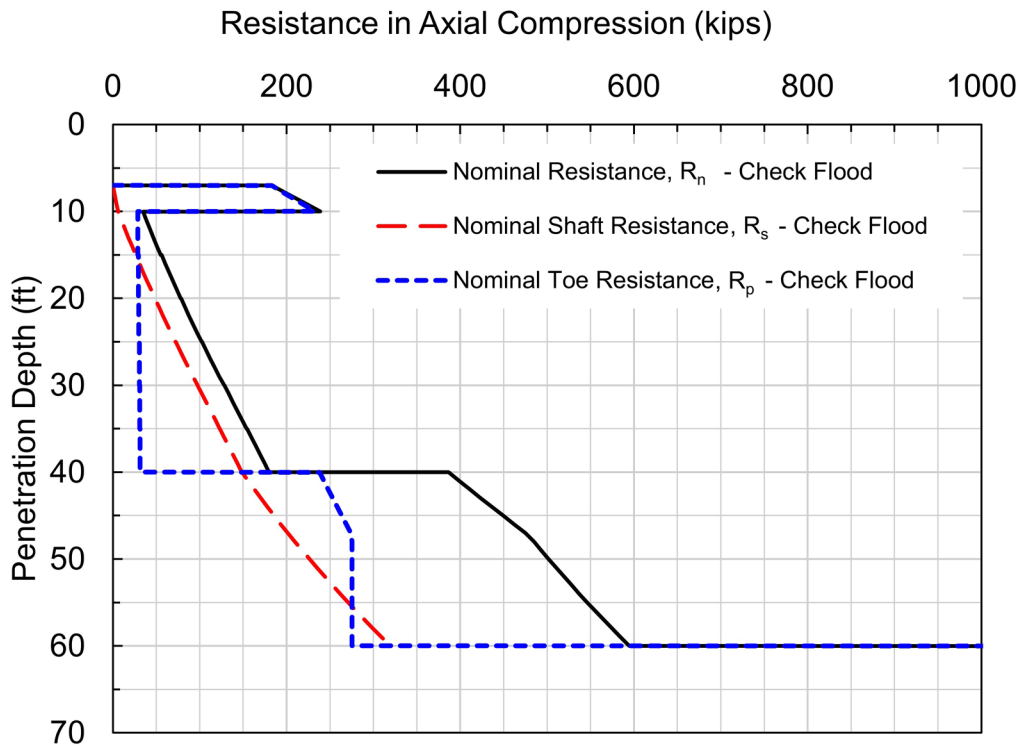

Figure D-48 Nominal geotechnical resistance in axial compression versus pile penetration depth for HP 12x74 at Pier 2 (check flood).

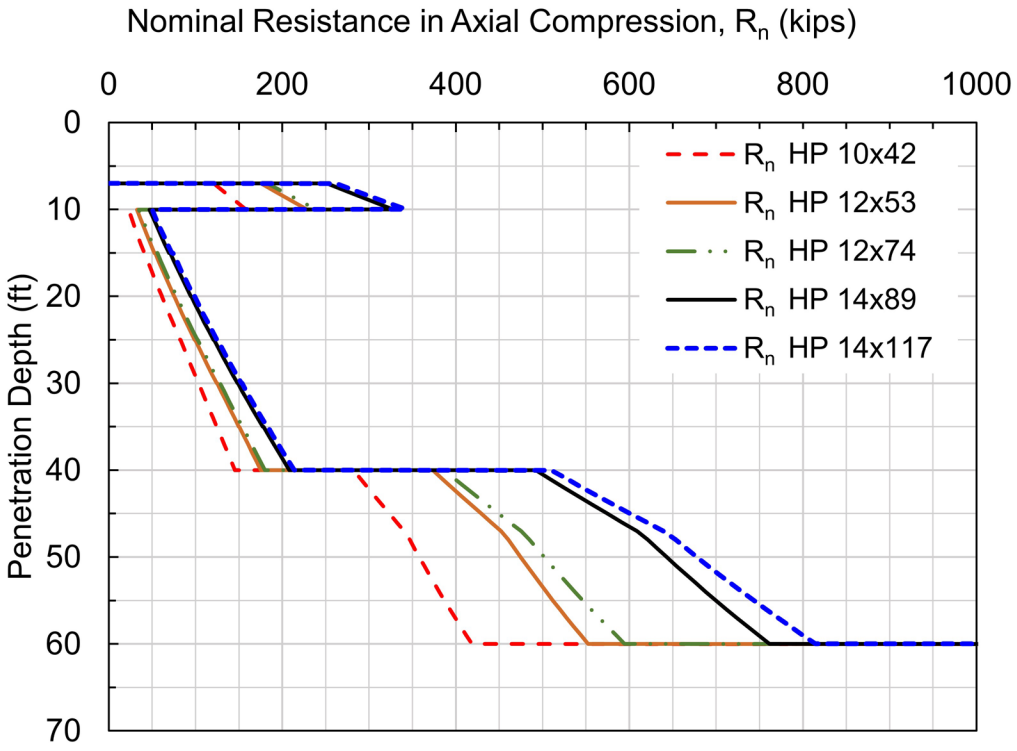

Figure D-49 Nominal geotechnical resistance in axial compression versus penetration depth for all candidate pile sections at Pier 2 (check flood).

Figure D-50 presents a design chart of the nominal and factored geotechnical resistance in axial compression versus depth during the check flood for the HP 12x74 candidate H-pile section. The design chart includes the nominal geotechnical resistance as well as the factored geotechnical resistance based on several resistance determination methods. The factored geotechnical resistance versus penetration depth is plotted for resistance determination by a static load test with dynamic testing of 2% of the piles (ϕ_{dyn}=0.80), by dynamic testing of at least two piles per site condition, but no less than 2% of the production piles, with signal matching (ϕ_{dyn}=0.65), and by wave equation analysis (ϕ_{dyn}=0.50). Also included is the factored geotechnical resistance based on the static analysis method used in this design example. For this, (ϕ_{stat}=0.45) was applied to the cohesionless soils as a result of using the Nordlund method while (ϕ_{stat}=0.35) was applied to the cohesive soils as a result of using the alpha method. For a single pile section (HP 12x74), this figure illustrates the effects the various resistance determination methods have on the pile length required for a given factored resistance, the factored resistance available from a given pile section, and the potential impact of these factors on the number of piles needed to resist axial compression loads.

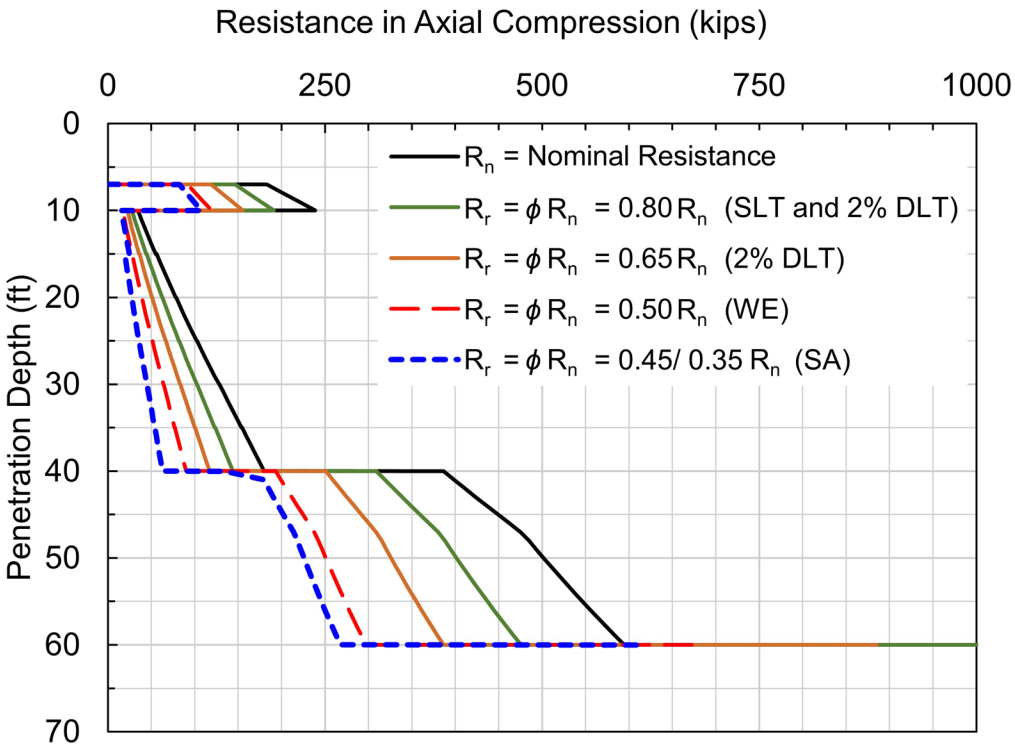

Figure D-50 Design chart of nominal and factored geotechnical resistance in axial compression versus pile penetration depth for HP 12x74 at the Pier 2 (check flood).

The factored geotechnical resistance in axial compression at the check flood for all candidate pile sections is presented in Figures D-51 through D-54. The presented factored geotechnical resistances are based upon on the field determination method or static analysis method used. Accordingly, these figures will be used to assess the effects of the various determination methods on pile length, pile section selection, and the required number of piles to resist axial compression loads.

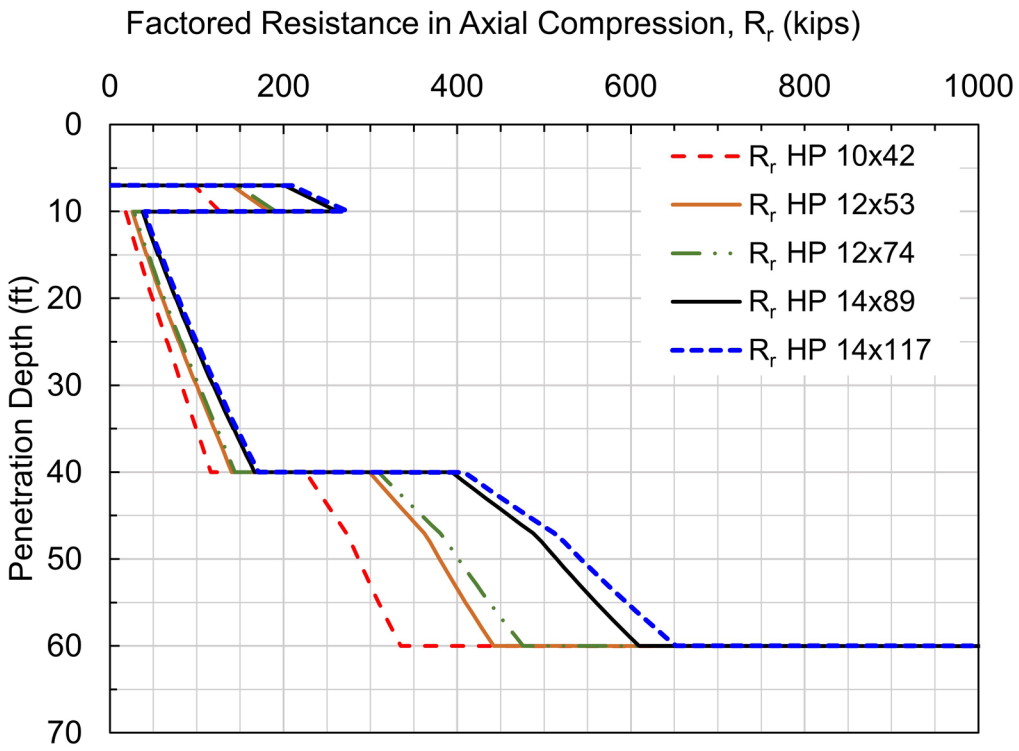

Figure D-51 Factored geotechnical resistance, R_r, in axial compression based on field determination by static load test and dynamic testing 2% of the piles, ϕ_{dyn}=0.80.

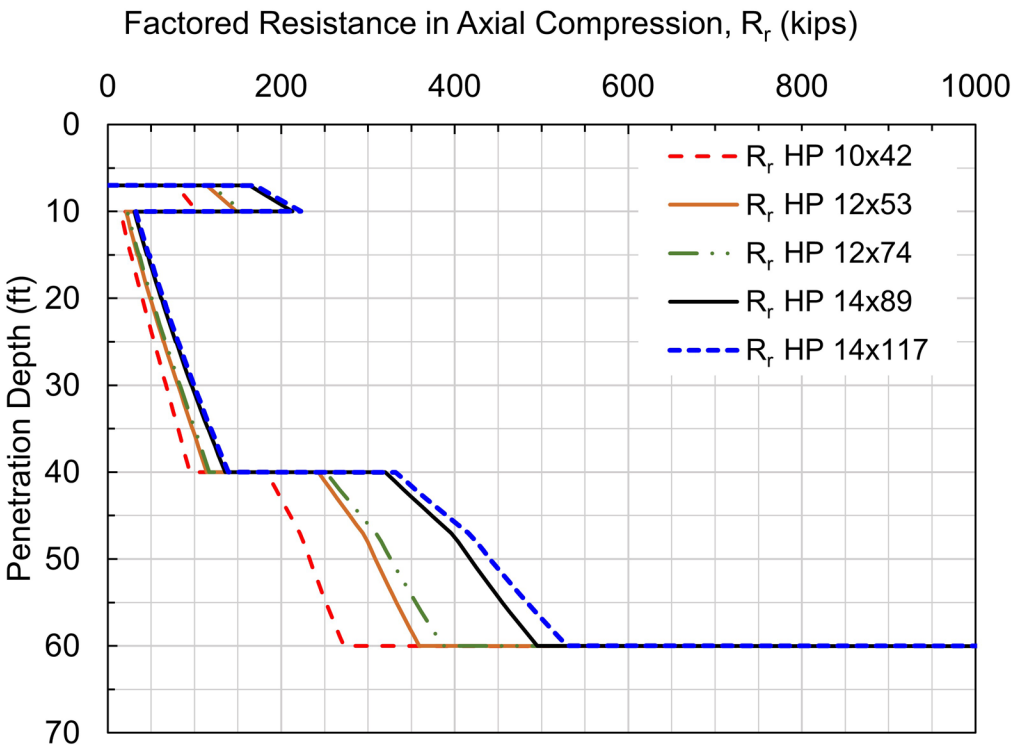

Figure D-52 Factored geotechnical resistance, R_r, in axial compression based on field determination by dynamic testing 2% of the piles, ϕ_{dyn}=0.65.

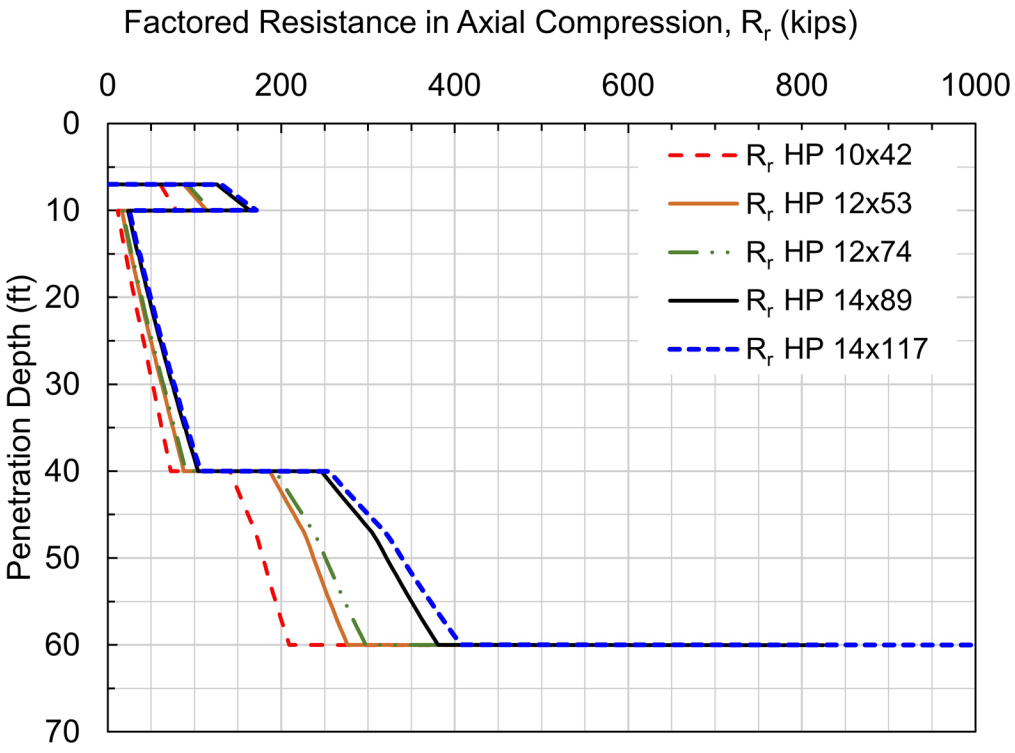

Figure D-53 Factored geotechnical resistance, R_r, in axial compression based on field determination by wave equation analysis, ϕ_{dyn}=0.5.

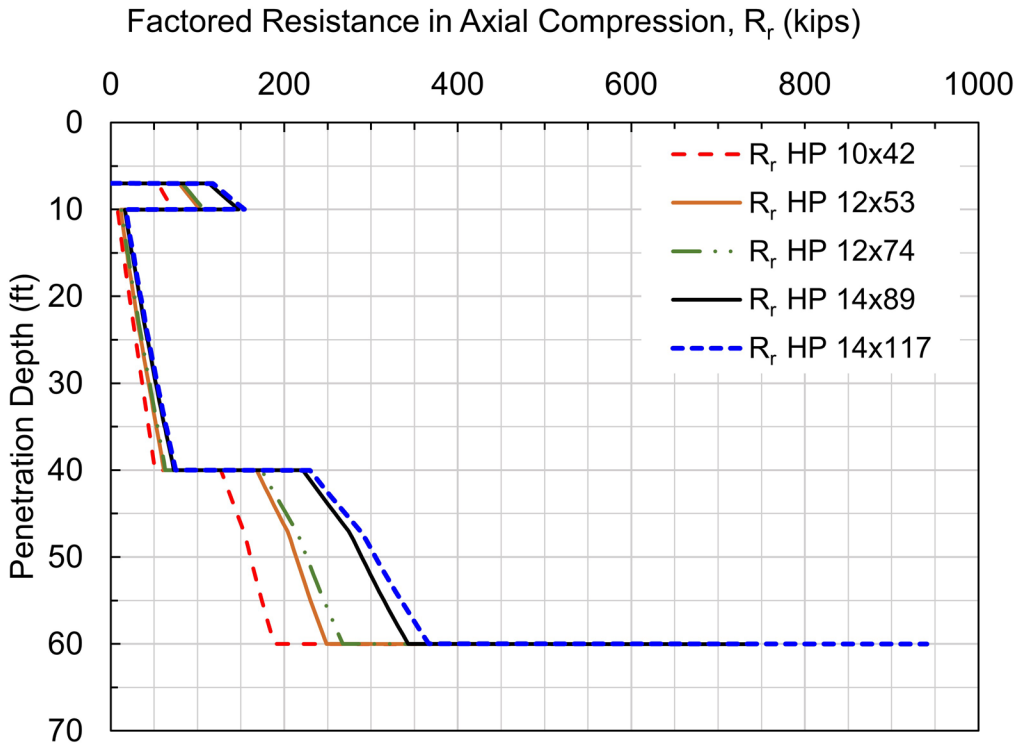

Figure D-54 Factored geotechnical resistance, R_r, in axial compression based on determination using static analysis, ϕ_{stat}=0.45 or ϕ_{stat}=0.35.

D.22.2 Geotechnical Resistance in Axial Tension

The nominal and factored geotechnical resistances in axial tension (uplift) are now calculated. The calculations were performed using the DrivenPiles program which utilized the Nordlund method in cohesionless soil layers and the alpha method in cohesive soil layers. For geotechnical resistance in axial tension, only the shaft resistance is considered. Therefore, the shaft resistance results calculated for the geotechnical resistance in axial compression can be re-used for axial tension. These tabular outputs of the nominal shaft resistance versus depth were previously presented in Table D-52 for the design flood and Table D-53 for the check flood.

D.22.2.1 Geotechnical Resistance in Axial Tension at the Design Flood

The nominal geotechnical resistance in axial tension at the design flood must be evaluated. In the design flood, 5 feet of channel degradation scour is anticipated. The channel degradation scour results in a change in vertical effective stress from the removal of 5 feet of channel materials. The channel degradation scour occurs above the bottom of the pile cap. Hence the channel degradation scour results in no loss of nominal resistance other than that caused by the reduction in overburden stress.

In addition to the channel degradation scour, 10 feet of local scour occurs during the design flood. This 10 feet of local scour occurring below the channel degradation scour results in the loss of frictional resistance on the upper 5 feet of the pile in the design flood event. Hence, these two scour mechanisms require a more rigorous analysis of the nominal resistance beyond simple subtraction of the shaft resistance within the scour prism.

The nominal geotechnical resistance in axial tension at the design flood (and associated factored geotechnical resistance based upon resistance determination method) will therefore be used to evaluate axial tension at the Strength limit state.

Figure D-55 presents plots of the nominal shaft resistance versus penetration depth for all the candidate pile sections during the design flood. As outlined in Section 7.2.3.2.1, the factored uplift resistance for a single pile is the shaft resistance multiplied by the appropriate resistance determination resistance factor, ϕ_{up}. Figure D-56 presents a design chart of the nominal and factored geotechnical resistance in axial tension for the HP 12x74 H-pile section. A resistance factor of 0.60 is used when the uplift resistance is determined by a static load test and 0.50 is used when determined by a dynamic test with signal matching. If the axial tension resistance is evaluated using static analysis methods, a resistance factor of 0.35 is applied to the nominal shaft resistance determined by the Nordlund static analysis method in cohesionless soil layers, and a resistance factor of 0.25 is applied to the nominal shaft resistance determined by the alpha static analysis method in cohesive soil layers.

For a single pile section (HP 12x74), Figure D-56 illustrates the effects the various resistance determination methods have on the pile length required for a given factored resistance, the factored resistance available from a given pile section, and the potential impact of these factors on the number of piles needed to resist axial tension loads.

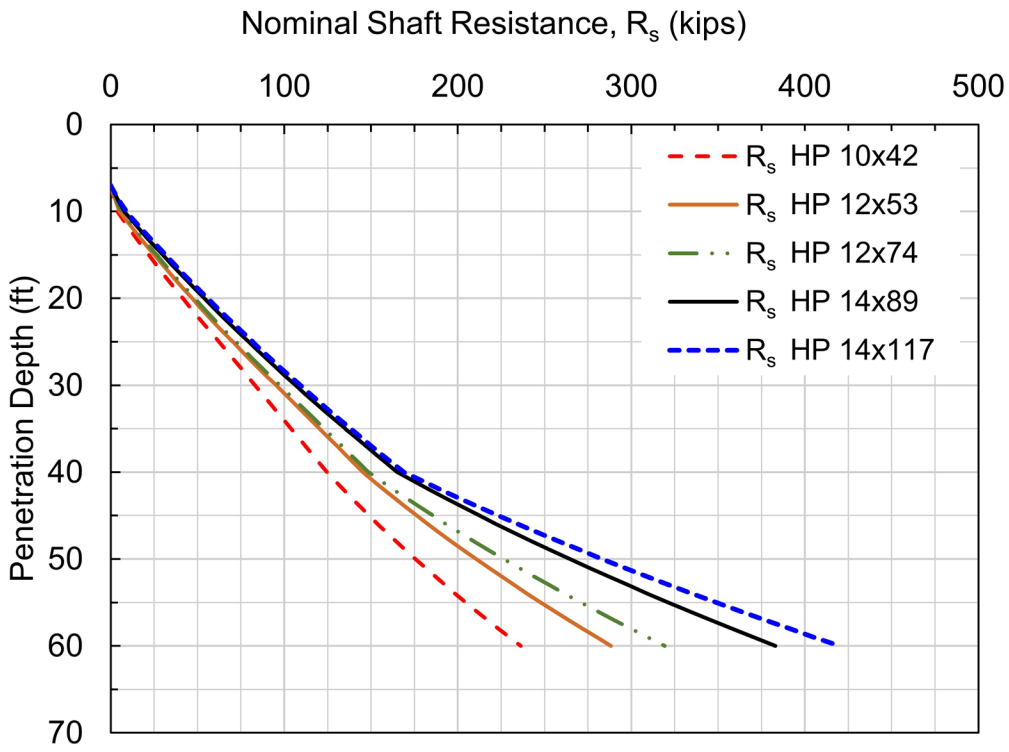

Figure D-55 Nominal shaft resistance versus pile penetration depth for all candidate pile sections at Pier 2 (design flood).

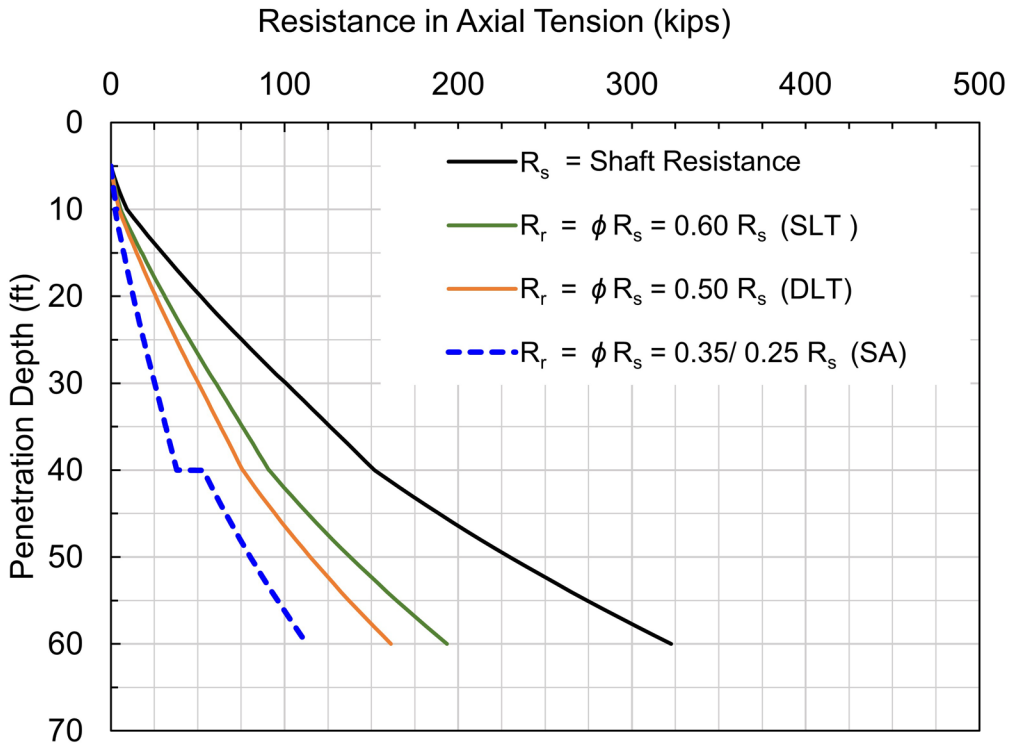

Figure D-56 Design chart of nominal and factored geotechnical resistance in axial tension versus pile penetration depth for HP 12x74 at the Pier 2 (design flood).

Figures D-57 to D-59 present the factored geotechnical resistance in axial tension versus penetration depth for all candidate pile sections at the design flood based on the resistance determination method. For all the candidate pile sections, these figures illustrate the effects the various resistance determination methods have on the pile length required for a given factored resistance, the factored resistance available from a given pile section, and the potential impact of these factors on the number of piles needed to resist axial tension loads.

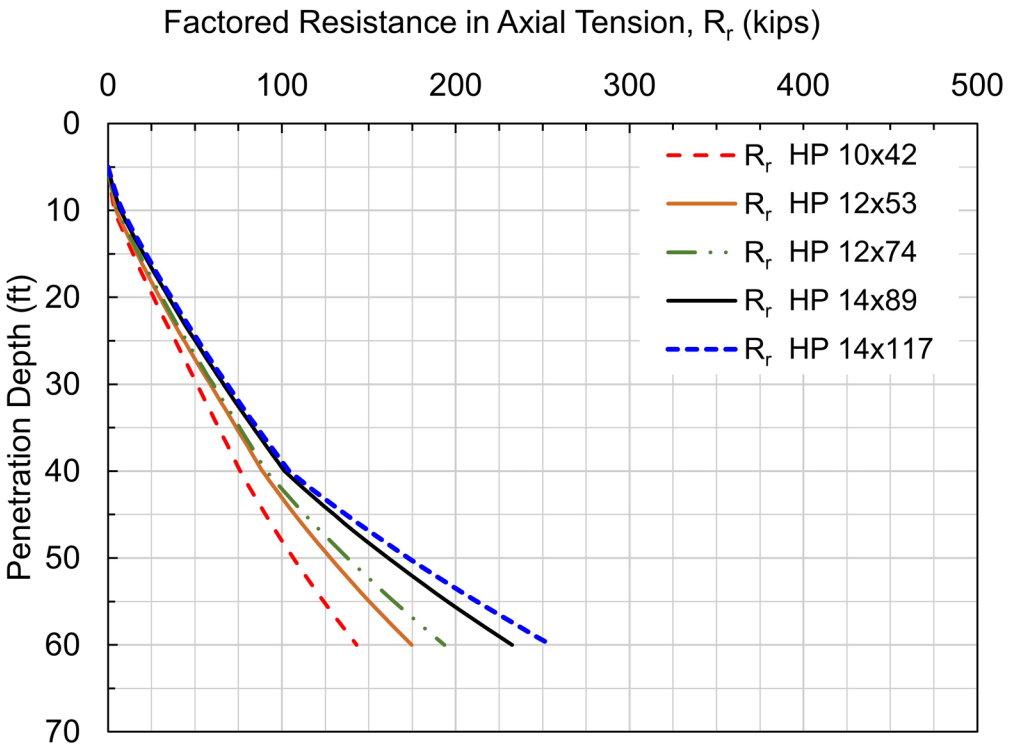

Figure D-57 Factored geotechnical resistance, R_r, in axial tension based on field determination by static load test, ϕ_{dyn}=0.60 (design flood).

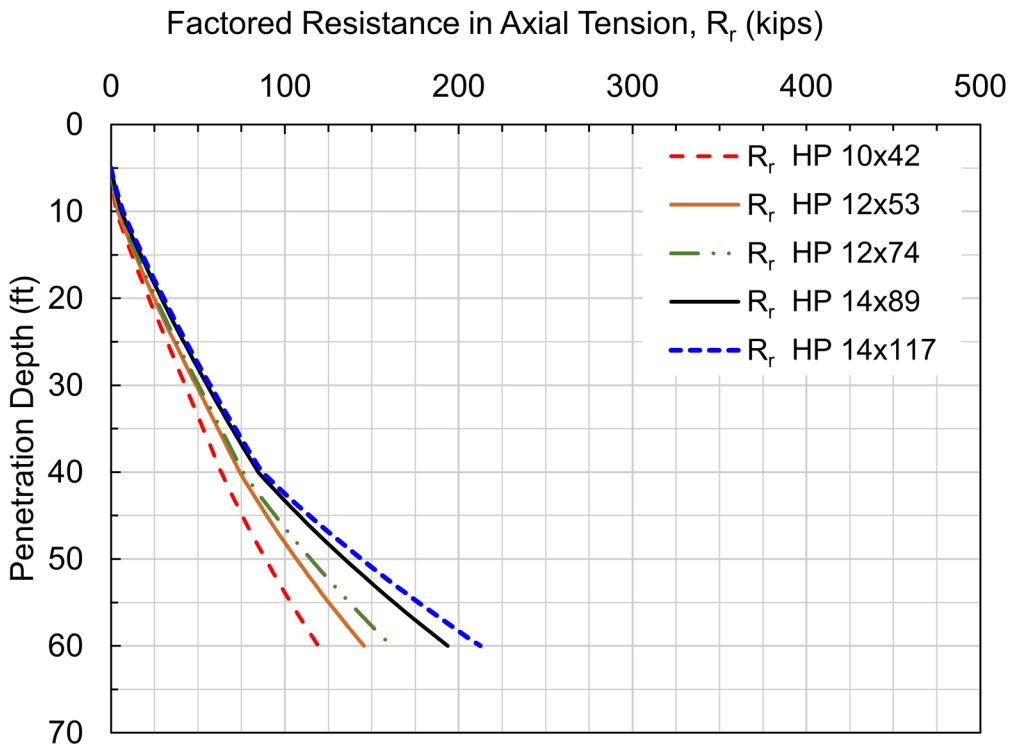

Figure D-58 Factored geotechnical resistance, R_r, in axial tension based on field determination by dynamic testing with signal matching, ϕ_{dyn}=0.50 (design flood).

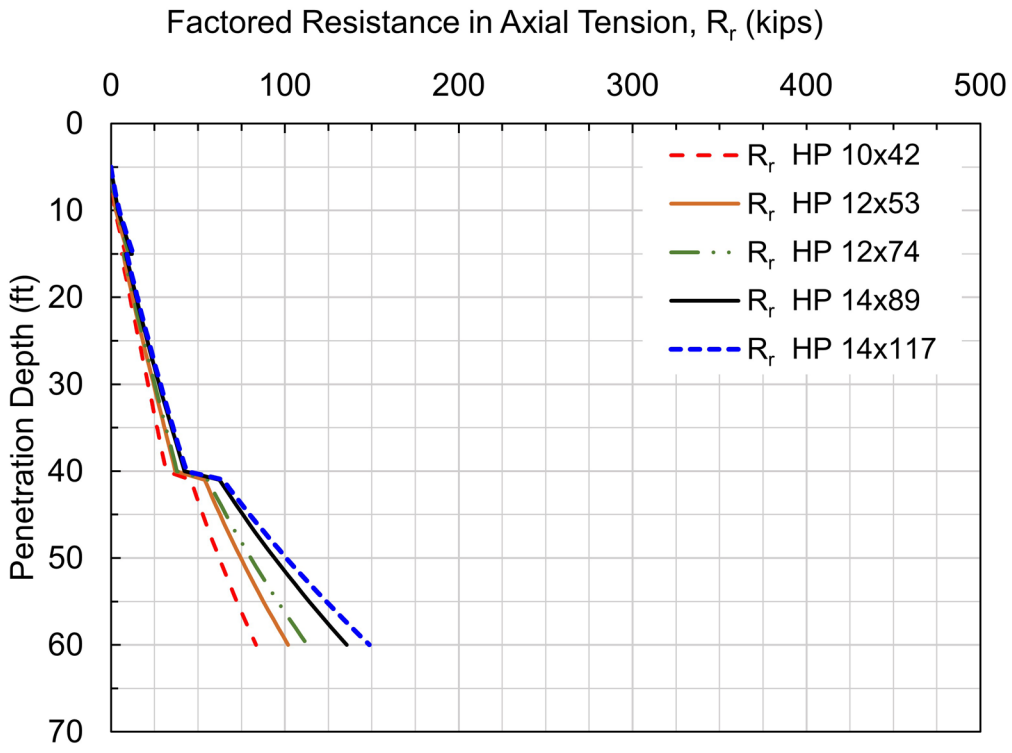

Figure D-59 Factored geotechnical resistance, R_r, in axial tension based on determination using static analysis, ϕ_{stat}=0.35 or ϕ_{stat}=0.25 (design flood).

D.22.2.2 Geotechnical Resistance in Axial Tension at the Check Flood

The nominal geotechnical resistance in axial tension at the Extreme Event check flood must also be evaluated. In the check flood, 5 feet of channel degradation scour is anticipated. The channel degradation scour results in a change in vertical effective stress from the removal of 5 feet of channel materials. The channel degradation scour occurs above the bottom of the pile cap. Hence the channel degradation scour results in no loss of nominal resistance other than that caused by the reduction in overburden stress.

In addition to the channel degradation scour, 12 feet of local scour occurs during the check flood. This 12 feet of local scour occurring below the channel degradation scour results in the loss of frictional resistance on the upper 7 feet of the pile in the check flood Extreme Event. Hence, these two scour mechanisms require a more rigorous analysis of the nominal resistance beyond simple subtraction of the shaft resistance within the scour prism.

The nominal geotechnical resistance in axial tension at the check flood (and associated factored geotechnical resistance based upon resistance determination method) will therefore be used to evaluate axial tension at the Extreme Event limit state.

Figure D-60 presents the nominal shaft resistance versus penetration depth for all the candidate pile sections. As outlined in Section 7.2.3.2.1 of Chapter 7, the factored uplift resistance for a single pile is the shaft resistance multiplied by the appropriate field determination resistance factor, ϕ_{up}. Figure D-61 presents a design chart of the nominal shaft resistance, R_s, and the factored geotechnical resistance, R_r, in axial tension versus pile penetration depth for the HP 12x74 H-pile section. A resistance factor of 0.60 is used when the uplift resistance is determined by a static load test, 0.50 when determined by a dynamic test with signal matching, 0.35 when determined by the Nordlund static analysis method and 0.25 when determined by the alpha static analysis method.

For a single pile section (HP 12x74), this figure illustrates the effects the various resistance determination methods have on the pile length required for a given factored resistance, the factored resistance available from a given pile section, and the potential impact of these factors on the number of piles needed to resist axial tension loads.

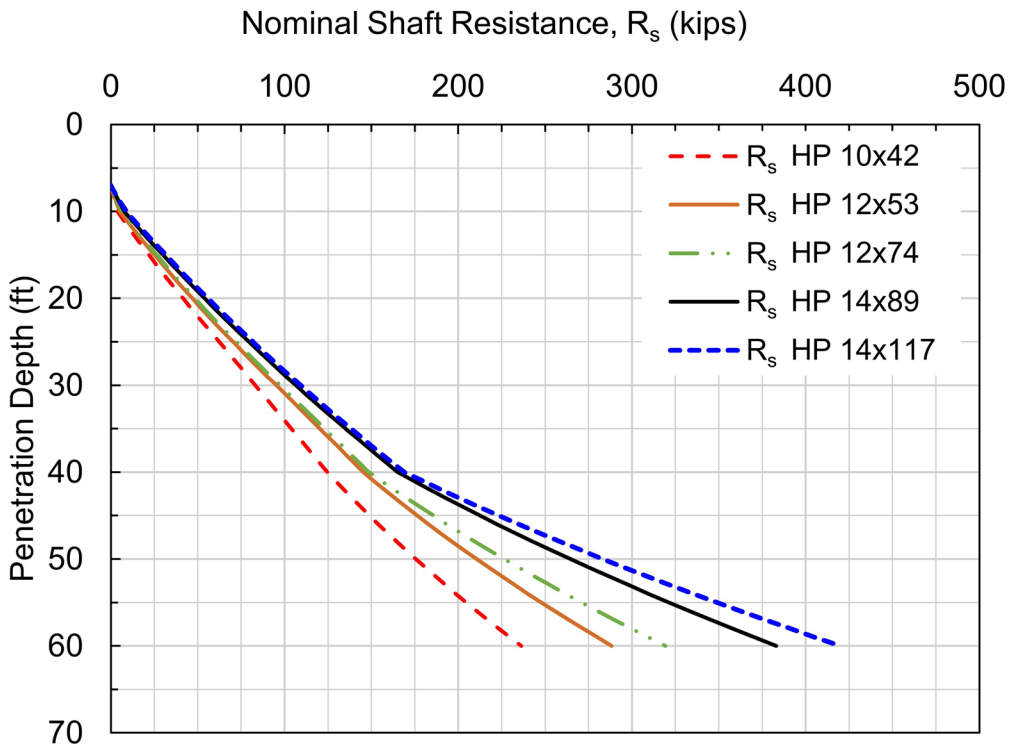

Figure D-60 Nominal shaft resistance versus pile penetration depth for all candidate pile sections at Pier 2 during Extreme Event (check flood).

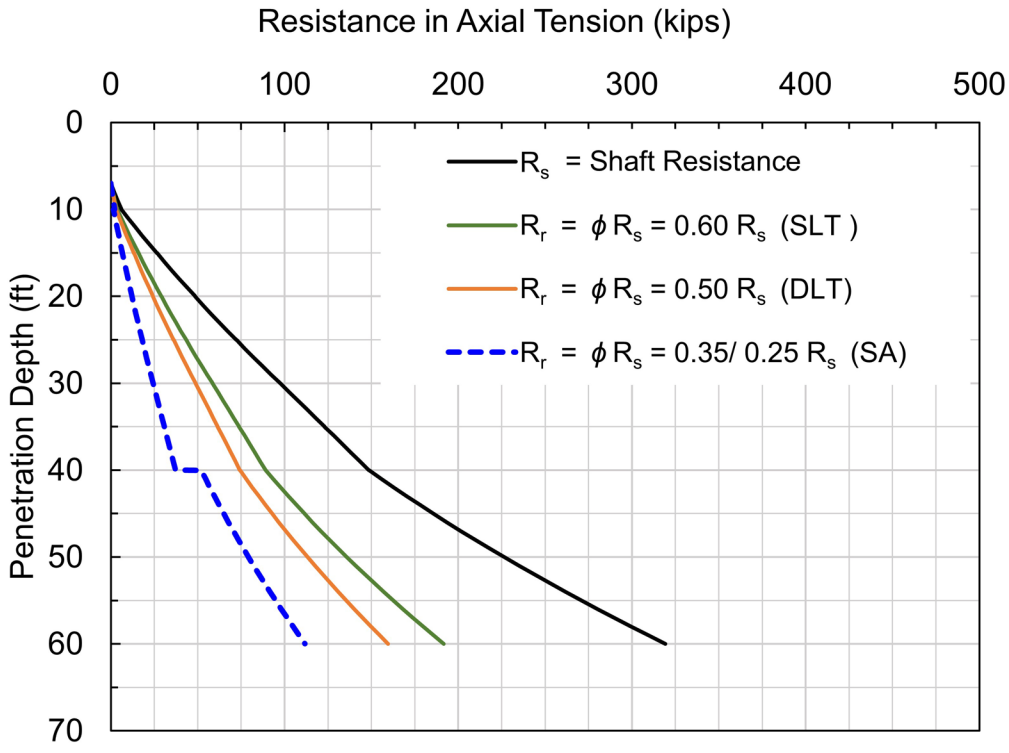

Figure D-61 Design chart of nominal and factored geotechnical resistance in axial tension versus depth for HP 12x74 at the Pier 2 during Extreme Event (check flood).

Figures D-62 to D-64 present the factored geotechnical resistance in axial tension versus penetration depth based on the field determination method for each of the candidate pile sections. For all the candidate pile sections, these figures illustrate the effects the various resistance determination methods have on the pile length required for a given factored resistance, the factored resistance available from a given pile section, and the potential impact of these factors on the number of piles needed to resist axial tension loads.

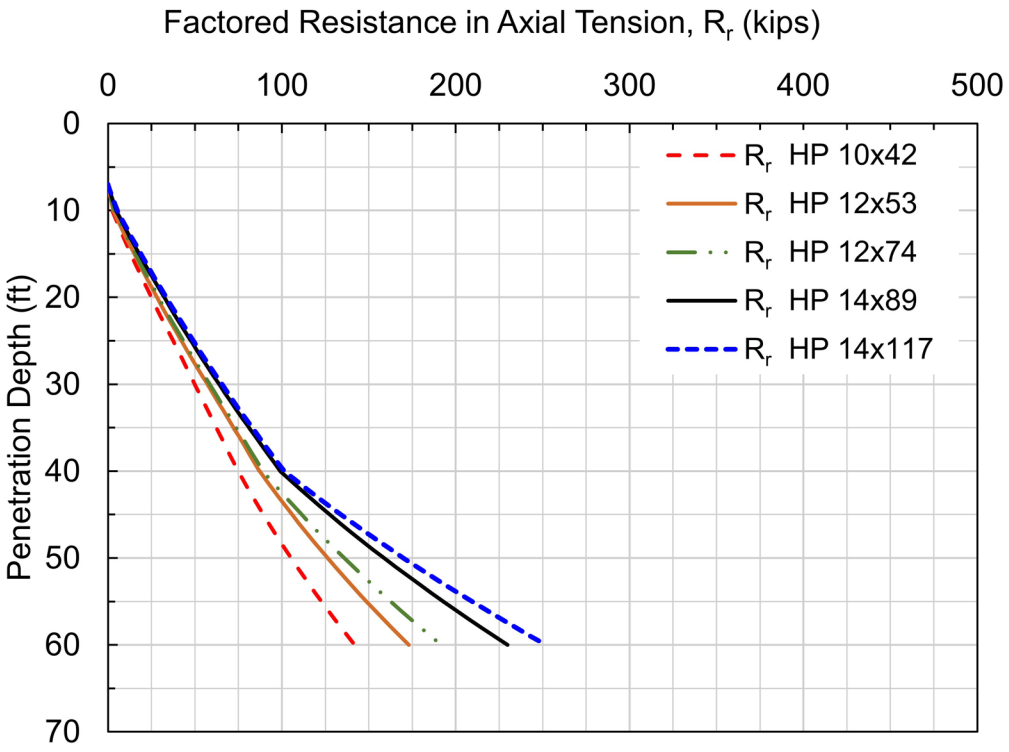

Figure D-62 Factored geotechnical resistance, R_r, in axial tension based on field determination by static load test, ϕ_{dyn}=0.60.

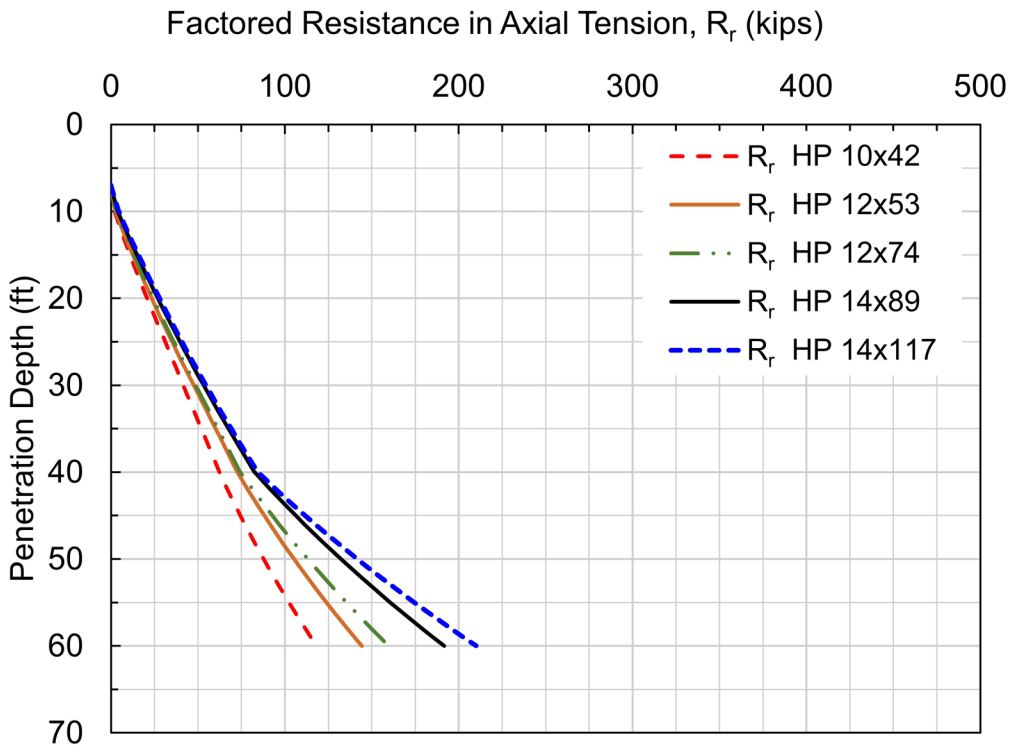

Figure D-63 Factored geotechnical resistance, R_r, in axial tension based on field determination by dynamic testing with signal matching, ϕ_{dyn}=0.50.

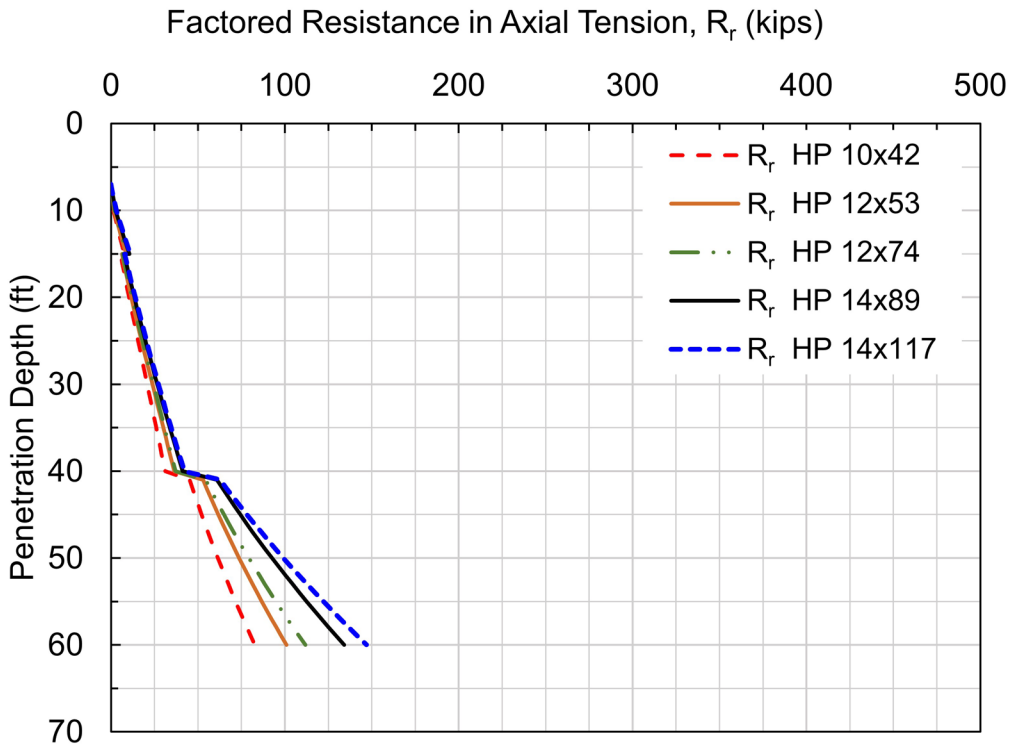

Figure D-64 Factored geotechnical resistance, R_r, in axial tension based on determination using static analysis, ϕ_{stat}=0.35 or ϕ_{stat}=0.25.

D.22.3 Preliminary Pile Drivability Assessment

Preliminary assessments of pile drivability are now performed at this stage of the design. A drivability check at this time is essential to assess the constructability of candidate pile types and/or sections and to eliminate sections with insufficient drivability. Section 12.4 provides a detailed discussion of wave equation drivability analyses and their applications.

A candidate pile section must be capable of being driven to the penetration depth necessary to achieve the nominal geotechnical resistance in axial compression and tension, to a penetration depth necessary to satisfy lateral load demands, as well as a penetration depth necessary to satisfy deformation requirements. A suitably sized pile hammer must be capable of driving the pile to its established minimum penetration depth and to the nominal resistance at a reasonable blow count without exceeding material stress limits. As detailed in Chapter 12, the blow count should be between 30 and 120 blows per foot at the nominal resistance. If the pile cannot be driven within these requirements, a larger pile hammer, a pile section with greater impedance, or pile installation aids such as predrilling or jetting may be required to satisfy or improve drivability.

Driving stresses during pile installation should remain below the driving stress limits tied to pile type and material strength. For the candidate steel H-piles, compression driving stress limits are given by Equation 8-33. As per ASTM A-572 requirements, new steel H-piles are rolled with a minimum yield stress of 50 ksi.

The driving stress limit, σ_{dr}, for candidate pile sections is then calculated as follows:

$$\sigma_{dr} = \varphi_{da}\left(0.9\,F_y\right) \qquad \text{[Eq. 8-33]}$$

Where: φ_{da} = resistance factor, 1.0 for steel piles.
F_y = yield stress, 50 ksi.

Therefore, the driving stress limit, σ_{dr}, is 45 ksi.

$$\sigma_{dr} = (1.0)\big(0.9\,(50\ ksi)\big) = 45\ ksi$$

Drivability analyses were performed for all five candidate pile sections. Since the specific pile hammer is often unknown at this point in the design, a reasonably sized, commonly available single acting diesel hammer was chosen for each of the candidate pile sections. As noted in Section 15.19, a hammer having a ram weight

of 1 to 2% of the larger of the required nominal resistance or required nominal driving resistance often provides a reasonable initial estimate of hammer size for wave equation analysis. Table D-54 summarizes the factored structural resistance in axial compression, P_r, and corresponding minimum and maximum nominal driving resistance associated with full section utilization and the full range of field determination methods resistance factors (static load test and dynamic testing (ϕ_{dyn}=0.80), and FHWA modified Gates dynamic formula (ϕ_{dyn}=0.40)). Given that full utilization of the structural section is uncommon, a reasonable initial estimate of the hammer size for a wave equation drivability analysis is 1% of the minimum R_{ndr}. Driving stress limits would likely be exceeded by choosing a significantly larger pile hammer. For each pile hammer, the wave equation default values were used for the helmet weight, hammer cushion materials, and the cushion material properties.

Table D-54 Summary of Pile Hammers Used in Drivability Analyses

Pile Section	Pile Cross Sectional Area (in^2)	Factored Structural Resistance, P_r (kips)	Minimum R_{ndr} ϕ_{dyn}=0.80 (kips)	Maximum R_{ndr} ϕ_{dyn}=0.40 (kips)	Ram Weight 1% of Min R_{ndr} (%)	Diesel Model	Ram Weight (kips)	Rated Energy (ft-kips)
HP 10x42	12.4	309	386	773	3.86	D25-52	5.51	62.0
HP 12x53	15.5	383	478	958	4.78	D30-52	6.62	74.4
HP 12x74	21.8	544	680	1360	6.80	D36-52	7.94	89.3
HP 14x89	26.1	652	815	1630	8.15	D46-32	10.14	114.1
HP 14x117	34.4	860	1075	2150	10.07	D50-52	11.03	124.0

For the soil resistance model, the output from DrivenPiles was converted to unit shaft resistance and unit toe resistance values and then input into the wave equation program. Similar soil resistances are thereby calculated versus depth by both the static analysis and wave equation analysis programs.

The dynamic soil properties for each soil layer were chosen in accordance with wave equation program recommendations. Selection of soil quake and damping parameters is discussed in Section 12.6.7. Pile driving at Pier 2 will commence at the bottom of pile cap excavation of Elevation 270 feet. Therefore dynamic soil properties for Layer 1 are not required for the preliminary drivability analyses. For the Pier 2 soil profile, a setup up factor of 2.0 was selected for the very stiff silty clay comprising Layer 3, while no setup is expected in the extremely dense gravel of Layer 2 or the dense gravel with sand of Layer 4. Soil setup is discussed in Section 7.2.4.2 and a summary of typical soil setup factors is provided in Table 7-16. The dynamic properties chosen are summarized in Table D-55.

Table D-55 Dynamic Soil Properties for Pier 2 Soil Profile

Soil Layer	Pile Section	Shaft Quake (in)	Toe Quake (in)	Shaft Damping (s/ft)	Toe Damping (s/ft)	Soil Set-Up Factor
2	HP 10 x 42	0.10	0.08	0.05	0.15	1.0
2	HP 12 x 53	0.10	0.10	0.05	0.15	1.0
2	HP 12 x 74	0.10	0.10	0.05	0.15	1.0
2	HP 14 x 89	0.10	0.12	0.05	0.15	1.0
2	HP 14 x 117	0.10	0.12	0.05	0.15	1.0
3	HP 10 x 42	0.10	0.17	0.20	0.15	2.0
3	HP 12 x 53	0.10	0.20	0.20	0.15	2.0
3	HP 12 x 74	0.10	0.20	0.20	0.15	2.0
3	HP 14 x 89	0.10	0.23	0.20	0.15	2.0
3	HP 14 x 117	0.10	0.23	0.20	0.15	2.0
4	HP 10 x 42	0.10	0.08	0.05	0.15	1.0
4	HP 12 x 53	0.10	0.10	0.05	0.15	1.0
4	HP 12 x 74	0.10	0.10	0.05	0.15	1.0
4	HP 14 x 89	0.10	0.12	0.05	0.15	1.0
4	HP 14 x 117	0.10	0.12	0.05	0.15	1.0

In soils that exhibit setup, the nominal resistance will be higher than the nominal driving resistance. Therefore, a gain/loss factor of 0.5 was used to estimate the nominal driving resistance versus depth in the drivability analyses. This gain/loss factor was determined from the inverse of the highest soil setup factor within the soil model (e.g., 1 divided by 2.0 equals 0.5). A gain/loss factor of 1 would be used if it was desired to model the nominal resistance instead of the nominal driving resistance and not consider the soil strength loss during driving and any subsequent soil setup. Refer to Chapter 12 for more detailed discussion on the selection of dynamic soil properties and soil setup factors.

The DrivenPiles program calculates the nominal driving resistance which models the soil strength lost during driving as well as the geotechnical nominal resistance once setup occurs. Figure D-65 presents the shaft resistance, toe resistance, and nominal driving resistance versus pile penetration depth for the HP 12x74 H-pile section at Pier 2. These nominal driving resistances are presented numerically in Table D-56. To quantify the expected soil setup at a given pile penetration depth, the values from Table D-56 can be compared against the nominal resistance previously presented in Table D-51. Figure D-66 illustrates the significant difference between the expected nominal driving resistance and the geotechnical nominal resistance after setup for the HP 12x74 candidate pile section.

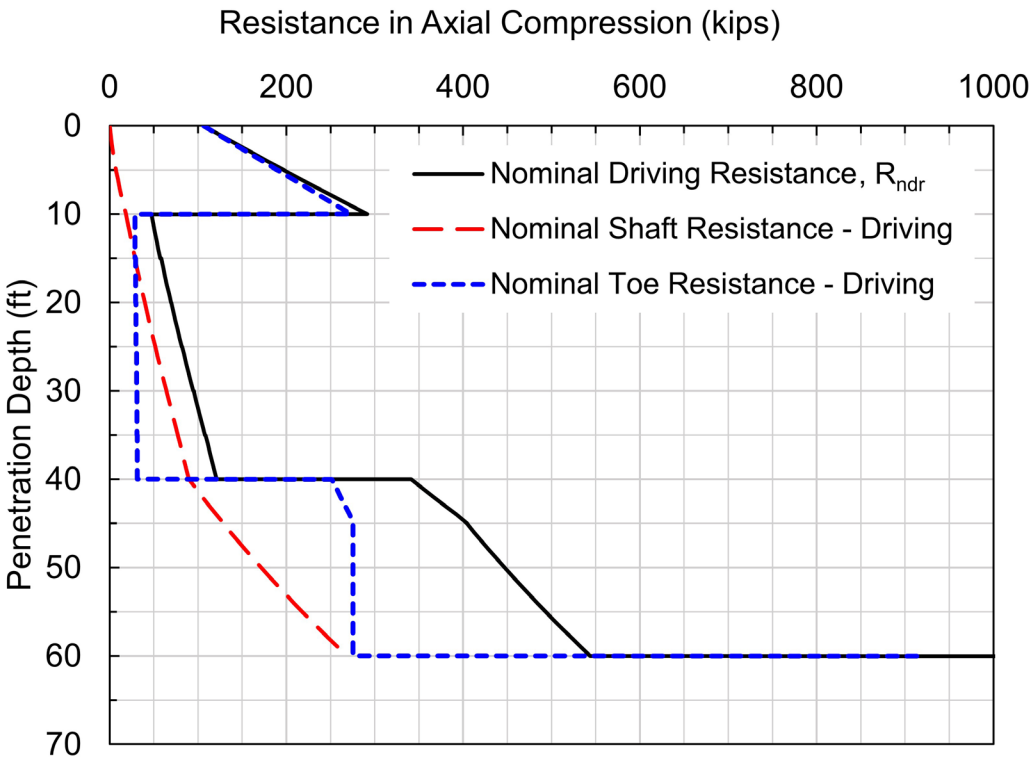

Figure D-65 Nominal driving resistance for HP 12x74 at Pier 2.

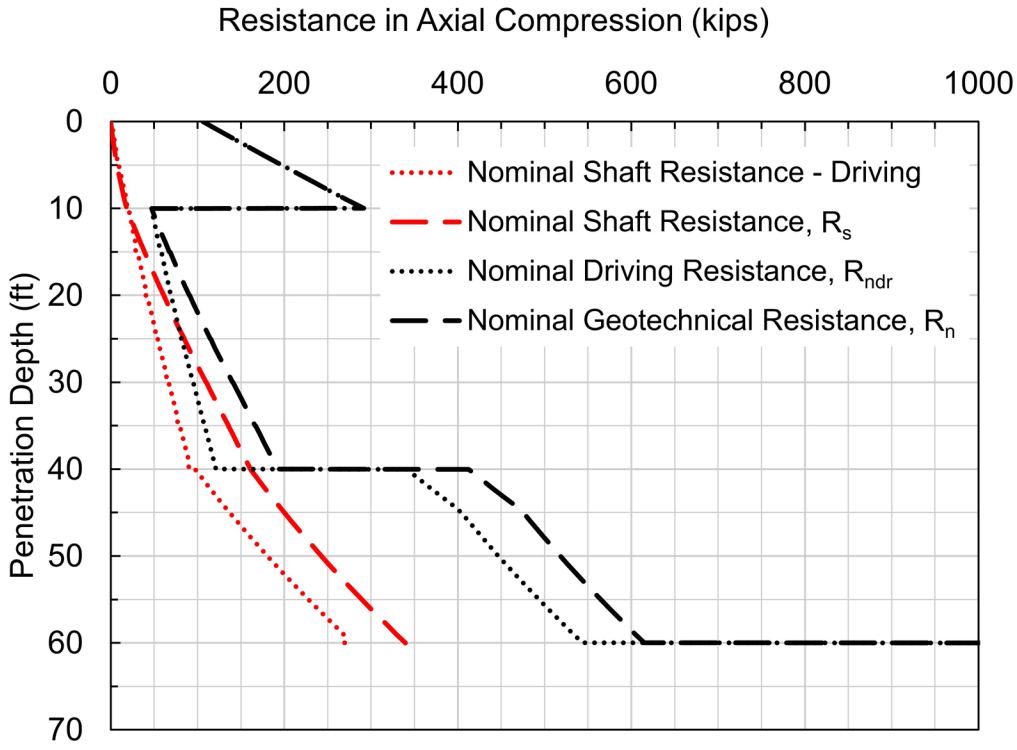

Figure D-66 Comparison of nominal driving resistance and nominal geotechnical resistance in axial compression for HP 12x74 at Pier 2.

Table D-56 Summary of Nominal Driving Resistance Versus Pile Penetration Depth for HP 12x74 at Pier 2

Depth (feet)	Nominal Shaft Resistance (kips)	Nominal Toe Resistance (kips)	Nominal Driving Resistance (kips)		Depth (feet)	Nominal Shaft Resistance (kips)	Nominal Toe Resistance (kips)	Nominal Driving Resistance (kips)
0.01	0.0	106.5	106.5		29.99	64.3	30.5	94.7
1	1.1	123.0	124.2		30.01	64.3	30.8	95.1
2	2.4	139.7	142.1		31	66.8	30.8	97.7
3	3.9	156.4	160.2		32	69.4	30.8	100.2
4	5.5	173.1	178.5		33	71.9	30.8	102.8
4.99	7.2	189.6	196.8		34	74.5	30.8	105.3
5.01	7.3	189.9	197.2		34.99	77.0	30.8	107.8
6	9.2	206.4	215.6		35.01	77.1	31.4	108.4
7	11.3	223.1	234.4		36	79.6	31.4	111.0
8	13.5	239.8	253.3		37	82.1	31.4	113.5
9	16.0	256.5	272.4		38	84.7	31.4	116.1
9.99	18.5	273.0	291.5		39	87.2	31.4	118.6
10.01	18.6	28.6	47.2		39.99	89.8	31.4	121.1
11	20.5	28.6	49.1		40.01	89.9	251.3	341.2
12	22.5	28.6	51.1		41	97.3	256.4	353.7
13	24.5	28.6	53.1		42	104.9	261.5	366.4
14	26.6	28.6	55.2		43	112.7	266.6	379.4
14.99	28.8	28.6	57.4		44	120.7	271.7	392.4
15.01	28.8	29.6	58.4		45	128.8	275.4	404.2
16	30.9	29.6	60.5		46	137.1	275.4	412.4
17	33.0	29.6	62.6		47	145.5	275.4	420.8
18	35.2	29.6	64.8		48	154.0	275.4	429.4
19	37.5	29.6	67.1		49	162.7	275.4	438.1
19.99	39.8	29.6	69.4		50	171.6	275.4	446.9
20.01	39.8	30.0	69.8		51	180.6	275.4	455.9
21	42.0	30.0	72.0		52	189.7	275.4	465.1
22	44.3	30.0	74.3		53	199.1	275.4	474.4
23	46.7	30.0	76.7		54	208.5	275.4	483.9
24	49.1	30.0	79.1		55	218.1	275.4	493.5
24.99	51.6	30.0	81.6		56	227.9	275.4	503.2
25.01	51.7	30.5	82.1		57	237.8	275.4	513.2
26	54.0	30.5	84.5		58	247.9	275.4	523.2
27	56.5	30.5	86.9		59	258.1	275.4	533.4
28	59.0	30.5	89.5		59.99	268.4	275.4	543.7
29	61.6	30.5	92.1		60.01	268.5	1042.6	1311.1

Graphical outputs of the preliminary drivability analyses are shown in Figure D-67. The nominal driving resistance, the blow count or pile penetration resistance, and the compression driving stress are presented versus pile penetration depth for each

of the five candidate pile sections. As previously noted, the recommended blow count limit is 120 blows per foot (10 blows per inch), and the recommended driving stress limit is 45 ksi. A circular reference marker is indicated on the blow count versus depth plot highlighting the depth where the blow count first exceeds 120 blows per foot. This marker is also shown at the same depth on the nominal driving resistance versus depth plot indicating the nominal driving resistance achieved when practical refusal driving conditions are encountered with the selected hammer in the modeled driving conditions. Similarly, the marker is shown at the same depth on the compression driving stress versus depth plot indicating the compression driving stress when practical refusal driving conditions are encountered.

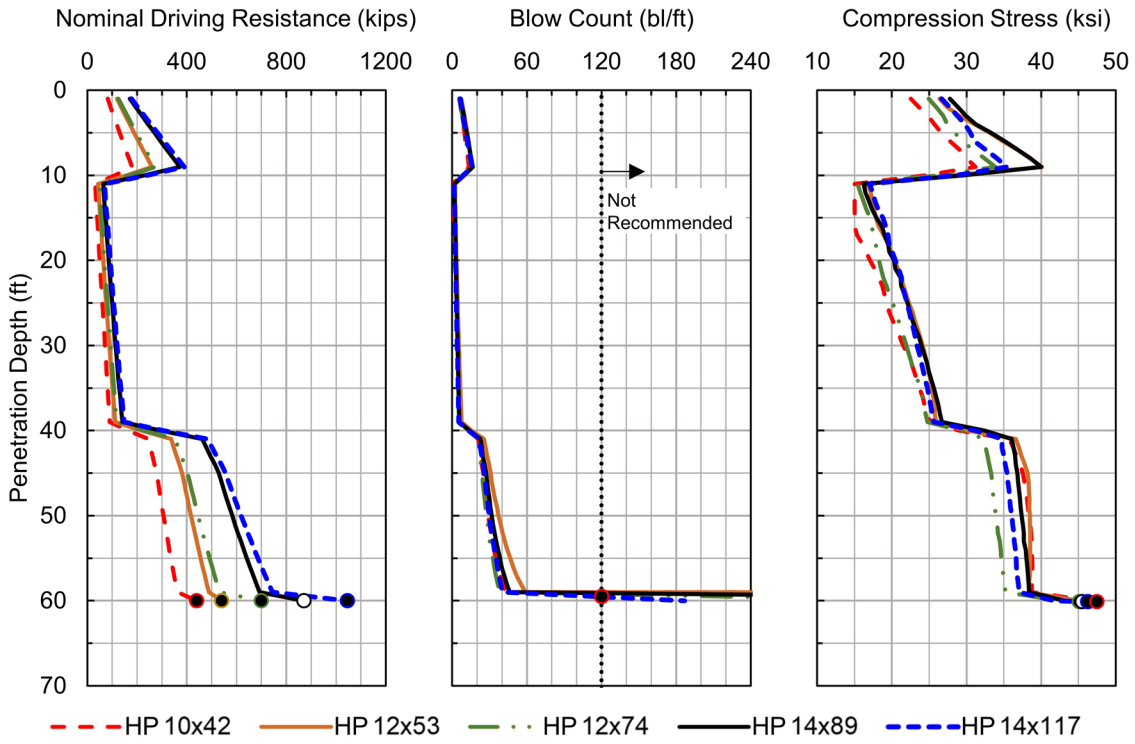

Figure D-67 Preliminary drivability results at Pier 2.

For all of the candidate pile sections and selected pile hammers, the blow count was 60 blows per foot or less before encountering hard rock at a penetration depth of 60 feet. Once bedrock was encountered, the blow count quickly transitioned to 120 blows per foot. Compression driving stresses for all candidate pile sections were also less than the 45 ksi driving stress limit prior to reaching bedrock.

If the final design requires piles be driven to hard bedrock, the driving criteria should be established to control compression stresses and prevent pile toe damage once hard rock is encountered (e.g., limit the number of blows at refusal driving

conditions). A summary of the preliminary drivability results is presented in Table D-57. The anticipated nominal resistance in this table is the expected resistance after soil setup that can be mobilized by the driving system at 10 blows per inch. For piles terminated on hard rock, a higher geotechnical nominal resistance, up to the structural resistance of the pile is actually available.

Once the estimated and/or minimum pile toe elevations are determined in Block 12 through Block 15 of the design process, the drivability results in Figure D-67 and Table D-57 should be reviewed to confirm that the candidate pile section can be driven to the estimated or required pile penetration depth, at reasonable blow counts, and with driving stress limits.

Table D-57 Summary of Preliminary Drivability Results at Pier 2

Pile Section	Pile Hammer	Fuel Setting	Pile Penetration Depth at Practical Refusal Limit (feet)	Nominal Driving Resistance at Practical Refusal Limit (kips)	Anticipated Nominal Resistance at Depth of Practical Refusal (kips)	Penetration Depth Exceeding Compression Driving Stress Limit (feet)	Maximum Compression Driving Stress (ksi)
HP 10x42	D25-52	4	60	440	500	60	46.4
HP 12x53	D30-52	4	60	540	610	60	44.9
HP 12x74	D36-52	4	60	700	770	60	42.6
HP 14x89	D46-52	4	60	870	950	60	43.2
HP 14x117	D50-52	4	60	1045	1125	60	41.8

D.23 Block 11: Pier 2 – Estimate Preliminary Number of Piles, Preliminary Pile Group Size, and Resolve Individual Pile Loads for All Limit States

The structural engineer has provided the anticipated loads for the controlling limit states at Pier 2. These limit state loads are restated in Table D-58. The Strength V limit state loads are used to evaluate geotechnical resistance in axial compression and tension, as well as for lateral loading. Although loads at Service I limit state were provided by the structural engineer, live loads should be removed when evaluating vertical deformation. Moreover, the Service I without live load includes only unfactored permanent loads such as the superstructure and wearing surface, pile cap and stem, utilities and vertical earth pressure among others. The Extreme Event II limit state must also be evaluated at this substructure location to consider effects of the check flood and associated loads.

Table D-58 Limit State Loads on Pier 2

Limit State	Q (kips)	V_{ux} (kips)	V_{uy} (kips)	M_{ux} (k-ft)	M_{uy} (k-ft)
Strength V	3456	18	109	-2981	3982
Service I	2682	15	100	-2749	2997
Service I, without LL	2172	0	0	0	0
Extreme Event II	3023	30	23	-797	1273

Pier construction will include a cofferdam and excavation of the existing geomaterials. The Agency practice for pier construction in a river is to use a substructure design with the smallest footprint. A minimum center to center pile spacing of 3 pile diameters is typical. Three potential pile group configurations for Pier 2 are under consideration. These are identified as Group Configurations 4, 5, and 6, respectively in Table D-59. Each group configuration has 5 rows of piles in the transverse direction. In the longitudinal direction, Group Configuration 4 has 3 rows of piles while Group Configurations 5 and 6 have 4 rows of piles. Furthermore, the distance from the center of any exterior pile to the pile cap edge must be at least 1.25 feet in both the transverse (x) and longitudinal (y) direction.

Table D-59 Potential Pile Group Configurations

Group Configuration	Piles per Row Y dir	Piles per Row X dir	Total Number of Piles	S_{bx}* (feet)	Total Footing Length (feet)	S_{by}* (feet)	Total Footing Width (feet)
4	3	5	15	3.0	14.5	3.0	8.5
5	4	5	20	3.0	14.5	3.0	11.5
6	4	5	20	5.0	22.5	4.0	14.5

* S_{bx} and S_{by} are illustrated in Figure D-68.

The following example calculation considers Group Configuration 6 and all applicable loads. For this alternative, 5 piles per row in the X direction and 4 piles per row in the Y direction are proposed. Thus the transverse pile spacing, $S_{bx,}$ is 3'-0" and the total footing length is 14'-6". The longitudinal pile spacing, $S_{by,}$ is 3'-0" and the total footing width is 11'-6". Figure D-68 shows the layout for the Group Configuration 6 pile cap.

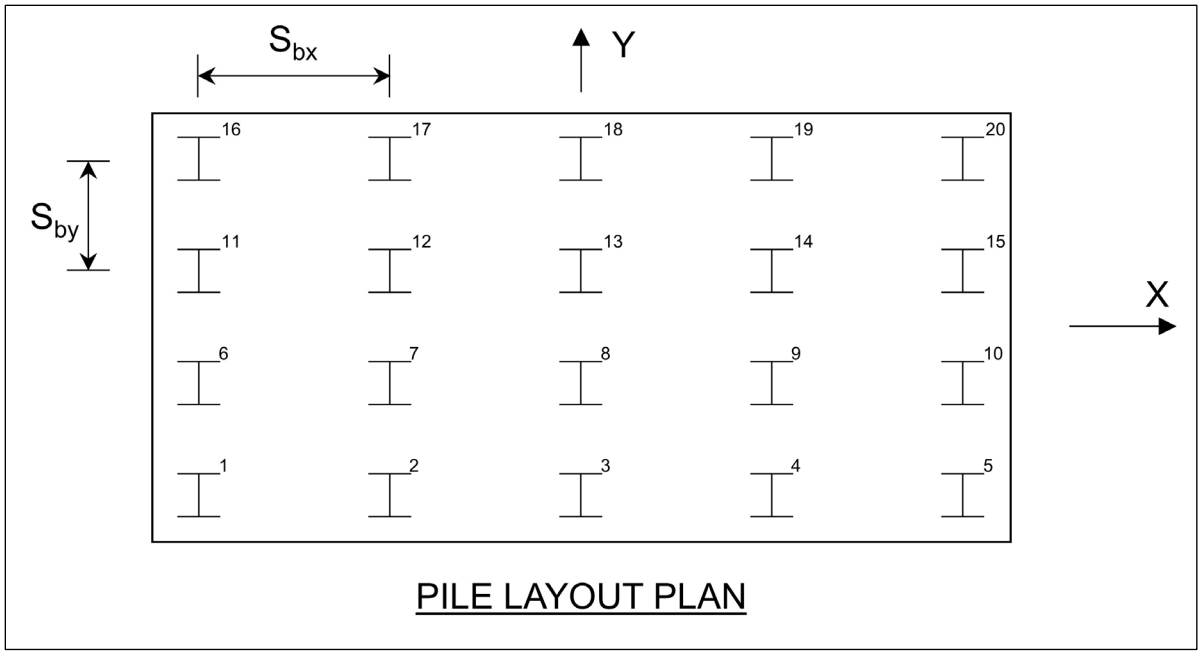

Figure D-68 Group Configuration 6 pile cap plan view.

For the trial pile group configuration in Figure D-68, loads for each pile in the group were determined using the limit state loads presented in Table D-58. The lateral load per pile in each direction was calculated by dividing the factored horizontal load V_{ux} or V_{uy} in Table D-58 by the number of piles, while the axial load per pile was calculated using Equation 8-79. For example, in Group Configuration 6, the lateral load per pile in the longitudinal direction is calculated by dividing 109 kips by 20 piles (i.e., 5.5 kips per pile). For the axial load per pile, an example calculation for the load applied to pile 5 at the Strength V limit state is presented below. Table D-60 shows the full calculation for all piles Group Configuration 6. The maximum individual pile load (on pile number 5) is 257 kips.

$$\mathrm{P}_{ui} = \frac{\mathrm{P}_{uz}+W_c+W_s}{n} + \frac{M_{ux}y}{\sum y^2} + \frac{M_{uy}x}{\sum x^2} \qquad \text{[Eq. 8-79]}$$

In this case, the factored limit state load, Q, replaces the factored axial load from superstructure/substructure acting upon pile cap, P_{uz}, estimated weight of pile cap, W_c and estimated weight of soil above pile cap, W_s as follows:

$$\mathrm{Q} = \mathrm{P}_{uz} + W_c + W_s$$

Calculate the individual pile axial load on pile number 5.

x = distance along x-axis from the center of the column to each pile center, 10 feet.

y = distance along y-axis from the center of the column to each pile center -6 feet.

$\sum x^2$ = sum of square distance along x-axis from the center of the column to each pile center, 1000 ft^2.

$\sum y^2$ = sum of square distance along y-axis from the center of the column to each pile center, 400 ft^2.

n = total number of piles, 20 piles (Group Configuration 6, Table D-59).

Q = factored axial load at Strength V limit state, 3456 kips (Table D-58).

M_{ux} = factored moment about the x axis acting on the pile cap, -2,981 kip-ft.

M_{uy} = factored moment about the y axis acting on the pile cap, 3,982 kip-ft.

$$\mathrm{P}_{ui} = \frac{\mathrm{Q}}{n} + \frac{M_{ux}y}{\sum y^2} + \frac{M_{uy}x}{\sum x^2} \qquad \text{[Eq. 8-79]}$$

$$\mathrm{P}_{ui} = \frac{(3{,}456\ \mathrm{kips})}{(20\ piles)} + \frac{(-2{,}981\ kip{-}ft)*(-6\ feet)}{(400\ ft^2)} + \frac{(3{,}982\ kip{-}ft)*(10\ feet)}{(1000\ ft^2)}$$

$$\mathrm{P}_{ui} = 257\ kips$$

Table D-60 Calculation of Individual Pile Load

Pile Number	x (feet)	y (feet)	x^2 (ft^2)	y^2 (ft^2)	$\frac{Q}{n}$ (kips)	$\frac{M_{ux}y}{\sum y^2}$ (kips)	$\frac{M_{uy}x}{\sum x^2}$ (kips)	P_{ui} (kips)
1	-10.0	-6.0	100.0	36.0	172.8	44.7	-39.8	177.7
2	-5.0	-6.0	25.0	36.0	172.8	44.7	-19.9	197.6
3	0.0	-6.0	0.0	36.0	172.8	44.7	0.0	217.5
4	5.0	-6.0	25.0	36.0	172.8	44.7	19.9	237.4
5	10.0	-6.0	100.0	36.0	172.8	44.7	39.8	257.3
6	-10.0	-2.0	100.0	4.0	172.8	14.9	-39.8	147.9
7	-5.0	-2.0	25.0	4.0	172.8	14.9	-19.9	167.8
8	0.0	-2.0	0.0	4.0	172.8	14.9	0.0	187.7
9	5.0	-2.0	25.0	4.0	172.8	14.9	19.9	207.6
10	10.0	-2.0	100.0	4.0	172.8	14.9	39.8	227.5
11	-10.0	2.0	100.0	4.0	172.8	-14.9	-39.8	118.1
12	-5.0	2.0	25.0	4.0	172.8	-14.9	-19.9	138.0
13	0.0	2.0	0.0	4.0	172.8	-14.9	0.0	157.9
14	5.0	2.0	25.0	4.0	172.8	-14.9	19.9	177.8
15	10.0	2.0	100.0	4.0	172.8	-14.9	39.8	197.7
16	-10.0	6.0	100.0	36.0	172.8	-44.7	-39.8	88.3
17	-5.0	6.0	25.0	36.0	172.8	-44.7	-19.9	108.2
18	0.0	6.0	0.0	36.0	172.8	-44.7	0.0	128.1
19	5.0	6.0	25.0	36.0	172.8	-44.7	19.9	148.0
20	10.0	6.0	100.0	36.0	172.8	-44.7	39.8	167.9
Sum	-	-	1000.0	400.0	-	-	-	3456.0

The process outlined above was used to determine the individual pile lateral and axial load for the remaining limit state loads presented in Table D-58. The maximum individual pile axial load is carried forward in the analysis for each group configuration. Based upon the applied loads and group configurations selected, no pile is put into axial tension. Therefore, only axial compression and lateral loads are required for the foundation design at Pier 2. Table D-61 presents the maximum factored axial compression load per pile based upon the number of piles in each group configuration. Table D-62 presents the maximum factored lateral load per pile based upon the number of piles in each group configuration.

Table D-61 Factored Axial Compression Load Per Pile for Alternative Pile Group Configurations

Group Configuration	Strength V, Q (kips)	Service I, without LL Q (kips)	Extreme Event II Q (kips)
4	418	145	256
5	299	109	188
6	257	109	176

Table D-62 Factored Lateral Load Per Pile for Alternative Pile Group Configurations

Group Configuration	Strength V, V_{uy} (kips)	Strength V, V_{ux} (kips)	Extreme Event II V_{uy} (kips)	Extreme Event II V_{ux} (kips)
4	8	2	2	2
5	6	1	2	2
6	6	1	2	2

D.24 Block 12: Pier 2 – Estimate Pile Penetration Depth for Maximum Axial Compression Loads. Check Group Efficiency in Axial Compression

The estimated minimum pile penetration depth necessary to obtain the factored geotechnical resistance equal to the maximum factored load per pile should now be determined. Note that the factored geotechnical resistance in axial compression and the resulting pile penetration depth is dependent upon the resistance determination method. Therefore, the influence of the field resistance determination method on the design is evaluated at this point in the design process. Thus, some resistance determination methods may be eliminated from further design consideration.

At Pier 2, drivability and potential damage when driving through the extremely dense gravel deposit is a concern. In addition, piles will also likely be driven into the gravel layer with cobbles encountered 40 feet below footing grade. This layer also presents a concern for pile damage. Therefore, it is determined that the factored geotechnical resistance will be substantiated by dynamic testing 2% of the piles. Figure D-45 illustrates the factored geotechnical resistance versus penetration depth for the 5 candidate pile sections based on this resistance determination method. From this plot, the estimated penetration depth for a factored geotechnical resistance of 257 kips in axial compression for the Group Configuration 6 ranges from 40 feet for the HP 14x117 to 57 feet for the HP 10x42. Results of this comparison for each pile section and group configuration are listed in Table D-63.

Table D-63 Estimated Pile Penetration Depths for the Factored Geotechnical Resistance in Axial Compression at the Strength V Limit State

Group Configuration	Factored Load per Pile (kips)	HP 10x42 (feet)	HP 12x53 (feet)	HP 12x74 (feet)	HP 14x89 (feet)	HP 14x117 (feet)
4	418	60	60	60	50	47
5	299	60	46	44	40	40
6	257	57	42	40	40	40

The Extreme Event II factored axial compression loads shown in Table D-61 were also used to estimate the pile penetration depth required to achieve the factored geotechnical resistance in axial compression. In this case, the nominal geotechnical resistance present in the check flood was used. Figure D-52 illustrates the factored geotechnical resistance versus penetration depth at the check flood for the 5 candidate pile sections based on determination testing by dynamic testing 2% of the piles. From this plot, the estimated penetration depth for the maximum factored geotechnical resistance of 176 kips in axial compression associated with Group Configuration 6 is 40 feet for all candidate pile sections except for the HP 10x42 section which requires approximately 57 feet. The 40 foot penetration depth is upper contact of the dense gravel layer. Results of this comparison for each pile section and group configuration are summarized in Table D-64.

Table D-64 Estimated Pile Penetration Depths for the Factored Geotechnical Resistance in Axial Compression at the Extreme Event II Limit State

Group Configuration	Factored Load per Pile (kips)	HP 10x42 (feet)	HP 12x53 (feet)	HP 12x74 (feet)	HP 14x89 (feet)	HP 14x117 (feet)
4	256	57	42	41	40	40
5	188	41	40	40	40	40
6	176	40	40	40	40	40

Based on the factored loads and estimated factored geotechnical resistances at Pier 2, the estimated pile penetration depth considering Strength V loads require the deepest pile penetration depth. Therefore, the estimated pile penetration depths presented in Table D-63 will be carried forward in the design.

Although a mixed soil profile appears at Pier 2, the stratum providing the majority of nominal geotechnical resistance is cohesionless soil, and will therefore be used as the controlling stratum for group efficiency. Per Section 7.2.2.1, the nominal geotechnical resistance of a pile group in cohesionless soil can be taken as the sum of the individual pile nominal geotechnical resistances. In a similar manner, the factored geotechnical resistance of the pile group in cohesionless soil is taken as the sum of the individual pile factored geotechnical resistances. This is recommended so long as 1) the bearing layer is not underlain by weak soil layers, 2) the piles are not installed at a pile spacing of less than 3 times the pile diameter, and 3) no special installation procedures are anticipated such as jetting or predrilling. Since all these conditions are met at Pier 2, the factored group resistances are satisfactory.

D.25 Block 13: Pier 2 – Establish Minimum Pile Penetration Depth for Axial Tension Loads. If Conditions Warrant, Modify Design and Return to Block 10

For the limit state loads identified in Table D-58 in combination with the group configurations at Pier 2 listed in Table D-59, no pile within any group configuration is loaded in tension. Therefore, the tension or uplift resistance is not evaluated, and there is no minimum pile penetration depth required for axial tension loads at Pier 2.

D.26 Block 14: Pier 2 – Establish Minimum Pile Penetration Depth for Lateral Loads. Determine p-y Models, Required Geomaterial Parameters, and Perform Lateral Load Analysis. If Conditions Warrant, Modify Design and Return to Block 10

Next, lateral analyses are performed to establish the required minimum pile penetration depth for lateral loading and to evaluate pile deflection and structural resistance for the applied limit state loads. No minimum penetration depth was required to satisfy the nominal geotechnical resistance requirements in axial tension in Block 13. A minimum pile penetration depth may be required for lateral loading based on the combination of factored lateral loads and structural resistances, or deflection limits. Excessive deflections and moments develop at relatively short pile lengths, where a depth to fixity is not achieved. Furthermore, the structural resistance of pile sections must be evaluated based upon the axial, lateral and moment loads. Factored structural resistances were presented in Table D-47 while a lateral deformation limit of 1 inch was established as a global performance requirement in Block 1 and confirmed in Block 4 as the design progressed.

As discussed in Section 7.3.7.6, p-multipliers are applied to the p-y curves to model pile group behavior. The p-multipliers depend on the center to center pile spacing within the pile group. For Group Configurations 6 at the Pier 2, the pile spacing in the longitudinal direction is 4 feet. Therefore, per Section 7.3.7.6 and AASHTO (2014) design specifications, interpolation was used to determine p-multipliers for a pile spacing of 4b. In this case, the front row p-multiplier is 0.90, the second row is 0.625, and the third and fourth rows are 0.5. For the same group configuration, piles in the transverse direction are spaced at 5 feet. Therefore p-multipliers for a pile spacing of 5b were used. In this case, the front row p-multiplier is 1.0, the second row is 0.85 and the third and fourth rows are 0.7.

Soil properties utilized for the lateral analysis are given in Figure D-39. Cyclic loading was performed for all rows using LPILE's Load Type 2 option, which uses shear and slope to model a fixed head condition. Considering loading conditions at this pier, lateral analyses in the longitudinal (y-direction) were performed about the pile section's strong axis. Figure D-68 shows the pile orientation within the trial pile cap design.

The following example is presented for the HP 12x74 pile section using a range of factored axial and lateral loads for Group Configuration 6. The Strength V limit state loads are applied in combination with the geotechnical resistance at the design flood, (i.e., 5 feet of scour below the pile head) Tables D-65 to D-67 provide LPILE output summaries for the longitudinal direction considering a pile penetration (from the bottom of pile cap) of 20 feet. Due to scour conditions, this is modeled as 15 feet of embedded pile length with 5 feet of pile stickup.

Table D-65 LPILE Summary Output at Pile Head for Front Row, p_m=0.90

Load Case	Load Type No.	Pile-Head Condition 1 V (kips)	Pile-Head Condition 2 S (rad)	Axial Load (kips)	Pile-Head Deflection (inches)	Maximum Moment in Pile (kip-ft)	Maximum Shear in Pile (kips)	Pile-Head Rotation (radians)
1	2	0	0	257	0.000	0.0	0.0	0
2	2	1	0	257	0.011	-5.4	-1.3	0
3	2	2	0	257	0.023	-10.8	-2.4	0
4	2	3	0	257	0.035	-16.3	-3.3	0
5	2	4	0	257	0.048	-21.8	-4.1	0
6	2	5	0	257	0.060	-27.3	5.0	0
7	2	6	0	257	0.073	-32.8	6.0	0
8	2	7	0	257	0.086	-38.3	7.0	0
9	2	8	0	257	0.099	-43.8	8.0	0
10	2	9	0	257	0.112	-49.3	9.0	0

Table D-66 LPILE Summary Output at Pile Head for Second Row, p_m=0.625

Load Case	Load Type No.	Pile-Head Condition 1 V (kips)	Pile-Head Condition 2 S (rad)	Axial Load (kips)	Pile-Head Deflection (inches)	Maximum Moment in Pile (kip-ft)	Maximum Shear in Pile (kips)	Pile-Head Rotation (radians)
1	2	0	0	257	0.000	0.0	0.0	0
2	2	1	0	257	0.012	-5.6	-1.2	0
3	2	2	0	257	0.026	-11.2	-2.2	0
4	2	3	0	257	0.040	-16.9	3.0	0
5	2	4	0	257	0.054	-22.7	4.0	0
6	2	5	0	257	0.069	-28.4	5.0	0
7	2	6	0	257	0.083	-34.2	6.0	0
8	2	7	0	257	0.098	-40.0	7.0	0
9	2	8	0	257	0.113	-45.7	8.0	0
10	2	9	0	257	0.128	-51.5	9.0	0

Table D-67 LPILE Summary Output at Pile Head for Third and Fourth Row, p_m=0.50

Load Case	Load Type No.	Pile-Head Condition 1 V (kips)	Pile-Head Condition 2 S (rad)	Axial Load (kips)	Pile-Head Deflection (inches)	Maximum Moment in Pile (kip-ft)	Maximum Shear in Pile (kips)	Pile-Head Rotation (radians)
1	2	0	0	257	0.000	0.0	0.0	0
2	2	1	0	257	0.013	-5.7	-1.2	0
3	2	2	0	257	0.028	-11.5	-2.1	0
4	2	3	0	257	0.043	-17.4	3.0	0
5	2	4	0	257	0.059	-23.3	4.0	0
6	2	5	0	257	0.075	-29.2	5.0	0
7	2	6	0	257	0.091	-35.1	6.0	0
8	2	7	0	257	0.107	-41.1	7.0	0
9	2	8	0	257	0.124	-47.0	8.0	0
10	2	9	0	257	0.140	-52.9	9.0	0

From LPILE's deflection results for individual rows, pile group deflection can be estimated. Factored load versus deflection for each row is plotted along with the average load for a given deflection as shown in Figure D-69. A discussion of this procedure is outlined in Section 7.3.7.6.

The rigid cap method assumes piles move together, and therefore experience the same shear and lateral load. Accordingly, at the resulting factored lateral load per pile, V_{uy}, of 6 kips (Table D-62), the estimated lateral group deflection at the pile head is determined as 0.085 inches. This lateral deflection is less than the 1 inch tolerance based upon project specific requirements.

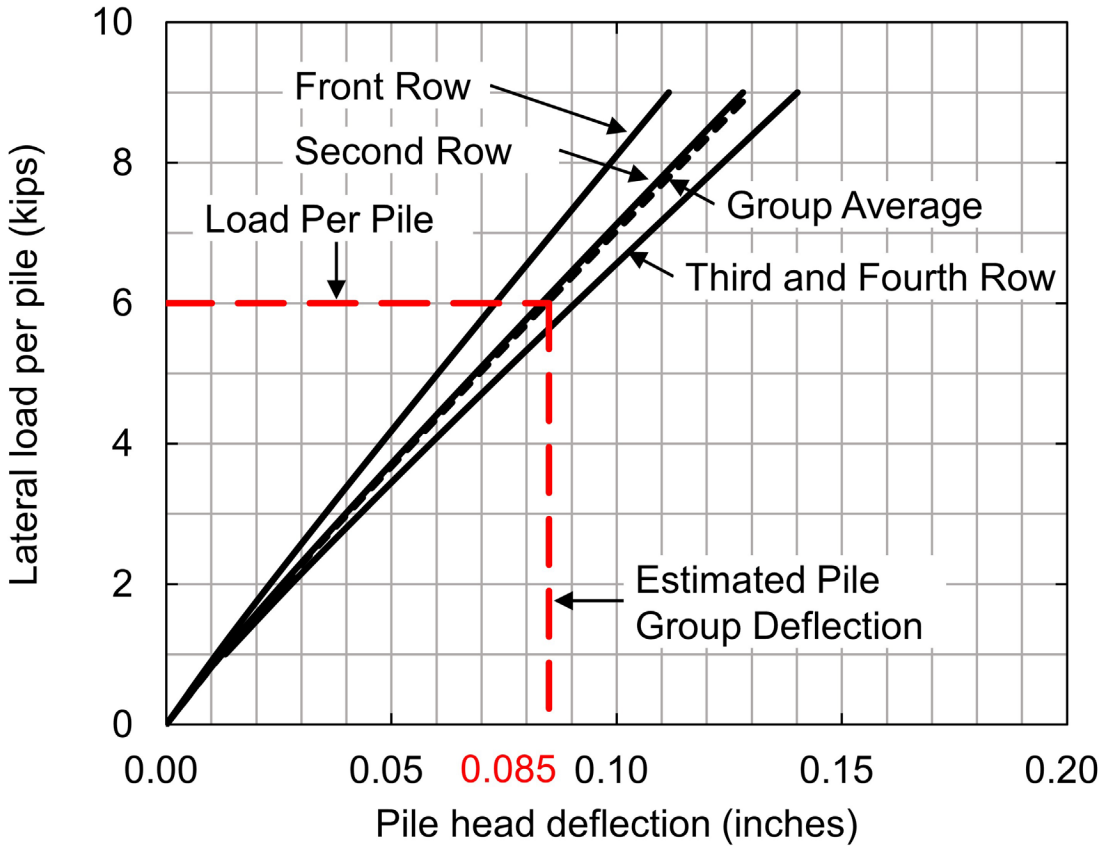

Figure D-69 Factored load versus deflection in longitudinal direction for HP 12x74 at Pier 2.

In addition to the lateral deflection limit, stresses from the resulting bending moment and shear must be evaluated to check that the pile section does not fail structurally. Using the LPILE tabular results, Figure D-70 plots the front row bending moment versus depth for a deflection of 0.085 inches.

Figure D-71 plots the maximum bending moment versus pile head deflection for all rows, however only the maximum bending moment for the front row is used as a "worst case" inspection of the structural resistance in combined axial compression and flexure. As illustrated in Figure D-71, at the estimated pile head deflection of 0.085 inches, the maximum bending moment, M_{uy}, is 38 kip-ft.

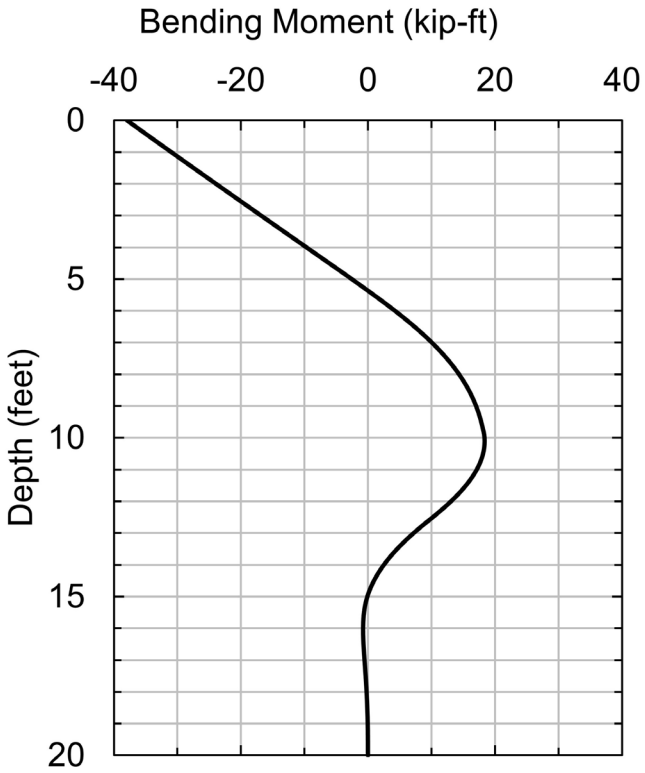

Figure D-70 Front row bending moment versus depth in longitudinal direction.

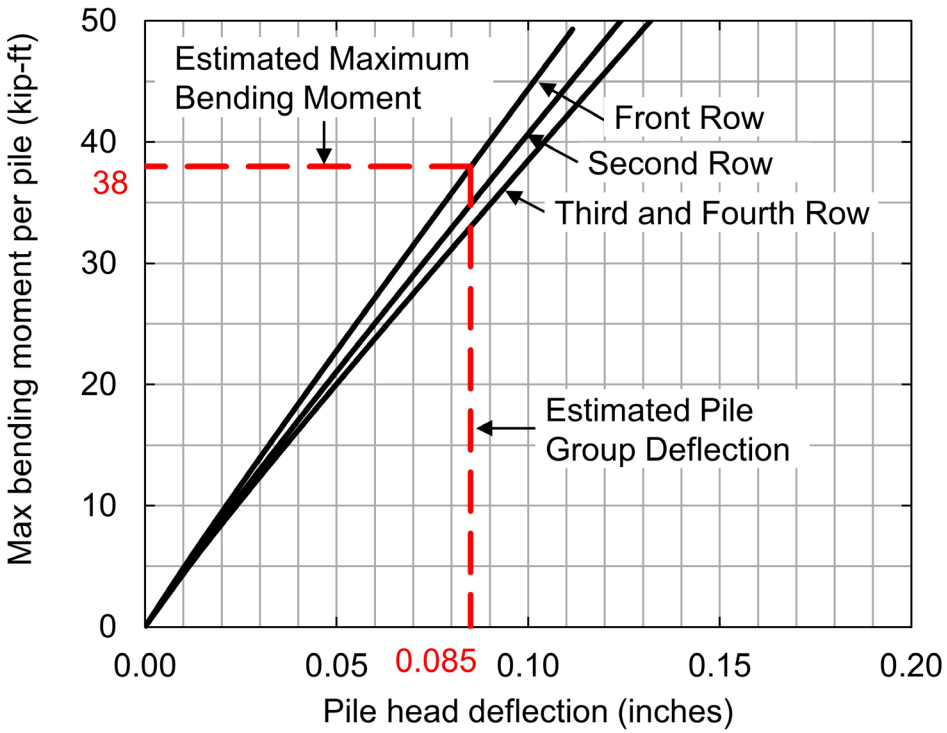

Figure D-71 Bending moment versus deflection in longitudinal direction for HP 12x74 at Pier 2.

The lateral analysis was also performed for the transverse direction with the Strength V limit state loads and the geotechnical resistance at the design flood, (i.e., 5 feet of scour below the pile head). Tables D-68 to D-70 provide LPILE output summaries for the transverse direction considering a pile penetration (from the bottom of footing) of 20 feet. Due to scour in the design flood, this is modeled as 15 feet of embedded pile length with 5 feet of pile stickup.

Table D-68 LPILE Summary Output at Pile Head for Front Row, p_m=1.0

Load Case	Load Type No.	Pile-Head Condition 1 V (kips)	Pile-Head Condition 2 S (rad)	Axial Load (kips)	Pile-Head Deflection (inches)	Maximum Moment in Pile (kip-ft)	Maximum Shear in Pile (kips)	Pile-Head Rotation (radians)
1	2	0.00	0	257	0.000	0.0	0.0	0
2	2	0.25	0	257	0.003	-1.3	-0.3	0
3	2	0.50	0	257	0.005	-2.6	-0.7	0
4	2	0.75	0	257	0.008	-4.0	-1.0	0
5	2	1.00	0	257	0.011	-5.3	-1.3	0
6	2	1.25	0	257	0.014	-6.7	-1.6	0
7	2	1.50	0	257	0.016	-8.0	-1.9	0
8	2	1.75	0	257	0.019	-9.3	-2.2	0
9	2	1.00	0	257	0.011	-5.3	-1.3	0

Table D-69 LPILE Summary Output at Pile Head for Second Row, p_m=0.85

Load Case	Load Type No.	Pile-Head Condition 1 V (kips)	Pile-Head Condition 2 S (rad)	Axial Load (kips)	Pile-Head Deflection (inches)	Maximum Moment in Pile (kip-ft)	Maximum Shear in Pile (kips)	Pile-Head Rotation (radians)
1	2	0.00	0	0	0.000	0.0	0.0	0
2	2	0.25	0	0	0.003	-1.3	-0.3	0
3	2	0.50	0	0	0.006	-2.7	-0.7	0
4	2	0.75	0	0	0.008	-4.0	-1.0	0
5	2	1.00	0	0	0.011	-5.4	-1.3	0
6	2	1.25	0	0	0.014	-6.8	-1.6	0
7	2	1.50	0	0	0.017	-8.1	-1.8	0
8	2	1.75	0	0	0.020	-9.5	-2.1	0
9	2	1.00	0	0	0.011	-5.4	-1.3	0

Table D-70 LPILE Summary Output at Pile Head for Third and Fourth and Fifth Rows, p_m=0.70

Load Case	Load Type No.	Pile-Head Condition 1 V (kips)	Pile-Head Condition 2 S (rad)	Axial Load (kips)	Pile-Head Deflection (inches)	Maximum Moment in Pile (kip-ft)	Maximum Shear in Pile (kips)	Pile-Head Rotation (radians)
1	2	0.00	0	0	0.000	0.0	0.0	0
2	2	0.25	0	0	0.003	-1.4	-0.3	0
3	2	0.50	0	0	0.006	-2.7	-0.7	0
4	2	0.75	0	0	0.009	-4.1	-1.0	0
5	2	1.00	0	0	0.012	-5.5	-1.3	0
6	2	1.25	0	0	0.015	-6.9	-1.5	0
7	2	1.50	0	0	0.018	-8.3	-1.8	0
8	2	1.75	0	0	0.022	-9.7	-2.0	0
9	2	1.00	0	0	0.012	-5.5	-1.3	0

From LPILE's deflection results for individual rows, pile group deflection can be estimated. Factored load versus deflection for each row is plotted along with the average load for a given deflection as shown in Figure D-72. A discussion of this procedure is outlined in Section 7.3.7.6.

The rigid cap method once again assumes piles move together, and therefore experience the same shear and lateral load. Accordingly, at the resulting factored lateral load per pile, V_{uy}, of 1 kip (Table D-62), the estimated lateral group deflection at the pile head is determined as 0.011 inches. This lateral deflection is less than the 1 inch tolerance based upon project specific requirements.

In addition to the lateral deflection limit, stresses from the resulting bending moment and shear must be evaluated to check that the pile section does not fail structurally. Using the LPILE tabular results, Figure D-73 plots the front row bending moment versus depth for deflection of 0.011 inches.

Figure D-74 plots the maximum bending moment versus pile head deflection for all rows, however only the maximum bending moment for the front row is used as a "worst case" inspection of the structural resistance in combined axial compression and flexure. As illustrated is Figure D-74, at the estimated pile head deflection of 0.011 inches, the maximum bending moment, M_{uy}, is 5.6 kip-ft.

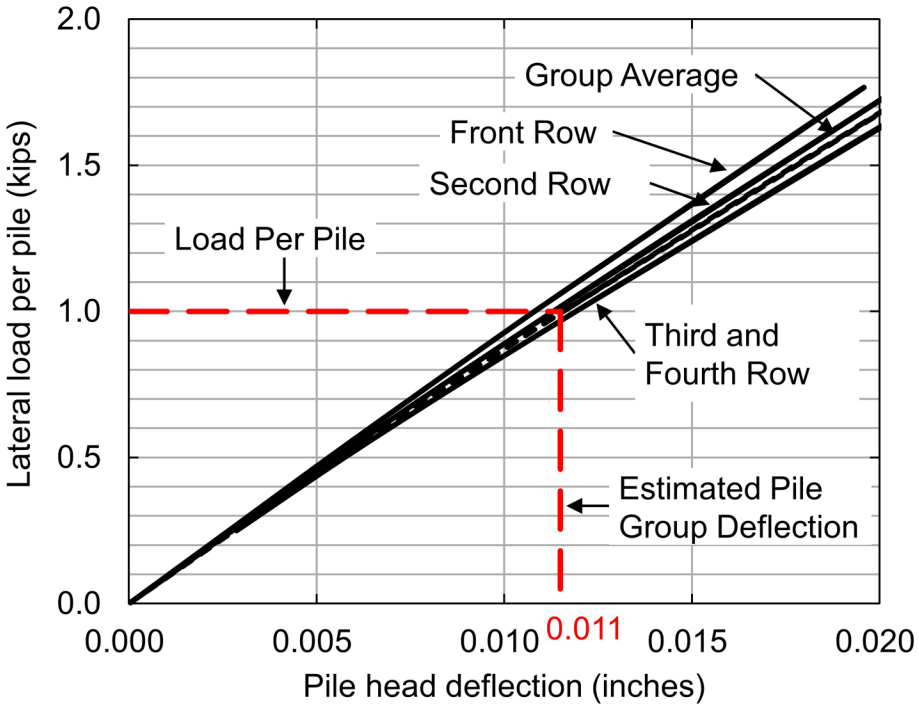

Figure D-72 Factored load versus deflection in transverse direction for HP 12x74 at Pier 2.

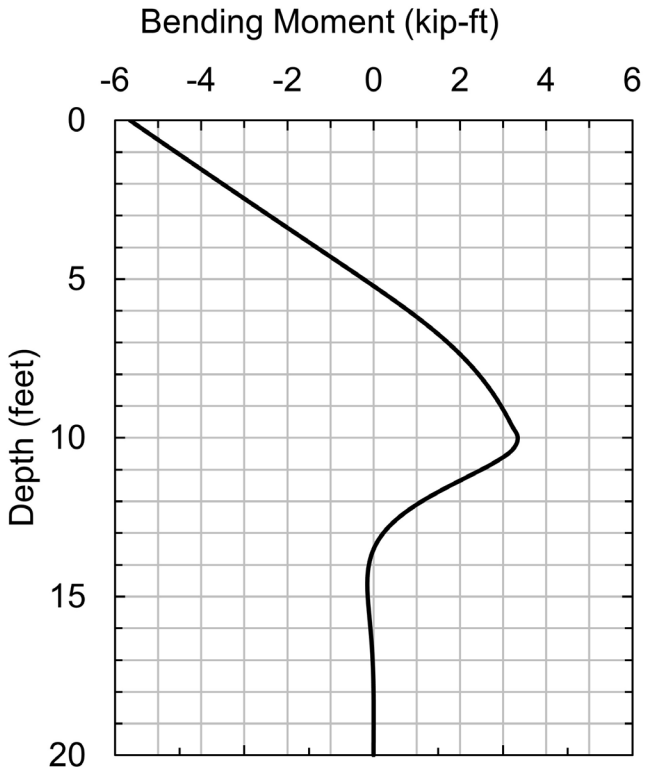

Figure D-73 Front row bending moment versus depth in transverse direction.

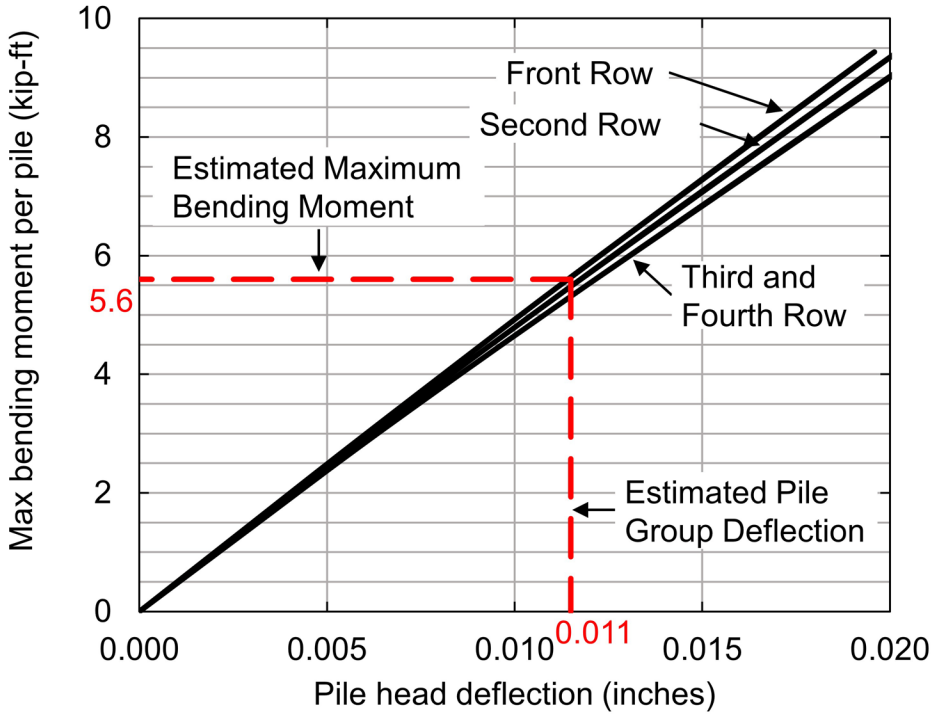

Figure D-74 Bending moment versus deflection in transverse direction for HP 12x74 at Pier 2.

The interaction shown in Equation 8-58 must be satisfied for the factored axial compression load and moment in the pile. Using results of the lateral analysis, the factored structural resistance was evaluated at the pile head using the factored axial compression load and maximum bending moment (determined using factored loads). The factored structural resistances were determined as shown in Table D-47.

Equation 8-58 must be satisfied for the pile section to be acceptable.

P_u = factored axial load, 257 kips (Table D-61).
P_r = factored axial resistance, 730 kips (Table D-47).
M_{ux} = factored moment about x-axis, 5.6 kip-ft (Figure D-74).
M_{rx} = factored flexural resistance about x-axis, 118 kip-ft (Table D-47).
M_{uy} = factored moment about y-axis, 38 kip-ft (Figure D-71).
M_{ry} = factored flexural resistance about y-axis, 433 kip-ft (TableD-47).

$$\frac{\mathrm{P}_u}{\mathrm{P}_r}+\frac{8.0}{9.0}\left(\frac{\mathrm{M}_{ux}}{\mathrm{M}_{rx}}+\frac{\mathrm{M}_{uy}}{\mathrm{M}_{ry}}\right)\leq 1.0 \qquad \text{[Eq. 8-58]}$$

$$\frac{(257\ kips)}{(730\ kips)} + \frac{8.0}{9.0}\left(\frac{(5.6\ kip{-}ft)}{(118\ kip{-}ft)} + \frac{(38\ kip{-}ft)}{(433\ kip{-}ft)}\right) \leq 1.0$$

$$0.47 \leq 1.0$$

The maximum shear from factored lateral loading was then compared to the factored shear resistance from Table D-47. The maximum shear within the pile occurred at the pile head. Based on the factored loads, the factored shear resistance is acceptable.

V_r = factored shear resistance, 214 kips (HP 12x74, Table D-47).
V_{uy} = factored shear load, 6 kips (Group Configuration 6, Table D-62).

$$V_{uy} < V_r$$

$$6\ kips < 214\ kips$$

The lateral analysis was also performed for each alternative pile section, and subsequently the deflection and factored structural resistance was evaluated considering the factored loads for group configurations shown in Table D-62. Pile head deflection must be limited to 1 inch, and based upon the applied loads and pile section, the factored structural resistance of the pile must also satisfy the structural resistance interaction equation presented as Equation 8-58. Furthermore, the pile should be embedded such that fixity is established, and for this case, the second crossing of the moment versus depth curve with the y-axis (i.e., moment is 0 kip-ft) is assumed as fixity for this design example. A review of Figure D-70 shows this depth to be approximately 20 feet. Pile sections satisfying these criteria were deemed acceptable, and furthermore as presented in Table D-71, a minimum required pile penetration depth was established based on lateral loads at the Strength V limit state. The minimum penetration depth is identified as "- - -" for candidate pile sections not meeting the lateral deformation or structural resistance requirements.

Table D-71 Minimum Pile Penetration Depth Required for Strength V Lateral Loads at Pier 2

Group Configuration	HP 10x42 (feet)	HP 12x53 (feet)	HP 12x74 (feet)	HP 14x89 (feet)	HP 14x117 (feet)
4	- - -	- - -	30	25	25
5	25	25	25	25	25
6	20	20	20	20	20

In a similar manner, the lateral analysis was repeated using the Extreme Event II limit state loads and the geotechnical resistance at the check flood. Although axial loads and lateral loads in the longitudinal direction decreased, further loss of geotechnical resistance from scour required an additional analysis. Table D-72 presents the minimum pile penetration depth required to satisfy lateral loading at the Extreme Event II limit state. As a result of reduced axial and lateral loads, the HP 10x42 and HP 12x52 pile sections in Group Configuration 4 would be acceptable. For the remaining candidate pile sections and group configurations, no additional pile penetration was required beyond the previously identified pile penetration depths in Table D-71.

Table D-72 Minimum Pile Penetration Depth Required for Extreme Event II Lateral Loads at Pier 2

Group Configuration	HP 10x42 (feet)	HP 12x53 (feet)	HP 12x74 (feet)	HP 14x89 (feet)	HP 14x117 (feet)
4	30	30	30	25	25
5	25	25	25	25	25
6	20	20	20	20	20

After evaluating lateral loads with the respective geotechnical resistance at the Strength and Extreme Event limit states, the established minimum pile penetration depth is taken as the worst case for each candidate section and group configuration. In this case, the more conservative depth for all candidate sections and group configurations is taken from the lateral loading evaluation at the Strength limit state. The established minimum pile penetration depth required for lateral loading is presented in Table D-73.

Table D-73 Established Minimum Pile Penetration Depth Required for Lateral Loading at Pier 2

Group Configuration	HP 10x42 (feet)	HP 12x53 (feet)	HP 12x74 (feet)	HP 14x89 (feet)	HP 14x117 (feet)
4	- - -	- - -	30	25	25
5	25	25	25	25	25
6	20	20	20	20	20

D.27 Block 15: Pier 2 – Establish Pile Penetration Depths that Satisfy Tolerable Deformations. Estimate Group Settlement over the Minimum and Maximum Range of Pile Penetration Depths From Blocks 12 to 14 and Identify All Pile Toe Elevations Which Result in Intolerable Deformations. If Conditions Warrant, Modify Design and Return to Block 10

Pile group settlement at Pier 2 was estimated using two methods, the Hough (1959) method and the Janbu Tangent modulus method. Ideally, the settlement method chosen by the designer is one that has shown good correlation with observed results. In order to obtain the factored geotechnical resistance in axial compression, the piles must be driven into the dense gravel with sand layer (Soil Layer 4, Figure D-39). As this is a cohesionless soil, pile group settlement was first estimated using the Hough (1959) Method. The Hough approach is a traditional settlement estimation method for pile groups in cohesionless soils and one that is referenced in the AASHTO (2014) design specifications. However, the soil conditions across the bridge substructure locations are quite variable and a settlement method that could be used at all substructure locations was also desired. Therefore, group settlement was also computed with the Janbu Tangent modulus approach using an equivalent footing placed at the neutral plane.

Compressibility properties for the silty clay layer were determined from one dimensional consolidation tests which were performed on undisturbed samples collected near the middle of the clay layer. Table D-74 presents the void ratio, e_o, overconsolidation ratio, OCR, compression index, C_c, and recompression index, C_r for the silty clay layer. The OCR of the soil was used to calculate the preconsolidation stress, σ'_p, at discrete depths.

Table D-74 Soil Properties Determined from One Dimensional Consolidation Test

Soil Layer	e_o	OCR	C_c	C_r
3	0.80	2.01	0.30	0.03

The Hough (1959) method as presented in Section 7.3.5.2 was used to estimate group settlement. As mentioned, piles must be driven to the dense gravel layer (Soil Layer 4) to achieve the required factored geotechnical resistance in axial compression. The settlement calculations were performed using only unfactored permanent loads. Therefore, the loads from the Service I limit state without live load were used to estimate settlement (i.e., load factor of 1.0 on permanent loads). The average contact stress for the trial pile group was calculated using the vertical load, *Q*, and pile group area *B x Z*. The following calculation is performed for Group

Configuration 6. Both the group width, *B*, and length, *Z*, were calculated from exterior pile edge to exterior pile edge.

An equivalent footing, with plan dimensions equal to those of the pile group, was evaluated at increasing pile penetration depths, and the resulting pile group settlement computed using the Hough (1959) method. The equivalent footing concept for piles driven to hard clay or sand through soft clay as presented in Figure 7-46a of Chapter 7 was utilized this analysis.

The following calculation is performed for the equivalent footing located at the silty clay / dense gravel interface at Elevation 235.0 feet. This location is 40 feet below the bottom of pile cap at Elevation 275.0 feet. Figure D-75 illustrates the pile group and resulting stress distribution at the equivalent footing. It was also assumed that vertical deformation below the gravel and bedrock interface at Elevation 215.0 feet is negligible. For Group Configuration 6, the length of the pile group is 21 feet, while the width is 13 feet. These dimensions are taken from exterior pile edge to exterior pile edge. This example calculation is therefore only suitable for this configuration. The soil profile was divided into 5 foot thick layers to evaluate settlement. Tabulated values for this group settlement analysis are presented in Table D-75. The elevation shown in Table D-75 references the midpoint of each respective soil layer, while z is the depth below the equivalent footing to the midpoint of each respective soil layer.

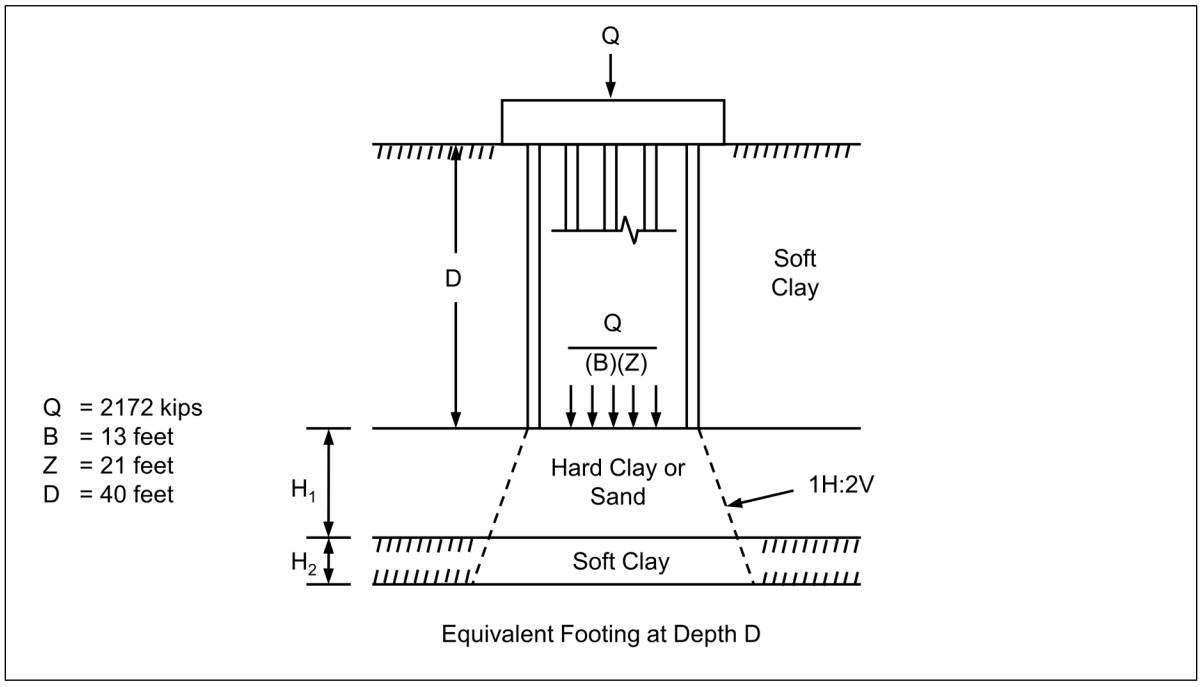

Figure D-75 Equivalent footing and stress distribution toe bearing piles in hard clay or sand considering Group Configuration 6 dimensions at Pier 2.

For the Hough (1959) method, the bearing capacity index must first be determined using the corrected SPT (N_1) value, however a review of the design soil profile in Figure D-39 shows SPT $(N_1)_{60}$ value as 46 for the dense gravel layer. To note, this value is corrected for both depth and energy. Figure D-76 presents the modified Hough (1959) method chart to determine the bearing capacity index from the respective soil layer's (N_1) value. Because the graph will be entered with a corrected SPT $(N_1)_{60}$ value, the x-axis scale consistent with the Safety hammer was used to enter the graph, while the soil type selected to determine the bearing capacity index was conservatively taken as the "clean, well graded fine to coarse sand." Based on these two assumptions, the bearing capacity index, *C'*, was determined as 180.

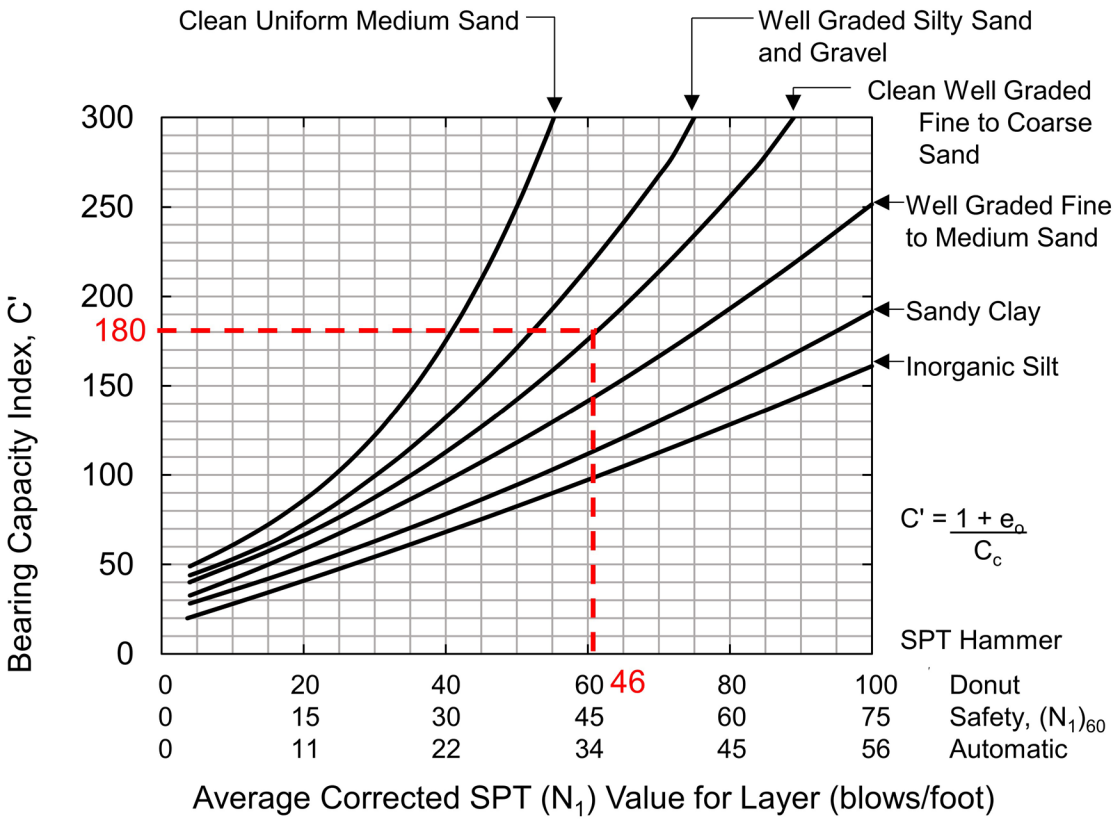

Figure D-76 Hough (1959) method chart to determine bearing capacity index from SPT (N_1) at Pier 2.

Considering only the unfactored permanent load, Q, calculate the vertical effective stress increase below the equivalent footing, $\Delta\sigma'_v$, at EL 235.0 feet.

Q = unfactored permanent load, 2182 kips (Service I, without LL, Table D-58).
B = pile group width, 13 feet.
Z = pile group length, 21 feet (Group Configuration 6 only)
z = depth below equivalent footing, 2.5 feet (Elev. 232.5 feet)

$$\Delta\sigma'_v = \frac{Q}{(B+z)+(Z+z))} \quad \text{[Eq. 7-55]}$$

$$\Delta\sigma'_v = \frac{(2182\ kips)}{((13\ feet)+(2.5\ feet))*((21\ feet)+(2.5\ feet)))}$$

$$\Delta\sigma'_v = 5.96\ ksf$$

Determine the percent stress increase by comparing σ'_{vo} and σ'_1

σ'_{vo} = initial vertical effective stress at depth z below the equivalent footing, 2.92 ksf.
σ'_1 = new vertical effective stress considering the unfactored permanent load, 2.92 ksf + 5.96ksf = 8.88 ksf.

$$Percent\ Stress\ Increase = \frac{\sigma'_1 - \sigma'_{vo}}{\sigma'_{vo}} * 100\% \quad \text{[Eq. D-5]}$$

$$Percent\ Stress\ Increase = \frac{(8.88\ ksf)-(2.92\ ksf)}{(2.92\ ksf)} * 100$$

$$Percent\ Stress\ Increase = 204\%$$

The stress increase is greater than or equal to 10%. Deformation for this depth increment should be estimated and included in the sum of all depth increments in which the stress increase is not less than 10%. A rock layer, which is considered incompressible, is located at Elev. 215.0 feet at this substructure location, and thus it is assumed that no settlement or compression occurs below this depth.

For the dense gravel at Elev. 232.5 feet, z = 2.5 determine deformation in the layer from the increase in vertical effective stress, S, with Equation 7-49.

H_o = initial soil layer thickness, 5 feet.
C' = dimensionless bearing capacity index, 180 (Figure D-76).
σ'_{vo} = vertical effective stress at midpoint of layer prior to stress increase, 2.92 ksf.
$\Delta\sigma'_v$ = vertical effective stress increase in the layer, 5.96 ksf.

$$S = H_o \left[\frac{1}{C'} \log \frac{\sigma'_{vo} + \Delta\sigma'_{vo}}{\sigma'_{vo}}\right] \quad \text{[Eq. 7-49]}$$

$$S = (5\ feet) \left[\frac{1}{(180)} \log \frac{(2.92\ ksf) + (5.96\ ksf)}{(2.92\ ksf)}\right] * \left(\frac{12\ inches}{1\ foot}\right)$$

$$S = 0.16\ inches$$

Table D-75 Settlement Estimate for Hough Method With Equivalent Footing Located at Elev. 235.0 feet

EL (feet)	z (feet)	H_o (ksf)	σ'_{vo} (ksf)	B (feet)	Z (feet)	$\Delta\sigma'_{v(ss)}$ (ksf)	σ'_1 (ksf)	Stress Incr. (%)	S (in)
232.5	2.5	5	2.92	15.5	23.5	5.96	8.88	204	0.16
227.5	7.5	5	3.23	20.5	28.5	3.72	6.95	115	0.11
222.5	12.5	5	3.54	25.5	33.5	2.54	6.08	72	0.08
217.5	17.5	5	3.85	30.5	38.5	1.85	5.70	48	0.06
								Total	0.41

The above analysis was performed for additional pile penetration depths considering pile group dimensions of all three group configurations. Table D-76 summarizes these analysis results for the Hough (1959) estimated settlement. For an equivalent footing at Elev. 240.0 feet, pile group settlement is magnified as 5 feet of silty clay remains below the equivalent footing, and thus consolidation settlement occurs. Conventional settlement equations as discussed in Section 7.3.5.6 were used to estimate settlement in this 5 feet thick layer in combination with the Hough (1959) method equations which were applied for the dense gravel. Elevation 235.0 feet is the upper contact of the dense gravel layer, and thus the comparatively smaller deformation below this depth is from elastic compression. A review of Table D-76 shows that for all group configurations, the vertical deformations reduce as the pile toe penetrates into the dense gravel layer at Elev. 235.0 feet. Therefore, the minimum pile penetration to design against intolerable deformations is 40 feet.

Table D-76 Summary of Pile Group Settlement Estimation Using Hough (1959) Method For All Pile Group Configurations at Pier 2

Equivalent Footing Elevation (feet)	Pile Toe Elevation (feet)	Pile Penetration Depth (feet)	Estimated Settlement For Group Configuration 4 (inches)	Estimated Settlement For Group Configuration 5 (inches)	Estimated Settlement For Group Configuration 6 (inches)
240.0	240.0	35.0	4.77	3.96	2.33
235.0	235.0	40.0	0.63	0.56	0.41
230.0	230.0	45.0	0.52	0.46	0.33

Pile group settlement was also calculated using the neutral plane method and Janbu tangent modulus as discussed in Section 7.3.5.6. An equivalent footing, with plan dimensions equal to those of the pile group, was evaluated at increasing pile penetration depths, and the resulting pile group settlement computed using the Janbu tangent modulus. This procedure allowed the shallowest depth of an equivalent footing to be determined that met vertical deformation requirements. The required minimum pile penetration depth was then determined based on the pile toe elevation that would place the neutral plane at this same equivalent footing depth where vertical deformation requirements were satisfied.

The following example calculation is performed for the neutral plane located 40 feet below the bottom of footing. Figure D-77 presents the pile group and resulting stress distribution at the equivalent footing. From Elev. 270.0 feet to 235.0 feet, strain calculations for cohesive soil (stress exponent of j=0) were applied for Soil Layer 3. Below Elev. 235.0 feet however, strain calculations for dense coarse grained soil (stress exponent of j=1) were applied for the Soil Layer 4. It was assumed that vertical deformation below the encountered bedrock at Elev. 215.0 feet is negligible. For Group Configuration 6, the length of the pile group is 21 feet, while the width is 13 feet. This example calculation is therefore only suitable for this configuration. Dimensions are taken from exterior pile edge to exterior pile edge. The soil profile was again divided into 5 foot thick layers. Tabulated values for this analysis are recorded in Table D-77. The elevation shown in Table D-77 references the midpoint of each respective soil layer, while z is the depth below the equivalent footing to the midpoint of each respective soil layer.

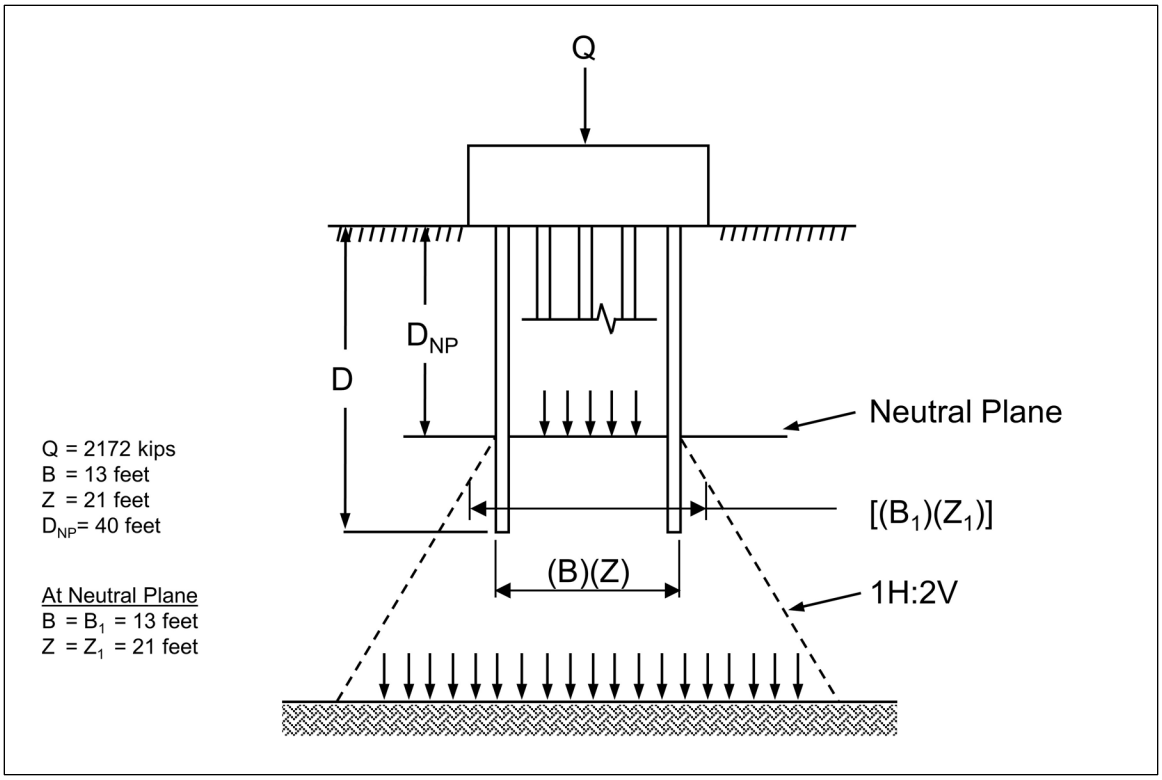

Figure D-77 Neutral plane at 40 feet below the pile cap and resulting stress distribution for Group Configuration 6.

Considering only the unfactored permanent load, Q, calculate the vertical effective stress increase below the equivalent footing, $\Delta\sigma'_v$, at EL 232.5 feet.

- Q = unfactored permanent load, 2182 kips (Service I, without LL, Table D-58).
- B = pile group width, 13 feet.
- Z = pile group length, 21 feet (Group Configuration 6 only).
- z = depth below equivalent footing, 2.5 feet (Elev. 232.5 feet).

$$\Delta\sigma'_{v(\mathrm{ss})} = \frac{Q}{(B+z)+(Z+z))} \qquad \text{[Eq. 7-55]}$$

$$\Delta\sigma'_{v(\mathrm{ss})} = \frac{(2182\ kips)}{((13\ feet)+(2.5\ feet))*((21\ feet)+(2.5\ feet)))}$$

$$\Delta\sigma'_{v(\mathrm{ss})} = 5.96\ ksf$$

Determine the percent stress increase by comparing σ'_{vo} and σ'_1.

σ'_{vo} = initial vertical effective stress at depth z below the equivalent footing, 2.92 ksf.

σ'_1 = new vertical effective stress considering the unfactored permanent load, 2.92 ksf + 5.96ksf = 8.88 ksf.

$$Percent\ Stress\ Increase = \frac{\sigma'_1 - \sigma'_{vo}}{\sigma'_{vo}} * 100\% \qquad \text{[Eq. D-5]}$$

$$Percent\ Stress\ Increase = \frac{(8.88\ ksf) - (2.92\ ksf)}{(2.92\ ksf)} * 100$$

$$Percent\ Stress\ Increase = 205\%$$

The stress increase is greater than or equal to 10%. Deformation for this depth increment should be estimated and included in the sum of all depth increments in which the stress increase is not less than 10%. A rock layer, which is considered incompressible, is located at Elev. 215 feet at this pier, and thus it is assumed that no settlement or compression occurs below this depth.

For the dense coarse grained soil at Elev. 232.5 feet, *z* = 2.5 (stress exponent of j = 1.0), determine the strain in the layer from the increase in vertical effective stress, ε, with Equation 7-61.

E_s = elastic modulus of soil, 1104 ksf (Figure D-39).

σ'_{vo} = initial vertical effective stress at depth z below the equivalent footing, 2.92 ksf.

σ'_1 = new vertical effective stress below the equivalent footing, 8.88 ksf.

$$\varepsilon = \frac{1}{E_s}[\sigma'_1 - \sigma'_{vo}] \qquad \text{[Eq. 7-61]}$$

$$\varepsilon = \frac{1}{(1104\ ksf)}[(8.88\ ksf) - (2.92\ ksf)]$$

$$\varepsilon = 0.0054$$

Calculate the layer compression denoted, *S*, with the initial height of the layer, H_o.

$$S = \varepsilon * H_o$$

$$S = 0.0054 * 5\ feet * \left(\frac{12\ inches}{1\ foot}\right)$$

$$S = 0.32\ inches$$

Table D-77 Settlement Estimation for Neutral Plane Method with the Neutral Plane at EL 235.0 feet

EL (feet)	z (feet)	H_o (ksf)	σ'_{vo} (ksf)	B (feet)	Z (feet)	$\Delta\sigma'_{v(ss)}$ (ksf)	σ'_1 (ksf)	Stress Incr. (%)	ε	S (in)
232.5	2.5	5	2.92	15.5	23.5	5.96	8.88	205	0.0054	0.32
227.5	7.5	5	3.23	20.5	28.5	3.72	6.95	115	0.0034	0.20
222.5	12.5	5	3.54	25.5	33.5	2.54	6.08	72	0.0023	0.14
217.5	17.5	5	3.85	30.5	38.5	1.85	5.70	48	0.0017	0.10
									Total	0.76

Table D-78 summarizes the settlement analysis results estimated using the neutral plane method and Janbu Tangent modulus approach. Although not yet determined, it is preliminarily estimated that elastic pile compression may be on the order of 0.3 inches, effectively limiting tolerable soil settlement to on the order of 1 inch. Therefore, to limit the total vertical deformation from elastic pile compression and settlement to less than 1.5 inches, the results in Table D-78 indicate that the neutral plane should be located 40 feet below the bottom of footing for Group Configuration 6. In a similar manner, the neutral plane should be located 55 feet and 50 feet below the bottom of footing for Group Configuration 4 and 5, respectively.

Table D-78 Estimated Pile Group Settlement Using Janbu Tangent Modulus with Neutral Plane Method For All Pile Group Configurations

Neutral Plane Elevation (feet)	Neutral Plane Depth (feet)	Estimated Settlement GC 4 (inches)	Estimated Settlement GC 5 (inches)	Estimated Settlement GC 6 (inches)
240.0	35	5.22	4.32	2.44
235.0	40	1.59	1.28	0.76
230.0	45	1.44	1.14	0.66
225.0	50	1.20	0.94	0.53
220.0	55	0.80	0.61	0.32

It is assumed that the equivalent footing acts at the same location as the neutral plane. Accordingly, an analysis was performed to determine the pile toe elevation necessary to locate the neutral plane at Elev. 235.0 (for piles in Group Configuration 6), thereby establishing the minimum required pile penetration depth to satisfy tolerable deformations.

The location of the neutral plane and the magnitude of drag force are evaluated following the procedure outlined in Section 7.3.6, using unfactored permanent loads and nominal geotechnical resistance. Because load factors for the Service limit state are 1.0, applicable loads at this limit state may be considered unfactored. The Service I, without LL limit state loads are therefore used for evaluation for the neutral plane. This example again utilizes the load for Group Configuration 6 (Q= 109 kips, Table D-61). Figure D-78 presents a graphical interpretation of the neutral plane for the HP 12x74 pile driven to 56 feet (pile toe at Elev. 219.0).

The unfactored permanent load and the cumulative shaft resistance are first plotted, followed by the mobilized toe resistance minus the cumulative shaft resistance (all vs. pile penetration depth). The exact percentage of toe mobilization is unknown at this stage of design, and therefore at least two of the toe mobilization curves should be evaluated to determine the neutral plane location. The 0% toe mobilization curve is the most conservative location to evaluate settlement (since it locates the neutral plane at the highest elevation), and the 100% toe mobilization curve should be used to check the pile section's structural strength (since it results in the greatest axial force in the pile). The structural strength check is performed in Block 17.

At Pier 2, it is expected that piles will be supported partially by toe resistance when driven to the dense gravel layer. Therefore the 0% toe mobilization curve presents

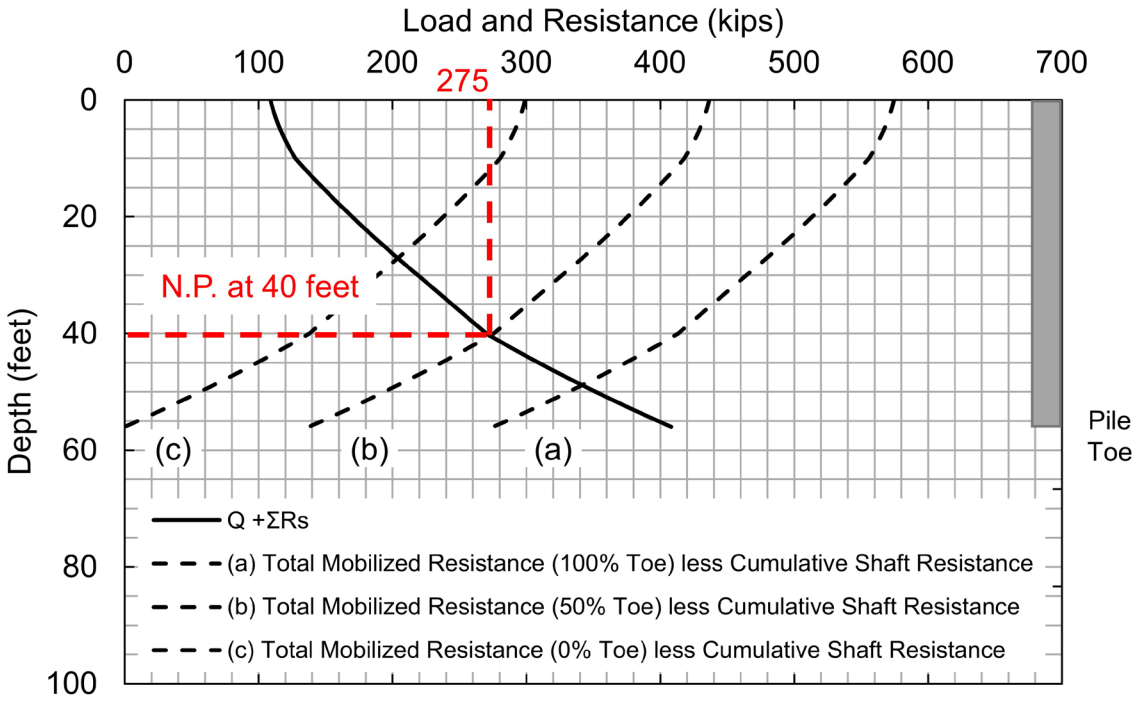

Figure D-78 Neutral plane location considering 50% toe mobilization for HP 12x74 at Pier 2.

an unreasonable baseline to evaluate settlement in this case. Some toe resistance is likely mobilized, and to remain consistent with the other substructure locations, the 50 % toe mobilization curve is again used to evaluate settlement.

Assuming 50 percent toe mobilization, the neutral plane is located 40 feet below the bottom footing with a resulting maximum load in the pile of 275 kips. For the remaining candidate pile sections and trial group configurations, the above analysis was also performed to determine the pile penetration depth required to locate the neutral plane at the depths indicated in Table D-78 for each respective pile group configuration. Table D-79 summarizes the results from these analyses.

Table D-79 Summary of Pile Penetration Depth Required to Locate Neutral Plane at Depth Determined From Settlement Estimation

Group Configuration	Load per Pile Q (kips)	HP 10x42 (feet)	HP 12x53 (feet)	HP 12x74 (feet)	HP 14x89 (feet)	HP 14x117 (feet)
4	145	60	60	60	60	60
5	109	60	60	60	58	60
6	109	60	58	56	52	49

To limit unacceptable settlement, it was decided that the method yielding the greatest settlement estimate would be used to establish the range of pile penetration depths to preclude unacceptable settlement. The neutral plane method illustrated above was therefore performed for additional equivalent footing depths until settlements within the project deformation criteria were estimated. Experience and judgement should be used to assess the required pile penetration depth with any settlement estimation approach.

A review of the soil profile at Pier 2 in Figure D-39 indicates no compressible soil layers below Soil Layer 4. Therefore, no effort is necessary to identify a maximum pile penetration depth to prevent punching though a dense layer into an unsuitable soil layer, or to apply a large stress increase on a lower compressible layer causing excessive settlement. Table D-80 presents the established minimum pile penetration depths to satisfy tolerable deformations at Pier 2.

Table D-80 Established Minimum Pile Penetration Depths to Satisfy Tolerable Deformations at Pier 2

Group Configuration	Load per Pile Q (kips)	HP 10x42 (feet)	HP 12x53 (feet)	HP 12x74 (feet)	HP 14x89 (feet)	HP 14x117 (feet)
4	145	60	60	60	60	60
5	109	60	60	60	58	60
6	109	60	58	56	52	49

Elastic shortening of the pile should be considered in the total pile deformation, noting that the drag force from negative shaft resistance adds to the axial compression force in the pile. Negative shaft resistance is determined from the previously discussed neutral plane calculation. For elastic compression, the load per pile from the Service I, without live load limit state (which is, in effect, and unfactored load) is applied at the pile head. As shown in Table D-61, this load is 109 kips.

Note that the drag force from negative shaft resistance increases the axial compression force in the pile. Negative shaft resistance above the neutral plane acts to increase axial compression force in the pile, whereas below the neutral plane, positive shaft resistance reduces the axial compression force in the pile. This effect must be accounted for in the elastic compression calculation. Accordingly, the unfactored axial load used to compute elastic compression, Q, changes for each pile

segment length, increasing equal to the unfactored permanent load plus the shaft resistance down to the neutral plane. In this example, the unfactored axial load is equal to the resistance distribution from 100% toe mobilization. The highest drag force magnitude results from this curve and represents the worst case.

Equation 7-48 is used to illustrate this example for the first 12 inch increment of the HP 12x74 pile section. The average shaft resistance and average load for each respective depth interval is used to estimate the elastic compression. For each 12 inch segment, the elastic modulus remains constant, and was evaluated as 29,000 ksi. The pile cross sectional area likewise remains constant as 21.8 in^2. Remaining calculations were performed using a spreadsheet; Table D-81 summarizes the elastic compression with depth.

Determine the unfactored axial load, Q, in segment.

Q_d = unfactored permanent load, 109.0 kips.
R_s^- = average (negative) shaft resistance, 1.1 kips.

$$\mathrm{Q} = Q_d + R_s^- = 109.0\ kips + 1.1\ kips$$

$$\mathrm{Q} = 110.1\ kips$$

Calculate elastic compression of segment with unfactored axial load from combined unfactored permanent load and negative shaft resistance.

L = segment length, 12 inches.
A = cross sectional area of pile material, 21.8 in^2.
E = elastic modulus of pile, 29,000 ksi.

$$\Delta = \frac{QL}{AE} \qquad \text{[Eq. 7-48]}$$

$$\Delta = \frac{(110.1\ kips)*(12\ inches)}{(21.8\ in^2)*(29{,}000\ ksi)}$$

$$\Delta = 0.00209\ inches$$

Table D-81 Elastic Compression Calculation

Depth Below Pile Head (feet)	Average Shaft Resistance (kips)	Average Unfactored Axial Load (kips)	Δ (inches)
0	0.0	109.0	0.00000
0-1	0.6	110.1	0.00209
1-2	1.8	110.8	0.00210
2-3	3.1	112.1	0.00213
3-4	4.7	113.7	0.00216
4-5	6.4	115.4	0.00219
5-6	8.2	117.2	0.00222
6-7	10.2	119.2	0.00226
7-8	12.4	121.4	0.00230
8-9	14.8	123.8	0.00235
9-10	17.3	126.3	0.00240
10-11	20.5	129.5	0.00246
11-12	24.4	133.4	0.00253
12-13	28.4	137.4	0.00261
13-14	32.5	141.5	0.00269
14-15	36.8	145.8	0.00277
15-16	41.1	150.1	0.00285
16-17	45.3	154.3	0.00293
17-18	49.6	158.6	0.00301
18-19	54.1	163.1	0.00310
19-20	58.7	167.7	0.00318
20-21	63.3	172.3	0.00327
21-22	67.8	176.8	0.00336
22-23	72.5	181.5	0.00344
23-24	77.3	186.3	0.00354
24-25	82.2	191.2	0.00363
25-26	87.1	196.1	0.00372
26-27	92.0	201.0	0.00381
27-28	97.0	206.0	0.00391
28-29	102.1	211.1	0.00401
29-30	107.4	216.4	0.00411
30-31	112.6	221.6	0.00421
31-32	117.7	226.7	0.00430
32-33	122.8	231.8	0.00440
33-34	127.9	236.9	0.00450
34-35	133.0	242.0	0.00459
35-36	138.1	247.1	0.00469
36-37	143.2	252.2	0.00479
37-38	148.3	257.3	0.00488

Table D-81 Elastic Compression Calculation (continued)

Depth Below Pile Head (feet)	Average Shaft Resistance (kips)	Average Unfactored Axial Load (kips)	Δ (inches)
38-39	153.4	262.4	0.00498
39-40	158.5	267.5	0.00508
40-41	164.8	273.8	0.00520
41-42	172.3	281.3	0.00534
42-43	180.1	289.1	0.00549
43-44	187.9	296.9	0.00564
44-45	196.0	305.0	0.00579
45-46	204.2	313.2	0.00594
46-47	212.5	321.5	0.00610
47-48	221.0	330.0	0.00626
48-49	228.4	337.4	0.00640
49-50	227.1	336.1	0.00638
50-51	218.2	327.2	0.00621
51-52	209.1	318.1	0.00604
52-53	199.9	308.9	0.00586
53-54	190.5	299.5	0.00568
54-55	180.9	289.9	0.00550
55-56	171.2	280.2	0.00532
		Total	0.23

For the pile head load of 109 kips (Group Configuration 1 loads), estimated elastic compression of the HP 12x74 pile section driven to 56 feet is 0.23 inches. Combined with 0.76 inches of deformation from settlement (Table D-78), it is estimated that total vertical deformation at Pier 2 is 0.99 inches.

D.28 Block 16: Pier 2 – Check pile drivability to maximum pile penetration depth requirements established in Blocks 12 through 15

Preliminary pile drivability was previously evaluated for the 5 candidate pile sections in Block 10. The plots of nominal resistance, blow count and compression stress versus depth in Figure D-67 should now be reviewed considering the established minimum pile penetration depths. A candidate pile section must be capable of being driven to the penetration depth necessary to achieve the nominal geotechnical resistance in axial compression and tension, and to a penetration depth necessary to satisfy lateral load demands as well as axial and lateral deformation requirements. However, no minimum pile penetration depth is required to satisfy axial tension

resistance. Minimum pile penetration depths have been previously established in Blocks 14 and 15 and are presented in Tables D-73 and D-80.

Although a minimum pile penetration depth is not established for nominal geotechnical resistance in axial compression, the pile should also be capable of being driven close to this estimated pile penetration depth. If the pile cannot be driven to the required depth within driving stress limits and at reasonable blow counts, a larger pile hammer, a pile section with greater impedance, or pile installation aids such as predrilling or jetting may be required to satisfy or improve drivability. Alternatively, substructure design modifications should be considered.

For the HP 12x74 candidate pile section in Group Configuration 6 the pile penetration depth for axial compression loading was estimated at 41 feet (Table D-64). There is no minimum penetration depth for axial tension loading since there was no tension demand. The minimum penetration depth for lateral loading was 20 feet (Table D-73). A minimum pile penetration depth of 56 feet is required to satisfy vertical deformation limits (Table D-80). Accordingly, candidate pile section must have sufficient drivability to the maximum of these depths, 56 feet.

A review of Figure D-67 indicates that the HP 12x74 pile section can be driven to bedrock at approximately 60 feet, if required. In addition, from the preliminary drivability evaluation (with soil and hammer model assumptions described in Block 10), it is estimated that the blow count will not exceed 120 blows per foot or 10 blows per inch before this penetration depth. Compression driving stresses are estimated to remain below driving-stress limits. Therefore, it is concluded that pile drivability to the estimated pile penetration depth is achievable.

D.29 Block 17: Pier 2 – Determine the Neutral Plane Location and Resulting Drag Force. Check Structural Strength Limit State for Pile Penetration Depth From Block 16

Previously in Block 15, the neutral plane was evaluated as part of the settlement calculations. The neutral plane and resulting drag force are now evaluated to check the structural strength limit state for candidate pile sections. Section 7.3.6 of Chapter 7 provides a reference for evaluating the neutral plane location and the magnitude of the drag force. Load using the Service I, without live load limit state (which are, in effect, unfactored loads) are considered. This example again utilizes the load for Group Configuration 6 (Q= 109 kips, Table D-61).

It is good practice that the drag force be evaluated for 100 percent toe mobilization. This results in the neutral plane at its lowest potential location, and thus the highest drag force magnitude. Accordingly, this is the toe mobilization curve that should be used to check the pile section's structural resistance. Figure D-79 presents a graphical interpretation of the neutral plane location for the HP 12x74 pile section driven to the estimated pile penetration depth of 56 feet. In this case the neutral plane is located 49 feet below pile head with a resulting maximum axial compression force in the pile of 342 kips.

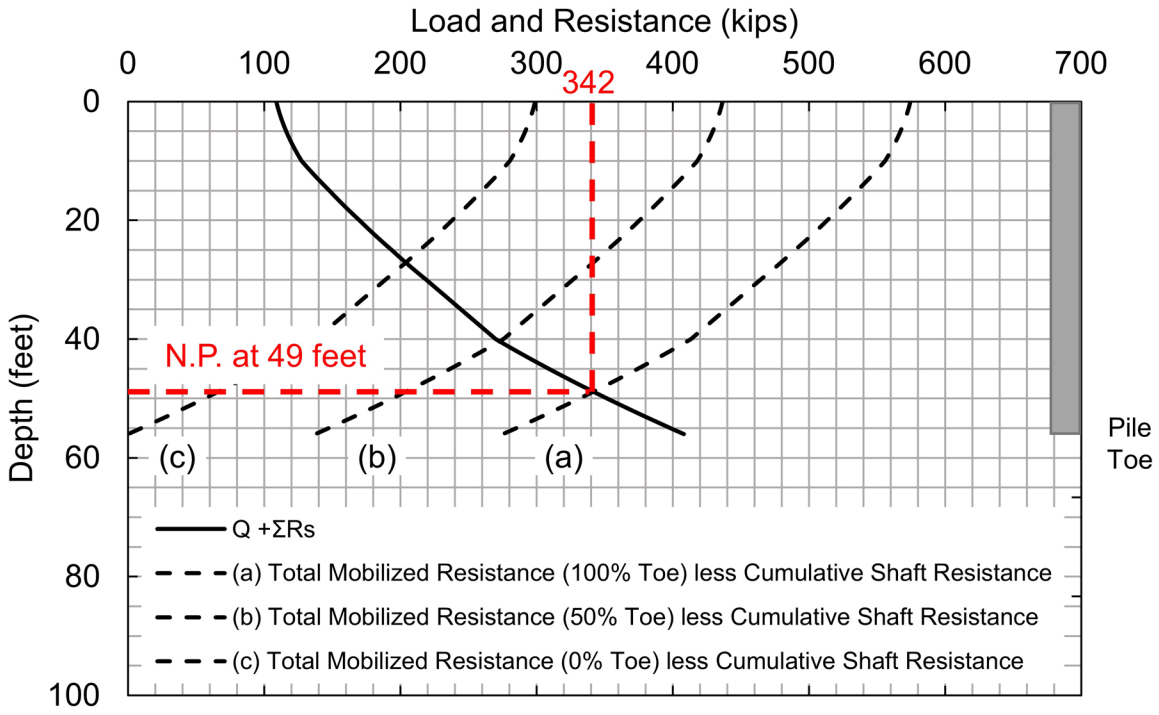

Figure D-79 Neutral plane location considering 100 percent toe mobilization for HP 12x74 at Pier 2.

The resulting unfactored drag force, DF, is the difference between the maximum unfactored axial compression force in the pile, Q_{max}, minus the unfactored permanent load (Q). In this case, the drag force is evaluated for 100 percent toe mobilization.

$$DF = Q_{max} - Q$$

$$DF = (342\ kips) - (109\ kips) = 233\ kips$$

Following this calculation, the structural resistance was checked with Equation 7-70. As discussed in Section 7.3.6 of Chapter 7, a load factor of 1.25 is applied to

the permanent load while a load factor of 1.1 is applied to the drag force. For H-piles which may be subject to damage during driving and require pile toe protection (i.e., as for piles driven to bedrock or through dense gravel, cobbles, etc.), the structural resistance factor in axial compression, ϕ_c, is 0.5. This applied to the nominal structural resistance of 1043 kips (Table D-46). For this assumption, the factored structural resistance, P_r, for the HP 12x74 section is 521 kips.

$$P_u = 1.25\ (Q) + \gamma_p(DF) < P_r \qquad \text{[Eq. 7-70]}$$

$$P_u = 1.25\ (109\ kips) + 1.1(233\ kips) = 393\ kips$$

$$393\ kips < 521\ kips$$

In this case, the factored structural resistance is greater than the factored load, and therefore the pile section is acceptable. It may be beneficial to review the ratio of the factored load to the nominal structural resistance or, P_u / P_n. The following evaluation serves to back calculate the minimum required structural resistance factor, $\phi_{c(\min)}$, for the section to be acceptable considering the factored load.

$$\phi_{c(\min)} = \frac{P_u}{P_n}$$

$$\phi_{c(\min)} = \frac{(393\ kips)}{(1043 kips)}$$

$$\phi_{c(\min)} = 0.38$$

The neutral plane and drag force analysis was also performed for each candidate pile section considering 100 percent toe mobilization. Factored structural resistance was subsequently evaluated considering the factored loads for group configurations shown in Table D-61. The pile penetration depth utilized for the structural resistance check was the required minimum penetration depth presented in Table D-80. Table D-82 presents the ratio of the factored load to nominal structural resistance, at the pile toe, for the all the candidate piles and group configurations. For H-piles which may be subject to damage during driving and require pile toe protection (i.e., as for piles driven to bedrock or through dense gravel, cobbles, etc.), the structural resistance factor in axial compression, ϕ_c, is 0.5. A review of Table D-82 shows several unacceptable candidate sections and group configurations. The HP 10x42 section is not acceptable in any group configuration, while the HP12x53 is not acceptable in Group Configuration 4 or 5. In a similar manner, the HP 12x74 section is not acceptable in Group Configuration 4.

Table D-82 Ratio of Factored Load to Nominal Structural Resistance in Axial Compression, $\phi_{c(\min)}$, at the Pile Toe

Group Configuration	HP 10x42 $\phi_{c(\min)}$	HP 12x53 $\phi_{c(\min)}$	HP 12x74 $\phi_{c(\min)}$	HP 14x89 $\phi_{c(\min)}$	HP 14x117 $\phi_{c(\min)}$
4	0.74*	0.68*	0.51*	0.50*	0.39*
5	0.66*	0.62*	0.49*	0.46*	0.37*
6	0.66*	0.38	0.26	0.38	0.27

Note: * - pile toe on rock.

For each combination, the ratio of the factored load to nominal structural resistance was also independently evaluated at the neutral plane. Table D-83 presents the ratio of the factored load to nominal structural resistance at the neutral plane

Table D-83 Ratio of Factored Load to Nominal Structural Resistance in Axial Compression, $\phi_{c(\min)}$, at the Neutral Plane

Group Configuration	HP 10x42 $\phi_{c(\min)}$	HP 12x53 $\phi_{c(\min)}$	HP 12x74 $\phi_{c(\min)}$	HP 14x89 $\phi_{c(\min)}$	HP 14x117 $\phi_{c(\min)}$
4	0.74*	0.68*	0.51*	0.50*	0.39*
5	0.66*	0.62*	0.49*	0.46*	0.35
6	0.66*	0.49	0.38	0.36	0.27

Note: * - neutral plane on rock.

Based on results of the drag force analysis, a candidate pile section may be eliminated from consideration if the factored loads are higher than the factored structural resistance. As noted in Table D-84, the larger candidate pile sections remained acceptable including drag force consideration.

Table D-84 Does Candidate Pile Section Meet Structural Resistance Requirement Considering Drag Force Associated with Minimum Pile Penetration Depth?

Group Configuration	HP 10x42	HP 12x53	HP 12x74	HP 14x89	HP 14x117
1	No	No	No	Yes	Yes
2	No	No	Yes	Yes	Yes
3	No	Yes	Yes	Yes	Yes

D.30 Decision 18: Does Estimated Total Settlement and Differential Settlement Between Adjacent Substructure Locations Satisfy Requirements and Angular Distortion Limits?

The North Abutment and Pier 2 have now been preliminarily designed and the estimated vertical deformations computed for both locations.

The vertical deformation limits and construction point concept detailed in Section 7.3 of Chapter 7 was used to first calculate tolerable differential settlement based upon angular distortion. Using Equation D-1, the angular distortion between substructure supports is limited to 0.004 radians, and for a 100 ft span on a multispan bridge, this equates to 4.8 inches of tolerable differential settlement.

Determine tolerable differential settlement, S_d, between substructure supports.

L_s = span length, 100 feet.
A = angular distortion limit, 0.004 radians (Table 7-18).

$$S_d = A * L_s \qquad \text{Eq. D-7}$$

$$S_d = (0.004) * (100\ feet) * \left(\frac{12\ inches}{1\ foot}\right)$$

$$S_d = 4.8\ inches$$

Although this differential settlement is tolerable for angular distortion, project performance requirements limited the settlement at each substructure location to a maximum of 1.5 inches, the differential settlement between adjacent substructure locations limited to 1.0 inch, an a maximum angular distortion of 0.0008 radians. These requirements were established for rideability, drainage, and attached utility damage considerations. The estimated substructure performance is summarized in Table D-85.

Table D-85 Summary of Foundation Total Settlement, Differential Settlement, and Angular Distortion

Substructure Location	Settlement Method	Total Settlement (inches)	Differential Settlement (inches)	Span Length (feet)	Angular Distortion
N. Abutment	N. Plane	1.17			
			0.18	100	0.0002
Pier 2	N. Plane	0.99			

The total settlement, differential settlement, and angular distortion for the two substructures designed so far are acceptable.

D.31 Block 19: Pier 2 – Evaluate Economics of Candidate Piles, Preliminary Group Configurations, and Other Factors

Until now, the design process has served to compare strength and service limits for several candidate pile types within trial group configurations. Some candidate pile types have not met all of the strength, service, or drivability requirements. It is useful to quickly review the suitable and unsuitable pile types and group configurations and then assess the cost of the viable foundation solutions.

Table D-86 summarizes the established minimum pile penetration depth based on analysis results from Blocks 12 through 15. For the candidate pile sections and group configurations at Pier 2, the established minimum pile penetration depth was, in some cases, based on meeting tolerable vertical deformations, and in other cases, based on satisfying the geotechnical resistance demand.

Several candidate sections did not meet structural resistance requirements for axial loading, lateral loading or both. The candidate pile sections and/or group configurations not meeting design requirements are identified with an asterisk in Table D-86. For all three group configurations, the HP 10x42 section did not meet all structural resistance requirements. In a similar manner, the HP 12x53 pile section is unacceptable in Group Configuration 4 or 5 and the HP 12x74 pile section is unacceptable in Group Configuration 4. These candidate pile sections and group configurations will therefore be eliminated for the final design.

Table D-86 Established Minimum Pile Penetration Depth at Pier 2

Group Configuration	HP 10x42 (feet)	HP 12x53 (feet)	HP 12x74 (feet)	HP 14x89 (feet)	HP 14x117 (feet)
4	60*	60*	60*	60	60
5	60*	60*	60	60	60
6	60*	58	56	52	49

Note: * - Did not meet structural resistance requirement.

Table D-87 presents the estimated minimum penetration depth for each candidate section to meet the factored geotechnical resistance requirements at the Strength V limit state. The larger pile sections require less pile penetration depth than the smaller pile sections to provide the same geotechnical resistance. In addition, the factored load per pile decreases from Group Configuration 4 to Group Configuration 6. However, from the analyses in Blocks 13 through 15, the established minimum penetration depth to preclude unacceptable vertical deformation requires all piles to be driven deeper than the depth needed for their factored geotechnical resistance. The minimum penetration depth requirement results in the additional geotechnical resistance gained by further pile embedment to be essentially wasted and therefore uneconomical.

Table D-87 Estimated Minimum Penetration Depth for Factored Geotechnical Resistance at Strength V Limit State

Group Configuration	HP 10x42 (feet)	HP 12x53 (feet)	HP 12x74 (feet)	HP 14x89 (feet)	HP 14x117 (feet)
4	60*	60*	60*	50	47**
5	60*	46*	44**	40**	40**
6	57*	42**	41**	40**	40**

Note: * - Did not meet structural resistance requirement.
Note: ** - Must be driven deeper to meet deformation requirements (Table D-80).

Reference should be made to Block 19 of the North Abutment for a discussion of individual pile cost. However Figure D-80 again presents the individual pile cost versus depth.

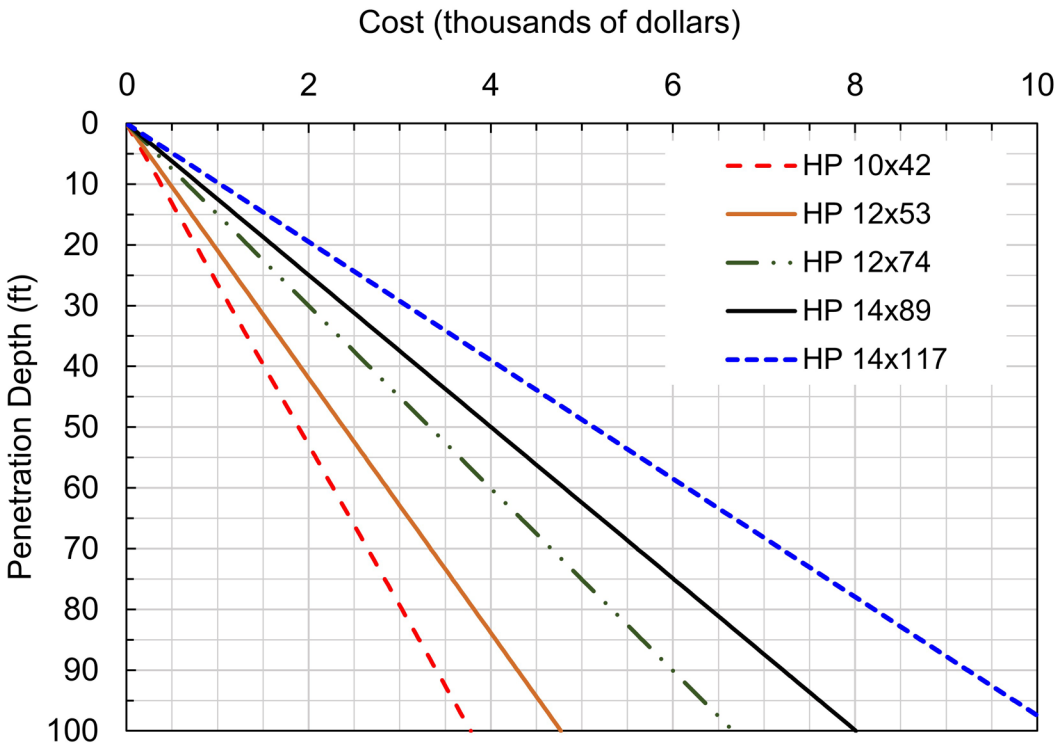

Figure D-80 Pile cost versus penetration depth.

Table D-88 shows the price per pile at Pier 2 with consideration of the established minimum pile penetration depth. For example, for the HP 12x 74 pile section in Group Configuration 6, the individual cost is determined by multiplying the cost per foot by the penetration depth. At the minimum pile penetration depth of 56 feet, the cost per pile is $3,730. To note, there will be additional pile length embedded in the cap, however for pile cost estimation it can be considered negligible. Furthermore Table D-89 shows the pile group cost reflecting the cost per pile and number of piles in the group.

Table D-88 Cost per Pile at Established Minimum Penetration Depth for Piles Meeting Structural Requirements

Group Configuration	HP 12x53	HP 12x74	HP 14x89	HP 14x117
4	-	-	$4,806	$6,156
5	-	$3,996	4,806	6,156
6	$2,767	3,730	4,165	5,027

Table D-89 Pile Group Cost at Established Minimum Penetration Depth for Piles Meeting Structural Requirements

Group Configuration	Number of Piles	HP 12x53	HP 12x74	HP 14x89	HP 14x117
4	15	-	-	$72,090	$92,340
5	20	-	$79,920	96,120	123,120
6	20	$55,332	74,600	83,304	100,548

Based upon this comparison, the HP 14x117 pile section proves to be least economical. Conversely, based upon pile cost alone, the HP 12x53 pile section in Group Configuration 6 appears to be the most economical, followed by the HP 14x89 in Group Configuration 4 and the HP 12x74 pile section in Group Configuration 6. Before selecting the lowest cost option solely considering the results in Table D-89, the cost of the pile cap should also be factored into the foundation cost, as discussed below.

Section 8.9 of Chapter 8 outlines a procedure to estimate the total pile cap thickness. Equation 8-77 is used to estimate this value along using the factored load per pile at the Strength limit state as previously presented in Table D-61. A sample calculation is shown for the HP 12x74 pile in Group Configuration 6, while tabulated results for each pile section and pile group permutation are presented in Table D-90.

Estimate the total pile cap thickness:

P_{ui} = maximum single pile factored axial load, Q =323 kips (Group Configuration 6, Table D-61).

$$t_{cap} = \frac{P_{ui}}{12} + 30 \qquad \text{[Eq. 8-80]}$$

$$t_{cap} = \frac{(257\ kips)}{12} + 30$$

$$t_{cap} = 51\ inches$$

Table D-90 Estimated Total Pile Cap Thickness

Group Configuration	HP 12x53 (inches)	HP 12x74 (inches)	HP 14x89 (inches)	HP 14x117 (inches)
4	-	-	65	65
5	-	55	55	55
6	51	51	51	51

Using the estimated total pile cap thickness, the volume of reinforce concrete required to construct the pile cap is determined. Total pile cap width and length values were previously provided in Table D-59. The resulting volume of reinforced concrete for each pile section and pile group permutation is presented in Table D-91 Note that pile cap volume is shown in cubic yards (CY).

Table D-91 Estimated Volume of Reinforced Concrete in Pile Cap

Group Configuration	HP 12x53 (CY)	HP 12x74 (CY)	HP 14x89 (CY)	HP 14x117 (CY)
4	-	-	24.7	24.7
5	-	28.2	28.2	28.2
6	51.8	51.8	51.8	51.8

To estimate the pile cap cost, past pricing information is generally the best guide; however, similar to estimating the pile cost, due to fluctuations in the market price of material and other factors, pile cap costs are subject to change. The cost of the reinforced concrete pile cap, furnished and constructed, is estimated to be $500 /CY. Using this estimated value, the volumes presented in Table D-91 were used to estimate the cost of the various reinforced concrete pile caps. The pile cap cost for each candidate section and group configuration permutation is shown in Table D-92.

Table D-92 Estimated Cost of Reinforced Concrete Pile Cap

Group Configuration	HP 12x53	HP 12x74	HP 14x89	HP 14x117
4	-	-	$12,331	$12,331
5	-	$14,110	14,110	14,110
6	$25,887	25,887	25,887	25,887

By adding the cost of the pile cap and piles for each permutation, the estimated total foundation cost is determined as presented in Table D-93. Additional construction costs should be accounted for such as excavations or required pile installation aides, however an exhaustive analysis is not presented in this design example. Considering both the pile and the pile cap costs, the HP 14x89 pile section in Group Configuration 4 is the more economical option.

Table D-93 Estimated Foundation Cost Including Piles and Pile Cap at Pier 2

Group Configuration	HP 12x53	HP 12x74	HP 14x89	HP 14x117
4	-	-	$84,421	$104,671
5	-	$94,030	110,230	137,230
6	$81,219	100,479	109,191	126,435

While the cost of pile over/underrun was evaluated at the North Abutment to account for inaccuracies in the assumed soil strength properties and estimated soil resistance, evaluation was not performed at Pier 2. Depending on the pile section and group configuration, piles must be driven to bedrock, or within 5 to 10 feet of bedrock, to satisfy tolerable deformations. These small variations, considering the total number of piles, reduce the risk of length over/underrun differences between the candidate sections. A further economic assessment is therefore not performed.

D.32 Decision 20: Is the Preliminary Design of All Substructure Foundations Complete?

No. The preliminary foundation design has been completed for the North Abutment and the Pier. The preliminary design needs to be completed for the South Abutment. Return to Block 9 and begin the preliminary design for the next substructure location.

D.33 Block 9: South Abutment – For all Candidate Piles, Calculate Nominal and Factored Structural Resistances

The nominal structural resistance is once again reviewed for the five candidate H-pile sections. The H-pile sections selected for evaluation at the South Abutment once again include a HP 10x42, a HP 12x53, a HP 12x74, a HP 14x89 and a HP 14x117. The piles at the South Abutment have the same unsupported length as those at the North Abutment. Therefore, the nominal structural resistances at the South Abutment are unchanged from those determined previously at the North Abutment. A detailed step by step example for calculation of the nominal structural resistance was previously presented in Section 8.5.3 for an HP 14x117 H-pile section. Therefore, this process is not repeated for the five candidate pile sections. Table D-94 once again presents the calculated nominal structural resistances in axial compression, flexure, and shear for the five candidate sections. An unbraced length of 1 foot was assumed in these calculations.

Table D-94 Nominal Structural Resistances in Axial Compression, Flexure and Shear

H-pile Section	HP 10x42	HP 12x53	HP 12x74	HP 14x89	HP 14x117
P_n, Nominal Resistance in Axial Compression (kips)	618	767	1088	1303	1718
M_{ny}, Nominal Resistance in Weak Axis Flexure (kip-ft)	82	114	118	257	380
M_{nx}, Nominal Resistance in Strong Axis Flexure (kip-ft)	176	295	433	592	807
$V_{n,}$ Nominal Resistance in Shear (kips)	118	149	214	246	331

At this time it has not been determined whether the piles at the South Abutment will be terminated in the very stiff clay or driven to bedrock. If driven to rock, pile shoes may be recommended to reduce the risk of damage. In this scenario, the applicable resistance factor, ϕ_c, would be 0.5 for resistance in axial compression. If terminated in the overlying clay where damage is unlikely to occur during driving, the applicable resistance factor, ϕ_c, would be 0.6 for resistance in axial compression. In any case, for combined resistance in axial compression and flexure (typically above fixity), the applicable resistance factor, ϕ_c, is 0.7. A resistance factor of ϕ_v =1.0 is used for shear, and a resistance factor of ϕ_f=1.0 is applicable for flexure only. Table D-95 summarizes the calculated factored structural resistances in axial compression, combined axial compression and flexure, flexure, and shear.

Table D-95 Factored Structural Resistance in Axial Compression, Flexure and Shear

H-pile Section	HP 10x42	HP 12x53	HP 12x74	HP 14x89	HP 14x117
P_r, Factored Resistance in Axial Compression, ϕ_c = 0.5 (kips)	309	383	544	652	859
P_r, Factored Resistance in Axial Compression and Flexure, ϕ_c = 0.7 (kips)	433	537	762	912	1203
M_{ry}, Factored Resistance in Weak Axis Flexure, ϕ_f=1.0 (kip-ft)	82	114	118	257	380
M_{rx}, Factored Resistance in Strong Axis Flexure, ϕ_f=1.0 (kip-ft)	176	295	433	592	807
V_r, Factored Resistance in Shear ϕ_v =1.0 (kips)	118	149	214	246	331

D.34 Block 10: South Abutment – For All Candidate Piles, Calculate Nominal and Factored Geotechnical Resistances in Axial Compression and Tension versus Depth. Perform Preliminary Pile Drivability Analyses

The engineering properties of the subsurface materials at the South Abutment were determined in Block 5. The results of the boring program and laboratory tests are now used to develop a design profile the South Abutment. Engineering judgement was used in developing the design profile to delineate the subsurface conditions into layers with similar properties. An effective stress diagram, depicted in Figure D-81, was then developed for this soil profile. This diagram includes the total stress, porewater pressure and effective stress versus depth. Figure D-81 also presents the basic soil profile for quick reference to the relevant soil layers. The effective stress diagram was computed using Equations 5-7 through 5-9 from Chapter 5. These equations are repeated below. For Figure D-81, the total stress, porewater pressure and effective stress were calculated at 1 foot increments using a spreadsheet.

$$\sigma_{vo} = \sum_i^n (\gamma_i h_i) \quad \text{[Eq. 5-7]}$$

$$u = \gamma_w h_w \quad \text{[Eq. 5-8]}$$

$$\sigma'_{vo} = \sum_i^n (\gamma_i h_i) - \gamma_w h_w \quad \text{[Eq. 5-9]}$$

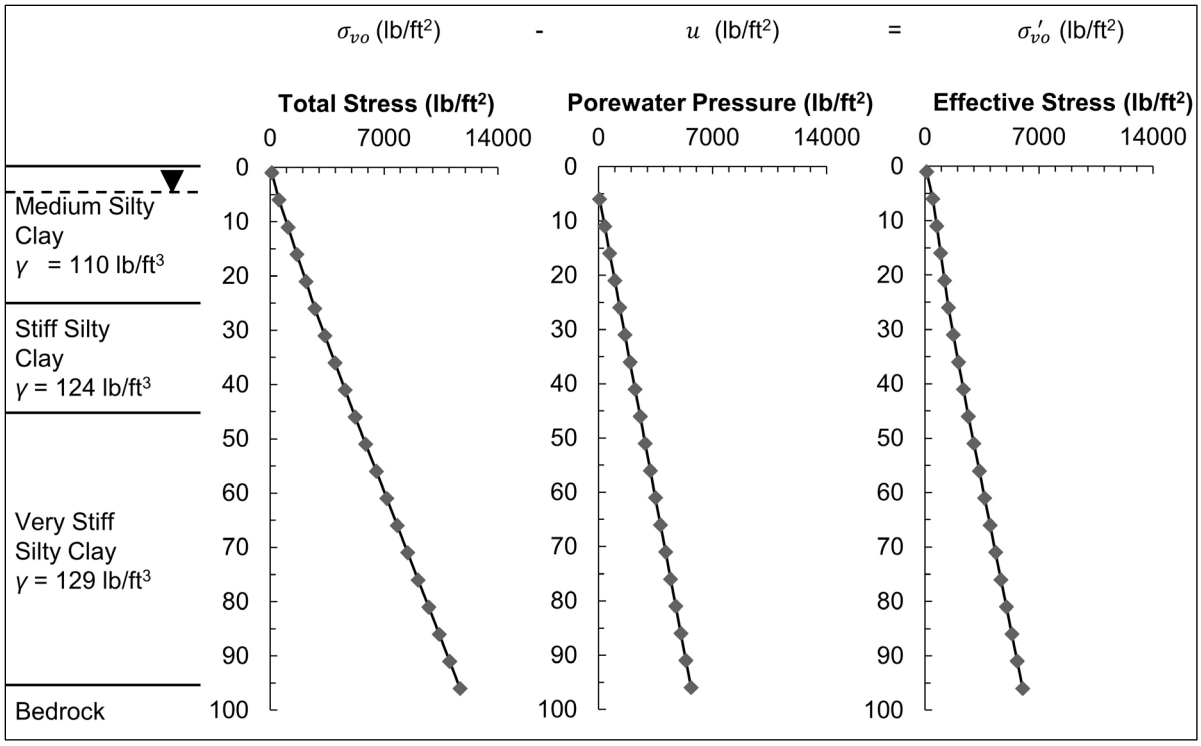

Figure D-81 Effective stress diagram for the South Abutment using Boring S-3.

As indicated by soil boring S-3 (Figures D-4), the soil conditions at the South Abutment consist of silty clay to a depth of 96 feet where bedrock is encountered. Unconfined compression strength tests were performed on each undisturbed cohesive soil sample. The undrained shear strength was then calculated by dividing the unconfined compression strength by 2.

Figure D-82 presents a plot of the undrained shear strength versus depth for the South Abutment soils. As illustrated, the undrained shear strength has distinct changes in undrained shear strength that can be used to identify three distinct soil layers and the layer boundaries. The undrained shear strength also increases approximately linearly with depth within each layer.

Table D-96 summarizes the undrained shear strength values for Soil Layer 1 as well as sublayers a through e. Similarly, Table D-97 and Table D-98 present the undrained shear strength values for Soil Layer 2 and Soil Layer 3 respectively, as well as the individual sublayers.

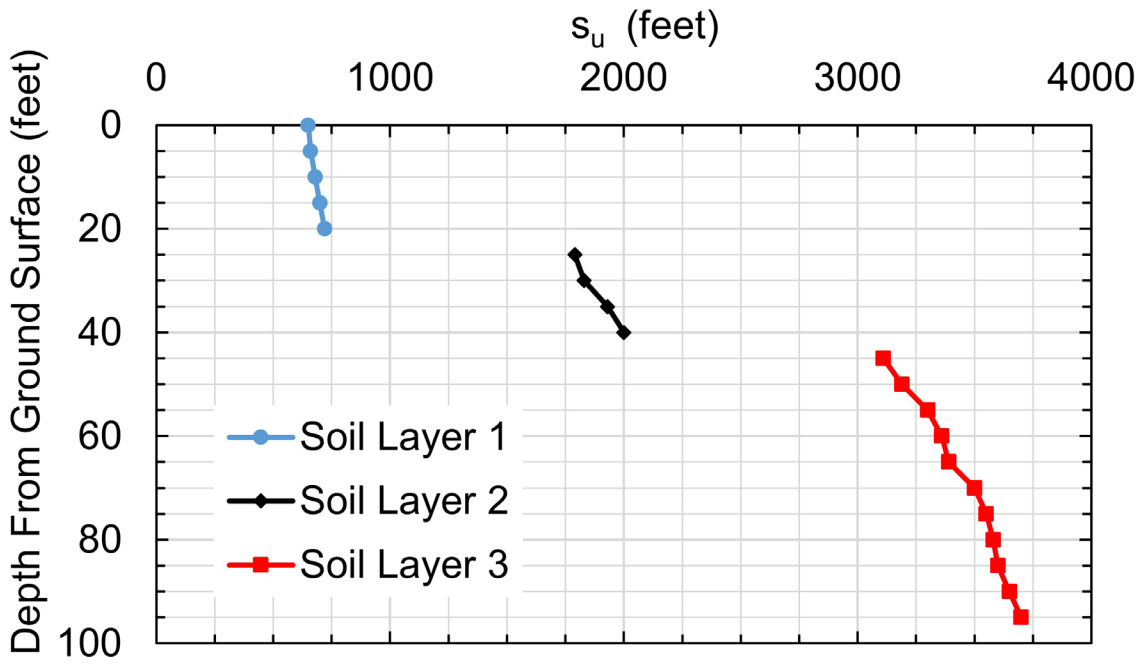

Figure D-82 Undrained shear strength, s_u, versus depth at the South Abutment.

Table D-96 Undrained Shear Strength, s_u, for Soil Layer 1 at the South Abutment

Soil Layer	Sample Depth (ft)	σ'_{vo} (ksf)	q_u (tsf)	s_u (ksf)
1a	1	0.110	0.650	0.650
1b	6	0.488	0.660	0.660
1c	11	0.726	0.680	0.680
1d	16	0.964	0.700	0.700
1e	21	1.202	0.720	0.720

Table D-97 Undrained Shear Strength, s_u, for Soil Layer 2 at the South Abutment

Soil Layer	Sample Depth (ft)	σ'_{vo} (ksf)	q_u (tsf)	s_u (ksf)
2a	26	1.440	1.79	1.79
2b	31	1.748	1.83	1.83
2c	36	2.056	1.93	1.93
2d	41	2.364	2.00	2.00

Table D-98 Undrained Shear Strength, s_u, for Soil Layer 3 at the South Abutment

Soil Layer	Sample Depth (ft)	σ'_{vo} (ksf)	q_u (tsf)	s_u (ksf)
3a	46	2.672	3.11	3.11
3b	51	3.005	3.19	3.19
3c	56	3.338	3.30	3.30
3d	61	3.671	3.36	3.36
3e	66	4.004	3.39	3.39
3f	71	4.337	3.50	3.50
3g	76	4.670	3.55	3.55
3h	81	5.003	3.58	3.58
3i	86	5.336	3.60	3.60
3j	91	5.669	3.65	3.65
3k	96	6.002	3.70	3.70

The design soil profile for the South Abutment is presented in Figure D-83. The bottom of pile cap (Elev. 305 feet) is 5 feet below ground surface. Some soil properties in the design soil profile such as the initial cyclic modulus of subgrade reaction, $k_{c,}$ have been selected based on published correlations in the absence of laboratory testing. For this particular soil profile, the initial cyclic moduli of subgrade reaction was selected based on the values given in Table 7-22 which are delineated by soil shear strength. Similarly, the 50% strain factor, $\varepsilon_{50,}$ was estimated based upon the values given in Table 7-21 which vary by soil shear strength. If piles will be driven to bedrock, strength properties of the limestone bedrock are needed. These rock parameters obtained from laboratory tests on recovered rock core samples are summarized in Table D-99.

Table D-99 Laboratory Determined Properties of Limestone Bedrock

Effective Unit Weight (kcf)	Undrained Shearing Resistance, s_u (ksf)	Friction Angle, ϕ (degrees)
0.165	476	35.5

D.34.1 Geotechnical Resistance in Axial Compression

The nominal geotechnical resistance in axial compression is now calculated for the selected candidate H-pile sections. The nominal geotechnical resistance can be calculated by hand or with computer software using an appropriate analysis method

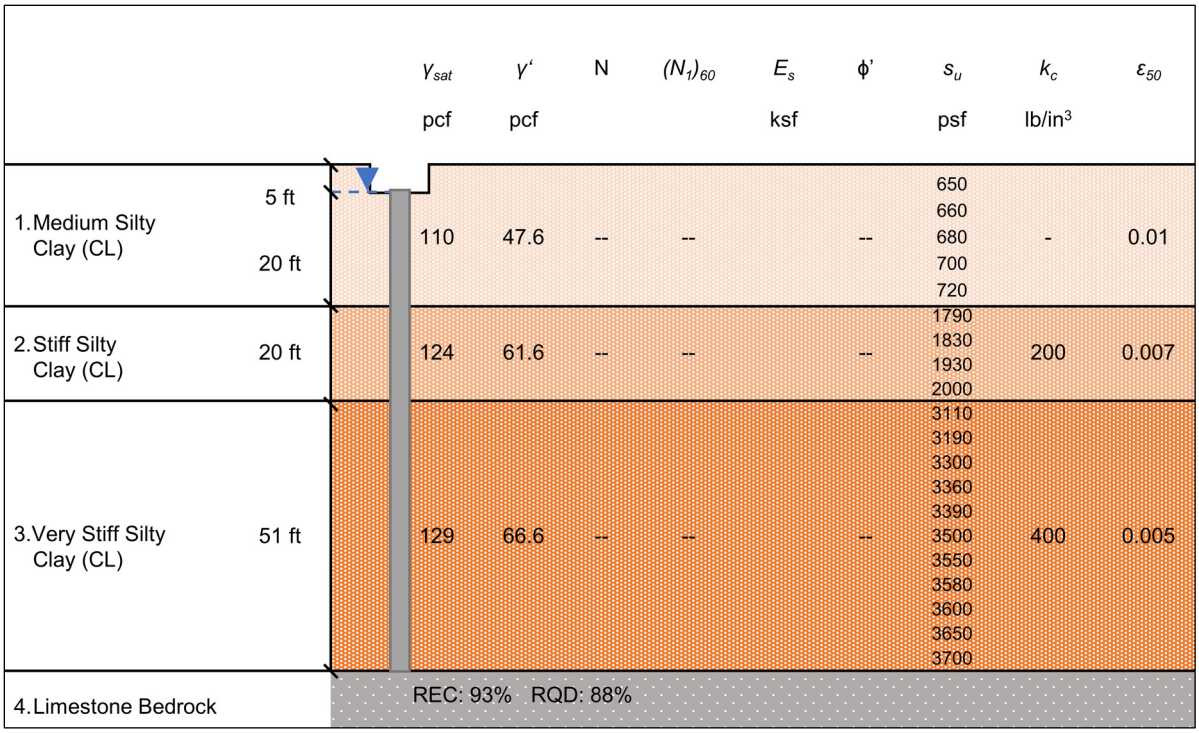

Figure D-83 Design soil profile at the South Abutment.

based upon soil, rock, and pile type. Chapter 7 describes appropriate methods for this purpose as well as computer programs available at the time of this manual's publication.

For this abutment, the DrivenPiles computer program was used to calculate the nominal resistance, shaft resistance, and toe resistance each as a function of depth for each of the five candidate H-piles. For nominal geotechnical resistance calculations, each cohesive sample depth in Soil Layers 1, 2, and 3 was treated as an individual layer with respect to shear strength. This software program was selected since it uses the FHWA recommended alpha method to calculate the nominal geotechnical resistance of H-piles in cohesive soils. A summary of the shaft, toe, and nominal geotechnical resistance is presented for the HP 12x74 H-pile section in Table D-100. The depth shown is taken from the bottom of pile cap.

In the DrivenPiles program, the selection of the geomaterial is limited to either cohesionless or cohesive soil. Hence, the program cannot calculate the nominal toe resistance on rock and the only choice is either to model rock as a hard cohesive soil or a very dense cohesionless soil. The nominal toe resistance presented in Table D-100 at depth 91.25 feet was not calculated using the DrivenPiles program but rather calculated using the procedure for hard rock presented in Section 7.2.1.4.2 of Chapter 7.

Table D-100 Nominal Shaft, Nominal Toe and Nominal Geotechnical Resistance for HP 12x74 at the South Abutment

Depth (feet)	Nominal Shaft Resistance (kips)	Nominal Toe Resistance (kips)	Nominal Geotechnical Resistance (kips)		Depth (feet)	Nominal Shaft Resistance (kips)	Nominal Toe Resistance (kips)	Nominal Geotechnical Resistance (kips)
0.01	0.02	6.09	6.11		32	116.23	17.81	134.03
1	2.21	6.09	8.3		33	122.25	17.81	140.05
2	4.42	6.09	10.51		34	128.36	17.81	146.16
3	6.63	6.09	12.72		34.99	134.49	17.81	152.3
4	8.85	6.09	14.93		35.01	134.62	18.45	153.07
4.99	11.03	6.09	17.12		36	140.69	18.45	159.14
5.01	11.08	6.27	17.35		37	146.83	18.45	165.28
6	13.35	6.27	19.62		38	152.96	18.45	171.41
7	15.67	6.27	21.95		39	159.1	18.45	177.55
8	18.03	6.27	24.3		39.99	165.17	18.45	183.62
9	20.42	6.27	26.69		40.01	165.28	28.69	193.98
9.99	22.81	6.27	29.08		41	170.34	28.69	199.03
10.01	22.86	6.46	29.32		42	175.44	28.69	204.13
11	25.27	6.46	31.73		43	180.54	28.69	209.24
12	27.75	6.46	34.21		44	185.65	28.69	214.34
13	30.25	6.46	36.71		44.99	190.7	28.69	219.39
14	32.79	6.46	39.25		45.01	190.8	29.43	220.23
14.99	35.34	6.46	41.79		46	195.85	29.43	225.28
15.01	35.39	6.64	42.03		47	200.95	29.43	230.39
16	37.96	6.64	44.6		48	206.06	29.43	235.49
17	40.58	6.64	47.23		49	211.16	29.43	240.59
18	43.24	6.64	49.89		49.99	216.21	29.43	245.64
19	45.94	6.64	52.58		50.01	216.31	30.45	246.76
19.99	48.63	6.64	55.28		51	221.37	30.45	251.81
20.01	48.71	16.51	65.23		52	226.47	30.45	256.92
21	53.96	16.51	70.48		53	231.57	30.45	262.02
22	59.34	16.51	75.85		54	236.68	30.45	267.12
23	64.8	16.51	81.31		54.99	241.73	30.45	272.17
24	70.33	16.51	86.84		55.01	241.83	31	272.83
24.99	75.89	16.51	92.4		56.00	246.88	31	277.88
25.01	76	16.88	92.88		57	251.98	31	282.98
26	81.48	16.88	98.37		58	257.09	31	288.09
27	87.1	16.88	103.99		59	262.19	31	293.19
28	92.8	16.88	109.69		59.99	267.24	31	298.24
29	98.59	16.88	115.47		60.01	267.34	31.28	298.62
29.99	104.39	16.88	121.27		61	272.4	31.28	303.67
30.01	104.51	17.81	122.31		62	277.5	31.28	308.78
31	110.29	17.81	128.1		63	282.6	31.28	313.88

Table D-100 Nominal Shaft, Nominal Toe and Nominal Geotechnical Resistance for HP 12x74 at the South Abutment (Continued)

Depth (feet)	Nominal Shaft Resistance (kips)	Nominal Toe Resistance (kips)	Nominal Geotechnical Resistance (kips)		Depth (feet)	Nominal Shaft Resistance (kips)	Nominal Toe Resistance (kips)	Nominal Geotechnical Resistance (kips)
64	287.71	31.28	318.98		78	359.15	33.03	392.18
64.99	292.76	31.28	324.03		79	364.25	33.03	397.28
65.01	292.86	32.29	325.15		79.99	369.3	33.03	402.33
66	297.91	32.29	330.2		80.01	369.4	33.21	402.62
67	303.01	32.29	335.31		81	374.46	33.21	407.67
68	308.12	32.29	340.41		82	379.56	33.21	412.77
69	313.22	32.29	345.51		83	384.66	33.21	417.88
69.99	318.27	32.29	350.56		84	389.77	33.21	422.98
70.01	318.37	32.75	351.13		84.99	394.82	33.21	428.03
71	323.43	32.75	356.18		85.01	394.92	33.68	428.59
72	328.53	32.75	361.28		86	399.97	33.68	433.65
73	333.63	32.75	366.39		87	405.07	33.68	438.75
74	338.74	32.75	371.49		88	410.18	33.68	443.85
74.99	343.79	32.75	376.54		89	415.28	33.68	448.96
75.01	343.89	33.03	376.92		90	420.33	33.68	454.01
76	348.94	33.03	381.97		91	420.43	33.68	454.11
77	354.04	33.03	387.07		91.25	420.43	1527.00	1947.43

For piles driven to hard rock, the nominal toe resistance should be determined using Equation 7-34 as described in Section 7.2.1.4.2. The strength properties of the limestone bedrock were presented in Table D-99. The unit toe resistance, q_p, of the hard rock can then be calculated using Equation 7-34.

$$q_p = P_s s_u N_c + \gamma D N_q + P_t \gamma \left(\frac{b N_\gamma}{2}\right) \quad \text{[Eq. 7-34]}$$

This computation requires determination of the bearing capacity factors N_c, N_q, and N_γ from Figure D-84. Entering the figure with a friction angle of 35.5 degrees, the bearing capacity factors N_c, N_q, and N_γ, were determined to be 17, 14, and 24, respectively. Because piles will likely be seated on bedrock, the pile penetration into the rock surface is assumed as 0.25 feet.

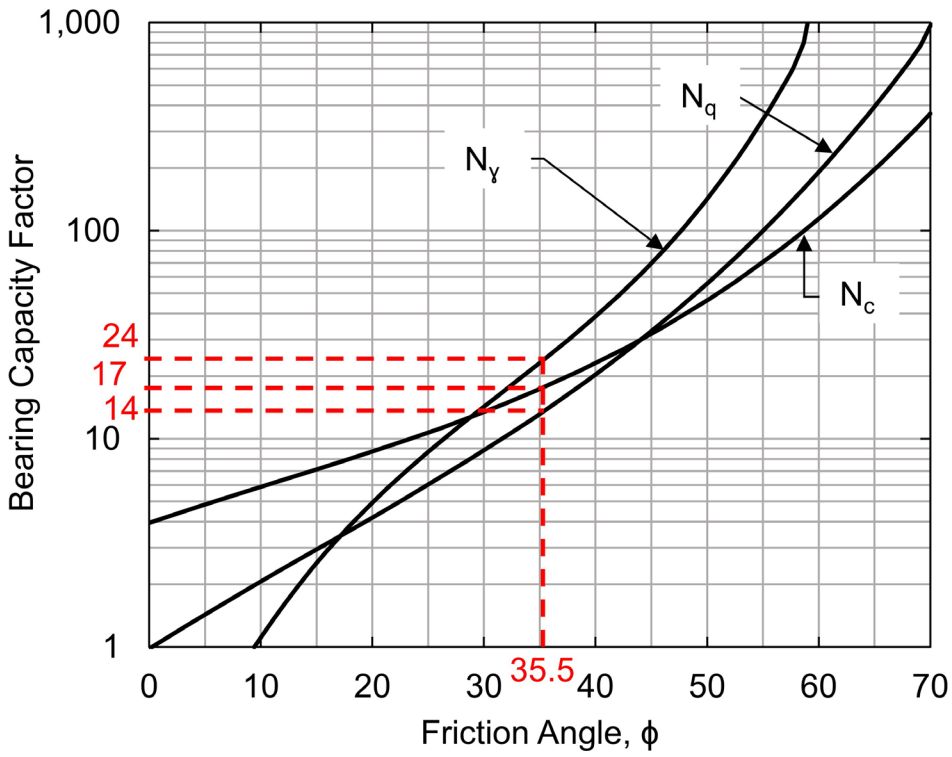

Figure D-84 Bearing capacity factors for foundations on rock.

Equation 7-34 is now used to determine the unit resistance, q_p, of the rock.

s_u = undrained shearing resistance of the rock, 476 ksf.
γ = effective density of the rock mass, 0.165 kcf.
D = pile penetration below the rock surface, assume 0.25 feet.
b = pile width or diameter 1 foot (HP 12x74).
P_s = pile shape factor of 1.25 for square pile toe.
P_t = pile base factor of 0.80 for a square pile toe.
N_c = bearing capacity factor, 17 (Figure D-84).
N_q = bearing capacity factor, 14 (Figure D-84).
N_γ = bearing capacity factor, 24 (Figure D-84).

$$q_p = P_s\, s_u\, N_c + \gamma D\, N_q + P_t\, \gamma \left(\frac{b\, N_\gamma}{2}\right) \qquad \text{[Eq. 7-34]}$$

$$q_p = (1.25) * (476\ ksf) * (17) + (0.165\ kcf) * (0.25\ feet) * (14) + (0.80) * (0.165\ kcf) * \left(\frac{(1\ foot) * (24)}{2}\right)$$

$$q_p = 10{,}117\ ksf$$

For the HP 12x74 pile section with toe area (area of steel, A_s) of 0.151 ft^2, the nominal toe resistance is then calculated as follows:

$$R_p = q_p * A_s$$

$$R_p = (10{,}117\ ksf) * (0.151\ ft^2)$$

$$R_p = 1{,}528\ kips$$

The nominal shaft, nominal toe, and nominal geotechnical resistance are also presented graphically in Figure D-85. A review of Table D-94 indicates the nominal structural resistance for the HP 12x74 section is 1088 kips, which is less than the nominal toe resistance when driven to hard limestone bedrock. Therefore, the nominal structural resistance will control the design. The penetration depth indicated in both Table D-100 and Figure D-85 is referenced from the bottom of footing, which is 5 feet below the original ground surface elevation. The nominal shaft, nominal toe, and nominal geotechnical resistances were calculated for all of the candidate pile sections in a similar manner. The nominal geotechnical resistances in axial compression versus pile penetration depth for all candidate pile types are presented in Figure D-86.

Once the nominal geotechnical resistance in axial compression versus pile penetration depth has been calculated, the factored geotechnical resistance in axial compression versus pile penetration depth can be determined. The factored geotechnical resistance depends on the resistance determination method selected for the design.

If the nominal resistance will be confirmed by a field determination method, the factored geotechnical resistance in axial compression as a function of pile penetration depth can be determined by multiplying the calculated nominal geotechnical resistance at a given depth by the resistance factor associated with the field determination method, ϕ_{dyn}. AASHTO (2014) resistance factors for field resistance determination methods are presented in Table 7-2.

If pile installation will be controlled by driving to a depth determined by static analysis method, then the factored geotechnical resistance in axial compression as a function of pile penetration depth can be determined by multiplying the calculated nominal resistance at a given depth by the resistance factor associated with the static analysis method, ϕ_{stat}. AASHTO (2014) resistance factors for static analysis methods are presented in Table 7-1 of this manual.

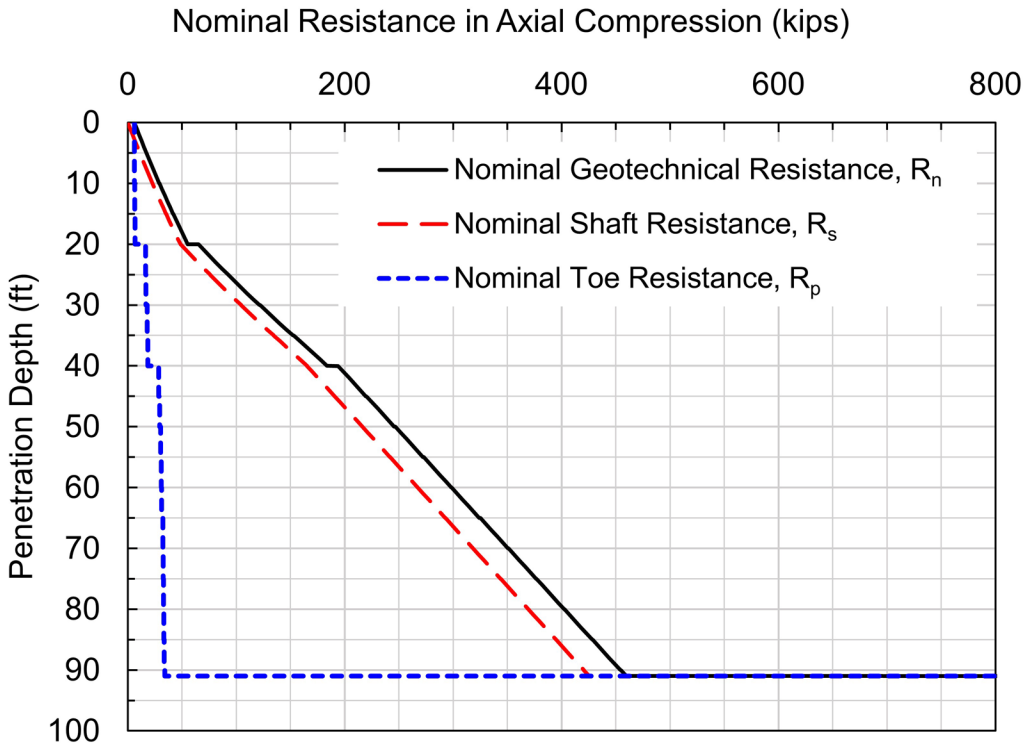

Figure D-85 Nominal geotechnical resistance in axial compression versus pile penetration depth for HP 12x74 at the South Abutment.

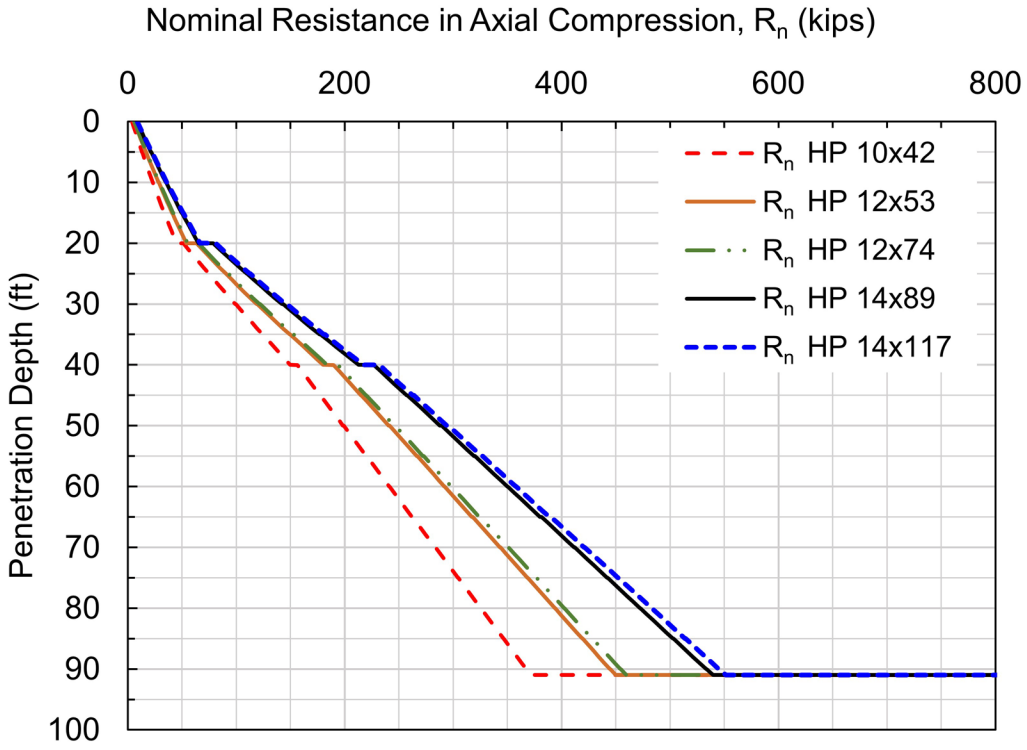

Figure D-86 Nominal geotechnical resistance in axial compression versus pile penetration depth for all candidate pile sections at South Abutment.

Figure D-87 presents a design chart of the nominal and factored geotechnical resistance in axial compression versus depth for the HP 12x74 candidate H-pile section. The design chart includes the nominal geotechnical resistance as well as factored geotechnical resistances based on several resistance determination methods. The factored geotechnical resistance versus penetration depth is plotted for resistance determination by a static load test with dynamic testing of 2% of the piles (ϕ_{dyn}=0.80), by dynamic testing of at least two piles per site condition, but no less than 2% of the production piles, with signal matching (ϕ_{dyn}=0.65), and by wave equation analysis (ϕ_{dyn}=0.50). Also included is the factored geotechnical resistance based on the static analysis method used at the abutment, the alpha method (ϕ_{stat}=0.35). An AASHTO resistance factor is not currently available for the static analysis method used for hard rock. Therefore, the field resistance determination method would control pile installation.

For the HP 12x74 section, Figure D-87 illustrates the effects that the various resistance determination methods have on the pile length required for a given factored compression resistance, the range of factored resistances available from a given pile section, and the potential impact of these factors on the number of piles needed to resist axial compression loads.

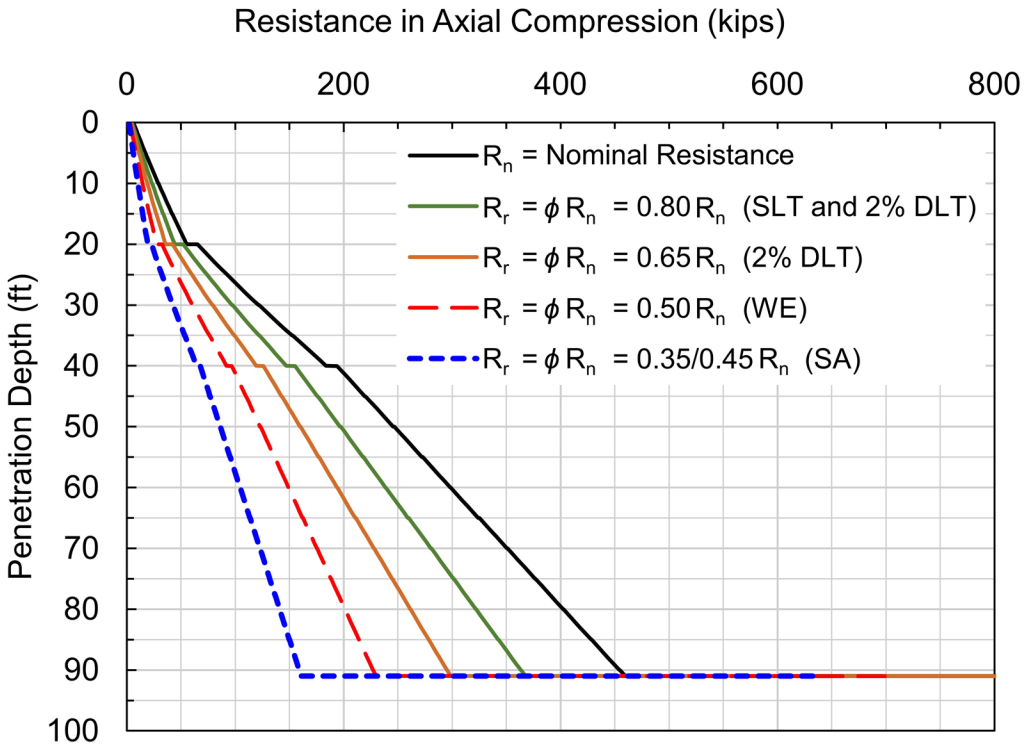

Figure D-87 Design chart of nominal and factored geotechnical resistance in axial compression versus pile penetration depth for HP 12x74 at the South Abutment.

The factored geotechnical resistance in axial compression for all candidate pile sections is presented in Figures D-88 through D-91 based on the same resistance determination method. For all the candidate pile sections, these figures illustrate the effects the various resistance determination methods have on the pile length required for a given factored resistance, the factored resistance available from a given pile section, and the potential impact of these factors on the number of piles needed to resist axial compression loads.

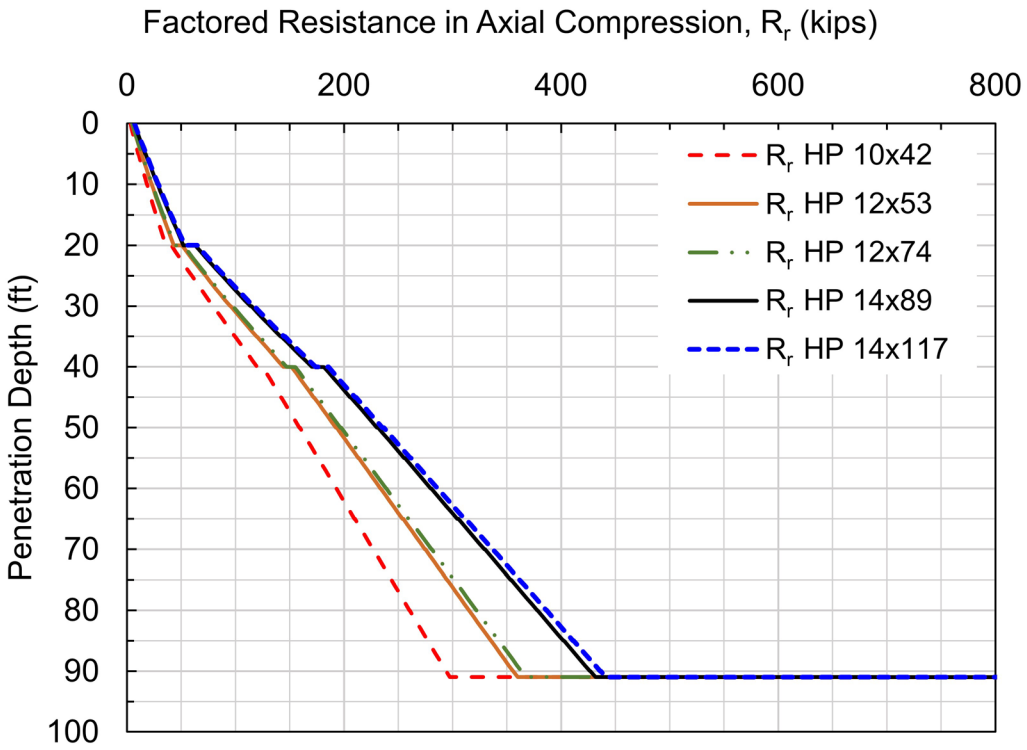

Figure D-88 Factored geotechnical resistance, R_r, in axial compression based on field determination by static load test and dynamic testing 2% of the piles, ϕ_{dyn}=0.80.

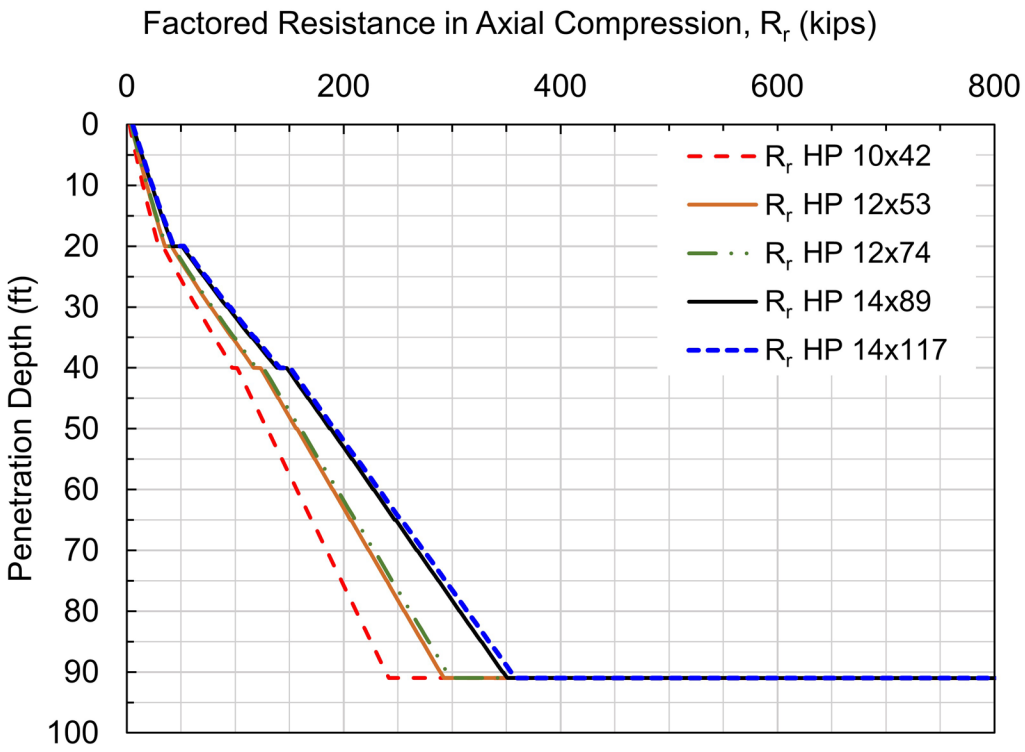

Figure D-89 Factored geotechnical resistance, R_r, in axial compression based on field determination by dynamic testing 2% of the piles, ϕ_{dyn}=0.65.

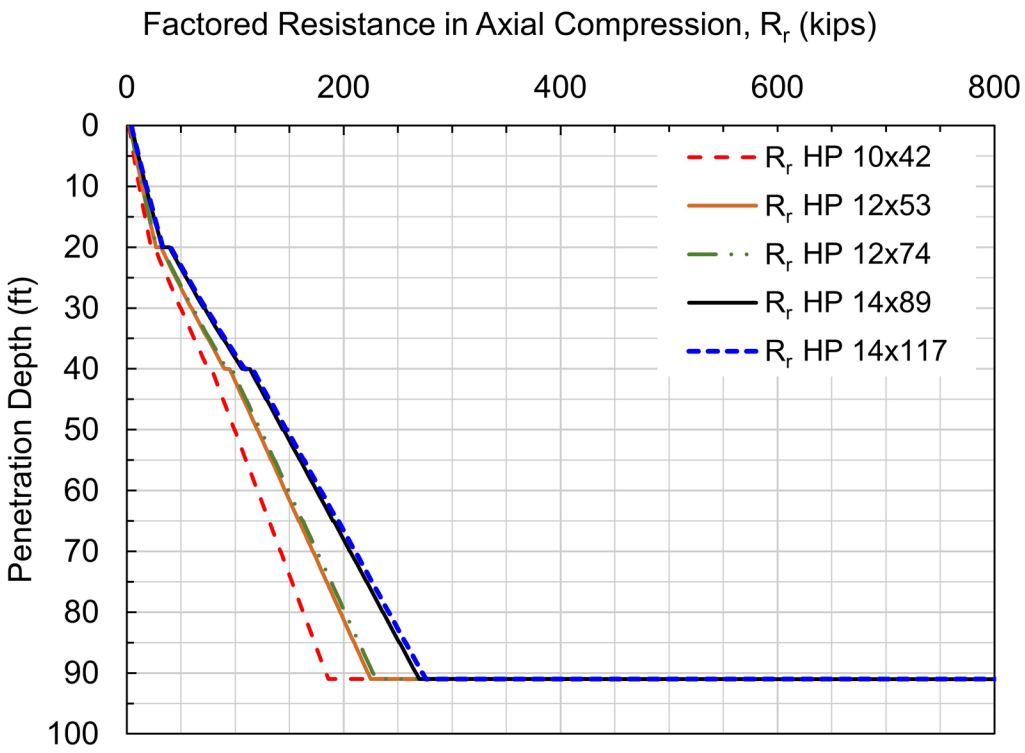

Figure D-90 Factored geotechnical resistance, R_r, in axial compression based on field determination by wave equation analysis, ϕ_{dyn}=0.50.

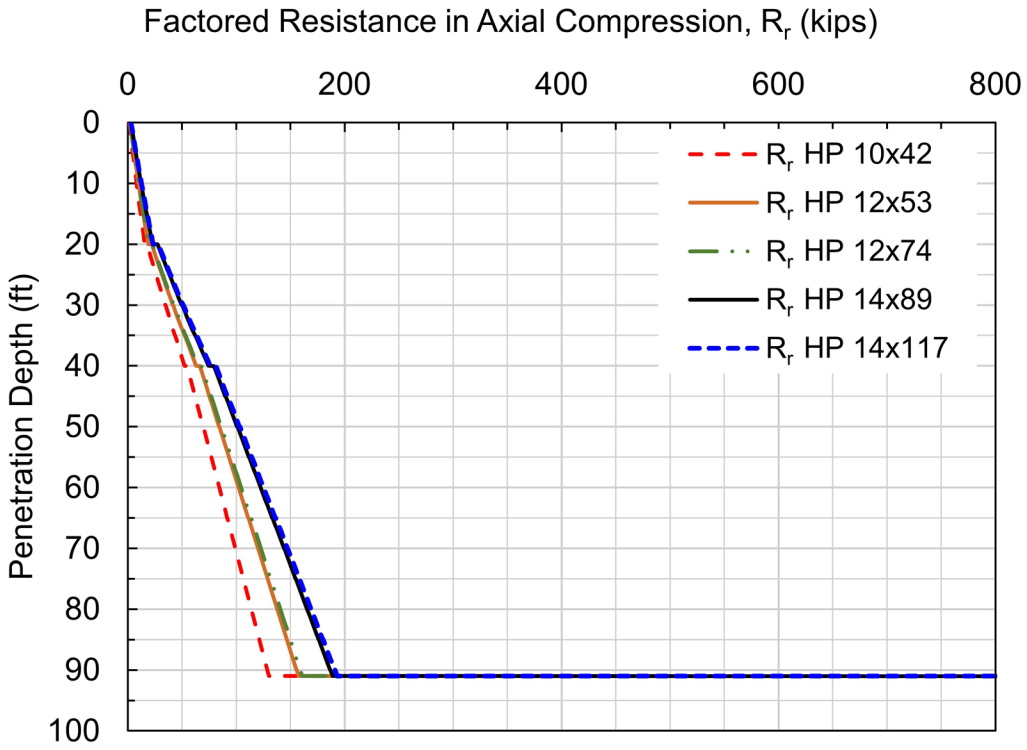

Figure D-91 Factored geotechnical resistance, R_r, in axial compression based on determination using alpha method static analysis, ϕ_{stat}=0.35.

D.34.2 Geotechnical Resistance in Axial Tension (uplift)

In a similar manner, the nominal and factored geotechnical resistances in axial tension (uplift) were calculated using the alpha method and with the DrivenPiles computer program. Figure D-92 presents the nominal shaft resistance versus penetration depth for all the candidate pile sections. As outlined in Section 7.2.3.2.1, the factored resistance in axial tension is the shaft resistance multiplied by the resistance factor, ϕ_{up}, for the resistance determination method.

Figure D-93 presents a design chart of the nominal and factored geotechnical resistance in axial tension versus pile penetration depth for HP 12x74 H-pile section. A resistance factor of 0.60 is used when the tension resistance is determined by a static load test, 0.50 when determined by a dynamic test with signal matching, and 0.25 when determined by the alpha method static analysis. For a single pile section (HP 12x74), this figure illustrates the effects the various resistance determination methods have on the pile length required for a given factored resistance, the factored resistance available from a given pile section, and the potential impact of these factors on the number of piles needed to resist axial tension loads.

Figures D-94 to D-96 present the factored geotechnical resistance in axial tension versus penetration depth based on the field determination method for each of the candidate pile sections. For all the candidate pile sections, these figures illustrate the effects the various resistance determination methods have on the pile length required for a given factored resistance, the factored resistance available from a given pile section, and the potential impact of these factors on the number of piles needed to resist axial tension loads.

A review of the soil profile at the South Abutment indicates no unsuitable soil layers are present that should be ignored for load support. Abutment scour and liquefaction due to a seismic event are also not considerations.

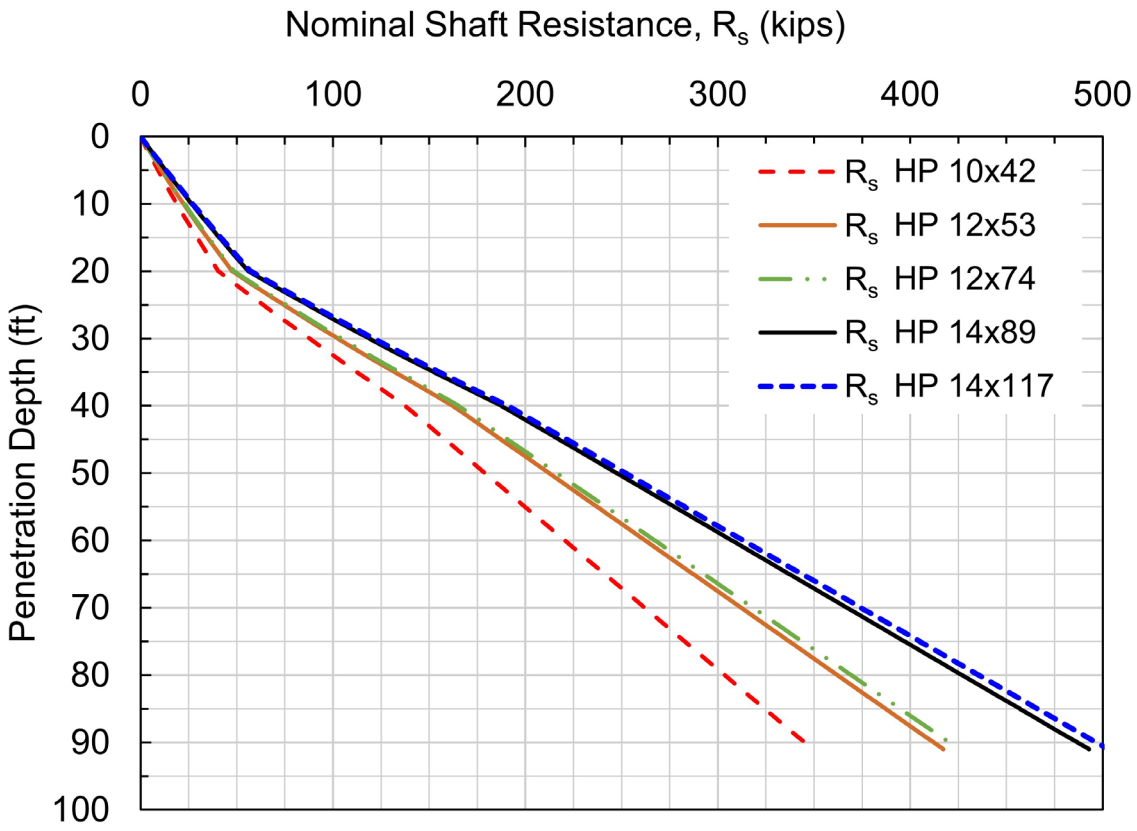

Figure D-92 Nominal shaft resistance versus penetration depth for all candidate pile sections at the South Abutment.

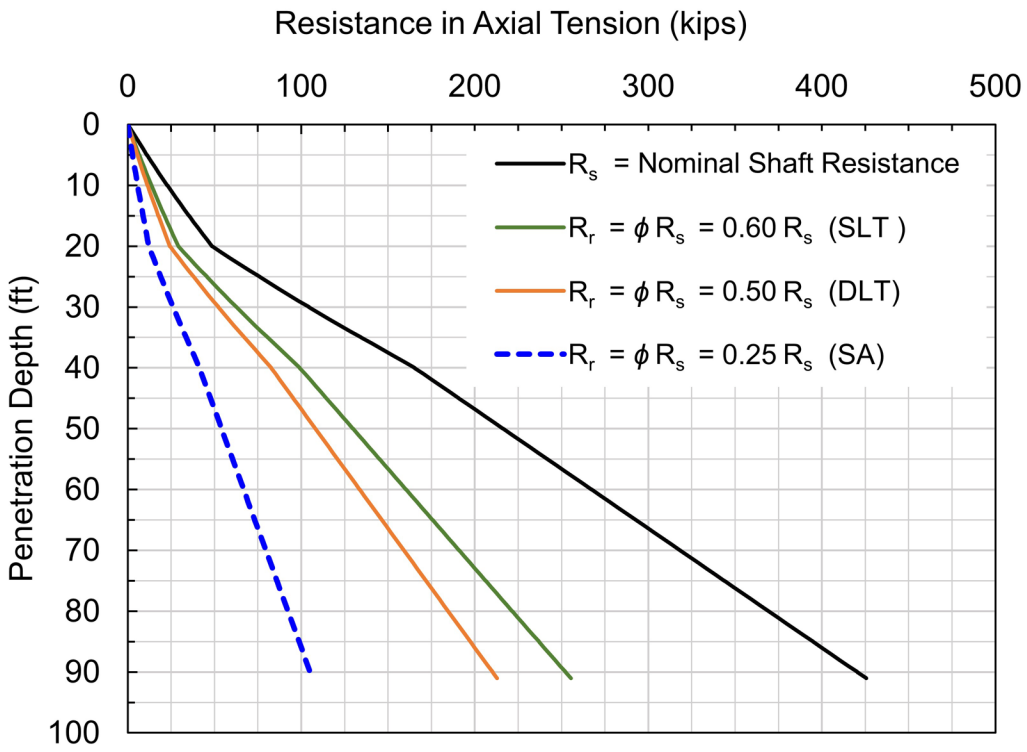

Figure D-93 Design chart of nominal and factored geotechnical resistance in axial tension versus pile penetration depth for HP 12x74 at the South Abutment.

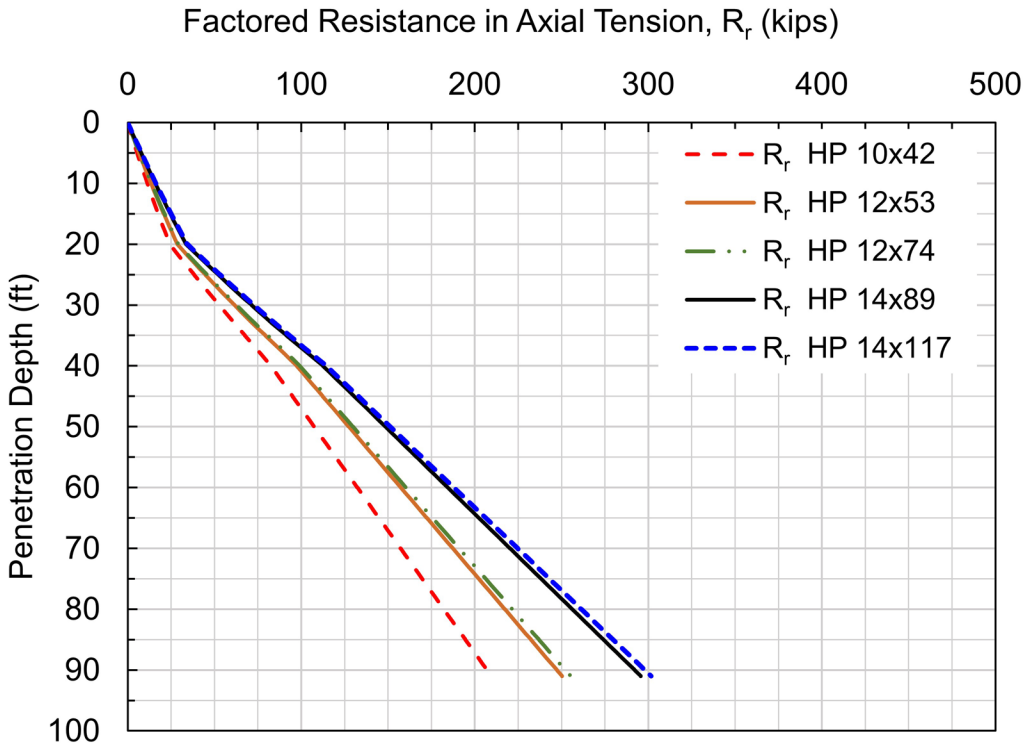

Figure D-94 Factored geotechnical resistance, R_r, in axial tension based on field determination by static load test, ϕ_{dyn}=0.60.

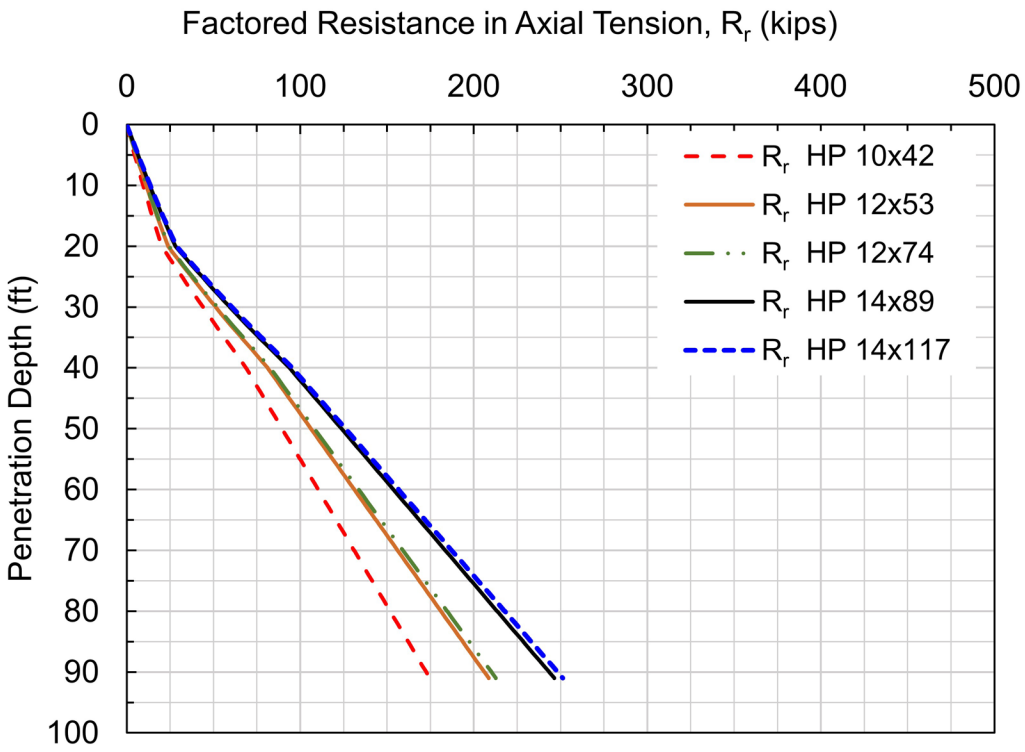

Figure D-95 Factored geotechnical resistance, R_r, in axial tension based on field determination by dynamic testing with signal matching, ϕ_{dyn}=0.50.

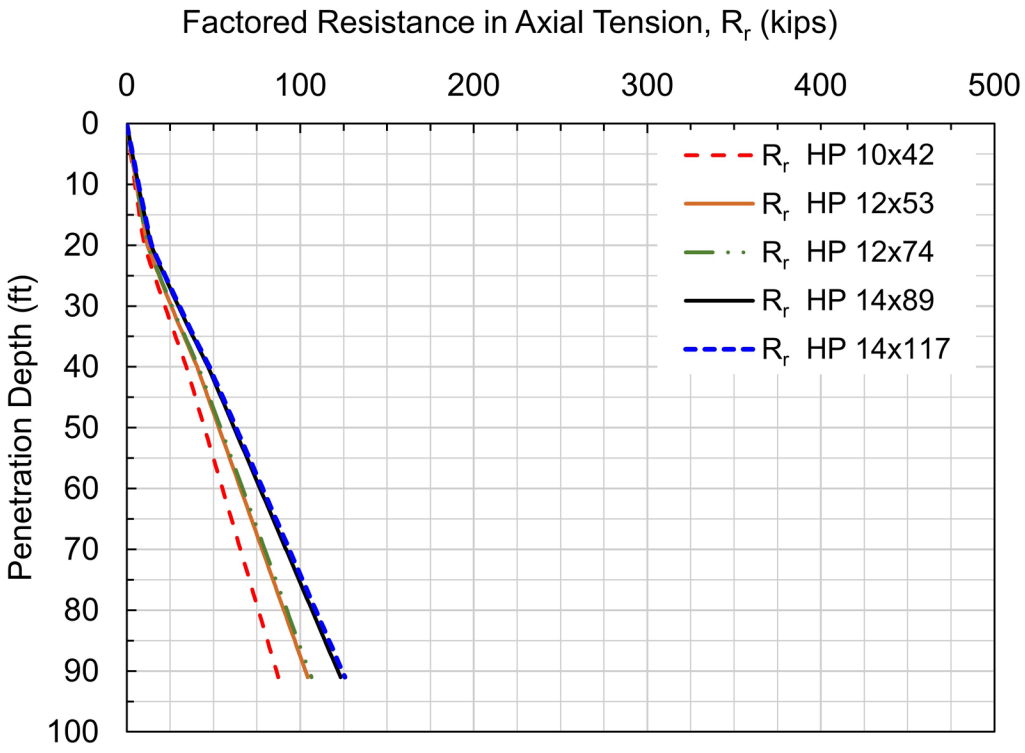

Figure D-96 Factored geotechnical resistance, R_r, in axial tension based on determination using alpha method static analysis, ϕ_{stat}=0.25.

D.34.3 Preliminary Pile Drivability Assessment

Preliminary assessments of pile drivability are now performed at this stage of the design. A drivability check at this time is essential to assess the constructability of candidate pile types and/or sections and to eliminate sections with insufficient drivability. Section 12.4 provides a detailed discussion of wave equation drivability analyses and their applications.

A candidate pile section must be capable of being driven to the nominal driving resistance. In this example, the nominal driving resistance is less than the nominal geotechnical resistance since soil set up will be incorporated into the design. In addition, a candidate pile section must be capable of being driven to the penetration depth necessary to achieve the nominal geotechnical resistance in axial tension, and to a penetration depth necessary to satisfy lateral load demands as well as axial and lateral deformation requirements. A suitably sized pile hammer must be capable of driving the pile to its established minimum penetration depth and to the nominal resistance at a reasonable blow count without exceeding material stress limits. As detailed in Chapter 12, the blow count should be between 30 and 120 blows per foot at the nominal resistance. If the pile cannot be driven within these requirements, a larger pile hammer, a pile section with greater impedance, or pile installation aids such as predrilling or jetting may be required to satisfy or improve drivability.

Driving stresses during pile installation should remain below the driving stress limits tied to pile type and material strength. For the candidate steel H-piles, compression driving stress limits are given by Equation 8-33. As per ASTM A-572 requirements, new steel H-piles are rolled with a minimum yield stress of 50 ksi.

The driving stress limit, σ_{dr}, for candidate pile sections is then calculated as follows:

$$\sigma_{dr} = \varphi_{da}\left(0.9\,F_y\right) \qquad \text{[Eq. 8-33]}$$

Where: φ_{da} = resistance factor, 1.0 for steel piles.
F_y = yield stress, 50 ksi.

Therefore, the driving stress limit, σ_{dr}, is 45 ksi.

$$\sigma_{dr} = (1.0)\left(0.9\,(50\ ksi)\right) = 45\ ksi$$

Drivability analyses were performed for all five candidate pile sections. Since the specific pile hammer is often unknown at this point in the design, a reasonably sized,

commonly available single acting diesel hammer was chosen for each of the candidate pile sections. As noted in Section 15.19, a hammer having a ram weight of 1 to 2% of the larger of the required nominal resistance or required nominal driving resistance often provides a reasonable initial estimate of hammer size for wave equation analysis.

Table D-101 summarizes the factored structural resistance in axial compression, P_r, and the corresponding minimum and maximum nominal driving resistance associated with full section utilization and field determination methods ranging from a static load test with dynamic testing (ϕ_{dyn}=0.80) to the FHWA modified Gates dynamic formula (ϕ_{dyn}=0.40). Given that utilization of the full structural resistance is uncommon for piles driven in soil, a reasonable initial estimate of the trial hammer size for a wave equation drivability analysis is 1 to 1.5% of the minimum R_{ndr}. Driving stresses could exceed specified limits by choosing a hammer with a ram weight significantly larger than 2% of the minimum R_{ndr}. For each pile hammer, the wave equation default values were used for the helmet weight, hammer cushion materials, and the hammer cushion material properties.

Table D-101 Summary of Pile Hammers Used in Drivability Analyses

Pile Section	Pile Cross Sectional Area (in^2)	Factored Structural Resistance, P_r (kips)	Minimum R_{ndr} ϕ_{dyn}=0.80 (kips)	Maximum R_{ndr} ϕ_{dyn}=0.40 (kips)	Ram Weight 1% of Min R_{ndr} (%)	Diesel Model	Ram Weight (kips)	Rated Energy (ft-kips)
HP 10x42	12.4	309	386	773	3.86	D25-52	5.51	62.0
HP 12x53	15.5	383	478	958	4.78	D30-52	6.62	74.4
HP 12x74	21.8	544	680	1360	6.80	D36-52	7.94	89.3
HP 14x89	26.1	652	815	1630	8.15	D46-52	10.14	114.1
HP 14x117	34.4	860	1075	2150	10.07	D50-52	11.03	124.0

For the soil resistance model, the output from DrivenPiles was converted to unit shaft resistance and unit toe resistance values and then input into the wave equation program. Similar soil resistances are thereby calculated versus depth by both the static analysis and wave equation analysis programs.

The dynamic soil properties for each soil layer were chosen in accordance with wave equation program recommendations. Selection of soil quake and damping parameters is discussed in Section 12.6.7. For the South Abutment profile, setup factors of 2.0 were selected for all of the silty clay layers. No setup was considered

for the hard rock. Soil setup is discussed in Section 7.2.4.2 and a summary of typical soil setup factors is provided in Table 7-16. A summary of the dynamic soil properties chosen for the drivability analyses are summarized in Table D-102.

Table D-102 Dynamic Soil Properties for South Abutment Soil Profile

Soil Layer	Pile Section	Shaft Quake (in)	Toe Quake (in)	Shaft Damping (s/ft)	Toe Damping (s/ft)	Soil Set-Up Factor
1	HP 10 x 42	0.10	0.17	0.20	0.15	2.0
1	HP 12 x 53	0.10	0.20	0.20	0.15	2.0
1	HP 12 x 74	0.10	0.20	0.20	0.15	2.0
1	HP 14 x 89	0.10	0.23	0.20	0.15	2.0
1	HP 14 x 117	0.10	0.23	0.20	0.15	2.0
2	HP 10 x 42	0.10	0.17	0.20	0.15	2.0
2	HP 12 x 53	0.10	0.20	0.20	0.15	2.0
2	HP 12 x 74	0.10	0.20	0.20	0.15	2.0
2	HP 14 x 89	0.10	0.23	0.20	0.15	2.0
2	HP 14 x 117	0.10	0.23	0.20	0.15	2.0
3	HP 10 x 42	0.10	0.17	0.20	0.15	2.0
3	HP 12 x 53	0.10	0.20	0.20	0.15	2.0
3	HP 12 x 74	0.10	0.20	0.20	0.15	2.0
3	HP 14 x 89	0.10	0.23	0.20	0.15	2.0
3	HP 14 x 117	0.10	0.23	0.20	0.15	2.0
4	HP 10 x 42	0.10	0.08	0.05	0.15	1.0
4	HP 12 x 53	0.10	0.10	0.05	0.15	1.0
4	HP 12 x 74	0.10	0.10	0.05	0.15	1.0
4	HP 14 x 89	0.10	0.12	0.05	0.15	1.0
4	HP 14 x 117	0.10	0.12	0.05	0.15	1.0

In soils that exhibit setup, the long term nominal resistance may be higher than the nominal driving resistance. Therefore, a gain/loss factor of 0.50 was used to estimate the nominal driving resistance versus depth in the drivability analyses. This gain/loss factor was determined from the inverse of the highest soil setup factor within the soil model (e.g., 1 divided by 2.0 equals 0.50). A gain/loss factor of 1 would be used if it was desired to model the nominal resistance instead of the nominal driving resistance and not consider the soil strength loss during driving and any subsequent soil setup. Refer to Chapter 12 for more detailed discussion on the selection of dynamic soil properties and soil setup factors.

The DrivenPiles program calculates the nominal driving resistance which models the soil strength lost during driving as well as the geotechnical nominal resistance once setup occurs. Figure D-97 presents the nominal shaft, toe, and driving resistance versus pile penetration depth for the HP 12x74 H-pile section at the South Abutment. These results are also presented numerically in Table D-103. To quantify the expected soil setup at a given pile penetration depth, the values from Table D-103 can be compared against the nominal resistance previously presented in Table D-100. Figure D-98 illustrates the significant difference between the expected nominal driving resistance and the geotechnical nominal resistance after setup for the HP 12x74 candidate pile section. For example, at a depth of 45 feet, the expected setup from shaft resistance is 95 kips. Where significant soil setup is expected, a smaller pile driving hammer may be acceptable for pile installation since the nominal driving resistance will be significantly lower than the nominal geotechnical resistance.

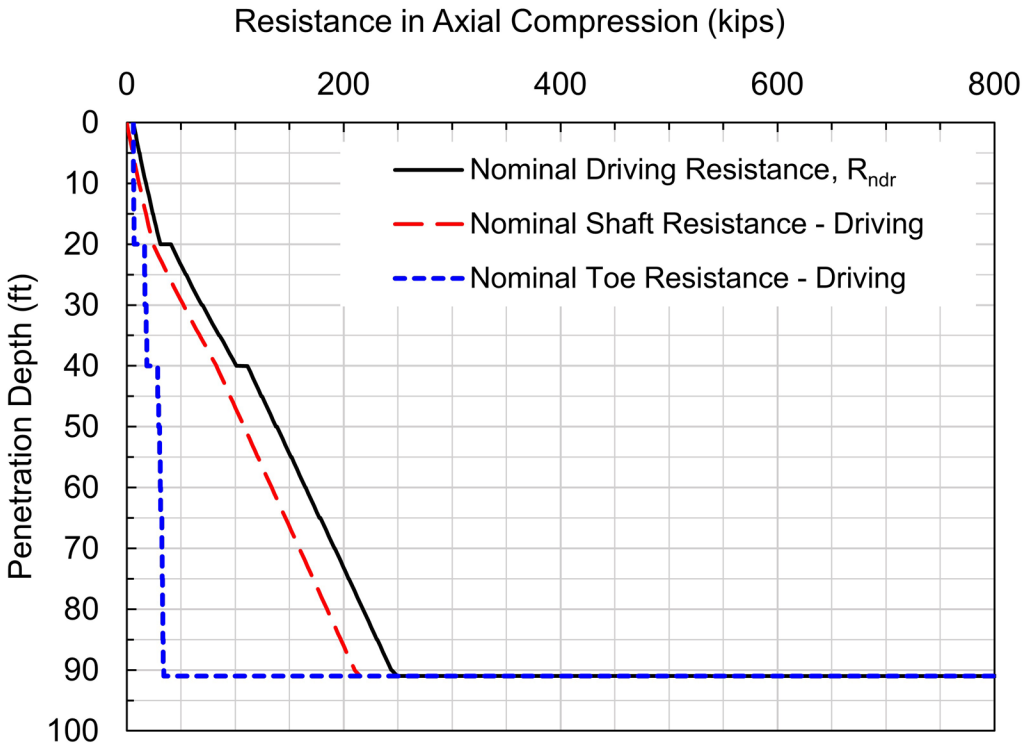

Figure D-97 Nominal driving resistance for HP 12x74 at the South Abutment.

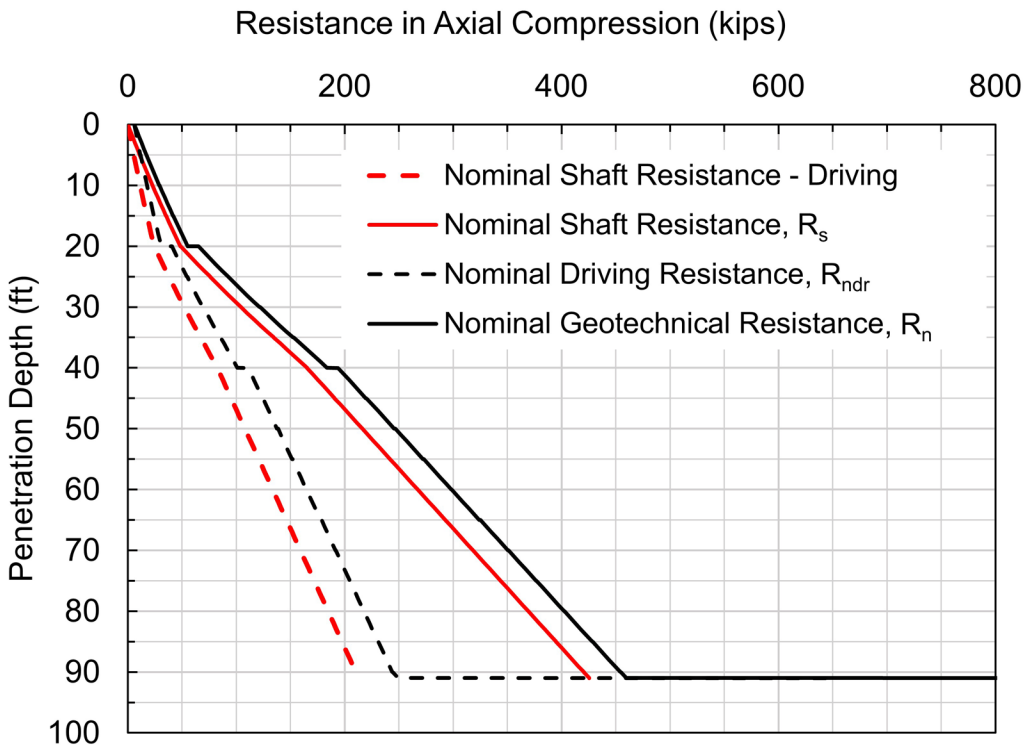

Figure D-98 Comparison of nominal driving resistance and nominal geotechnical resistance in axial compression for HP 12x74 at the South Abutment.

Table D-103 Nominal Shaft, Nominal Toe and Nominal Driving Resistance for HP 12x74

Depth (feet)	Nominal Shaft Resistance (kips)	Nominal Toe Resistance (kips)	Nominal Driving Resistance (kips)		Depth (feet)	Nominal Shaft Resistance (kips)	Nominal Toe Resistance (kips)	Nominal Driving Resistance (kips)
0.01	0.01	6.09	6.1		32	58.11	17.81	75.92
1	1.1	6.09	7.19		33	61.12	17.81	78.93
2	2.2	6.09	8.3		34	64.18	17.81	81.99
3	3.3	6.09	9.41		34.99	67.25	17.81	85.05
4	4.4	6.09	10.51		35.01	67.31	18.45	85.76
4.99	5.52	6.09	11.61		36	70.35	18.45	88.8
5.01	5.54	6.27	11.81		37	73.41	18.45	91.87
6	6.67	6.27	12.95		38	76.48	18.45	94.93
7	7.84	6.27	14.11		39	79.55	18.45	98
8	9.01	6.27	15.29		39.99	82.59	18.45	101.04
9	10.21	6.27	16.48		40.01	82.64	28.69	111.34
9.99	11.4	6.27	17.68		41	85.17	28.69	113.86
10.01	11.43	6.46	17.89		42	87.72	28.69	116.41
11	12.64	6.46	19.1		43	90.27	28.69	118.96
12	13.87	6.46	20.33		44	92.82	28.69	121.52
13	15.13	6.46	21.59		44.99	95.35	28.69	124.04
14	16.4	6.46	22.85		45.01	95.4	29.43	124.83
14.99	17.67	6.46	24.13		46	97.93	29.43	127.36
15.01	17.69	6.64	24.34		47	100.48	29.43	129.91
16	18.98	6.64	25.62		48	103.03	29.43	132.46
17	20.29	6.64	26.93		49	105.58	29.43	135.01
18	21.62	6.64	28.26		49.99	108.11	29.43	137.54
19	22.97	6.64	29.61		50.01	108.16	30.45	138.6
19.99	24.32	6.64	30.96		51	110.68	30.45	141.13
20.01	24.36	16.51	40.87		52	113.23	30.45	143.68
21	26.98	16.51	43.5		53	115.79	30.45	146.23
22	29.67	16.51	46.18		54	118.34	30.45	148.78
23	32.4	16.51	48.91		54.99	120.86	30.45	151.31
24	35.16	16.51	51.68		55.01	120.91	31.00	151.91
24.99	37.94	16.51	54.46		56	123.44	31.00	154.44
25.01	38.0	16.88	54.88		57	125.99	31.00	156.99
26	40.74	16.88	57.63		58	128.54	31.00	159.54
27	43.55	16.88	60.44		59	131.1	31.00	162.1
28	46.4	16.88	63.29		59.99	133.62	31.00	164.62
29	49.29	16.88	66.18		60.01	133.67	31.28	164.95
29.99	52.19	16.88	69.08		61	136.2	31.28	167.48
30.01	52.25	17.81	70.06		62	138.75	31.28	170.03
31	55.15	17.81	72.95		63	141.3	31.28	172.58

Table D-103 Nominal Shaft, Nominal Toe and Nominal Driving Resistance for HP 12x74 (continued)

Depth (feet)	Nominal Shaft Resistance (kips)	Nominal Toe Resistance (kips)	Nominal Driving Resistance (kips)		Depth (feet)	Nominal Shaft Resistance (kips)	Nominal Toe Resistance (kips)	Nominal Driving Resistance (kips)
64	143.85	31.28	175.13		78	179.57	33.03	212.6
64.99	146.38	31.28	177.66		79	182.13	33.03	215.15
65.01	146.43	32.29	178.72		79.99	184.65	33.03	217.68
66	148.96	32.29	181.25		80.01	184.7	33.21	217.92
67	151.51	32.29	183.8		81	187.23	33.21	220.44
68	154.06	32.29	186.35		82	189.78	33.21	222.99
69	156.61	32.29	188.9		83	192.33	33.21	225.55
69.99	159.14	32.29	191.43		84	194.88	33.21	228.1
70.01	159.19	32.75	191.94		84.99	197.41	33.21	230.62
71	161.71	32.75	194.47		85.01	197.46	33.68	231.14
72	164.26	32.75	197.02		86	199.99	33.68	233.66
73	166.82	32.75	199.57		87	202.54	33.68	236.21
74	169.37	32.75	202.12		88	205.09	33.68	238.76
74.99	171.89	32.75	204.65		89	207.64	33.68	241.32
75.01	171.94	33.03	204.97		90	210.17	33.68	243.84
76	174.47	33.03	207.5		91	210.24	33.68	243.92
77	177.02	33.03	210.05		91.25	210.24	1527.00	1737.24

Graphical outputs of the preliminary drivability analyses are shown in Figure D-99. The nominal driving resistance, the blow count or pile penetration resistance, and the compression driving stress are presented versus pile penetration depth for each of the five candidate pile sections. As previously noted, the recommended blow count limit is 120 blows per foot (10 blows per inch), and the recommended driving stress limit is 45 ksi. A circular reference marker is indicated on the blow count versus depth plot highlighting the depth where the blow count first exceeds 120 blows per foot. This marker is also shown at the same depth on the nominal driving resistance versus depth plot indicating the nominal driving resistance achieved when practical refusal driving conditions are encountered with the selected hammer in the modeled driving conditions. Similarly, the marker is shown at the same depth on the compression driving stress versus depth plot indicating the compression driving stress when practical refusal driving conditions are encountered.

In Figure D-99, preliminary drivability results illustrate all candidate pile sections can be driven to the hard rock layer without reaching the blow count limit of 120 blows per foot. Compression driving stresses are also well below the driving stress limit of 45 ksi prior to reaching bedrock.

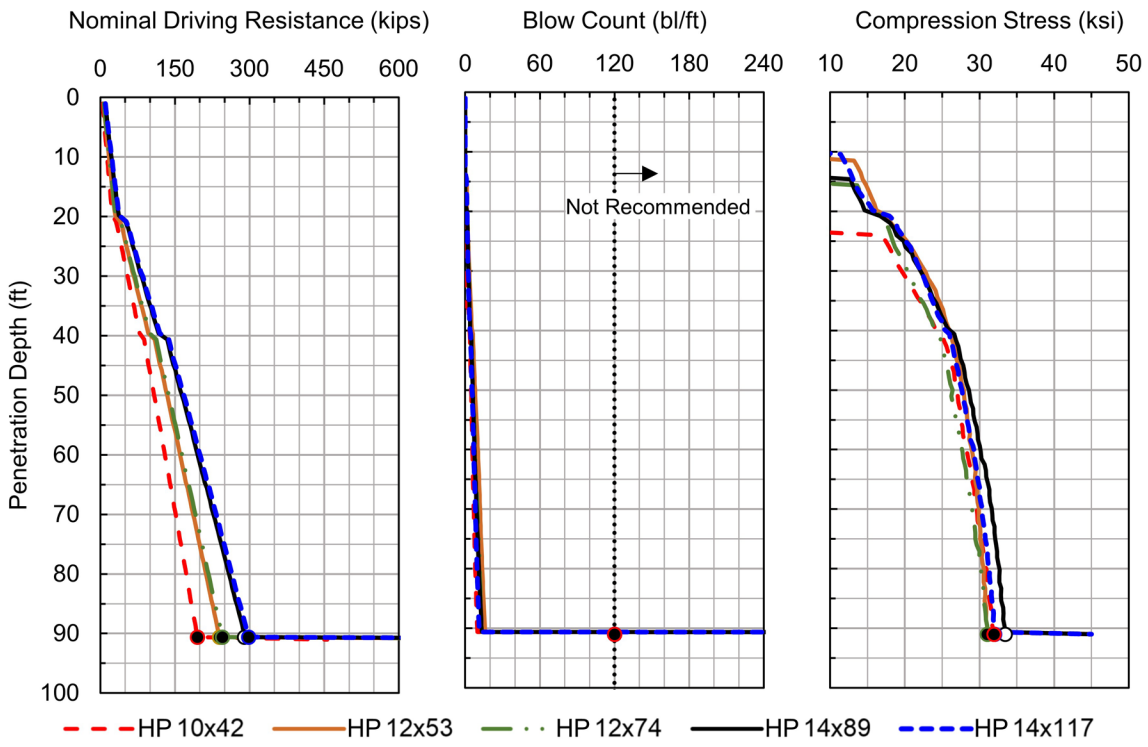

Figure D-99 Preliminary drivability results for five candidate H-pile sections at the South Abutment.

For piles driven to hard rock, the driving criteria should be established to control compression stresses and prevent pile toe damage (e.g., limit the number of blows at refusal driving conditions). A summary of the preliminary drivability results is presented in Table D-104. The anticipated nominal resistance in this table is the expected resistance after soil setup that can be mobilized by the driving system at 10 blows per inch. Since the piles terminate on hard rock, a higher geotechnical nominal resistance, up to the structural resistance of the pile, is actually available.

Once the estimated and/or minimum pile toe elevations are determined in Block 12 through Block 15 of the design process, the drivability results should be reviewed to confirm that the candidate pile section can be driven to the required nominal driving resistance, at the estimated or required pile penetration depth, at a reasonable blow count, and within driving stress limits. Upon determination of the estimated toe elevation, these plots should be reviewed to confirm that the pile can be driven to the estimated toe elevation at reasonable blow counts and stresses.

Table D-104 Summary of Preliminary Drivability Results at South Abutment

Pile Section	Pile Hammer	Fuel Setting	Pile Penetration Depth at Practical Refusal Limit (feet)	Nominal Driving Resistance at Practical Refusal Limit (kips)	Anticipated Nominal Resistance at Depth of Practical Refusal (kips)	Penetration Depth Exceeding Compression Driving Stress Limit (feet)	Maximum Compression Driving Stress (ksi)
HP 10x42	D25-52	4	91.1	362	536	> 91.1	34.1
HP 12x53	D30-52	4	91.1	446	649	> 91.1	34.6
HP 12x74	D36-52	4	91.1	590	806	> 91.1	36.7
HP 14x89	D46-52	4	91.1	729	975	> 91.1	39.5
HP 14x117	D50-52	4	91.1	896	1143	> 91.1	39.2

D.35 Block 11: South Abutment – Estimate Preliminary Number of Piles, Preliminary Pile Group Size, and Resolve Individual Pile Loads for All Limit States

The structural engineer has provided the anticipated loads for the controlling limit states at the South Abutment. These limit state loads are restated in Table D-105. The Strength I limit state loads are used to evaluate geotechnical resistance in axial compression and tension, as well as for lateral loading. Service I limit state loads were also provided by the structural engineer without live loads. The Service I without live load (LL) includes only unfactored permanent loads such as the superstructure and wearing surface, pile cap and stem, utilities, and vertical earth pressure among others. The Service I without live load should be used for evaluating vertical deformation. There are no loads in the transverse direction at this abutment.

Table D-105 Limit State Loads on South Abutment

Limit State	Q (kips)	V_{uy} (kips)	M_{uy} (k-ft)
Strength I	-2815	946	6732
Service I	-2082	629	3931
Service I, without live load	-1783	546	3024

Based on past experience, the agency generally utilizes 2 rows of piles at abutments with a minimum center to center pile spacing of at least 3 pile diameters. Three potential pile group configurations are therefore being considered: 2 rows of 9 piles, 2 rows of 11 piles, and 2 rows of 13 piles. These group configurations are identified as Group Configuration 1, 2, and 3, respectively in Table D-106. Because of site constraints, the pile cap length is limited to 43 feet. Furthermore, the distance from the center of any exterior pile to the pile cap edge must be at least 1.25 feet in both the transverse (x) and longitudinal (y) direction.

Table D-106 Potential Pile Group Configurations

Group Configuration	Piles per Row	Total Number of Piles	S_{bx}* (feet)	Total Footing Length (feet)	S_{by}* (feet)	Total Footing Width (feet)
1	9	18	5.0	42.5	4.0	6.5
2	11	22	4.0	42.5	4.0	6.5
3	13	26	3.0	38.5	4.0	6.5

Note: * - S_{bx} and S_{by} are illustrated in Figure D-100

The following calculation is for the Group Configuration 3 and all applicable loads. For this alternative, 13 piles per row are used in two separate rows, thus the transverse pile spacing, $S_{bx,}$ is 5'-0" and the total footing length is 38'-6". The longitudinal pile spacing, $S_{by,}$ is 4'-0". Figure D-100 shows the layout for the Group Configuration 3 pile cap.

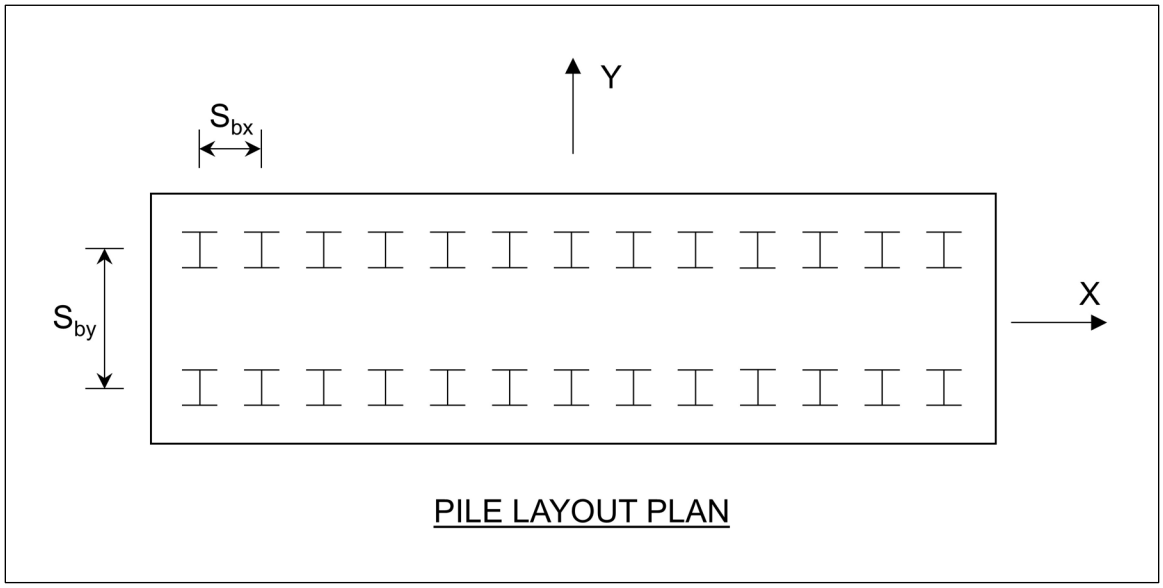

Figure D-100 Group Configuration 3 pile cap plan view.

For the established limit state loads and the trial pile group configuration in Figure D-100, reactions for both the front and the back rows of piles were determined. Compression loads are taken as positive. The maximum factored load applied to each pile was subsequently calculated by dividing the reactions by the number of piles. Figure D-101 shows the free body diagram for determining the factored load for both the front and the back row.

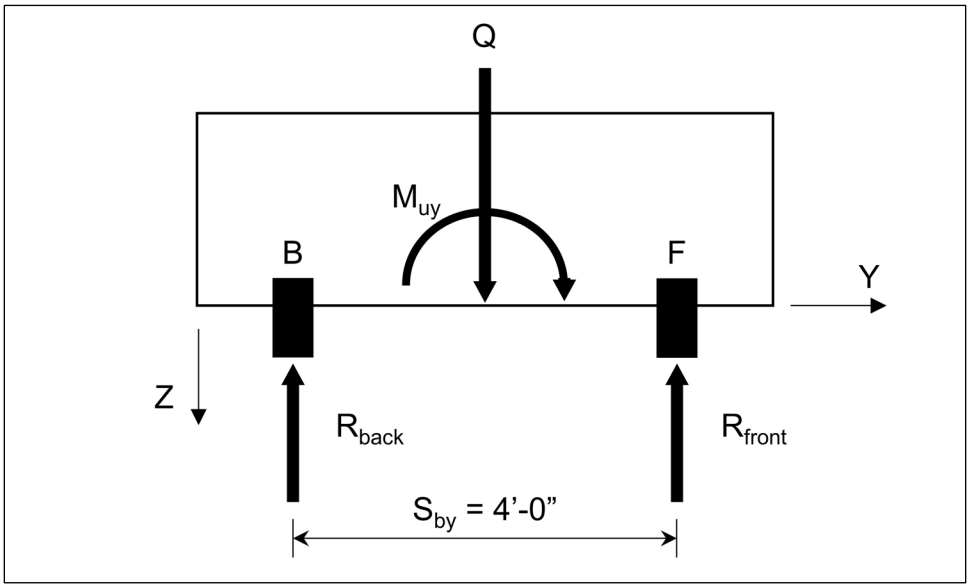

Figure D-101 Elevation view of cap free body diagram.

Table D-107 summarizes the limit state loads and the front and back row reactions. Strength I loads, Service I loads and the Service I loads without live load (LL) are provided. The Service I load without live load is used for settlement calculations.

Table D-107 Factored Loads and Row Reactions

Limit State	Q (kips)	M_{uy} (k-ft)	R_{front} (kips)	R_{back} (kips)
Strength I	-2815	6732	3091	-276
Service I	-2082	3931	2037	46
Service I, without LL	-1783	3024	1648	136

Table D-108 presents the maximum factored load per pile based upon the number of piles in each group configuration. For example, considering Group Configuration 3, the Service I, without live load, front-row reaction of 1648 kips is divided by 13 piles to yield a front-row factored load per pile equal to 127 kips. Table D-108 also provides the factored load per pile for other limit states and group configurations.

Table D-108 Factored Load Per Pile for Alternative Pile Group Configurations

Group Configuration	Strength I, Q (kips)	Strength I, Q (tension) (kips)	Strength I, V_{uy} (kips)	Service I, without LL Q (kips)
1	344	-31	53	183
2	281	-25	43	150
3	238	-21	37	127

D.36 Block 12: South Abutment – Estimate Pile Penetration Depth for Maximum Axial Compression Loads. Check Group Efficiency in Axial Compression

The estimated minimum pile penetration depth necessary to obtain a factored geotechnical resistance that is equal or greater than the maximum factored load per pile is now determined. Note that the factored geotechnical resistance in axial compression and the resulting pile penetration depth is dependent upon the resistance determination method. Therefore, the influence of the field resistance determination method on the design needs to be evaluated at this point in the design process and some resistance determination methods may be eliminated from further design consideration.

Since setup in the cohesive soils will be a significant component of the nominal resistance, it is determined that the nominal geotechnical resistance will be substantiated by dynamic testing 2% of the piles. Figure D-89 illustrates the nominal geotechnical resistance versus penetration depth for the 5 candidate pile sections based on this resistance determination method. From this plot, the estimated penetration depth for a factored geotechnical resistance of 238 kips in axial compression for the Group Configuration 3 ranges from 62 feet for the HP 14x117 H-pile section to 91 feet for the HP 10x42 H-pile section. The estimated pile penetration depth needed for the factored load associated with each group configuration is provided for all candidate pile sections in Table D-109.

Table D-109 Estimated Pile Penetration Depths for the Factored Geotechnical Resistance in Axial Compression at the Strength I Limit State

Group Configuration	Factored Load per Pile (kips)	HP 10x42 (feet)	HP 12x53 (feet)	HP 12x74 (feet)	HP 14x89 (feet)	HP 14x117 (feet)
1	344	91	91	91	90	88
2	281	91	90	86	74	72
3	238	91	74	73	63	62

As described in Section 7.2.2.2, the nominal geotechnical resistance of a pile group in cohesive soil can be taken as the sum of the individual pile nominal geotechnical resistances. In a similar manner, the factored geotechnical resistance of the pile group in cohesive soil is taken as the sum of the individual pile factored geotechnical resistances. This is recommended so long as 1) the pile cap is in firm contact with the ground and 2) the piles are not installed at a pile spacing of less than 3 times the pile diameter or 3 feet. Since both conditions are met at the South Abutment, by inspection, the nominal and factored group resistances are satisfactory.

As will be discussed later in Block 15, in order to satisfy tolerable deformations, the piles at the South Abutment will be driven to bedrock. Therefore, piles at the South Abutment are not subject to block failure as outlined in Section 7.2.2.3 of Chapter 7.

D.37 Block 13: South Abutment – Establish Minimum Pile Penetration Depth for Axial Tension Loads. If Conditions Warrant, Modify Design and Return to Block 10

The factored geotechnical resistance in axial tension must also be evaluated as the back row of piles will be loaded in tension (Table D-107). In this case, the minimum required factored geotechnical resistance in axial tension is established using the Strength I limit state and is determined following the procedure outlined in Section 7.2.3.2. The analysis presented in this appendix slightly differs from the procedure outlined in Chapter 7 in that only a single row of piles is providing the tension resistance rather than the entire pile group. Two analyses are performed; one that considers the factored shaft resistances from individual piles, and one that considers the weight of a soil block acting with the piles. The lesser tension resistance determined from either method controls the design.

As noted in Table D-107, the Strength I limit state tension load on the back row of piles for the Group Configuration 3 is 276 kips. Therefore, the minimum factored geotechnical resistance in axial tension required from an individual pile is this factored load divided by the 13 piles in the rear row or 21 kips. In a similar manner, the minimum factored geotechnical resistance required from an individual pile in axial tension is 31 kips for Group Configuration 1, and 25 kips for Group Configuration 2.

As noted earlier, dynamic testing with signal matching will be used as the resistance determination method in the field. Therefore, the AASHTO recommended resistance factor, ϕ_{up}, is 0.5 (Table 7-2 of Chapter 7). Figure D-95 provides plots of the factored geotechnical resistance in axial tension versus depth for all of the candidate pile types based on this resistance determination method. For each candidate section, Figure D-95 should be entered on the x-axis at the required factored axial tension resistance to determine the corresponding pile penetration depth.

Following this procedure, the estimated pile penetration depth to achieve the factored geotechnical resistance in axial tension for each candidate pile section and group configuration is summarized in Table D-110.

Table D-110 Estimated Minimum Pile Penetration Depth Required for Factored Geotechnical Resistance in Axial Tension at the Strength I Limit State

Group Configuration	Required Factored Resistance in Axial Tension (kips)	HP 10x42 (feet)	HP 12x53 (feet)	HP 12x74 (feet)	HP 14x89 (feet)	HP 14x117 (feet)
1	31	25	23	23	21	21
2	25	23	21	21	19	18
3	21	21	19	18	16	16

Next, the tension resistance of the pile row when considered as a soil block is calculated. For Group Configuration 3, the required factored tension resistance of the back row remains 276 kips (Table D-107) and the resistance is derived from the weight of soil as a block and an average of the soil shear strength. Equation 7-39 is used to determine the required nominal group resistance in axial tension.

$$R_r = \phi R_n = \phi_{ug} R_{ug} \quad \text{[Eq. 7-39]}$$

Where:

R_n = nominal resistance (kips).
ϕ_{ug} = resistance factor for tension per Table 7-1, 0.50.
R_{ug} = nominal uplift resistance of the pile group (kips).

$$R_{ug} = \frac{R_r}{\phi_{ug}} \quad \text{Eq. [7-39 modified]}$$

$$R_{ug} = \frac{(276\ kips)}{(0.5)}$$

$$R_{ug} = 552\ kips$$

The minimum required nominal uplift resistance is 552 kips.

Equation 7-41 is then used to determine the minimum embedded length required to satisfy the nominal group tension resistance for soil acting as a block. The length of the pile group will change depending upon the group configuration. For Group Configuration 1 and 2, the pile group length is 41 feet from exterior pile edge to exterior pile edge assuming a 12 inch pile width/diameter. For Group Configuration 3, the pile group length is 37 feet using the same pile dimension. The effect of a smaller pile size on the pile group length is negligible (e.g. for HP 10x42 section, the pile group length is 40.83 feet).

$$R_{ug} = 2\ \mathrm{D}\ (\mathrm{B} + \mathrm{Z}) s_u + W_g \quad \text{[Eq. 7-41]}$$

D = embedded length of piles (feet).
B = width of pile group, assume 1 foot (1 row in tension).
Z = length of pile group, 37 feet (Group Configuration 3).
s_u = weighted average of the undrained shear strength over the depth of pile embedment along the pile group perimeter (ksf) (Figure D-83).
W_g = effective weight of the pile/soil block including pile cap weight (kips).

The calculation is performed for the HP 12x74 pile section in Group Configuration 3. The back row contains 13 piles, and the group length is 37 feet. Figure D-102 provides a visual representation of the soil volume used to determine tension resistance. The block of soil being evaluated is only as wide as, and lies between, the piles. Therefore it is not visible in the transverse elevation view in Figure D-102.

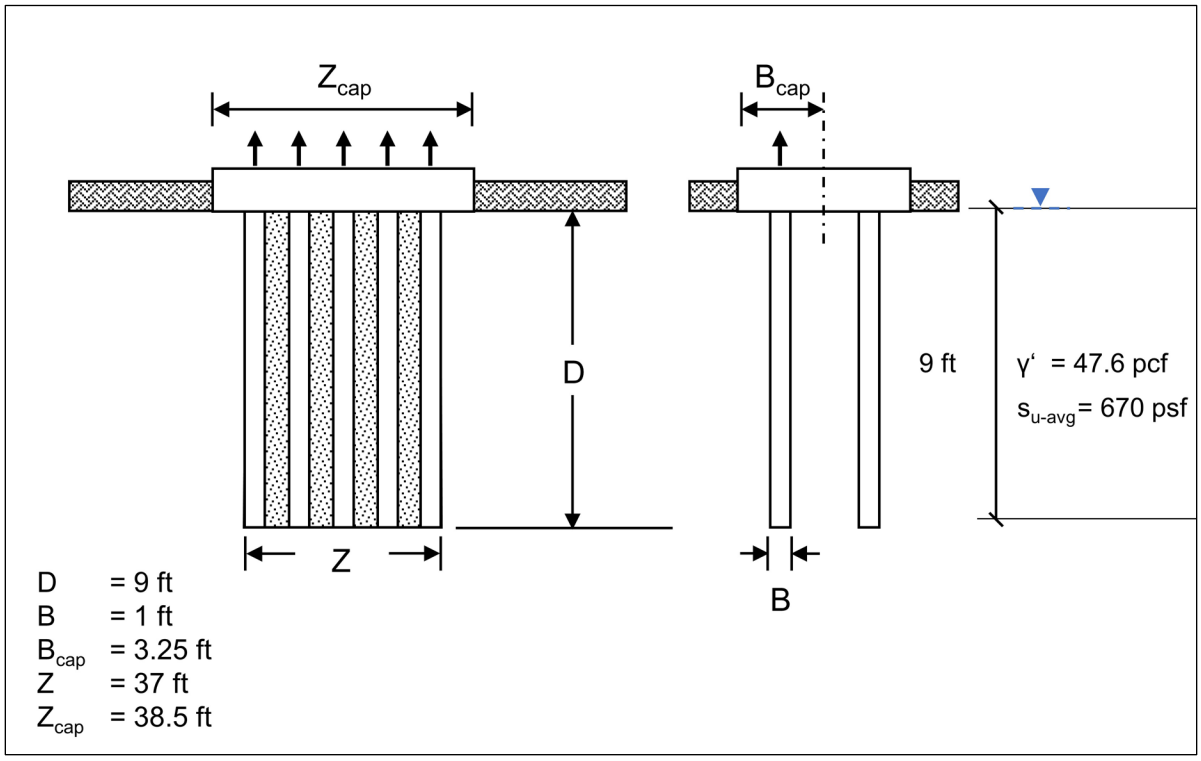

Figure D-102 Tension resistance of pile group in cohesive soil.

Several iterations were performed to incrementally increase the pile length and evaluate the nominal uplift resistance of the pile group. The minimum required embedded length of piles was determined to be 9 feet, and therefore, that calculation is presented below.

Calculate the weight of piles:

D = embedded length of piles, 9 feet.
W/ft = weight per linear foot of HP 12x74 pile section, 0.074 kip/ft.

$$W_{piles} = (\text{Weight/ linear foot}) * D * Number\ of\ Piles$$

$$W_{piles} = \left(0.074 \frac{kip}{ft}\right) * (9\ feet) * (13\ piles)$$

$$W_{piles} = 8.66\ kips$$

Calculate the weight of soil:

D = embedded length of piles, 9 feet.
B = width of pile group, assume 1 foot (1 row in tension).
Z = length of pile group, 37 feet (Group Configuration 3).
γ'_{soil} = effective unit weight of soil, 47.6 pcf (Figure D-83).

$$W_{soil} = \mathrm{D} * B * \mathrm{Z} * \gamma'_{soil}$$

$$W_{soil} = (9\ feet) * (1\ feet) * (37\ feet) * (47.6\ pcf) * \left(\frac{1\ kip}{1000\ lbs}\right)$$

$$W_{soil} = 15.85\ kips$$

Calculate weight of the pile cap, conservatively taken as the tributary are over piles in tension:

B_{cap} = width of pile cap, half of cap width 6.5 feet /2 = 3.25 ft (Table D-106).
Z_{cap} = length of pile group, 38.5 feet (Table D-106).
t_{cap} = thickness of pile cap, preliminary estimate, 4.2 feet.
$\gamma_{concrete}$ = unit weight of reinforce concrete, 150 pcf.

$$W_{cap} = B_{cap} * Z_{cap} * t_{cap} * \gamma_{concrete}$$

$$W_{cap} = (3.25\ feet) * (38.5\ feet) * (4.2\ feet) * (150\ pcf) * \left(\frac{1\ kip}{1000\ lbs}\right)$$

$$W_{cap} = 78.83\ \mathrm{kips}$$

Calculate the effective weight of the pile/soil block including pile cap weight:

$$W_g = W_{piles} + W_{soil} + W_{cap}$$

$$W_g = (8.66\ kips) + (15.85\ kips) + (78.83\ kips)$$

$$W_g = 103.3\ kips$$

Equation 7-41 is next used to calculate the group tension resistance for soil acting as a block. A weighted average shear strength value of 0.67 ksf was used for the first 10 feet below the footing in the silty clay soil layer (Figure D-83).

D = embedded length of piles, 9 feet.
B = width of pile group, assume 1 foot (1 row in tension).
Z = length of pile group, 37 feet (Group Configuration 3).
s_u = weighted average undrained shear strength, 0.67 ksf (Figure D-83).
W_g = effective weight of the block, 103.3 kips.

$$R_{ug} = 2\,\mathrm{D}\,(\mathrm{B}+\mathrm{Z})s_u + W_g \qquad \text{[Eq. 7-41]}$$

$$R_{ug(9\,ft)} = 2 * (9\,feet) * \big((1\,foot) + (37\,feet)\big) * (0.67\,ksf) + (103.3\,kips)$$

$$R_{ug(9\,ft)} = 561.6\,kips$$

Therefore:

$$R_{ug(9\,ft)} > R_{ug}$$

$$561.6\,kips > 552\,kips$$

The required soil block weight is achieved at approximately 9 feet of pile penetration. Accordingly, any additional pile penetration would satisfy this requirement. For a pile group length of 41 feet (i.e., Group Configuration 1 and 2), the minimum pile penetration depth to achiegve a soil block weight in excess of the required 552 kips is also 9 feet.

As noted earlier, two analyses are performed to determine the minimum pile penetration depth for nominal tension resistance. The first one considers the shaft resistances from individual piles, and the second one considers the weight of a soil block acting with the piles. The required minimum pile penetration depth to achieve geotechnical resistance in axial tension is the greater depth of the above calculated resistances. The estimated minimum penetration depth required for the factored geotechnical resistance in axial tension was summarized in Table D-110. For the HP 12x74 pile section in Group Configuration 3, the minimum pile penetration depth is 18 feet for the factored tension load of 21 kips.

$D_{(individual)}$ = minimum pile penetration depth based on sum of individual pile resistance = 18 feet (Table D-110).

$D_{(block)}$ = minimum pile penetration depth based on weight of soil block
= 9 feet. (calculated above).

$$D_{(individual)} > D_{(block)}$$

$$18\ feet > 9\ feet$$

Therefore, the minimum penetration depth $D_{(min-tension)}$ is as follows:

$$D_{(min-tension)} = 18\ feet$$

In a similar manner, this check was performed for all candidate pile sections and group configurations. The resulting established minimum required pile penetration depth to meet axial tension requirements for each candidate pile section within the specified group configuration is presented in Table D-111.

Table D-111 Established Minimum Pile Penetration Depth Required for Factored Geotechnical Resistance in Axial Tension at South Abutment

Group Configuration	HP 10x42 (feet)	HP 12x53 (feet)	HP 12x74 (feet)	HP 14x89 (feet)	HP 14x117 (feet)
1	25	23	23	21	21
2	23	21	21	19	18
3	21	19	18	16	16

D.38 Block 14: South Abutment – Establish Minimum Pile Penetration Depth for Lateral Loads. Determine p-y Models, Required Geomaterial Parameters, and Perform Lateral Load Analysis. If Conditions Warrant, Modify Design and Return to Block 10

Next, lateral analyses are performed to establish the required minimum pile penetration depth for lateral loading and to evaluate pile deflection and structural resistance for the applied limit state loads. The minimum required pile penetration depth required to satisfy the nominal geotechnical resistance requirements in axial tension was determined to be 18 feet in Block 13. A deeper minimum required pile penetration depth for lateral loading can result based on the combination of factored lateral loads and structural resistances, or deflection limits. Excessive deflections and moments develop at relatively short pile lengths, where a depth to fixity is not

achieved. Furthermore, the structural resistance of pile sections must be evaluated based upon the axial, lateral and moment loads. Factored structural resistances were presented in Table D-95 while a lateral deformation limit of 1 inch was established as a global performance requirement in Block 1 and confirmed In Block 4 as the design progressed.

The soil profile at the South Abutment was presented in Figure D-83. For lateral load analyses, appropriate p-y models must be selected for each soil layer. The input parameters necessary for lateral load analysis using the LPILE computer program are included in the South Abutment soil profile.

As discussed in Section 7.3.7.6, p-multipliers are applied to the p-y curves to model pile group behavior. The p-multipliers depend on the center to center pile spacing within the pile group. For all group configurations at the South Abutment, the pile spacing in the longitudinal direction is 4 feet. Therefore, per Section 7.3.7.6 and AASHTO (2014) design specifications, interpolation was used to determine p-multipliers for a pile spacing of 4b. In this case, the front row p-multiplier is 0.90, while the second row is 0.625.

Cyclic loading was performed for both rows using LPILE's Load Type 2 option, which uses shear and slope to model a fixed head condition. Considering loading conditions at this abutment, lateral analyses in the longitudinal (y-direction) were performed about the pile section's strong axis. Figure D-100 shows the pile orientation within the trial pile cap design.

The following example is presented for the HP 12x74 pile section using a range of factored axial and lateral loads for Group Configuration 3. Tables D-112 and D-113 provide LPILE output summaries for both rows at the pile head considering a pile penetration for lateral loading of 30 feet. The pile head is assumed to terminate at the ground surface (i.e. no stickup).

Table D-112 LPILE Summary Output at Pile Head for Front Row, p_m=0.90

Load Case	Load Type No.	Pile-Head Condition 1 V (kips)	Pile-Head Condition 2 S (rad)	Axial Load (kips)	Pile-Head Deflection (inches)	Maximum Moment in Pile (kip-ft)	Maximum Shear in Pile (kips)	Pile-Head Rotation (radians)
1	2	0	0	238	0.000	0.0	0	0
2	2	15	0	238	0.116	-56.6	15	0
3	2	30	0	238	0.451	-141.7	30	0
4	2	35	0	238	0.611	-173.8	35	0
5	2	36	0	238	0.646	-180.4	36	0
6	2	37	0	238	0.682	-187.1	37	0
7	2	38	0	238	0.719	-193.9	38	0
8	2	40	0	238	0.796	-207.6	40	0
9	2	42	0	238	0.876	-221.5	42	0
10	2	50	0	238	1.344	-292.1	50	0

Table D-113 LPILE Summary Output at Pile Head for Second Row, p_m=0.625

Load Case	Load Type No.	Pile-Head Condition 1 V (kips)	Pile-Head Condition 2 S (rad)	Axial Load (kips)	Pile-Head Deflection (inches)	Maximum Moment in Pile (kip-ft)	Maximum Shear in Pile (kips)	Pile-Head Rotation (radians)
1	2	0	0	238	0.000	0.0	0	0
2	2	15	0	238	0.196	-67.5	15	0
3	2	30	0	238	0.769	-169.8	30	0
4	2	35	0	238	1.060	-211.2	35	0
5	2	36	0	238	1.138	-221.2	36	0
6	2	37	0	238	1.223	-231.8	37	0
7	2	38	0	238	1.317	-242.9	38	0
8	2	40	0	238	1.531	-266.6	40	0
9	2	42	0	238	1.793	-292.7	42	0

The pile group deflection can be estimated from the above LPILE's deflection results for the front and second rows. The factored load versus pile head deflection for each row is plotted in Figure D-103 along with the group average. The average lateral load per pile for a given group deflection is shown. A step by step discussion of this procedure is provided in Section 7.3.7.6.

The rigid cap method assumes piles move together, and therefore experience the same shear and lateral load. Accordingly, at the resulting factored lateral load per pile, V_{uy}, of 37 kips (Table D-108), the estimated lateral group deflection at the pile head is determined as 0.96 inches. This lateral deflection is less than the 1 inch tolerance based upon project specific requirements.

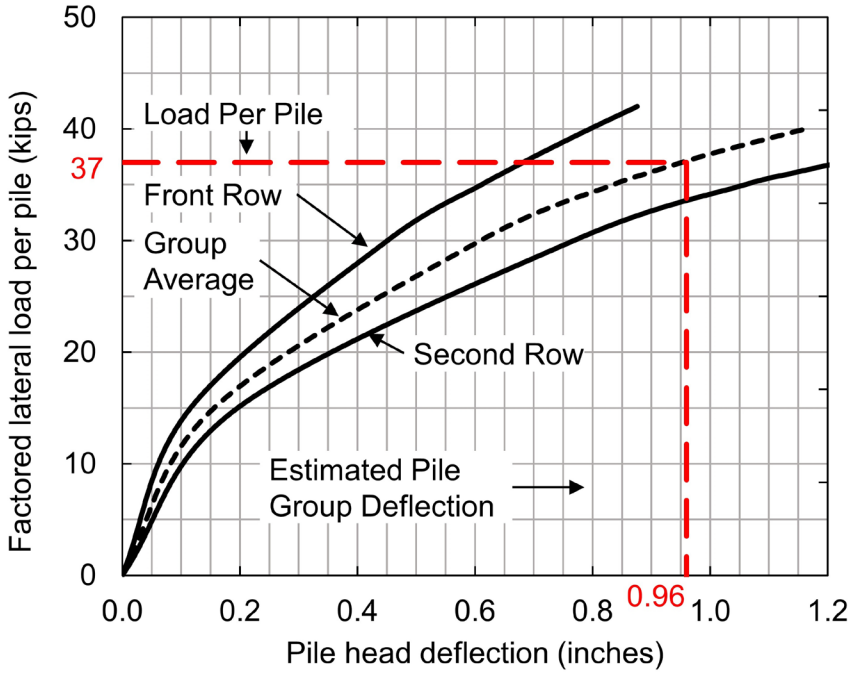

Figure D-103 Factored load versus deflection for HP 12x74 at South Abutment.

In addition to the lateral deflection limit, stresses from the resulting bending moment and shear must be evaluated to check that the pile section does not fail structurally. Using the LPILE tabular results, Figure D-104 plots the front row bending moment versus depth for a deflection of 0.96 inches.

Figure D-105 plots the maximum bending moment versus pile head deflection for both the front and back rows, however only the maximum bending moment for the front row is used as a “worst case” evaluation of the structural resistance in combined axial compression and flexure. As illustrated in Figure D-105 for the front row piles, at the estimated pile head deflection of 0.96 inches, the maximum bending moment, M_{uy}, is 235 kip-ft.

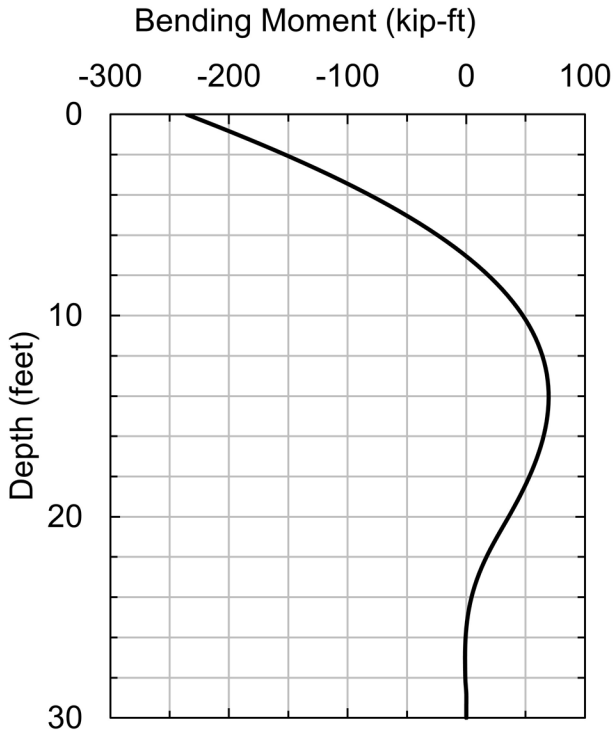

Figure D-104 Front row bending moment versus depth.

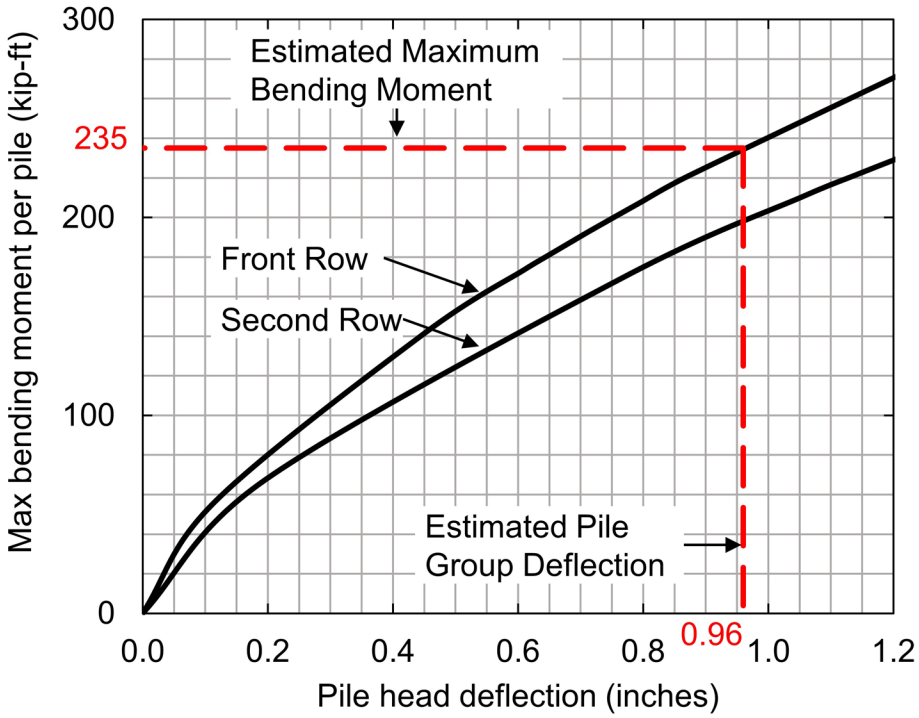

Figure D-105 Bending moment versus deflection for HP 12x74 at South Abutment.

The interaction shown in Equation 8-58 must be satisfied for the factored axial compression load and moment in the pile. Using results of the lateral analysis, the factored structural resistance was evaluated at the pile head using the factored axial compression load and maximum bending moment (determined using factored loads). The factored structural resistances were determined as shown in Table D-95.

Equation 8-58 must be satisfied for the pile section to be acceptable.

P_u = factored axial load, 238 kips (Table D-108).
P_r = factored axial resistance, 762 kips (Table D-95).
M_{ux} = factored moment about x-axis, 0 kip-ft (Block 11).
M_{rx} = factored flexural resistance about x-axis, 118 kip-ft (Table D-95).
M_{uy} = factored moment about y-axis, 235 kip-ft (Figure D-105).
M_{ry} = factored flexural resistance about y-axis, 433 kip-ft (Table D-95).

$$\frac{\mathrm{P}_u}{\mathrm{P}_r}+\frac{8.0}{9.0}\left(\frac{\mathrm{M}_{ux}}{\mathrm{M}_{rx}}+\frac{\mathrm{M}_{uy}}{\mathrm{M}_{ry}}\right)\leq 1.0 \qquad \text{[Eq. 8-58]}$$

$$\frac{238\ \text{kips}}{762\ \text{kips}}+\frac{8.0}{9.0}\left(\frac{0}{118\ \text{kip}-\text{ft}}+\frac{235\ \text{kip}-\text{ft}}{433\ \text{kip}-\text{ft}}\right)\leq 1.0$$

$$0.79\leq 1.0$$

The maximum shear from factored lateral loading was then compared to the factored shear resistance from Table D-95. Based on the factored loads, the factored shear resistance is acceptable.

V_r = factored shear resistance, 214 kips (HP 12x74, Table D-95).
V_{uy} = factored shear load, 37 kips (Group Configuration 3, Table D-108).

$$V_{uy} < V_r$$

$$37\ kips < 214\ kips$$

The lateral analysis was also performed for each alternative pile section. The deflection and factored structural resistance were evaluated considering the factored loads for group configurations shown in Table D-108. Pile head deflection must be limited to 1 inch, and based upon the applied loads and pile section, the factored structural resistance of the pile must also satisfy the structural resistance interaction

equation presented as Equation 8-58. Pile sections satisfying both criteria were deemed acceptable, and furthermore as summarized in Table D-114, a minimum required pile penetration depth was established based on lateral load resistance considerations. The minimum penetration depth is identified as "- - -" for candidate pile sections not meeting the lateral deformation or structural resistance requirements.

Several of the larger pile sections provided sufficient stiffness to resist the applied loads, while less stiff sections did not (they failed the structural resistance check in Equation 8-58). Factored axial compression loads, in combination with moments caused by factored lateral loads, resulted in some sections' factored structural resistance being exceeded. Although the HP 12x53 pile section satisfied structural resistance requirements considering Group Configuration 3 factored loads, the pile section did not satisfy the 1 inch pile head deflection requirement for any pile penetration depth.

Table D-114 Established Minimum Required Pile Penetration Depth for Lateral Loading at the South Abutment

Group Configuration	HP 10x42 (feet)	HP 12x53 (feet)	HP 12x74 (feet)	HP 14x89 (feet)	HP 14x117 (feet)
1	- - -	- - -	- - -	- - -	40
2	- - -	- - -	- - -	35	35
3	- - -	- - -	35	35	35

D.39 Block 15: South Abutment – Establish Pile Penetration Depths that Satisfy Tolerable Deformations. Estimate Group Settlement over the Minimum and Maximum Range of Pile Penetration Depths From Blocks 12 to 14 and Identify All Pile Toe Elevations Which Result in Intolerable Deformations. If Conditions Warrant, Modify Design and Return to Block 10

For the cohesive soils at the South Abutment, pile group settlement was estimated using two methods, classic consolidation theory in cohesive soils and the Janbu Tangent modulus method. Ideally, the settlement method chosen by the designer is one that has shown good correlation with observed results. The pile group settlement at the South Abutment was first calculated using classic consolidation theory with an equivalent footing per AASHTO (2014) design specifications. However, the soil conditions across the bridge substructure locations are quite variable and a settlement method that could be used at all substructure locations was also desired. Therefore, group settlement was also computed with the Janbu Tangent modulus approach using an equivalent footing placed at the neutral plane.

As established by global project performance requirements, vertical deformation (including both settlement and elastic compression) should be limited to 1.5 inches at each substructure location.

The deformation analysis must consider all loads and resulting changes in vertical effective stress. Thus the analysis begins considering construction of the new embankment and the subsequent increase in vertical effective stresses below the abutment. For simplification, the vertical effective stress increase is determined by treating the embankment surcharge as a strip load. Figure D-106 demonstrates this concept and defines symbols, while the change in vertical effective stress with depth is determined using Equation D-2 through D-4.

$$\Delta\sigma_v = \frac{q}{\Pi}[\beta + \sin(\beta) * \cos(\beta + 2\delta)] \quad \text{[Eq. D-2]}$$

Where:

$$\beta = tan^{-1}\left(\frac{x+b}{z}\right) - tan^{-1}(\frac{x-b}{z}) \quad \text{[Eq. D-3]}$$

and

$$\delta = tan^{-1}(\frac{x-b}{z}) \quad \text{[Eq. D-4]}$$

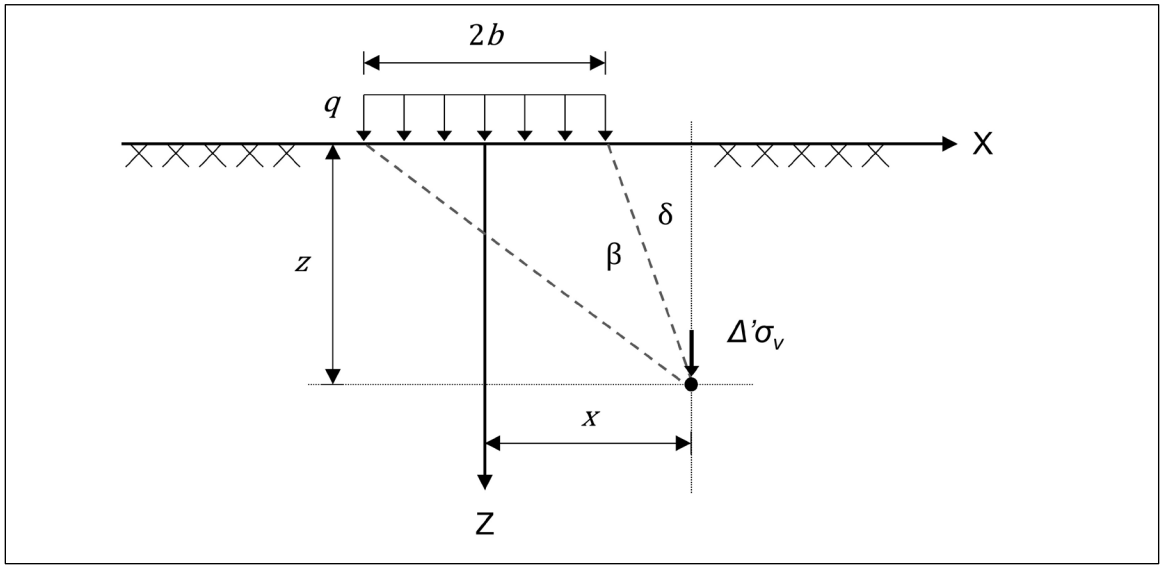

Figure D-106 Vertical effective stress increase due to strip load.

The 15 foot high embankment, with a soil unit weight 120 pcf, results in a surcharge stress at the embankment base of 1.8 ksf, and is assumed to extend 100 feet behind

the abutment. Fill directly above the footing is already included in design as a permanent vertical load, EV, and therefore the embankment surcharge is assumed to act as a strip load beginning at the footing edge. The change in vertical effective stress from the embankment surcharge, $\Delta\sigma'_{v(e)}$, is determined under the footing centerline as depicted in Figure D-107.

An example calculation is shown for a depth below footing, *z*, of 2.5 feet, while complete calculations were performed using a spreadsheet and are shown in Table D-115. The bottom of footing is at Elevation 305 feet. Therefore, although the value of z in the following series of analyses may vary based upon the equivalent footing or neutral plane location, the elevation is used to provide a comparison of effective stress change with depth.

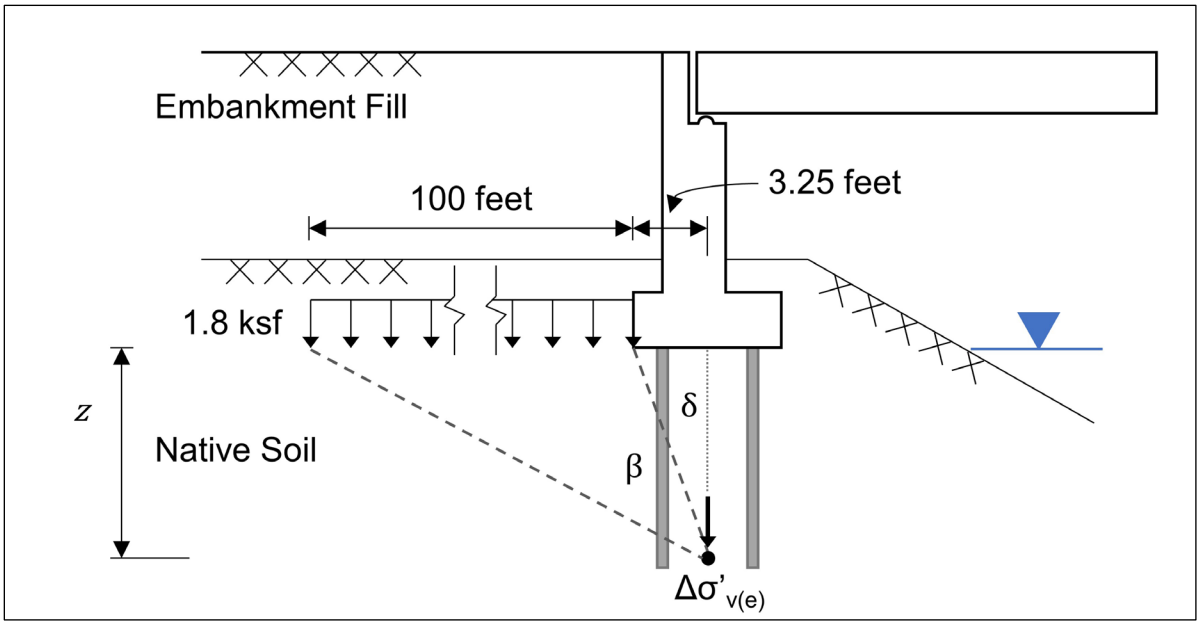

Figure D-107 Profile of vertical stress increase due to embankment surcharge.

Determine geometry of profile.

$$x = 3.25\ feet + \frac{100\ feet}{2} = 53.25\ feet$$

$$b = \frac{100\ feet}{2} = 50\ feet$$

Determine angle β.

$$\beta = tan^{-1}\left(\frac{x+b}{z}\right) - tan^{-1}\left(\frac{x-b}{z}\right) \qquad \text{[Eq. D-3]}$$

$$\beta = tan^{-1}\left(\frac{53.25\ feet+50\ feet}{2.5\ feet}\right) - tan^{-1}\left(\frac{53.25\ feet-50\ feet}{2.5\ feet}\right)$$

$$\beta = 0.63$$

Determine angle δ.

$$\delta = tan^{-1}(\frac{x-b}{z}) \qquad \text{[Eq. D-4]}$$

$$\delta = tan^{-1}\left(\frac{53.25\ feet-50\ feet}{2.5\ feet}\right)$$

$$\delta = 0.92$$

Calculate the change in vertical effective stress due to embankment surcharge.

q = stress per unit length, 1.8 ksf.

$$\Delta\sigma'_{v(e)} = \frac{q}{\Pi}[\beta + \sin(\beta) * \cos(\beta + 2\delta)] \qquad \text{[Eq. D-2]}$$

$$\Delta\sigma'_{v(e)} = \frac{1.8\ ksf}{\Pi}[0.63 + \sin(0.63) * \cos(0.63 + 2 * (0.92))]$$

$$\Delta\sigma'_{v(e)} = 0.10\ ksf$$

Table D-115 Vertical Effective Stress Increase from Embankment Surcharge

Elevation (feet)	Soil Layer	z (feet)	δ	β	$\Delta\sigma'_{v(e)}$ (ksf)
304.99	1	0.01	1.57	0.00	0.00
302.5	1	2.5	0.92	0.63	0.10
297.5	1	7.5	0.41	1.09	0.46
292.5	1	12.5	0.25	1.20	0.61
287.5	1	17.5	0.18	1.22	0.69
282.5	2	22.5	0.14	1.21	0.73
277.5	2	27.5	0.12	1.19	0.76
272.5	2	32.5	0.10	1.17	0.78
267.5	2	37.5	0.09	1.14	0.79
262.5	3	42.5	0.08	1.10	0.79
257.5	3	47.5	0.07	1.07	0.79
252.5	3	52.5	0.06	1.04	0.79
247.5	3	57.5	0.06	1.01	0.79
242.5	3	62.5	0.05	0.97	0.78
237.5	3	67.5	0.05	0.94	0.78
232.5	3	72.5	0.04	0.91	0.77
227.5	3	77.5	0.04	0.88	0.76
222.5	3	82.5	0.04	0.86	0.75
217.5	3	87.5	0.04	0.83	0.74
214.5	3	90.5	0.04	0.82	0.73

The increase in vertical effective stress with depth is relatively sustained due to the long embankment length, and, as a result, settlement will be adversely affected. Therefore, the designer should determine if the construction schedule can accommodate the time required for embankment induced settlements to occur before the start of pile driving and superstructure construction. This example calculation assumes construction cannot be delayed, and therefore, the stress increase from embankment construction and foundations loads are applied concurrently.

Compressibility properties for the three silty clay layers were determined from one dimensional consolidation tests which were performed on undisturbed samples collected near the middle of each respective soil layer. Table D-116 presents the void ratio, e_o, overconsolidation ratio, OCR, compression index, C_c, and recompression index, C_r for the three silty clay layers. The OCR of the various soil layers were used to calculate the preconsolidation stress, σ'_p, at discrete depths.

Table D-116 Soil Properties Determined from One Dimensional Consolidation Test

Soil Layer	e_o	OCR	C_c	C_r
1	0.94	1.68	0.34	0.03
2	0.80	2.01	0.30	0.03
3	0.54	1.71	0.20	0.02

The settlement at the South Abutment was first evaluated using an equivalent footing with stress distribution considering piles supported by shaft resistance in clay as depicted by Figure D-108. A discussion of this approach is provided in Section 7.3.5.3 of Chapter 7. Classic consolidation settlement equations were used to estimate pile group settlement. For this approach, an equivalent footing was placed at increasing pile penetration depths and resulting pile group settlements were estimated. Figure D-108 presents the equivalent footing concept with the appropriate stress distribution. The displayed group length dimension, Z, is 37 feet and is appropriate for only Group Configuration 3. The shallowest depth of an equivalent footing which satisfied vertical deformation requirements was thus determined. After calculating settlement, the location of the equivalent footing location was correlated to the required pile penetration depth. This depth was then used to establish the minimum required pile penetration depths to satisfy deformation requirements.

The following example calculation is performed for an equivalent footing located 35 feet below the bottom of footing. From Elev. 270.0 feet to Elev. 214.0 feet, settlement calculations for cohesive soil were performed for the silty clay layers. The stress increase from the superstructure and embankment loads was less than the preconsolidation stress at each layer. Therefore, Equation 7-57 was used to estimate recompression settlement for overconsolidated soil. It was furthermore assumed that compression of the underlying limestone bedrock is negligible.

The length of the pile group in Group Configuration 3 is 37 feet from exterior pile edge to exterior pile edge, and therefore this example is suitable for only this configuration. The same dimension for Group Configuration 1 and 2 is 41 feet. Similar to the stress increase calculations from embankment loading, the soil profile was again divided into 5 foot thick layers with the exception of the final layer which is 1 foot thick. The elevation shown in Table D-117 references the midpoint of each respective soil layer, while z is the depth below the equivalent footing to the midpoint of each respective soil layer. Tabulated values for this analysis are recorded in Table D-117 with a total settlement estimated of 1.21 inches.

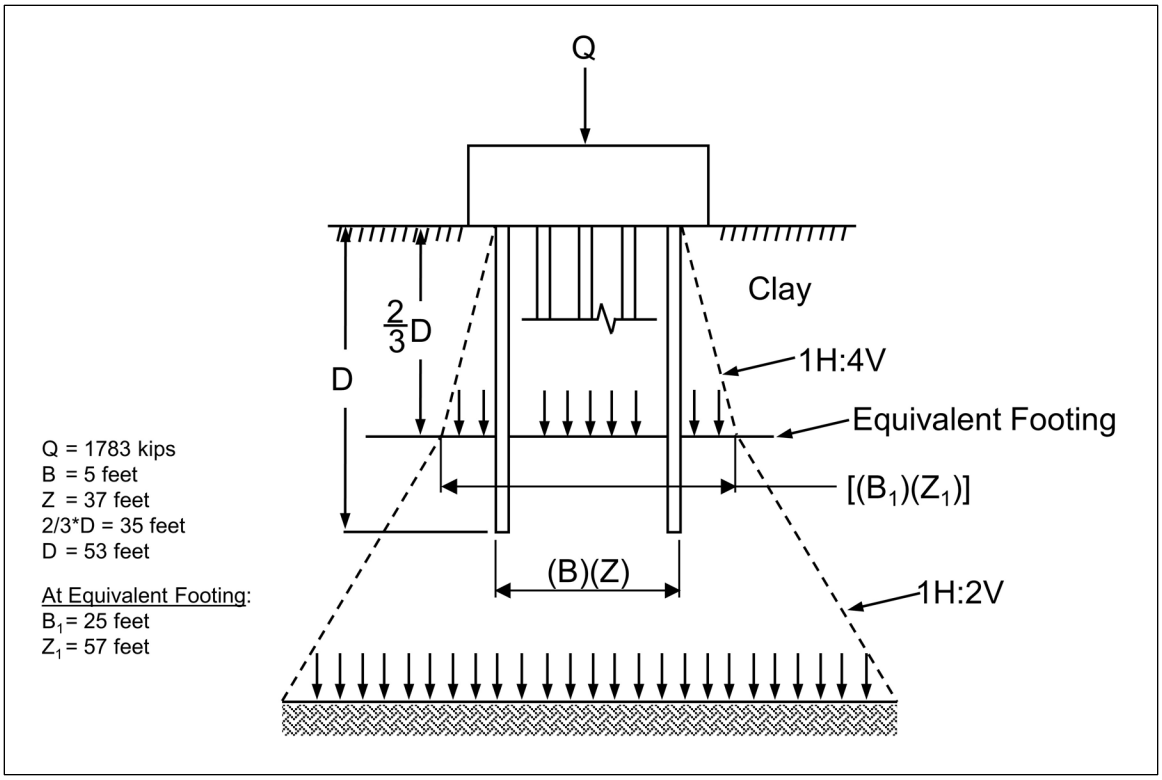

Figure D-108 Equivalent footing at 35 feet below the pile cap with respective stress distribution for conventional settlement analysis.

Considering only the unfactored permanent load, Q, calculate the vertical effective stress increase below the equivalent footing resulting from superstructure loads, $\Delta\sigma'_{v(ss)}$, at Elev. 267.5 feet.

- Q = unfactored permanent load, 1783 kips (Service I, without LL, Table D-105).
- B_1 = pile group width at equivalent footing, 25 feet.
- Z_1 = pile group length at equivalent footing, 57 feet (Group Configuration 3 only).
- z = depth below equivalent footing, 2.5 feet (Elev. 267.5 feet).

$$\Delta\sigma'_{v(ss)} = \frac{Q}{(B_1+z)+(Z_1+z))} \qquad \text{[Eq. 7-55]}$$

$$\Delta\sigma'_{v(ss)} = \frac{(1783\ kips)}{((25\ feet)+(2.5\ feet))*((57\ feet)+(2.5\ feet))}$$

$$\Delta\sigma'_{v(ss)} = 1.09\ ksf$$

Including the vertical effective stress increase from the embankment and superstructure, calculate the total vertical effective stress increase below the equivalent footing at Elev. 267.5 feet.

$\Delta\sigma'_{v(e)}$ = change in effective stress at depth z below the equivalent footing from embankment loading, 0.79 ksf (Table D-115).

$\Delta\sigma'_{v(\mathrm{ss})}$ = change in effective stress at depth z below the equivalent footing from superstructure loading, 1.09 ksf.

$$\Delta\sigma'_{v(e+ss)} = \Delta\sigma'_{v(e)} + \Delta\sigma'_{v(\mathrm{ss})}$$

$$\Delta\sigma'_{v(e+ss)} = (0.79\ ksf) + (1.09\ ksf)$$

$$\Delta\sigma'_{v(e+ss)} = 1.88\ ksf$$

Determine the preconsolidation stress from the initial vertical effective stress and overconsolidation ratio at depth z below the equivalent footing (Elev. 267.5 feet).

σ'_{vo} = initial vertical effective stress at depth z below the equivalent footing, 2.24 ksf.

OCR = overconsolidation ratio, 2.01 (Soil Layer 2, Table D-116).

$$\sigma'_p = \sigma'_{\mathrm{vo}} * \mathrm{OCR}$$

$$\sigma'_p = (2.24\ \mathrm{ksf}) * (2.01)$$

$$\sigma'_p = 4.50\ ksf$$

Evaluate the stress increase at depth z below the equivalent footing (Elev. 267.5 feet) relative to the preconsolidation stress.

σ'_{vo} = initial vertical effective stress below equivalent footing, 2.70 ksf.

$\Delta\sigma'_{v(e+ss)}$ = change in effective stress below equivalent footing, 1.88 ksf.

σ'_p = preconsolidation stress below equivalent footing, 4.50 ksf.

$$\sigma'_{\mathrm{vo}} + \Delta\sigma'_{v(e+ss)} \leq \sigma'_p$$

$$(2.24\ ksf) + (1.88\ ksf) \leq (4.50\ ksf)$$

Determine the stress increase by comparing σ'_{vo} and $\sigma'_{1(\mathrm{ss+e})}$.

$$Stress\ Increase = \frac{\sigma'_{1(\mathrm{ss+e})} - \sigma'_{\mathrm{vo}}}{\sigma'_{\mathrm{vo}}} * 100\% \qquad \text{[Eq. D-5]}$$

$$Stress\ Increase = \frac{(4.12\ ksf) - (2.24\ ksf)}{(2.24\ ksf)} * 100\%$$

$$Stress\ Increase = 84\%$$

The stress increase is greater than or equal to 10%. Deformation for this depth increment should be estimated and included in the sum of all depth increments in which the stress increase is not less than 10%.

Estimate consolidation settlement of layer for overconsolidated soil using Equation 7-57 for ($\sigma'_{vo} + \Delta'\sigma \leq \sigma'_{p}$).

e_o	=	initial soil layer void ratio, 0.80 (Soil Layer 2, Table D-116).
C_r	=	recompression index, 0.03 (Soil Layer 2, Table D-116).
H_o	=	initial height of soil layer, 5 feet.
σ'_{vo}	=	initial vertical effective stress at depth z below the equivalent footing, 2.24 ksf.
$\Delta\sigma'_{v(e+ss)}$	=	change in vertical effective stress at depth z below the equivalent footing, 1.88 ksf.

$$S_c = \frac{C_r}{1+e_o} H_o \log\left(\frac{\sigma'_{vo} + \Delta\sigma'_{v}}{\sigma'_{vo}}\right) \qquad \text{[Eq. 7-57]}$$

$$S_c = \frac{(0.03)}{1+(0.80)} (5\ feet) * log\left(\frac{(2.24\ ksf) + (1.88\ ksf)}{(2.24\ ksf)}\right)$$

$$S_c = 0.0221\ feet * \left(\frac{12\ inches}{1\ foot}\right) = 0.26\ inches$$

Table D-117 Calculation of Settlement using Equivalent Footing and Conventional Primary Consolidation Equations

EL (feet)	z (feet)	H_o (feet)	σ'_{vo} (ksf)	OCR	σ'_p (ksf)	B (feet)	Z (feet)	$\Delta\sigma'_{v(ss)}$ (ksf)	$\Delta\sigma'_{v(e+ss)}$ (ksf)	Stress Incr. (%)	S (in)
267.5	2.5	5	2.24	2.01	4.504812	27.5	59.5	1.09	1.88	84	0.26
262.5	7.5	5	2.54	1.71	4.3398945	32.5	64.5	0.85	1.64	65	0.17
257.5	12.5	5	2.87	1.71	4.902912	37.5	69.5	0.68	1.48	51	0.14
252.5	17.5	5	3.20	1.71	5.472342	42.5	74.5	0.56	1.35	42	0.12
247.5	22.5	5	3.53	1.71	6.041772	47.5	79.5	0.47	1.26	36	0.10
242.5	27.5	5	3.87	1.71	6.611202	52.5	84.5	0.40	1.18	31	0.09
237.5	32.5	5	4.20	1.71	7.180632	57.5	89.5	0.35	1.12	27	0.08
232.5	37.5	5	4.53	1.71	7.750062	62.5	94.5	0.30	1.07	24	0.07
227.5	42.5	5	4.87	1.71	8.319492	67.5	99.5	0.27	1.02	21	0.06
222.5	47.5	5	5.20	1.71	8.888922	72.5	104.5	0.24	0.98	19	0.06
217.5	52.5	5	5.53	1.71	9.458352	77.5	109.5	0.21	0.95	17	0.05
216.5	53.5	1	5.21	1.71	8.9038845	78.5	110.5	0.21	0.94	18	0.01
										Total:	1.21

The above analysis was performed for additional equivalent footing locations considering dimensions of the three trial group configurations. Table D-118 summarizes the analysis results for pile group settlement using the equivalent footing with conventional primary consolidation. As established by global project performance requirements, total vertical deformation should be limited to 1.5 inches at each substructure location. To account for the additional deformation from elastic pile compression, the equivalent footing should be located 35 feet below the bottom of pile cap (i.e., located at Elev. 270.0 feet). Using the equivalent footing to pile penetration depth relationship displayed in Figure D-108, the respective pile penetration depth, *D*, is 53 feet ((3/2) *35 feet ≈ 53 feet) for an equivalent footing at a depth of 35 feet.

Table D-118 Summary of Pile Group Settlement Estimates Based on Equivalent Footing Depth and Conventionally Settlement Computations

Equivalent Footing Elevation (feet)	Equivalent Footing Depth (feet)	Pile Toe Elevation (feet)	Pile Toe Depth (feet)	Estimated Settlement Group Configuration 1 and 2 (inches)	Estimated Settlement Group Configuration 3 (inches)
280.0	25	267.0	38	5.63	6.22
275.0	30	260.0	45	1.46	2.85
270.0	35	252.0	53	1.20	1.21
265.0	40	245.0	60	0.97	0.99

Pile group settlement was also evaluated using the neutral plane method and Janbu tangent modulus approach as outlined in Section 7.3.5 of Chapter 7. To compare settlement estimates using this approach with the conventional consolidation theory results presented in Table D-118, the neutral plane was placed at the same elevation as the equivalent footing location that resulted in the estimated settlement of 1.21 inches (i.e., the neutral plane was placed at 35 feet). Figure D-109 illustrates the neutral plane location and stress distribution used with this approach. To highlight the differences between these two methods, the equivalent footing at 35 feet in Figure D-109 has plan dimension of 5 feet by 37 feet. However, the equivalent footing in Figure D-108 used with the conventional consolidation theory has an equivalent footing plan dimension of 25 feet by 57 feet. As a result of the greater contact stress, the neutral plane calculated settlements are significantly greater.

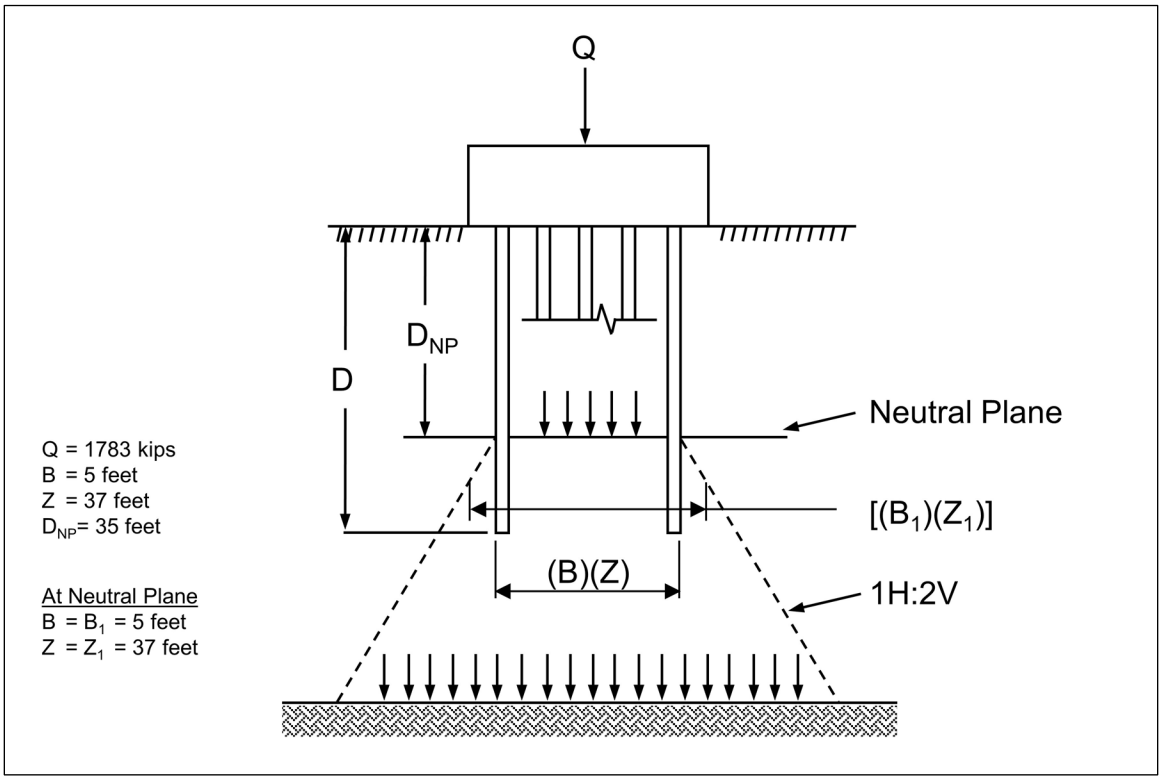

Figure D-109 Neutral plane at 35 feet below the pile cap and resulting stress distribution.

The following settlement calculation is performed for the neutral plane located 35 feet below the bottom of footing. From Elev. 270.0 feet to 214.0 feet, strain calculations for cohesive soil (stress exponent of j=0) were applied for Soil Layers 1 to 3. It was assumed that vertical deformation below the encountered bedrock at Elev. 214.0 feet is negligible. The length of the pile group in Group Configuration 3

is 37 feet from exterior pile edge to exterior pile edge, and therefore this example is suitable for only this configuration. The same dimension for Group Configuration 1 and 2 is 41 feet. Similar to the stress increase calculations from embankment loading, the soil profile was again divided into 5 foot thick layers with the exception of the final layer which is 1 foot thick. The elevation shown in Table D-119 references the midpoint of each respective soil layer, while z is the depth below the equivalent footing to the midpoint of each respective soil layer. Tabulated values for this analysis are recorded in Table D-119.

Considering only the unfactored permanent load, Q, calculate the vertical effective stress increase below the equivalent footing resulting from superstructure loads, $\Delta\sigma'_{v(\mathrm{ss})}$, at EL 267.5 feet.

Q = unfactored permanent load, 1783 kips (Service I, without LL, D-105).
B = pile group width, 5 feet.
Z = pile group length, 37 feet (Group Configuration 3 only).
z = depth below equivalent footing, 2.5 feet (Elev. 267.5 feet).

$$\Delta\sigma'_{v(\mathrm{ss})} = \frac{Q}{(B+z)+(Z+z))} \qquad \text{[Eq. 7-55]}$$

$$\Delta\sigma'_{v(\mathrm{ss})} = \frac{(1783\ kips)}{((5\ feet)+(2.5\ feet))*((37\ feet)+(2.5\ feet)))}$$

$$\Delta\sigma'_{v(\mathrm{ss})} = 6.02\ ksf$$

Including the vertical effective stress increase from the embankment and superstructure, calculate the total vertical effective stress increase below the equivalent footing at EL 267.5 feet.

$\Delta\sigma'_{v(e)}$ = change in effective stress at depth z below the equivalent footing from embankment loading, 0.79 ksf (Table D-115).
$\Delta\sigma'_{v(\mathrm{ss})}$ = change in effective stress at depth z below the equivalent footing from superstructure loading, 6.02 ksf.

$$\Delta\sigma'_{v(e+ss)} = \Delta\sigma'_{v(e)} + \Delta\sigma'_{v(\mathrm{ss})}$$

$$\Delta\sigma'_{v(e+ss)} = (0.79\ ksf) + (6.02\ ksf)$$

$$\Delta\sigma'_{(e+ss)} = 6.81\ ksf$$

Determine the preconsolidation stress from the initial vertical effective stress and overconsolidation ratio at EL 267.5 feet.

σ'_{vo} = initial vertical effective stress at depth z below the equivalent footing, 2.24 ksf.

OCR = overconsolidation ratio, 2.01 (Soil Layer 2, Table D-116).

$$\sigma'_p = \sigma'_{\mathrm{vo}} * \mathrm{OCR}$$

$$\sigma'_p = (2.24\ \mathrm{ksf}) * (2.01)$$

$$\sigma'_p = 4.50\ ksf$$

Evaluate the stress increase at depth at EL 267.5 feet relative to the preconsolidation stress.

σ'_{vo} = initial vertical effective stress at depth z below the equivalent footing, 2.24 ksf.

$\Delta\sigma'_{v(e+ss)}$ = change in effective stress at depth z below the equivalent footing, 6.81 ksf.

σ'_p = preconsolidation stress at depth z below the equivalent footing, 4.50 ksf.

$$\sigma'_{\mathrm{vo}} + \Delta\sigma'_{v(e+ss)} \geq \sigma'_p$$

$$(2.24\ ksf) + (6.81\ ksf) \geq (4.50\ ksf)$$

Determine the percent stress increase by comparing σ'_{vo} and $\sigma'_{1(\mathrm{e+ss})}$.

σ'_{vo} = initial vertical effective stress at depth z below the equivalent footing, 2.24 ksf.

$\sigma'_{1(\mathrm{e+ss})}$ = new vertical effective stress considering both superstructure and embankment loads, 2.24 ksf + 6.81 ksf = 9.05 ksf.

$$Percent\ Stress\ Increase = \frac{\sigma'_{1(\mathrm{e+ss})} - \sigma'_{\mathrm{vo}}}{\sigma'_{\mathrm{vo}}} * 100 \qquad \text{[Eq. D-5]}$$

$$Percent\ Stress\ Increase = \frac{(9.05)-(2.24)}{2.24} * 100$$

$$Percent\ Stress\ Increase = 304\%$$

For cohesive soil at Elevation 272.5 feet, *z* = 2.5 (j = 0), the modulus number is determined by Equation 7-68.

e_o = void ratio, 0.80 (Soil Layer 2, Table D-116).
C_c = compression index, 0.30 (Soil Layer 2, Table D-116).

$$m_n = 2.30\left[\frac{1+e_0}{C_c}\right] \quad \text{[Eq. 7-68]}$$

$$m_n = 2.30\left[\frac{1+(0.80)}{(0.30)}\right]$$

$$m_n = 13.8$$

For cohesive soil at Elevation 272.5 feet, *z* = 2.5 (j = 0), the recompression modulus number is determined by Equation 7-69.

e_o = initial soil layer void ratio, 0.80 (Soil Layer 2, Table D-116).
C_c = recompression index, 0.03 (Soil Layer 2, Table D-116).

$$m_{nr} = 2.30\left[\frac{1+e_0}{C_r}\right] \quad \text{[Eq. 7-69]}$$

$$m_{nr} = 2.30\left[\frac{1+(0.80)}{(0.03)}\right]$$

$$m_{nr} = 138$$

For overconsolidated cohesive soils (j = 0) in which the new vertical effective stress exceeds the preconsolidation stress, determine strain in layer with Equation 7-65.

σ'_p = preconsolidation stress, 4.50 ksf.
σ'_{vo} = initial vertical effective stress at depth z below the equivalent footing, 2.24 ksf.
$\sigma'_{1(\mathrm{e+ss})}$ = new vertical effective stress, 9.05 ksf.
m_{nr} = recompression modulus, 138.
m_n = compression modulus, 13.8.

$$\varepsilon = \frac{1}{m_{nr}}\ln\left[\left(\frac{\sigma'_p}{\sigma'_{v0}}\right)\right] + \frac{1}{m_n}\ln\left[\left(\frac{\sigma'_1}{\sigma'_p}\right)\right] \quad \text{[Eq. 7-65]}$$

$$\varepsilon = \frac{1}{(138)} \ln\left[\left(\frac{(4.50\ ksf)}{(2.24\ ksf)}\right)\right] + \frac{1}{(13.8)} \ln\left[\left(\frac{(9.05\ ksf)}{(4.50\ ksf)}\right)\right]$$

$$\varepsilon = 0.0557$$

Calculate the layer compression denoted, *S*, with the initial height of the layer, H_o.

$$S = \Delta\varepsilon * H_o$$

$$S = 0.0557 * (5\ feet)\left(\frac{12\ inches}{1\ foot}\right)$$

$$S = 3.34\ inches$$

For overconsolidated cohesive soils (j = 0) in which the new effective stress does not exceed the preconsolidation stress, such as at EL 252.5, determine strain in layer with Equation 7-66.

σ'_p	=	preconsolidation pressure, 5.47 ksf (Table D-119).
σ'_{vo}	=	initial vertical effective stress at depth z below the equivalent footing, 3.20 ksf (Table D-119).
$\sigma'_{1(\mathrm{e+ss})}$	=	new vertical effective stress, 5.45 ksf (Table D-119).
m_{nr}	=	recompression modulus, 177.1 (Calculation not presented for Soil Layer 3).

$$\varepsilon = \frac{1}{m_{nr}} \ln\left[\left(\frac{\sigma'_1}{\sigma'_{\mathrm{v0}}}\right)\right] \qquad \text{[Eq. 7-66]}$$

$$\varepsilon = \frac{1}{(177.1)} ln\left[\left(\frac{(5.35\ ksf)}{(3.20\ ksf)}\right)\right]$$

$$\varepsilon = 0.0030$$

Calculate the layer compression denoted, *S*, with the initial height of the layer, H_o.

$$S = \varepsilon * H_o$$

$$S = 0.0030\ feet * (5\ feet)\left(\frac{12\ inches}{1\ foot}\right)$$

$$S = 0.18\ inches$$

Table D-119 Settlement Estimate for Neutral Plane Method with the Neutral Plane at EL 270.0 feet

EL (feet)	z (feet)	H_o (ksf)	σ'_{vo} (ksf)	OCR	σ'_p (ksf	B (feet)	Z (feet)	$\Delta\sigma'_{ss}$ (ksf)	σ'_{1e+ss} (ksf)	Stress Incr. (%)	ε	S (in)
267.5	2.5	5	2.24	2.01	4.50	7.5	39.5	6.02	9.05	304	0.0556	3.34
262.5	7.5	5	2.54	1.71	4.34	12.5	44.5	3.21	6.53	157	0.0261	1.57
257.5	12.5	5	2.87	1.71	4.90	17.5	49.5	2.06	5.72	99	0.0117	0.70
252.5	17.5	5	3.20	1.71	5.47	22.5	54.5	1.45	5.45	70	0.0030	0.18
247.5	22.5	5	3.53	1.71	6.04	27.5	59.5	1.09	5.41	53	0.0024	0.14
242.5	27.5	5	3.87	1.71	6.61	32.5	64.5	0.85	5.50	42	0.0020	0.12
237.5	32.5	5	4.20	1.71	7.18	37.5	69.5	0.68	5.66	35	0.0017	0.10
232.5	37.5	5	4.53	1.71	7.75	42.5	74.5	0.56	5.86	29	0.0015	0.09
227.5	42.5	5	4.87	1.71	8.32	47.5	79.5	0.47	6.10	25	0.0013	0.08
222.5	47.5	5	5.20	1.71	8.89	52.5	84.5	0.40	6.35	22	0.0011	0.07
217.5	52.5	5	5.53	1.71	9.46	57.5	89.5	0.35	6.61	20	0.0010	0.06
214.5	53.5	1	5.21	1.71	8.90	58.5	90.5	0.34	6.27	20	0.0011	0.01
											Total	6.46

For the same equivalent footing location of Elev. 270 feet, the above results of 6.46 inches of estimated settlement using the neutral plane approach is significantly larger than the 1.23 inches of settlement (Table D-118) based on consolidation theory. For this example calculation, it was decided that the settlement method yielding the greatest settlement magnitude would be used to establish the range of pile penetration depths that satisfy tolerable deformations. The neutral plane method illustrated above was performed for additional equivalent footing depths until tolerable settlements were estimated.

Table D-120 summarizes analysis results for pile group settlement estimated using the neutral plane method and Janbu Tangent modulus approach. Although not yet calculated, it is preliminarily estimated that elastic pile compression may be on the order of 0.5 inches, effectively limiting tolerable soil settlement to on the order of 1 inch. Therefore, to limit the total vertical deformation including elastic pil compression and settlement to less than 1.5 inches, analysis results in Table D-120 indicate that the neutral plane should be located at Elev. 215.0 feet, 90 feet below the bottom of pile cap.

Table D-120 Summary of Pile Group Settlement Estimates Based on Janbu Tangent Modulus with Neutral Plane Method For All Group Configurations

Neutral Plane Elevation (feet)	Neutral Plane Depth (feet)	Estimated Settlement Group Configuration 1 and 2 (inches)	Estimated Settlement Group Configuration 3 (inches)
235.0	70	1.85	2.13
230.0	75	1.50	1.77
225.0	80	1.23	1.41
220.0	85	1.07	1.25
215.0	90	0.28	0.35

It is assumed that the equivalent footing acts at the same location as the neutral plane. Accordingly, an analysis was then performed to determine the pile toe elevation necessary to locate the neutral plane at Elev. 215.0, thereby establishing the minimum required pile penetration depth to satisfy tolerable deformations.

The location of the neutral plane and the magnitude of drag force are evaluated following the procedure outlined in Section 7.3.6 of Chapter 7, using unfactored permanent loads and nominal geotechnical resistance. Because load factors for the Service limit state are 1.0, applicable loads at this limit state may be considered unfactored. The Service I, without LL limit state loads are therefore used for evaluation for the neutral plane. This example again utilizes the load for Group Configuration 3 (Q= 127 kips, Table D-108). Figure D-110 presents a graphical interpretation of the neutral plane for the HP 12x74 pile driven to 91 feet (seated on bedrock at Elev. 214.0).

First, the sustained load plus the cumulative shaft resistance versus depth is plotted. Next, the mobilized toe resistance minus the cumulative shaft resistance versus pile penetration depth is plotted. The exact percentage of toe mobilization is unknown at this stage of design, and therefore multiple toe mobilization curves should be evaluated to determine the neutral plane location. The 0% toe mobilization curve is the most conservative location to evaluate pile settlement since it locates the neutral plane at the highest elevation. The 100% toe mobilization curve should be used to check the pile section's structural strength since it results in the greatest axial force in the pile. The structural strength check is performed in Block 17.

At the South Abutment, it is expected that piles will be supported partially by toe resistance on bedrock, and therefore the 0% toe mobilization curve presents an unreasonable baseline to evaluate settlement in this case. Some toe resistance is likely mobilized, and to remain consistent with the other substructure locations, the 50 % toe mobilization curve is again used to evaluate settlement.

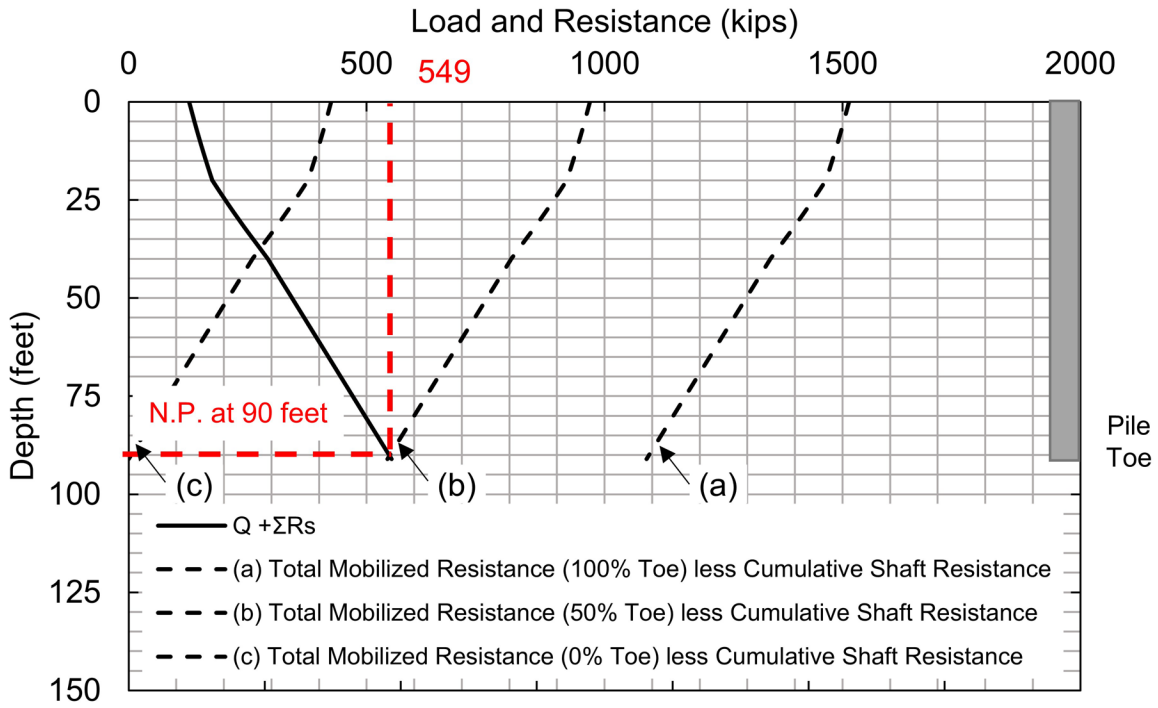

Figure D-110 Neutral plane location considering 50% toe mobilization for HP 12x74 at the South Abutment.

Assuming 50 % toe mobilization, the neutral plane is located 90 feet below the bottom footing with a resulting maximum load in the pile of 549 kips. Since the pile toe is seated on bedrock at EL 214.0, vertical deformation will be limited to elastic shortening of the pile and elastic compression of the bedrock which is expected to be negligible. The minimum pile penetration required to satisfy tolerable deformations is therefore approximately 91 feet resulting in the piles being driven to bedrock to control vertical deformations.

This procedure was performed for the remaining candidate pile sections and trial group configurations. , the above analysis was also performed to determine the pile penetration depth required to locate the neutral plane below a depth of 90 feet (EL 215.0 ft). The results of these analyses indicate that all the candidate pile sections and trial group configurations require the pile to be driven to bedrock (i.e., at an approximate depth of 91 feet.

As previously noted, a comparison of the required pile penetration depth determined from both settlement estimation methods yielded significantly different results. This is a direct result of the equivalent footing dimensions and stress distribution for each respective method. Previously, Table D-118 summarized the minimum pile penetration depth based on conventional settlement estimates for piles supported by shaft resistance in clay. Table D-121 presents the minimum pile penetration depth for all pile sections and group configurations based on settlement estimation using the neutral plane method with Janbu Tangent modulus. In the latter settlement approach, for all candidate pile sections and group configurations, the piles must be driven to bedrock at approximately 91 feet.

Experience should be used to establish a penetration depth with either settlement estimation approach. For this design example, the established minimum pile penetration depth to satisfy tolerable vertical deformations will be based solely on the settlement results using the neutral plane and Janbu tangent modulus. Table D-121 presents the established pile penetration depths to satisfy tolerable deformations at the South Abutment.

Table D-121 Established Minimum Required Pile Penetration Depths to Satisfy Tolerable Deformations at the South Abutment

Group Configuration	All Candidate Pile Sections (feet)
1, 2 and 3	Bedrock (≈ 91)

Elastic shortening of the pile should be considered along with settlement. For elastic compression, the load per pile from the Service I, without live load limit state is applied at the pile head. As shown in Table D-108, this load is 127 kips.

Note that the drag force from negative shaft resistance increases the axial compression force in the pile. Negative shaft resistance above the neutral plane acts to increase axial compression force in the pile, whereas below the neutral plane, positive shaft resistance reduces the axial compression force in the pile. This effect must be accounted for in the elastic compression calculation. Accordingly, the unfactored axial load used to compute elastic compression, Q, changes for each pile segment length, increasing equal to the unfactored permanent load plus the shaft resistance down to the neutral plane. In this example, the unfactored axial load is equal to the resistance distribution from 100% toe mobilization. The highest drag force magnitude results from this curve and represents the worst case.

Equation 7-48 is used to illustrate this example for the first 12 inch increment of the HP 12x74 pile section. The average shaft resistance and average load for each respective depth interval is used to estimate the elastic compression. For each 12 inch segment, the elastic modulus remains constant, and was evaluated as 29,000 ksi. The pile cross sectional area likewise remains constant as 21.8 in^2. Remaining calculations were performed using a spreadsheet; Table D-122 summarizes the elastic compression with depth.

Determine the unfactored axial load, Q, in segment.

Q_d = unfactored permanent load, 127.0 kips.
R_s^- = average (negative) shaft resistance, 1.1 kips.

$$\mathrm{Q} = Q_d + R_s^- = 127.0\ kips + 1.1\ kips$$

$$\mathrm{Q} = 128.1\ kips$$

Calculate elastic compression of segment with unfactored axial load from combined unfactored permanent load and negative shaft resistance.

L = segment length, 12 inches.
A = cross sectional area of pile material, 21.8 in^2.
E = elastic modulus of pile, 29,000 ksi.

$$\Delta = \frac{QL}{AE} \qquad \text{[Eq. 7-48]}$$

$$\Delta = \frac{(128.1\ kips)*(12\ inches)}{(21.8\ in^2)*(29{,}000\ ksi)}$$

$$\Delta = 0.00243\ inches$$

Table D-122 Elastic Compression Calculation

Depth Below Pile Head (feet)	Average Shaft Resistance (kips)	Average Unfactored Axial Load (kips)	Δ (inches)
0	0.0	127.0	0.00000
0-1	1.1	128.1	0.00243
1-2	3.3	130.3	0.00247
2-3	5.5	132.5	0.00252
3-4	7.7	134.7	0.00256
4-5	10.0	137.0	0.00260
5-6	12.2	139.2	0.00264
6-7	14.5	141.5	0.00269
7-8	16.9	143.9	0.00273
8-9	19.2	146.2	0.00278
9-10	21.6	148.6	0.00282
10-11	24.1	151.1	0.00287
11-12	26.5	153.5	0.00291
12-13	29.0	156.0	0.00296
13-14	31.5	158.5	0.00301
14-15	34.1	161.1	0.00306
15-16	36.7	163.7	0.00311
16-17	39.3	166.3	0.00316
17-18	41.9	168.9	0.00321
18-19	44.6	171.6	0.00326
19-20	47.3	174.3	0.00331
20-21	51.3	178.3	0.00339
21-22	56.7	183.7	0.00349
22-23	62.1	189.1	0.00359
23-24	67.6	194.6	0.00369
24-25	73.2	200.2	0.00380
25-26	78.7	205.7	0.00391
26-27	84.3	211.3	0.00401
27-28	90.0	217.0	0.00412
28-29	95.7	222.7	0.00423
29-30	101.6	228.6	0.00434
30-31	107.4	234.4	0.00445
31-32	113.3	240.3	0.00456
32-33	119.2	246.2	0.00467
33-34	125.3	252.3	0.00479
34-35	131.5	258.5	0.00491
35-36	137.7	264.7	0.00502
36-37	143.8	270.8	0.00514
37-38	149.9	276.9	0.00526

Table D-122 Elastic Compression Calculation (continued)

Depth Below Pile Head (feet)	Average Shaft Resistance (kips)	Average Unfactored Axial Load (kips)	Δ (inches)
38-39	156.0	283.0	0.00537
39-40	162.2	289.2	0.00549
40-41	167.8	294.8	0.00560
41-42	172.9	299.9	0.00569
42-43	178.0	305.0	0.00579
43-44	183.1	310.1	0.00589
44-45	188.2	315.2	0.00598
45-46	193.3	320.3	0.00608
46-47	198.4	325.4	0.00618
47-48	203.5	330.5	0.00627
48-49	208.6	335.6	0.00637
49-50	213.7	340.7	0.00647
50-51	218.8	345.8	0.00656
51-52	223.9	350.9	0.00666
52-53	229.0	356.0	0.00676
53-54	234.1	361.1	0.00685
54-55	239.3	366.3	0.00695
55-56	244.4	371.4	0.00705
56-57	249.4	376.4	0.00715
57-58	254.5	381.5	0.00724
58-59	259.6	386.6	0.00734
59-60	264.8	391.8	0.00744
60-61	269.9	396.9	0.00753
61-62	275.0	402.0	0.00763
62-63	280.1	407.1	0.00773
63-64	285.2	412.2	0.00782
64-65	290.3	417.3	0.00792
65-66	295.4	422.4	0.00802
66-67	300.5	427.5	0.00811
67-68	305.6	432.6	0.00821
68-69	310.7	437.7	0.00831
69-70	315.8	442.8	0.00840
70-71	320.9	447.9	0.00850
71-72	326.0	453.0	0.00860
72-73	331.1	458.1	0.00869
73-74	336.2	463.2	0.00879
74-75	341.3	468.3	0.00889
75-76	346.4	473.4	0.00899

Table D-122 Elastic Compression Calculation (continued)

Depth Below Pile Head (feet)	Average Shaft Resistance (kips)	Average Unfactored Axial Load (kips)	Δ (inches)
76-77	351.5	478.5	0.009082
77-78	356.6	483.6	0.009179
78-79	361.7	488.7	0.009276
79-80	366.8	493.8	0.009373
80-81	371.9	498.9	0.009470
81-82	377.0	504.0	0.009567
82-83	382.1	509.1	0.009664
83-84	387.2	514.2	0.009760
84-85	392.3	519.3	0.009858
85-86	397.4	524.4	0.009955
86-87	402.5	529.5	0.010051
87-88	407.6	534.6	0.010148
88-89	412.7	539.7	0.010245
89-90	417.9	544.9	0.010342
90-91	423.0	550.0	0.010439
			0.55

For the pile head load of 127 kips (Group Configuration 3 loads), estimated elastic compression of the HP 12x74 pile section driven to 91 feet is 0.55 inches. As the piles are driven to bedrock, it is assumed no settlement will occur, and therefore it is estimated that total vertical deformation at the South Abutment is 0.55 inches.

D.40 Block 16: South Abutment – Check pile drivability to maximum pile penetration depth requirements established in Blocks 12 through 15

Preliminary pile drivability was previously evaluated for the 5 candidate pile sections in Block 10. The plots of nominal resistance, blow count and compression stress versus depth in Figure D-99 should now be reviewed considering the established minimum pile penetration depths. A candidate pile section must be capable of being driven to the penetration depth necessary to achieve the nominal geotechnical resistance in axial compression and tension, and to a penetration depth necessary to satisfy lateral load demands as well as axial and lateral deformation requirements. Minimum pile penetration depths have been previously established in Blocks 13, 14 and 15 and are presented in Tables D-111, D-114 and D-126.

Although a minimum pile penetration depth is not typically established for nominal geotechnical resistance in axial compression, the pile should also be capable of being driven reasonably close to the estimated pile penetration depth where the nominal resistance is expected to develop. If the pile cannot be driven to the required depth within driving stress limits and at reasonable blow counts, a larger pile hammer, a pile section with greater impedance, or pile installation aids such as predrilling or jetting may be required to satisfy or improve drivability. Alternatively, substructure design modifications should be considered.

For the candidate HP 12x74 pile section in Group Configuration 3, the pile penetration depth for axial compression loading was estimated at 73 feet (Table D-110), the minimum penetration depth for axial tension loading was 18 feet (Table D-111), the minimum penetration depth for lateral loading was 25 feet (Table D-114) and the estimated minimum penetration depth to satisfy vertical deformation limits was 91 feet (Table D-126). Accordingly, candidate pile section must have sufficient drivability to the maximum of these depths, 91 feet, where driving is anticipated to terminate on bedrock.

A review of the preliminary drivability in Figure D-99 indicates that the HP 12x74 pile section can be driven to bedrock at approximately 91 feet. In addition, from the preliminary drivability evaluation (with soil and hammer model assumptions described in Block 10), it is estimated that the blow count will not exceed 120 blows per foot or 10 blows per inch before this penetration depth. Compression driving stresses are estimated to remain below driving-stress limits. Therefore, it is concluded that pile drivability to the estimated pile penetration depth is acceptable.

D.41 Block 17: South Abutment – Determine the Neutral Plane Location and Resulting Drag Force. Check Structural Strength Limit State for Pile Penetration Depth From Block 16

Previously in Block 15, the neutral plane was evaluated as part of the settlement calculations. The neutral plane and resulting drag force are now evaluated to check the structural strength limit state for candidate pile sections. Section 7.3.6 provides guidance for evaluating the neutral plane location and the magnitude of the drag force. Load using the Service I, without LL limit state are considered for the applied pile head load. This example again utilizes the load for Group Configuration 3 (Q = 127 kips, Table D-108).

At 100 percent toe mobilization, the neutral plane is at its lowest potential location, and thus the highest drag force magnitude results. Accordingly, this is the toe

mobilization curve that should be used to check the pile section's structural strength. Figure D-111 presents a graphical interpretation of the neutral plane for the HP12x74 pile section driven to the estimated pile penetration depth of 91 feet (seated on bedrock). In this case the neutral plane is located 91 feet below pile head with a resulting maximum axial compression force in the pile of 552 kips.

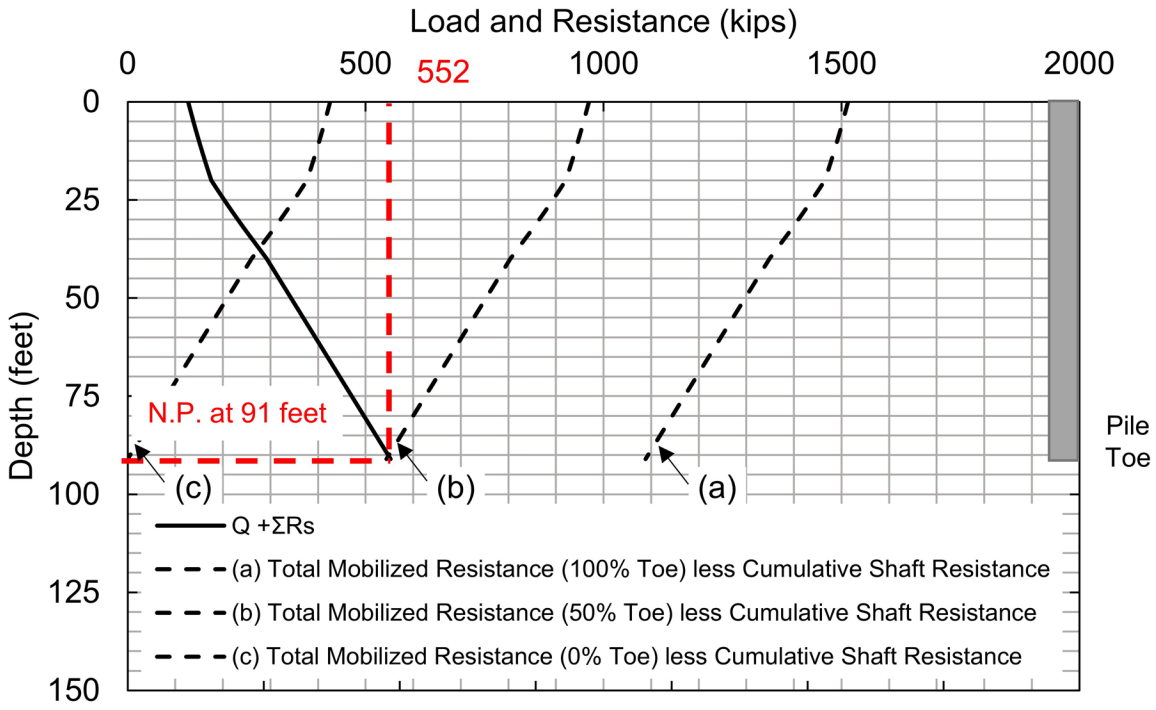

Figure D-111 Neutral plane location considering 100 percent toe mobilization for HP 12x74 at the South Abutment.

The resulting unfactored drag force, DF, is the difference between the maximum unfactored axial compression force in the pile, Q_{max}, minus the unfactored permanent load (Q). In this case, the drag force is evaluated for 100 percent toe mobilization.

$$DF = Q_{max} - Q$$

$$DF = (552\ kips) - (127\ kips) = 425\ kips$$

Following this calculation, the structural resistance was evaluated with Equation 7-70. As discussed in Section 7.3.6 of Chapter 7, a load factor of 1.25 is applied to the permanent load while a load factor of 1.1 is applied to the drag force. When driving through dense soil to rock, it may be generally appropriate to assume that the pile toe may be subject to damage during driving. Therefore, a structural resistance

factor for axial compression, ϕ_c, of 0.5 is applied to the nominal structural resistance of 1088 kips (Table D-94). For this assumption, the factored structural resistance, P_r, for the HP 12x74 section is 544 kips.

$$P_u = 1.25\ (Q) + \gamma_p(DF) < P_r \qquad \text{[Eq. 7-70]}$$

$$P_u = 1.25\ (127\ kips) + 1.1(425\ kips) = 626\ kips$$

$$626\ kips > 544\ kips$$

In this case, the factored structural resistance is less than the factored loads, and therefore the pile section is unacceptable.

It may be appropriate to reconsider the structural resistance factor used above based upon the driving conditions. The pile is driven through silty clay for approximately 91 feet, and the probability of damage in this zone is very low. In addition, a review of the boring logs (Figure D-2) indicates the transition from silty clay to bedrock is relatively abrupt, and there will be little difficulty seating the pile on bedrock. If an appropriately sized hammer (or appropriate energy setting) is selected, dynamic testing is performed to monitor and control driving stresses, and driving criteria is established such that the risk of pile toe damage is low, the use of a higher structural resistance factor may be warranted. Consideration could also be given to dynamically testing 100% of the piles as a further means of identifying and mitigating any damaged piles. AASHTO (2014) design specifications allow a structural resistance factor for axial compression of 0.6 for H-pile sections with good driving conditions where damage is unlikely.

Proceeding with the drag force analysis, if a structural resistance factor for axial compression, ϕ_c, of 0.6 is applied to the nominal structural resistance of 1088 kips (Table D-94), the factored structural resistance, P_r, for the HP 12x74 section is 652 kips. Equation 7-68 is used to evaluate the structural resistance.

$$P_u = 1.25\ (Q) + \gamma_p(DF) < P_r \qquad \text{[Eq. 7-70]}$$

$$P_u = 1.25\ (127\ kips) + 1.1(425\ kips) = 626\ kips$$

$$626\ kips < 652\ kips$$

In this case, the factored structural resistance is greater than the factored load, and therefore the pile section is acceptable.

It may be beneficial to review the ratio of factored load to nominal structural resistance or, P_u / P_n. The following evaluation serves to back calculate the minimum required structural resistance factor, $\phi_{c(\min)}$, for the section to be acceptable considering the factored load.

$$\phi_{c(\min)} = \frac{P_u}{P_n}$$

$$\phi_{c(\min)} = \frac{(626\ kips)}{(1088\ kips)}$$

$$\phi_{c(\min)} = 0.58$$

The neutral plane and drag force analysis was also performed for each candidate pile section using 100 percent toe mobilization. Factored structural resistance was subsequently evaluated considering the factored loads for group configurations shown in Table D-108. The pile penetration depth utilized for the structural resistance check was the required minimum penetration depth presented in Table D-126 (91 feet for all piles and group configurations at the South Abutment). It was again assumed that the probability of pile damage is reduced using the means discussed above. Therefore, a structural resistance factor in axial compression, ϕ_c, of 0.6 was applied to the nominal structural resistance for each candidate pile section. Table D-123 presents the ratio of the factored load to nominal structural resistance, at the neutral plane (also the pile toe), for all the candidate piles and group configurations.

Table D-123 Ratio of Factored Load to Nominal Structural Resistance in Axial Compression, $\phi_{c(\min)}$, at the Neutral Plane

Group Configuration	HP 10x42 $\phi_{c(\min)}$	HP 12x53 $\phi_{c(\min)}$	HP 12x74 $\phi_{c(\min)}$	HP 14x89 $\phi_{c(\min)}$	HP 14x117 $\phi_{c(\min)}$
1	0.99**	0.90**	0.64**	0.59	0.46
2	0.93**	0.84**	0.60**	0.56	0.43
3	0.88**	0.81**	0.58	0.54	0.41

The neutral plane is located at the pile toe for all sections and group configurations.
Note: ** - Section not acceptable considering ϕ_c equal or greater than 0.60.

Based on results of the drag force analysis, a candidate pile section may be eliminated from consideration if the factored loads are higher than the factored structural resistance. Table D-124 summarizes results of the drag force analysis.

The HP 12x74 pile section is acceptable in Group Configuration 3, while the HP 14x89 and HP 14x117 pile sections are acceptable in all three group configurations.

Table D-124 Does Candidate Pile Section Meet Structural Resistance Requirements Considering Drag Force at Minimum Pile Penetration Depth?

Group Configuration	HP 10x42	HP 12x53	HP 12x74	HP 14x89	HP 14x117
1	No	No	No	Yes	Yes
2	No	No	No	Yes	Yes
3	No	No	Yes	Yes	Yes

D.42 Decision 18: Does Estimated Total Settlement and Differential Settlement Between Adjacent Substructure Locations Satisfy Requirements and Angular Distortion Limits?

All substructures have now been preliminarily designed and the estimated vertical deformations computed for each location.

The vertical deformation limits and construction point concept detailed in Section 7.3 of Chapter 7 was used to first calculate tolerable differential settlement based upon angular distortion. Using Equation D-5, the angular distortion between substructure supports is limited to 0.004 radians, and for a 100 ft span on a multispan bridge, this equates to 4.8 inches of tolerable differential settlement.

Determine tolerable differential settlement, S_d, between substructure supports.

L_s = span length, 100 feet.
A = angular distortion limit, 0.004 radians (Table 7-18).

$$S_d = A * L_s \qquad \text{[Eq. D-7]}$$

$$S_d = (0.004) * (100\ feet) * \left(\frac{12\ inches}{1\ foot}\right)$$

$$S_d = 4.8\ inches$$

Although this differential settlement is tolerable for angular distortion, project performance requirements limited the settlement at each substructure location to a maximum of 1.5 inches, the differential settlement between adjacent substructure locations limited to 1.0 inch, and a maximum angular distortion of 0.0008 radians. These requirements were established for rideability, drainage, and attached utility damage considerations. The estimated substructure performance is summarized in Table D-125.

Table D-125 Summary of Foundation Total Settlement, Differential Settlement, and Angular Distortion for HP 12x74 Pile Section

Substructure Location	Settlement Method	Total Settlement (inches)	Differential Settlement (inches)	Span Length (feet)	Angular Distortion
N. Abutment	N. Plane	1.17			
			0.18	100	0.0002
Pier 2	N. Plane	0.99			
			0.44	100	0.0004
S. Abutment	N. Plane	0.55			

As illustrated in Table D-125, the total settlement, differential settlement, and angular distortion requirements are all satisfied.

D.43 Block 19: South Abutment – Evaluate Economics of Candidate Piles, Preliminary Group Configurations, and Other Factors

The design process has served to compare strength and service limits for several candidate pile types within trial group configurations. Some candidate pile types have not met all of the strength, service, or drivability requirements. It is useful to quickly review the suitable and unsuitable pile types and group configurations and then assess the cost of the viable foundation solutions.

The number of initial candidate pile types has been reduced through evaluations of strength or drivability requirements while remaining candidate pile types are now subject to an economic analysis. Foundation cost and related economics are discussed in Section 3.4 of Chapter 3. Final selection of a pile type and group configuration is therefore based not only upon limit state requirements, but considers the associated cost.

Table D-126 summarizes the established minimum pile penetration depth based on analysis results from Blocks 12 through 15. For all candidate pile sections and group configurations at the South Abutment, the established minimum pile penetration depth was based on meeting tolerable vertical deformations.

Several candidate sections did not meet structural resistance requirements for axial loading, lateral loading or both. The candidate pile sections and/or group configurations not meeting design requirements are identified with an asterisk in Table D-126. For all three group configurations, the HP 10x42 and HP 12x52 pile sections did not meet all structural resistance requirements. The HP 12x74 section was also structurally unacceptable for Group Configurations 1 and 2. These candidate pile sections and group configuration were eliminated for the final design.

Table D-126 Established Minimum Pile Penetration Depth at the South Abutment

Group Configuration	HP 10x42 (feet)	HP 12x53 (feet)	HP 12x74 (feet)	HP 14x89 (feet)	HP 14x117 (feet)
1	91*	91*	91*	91*	91
2	91*	91*	91*	91	91
3	91*	91*	91	91	91

*Did not meet structural resistance requirement

Table D-127 presents the estimated minimum penetration depth for each candidate section to meet the factored geotechnical resistance requirements at the Strength I limit state. The larger pile sections require less pile penetration depth than the smaller pile sections to provide the same geotechnical resistance. In addition, the factored load per pile decreases from Group Configuration 1 to Group Configuration 3. However, from the analyses in Blocks 13 through 15, the established minimum penetration depth to preclude unacceptable vertical deformation requires all piles to be driven deeper than the depth needed solely for their factored geotechnical resistance. The minimum penetration depth requirement results in the additional geotechnical resistance gained by further pile embedment to be essentially wasted and therefore uneconomical.

Table D-127 Estimated Minimum Penetration Depth for Factored Geotechnical Resistance at Strength I Limit State

Group Configuration	HP 10x42 (feet)	HP 12x53 (feet)	HP 12x74 (feet)	HP 14x89 (feet)	HP 14x117 (feet)
1	91*	91*	91*	90*	88**
2	91*	90*	86*	74**	72**
3	91*	74*	73**	63**	62**

Note: * -Did not meet structural resistance requirement

Note: ** -Must be driven deeper to established minimum penetration depth (min. 91 feet).

Reference should be made to Block 19 of the North Abutment for a more detailed discussion of individual pile cost. Figure D-112 again presents the estimated individual pile cost versus pile penetration depth.

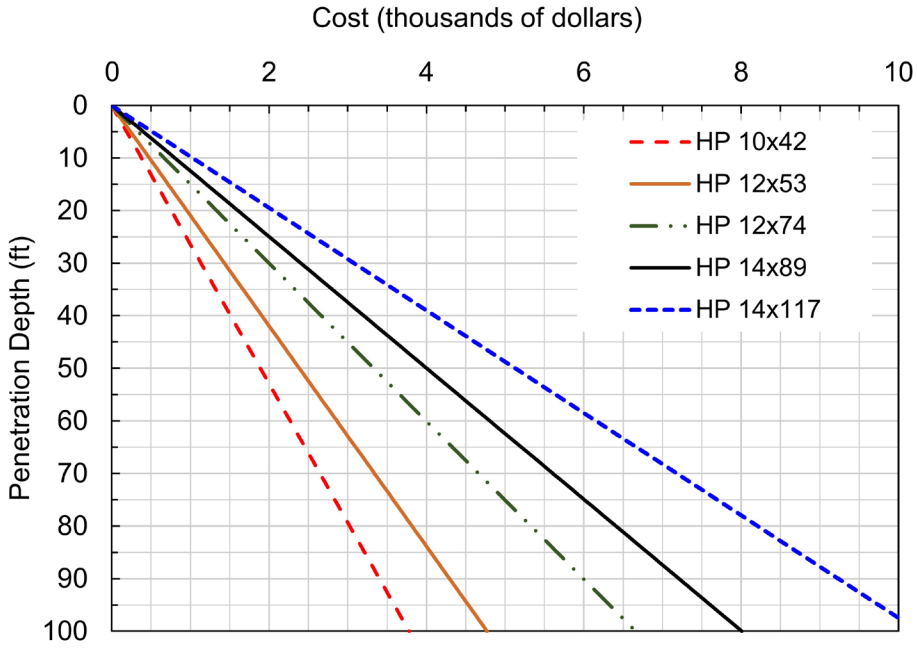

Figure D-112 Pile cost versus penetration depth.

For the South Abutment, Table D-128 shows the price per pile when considering the established minimum pile penetration depth. For example, for the HP 12x74 pile section in Group Configuration 3, the individual cost is determined by multiplying the cost per foot by the penetration depth. At the minimum pile penetration depth of 91 feet, the cost per pile is $6,061. To note, there will be additional pile length embedded in the cap, however for pile cost estimation it can be considered negligible. Furthermore, Table D-129 shows the pile group cost reflecting the cost per pile and number of piles in the group.

Table D-128 Cost per Pile at Established Minimum Penetration Depth for Piles Meeting Structural Requirements

Group Configuration	HP 12x74	HP 14x89	HP 14x117
1	-	-	$9,337
2	-	$7,289	9,337
3	$6,061	7,289	9,337

Table D-129 Pile Group Cost at Established Minimum Penetration Depth for Piles Meeting Structural Requirements

Group Configuration	Required Number of Piles	HP 12x74	HP 14x89	HP 14x117
1	18	-	-	$168,059
2	22	-	$160,360	205,405
3	26	$157,576	189,517	242,752

Based upon this comparison, the HP 14x117 pile section proves to be least economical. Based upon pile group cost, the HP 14x89 pile section in Group Configuration 1 appears to be the most economical followed by the HP 12x74 pile section in Group Configuration 3. However, before selecting the lowest cost option considering solely the results in Table D-129, the cost of the pile cap should also be estimated and factored into the foundation cost, as discussed below.

Section 8.9 of Chapter 8 outlines a procedure to estimate the total pile cap thickness. Equation 8-80 is used to estimate this value along using the factored load per pile at the Strength limit state as previously presented in Table D-108.

A sample calculation is shown for the HP 12x74 pile in Group Configuration 3. Table D-130 summarizes the estimated cap thickness for each pile section and pile group permutation calculated using this procedure.

Estimate the total pile cap thickness.

P_{ui} = maximum single pile factored axial load, Q =238 kips (Group Configuration 3, Table D-108).

$$t_{cap} = \frac{P_{ui}}{12} + 30 \qquad \text{[Eq. 8-80]}$$

$$t_{cap} = \frac{(238\ kips)}{12} + 30$$

$$t_{cap} = 50\ inches$$

Table D-130 Estimated Total Pile Cap Thickness

Group Configuration	HP 12x74 (inches)	HP 14x89 (inches)	HP 14x117 (inches)
1	-	-	59
2	-	53	53
3	50	50	50

Next, the volume of reinforce concrete required to construct the pile cap is determined from the estimated total pile cap thickness. The total pile cap width and length values were previously provided in Table D-106. The resulting volume of reinforced concrete for each pile section and pile group permutation is presented in Table D-131. Note that pile cap volume is shown in cubic yards (CY).

Table D-131 Estimated Volume of Reinforced Concrete in Pile Cap

Group Configuration	HP 12x74 (CY)	HP 14x89 (CY)	HP 14x117 (CY)
1	-	-	50.0
2	-	45.5	45.5
3	38.5	38.5	38.5

To estimate the pile cap cost, past pricing information is generally the best guide; however, similar to estimating the pile cost, due to fluctuations in the market price of material and other factors, pile cap costs are subject to change. The cost of the reinforced concrete pile cap, furnished and constructed, is estimated to be $500 /CY. Using this estimated value, the volumes presented in Table D-131 were used to estimate the cost of the various reinforced concrete pile caps. The pile cap cost for each candidate section and group configuration is shown in Table D-132.

Table D-132 Estimated Cost of Reinforced Concrete Pile Cap

Group Configuration	HP 12x74	HP 14x89	HP 14x117
1	-	-	$25,010
2	-	$22,772	22,772
3	$19,245	19,245	19,245

By adding the cost of the pile cap and piles for each permutation, the estimated total foundation cost is determined as presented in Table D-133. Additional construction costs should be considered and included, if applicable, such as excavations support, dewatering, and utility relocation or other environmental impacts. However, an exhaustive analysis of the other considerations is not presented in this example. Considering both the pile and the pile cap costs, the HP 12x74 section in the Group Configuration 3 is the most economical solution at the South Abutment followed by the HP 14x89 section in Group Configuration 2. Contractor equipment considerations, potential economies from use of only one pile section across the project, and other factors should be weighed in deciding between the HP 12x74 and HP 14 x 89 section use at the three substructure locations.

Table D-133 Estimated Foundation Cost Including Piles and Pile Cap at South Abutment

Group Configuration	HP 12x74	HP 14x89	HP 14x117
1	-	-	$193,069
2	-	$183,132	228,177
3	$176,821	208,762	261,997

While the cost of pile over/underrun at other substructure locations was evaluated to account for inaccuracies in the assumed soil strength properties and estimated soil resistance, this is not the case at the South Abutment. Piles must be driven to bedrock (approximately 91 feet) at the South Abutment to satisfy a tolerable deformation, which effectively eliminates risk of length over/overrun differences between any candidate pile sections and a further economic assessment is therefore not needed.

D.44 Decision 20: Is the Preliminary Design of All Substructure Foundations Complete?

Yes, the preliminary foundation design has now been completed at all three substructure locations; North Abutment, Pier 2, and South Abutment.

D.45 Block 21: Refine Structural Modeling and Determine Loads at Foundation Top and Lateral Earth Pressure Loads on Abutments

The structure and foundation response to the loading cases is now further refined based on the structural and geotechnical analyses completed in Block 9 through

Block 17. The structural model is reanalyzed using the results from these preliminary substructure analyses to better define the structure loads at the foundation top, and lateral earth pressure loads on the abutments.

D.46 Decision 22: Did Loads Significantly Change, and Require Reevaluation of the Foundation Design?

No. The refined structural modeling determined that the structural loads provided in Block 11 are suitable for the final design.

D.47 Block 23: For Dynamic Elastic Analyses, Reevaluate Foundation Stiff nesses Using Unfactored Loads in Structural Model to get New Foundation Loads

Dynamic elastic analyses are not required since the structure is not subject to seismic events.

D.48 Decision 24: Did Loads Significantly Change, and Require Reevaluation of the Foundation Design?

Since dynamic analyses are not required, re-evaluation of the foundation design is not necessary.

D.49 Decision 25: Does the Design Meet All Limit State Requirements?

All strength, service, and extreme limit state requirements have been satisfied by one or more candidate piles and associated group configurations as demonstrated in Blocks 9 through 18.

To complete the final design, a candidate pile section and associated pile group configuration must be selected at each substructure location. Table D-134 summarizes the total foundation cost for HP 12x74, HP 14x89 and HP 14x117 at each respective substructure location. If one pile section is used at all substructure locations for the bridge, the lowest cost foundation selection is the HP 12x74 at $367,043 followed by the HP 14x89 at $369,674. The most economical solution is to use HP 12x74 H-piles at both abutments and HP 14x89 H-piles at Pier 2. This solution has an estimated foundation cost of $357,434.

Table D-134 Estimated Total Foundation Cost at All Substructures Locations on the Southbound Bridge

Location	Most Economical HP 12x74 Cost	Associated HP 12x74 Group Configuration	Most Economical HP 14x89 Cost	Associated HP 14x89 Group Configuration	Most Economical HP 14x117 Cost	Associated HP 14x117 Group Configuration
North Abutment	$96,192	1	$102,121	1	$122,145	1
Pier 2	94,030	5	84,421	4	104,671	4
South Abutment	176,821	3	183,132	2	193,069	1
Total	367,043	-	369,674	-	419,885	-

Although the results of the above economic assessment suggests the final design use different H-pile sections at different substructure locations, the $9,609 savings in the estimated foundation cost is likely insufficient to address potential increased costs from varying installation equipment or accessories as well as pile quantity discounts. Therefore, the final design will be based on the HP 12x74 section for the entire structure.

D.50 Block 26: Design Pile Caps and Abutments

Preliminary design of pile caps is discussed in Section 8.9. Preliminary pile cap design was performed for this design example in Block 13. Final pile cap and abutment design is now performed by the structural engineer and is not detailed herein.

D.51 Block 27: Finalize Plans and Specifications Including Pile Quantities, Minimum Pile Penetration Requirements from Blocks 13 through 15, and Required Nominal Resistances

Plans and specifications are finalized based upon the analyses and results from the previous design blocks. A summary of the final design is presented in Table D-135. At Pier 2, Group Configuration 6 was selected over Group Configuration 5 to reduce the risk of pile damage from driving piles through the dense gravel with cobbles to the bedrock. This decision increases the estimated final foundation cost from $367,043 to $373,492. This modest increase is justified by the replacement and redesign costs anticipated to accommodate a damaged pile.

Table D-135 Final Design Foundation Summary and Associated Penetration Depths for the Southbound Bridge

Location	Group Configuration	Estimated Penetration Depth for Axial Compression (feet)	Minimum Penetration Depth for Axial Tension (feet)	Minimum Penetration Depth for Lateral Deformation (feet)	Minimum Penetration Depth for Vertical Deformation (feet)	Pile Section Drivability Limit (feet)
North Abutment	1	45	28	25	60*	62
Pier 2	6	40	0	20	56*	60
South Abutment	3	73	18	35	91*	91

Note: * - Penetration depth controls the foundation design.

Plans and specifications are developed detailing the factored load, the nominal resistance determination method, the required nominal driving resistance, and associated estimated or minimum pile penetration depth estimates for strength or deformation requirements. As decided earlier in the design, dynamic testing with signal matching of at least 2% of the piles per location will be used for the resistance determination method in the field.

D.51.1 Required Nominal Resistance at the North Abutment

At the North Abutment, the required factored load per pile at the Strength I limit state is 323 kips (Table D-14 of Block 10). Therefore the minimum required factored resistance in axial compression is 323 kips. Using the AASHTO resistance factor for nominal resistance determination by dynamic testing, ϕ_{dyn}= 0.65, the nominal resistance per pile is calculated with Equation 7-3.

R_r = required factored resistance per pile, 323 kips (Table D-14).
ϕ_{dyn} = resistance factor (based on the static analysis method).

$$R_r \leq \phi_{dyn} R_n \qquad \text{[Eq. 7-3]}$$

Rearranging terms for R_n:

$$R_n \geq \frac{R_r}{\phi_{dyn}} \qquad \text{[Eq. 7-3]}$$

$$R_n \geq \frac{(323\ kips)}{(0.65)}$$

$$R_n \geq 497\ kips$$

The nominal resistance, R_n, must therefore be greater than 497 kips per pile and this value is included on plan documents. As noted in Table D-6 and Figure D-9, for the HP 12x74 section in Group Configuration 1, the estimated depth to achieve this nominal resistance is 45 feet below the bottom of pile cap.

At the North Abutment, a limited amount of soil setup may also be considered in establishing the driving criteria. Figure D-21 illustrates the estimated soil setup at a depth of 45 feet is 35 kips. However, for tolerable deformations, a minimum pile penetration depth of 60 feet was specified. No additional setup occurs in the soils below 45 feet so the estimated setup at 60 feet is also 35 kips. Hence, production piles achieving a nominal driving resistance, R_{ndr}, of 462 kips should attain the required nominal resistance of 497 kips during restrike. Based on the geomaterials, a restrike test interval of 1 day is specified. The required nominal driving resistance, R_{ndr}, of 462 kips, the nominal resistance, R_n, of 497 kips, the minimum penetration depth, and restrike interval are included on plan documents.

D.51.2 Required Nominal Resistance at Pier 2

At Pier 2, the required factored load per pile at the Strength V limit state is 257 kips (Table D-61 of Block 10). Therefore the minimum required factored resistance in axial compression is 257 kips. Using the AASHTO recommended resistance factor ϕ_{dyn}=0.65, the nominal resistance per pile to be determined from field determination is calculated with Equation 7-3.

R_r = required factored resistance per pile, 257 kips (Table D-61).
ϕ_{dyn} = resistance factor (based on the static analysis method).

$$R_r \leq \phi_{dyn} R_n \qquad \text{[Eq. 7-3]}$$

Rearranging terms for R_n:

$$R_n \geq \frac{R_r}{\phi_{dyn}} \qquad \text{[Eq. 7-3]}$$

$$R_n \geq \frac{(257\ kips)}{(0.65)}$$

$$R_n \geq 395\ kips$$

The nominal resistance, R_n, must therefore be greater than 395 kips per pile (this value is included on plan documents). As noted in Table D-63 and Figure D-41, for

the HP 12x74 section in Group Configuration 6, the minimum estimated depth to achieve this nominal resistance is 40 feet from the bottom of pile cap.

At Pier 2, more soil setup is anticipated due to the cohesive layer. Table D-52 and Table D-56 indicate the estimated soil setup at a depth of 40 feet is 71 kips. However, for tolerable deformations, a minimum pile penetration depth of 56 feet was specified. No additional setup occurs in the soils below 40 feet so the estimated setup at 60 feet is also 71 kips. Hence, production piles achieving a nominal driving resistance, R_{ndr}, of 324 kips should attain the required nominal resistance of 395 kips during restrike. Based on the geomaterials and project size, a restrike test interval of 3 days is specified. The required nominal driving resistance, R_{ndr}, of 324 kips, the nominal resistance, R_n, of 395 kips, the minimum penetration depth, and the restrike interval are included on plan documents.

D.51.3 Required Nominal Resistance at the South Abutment

At the South Abutment, the required factored load per pile at the Strength I limit state is 238 kips (Table D-108 of Block 10). Therefore the minimum required factored resistance in axial compression is 238 kips. Using the AASHTO recommended resistance factor ϕ_{dyn}=0.65, the nominal resistance per pile to be determined from field determination is calculated with Equation 7-3.

R_r = required factored resistance per pile, 238 kips (Table D-108).
ϕ_{dyn} = resistance factor (based on the static analysis method).

$$R_r \leq \phi_{dyn} R_n \qquad \text{[Eq. 7-3]}$$

Rearranging terms for R_n:

$$R_n \geq \frac{R_r}{\phi_{dyn}} \qquad \text{[Eq. 7-3]}$$

$$R_n \geq \frac{(238\ kips)}{(0.65)}$$

$$R_n \geq 366\ kips$$

The nominal resistance, R_n, must therefore be greater than 366 kips per pile (this value is included on plan documents). As noted in Table D-100 and Figure D-85, for the HP 12x74 section in Group Configuration 3, the minimum estimated depth to achieve this nominal resistance is 73 feet from the bottom of pile cap (Table D-109).

At the South Abutment, a significant amount of soil setup is anticipated. The nominal resistances in Table D-100 and Table D-103 indicate the estimated soil setup at a depth of 73 feet is 167 kips. However, for tolerable deformations, a minimum pile penetration depth of 91 feet was specified. This depth corresponds to the interface between the silty clay and bedrock layer. The estimated setup in the soil profile to 91 feet is 210 kips. Hence, production piles achieving a nominal driving resistance, R_{ndr}, of 156 kips should attain the required nominal resistance of 366 kips with time. In clay soils, restrikes are often performed 1 week after initial driving. However, to satisfy the tolerable deformation requirements the piles will be driven to hard rock, the piles will have more than sufficient nominal resistance without setup. Hence, waiting 1 week to conduct restrike tests is not realistic or needed. Based on the geomaterials and project size, a restrike test interval of 1 days is specified. The required nominal driving resistance, R_{ndr}, of 156 kips, the nominal resistance, R_n, of 366 kips, the minimum penetration depth, and the restrike interval are included on plan documents.

D.52 Block 28: Perform Evaluation of Contractor's Proposed Equipment

Project specifications require the Contractor to provide documentation for the pile driving hammer to be used. The drive system submittal form shown in Figure 15-50 of Chapter 15 is typically completed by the Contractor, and provided to the Engineer. A preconstruction wave equation is then performed considering the contractor's specific hammer, selected pile section and respective soil model.

The Contractor has submitted an ICE I-36 V2 single acting diesel hammer for hammer approval. Figure D-113 presents a copy of the hammer submittal form.

Contractor No.: 105589
Project: Sunrise Expressway
County: Sussex

Structure Name and/or No.: Freedom Bridge
Pile Driving Contractor or Subcontractor: CJG Construction
(Piles driven by)

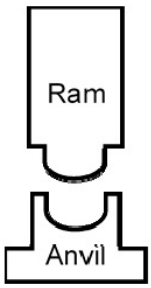

Hammer
Manufacturer: ICE Model No.: I-36v2
Hammer type: Single Acting Diesel Serial No.: 16456
Manufacturer Maximum Rated Energy: 93.74 (kip-ft)
Stroke at Maximum Rated Energy: 11.81 (ft)
Range in Operating Energy: 67.7 to 93.74 (kip-ft)
Range in Operating Stroke: 8.5 to 11.81 (ft)
Ram Weight: 7.94 (kips)
Modifications: N/A

Striker Plate
Weight: N/A (kips) Diameter: (in)
Thickness: (in)

Hammer Cushion
Material#1
Name: Nylon
Area: 490.87 (in^2)
Thickness/Plate: 4 (in)
No. of Plates: 1

Material#2 (for composite cushion)
Name:
Area: (in^2)
Thickness/Plate: (in)
No. of Plates:

Total Thickness of Hammer Cushion: 4

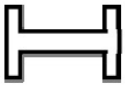

Helmet
Weight: 3.338 (kips)

Insert (If Any)
Weight: N/A (kips)
Total Weight of Helmet and Insert: 3.338 (kips)

Pile Cusion
Material: N/A
Area: (in^2) Thickness/Sheet: (in^2)
No. of Sheets:
Total Thickness of Pile Cushion:
Maximum Thickness Accommodated by Helmet: (in)

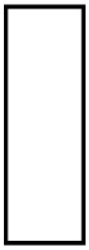

Pile
Pile Type: HP 12x74
Wall Thickness: 0.61 (in) Taper: N/A
Cross Sectional Area: 21.8 (in^2) Weight/ft: N/A
Ordered Length: 90 (ft)
Factored Resistance: N/A (kips)
Nominal Resistance: varies by substructure (kips)
Description of Splice: N/A

Driving Shoe/Closure Plate Description: N/A

Submitted By: Christian J. Logan Date: 11/8/2012
Telephone No.: Email:

Figure D-113 Contractor's ICE I-36 V2 hammer submittal form.

D.52.1 Wave Equation for the North Abutment

At the North Abutment, the design stage drivability file was modified to evaluate the Contractor's proposed driving system. The drivability results, presented in Figure D-114, show that the ICE I-36 V2 appears suitable to drive the HP 12x74 pile section to the required minimum penetration depth of approximately 60 feet, within specified blow count range of 30 to 120 blows per foot, and with driving stresses below the maximum driving stress limit of 45 ksi.

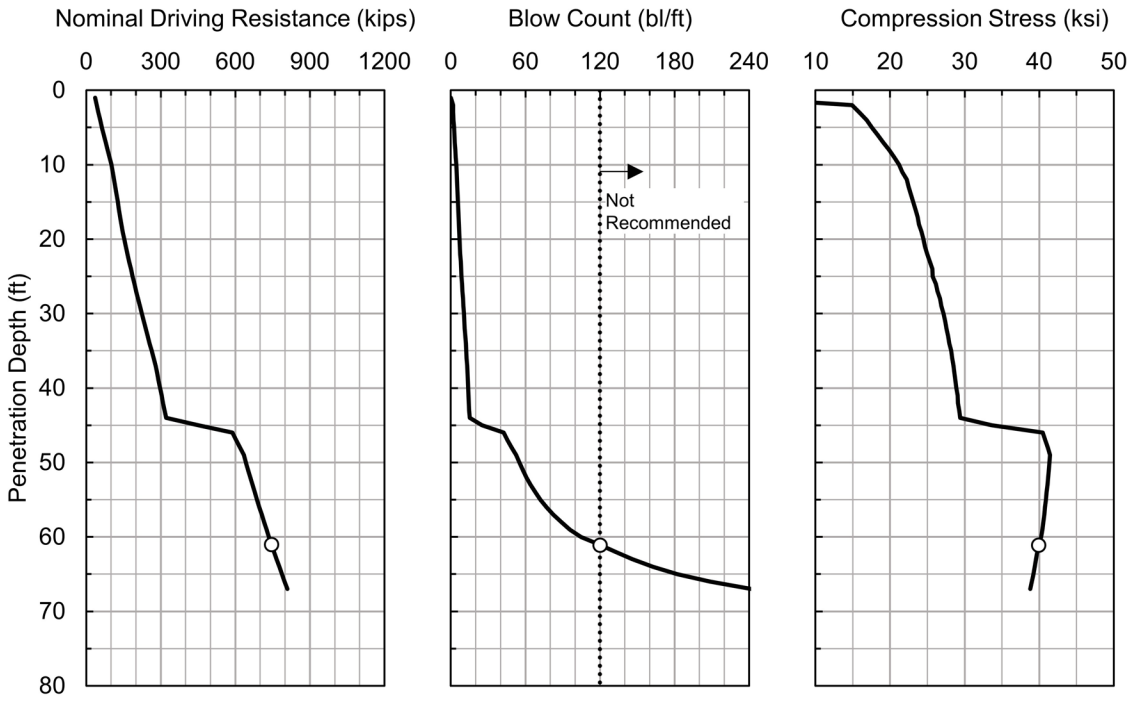

Figure D-114 Preliminary drivability with Contractor's hammer at the North Abutment.

A wave equation bearing graph was also developed for the proposed driving system and HP 12x74 pile section at the required minimum pile penetration depth of 60 feet. The plot of compression stress and tension stress versus blow count is shown as Figure D-115. Driving stresses are less than the 45 ksi specification limit. Figure D-116 presents the bearing graph of the nominal resistance versus blow count, and the calculated hammer stroke versus blow count. In this, it is important to note that the required nominal driving resistance of 462 kips as well as the nominal resistance of 497 kips are well within the blow count range of 30 to 120 blows per foot.

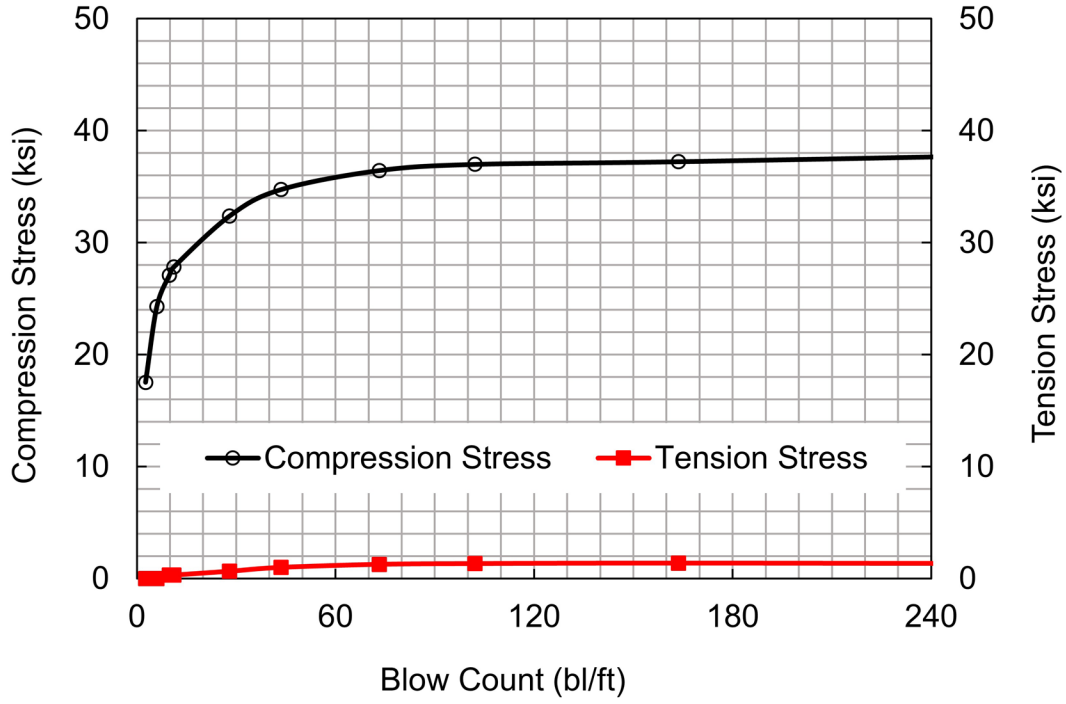

Figure D-115 Compression and tension stress versus blow count.

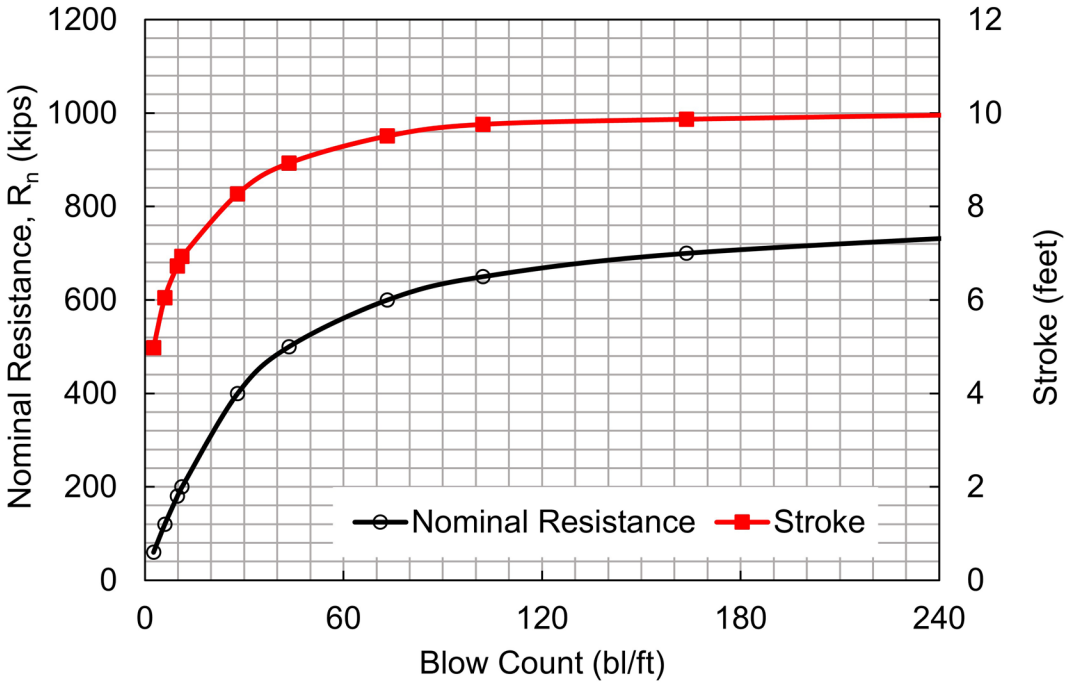

Figure D-116 Nominal resistance and stroke versus blow count.

Figure D-117 provides a preliminary Inspectors Chart of hammer stroke versus blow count for the ICE I-36 V2 and a nominal driving resistance, R_{ndr}, of 462 kips. This plot provide pile inspector with an additional tool to determine the necessary blow count at the observed hammer stroke. For example, the 462 kip nominal driving resistance is achieved at 62 blows per foot with a hammer stroke of 6 feet and at a blow count of 28 blows per foot at a hammer stroke of 11 feet.

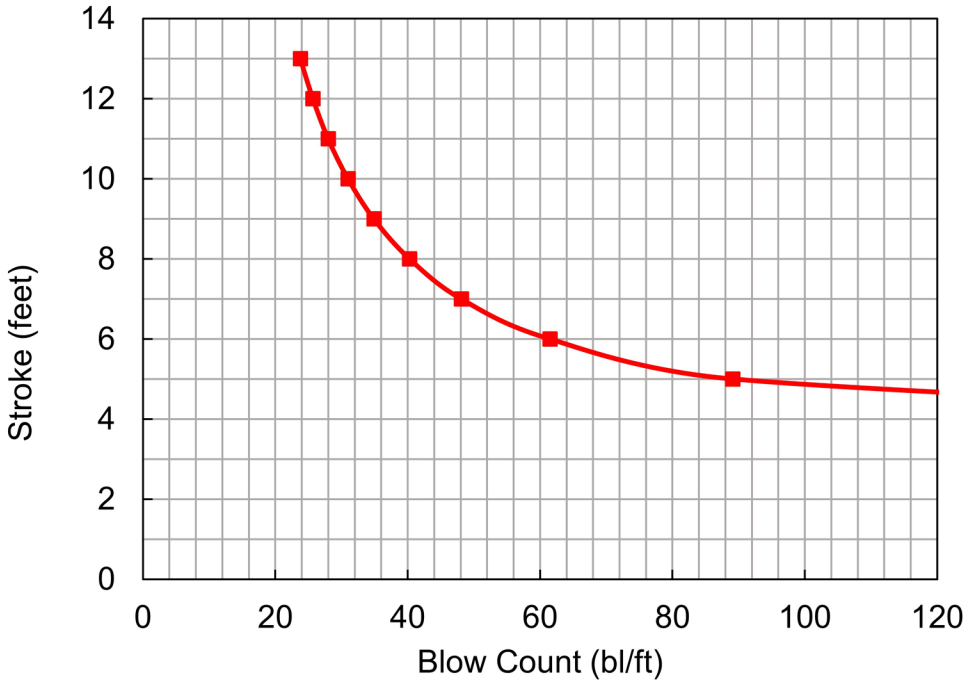

Figure D-117 Inspectors Chart for ICE I-36 V2 at the North Abutment.

D.52.2 Wave Equation for Pier 2

At the Pier 2, the design stage drivability file was again modified to evaluate the Contractor's proposed driving system. The drivability results presented in Figure D-118 show that the ICE I-36 V2 appears suitable to drive the HP 12x74 pile section to the required minimum penetration depth of approximately 56 feet, within specified blow count range of 30 to 120 blows per foot, and with driving stresses below the maximum driving stress limit of 45 ksi.

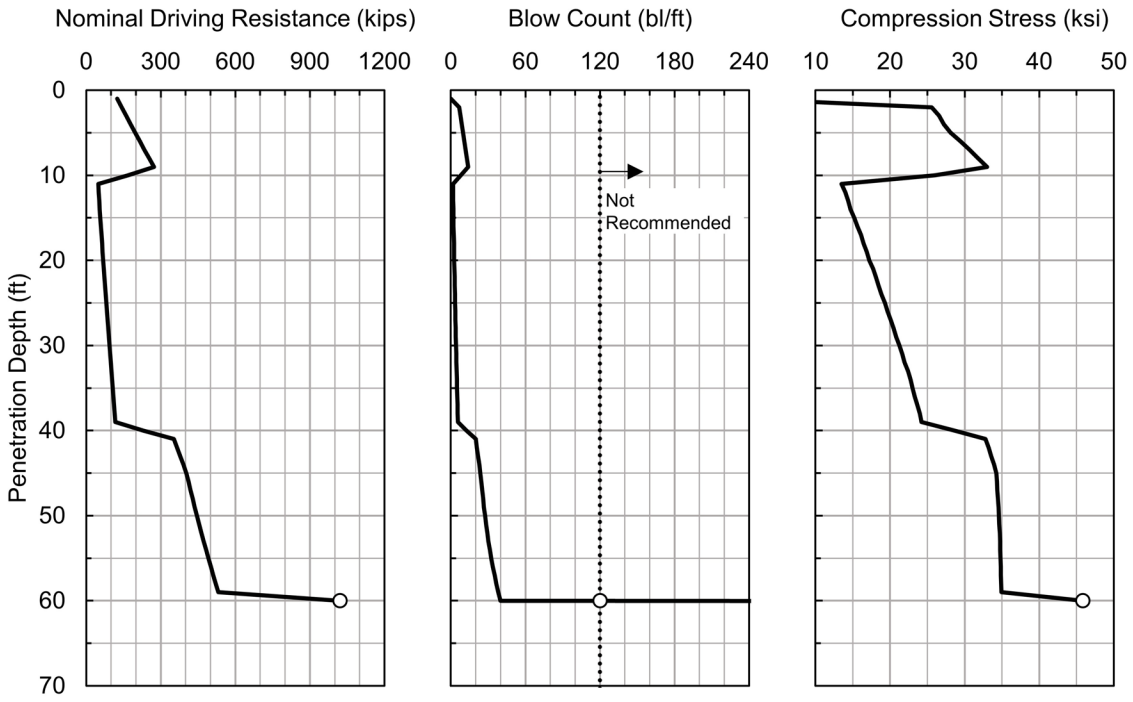

Figure D-118 Drivability with Contractor's hammer at Pier 2.

A wave equation bearing graph was also developed for the proposed driving system and HP 12x74 pile section at the required minimum pile penetration depth of 56 feet. The plot of compression stress and tension stress versus blow count is shown as Figure D-119. Driving stresses are less than the 45 ksi specification limit. Figure D-120 presents the bearing graph of the nominal resistance versus blow count, and the calculated hammer stroke versus blow count. In this, it is important to note that the required nominal driving resistance of 324 kips as well as the nominal resistance of 395 kips are within slightly less than acceptable blow count range of 30 blows per foot. However, the analysis was performed using the maximum fuel setting. If it is desired to have the blow count above 30 blows per foot at the nominal driving resistance, a reduced fuel setting could be used. Also, the nominal driving

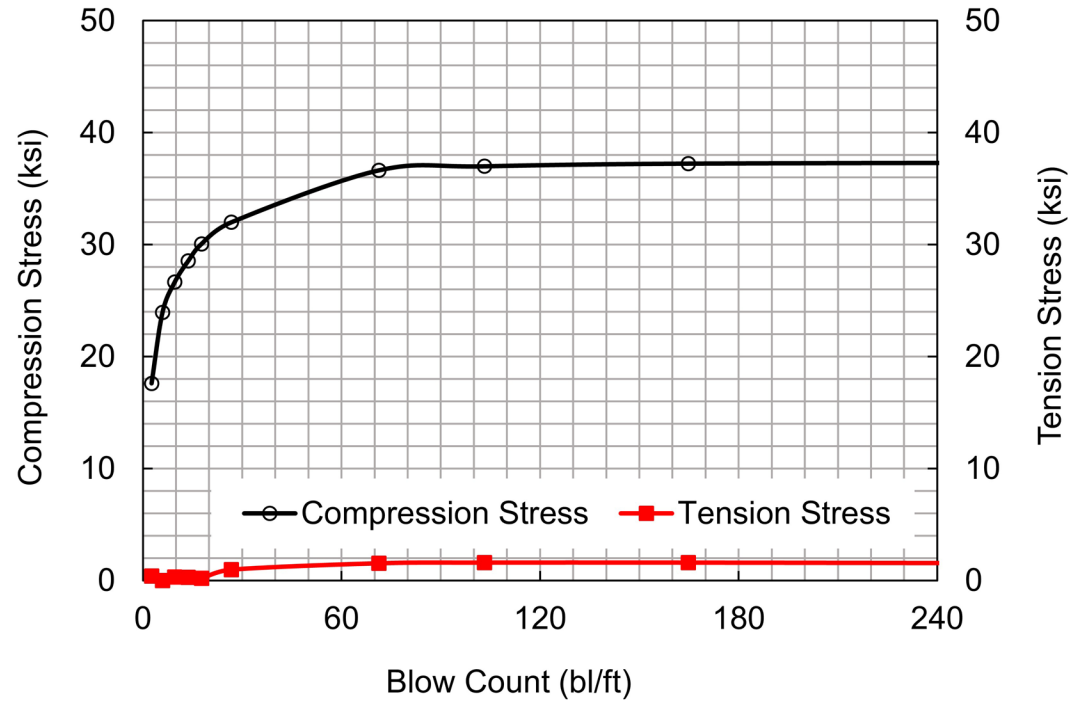

Figure D-119 Compression and tension stress versus blow count.

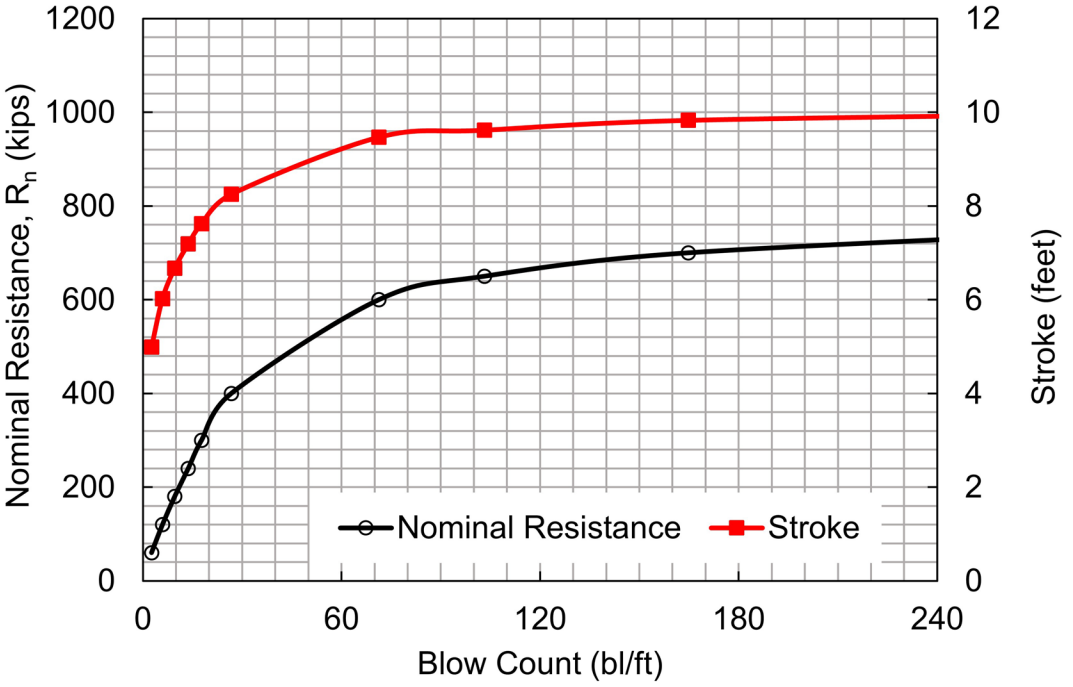

Figure D-120 Nominal resistance and stroke versus blow count.

resistance is expected to be on the order of 500 kips at the minimum pile penetration depth where the blow count is above 30 blows per foot.

Figure D-121 provides a preliminary Inspectors Chart of hammer stroke versus blow count for the ICE I-36 V2 and a nominal driving resistance, R_{ndr}, of 324 kips. This plot provide pile inspector with an additional tool to determine the necessary blow count at the observed hammer stroke. For example, the 324 kip nominal driving resistance is achieved at 37 blows per foot with a hammer stroke of 5 feet and at a blow count of 20 blows per foot at a hammer stroke of 9 feet.

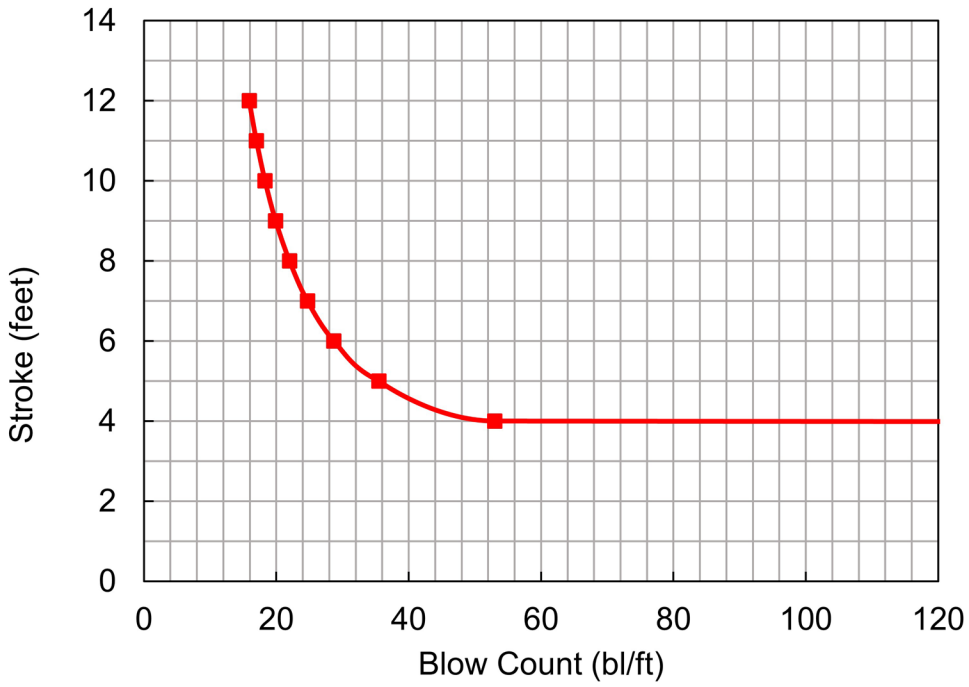

Figure D-121 Inspectors Chart for ICE I-36 V2 at Pier 2.

D.52.3 Wave Equation for the South Abutment

At the South Abutment, the design stage drivability file was revisited and modified to evaluate the Contractor's proposed driving system. The drivability results, presented in Figure D-122 show that the ICE I-36 V2 appears suitable to drive the HP 12x74 pile section to the required minimum penetration depth of approximately 91 feet, within specified blow count range of 30 to 120 blows per foot, and with driving stresses below the maximum driving stress limit of 45 ksi.

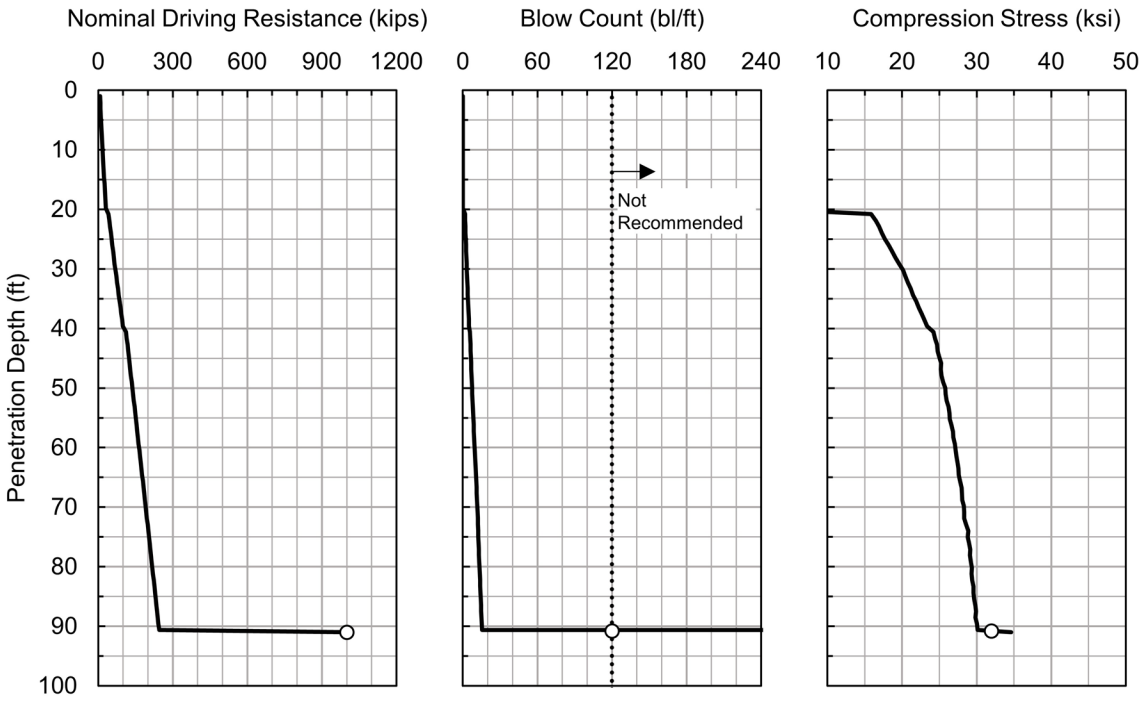

Figure D-122 Drivability with Contractor's hammer at the South Abutment.

A wave equation bearing graph was also developed for the proposed driving system and HP 12x74 pile section at the required minimum pile penetration depth of 91 feet. The plot of compression stress and tension stress versus blow count is shown as Figure D-123. Driving stresses are less than the 45 ksi specification limit. Figure D-124 presents the bearing graph of the nominal resistance versus blow count, and the calculated hammer stroke versus blow count. In this, it is important to note that the required nominal driving resistance of 156 kips as well as the nominal resistance of 366 kips are below the recommended blow count range of 30 to 120 blows per foot. However, the analysis was performed using the maximum fuel setting. If it is desired to have the blow count above 30 blows per foot at the nominal driving resistance, a reduced fuel setting could be used. It should also be noted that the

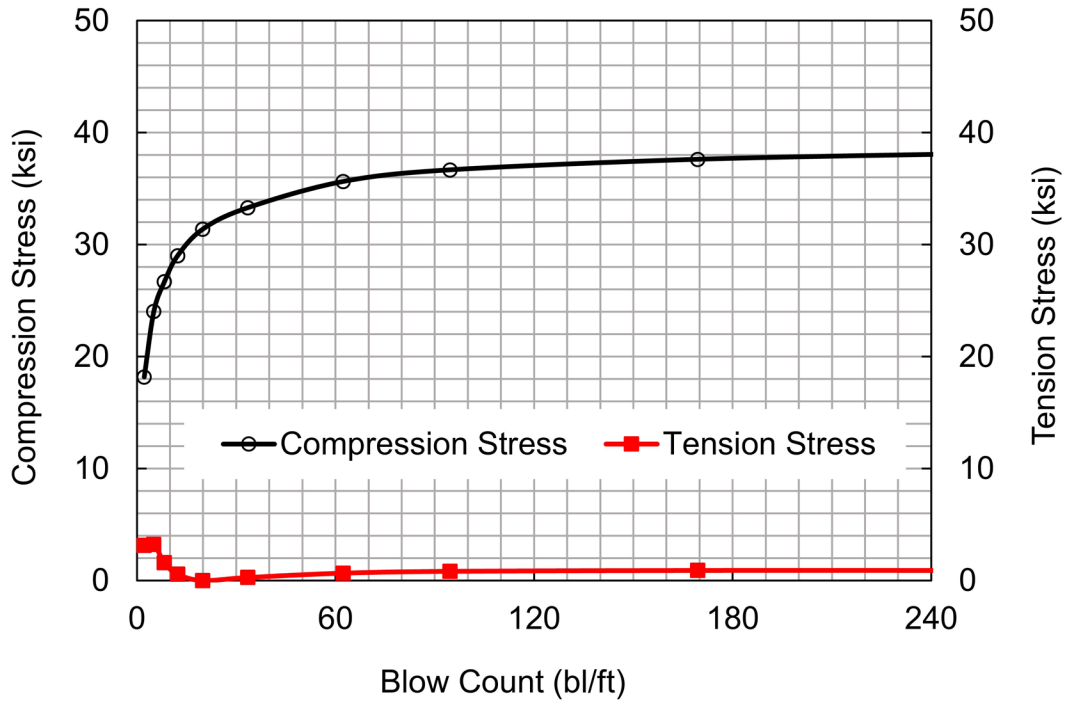

Figure D-123 Compression and tension stress versus blow count.

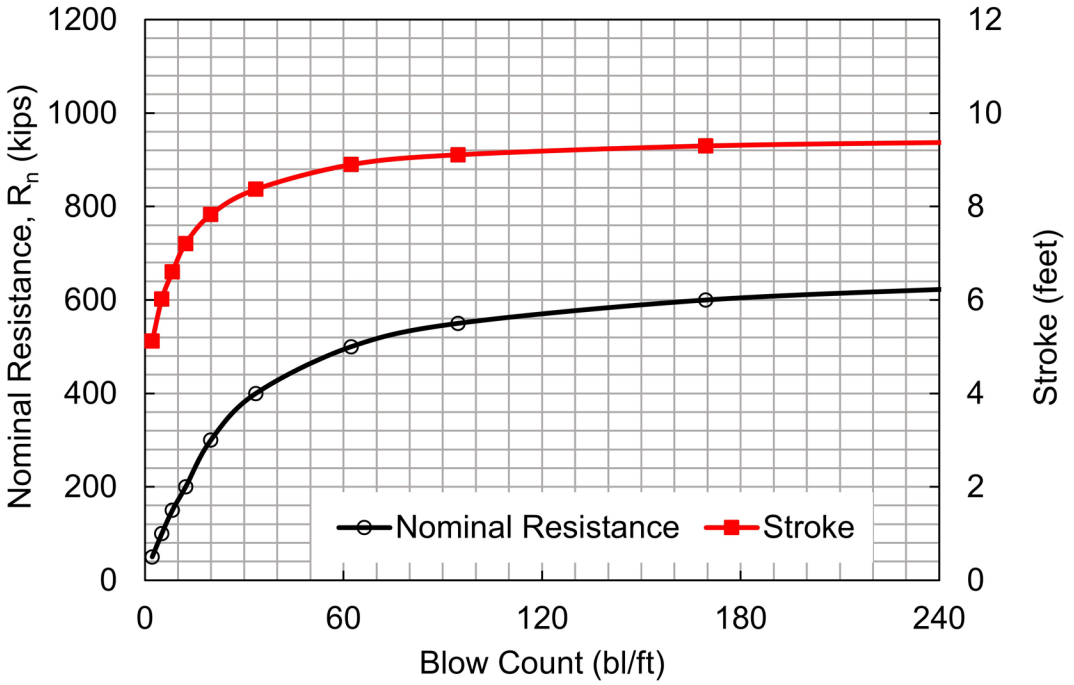

Figure D-124 Nominal resistance and stroke versus blow count.

nominal driving resistance will quickly transition from approximately 240 to 250 kips above rock to well in excess of 900 kips on rock. Hence, hammer operation at a reduced fuel setting is preferred to better control driving stresses.

Figure D-125 is a preliminary Inspectors Chart for the IC I-36 V2. For the nominal driving resistance, R_{ndr}, of 156 kips, Figure D-125 plots the stroke and respective blow count determined from the wave equation analysis. This chart provides the inspector with an additional tool to compare the relative stroke and penetration resistance for a hammer varies in performance. For example, 156 kips of nominal resistance is achieved at 8 blows/ft with a hammer stroke of 6 feet and also at 11 blows/ft with a hammer stroke of 4 feet.

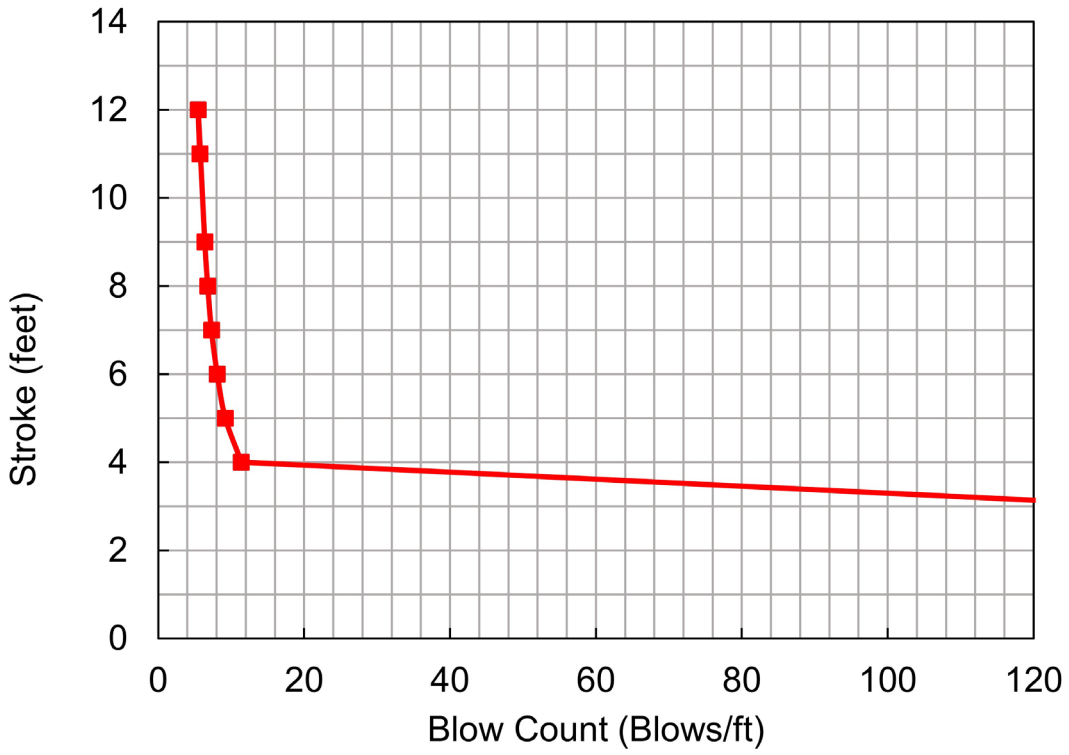

Figure D-125 Inspectors Chart for ICE I-36 V2 at the South Abutment.

D.53 Block 29: Set Preliminary Driving Criteria, Drive Test Pile(s) and Assess Constructability

The required nominal driving resistance at each substructure location was determined in Block 27. These nominal driving resistances consider the selected resistance determination method as well as changes in the long term geotechnical resistance due to soil setup, scour, or construction activities. The wave equation analyses performed for each substructure location in Block 28 will be used to set the preliminary driving criteria.

Two test piles are driven at production pile locations for each substructure. Dynamic monitoring is performed on these two piles during initial driving and again during restrike after an appropriate waiting period. Signal matching analysis is also performed on the initial driving and restrike dynamic test results to determine the magnitude of soil setup. The dynamic testing and signal matching results substantiate the constructability of the design..

D.54 Block 30: Adjust Driving Criteria or Design

Refined wave equation analyses are now performed based on the dynamic test results. The refined wave equation analyses establish the production pile installation criteria at each substructure location. The required nominal driving resistance considers the magnitude of soil setup substantiated by the test pile monitoring during initial driving and restrike. The test pile results confirmed that design modifications are not required.

D.55 Block 31: Drive Production Piles with Construction Monitoring, Resolve any Pile Installation Problems

Production piles are installed using the final driving criteria. Pile installation is documented in accordance with established quality control procedures.

D.56 Block 32: Perform Post-Construction Evaluation and Refinement For Future Designs

After completion of the foundation construction, the design is reviewed and evaluated for its ability to satisfy the design requirements cost effectively.